Water Science and Technology Library

VOLUME 41

The titles published in this series are listed at the end of this volume.

HYDROLOGY AND WATER RESOURCES OF AFRICA

by

MAMDOUH SHAHIN

Water Resources Engineering Consultant
Formerly Professor Cairo University, Giza, Egypt
and
IHE-Delft, The Netherlands

KLUWER ACADEMIC PUBLISHERS
NEW YORK, BOSTON, DORDRECHT, LONDON, MOSCOW

CD-ROM only available in print edition
eBook ISBN: 0-306-48065-4
Print ISBN: 1-4020-0866-X

Created in the United States of America

Visit Kluwer Online at: http://kluweronline.com
and Kluwer's eBookstore at: http://ebooks.kluweronline.com

To: AFRICA

A Continent Rich in Development Potential

PREFACE

Africa, the cradle of many old civilizations, is the second largest world continent, and the homeland of nearly one-eighth of the world population. Despite Africa's richness in natural resources, the average income per person, after excluding a few countries, is the lowest all over the world, and the percentage of inhabitants infected with contagious diseases is the highest.

Development of Africa to help accommodate the ever-increasing population and secure a reasonable living standard to all inhabitants, though an enormous challenge is extremely necessary. Water is the artery of life, without it all living creatures on earth cannot survive. As such, a thorough knowledge of the meteorological and hydrological processes influencing the yield and quality of the water resources, surface and subsurface, and their distribution and variability in time and space is unavoidable for the overall development of any part of the world. It is highly probable that the said knowledge is at present a top priority to Africa, a continent that has been for so long-and probably still-devastated by the endless ambitions of colonial powers not to forget the corruption and destruction practiced by the internal powers, at least in some countries.

The present book "Hydrology and Water Resources of Africa" is written with the aim of bringing together in one volume a fair amount of knowledge any professional involved in hydrology and water resources of Africa needs to know. African hydrology, after all, covers a wide range of subdivisions ranging from Hyper-arid and arid (Saharan) to very humid (Tropical). With this aim in mind, the material covering the book is distributed among fourteen chapters. The first chapter, as usual, serves as a general introduction. The second, third, fourth and fifth chapters outline and discuss the basic items relevant to climate such as precipitation, evaporation and evapotranspiration. These four chapters are presented from the angle of applied climatology rather than theoretical meteorology.

Chapter 6 deals with the processes of runoff and streamflow. Such processes combined with the contents of Chapters 2 to 5 help elaborate a reasonable estimate of the water balance of each of the main hydrologic sub-systems of the continent. Chapters 7 and 8 deal with hydrology of large river basins in East and West Africa, and Central and Southern Africa respectively. Certain aspects of hydrological interest concerning intermediate and small river basins, including ephemeral streams (wadis), are outlined and discussed in Chapter 9.

The built-up of Africa includes some areas of wetlands in the form of permanent and seasonal swamps, marshes, and floodplains. The Great Rift Valleys already formed as a result of the tectonic movements and volcanic activities during the Miocene era have created depressions and lakes of depths up to 1,000 m. The volumes of the African Lakes are about eleven times as

much as the annual volume of river flows. No wonder then that the world of Tropical Africa is not dominated by its rivers but rather by its lakes. The principal hydrologic, morphometric and physico-chemical parameters, and the mass balance of several of the wetlands including natural lakes are dealt with in Chapter 10.

Due to the geographic location of Africa, thereupon its climate, the flow of many an African river is highly seasonal. To satisfy the demand on water, the natural supply of several rivers is regulated through storage reservoirs created by the dams built across these rivers. A description of some of the large African dams, their dimensions, functions and the relevant particulars underlying the design of their respective reservoir storage capacities are given in Chapter 11.

The African ground is underlain by groundwater reservoirs some of which have huge dimensions and storage volumes. Classification of these reservoirs according to their geology, and estimates of the hydrogeological parameters of the water-bearing formations and their productive aquifers are given in Chapter 12. Of particular interest are the types of aquifers encountered, rates and means with which aquifers are being recharged. The comparison between the rates of recharge to and extraction from an aquifer serves as a criterion for distinguishing between rejuvenated and non-rejuvenated or fossil water. The quality of groundwater and its suitability for drinking and domestic purposes too are reviewed. The survey and analysis presented in Chapter 12 cover a rather large number of areas of Africa.

Africa consists of a main or fast land and a number of sets or groups of islands. Despite the fact that most of the islands are geographically located at a large distance from the fast land, and are administered by European countries such as France, Portugal, etc, yet in a way they are regarded as part of Africa. With the exception of Madagascar, the fourth largest island of the world, all African islands can be classified as small. Chapter 13 deals mainly with the climate, hydrology and water resources of all African islands whether small or large.

Chapter 14, the last chapter of the book, deals with the development of Africa from the point of view of water resources. The present state of Africa, the water resources development and management projects implemented in the 20th century, and the possible future development and management of water resources are presented. The effects of flow regulation and control works on land irrigation, hydropower development, fisheries, and river navigation are highlighted. Emphasis is laid on both the negative and positive aspects of water sources and storage of water in reservoirs on vector water-related diseases. The discussion is illustrated with a number of field surveys and case studies.

The presentation, analysis and discussion of the contents of the book would not have been possible without using a wide range of data: basically meteorological, hydrological, geohydrological and water quality data. Most, not all, of the data used and the relevant sources of information are made available

to the user of the book on a compact disc (CD Rom) and the rest can be found in the text itself. Classification of the data on the disc is described in the few pages at the end of Chapter 14. It is unfortunate that most of the available data can be fairly described as inadequate, both in quantity and quality. Furthermore, some of the data that used to be continuously recorded or periodically collected are already suffering for sometime from gaps of different widths, and some of them even stopped. The authorities concerned are strongly advised to pay considerable attention, and secure the necessary means for data collection, dissemination and processing.

The preparation of the book contents has certainly required considerable effort and long time. A large number of books, research papers, technical bulletins, reports and documents, all added to the author's professional experience in certain parts of Africa, were assembled, reviewed and worked out. As the book publication is now in sight the author wishes to express his heart-felt thanks to all who have contributed in a way or another to bring it to almost completion. It is impossible to mention the name of each one of them. However, a few names have to be mentioned in recognition of their unforgettable and undeniable services. The author is grateful to Professor V.P. Singh for recommending to Kluwer Academic Publishers, The Netherlands, to consider the publication of the book. Thanks are also due to the staff of the libraries of water resources divisions in many of the World Organizations and Universities. Mrs. P. Franken and the staff of the library of the IHE, Delft, The Netherlands, deserve special mention. Thanks are extended to Mr. Z. Salty and Mr. A. Botrous for their unfailing assistance to solve computer-related problems. Last, but not least, the author is grateful to the publisher for the encouragement as well as useful suggestions to improve the manuscript.

Mamdouh Shahin
Voorburg, The Netherlands

March 2002

SELECTED THEORIES AND PHRASES

"And the name of the second river [is] Gihon: the same [is] it compasseth the whole land of Ethiopia".
(Genesis 2:13, King James Version of the Bible).

And do We not send down
From the clouds water
In abundance,
That We may produce
Therewith grain and vegetables,
And gardens of luxurious growth?
(Verses 14, 15 and16, Sūrat 78: An-Nabaa, The Holy Qur-ān)

It is said that the Greeks used to call the continent Libya. It is also suggested that Africa could be ascribed to the Greek word aphrike ("without cold") or the Latin aprica ("sunny"). The Romans, who for a time ruled the North African coast, are also said to have called the land south of their settlements Afriga, or the land of the Afrigs – the name of a Berber community south of Carthage *(The 1994 – 2001 Encyclopædia Britannica).*

According to Aristotle, Thales of Miletos (624 – 548 B.C.) the chief of the seven wise men of ancient Greece believed that water is the primary element and the world is a flat disc floating upon the seas and oceans.

"And what fun to make the immemorial Nile begin its journey by diving through a turbine!" *(from: My African Journey by Sir Winston Churchill, 1907).*

"If the hungry could eat words, Africa would recover" *(BBC Television commentary on Africa, 1985).*

"La Guinée Equatoriale, bien que petite, sera un pays comme la Suisse en Europe, si elle travaille en paix et dans l'unité" *(d'après S. Eñeso Neñe, Ebano, Santa Isabel, 28 Janvier 1966, p. 2).*

Clean water is a key to poverty alleviation *(the author, 2001).*

CONTENTS

	Page
DEDICATION	v
PREFACE	vii
SELECTED THEORIES AND PHRASES	xi
CHAPTER 1 INTRODUCTION	1
1.1- Geography, Relief and Physical Setting of Africa	1
1.2- Brief Account of Geology, Soils,Natural Vegetation and Agriculture	6
1.3- Exploring Africa's Surface Water Resources	11
1.4- Irrigated Surface and Water Resources	18
1.5- Population Growth, Share per Capita in Water Resources, Supply and Demand	19
CHAPTER 2 CLIMATE	25
2.1- Factors Affecting the Climate	25
2.2- Climatic Data	28
2.2.1 Development of observation stations	28
2.2.2 Data used in the present study	29
2.3- Aridity	54
2.4- Climatic Classification and Regions	57
CHAPTER 3 ANALYSIS OF RAINFALL DATA	65
3.1- Annual Rainfall	65
3.1.1 Rainfall fluctuation in the last twenty millenia	65
3.1.2 Evaluation of the variation of annual rainfall in the 20th century/Drought in Africa	66
3.1.3 Teleconnection of annual rainfall in Africa	80
3.1.4 Frequency distribution of annual rainfall	82
3.1.5 Results of drought risk	87
3.2- Monthly Rainfall	88
3.2.1 Distribution of annual rainfall between the months of the year	88
3.2.2 Statistical analysis of monthly rainfall	93

Chapter 3 Cont'd
3.2.3 Statistical analysis of (maximum) monthly rainfall 95
3.3- Daily Rainfall 98
3.4- Short Duration Rainfall (less than 24 hours) and Intensity-Duration-Frequency Relationships 104

CHAPTER 4 EVAPORATION 113

4.1- Definitions and Background 113
4.2-Instrumental Measurements of Evaporation 114
4.2.1 Piche atmometer 114
4.2.2 Wild evaporimeter 114
4.2.3 Colorado sunken pan 115
4.2.4 Kenya ground pan 115
4.2.5 Symons sunken pan 115
4.2.6 Nigeria ground pan 115
4.2.7 USWB Class A ground pan 115
4.2.8 The Sudan Tank 115
4.2.9 GGI-3000 Tank 115
4.2.10 Comparisons between evaporation measurements using different instruments 115
4.2.11 Concluding remarks 121
4.3- Estimation Methods 122
4.3.1 The Water balance method 122
4.3.2 Energy budget method 124
4.3.3 Combination (Penman) method 126
4.3.4 Kohler's methods 128
4.3.5 Morton's method 129
4.4- Evaporation From Some of the Natural Lakes and Storage Reservoirs in Africa 132
4.4.1 Mean monthly and annual evaporation using different estimation methods 132
4.4.2 Annual evaporation series 136
4.5- Review of Evaporation Data of Some African Countries and Islands 137
4.5.1 Egypt 138
4.5.2 The Sudan 139
4.5.3 Zimbabwe 142
4.5.4 Malawi and Zambia 144
4.5.5 South Africa 145
4.5.6 Madagascar 146
4.5.7 Nigeria 147
4.5.8 Chad and Congo Brazzaville 148
4.5.9 Tunisia 152
4.5.10 Mauritania 154

CHAPTER 5 EVAPOTRANSPIRATION 157

5.1- Definitions and Background 157
5.2- Measurement of Evaporation 158
5.2.1 Gravimetric lysimeters 160
5.2.2 Volumetric lysimeters 161
5.3- Estimation of Evapotranspiration Using Climatic Data 162
5.3.1 Temperature methods 164
5.3.2 Radiation methods 167
5.3.3 Combination methods 168
5.3.4 Evaporation pan methods 169
5.4- Relation Between Evapotranspiration and Potential Evapotranspiration 170
5.5- Country Practices and Experiences 174
5.5.1 Egypt 174
5.5.2 The Sudan 179
5.5.3 Ethiopia 183
5.5.4 Niger 185
5.5.5 Some northwest African countries 188
5.5.6 Chad, Congo (Brazzaville) and Central African Republic 189
5.5.7 Tunisia 193
5.5.8 Morocco 194
5.5.9 Congo (Kinshasa), Rwanda and Burundi 194
5.5.10 Uganda and Kenya 198
5.5.11 Zambia, Zimbabwe and Malawi 199
5.5.12 South Africa 201
5.6- Evapotranspiration from Wetlands 202
5.6.1 Brief description and background 202
5.6.2 Swamps in southern Sudan 205
5.6.3 East Africa (Kenya and Uganda) 205
5.6.4 Zambia 207
5.6.5 Senegal, Niger and Botswana 209
5.7- Evapotranspiration from Woodlands and Forests 209

CHAPTER 6 RUNOFF, STREAMFLOW, EROSION AND SEDIMENTATION 213

6.1- Introduction 213
6.2- Runoff and Runoff Coefficient 215
6.2.1 Water balance of Africa 215
6.2.2 Regional water balance 216
6.2.3 River basins 219
6.2.4 Index catchments 220
6.2.5 Representative basins 222

Chapter 6 Cont'd
6.2.6 Preliminary estimate of flood flow for a given return period 226
6.3- Streamflow 230
6.3.1 Streamflow data 232
6.3.2 Patterns of mean monthly discharges 232
6.3.3 Annual extreme discharges 235
6.3.4 Interannual variability of river flow and analyses of annual flow series 243
6.4- Filling Gaps or Supplementing Missing Runoff/Streamflow Data 256
6.4.1 Recession equation 256
6.4.2 Interpolation equation 256
6.4.3 Recursive models 257
6.4.4 Autoregressive models 257
6.4.5 Extended autoregressive models 257
6.4.6 Regression models 258
6.4.7 Unit hydrograph 258
6.4.8 Storage models 260
6.5- Erosion and Sedimentation 263
6.5.1 Relationship between discharge and suspended sediment load 266
6.5.2 Relationship between sediment yield and drainage area 268
6.5.3 Other factors influencing erosion and sediment yield 268
6.5.4 Sedimentation in storage reservoirs 269
6.5.5 Sedimentation in canals and around hydraulic sructures 270

CHAPTER 7 HYDROLOGY OF LARGE RIVER BASINS: Eastern and Western Africa 271

7.1-The Nile Basin 272
7.1.1 Short description of the basin 272
7.1.2 Water balance of the basin 281
7.1.3 River stage 294
7.1.4 Models related to discharge and discharge forecasting 299
7.2- The Niger Basin 303
7.2.1 Brief description of the basin 303
7.2.2 Availability of hydrological data 309
7.2.3 Hydrology of the Niger Basin 311
7.2.4 Some models for simulating the flow of the Niger and its tributaries 316
7.2.5 Water quality 320

Chapter 7 Cont'd
7.3- Lake Chad Basin 322
7.3.1 Brief description of the basin 322
7.3.2 Hydrology of Lake Chad Basin 326
7.3.3 Water quality 331

CHAPTER 8 HYDROLOGY OF LARGE RIVER BASINS; Central and Southern Africa 335

8.1- The Congo (Zaire) Basin 335
8.1.1 General description of the basin 335
8.1.2 Hydrology of the Congo Basin 339
8.1.3 Stochastic analysis of the mean monthly discharge series, 1903-83, of the Congo River at Kinshasa 346
8.1.4 Water quality 349
8.2- The Zambezi Basin 350
8.2.1 General description of the basin 350
8.2.2 Hydrology of the Zambezi Basin 353
8.2.3 Water quality of the Zambezi River 359
8.3- The Orange Basin 360
8.3.1 Brief description of the basin 360
8.3.2 Hydrology of the Orange Basin 363
8.3.3 Cyclic oscillation of streamflow and runoff prediction 368
8.3.4 Response of streamflow to land use 371
8.3.5 Water quality 372
8.4- Summary Statistics of Large African Basins 374

CHAPTER 9 HYDROLOGY OF SELECTED INTERMEDIATE AND SMALL RIVER BASINS 377

9.1- The Senegal River 377
9.1.1 Brief description of the basin 377
9.1.2 Hydrology of the Senegal Basin 380
9.1.3 Extreme values of stage and discharge of the Senegal River 386
9.1.4 Water quality 388
9.2- The Volta Basin 389
9.2.1 Brief description of the Volta Basin
9.2.2 Hydrology of the Volta Basin 390
9.2.3 Water quality 395
9.3- Sanaga River Basin 395
9.3.1 Brief description of the basin 395
9.3.2 Hydrology of the Sanaga Basin 397

Chapter 9 Cont'd
9.4- Ogooue River Basin 399
9.4.1 Brief description of the basin 399
9.4.2 Hydrology of the Ogooue Basin 400
9.5- Limpopo Basin 402
9.5.1 Brief description of the basin 402
9.5.2 Hydrology of the Limpopo Basin 403
9.6- The Oued (Wadi) Zeroud Basin 405
9.6.1 Brief description of the basin 405
9.6.2 Hydrology of the Oued Zeroud Basin 407
9.6.3 Water quality 409
9.7- The Oued (Wadi) Sebou Basin 412
9.7.1 Brief description of the basin of Oued (Wadi) Sebou 412
9.7.2 Hydrology of the Sebou Basin 413
9.7.3. Erosion and sedimentation 415
9.8- The Gambia River Basin 416
9.8.1 Brief description of the basin 416
9.8.2 Hydrology of the Gambia Basin 417
9.8.3 Water quality of the Gambia River 418
9.9- The Tana Basin 419
9.9.1 Brief description of the Tana Basin 419
9.9.2 Hydrology of the Tana Basin 421
9.9.3 Sediment yield of the Tana Basin 425

CHAPTER 10 HYDROLOGY OF WETLANDS AND NATURAL LAKES 427

10.1- Wetlands 427
10.1.1 Definitions and physical features 427
10.1.2 El-Sudd area in Southern Sudan 431
10.1.3 Wetlands in West Africa 436
10.1.4 Wetlands in southern Africa 437
10.2- Natural Lakes 439
10.2.1 Definitions and physical aspects 439
10.2.2 Sahelian Lakes 443
10.2.3 Nile Basin Lakes 450
10.2.4 Kenyan Lakes 462
10.2.5 South-east African Lakes 464

CHAPTER 11 LARGE DAMS AND STORAGE RESERVOIRS, AND THEIR IMPACTS 475

11.1- Introduction 475
11.2 Some Methods of Determining the Capacity of a Storage Reservoir 476

Chapter 11 Cont'd
11.2.1 Seasonal/annual storage 476
11.2.2 Long-term storage 478
11.2.3 Rippl method applied to synthetically-generated flow data 479
11.2.4 Century storage and the Hurst phenomenon 481
11.3- Large Dams and Reservoirs in Africa 483
11.3.1 Aswan High Dam 483
11.3.2 The Roseires Dam 489
11.3.3 Owen Falls Dam/Lake Victoria 494
11.3.4 Manantali Dam 495
11.3.5 Akasombo Dam/Volta Reservoir 496
11.3.6 Kainji Dam 499
11.3.7 Inga Dam 500
11.3.8 Kariba Dam 501
11.3.9 Cabora Bassa Dam 503
11.3.10 Gariep Dam 505

CHAPTER 12 GROUNDWATER RESOURCES OF AFRICA 509

12.1- Introduction 509
12.2- Types of Aquifers and Their Hydrogeological Characteristics 511
12.2.1 Types of aquifers 511
12.2.2 Hydrogeologic constants 513
12.2.3 Recharge 514
12.3- Groundwater Provinces and Basins 515
12.3.1 The Basement Shield 517
$12.3.2_a$ Sedimentary Province (Sandy formations) 518
$12.3.2_b$ Sedimentary Province (Nubian sandstone) 520
$12.3.2_c$ Sedimentary Province (Limestone formations) 521
12.3.3 The Volcanic Province 521
12.3.4 The Chad Basin 522
12.4- Groundwater in Selected Regions and Countries 522
12.4.1 The Nile Basin Region 522
12.4.2 North and West Africa 529
12.4.3 East Africa 542
12.4.4 Equatorial Africa 543
12.4.5 Southern Africa 546
12.5- Vulnerability and Impacts of Groundwater Exploitation 556
12.5.1 Vulnerability of groundwater 556
12.5.2 Impacts of groundwater exploitation 557

CHAPTER 13 HYDROLOGY AND WATER RESOURCES OF AFRICAN ISLANDS 565

13.1- Introduction 565
13.2- North Atlantic Islands 566
13.2.1 The Azores (Acores) Islands 566
13.2.2 The Madeira (Funchal or Madeiras) Islands 566
13.2.3 The Canary Islands (Canaries) 568
13.2.4 Cape Verde Islands 568
13.3- Equatorial Islands 570
13.3.1 Principe and Sao Tome 570
13.4- South Atlantic Islands 571
13.4.1 Ascension Island 572
13.4.2 Saint Helena Island 572
13.4.3 Tristan da Cunha Island 572
13.5- Indian Ocean Islands 573
13.5.1 Seychelles Island 574
13.5.2 The Comoros Islands (Comoros) 576
13.5.3 Mauritius Island 577
13.5.4 Rodriguez Island 579
13.5.5 Reunion (Bourbon) Island 579
13.5.6 Madagascar Island 579

CHAPTER 14 WATER RESOURCES AND DEVELOPMENT OF AFRICA 583

14.1- Africa at Present 583
14.1.1 Africa's population and gross national product 583
14.1.2 Agriculture, forestry, fishing and food 584
14.1.3 Water resources 586
14.1.4 Water-related diseases 588
14.2- Water Resources Development and Management Projects in the 20th Century 591
14.2.1 River flow regulation for land irrigation 591
14.2.2 Management of river flow for hydropower development 593
14.2.3 River flow regulation and flood protection 594
14.2.4 Effect of storage reservoirs on fish 594
14.2.5 Impacts of storage reservoirs on the upstream and downstream of rivers 595
14.2.6 Impacts of large-scale river management schemes on water-related diseases 595
14.2.7 Social impacts of reservoir construction 595
14.3- Future Development and Management of Water Resources 596
14.3.1 Combating water-related diseases 596
14.3.2 Sharing water resources 597
14.3.3 Water management for irrigation 598
14.3.4 Water management for hydropower development 599
14.3.5 River (inland) navigation as a means of development 599

REFERENCES 603

GUIDE TO METEOROLOGICAL, HYDROMETRIC AND WATER QUALITY DATA USED IN THE BOOK 629

Note to the Reader 631
Abbreviation of Country and Island Names 632
Nomenclature and Units used in Appendixes A and B 633
Key to Meteorological Data (Appendix A) 634
Key to Hydro and Water Quality Data (Appendix B) 635
Part I 635
Part II 636

REFERENCE INDEX 639
GEOGRAPHICAL INDEX 645

CD-Rom with raw meteorological, hydrometric and water quality data: inside back cover

CHAPTER 1

INTRODUCTION

1.1- Geography, Relief and Physical Setting of Africa

Africa is the second largest continent in the world. Together with the islands belonging to it, Africa has a surface area of about $30.65*10^6$ km^2. The largest distance from north to south is about 8,000 km, and the largest width (Cape Hafun, Somalia,- Cape Verde Isl.) is 7,600 km. Since Africa is situated between the latitudes $\varphi = 37^o\ 21'$ N and $\varphi = 4^o\ 51'$ S, the continent is nearly equally bisected by the Equator. The surface area of the northern half, however, is about 68% of the total area i.e. nearly two times the size of the southern half. Additionally, nearly 75% of the total surface is situated between the Tropics of Cancer in the north and Capricorn in the south, rendering Africa a tropical terrain. Tropical areas as a rule are described as the least developed parts of the world. The tropical surface of Africa is definitely no exception to this rule.

As of 1993, the landmass of Africa comprises 48 countries. The surface area per country varies from a maximum of about $2.5*10^6$ km^2 to a minimum of about $11*10^3$ km^2. Nearly 55% of the countries have an area of less than $0.5*10^6$ km^2 each, 75% less than $1*10^6$ km^2, 94% less than $2*10^6$ km^2 and the remaining 6% larger than $2*10^6$ km^2. Furthermore, some countries have long seacoasts in proportion to their size; e.g. the ratio for each of Equatorial Guinea and Guinea-Bissau is 7-8, Somalia 5.6 and Mozambique 3.1 km/ km^2. As nearly 30% of the African countries are land-locked, the overall average ratio is in the order of 1km/ km^2.

Next to the landmass, the makeup of Africa comprises a number of islands. These are the Canaries, Cape Verde, Comoros, Madagascar, Madeiras, Mauritius, Réunion, São Tomé and Principe, and the Seychelles. The map in Figure 1.1 shows the international frontiers and capitals of the countries within the landmass. Additionally, the code name, hemisphere, name of the capital city, surface area and length of the sea/ocean coastal line are given in Tables 1.1_a and 1.1_b for the land mass and islands, respectively.

The surface of Africa is covered by an alternation of tablelands or plateaus and shallow depressions or basins at varying elevations The plateaus in the south and east have a higher elevation (above 1,000 m) than the rest of the continent. The Lowlands and the Higher lands can be conveniently separated by a line extending from the Nile valley southwards across the upper Congo Basin. The area situated northwest of this line constitutes lowland plains, from 150 to 600 m in altitude. The major drainage basins in this area are those of the middle and lower Nile, the Sénégal,

the Niger and the Chad inland drainage systems. Higher altitudes are limited to the Atlas Mountains (up to 4,200 m), the Ahaggar and the Tibesti massifs, the Highlands of the Cameronian Range (above 3,000 m) and the Guinean Highlands. Most of the land located southeast of the dividing line is higher than 1,000 m in altitude. However, exceptions from this division can be found in the coastal strip extending southeast from Somalia, adjacent to the Indian Ocean (Martins & Probst, 1991)

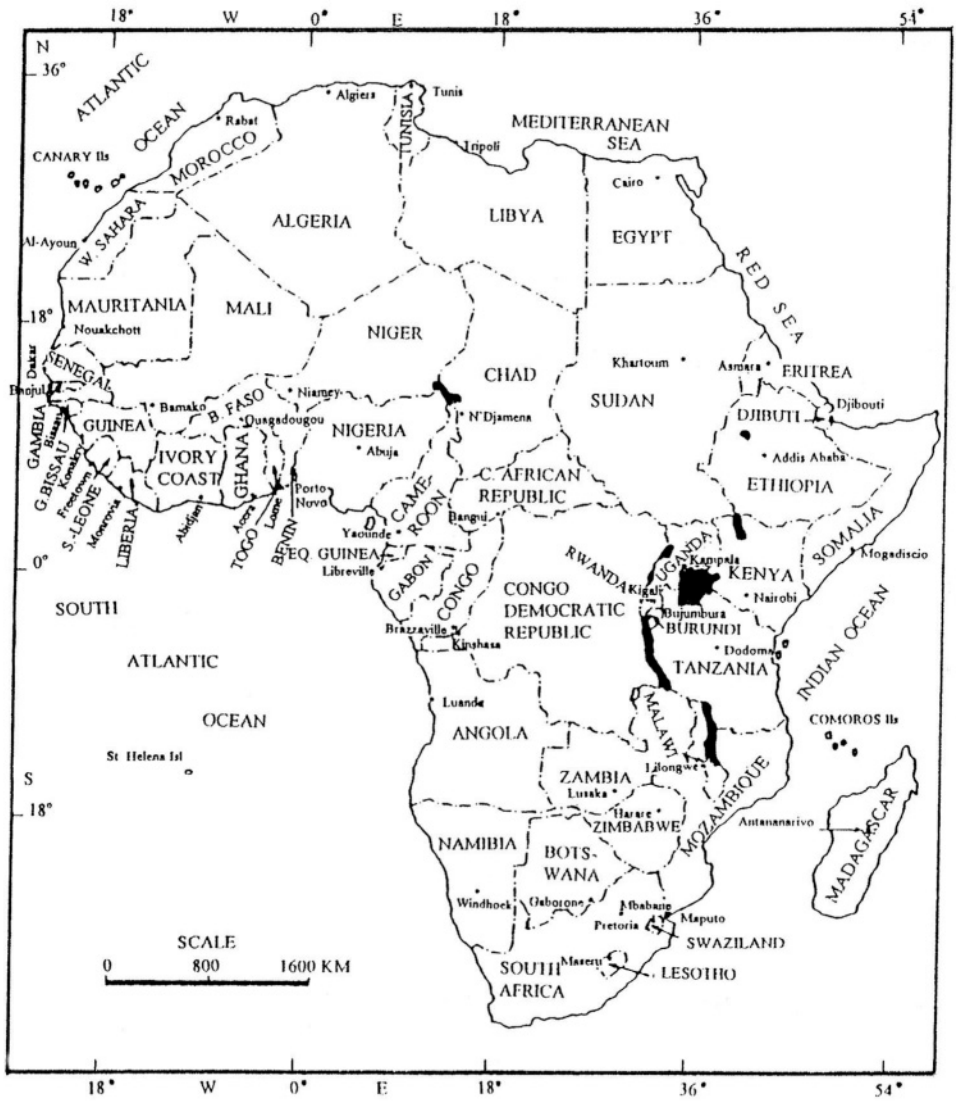

Figure 1.1- Political map of Africa after 1993

Table 1.1$_a$- Geographic locations, capitals, surface areas and lengths of sea/ ocean coast of African countries

Country	Code name	Hemi-sphere	Capital city	Area (km^2)	Length of coast$^+$ (km)
Algeria	Alg	N	Algiers	2,381,741	1,200
Angola	Ang	S	Luanda	1,246,700	1,380
Benin	Ben	N	Porto Novo	112,622	110
Botswana	Bot	S	Gaborone	581,730	0
Burkina Faso	BrF	N	Ouagadougou	274,200	0
Burundi	Bur	S	Bujumbura	27,834	0
Cameroon	Cmn	N	Yaounde	475,442	420
Central African Republic	CAR	N	Bangui	622,984	0
Chad	Chd	N	N=Djamena	1,284,000	0
Congo (Brazzaville)	CnB	N/S	Brazzaville	342,000	180
Congo (Kinshasa)	CnK	N/S	Kinshasa	2,344,885	60
Djibouti	Djb	N	Djibouti	23,200	315
Egypt	Egy	N	Cairo	1,001,449	2,395
Equatorial Guinea*	EqG	N	Bata	28,051	255
Eritrea	Ert	N	Asmara	124,320	900
Ethiopia	Eth	N	Addis Ababa	1,221,900	0
Gabon	Gab	N/S	Libreville	267,667	1330
Gambia, The	Gam	N	Banjul	11,295	260
Ghana	Ghn	N	Accra	238,537	650
Guinea	Gun	N	Conakry	245,857	400
Guinea Bissau	GnB	N	Bissau	36,125	340
Ivory Coast	IvC	N	Abidjan	322,463	890
Kenya	Ken	N/S	Nairobi	580,370	470
Lesotho	Les	S	Maseru	30,355	0
Liberia	Lbr	N	Monrovia	111,369	540
Libya	Lib	N	Tripoli	1,759,540	1,780
Malawi	Mlw	S	Lilongwe	118,484	0
Mali	Mal	N	Bamako	1,240,190	0
Mauritania	Mrt	N	Nouakchott	1,025,500	610
Morocco	Mor	N	Rabat	446,550	1,680
Mozambique	Moz	S	Maputo	801,590	2,450
Namibia	Nmb	S	Windhoek	824,292	1,310
Niger	Ngr	N	Niamey	1,267,000	0
Nigeria	Nig	N	Abuja	923,768	850
Rwanada	Rwd	S	Kigali	26,330	0
Senegal	Sng	N	Dakar	196,720	590
Sierra Leone	SrL	N	Freetown	71,740	550
Somalia	Som	N	Mogadiscio	637,657	3,400
South Africa	Saf	S	Pretoria	1,221,042	2,300
Sudan, The	Sud	N	Khartoum	2,505,813	720
Swaziland	Swz	S	Mbabane	17,363	0
Tanzania	Tnz	S	Dodoma	945,087	770
Togo	Tog	N	Lome	56,790	75

Table 1.1_a- Cont'd.

Country	Code name	Hemi sphere	Capital city	Area (km^2)	Length of Coast[+] (km)
Tunisia	Tun	N	Tunis	163,610	1380
Uganda	Ugd	N/S	Kampala	235,880	0
Western Sahara	WSH	N	Al-Aaiún	266,000	975
Zambia	Zmb	S	Lusaka	752,614	0
Zimbabwe	Zmw	S	Harare	390,580	0
Total				30,040,056	31,535

Source of information about capital cities, surface areas and 1994 population figures is the World Guide 1997-1998 (1997)

[+]*Length of coastalline at mean sea level*

[*]*Including the islands of Fernando Poo and Annobon*

Table 1.1_b- Geographic location, capital, surface area and length of coast of African islands

Island/group of islands	Code name	Hemi-sphere	Capital city	Area (km^2)	Length of coast[+] (km)
Canaries	CnI	N	Las Palmas	7,273	-
Cape Verde	CvI	N	Praia	4,033	810
Comoros	CmI	S	Moroni	2,238	-
Madagascar	Mdg	S	Tananarive	587,040	4,100
Madeiras	M	N	Funchal	797	-
Mauritius	MtI	S	Port Louis	1,860	190
Reunion	RnI	S	St. Denis	2,512	240
Sao Tome & Principe	STP	N	Sao Tome	960	100
Seychelles	SyI	S	Victoria	280	66
Total				606,993	

Source of information about capital citie, surface areas and 1994 population figures is the World Guide 1997-1998 (1997)

+ Length of coastalline at mean sea level

Some mountains rise from the surface of the East African plateau, of which the Kilimanjaro (5,895 m) and Elgon (4,300 m) are the most notable ones Farther to the northeast, certain peaks in the Ethiopian Highland, such as Ras-Dashen, reach 4,620m. Down to the southeast, one can observe that Lesotho is bordered on the eastern side by mountain peaks well above 3,200 m. Remarkable enough that these mountain ranges are at a distance of 200 km or less from the ocean coast. At a large distance to the west, the Ruwenzori Range rises north of Lakes George and Edward in the extreme west of Uganda with peaks reaching 5,120 m.

Some of the shallow depressions form inland drainage basins for certain parts of the plateaus on which these depressions are scattered. Other parts of the plateaus are drained by rivers basically formed by erosion processes, which pass through canyons or falls on their way to coastal plains. It is quite common to identify a certain area that collects precipitation water and supplies it to a drainage network by its watershed.

The Food and Agriculture Organization (FAO, 1987) has identified 335

watersheds in Africa. These watersheds are aggregated into 25 major basins. Some of the relevant details about these basins are summarized in Table 1.2. It can be seen from this Table that more than half the surface of Africa is drained by the basins of nine rivers and one lake, namely: The rivers Congo/Obangui, Nile, Niger, Zambezi, Orange (including the Vaal), Shibeli and Juba, Sénégal, and Limpopo along with Lake Chad.

Africa is characterized by the hot climate of most of its regions and for most of the time of the year. The average air temperature at sea level for January and July varies from less than 15°C to more than 35°C, depending on the geographic location and the season of the year (Nieuwolt, 1977). According to Paffen (1966), the mean daily range of temperature does not exceed 10° C for the coastal strips as well as along the Equator. This range increases with distance towards the heart of the continent to reach or exceed 20° C.

The mean annual rainfall in Africa varies from less than 100 mm to more than 3,000 mm. The remarkable feature is that the climatic divisions or classes can be approximated by more or less parallel bands extending from west to east, with the heaviest rainfall (tropical wet climate) around the Equator. Rodier (1964) suggested that these bands can be classified according to the annual rainfall into desert (100-150 mm), sub-desert (150-300 mm), sahelian (300-750 mm), tropical (750-1,200 mm) and tropical-equatorial (more than 1,200 mm).

Most of the major rivers of Africa run in a lateral direction from west to east. The Nile and its tributaries are probably the only exception to this rule, as they run from south to north. This state of affairs, added to the heavy losses incurred in the vast areas covered by swamps, is causing the average natural supply of the Nile per unit basin area to be the lowest for all African Rivers, perhaps for all world major rivers.

A special feature of Tropical Africa is the permanent and intermittent swamps. The surface covered by these swamps has been estimated at $340{,}000\ km^2$, i.e. about 1.1% of the total area of Africa. The swamps are distributed over the drainage basins of major rivers like the Zambezi, Congo, and the Upper Nile, as well as lakes Victoria, Kyoga, Chad and Mweru. The different kinds of the swamps and their respective hydrological and ecological characteristics will be presented in a later chapter.

Quite different from the swamps are the Chotts and depressions, which cover certain parts of the surface of North Africa. Among the well-known Chotts are the Jerid ($5{,}000\ km^2$ in area and 16 m in depth), Gharsa (23 m in depth in Tunisia). These are important salt lakes. Many Chotts can be found as well in Algeria. When a low-lying coastal strip extends into the desert, the salt lake is often called a Sabkha (sometimes Sabhat). An excellent example of this is Sabhat Ghuzzayil, which is a large salt lake situated 47-m below mean sea level. This is the level of the lowest point in Libya. The deepest depression in Africa, with its lowest point at 153 m below mean sea level, lies in the Western Desert of Egypt, and is known as Quattara depression. This very deep depression comprises multiple Sabkhats.

Table 1.2- Data about the watersheds and major basins in Africa (FAO, 1987)

Major basin	Surface area (km^2)	Number of watersheds	Number of riparian countries	Annual rainfall (mm)
Senegal (R)	486,438	1	-	592
Niger (R)	2,228,110	5	12	720
Chad (L)	2,370,307	3	7	437
Nile (R)	3,106,130	12	10	649
Rift	620,308	13	10	660
Shibeli/ Juba (R)	827,205	3	3	400
Congo/ Obangui (R)	3,774,248	10	10	1,570
Zambezi (R)	1,300,000	7	9	936
Okavango (R)	321,121	2	3	685
Limpopo (R)	404,567	3	4	524
Orange (R)	637,839	4	4	354
South Interior	920,401	3	4	-
North Interior	5,775,608	12	-	48
Med. Sea Coast	728,723	19	4	266
North West Coast	685,858	11	4	142
West Coast	1,443,758	26	11	1,544
West Central Coast	703,049	16	8	1,940
South West Coast	513,983	24	2	906
South Atlantic Coast	367,377	23	2	175
Indian Ocean Coast	675,530	34	4	686
East Central Coast	1,026,011	41	4	946
North East Coast	750,344	10	5	158
Madagascar West	398,078	21	1	1,275
Madagascar East	188,950	22	1	1,815
Islands [+]	188,950	11	-	
Total	30,308,967	325		

[+] *Canaries, Madeiras, Cape Verde, SaoTome & Principe, Fernando Poo, Mascarene, Comoros, Pemba, Zanzibar, Mafia and Ilha Inhaca.*

A remarkable feature of the surface of the Western Desert, especially in Egypt and Libya, are the oases. The artesian flowing groundwater allows the oases to be well-inhabited areas. The local population is surviving on irrigated agriculture, grazing and production of simple rural commodities.

1.2- Brief Account of Geology, Soils, Natural Vegetation and Agriculture

The greater part of Africa consists of a very ancient mass originating from the Precambrian crystalline and metamorphic rocks. The Precambrian can be subdivided into three major units. These are the Lower Precambrian, predominantly consisting of granitoids and granite gneisses; the Middle Precambrian, essentially schist quartzic and eruptive material; and the Upper Precambrian with schist, sandstone, lava and conglomerates.

The basal complex is exposed over very large areas. Its outcroppings correspond

to the uplift areas, which encircle the low-lying basins with sedimentary formations. Typical examples can be found in the basins of the Zambezi, Congo, Niger and Nile Rivers. Within these areas the ancient formations are mainly calcero-dolomitic rocks and calcareous shales of marine origin. The more recent formations consist of shales and sandstones. Sandstone deposits filled most of the coastal sedimentary basins during the Intercalary period (Jurassic and Lower Cretaceous). Sandstone formations developed further in the Tertiary period.

Paleozoic rocks, mainly carboniferous, are folded and appear in the form of mountain ranges in two places: northwest in Algeria and Morocco, and deep south in South Africa close to the ocean coast. The strain exerted on the rigid mass of Africa for a long time resulted in the rift system. This system consists of two great fractures extending from north to south, mainly on the eastern side of the continent.

The rift extends from Jordan and the Red Sea in the north down to South Africa. The western rift runs through or very closely parallel to Lakes Albert, Edward, Tanganyika and Malawi. The faulting and fracturing processes were associated with volcanic eruptions. There are many areas in Ethiopia and Kenya covered with lava. Examples of the volcanic cones in East Africa are Mount Kenya, Kalimanjaro and Mount Elgon. The map in Figure 1.2 shows the approximate boundaries of the fold mountains, sedimentary basins, volcanic terrains and the basement shield in Africa (based on Wright, 1983).

Soils are the product of all processes exercised by the prevailing climates on the parent materials. As such, African soil types are widely variable, and for each climatic type there can be rich as well as poor soils.

Generally speaking, sands, gravels and pebbles cover desert regions. The soils of the highly elevated areas are usually shallow and mostly covered with stones. The African deserts represent no less than one-third of the total surface area of the continent. All or parts of some eleven countries in North Africa are considered to belong to desert. These countries are Algeria, Chad, Egypt, Libya, Mali, Mauritania, Morocco, Niger, Sudan, Tunisia and Western Sahara. Arid or desert areas are also to be found in southwestern Africa (Namib) and central southern Africa (Kalahari).

Despite the marked absence of surface water resources, nearly all deserts have some stored water at some depth. This water may be moving through underground channels, whenever a gradient exists, In other cases, groundwater may be old and non-rejuvenated (fossil water). Fog and dew are important items in the hydrological cycle of the desert areas. The condensed dew water in the Namib hyper desert has been estimated at $40\ mm\ y^{-1}$ (WMO, 1973). Such an amount can support the growth of short-lived plants. The natural vegetation that exists in all desert countries is widely dispersed and very poor in species. As mentioned earlier, oases are extremely essential for the nomadic and sedentary populations of the desert. Palm dates and some irrigated fields covered with cereals and vegetables provide the necessary foodstuffs.

Steppe, which is typically semi-arid in climate (up to $400\text{-}mm\ y^{-1}$ rainfall), is

located to the south of the hyper-arid Sahara. One can list no less than seven countries included in this region. These are Chad, Mauritania, Niger, Nigeria, Senegal, Somalia and Sudan. This geographic fearure is also to be found in the southern part of Africa under the name of middle latitude steppe. The steppe region is characterized by its ferruginous soils. These are often alkaline, but may become slightly acidic if heavily leached with water. The natural vegetation here is a thorny Acacia and certain local grasses. This natural vegetation supports the nomadic pastoral economy in the Sahel region, which is the steppe region situated in northwest and part of West Africa. Steppe is usually classified into semi-desert steppe and wooded steppe. The latter is an extension of the woodland and savanna.

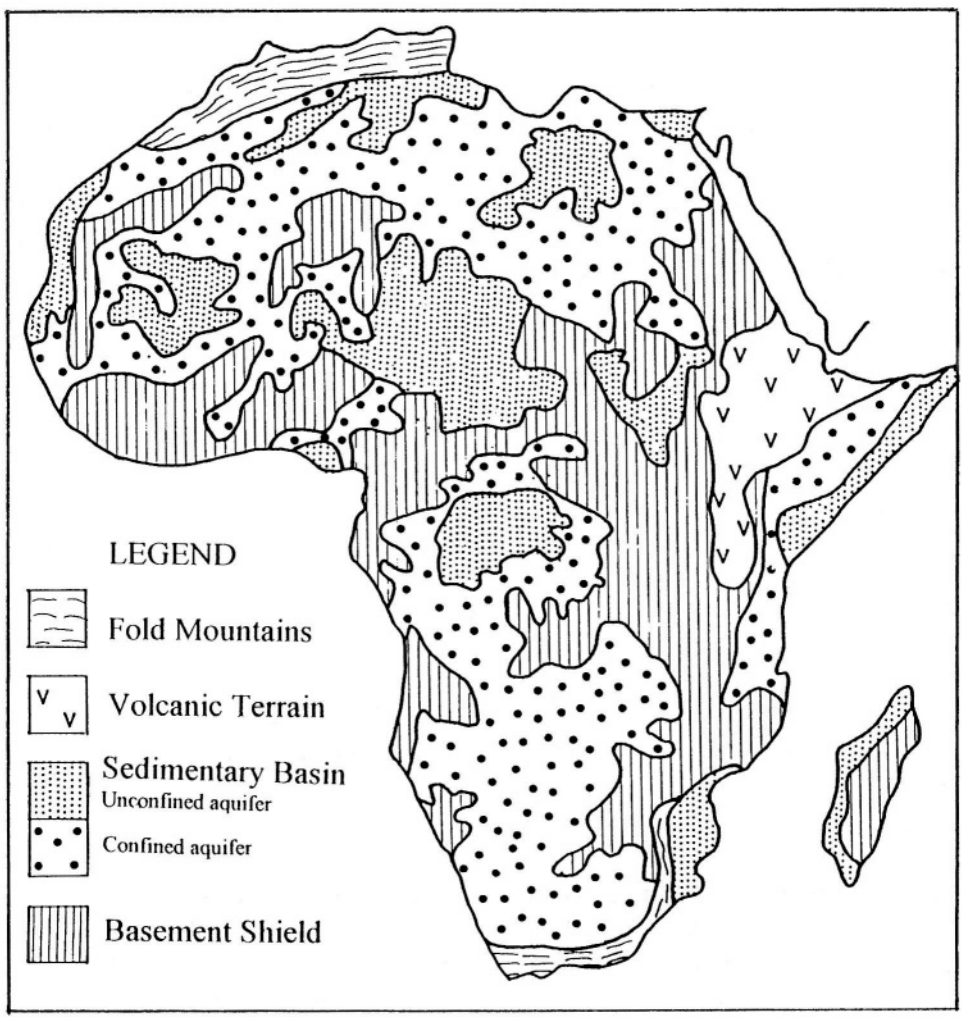

Figure 1.2- Generalized geohydrological divisions of Africa (based on Wright, 1983)

Savanna is the name given to those areas where dry and wet climates alternate, i.e., seasonally well-watered areas. As such, savannas are in fact subject to unfavourable land drainage conditions. Savannas cover at least one-third of the African tropics. The main countries concerned are, from west to east: Senegal, Mali, Burkina Faso, Ghana, Nigeria, Cameroon, Sudan and lowland Ethiopia. Certain parts of Kenya, Tanzania, southern Africa and Madagascar can be included in this group, Most of the soils found in the northern part of Ivory Coast, Burkina Faso, some parts of Ghana, Togo, Angola, Zimbabwe and Mozambique are ferruginous tropical soils (ferric Luvisols and Cambisols). These are easily cultivated but they also lose their structure easily, In many types of savanna, a differentiation is made between grass savanna, shrub savanna and woodland savanna. This differentiation is essentially based on the quantity and duration of available water.

Contrary to the savanna a tropical rainforest is a perennially well-watered region. As such, a rainforest is an area where the annual rainfall is in excess of the water needs of forest plants. The African equatorial rainforest together with savanna occupy more than half the area of Africa. The equatorial rainforest can be found in Guinea, Guinea Bissau, Sierra Leone, Liberia, Ivory Coast, Ghana, Cameroon, Togo, Benin, Nigeria, Congo (Kinshasa and Brazzaville), Equatorial Guinea and Gabon. Some of the significant rivers of tropical Africa are fed from the runoff of the equatorial forest area. These are the Middle Niger, Tana, Rujiji and the most important sub-basins of the Congo and Bangui (Balek, 1977) Acid soils (Ferralsols and Acrisols) are found in the low-lying parts of the Congo and the Niger basins. These soils are known to have good physical properties and are resistant to erosion. Almost all forests have been affected by human activities. The rate of deforestation has become a matter of concern on both the African and world levels because of its impact on climate, land and water resources (UNEP, 1985).

Highland grasses and mountain forests are found in volcanic areas and where the elevation of the ground is at or above 1,500 m. They cover certain parts of Ethiopia, Kenya and southern Africa soils (Nitosols and Ondosols). These soils are heavily erodible on steep hills,

The above classification of vegetation zones in Africa is a rather simplified one. The map shown in Figure 1.3 has been developed from a number of source maps, of which the one published by Grove (1978) can be regarded as the main one. More detailed classifications of vegetation belts, especially in tropical Africa, can be found in specialized literature (e.g. Aubreville et al., 1959)

Most of Africa's farming communities already grow trees. In Malawi, a 1982 Survey showed that 40% of families had planted trees during the past five years, and some had planted up to 100. In Kenya, many people plant trees for fruit, timber, shade and ornament. The thorn tree *Acacia albida* is valued highly in Senegal and other parts of the Sahel; it is either deliberately planted or left standing when land is cleared for agriculture. The role of this tree in the farming system has been reported as follows by the FAO (1981): The tree roots, by penetrating deep into the soil, can

draw up nutrients and use water that would otherwise be lost. The trees themselves shed their leaves in the wet season when agricultural crops are growing. They also provide shade for cattle in the dry season. The local people depend on these trees to produce the firewood and fodder they need.

A wide variety of crop agriculture is practiced in most African countries though at a varying extent. Millet, sorghum, maize, cassava, corn and other grain crops provide the necessary carbohydrates and are used for local consumption. Rice, though planted and consumed in some countries, is not a popular foodstuff for the Africans as it is for the Asians. Cocoa and coffee beans, tea, groundnuts, sesame, cotton, tobacco, oil palm date palm and rubber are among the chief means of earning foreign currency earning. A considerable proportion of the annual yield is kept for export The same applies to such other fruits as mangos, bananas, coconut, pineapple and papaya.

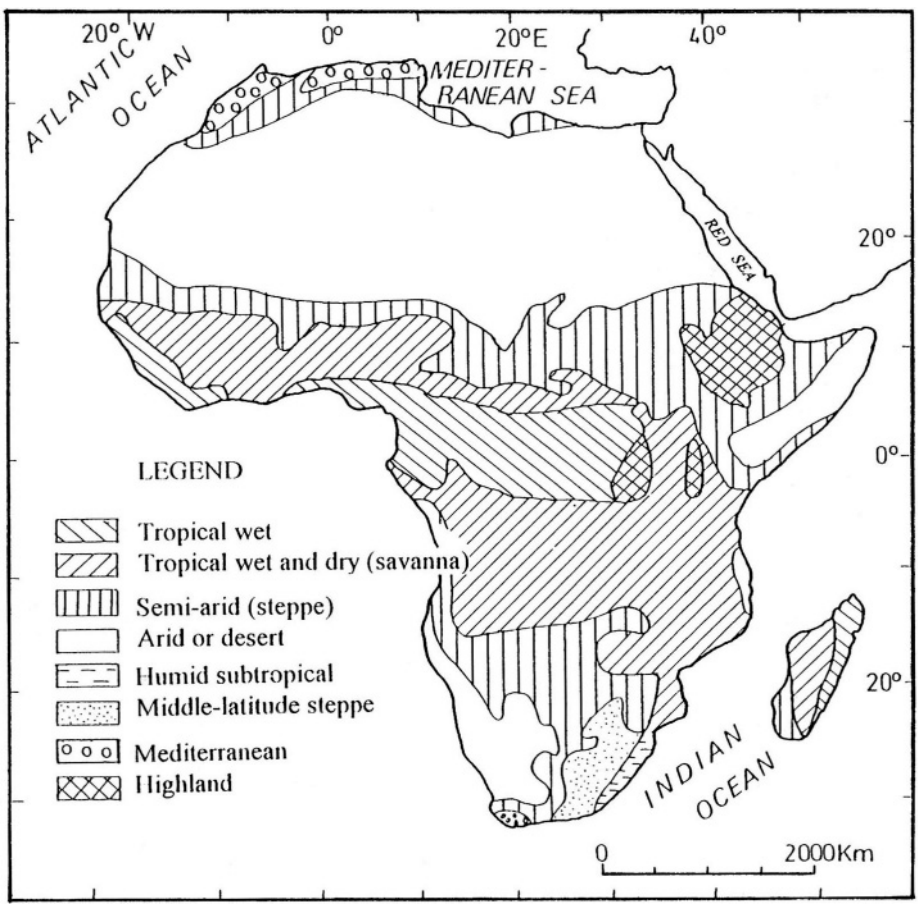

Figure 1.3- A simplified map of the vegetation belts in Africa

One should realize that the above-mentioned crops are not necessarily grown under irrigation; they can be grown fully or partly under rain. Whereas cotton in Egypt gets all the water it needs for growth through irrigation, it is grown under rain in Uganda and Mozambique. The quality and yield of rice, which is used to be grown under rain alone in the Gambia have shown a remarkable improvement when supplementary irrigation was applied.

Since the greater part of Africa, considering the predominantly hot climate, is quite limited, plant growth and crop production depend to a large extent on irrigation. Even in the wet parts, the distribution of rainfall does not always help to supply the right amount of water to the crops at the right time that they need it for their proper growth. This state of affairs has led many of the authorities in charge of agricultural development to consider seriously the importance of land irrigation for their respective countries.

1.3- Exploring Africa's Surface Water Resources

The African continent is one of the most ancient continents in the world. It is bounded on the north by the southern shores of the Mediterranean Sea, on the west and south west by the Atlantic Ocean, on the south east and east by the Indian Ocean and by the Red Sea on the north east. Without the Sinai Peninsula, which separates it from Asia, Africa would have been the world's largest island.

By virtue of its geographical location, the contact between North Africa and Europe and Asia is as old as history itself. This contact has, among other things, a long-lasting influence on some of the hydrological factors affecting the continent's surface water resources. Probably the most impressive example in this respect is the measurement of the annual flood stages of the Nile River at certain gauging sites called Nilometers. The ancient gauge levels of the Memphis Nilometer from the first dynasty (about 3050 B.C.) till the fifth dynasty (about 2500 B.C.) are engraved on the Palermo stone. For the Greco-Roman period in Egypt only few quantitative data are known about the level of the Nile. The ancient gauging sites, however, remained in operation guarded by the Copts (Christians of Egypt) till the Arab conquest of North Africa. Though the Arabs control of these sites in 641 A.D., the Copts remained as guardians for two more centuries. The Arabs used a number of gauging sites around Cairo till the Nilometer on the island of Roda, better known as the Roda Nilometer, was constructed. The maximum and minimum levels of the Nile at Roda have been gauged and recorded regularly and accurately till the conquest of Egypt by the Ottoman Turks in 1517. From thsat time and until the Napoleonic expedition of 1798 reached Egypt, on even later, many records are either missing or of poor quality. More elaborate discussion of river water gauging in Africa shall be presented in a later chapter.

Before we dwell on the history of exploring Africa's surface water resources (rivers and lakes), it might be worthwhile to highlight some of the dynamic processes

underlying the formation of river drainage basins. Stream erosion of the landmass during the heavy pluvial episodes of the early Miocene ($20*10^6$ y B.P.) created the ancient drainage patterns, which still form the basis of the hydrology of a large part of the continent. This had been effected by rivers flowing from a higher central region to lower areas eastward and westward. On the other hand, the upward earth movements and volcanic activities in the Miocene period also created depressions and minor lake basins distributed approximately along a north-south axis. Those activities also caused a wide stretch of land extending from Eritrea to the Zambezi River to be lifted up more than 1,000 m. As a result of the gradual sagging of the center of that stretch, Lake Victoria was formed and the two edges were raised further to form two great rifts. Tectonic activities in and near these valleys formed a series of splits in the earth's crust, some of which were more than 1,000 m deep, and filled in with water. As such all Great Lakes in East Africa, except Victoria, were then formed (Crul, 1997).

Despite the early-established contacts between Europe and North Africa, the waters and shores circumscribing Africa did not become well known to the European sailors until the 15th century. Navigation from Europe to east and south east Asia around Africa seems to have been encouraged by the legendary voyage of Vasco da Gama from Portugal to India about 1497.

To reduce the risk associated with sea voyages from west to east, the navigators established some control posts and service points for their ships on the shores of the continent and the surrounding islands. Despite the experience they gained with the African coasts, it took no less than three centuries before successful exploration missions could occur. Contrary to the Europeans, the Asians and Arabs crossed the Indian Ocean from east to west much earlier. Immigrants from Southeast Asia settled in Madagascar, and Arabs invaded the East African coast, some of them penetrating deep inland and settling there.

It is recorded that a Portuguese missionary, Father Lobo, reached Ethiopia in the year of 1622. Unfortunately nothing of substance is known about his achievements there. It was nearly 150 years later when James Bruce, a Scottish explorer, sailed down the Blue Nile to its confluence with the White Nile. In 1795 another Scottish explorer, M. Park entered Africa from the mouth of the Gambia River and traveled down the Niger eastward for some distance before stopping his expedition. Ten years later he again traveled the same route and was probably murdered before completing his mission.

Some Dutch retirees from the Royal Dutch East India Company, instead of going back home, preferred to stay overseas. They formed a community of farmers (Boers) and settled in Cape Town (Cape of Good Hope) in the middle of the seventeenth century. After Cape Town became a British colony in 1814 they were forced to leave the place. They took the hardship to cross what is now known as the Orange River and migrated inland to establish for themselves the Orange Free State. Those who sailed further and crossed the Vaal River established what became later known as the

Transvaal Republic. The Boers used both rivers to irrigate the lands they occupied. There is hardly any information of the hydrology of these rivers or their respective basins from that time.

In 1828 a Frenchman, Auguste Caille, entered Africa from Guinea and after crossing the North African Sahara (desert) was able to reach Morocco. French interests in West and Equatorial Africa began as early as 1643, when they took possession of the Island of Reunion in the Indian Ocean. In 1658 they founded Saint Louis, which later became the capital of the Sénégal (at present the second town after Dakar). They kept Mauritius Island in their possession for almost a century (1715-1810). The French resumed, even accelerated, the speed of their penetration in Africa after the Napoleonic wars came to an end. This situation can be evidenced by their discovery of the River Gabun in 1841 and their founding of the principal town and port of Libreville. About the same time they imposed their influence on the Ivory Coast and a little later on Benin (formerly Dahomey). The military difficulties caused to France by Germany and the resulting loss of Alsace-Lorraine prompted further the French expansion and possession of townships along the West Coast of Africa. This has been well described by Stamp & Morgan (1972) in "Everywhere the story is the same; coastal settlements followed much later by extension inland". Surprising enough that the occupation of West Africa by France went on without any mentionable resistance from Great Britain. Probably that was the case so that Britain, in return, would be left a free hand in implementing her policy of expansion in the remaining parts of Africa

Livingstone, a British missionary, after having spent about ten years in the southern part of Africa, sailed up the Zambezi River and reached Victoria Falls. Two years later Richard Burton and John Speke traveled from Zanzibar, on the east coast, westward till they overlooked the East African rift valley and Lake Tanganyika. Due to the sickness of Burton, Speke continued the route northward and was fortunate to discover alone Lake (Nyanzna)Victoria before returning back to Burton. In 1858, D. Livingstone started his second Zambezi expedition. He sailed together with J. Kirk up the Zambezi through the Shire River and in 1859 they discovered Lake Nyassa, the third largest lake in East Africa. Two years later Speke, joined by A.Grant, visited Rippon Falls, at the outfall of Lake Victoria. In 1863, Speke declared that he had already discovered the source of the Nile River. In the same year, another explorer named Samuel Baker sailed up the White Nile through the vast swamps of the Sudd region (southern Sudan). Exploration of the River Atbara, a tributary of the Nile, around 1862, and two years later Albert Nyanza are both credited to Baker.

Livingstone started his third and last expedition from Zanzibar in 1866. He was able to reach the mouth of the Ruvuma River and Lake Nyassa (presently known as Lake Malawi). He continued his expedition by turning west and northwest to discover Lakes Mweru and Bangweulu. In 1871, Stanley went to meet Livingstone somewhere in the vicinity of Lake Tanganyika, but he found him seriously ill. One year after the death of Livingstone in 1873, Stanley Baker crossed Lake Victoria then traveled

westward and discovered the Lualaba River, a tributary of the Congo. From the Lualaba he continued his voyage to discover the main stream of the Congo down to its mouth on the Ocean. These discoveries motivated the Belgian Monarch then to develop strong ties with Stanley; a situation that enabled the King of Belgium to possess the Congo as one of his territories. Later Congo became a colony under the Belgian rule.

In 1878-1880 and 1890-1891, the Scottish explorer J. Thompson passed Lake Nyassa, both on the north and the south, on his way to other Central African Lakes (Crul, 1997). Later expeditions to Africa were basically for political purposes. Geographical expeditions associated with the discovery of surface water resources (rivers and lakes) became exceptional. Some of the exploration routes already described in this section are shown on the maps, Figure 1.4.

Shortly after the beginning of the twentieth century, Africa became divided into colonies under the rule of the then leading European powers; Belgium, Great Britain, France, Germany, Italy, Portugal and Spain. Liberia and the Union of South Africa were the only exceptions. The partition of Africa into a large number of colonies separated by boundaries not based on sound physical features or tribal origins remains a legacy of the hard struggle between those powers. What really matters here is that a major component of the African water problem is essentially caused by the non-uniform spatial distribution of the water resources of the continent.

For some reason, basically the deep interest in developing and expanding agriculture in some parts of Africa, the colonizing powers made the necessary effort to learn of the features of African hydrology, that could be useful to them. Not only lake and river levels and discharges were the hydrologic parameters to be recorded, interests and needs extended to cover items like evaporation, evapotranspiration, land use, soil-moisture movement, and erosion and sedimentation. This wealth of information has proven to be useful for designing water conveyance, distribution and management structures, such as storage reservoirs, flood protection dikes, irrigation and drainage canals, pumping stations and hydro-power plants. Groundwater, Wadi flow and sedimentation have remained mostly specialities that have been studied mainly in North Africa. Regrettably the collected data were not always disseminated nor made available to users, even from countries to which the data belong.

It seems appropriate in this introduction to hint to the state of affairs regarding the collection of hydrological data; namely, water levels and discharges of some of the major rivers and lakes in the occupied countries during their period of colonization. Table 1.3 lists resource names, measured variables, gauging stations and approximate years in which systematic records of hydrologic variables in question began.

The United Nations Organization was founded after the end of the Second World War, 1939-1945. One of its primary goals was to establish a free world. Occupation and colonization were to be abolished, and all countries were to become independent and sovereign. Between 1955 and 1965, most of the African countries became independent and the rest followed shortly thereafter.

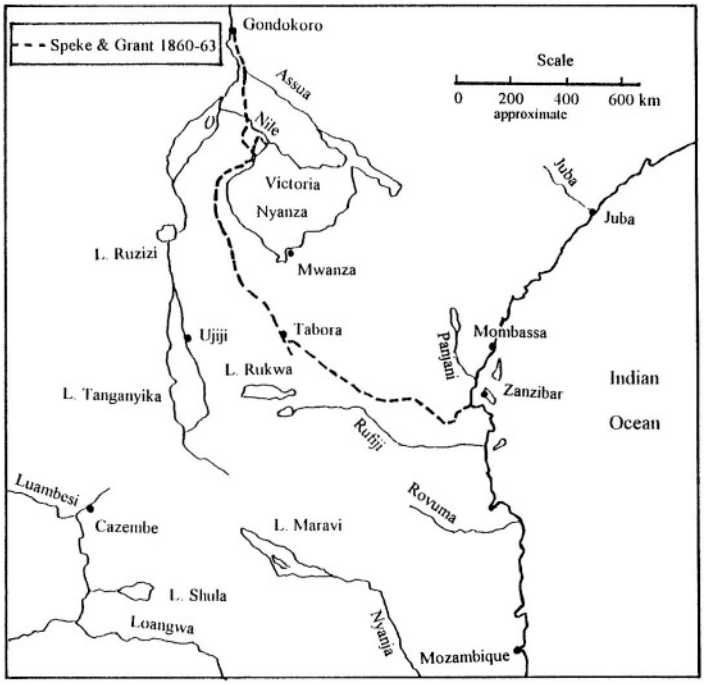

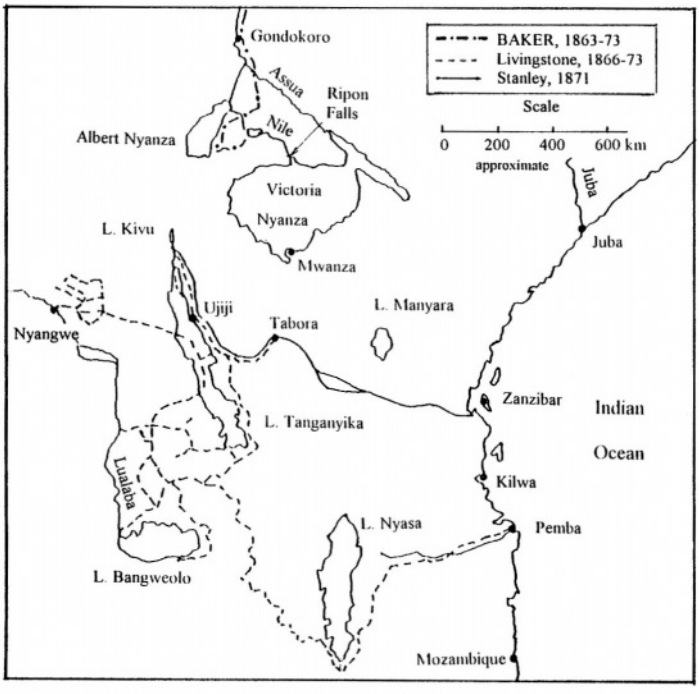

Figure 1.4- Routes taken by the explorers of the Nile (Moorehead, 1983)

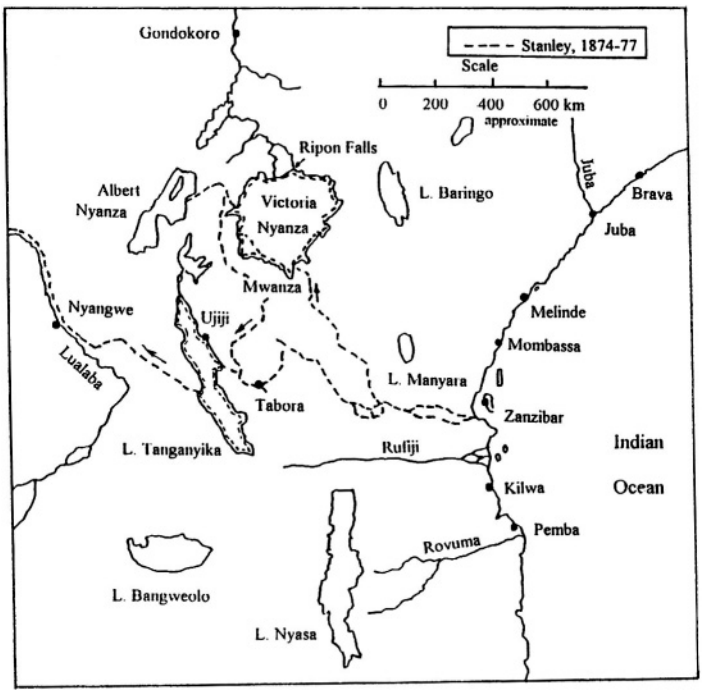

Figure 1.4 (Cont'd)- The routes taken by the Nile explorers (Moorehead, 1983)

Many of the former colonies, despite their official independence, do not really enjoy any real independence. Instead, they remain till present largely dependent on their former colonizers: technically, culturally, militarily and most important economically. The disturbing levels of poverty, illiteracy and sickness combined with lack of professional expertise are still dominating and affecting every aspect of life.

The thirst of some individuals or groups for power is strong, at least in certain countries. The military governments, ethnic and racial differences and lack of democracy are serious problems in these countries, making them almost uninhabitable. In 1985 Timberlake notes how such circumstances had created difficulties in southern Sudan, the war turned nastier with the arming of various tribal factions traditionally hostile to one another, assuring more atrocities and human-rights violations. In Mozambique war and associated food scarcities affected at least four million people, a quarter of the national population. Relief agencies are getting food in by expensive and inefficient airlifts because rebel activity made roads and rails unusable. In Angola, civil war, which raged since independence, make it impossible for relief agencies to even judge the extent of the need.

The United Nations Organization (UN), the Organization of African Unity, recently the African Union and several action groups are spending tremendous efforts to bring peace to conflicting countries and parties in Africa Despite all these efforts

violence is still dominating life in these areas. No wonder then that the average rate of general development all over Africa is rather insignificant. One should not forget that water resources and transportation are the principal keys to African development. The development of water resources is the area of interest of this book.

The conditions in the troubled areas of Africa have definitely led to interruption in the hydrological records and either decapitated or destroyed some of the old gauging sites. This situation does not confine itself to hydrological records only but extends itself to records of meteorological and/or agricultural relevance. Substantial breaks in the data-time series and erratic or unreliable measurements are responsible for the poor quality of available data. Examples illustrating such defective data will be presented in the chapters concerned with analysis and discussion of climatic, runoff and streamflow series.

It goes without saying that some of the missing data can be supplemented using certain techniques or models. However, one must never expect that the quality of supplemented data will ever be equivalent to the quality of the original data themselves.

Table 1.3- Beginning year of systematic collection of hydrological data

Source of water	Beginning of record	Variable measured and specification
River Nile at Roda	641	Water level (maxima and minima)
River Nile at Aswan	1869	Discharge
Lake Tanganyika	1909	Water level
Lake Victoria at Jinja	1900	Water level
Lake Victoria near Jinja	1902	Inflow to Upper Victoria Nile
Lake Malawi	1900	Water level
Lake Kyoga at Lale Port	1917	Water level
Lake Albert at Butiaba	1912	Water level
Lake Albert at Butiaba	1904	Outflow from the lake
Bahr el-Jebel at Mongalla	1905	Discharge
White Nile at Malakal	1905	Discharge
Blue Nile at Khartoum	1905	Discharge
River Atbara at Kilo.3	1911	Discharge
River Niger at Koulikoro	1907	Discharge
River Sénégal at Bakel	1904	Discharge
River Falémé at Kidira	1930	Discharge
River Oubangui at Bangui	1911	Discharge
River Congo (Zaïre) at Kinshasa	1903	Discharge
River Ogooue at Lambaréné	1930	Discharge
River Tana at Gaissa	1934	Discharge
River Chari at N'Djamena	1933	Discharge
River Sanaga at Edéa	1943	Discharge

1.4- Irrigated Surface and Water Resources

Table 1.4 gives the 1982 statistics of rainfed and irrigated areas for each region in Africa. This table has been prepared using some of the relevant data published by the International Commission on Irrigation and Drainage (ICID, 1987). These statistics together with the corresponding figures for 1989 given by Postel (1992) show that half of the irrigated land in Africa is located in Egypt and the Sudan. Additionally, the total surface of irrigated land in Africa is in the order of 4 % of the world irrigated area. Table 1.4 includes also estimates of the potential areas of agricultural land to be supplied with water by rain and by irrigation. These estimates are based on short as well as long water-transport distances.

The 1982 rainfed and irrigated croplands were estimated at about $1.43*10^6$ km^2 and $0.09*10^6$ km^2, respectively, i.e. about 4.6 and 0.3 % of the total surface of Africa, respectively. The corresponding estimates of the potential areas are about six times as large for the 1982 rainfed area, four times for the irrigated area with short transport distance and five times for the long-transport distance of water.

More detailed information is to be found in Table 1.5, which has been prepared using some of the data collected and published by the Food and Agriculture Organization (FAO, 1987). It gives the total water resources (surface and ground-water) per major water basin, the then actual as well as the potential water requirements, and the areas of the then actual as well as the potentially irrigable soils (best plus suitable). The reader should be alerted to the fact that Table 1 of Part I, Appendix B, placed at the end of the book gives three more estimates of the freshwater resources of Africa. The four estimates do not all entirely agree. We shall discuss the differences between the different estimates in the next section.

What interests us here is that by the mid-nineteen-eighties the area of soil under irrigation in both the uplands and lowlands of all water basins in Africa did not exceed $4.15*10^6$ km^2, or just 13.5 % of the surface area of the continent. The same source estimated the area of potentially irrigable soils at about $10.5*10^6$ km^2, or 34.5 % of the total surface area of Africa. The information reported by the Committee on Water Research (COWAR, 1993) to UNESCO indicates clearly that the 1962 rate of increase of irrigated land in Africa, 2.3 %, declined steeply with lime to reach about 1.3 % by 1977. This decline has been followed by a very slow rise to reach slightly more than 1.5 % in 1987. The deteriorating economic situation and the large-scale violence exercised in many countries and between neighbouring countries are among the main reasons behind the fall in the rate of increase in irrigated land. Postel (1993), in making a worldwide comparison, reported that developing a new capacity costs the most in parts of Africa. Lack of adequate infrastructure, the relatively small parcels of irrigable land, and the seasonal nature of river flows have driven the costs per hectare in many projects to between US $10,000 and $20,000, or even higher. The same reference continues: "Not even double-cropping of higher-valued crops can make irrigation systems at the top end of this spectrum economical. Consequently, irrigated area in sub-Saharan Africa has expanded minimally since 1980, even though less than 5 % of the region's cropland is irrigated".

Table 1.4-- Areas occupied by rainfed and irrigated agriculture in Africa (ICID, 1987)

Region	1982-Estimates of		Estimated potential areas of		
Area	Rainfed land	Irrigable land	Rainfed land	Irrigable land (a)	Irrigable land (b)
Mediterranean, North & North East Africa	294.9	54.3*	34.3	48.6	294.9
West Africa	620.4	18.1**	2,689	79.7	120.2
East & Central Africa	319.5	4.5	2,621	80.1	100.2
Southern Africa	197.0	13.2	2,263	145.4	178.5
Total	1,432	90.1	8,360	339.5	447.5

Explanation

All areas are expressed in 10^3 km.^{2}

*(a) = shorter transport of water, (b) = longer transport of water, both a and b do not include imported or fossil sources of water, * includes imported water, ** probably includes some imported water.*

In conclusion one can accurately divide the total surface area of Africa according to the existing uses of land and water as follows:

Area of woodland	$= 6.1*10^6$ km^2
Area of forestland	$= 7.2*10^6$ km^2
Area covered with pastures	$= 7.8*10^6$ km^2
Cropped area	$= 1.1*10^6$ km^2
Area covered with swamps, Natural and artificial lakes	$= 0.6*10^6$km^2
Area covered by desert and waste	$= 8.3*10^6$ km^2.

1.5- Population Growth, Share per Capita in Water Resources, Supply and Demand

The previous sections have been prepared with the aim of providing the reader with brief accounts of the exploration of African Rivers and Lakes, the geography of the continent and its physical setting, climate, natural vegetation and some of the agricultural aspects relevant to water resources. Most of the contents of the previous sections will be presented and discussed in more detail in subsequent chapters

The present section aims at briefly presenting the consumption and demand per capita of fresh water. In order to have a systematic presentation it is worthwhile to begin with the demography of Africa and the growth of its population.

Table 1.6 contains five sets of figures: the 1955, 1990 and 2025 sets are from Engelman & Le Roy (1994), the UN estimates for mid-1969 cited in Stamp & Morgan (1972) and the 1994 set taken from the World Guide (1997-1998). The predicted populations for 2025 are based on the UN medium projection.

The few missing estimates in the references have been supplemented using the general trends of population growth in the respective countries or islands.

The data presented in Table 1.6 show affirmatively that the population growth rate on a continental scale is in the order of 2.6%. It goes without saying that the growth rate varies considerably from one country to another; e. g, 2.0-2.1% for Chad, Central African Republic and Mozambique, 2.4% for Somalia, 2.5-2.6 % for Mali and Lesotho, 2.71% for Nigeria, 3.0-3.1% for Niger, Tanzania and Uganda, etc.

Table 1.5- Total water resources, water requirements, potential water requirements, irrigated area and potentially irrigable area by basin (FAO, 1987)

Major Water Basin	Tot. Wat. Resourc. 10^9 m^3	Upland crops WR 10^9 m^3	IA 10^3 km^2	PWR 10^9 m^3	PIA 10^3 km^2	Lowland crops WR 10^9 m^3	IA 10^3 km^2	PWR 10^9 m^3	PIA 10^3 km^2
Senegal	25.16	22.22	18.2	23.42	19.14	22.22	18.06	24.22	19.6
Niger	219.32	150	157	184	184	141	155	177	183
Chad	156,55	150	144	237	212	148	142	301	264
Nile	282.80	271	260	610	531	271	262	719	617
Rift	39.71	31.94	28.14	120	97.14	34.45	30.70	143	116
Shibeli/ Juba	17.31	17.31	12.9	206	153	17.31	13	272	203
Congo/ Obangui	1,101.8	427	600	444	615	557	765	594	801
Zambezi	174.94	146.47	139.2	232	214	149	143	308	286
Okav.go	24.14	24.14	21.03	61.95	50.68	24.14	21.17	24.14	52.5
Lim.po	8.53	8.53	6.68	94.5	73	8.5	6.73	103	79.4
Orange	6.86	6.86	5.65	133	96.87	6.86	5.68	147	108
S. Inter.	24.57	24.57	18.82	213	155	24.57	18.84	237	173
N. Inter.	2.13	2.02	1.31	267	165	2.13	1.35	300	186
Med. C	10.83	10.63	8.73	165	115	10.71	8.80	166	116
N.W.C.	2.65	2.65	2.06	104	68.46	2.65	2.05	117	76.7
West C.	361.04	112	154	114	156	120	177	125	182
W.C.C.	237.28	50.65	109.4	50.66	109	57.90	125	57.95	125
S.W.C.	57.57	54.64	54.72	105	94	57.37	57.90	117	106
S. Atl. C	.0.39	0.39	0.28	56.24	37.72	0.39	0.28	61.57	41.2
I. O. C.	47.22	40.89	37.19	138	113	43.16	39.73	153	128
E.C.C.	131.54	89.16	85.96	148	133	107	104	194	176
N.E.C.	2.09	2.09	1.44	113	75.83	2.09	1.42	133	88.3
Mad. W.	73.63	48.77	57.36	67.4	73.68	54.18	64.03	76.31	84.0
Mad. E.	56.74	11.21	29.52	23.39	39.90	114	29.85	23.77	40.4
Islands	4.85	0.56	0.94	4.16	3.28	0.63	1.12	4.10	3.37

Explanation

Tot. Wat. Resourc. = Total water resources, WR = Water requirements, IA = Irrigated area
PWR = Potential water requirements, PIA = Potentially irrigable area,
S Inter. = South Interior, N. Inter. = North Interior, Med. C. = Mediterranean Coast,
N.E C. = Northeast Coast, N.W.C. = Northwest Coast
W.C.C. = West Central Coast, S.W.C. = Southwest Coast,
S.Atl.C. = South Atlantic Coast, I.O.C. = Indian Ocean Coast, E.C.C. = East Central Coast,
Mad W. = Madagascar West and Mad. E. = Madagascar East,

Table 1.6- Population of African countries and Islands

Country/ Island	Population estimates (10^6) for the years 1955	1969	1990	1994	2025
Algeria	9.715	13.349	24.935	27.422	45.475
Angola	4.437	5.430	9.194	10.442	26.619
Benin	2.111	2.640	4.633	5.325	12.252
Botswana	0.433	0.629	1.276	1.443	2.980
Burkina Faso	4.012	5.128	8.987	10.118	21.654
Burundi	2.687	3.475	5.503	6.183	13.490
Cameroon	4.843	5.680	11.526	12.986	29.173
Canary Islands	(0.825)	0.950	(1.200)	(1.280)	(2.030)
Cape Verde Islands	0.169	0.250	0.341	0.372	0.735
Central African Republic	1.414	2.256	2.927	3.234	6.360
Chad	2.8838	3.510	5.553	6.288	12.907
Comoros Islands	0.194	0.275	0.543	0.485	1.646
Congo (Brazzaville)	0.889	0.870	2.232	2.577	5.677
Congo (Kinshasa)	13.604	21.638	37.436	42.540	104.639
Djibouti	0.069	0.091	0.517	0.603	1.055
Egypt	24.692	32.500	56.312	56.767	97.301
Equatorial Guinea	0.238	0.320	0.352	0.386	0.798
Eritrea	-*	-	-	3.482	-
Ethiopia	20.418	24.769	47.423	54.890	126.886
Gabon	0.477	0.485	1.146	1.301	2.697
Gambia, The	0.313	0.357	0.923	1.079	2.102
Ghana	5.759	8.546	15.020	16.639	37.998
Guinea	2.826	3.795	5.755	6.425	15.088
Guinea Bissau	0.522	0.530	0.964	1.044	1.978
Ivory Coast	3.221	4.764	11.974	13.841	36.817
Kenya	7.190	10.943	23.613	26.017	63.360
Lesotho	0.794	0.935	1.792	1.942	4.172
Liberia	0.914	1.150	2.575	2.719	7.240
Libya	1.126	1.905	4.545	5.218	12.885
Madagascar	4.747	6.643	12.571	13.100	34.419
Madeira Islands	0.225	0.269	(0.415)	(0.450)	(0.630)
Malawi	3.169	4.398	9.367	9.532	22.348
Mali	3.911	4.831	9.212	9.524	24.575
Mauritania	0.901	1.140	2.003	2.215	4.443
Mauritius Islands	0.571	0.870	1.057	1.115	1.481
Morocco	10.132	15.030	24.334	26.367	40.650
Mozambique	6.744	7.376	14.187	15.463	35.139
Namibia	0.562	0.749	1.349	1.508	3.049
Niger	2.689	3.909	7.731	8.730	22.385
Nigeria	37.094	65.820	96.154	108.014	238.397
Reunion Island	(0.275)	0.445	(0.575)	0.640	(0.870)
Rwanda	2.391	3.500	6.986	7.755	15.797
Sao Tome & Principe	(0.058)	0.066	(0.095)	0.125	(0.175)
Senegal	2.811	3.780	7.322	8.263	16.896

Table 1.6- Cont'd

Country/ Island	Population estimates (10^6) for the years 1955	1969	1990	1994	2025
Seychelles Islands	(0.045)	0.053	(0.065)	0.072	(0,098)
Sierra Leone	2.081	2.510	2.999	4.399	8.690
Somalia	3.401	2.730	8.677	8.775	21.276
South Africa	15.385	21.282	37.066	40.503	70.951
Sudan, The	10.150	15.186	24.585	27.585	58.388
Swaziland	0.291	0.423	0.744	0.906	1.647
Tanzania	8.915	12.926	25.600	28.817	62.894
Togo	1.414	1.956	3.531	4.007	9.377
Tunisia	3.860	4.925	8.080	8.792	13.290
Uganda	5.556	9.526	17.949	18.592	48.056
Zambia	2.753	4.220	8.150	9.203	19.130
Zimbabwe	3.257	5.090	9.903	10.778	19.631
Western Sahara	(0.042)	0.061	(0.400)	1.000	(1.360)
Total	250.118	356.884	631.309	699.055	1491.956

Explanation
Population figures for 1955, 1990 and 2025 are taken from Le Roy & Engelman (1994)
Population figures for mid-1969 are UN estimates (cited in Stamp & Morgan, 1972)
Population figures for 1994 are taken from The World Guide, 1997-1998 (1997)
**Population estimates are for Eritrea and Ethiopia combined*

: Stamp & Morgan (1972) give the population estimates for the years 1900,1920, 1930, 1940 and 1950 as 120, 141, 157, 176 and 206, (all in 10^6 inhabitants), respectively. The same reference adds that the population of Africa in 1850 represented only 8% of the then world population. For the purpose of the present study, an overall average rate of 2.6% is used to obtain the so-called medium projection of the population for the year 2025 This rate based on the figure of $250*10^6$ for the base year 1955 means that there will be about $1,500*10^6$ inhabitants in the year 2025.

Regardless of the rapid growth of its population, it is well known that the rate of mortality, in Africa, especially among the children, is probably the highest in the world. Water-related, and water-borne and transmitted diseases such as cholera, typhoid, dysentery and Malaria are among the common diseases causing mortality at an early age. Schistosomiasis, onchocirciasis, which are wide spread in most parts of Africa and the southern Saharan region respectively, also constitute major causes of mortality. Unfortunately there is no overwhelming evidence that the near future will witness any drastic reduction in the numbers of population earning one or more of these sicknesses. Additionally, as already stated in an earlier section, extreme violence and bloodsheds dominate life in a number of countries and the death toll sometimes can be quite high. Despite these adverse factors the percentage of Africans constituting the total world population has kept growing: it reached about 9% in 1970 and is expected to jump to 12% or more by the year 2025.

The estimates of the freshwater potential listed in Table 1, Part I Appendix B, are

not all in good agreement with each other. The estimate given by FAO (1987) is the least of the four, whereas the estimate given by Engelman & Le Roy (1994) is the largest one. The ratio of the largest estimate to the smallest estimate is about 1.5: 1. The other two estimates, which have been suggested by L'vovich (1974) and Gleick (1993), are nearly the same, each $4.2*10^{12}$ m^3. They lie halfway between the two extreme estimates. This situation has led us to proceed further by presenting the detailed figures included in the FAO estimate (1987) and the L'vovich estimate (1974).

Table 2, Part I Appendix B, which contains the L'vovich and the FAO estimates, shows considerable disagreement between the respective figures for each country, no matter if the source of water is underground or surface. The totals given at the end of the table show that the surface runoff estimated by the FAO is about 82.8% of that given by L'vovich and only 53.6% of the total groundwater resources. Since the figures suggested by Engelman & Le Roy form a certain part of a worldwide estimate, they have been used for preparing Table 1.7, regardless of their being the highest of all available estimates. This table gives the share per capita per African country/island of freshwater in 1955,1990 and 2025 (using UN medium projection).

The high seasonal fluctuation of discharge is a typical characteristic of most of the African Rivers outside the equatorial belt. Water management through storage reservoirs and other appropriate means is necessary to guarantee the required supply at the right time. Despite the problems with big dams, Africa badly needs hundreds of small dams. Small dams are manageable. Systems can be changed and rebuilt as change and repair become necessary, by groups of natives rather than by outside contractors and expensive machinery.

Water management schemes are unavoidable for increasing the land return in the form of foodstuff. This return is basically and urgently needed to ensure a bottom line of food self-sufficency. They can also be used for energy production and other purposes if they are brilliantly designed. As such it is fairly safe to conclude that proper management of water resources is one of the major issues of relevance to the overall, especially the economic, development of Africa. A brief description of some of the existing dams in Africa and the role they play in the management of its water resources will be presented in one of the next chapters.

Table 1.7- Share per capita of freshwater and its decline with time between 1955 and 2025

Country/ Island	Share per capita (m^3yr^{-1}) for the years 1955	1990	2025
Algeria	1,770	690	378
Angola	35,610	17,185	5,936
Benin	12,316	5,612	2,122
Botswana	41,570	14,107	6,040
Burkina Faso	6,979	3,116	1,293
Burundi	1,340	654	267
Cameroon	42,949	18,046	7,130

Table 1.7- Cont'd

Country/ Island	Share per capita (m^3yr^{-1}) for the years 1955	1990	2025
Cape Verde Islands	1,183	587	272
Central African Republic	99,717	48,172	22,170
Chad	13,390	6,843	2,944
Comoros Islands	5,258	1,878	620
Congo (Brazzaville)*	902,137	359,319	141,272
Congo (Kinshasa)	74,904	27,220	9,378
Djibouti	145	19	9
Egypt	2,385	1,046	605
Equatorial Guinea	126,050	85,227	37,594
Eritrea	5,387	2,320	
Ethiopia	5,387	2,320	867
Gabon	343,816	143,106	60,808
Gambia, The	70,288	23,835	10,466
Ghana	9,203	3,529	1,395
Guinea	79,972	39,270	14,979
Guinea Bissau	59,387	32,158	15,672
Ivory Coast	22,974	6,180	2,010
Kenya	2,086	635	237
Lesotho	5,038	2,232	959
Liberia	253,829	90,097	32,044
Libya	4,103	1,017	359
Madagascar	8,426	3,182	1,162
Malawi	2,840	961	403
Mali	15,853	6,730	2,523
Mauritius Islands	3,853	2,081	1,485
Morocco	2,764	1,151	689
Mozambique	8,600	4,088	1,651
Namibia	16,014	6,672	2,952
Niger	16,363	5,691	1,966
Nigeria	8,303	3,203	1,292
Rwanda	2,635	902	399
Senegal	12,451	4,777	2,071
Sierra Leone	76,886	40,010	18,412
Somalia	2,499	980	400
South Africa	3,250	1,349	705
Sudan, The	11,900	4,913	2,069
Swaziland	23,918	9,355	4,226
Tanzania	7,864	3,220	1,208
Togo	8,487	3,398	1,280
Tunisia	1,130	540	328
Uganda	11,879	3,677	1,373
Zambia	34,871	11,779	5,018
Zimbabwe	7,062	2,323	1,172

CHAPTER 2

CLIMATE

2.1- Factors Affecting the Climate

The general climate of Africa is mainly influenced by its geographic location. The Equator, as mentioned earlier, bisects the continent into two halves of nearly equal longitudinal dimension. The two halves, however, are not equal or nearly equal in surface area. Since almost two-thirds of the total surface of the continent is confined between the two tropics the tropical climate prevails over most of Africa. It is well known that the activity of the sun and its influence on the hydrology of a certain area is more pronounced in the tropics than elsewhere. Furthermore, Africa's position in low latitudes means that the amount of insolation is nearly the same throughout the year.

The second factor is related to the geometrical form of the outline of the continent. The northern half has a very wide stretch of land between the Atlantic Ocean and the Red Sea, the bounding water surfaces. This situation renders most of the surface of this half free of the ocean humidifying effect. Contrarily, the southern half, which is confined between the South Atlantic and the Indian Oceans, has an average width less that is than 40% of the average width of the northern half. This situation makes the southern half of the continent, in general, more humid compared to most of the surface of the northern half.

The third important factor is the location of the Inter-Tropical Convergence Zone (ITCZ), a surface of discontinuity separating a generally warm, dry air mass and a cooler, moist one. It undergoes a seasonal migration related to the movement of the sun as can be seen in Figure 2.1. This figure comprises four maps: A, B, C and D for January, April, July and October, respectively (Griffiths, 1972). Each of these four maps shows the position of the ITCZ and the boundaries of wind convergence. The nature of precipitation and its annual variation is linked to the movement of the ITCZ and the airflow patterns.

In January the position of the ITCZ over West Africa is parallel to 5°N (map A). Above the eastern edge of the Congo Basin the ITCZ is forced by orography of the region to assume a longitudinal position, but from 18°S it bends to the east. In April the ITCZ (map B), with its accompanying high temperature over the Sahara, moves northwards till all of its eastern section becomes situated north of the Equator.

By July, the ITCZ has moved farther to the north and all of its extent has nearly coincided with latitude 18°N (map C). In October the ITCZ (map D) is still north of the Equator, though compared to its position in July, it is at least 5° to the south

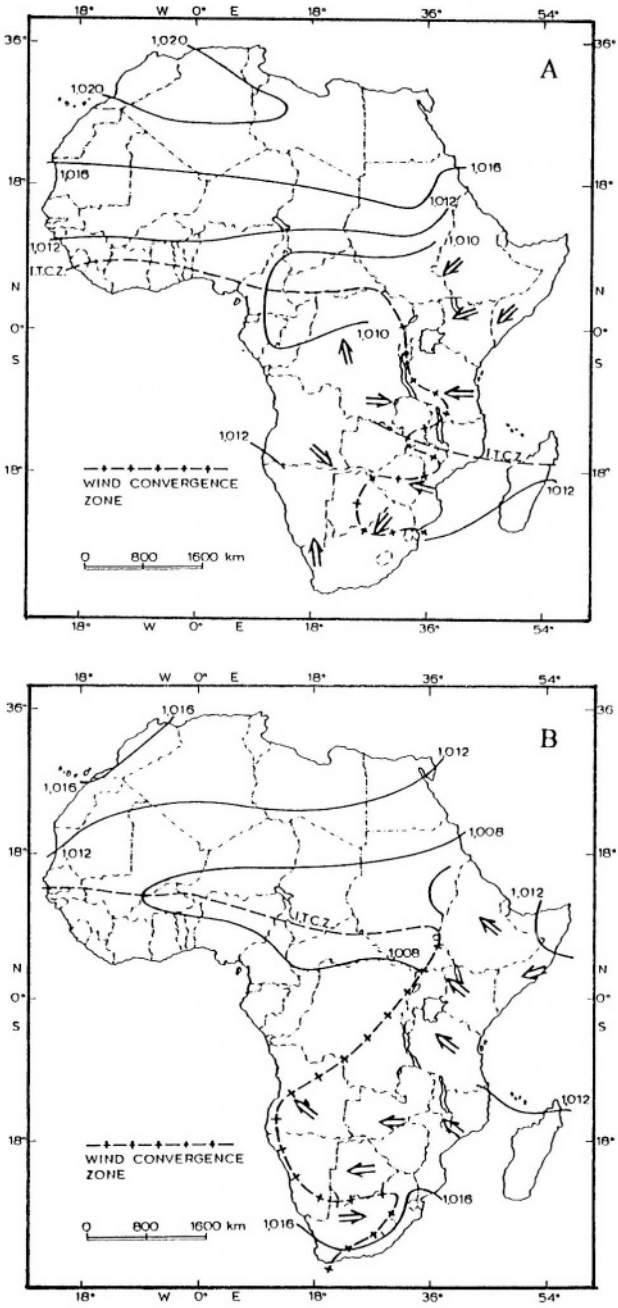

Figure 2.1- Mean pressure and airflow patterns for: A. January, B. April (Griffiths, 1972)

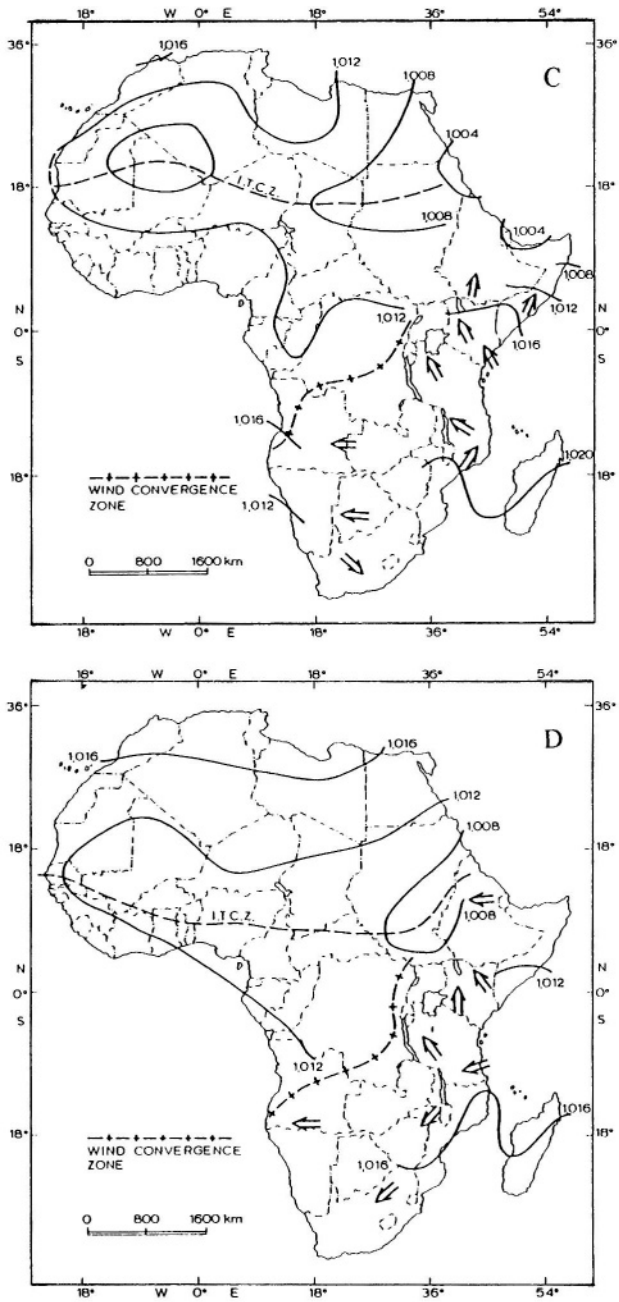

Figure 2.1 (Cont'd) Mean pressure and airflow patterns for: C. July and D. October (Griffiths, 1972)

The relief of the continent influences the atmospheric circulation, which is responsible for transporting air masses of different types. The continent is sheltered from the north by the Atlas Mountain range, which extends along the western Mediterranean coast. Likewise, the chain of mountains in the cast and south of the southern half of Africa provides similar protection. The atmospheric circulation is another factor playing a significant role in the climates of Africa. The moisture content of the transported air masses is the reason behind the wet and dry seasons. Some ocean currents can be very effective in this respect. The cold Benguela and Canary Currents (southern winter), the Equatorial Counter and the Guinea Currents (northern summer) and in winter only the Guinea Current are active on the Atlantic side. The southern Indian Ocean coast above 10°S is affected the whole year round by the Somali Current and, below it, by the warm Mozambique and Agulhas Currents.

2.2- Climate Data

2.2.1 Development of observation stations- Climate data are part of the national wealth of every nation. These data help understand the far-reaching effects of climate on the economy and welfare of mankind. Climate is distinguished from other natural resources by its strongly felt temporal as well as spatial variations. As such, climate cannot be assessed by a single-time survey or an occasional sampling every year or over a limited number of years. Trends, which short-term data might show, cannot be easily extrapolated to provide reasonable forecasts of future changes. For these reasons climate monitoring must be continuous, and accumulation of reliable data over long periods is essential for interpreting spatial as well as temporal changes.

A survey was carried out by the World Meteorological Organization (WMO) in 1978 on the number of stations with homogeneous climatological series. Only 13% of the countries of Africa answered that questionnaire. It is very likely that this small sample has a heavy bias towards those countries having stronger services. Moreover, the answers to that questionnaire have shown tremendous inconsistencies, which indicate the need for a more thorough planning, better use and presentation of the data collected.

Rainfall data are probably the variable most of the regions of Africa need to have. The only exception is the tropical cyclones and the associated hurricane winds in the south west of the continent. The second important climate variable next to rainfall is air temperature

It is well documented that Eastern Africa is rather richer in old data than Western Africa and much richer than Central Africa. Tanzania began its rainfall series prior to 1850, and a few more countries have by now rainfall data covering more than 100 years. In contrast with the extreme north and south and other temperate regions. Tropical Africa together with other low-latitude regions generally suffer from a paucity of data in the period before 1931.

By the beginning of the 1931-1960 period, often referred to as the “normal

period", every country in Africa had established some rainfall and climate stations. In many instances, hardly any attention was paid to recommended guidelines for network design. With urban extension, changes of authority and deterioration of internal affairs, breaks in the records became inevitable in some countries. Many countries did not then have national meteorological services to safeguard continuity of operation of measurement stations, to store and process the data collected and to ensure rational distribution of stations in networks covering the whole country.

The period 1961-1990 witnessed a rapid increase in the number of measurement stations in several African countries: old networks have been updated and new networks established. Hydromet, in the Equatorial Lakes region, and Agrymet, in the Sahel region, are two examples to mention. Additionally, a number of national meteorological services have been established in the said period. These developments made the proportions of existing stations in Africa jump from 20 to 50 to 100 in the periods prior to 1931, 1931 -1960 and 1961 -1990, respectively. As can be expected, the increase in the number of rain gauging stations exceeded the increase in the number of other climate stations.

2.2.2 Data used in the present study- Certain climatic variables are usually needed and used for describing and typifying the climate. The standard variables of direct relevance to the natural yield and management of water resources, surface or groundwater are: precipitation and the group of variables partly or fully responsible for free water evaporation and evapotranspiration. This group includes atmospheric temperature, relative humidity, radiation, duration of sunshine, cloudiness, and wind speed and direction.

Series of annual rainfall and series of maxima and minima rain depths have been collected for a number of stations with long and uninterrupted records. These series will be used in frequency analyses and extrapolation to return periods much longer than the period of record itself.

In order to develop a clear portrait of the climates of Africa, the available climatic data at 271 meteorological stations distributed all over the continent, land and islands, have been gathered and analyzed for the purposes of the present study. The locations of these stations are shown on the map in Figure 2.2. Most of the data used in the text are given at the end of this book in Appendix A. The contents of this Appendix are as follows:

Table 1: Number, name and coordinates of each station
Table 2: Daytime hours
Table 3: Air temperature
Table 4: Relative humidity
Table 5: Global radiation
Table 6: Sunshine hours
Table 7: Cloudiness

Table 8: Wind speed
Table 9: Annual rainfall
Table 10a: Mean and coefficient of variation of annual rainfall
Table 10b: Annual precipitation series
Table 11a: Number of rainy days
Table 11b: Maximum monthly and annual rainfall
Table 11c: Minimum monthly and annual rainfall
Table 12: Evaporation rate
Table 13a: Potential evapotranspiration
Table 13b: Additional estimates of potential evapotranspiration

The sources of data in Appendix A are available in the list of references accompanying Appendixes A and B. The sources of any additional data that might appear in the text are included in the bibliography at the end of the book The next sections define and briefly discuss each climate variable listed in these tables.

Daytime- The duration or length of time is the number of hours between sunrise and sunset. The sum of hours for all days of each month divided by the number of days gives the respective monthly average of daytime hours. The monthly averages are given in Table 1, Appendix A. Though not as effective as the duration of bright sunshine, the length of daytime is used in some methods to estimate evapotranspiration because it is more available.

The shortest and longest days in the northern hemisphere are in December and June respectively. The lag or lead between the two hemispheres is six months. The difference between the longest and shortest days of the year at a certain location is a function of the latitude of that location. The difference at station 3 (36° 50'N) is 4.96 h; station 123 (6° 27'N) 0.71 h; station 201 (12° 48'S) 1.49 h and station 271 (33° 59'S) 4.44 h. These figures show that the difference increases or decreases by about 1.25 h per 10° further from or nearer to the Equator

Temperature- The air temperature in Africa is influenced by some factors such as the continentality (proximity of a certain location from the sea or ocean coast), the geographic location (latitude and hemisphere whether N or S), elevation and month of the year.

Africa is, generally speaking, a warm-climate continent Without paying much attention to the non ideal distribution of the observation stations shown in the map, Figure 2.2, the mean annual temperature at all stations is very close to 22°C and the coefficient of variation is about 0.21. The highest mean annual temperature is 30.7°C at Nema, Mauritania and the lowest is 14.5°C at each of Debra Marcus, Ethiopia and Grootfontein, South Africa. As the period and length of record are not the same for all stations, these figures should be used somewhat conservatively.

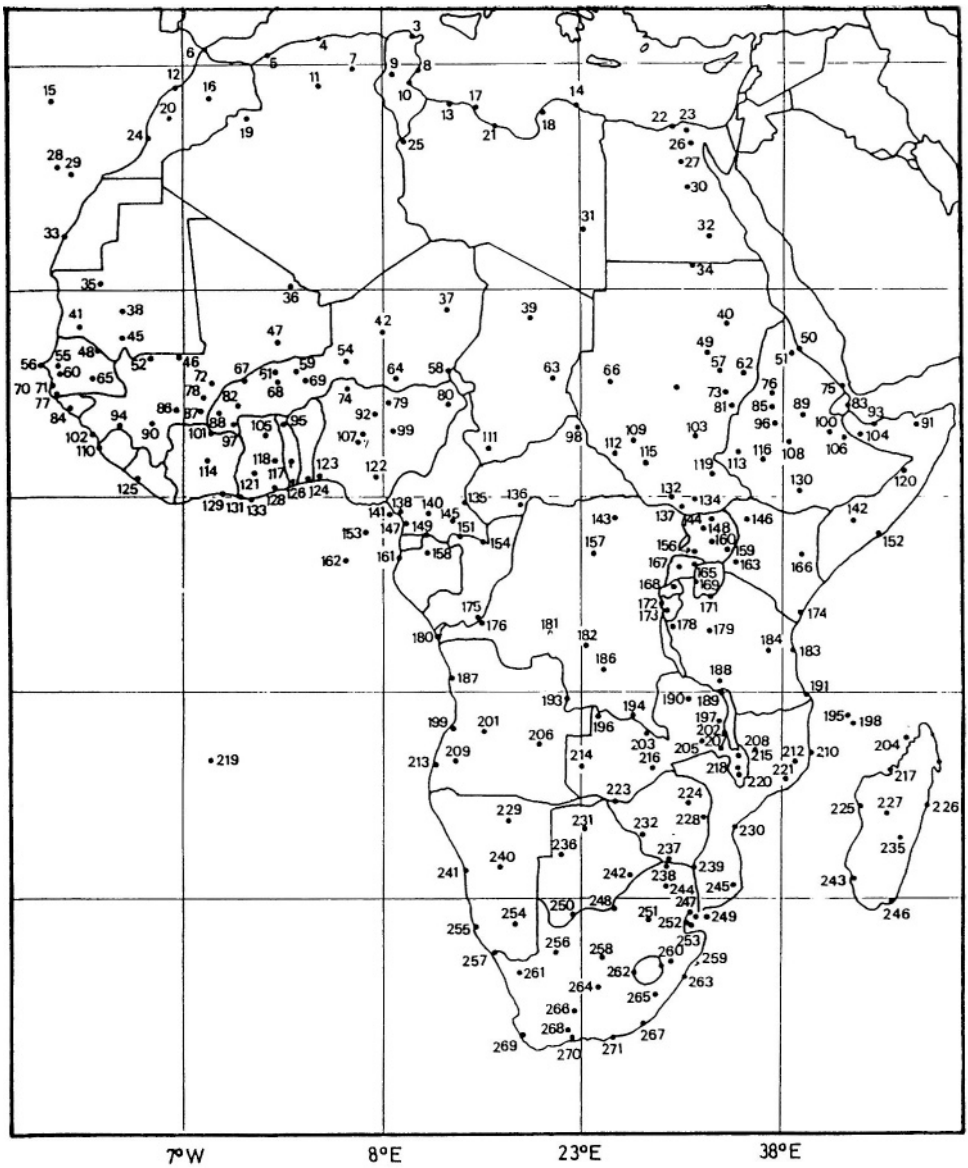

Figure 2.2- Map showing the locations of climate stations listed in Appendix A

The effect of distance from the sea or ocean (continentality) can be seen from the figures in Table 2.1 for some stations located along the longitudinal line 21° 30'E In fact, the temperature at some of these stations are under the combined effects of continentality and elevation.

Table 2.1- Mean annual temperature, distance from sea/ocean and elevation of some stations

Station No.	Country	Annual Temperature (°C)	Distance from Sea/Ocean* (km)	Elevation (m)
14	Libya	20.1	0/7160	7
31	Libya	23.1	960 /6200	381
98	C. African Republic.	26.3	2470/4690	465
157	Congo (Kinshasa)	24.6	3400/3760	487
181	Congo (Kinshasa)	24.5	4060/3100	60
214	Zambia	21.9	5050/2110	1052
231	Botswana	22.5	5540/1620	942
250	Botswana	19.9	6180/980	962
266	South Africa	18.0	6930/230	857
270	South Africa	16.0	7140/20	221

* *Sea =Mediterranean, Ocean = South Atlantic*

The latitude of a certain location dictates the months of the warmest and coldest temperatures of the year. June, July and August are the warmest months in the high-latitude regions in the northern hemisphere. Examples can be found in Sfax (8), Funchal (15), Agadir (24), Aswan (32), Atar (35) and Bilma (37) all located above 18° N. The warmest month moves to May at Tillabery (59), Dori (61) and Arbecher (63) where the latitude is around 14°N. The summer month moves further to April at Kuotiala (78) and Boromo (82), located at about 12° N latitude. In the period January-March the warmest regions are the equatorial parts of the Gulf of Guinea, the Chad Basin, the southern Sudan and the lowlands of Somalia. Our observation is somewhat different from what has been reported by Martyn (1992) that January is the warmest month for the said region. This is true, i.e. January for the stations in the southern hemisphere as Beitbridge (237), Panda (245), Tsabong (250) and Grootfontein (264), all below 22° S. Between this latitude and the Equator the warmest month can be as early as October or November

On the other hand, January is the coldest month for all observation stations in the region situated in the northern hemisphere down to nearly 10°N latitude. This region includes the coastal desert of the Mediterranean and the northern Sahara. Griffiths (1972) reported: "In northern Africa the boundary of a winter (December-February) minimum of mean monthly temperature extends down to about 12°N and even as far as 6°N in Somalia. In contrast, the lowest temperature is recorded in July or August over a region extending from Cape Town to as far as 12°N, in extreme West Africa. The month of the minimum mean monthly temperature in the highland of Ethiopia is July. The remarks stated here can be observed from the graphs in Figure 2.3, which show the mean monthly air temperature averaged over a long period for some stations in northern as well as southern Africa.

It may be of interest to present here the range between the highest and lowest monthly temperatures. Griffiths (1972) reported that about one-third of the continent

experiences an annual range of less than 6°C. As can be seen from the figures listed in Table 2.2, the range can reach as much as 18°C or higher in the interior desert. In savanna and woodland highlands, the seasonal range is often less, but in arid highland this range can easily reach 15°C

Conrad (1946) suggested the use of the mean annual temperature range as the best index or measure of continentality. This can be expressed as:

$$K = 1.7A/\sin(\Phi + 10) - 14 \qquad (21)$$

where K = index of continentality, A = average annual temperature range in °C and Φ = latitude. K should be zero for a completely oceanic earth and 100 for the corresponding continental planet.

Applying Conrad's expression, Eq. (2.1) to the data in Table 2.2, one gets K-values ranging from (-) 1.32 for station 157 (Yangambi, Congo Kinshasa) to 39.5 for station 31 (Kufra, Libya). The former is about 400 km from the Atlantic Ocean whereas Kufra is located at a distance of about 4,000 km from the ocean, 800 km from the Mediterranean Sea and 1,200 km from the Red Sea.

The considerable diurnal variation in some large areas is one of the remarkable characteristics of temperature in Africa. The difference between day and night temperatures in these areas can be more than 20° C. For example, the average range at Wad-Medani (Station 57), El-Fasher (Station 66) and Raga (Station 112), all in the Sudan, is 20.8°C (March), 22.2 (March) and 22.8 (January), respectively for the period 1931-1960 (Shahin, 1985).

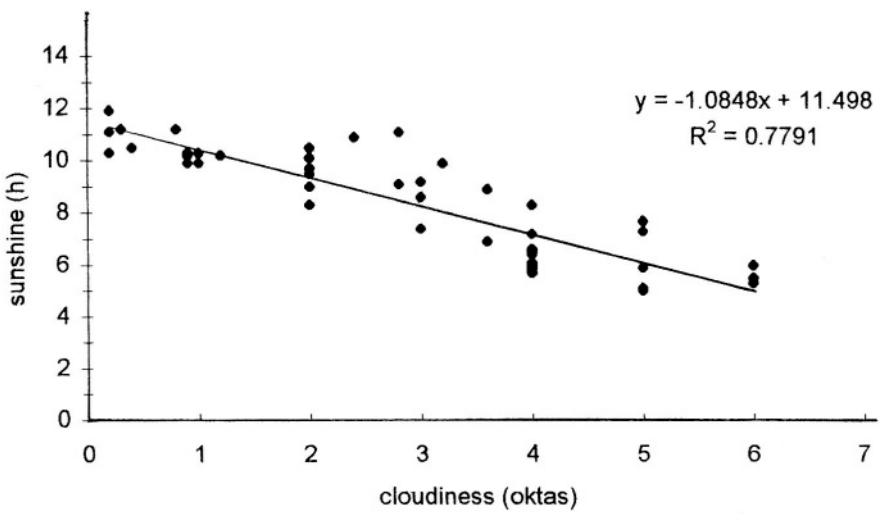

Figure 2.3- Distribution of long-term average monthly temperature at some meteorological stations in northern and southern Africa

Table 2.2- The range between the mean temperatures of warmest and coldest months for the stations listed in Table 2.1

Station No	Coldest Temp.(°C)	Warmest Temp. (°C)	Range (°C)	Latitude N/S	Remarks
14	14.1	26.2	12.1	32° 49' N	Coastal desert
31	12.9	30.6	17.7	24° 13' N	Interior desert
98	23.6	30.6	7.0	10° 17' N	Interior humid
157	23.9	25.3	1.4	00° 49' N	Equatorial zone
181	24.0	25.0	1.0	05° 53' S	Equatorial zone
214	17.2	25.5	8.3	15° 15' S	Savanna
231	16.0	26.4	10.4	19° 57' S	Semi-arid highland
250	11.7	26.7	15.0	26° 03' S	Arid highland
266	11.5	24	12.5	32° 21' S	Arid highland near sea coast
270	13.0	19.5	6.5	33° 58' S	Semi-arid coastal area

Recent change of temperature: Hastenrath and Kruss (1992) reported that there is evidence for a rising trend in the temperature of East Africa since 1990. The most consistent warming is found in subtropical and tropical regions, especially the Indian Ocean and the nearby regions Plisnier (1998) mentioned that since the 1960s an increase in the air temperature has been noted in two stations at each end of Lake Tanganyika. At Bujumbura airport (northern end), the average increase, assuming a linear trend for the data between 1964 and 1990, was 0.7°C (coefficient of correlation, r = 0.69). At Mbala airport (southern end) the average increase for the same period was 0.9°C (r = 0.79).

The linear trend approach was earlier used by El-Agib (1995) for detecting and analyzing the trend in the annual temperature series at twelve stations in the Sudan. The results he obtained for the period 1962-91 were: -0.028,0.008,0.18,0.22,0.020, 0.007, 0.018,0.019, 0.010,0.010, 0010 and 0.011 $^{o}C\ y^{-1}$ for Port Sudan, Khartoum, Kassala, Wad-Medani, El-Gadaref, El- Fasher, El-Obeid, Nayala, Ed-Damazin, Malakal, Wau and Juba, respectively. The average of these results shows an increase of about 0.3°C over a 30-year period. When the decline in temperature at Port Sudan is neglected, the average temperature increase for the remaining 11 stations rises to about 0.42°C.

Shahin (1997) analyzed the annual temperature series at two places in Egypt: Alexandria and Al-Minya. The former is located along the Mediterranean Coast whereas Al-Minya is located inland on the Nile. The annual series cover 54 years (1942-95) and 51 years (1945-95) for the two stations in their respective order. First of all, the change in temperature at either station does not appear to be statistically significant, instead it lies within the range of climate noise. Secondly, the station along the seacoast shows a falling trend and the inland station shows a rising one. The apparent cooling shown by the data from Alexandria amounts to 0 4°C for the period 1942-95. This can be seen in Figure 2.4, which shows the trend in the modular series of this station (annual temperature divided by the mean of the series).

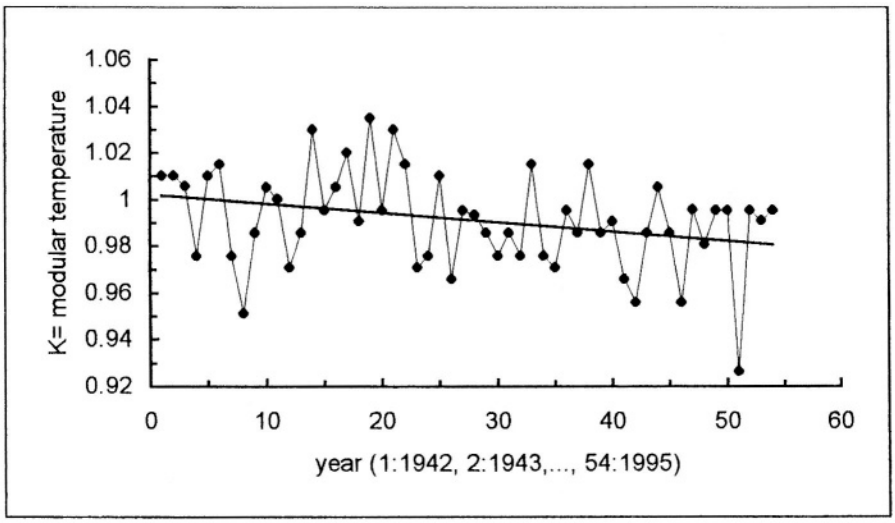

Figure 2.4- The apparent falling trend in the air temperature at Alexandria (Shahin, 1999)

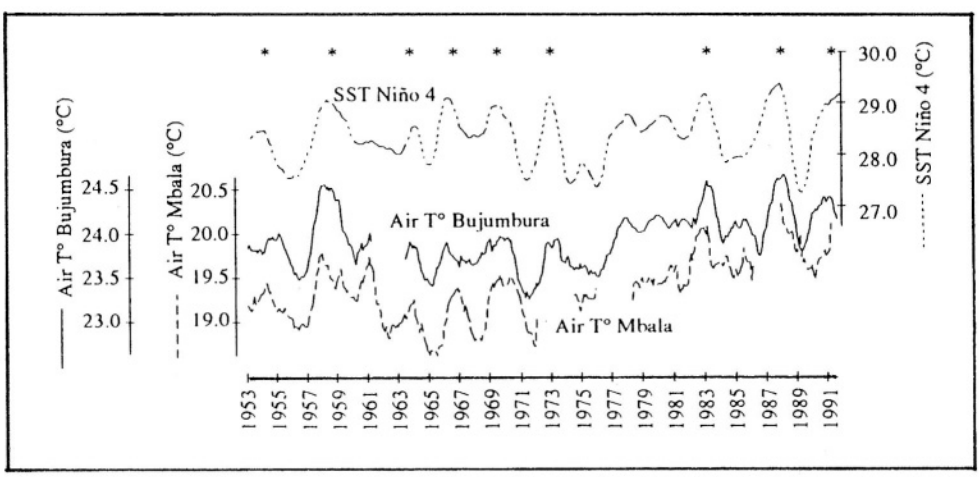

Figure 2.5- Monthly air temperature at Bujumbura and Mbala and sea surface temperature (SST) in the Niño 4 area of the Pacific Ocean (150° W to 160° E and 5° S to5° N) from January 1953 to July 1991. Observed Niño events are marked with asterisks. Running averages of 12 months are shown (Plisnier, 1998)

In addition to the general increasing trend in the air temperature at Lake Tanganyika, oscillations around the general mean were noted. There is a significant correlation between the air temperature at the climate stations and the sea surface temperature (SST) of the Pacific Ocean. The strongest correlation corresponds to a lag of four months between the SST peak and the next temperature peak in the lake environment. The coefficients of correlation are 0.67 and 0.41 for Bujumbura and Mbala, respectively. Plisnier (1998) reported that recent El- Niños were observed at Lake Tanganyika in 1954, 1958, 1966, 1969, 1973, 1983, 1988 and 1991-1994. Increase in air temperature for years corresponding to El-Niño events could reach 1.0°C in Bujumbura and 0.83°C in Mbala (Figure 2.5).

Atmospheric Humidity- In this context humidity refers to the mean relative humidity of air at a certain time in a certain area. Mean monthly relative humidity for 200 stations are given in Table 4, Appendix A. It has been indicated in this Table that some of the tabulated figures are based on three measurements per day, others on two and the rest on just a single measurement per day. This is a very crucial factor, as humidity can undergo a rapid change, especially at certain hours of the day. The diurnal variation of both relative humidity and temperature at Lusaka (station 216), Zambia, are shown in Figure 2.6 $_a$ (Nieuwolt, 1977). Some methods for computing evapotranspiration are based on the daily mean humidity (H_m), others on daily minimum humidity (H_n). The two humidities can be combined in one expression like the given by Eq. (2.2)

$$H_n = a + bH_m + cH^2_m \qquad (2.2)$$

where *a, b* and *c* are parameters varying from one region to another. The respective values found for Egypt are 9.788, 0.1396 and 0.004382, and H_n and H_m are indicated as percentages (Shahin, 1985)

The relative humidity at a certain location depends on its altitude and proximity from a large body of water like a sea or ocean. These reasons bring the air humidity in a close though inverse correlation with temperature. Relative humidity records should be thus associated with the corresponding temperatures so as to specify the state of the atmosphere completely. The mean annual relative air humidity varies according to the latitude of the place considered. Nieuwolt (1977) developed Figure 2.6$_b$ for latitudes from 60°N to 60°S. Obviously, the region of interest for us is the one between 37°N and 37°S. The mean relative humidity varies from one month to another within the year. The pattern and extent of variation is not the same for every location. Examples of this variation are shown by the curves presented in Figure 2.6$_c$.

Radiation, Sunshine and Cloudiness- The average monthly and annual global radiation for fifty-five selected stations are given in Table 5, Appendix A. The mean annual radiation is nearly 472 cal. cm^2 d^{-1} and the coefficient of variation is 0.114.

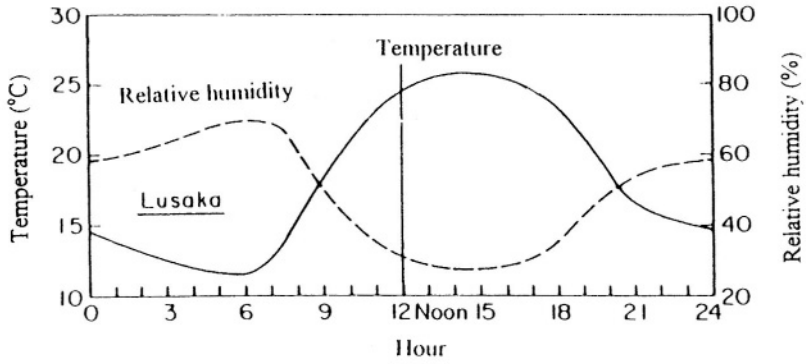

Figure 2.6$_a$- Diurnal variation of air temperature and relative humidity at Lusaka, Zambia, in August (Nieuwolt, 1977)

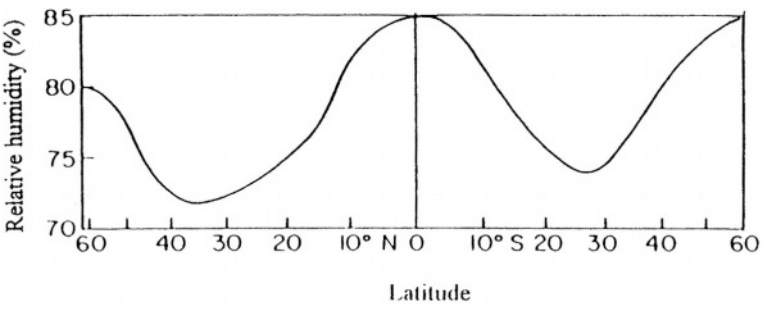

Figure 2.6$_b$- Latitudinal distribution of mean annual relative humidity (Nieuwolt, 1977)

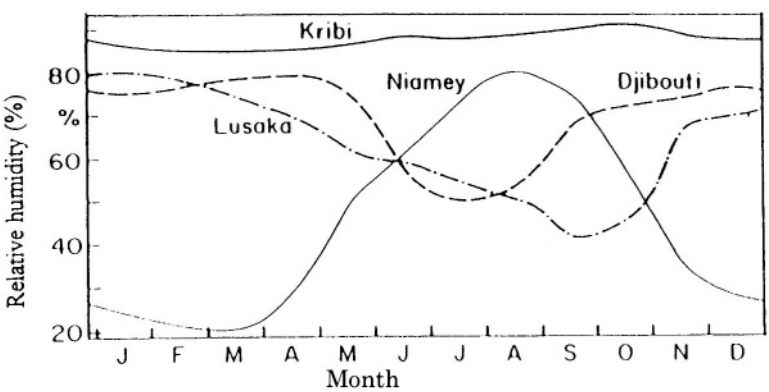

Figure 2.6$_c$- Monthly distribution of relative humidity at Djibouti (Djibouti), Kribi (Cameroon), Lusaka (Zambia) and Niamey (Niger)

The minimum and maximum values of the mean annual radiation for the stations considered are 355 (Algiers) and 567 (Aswan) cal cm^{-2} d^{-1}, respectively. Stations in the northern hemisphere receive the largest radiation in the season June-August whereas stations very close to the Equator, yet in northern Africa, have their monthly highest figures between February and April. The stations on or around the Equator hardly show any substantial difference between the months of the year. December amounts in South Africa are close to 700 cal cm^{-2} d^{-1} and fall down to 250 cal cm^{-2} d^{-1} or less in June and/or July. The monthly distribution of global radiation and the corresponding sunshine hours at four climate stations are shown graphically in Figures 2.7_a and 2.7_b.

Table 6, Appendix A, gives the monthly and annual sunshine hours at some stations. The stations located in the Sahara of northern Africa receive some 4,000 sunshine hours per year; 350-380 h in June and 250-280 h in December. Southwards, the sunshine decreases rapidly as the rainy season becomes longer. The annual number of sunshine hours does not exceed 3,000 in southern Mauritania, 2,600 south of Chad and 2,300 in southern Sudan. The cloudiest regions south of 10°N, the Gulf of Guinea coast, and a belt running along the western slopes of the Ethiopian Plateau and East Africa Mountains have 100-150 h of monthly sunshine. Around Guinea itself this figure decreases to 100 h and less (Martyn, 1992). The monthly number of sunshine hours rises to 150-200 south of the Equator in the belt between 5 and 12°S. The Kalahari Basin and the southern edges of the Congo Basin receive each month between 250 and 300 h. Namibia is the sunniest part of southern Africa with over 3,600 h. Due to its proximity to the polar front in certain months, the annual sunshine hours drop to 2,500-2,800 h in the southernmost part of the continent.

The seasonal changes in sunshine are basically connected to the variation in cloudiness. The Mediterranean region gets its maximum cloudiness in the winter season (December-February), consequently the least number of sunshine hours. The considerable amount of cloudiness in this region during winter is of cyclonic origin. However, the situation is reversed in June-July. The southern part of North Africa is an exception to this trend. It receives less sun in July due to the northward movement of the ITCZ. The cloudiness for selected climate stations is given in Table 7, Appendix A.

The January cloudiness in several parts of Burkina Faso, Mauritania, Eritrea and southern Sudan is the least and the duration of bright sunshine the longest. The weather in January in the Cameroon and the Central African Republic is quite pleasant, relatively dry with a monthly duration of 200-250 h sunshine. The movement of the ITCZ causes a considerable increase in the cloudiness, up to 80% in the period June-August in many west African countries. Examples can be found in Liberia, southern Nigeria, Guinea, Ivory Coast, Togo and Benin. The same observation extends to the Cameroon, southern Sudan and some parts of Ethiopia and Somalia. This situation results in a corresponding reduction in the number of sunshine hours. For example, the July sunshine at Lagos (Nigeria) is about 90 h,

while at Douala (Cameroon) and St. Isabel (Equatorial Guinea), it is less than 40 h.

Bultot (1971-77) produced figures for the mean frequency of overcast sky (cloudiness ≥ 90%) in the Congo Basin. The interesting thing in the statistics he produced is the hourly variation of the cloudiness. Clear sky prevails between 0600 and 1800 hours, especially from June to September and, in the south of the basin, from April to October. In the dry season, the early morning hours are the cloudiest time of the day. After sunrise the fog that has been formed by cooling during the night disappears and the sky becomes clear again.

The least amount of cloudiness in Angola occurs in the June-August season, with more than 260 hours of sunshine per month. The situation is reversed in the December-February period. The cloudiness then can reach 70% or more, especially along the ocean coast. Consequently, the monthly duration of sunshine reduces to 150-160 hours. The same observation applies to countries east of Angola, like Zambia and Malawi. The monthly distribution of the sunshine hours in these two countries is less uniform than in Zimbabwe. Cloudiness and sunshine do not show much irregularity in the Island of Madagascar. August-October is the period with clearest skies.

Windhoek (Station 240), Namibia, and Ghanzi (Station 236), Botswana, show the least cloudiness from May to September. The sunshine in this period is 310-320 h mo^{-1} and the annual number of hours is in the order of 3,600. The monthly distribution of the cloudiness in the southern part of South Africa is not uniform. It is rather limited in June-July and increases substantially in the rest of the year.

Sunshine and cloudiness are connected. Yet, one should not expect that sunshine and cloudiness will be strictly complementary as implied by the expression:

$$(SS)_o/(SS)_m + Cl = 1 \tag{2.3}$$

where $(SS)_o$ = observed sunshine hours, $(SS)_m$ = maximum possible number of sunshine hours and Cl = cloudiness expressed in oktas.

The Department of Meteorological Services of Zimbabwe (1981) has introduced some empirical adjustment to the left-hand side of Eq. (2.3) to bring the sum as close to 1 as possible. The adjustment as obtained from data covering 35 stations in Zimbabwe can be written as:

$$(SS)_o/(SS)_m + 0.62(Cl + 0.07) \cong 1 \tag{2.4}$$

As an example, the July mean ratio of observed to maximum possible sunshine is 0.81 and the cloudiness is 0.26. The unadjusted sum, 1 07, becomes after adjustment 0.81+ 0.62 (0.26+0.07) =1.01 Similarly, the observed cloudiness in April is 0.45 and $(SS)_o/(SS)_m = 0.70$ bringing the sum to 1. 15 and the adjusted sum to 1.02.

Christiansen (1966) developed an expression which can be used for estimating the percentage relative duration of sunshine, n/N (%) = 100 $(SS)_o/(SS)_m$, using the

cloudiness, Cl (scale 0 to 10, i.e. 1.25 oktas). This expression is written as:

$$n/N = 100 - 1.6Cl - 0.84Cl^2 \quad (2.5)$$

The estimates of n/N from Eq. (2.5) for the above examples using the given Cl are 0.9 and 0.76, respectively. The corresponding measurements of n/N were 0.81 and 0.70. The sunshine hours and the cloudiness data of the four stations 32, 103, 182 and 269 (Figure 2.7_b) have been used to develop a regression relation between n (h d^{-1}) and Cl (oktas). The linear regression (Figure 2.7_c) obtained from those data is:

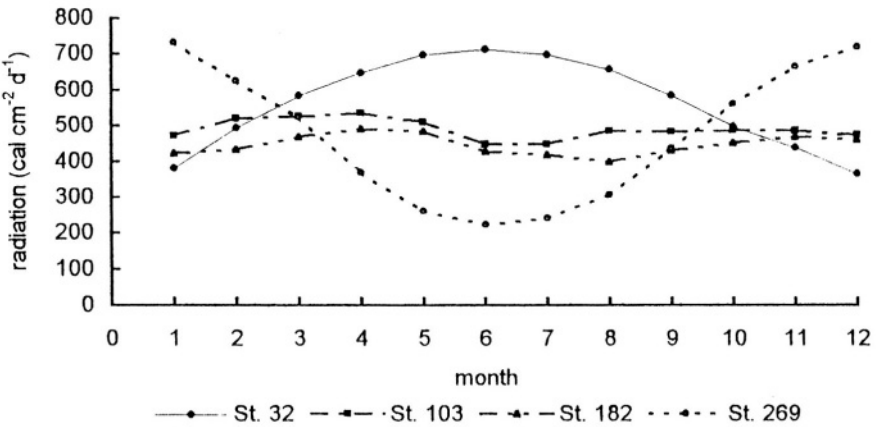

Figure 2.7_a- Monthly distribution of global radiation at four climate stations

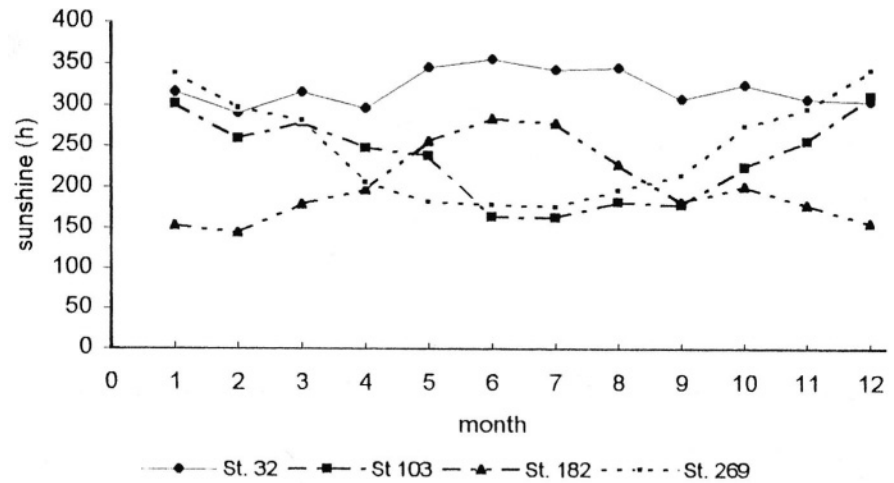

Figure 2.7_b- Monthly distribution of sunshine hours at the same four stations used in Figure 2.7_a

$$n = 11.5 - 1.0867Cl \tag{2.6}$$

The fact that Eq. (2.6) yields $n = 11.5$ h for a clear sky ($Cl = 0$) and $n = 2.8$ h for an cast sky ($Cl = 8$) reflects the approximate nature of this relationship. However, the correlation between the two variables, i.e. n and Cl is rather strong (r = 0.88).

Evaporation and evapotranspiration, which will be discussed in Chapters 4 and 5, are strongly affected by the net radiation, R_n. In the absence of direct measurements, R_n can be estimated from the global radiation using the expression:

$$R_n = R_s(1 - \alpha_s) - R_{nl} \tag{2.7}$$

where R_s = global (short-wave) radiation, α_s = albedo of the surface and R_{nl} = net long-wave radiation. The terms appearing in the right-hand side of Eq. 2.7 can be obtained from empirical formulas or theoretical models whenever available. For example R_s can be estimated from the relationship, originally developed by Ångstrom (1924), or any of its modified forms:

$$R_s = R_{se}[a + b(n/N)] \tag{2.8}$$

where R_{se} = extraterrestrial radiation depending on latitude and time of the year, a and b are constants depending on the geographic location, season and the state of the atmosphere and $n/N = (SS)_o/(SS)_m$ is the relative sunshine. Values of a and b have been determined for many locations, The average values of a and b reported by Doorenbos and Pruitt (1977), and Brutsaert (1982) are 0.25 and 0.50, respectively.

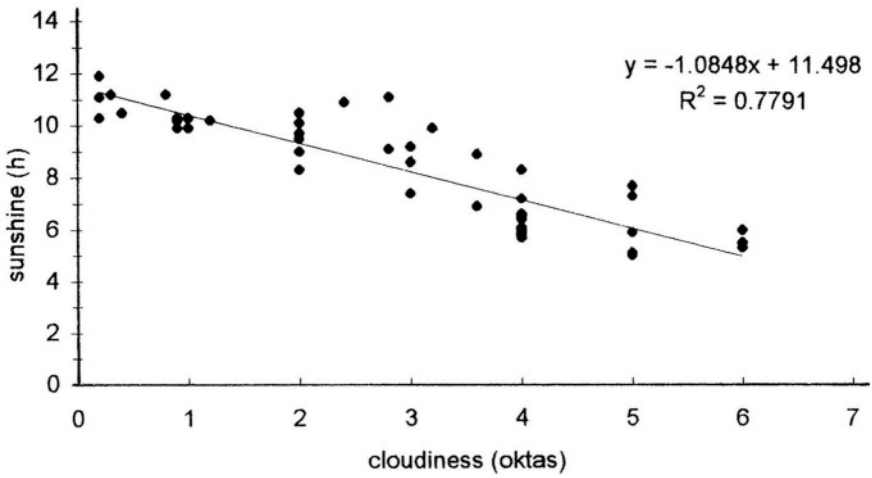

Figure 2.7$_c$- Regression relation between sunshine and cloudiness for the stations in Figures 2.7$_a$ and 2.7$_b$

Glover and McCulloch (1958) using data from East Africa showed that sunshine and radiation are significantly linked by the equation:

$$R_s / R_{st} = 0.29 \cos \Phi + 0.52 n / N \tag{2.9}$$

where R_s = short-wave radiation for a cloudy sky, R_{st} = same as R_s, except for a transparent atmosphere at the same time and location, φ = latitude and n/N as defined before. Substituting R_{se} for R_{st} and $\cos \varphi = 1$, a and b for East Africa become 0.29 and 0.52, respectively. Using the data given by Shahin (1985) for the Nile Basin in Egypt and northern Sudan, the best fit of the regression line gives 0.28 for a and 0.45 for b (Sadek, 1992). Again, Eq. 2.7 can be rewritten as

$$R_n = R_{ns} - R_{nl} \tag{2.10}$$

where R_{ns} = net short wave radiation Yin and Nicholson (1998) while investigating the water balance of Lake Victoria, substituted 0.07 for the albedo α_s of the lake surface and for R_{ns} used the expression:

$$\begin{aligned} R_{ns} &= (1-\alpha_s) R_{se} (0.803 - 0.34c - 0.458c^2) = \\ &= 0.93 R_{se} (0.803 - 0.34c - 0.458c^2) \end{aligned} \tag{2.11}$$

where c = fractional cloud cover and the rest as before. The expression for net long wave radiation used by Yin and Nicholson (1998) is that developed by Budyko (1974) and written as:

$$R_{nl} = \varepsilon \sigma T_w^4 (0.39 - 0.05\sqrt{e_s})(1 - 0.53c^2) \tag{2.12}$$

where ε = emissivity of water taken as 0.96, σ = Stefan-Boltzman constant = $5.67 * 10^{-8}$ W m^{-2} K^{-4}, T_w = water temperature in degrees Kelvin (Centigrade+ 273) and e_s is the saturated vapour pressure for the monthly surface temperature Substituting the climatic data of Lake Victoria in Eqs. 2.10, 2.11 and 2.12 the total net radiation has been found in the order 125-150 W m^{-2} throughout the year. Measured solar radiation at the surface likewise validates our calculations (Shahin, 1985; Yin and Nicholson, 1998)

Air Movement- Africa is dominated by a system of permanent pressure belts. This system comprises two subtropical high-pressure belts with a central, equatorial low-pressure belt or equatorial trough in between. The equatorial trough has been earlier referred to as the Inter-Tropical Convergence Zone (ITCZ) The pressure belts move northward in the summer of the northern hemisphere and southward in the summer of

the southern hemisphere. The seasonal movement of the ITCZ has already been discussed at the beginning of the present chapter, and its corresponding locations are shown on the four maps in Figure 2.1. As such the discussion in the present section will be confined to the different air streams and their movement. While doing so, the wintertime will be represented by January and the summertime by July, in the northern hemisphere whereas, July and January will represent the winter and summer seasons for the southern hemisphere, respectively.

The high-pressure belts, known as subtropical highs, are areas of descending air. They lie over the Sahara in northern Africa and the Namib Desert in southern Africa. The convergence of air means that more air is entering an area at the surface than leaving it. The surplus heat energy is transformed into kinetic energy near the Equator. A certain proportion is also involved in consumed by evaporation and carried with the moving air masses. The heated air masses are uplifted and transported to higher elevations by upper air currents known as anti-trades, and there the air cools to saturation point. This process is very likely to produce rainfall in the tropics. The air movement gradually slows down at about 20-30° latitude. The subsiding air movement, which prevails there, carries the air back down to the earth's surface. This process helps to maintain the subtropical highs. A massive air stream, the trade winds, moving at low levels towards the Equator, closes the circulation. The two wind systems, trade and anti-trade, converge at the ITCZ. The divergence, which brings about subsiding air masses, is likely to result in aridity.

On the poleward side of the high-pressure belts, alternating cyclones and wedges of high pressure move from west to east. The rain-inducing fronts associated with these cyclonic activities bring rain to areas outside the Equator.

Figures 2.8_a and 2.8_b show the directions of seven air streams, a through f, which have been distinguished by Brooks and Mirrlies (cited in Stamp and Morgan, 1972). These air streams are as follows:

(a) The Atlantic Northeast Trades, blowing toward the southwest from the Azores high-pressure system;

(b) The north-easterly trade winds (harmattan), an air system blowing from the Saharan high-pressure belt across the southern Sudan and toward West Africa;

(c) The Egyptian air stream, blowing up the Nile Valley as a northerly wind and reaching as far as Botswana;

(d) The Atlantic Southeast Trades, blowing toward the equatorial low-pressure belt over the South Atlantic. On crossing the equator, which they do especially during the northern summer, these winds become southwesterly and produce a monsoon effect in West Africa, but penetrate in January only a short distance inland;

(e) The Arabian or Indian Northeast Trades, blowing from the high pressure system of Southwest Asia in the winter months only, being eliminated and reversed by the monsoon currents for the other half of the year;

(f) The Indian Ocean Southeast Trades, the dominant influence over the southeast part of the continent;

Stamp and Morgan (1972) have suggested the addition of two more air streams; (i) and (h) to indicate cyclone activities. The one over the Mediterranean (h) is a cyclonic belt of alternating depressions and wedges of high pressure, responsible for the winter fall from Morocco to Egypt. The other one, (i), moving over the southern ocean, is associated with strong, more regular winds, and is responsible for the winter fall of the Cape. In the following paragraphs we shall briefly describe the role each of these streams play in developing the climates of Africa.

In the wintertime of the northern hemisphere, atmospheric activities (h) over North Africa are connected with the wedges of the Azores High, Saharan anticyclone, Arabian High, Mediterranean depressions and Equatorial lows over central Africa. Accordingly, with the exception of the Mediterranean region where the westerly winds prevail, northerly, northeasterly and harmattan winds (b) dominate the rest of the region. Certain depressions known as gibli (Sirocco) and Khamasin (50 days) cause the most serious desert winds, which occur during the winter and early spring times in Libya and Egypt. These winds bring considerable amounts of fine dust and are largely responsible for the aridity of the region.

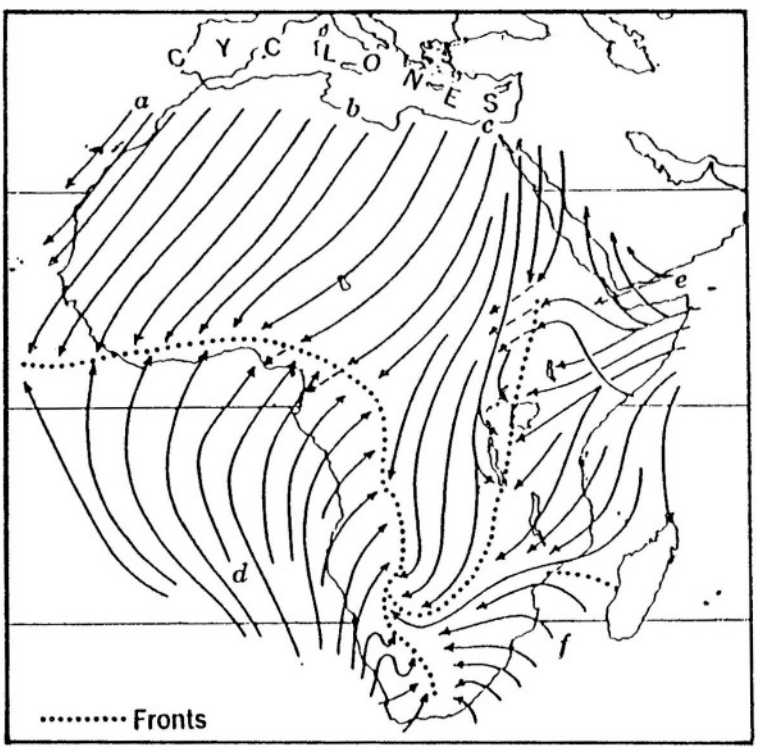

Figure 2.8a- Air movement over Africa in January (based on Brooks and Mirrlees, cited in Stamp and Morgan, 1972)

In January, the harmattan winds do not go beyond 5°N, and do not usually reach the Gulf of Guinea in West Africa. At the same time the Egyptian current (c) blows off the Sahara from the north and northeast and the Arabian stream (e) from the east. Both air streams are received at many areas in Ethiopia, Somalia and Djibouti. Moist-laden air masses blowing across the Indian Ocean reach the southern parts of East Africa and influence the weather there. Some of these parts lie within reach of the dry northeasterly winds blowing from the Arabian Peninsula and Somalia. In April (mid-autumn) moist air masses (f) blow off the Indian Ocean normally onto the Kenyan and Tanzanian coasts and the mountain barriers. The result is intensive rain.

Southwesterly winds coming from the South Atlantic prevail most of the time in the northwestern part of Angola. East Angola, however, remains mostly under the influence of the Indian Ocean High. In winter (July), the cool Benguela Current that sweeps over the Angolan coast affects the climate of the coastal plain up to Gabon. The autumn and winter climate in nearly all of Angola is dominated by the South African High together with the Indian Ocean High.

The Indian Ocean High as well as the South African High influence the winter (July) in the southeastern part of Africa. The southeast Trades, (f), dominate that part of Africa. Since most of its moisture is precipitated over Madagascar, what reaches southeast Africa (Mozambique, Zambia, Zimbabwe and Malawi) hardly brings any rainfall there.

The atmospheric circulation over southern Africa, similar to the southeast, is controlled by the South Atlantic and South Indian Ocean Highs centered on latitude 30° S. The anticyclone activities and the eastern winds, which prevail in wintertime over Lesotho, Botswana and Namibia, are the factors behind the arid climate of southern Africa.

In July, the Azores High, which stretches to the north over the Mediterranean and southwest Europe, together with the depressions over the southern Sahara, southern Sudan and the highs over central Africa, block the entry of the cyclonic system from the Atlantic and bring dry summers to North Africa.

Contrary to the situation in North Africa, the convergence of the harmattan (b) and the Guinea monsoon in July can penetrate northward up to latitude 20°N and eastward to northern Sudan causing precipitation. Climate stations at Khartoum (49), Gedaref (62) and Roseires (81) receive 75, 60 and 50% of their respective annual rainfall in July and August each year. At the same time rainfall in southern Sudan is linked with the Indian monsoon.

Since the central part of West Africa in the northern hemisphere is contained between the Atlantic Ocean from the west and south and the Sahara from the north, the climate of this region is dominated by these two factors. In July, the southwest monsoon has already extended itself north to reach almost 20° N. The areas where the monsoon is quite deep, like the belt from 8 to 10°N, receive heavy summer rain. The July and August rainfall at stations 102 (Guinea) and 110 (Sierra Leone) forms 55 and 45% of their annual rainfall, respectively.

The climate conditions in East Africa (Ethiopia, Kenya, Djibouti and Somalia) are more complex. The northeast Trades dominate the northeast of Ethiopia. Dry masses of air blowing off the Arabian Peninsula, from Kenya and across the Indian Ocean meet over the Somali Plateau. At the same time, West Ethiopia is exposed to the moist monsoon air blowing over the Congo Basin, whereas southern Ethiopia and southeastern Sudan receive moist air masses from the Indian Ocean.

While Northwest Angola is dominated by southwesterly winds alone, the southern parts of the country are exposed to northwesterly, westerly and southwesterly winds. Differently, East Angola is under the mutual influence of the Indian and South Atlantic Oceans. Air masses from both oceans meet at a meridional front whose location varies according to the season. As a consequence to the strong variation in moisture content of the blowing winds over the different areas, the northern part of Angola receives a lot more rain than the south. The weakening of the Benguela Current is reflected in the precipitation along the coast (Martyn, 1992)

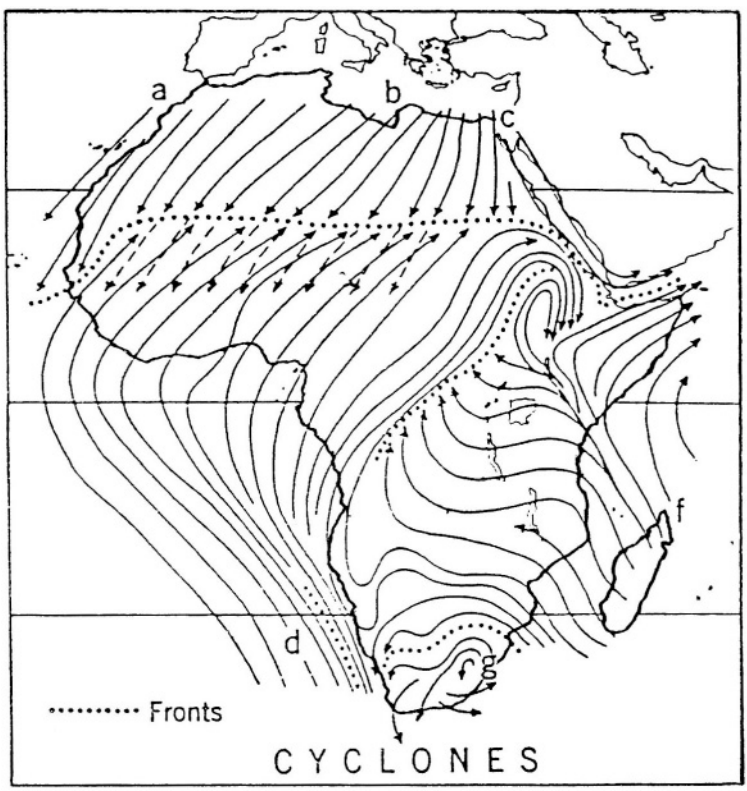

Figure 2.8$_b$- Air movement over Africa in July (based on Brooks and Mirrlees, cited in Stamp and Morgan, 1972)

In summer (January), a center of low atmospheric pressure is formed over southern Zambia. The pressure gradient draws air masses from the Congo (moist), northeast Monsoon (dry), Somalia and east Africa. Trade winds from the Indian Ocean High reach parts of Zambia, Zimbabwe and Mozambique, mostly from the south.

Botswana, Namibia and central South Africa are under the influence of a high-pressure belt over the Transvaal during the wintertime. By July, Namibia is hit by easterly winds, turning into northerly over the Cape Province and Kalahari Desert. Westerly, northwesterly and southwesterly winds blow parallel to the different parts of the curved shoreline of South Africa.

Thunderstorms: A thunderstorm is a culmination of atmospheric convective processes when cumulus clouds have grown beyond their single-cell structure to become towering cumulonimbus clouds penetrating layers of atmosphere colder than - 30° C and finally maturing as thunderstorm rain, hail and lightning. Their small size and short duration characterize thunderstorms. They hardly reach a diameter of more than 10 km and their duration is mostly limited to 1-2 hours. As such, the impression of thunderstorms on the general pressure distribution and wind pattern is minor and temporary. However, thunderstorms can be climatically important in view of the high-intensity rain they cause.

Most of the thunderstorms occur in the tropics. About 20% of Africa experiences more than 100 thunderstorm days per year. Certain parts of Congo (Kinshasa), Nigeria and Uganda can have more than 200 days per year. The smallest frequency occurs in the Sahara in the north and in Southwest Africa.

The monthly distribution of the mean number of thunderstorm days is basically non-uniform. For example, the 20-y mean number of days at Harare, Zimbabwe (St. 224), are: 0.0, 0.7, 1.8, 5.9, 10.7, 13.7, 13.9, 13.0, 7.1, 4.2, 1.2 and 0.6 for July, August, ... May and June, respectively. The total number of days varies considerably from one location to another, and so does the percentage of thunder days to raindays. Examples of these variations over Zimbabwe are shown in Figures 9_a and 9_b (Department of Meteorological Services of Zimbabwe, 1981).

Surface Wind- Table 8 in Appendix A gives the monthly and annual average figures of wind speed at selected locations. The wind speed is given in $km\ h^{-1}$ at a standard height of 2 m above the surface of ground or water. The figures presented in that table show the average over the year varies from a minimum of $3\ km\ h^{-1}$ in Cameroon to a maximum of $21\ km\ h^{-1}$ in Madagascar

The distribution of the annual average wind speed is bimodal with a higher peak at $7\ km\ h^{-1}$ and the other peak at $14\ km\ h^{-1}$ (Figure 2.10_a). The mean of the distribution is about $10.15\ km\ h^{-1}$, with a coefficient of variation of 0.4. The wind speed and direction can vary significantly for the same location from one time interval to another, even if it is short. In this subsection, only monthly variation will be

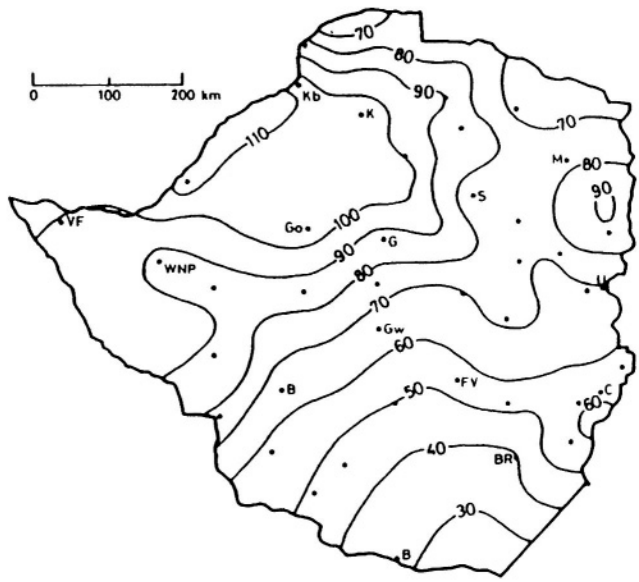

Figure 2.9$_a$- Mean number of thunder days per year in Zimbabwe

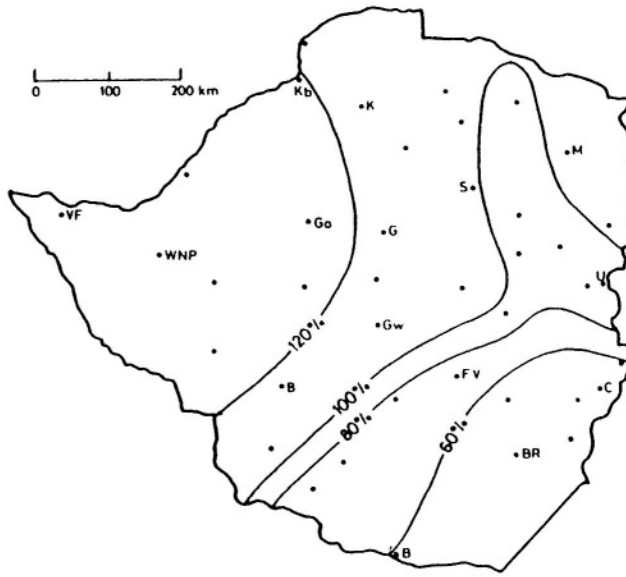

Figure 2.9$_b$- Ratio of annual thunderstorm days to rainy days

presented. Figure 2.10$_b$ shows the monthly distribution at four stations. Station 6 (Tangier, Morocco) is located on the Atlantic/Mediterranean coast showing a nearly uniform distribution where the maximum to minimum wind speed is 1.2:1. Station 88 is an inland station at Bobo Dioulasso, Burkina Faso. It shows a heavy non-uniform distribution with a ratio of maximum to minimum wind speed of 10:1. Stations 191 and 259 are at Mtwara, Tanzania, and Estcourt, South Africa, respectively. The former is on the coast of the Indian Ocean, whereas Estcourt is more of an inland station. The corresponding ratios are 1.6:1 and 2.3:1, respectively.

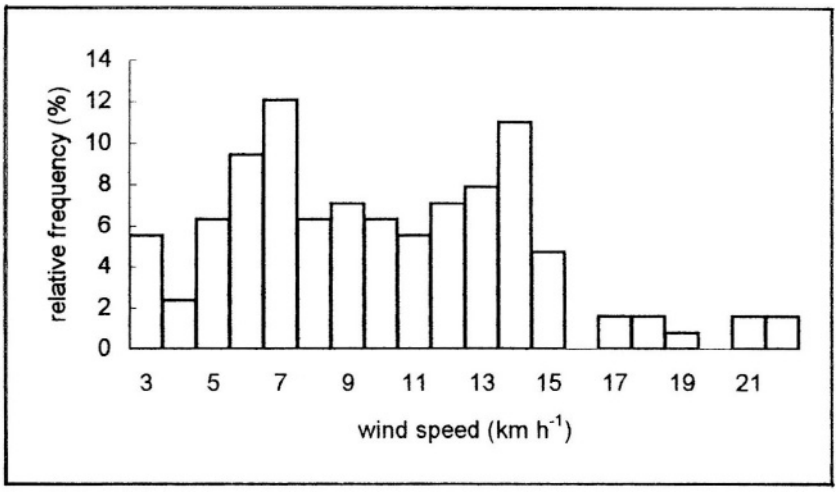

Figure 2.10$_a$- Distribution of mean annual wind speed at selected stations in Africa

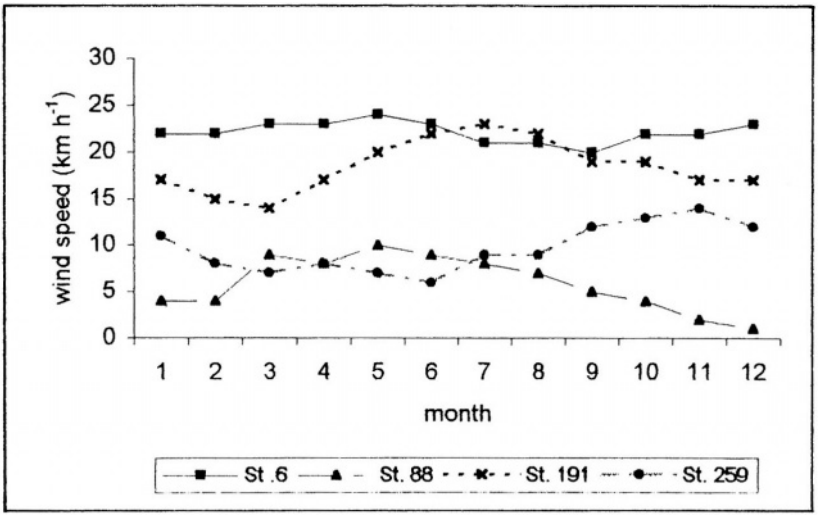

Figure 2.10$_b$- Monthly distribution of wind speed at four stations

The literature on Africa's meteorology is full of examples about wind direction and its variability. An example of the monthly as well diurnal change of the percentage duration of the northeast wind in Djibouti quoted from Griffith's (1972) is as follows:

Month	6.00 a m	12.00 noon	Month	6.00 a m	12.00 noon
Jan	8	28	Jul	2	14
Feb	18	40	Aug	5	13
Mar	30	55	Sep	5	33
Apr	9	50	Oct	11	51
May	11	53	Nov	9	32
Jun	10	39	Dec	10	34

It is common to represent the wind direction and its frequency graphically on a diagram called the wind rose. As the wind force measured on the Beaufort scale reaches or exceeds 8, the wind is called then a gale. The number of days with gales varies with time and space. Locations with 50 or more days of gales are not unusual in the African Horn.

Rainfall- Rainfall is the most common form of precipitation in Africa. Despite this fact there is always the chance, al least for some locations to get precipitation in the form of hail. As mentioned earlier, the African deserts can benefit from condensed water (dew).

Table 9 in Appendix A gives monthly and annual rainfall at chosen stations. Furthermore, Table 10_a indicates the mean annual precipitation depth over a certain period of years together with the coefficient of variation for all meteorological stations (271) considered in the book. The tabulated data supported by figures from additional stations, not included in the said tables, have been used for preparing the annual rainfall map shown in Figure 2.11.

The annual rainfall at some locations is practically zero and at other stations is above 4,000 mm. Moreover, the period of record for all stations is not the same. For these reasons it has been found more realistic to divide Africa into zones, each having a certain range of rainfall depth, 8, e.g. $8< 100$ mm, $100 \leq 8<200$, $200 \leq 8<400$, etc. Based on the map in Figure 2.11, the following results have been obtained:

Percentage of total surface area	Average depth, mm	Fractional depth of rainfall, mm
32	25	8
5	180	9
6	300	18
14	600	84
30	1,000	300

12	2,000	240
1	3,000	30
Total depth		689

The calculated annual depth, 689 mm, is very close to the 686 mm estimated earlier by L'vovich (1979). Multiplying the surface area of the continent ($30*10^{12}$ m^2) by an annual depth, say 0.69 m, yields an annual volume of rainfall of about $20.7*10^{12}$ m^3 or 20,700 km^3.

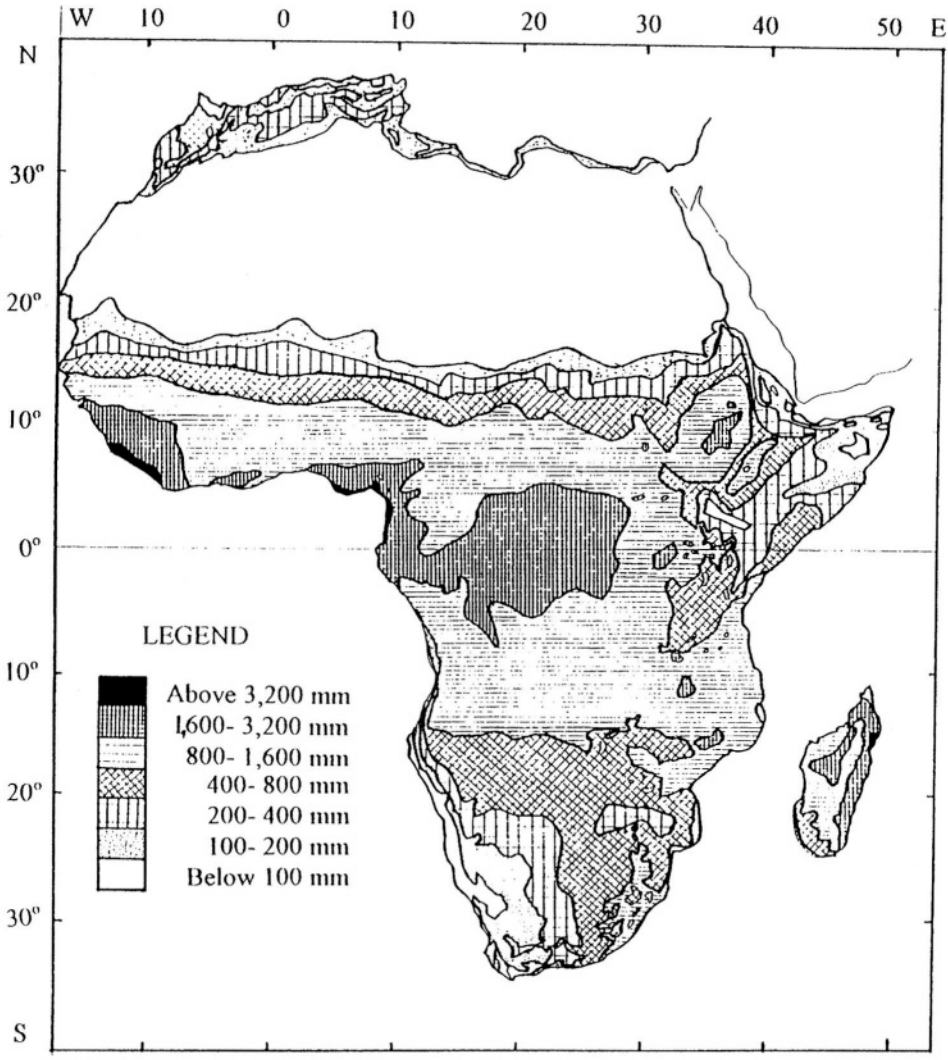

Figure 2.11- Mean annual rainfall in Africa

The division of the continent into zones of equal annual depth might help to identify the extent of aridity/humidity of climate in each zone. Obviously this identification will require additional climatic data such as atmospheric temperature and evapotranspiration, as will be discussed in the next section.

Convective, frontal, orographic, monsoonal, cyclonic, etc are terms associated with the processes causing precipitation. In the subsection on atmospheric disturbance, precipitation resulting from thunderstorms has been discussed. The number of monthly and annual rain days listed in Table 11, does not really specify the process underlying precipitation. This Table gives a minimum of 0.2 day for Aswan, Egypt and a maximum of 213 days per year for Antalaha, Madagascar.

The different climate stations show different distribution patterns of the monthly number of rainy days. This is basically due to the geographic location as well as the elevation of each station. The graphs in Figure 2.12 are for four stations: 21 (Sirte, Libya), 84 (Bolama, Guinea Bissau), 147 (Kribi, Cameroon) and 203 (Ndola, Zambia). Station 21 gives a total of 28 rain days with 0 and 1 day in the summer period May-September. The annual rainfall at this station is 193 mm. The second station, 84, receives annual depth of 2,167 mm in 108 days concentrated in the season from June-to November. Station 147, with an annual average rainfall of 2,934 mm and 205 rainy days, has a bimodal distribution with one peak in May and the second in September-October. According to the available data, there is no dry season in the area represented by this station. The fourth station, 203, receives annual rainfall of 1,200 mm in just 94 days from October to April each year. As such, one can fairly conclude that the average rainfall in each of the rainy days varies from about 7 mm at Sirte to about 20 mm at Bolama. This range is expected to increase as the number of gauges used in the analysis increases. Remarkable enough is that the average depth per rainy day shows a reasonable degree of consistency for fairly wide

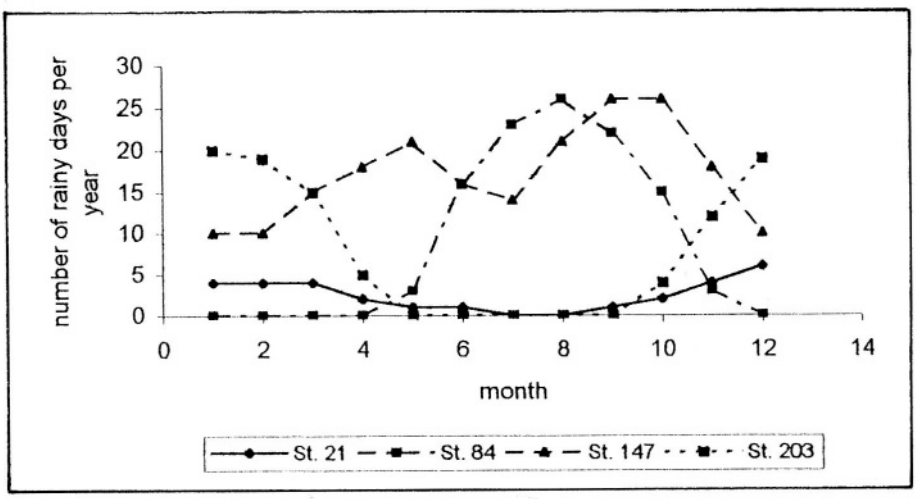

Figure 2.12- Distribution of the monthly number of rain days at four stations

intervals of rainfall. Despite the obvious high rate in the west and low rate in the east, the mean and coefficient of variation for the interval 1,000-2,000 mm are 13.2 $mm\,d^{-1}$ and 0.25, respectively. The mean for the interval 2,000-3,000 mm is 15.1 $mm\,d^{-1}$ and so on.

The rest of the rainfall data in Tables 9, 10 and 11 of Appendix A will be discussed in Chapter 3, which deals with analysis of rainfall data.

Evaporation and Evapotranspiration-By evaporation, it is here meant the direct transfer of water from the surface of such water bodies as lakes, reservoirs, depressions, etc. to the atmosphere (Shaw, 1984). Certain devices, such as the Piche evaporimeter, USWB class A evaporation pan, etc, are used for measuring the evaporativity of a given environment. Moreover, since evaporation influenced by climatic factors such as temperature, radiation, humidity, wind speed, etc, it can be estimated using any of the currently available expressions based on these factors. Table 12 in Appendix A, includes measured as well as well as estimated evaporation rates.

When the evaporation loss is caused by transpiration from vegetation and the intercepted precipitation on plant surfaces is also included the process is called evapotranspiation. As such, evapotranspiration can be regarded as the total loss by evaporation and transpiration. When evapotranspiration occurs under the condition of unlimited water, the (actual) evapotranspiration reaches a level known as potential evapotranspiration. Tables 13_a and 13_b include measurements and estimates of potential evaporation from cropped surfaces at a number of locations. Table 13_c is concerned with evapotranspiration from swamps and forest areas.

Africa, because of its geographic location receives a large amount of solar heat and has a positive radiation balance. With this large amount of energy, one can expect the potential evapotranspiration to reach high values. The map showing the contour lines of equal potential evapotranspiration in Africa (Kurzon, 1978) gives a minimum of 1,250 $mm\,y^{-1}$ in the very humid parts of West Africa to more than 2,500 $mm\,y^{-1}$ for the hyper arid parts of the Sahara in North Africa. A simplified version of this map is shown in Figure 2.13. In view of the reduced continentality in southern Africa compared to northern Africa, the northern latitudes are more susceptible to higher potential evapotranspiration than the corresponding southern latitudes

The map of potential evapotranspiration, ET_o, when compared to the map of actual evapotranspiration, ET_a, shows that, for hyper-arid areas, the ratio ET_a/ET_o is in the order of say 25/2,500, i.e. 1%. The same ratio, ET_a/ET_o, for the humid parts of the continent is commonly around 1,000/1,250, i.e. 80%. Furthermore, when the map of potential evapotranspiration is compared to the map of annual precipitation, the difference will be either positive or negative. The positive difference indicates surplus or excess. Conversely, a negative difference is termed a shortage or deficit. Since the difference, $P - ET_o$, for the largest part (>85%) of Africa is negative, Africa can be truly described as the continent of water shortage.

The analysis and discussion of water loss by evaporation and evapotranspiration will be presented in Chapters 4 and 5, respectively. However, the available figures of potential evapotranspiration will be used together with temperature and precipitation data for determining the extent of aridity/humidity and thereupon the climate of the different regions of Africa.

2.3- Aridity

Agroclimatological research and development have considerable potential in the less well-defined subtropical and tropical environments of the world. There is an urgent need for increased agricultural production as well as more information about desert environments, pasture plants and tropical crops. With these needs in mind, climate

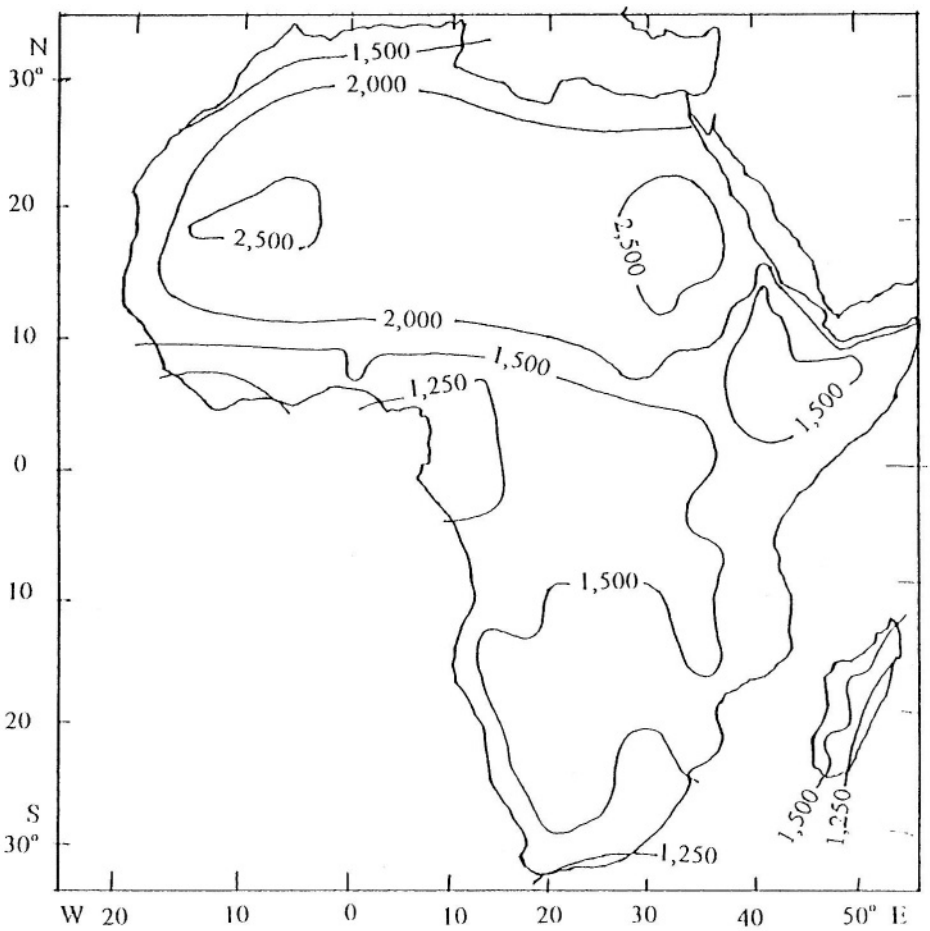

Figure 2.13- Map of potential evapotranspiration in Africa (Kurzon, 1978)

classification is important in developing a broad understanding of factors affecting soil and crop patterns in various environments. Gentilli (1972) specified the criteria used in climatic classification as listed in Table 2.3. Since the climate of a considerable surface of Africa is hyper-arid to semi-arid, it seems unavoidable to discuss the issue of aridity before dealing with the classification of the climate.

Lack of precipitation in relation to the prevailing temperature and evapotranspiration values is one of the principal factors in the creation of desert and semi-desert areas. The lack of adequate climatological information is, in part, responsible for the unsatisfactory attempts to delimit the margins of the arid zone by climatic data. The same remark applies to the division of the arid area into its more or less humid components (Walton, 1969).

De Martonne (1926) introduced a slight modification to de Lang's *P/T* ratio to produce the Index of Aridity, *IA,* as:

$$IA = P \big/ (T + 10) \tag{2.13}$$

where *P* and *T* are the annual precipitation expressed in mm, and T the annual mean temperature in °C. The limit of the true desert was set by De Martonne at *IA* = 5. The dry steppe boundary, or the limit of dry farming without irrigation, was drawn where the aridity index has a value of 10.

Köppen (1931) followed the same approach as de Lang and de Martonne. He too concluded that the boundaries of the arid regions can be established in terms of P and T, though using different expressions. The limit of semiarid regions in the subtropics could be expressed as:

Table 2.3- Classification criteria used in climatic classification

Time	Frequency or duration	Climatic elements	Examples of criteria
Independent		Single	Temperature
			Rainfall
			Wind direction
		Combined	Temperature and rainfall
		Ratios	Temperature/rainfall
			Rainfall/evaporation
Dependent	Frequency or probability	Single	Annual wet days
			Percentage of wet days
		Combined	Wet days with certain wind patterns
			Temperature and humidity
		Ratio	Frequency of years with R/T+10>0
			Probability of years R<T+7
	Seasonal duration	Single	Frost-free season
		Ratio	Months with r/e.0.75>0.4

$$P = 2(T + 7) \tag{2.14}$$

where T is the same as in Eq. (2.13) but P is in cm.. The limit he set for arid conditions is half that to be obtained from Eq. (2.14). Köppen, later, corrected the expression given by Eq. (2.14) to read

$$P = 2(T + 14) \tag{2.15a}$$

in areas with summer rainfall, and

$$P = 2T \tag{2.15b}$$

in areas with winter rainfall. Köppen's index has been applied to the Mediterranean region of Africa. Bagnouls and Gaussen (1959) established a system of aridity based on the number of dry months in the year. He applied Eq. (2.15b) on a monthly scale, i.e. $p < 2t$, to define a dry month, where p and t are the monthly precipitation and temperature, respectively. The above expressions were often criticized on the grounds that temperature alone is inadequate to describe evaporation, which has to appear in any expression aiming at defining the aridity

Thornthwaite (1948) developed a new expression introducing the Precipitation-Evapotranspiration Index. This index, *PEI,* can be written as:

$$PEI = 10\Sigma^{12} p/et_o = \Sigma^{12} 115[p/(t-10)]^{0.9} \tag{2.16}$$

where p, et_o and t are monthly precipitation (in), potential evapotranspiration (in) and temperature (°F), respectively, summed up for the 12-months of the year. Using this approach Meigs (1951) constructed for UNESCO a map of the world's arid lands divided into semi-arid, arid and extremely arid climates. This classification has been recently expanded by UNEP (1993) to become as follows:

Hyper-arid	$0.00 \leq P/ET_o < 0.05$
Arid	$0.05 \leq P/ET_o < 0.20$
Semi-arid	$0.20 \leq P/ET_o < 0.50$
Semi-humid	$0.50 \leq P/ET_o < 0.65$
Humid	$0.65 \leq P/ET_o$

Budyko (1956) developed the so-called dryness ratio, D, as a measure of aridity. This measure depends on the relative magnitudes of energy supply and rainfall. The expression for it is as follows:

$$D = R_n / LP \tag{2.17}$$

where R_n is the net radiation, L is the latent heat of vaporization and P is the mean annual rainfall. The guide lines for classification of aridity are: $D \geq 3.4$ for deserts, $2.3 \leq D < 3.4$ for semi-deserts and $1.1 \leq D < 2.3$ for steppe or savanna.

Nearly 100 stations have been tested for the aridity using the expressions of De Martonne, Köppen and Thornthwaite. The results obtained are given in Table 2.4. It goes without saying that the results obtained from the three approaches are always identical for every station. Köppen's approach seems to yield more discriminating results than de Martonne's whereas Thornthwaite's method distinguishes between arid and hyper-arid climates. Anyhow, the inconsistency between the results obtained for some stations using different expressions indicates clearly the need for adequate agroclimatic information and a research methodology addressing the problem of aridity. A general map showing the contour lines of equal values of dryness ratio in Africa as a whole as developed by Budyko (1956), is shown in Figure 2.14.

Ayabotelle (1984) applied the data available in the Atlas of World Water Resources (Kurzon, 1978) to obtain values of the mean annual aridity index for arbitrarily formed subdivisions of Africa. He used the annual precipitation/potential evapotranspiration ratio of Thornthwaite for this purpose. The subdivisions that were considered are in fact the cells formed by intersection of 10° wide latitudinal bands with 10° wide longitudinal bands covering the surface of Africa. The results obtained after rearrangement and some additions are summarized in Table 2.5.

2.4- Climatic Classification and Regions

Of the currently available climatic classification systems, those of Köppen and Thornthwaite are probably the most widely used ones. These two systems have already been discussed in Sec. 2.3 in connection with the aridity issue. It seems, therefore, relevant to start by further applying them to areas other than arid and semi-arid areas before delineating the climatic regions of Africa.

Köppen climatic classification as applied to Africa consists of three classes to be denoted A, B and C. Each class has a number of subdivisions as follows:

A climates: mean temperature of coldest month of the year is at least 18° C
f = monthly rainfall exceeds 60 mm
w = mean annual rainfall < 100 + 10 (6 - amount in driest month)

B climates:
BS = $P < 2T$ (winter rains)
$P < 2(T + 14)$ (summer rains)
$P < 2(T + 7)$ (other patterns)
BW = $P < T$ (winter rains)
$P < (T + 14)$ (summer rains)
$P < T + 7$ (other patterns)
h = mean annual temperature above 18°C
k = mean annual temperature below 18°C

Table 2.4- Extent of aridity at a number of selected stations as obtained from the methods established by De Martonne, Koppen and Thornthwaite

Station No	Location	Extent of aridity according to						
		De Martonne		Koppen		Thornthwaite		
		Arid	D. St.	Arid	S. Arid	H. Arid	Arid	S. Arid
7	Biskra	x		x			x	
8	Sfax		x	x			x	
9	Gafsa		x	x			x	
10	Gabes		x	x			x	
11	Laghouat		x	x			x	
12	Casablanca							x
13	Tripoli		x		x		x	
14	Derna		x	x			x	
15	Funchal							x
17	Misurata		x	x			x	
18	Benghazi		x	x			x	
19	C.Bechar	x		x		x		
20	Marrakech		x	x			x	
21	Sirte		x	x			x	
22	Alexandria		x	x			x	
23	Mansoura	x		x		x		
24	Agadir		x	x			x	
25	Ghadames	x		x		x		
26	Giza	x		x		x		
27	El- Fayoum	x		x		x		
28	St. C. Tenerif		x	x			x	
29	Las Palmas	x		x			x	
30	Assiut	x		x		x		
31	Kufra	x		x		x		
32	Aswan	x		x		x		
33	V. Cisneros	x		x		x		
34	Wadi Halfa	x		x		x		
35	Atar	x		x		x		
36	Tessalit	x		x		x		
37	Bil,a	x		x		x		
38	Tidjikja	x		x			x	
39	F. Largeau	x		x		x		
40	Atbara	x		x		x		
41	Boutilimit	x		x			x	
42	Agades	x		x			x	
43	Porto Grande	x		x			x	
44	Sal	x		x		x		
45	Kiffa		x	x			x	

Table 2.4- Cont'd

Station No	Location	Extent of aridity according to						
		De Martonne		Koppen		Thornthwaite		
		Arid	D. St.	Arid	S .Arid	H. Arid	Arid	S. Arid
46	Nema		x	x			x	
47	Gao		x	x			x	
48	Matam		x		x			x
49	Kharatoum	x		x			x	
50	Massawa		x	x			x	
	Port Sudan	x		x		x		
	Kassala		x	x			x	
51	Asmara							x
53	Praia		x	x			x	
54	Tahoua			x			x	
57	Wad Medani		x		x		x	
58	N'Guimi		x	x			x	
59	Tillabury				x			x
61	Dori				x			x
62	Gedaref							x
63	Arbecher				x			x
64	Zinder				x			x
66	El-Fasher		x	x			x	
	El-Obeid		x	x			x	
	Nyala		x		x			x
73	Singa				x			x
75	Assab	x				x		
83	Djibouti	x		x			x	
91	Erigavo							x
93	Berbera	x		x		x		
100	Dire Dawa							x
104	Hargeisa				x			x
120	Galcaio	x		x			x	
130	Negelli							x
142	L. Ferrandi		x	x			x	
146	Lodwar.	x		x			x	
152	Mogadiscio				x			x
166	Garissa		x	x			x	
185	Wideawake	x		x			x	
187	Luanda				x		x	
199	Lobito		x	x			x	
213	Mossamedes	x		x		x		
229	Tsumeb							x
231	Maun							x

Table 2.4- Cont'd

Station No	Location	Extent of aridity according to						
		De Martonne		Koppen		Thornthwaite		
		Arid	D. St.	Arid	S .Arid	H. Arid	Arid	S. Arid
232	Bulawayo							x
236	Ghanzi							x
237	Beitbridge				x			x
238	Messina				x			x
239	Pafuri				x			x
240	Windhoek				x		x	
241	Swakopmond	x		x		x		
242	Mahalapye							x
243	Tulear				x			x
244	Pietersburg							x
248	Zeerust							x
250	Tsabong				x		x	
254	Keetmanshoop		x	x			x	
255	Ludritz Bay	x		x		x		
256	Upington		x	x			x	
257	Alexander Bay	x		x		x		
258	Kimberly							x
261	Okiep		x	x			x	
264	Grootfontein				x			x
266	Beaufort West		x	x			x	
268	Oudtshoorn		x	x			x	

Abbreviations

D. St.= Dry steppe, S. Arid= Semi-arid and H. Arid= Hyper-arid

C climates: One or more months with mean temperature less than 18° C

a = hot summer, mean of hottest month > 22° C

b = warm summer, mean of hottest month below 22° C

w = winter dry, rainfall in winter season's driest month < 0.1 of the wettest summer month

s = summer dry, rainfall in summer's driest month < 1/3 of the wettest winter month

f = uniform rain, neither w nor s.

The climatic regions of Africa, as obtained from Köppen's classification system, are shown in the map in Figure 2.15 (cited in Griffith's, 1972). The boundaries between the different climatic classes in this map, except for the area below 10° S, resemble closely the contour lines of dryness ratio of Budyko shown in the map in Figure 2.14. The classification approach or system of Thornthwaite, as mentioned earlier, is based on the Temperature Efficiency, *TE*, and Precipitation Effectiveness Index, *PEI*. These are expressed as:

$$TE = \Sigma^{12}(5t/36) \tag{2.18}$$

and *PEI* as expressed earlier by Eq. (2.16). Thornthwaite's original classification is based on the following guideline

TE	Class name	*PEI*	Class name
>127	Tropical	>127	Wet
64-127	Mesothermal	64-127	Humid
32-63	Microthermal	32-63	Sub-humid
16-31	Taiga	16-31	Semi-arid
1-15	Tundra	<16	Arid
0	Frost		

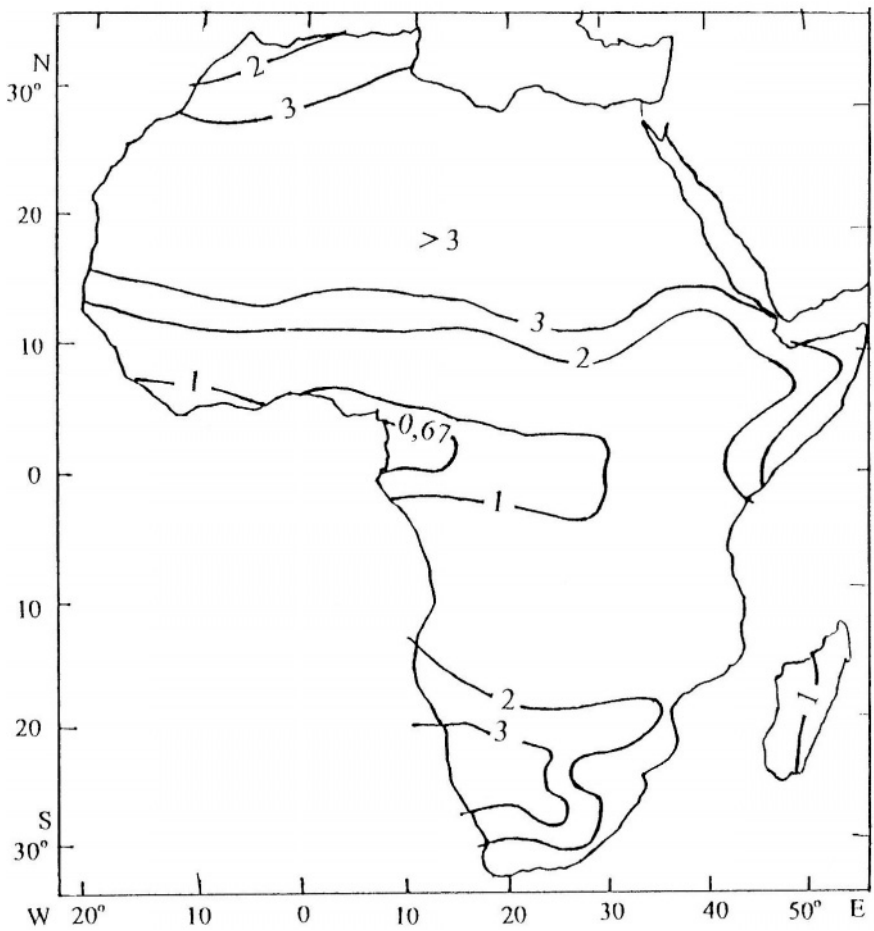

Figure 2.14- Contour lines of equal dryness ratio in Africa (Budyko, 1956)

Table2.5- Distribution of mean annual Thornthwaite's aridity index over Africa

Latitude	Index and class of aridity fot the given longitudes						
N/S	W_2	W_1	E_1	E_2	E_3	E_4	E_5
N_4		0.21/SA	0.12/Ar	0.19/Ar	0.05/HA	0.04/HA	
N_3	0.04/HA	0.02/HA	0.02/HA	0.01/HA	<0.01/HA	<0.01/HA	
N_2	0.50/SA	0.30/SA	0.20/SA	0.20/SA	0.16/Ar	0.21/SA	< 0.20/Ar
N_1	2.50/Hu	1.40/Hu	1.10/Hu	1.40/Hu	1.00/Hu	0.62/SH	0.24/SA
S_1				1.10/Hu	>1.00/Hu	0.67/HU	0.53/SH
S_2				0.48/SA	0.59/SH	0.71/Hu	1.40/Hu
S_3				0.10/Ar	0.26/SA	0.56/SH	0.77/Hu
S_4				0.33/SA	0.34/SA		

Definition of the notations used in the table

N_4 = 40-30° N, N_3 = 30-20° N, N_2 = 20-10° N, N_1 = 10-0° N,

S_1 = 0-10° S, S_2 = 10-20° S, S_3 = 20-30° S, and S_4 = 30-40° S.

HA = hyper-arid, Ar = arid, SA = semi-arid, SH = semi-humid, and Hu = humid

Example: The monthly mean temperatures at Mogadiscio, Somalia (Station 152), as given in Table 3 of Appendix A are 26.5, 26.8, 28.0, 28.4, 27.5, 26.5, 25.8, 25.5, 26.1, 26.8, 26.6 and 26.7oC for the months January, February, ..., December, respectively. The monthly precipitation for the 12 months in the same sequence are 0.1, 0.0, 0.9, 5.8, 5.6, 8.2, 5.8, 4.0, 2.3, 2.7, 3.6 and 0.9 cm. Substitution of these data in Eqs. (2.18) and (2.16) yields values 44.6 for *TE* and 37.12 for *PEI.* According to the aforementioned guidelines, the climate of Mogadiscio can be described as microthermal sub-humid. The classifications of Köppen and Thornthwaite using mean annual figures of precipitation, temperature and potential evapotranspiration define the climate of Mogadiscio as semi-arid. The De Martonne approach, however, moves the climate slightly outside the class of semi-arid to bring it into semi-humid. As such, it can be fairly concluded that Mogadiscio falls on the boundary between the semi-arid and semi-humid climates.

Trewartha (1963) devised a simplified classification system based on the original system developed by Köppen. The simplified version consists of four classes: A for tropical humid climates, B for dry climates, C for humid mesothermal climates and H for Highland climates. Class A is subdivided into equatorial or rainforest climate and tropical wet and dry savanna climate. These two subdivisions correspond to Af and Aw in Köppen's classification, respectively. The tropical rainforest is characterized by almost constant temperature, humidity and rainfall (P >2,000 mm). These characteristics provide an excellent opportunity for plants to grow throughout the year. The tropical wet and dry is characterized by significant variations in precipitation within the year and between years. The savanna region stretches from the edges of the equatorial rainforest to the margins of semi-arid regions. As such, the range of annual precipitation in this region can be from 2,000 to 400 mm.

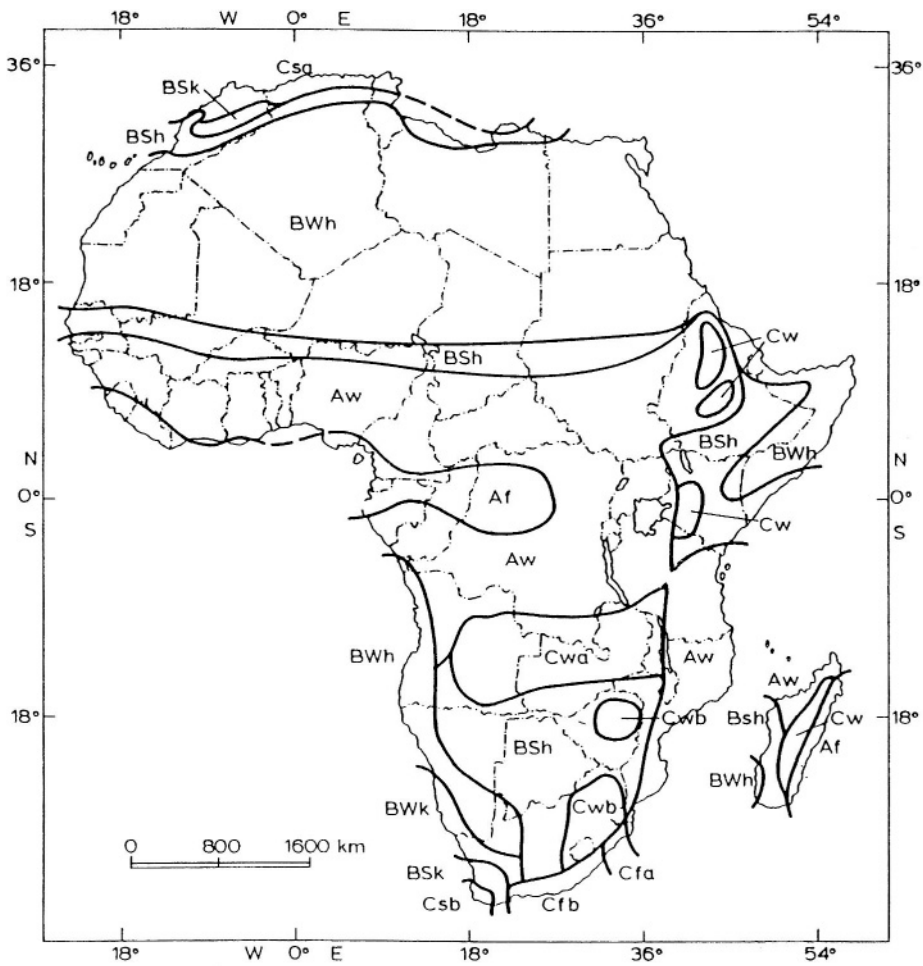

Figure 2.15- Climatic classification of Africa according to Köppen's system

Class B comprises the semi-arid (tropical steppe) and arid or desert climates, i.e. the BSh and BW in Köppen's classification system. Again, the trouble here is the difficulty in drawing a sharp line of demarcation between the semi-arid and the desert zones. It is customary, however, to use the 400-mm isohyet as the dividing line between the steppe and savanna, and the 200 or 250-mm isohyet as the dividing line between the steppe and the desert. Long hours of bright sunshine and wide diurnal as well as seasonal ranges of temperature characterize this class of climate.

Class C includes three subdivisions: humid subtropical climate, middle latitude steppe and Mediterranean climates. These compare to Köppen's Ca, BSk and Cs climate subdivisions, respectively. The humid subtropical climate applies to the Natal province and the neighbouring southeastern coastal plains at about latitude 30°S. The climate of middle latitude steppe applies to the wetter parts of the South African High Veld (field). Low temperature, especially in the winter season where snowfall might

occur, is the main characteristic of this zone. The Mediterranean climate is prevailing in the extreme northwest and extreme southeast of the continent. These areas are typified by their mountain ranges, coastal strips and deep valleys, all of which cause significant local variations in rainfall, humidity, sunshine and rainfall.

The last class, H, is concerned with the undifferentiated highlands of Africa. The high elevation of the ground helps to modify the temperature of a large surface around the Equator in East Africa. This is especially true for Kenya and Uganda. The situation of Ethiopia is not exactly the same. It is somewhat complicated due to the special topography and relief of the ground surface. The same applies to the volcanic parts of East Africa.

The map in Figure 2.16 shows clearly the boundaries between the different classes of climate in Africa as developed by Trewartha (1962).

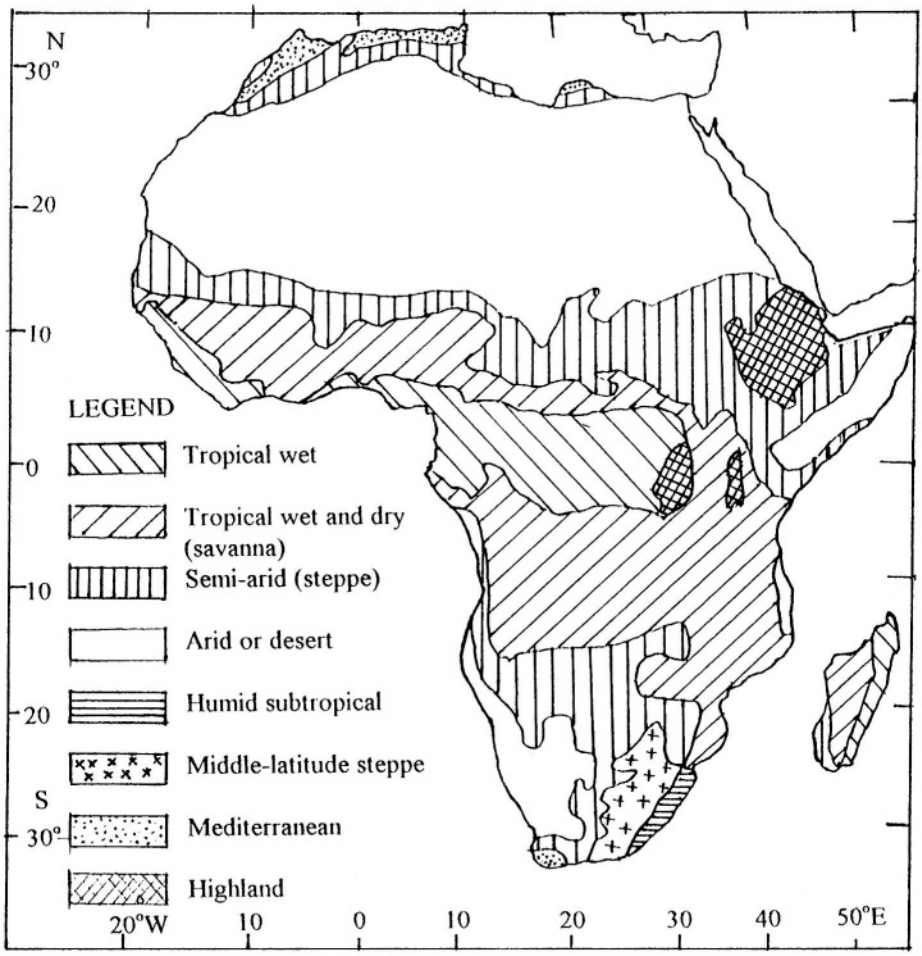

Figure 2.16- The climates of Africa as suggested by Trewartha (1962)

CHAPTER 3

ANALYSIS OF RAINFALL DATA

3.1- Annual Rainfall

3.1.1 Rainfall fluctuation in the last twenty millennia- The history of the earth's climate and periods of high humidity and aridity have been revealed and dated. Evidence was gathered from archeological remnants at prehistoric sites, palynological analysis of lake deposits and levels, deep-water ocean cores and dating of geological events using radioactive isotope techniques

Palynological and geochemical investigations have provided most of the relevant information regarding the fluctuation of precipitation in Africa (mainly the Sahara, the Sudano-Sahelian region and surrounding areas). Palynological analysis of deep-water ocean cores taken from the Atlantic near the west coast, deposits and levels of Lake Chad, and evidence gathered from prehistoric sites along the White Nile above Khartoum are just a few examples worth mentioning. The results of the various investigations lead us to believe that the African Sahara and the surroundings were relatively humid during the Middle Würm (40,000-20,000 years BP) The maximum humidity occurred in the period 40,000-35,000 years before present (BP). As a consequence of the global cooling, the climatic zones moved southward (20,000-12,000 years BP). The extreme cooling, between 20,000 and 18,000 years ago caused a high level of aridity. The greatest changes in precipitation occurred in the Sahara and surroundings in the Lower Holocene (11,000-6,000 years BP). The "climatic optimum" of the Holocene, some 6, 000 years ago, produced a considerable state of humidity in the Sahara region and surroundings. In general, the highest levels of Lake Chad correspond to global warming, while a drop in global temperature results in less precipitation and a lower lake level. During the sufficiently wet period (Neolithic I), some 7,000-5,300 years BP, the level of the oceans rose by 2 to 3 m. This wet episode was followed by a period of cold and dry climate (Neoglacial I) from 5,300 to 4,000 years ago. In that period the level of many African lakes and the Nile River dropped sharply. The next dry and cool episodes occurred in the periods. 3,600-3,400 (Neoglacial II), 3,100-2,400 (Neoglacial III) and 2,100-1,800 (Neoglacial IV), all in years BP. More information about these sequences of wet and dry periods have been presented and discussed by Borzenkova (1980).

Figure 3.1 illustrates the strength of precipitation over Central Africa in the period from 1750-1940 as suggested by Tilho and cited in Roche et al. (1976).

Again, palynological and geochemical investigations have shown that Lake Victoria before 14,500 years ago did not have an outlet. The climate of the Equatorial Lakes' region remained dry. About 12,000 BP Lake Victoria overflowed and the White Nile was high. Between 12,000 and 8,000 BP, especially during the last 2,000 years of that period, the flows of the White Nile were extremely high. After 8,000 BP the level of the White Nile fell sharply and climatic desiccation accelerated the trend towards a semi-desert condition. From ancient records and other evidence, Butzer (1966) concluded that a fluctuating wet period lasted from 5,000 to 2,700 BC, with submaxima centered on 4,500, 3,700 and 3,000 BC. After 2,700 BC lake levels and flows were considerably reduced until wetter conditions returned around 1,850 BC. This wet episode terminated around 1,200 BC.

Evans (1994) reported that during the atmospheric warming of some 9° C, which took place in the period between 18,000 and 7,000 years BP, there were numerous trends, oscillations, persistences and long and short-term cycles in the climate. All these characteristics are highly significant in relation to long-term changes over many millennia.

3.1.2 Evaluation of the variation of annual rainfall in the 20th century/Drought in Africa- While investigating climate changes, one should distinguish major changes in or out of pluvial episodes lasting thousands of years from minor changes lasting hundreds of years, and from variations that are experienced for some decades. Needless to say each episode has its own biological significance. Since, the shorter period variations are not isolated, but rather superimposed on the longer period fluctuations, deep historical analysis of climate change often leads to detection of major fluctuations at the expense of the minor ones.

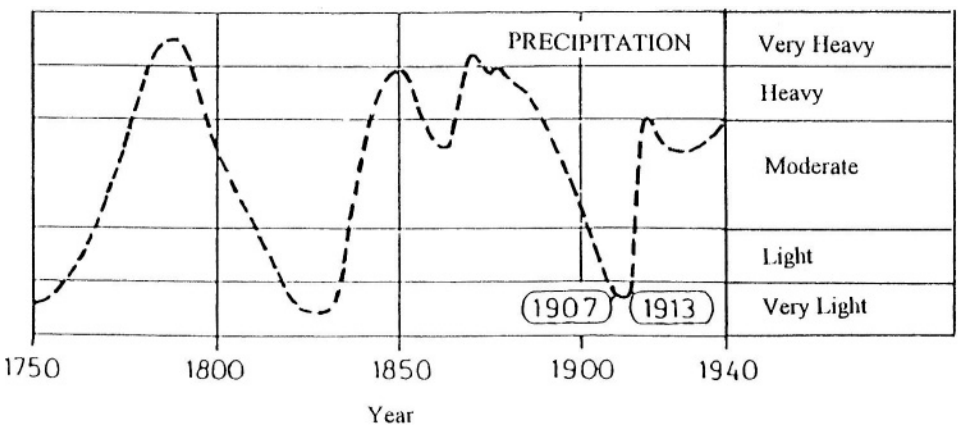

Figure 3.1- Level of precipitation over Central Africa in the period 1750-1940 (cited in Roche et al, 1976)

A variety of case studies dealing with variation of rainfall totals in the period from the last decades of the past century till present are discussed in this subsection. As the rainfall in this period is characterized by decline in the annual total over wide spans of time and in several parts of the continent, the situation is often referred to as "drought".

According to the classification of droughts suggested by Glantz (1987), what is dealt with here is meteorological drought. This can be defined in terms of the degree of dryness (percentage reduction from the long-term average annual rainfall). The definition includes also the duration of dryness in a given region.

Jenkinson (1973) reported on the variations in May to September (rain season) rainfall in West-African marginal rainfall areas. The area considered extends from 12 to 14° N and from 6° W to 15° E, and the stations investigated were eight, located in Chad, Mali, Niger and Nigeria. The conclusions drawn from that investigation emphasized the notable fluctuation in seasonal rainfall, with well marked maxima centered about 1920, 1931 and 1959, and well marked minima centered about 1913, 1942 and 1971, with shorter periods of marked deficit 1925-26 and 1947-49. The longer periods of marked deficit have occurred at roughly thirty-year intervals.

Bunting et al. (1976) presented an analysis of long-term rainfall records in West Africa. Two rainfall series were used; one based on 5 stations, in Niger and Nigeria, from 1905 to 1974 and the second on 50 stations, in Sénégal, Mali, Burkina Faso, Niger, Nigeria and Chad, from 1953 to 1972. It is noteworthy that some of the stations used in this investigation are the same stations used earlier by Jenkinson (1973). The conclusion was that the succession of drought years experienced in the Sahel between 1968 and 1974 could not be distinguished statistically from a random series and did not indicate a changing climate

Roche et al. (1976) commented on the hydrological aspects of the 1968 drought in West Africa saying: "The drought became perceptible in certain regions in 1965 and the effects have been noticeable in Mauritania, Sénégal and the regions north of Mali and Niger since 1968. In 1970 the drought became more extreme and extended to Burkina Faso and Chad, and at many rainfall stations absolute extreme low precipitation amounts were recorded. In many parts of the Sahel the driest year was 1972 when the frequency of rainfall was close to the 100-yr low, but in the southern humid tropical regions there was more rainfall than normal. Although there has been near normal rainfall since 1974, the effects of the drought have hardly begun to disappear". It is interesting to know that the deficit in a certain area has been coupled with surplus in another area.

As rainfall in West Africa remained low and drought continued for some years after 1974, Dennett et al. (1985) updated the rainfall data used by Jenkinson (1973) and Bunting et al. (1976), and reanalyzed the updated series

to assess whether the original conclusions remained valid. The series used was the average of the percentage deviations from the 1931-1960 mean at each station. The rainfall recovered somewhat in the late 1970s after the severe drought of 1971-1973 but rainfall remained below the 1931-1960 average. The annual series for the 5 stations was examined for trends and periodicities. There were no spikes in the power spectrum, and the expected and observed number of runs of years above or below the median did not differ significantly. However, rank correlation showed a weak, though statistically significant, downward trend. A significant feature is an 11-yr run (1968-1978) of years below the median. Rainfall in 1979 was just 3% above the median; otherwise all the years between 1968 and 1983 have been below. The results obtained from that study are shown in Figures 3.2$_a$ and 3.2$_b$. In the former, the ordinate R_5 represents the percentage deviations of the average of the 5 stations from the 1931-1960 mean. In Figure 3.2$_b$, R_{50} represents the June-September rainfall averaged over the 50 stations expressed as deviations from the 1931-1960 mean. The relationship between the two series was given by the expression:

$$R_5 = 0.94R_{50} + 0.7 \tag{3.1}$$

with a coefficient $r^2 = 0.72$

As already mentioned before, the steady decrease of rainfall, which began in the 1950s in the West-African Sahel and reached it's culmination point around 1968, did not terminate in the mid 1970s as was then thought. Instead, it continued to the 1980s, a situation that urged many researchers, notably Nicholson (1983, 1985), to investigate the sub-Saharan rainfall in the periods 1976-1980 and 1981-1984.Investigation of the rainfall during the period 1976-80 confirmed the fact of continued drought. It also showed that there is a generally consistent relationship between the Sahel and the Kalahari regions of Africa. This consistency can be seen from the series of annual rainfall departures for the period 1901-1975 in the Sahel, and northern and southern Kalahari regions (see Figure 3.3).

For the purpose of another investigation, Nicholson (1985) used the standardized rainfall departure from the mean, which can be expressed as:

$$X_{ij} = (P_{ij} - P_{mi})/\sigma_i \tag{3.2}$$

where, P_{ij} is the annual total for the station i in the year j, P_{mi} is the annual mean at station i and σ_I is the standard deviation of the annual totals for the station i.

Nicholson subdivided the sub-Saharan region into three zones according to the long-term mean annual rainfall: Sahelo-Sahara, 50-100 mm; Sahel, 100-400 mm and Sudan, 400-1,200 mm. The inadequacy of data above the 1,200 mm level made it difficult to extend the investigation to the Guinean zone. For each zone the areally integrated rainfall R_j for the year j is represented by:

$$R_j = (N_j)^{-1} \Sigma^i X_{ij} \tag{3.3}$$

where, N_j is the number of stations available for the year j and X_{ij} as given by Eq (3.2) The results obtained for the three investigated zones are shown in Figure 3.4, where 100 R_j is plotted versus time in years from 1900 to 1984.

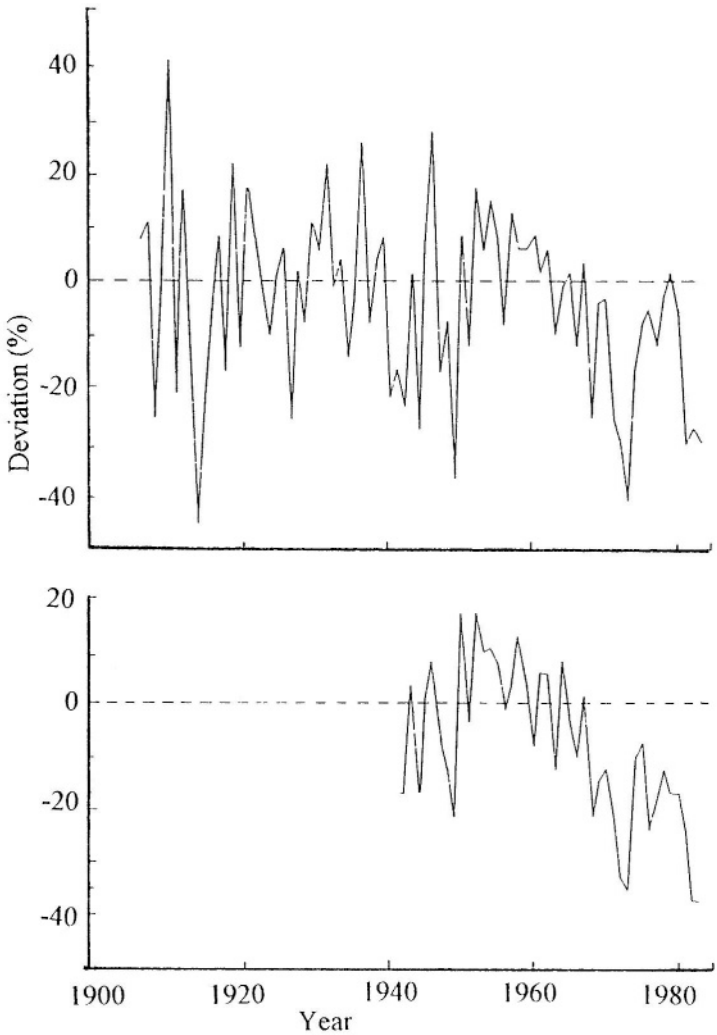

Figure 3.2- (a) Annual rainfall averaged over 5 stations between 12°N and 14°N expressed as a percentage deviation from the 1931-1960 mean; (b) June to September rainfall averaged over 50 stations between 10°N and 20°N expressed as a percentage deviation from the 1931-1960 mean

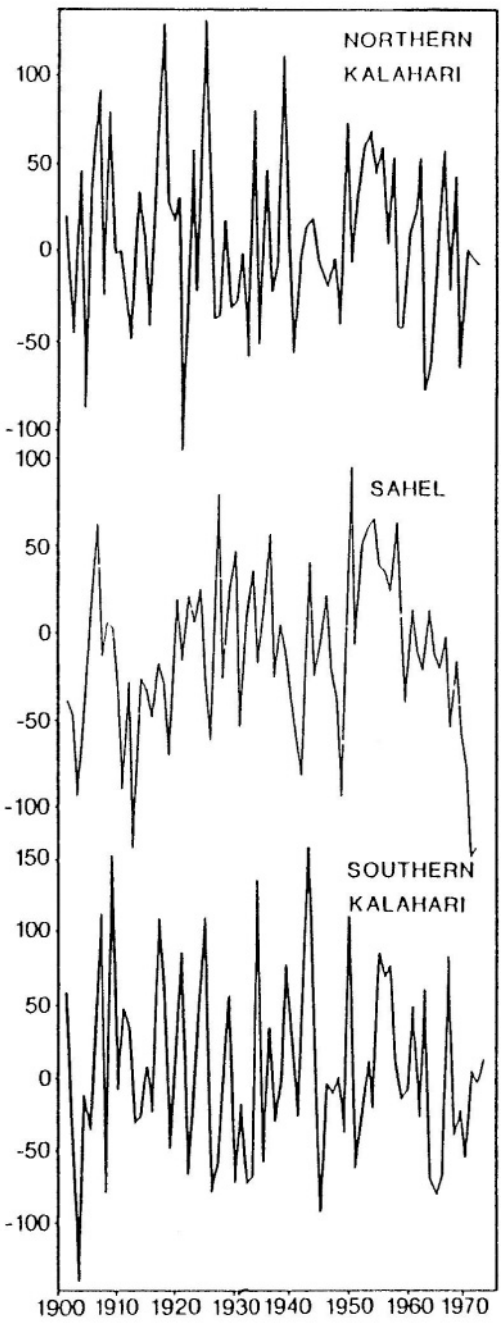

Figure 3.3- Rainfall percentage standard departures, 1901-1975, for the Sahel, and the northern and southern Kalahari (taken from Nicholson, 1983)

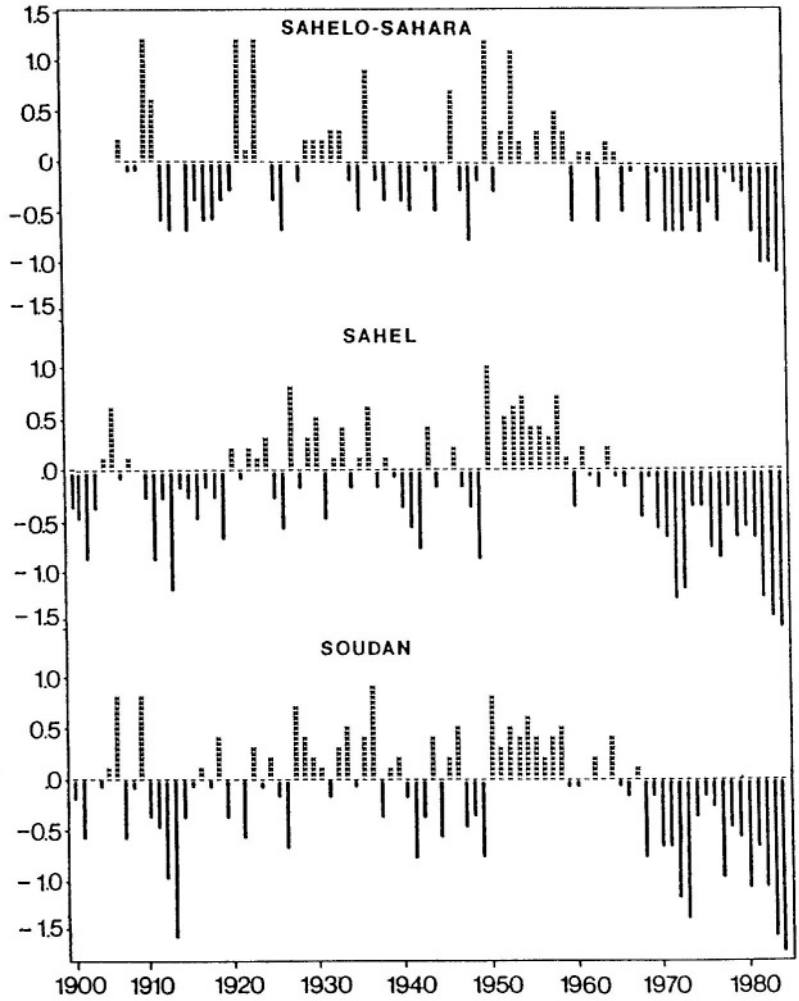

Figure 3.4- Standardized annual rainfall departures for three sub-Saharan zones, 1901-84

Figures 3.5_A and 3.5_B show the secular pattern of precipitation anomalies in the period 1891-1976 for two climatic zones of Africa (Borzenkova, 1980): (a)- the Mediterranean Coast and (b)- the Sudano-Sahelian zone. Line 1 refers to the unsmoothed values of the anomalies and line 2 gives the 5-yr moving averages. The graphs show that a positive rainfall anomaly in one of the zones is usually accompanied by a reduction in precipitation in the other zone and vice versa. This confirms the finding of Roche et al. (1976) that a reduction in the rainfall in the Sahel was counteracted by an increase in the rainfall in the equatorial belt. Whereas there was sufficient rainfall in the Sudano-Sahel zone in the

1930s and 1950s, the territory of North Africa bordering the Mediterranean Sea had a marked rainfall deficit at that time. Equally important is that periods with adequate precipitation in the Sudano-Sahel zone (1930s-1950s) correspond to periods with the highest air temperatures in the entire northern hemisphere and vice versa. The sharp decrease in precipitation (1960s-1970s) corresponded to a decrease in the air temperature in the northern hemisphere in the same period (1960s-1970s).

De Marée & Nicolis (1990) applied certain statistical techniques for analyzing and interpreting the Sahelian drought. They used the annual precipitation time series, 1904-1987, of the Kaédi meteorological station in Mauritania on the Sénégal River (Figure 3.6). The Mann-Kendall-Sneyers test showed a highly significant downward trend. A change point test was then applied to locate the time of transition. An abrupt transition in the series was located around 1967.

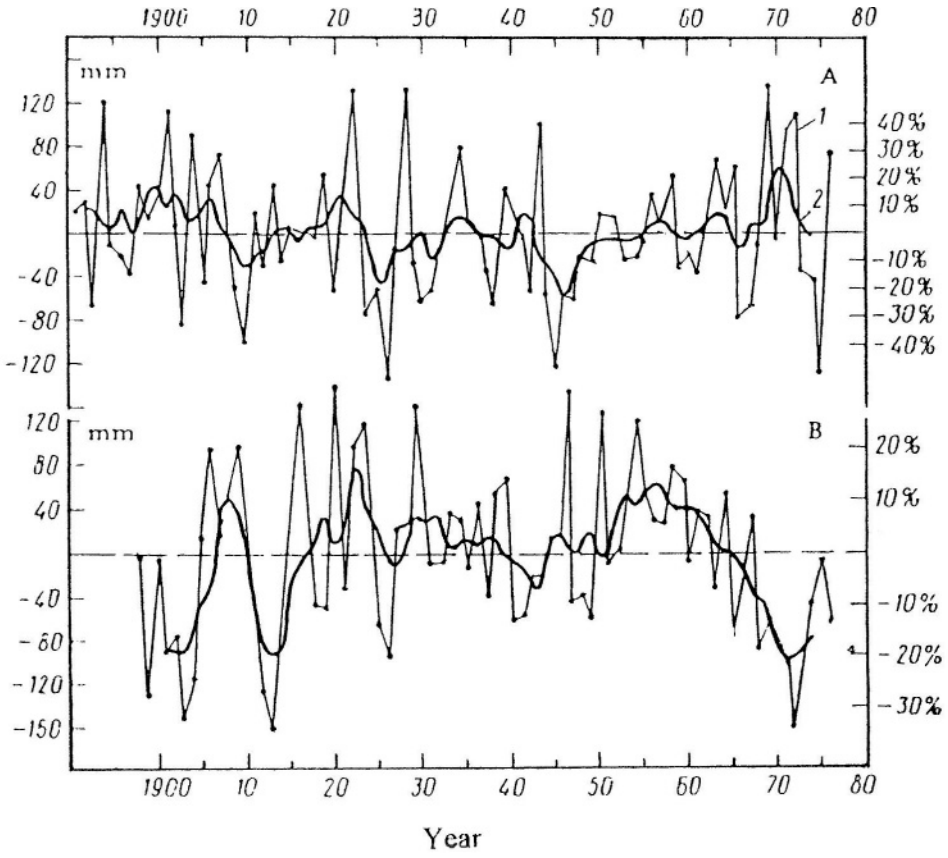

Figure 3.5- Secular pattern of mean annual precipitation anomalies in two climatic zones of Africa in the northern hemisphere.

Snijders (1986) reported evidence of nonstationarity of an areal index of the wet season precipitation over the period 1953-1983 in Burkina Faso. Similarly, Hubert & Carbonel (1987), upon studying long-term precipitation series (37 to 97 years long) from 42 stations spread from the Senegal to Niger, pointed out the non-stationarity of those series and suggested a climatic jump around 1969-1970.

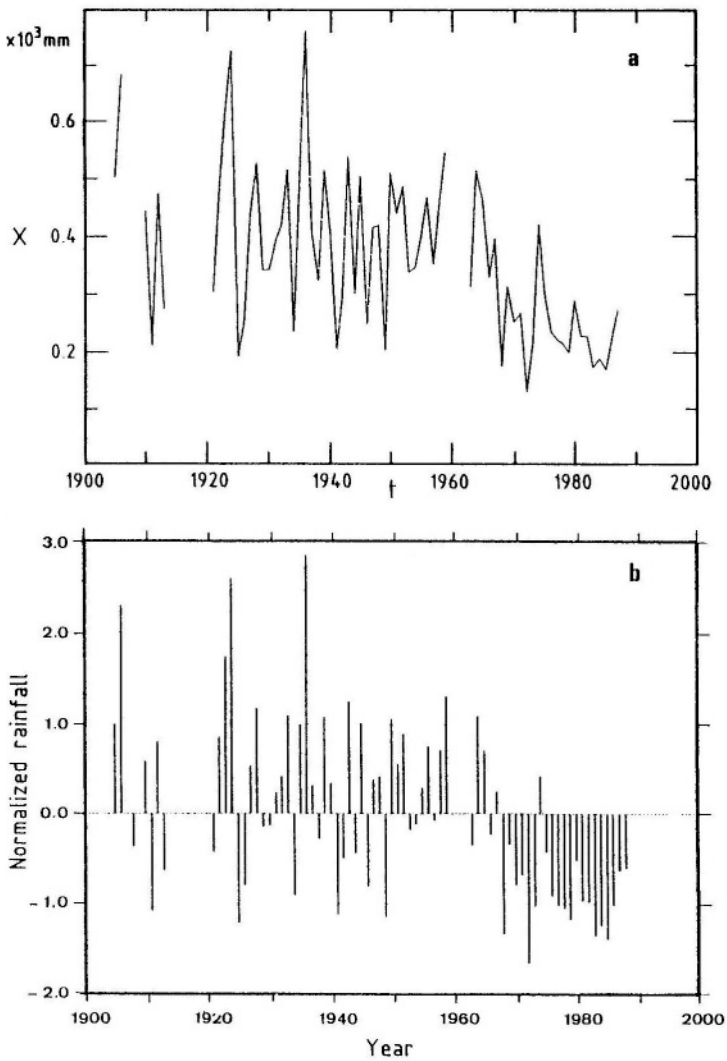

Figure 3.6- (a)- Annual rainfall at Kaédi, Mauritania, 1904-1987. (b)- Normalized departures in standard deviations (De Marée & Nicolis, 1990)

At this point it is clearly evident that African drought, seen as a major climatic event, is characterized by (a)- strong persistence, about two decades; (b)- spatial range extending over the entire sub-Saharan region; (c)- nearly synchronous occurrence of similar events in the subtropics of southern Africa; and (d)- associated with the record used, there is an additional induced transition between two stable regimes of humid and dry states.

The continuation of the drought in the 1980s and its expansion to more areas have attracted widespread interest among several research agencies and individuals. The variations of precipitation and runoff in West and Central Africa in the period 1951-1989, as an example, have been analyzed and discussed by Mahé & Olivry (1995). The precipitation data used in that investigation belonged to about 900 stations distributed between Sénégal-Fouta, Guinea, Sierra Léone, Liberia, Ivory Coast, Ghana, Burkina Faso, Mali, Niger, Nigeria, Chad, Central African Republic, Togo, Benin, Cameroon, Congo (Brazzaville), Congo Kinshasa and Angola. The so-called Regional Vector Method (RVM) developed by ORSTOM was applied to supplement missing annual precipitation for some years or at certain locations. The annual precipitation series for Central and West Africa are shown in Figures 3.7$_a$ and 3.7$_b$, respectively. In the period from 1951 to 1989, the years of considerable deficit over West and Central Africa not just the Sahel region alone were 1958, 72, 73, 77, 82, 83, 84, 86 and 1987.

To specify the characteristics of the rainfall variability in non-Sahelian West Africa, time series of the annual rainfall, duration of rainy season, rainfall in dry seasons and number of rainy days have been generated with a one year-time step from 1950 to 1989. Using a special computer program, statistical methods have been applied to test the presence of a shift in the mean. To characterize the change in space and in time, the results of the tests have been synthesized using multiple correspondence analyses. This study has led to the conclusion that the rainfall regime began to change around 1966 in Sénégal and Guinea Bissau, then Guinea, Mali, Burkina Faso and the northern part of Bénin. The Ivory Coast, Togo and the south of Bénin have been affected to various degrees. The rainfall variability in the Cameroon and the Central African Republic has not been uniform or has been slight (Gautier et al., 1998)).

Quaye (1993) applied two methods of drought analysis to the rainfall data in the West African region comprising Mauritania, Sénégal, Mali, Niger, Burkina Faso and Ghana. The investigated rainfall data covered the period 1921-1980, although for Ghana the data extended to 1990. It is very unfortunate that the many missing rainfall data for Chad caused by the long civil war in that country made it rather senseless to have Chad included in this investigation.

Standard statistical tests were first applied to the annual rainfall series and the revised results are given in Table 3.1. Drought analysis was then carried out using the so-called Herbst technique. This technique consists of a set of procedures for testing the onset of drought, termination of drought, duration of

drought, drought intensity and drought index. The details of these procedures are described in Herbst et al. (1966). The same data were analyzed a second time using the method of runs, which has been described by Yevjevich (1967). The main drought characteristics as obtained from the Herbst technique and the method of runs are summarized in Tables 3.2 and 3.3, respectively. The parameters describing the drought characteristics listed in these tables are presented graphically in Figure 3.8. The principal conclusions that can be fairly drawn from Tables 3.2 and 3.3 are as follows:

i- all investigated countries, including Ghana (mostly tropical), have been stricken by drought, though to a varying extent

ii- the Herbst method gives total drought duration of 17 to 43 years out of 60 years. The corresponding range as given by the run method is 26-34 years.

iii- the longest duration of a single dry spell varied from 2 to 12 years and 4 to 14 years as obtained from the Herbst and the run methods respectively.

iv- based on drought occurrences of 1913-1914 (literature), the 1940s and the late 1960s (investigation), it can be suggested that the Sahel region is likely to be hit by an intense drought with a recurrence interval of about 30 years.

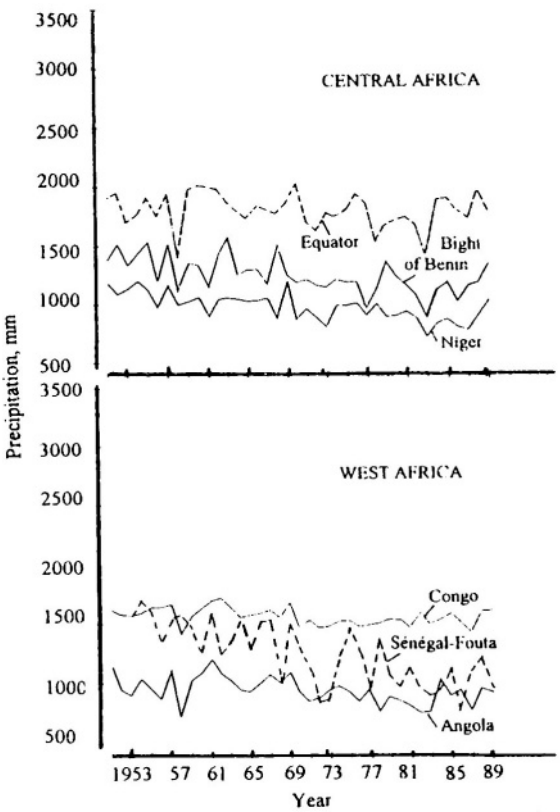

Figure 3.7- Mean regional annual rainfall, 1951-1989 (Mahé & Olivry, 1995)

Table 3.1- Basic statistical descriptors and results of indepence test of the annual rainfall series used by Quaye (1993)

Station No.	Mean, mm	Cv %	r_1	r_2	r_3	r_4	r_5	I / D	T / NT
37	18	84	0,150	0,050	0,163	0,089	-0,283	I	NT
38	150	51	0,219	0,043	0,171	-0,112	-0,092	I	NT
41	173	48	0,016	-0,037	0,225	0,049	0,041	I	NT
42	152	37	0,230	0,236	0,292	0,195	0,258	I	NT
45	333	38	0,120	0,088	0,212	-0,910	0,026	I	NT
46	278	29	0,242	0,250	0,318	0,194	0,032	D	T
48	477	35	0,369	0,387	0,302	0,231	0,157	D	T
52	631	42	0,734	0,548	0,375	0,240	0,051	D	T
54	397	24	0,158	0,066	0,208	0,232	-0,086	I	NT
55	639	29	0,143	0,178	0,167	0,097	0,070	I	NT
56	627	33	0,170	0,113	0,143	0,167	0,239	I	NT
58	216	46	0,056	0,195	0,196	0,015	0,106	I	NT
59	481	22	-0,015	0,363	0,228	0,229	0,106	D	NT
60	765	30	0,270	0,364	0,359	0,066	0,251	D	T
61	519	24	0,191	0,279	0,195	0,085	0,084	D	NT
64	501	24	0,141	0,150	0,142	0,229	-0,033	I	NT
65	884	20	0,242	0,225	0,191	0,044	0,079	D	NT
67	690	20	0,288	0,078	0,147	0,149	0,037	D	T
68	874	17	0,385	0,410	0,372	0,301	0,441	D	T
69	590	21	-0,012	0,106	-0,015	-0,230	0,037	I	NT
72	747	16	-0,084	-0,158	0,254	0,153	-0,001	I	NT
77	1488	22	0,089	0,175	0,256	0,198	0,248	I	NT
78	975	18	0,121	0,063	0,202	-0,007	0,100	I	NT
82	970	22	0,087	0,131	0,048	-0,046	0,094	I	NT
86	1251	20	0,271	0,321	0,081	0,219	0,093	D	T
87	1310	17	0,396	0,396	0,286	0,335	0,270	D	T
88	1129	18	0,108	0,210	0,308	-0,037	-0,034	I	NT
97	1180	21	0,281	0,175	0,215	0,270	0,203	D	T
UCL			0,236	0,238	0,240	0,242	0,244		
LCL			-0,270	-0,272	-0,275	-0,277	-0,280		

Cv = coefficient of variation, r = serial correlation, suffix 1, 2,.. refers to the lag number in years, I = independent series, D = dependent series, T = trend NT = no trend, UCL = upper confidence limit and LCL = lower confidence limit at 2.5% and 97.5% levels.

Tabulated results are revised version of those obtained by Quaye (1993)..

All aforementioned case studies have been limited to West and Central Africa. To extend the area covered by the analysis to Eastern and Southern Africa, the author considered 21 stations representing different regions of the continent. The basic statistics of these series are listed in Table 3.4.

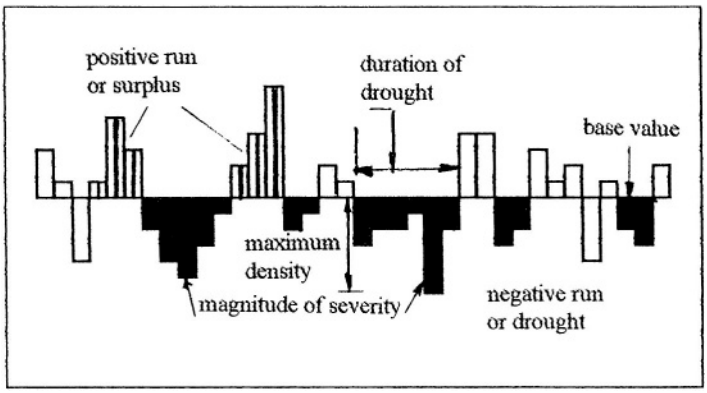

Figure 3.8- Definition sketch of the parameters characterizing a drought

Table 3.2- Drought characteristics as obtained from Herbst technique (Quaye, 1993)

Country	No. of stations	Range of number of spells	Total duration, months	Longest spell, months	Maximum drought density
Niger	6	(9-15)	293-407	60-141	1.00-3.75
Bur. Faso	6	(11-79)	324-520	30-92	0.98-2.45
Bur. Faso*	7	(6-10)	199-273	54-150	1.04-2.26
Mali	6	(11-65)	350-535	40-139	0.98-2.58
Senegal	4	(10-13)	310-390	67-132	1.28-2.98
Mauritania	4	(12-16)	371-417	63-121	1.37-1.56
Ghana**	17	(7-18)	199-274	23-108	1.26-2.41

*Record: * 1921-1990, ** 1951-1990 and the rest 1921-1980.*

Table 3.3- Drought characteristics as obtained from the method of runs (Quaye, 1993)

Country	No. of stations	Range of number of spells	Total duration, years	Longest spell, years	Maximum severity in any run	Total Magnitude of severity
Niger	6	10.0-18.0	29-32	(4-13)	4.2-12.0	23.1-24.5
Bur. Faso	6	13.0-17.0	26-34	(4-10)	3.4-9.0	20.4-25.2
Mali	6	7.0-18.0	29-34	(4-14)	4.1-11.8	21.6-25.8
Senegal	6	12.0-17.0	28-33	(4-11)	5.6-13.7	23.2-24.9
Mauritania	4	12.0-16.0	28-31	(5-7)	4.4-5.6	22.8-24.5

"Runs" refer here to negative runs when the rainfall is below the mean.

Table 3.4- Results of statistical tests applied to annual rainfall series at twenty different stations

Station No./Name	Period of record	Parameters a	b	Mean mm y^{-1}	R^2	Z	T / NT
42- Agades	1921-1980	1,136	-0,0044	153	0,0430	1,950	NT*
46- Nema	1921-1980	1,006	-0,0002	278	0,0001	0.277	NT
48- Matam	1921-1980	1,294	-0,0097	485	0,2330	3,725	T
49- Khartoum	1938-1989	1,210	-0,0082	150	0,0640	1,819	NT
52- N. de Sahel	1921-1980	1,308	-0,0105	631	0,2130	3,312	T
53- Praia	1885-1982	1,156	-0,0034	227	0,0240	2,409	T
62- Gedaref	1904-1982	0,923	0,0019	586	0,0530	2,577	T
66- EL-Fasher	1938-1992	1,243	-0,0098	253	0,1300	3,761	T
67- Ouahigouya	1921-1990	1,102	-0,0041	690	0,1480	2,833	T
69- Niamey	1921-1980	1,047	-0,0017	590	0,0170	0,607	NT
70- Banjul	1886-1982	1,154	-0,0031	1146	0,1180	3,185	T
72- San	1921-1980	1,012	-0,0004	747	0,0021	0,124	NT
83- Djibouti	1901-1984	0,893	0,0025	135	0,0080	0,205	NT
108- Ad. Ababa	1900-1990	1,048	-0,0010	1207	0,0250	0,024	NT
117- Atakpame	1928-1990	1,044	-0,0013	1400	0,0110	0,647	NT
121- Kumasi	1921-1990	1,044	-0,0012	1423	0,0200	1,634	NT
N'Djamena	1932-1988	1,164	-0,0055	580	0,1090	2,290	T
El-Obeid	1938-1990	1,249	-0,0093	355	0,1850	3,203	T
St.Louis	1890-1982	1,215	-0,0047	366	0,0680	0,972	NT
Dakar	1898-1982	1,021	-0,0005	540	0,0012	0,021	NT
Ft. Victoria	1901-1980	0,985	0,0003	636	0,0070	0,341	NT

R^2 = Square of the coefficient of correlation, a and b are the constant and slope of the regression line Y = a+bX, z = standard normal deviate, N/NT = trend/no trend

** very close to the critical value the series in question needs to have a trend.*

Stations No. 42, 46, 48, 52, 53, 67, 69,70, 72, N'Djamena, Saint Louis and Dakar are situated in the sub-Saharan/Sahelian region. Stations 49, 62, 66 and El-Obeid are in the Sudan region, 117 and 121 are in a wet region close to the Equator, 83 and 105 are in the Horn of Africa and the Highland of Ethiopia, respectively, and Ft. Victoria is in Zimbabwe. The statistical analysis of the investigated series shows that, for the tabulated periods of record and the assumed significance level (5%), more than half of the sub-Saharan stations suffer from a falling trend (Figure 3.9). In the Sudan three stations out of four have shown trends, falling in two series (Figure 3.10a and 3.10 b), and rising at Gedaref station. The two series of the wet region close to the Equator and those in East Africa and Zimbabwe appear to be trend-free. As such, the number of the trend-free series in Table 3.4 is 12, one of which can be regarded as a critical case, and the remaining 9 series are not trend-free.

One should not forget, however, the difference in data analysis between Table 3.4 and the previously presented case studies. In most of these cases the means of the later half of the series, i.e. from about 1950-1960 onwards have

been tested against the means or medians of the earlier half of the respective series, which are usually significantly larger. In the case presented in Table 3.4, the full series for each station has been examined and a linear regression relation assumed to exist between the annual rainfall and time. The null hypothesis is that the slope of the regression line is not significantly different from zero unless proven otherwise.

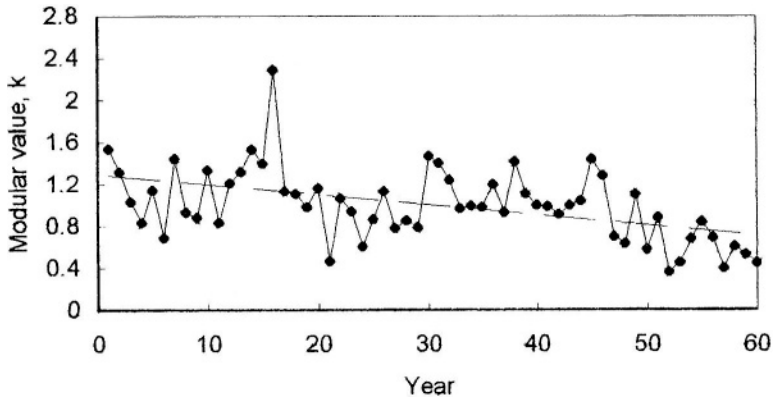

Figure 3.9- The annual rainfall in Matam,, 1921-1980, and the fitted trend line

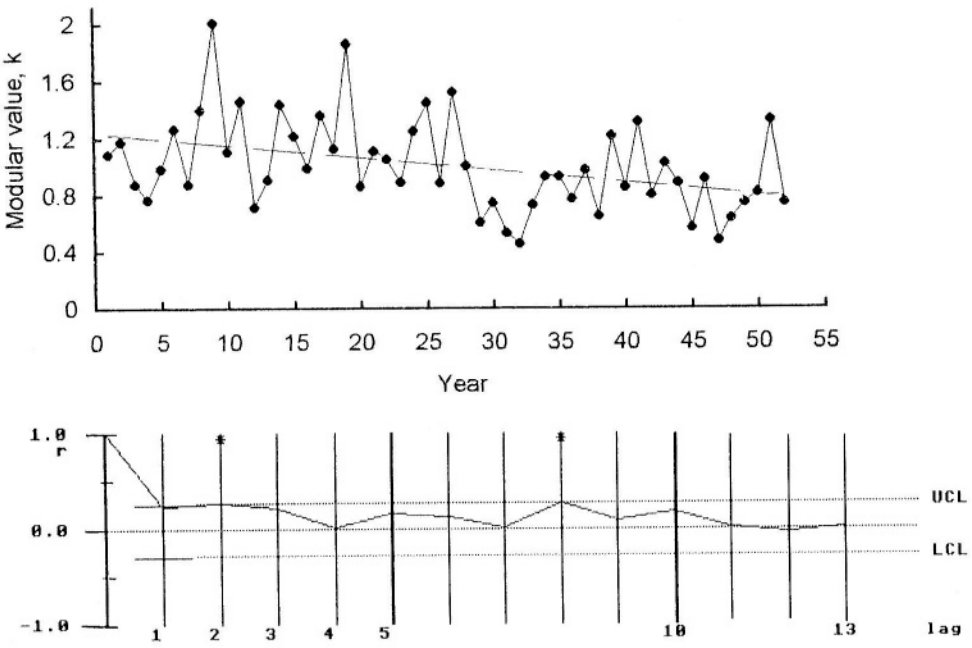

Figure 3.10- The annual rainfall in El-Obeid, 1938-1990, (a)- plots of time series and trend line and (b)- serial correlogram and confidence limits

While commenting on atmospheric pressure variations in the northern hemisphere, Lamb (1973) asserted that the cycles of 2 years, 5.5 years, 9.5 years, 11 years and 20-22 years duration have nothing to do with the African drought that began in the 1960s.

Anyadike (1992) analyzed the variation in rainfall in Nigeria over the period 1916-1987 using 28 stations, 10 stations in each of the northern and southern regions and 8 in the middle belt of the country. In order to reveal the existence of any significant cycles, the seasonal rainfall series were first detrended, then subjected to power spectrum analysis. The spectral peaks indicate the presence of some cycles in all series, with the major ones being of 2.53 to 2.67 years and 3.69 to 4.36 years (for the middle belt only) and 8.00 to 9.60 years for all the regions. The detection of the 2.53 and 2.67 years cycles in the middle belt suggest that a significant quasi-biennial oscillation (QBO) is present in the middle belt of Nigeria.

3.1.3 Teleconnection of annual rainfall in Africa- Large-scale teleconnection designates the relationship between temporal fluctuations of meteorological parameters at widely distant locations. Nicholson (1986), using a regionally averaged data set comprising the records of 1087 stations, examined the spatial patterns of rainfall variability over the African Continent. Large-scale teleconnections have been indicated by both the extreme spatial coherence of rainfall anomalies in the low latitudes and the interrelationship between tropical and extratropical regions.

For northern Africa, most of the years in the investigated period 1901-73 fell into one of six types; two showing the same sign over the whole region and four showing strong opposite signs between the equatorial and subtropical latitudes. For the continent as a whole, Nicholson (1986) developed six types for the anomaly pattern. These types reflect the patterns derived using northern Africa alone, with conditions in the southern subtropics resembling those in subtropical latitudes north of the Equator. The map in Figure 3.11 represents Type 2, which illustrates nearly continental drought. The graphic plots of the rainfall time series shown in Figure 3.3 (Nicholson, 1983) show the generally consistent resemblance of the annual rainfall departures, 1901-1975, between the Sahel and the Kalahari.

On the other hand the values of annual maximum rainfall, P_{mx}, and the annual minimum, P_{mn}, in Tables 11_b and 11_c of Appendix A respectively have been used to calculate the corresponding, k_{mx} and k_{mn} values, where:

$$k_{mx} = P_{mx} / P_m \tag{3.4}$$

$$k_{mn} = P_{mn} / P_m \tag{3.5}$$

respectively, and P_m is the mean rainfall listed in Table 10_a of Appendix A.

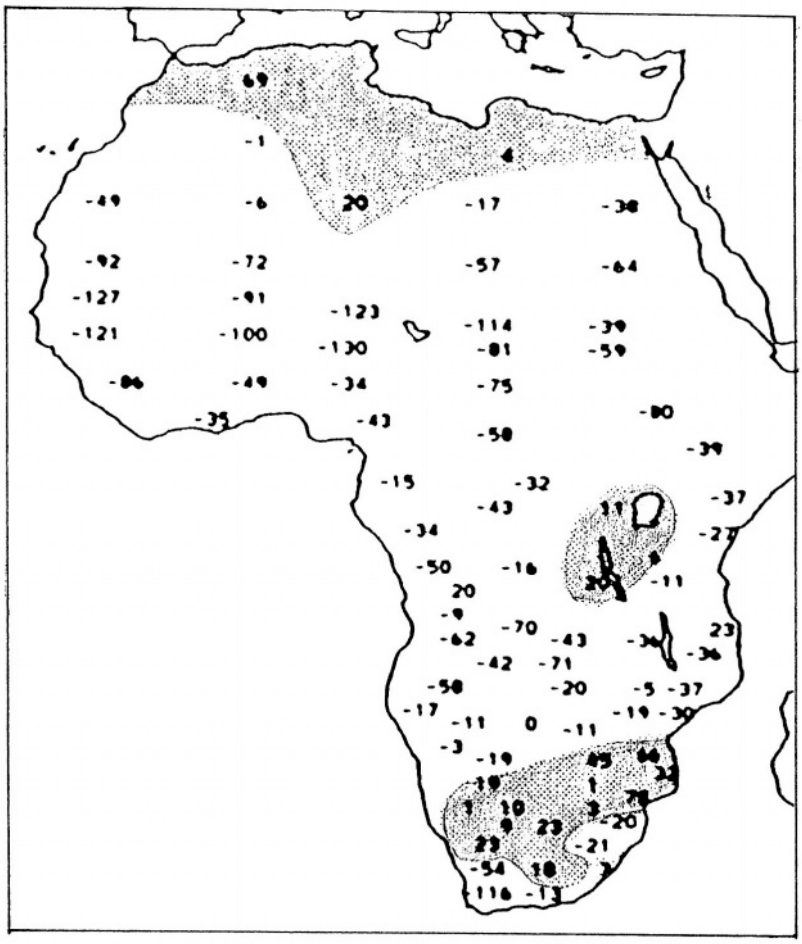

Figure 3.11- Continental anomaly type 2 (based on 75 regions) as developed by Nicholson (1986); shading indicates positive departures

The stations with $k_{mx} \leq 1.5$ represent 38.7% of all investigated stations, $\leq$ 2.0 are 78.5% and ≤ 3.0 comprise 96.3%. The ratio of stations in proportion of the total number of stations used with $0.75 \leq k_{mn} < 1.0$ is 12.5%, $0.50 \leq 1.0$ 65.9% and $0.25 \leq 1.0$ is $\approx$ 83%. More details about the joint frequencies of the percentage ratios of k_{mx} and k_{mn} are shown in Table 3.5. The joint frequencies show that the conditional probability $[1.0 \leq k_{mx} < 2.00 | 0.5 < k_{mn} \leq 1.0] = 51.8\%$. As such, it can be fairly concluded that a large number of the investigated stations have a fairly uniform range of variation, no matter their location. This does not, however, eliminate the fact that locations with limited annual rainfall are more susceptible to larger departure from the long-term mean compared to those locations with heavier rainfall.

Table 3.5- Joint frequencies of occurrence of certain ranges of k_{mn} given specified ranges of k_{mx}

k_{mn}	k_{mx}						
	1.00-1.25	1.25-1.50	1.50-1.75	1.75-2.00	2.00-2.50	2.50-3.00	>3.00
0.00-0.25	1.1	5.5	4.22	2.57	1.83	1.28	0.55
0.25-0.50	1.1	5.5	4.22	2.57	1.83	1.28	0.55
0.50-0.75	3.44	17.23	13.21	8.03	5.74	4.03	1.72
0.75-1.00	0.81	4.03	3.09	1.88	1.35	0.94	0.41

It has already been mentioned that Anyadike (1992) published the results of rainfall analyses in Nigeria over the period 1916-1987. The 72-yr mean rainfall was 840 mm for the northern region, 1,230 mm for the middle belt, 1981 mm for the southern region and 1,351 mm for all of Nigeria. From the Mann-Kendall rank statistics it has been shown that northern Nigeria and the Nigeria as a whole suffer from a significant falling trend in annual rainfall. Despite the decline of annual rainfall in the middle belt and southern region the decrease did not prove to be significant.

It is remarkable that the k_{mx}/k_{mn} ratios for the northern region, middle belt, southern region and the whole country were 124/78 = 1.59, 121/77 = 1.57, 119/71 = 1.68 and 118/77 = 1.53, respectively. Such a consistency over a large surface area like that of Nigeria, about $0.923*10^6$ km^2, is quite amazing.

3..1.4 Frequency distribution of annual rainfall- It is often interesting to have reasonable estimates of variate values for the variable in question for probabilities of exeedance/non-exceedance or simply return periods other than those available in the record. A fairly large number of series have been examined for statistical dependence. Some of the independent series only have been further elaborated and the results obtained are listed in Table 3.6, as well as in Figures 3.13 and 3.14. With the exception of stations no. 192 and 200 at Agalega, Mauritius Island and 200 at Diego Suarez, Madagascar the shortest length of record for any station is 46 years. Table 3.6 gives annual rainfall estimates for return periods of 1.25, 2 5, 10, 50, 100 and 200 years. This study has led to the following results:

i- The distribution functions that best fit the examined records are the normal, 2-parameter lognormal, 2-parameter Gamma and Pearson Type III.

ii- The coefficient of variation C_v decreases with increasing mean annual rainfall P_m. This result is very much in agreement with the relation developed by WMO (1981). For $P_m < 100$ mm C_v may reach or exceed 1.0 and for P_m above 1,000 mm, C_v is between 0.1 and 0.2.

iii- The grouping of the sub-Saharan stations according to median values, consequently the large number of station years obtained for each group, has helped to establish a relationship between the median and mean of the

deviation between the mean and the median diminishes from north to south (personal communication). This deviation reduces to 3.7% for median values of 300 mm. This result is not strongly supported by the relative difference between the medians and means of the stations presented in Table 3.6 and the graphs in Figures 3.13 and 3.14. To give just a few examples here, the relative differences for St. Louis (Senegal), Wad-Medani (Sudan) and Atakpame and Sokode (Togo) are 7.5, 6.6, 1.1 and 4.5, respectively. Of these four examples, only the station of Atakpame is the one to which the normal distribution has been fitted.

It should be noted that whereas frequency distribution techniques help to estimate the variate values for certain average recurrence intervals, especially beyond the length of the record, yet the times of occurrence of these estimates, especially the extremes, remain always unknown. As such, the estimates obtained from these techniques can be quite useful only for certain purposes. Water management is one of the areas where estimates of average and extreme values are used extensively.

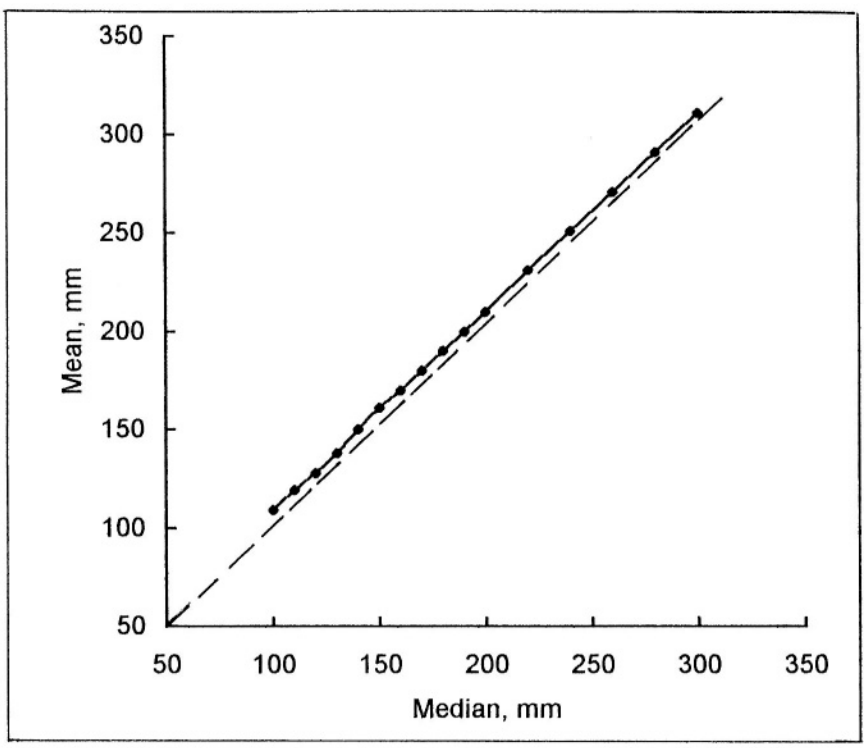

Figure 3.12- The median versus the mean annual rainfall of the three sub-Saharan groups

Table 3.6- Estimted annual rainfall correponding to a number of return periods at selected stations

Location	Period of record	P_m, mm	Cv	DF+	Annual rainfall, mm, corresponding to T_r, yr						
					1.25	2	5	10	50	100	200
St. 22	1938-1982	186	0.36	P III	129	182	274	303	336	359	264
S.Tunisia*	1900-1980	151	0.32	P III	110	148	191	214	258	275	280
St. 42 °	1921-1980	153	0.37	N	105	153	201	226	269	285	299
St. 49	1938-1989	150	0.48	G II	88	140	206	248	331	369	394
Saint.Louis	1890-1982	362	0.51	LN II	215	322	483	597	865	988	1112
Sub-Saharan[x]											
Group 1		150			90	140	200	239	315	345	380
Group 2		210			121	200	280	325	415	458	490
Group 3		281			166	270	360	420	540	580	630
St. 68	1921-1980	874	0.17	P III	750	863	991	1066	1207	1260	1300
St. 69	1921-1980	590	0.21	N	486	590	694	749	845	878	909
St. 72	1921-1980	747	0.16	G II	648	740	842	899	1006	1046	1092
St. 83	1901-1984	135	0.68	G II	58	115	219	277	401	452	500
St.108	1900-1990	1207	0.17	P III	1030	1166	1361	1488	1758	1868	2000
St. 112 °	1938-1982	1188	0.14	P III	1041	1173	1325	1415	1585	1650	1701
St. 117	1928-1990	1399	0.23	P III	1122	1360	1653	1830	2181	2348	2480
St. 121	1921-1990	1423	0.21	P III	1178	1392	1661	1825	2155	2284	2400
St. 148	1938-1972	1553	0.15	N	1357	1553	1749	1852	2032	2094	2153
St. 165	1938-1972	1840	0.16	N	1600	1840	2080	2205	2425	2503	2574
St. 171	1922-1992	1021	0.18	P III	873	977	1144	1259	1512	1617	1790
St. 192	1961-1990	1647	0.14	N	1454	1674	1866	1940	2116	2179	2235
St. 200	1961-1987	1210	0.26	N	942	1210	1478	1618	1863	1950	2029
N. E. Zambia[xx]	(46 yr)	1091	0.17	LN II	933	1076	1239	1335	1520	1591	1640
Ft. Victoria	1901-1980	636	0.32	N	465	636	807	897	1054	1109	1160
S. Africa**	1921-75	1	0.19	LN II	0.839	0.983	1.151	1.25	1.446	1.523	1.625

Explanation

DF+ :Distribution function of best fit to data in record; N: normal, LN II: 2-parameter lognormal G II: 2-parameter Gamma and P III: Pearson type III.

** Areal average of 10 stations in southern Tunisia (Flohn/WMO, personal communication).*

° The series is just above the level at which the data would be significanly dependent.

x Group I: Stations of Agades, Kidal, Nouakchott, Tidjikja, Oualata plus 206 station-year values. Group 2: Boutilimit, In Gali, Moudjeria, Nguimi, Tamchakett plus 196 station-year values. Group 3: Aleg, Biltine, Iribo, Mao, Mederda, Menaka, Nema, Tanout plus 311 station year-values. The ranges of median values are 100-160 for Gr. 1, 160-220 for Gr. 2 and 220-300/310 for Gr. 3. Data about the 3 sub-Saharan groups were obtained through personal comunnication with ORSTOM.

xx Areal average of 10 stations in the Chambeshi basin (Sharma, 1985).

*** Spatial average for quaternary subcatchments in the upper reach of the Pongola River (Paling & Stephenson,1988). Annual rainfall depths are given in modular form, I.e. individual values are divided each by the sample mean. By this technique the sample mean is reduced to the modular mean, i.e. 1.0 as given in Table 3.6.*

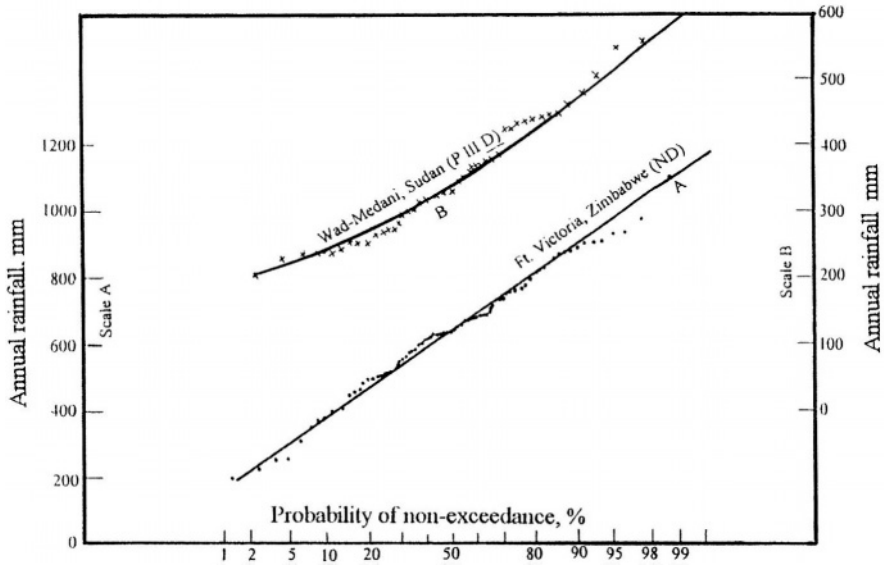

Figure 3.13- Normal and Pearson Type III distribution functions fitted to the annual rainfall series at Ft. Victoria, Zimbabwe, and Wad-Medani in the Sudan

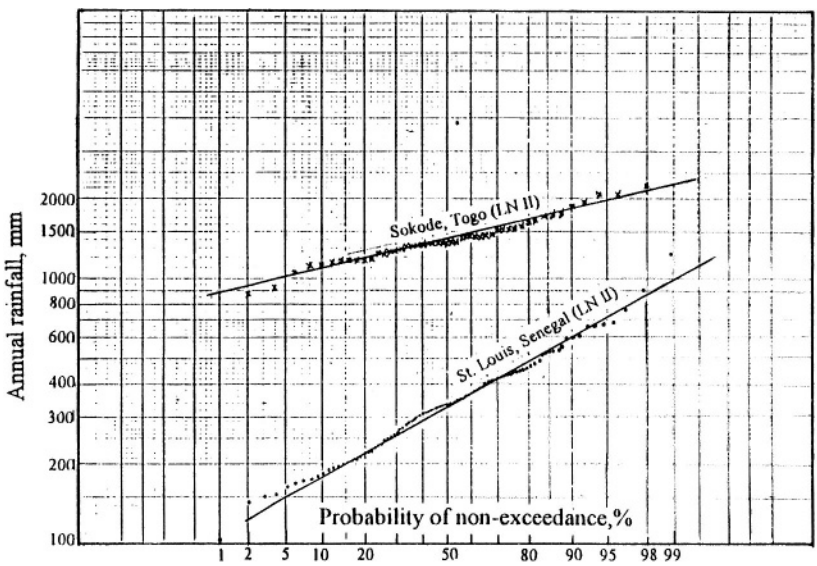

Figure 3.14- Two-paraameter lognormal distribution function fitted to the annual rainfall series at St. Louis, Senegal, and Sokode, Togo

3.1.5 Results of drought risk- The Food and Agriculture Organization (FAO) while investigating the possibility of expanding irrigation in Africa, undertook, as a study component, the probability analysis of rainfall. From irrigation practices it is known that the mean value for the available water is not an appropriate design factor, unless there is considerable carry-over storage. FAO is therefor arbitrarily adopting the level of 80% for rainfall occurrence, i.e. a certain amount is reached or exceeded in 4 out of 5 years.

For this purpose the FAO analyzed the records of 200 rain gauging stations. From these records and the 80% non-exceedance probability calculated, it became possible to determine the number of times in 50 years that the 80% rainfall figure was not reached in two or more successive years. We shall call this number the absolute frequency of failure. The results obtained from that investigation are as follows (FAO, 1987):

Mean annual rainfall range, mm	Frequency of failure in 50 years	Probability of failure, %	Rank of drought risk
200-250	10	20	Very high
250-300	9	18	-
300-350	8	16	High
350-450	7	14	Strong
450-700	6	12	-
700-1,300	5	10	Moderately strong
1,300-2,000	4	8	Moderate
2,000-2,600	3	6	-
2,600-3,300	2	4	Low
>3,300	1	2	Very low

The above figures show that regions with long-term low rainfall such as vast areas in Mauritania, Mali, Angola,... are subject to high drought risk. The extent of the risk diminishes with increase of the long-term average rainfall. This brings the drought risk in a vast surface in West, Central and East Africa, and Madagascar to moderate. The zones in between the regions with high and moderate risks, e.g. a large surface in Zambia, Zimbabwe and South Africa, have been termed strong and moderately strong. A relatively small surface along the western coast, middle and east of Congo has a very limited risk or probability of failure in fulfilling the requirement of the 80% level of rainfall. Anyhow these areas by virtue of their heavy precipitation need no irrigation.

3.2-Monthly Rainfall

3.2.1 Distribution of annual rainfall between the months of the year- In the subsection on rainfall in Chapter 2, a brief description of the distribution patterns of monthly number of rain days at four stations is given. The station no. 21 at Sirte, Libya, shows a limited rainfall in the period between October and April, the remaining months being practically dry. The station in Guinea-Bissau shows just one rainy season, April-December. Kribi, station no. 147 in Cameroon, shows two rainy seasons, of which the second seems to be wetter than the first. The fourth station, no.203, is situated in Zambia, Southern Africa and shows a long dry season from May to September. These four stations are typical examples of the climates in the Mediterranean Coast in North Africa, wet and dry Tropical zone, Equatorial rain forest and the central part of Southern Africa, respectively.

For the sake of completion the map in Figure3.15, taken from Martyn (1992), is included here. This map shows the distribution of the total rainfall over the months of the year at 66 stations covering Africa and some of its islands. The explanation underneath the map gives the average number of rainy days per year. The number of rainy months varies from practically zero to twelve, and the number of rainy days from zero or close to zero in the desert to 246 days in Toamasina on the eastern coast of Madagascar. The rainy season, in general, seems to occur during the period of high sun, obviously to be followed by a dry season.

Thompson (1965) prepared a map showing the length of rainy season in months. He considered a month to belong to the rainy season when the rainfall in that month equals or exceeds 50 mm. The rainy season in Somalia and certain parts of Kenya has been described as variable, twin season of duration 1 to 5 months. Some areas in the western part of that region receive insignificant rain. Other areas of insignificant rainfall are about the top half of Northern Africa and the western strip of the lower half of Southern Africa (Figure 3.16).

Griffith's (1972) presented some maps that indicated the parameters describing the monthly rainfall in Africa, such as the duration of the rainy season, the wettest quarter of the year and the contribution of the rainy season to the annual total rainfall. One of those maps is shown in Figure 3.17. He, like Thompson, considered a certain month to be part of the rainy season whenever the depth of rain in that month is equal to 50 mm or more. As such, no wonder then that both maps in Figures 3.16 and 3.17 have many features in common.

Figure 3.17, in addition to the length of rainy season(s), indicates the central month of the wettest quarter of the year. Furthermore, it shows two classes for the wettest quarter of the year; one class with contribution of 40-60% of the annual total and the other with contribution above 60%. The contribution of the wettest quarter to the annual rainfall of less than 40% either does not exist or has been dropped.

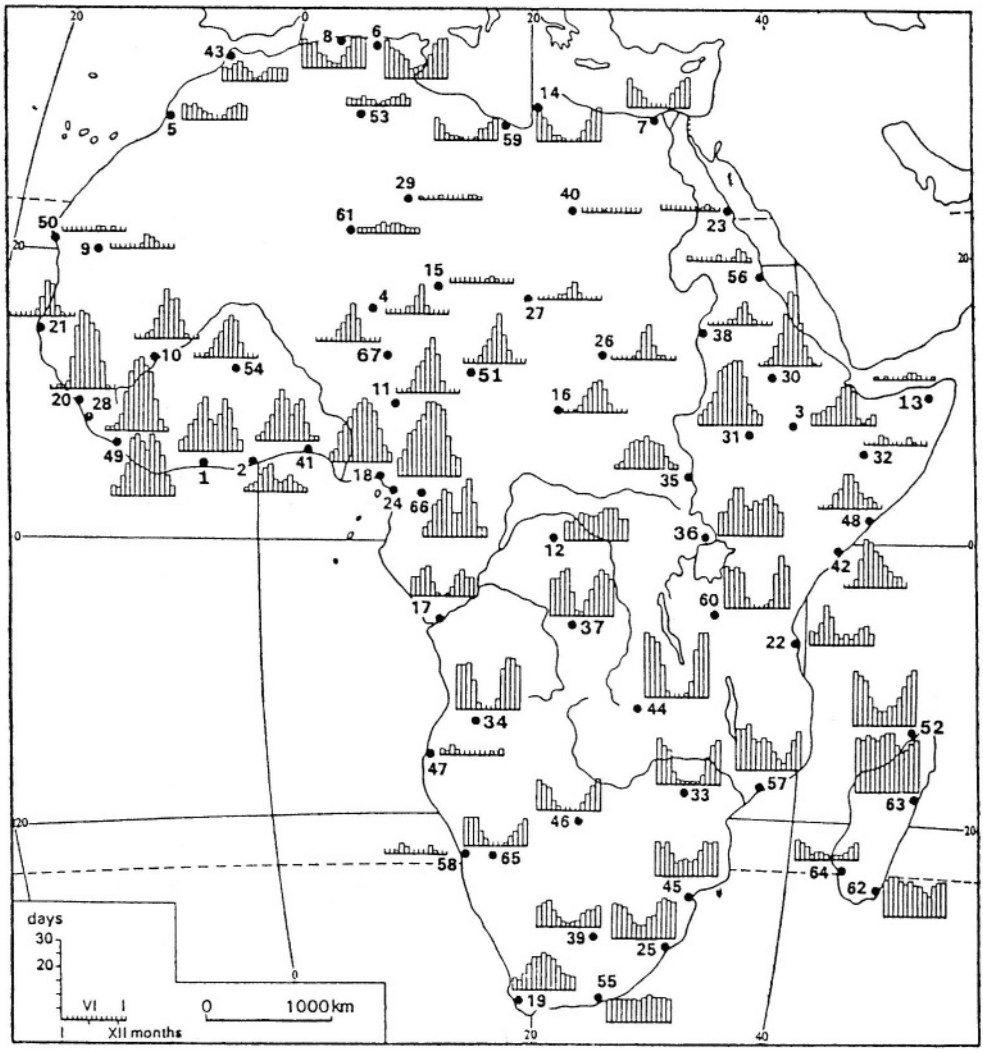

Number of precipitation days per year in brackets: 1—Abidjan (153), 2—Accra (54), 3—Addis Ababa (138), 4—Agades (22), 5—Agadir (34), 6—Ain el Kasar (99), 7—Alexandria (44), 8—Algiers (76), 9—Atar (16), 10—Bamako (76), 11—Bauchi (84), 12—Befale (117), 13—Bender Cassim (8), 15—Benghazi (56), 15—Bilma (2), 16—Birao (53), 17—Boma (70), 18—Calabar (173), 19—Cape Town (112), 20—Conakry (158), 21—Dakar (47), 22—Dares-Salaam (113), 23—Dongonab (6), 24—Douala (208), 25—Durban (116), 26—El Fasher (34), 27—Faya (10), 28—Freetown (167), 29—Ghat (4), 30—Gondar (127), 31—Gore (177), 32—Gorrahey (11), 33—Harare (87), 34—Huambo, 35—Juba (87), 36—Kampala (159), 37—Kananga (152), 38—Khartoum (18), 39—Kimberley (61), 40—Kufra (0.7), 41—Lagos (123), 42—Lamu (91), 43—Llano Amarillo (59), 44—Lubumbashi (135), 45—Maputo (108), 46—Maun (52), 47—Moçâmedes (9), 48—Mogadishu (78), 49—Monrovia (207), 50—Nauadhibu (8), 51—Ndjamena (61), 52—Nossi-Bé Island (152), 53—Ouagadougou (72), 54—Ouargla (16), 55—Port Elizabeth (103), 56—Port Sudan (13), 57—Quelimane (129), 58—Swakopmund (11), 59—Sirte (33), 60—Tabora (100), 61—Tamanrasset (21), 62—Taolanaro (151), 63—Toamasina (246), 64—Toliara (35), 65—Windhoek (55), 66—Yaounde (142), 67—Zinder (44).

Figure 3.15- Monthly distribution of annual rainfall in Africa (taken from Martyn, 1992)

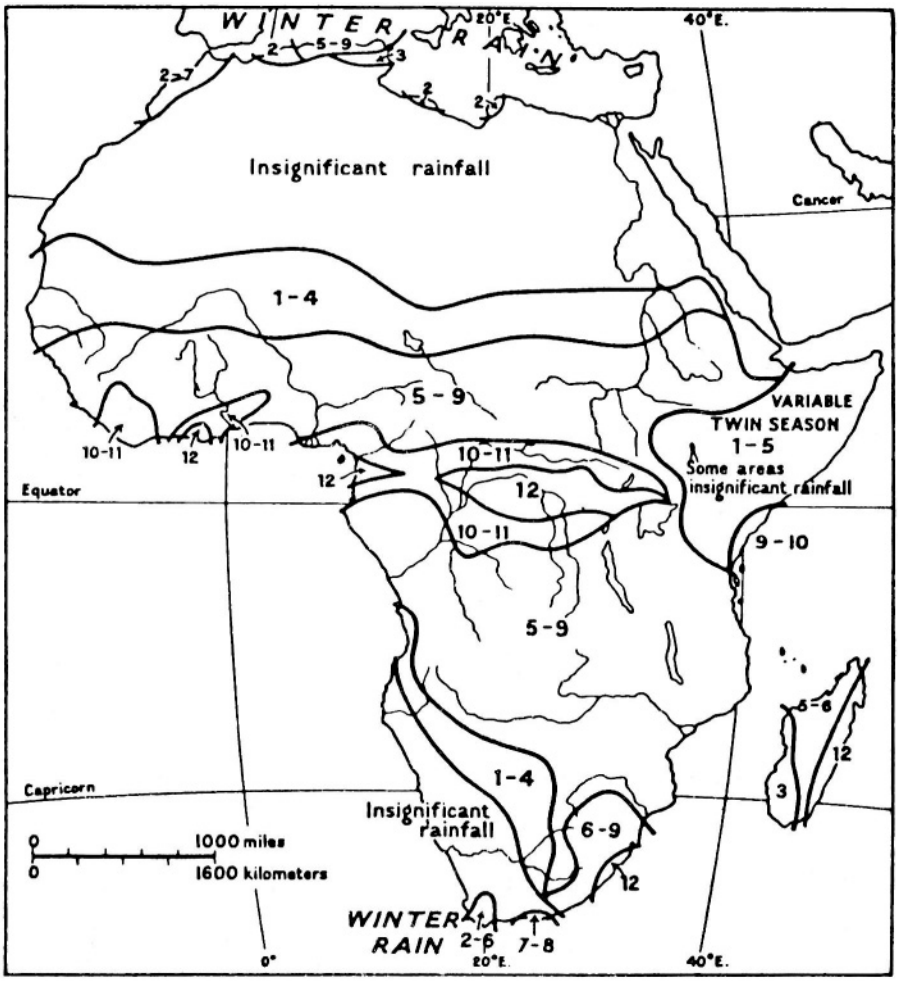

Figure 3.16- Map of Africa showing the length of rainy season in months per year. A month is considered part of the rainy season when the mean rainfall exceeds 50 mm (derived from Thompson, 1965)

Griffith's (1972) commented on Figure 3.17 mentioning that the choice of a 50-mm threshold is based on vegetal considerations, but if another threshold were taken, the zones would show mainly a change in the Arabic numerals and not in the boundary locations. Additionally, the real and practical concentration of short-duration rainfall is indicated in the 4-6 months and in the I', II', VI', XII', I" and II" areas. This concentration lays much stress on these short

seasons and failure of the rain inevitably leads to crop failure and subsequently to social-economic hardships.

For a large surface in Africa, monthly rainfall of 50-mm or more hardly occurs. Wallén (1968), upon investigating the possibility of dry-land farming in the Middle East, reported that the minimum annual rainfall at which dry-land farming is possible varies from region to region. This is because the extent of variability of the annual rainfall is larger in some areas than in others. Wallén introduced the term interannual variability (IAV), which can be expressed as:

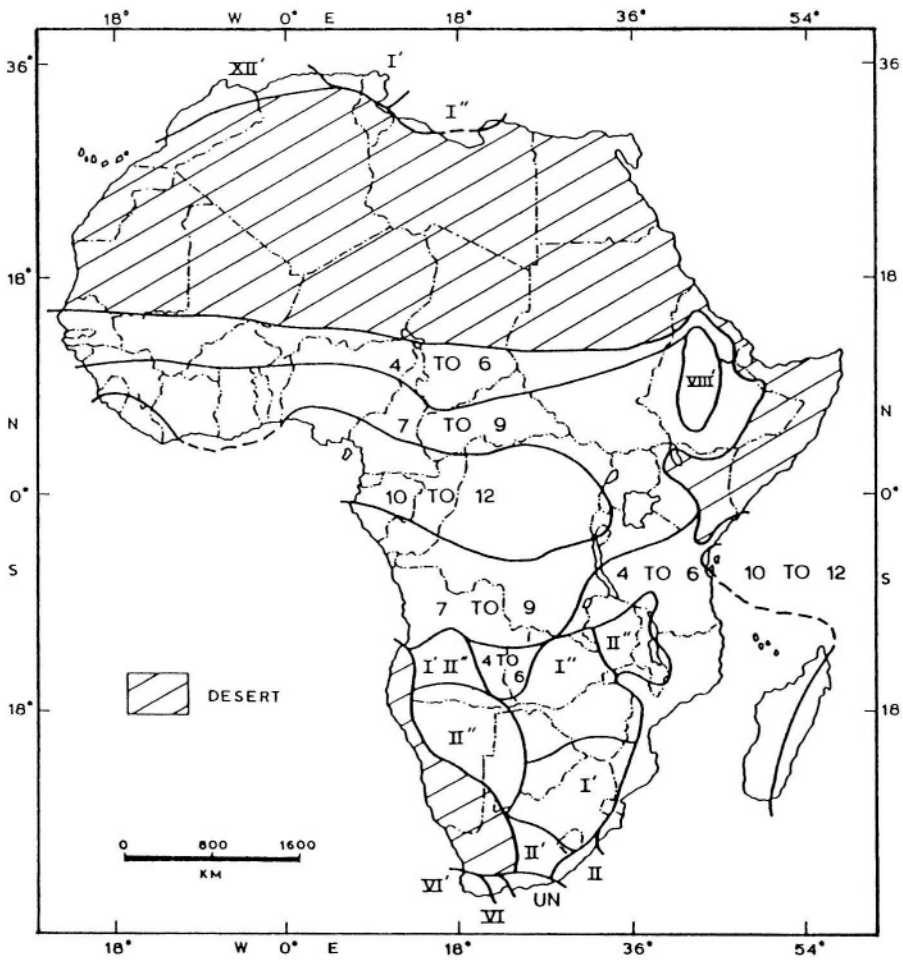

Figure 3.17- Rainfall distribution. Arabic numerals refer to number of months receiving at least 50 mm of rain. Roman numerals denote central month of wettest quarter. ' indicates 40-60% annual total received rainfall received in wettest quarter; " indicates over 60%

$$IAV_{rel} = \frac{100\Sigma_{i=2}^{i=n}(P_{i-1} - P_i)}{P_m(n-1)} \tag{3.6}$$

where, P_i = annual rainfall in year i, n= number of years of record and P_m= mean annual rainfall.

Wallén calculated IAV_{rel} for a variety of stations in the Middle East and fitted an average curve or primary curve to the scatter of points representing IAV_{rel} against P_m. This curve, though different from the curve of C_v versus P_m, shows a decline of IAV_{rel} with increase in the mean total precipitation, P_m. He fitted further curves to his diagram separating stations where dry-land farming is possible from those where it is not possible. The intersection of these two curves and the primary curve gave the approximate value of annual precipitation at the limit of dry-land farming in the Middle East at 240 mm with an interannual variability of 37%.

In the Middle East, which has winter rainfall, Wallén considers that the start and end of the reliable rainfall season correspond to a monthly rainfall of 25 mm and a variability of 100%. He introduced for the monthly precipitation a certain parameter, q, which can be calculated from the formula:

$$q = \frac{p_m}{IAV_{rel}} \tag{3.7}$$

where, p_m = long-term mean precipitation for a certain month and IAV_{rel} = interannual variability of precipitation in the same month. Substituting in Eq. (3.7) 0.25 for q and 100% for IAV_{rel} one gets a monthly rainfall of 25 mm

Since certain parts of Africa, especially in the north and south, have Mediterranean, Saharan and sub-Saharan climates like the Middle East, it seemed useful to develop two new maps for the monthly rainfall in Africa. In a manner rather similar to those previous investigations, we began by counting the number of rainy months at each of the 271 stations listed in Appendix, A. A month has been considered to belong to the rainy season when its p_m is equal to or more than 25 mm. Other than the Saharan zone, where the duration of rainy season is zero, six zones have been developed with a 2-month step, i.e., 1-2, 3-4,... and 11-12. Despite the fact that more zones are shown on the map in Figure 3.18, both maps nearly have the same basic features.

The ratio of rainfall in the rainy season to the total rainfall is important for the management of water resources, especially in areas with alternating wet and dry climates. Storage of excess water, urban drainage and land irrigation are just a few examples are worth mentioning. As such, the map in Figure 3.19 has been prepared using the 271 meteorological stations listed in Appendix A so as to take this objective in to account. Five zones or classes have been developed,

each comprising a certain range of ratios of the rainfall in the wet season to the annual rainfall. Zone 5 (95-100%) covers over 40% of the surface of Africa. On the other hand, about 30% of the area of the continent is covered by zone 1 (< 50%). The rest of the area of Africa and Madagascar is covered by classes 2, 3 and 4 with ratios of 50-80, 80-90 and 90-95% respectively.

3.2.2 Statistical analysis of monthly rainfall- The family of Gamma (distribution functions, particularly the Gamma two and three parameters; sometimes called Pearson III are comparable to the lognormal, being distribution functions that serve as a good fit to monthly rainfall (Shahin, 1993)

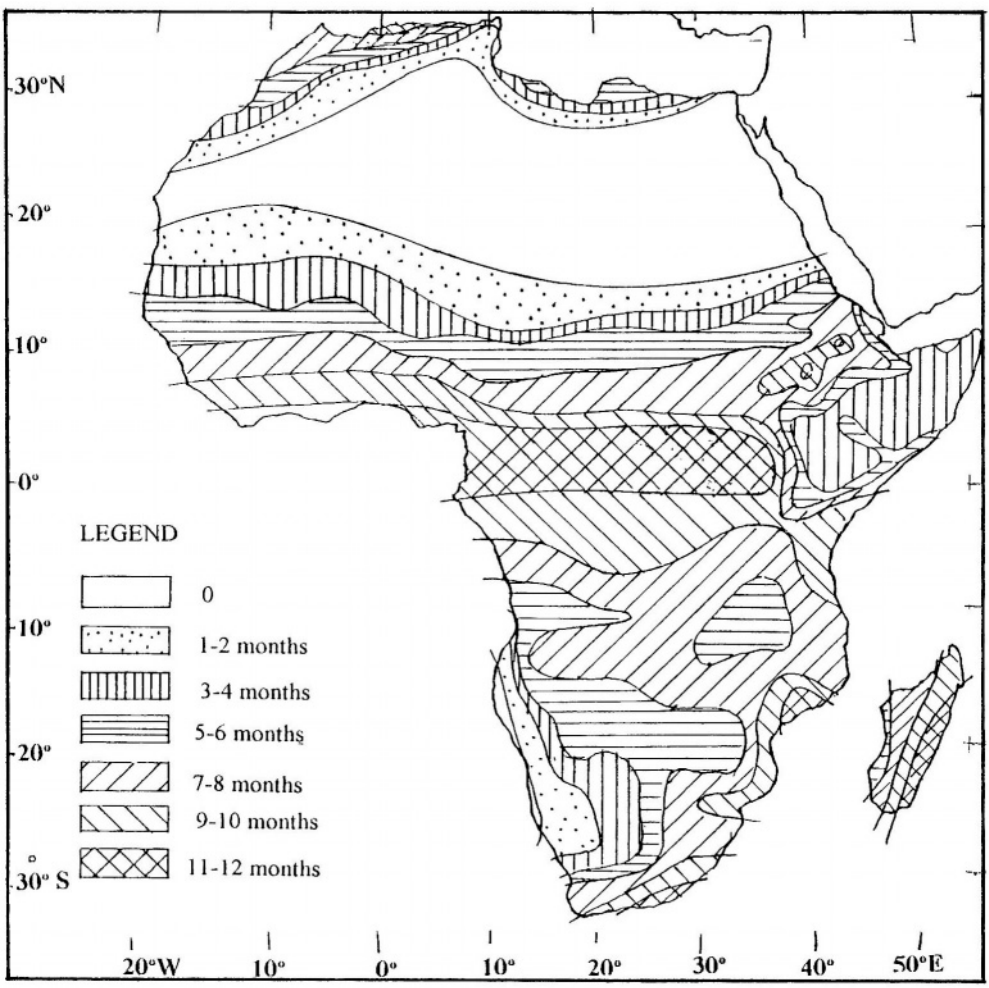

Figure 3.18- Areal distribution of the length of rainy season(s) in Africa

The 2-parameter Gamma distribution function has proven to be a useful representation of rainfall frequencies under the conditions in the Equatorial Lakes area (WMO, 1974). The probability density function can be written as:

$$f(x) = \frac{\lambda\eta}{\Gamma(\eta)} x^{\eta-1} e^{-\lambda x} \qquad \text{if } x \geq 0 \qquad (3.8)$$

$$= 0 \quad \text{elsewhere}$$

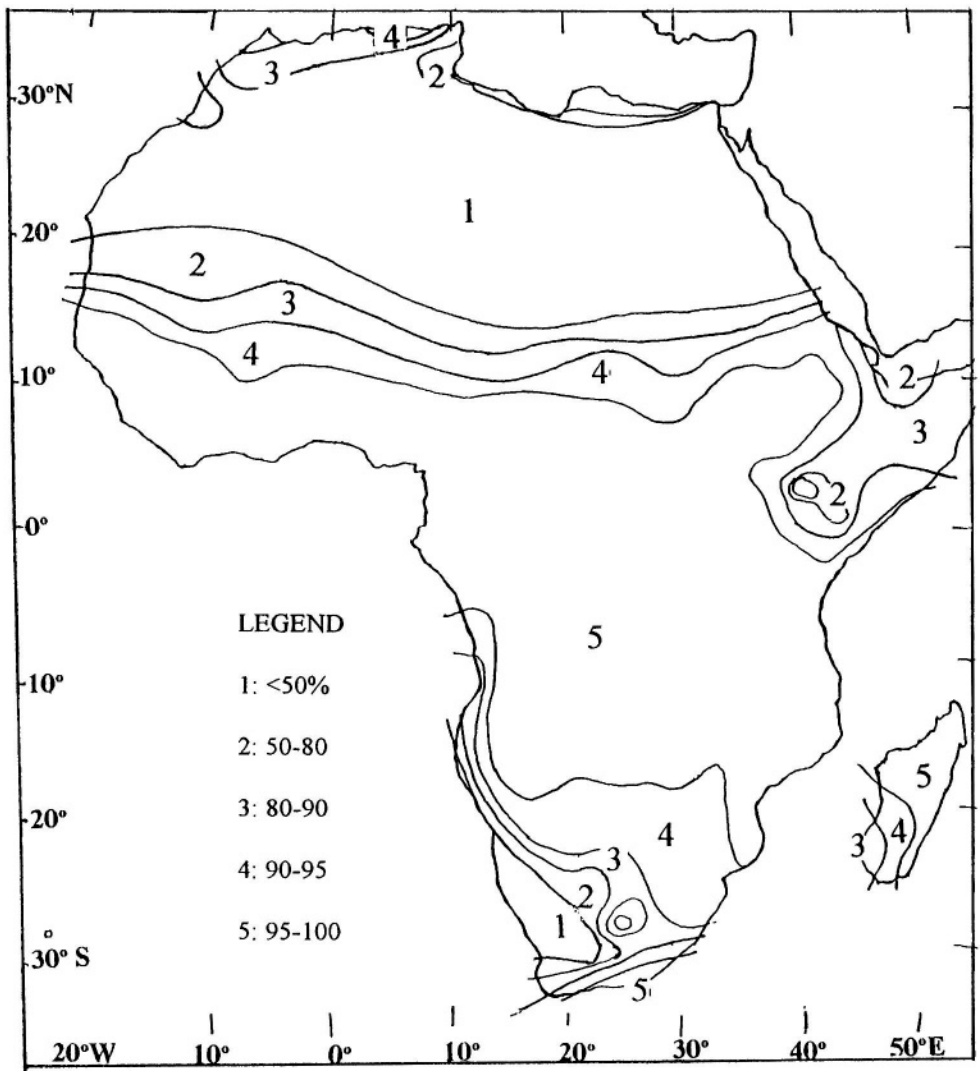

Figure 3.19- Contribution of the rainy season to the annual total precipitation

where, λ = scale parameter > 0 and η = shape parameter of the distribution. The normalizing factor $\Gamma(\eta)$ can be defined such that the total area under the density curve equals 1. Hence:

$$\Gamma(\eta) = \int_0^{\infty} \lambda^{\eta} x^{\eta-1} e^{-\lambda x} dx \qquad (3.9)$$

The mean and variance of this distribution are given by η/λ and η/λ^2 respectively. The maximum likelihood estimates of the parameters of the Gamma function have been obtained for seven rain gauging stations, 3 in Uganda, 2 in Kenya and 2 in Tanzania. These estimates are listed in Table 3.7.

3.2.3 Statistical analysis of (maximum) monthly rainfall- While discussing the (maximum) monthly rainfall over a consecutive number of years, two problems become apparent. The maximum monthly depth of rain does not always fall in the same month, causing the interval between two successive elements in the monthly rainfall series to be variable If this interval has to be kept constant, the rain depths in the month with highest frequency of maximum monthly rainfall should be used. The disadvantage of this approach is that not all elements in the series will then represent the maximum monthly rainfall.

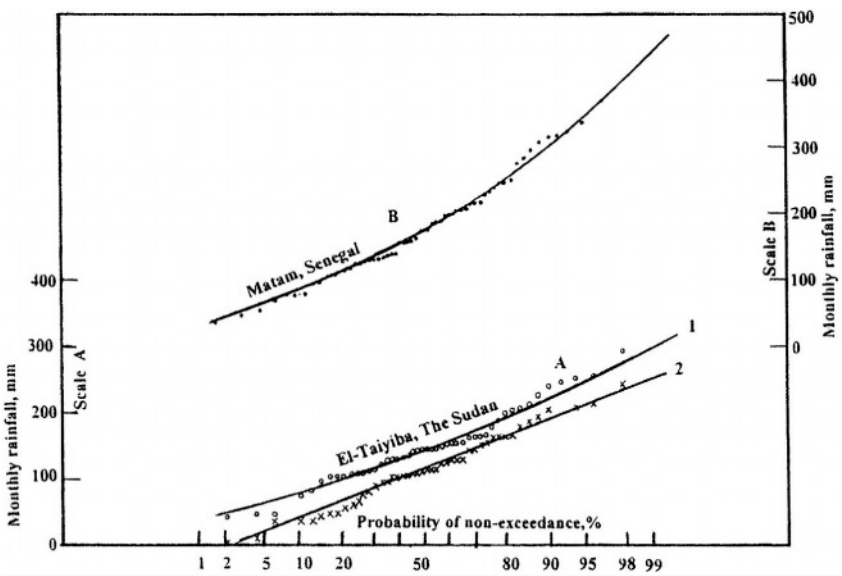

Figure 3.20$_a$- Frequency distribution of maximum monthly rainfall (1) at Taiyiba, the Sudan, and rainfall in the month with most frequent maximum rainfall at Taiyiba, The Sudan (2) and Matam (upper curve), Sénégal

As an example consider the monthly rainfall at Al-Taiyiba (Φ = 14°28'N, λ =33°26'E, z=405 m) close to Wad Medani, the Sudan. The length of record considered is 48 years, 1934-1981. The frequency of maximum rainfall is 1 for June, 21 for July, 25 for August and 1 for September. The mean of the maximum values is 147.8 mm and the data can be fitted by the Gamma function, curve 1 in Figure 3.20$_a$. This result prompted us to investigate more monthly series using other stations in northern Africa. It appeared that the case of Al-Taiyiba station is somewhat extreme. Other stations showed that August is by far the month with largest mean rainfall. Furthermore, the frequency of maximum monthly rainfall in August is larger than any other month, and counts to over two-thirds of the total number of maximum monthly rainfall on record. Two examples to mention here are:

Station no. 64: Zinder, Niger, August rainfall = 41.2% of the annual total
relative frequency of maximum monthly rainfall = 73.5%
July rainfall = 29.2% of the annual total
relative frequency of maximum monthly rainfall = 26.5%

Station no. 48: Matam, Senegal, August rainfall = 38.2% of the annual total
relative frequency of maximum monthly rainfall = 76.6%
July rainfall = 23.7% of the annual total
relative frequency of maximum monthly rainfall = 23.4%

Again, the function best fitting the August rainfall of the stations under investigation has been found to be the 2-parameter Gamma. In addition to the two series presented in Figure 3.20$_a$, the rainfall series for Zinder in Niger and Bougouni in Mali are shown in Figure 3.20$_b$.

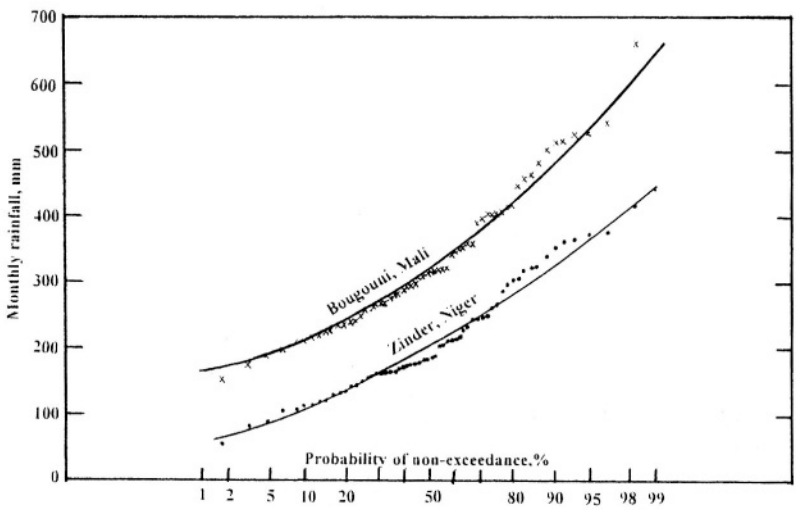

Figure 3.20$_b$- Frequency distribution of the rainfall in August at Zinder, Niger and Bougouni, Mali and the fitted 2-parameter Gamma functions

Table 3.7-Distribution parameters of the Gamma function fitted to monthly and annual rainfall data at certain stations in the Equatorial Lakes area (WMO, 1974)

Month	Shape parameter of rainfall at stations							Scale parameter of monthly rainfall at stations						
	148	163	164	165	167	169	171	148	163	164	165	167	169	171
Jan	1.01	1.01	1.28	1.58	1.6	4.32	4.17	21.7	52.4	42.7	50.5	33.4	34.5	24.3
Feb	0.91	2.08	2.76	2	2.31	3.25	2	52.5	40.7	21.7	47.6	29.3	49	51.6
Mar	3.38	4.08	4.58	2.64	7.22	9.63	2.51	28.3	34	26.6	63	13.9	24.3	61.2
Apr	8.43	5.57	5.9	6	5.76	12.6	7.59	20.4	33.4	31.9	41.5	21.1	29.6	24
May	9.22	4.87	3.04	11.2	2.88	8	2.52	19.7	29.9	60.2	19.9	29.7	40.1	35
Jun	5.75	2.31	1.39	9.6	0.86	2.52	0.95	26.3	32.9	37.5	14.4	34.3	34.2	25.4
Jul	6.26	2.72	1.67	4.3	0.93	1.42	0.75	27.1	19.9	24	26.4	22.6	38.4	27.1
Aug	10.1	2.3	1.77	8.68	2.4	2.78	0.18	24.5	31.8	31.8	16	23.4	26	24.9
Sep	4.35	3.23	3.14	4.87	3.41	3.75	1.46	41.4	18.6	29.3	24.3	27.3	29.4	25.9
Oct	7.02	1.97	5.4	4.52	4.25	5.41	1.19	24.2	27.2	20.3	24.9	23.5	26.4	57.1
Nov	1.48	1.22	4.5	2.46	3.69	6.2	2.27	64.5	75.1	23.2	47.7	32.2	29.4	56.9
Dec	1.28	2.19	2.21	2.39	2.35	4.54	2.59	36.5	43.7	44.5	45.8	31.5	42.9	56.6
Year	45.2	28.2	19.1	42.1	34.2	53.6	20.3	34.7	38.8	62	39.4	26.8	38.7	52

Explanation

Denote the number of months in the record at any station by n, given below are n values used in the analysis:
Years indicating the beginning and end of record are not indicated in the reference.
St. 148: Gulu, Uganda, n=31-40, St. 163: Kisumu, Kenya, n=37-40, St.164:Massake, Uganda, n=38-40,
St. 165: Kericho, Kenya, n=40, St. 167: Mbarara, Ugandaa, n=33-40, St. 169: Bukoba, Tanzania, n=37-40,
St. 171: Mwanza, Tanzania, n=(19)-40. For more details, the reader is refered to Vol.I, Part I of the report of WMO on Hydro-meteorological survey of the catchments of Lakes Victoria, Kyoga and Albert (1974).

3.3-Daily Rainfall

In this section, the results of some studies about daily rainfall in certain parts of Africa will be reviewed. For agricultural purposes as well as design of certain urban structures, emphasis is usually laid on maximum daily precipitation.

According to Griffith's (1972), north of Morocco in the area between Tangier and Mellila, essentially Mediterranean climate, falls of over 150 mm in a day have been recorded. The Algerian coast, which is characterized by a transitional Mediterranean climate, has much in common with temperate climate in winter, and experiences a considerable number of heavy rain falls, over 30 mm d^{-1}, all occurring in December. Locations east of Greenwich Meridian receive amounts in excess of 100 mm d^{-1}. In contrast, in the predominantly dry zone of southern Morocco, falls of more than 60 mm d^{-1} have never been experienced.

Table 3.8 has been prepared using some of the Griffith's findings (1972). It gives the two highest daily rainfalls at some rain gauging stations. Belloum (1993) discussed the maximum daily rainfall at Skikda, on the Mediterranean coast in Algeria. He pointed out that both Galton (2-parameter lognormal) and Gumbel (Type I extreme value [EV]) are adequately suitable for modeling the frequency distribution of the maximum daily rainfall. It goes without saying that Gumbel's function is a special case of the lognormal distribution when the coefficient of variation, C_v, is about 0.37. The maximum daily precipitation depths at Skikda, for the 30-yr period, 1958-1987 are plotted on Type I EV probability paper, and a straight line is fitted as shown in Figure 3.21. The highest value in the 30-yr record is about 104 mm d^{-1}. Extrapolating the theoretical distribution to return periods of 50 and 100 years the estimates of the corresponding falls are 113 and 125 mm a day respectively. According to the general relationship of depth-duration-frequency (sometimes referred to as the law of Montana), the depth d_{Tr} corresponding to a certain return period Tr can be estimated from the expression:

$$d_{Tr} = aTr^{n} \tag{3.10}$$

where a and n are dimensionless parameters varying from one return period to another. For rain duration, t = 24 hours, and Tr = 100 yr, a - 32 and n = 0.30, Eq (3.10) gives a maximum daily fall of 127.5 mm. This value is the same as that can be obtained from Figure 3.21. Likewise, assuming for Tr = 50 yr that a = 32 and n = 0.32 d_{50} will be 112 mm, a value which is very close to the one to be obtained from the graph in Figure 3.21. Obviously, considerable amount of data about heavy rainstorms of 24h-duration each are needed before reliable estimates of the parameters a and n are obtained. The same has to be done for other rain duration such as 2, 3 days, even longer. The need for these estimates

becomes more pressing, especially when regional rainfall is considered. This procedure will be further discussed in the next section.

In Nigeria too, statistical analyses and distribution functions that best fit annual series of maximum daily rainfall have been worked out. It has been reported by Ayoade (1976) that the normal and the EV Type I distribution functions yield about the same results. Based on this conclusion, Figures 22 a and b are shown here as examples of the good fit provided by the EV Type I function in approximating the maximum daily rainfall in Lagos, 1915-62 and Ibadan, 1926-63.

Table 3.8- Two highest rainfalls in mm (Griffith's, 1972)

Stat.	Maxima		Stat.	Maxima	
no.	first	second	no.	first	second
3	86 (Nov.)	81 (Dec.)	13	129 (Nov.)	125 (Feb.)
4	135 (Oct.)	81 (Nov.)	14	61 (Nov.)	51 (Sep.,Oct.)
5	81 (Feb.)	72 (Nov.)	16	53 (Dec.)	31 (Apr., May)
6	122 (Dec.)	112 (Oct.)	17	78 (Oct.)	31 (Feb., Mar.)
8	89 (Mar.)	69 (Oct.)	18	43 (Nov.)	38 (Oct.)
9	46 (Apr.)	41 (Mar.)	20	41 (Jun.)	38 (Nov.)
10	105 (Oct.)	102 (Nov.)	21	66 (Sep.)	43 (Nov.)
12	41 (Nov.)	38 (Mar.)	22	63 (Nov.)	56 (Dec.)

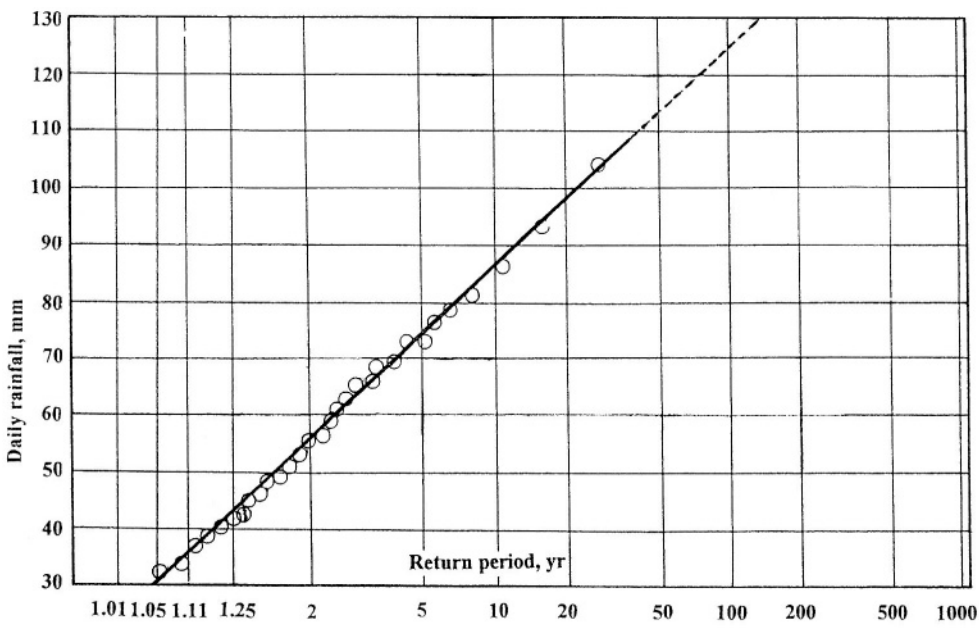

Figure 3.21- Fitting Gumbel's distribution to the maximum daily rainfall at Skikda, Algeria (Belloum, 1993)

The maximum daily rainfall totals at 19 stations for each year over the period 1951-65 were subjected to the same analysis. Using Gumbel's distribution function the estimates for 100-yr return period have been found to vary from 225 to 250 mm d^{-1} for the coastal strip, from 175 to 200 mm d^{-1} for the middle belt and from 125 to150 mm d^{-1} for the northern and eastern parts of Nigeria.

Additionally, values of probable maximum precipitation (PMP) have been estimated using Ven te Chow's general frequency formula (1951), which can be written as:

$$X = X_m + k\sigma \tag{3.11}$$

where, X = estimate of the variate value corresponding to a given return period, X_m = mean, σ = standard deviation and k = frequency factor depending on the kind of distribution, return period and the coefficient of variation, C_v, of the data. For estimating the PMP, k is usually substituted as 15 in Eq. (3.11). Furthermore, substitute in Eq. (3.11) for X_m; 100-110 for the coastal zone, 80-90 for the middle belt and 60-70 mm d^{-1} for the northern and eastern parts, and for σ; 25, 20-30 and 15-20 mm d^{-1} for the three zones in their respective order. Eq (3.11) yields values about 500, 425 and 250 mm d^{-1} for PMP for the three zones respectively.

While discussing the 1-day maximum rainfall in the report of the Hydro-meteorological survey of the catchments of Lakes Victoria, Kyoga and Albert (WMO, 1974), distinction has been made between the maximum rainfall over a period of any 24 hours at a stretch and the maximum during a fixed 24hour period. The former is likely to be larger than the rainfall over a constant period of 24 hours. The method that has been followed was to estimate the 24-h maximum from the relationship:

$$X = X_{obs} + \frac{1}{2}R' \tag{3.12}$$

where, X = any continuous 24-h maximum, X_{obs} = observed day maximum and R' is the highest daily rainfall on the preceding or following day. As such, if the statistics for 24-h periods are available, the corresponding statistics for 24-h maxima can be obtained by appropriate stepping up. Again, the method of analysis adopted in that investigation involved fitting the Gumbel Type I EV distribution to the X-series. Two charts giving I-day extreme precipitation, one for 2 years and the second for 100 years, were used to construct a general nomogram for estimating the 1-day extreme rainfalls for other return periods. By this procedure estimates of 1-day extreme rainfall have been obtained for 21 locations in the catchments of Lakes Victoria, Kyoga and Albert (WMO, 1974).

The estimates are given for Tr = 10, 20, 50 and 100 years. Those for station no. 163 at Kisumu in Kenya are shown in Figure 3.23 for all months of the year.

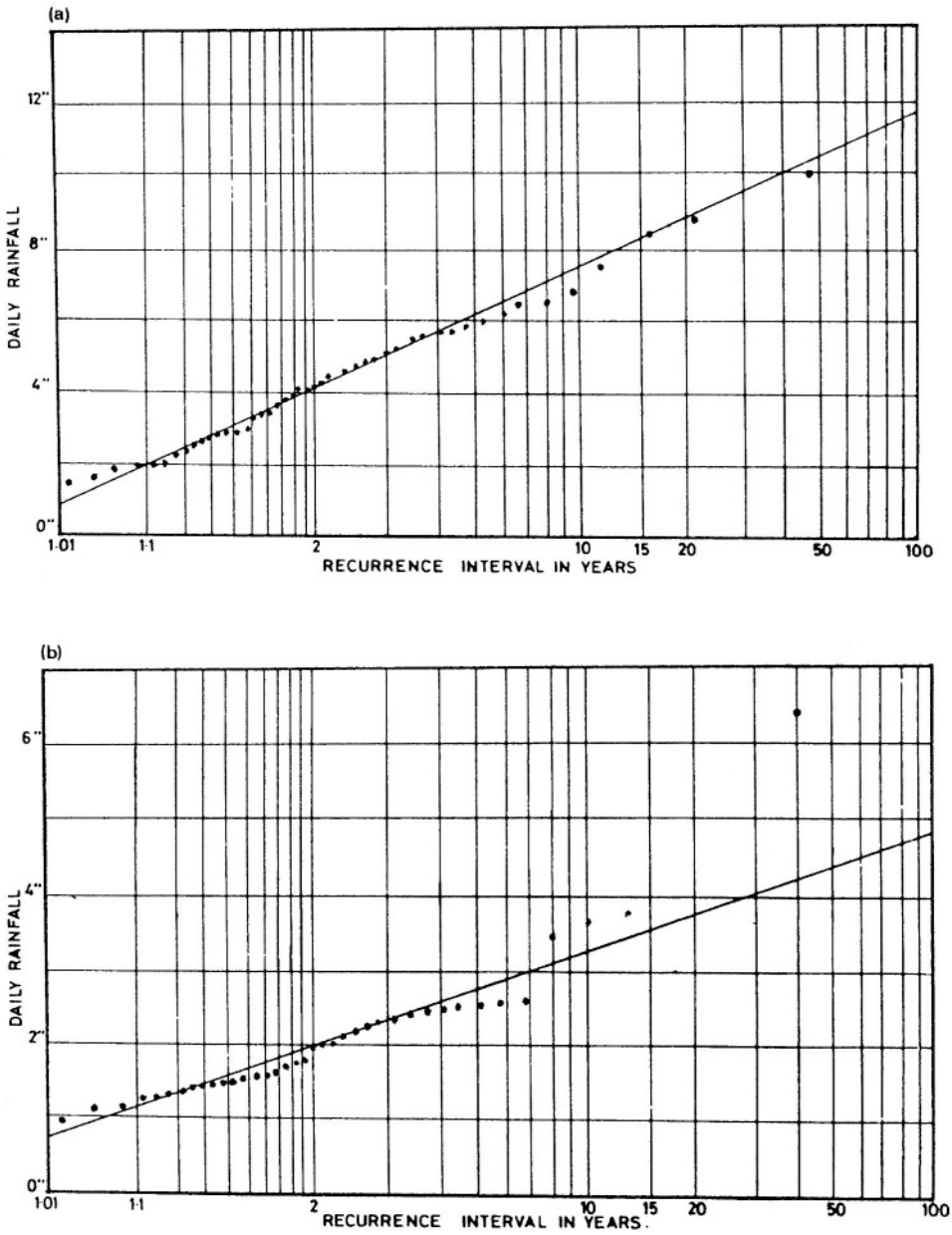

Figure 3.22- June maximum daily rainfall (in inches, 1 inch= 25.4 mm) in Lagos, 1915-1962 (a), and in Ibadan, 1926-1963 (b)

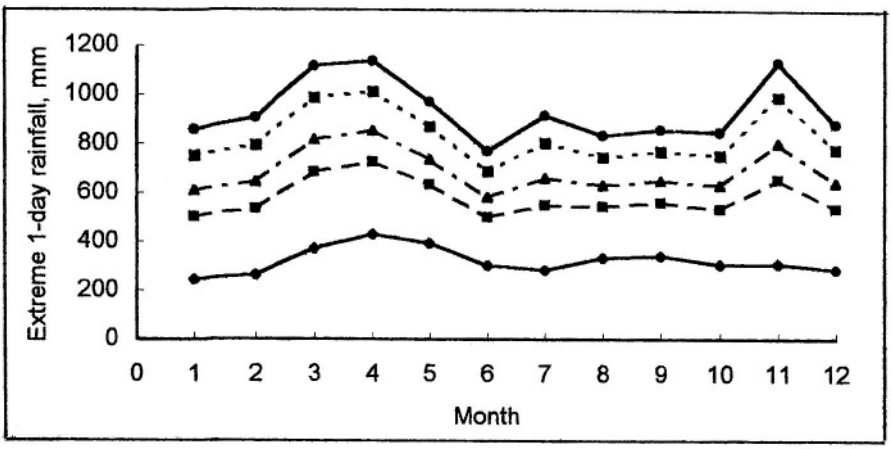

Figure 3.23- Extreme 1-day rainfalls in Kisumu, Kenya, for all months of the year. The graphs, from top to bottom, are for return periods of 100, 50, 20, 10 and 2.33 (mean) years

In an effort to investigate the phenomena of persistence of the states of wetness and dryness in some West African countries, Afouda Abel (1989) used a linear discrete model based on the usual Markov chain For the operation of the model he used rainfall data of 13 stations over a period of 20-45 years to derive the marginal and conditional probabilities of having 1, 2, 3 and 4 consecutive rainy days The same procedure was repeated to get the corresponding probabilities for dry days. From principles of statistics, the sum of the two marginal probabilities must equal 1, but not the sum of a number of consecutive rainy days and the same number of consecutive dry days. Table 3.9 gives the results obtained for 8 stations

Last, but not least, we like to end this section by reviewing the hydrological practices in Zimbabwe of recording daily rainfall According to the Department of Meteorological Services (1981), a month is too long to show clearly the variations in the incidence of rainfall, and yet the fine details given by daily falls tend to be excessive. "Since rain tends to occur in spells of a few days' duration followed by dry spells lasting a few days, there is a merit in using a five-day period as a unit for rainfall incidence" As such, the rainy season can be better described by 42 pentads than by 7 months, and less complicated than by 210 days. The probability of having a rainy pentad during the wet season can be obtained from the relative frequency of rainy pentads. Table 3.10 has been prepared for Harare, the Capital of Zimbabwe, based on the data published by the said department. From this table it is clear that the probability of giving pentad no. 68 a value not exceeding 10 (80 days) is not less than 70%.

As pentads are linked to fixed calendar dates, they do not always coincide with wet and dry spells, and a threshold value is needed in order to classify a particular pentad as 'rainy' or 'dry'. The criterion in use is to define the middle pentad of a group of three pentads as rainy if there is at least 8 mm in each of at least two pentads in the group, and the total rainfall in all three pentads is at least 40 mm. The frequency distribution of rainfall in the rainy season pentad-wise at Harare using the 1901-61 data has been approximated by a compound distribution. This is composed of two normal distributions, one is centered at pentad 68 with a standard deviation of 4.8, and the second centered at pentad 7 with a standard deviation of 6.8.

Table 3.9- Marginal and conditional probabilities of rainy and dry days for some West African countries (Afouda Abel, 1989)

Country/	State: rain				State: dryness			
Station	a_1	b_{11}	b_{111}	b_{1111}	a_0	b_{00}	b_{000}	b_{0000}
Benin (1961-80)								
Cotonou	0.25	0.36	0.45	0.53	0.75	0.79	0.81	0.84
Kandi	0.24	0.51	0.56	0.57	0.76	0.84	0.89	0.92
B. Faso (1955-82)								
Goromo-Goromo	0.09	0.21	0.26	0.37	0.91	0.92	0.93	0.94
Niger (1922-65)								
Niamey	0.13	0.31	0.41	0.52	0.87	0.90	0.92	0.94
Zinder	0.12	0.31	0.41	0.52	0.86	0.91	0.93	0.95
Senegal (1921-65)								
Kaolack	0.16	0.33	0.57	0.62	0.84	0.91	0.94	0.95
Mali (1925/33-65)								
San	0.16	0.34	0.41	0.46	0.84	0.88	0.91	0.93
Nioro du Sahel	0.14	0.36	0.38	0.41	0.86	0.90	0.92	0.94

Explanation

a_1 and a_0 are the marginal probabilities of rainy and dry days respectively.

b_{11}, b_{111} and b_{1111} are the conditional probabilities of having 2, 3 and 4 consecutive rainy days, respectively. Likewise, b_{00}, b_{000} and b_{0000} are the *conditional probabilities of having 2, 3 and 4 consecutive dry days, respectively.*

Table 3.10- Percentage relative frequency (approximate probability) of a certain pentad in the wet season being rainy, Harare, Zimbabwe, 1901-1961

Pentad no.	56	57	58	59	60	61	62	63	64	65	66	67	68	69
Rel. frequency*	3	3	7	10	12	17	28	37	28	33	43	58	73	77
Pentad no.	70	71	72	73	1	2	3	4	5	6	7	8	9	10
Rel. frequency*	80	80	82	77	73	70	77	77	75	78	82	83	70	72
Pentad no.	11	12	13	14	15	16	17	18	19	20	21	22	23	24
Rel. frequency*	67	62	60	47	52	45	33	25	22	15	8	3	8	3

** The tabulated relative frequencies are in percent .*

3.4- Short Duration Rainfall (less than 24 hours) and Intensity-Duration Frequency Relationships

Rainfall depth refers to the total amount of rain falling at a certain point during a particular rainstorm. This parameter is expressed in length units such as mm or cm. The rate of fall of rain during a certain period of time is called the intensity of rain. The intensity is given in unit of length per unit of time such as $mm\ h^{-1}$, $mm\ min^{-1}$ or any other appropriate units. If this rate is computed for the full duration of the storm, it is called then the mean rainfall intensity. This is usually less than the maximum intensity, which occurs in a relatively short period. The duration is the period of time during which rain falls, expressed in min (minute), h (hour) or day (d). The greater the intensity of rainfall, in general, the shorter length of time (duration) it lasts. The frequency of occurrence (absolute) is the number of times a certain event occurs in a total number of times of occurrence and non-occurrence. The relative frequency of occurrence is simply the ratio of number of occurrences divided by the sum of occurrences and non-occurrences. In the analysis of several hydrological and meteorological data, one often talks about probabilities of exceedance and non-exceedance. The probability of exceedance is the limiting value of the relative frequency, having a certain value equaled or exceeded, in an infinitely long lapse of time. Both probabilities of exceedance and non-exceedance are complementary, i.e. their sum is equal to 1. As a common practice in hydrological sciences the term return period is used. The return period is simply the reciprocal of the probability of occurrence. In this section we shall denote the depth of rain by *R,* rainfall intensity by *i*, duration of rainstorm by *d* and return period by *Tr.*

Before we embark on a discussion of the intensity-duration frequency relationship it may be of interest to present some of the greatest observed rain depths in Africa, which have been collected by Paulhus (1965). Table 3.11 includes these depths and the corresponding average rainfall intensities.

The analysis of continuous rainfalls, usually lasting for periods of less than 1-day, entails the abstraction of rainfall depths over specified durations. The standard relationship between the parameters of the rainstorm often used is:

Table 3.11- Africa's greatest observed rainfall depths (as of 1965, according to Paulhus, 1965)

Duration	Depth, mm	Intensity, mmh^{-1}	Location	Date
9 h	1,086.9	120.8	Belouve, La Reunion	28-29 Feb, 1964
12 h	1,340.1	111.7	Belouve, La Reunion	28-29 Feb, 1964
18.5 h	1,688.8	91.3	Belouve, La Reunion	28-29 Feb, 1964
24 h	1,869.9	77.9	Cilaos, La Reunion	15-16 Mar, 1952
2 d	2,500.0	52.1	Cilaos, La Reunion	16-17 Mar, 1952
7 d	4,110.0	24.5	Cilaos, La Reunion	12-19 Mar, 1952

$$R = \frac{at}{b+t} \qquad \text{for a few min} < t < \text{2-3 h} \qquad (3.13)$$

Belloum (1993) used Eq. (3.13) for long rains (> 5 h) at Azzaba and short rains (< 5 h) at Bouati Mahmoud, both in northern Algeria. He obtained four sets of values for a and b at each location corresponding to return periods of 1, 2, 5 and 10 years. For example a = 171 and 111, and b = 3 and 2 for Azzaba and B. Mahmoud respectively. Unfortunately, the limited amount of available data did not permit extrapolation to a return period greater than 10 years. Figures 3.24_a and 3.24_b show the corresponding sets of curves.

Classical studies of short rainfalls (not exceeding 120 min) have resulted in a general formula, which gives the intensity i in terms of the return period and rainstorm duration as:

$$i = k(Tr)^c t^d \qquad (3.14)$$

The three parameters, k, c and d vary from one location to another, and so from one storm to another. Depending on the number of storms in the record and the units used, each parameter is evaluated and the mean found. Taking the logarithms of the two sides of Eq. (3.14) often linearizes the relationship.

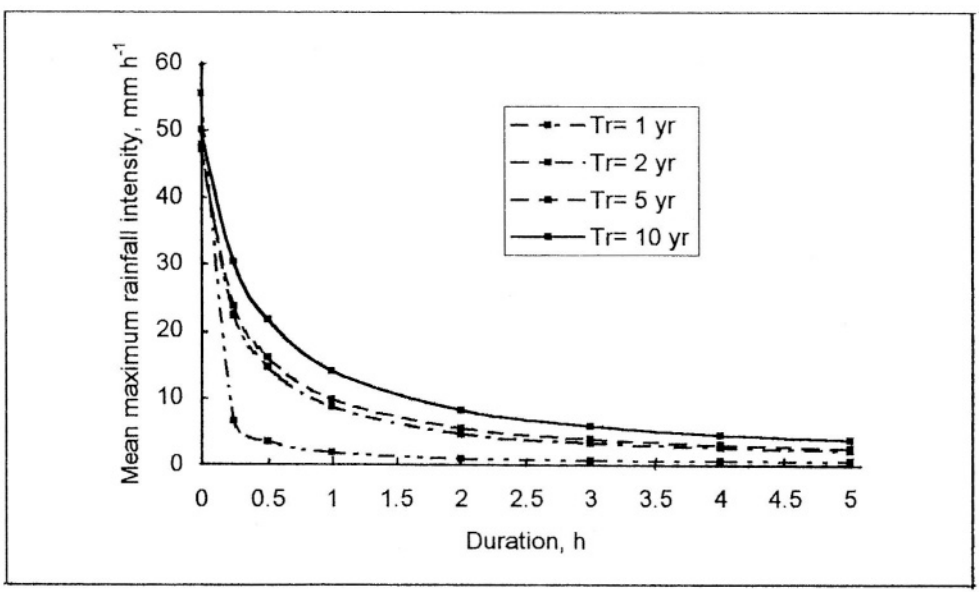

Figure 3.24_a- Mean maximum rainfall intensity for long rains at Bouati Mahmoud, Northern Algeria (from Belloum, 1993)

The intensity of rains recorded for three years at Lubumbashi, Congo (Kinshasa), were studied and diagrams representing intensity-duration-probability and intensity-duration-frequency relationships have been drawn **Figure 3.25$_a$** shows four curves prepared for return periods of 1, 2, 5 and 10 years and rainfall durations of 10, 15, 30 min, 1, 2, 3, 6, 12 h and 1, 2, and 4 d. Likewise, the maximum intensity-duration-frequency relationship for Lubumbashi (station no. 194, wet tropical climate) was included in that study. The curve in **Figure 3.25$_b$** is compared to curves obtained for Mediterranean and subtropical climates (Kanutanda, 1979). From this figure, it is clear that curve 1 for Idenau, Cameroon, compared to curve 2 for Lubumbashi, Congo, gives lower intensities for durations up to 30 min, beyond which, the ordinates of curve 2 fall well below the ordinates of curve 1. Both curves 1 and 2 overlie curve 3 for the Mediterranean coast of Algeria.

The linear form of Eq. (3.14) can be written as:

$$\log i = \log k + c \log Tr + d \log t \qquad (3.15)$$

From Eq. (3.15), $k = i$ when Tr and t are equal to 1. The slope of the line = change in log i per log-cycle of t. In some cases, however, the slope varies to such extent that it is necessary to provide a break in the line

The ratios of 1-h rainfalls for selected return periods to the 1-h, 10-yr rainfall are consistent for each return period. Similarly, the ratios of the 1-h

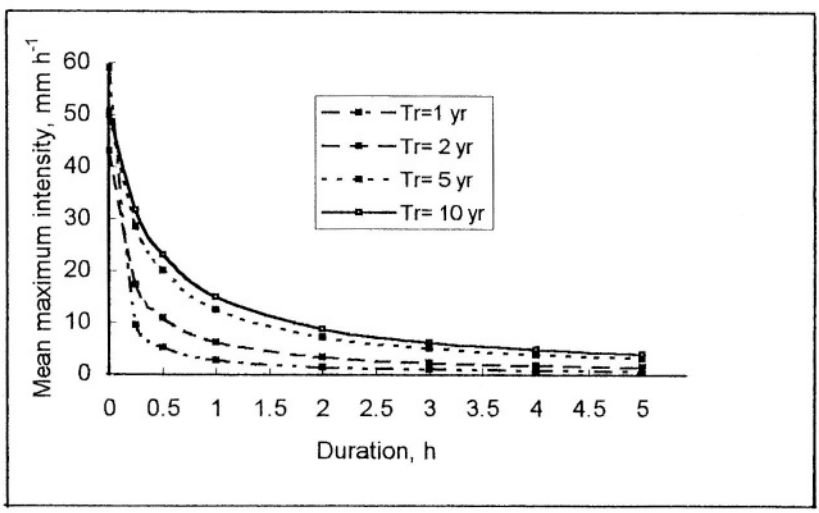

Figure 3.24$_b$- Mean maximum rainfall intensity for short rains at Azzaba, northern Algeria (from Melloum, 1993)

rainfalls for selected return periods to the 1-h, 2-yr rainfall can also give a good constant relationship, though with greater variability (Shaw, 1983). These observations help the designer to get a fair estimate for missing rain depths whenever the record is short or inadequate.

When the extreme intensities of rainfall in the catchments of the Equatorial Lakes were plotted versus the corresponding durations on log-log graph paper, the points were generally found aligned in straight lines characteristic of the different months and stations (WMO, 1974). This indicated that for durations between 15 min and 24 h the relationship is adequately represented by:

$$(i_{mx})_t = i_o t^{-\alpha} \tag{3.16}$$

where $(i_{mx})_t$ is the maximum intensity in mm h^{-1} during a time interval of t min, t is the duration in min and α is the damping or attenuation rate of the intensity. As an example, Figure 3.26 shows the frequency extrapolation nomogram for extreme rainfall intensities at Gulu station, Uganda (WMO, 1974).

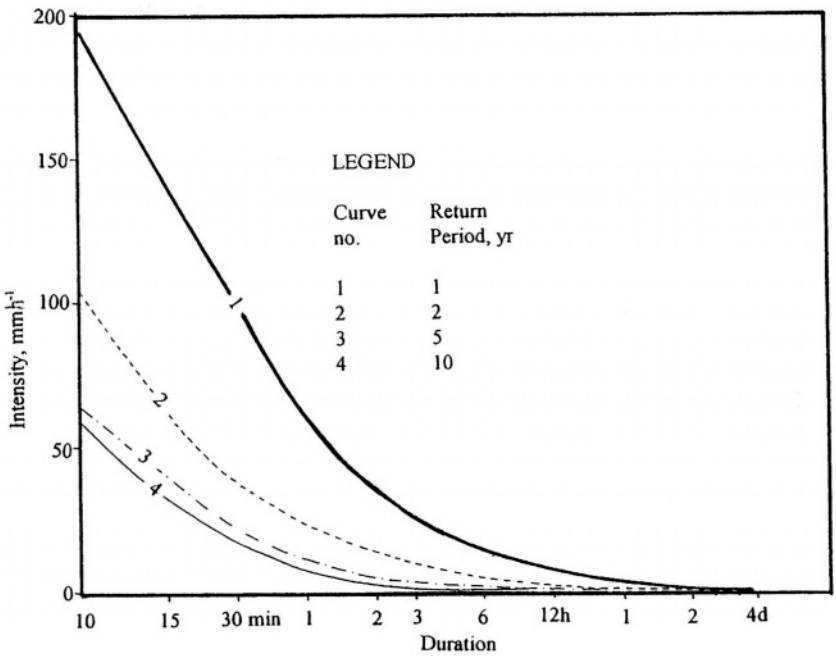

Figure 3.25.- Intensity-duration-frequency curves for Lubumbashi, Congo Kinshasa (from Kanutanda, 1979)

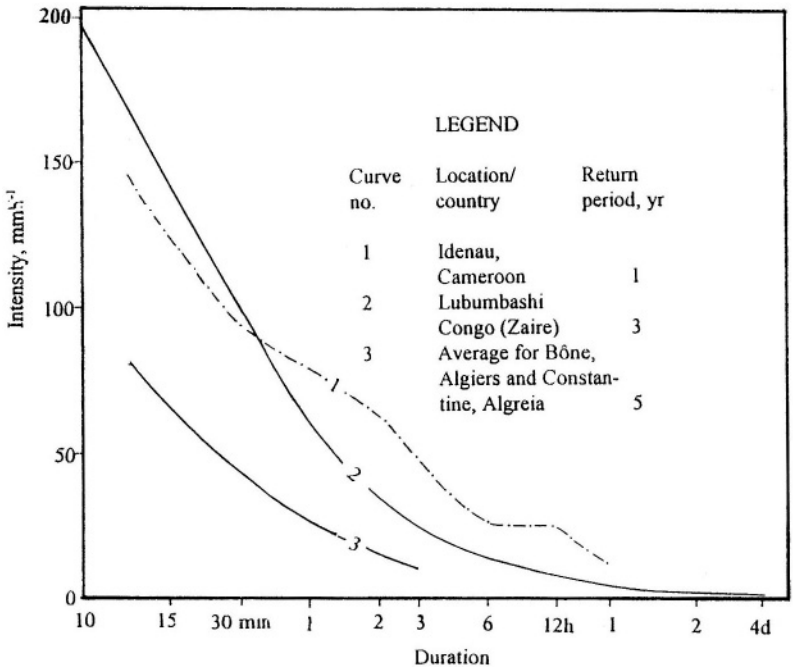

Figure 3.25$_b$- Intensity-duration curves for Idenau, Cameroon, Lubumbashi, Congo (Kinshasa), and Bône, Algiers and Constantine, Algeria (from Kamutanda, 1979)

The bulk of the rainfall in Zimbabwe occurs in the form of showers and thunderstorms, which are mostly of high intensity and short duration. However, low-intensity drizzle and rain occur sufficiently often to be a noticeable feature of the climate in certain parts of the country. The usual types of recording rain gauges show time and depth of rain, from which the greatest amount of rain falling in specified time intervals can be obtained. The analyses of rainfall data for duration from 15 to 120 min have led to the following relationship (Climate Handbook of Zimbabwe, 1981):

$$i = \frac{2{,}050\log(TrR) - 3{,}000}{t + 20} \qquad (3.17)$$

where, R is the annual rainfall in mm, Tr is the return period in year and t is the duration of fall in min. So, for Tr = 100-yr and t = 30-min and R = 800 mm, Eq. (3.17) yields intensity i of about $141\,\text{mm h}^{-1}$.

For extreme rainfalls the return period Tr in Eq. (3.17) is changed to $T'r$, which is given by:

$$T'r = \frac{1}{1-(1-p)^{1/Tr}} \qquad (3.18)$$

Supposing that *p,* the outside probability of occurrence, is 0.05 (1 in 20 chance of occurrence) and using the data in the previous example, Eq. (3.18) gives *T'r* as 995 yr. This value upon substitution in Eq. (3.17) yields an extreme intensity of about 223 mm h^{-1}. This figure is about 58% greater than the standard intensity found from Eq. (3.17) without changing *Tr*. As such, the Department of Meteorological Services of Zimbabwe is using a number of pairs of sets of curves; one for the standard intensity and the second for the extreme rainfall intensity, referred to as safe curves. Each set consists of 5 curves, 1, 2,5, 10, 20 and 30 years return period. Pairs of sets of curves are available for different annual rainfalls. The pair shown in Figure 3.27 is for 800 mm annual rainfall.

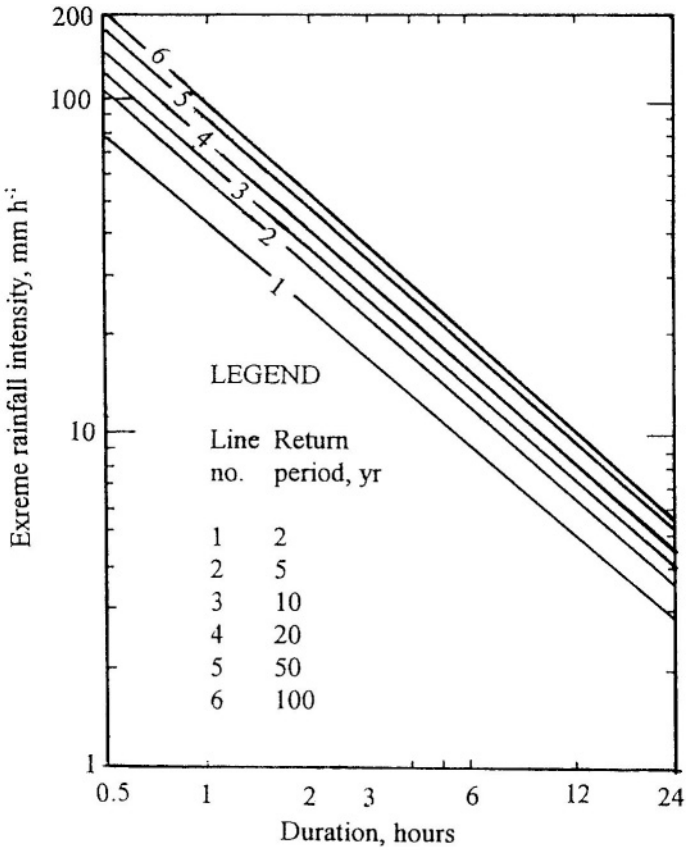

Figure 3.26- Frequency interpolation nomogram for extreme intensities of rainfall in the catchments of the Equatorial Lakes, Gulu station Uganda (WMO, 1974)

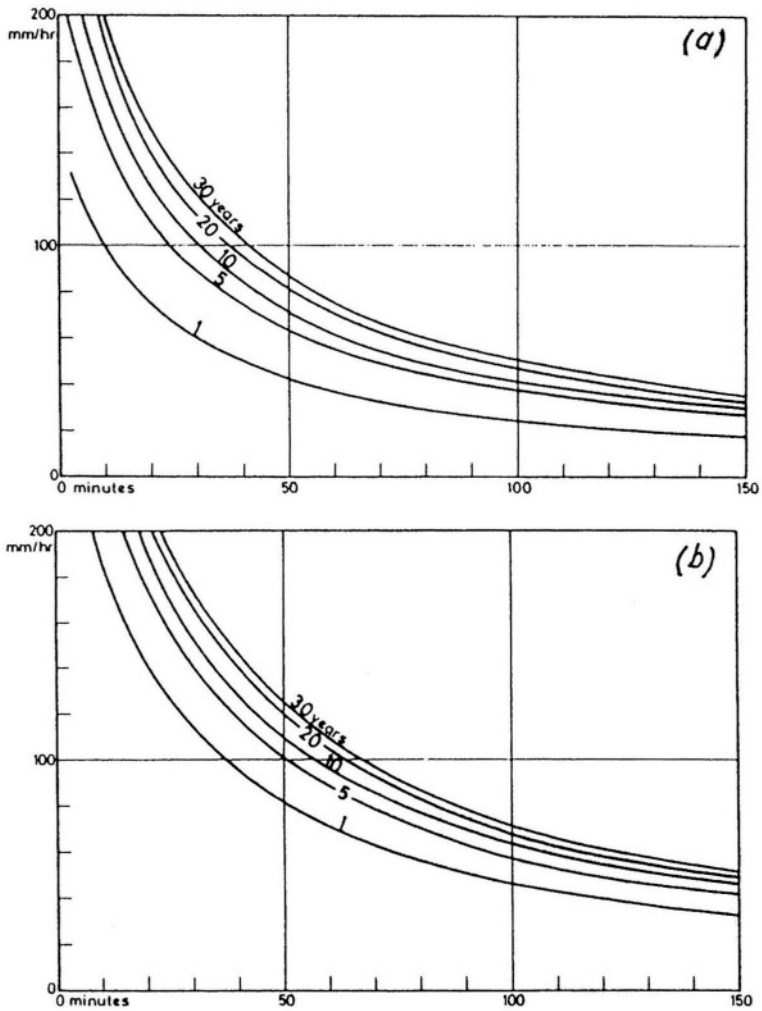

Figure 3.27- Intensity-duration-frequency curves for Zimbabwe, (a) standard curves and (b) safe or extreme intensity curves, both for 800 mm annual rainfall (redrawn from Climate Handbook of Zimbabwe, 1981)

Oyebande (1982), upon studying the derivation of rainfall intensity-duration-frequency relationships for Nigeria, used 35 stations representing 11 rainfall zones. To illustrate the extent of the inadequacy of the data from those stations, he reported that the length of the record exceeded 25 years for 3 stations only and 20 years for 18 stations out of 35 stations used in the study. For engineering designs as well as other purposes it is quite often necessary to have reasonable estimates of design values for return periods of 50 years or

more. From the then available data, he got 10-yr, 10-min and 30-min falls, 2-yr, 15-min and 60 mm falls, and 25-yr, 1-h and 24-h falls for each of the 11 zones of the country. The Gumbel extreme value Type 1 distribution was fitted to the annual maxima series to obtain the intensity-duration-frequency relationships. The distribution parameters α and β were obtained for each zone and durations of 0.2, 0.4, 1, 3, 6, 12 and 24 h. These estimates were then substituted in Eq. (3.19):

$$y = \alpha(x - \beta) \tag{3.19}$$

where y is a reduced variate given by:

$$y = -\ln[\ln(Tr / Tr - 1)] \tag{3.20}$$

and x is the estimate of the rainfall intensity given the return period Tr. As an example, Eq. (3.20) gives y as 4.6 and 3.9 for Tr = 100 and 50 years, respectively. Assuming that α = 0,04 and β = 120, Eq. (3.19) yields x = 235 and 217.5 mm h^{-1} respectively. Figure 3.28 is an example of the intensity-duration-frequency relationship for Zone II in Nigeria, as represented by Lagos.

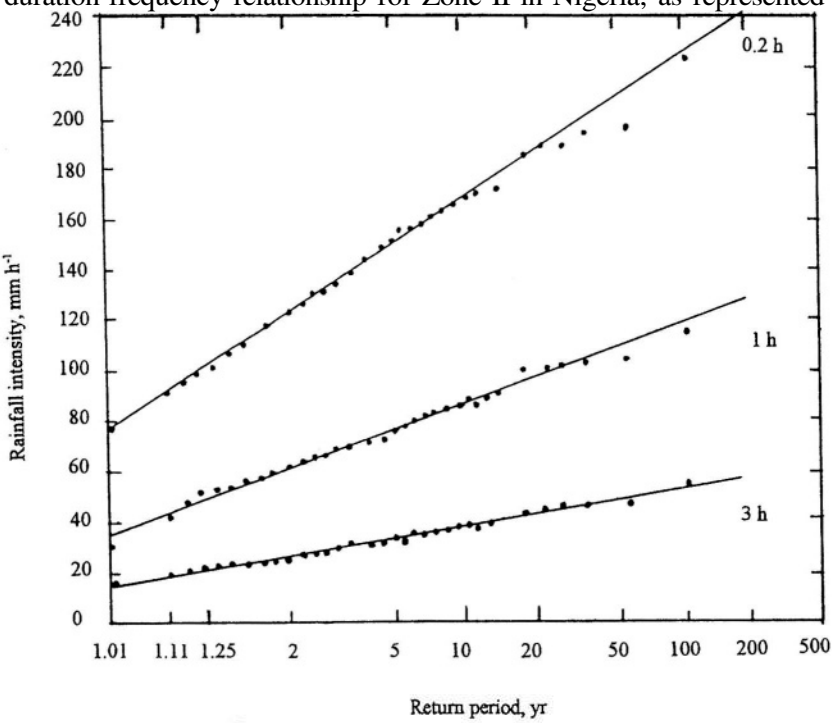

Figure 3.28- Rainfall intensity-duration-frequency relationship for Zone II in Nigeria, represented by Lagos (from Oyebande, 1982)

CHAPTER 4

EVAPORATION

4.1- Definitions and Background

Evaporation can generally be defined as a process by which a liquid or solid is transformed into vapour. Although there is always a continuous exchange of water molecules to and from the atmosphere, the hydrologic definition of evaporation is restricted to the net rate of vapour transport to the atmosphere. Penman (1948) defined open water evaporation as "The amount evaporated in unit time by a shallow layer of open water, for which reflection of radiation is determined by the surface only, and sufficiently extensive for edge effects to be negligible, under the atmospheric conditions measured above it". Stigter and Kisamo (1978) have criticized this definition on the grounds that it does not apply to lake evaporation, since a lake is not a shallow layer of water.

By evaporation, we are here referring to evaporation from open water systems, like natural lakes and man-made pools and reservoirs, flowing streams, bare soil with water tables at or close to the land surface, and impervious surfaces like roofs and roads. Evaporation from vegetated surfaces, forests and woodland, where evaporation is accompanied by transpiration, referred to as evapotranspiration, will be dealt with in the next chapter. The total annual volume of evaporation and evapotranspiration has been estimated for Africa by L'vovich (1974/79) as $16.555*10^{12}$ m^3 or about 80% of the total precipitation.

According to Wisler & Brater (1957), evaporation is ranked under the category of water losses, which are defined as the difference between the total precipitation and total runoff from a given area. African river basins contain a considerable number of storage reservoirs added to an extensive network of streams, canals, and natural lakes all contributing to the quite extensive amount lost annually by evaporation.The annual loss of water by evaporation from Lake Victoria alone is in the order of $100*10^9$ m^3 and from the High Aswan Dam in Egypt is in the range $10\text{-}11*10^9$ m^3. These figures are enough to show the importance of determining the amounts of evaporation as accurately as possible.

The change of state from liquid to vapour requires an exchange of approximately 600 cal for each gram of water evaporated. If the temperature of the surface is to be maintained, these large quantities of heat must be supplied by radiation and conduction from the overlying air or at the expense of energy stored below the surface (Linsley et al, 1958). As such, evaporation is basically influenced by the prevailing climate. The main climatological factors affecting the rate of evaporation are:

radiation, atmospheric temperature and relative humidity, wind speed and direction, and degree of cloudiness. All these factors have already been discussed in Chapter 2 Monthly and annual values of these factors for selected stations are included in Appendix A.

The factors affecting evaporation can be grouped under two distinct classes. These are the meteorological factors affecting the process and the physical nature of the body containing the water. Measurement and/or estimation of evaporation can be obtained using different methods. Examples of these methods are the water balance, heat budget, bulk aerodynamic, atmometers, pans and tanks, and evaporation models. The methods in frequent use for measuring and/or estimating evaporation from open water systems in Africa are briefly reviewed in the next sections and the results obtained are tabulated and discussed

4.2- Instrumental Measurements of Evaporation

Although the instrumental measurements are not so simple and straightforward as for rainfall, it is a compensating factor that evaporation quantities are less variable from one season to another, and therefore more easily predicted than rainfall amounts (Shaw, 1983). Measurement of evaporation, mostly the evaporative capacity of the air rather than evaporation itself, began quite sometime ago. Several instruments have been in use in Africa, where every now and then a more recent instrument replaces an old one.

In the course of the 20^{th} century, the widely used instruments have been the Wild. Piche, sunken pans, tanks, USWB Class A pan and the Russian GGI-3000 tank. At present, the evaporimeter in common use is the Class A pan.

4.2.1 Piche atmometer- It consists of a calibrated glass tube 225 mm long with a closed end, internal diameter of 11 mm and external diameter of 14 mm. A circular disc of blotting paper 32 mm in diameter is held against the open end of the tube by a spring fitted with a disc and a collar (Figure 4.1$_a$). The tube is filled with water and the loss of water in $cm^3\ d^{-1}$ is a measure of the evaporation rate. The total evaporation surface (two sides) is $1{,}300\ mm^2$ The Piche atmometer is frequently installed with the evaporating surface at a height of 1.22 m (4 ft) above the ground surface and placed in a screen. This atmometer used to be installed in many of the former British colonies.

4.2.2 Wild evaporimeter- This is a small pan 17.8 cm in diameter (surface area = 250 cm^2) and 25 mm depth. It is set on a weighing balance equipped with a recording chart, which turns one revolution every 24-h. The equipment is placed on a platform with a roof cover, but freely exposed to air movement The surface of the pan is at height of 2 m above the ground.

4.2.3 Colorado sunken pan- This is a 92 cm (3 ft) square and 46 cm (1.5 ft) deep pan.The pan is made of galvanized iron and set in the ground with a rim 50 mm above the ground surface. The water level in the pan is usually maintained at or slightly below the ground level (Figure 4.1$_b$). Many of the former French colonies are, or used to be, equipped with this pan.

4.2.4 Kenya ground pan- This evaporimeter is made of galvanized iron, 1.22 m (4 ft) in diameter and 35.5 cm deep. The inside of the pan is painted with bitumastic and screened with 25 mm mesh chicken wire netting. The pan is mounted on timber supports and placed above the ground surface. The Kenya pan has been installed by the East Africa Meteorological Department (EAMD) in what currently are known by Uganda, Tanzania and Kenya (Figure 4.1$_c$).

4.2.5 Symons sunken pan- This pan is square in geometry with a side length of 1.83 m (6 ft) and 0.61 m (2 ft) in depth. This pan is installed in the ground with the rim 76 mm above the ground level. The Symons pan used to be operating in the countries of the Union of South Africa, Zimbabwe, Zambia, Lesotho Botswana, Swaziland and South Africa.

4.2.6 Nigeria ground pan- This is a rectangular pan 1.28m (4 ft) long by 0.92 m (3ft) in width and 0.43 m in depth. The inside of the pan is painted black. It is placed in a timber construction on the ground surface. This pan has been in use in Nigeria for quite sometime.

4.2.7 USWB Class A ground pan- The pan is cylindrical in form, 1.23 m (4 ft) in diameter, and 255 mm (10 inches) in depth. It is usually made of galvanized iron and mounted on a wooden frame platform placed on the ground. The pan is filled to within 50 mm of the rim (Figure 4.1$_d$). Evaporation measurements are made by a hook gauge or by refilling to a fixed point. The Class A pan is used for measuring evaporation practically everywhere.

4.2.8 The Sudan tank- It is a simple cylindrical tank 3.65 m (12 ft) in diameter and 1.22 m (4 ft) sunken in the ground.

4.2.9 GGI-3000 tank- This is a cylindrical tank with a conical base made of galvanized sheet iron. The diameter of the cylinder is 61.8 cm; the depth at the wall is 60 cm and 68.5 at the center (Figure 4.1$_e$). The tank is sunk in the ground, with the rim approximately 76 mm above ground level.

4.2.10 Comparisons between evaporation measurements using different instruments - The relationships between Class A pan and other evaporimeters as obtained from a number of locations in Africa are as follows (WMO, 1966):

Figure 4.1$_a$- Piche evaporimeter

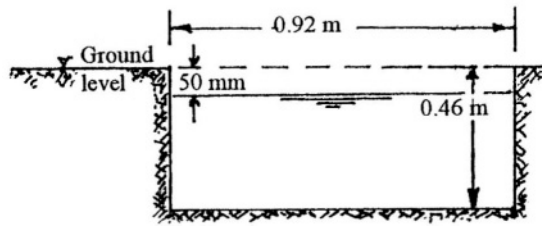

Figure 4.1$_b$- Sunken evaporation pan

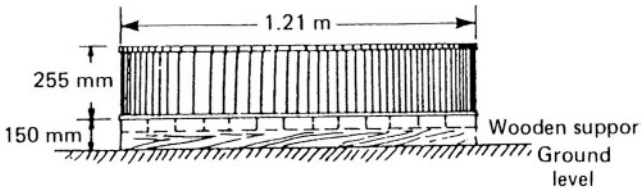

Figure 4.1$_c$- US Class A pan

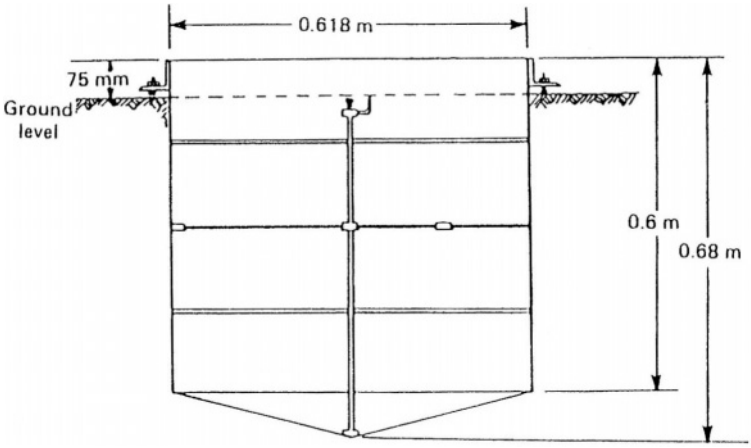

Figure 4.1$_d$- USSR GGI-3000 evaporation tank

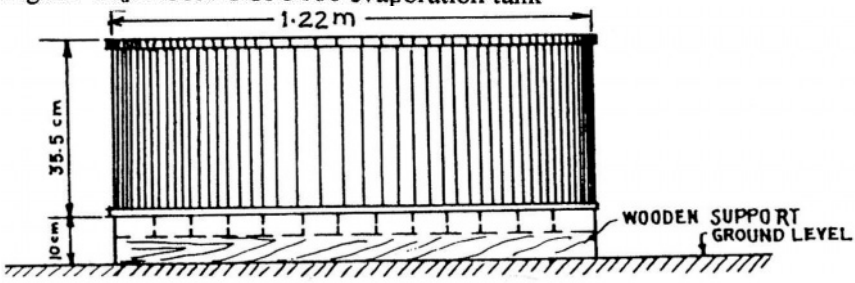

Figure 4.1$_e$- Kenya evaporation pan

i- East African Territories

Class A pan (mm d^{-1}) = 0.87 Piche +610 mm y^{-1}

ii- Egypt. Class A pan evaporation/ Piche evaporation

Piche in free air:	mean,	0.53-0.74	avg. 0.623
	maximum,	0.57-0.79	avg. 0.672
	minimum	0.41-0.71	avg. 0.570
Piche in screen:	mean,	0.86-1.24	avg. 1.020
	maximum,	0.91-1.26	avg. 1.102
	minimum	0/70-1.21	avg. 0.923

(December and January are months of the minimum, and July and August are the months of the maximum evaporation)

iii- Kenya

Class A (unscreened, mm d^{-1}) = 1.3 Kenya pan (screened) + 0.51 mm d^{-1}

Number of days of record = 1384 (4 years), correlation coefficient = 0.95

Ratios (computed over 2 years)

Class A (unscreened)	= 100	
Class A (screened)	= 86	(84-88)
Class A (painted and screened)	= 84	(82-86)
Kenya (unscreened)	= 95	(only few months of record)
Kenya (screened)	= 71	(69-74)
Kenya (painted and screened)	= 69	(65-72)

iv- The Sudan: The results obtained from the comparison carried out at the Khartoum Observatory of a 3.66 m (12-ft) pan with a Class A pan, as well as with Piche, Penman and Kohler formulas are listed in Table 4.1. The evaporation measuring techniques formulas developed by Penman and Kohler will be discussed in a subsequent section. The remarkable result one can draw from this comparison is that the formula of Kohler yields evaporation amounts very close to those measured using the 12-ft pan.

The average decadal evaporation values using two Piche instruments, one installed at the shore of the lake formed by the storage reservoir on the Blue Nile at Sennar in the Sudan (P_{sh}) and the other placed in a floating station in the lake itself (P_l) is shown in Figure 4.2. Abdulai (1989) found the regression relation between the two sets of Piche evaporation readings, mm d^{-1}, for the period February-June 1988 as:

$$P_l = 0.23 + 0.93 P_{sh} \qquad (4.1)$$

with a correlation coefficient of 0.96

v- Uganda: Comparative measurements of three evaporimeters: USSR 20 m^2 tank (5

m in diameter, 2 m in depth, buried in the ground to within 75 mm of its rim height); USSR GGI 3000 and USA Class A pan, both described earlier, have been collected from different stations in 13 countries and analyzed statistically (WMO, 1976). The results of the regression analysis performed on the measurements in Entebbe, Uganda are listed in Table 4.2. A comparison between the average readings of two Piche instruments and the readings of a tank evaporimeter, all placed in Namulonge Cotton Research station, Uganda, is shown graphically in Figure 4.3. The scatter of points in this particular case is so enormous that any attempt to relate the two sets of evaporation to each other does not make any sense.

Table 4.1- Ratio of measured 12-ft pan evaporation to measured/estimated evaporation using other devicesat Khartoum, The Sudan (WMO, 1968)

Month, average (1960-61)	12-ft pan/ Class A pan	12-ft pan/ Piche	12-ft pan/ Penman	12-ft pan/estimated evaporation*
January	0.675	0.505	1.215	1.065
February	0.630	0.465	1.185	1.000
March	0.645	0.490	1.195	1.010
April	0.620	0.475	1.265	0.975
May	0.615	0.505	1.365	0.980
June	0.640	0.555	1.220	0.990
July	0.650	0.660	1.015	0.960
August	0.695	0.615	1.050	1.015
September	0.690	0.620	1.185	1.025
October	0.680	0.540	1.280	1.030
November	0.650	0.475	1.210	0.990
December	0.650	0.485	1.190	1.005
Year	0.645	0.505	1.200	1.000

Explanation : Estimated evaporation is the Class A pan evaporation correctedfor he for heat exchange through sides and bottom of the pan (Kohler)

Table 4.2- Statistical analysis of evaporation relationships under all rainfall conditions for Entebbe, Uganda (WMO, 1976)

Y	X				X				X			
Measured evaporatior	GGI evaporimeter b	a	r	cv*	Class A pan b	a	r	cv	20 m^2 tank b	a	r	cv
20 m^2 tank	0.75	0.2	0.89	5	0.62	0.62	0.84	6	1	0	1	0
Estimated open water loss	0.58	1.4	0.78	5	0.46	1.78	0.71	6	0.57	1.94	0.65	7

Explanation

Y and X are related together by the linear regression relationship Y = a +b X, where, Y and X and b are expressed in mm d^{-1}, r = coefficient of correlation and cv = coefficient of variation around regression line, % of the mean of Y's.

vi- South Africa: The regression relation between screened and unscreened US Class A evaporation pans has been studied using monthly evaporation data from certain meteorological stations in South Africa. The relationship obtained using the data of station at Lydenburg ($\phi = 24^{o}\,54'$ S, $\lambda = 30^{o}\,26'$ E) is shown graphically in Figure 4.4.

vii- Zambia/Congo (Kinshasa): Evaporation has been observed in the period 1968-1969 in the Luano catchments, located along the boundary between Zambia and Congo (Kinshasa). A comparison between a US Class A pan (galvanized) and a pan made of fiberglas was carried out as reported by Balek (1977). By using fiberglas, the influence of the sun on the heating and cooling of the material has been reduced. As such, the data obtained from both pans differ significantly, as can be seen in Table 4.3. The tabulated data show that the largest difference, up to 30%, occurred in October and did not exceed 20% in the rest of the months. The difference between the annual evaporations in the two sets of data is limited to about 17%. This example clearly shows that next to the size and colour of the evaporation pan, the material of construction of the pan plays an important role in the estimation of evaporation.

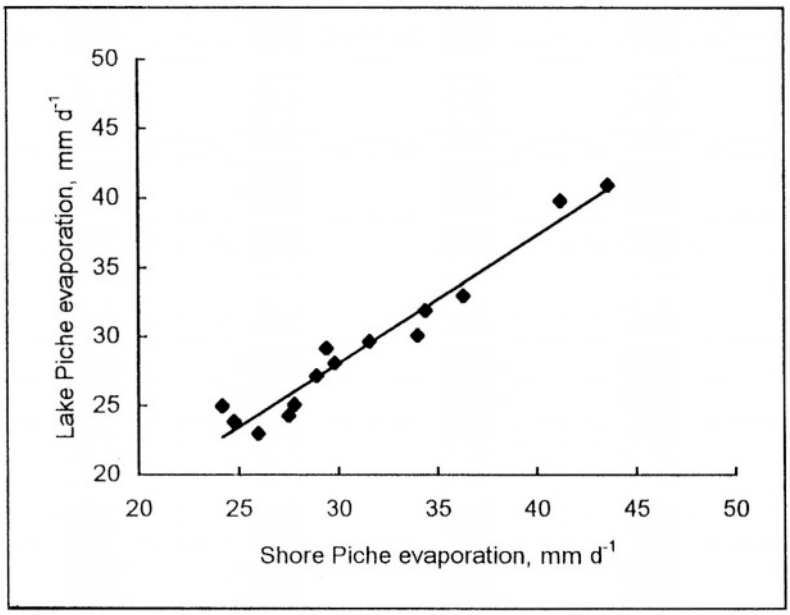

Figure 4.2- Regression relation between lake Piche evaporation and shore Piche evaporation, Sennar reservoir on the Blue Nile, the Sudan (Abdulai,1989)

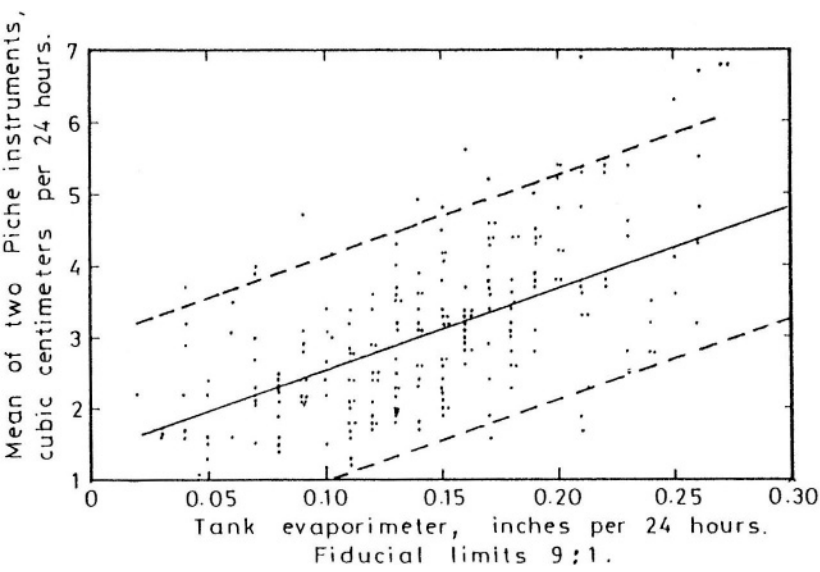

Figure 4.3- Comparison of readings of Piche and tank evaporimeters at Namulonge Cotton Research Station, Uganda (Olivier, 1961)

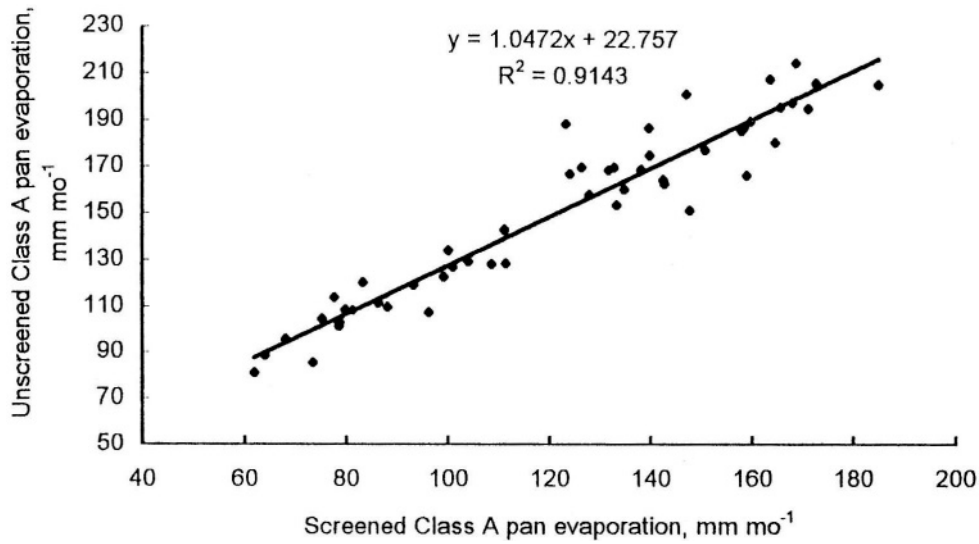

Figure 4.4- Regression relation between monthly measurements of screened and unscreened Class A evaporation pans at Lydenburg Station, South Africa, for the period August 1966- September 1970

Table 4.3- Observed evaporation, expressed in mm mo^{-1}, at the Luano catchments (12° 34' S, 28° 01' E) near Lubumbashi, on the boundary between Congo (Kinshasa) and Zambia (cited in Balek, 1977)

Month	Measured evaporation		Month	Measured evaporation	
	Pan (1)	Pan (2)		Pan (1)	Pan (2)
October	227.5	170.4	April	136.7	127.7
November	135.9	120.2	May	138.5	122.6
December	129.9	106.4	June	120.0	102.2
January	111.1	99.3	July	135.1	117.0
February	127.9	103.2	August	173.5	155.0
March	127.4	115.1	September	162.5	161.5
Total				1757	1502

Explanation

Pan (1) = galvanized Class A pan and Pan (2) = fiberglas pan

4.2.11 Concluding remarks- The above mentioned comparative measurements using different evaporimeters show clearly the difficulty in depending on any instrumental measurement without having a proper means to convert it to its equivalent of evaporation from a large body of water. The size, setting, exposure, colour and material of the evaporimeter are the basic items affecting the magnitude of the conversion factor.

The current literature on free water evaporation suggests that evaporation estimates from tanks of a size ranging between 20 and 100 m^2 can be accepted as standard, i.e. very close to lake evaporation. Since tanks of such sizes are too bulky and not easy to maintain, the use of smaller evaporimeters can be recommended together with an appropriate conversion factor. As early as 1931, Hurst & Philips recommended considering evaporation from a 2 m square floating tank as a close approximation to evaporation from an extended water surface. They recommended also that evaporation from the said pan be taken as equal to 0.5 times evaporation from the Piche instrument and 0.88 times the evaporation from a 1 m square floating tank (Hurst & Philips, 1931). The Irrigation Department of the Sudan used to regard the lake evaporation as 0.50-0.56 times the Piche evaporation. Linsley et al. (1958) found that the annual lake evaporation to Class A pan ratio or coefficient falls in the range of 0.60-0.82, with a recommended mean of 0.70. Part-year coefficients are more variable because energy storage in the lake can be appreciably different at the beginning and end of the period. So, if the size is the only factor considered the relationship between the size of the evaporimeter and the ratio of evaporimeter to lake evaporation can generally be described as shown in Figure 4.5.

Pans are usually made of galvanized steel. Measurements from white painted pans have shown to be 82.7% of the corresponding measurements from new galvanized pans, whereas the percentage evaporation for black painted pans easily reaches 105.7%. An example of the effect of the material has already been discussed.

galvanized pans, whereas the percentage evaporation for black painted pans easily reaches 105.7%. An example of the effect of the material has already been discussed.

4.3- Estimation Methods

4.3.1 The water balance method- Estimation of evaporation from an open water system, like a lake or reservoir, depends largely on the availability and reliability of certain data. These comprise the direct precipitation on the system, tributary flow and surface runoff and/ or surface water extraction or diversion from the system, groundwater inflow to and from the system, and the volume of water in storage at the beginning and end of the balance period (Morton, 1979). In certain situations, e.g. where errors in measuring inflow, outflow and storage are large compared to evaporation, the water balance (budget) method becomes impracticable. Furthermore, seepage, ungauged local flow and bank storage are uncertain and often immeasurable items (WMO, 1983).

Several lakes and reservoirs in Africa have large surface areas causing their annual losses by evaporation to be considerable. Therefore, application of the water balance method can be reasonably successful whenever the data needed for balance calculations are available and of high quality. From the principle of continuity between the inflow and outflow components to and from an open water system over a certain period of time Δt, the loss by evaporation E can be expressed as follows:

$$E = I + P + (Gi - Go) - O - L \pm \Delta S \qquad (4.2)$$

where I is the inflow of surface water to the system, P is the direct precipitation on the water body, G_i is the inflow of groundwater and G_o the outflow of groundwater to and from the system, O is the surface water outflow (including any extraction and/or diversion), L is the loss by leakage and ΔS is the change in storage over Δt.

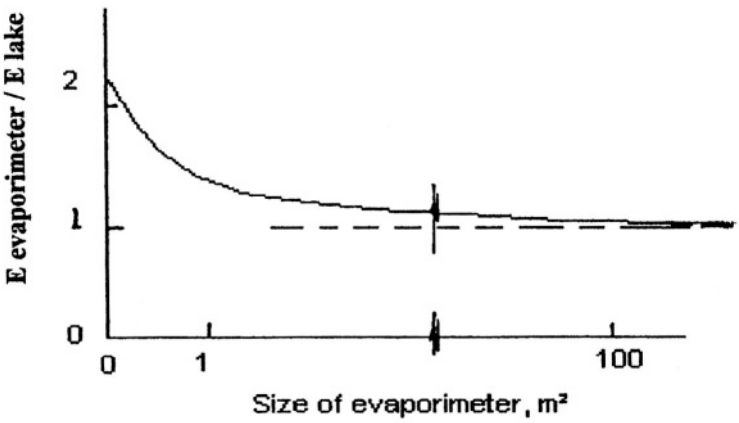

Figure 4.5- Approximate relationship between size of the evaporimeter and the ratio of evaporimeter measurement to lake evaporation

to and from the system, O is the surface water outflow (including any extraction and/or diversion), L is the loss by leakage and ΔS is the change in storage over Δt. It should be clearly understood that Eq. (4.2) is strictly valid in theory only. The errors associated with measurement or estimation of the different inflow and outflow items make it necessary to rewrite it as:

$$E \pm \delta = I + P + (Gi - Go) - O - L \pm \Delta S \tag{4.3}$$

where δ is the resultant error term bringing the two sides of the equation into equality. A small value of δ, if it occurs, should not be interpreted as indication of the smallness of the errors contained in the measurement or estimation of each of the individual items in the balance equation. As some of the errors are positive in sign and the rest are negative, the sum of all errors may simply become too small.

Suppose that in a particular situation the estimated error of the individual water balance terms are represented by $\delta_1, \delta_2, \ldots \delta_j \ldots, \delta_m$, where these error limits may be either positive or negative. There is usually a degree of uncertainty in estimating the magnitude of each error limit δ_j for any component. This error limit specifies the range within which the actual, yet unknown, error is expected to fall. The probable maximum discrepancy δ will be the sum of the absolute values of the error limits of all water balance components, $\Sigma|\delta j|$. A recommended criterion is that δ should not exceed the square root of the sum of the squares of the error limits of the water balance components (UNESCO, 1981):

$$\delta = \sqrt{\delta_1^2 + \delta_2^2 + \ldots\ldots + \delta_m^2} \tag{4.4}$$

Eq. (4.4) is often recommended as a useful practical approach while dealing with evaporation estimates using the water balance method. In a simple application of this equation, where it is assumed that the limits of errors in each of I, P, O and ΔS are 2% and in $(G_i\text{-}G_o)$ and I are 5%, Eq. (4.4) yields $\delta = 8.12\%$. If the error limits for the first four terms increase to 5% and for the remaining two terms to 10%, the resulting error limits of evaporation estimate will rise to 17.3%.

Despite the frequent use of the water balance approach to hydrologic estimates related to the Equatorial lakes, in some cases it was applied to items other than evaporation. Next to the old material in the Nile Basin volumes (e.g. Hurst & Philips, 1931), the most notable work is probably that of WMO (1974), which reported on the monthly evaporation in a normal year, average over the period 1946-70, and for the years 1969 and 1970 for Lakes Victoria, Kyoga and Albert. Whereas the difference between the total annual evaporation is not too different from year to year, the differences for the same month between years of record are sometimes too enormous to be trusted. The results included in Table 4.4 show that the ratio of the November 1970 evaporation from Lake Kyoga counts only to 0.169 of the average

for the period 1946-1970 for the same month. For the same lake and the same month the evaporation from Lake Albert is three times as much as the average for the standard period, 1946-1970. Another striking example to mention is the evaporation from the reservoir formed by the High Aswan Dam in Egypt. Sadek (1992) estimated the monthly and annual evaporation from this reservoir for 22 years, 1968-1989 using the water balance method. The smallest figure, 2.61 mm d^{-1}, occurred in 1987 and the largest, 12.01 mm d^{-1}, occurred in 1971. Arranging the annual evaporation in classes of 2 mm d^{-1} width, the class frequencies for those 22 years are 2, 7, 6, 4, 2 and 1 for the respective classes with limits 2-4, 4-6, 6-8, 8-10, 10-12 and 12-14 mm d^{-1}. Even for the 7-year period 1976-1982, in which the reservoir level can be described as stable, the average annual rate of evaporation varied from 4.27 mm d^{-1} as a minimum to 7.29 mm d^{-1} as a maximum, with a mean of 5.88 mm d^{-1} and coefficient of variation of 0.23. These examples serve to illustrate the difficulty in obtaining a reasonable estimate of evaporation from the water balance method in the absence of reliable data covering a long period of record.

4.3.2- Energy budget method- This method is somewhat comparable to the water balance method. Whereas hydrologists and water resources engineers favour the latter the energy budget, which is favoured by physicists and meteorologists, is based on the inflow, outflow and energy storage in a given system. After some minor simplifications the basic expression (WMO, 1983) can be written as:

$$Q_E = \Delta G - (R_n + A + Q_h + Q_w) \tag{4.5}$$

Tabla 4.4- Monthly and annual ratios of evaporation for 1969 and 1970 from Lakes Victoria, Kyoga and Albert to the average for the period 1946-1970

	Ratio of monthly evaporation in a given year to a normal year					
Year/	L. Victoria		Lake Kypga		Lake Albert	
Month	1969	1970	1969	1970	1969	1970
January	0.958	0.76	0.9	1.691	1.025	1.026
February	0.623	1.208	0.745	0.745	0.275	1.406
March	0.748	0.637	0.781	1.329	1.201	1.51
April	0.518	0.609	0.969	1.019	1.508	1.093
May	0.654	0.89	0.854	0.55	1.723	2.232
June	1.237	0.974	0.821	0.598	0.914	0.862
July	1.168	0.804	0.791	0.923	2.458	1.187
August	1.479	0.866	0.724	1.146	0.794	0.109
September	1.179	1.321	0.964	0.655	2.657	2.791
October	1.783	1.349	1.229	0.716	2.151	1.871
November	1.109	0.961	1.223	0.169	1.032	3
December	1.771	1.131	1.577	1.587	0.819	2.187
Year	1.088	1.036	0.937	0.908	1.237	1.438

where Q_E is the latent heat used for evaporating water, ΔG is the net increase in energy stored in the body of water, R_n is the net radiation (Eq. [2.4]), A is the net heat input into or output from the water body, Q_h is the sensible heat flow from or to the water and Q_w is the energy due to replacing the evaporating water.

Each term in Eq.(4.5) is obtained either by direct measurement or estimated from a known relationship. Reliable readings are hardly available, and some relationships contain coefficients or parameters, which vary from place to place or from experience to another, making the results obtained from this method too questionable.

For computational purposes the following relationships have been suggested.

$$Q_E = \rho_w E L \tag{4.6}$$

$$Q_h = \beta Q_E \tag{4.7}$$

$$Q_w = \rho_w C_w E (T_{ws} - T') \tag{4.8}$$

$$\beta = \frac{0.61(T_{ws} - T_a)P_A}{1000(e_o - e_a)} \tag{4.9}$$

where

ρ_w = density of water in kg m^{-3}
E = rate of evaporation in cm d^{-1}
L = latent heat of vaporization in J Kg^{-1}
β = Bowen's ratio
C_w = specific heat of water in J kg^{-1} $°C^{-1}$
T_{ws} = temperature of water surface in °C
T' = temperature of inflowing water which replaces the evaporated water in °C
T_a = air temperature in °C
P_A = atmospheric pressure in hPa (hecto Pascal)
e_o = saturation vapour pressure at T_{ws} in hPa
e_a = saturation vapour pressure of air in hPa

Eqs. (4.5) thru' (4.9) together with a slight modification yields a general expression for E as follows:

$$E = \frac{R_n + A - \Delta G}{\rho_w [L(1+\beta)(1+r) + C_w(T_{ws} - T')]} \tag{4.10}$$

The accuracy of evaporation estimates by the energy budget method as already

mentioned depends, among others, on the inherent accuracy of the measuring instruments, as well as on the completeness of the data. The error in the estimate can be up to 10% in summer and 20% in the winter, whenever sampling is done appropriately. In practice, the energy budget method is difficult to apply because of the complexity of the required field measurements. However, for quite sometime it has been known to yield the best results over a wide range of conditions as compared to other methods, when data sampling is carried out in an optimal way (e.g. de Bruin and Keijman, 1979)

The estimates of monthly and annual evaporation for Lake Victoria, averaged over the period 1946-1970 (WMO, 1974) as obtained by the energy budget method are included in Table 4.9. The same table includes also the corresponding estimates for the period 1969-1972 (Bakry, 1975). Not withstanding the difference between the two periods of record, the agreement between the two sets of results can be described as excellent for the annual figure and average to good for the monthly estimates.

Omar & El-Bakry (1981), using the energy budget method, estimated the monthly and annual evaporation rates for the reservoir of the High Aswan Dam. They used the average monthly estimates of the different meteorological elements over the reservoir based on measurements taken during survey trips in the period 1970-1971. The survey period was, unfortunately, not long enough to give a reasonable average for the seasonal variation of water temperatures over the reservoir. Additionally, the formula they used for calculating the net long-wave radiation has been criticized by Morton (1983) as being unrealistic as long as it ignores the need to calibrate the effect of the atmospheric vapour pressure. To show the effect of changing the net radiation R_n on monthly and annual evaporation estimates, keeping other items in the energy budget equation unchanged, Table 4.5 has been prepared.

4.3.3- Combination (Penman) method- A powerful method for the estimation of evaporation is the combination of the energy balance and a bulk aerodynamic equation. The combination method introduced by Penman (1948) combined the energy budget with the Dalton aerodynamic expression:

$$E' = f(u)(e_o - e_a) \qquad (4.11)$$

where, E' is the evaporation rate in $\mathrm{mm\ d^{-1}}$, $f(u)$ is a function of the prevailing wind speed, e_o is the saturated vapour pressure, in h Pa, corresponding to the temperature at the water surface, and e_a is the actual vapour pressure in hPa corresponding to the air temperature above the water surface.

Penman combined the energy budget equation with the bulk aerodynamic expression as in Eq. (4.11) and with an approximate analytical solution developed the expression known as Penman's equation:

Table 4.5- Annual and monthly estimates of evaporation for the reservoir formed by tha High Aswan dam, Egypt, as obtained from the energy budget method using different values for the net radiation (Sadek, 1992)

Month	R_n, mm d^{-1}			E, mm d^{-1}		
	1	2	3	1	2	3
January	2.61	3.25	3.16	3.59	4.15	4.07
February	4.47	4.1	4.12	4.95	4.56	4.59
March	6.73	5.12	5.22	5.4	3.94	4.03
April	7.89	6.15	6.08	5.52	3.61	3.54
May	9.07	6.65	6.49	8.95	6.26	6.09
June	9.87	6.96	6.83	11.66	8.2	8.05
July	9.62	7.15	6.95	10.42	7.54	7.31
August	8.88	6.86	6.47	8.39	6.08	5.63
September	7.57	5.91	5.44	8.61	6.74	6.2
October	5.78	4.71	4.37	8.98	7.8	7.42
November	3.66	3.49	3.44	6.87	6.7	6.65
December	2.68	2.93	2.79	4.9	5.12	4.99
Year	6.57	5.27	5.11	7.35	5.89	5.72

Explanation

1-Values used by Omar and El-Bakry (1981)

2- Values suggested by Sadek (1992)

3- Values suggested by Morton (1983)

$$E = \frac{\Delta R_n + \gamma E'}{\Delta + \gamma} \tag{4.12}$$

where E is the free water evaporation expressed in cal cm^{-1} d^{-1}, Δ is the slope of the saturated vapour pressure-temperature curve at the specified air temperature, R_n is the net radiation or heat budget expressed in cal cm^{-1} d^{-1} and computed from Eqs. (2.6) thru' (2.11), E' is the isothermic evaporation given by Eq. (4.11) and γ is the psychrometer constant corresponding to a given wind speed.

Since the latent heat of vaporization is approximately 600 cals gm^{-1}, the evaporation estimated from Eq. (4.12) can be converted to its equivalent in mm d^{-1} by dividing it by an amount very close to 60.

The wind function in Eq. (4.11) is one of the sources of discrepancy between the various researchers. The expression proposed by Penman (1956):

$$f(u) = 0.26[0.5 + (u_2 / 160)] \tag{4.13}$$

where u_2 is the wind speed in km d^{-1} at a height of 2 m above the water surface has been reported to give satisfactory results in East Africa (Stigter and Kisamo, 1978).

Yin and Nicholson (1998), while investigating the water balance of Lake Victoria in East Africa, have recently used the same expression for the wind function.

Morton (1983) reported that Penman's analytical solution (1948) and the modification suggested by Kohler and Parmele (1967) are accurate only under relatively humid conditions. In very arid climates, where advective conditions can be strong, Brutsaert (1982) did not recommend the application of Penman's equation for estimating evaporation. To illustrate the differences caused by different wind functions the evaporation from the reservoir of the Aswan High Dam in Egypt has been estimated by Sadek (1992) as shown in Table 4.6.

4.3.4 Kohler's methods- Kohler, Nordson and Fox (1955) suggested a scheme for estimating lake evaporation based on computed pan evaporation and certain meteorological data. Their formulation is essentially based on the original formula developed by Penman (1948). The pan concept is based on the following criteria:

i- any net advection into the lake is balanced by the change in heat storage
ii- the net transfer of sensible heat through the pan is negligible
iii- the exposure of the pan is representative.

On the basis of the above criteria, they suggested a Class A pan coefficient equal to 0.70 to be introduced in the formula for estimating the lake evaporation, E_l, as:

$$E_l = 0.70\left[E_p + 0.00051 p \alpha_p (0.37 + 0.003u_2)(T_o - T_a)^{0.88}\right] \tag{4.14}$$

where E_p is the pan evaporation expressed in d^{-1}, p is the atmospheric pressure in Hg (28.6 in Hg = 954 h Pa), u_2 is the wind speed in mi d^{-1}, T_o is the mean daily pan water surface temperature in °F, T_a is the mean daily air temperature in °F, and α_p is the proportion of advected energy into Class A pan utilized in evaporation and can be calculated as follows:

$$\alpha_p = \frac{\left[(e_o^* - e_d^*)^{0.88} - (e_o - e_d)^{0.88}\right] - (0.37 + 0.003u_2)}{\left[(e_o^* - e_d^*)^{0.88} - (e_o - e_d)^{0.88}\right] + (0.37 + 0.003u_2)(7.6 * 10^{-11})\left[(K_o^*)^4 - K_o^4\right]}$$

$$x \frac{1}{+ 0.000367 p\left[(T_o^* - T_a^*)^{0.88} - (T_o - T_a)^{0.88}\right](0.37 + 0.003u_2)} \tag{4.15}$$

where $T_o^* = (T_o + 1)$ in F°, K_o^* = absolute temperature corresponding to T_o^*,
K_o = absolute temperature corresponding to T_o,
e_o = saturated vapour pressure over the pan water surface
e_o^* = saturated vapour pressure corresponding to T_o^*, and
e_d = saturated vapour pressure at the dew point of the given temperature

To avoid the complexity caused by using Eq (4.15), Kohler and Parmele (1967) developed two charts, each including certain sets of curves. The first chart gives α_p for known pan water temperature, pan wind movement and elevation. The second set converts the Class A pan evaporation to Lake evaporation given the pan evaporation E_p, difference in temperature $(T_o\text{-}T_a)$, the portion of advected energy α_p and the elevation above mean sea level in ft.

Kohler's method (1955) together with the curves he and Parmele developed (1967) have been applied using the available data for a number of stations located in the catchments of Lakes Victoria, Kyoga and Albert. The estimates obtained are published in the WMO report on the hydrometeorologial survey of these catchments (1974). As an example, the monthly evaporation rates at Butiaba on the shore of lake Albert were estimated for 1970 as: 3.6, 4.0, 3.2, 3.7, 3.4, 3.3, 2.8, 2.9, 3.4, 3.6,3.4 and 3.7 mm d^{-1} for the months January thru' December. These rates sum up to a total evaporation of 1,365 mm, which counts for just 61.4% of the lake evaporation for the same year estimated by the water balance method.

The monthly and annual ratios of evaporation from a 3.66 m (12 ft) pan to evaporation estimates obtained from Kohler's method as developed at the Khartoum Observatory in the Sudan are included in Table 4.1. Remarkable enough is the fact that each of those ratios is very close to unity.

4.3.5 Morton's method- Nash (1989) stated that the work of Penman (1948) on evaporation constitutes a major contribution to modern applied hydrology. It is likely that Morton's contribution (1983) will attract the same recognition. According to Doyle (1990): Morton's work is based on two hypotheses: the energy balance as in Penman and the other is a new concept developed by Bouchet (1963). This concept states that any energy unused for actual evaporation due to lack of available moisture acts so as to increase the potential evaporation over the system in question.

Table 4.6- Annual evaporation from the reservoir of the High Aswan Dam, Egypt, using different wind functions (Sadek, 1992)

Reference	Wind function	Penman evaporation, mm y^{-1}	
	f (u)	A	B
Koopman (cited in Sweers, 1976)	$0.093\ u_2$	2121	2182
Sweers (1976)	$0.13+ 0.094\ u_2$	2390	2449
Penman (1956)	$0.13+ 0.140\ u_2$	2713	2774

Explanation

A: heat storage and energy advection to the reservoir by inflow and/or outflow are neglected.

B: heat storage and energy advection to the reservoir by inflow and/or outflow, as given by Omar & El-Bakry (1981), are taken into account

The estimate of areal evapotranspiration E_T can be based on the negative or complementary responses of potential evapotranspiration E_{TP} to changes in the availability of water for areal evapotranspiration. Denoting the wet environment areal evapotranspiration by E_{TW} one can express the complementary relation by:

$$2E_{TW} = E_T + E_{TP} \tag{4.16}$$

Eq. (4.16) shows that under completely arid conditions (moisture supply = zero), the actual evapotranspiration would be zero and the potential evapotranspiration would be very high, $2\ E_{TW}$. For less than abundant supply, the actual evapotranspiration would equal the supply, and for abundant supply, the actual and potential evapotranspirations would be equal.

Despite the controversy embracing the complementary hypothesis, Morton used Eq. (4.16) with the energy balance and the vapour transfer equation to build the model known as complementary relationship for areal evapotranspiration (CRAE). This relationship will be discussed further in Chapter 5 "Evapotranspiration"

Minor changes have been introduced by Morton (1983) so as to transform the CRAE model to a complementary relationship for lake evaporation (CRLE) model. The relationship between shallow-lake evaporation and potential evaporation in a land environment receiving a constant supply of radiant-energy is shown in Figure 4.6.

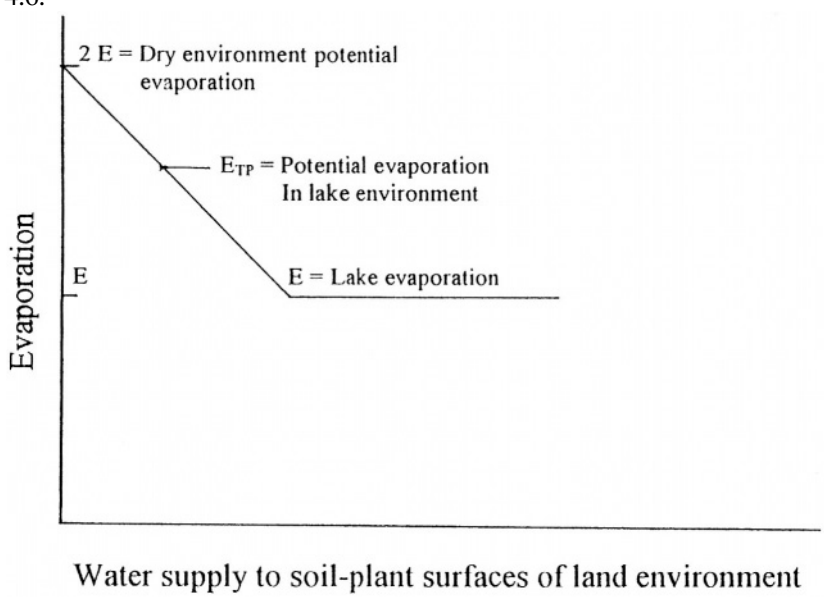

Figure 4.6- Schematic representation of the relationship between shallow-lake evaporation and potential evaporation in a land environment with constant radiant energy supply (Morton, 1983)

Morton (1986) introduced some changes to the CRLE model so as to convert evaporation estimates for a shallow lake to evaporation estimates for a deep lake. To do this, Morton suggested the routing of solar and water-borne heat input through a hypothetical heat reservoir with time lag and storage constants depending on the depth and salinity of the lake water. The energy routing concept used here is very much parallel to the concept of flood routing in lakes and reservoirs.

Morton's model was run in four forms for estimating the evaporation from the reservoir formed by the high Aswan Dam at both Aswan and Wadi Haifa, almost the two ends of the reservoir. The first model was run assuming that the reservoir was a shallow lake. In the second model, the storage and advective heat terms, employed by Omar & El-Bakry in their earlier study (1981), were included. In the third run routing was applied to the incoming radiation only, and the advective heat was not taken into account. In the fourth model, the routing technique was applied to both incoming radiation and net water-borne energy (advective heat), as in the second model.

The models give comparable results at the annual level; 2,081, 2,150, 2,080 and 2,244 mm for numbers 1, 2, 3 and 4 respectively, in contrast to 2,151 mm y^{-1} as obtained from the water balance method for the stable period 1976-1982. The monthly evaporation estimates obtained from the four models are not in good agreement with each other or with water balance estimates. The results obtained from the third model, however, are probably the nearest to the results obtained from the water balance method (Sadek, 1992 and Sadek et al., 1997). The extent of agreement between the two can be seen in Figure 4.7.

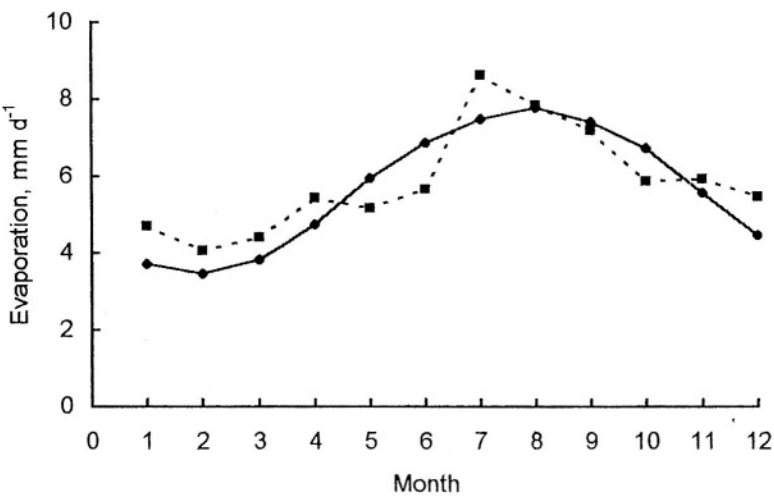

Figure 4.7- Monthly evaporation estimates for the reservoir formed by the Aswan High Dam, Egypt including the average for Aswan and Wadi-Halfa as obtained from the third CRLE model of Morton ●—● and the water balance average for the period 1976-82 ■-----■ (Sadek, 1992 and Sadek et al., 1997)

4.4- Evaporation From Some of the Natural Lakes and Storage Reservoirs in Africa

4.4.1 Mean monthly and annual evaporation using different estimation methods-
The present subsection lists in table form the mean monthly and annual evaporation rates from 14 natural lakes and 2 storage reservoirs as obtained by different sources using different methods and periods of investigation. The geographic locations of these lakes and reservoirs are shown on the map in Figure 4.8. More information about these water bodies and their water balance, average depth, surface area and water levels are given in one or more of the following chapters.

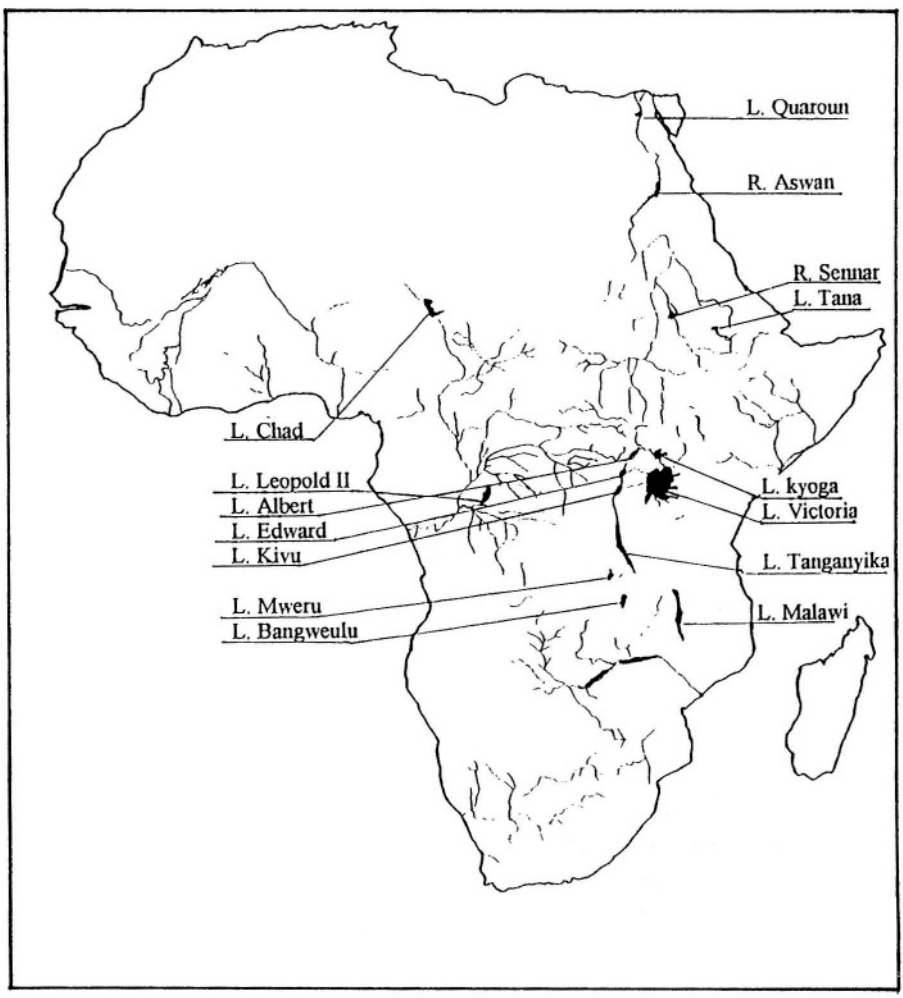

Figure 4.8- Location map of the storage reservoirs and natural lakes mentioned in Tables 4.7 thru' 4.13

Table 4.7- Estimates of monthly and annual evaporation in mm d^{-1} from the Aswan old reservoir and the High Dam reservoir, Egypt

Source	Jan	Feb	Mar	Apr	May	Jun	Jul	Aug	Sep	Oct	Nov	Dec	Yr
aA	3,8	X	X	8,7	X	X	10	X	X	7,8	X	X	7,5
aH	4,5	X	X	9,3	X	X	9,9	X	X	8,1	X	X	7,9
bA	3,8	4,6	6,5	8,4	9,3	10,8	9,8	9,6	9,1	7,8	5,4	3,7	7,4
bH	4,4	5,5	7,2	9,1	9,2	10,7	9,7	8,8	9,1	8	5,9	4,3	7,6
c	5,8	4,9	3,4	5	6,3	7,9	8,9	4	10,9	10	9	7	7,4
d1	3,9	5,4	7,4	8,9	10	11,2	11	10,6	9,5	7,3	6,3	4,1	7,9
d2	3,8	4,5	5,1	6,4	9,2	10,9	10	9,6	9,5	6	6	4,7	7,4
e1	3,3	3,9	4,5	5,2	5,8	6,1	5,7	5,5	5	4,3	3,7	3,2	4,7
e2	3,7	4,3	5,1	5,8	6,1	6,4	6,6	6,4	5,7	5,1	4,2	3,7	5,2
f1	3,4	4,2	5,3	6,4	7,5	7,9	7,4	7,3	6,5	5,4	4,1	3,3	5,7
f2	4,4	4,5	4,8	4,4	6,8	7,8	7	6,1	6,6	7,2	6,4	5,3	5,9
g	4,1	5	6,9	8,8	9,5	10,8	9,8	9,2	9,1	7,9	5,6	4	7,5
iA	3,5	4,6	6,2	7,7	8,5	9,4	9,3	8,8	8,2	6,5	4,5	3,7	6,7
iH	4,5	5,8	7,1	8,7	9,3	9,8	9,6	9,3	8,6	7,7	6,1	4	7,5
j1	4,7	4,1	4,4	5,4	5,2	5,7	8,7	7,9	7,2	5,9	6	5,5	5,9
j2	4,2	4,6	3,9	3,6	6,3	8,2	7,5	6,1	6,7	7,8	6,7	5,1	5,9
j3	4,6	4,9	5,3	5,1	7,5	8,7	8,1	7	7,6	8	6,8	5,2	6,6
j4	4,2	4,3	4,7	4,4	6,7	8	7,3	6,3	6,6	7,1	6,2	5	5,9

Source

aA: 0.5x Piche evaporation at Aswan, 1920-1929 (Hurst& Philips,1931)

aH: 0.5x Piche evaporation at Wadi Halfa, 1905-1929 (Hurst& Philips,1931)

bA: 0.5x Piche evaporation at Aswan, 1920-1950 (Hurst et al.1959)

bH: 0.5x Piche evaporation at wadi Halfa, 1905-1950 (Hurst et al.,1959)

c: monthly distribution of evaporation is based on Dalton's law (Attia et al., 1979)

d1: bulk aerodynamics and heat budget (Omar& Bakry, 1970)

d2: based on a few lake measurements taken in 1970-1971(Omar& Bakry, 1981)

e1: Morton's original Crle model (Morton, 1979)

e2: same as in e1 except using net heat input of Lake Mead, USA (Morton, 1979)

f1: Morton's modified CLRE model (Morton, 1983)

f2: same as in f1 except using heat data as in d2 (Morton,1983)

g: Ministry of Public Works and Water Resources of Egypt (cited in Whittington& Guarisso, 1983)

Source (Cont'd)

iA: estimated evaporation at Aswan, Penman's original formula (Shahin, 1985)
iH: similar to iA except that the estimate is for Wadi Halfa (Shahin, 1985)
j1: water balance method,1976-1982 (Sadek, 1992)
j2: heat budget method of the reservoir (Sadek, 1992)
j3: Peman's method using heat storage, advective energy and wind function as in d2 (Saadek, 1992)
j4: average of estimates for Aswan and Wadi Halfa applying the CRLE model and the same advective energy and heat storage as in d2 (Sadek, 1992)

Table 4.8- Average monthly and annual estimates of evaporation from the reservoir formed by the Sennar Dam on the Blue Nile, the Sudan

Source	Jul	Aug	Sep	Oct	Nov	Dec	Jan	Feb	Mar	Apr	May	Jun	Year
a	8,1	8,7	11	10	9,3	7,4	4,5	3,2	3,5	5,7	7,4	7,3	7,2
b	7,9	5,1	6,6	9,9	15	14	15	19	22	21	16	14	14
c	6,6	4,2	5	7,2	9,6	7,9	7,8	9,5	11	12	9,2	9,5	8,4
d								7,2	7,7	9,2	8,4		

Source

a =estimates adopted by Ministry of Irrigation, the Sudan (cited in Ali, 1990)
b = Piche evaporation, average for the period 1921-1950 (Hurst et al., 1959)
c = Piche evaporation corrected to free water evaporation (Shahin, 1985)
d = Modified Penman using lake data, Feb-Jun 1988 and Feb 1989 (Abdulai, 1989)

Table 4.9- Evaporation estimates in mm for Lake Victoria

Source	Jan	Feb	Mar	Apr	May	Jun	Jul	Aug	Sep	Oct	Nov	Dec	Year
a1	109			87			136			115			1315
a2	109	106	102	78	76	93	89	88	87	99	98	91	1116
b1	96	106	135	133	135	156	143	119	106	106	128	109	1473
b2	115	101	112	102	115	129	140	136	153	143	123	112	1481
b3	116	102	113	103	116	130	142	137	155	145	124	113	1496
c1	107	94	130	151	143	156	170	131	104	108	104	104	1502
c2	96	106	135	133	136	156	143	119	106	106	128	109	1473
d	119	112	139	154	151	166	175	137	109	114	107	110	1590
e	135	135	145	130	125	120	135	140	145	130	130	130	1595

Table 4.9- Cont'd

Source	Jan	Feb	Mar	Apr	May	Jun	Jul	Aug	Sep	Oct	Nov	Dec	Year
f1	135	127	144	132	123	109	113	126	135	145	132	129	1551
f2	150	145	162	146	138	130	135	144	148	154	145	146	1743

Explanation

a1: Water balance method, 1902-1923 (Hurst & Philips, 1931)
a2: Water balance method, 1906-1932 (Hurst & Philips, 1938)
b1: Water balance method, 1946-1970 (WMO, 1974)
b2: Mass transfer method, 1946-1970 (WMO, 1974)
b3: Energy balance method, 1946-1970 (WMO, 1974)
c1: Heat budget method, 1969-1972 (Bakry, 1977)
c2: Water balance method, 1946-1970 (Bakry, 1977)
d: Water balance method, 1970-1974 (Kite, 1981)
e: Water balance method, 1956-1978 (Piper et al., 1986)
f1: Radiation method (Yin & Nicholson, 1998)
f2: Penman method (Yin & Nicholson, 1998)

Table 4.10- Evaporation estimates in mm for Lake Kyoga

Source	Jan	Feb	Mar	Apr	May	Jun	Jul	Aug	Sep	Oct	Nov	Dec	Year
a	121			99			133			115			1425
b1	110	141	146	161	171	117	91	123	113	109	130	104	1516
b2	161	152	156	127	137	125	113	126	130	132	129	135	1623

Source

a: Water balance method, 1902-1923 (Hurst & Philips, 1931)
b1: Water balance method, 1946-1970 (WMO, 1974)
b2: Penman's formula

Table 4.11- Evaporation estimates in mm for Lake Albert

Source	Jan	Feb	Mar	Apr	May	Jun	Jul	Aug	Sep	Oct	Nov	Dec	Year
a	143			111			133			112			1425
b	160	138	149	118	112	116	107	238	67	93	93	155	1546

Source

a: Water balance method, 1902-1923 (Hurst & Philips, 1931)
b: Water balance method (WMO, 1974)

Table 4.12- Evaporation measurements/estimates in mm for Lake Quaroun, Egypt (Mankarious, 1979)

Source	Jan	Feb	Mar	Apr	May	Jun	Jul	Aug	Sep	Oct	Nov	Dec	Year
a	52	65	110	151	208	233	227	208	168	130	80	51	1683
b	60	77	121	152	199	226	229	224	187	147	101	62	1685

Source

a: observations of a floating pan (1mx1mx1m) adjusted by a coefficient (0.75-0.90)
b:evaporation measurements using a masonary basin (12mx12 mx12m) corrected by a constant value of 0.9

Table 4.13- Monthly and annual evaporation in mm from some African Lakes

Lake	Jan	Feb	Mar	Apr	May	Jun	Jul	Aug	Sep	Oct	Nov	Dec	Year
Tana	121	136	158	171	127	72	34	34	42	68	72	99	1134
Bam	177	178	217	228	242	222	205	161	156	195	192	171	2344
Chad	136	155	211	228	226	201	177	149	159	198	177	149	2166
Edward	144	134	112	120	111	107	95	89	100	114	110	140	1376
Tanganyika	132	124	138	130	149	147	144	147	167	153	135	130	1696
Mweru	137	119	138	141	150	136	138	144	159	164	141	134	1701
Bangweulu	136	115	136	134	134	114	118	134	163	175	147	134	1642
Leopold II*	112	104	124	124	114	107	98	102	115	125	120	111	1356
Kivu	116	107	122	117	121	111	110	116	124	127	122	119	1412

Explanation

Lake Tana: Piche evaporation multiplied by 0.5 (Shahin, 1985)
Lake Edward: Water balance method (cited in Balek, 1977)
Lakes Bam (1966-1975) and Chad (1965-1978): water balance (Pouyaud, 1989)
Other lakes: Evaporation measurements were taken from Colorado sunken pans
** Lake Leopold II is presently known as Lake Mai Ndombe*

4.4.2 Annual evaporation series- Contrary to precipitation and runoff, it is not common to find in any published material relevant to hydrology and/or climatology any mention of monthly or annual evaporation series. Instead, it is quite usual to find evaporation figures given as averages for certain periods of time. This is probably so because evaporation rates do not vary significantly from year to year in a relatively short continuum of time. This conclusion can be reached upon examining the annual evaporation figures presented in Tables 4.14 and 4.15. The former includes annual evaporation from Lake Quaroun, Egypt, for the period 1960-1977. The latter, Table 4.15, also gives the annual evaporation from Lake Malawi in Malawi from 1954 up to 1979. The series of the two lakes in their respective order give an annual mean of 1725 and 1,605 mm y^{-1}, both showing nearly the same coefficient of variation: 3.5-3.8%. In view of its changing hydrologic environment, the annual evaporation series of Lake Quaroun, however, indicated a somewhat rising trend with time. The correlation between the annual depth of evaporation and time is fairly high, 68.8%. It is regrettable that measurement/estimate of evaporation from this lake was not continued on a regular basis after 1977, so as to decide whether this increase stopped or is continuing.

Table 4.14- Annual evaporation from Lake Quaroun, Egypt (Mankarious, 1979)

Year	E, mm	Year	E, mm	Year	E, mm
1960	1684	1966	1649	1972	1750
1961	1656	1967	1728	1973	1767
1962	1670	1968	1766	1974	1735
1963	1650	1969	1804	1975	1750
1964	1646	1970	1791	1976	1857
1965	1705	1971	1742	1977	1703

Mean of the series = 1725 mm y^{-1}, standard deviation = 60 mm y^{-1}

Table 4.15- Annual evaporation from Lake Malawi as obtained from the water balance method (Neuland, 1984)

Year	E, mm	Year	E, mm	Year	E, mm
1953	X	1962	1585	1971	1582
1954	1712	1963	1565	1972	1659
1955	1598	1964	1590	1973	1707
1956	1593	1965	1638	1974	1631
1957	1524	1966	1661	1975	1577
1958	1613	1967	1549	1976	1562
1959	1683	1968	1534	1977	1496
1960	1524	1969	1577	1978	1623
1961	1560	1970	1720	1979	1643

Mean of the series = 1605 mm y^{-1}, standard deviation = 61 mm y^{-1}

4.5- Review of Evaporation Data of Some African Countries and Islands

The average annual precipitation over the continent of Africa, including islands, has been estimated as 686 mm, of which 547 mm y^{-1} or $16.465*10^{12}$ m^3 y^{-1} goes back to the atmosphere by evaporation and evapotranspiration (L'vovich, 1974/79 and Shiklomanov, 1990). Since these two processes mostly occur concurrently, it is quite difficult to assess separately the volume of water lost by evaporation from free water systems and the volume lost by evapotranspiration . If we assume that the sum of the surface areas of all open water systems counts to say 3% of the total surface and the overall average rate of evaporation to about 1.5 m y^{-1}, the annual volume of water lost by evaporation will be then $1,350*10^9$ m^3 y^{-1}. From the previous sections it has already been shown that the annual evaporation from the Equatorial Lakes all alone is about $120*10^9$; from Lake Tanganyika, $44*10^9$ (Krul, 1997); Lake Malawi, $54*10^9$ (Krul, 1997): Lake Chad, $47*10^9$ (UNESCO, 1970); Lake Nasser formed above the Aswan High Dam $(10\text{-}11)*10^9$ all in m^3 y^{-1}. It goes without saying in Africa that there are many more lakes, though smaller in size than the ones already mentioned.

Moreover, there are too many storage dams of all sizes in Africa as well as large rivers and tributaries, wadies (seasonal and ephemeral streams), irrigation and drainage canals, which undoubtedly contribute to evaporation losses by large quantities. For example, a stream 1000 km long having a hydraulic section with an average surface width of 1 km traversing a region where the annual rate of evaporation is estimated at 1.5 m loses $1.5*10^9$ m^3 y^{-1}.

As already mentioned earlier in this chapter, several types of instruments have been used to measure evaporation. Likewise, many estimation methods have been used and are still in use. This wide diversity of measuring devices and estimation methods and formulas makes it extremely difficult to perform a consistent comparison between the evaporation rates and magnitudes over the different parts of the continent. Nevertheless, we shall try in the next subsections to present a brief survey of the practices and/or research results relevant to evaporation from the open water surfaces in some countries and islands of Africa.

4.5.1 Egypt- In Egypt and the Sudan, the Piche, Wild and tank evaporation measuring instruments have been in use for quite some time, later most of these instruments have been gradually replaced by Class A pans. Before 1919, the Wild instrument was much in use. Sutton (1950) reported that on the grounds of the results obtained from the experiments carried out in Egypt, the Piche reading is about 1.42 times the reading of the standard Wild instrument. Since 1920, the use of the Wild instrument stopped to give way to the Piche evaporimeter. Additionally, the observations from floating tanks at Khartoum, Wadi Halfa, Aswan and Giza were compared to readings from screened Piche tubes and the ratio tank to Piche was found to be 0.58 for Khartoum, 0.54 for Wadi Halfa, 0.45 for Aswan and 0.63 for Giza. Other experiments were carried out at Helwan Observatory in Egypt, except that the tanks used were of the ground sunken type and the ratios obtained were 0.72 for tank to Piche and 1.12 for Piche in a single-louvered screen to Piche in a double-louvered screen. In 1924, more experiments were earned out at Abbassiya in the vicinity of Cairo to determine the ratio between floating square tanks of different sizes and Piche tubes to evaporation from a much bigger standard square tank. The ratios were determined for each month of the year, and they did not show any seasonal variation. The probable departure of the monthly ratios from the annual mean was limited to 3% for the tanks and 10% for the Piche. The results of all those experiments have shown clearly that evaporation from a square floating tank 1.0 m* 1.0 m bears an average ratio of 0.58 to Piche evaporation. As this tank has proven to be more convenient from the practical point of view, it was installed at a number of stations on the Nile, such as Malakal, Sennar and Khartoum in the Sudan and at Aswan and Lake Quaroun in Egypt. The tank is 1 m*1 m* 1 m in size, constructed of galvanized steel plates and has a centrally fitted scale of thermometer type.

During the 1960s, the USWB Class A pan, alone or together with other evaporation measuring instruments, was introduced at some meteorological stations

with the purpose of collecting and analyzing pan evaporation data. Some of these data have been reviewed and discussed by Shahin (1969). The monthly pan evaporation at four stations is summarized in Table 4.16. These are Giza at the apex of the Nile Delta; El-Tahrir, a newly desert reclaimed area; El-Kasr, close to the Mediterranean coast west of Alexandria and El-Kharga, an oasis in the Western Desert.

The tabulated evaporation varies from month to month but is similar to the pattern of variation of monthly temperature, with the maximum evaporation occurring in June-July and the minimum December-January. The annual pan evaporation increases from about 2,500 mm in Giza to 2,800 in El-Tahrir to 3,400 mm in El-Kasr to about 5,400 mm in El-Kharga Oasis. Assuming that the conversion factor lake to pan is 0.7, these four values will reduce to 1,750, 2,000, 2,400 and 3,750 mm respectively. All estimates seem to be reasonable, except the estimate for El-Kharga Oasis, which seems to be a bit too high. Probably a conversion factor of 0.55-0.60 will be more appropriate.

The above-summarized work (Shahin, 1969) wae subsequently followed by a study of evaporation at Lake Quaroun (Mankarious, 1979) and a year later by a study of the evaporation from the Quattara Depression (Flohn & Wittenberg, 1980). The evaporation from Lake Quaroun has already been presented and discussed in an earlier subsection.

The Quattara depression is a depression in the northwestern part of Egypt. It is located at a distance of 75 km from the town of Alamain on the Mediterranean coast. The deepest point of the depression is about 150 m below mean sea level (b. m. s. 1.) and the surface area at mean sea level is about $25{,}000\ km^2$. Since 1916, a plan has been drawn to use this depression for generating hydropower. The basic idea is to supply the depression with water from the sea through a conduit (canal/tunnel) at a rate equal to the rate of loss by evaporation. As such, the hydraulic and structural designs depend largely on accurate evaporation estimates. Flohn & Wittenberg (1980) carried out a study on evaporation using different estimation methods. Some of the results they obtained are included in Table 4.17. The four methods agree quite well as far as the annual depth of evaporation is concerned, the largest difference being about 4%. The differences between the different estimates reach 44% in December, 36% in November and less than 20% for the remaining months. Quite remarkable is that the ratio of monthly maximum to monthly minimum is the largest at 5.4 for Penman evaporation method, second largest for McIlroy at 4.1 and at about 3.75, average for Dalton and the heat budget methods. This is because Penman, compared to other methods, gives the lowest of minimum evaporation and the largest maximum evaporation.

4.5.2 The Sudan- The history of evaporation research in the Sudan, especially in the early part of the 19^{th} century, is more or less similar to that in Egypt. This is because of the mutual interest of both countries in the Nile water. This state of affairs does not eliminate at all the fact that the Sudan has more climates than Egypt does.

Table 4.16- Monthly Class A pan evaporation mm d^{-1} at four locations representing different climates in Egypt (Shahin, 1969)

Stat	Jan	Feb	Mar	Apr	May	Jun	Jul	Aug	Sep	Oct	Nov	Dec
Gz*	2,9	3,9	5,8	8,1	10,3	11,4	10,4	9,5	8,1	6,1	4,1	3
Th°	3,8	4,8	6,8	9,1	10,8	12,5	11,4	10,3	8,7	6,3	4,2	3,3
Ks^{x}	4,9	5,8	6,9	8,4	8,2	10,4	10,9	10,6	9,6	7,8	5,4	5,1
Kg^{xx}	6,4	8,5	12	16,1	20	23,3	21,7	19,5	18,2	14,4	9,9	6,8

Description of locations

**Giza; latitude 31° 02' N, longitude 31° 13' E and elevation 21 m a.m.s.l*

° El-Tahrir; latitude 30° 42' N, longitude 30° 36' E and elevation 22 m a.m.s.l.

^{x} El-Kasr; latitude 30° 10'N, longitude 27° 38' E and elevation 26 m a.m.s.l.

^{xx} El-Kharga; latitude 25° 26' N, longitude 30° 34' E and elevation 72 m a.m.s.l.

N.B. a.m.s.l.= above mean sea level

Table 4.17- Estimates of monthly and annual evaporation from the Quattara depression, Egypr (Flohn & Wittenburg, 1980)

Met-	Monthly evaporation, mm											
hod	Jan	Feb	Mar	Apr	May	Jun	Jul	Aug	Sep	Oct	Nov	Dec
D°	59	62	103	137	177	228	201	190	190	164	119	71
B°°	62	70	121	150	195	204	217	226	189	152	105	81
P^{x}	49	75	129	175	220	237	236	221	178	128	76	44
M^{xx}	52	68	115	148	191	210	214	217	189	155	109	78

Explanation

D°: Dalton's law; total evaporation = 1,701 mm

B°°: Heat budget, total evaporation = 1,772 mm

P^{x}: Penman method, total evaporation =1,768 mm

M^{xx}: McIlroy method, total evaporation = 1,756 mm

The results of the comparative study conducted in 1960-1961 at the Khartoum observatory have already been listed in Table 4.1. Evaporation estimates in the last decades are swinging much in favour of Penman's method. Recently, a hydrological study comprising twelve stations representing the different climates of the Sudan was performed by El-Agib (1995). The maximum estimate of daily evaporation was found to be 9.8 mm in June for Wad-Medani and the minimum around 4.1 mm in December for Kassala. The mean Penman evaporation for the period 1961-1990 at each of those 12 stations and the corresponding climates are given in Table 4.18. The tabulated figures show that the annual evaporation according to Penman's method varies from 1,840 mm for semi-arid regions to 2,930 mm for arid regions, both in the Sudan. The difference in climate is reflected not only on the total evaporation but extends itself to the pattern of distribution of the monthly values. The months of maximum and

minimum evaporation are not the same for the two types of climates nor the ratio of maximum to minimum evaporation. This result is evident from Figure 4.9, which illustrates the monthly rainfall for Port Sudan, in an arid region, and the other for Wau, in a semi-arid region. The former is located on the coast of the Red Sea, whereas Wau is located in the middle of the Bahr el-Ghazal swamps. Sutcliffe & Parks (1994) while examining the water balance of the Bahr el-Ghazal swamps, developed open water evaporation estimates for the Sudd (swamps) area. The twelve monthly values from January to December are: 217, 190, 202, 186, 183, 159, 140, 140, 150, 177, 189 and 217 mm, with a total annual evaporation of 2,150 mm. This estimate is about 17% higher than the one in Table 4.18.

Table 4.18- Annual evaporation in mm at different locations in the Sudan as obtained from Penman method, average for 1961-1990 (Al-Agib, 1995)

Location	Stat. no.	E, mm	Climate	Location	Stat.no.	E, mm	Climate
Pt. Sudan	x	2,423	Arid	El-Obied	x	2,004	Arid
Khartoum	49	2,932	Arid	Nyala	x	x	Arid
Kassala	x	2,045	Arid	Roseires	81	2,532	S.-arid
W.-Medani	57	2,772	Arid	Malakal	103	2,302	S.-arid
Gadaref	62	2,457	S.-arid	Wau	115	2,064	S.-arid
El-Fasher	66	2,34	Arid	Juba	134	1,84	S.-arid

Explanation

Stat.= Station, E= evaporation, S.-arid= Semi-arid

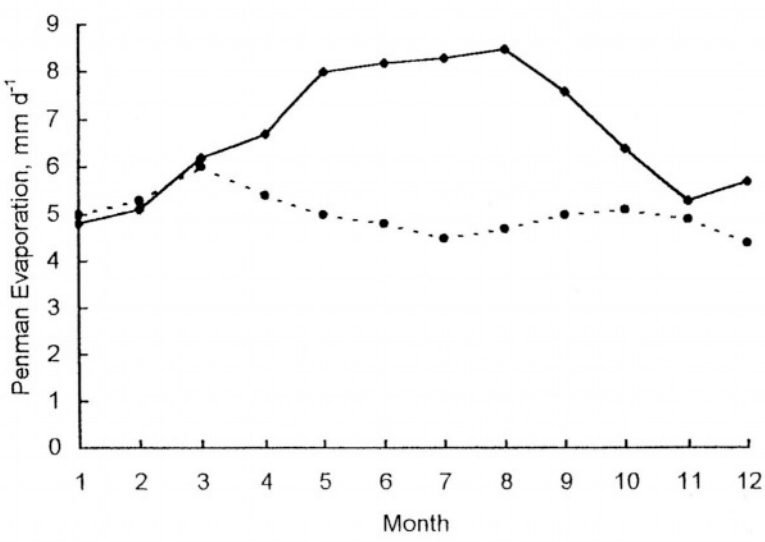

Figure 4.9- Monthly evaporation at Port Sudan●—● and Wau o-----o in the Sudan, as estimated using the Penman method, average for 1961-1990, (Al-Agib, 1995)

4.5.3 Zimbabwe- Zimbabwe has a fairly wide experience with measuring and estimating evaporation from open water bodies. Since the use of the old Symons pan has come to an end, evaporation measurement in Zimbabwe depends heavily on the US Class A pan. It is customary to estimate or calculate open water evaporation using any of Penman, Walker or Torrence formulas. Whereas Penman's expression, as discussed earlier, contains terms related to radiation, temperature, sunshine, saturation vapour pressure and wind speed, the Walker expression utilizes sunshine and radiation only. There are two expressions that have been developed by Torrence; the first uses air temperature, vapour pressure deficit and elevation of the location in question above mean sea level, and the second uses pressure and vapour pressure deficit

The comparison between calculated and measured evaporation at Bulawayo shows that the Penman evaporation tended to run low for most of the year, even though that the pan measurements were taken from a screened pan, which is usually 10% lower than the measurements from an unscreened pan. There is no evidence from the literature that the screened pan measurements are reduced by any factor to convert it into free water evaporation. Last but not least, the two Torrence expressions have been claimed to fit generally well to local conditions, but not specifically to Bulawayo.

Depending on the prevailing climatic conditions, most areas experience the peak evaporation in mid-October. This coincides basically with the peak temperature in the country. The diagram in Figure 4.10 illustrates the change of evaporation throughout the year averaged over 16 years at Makoholi experiment station. It should be noted here that the year begins with July and ends with June.

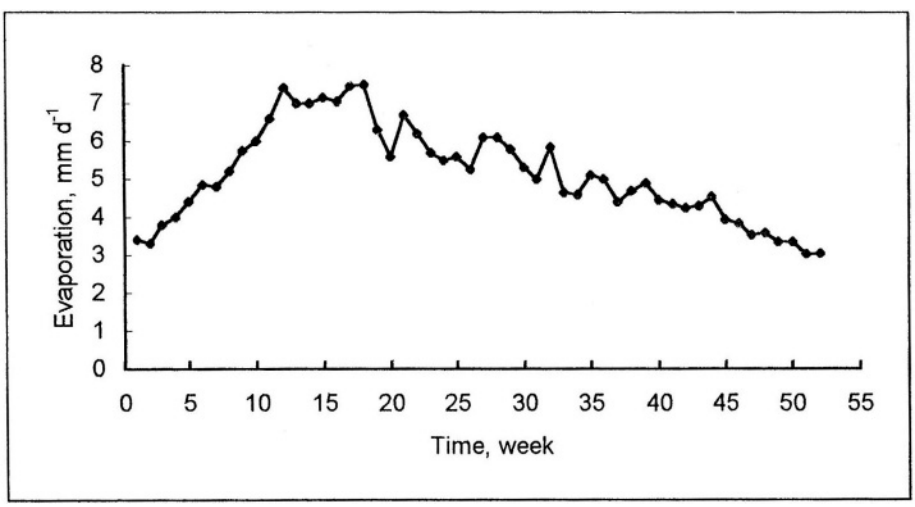

Figure 4.10- Mean monthly evaporation at Makoholi station, Zimbabwe, average for 1965-1980 (Department of Meteorological Services of Zimbabwe, 1981)

The annual pan evaporation in Zimbabwe varies from about 1.75 m to 2.25 m, being greatest at low altitudes and in the north west and west of the country, and least at high latitudes and along the eastern border. Figure 4.11 shows one version of the annual evaporation; the exact values differ according to the particular years used, but they all agree in the general distribution and pattern of isoplethes (Department of Meteorological Services of Zimbabwe, 1981).

Table 4.19- Effect of cloudiness on evaporation in Zimbabwe (Department of Meteorological Services of Zimbabwe, 1981)

Period,	Cloudiness, oktas								
months	0.0-0.9	1.0-1.9	2.0-2.9	3.0-3.9	4.0-4.9	5.0-5.9	6.0-6.9	7.0-7.9	8
Jan-Feb	7.3*	7	6.7	6.3	6.2	5.3	6.4	3.6	2.1
Mar-Apr	6.3	5.7	5.8	5.4	4.9	4.8	4.2	3.4	3.6
Jun-Jul	6.4	4.5	4.2	4	4	3.7	3.1	2.5	1.3
Sep-Oct	8.7	8.6	8.5	8.3	7.7	6.8	6.7	4.4	x
*Plateau stations, *evaporation rates are in mm d^{-1}*									
Jan-Feb	7.6	7.4	7	6.7	6.1	5.7	5	4	2
Mar-Apr	6.1	6.4	6.1	5.7	5.2	5.1	4.8	3.6	2.8
Jun-Jul	3.9	3.8	3.7	3.3	2.9	2.9	2.7	1.7	x
Sep-Oct	8.3	9.4	8.7	7.6	6.5	6.3	5.8	4.6	1.8
*Lowveld stations, *evaporation rates are in mm d^{-1}*									

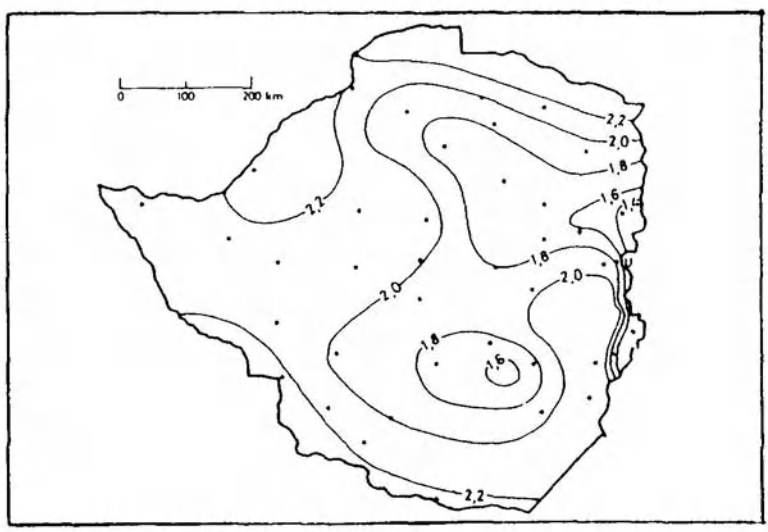

Figure 4.11- Contour lines of equal annual evaporation in Zimbabwe (marked in m; taken from the Department of Meteorological Services of Zimbabwe, 1981)

Table 4.19 shows interesting results as far as the effect of cloudiness on evaporation is concerned. It is possible that the rate of decline in evaporation is different for the different periods. Nevertheless, all stations show significant decline with increasing cloudiness, regardless of the period of time or the geographic region.

4.5.4 Malawi and Zambia- The annual evaporation from Lake Malawi for a period of 16 consecutive years, 1954-1979, using the water balance method is already given in Table 4.15. The mean of the series is close to 1,610 mm y^{-1} and the variation coefficient is about 3.75%. In a modeling study Calder et al. (1995) reported that evaporation from the land and lake catchment is calculated using the Penman open water method. Further, the monthly Penman values have been computed for the same period and normalized to give the annual total of 1,610 mm. The open water evaporation for the periods 1896-1953 and 1980-1994, a monthly Penman series, was synthesized using the same constant annual figure of 1,610 mm. This was achieved by distributing this annual value according a given distribution of the mean monthly evaporation.

Screened US Class A pans are placed in several meteorological stations in both Malawi and Zambia. Very much similar to the situation in Zimbabwe, there is a common opinion in Zambia and Malawi that evaporation from a screened Class A pan can be applied directly to evaporation from an extended open water surface without any correction. Screened Class A pans, which are painted black inside, give evaporation rates 10% lower than unscreened unpainted pans.

The considerable amounts of solar radiation are reflected on the high evaporation rates, bringing the annual evaporation to no less than 1.75 m and in some places reaching 2.0 m. The prevailing temperature and wind conditions render September and October to be the months of peak evaporation. In these months, it is common to have evaporation up to 10 mm d^{-1}. This rate drops to 3 mm d^{-1} or less in the rainy season.

Penman's method is generally accepted in Zambia and Malawi, though with some reservation. Similar to the case of Zimbabwe, there are locally modified versions of Penman's formula, e. g . the expressions of Aune and McCulloch, which are used in Zambia. The results obtained from these expressions for estimating the monthly and annual evaporation from the Luano catchment can be found in Balek (1979). The estimate of annual evaporation obtained from Aune's method for 1967-1968 is nearly the same as the figure measured from the galvanized Class A pan, given in Table 4.3. For the same year the estimate obtained from McCulloch's expression is about 3.5% larger than the pan measurement. Aune used two expressions for the 1969-1970 evaporation. The expression that depends on sunshine as a basic parameter gave a yearly value of 1,818 mm, whereas the other expression, which depends largely on radiation gave 1,609 mm only, i.e. 11.5% less. The two Aune expressions gave as well different estimates for the monthly evaporation. The difference between the two sets of estimates varies from a minimum of about 9% to a maximum of about 18%.

Table 4.20- Penman evaporation at a number of locations in Malawi and Zambia for the period from October to April

Location	Stat. No.	Oct	Nov	Dec	Jan	Feb	Mar	Apr
Blantyre	218	228	202	200	166	141	140	53
Karonga	189	203	203	155	144	126	137	120
Mzimba	197	229	205	168	150	134	155	123
Nkhotakota	202	232	207	182	162	148	166	165
Lilongwe	207	218	193	171	153	154	139	139
Zomba	215	210	188	167	168	153	158	152
Mlanje	220	170	201	273	151	175	59	65
These stations are located in Malawi								
Karonga	190	214	184	146	139	131	154	146
Mwinilunga	196	185	149	152	135	135	137	131
Ndola	203	207	179	149	72	153	139	144
Kasempa		199	178	148	145	138	137	132
Chipata	205	214	199	166	179	158	153	181
Mongou	214	204	192	184	168	183	171	179
Livingstone	223	223	211	191	175	176	173	144
These stations are located in Zambia								

More insight into monthly open water evaporation at a number of locations in both Malawi and Zambia for the period October-April can be obtained from Table 4.20.

4.5.5 South Africa- Data on water loss from a free water surface in South Africa date back to the 1930s. In those years, the British Symon's evaporation pan, already discussed in subsection 4.2.5, was widely used for measuring evaporation losses from the storage reservoirs built for irrigation and water-supply purposes, in the 1960s the Symon's sunken pan began to give way to the US Class A pan. Studies were carried out to quantify the difference in reading between screened and unscreened pans. An example of the results obtained is shown in Figure 4.4. This figure and the accompanying regression equation show clearly that the screened pan gives a reading 6 to 7% less than the unscreened pan for the range of 1,000 to 2,000 mm. Other studies were carried out with the object of establishing a relationship between the two types of evaporation pans, i.e. the Symon and the Class A pans. Over the greater part of South Africa, the average annual values obtained from the Symon's pan are roughly 75% of the evaporation from the A pans; only on the southern and southwestern coastal areas is the relation somewhat closer, namely of the order of 85%. The results of those other studies were helpful for preparing a map of the contour lines of equal annual Class A pan evaporation shown in Figure 4.12. This map can also be found in the book on *Climates of Africa* (edited by Griffiths, 1972). From the map it is clear that evaporation is greatest on the western interior plateau

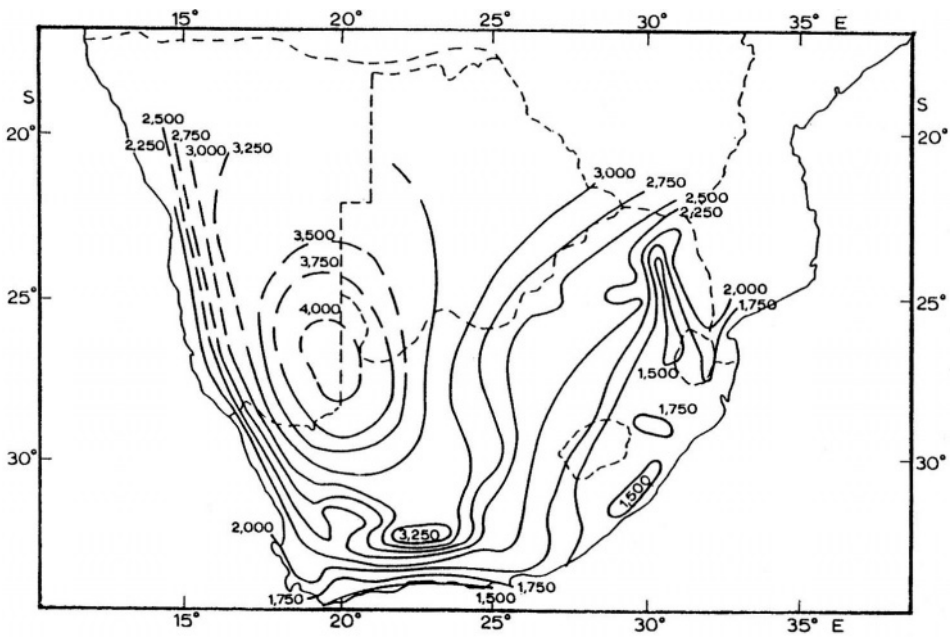

Figure 4.12- Average annual evaporation in mm as obtained from Class A pans in South Africa (from Schulze, cited in Griffiths, 1972)

and the least along the eastern escarpment. Assuming that the lake-pan coefficient for the coastal areas in the east and south is about 0.8 and in the interior 0.7 the open water evaporation in South Africa will fall then in the range 1.2-2.8 m.

As a rule, the pattern of monthly evaporation is quite similar to the pattern of monthly temperature unless interrupted by the fall of rain. As such, the maximum monthly evaporation in the southern region occurs during mid-summer (December-January) and the minimum during the mid-winter (June-July). The northerly stations achieve the maximum evaporation in October-November and the minimum in June

4.5.6 Madagascar- The central parts of Madagascar are occupied by highland plateaus running from north to south along the length of the island at elevations between 800 and 1, 500 m above mean sea level (a. m. s. l.). Three isolated massifs rise from these plateaus and reach a height above 2,500 m. The geography, relief of the island and the ocean and wind regimes are the principal causes underlying the varied climatic conditions of Madagascar.

The variable climate from part to part of the island is strongly reflected on the evaporation from free water there. There is hardly any uniform or clear pattern except that annual evaporation increases steadily along most of the eastern coast from north to south to reach about 1.5 m at Fort Dauphin. It turns with the coast to the south west where an annual evaporation of about 1.8 m is reached at Tulear. North of

Tulear, it decreases rapidly to say 1.1 m along the rest of the western coast, except at some stations like Majunga, where the total evaporation is normally above 1.8 m. Monthly and annual evaporation figures at a number of meteorological stations are included in Table 12, Appendix A. Another characteristic is the limited range in which monthly evaporation changes from month to month. The ratio of maximum to minimum monthly evaporation at any station does not exceed 1.5 to 1. This is basically due to the limited range of temperature variation from one to another.

4.5.7 Nigeria- Evaporation in Nigeria used to be measured using the Piche evaporimeter, the Nigeria ground pan and later the US Class A pan, all of these instruments have been described in sec. 4.2

In view of its large surface area (about $0.924*10^6$ km^2) and geographical location as well as extent in the continent, Nigeria experiences all the West African climates within its boundaries. Sokoto, in the very north of the country, has an average annual temperature of 28.5°C reaching to an average of 33.5° C in the hottest month. These figures, when combined with an average annual humidity of 40%, dropping to say 16% in the warmest months, and 8.8 h d^{-1} of sunshine definitely results in excessively high pan evaporation. The annual pan evaporation is close to 4,400 mm. The daily evaporation varies from about 6 mm d^{-1} in August to 17 mm d^{-1}. Maiduguri, in the northeastern part of Nigeria, presents nearly the same conditions as Sokoto, except that the annual figure for evaporation is about 10% less. The decline with respect to Sokoto increases in a southerly direction to reach say 20% at Kano, where the pan evaporation is close to 3,500 mm.

Unlike Sokoto, Maiduguri and Kano, which are located in the arid northern belt of Nigeria, Lagos is located in the south on the coast of the Bight of Benin. There the climate is wet, 80% average annual relative humidity, 5.2 h d^{-1} sunshine and 26.5°C temperature. These figures cause the annual evaporation in Lagos and Benin City, i.e. the southern coastal belt to be in the order of 1,500 mm d^{-1}. A narrow range of variation characterizes the monthly evaporation in this belt, the ratio maximum to minimum evaporation is in the order of 1.5:1.

Between the northern and southern belts there is a middle belt, where annual pan evaporation falls in the range of say from 2,000 to 3,000 mm. At Jos, it is slightly above 3,000 mm, at Yelwa on the River Niger, not far from the Kainji reservoir, about 2,750 mm and at Makurdi 2,350 mm. These three stations are arranged in location from north to south.

From the given pieces of information, it is fairly safe to conclude that pan evaporation in Nigeria varies between 1.5 and 4.5 m y^{-1}. It is unfortunate that the lake-pan factor for Nigeria is unknown, or at best not published, so as to convert the pan data to their equivalent of lake evaporation. However, if this unknown factor can be assumed as 0.7 for the annual values, the annual lake evaporation will be then from 1.0 or 1.1 m along the coast and increases steadily to reach 3.0 m in the far north of the land.

4.5.8 Chad and Congo Brazzaville- The former ORSTOM (French Office for Overseas Scientific and Technical Research) conducted in the 1950s and 1960s extensive theoretical and experimental research work on evaporation and potential evapotranspiration. In this subsection, discussion will be limited to the theoretical and instrumental work on evaporation conducted in Central Africa in the area extending from northern Chad to south of the Equator.

Part of the said study focused on the readings of screened Piche evaporimeters and the effect of wind or ventilation inside the screen (by screen here is meant a shelter) on those readings. The screened Piche evaporation V was preliminarily expressed as a linear function of the temperature difference $(\theta_a - \theta_w)$ between the dry and wet thermometers and the wind speed. The suggested expression is written as:

$$V/(\theta_a - \theta_w) = \gamma d \tag{4.17}$$

Rigorously speaking, γ is not a constant but rather a function of the wind speed. To check the relationship given by Eq. (4.17) experimentally, monthly values of V from screened (sheltered) evaporimeters were plotted versus the difference $(\theta_a - \theta_w)$ for three stations. These are N'Djamena (formerly Fort Lamy, Chad), Bol-Dune (Chad) and Brazzaville (Congo Brazzaville). An example of these plots is shown in Figure 4.13. The results obtained were as follows:

N'Djamena: 1965-1970, regression coefficient = 0.755
Bol-Dune: 1965-1970, regression coefficient = 0.860
Brazzaville. 1968-1970, regression coefficient = 0.690

The scatter of the points was partly attributed to the influence of wind. This also reacted on the regression coefficients for the three stations. Riou (±1975, exact year is unknown) reported that the screen ventilation at the station of Bol-Dune was the most and the one at Brazzaville the least.

Again, the monthly evaporation amounts for the three stations combined were plotted versus the wind speed at a height of 2.0 m and the relation obtained was:

$$V/(\theta_a - \theta_w) = 0.59u_2^{0.78} \tag{4.18}$$

where u_2 is the wind speed in $\mathrm{m\,s^{-1}}$. The same relation applied much better to the plot of average decadal (10-days) values of $V/(\theta_a - \theta_w)$, 1966-1970, against u_2 for N'Djamena, Chad (Figure 4.14). From Eq. (4.18) one can express the evaporimeter reading, V in mm $\mathrm{d^{-1}}$, directly as:

$$V = 0.59(\theta_a - \theta_w)u_2^{0.78} \tag{4.19}$$

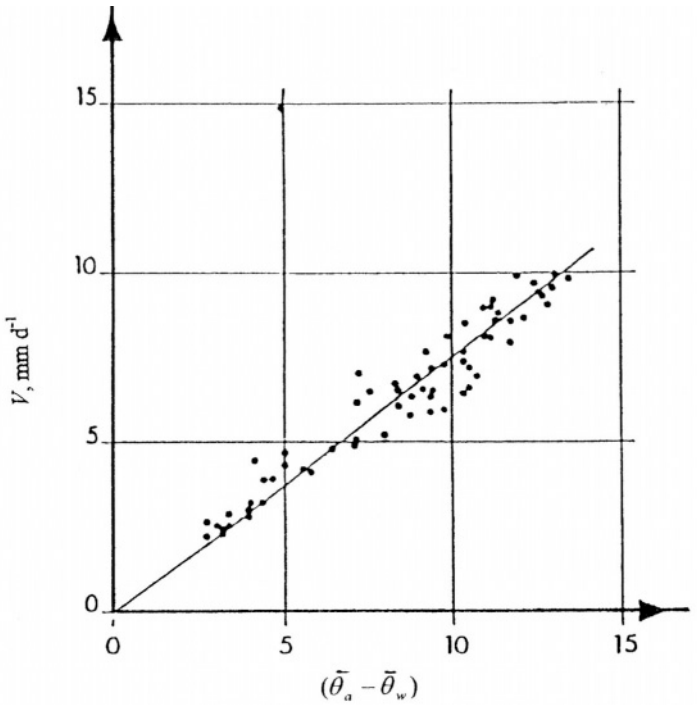

Figure 4.13- Monthly evaporation (Piche in screen) versus temperature difference between dry and wet thermometers at N'Djamena, Chad, from 1965 to 1970 N'Djamena, Chad (after Riou, ± 1975)

Figure 4.14 shows clearly that the ratio $V/(\theta_a - \theta_w)$ increases at a rate less than the rate of increase of the wind speed.

Another component of the study relevant to the performance of the Piche evaporimeter was to examine the effect of the extent of ventilation on the reading of the Piche. This was implemented through a comparison between the readings, V, of Piche instruments placed in the so-called standard, classic or english screen and the readings, V_v, of other Piche instruments placed in well-ventilated screen. An example of the latter is AMPS, at the National Center of Atmospheric Research, Versailles The results obtained from both types of screen in Brazzaville and N'Djamena yielded a simple linear relationship, which can be expressed as:

$$V_v = 1.48V \tag{4.20}$$

It is of interest to observe the joint effect of the extent of ventilation inside the screen and wind speed on the reading of the Piche instrument. The results obtained from both the classical and the well-ventilated screens (shelters) at N'Djamena and

Brazzaville are plotted in Figure 4.15.

In another study on evaporation by the same agency (ORSTOM) and research leader Riou, the evaporimeter investigated was the Colorado sunken pan already described in subsection 4.2.3. The probblem statement was as follows:

> Is it possible to derive a general expression for evaporation from an evaporating surface as a function of the traditional data obtained from a sheltered or screened evaporimeter and the dimensions of that surface? Is it possible using this expression for estimating the evaporation from a large surface

The procedure underlying the theoretical approach comprised expressions for the flux of water vapour overlying the evaporating surface, heat exchange above the evaporating surface, Bowen's ratio and wind function and E' (hypothetical evaporation in case of equal air and water temperature). A great deal of this procedure is similar to the combination method using the heat budget and aerodynamic concepts already developed by Penman.

Denote the evaporation measured by a Colorado sunken pan as E_{Csp} and the evaporation from an extended surface of water like a reservoir or a lake by E_l. The term E' is the same as the one given be Eq. (4.11). The measured pan evaporation E_{Csp} was compared to the evaporation E computed from the expression:

$$E = \frac{\Delta R_n + 2\gamma E'}{\Delta + 2\gamma} \tag{4.21}$$

where Δ is the slope of the saturation-vapour pressure curve at the temperature of the air just overlying the water surface and γ is the psychrometer constant already explained above. The results employed in the said comparison belong to station Bol-Dune, installed on the shore of Lake Chad. The monthly evaporation E computed from Eq. (4.21) and the corresponding measurement from the Colorado sunken pan, E_{Csp}, are included in Table 4.21. Since the maximum difference for a month did not exceed 4.5% and the year 2.7%, Eq. (4.21) has been recommended for estimating the evaporation from the Colorado sunken pan

Further theoretical elaboration of the problem has led to:

$$E_l = \frac{\Delta R_n + 0.59\gamma E'}{\Delta + \gamma} \tag{4.22}$$

where E_l = lake or open water evaporation and the remaining notations as explained earlier. Obviously Eq. (4.22) is similar to the equation of Penman, except that the weight of the term containing the hypothetical evaporation E' is less compared to that introduced by Penman. The lake (Chad) evaporation estimated from Eq. (4.22) is also included in Table 4.21 The monthly E_l values have been divided by the

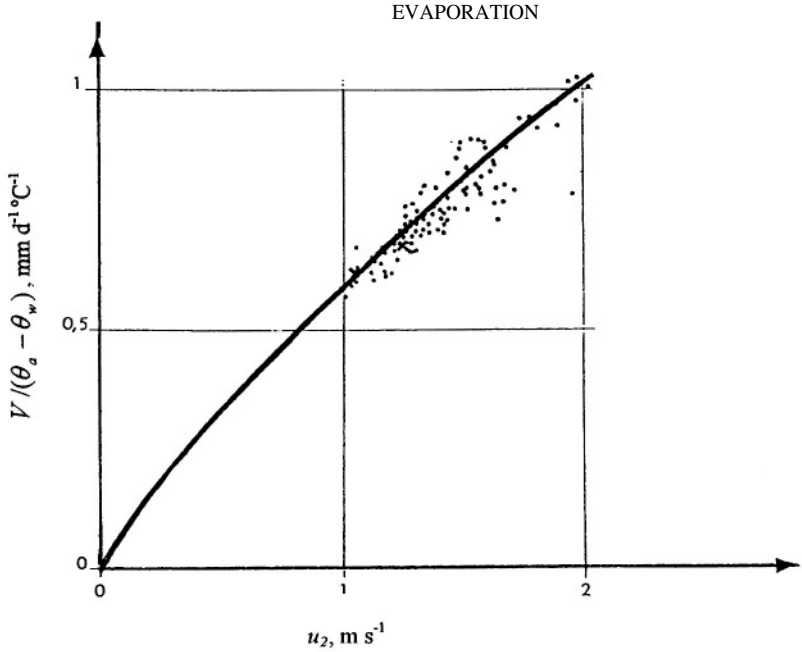

Figure 4.14- Readings of screened evaporimeter against wind speed at a height of 2 m above the ground level, decadal means for the period 1966-70, at N'Djamena, Chad (Riou, ± 1975)

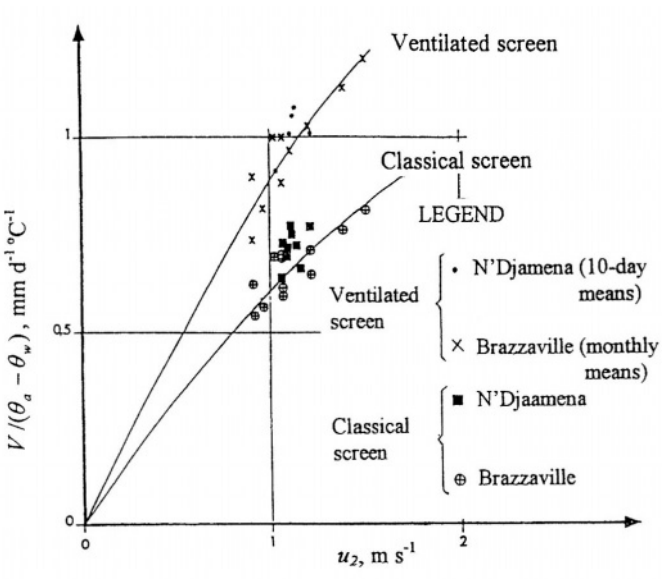

Figure 4.15- Comparison of Piche evaporation in mm d^{-1} °C^{-1} versus wind speed in m s^{-1} between classical and well-ventilated screens (Riou, ±1975)

Table 4.21- Estimated evaporation from theory, E, measured evaporation using Colorado sunken pan, E_{Csp}, estimated lake evaporation, E_l, and pan-lake coefficient, a_p, for Bol-Dune, Chad (average for !957-1966)

Month	E	E_{Csp}	E_l	a_p	Month	E	E_{Csp}	E_l	a_p
Jan	270	267	155	0,577	Jul	223	233	210	0,921
Feb	288	285	165	0,576	Aug	183	189	183	0,984
Mar	350	350	217	0,62	Sep	210	207	192	0,921
Apr	327	327	217	0,664	Oct	267	282	221	0,805
May	307	304	232	0,759	Nov	270	279	180	0,656
Jun	252	255	213	0,84	Dec	248	251	150	0,601
Year						3,195	3,230	2,339	0,728

Explanation

Results were obtained by Riou (@ 1975), all values are given in mm

ap = pan-lake coefficient obtained by dividing E_l by the mean of E and E_{Csp} for each month and for the year

corresponding average values of E and E_{Csp} to get the monthly and annual pan-lake coefficient α_p. Table 4.21 includes as well the pan-lake coefficients. The annual value being equal to 0.728 is within the known range for such a coefficient. The monthly values show a wide range of variation from month to month. The minimum is slightly less than 0.58 for January and February, and the maximum is a bit over 0.92 and occurs in August. If these results are accepted, it means that the pan overestimates the open water evaporation in the winter months and gives a better or closer estimate in the summer months.

It is quite remarkable that the estimates of evaporation from Lake Chad are highly consistent for the different periods. The estimate given by Roche (1975) for the period 1953-1956 is 2,285 mm y^{-1} and Riou (± 1975) using a modified Penman equation got 2,239 mm y^{-1} as an average for the period 1957-66 (Table 4. 21). The estimate made by Pouyaud (1989) from the water balance of the lake for the period 1965-78 is about 2,166 mm y^{-1}. As such, the annual average of the period of 26 years, 1953-78, is about 2,200 mm y^{-1} or $45*10^9\ m^3\ y^{-1}$. The figures often mentioned in the literature are between 44 and $47*10^9\ m^3\ y^{-1}$.

4.5.9 Tunisia- While carrying out certain research projects aiming at land irrigation with saline water in Tunisia, evaporation from free water surfaces was put under investigation. Five stations and four methods were used. The five stations are:as follows: Cherfech ($\varphi = 36°50'$ N) in the Low Medjerda Valley, top north of Tunisia, with annual precipitation of 420 mm, Messouadia station ($\varphi = 35°40'$ N) with annual precipitation of 280 mm, Ksar Geriss ($\varphi = 34°39'$ N) with annual precipitation of 150 mm and Nakta station ($\varphi = 34°19'$ N) with annual precipitation of 200 mm are all situated in the middle of the northern part of the country and Tozeur station in Tozeur

oasis in the south west ($\varphi = 33°55'$ N) where the annual precipitation is just 90 mm. The monthly and annual figures in mm d^{-1} as obtained from the four methods are listed in Table 4.22. From these results, one can reach the following conclusions:

- All methods applied to all stations give July as the month of maximum evaporation and January-February as the period of minimum evaporation.
- The ratio of the Penman evaporation to the sunken pan evaporation varies from 0.83 to 0.93 with an average of 0.895 for the year.
- From the five stations used in the investigation, the most southerly and arid station, Tozeur, Tz* (chott = wetland / salt lake), produces the largest figure

Table 4.22- Measurements /estimates of evaporation in mm d^{-1} at four meteorological stations in Tunisia (UNESCO/UNDP, 1970)

Method	Jan	Feb	Mar	Apr	May	Jun	Jul	Aug	Sep	Oct	Nov	Dec	Year
Piche													
Stat .Ch	2,6	2,7	3	4,2	5,7	7,5	8	6,5	5,3	5	3,9	2,9	4,8
Stat. KG	4,2	4,6	4,6	6	7,9	8,4	11	8,5	6,3	5,5	5,6	4,3	6,4
Stat.Tz	x	x	x	x	x	x	x	x	x	x	x	x	x
Stat. Ms	3,3	2,7	3,5	3,9	7	6,4	8	7,3	4,5	4,5	3,5	3,6	4,8
Stat. Nk	4	4,4	4,2	4,3	5	5	5,4	6,5	5,9	4,4	4,7	4,2	4,8
G. Pan													
Stat. Ch	1,4	2,1	3	4,3	6,3	7,5	8,2	7,2	5	3,8	2,2	1,7	4,4
Stat. KG	3,3	4,2	5	6,5	8,4	9,3	11	9,7	7,3	5,1	4	3,1	6,4
Stat. Tz	2,4	3,8	6	8,2	10	13	14	13	8,8	6,2	3,4	2,1	7,6
Stat. Ms	x	x	x	x	x	x	x	x	x	x	x	x	x
Stat. Nk	x	x	x	x	x	x	x	x	x	x	x	x	x
S. Pan													
Stat. Ch	1,1	1,5	2,4	3,5	5,1	5,7	6,3	5,7	3,8	2,8	1,7	1,4	3,4
Stat. KG	2,4	3	3,9	5,1	6,7	7,6	8,9	7,9	5,7	3,9	2,9	2,4	5
Stat. Tz*	1,9	3	4,8	7	9	11	12	11	7,8	5,1	3	1,8	6,5
Stat. Tz**	1	1,9	3,6	5,1	6,8	8	8,7	7,5	5,2	3,1	1,7	1	4,5
Stat. Ms	1,6	2,4	3,4	4,2	6,7	6,5	8,4	8,5	6,1	4,7	2,9	2,4	4,8
Stat. Nk	2,6	2,5	3,4	4,4	5,5	6,5	7,4	7,3	5,3	4	3,1	2,4	4,5
Penman													
Stat. Ch	1,1	1,7	2,6	3,9	5,5	6,4	7,4	6,4	4,5	3,2	1,8	1,1	3,8
Stat. KG	2	2,9	3,7	4,6	6,3	6,8	8,2	7,3	5,3	3,8	2,6	1,9	4,6
Stat. Tz	1,5	2,5	4,3	5,9	7,6	9,3	9,9	9,1	6,5	4,1	2,3	1,3	5,4
Stat. Ms	1,5	2,4	3,1	4,5	6,1	6,4	7,8	6,9	5,1	3,6	2,2	1,7	4,3
Stat. Nk	1,4	2,1	3,3	4,5	5,7	6,4	7,4	6,9	5,2	3,5	2,2	1,4	4,2

Explanation

The tabulated results for stations Cherfech (Ch), Ksar Geriss (KG) and Tozeur (Tz) are for the period May 1964-May 1969. The remaining results for Messaoudia (Ms) and Nakta (Nk) stations are for the period May 1967-May 1969.

Tz = Tozeur chott (wetland) and Tz** = Tozeur oasis*

for evaporation. This is probably due to the availability of water all the time. The measurement obtained from the sunken pan in the oasis, Tz**, counted to about 70% of the corresponding measurement from the pan placed at the edge of the chott. The latter counted only to 83.3 % of the evaporation from the free water surface as estimated by the method of Penman.

- The evaporation measured by means of the sunken pan is less than the estimate given by Penman's method for all stations, except for Cherfech station, which is close to the Mediterranean coast. So, if it is accepted that Penman's method gives a reasonable estimate of open water evaporation in Tunisia, the annual amounts will be then about 1,390 mm in the very north, 1,600 mm in the middle and 1,970 mm in the southern part of the area investigated.
- According to the report of UNESCO/UNDP (1970) that the yearly averages obtained from the few years of records at those agroclimatic stations are almost the same as those calculated over a period of 50 years by the Meteorological Services for neighbouring stations.

4.5.10 Mauritania- With the exception of the coastal area overlooking the Atlantic, the inland of Mauritania is hot and relatively dry for most of the year. Radiation and sunshine too being of substantial amounts lead to excessive amounts of evaporation. Most of the evaporation measurements in Mauritania as well as the neighbouring countries are taken by the Piche evaporimeter exposed in an instrument shelter.

The map in Figure 4.16 shows contour lines of equal annual Piche evaporation for a large area of the northwestern Sahara (Griffiths & Soliman in Griffiths, 1972). These lines represent minimum of 1.0 to 2.0 m Piche evaporation along the water-side, whether it is the Mediterranean or the Atlantic. From the coast, the evaporation increases in a uniform pattern towards the inland. The map shows further that the mean annual Piche evaporation can reach as much as 5 m in the central Sahara. The surface of Mauritania, as seen on the map, is traversed by contour lines of annual evaporation increasing from 2.0 m to 5.0 m.. The map shows that the annual Piche evaporation at Nouakchott is about or slightly less than 2.0 m. The mean for the period 1951-1990 is 2,359 mm y^{-1} (Ould el-Joud, 1993).

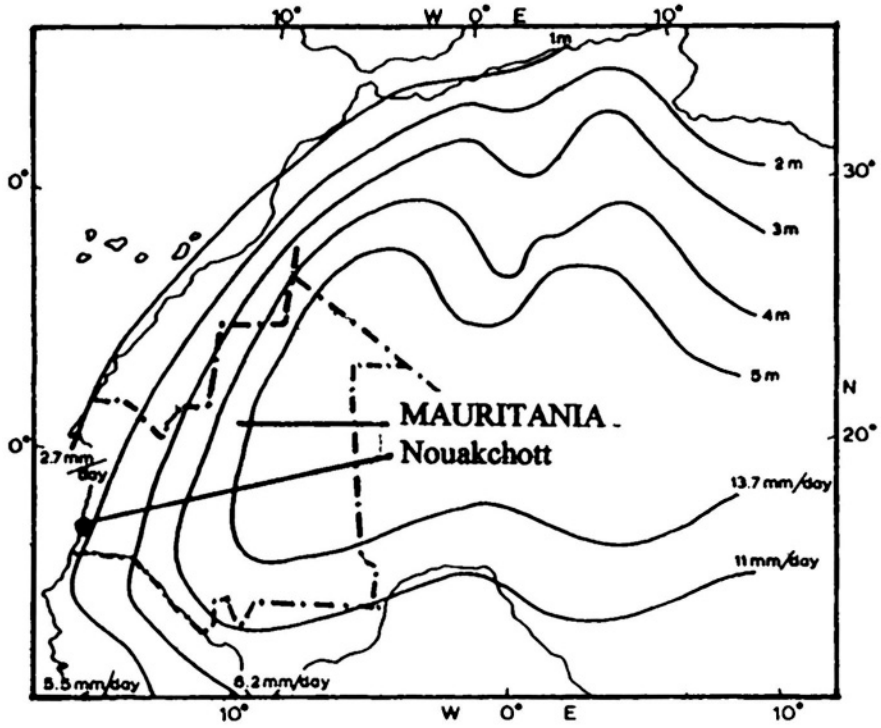

Figure 4.16- Map showing contour lines of mean annual Piche evaporation (Griffiths, 1972)

CHAPTER 5

EVAPOTRANSPIRATION

5.1- Definitions and Background

Evapotranspiration, *ET,* has been defined by the World Meteorological Organization (WMO, 1966) as the difference between precipitation and / or irrigation minus surface runoff minus underground drainage minus change in water storage in the mass of soil concerned. This definition is strictly hydrological in nature. From the stand point of physical meteorology evapotranspiration can be defined as the combined process of both evaporation from soil and plant surfaces and transpiration through the stomata of the plant surfaces. The term consumptive use *CU* is the same as *ET* except that it includes water needed for the building of the plant tissue.

In the previous chapter, distinction has been made between actual and potential evapotranspiration. The potential ET_p is the rate at which water is removed from the soil surface or profile by evapotranspiration if there is no restriction on the available water. The potential ET_p and the maximum ET_{mx} are often viewed as synonymous since the latter describes the maximum ET for a specified crop at a designated time where *ET* is not limited by dry soil water conditions. The actual evapotranspiration ET_a is the actual *ET* for a specified crop at a designated time where ET_a has been corrected for the possible condition of dry soil water.

The term reference crop evaotranspiration can be defined as the water requirements of a disease-free crop, growing in large fields under non-restricting soil conditions including soil water and fertility and achieving full production potential under the given growing environment (Doorenbos & Pruitt, 1977). According to Allen et al. (1994) the reference evapotranspiration ET_r approach to calculating crop evapotranspiration is widely accepted by engineers, agronomists and managers in field practice, design and research. For example, grass reference evapotranspiration is the maximum water loss from a clipped grass surface having a height of 0.12 m and bulk surface resistance of about 70 $s\ m^{-1}$, both at the same prevailing weather conditions (Allen et al., 1994). Burman & Pochop (1994) mentioned that ET_r is similar to ET_p except that it is applied to an identifiable crop, such as alfalfa or grass. ET_r is *ET* from a well-adapted local crop grown under the same conditions as for ET_p.

The crop coefficient, K_c, is a dimensionless coefficient used to relate ET_r to *ET* from a specific crop or plant at a specific time. Formerly, K_c used to relate ET_p to *ET*. Crop coefficients are generally derived from experimental data.

The determination of a reference evapotranspiration or ET_r for a single reference crop like alfalfa and the use of empirical crop coefficients provide a conservative means of estimating *ET* for other crops at progressive stages of growth. The distribution of the crop coefficients for a particular crop as a function of time constitutes a crop curve (Wright, 1982).

The crop evapotranspiration, ET_a, is *ET* from a specified plant grown under defined conditions including soil water, fertility, and other cultural conditions. Evapotranspiration in Africa occurs from a wide variety of ecosystems with different biomass productivity. Basically, these are cultivated lands, tropical rain forests, wetlands (swamps, marshes and dambos) covered fully or partly with water plants, grasslands, woodlands, scrubs and deserts. Estimates of evapotranspiration, no matter the nature of the ecosystem, are important in irrigation planning, scheduling, hydrologic balance studies, onsite wastewater treatment and watershed hydrology (Katul et al, 1992).

The rates of evapotranspiration can be measured or estimated from certain models and / or empirical approaches. Measurements of evapotranspiration from a vegetative surface are a difficult and time-consuming task. All measuring techniques so far available are open to criticism. In addition to the measurements of *ET,* climatic data are indispensable for developing or calibrating methods off estimation of *ET.* When using an empirical method to estimate *ET* from climatic data, it is important that the climatic data used in calibrating methods represent the prevailing climate of the system for which the estimate is made. For example, data collected within a large moist irrigated area will not be compatible with data collected within a dry desert or that collected at an airport. Unfortunately, airport data are often the only data available (Burman & Pochop, 1994). The last years have witnessed the development of new measuring systems of meteorological data. These systems are capable of making many more measurements with greater frequency and accuracy, and are capable of processing and summarizing the data. Additionally, fairly good methods for estimating evapotranspiration using a few climatic data have been developed some years ago (Shih, 1984).

5.2- Measurement of Evapotranspiration

Evapotranspiration can be determined from the water balance of a given system if other items are known accurately. The hydrologic budget can be formulated by the mass balance equation:

$$ET = (I + P_e) - (O + DR) \pm \Delta SM \pm (GW)_r \qquad (5.1)$$

where I = inflow to the system (e.g. irrigation), P_e = effective precipitation, O = outflow from the system, DR = drainage, ΔSM = increase or decrease of soil moisture in storage and $(GW)_r$ = increase or decrease of groundwater runoff.

A special case of Eq. (5.1) develops when both terms I and O are equal to zero. In such a case the balance reduces to:

$$ET = P_e + \Delta SM - DR \pm (GW)_r \tag{5.2}$$

In Eq. (5.2), P_e can be either the effective precipitation or the irrigation supply to the plant or both. The remaining symbols have the same meaning as used in Eq. (5.1). Eq. (5.2) have been applied to rain-fed or irrigated fields without lysimeters. Soil samples are taken before and after application of water at specific time intervals to assess the change in soil moisture content. It is strongly recommended that this method be applied to areas with deep water table, much deeper than the plant root zone. Excessive application of irrigation water should be avoided and soil moisture determinations should be confined to periods with light showers.

According to Israelsen (1956), the early measurements of crop water use were taken from irrigated field plots where the water table was at a considerable depth below the soil surface. The depth of soil moisture removed from the root zone was obtained from the equation:

$$D = \Sigma \frac{(\theta_{fc} - \theta_r)\rho_s h}{100} \tag{5.3}$$

where

D = depth in mm of moisture removed from the root zone
θ_{fc} = % moisture content at field capacity
θ_r = % remaining soil moisture
ρ_s = apparent specific gravity of soil
h = thickness of soil layer

The results obtained from the use of this in Egypt have been summarized in Shahin(1985).

It often appeared, however, that percolation of water below the root zone was difficult to control. This difficulty affected the measurements obtained from the experimental field plots. As a consequence, it was thought more practical to apply the general balance method, Eq. (5.1), to certain devices known as evapotranspirometers or lysimeters.

Lysimeters have been used for many years in numerous countries to supply data to meet specific needs for evapotranspiration problems. According to Harrold (1966), the interest in the use of lysimeters developed early in the 1900s. A lysimeter is basically a container in which soil is placed and water is supplied through precipitation and / or irrigation. A plant is grown in the

container and water table level as well as drainage quantity (if any) are observed or measured.

Constant shallow-depth, water table lysimeters were used to obtain *ET* values by assuming no water storage change during a certain period and equating *ET* to the total water added to the lysimeter soil (special case of Eq. 5.2). Those limitations often caused a confusion about the measured ET values, whether they were actual or potential. If *ET* measurements are to be reliable, there are certain requirements that have to be fulfilled. These requirements are related to the size (area and depth), crop cover, siting, material of construction and isolation, water table and drainage conditions, etc. Lysimeters depending upon their constructional design and operation can be classified into gravimetric and volumetric.

5.2.1 Gravimetric lysimeters-

- Weighable lysimeters are described as complex and expensive, yet produce the most reliable *ET* measurements provided that all necessary precautions in design, operation and siting have been taken (WMO, 1966) In these lysimeters, the whole setup is provided with a system of balances (Figure 5.1) and any change in weight is recorded against time.
- Floating lysimeters, compared to weighable lysimeters, are relatively less expensive. In this type the system of balances that is available in the weighable lysimeters is replaced by a hydraulic system. Small floating lysimeters ($1.0\ m^2$ surface area and 1.83 m deep) have been used in East Africa. One of the earliest floating lysimeters put into use is the one developed by King et al.(1956). It was used to obtain a continuous record of evapotranspiration from an irrigated pasture. The results obtained by this method were compared to evapotranspiration found from the heat budget method. The agreement between the two sets of results depended largely on the lysimeter's effective area. This will be shown in a later section of this chapter. Most important here is to conclude that without an area calibration results from any lysimeter are likely to be unreliable.
- A smaller and definitely a much cheaper lysimeter compared to the previous two types is the one known as Popov lysimeter. This device has long been in use and is very likely still in use in certain parts of Africa (e.g. The Sudan). The device is essentially a metal cylinder $500\ cm^2$ in area and 26 cm deep, closed at the bottom by fine wire netting and filled with soil. Because of its limited depth it is suitable only for short-rooted plants. To prevent sagging of the wire-netting base this cylinder is made to rest on another fine wire net placed at the top of a funnel-shaped cylinder filled with soil which has along its axis an open pipe to permit percolation of water into a container. The daily evapotranspiration is calculated as the difference between the weight of the whole device plus the added water (if any) and the weight of the whole device plus the percolated water on the next day plus rainfall (if any). The Popov lysimeter, next to the

measurement of evapotranspiration, can be used for measuring evaporation from a bare soil surface.

5.2.2 Volumetric lysimeters- In volumetric lysimeters the supply of water to the lysimeter is measured and so is the outflow water collected at the bottom of the soil tank. By maintaining the soil moisture at the field capacity level at the beginning and end of the balance period, the difference between the supply and outflow represents the amount of evapotranspiration in the said period

- Thomthwaite designed an evapotranspirometer (Figure 5.2) for measuring ET_p. The device consists of a field tank of $4\ m^2$ cross-sectional area and 0.70 m in depth, a water supply arrangement and a percolation tank. The system is provided with a regulating mechanism to limit the fluctuation of the water level to within 1cm. Dupriez (1959) reported that the National Institute for Agronomical Studies (INEAC) has installed in 24 of its stations in Congo (Kinshasa), Rwanda and Burundi a network of evaporation measurements based on the principles laid down by Thomthwaite. Each installation consisted of two lysimeters. Some of the results obtained from those experiments using grasses and field crops are summarized in Table 13_a, Appendix A.
- Modified lysimeters have been used by different authorities. The Mather lysimeter (1954, cited in WMO, 1968) has proven to be superior to that of Thomthwaite. The water level regulation device in the latter gave much trouble through clogging. Also, the watering of the field tank from above eliminated many problems resulting from the fixed water table method. Nigeria and Egypt are among the African countries using differently modified lysimeters; e.g. The ones used in Egypt are 1.3 x 0.9 m in surface area and 0.7 m in depth.

Lysimeter measurements of evapotranspiration are generally too expensive, time consuming and not always reliable unless special care is undertaken. In arid areas, particularly, the sparse and irregular nature of vegetation distribution added to the small depth of rainfall and the errors associated with its measurement render the overall reliability of the measurements obtained from

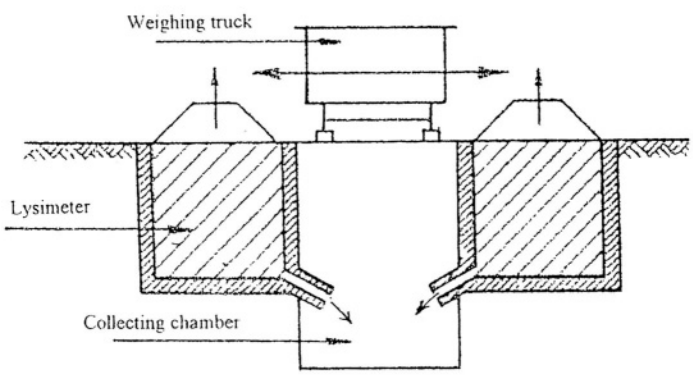

Figure 5.1- A simplified sketch of the weighable lysimeter

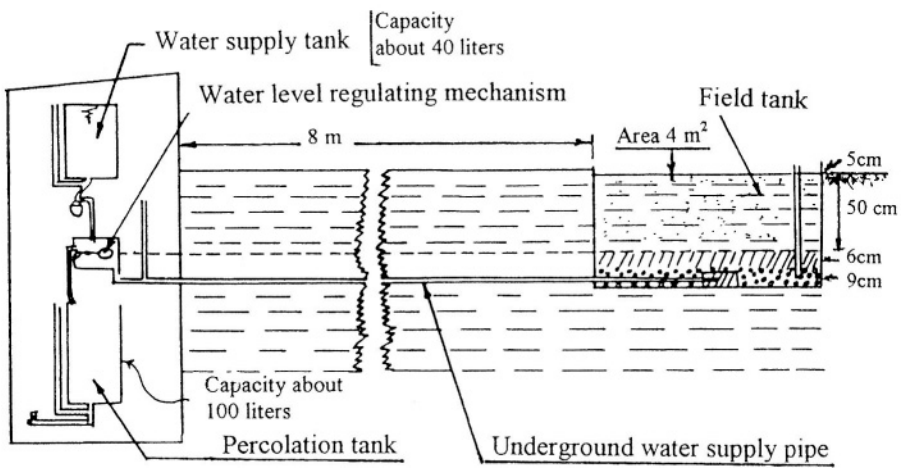

Figure 5.2- Diagrammatic sketch of Thornthwaite's lysimeter

lysimeters too questionable. These zones need too large, properly installed and maintained lysimeteric installations to get sufficiently accurate results. It will be favourable to calibrate these results against results obtained from other methods

5.3- Estimation of Evapotranspiration using Climatic Data

The last 60 years or so have witnessed the development of a considerable amount of methods all aiming at estimation of free water evaporation, pan evaporation, potential/reference and crop evapotranspiration. It should be clearly stated here that not all these methods require the same amount of climatic data. The results obtained from estimation methods requiring much data can be produced equally as well, at least under certain conditions, with less climatic data. According to Shih (1984), the lack of basic data and the difficulties in measurement required in the field methods have accounted for the great efforts made to develop evapotranspiration equations that can relate evapotranspiration some readily available climatic data.

Review and discussion of estimation methods available in the current literature will be basically confined to those methods in current use in Africa. Some of the symbols and notations needed for this purpose have already appeared in Chapter 4 in relation to free water surface evaporation However, for the sake of completeness, it has been found more appropriate to list all notations needed in this section and their respective meanings here below as follows:

A_w = available soil water, percent
Cl = cloudiness

CU = seasonal or annual consumptive use
Cu = monthly consumptive use
E_p = measured pan evaporation
ET = evapotranspiration
ET_a = actual evapotranspiration
ET_p = potential evapotranspiration
ET_r = reference evapotranspiration
F = seasonal or annual consumptive use factor
G = soil heat flux density
H = relative humidity of the air, in percent
H_n = relative humidity at noon, in percent
H_m = minimum relative humidity in percent, quite often $H_m = H_n$
Ka, K' = adjustment coefficient depending on the available soil water
K_c = seasonal or annual consumptive use coefficient
K_c' = crop coefficient adjusted according to the availability of soil water
K_c'' = crop coefficient adjusted to the availability of soil water and degree of wetness of the soil surface
K_{cb} = basal crop coefficient
K_{co} = crop coefficient
K_s = coefficient depending on the degree of wetness of the soil surface
N_{hm} = number of hours in month m (m: 1 for January, 2 for February, etc)
R_s = global short-wave radiation
R_{se} = extraterrestrial radiation
R_n = net radiation
R_{ns} = net short-wave radiation
SS_o = observed number of sunshine hours
R_{nl} = net long-wave radiation
SS_m = maximum possible number of sunshine hours
T = temperature
TD = difference between mean maximum and mean minimum temperatures in ° C
T_K = temperature in degrees Kelvin or absolute, $T_K = T°\,C + 273$
T_m = mean monthly temperature in month m
Z = height in ft
a = calibration factor
b = calibration factor
c = adjustment factor
e = vapour pressure
e_1 = saturation vapour pressure at the mean minimum temperature in mb
e_2 = saturation vapour pressure at the mean maximum temperature in mb
e_a = saturation vapour pressure at the mean air temperature in mb
e_d = actual air pressure at the mean air temperature in mb
f = Blaney-Criddle factor
$f(u)$ = aerodynamic wind function
k_c = monthly consumptive use coefficient
k_p = evaporation pan coefficient
ln = natural logarithm
n/N = $(SS)_o / (SS)_m$ = relative duration of sunshine

p = mean monthly percent of daytime hours of the year
u_z = wind speed, $m\ s^{-1}$, at a height z meters above soil surface
w = temperature-related weighting factor
Δ = slope of the saturation vapour pressure-temperature function at a given T
α = conversion factor
α_s = surface albedo
γ = psychrometric constant
σ = Stefan-Boltzman's constant
ε = emissivity of water

Methods for estimating evapotranspiration (consumptive use) using climatic data are subdivided into groups. Each group appearing in any of the next subsections will be termed after the basic climate parameter it contains

5.3.1 Temperature methods- Of this group of methods, only those developed by Blaney-Criddle, Thornthwaite and Hagreaves will be reviewed here.

a- The *Blaney-Criddle* (B-C) consumptive use formulas (1950/52) can be expressed as:

$$Cu = k_c f = k_c Tp/100 \tag{5.4}$$

and

$$CU = \Sigma Cu = K_c F = K_c \Sigma f = \Sigma k_c f \tag{5.5}$$

where, *Cu and CU* are in inches per month respectively and *T is* the mean air temperature in degrees Fahrenheit. Consider as an example three consecutive months of a crop-growing season with mean temperatures of 68, 71.6 and 77 ° F, respectively. Given k_c as 0.5, 0.75 and 0.85 for the 3 months in their respective order, the corresponding *Cu* values will be 70.6 mm (2.78 in), 128.3 mm (5.05 in) and 174.5 mm (6.87 in). These given data also yield F = 20.39, K_c = 0.721 and *CU*= 373.4 mm (14.7 in).

Several publications by Blaney and Criddle (e.g. 1950/52, 1966) give values of seasonal consumptive use coefficient for a wide variety of crops in the USA. For example, K_c = 0.6-0.7 for cotton (7 months growing season), 0.7-0.8 for sorghum (4 to 5 months growing season) and 1.0-1.1 for rice (3 to 5 months growing season). Those publications included as well the monthly p-values for different geographical latitudes. These can also be obtained for any of the 271-meteorological stations used in this book, using the data in Table 2, Appendix A. For example, the monthly p-values for station no. 26 in Giza, Egypt, are; 7.27, 7.07, 8.33, 8.68, 9.50, 9.47, 9.93, 9.38, 8.37, 7.89, 7.19 and 7.14 % for

January through December. These values are hardly different from those given by Blaney and Criddle (1966).

The B-C formulas proved not to be complicated, instead they are too easy to apply. As someone said, all you need is a kitchen thermometer and a calendar. It certainly gained a wide success in many parts of the world including Africa. To make it even more practical, the structure of Eq. (5.4) has been slightly changed to read:

$$Cu = k_c p(0.46T + 8.13) \tag{5.6}$$

where, Cu = monthly consumptive use in mm and T is the mean air temperature in degrees Centigrade. Many countries tried to develop their own values of monthly and seasonal consumptive use coefficients for the crops growing locally through calibration with other methods, e.g. soil moisture studies. Phelan proposed a modification of the B-C formula, as given by Quackenbush and Phelan (1965), where $k_c' k_T$ is substituted for the k_c in the B-C formula., i.e

$$Cu = k_c' k_T pT/100 \tag{5.7}$$

and

$$k_T = 0.0173T - 0.314 \tag{5.8}$$

where, k_c' is a coefficient reflecting the extent of growth of the plant and k_T is a function of the mean air temperature. The Soil Conservation Service (SCS) of the United States Department of Agriculture (USDA) adopted the modification given by Eq.(5.7) but changed Eq. (5.8) to read (SCS, TR-21, 1967):

$$k_T = 0.0311T + 0.24 \tag{5.8}$$

The FAO Paper-24 introduced a further adjustment to the B-C formula (Doorenbos & Pruitt, 1977) to give the reference evapotranspiration, ET_r, as:

$$ET_r = a + b[p(0.46T + 8.13)] \tag{5.10}$$

where,

$$a = 0.0043H_m - \frac{n}{N} - 1.41 \tag{5.11}$$

and

$$n/N = 2(R_s / R_{se}) - 0.5 \tag{5.12}$$

Once *n/N* is estimated, Eq. (5.12), and the day wind speed at 2 m height above the soil surface is given, the coefficient *b* can be obtained from the tables prepared by Allen and Pruitt (1991). For example; given *n/N* = 0.6, H_m = 40% and $u_2 = 2\ \mathrm{m\ s^{-1}}$, *b* can be found equal to 1.25.

b- The original form developed by *Hargreaves* (1956) for estimating evaporation has been adjusted later by *Hargreaves and Semani* (1982) to yield estimates for potential evapotranspiration using the expression:

$$ET_p = 0.0135 R_s (T + 17.8) \tag{5.13}$$

where

$$R_s = [0.055 + 0.00042(100 - H)] R_{se} \sqrt{n/N} \tag{5.14}$$

where *n/N* in Eq. (5.14) is a percentage. The extraterrestrial radiation R_{se} in units of evaporation can be obtained for any given latitude from the standard tables available in current literature, e.g., FAO-Paper 24 (Doorenbos & Pruitt, 1977), ASCE Report on Consumptive Use of Water and Irrigation Water Requirements (M. Jensen et al., eds, 1990)

The data obtained from 29 $\mathrm{m^2}$ weighable lysimeters at Davis, California, raising Alta fescue grass, were used by Hargreaves and Semani (1985) to rewrite Eq. (5.13) as:

$$ET_p = 0.00023 R_{se} (T + 17.8) \sqrt{TD} \tag{5.15}$$

In the absence of actual measurements of *TD* one can use the expression:

$$TD = 5.56 + 0.178(100 - H) \tag{5.16}$$

For example; when H is given as 75%, the temperature difference TD can be taken as 10 °C.

c- *Thornthwaite* (1948) devised a procedure for estimating potential evapotranspiration from short, close-set vegetation with an adequate water supply in certain parts of the USA. This procedure uses the mean air temperature and number of hours of daylight between sunrise and sunset. The procedure suggested consists of the following computations:

$$ET_p = \frac{N_{hm}}{360} 1.6 \left[\frac{10 T_m}{\Sigma_{m=1}^{12} (0.2 T_m)^{1.514}} \right]^a \tag{5.17}$$

where,

$$a = (675 * 10^{-9}) J^3 - (771 * 10^{-7}) J^2 + (178 * 10^{-4}) J + 0.498 \tag{5.18}$$

and

$$J = \Sigma_{m=1}^{12} (0.2 T_m)^{1.514} \tag{5.19}$$

Consider the monthly day time data in Table 2 and the temperature data in Table 3, Appendix A, both for station No. 125 at Monrovia, Liberia. Substituting these data in Eqs. (5.17), (5.18) and (5.19), the monthly ET_p there can be found as: 79.4, 78.1,... and 80.0 mm for January, February,... and December, with a total annual of 933 mm. The estimates for all months of the year are given in Table 5.1. It also includes the monthly estimates as obtained from Hargreaves formula, Eq. (5.14) and from the radiation method by Jensen and Haise, Eq.(5 20), given in the next subsection.

5.3.2 Radiation methods- This group comprises a number of methods such as those by Makkink, Turc, Grassi, Stephens-Stewart, Stevens, etc. The only method that will be reviewed here is the original Jensen-Haise formula and its subsequent developments

a-: *Jensen and Haise* (1963) began by collecting and re-evaluating the available measurements of ET_p from irrigated areas in the western states of the United States. Those measurements were combined with measurements of temperature and estimates of the solar radiation. The relationship between the three variables, expressed in CGS units, and the solar radiation in evaporation units, has been found as:

$$ET_p = (0.025T + 0.08) R_s \tag{5.20}$$

The original work of Jensen and Haise provides a calculation procedure to get R_s given the cloudiness *Cl* and the solar and sky radiation flux on cloudless days. The estimates obtained from the Jensen-Haise method, Eq (5.20), and Hargreavse method, Eq. (5.14), which are listed in Table 5.1, have all been influenced by the assumed *n/N* values. Due to the absence of local observations

Table 5.1- Monthly and annual estimates of potential/reference evapotranspiration at Monrovia (Stat.no.125), Liberia, using three different methods

Method	Jan	Feb	Mar	Apr	May	Jun	Jul	Aug	Sep	Oct	Nov	Dec	Year
Thorn.	79	78	93	85	78	76	68	72	69	75	79	80	933
Harg.	98	74	87	84	74	60	62	64	61	73	76	95	908
J-H	121	92	109	104	90	73	75	78	74	89	94	117	1116

Explanation

Thorn. = Thornthwaite, Harg. = Hagreaves and Semani (1982) and J-H (Jensen-Haise, 1963). All estimates are expressed in mm. For estimating the monthly solar radiation R_s, the average relative duration of bright sunshine n/N at the neighbouring stations has been used. The ratios used are: Dec-Jan = 0.40, Feb-Apr Apr = 0.25, May = 0.20, Jun-Sep = 0.15, Oct = 0.20 and Dec = 0.25

data from neighbouring stations have been used. The annual ET_p estimated by Hargreaves method is about 2.7% less than that estimated by Thomthwaite's. On the other hand ET_r obtained from The Jensen-Haise formula is 123% larger than the ET_p estimated by the Thornthwaite method. The differences between monthly estimates using the three methods reach as much as 50%.

Jensen (1966) reviewed the energy balance underlying the derivation of Eq. (5.20) and developed other expressions for the reference evapotranspiration ET_r as follows:

$$ET_r = C_T (T - T_x) R_s \tag{5.21}$$

where

$$C_T = 1/\left[C_1 + (650/(e_2 - e_1)\right], \tag{5.22}$$

$$C_1 = 68^o F - (3.6^o F.0.001Z), \tag{5.23}$$

$$T_x = 27.5^o F - \left[0.25(e_2 - e_1) - 0.001Z\right] \tag{5.24}$$

The *Jensen-Haise* method has been used for periods ranging from just 1-day to a month. ASCE recommends its use for a minimum time period of 5 days (Jensen et al., 1990).

5.3.3 Combination methods- The original *Penman's formula,* the adjusted expressions referred to as the *FAO-Penman* and the *FAO-Penman-Monteith* are the only methods from the combination group which will be reviewed here.

a- The original formula developed by *Penman* (1948) aimed at predicting evaporation losses *E* from an open water surface. This formula combines the

energy (radiation) term with an aerodynamic (wind and humidity) term. combined formula has already been given in Chapter 4 by the set of Eqs. (4.11), (4.12) and (4.13).

b- The *FAO-Penman* formula, sometimes referred to as the modified formula (1977), has been developed with the aim of using for predicting grass reference evapotranspiration. The adjusted expression is as follows:

$$ET_r = c[wR_n + (1-w)f(u_2)(e_a - e_d)] \tag{5.25}$$

The factors *c* and *w* can be obtained according to the instructions given in the ASCE manual on Consumptive Use of Water and Irrigation Water Requirements (Jensen et al., 1990). The ET_r calculated from Eq. (5.25) can be expressed in terms of free water surface evaporation *E* by the relationship:

$$ET_r = \alpha E \tag{5.26}$$

c- The *updated FAO-Penman-Monteith formula* (ICID/Allen et al.,1994) can be written as:

$$ET_r = 0.408\Delta(R_n - G) + [900\gamma u_2(ea - ed)/(T_K)]/[\Delta + \gamma(1 + 0.34u_2)] \tag{5.27}$$

where R_n and *G* are in MJ m^{-2} d^{-1}, γ in $kPa^{\circ}C^{-1}$, and e_a and e_d in kPa.

For monthly temperature fluctuations (effective soil depth 2.0 m), Jensen et al. (1990) have suggested expressing the term G as:

$$G = 0.07(T_{m=i+1} - T_{m=i-1}) or = 0.14(T_{m=i} - T_{m=i-1}) \tag{5.28}$$

where m is an arbitrary month, $m = i$ is the number of the month in question, $m = i-1$ is the number of the preceding month and $m = i+1$ is the number of next month. All parameters used in the calculation of evapotranspiration are given by Jensen et al. (ASCE, 1990) as well as Allen et al. (ICID, 1994).

5.3.4 Evaporation pan methods- Water loss from an evaporation pan and evapotranspiration from a vegetated surface both involve evaporation processes As measurement of water loss from an evaporation pan is more feasible than from vegetation, it is easier to estimate evapotranspiration from pan evaporation together with a conversion coefficient, usually less man unity, i.e.

$$ET_r = k_p E_p \tag{5.29}$$

The pan coefficient k_p depends on the kind of pan used (US Class A pan or Colorado sunken pan), the wind run and the environment surrounding the pan (case A or B). It should be noted that k_p increases with increasing relative humidity and decreasing wind speed.

The FAO-Paper 24 (Doorenbos & Pruitt, 1977) and ASCE manual (Jensen et al., 1990), are among the currently available literature which includes special tables for k_p. From these tables, it can be seen that the pan coefficient varies from a minimum of 0.4 to a maximum of 0.85 for class A pans and from a minimum of 0.45 to a maximum of 1.1 for the sunken pans.

5.4- Relation between Evapotranspiration and Potential Evapotranspiration

The current literature presents a number of methods and models describing the relationship between the evapotranspiration and potential evapotranspiration. A number of concepts describing this relationship has been mostly collected and summarized by Tanner (1967), as illustrated in Figure 5.3. Boonyatharokul & Walker (1979) and Hillel (1980) have also presented some models of the classical concepts for the ratio ET_a/ET_p as functions of the available soil moisture, though in hypothetical idealized forms.

Jensen (1968) suggested a more practical approach. He introduced a new coefficient termed the crop coefficient K_{co} which can be expressed as:

$$K_{co} = \frac{ET}{ET_p} = \frac{R_n + G + A}{R_{no} + G_o + A_o} \tag{5.30}$$

where the "$_o$" subscript designates concurrent values for the reference crop. Crop coefficients can be used to estimate actual water use for a particular crop from estimates or measurements of a potential or reference evapotranspiration. They are empirical ratios of crop *ET* and are generally derived from experimental data. The determination of a reference evapotranspiration ET_r for a single reference crop, like alfalfa, and the use of empirical crop coefficients provides a conservative means of estimating *ET* for other crops at progressive stages of growth. The distribution of the crop coefficients for a particular crop as a function of time constitutes a crop curve.

Some investigators favour alfalfa over grass as a reference crop because the aerodynamic characteristics of alfalfa are more like most agricultural crops. Furthermore, the height of the plant canopy and the greater depth of the root system are additional merits. On the other hand, grasses can be clipped and thus be maintained at a constant height throughout the growing season.

Table 5.2 gives experimental crop coefficients K_{co} for a number of field crops and pasture as can be found in literature, e.g. Jensen et al (1990). Values are given on 10% intervals for the pre-effective plant cover periods and for 10-

day intervals throughout the post-effective cover period. When soil water limits plant growth including *ET,* the crop coefficient K_{co} has to be adjusted according to the available water A_w. One of the possible ways of adjustment is to use an adjusted crop coefficient $K_c^{'} \leq K_{co}$ expressed as:

$$K'_c = K_{co} K_a = K_{co} \ln(A_w + 1) / \ln(101) \tag{5.31}$$

Eq. (5.31) gives the reduction coefficient, K_a, as 0.852, 0.891, 0.924, 0.952, 0.977 and 1.00 for A_w = 50, 60, 70, 80, 90 and 100%, respectively.

Wright (1982) developed a different procedure to replace K_{co} by $K_c^{"}$. He claimed that this procedure permits helps to get a more accurate estimation of the daily *ET* whenever the state of wetness of the soil surface can be described, e.g. after rainfall or irrigation. The proposed coefficient can be expressed as:

$$K_c^{"} = K_{cb} K_a^{'} + K_s \tag{5.32}$$

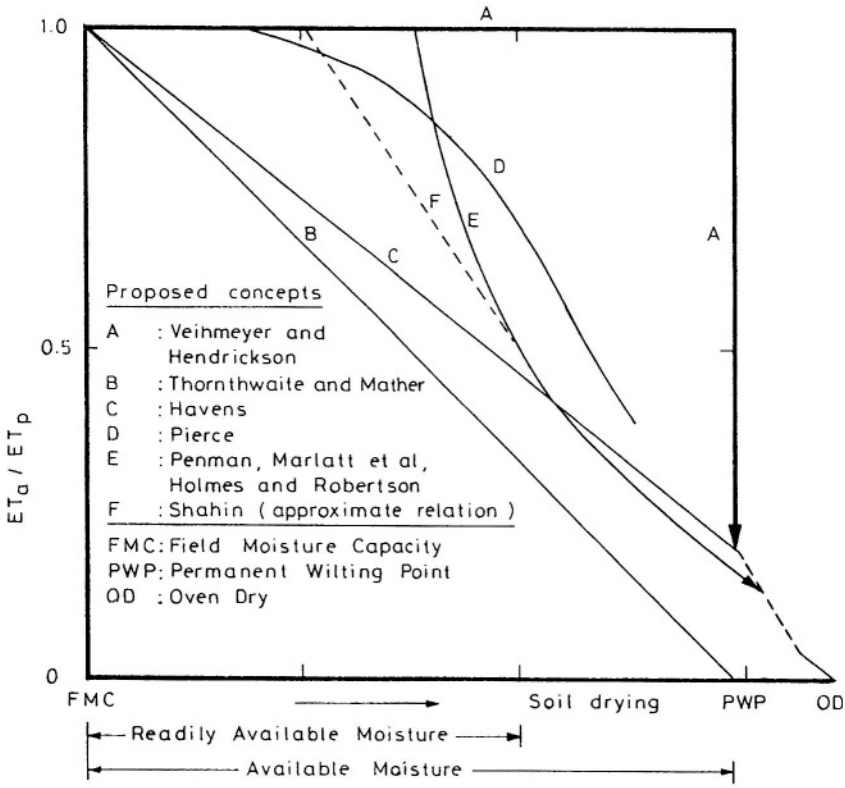

Figure 5.3- The ratio ET_a / ET_p as a function of the soil moisture content (Taner, 1967)

Table 5.2- Experimental crop coefficients, K_{co} (from Jensen et al., 1990)

	Planting to effective cover in percent									
Crop	10	20	30	40	50	60	70	80	90	100
Small grains	0.16	0.18	0.25	0.37	0.51	0.67	0.82	0.94	1.02	1.07
Beans	0.20	0.23	0.30	0.39	0.51	0.63	0.76	0.88	0.98	1.07
Peas	0.20	0.24	0.31	0.40	0.51	0.63	0.75	0.87	0.97	1.05
Potatoes	0.10	0.13	0.20	0.30	0.41	0.53	0.65	0.76	0.85	0.91
Sugar beets	0.10	0.13	0.20	0.30	0.41	0.53	0.65	0.76	0.85	0.91
Corn	0.20	0.23	0.29	0.38	0.49	0.61	0.72	0.82	0.91	0.96
Alfalfa	0.36	0.47	0.58	0.68	0.79	0.90	1.00	1.00	1.00	1.00
Pasture	0.87	0.87	0.87	0.87	0.87	0.87	0.87	0.87	0.87	0.87
	Days after effective cover									
	10	20	30	40	50	60	70	80	90	100
Small grains	1.04	0.94	0.74	0.49	0.19	0.10	0.10	0.10	0.10	0.10
Beans	1.02	0.96	0.85	0.73	0.59	0.45	0.31	0.19	0.10	0.10
Peas	0.98	1.02	0.99	0.76	0.20	0.10	0.10	0.10	0.10	0.10
Potatoes	0.90	0.85	0.75	0.60	0.38	0.10	0.10	0.10	0.10	0.10
Sugar beets	0.90	0.90	0.90	0.90	0.90	0.90	0.90	0.90	0.90	0.90
Corn	0.99	0.99	0.93	0.82	0.68	0.54	0.40	0.28	0.20	0.17
Alfalfa	0.75	1.00	1.00	1.00	1.00	1.00	1.00	1.00	1.00	1.00
Pasture	0.87	0.87	0.87	0.87	0.87	0.87	0.87	0.87	0.87	0.87

where K_{cb} = basal crop coefficient (e.g. Jensen et al., 1990), K'_a is a function of A_w. From an earlier study by Boonyatharokol and Walker (1979), it has been recommended that K'_a can be taken equal to 1 for $A_w > 50\%$ and $A_w / 50$ for $A_w < 50\%$. K_s = adjustment coefficient for the degree of wetness of the soil surface; $K_s > 0$ when the surface is wet and zero when it is dry.

The FAO-Paper No.56 (Allen et al., 1998) went another step further by slightly changing Eq. (5.31) to read:

$$K_c^{"} = K_{cb} + K_e \qquad (5.32')$$

The basal crop coefficient K_{cb} as given in Eq. (5.32'), can be defined as the ratio of crop evapotranspiration, *ET,* over the reference evapotranspiration (ET/ET_r) when the soil surface is dry but transpiration is occurring at a potential rate, i.e. water is not a limiting transpiration. The other coefficient, K_e in the dual crop coefficient approach, serves to get values for surface evaporation.

An example of the dual crop coefficient approach can be found in the case study shown below. The main features of the case considered are as follows:

- sandy loam soil having moisture levels of 0.23 $m^3\ m^{-3}$ and 0.10 $m^3\ m^{-3}$ at the field capacity and wilting point respectively,
- depth of surface soil layer that is subject to drying by way of evaporation is 0.10m,

- height of vegetation is 0.30 m, $u_2 = 1.6\ m\ s^{-1}$, $H_m = 35\%$,
- $K_{cb} = 0.3$ on day 1 and 0.4 on day 10,
- the exposed soil fraction decreases from 0.92 on day 1 to 0.86 on day 10,
- all evaporable water has been depleted from the evaporation layer at the beginning of calculations,
- irrigation occurs at the beginning of day 1, depth of irrigation water is 40 mm, and the fraction of soil surface wetted by irrigation = 0.80,
- a rain of 6 mm occurred at the beginning of day 6.

The calculation of the daily crop coefficient is done according to the procedure described in the FAO-Paper 56 (Allen et al., 1998). The results obtained are shown graphically in Figure 5.4.

Before bringing the present section to an end, it might be worth while revisiting Morton's hypothesis in relation to evapotranspiration. This hypothesis has already been presented in Chapter 4 while discussing evaporation from free water surfaces. Morton in his hypothesis suggested that the estimate of the so-called areal evapotranspiration $(ET)_A$ can be based on the complementary response of the potential evapotranspiration ET_P to changes in the availability of water to areal evapotranspiration. So, would the relation be truly complementary it can then be represented as:

$$(ET)_A + ET_p = 2ET_W \tag{5.33}$$

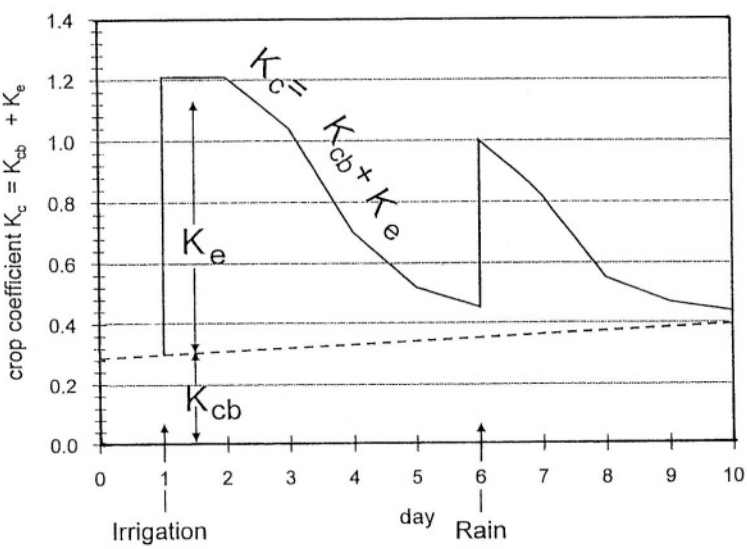

Figure 5.4- Example of the dual crop evapotranspiration coefficient approach (Allen et al., 1998)

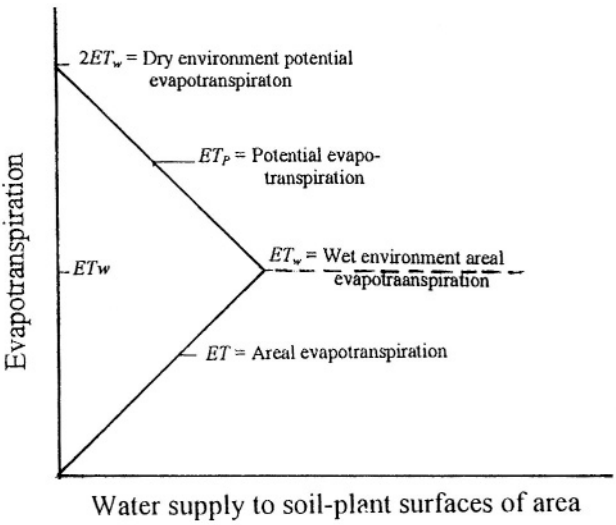

Figure 5.5- Schematic representation of the complementary relationship between areal and potential evapotranspiration with constant energy supply (Morton, 1983)

where $(ET)_A$ is the actual evapotranspiration from an area so large that the effects of upwind boundary transitions are negligible, ET_P is the potential evapotranspiration, and ET_W is the wet environment areal evapotranspiration. The relation expressed by Eq. (5.31) can be clearly seen from the diagrammatic representation shown in Figure 5.5. This figure shows that under completely arid conditions (zero supply) the areal evapotranspiration would be zero and the potential evapotranspiration would be high. For a less than abundant supply, ET_A would equal the supply, and for an abundant ET_A and ET_P would be equal. Morton's hypothesis, as cited in Nash (1989), is that for all intermediate supply rates the slope of the two curves would be equal in magnitude and opposite in sign, thus implying a constant sum of ET_A and ET_p.

5.5- Country Practices and Experiences

The previous section dealt with the main features of the methods for measuring or estimating evapotranspiration which have been used and are still in common use in many of the African countries. The experiences already gained by some of these countries can be summarized in the next subsections.

5.5.1 Egypt- Most of agriculture in Egypt is totally dependent on irrigation water. In 1920, the Water Requirements Committee of Egypt recommended to the then State Irrigation Department certain figures for the (irrigation) water

requirements of both Lower and Upper Egypt to ensure reasonably high crop yields. For example the seasonal water requirements for sugar cane (summer crop) were set at 1,330 mm and 1,695 mm per acre (4,200 m^2) for Lower Egypt and Upper Egypt respectively. The corresponding crop consumptive use of water can be obtained by dividing the irrigation water requirement by the overall efficiency of irrigation. So, if it is 60% in the case of the sugar cane crop, the corresponding figures for the consumptive use (evapotranspiration) will be about 800 mm for Lower Egypt and 1,020 for Upper Egypt respectively, the difference is due to the significant difference in climate between the two regions.

Experimental work aiming at the direct determination of crop consumptive use of water began in the 1940s at a number of State and University experimental farms where soil moisture depletion measurements from controlled plots and lysimeters were the main technique then used. The contribution of the water table to the cyclic as well as total consumption remained, however, difficult to assess.

As the results of the research works of Blaney and Criddle, Hargreaves, Thomthwaite and Penman became known from the relevant literature, the available soil moisture depletion figures were used to obtain the corresponding consumptive use coefficients. A relatively large sample of crop water use coefficients, K_o, have been obtained from the calibration of each of the original *Blaney-Criddle* formula, Eq. (5.5) or (5.6) and the original formula of *Hargreaves* (1956)*, expressed as:

$$ET_p = 0.38K_c p(T - 32)(1 - H_n) \tag{5.34}$$

where T = average monthly temperature in °F, and H_n = relative humidity at noon, expressed decimally, The *Thornthwaite* formula given by Eqs. (5.17), (5.18) and (5.19), and the original *Penman's* method expressed by Eq. (4.12), (4.13) and (4.14). Some of the results obtained are summarized in Table 5.3.

*Due to its limited use, this formula was not discussed in sec. 5.3.

The crop consumptive use coefficients obtained by the above mentioned estimation methods, i.e. Blaney-Criddle, Hargreaves, Thornthwaite and Penman, were in reasonable agreement with those obtained from areas in the United States having a similar climate to that of Egypt. This result encouraged the concerned authorities to continue the same procedure in the late 1960s and 1970s aiming at determining consumptive use coefficients for more crops and other locations in Egypt. The simplicity and ease of application of the Blaney-Criddle formula in particular have made its use so popular that it covered many countries in the Middle East and the Southern Mediterranean. Despite the physical grounds (energy budget and aerodynamic component) on which

Penman's formula is founded, its application remained restricted only to those locations where adequate and reliable climatic data are available.

Fathi (1995) examined the applicability of the consumptive use coefficients recommended by Doorenbos and Pruitt (FAO, 1977) to four crops raised in a desert environment in Egypt. The crops were sorghum, wheat, barley and peanuts raised in two volumetric lysimeters each installed in desert sandy soils. The experiments were conducted at south Tahrir (φ = 30° 39'N, λ = 30° 35'E and z = 31 m). The average figures for climatic data over 10 consecutive years were 19. 5°C for air temperature, 63% mean relative humidity, 28 km d^{-1} wind speed, 9.1 h d^{-1} sunshine and 4.2 mm d^{-1} radiation. These data were fed into the computer program CROPWAT developed by FAO (1989). The daily values of potential evapotranspiration ET_p thus obtained are: 1.75, 2.36, 3.23, 4.52, 5.41, 6.14, 6.06, 5.55, 4.54, 3.26, 2.16 and 1.67 mm for January, February, ..., December, respectively.

The coefficients K_c/Exp were obtained by dividing the average loss of moisture from the two lysimeters raising each crop by the FAO ET_p, whereas the FAO recmmended coefficients K_c/FAO are available in the FAO-Paper 24 (Doorenbos and Pruitt, 1977). The two sets of coefficients for each of the four crops are listed in Table 5.4. In general, the seasonal coefficients are almost the same for all crops. The experimentally found coefficients are significantly less than those published by FAO for the initial stage of crop growth, and just the opposite for the late stage except for the peanuts. The figures for developed and middle stages of growth are slightly different for all crops.

Semaika and Rady (1988) reported the results of an interesting study on the consumptive use of cotton. The experimental work covered the growing seasons of 1983 and 1984 at Bahteem station in the southern part of the Nile Delta, not far from Cairo. The depletion of soil moisture was observed closely in five treatments where the intervals between two successive irrigation applications were 9, 12, 15, 18 and 21 days. The average figures for the two seasons showed a drastic fall in the seasonal consumption from 725 mm for the 9-days interval to 485 mm for the 21-days interval, i.e. a drop of about one-third. The line of best fit to the 10 consumptive use figures is shown in Figure 5.6.

Almost similar results were obtained from a different set of irrigation experiments performed in 1991 and 1992 on sugar beets in the Middle part of the Nile Delta area. The treatments irrigated once every 7 days lost more soil moisture than the treatments irrigated once in 14 days and much more than those irrigated once every 21 days. On the other hand the contribution of the water table to the crop water use increased with increased irrigation interval (Ibrahim et al., 1995). The average reductions in water use caused by increasing the irrigation interval to two and three weeks instead of one week were about 20 and 30% respectively.

Table 5.3- Monthly crop consumptive use coeffisients (single), average for the Nile Delta and Middle Egypt (El-Shal, 1966, and Shahin & El-Shal, 1969)

Crop / method	Monthly and seasonal crop consumptive use coefficients												
	Jan	Feb	Mar	Apr	May	Jun	Jul	Aug	Sep	Oct	Nov	Dec	Season
*Cotton**													
Blaney-Criddle			0,26	0,39	0,66	1,07	1,03	0,56	0,51				0,71
Hargreaves			0,19	0,23	0,39	0,65	0,6	0,34	0,34				0,42
Thornthwaite			0,75	0,72	0,98	1,33	1,23	0,66	0,73				0,99
Penman			0,4	0,65	0,86	1,35	1,31	0,74	x				0,95
*Wheat***													
Blaney-Criddle	0,49	0,59	0,67	0,49	0,32						0,46	0,47	0,51
Hargreaves	0,47	0,6	0,49	0,27	0,14						0,34	0,45	0,38
Thornthwaite	2,15	2,78	1,89	0,89	0,42						0,97	1,57	1,3
Penman	2,5	2,24	1,3	0,8	0,53						1,57	3,05	1,34
*Maize (late)****													
Blaney-Criddle								0,58	1,11	1,25	0,48		0,84
Hargreaves								0,34	0,75	0,89	0,38		0,59
Thornthwaite								0,68	1,56	2,22	1,1		1,29
Penman								0,87	2	1,97	1,626		1,56
Berseem°													
Blaney-Criddle	0,31	0,42	0,79	0,82	0,64	0,25				0,31	0,37	0,62	0,56
Hargreaves	0,32	0,39	0,49	0,39	0,35	0,13				0,19	0,27	0,61	0,37
Thornthwaite	1,49	1,65	2,18	1,59	0,98	0,5				0,28	0,82	2,43	1,29
Penman	0,48	0,68	0,79	0,8	0,61	0,22				0,43	0,62	1,3	0,73
Maize (early)°°													
Blaney-Criddle				0,36	0,71	1,06	0,87	0,6					0,79
Penman				0,34	0,62	0,89	0,8	0,52					0,7

Table 5.3- Cont'd

Crop / method	Monthly aand seasonal crop consumptive use coefficients												
	Jan	Feb	Mar	Apr	May	Jun	Jul	Aug	Sep	Oct	Nov	Dec	Season
Citrus trees ^{ooo}													
Blaney-Criddle	0,35	0,51	0,55	0,57	0,6	0,64	0,7	0,64	0,59	0,56	0,42	0,32	0,54
Penman	0,54	0,56	0,6	0,55	0,56	0,57	0,62	0,62	0,6	0,77	0,71	0,67	0,62

Explanation

** Averages over the period 1957-1960, data from Abd el-Samie &Barraada (1960), Abd el Warith (1965) and El-Shal (1966)*

*** Averages over the period 1957-1960, data from Abd el-Warith (1965) and El-Shal (1966)*

**** Averages over the period1959-1964, data from El-Shal (1966), El- Gibali (1966) ang Shenouda et al. (1966)*

^{o} Averages over the period 1957-1959, data from Shahin (1959) and El- Shal (1966). Irregulaities in figures are oaused by cutting the crop (Berseem is an Egyptian clover)

^{oo} Averages for 1964-1965, data from Shenouda et al. (1966)

^{ooo} Averages for the period 1957-1959, data from Shahin (1959) and El- Nokrashy (1963)

Table 5.4- Consumptive use coefficients for sorghum, wheat, barley and peanut grown under desert conditions in Egypt, 1987-1990 (Fathi, 1995)

Stage of growth	Sorghum		Wheat		Barley		Peanut	
	K_c/Exp	K_c/FAO	K_c/Exp	K_c/FAO	K_c/Exp	K_c/FAO	K_c/EXp	K_c/FAO
Initial	0.5	0.7	0.58	0.9	0.6	0.9	0.57	0.65
Developed	0.63	0.85	0.71	0.97	0.69	0.97	0.9	0.8
Middle	0.99	1	1.03	1.05	1.09	1.05	1.1	0.95
Late	0.8	0.5	0.67	0.25	0.66	0.25	0.45	0.55
Average	0.73	0.76	0.75	0.79	0.76	0.79	0.76	0.74

Explanation

K_c/Exp = Consumptive use, average of 2 lysimeters divided by ET_p as obtained from FAO CROPWAT computer program using 10 years agrometeorological data, ETp = potential evapotranspiration, and K_c/FAO = crop coefficient as suggested by FAO (Doorenbos & Pruitt/FAO, 1977)

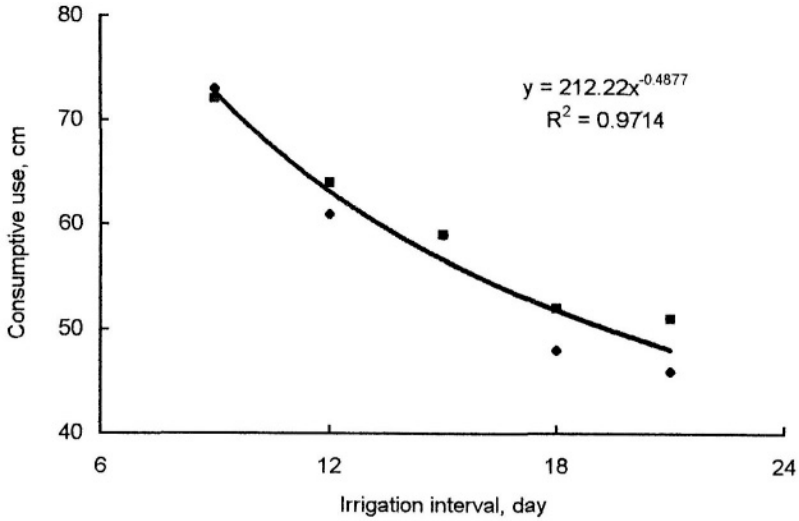

Figure 5.6-Seasonal consumptive use of water for cotton in the upper part of the Nile Delta area against the interval between irrigation applications

5.5.2 The Sudan- Various crops grow in the Sudan, of which cotton is the most important crop, as it is the chief source of foreign earnings for the country. The area raising cotton in the Gezira region (the northern part of the triangle of land contained between the White and the Blue Niles (Figure 5.7), has grown from just 100 ha in 1912 to more than 420,000 ha by the end of the 1960s.

The weighable, volumetric and floating types of lysimeters were engaged for measuring evapotranspiration from a number of crops such as cotton, wheat, sorghum (dhura), kidney beans and grasses. Olivier (1961) applied his own method for estimating the consumptive use of certain crops grown in Wad-Medani (Station No.57) and grass at Malakal (Station No. 103). The results obtained are included in Table 5.5. His estimate for evapotranspiration from the swamps in southern Sudan is given in a later section.

Rijks carried out a series of investigations into the use of water by irrigated cotton in the Gezira area of the Sudan. The results of his experimental work were published in four parts. The first part dealt with a detailed analysis of the radiation balance over the crop and over the desert soil (1967). In the second part (1968), he aimed at estimating the energy available for evaporation and for heating of the air. Additionally, he tried to develop a method of estimating the components of the radiation balance from the available meteorological data. The third part of the study dealt mainly with Bowen ratios and estimates of advective energy. It also presents the estimates of evaporation obtained by micrometeorological methods. The amount of water used by irrigated cotton in the Sudan Gezira was estimated by three methods: a combination of micrometeorological techniques, gravimetric sampling of soil water, and lysimetry. The fourth part (1971) compares the evapotranspiration estimates obtained by these three methods and relates them to potential evapotranspiration

Table 5.5- Estimates of monthly evapotranspiration and Class A pan evaporation in mm d^{-1}, in the Sudan

Crop / Location	Method	Jan	Feb	Mar	Apr	May	Jun	Jul	Aug	Sep	Oct	Nov	Dec	Season mm
*Wad-Medani**														
Cotton	Olivier	4.65	6.16	8.69	10.08				2.23	2.95	4.75	5.06	3.92	1,265
Wheat		4.65	6.16	8.69								5.06	3.92	690
Sorghum								3.46	2.23	2.95	4.75			260
K. Beans		4.65								2.95	4.75	5.06	3.92	562
*Malakal**														
Grass	Olivier	6.10	7.60	8.69	5.99	3.61	2.22	1.40	1.35	1.72	1.98	4.12	5.28	1,521
*Wad-Medani***														
Cotton	Blaney	4.71	3.75	1.93	1.37				1.00	3.45	5.40	5.75	5.32	965
Wheat	&	5.41	4.44	2.23								1.88	3.61	480
Sorghum	Criddle							1.83	5.14	4.80	1.34			350
K. Beans		2.65								0.86	3.43	5.36	3.92	461
Class A Pan	Har-greaves	11.14	12.43	14.57	18.43	17.86	16.14	11.57	8.14	9.29	13.57	13.14	11.57	4,803
*Khartoum***														
Class A Pan		14.43	16.57	19.43	23.71	24.28	21.71	15.43	10.86	12.29	18.00	18.00	15.71	6, 403
*Wad-Medani****														
Cotton	Energy balance	6.70									5.76	6.08	5.71	

Explanation

*Figures are quoted from: *Olivier (1961), ** Shahin (1985) and ***Rijks (1971)*

and to plant growth. The graphic plot of the daily *ET* of cotton for 79 days, from 18.10.1965 to 04.01.1966, is shown in Figure 5.8. It is of interest to observe how *ET* fluctuates from day to day depending on the wetness of the surface.

The average figures for October, November, December and January are given in Table 5.5. The same table includes estimates not only for cotton but also for wheat, sorghum and kidney beans under conditions at Wad-Medani and Khartoum (Station No. 49). Remarkable enough that the monthly estimates from the Blaney-Criddle method and those obtained by Rijks do not differ by more than 7.3%. The larger difference for January is probably due to the small number of days over which the comparison is made.

The traditional irrigation practice in El-Gezira region is to apply 100 mm of water at an interval of two weeks regardless of the crop raised or its stage of growth. Cotton is the main crop raised in the Gezira plain. However, other crops such as sorghum, wheat and groundnuts have been introduced since 1975. The Gezira black cotton soil (vertisol) is well known with its deep fractures when dry they expand and seal off upon wetness, thereby stopping any further infiltration. Since the land is almost flat, any excess water left on the soil surface is left to evaporate. This means that the empty volume in the soil moisture reservoir is filled during each wet-dry cycle with the same volume of water. As such, it is the rate of moisture exhaustion that varies from one cycle to another. In other words, the duration of the irrigation interval is the decisive parameter in scheduling irrigation (Hussein & El-Daw, 1989).

Extensive research work at Gezira Agricultural Research Station (at Wad-Medani) was carried out between 1965 and 1975 aiming at the determination of water requirements of all crops raised in the Gezira area. The method that has been used to determine *ET* was to observe the depletion of soil moisture through standard neutron probe techniques. Furthermore, the available meteorological data at Wad-Medani (Station No. 57) were substituted in the original formula of Penman (1948) for estimating open water evaporation, EV_P. The so-called crop coefficient, K_c, was then determined from the expression:

$$K_c = ET / EV_P \tag{5.35}$$

The crop coefficients thus obtained have been adhered to, though strongly criticized because they are related to Penman's open water evaporation instead of a reference crop. Additionally, the free water evaporation as obtained from Penman's formula was not calibrated against the local conditions.

The informative study carried out by Hussein and El-Daw (1989) aimed at an investigation into the crop to be considered as a standard reference crop, the method (s) which can be used for estimating the crop evapotranspiration and finally to establish a well-documented set of consumptive use coefficients, all under the local conditions of the Gezira plain. The crops put under investigation were cotton, Sorghum and groundnuts.

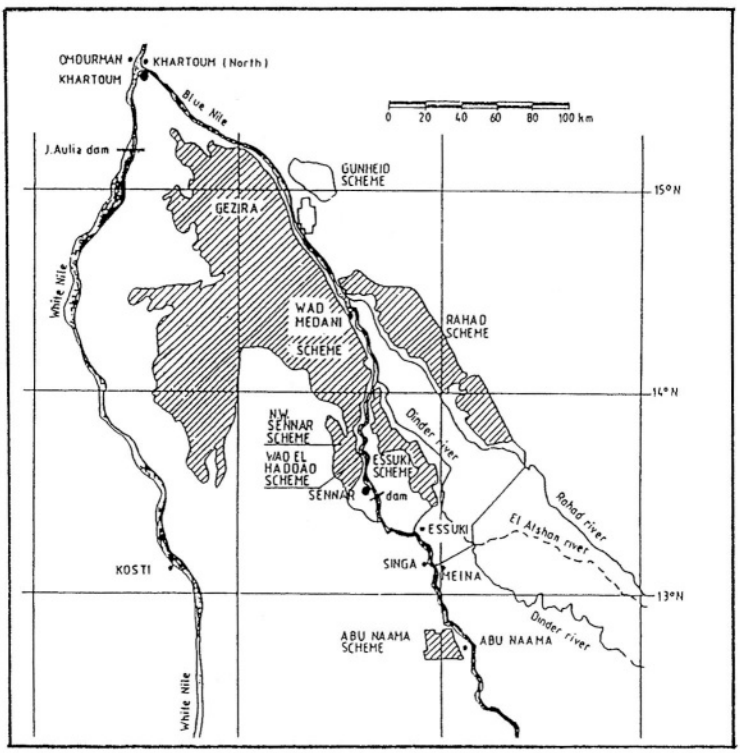

Figure 5.7- Plan of irrigation schemes on the Blue Nile dominated by the vast Gezira scheme

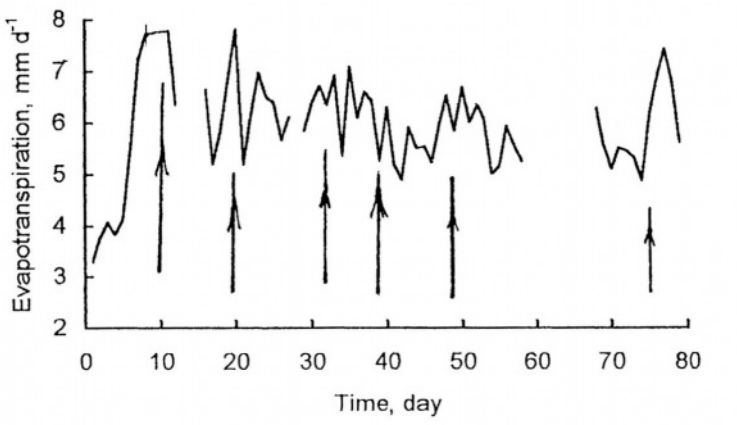

Figure 5.8- Fluctuation of daily evapotranspiration of cotton at Wad-Medani, The Sudan. Day 0 corresponds to 17.10.1965 and day 80 to 05.01.1966, the vertical arrows refer to the times of irrigation (data are from Rijks, 1971)

Since there were hardly any reliable *ET* measurements of a standard reference crop available for use other than those of a local warm-season short grass it has been regarded as the reference crop. Those were obtained through soil moisture depletion techniques using a neutron probe. The methods used for predicting crop evapotranspiration were the FAO/Penman, using the Penman (1948) wind function and the Hargreaves formula. The effect of temperature on the evapotranspiration from a warm-season short grass as a reference crop was investigated and a temperature correction coefficient C_T suggested. For temperatures less than 28.3° C, the coefficient C_T can be taken as unity, whereas for temperatures above 28.3°C, ET_r must be adjusted by $C_T = 0.635$. The improvement in the strength of agreement between the measured and estimated rates of ET_r can be assessed from Figures 5.9_a and 5.9_b.

Hussein & El-Daw (1989) upon considering Eq. (5.32) given by Wright (1982), suggested that the crop evapotranspiration *ET* could be expressed as:

$$ET = K_{cc} ET_{rc} = K_{cw} ET_{rw} \tag{5.36}$$

where K_{cc} = crop water use coefficient associated with cool-season reference grass, ET_{rc} = evapotranspiration of cool-season reference grass (case of Hargreaves formula), K_{cw} = crop water use coefficient associated with warm-season reference grass, ET_{rw} = evapotranspiration of warm-season reference grass (like the present case). It should be well remembered that ET_r of alfalfa, when taken as a reference crop (case of Jensen and Haise formula), is close to 1.15 times ET_r of grass when used as a reference crop. Eq. (5.36) can be rewritten as expressed given by Eq. (5.37):

$$K_{cc} / K_{cw} = ET_{rw} / K_{cw} = C_T \tag{5.37}$$

Using Eq. (5.37) together with ET_{rw} (adjusted expression of FAO/Penman (1948) or Hargreaves and published values of K_{cc} the coefficient K_{cw} can be obtained. By this way the crop water use coefficients and rates (average for 10-days) for cotton, wheat and groundnuts have been determined.

5.5.3 Ethiopia- Other than Piche evaporation, temperature, rainfall and discharge data at some locations for a number of years, the reader hardly finds any published information about evapotranspiration and crop water use in Ethiopia. Using Thornthwaite's formula, Gamachu (1977, cited in Johnson & Curtis, 1994) computed the long-term monthly average potential evapotranspiration ET_p for 55 stations. Thonthwaite's ET_p formula is a function of temperature and hours of daylight.

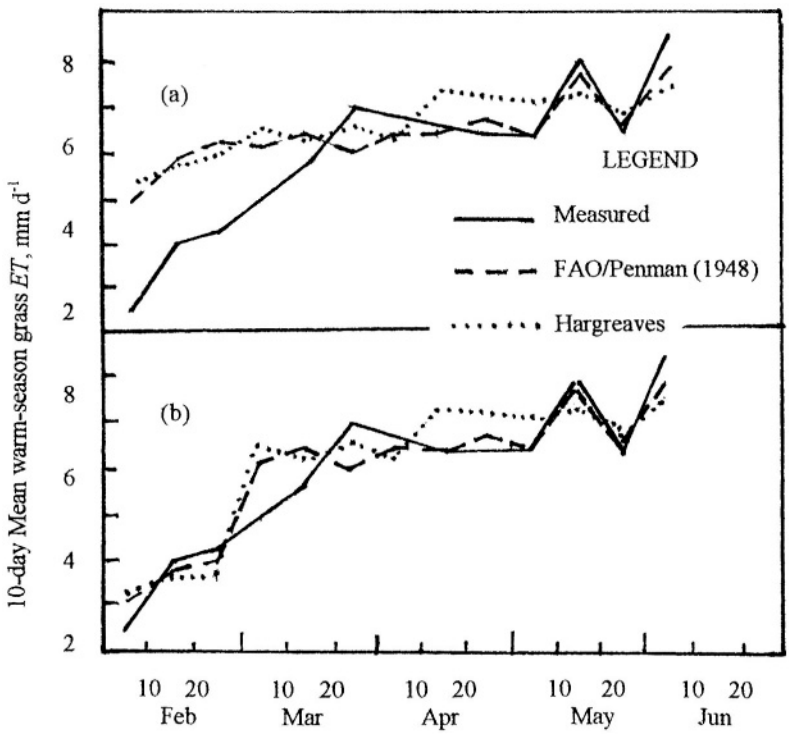

Figure 5.9- Comparison between measured ET of warm-season grass grown in El-Gezirah, The Sudan, and estimated ET_r using FAO/Penman (1948) and Hargreaves formulas, both before and after introducing the temperature correction coefficient, C_T (prepared from Hussein & El-Daw, 1985)

Using Thornthwaite's formula, Gamachu (1977, cited in Johnson & Curtis, 1994) computed the long-term monthly average potential evapotranspiration, ET_p, for 55 stations. Thornthwaite's ET_p formula is a function of temperature and hours of daylight. Monthly values of ET_p for 7 stations (No. 76, 85, 89, 96, 100, 106 and 108) are included in Table 13$_a$ of Appendix A.

While dwelling upon the hydrology of the Blue Nile Basin, Johnson and Curtis (1994) depended on data and figures obtained by Hurst & Philips (1931), US Bureau of Reclamation (1964), Gamachu (1977, cited in Johnson & Curtis, 1949 and Shahin (1985). Those were used as input data to water balance model, which obviously contains ET_a as a component. The assumption that was considered to hold then was that ET_a is a linear function of relative soil moisture

$$ET_a = ET_p\left(\frac{S}{S_{max}}\right) \qquad (5.38)$$

where S = soil moisture and S_{max} = maximum soil moisture. A nonlinear version of the model was also used.

The estimates of the annual values of ET_a for 15 locations as obtained from the two versions of the model, A and B, are given in Table 5.6. These estimates show that in 36.7%, 60%, 73.3% and 76.7% of the cases, for the two versions of the model, the ratio ET_a/ET_p was above 50%, 60%, 70% and 80%, respectively. Secondly, the percentage ratio $(ET_a)_A/(ET_p)_B$ varies from a minimum of 64.3 to 132.4 with a mean of 100.27. In fact in 5 cases out of 15, it was above 100%; in 7 cases out of 15, it was between 90 and 100%; and in 3 cases it went below 50%. As such, one can conclude that the two versions do not yield strictly identical figures but fairly close results for the annual evapotranspiration.

The average monthly ET_a values for the Chemoga River Basin (a tributary of the Blue Nile) represented by the station at Debre Markos (Station No.96), were estimated as: 77, 69, 57, 50, 52, 51, 64, 64, 67, 61, 61, and 61 mm for months 1, 2, 3,...and 12, with a total of 734 mm. The corresponding ET_p values are: 78, 77, 95, 82, 71, 72, 65, 64, 67, 61, 61, 61 mm for the 12 months in their respective order, and 854 mm for the year. The actual and potential evapotranspirations are equal or very nearly equal in the wet months or in months with adequate soil moisture. This is more so in low-temperature months.

5.5.4 Niger- The International Research Institute for the Semi-Arid-Tropics (ICRISAT) prepared a report on agroclimatology of the Niger (Sivakumar et al., 1993). The said report gives potential evapotranspiration rates for 13 stations. These were computed from maximum and minimum air temperatures, vapour pressure deficit, sunshine hours and wind speed. The computed values of average monthly ET_p for 7 stations (Stations No. 37, 42, 54, 58, 59, 64 and 59) are included in Table 13, of Appendix A. The report authors used a certain water balance model to be able to estimate the soil moisture assuming two different water holding capacities. The model computed the average 10-days actual evapotranspiration, ET_a, for those two levels. Table 5.7 gives ET_a and the ratio ET_a/ET_p for three stations, namely; Tahoua, Tillabery and Zinder. The remarkable observations about the tabulated results are:

- The decadale ratio, *a,* is above 0.40 for the period from decade 19 to decade 27. This period corresponds with the months of July, August and September in which 85% or more of the rain falls. By the end of July and beginning of August it reaches as much as 0.85 but does not reach unity. Other than these three months, the ratio a is well below 0.40 and reaches 0.02 in January, February and March. The distribution of the monthly ET_a is reasonably parallel to the distribution of the monthly rainfall.
- The annual ratio a* varies between 0.19 and 0.24 for the assumption of 100 mm water holding capacity, and between 0.18 and 0.23 for 150 mm water holding capacity. This is not unexpected in a semi-arid climate with annual rainfall of 180-700 mm with mean annual temperature of 25-30°C.

Table 5. 6- Actual evapotranspiration for the subwatersheds of the Blue Nile Basin, Ethiopia, as obtained from a water balance model using two versions (Johnson & Curtis, 1994)

Station	Period	ET_p,	ET_a, mm		ET_a / ET_p, %		a^*_A / a^*_B
		mm	A	B	a^*_A	a^*_B	A / B, %
Andassa	1961-62	1,509	1,265	1,337	83.8	88.6	94.6
Arera	1960-61	1,095	929	703	84.8	64.2	132.1
Bello	1961	1,099	343	415	31.2	37.8	82.7
Beressa	1960-61	1,175	894	956	76.1	81.4	93.5
Chemoga	1965-69	854	725	732	84.9	85.7	108.8
Finchas	1961-62	1,128	1,226	1,127	108.7	99.9	132.4
G. Abbay	1965-69	1,208	331	250	27.4	20.7	113.3
Gumara	1961-62	1,646	840	740	51.0	45.0	90.9
Lah	1961-62	1,217	816	898	67.1	73.8	99.4
Leza	1961-62	1,204	1,048	1,054	87.0	87.5	122,2
Megech	1961	1,055	813	666	77.1	63.1	92.8
Mugher	1959-62	1,095	776	801	70.9	73.2	95.6
Ribb	1961-62	1,237	852	890	68.9	71.2	96.8
Selale	1961-62	1,265	999	1,183	79.0	93.5	84.5
Temcha	1961-62	1,155	297	480	25.7	41.5	64.3

Explanation

ET_a = actual evapotranspiration, ET_p = potential evapotranspiration

a^* = annual ratio ET_a / ET_p,

A = actual evapotranspiration is a linear function of the available soil moisture, and

B = nonlinear version of the model used in A (Schaake and Chunzehn, 1989)

Table 5.7- Actual evapotranspiration in mm, and its ratio to the correspoding potential evapotranspiration at three stations in Niger under two levels of of soil water holding capacity (ICRISAT, 1939)

Deca-	Water holding capacity = 100 mm						Water holding capacity = 150 mm					
de	Stat. 54		Stat. 59		Stat. 64		Stat.54		Stat. 59		Stat. 64	
No.	ET_a	a	ET_a	a	ET_a	a	ET_a	a	ET_a	a	ET_a	a
1	4.51	0.08	0.75	0.02	0.81	0.02	3.69	0.07	0.90	0.02	0.97	0.02
2	3.87	0.07	0.75	0.02	0.83	0,02	3.73	0,07	0.90	0.02	0.99	0.02
3	1.10	0.02	0.92	0.02	0.94	0.02	1.96	0.03	1.10	0.02	1.13	0.02
4	1.06	0.02	0.89	0,02	0.94	0.02	1.27	0.02	1.06	0.02	1.13	0.02
5	1.13	0.02	7.83	0.14	0.96	0.02	1.35	0.02	6.54	0.12	1.15	0.02
6	1.01	0.02	1.24	0.03	1.18	0.02	1.22	0.02	2.00	0.04	1.14	0.02
7	1.13	0.02	2.10	0.04	1,04	0.02	1.35	0.02	2.41	0.04	1.25	0.02
8	1.97	0.03	2.79	0,05	1.79	0.03	1.88	0.03	2.66	0.04	1.86	0.03
9	1.53	0.02	9.03	0.12	1.63	0.02	1.72	0.02	8.05	0.11	1.79	0.02
10	3.97	0.02	3.05	0.05	1.97	0.03	3.21	0.04	2.77	0.04	1.86	0.03

Table 5.7- Cont'd

Decade No.	Water holding capacity = 100 mm						Water holding capacity = 150 mm					
	Stat.54		Stat. 59		Stat. 64		Stat. 54		Stat. 59		Stat. 64	
	ET_a	ET_p	ET_a	ET_p	ET_a	ET_p	ET_a	ET_p	ET_a	ET_p	ET_a	ET_p
11	5.70	0.08	3.95	0.06	2.23	0.03	5.00	0.07	3.69	0.06	2.12	0.03
12	4.01	0.05	4.13	0.06	7.46	0.10	3.47	0.04	3.80	0.06	5.86	0.08
13	6.15	0.08	5.70	0.08	12.07	0.16	5.32	0.07	5.02	0.07	10.35	0.14
14	10.80	0.13	8.54	0.12	6,65	0.09	8.73	0.11	7.32	0.10	5.85	0.08
15	10.60	0.12	18.09	0.23	14.22	0.18	8.76	0.10	15.60	0.20	12.02	0.15
16	19.06	0.27	18.35	0.30	16.07	0.23	16.04	0.22	14.90	0.24	13.27	0.19
17	15.30	0.21	20.52	0.31	15.80	0.22	12.99	0.18	19.50	0.03	14.02	0.20
18	25.10	0.35	18.65	0.28	19.30	0.28	21.48	0.30	17.20	0.26	16.50	0.24
19	32.90	0.46	32.42	0.53	37.38	0.57	28.46	0.40	29.50	0.48	33.21	0.51
20	38.00	0.56	29.32	0.48	39.21	0.63	33.68	0.49	28.90	0.48	37.35	0.60
21	40.40	0.58	46.50	0.73	47.46	0.74	37.52	0.54	44.80	0.70	45.95	0.72
22	44.20	0.65	42.30	0,75	47.30	0.80	40.76	0.60	41.50	0.74	46.47	0.78
23	41.00	0.64	45.95	0.81	50.66	0.85	38.06	0.59	45.90	0.81	50.30	0.84
24	48.10	0.69	53.41	0.85	56.45	0.87	46.31	0.67	52.90	0.84	55.85	0.86
25	29.40	0.46	38.92	0.70	39.47	0.67	27.78	0.43	39.06	0.71	39.81	0.68
26	23.61	0.38	33.78	0.58	33.10	0.57	23.21	0.37	34.84	0.60	34.70	0.60
27	17.70	0.27	25.11	0.44	24.86	0.42	18.61	0.29	27.67	0.48	29.70	0.50
28	10.70	0.16	12.32	0.21	12.90	0.22	11.46	0.18	16.01	0.27	17.00	0.28
29	9.60	0.15	10.40	0.19	9.22	0.15	8.85	0.14	12.28	0.22	11.14	0.19
30	3.94	0.05	4.80	0.08	2.84	0.05	4.69	0.06	6.79	0.11	4.67	0.08
31	1.08	0.02	1.23	0.02	2.29	0.04	1.29	0.02	2.11	0.04	2.74	0.05
32	1.02	0.02	1.24	0.03	1.06	0.02	1.22	0.02	1.42	0.03	1.23	0.02
33	1.05	0.02	1.13	0.02	1.02	0.02	1.26	0.02	1.24	0.03	1.20	0.02
34	0.98	0.02	0.76	0.02	0.83	0.02	1.18	0.02	0.99	0.02	1.00	0.02
35	0.90	0.02	0.69	0.02	1.89	0.04	1.09	0.02	0.83	0.02	1.82	0.04
36	0.97	0.02	0.85	0.02	0.92	0.02	1.16	0.02	0.99	0.02	1.20	0.02
Total	464		498		525		428		428		509	
Et_p	2436		2096		2221		2436		2096		2221	
a*	0.19		0.24		0.24		0.18		0.20		0.23	

Explanation

ET_a = actual evapotranspiration in mm, ET_p = potential evapotranspiration in mm

a = ratio of actual evapotranspiration to potential evapotraanspiration = ET_a / ET_p

a = ratio of annual ET_a to annual ET_p*

Stations No. 54, 59 and 64 are located situated at Tahoua, Tillabery and Zinder

5.5.5 Some northwest African countries (Senegal, Mali and Mauritania)- While investigating future irrigation project management in the Senegal River Basin, Hargreaves et al. (1985) considered the climate data from four stations in Senegal and Mauritania. The available data confirmed the applicability of Eq. (5.15) for estimating reference crop evapotranspiration, ET_r. The reference crop here is a cool-season short grass (Alta fescue grass). The crop coefficients given by Doorenbos and Pruitt (FAO-Paper 24, 1977) have been recommended for use with the calculated ET_r. Additionally, procedures given by the same reference for estimating the readily available water and managing allowable soil moisture depletions were also recommended for use by the project management so as to determine the proper rotation periods and the required water deliveries.

Hagreaves (1975) using experimental results obtained the following crop response function:

$$Y = 0.8X + 1.3X^2 - 1.1X^3 \tag{5.39}$$

where, Y = actual crop yield relative to the maximum yield and X = amount of water applied relative to the amount required to produce maximum yield. The first derivative of Eq. (5.39) gives the maximum yield for a relative amount of water X equal to 0.4. Practically the maximum yield is obtained when X falls in the range 0.4-0.6. This means that would precipitation be able to supply the unsaturated zone by a certain amount of moisture, a small increase in the water available to the crop through a limited amount of irrigation water will result in a considerable increase in crop production.

A certain soil moisture model related to dryland farming and water conservation in West Africa adopted a similar procedure to the previous one. The data of the experimental farm at Kita, Mali, where the agroclimate belongs to the Sudano-Sahelian zone (annual rainfall 800-1,000 mm) were applied. The basic relationship between moisture depletion, evapotranspiration and crop response is:

$$(1 - Y) = k_y\left(1 - \frac{ET_a}{ET_m}\right) \tag{5.40}$$

where Y has the same meaning as in Eq. (5.39), k_y is a coefficient relating the crop response to the relative evapotranspiration and ET_m is the maximum evapotranspiration and can be taken equal to ET_p or ET_r. The k_y values reported by Doorenbos and Kassam (FAO-Paper 33, 1979), calibrated to reflect crop varieties and farming practices traditionally followed by the farmers in the Kita area, formed the basis of the moisture stress-crop yield computations which have been carried out in this case study.

Assuming the water holding capacity in root zone as 60 mm, the estimated ET_a of long season sorghum at Kita station was obtained. The estimates in mm were: 35 for the period 01.06-15.06, 42 for the period 16.06-30.06, 38 for the period 01-07, 56 for the period 16.07-31-07, 66 for the period 01.08-15-08, 88 for the period 16.08-31.08, 86 for the period 01.09-15.09, 73 for the period 16.09-30.09 and 59 for the period 10.10-15.10. These figures when summed up give a seasonal use of 543 mm for sorghum, which is quite usual for the area under investigation.

While discussing the water management issue of the Sahelian zone of Mauritania, the figures of 4,300 mm and 3,900 mm were used to represent the annual Class A pan evaporation for Atar (Station No.35) and Kiffa (Station No. 45) respectively. These figures have already been mentioned in subsection 4.5.10. The monthly distribution of the average pan evaporation was estimated as a function of temperature and wind speed. The reference evapotranspiration ET_r was obtained by multiplying the evaporative demand by the corresponding pan coefficient to get the monthly crop water use. Remarkable enough is that the total consumptive use of water by long season sorghum (150 days starting 1st of June) was about 530 mm. This figure is nearly the same as that obtained for sorghum at Kita station, Mali (135 days growing season).

5.5.6 Chad, Congo (Brazzaville) and Central African Republic- In subsection 4.5.8 of Chapter 4, "Evaporation", the theoretical backgrounds underlying Piche evaporation (usual and sheltered or screened) and the Colorado sunken pan have been described in a summarized form. A number of case studies verifying the relevant theorems have been presented as well. The research work developed by Riou (1970) extended to cover the possible relationship between evaporation measurements using Colorado sunken pan, E_{sp}, and potential evapotranspiration ET_p. The resulting relationship between these two variables can be expressed as:

$$ET_p = \frac{1}{1.04}\left(E_{sp} - \frac{\gamma E_a}{\Delta + 2\gamma}\right) \tag{5.41}$$

where all other notations have the same meaning as explained in relation to free water evaporation. Eq. (5.41) can be simplified to read:

$$ET_p = \left(E_{sp} - \frac{\gamma E_a}{\Delta + 2\gamma}\right) \tag{5.42}$$

with less than 4% approximation.

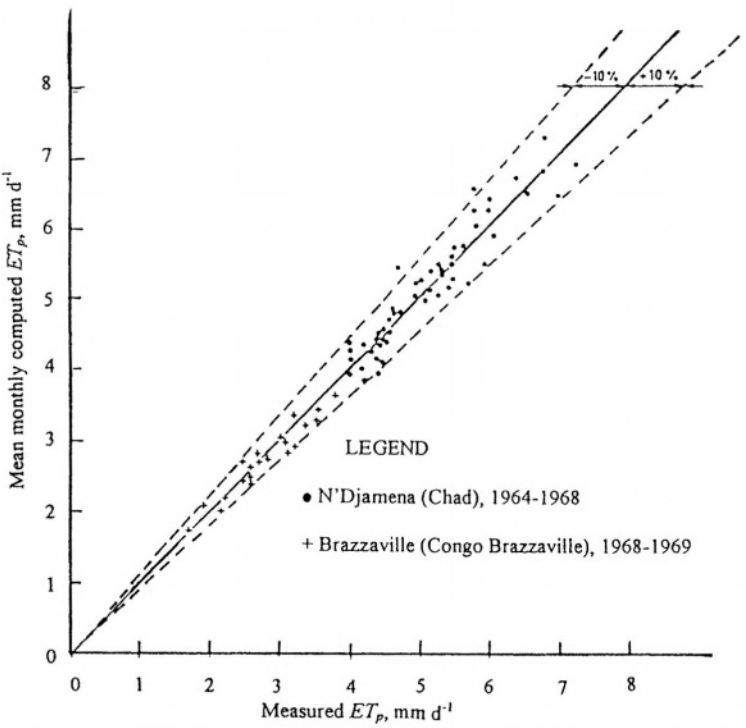

Figure 5.10- Calculated ET_p versus measured ET_p for N'Djamena, Chad and Brazzaville, Congo Brazzaville, (Riou, 1970)

Eq. (5.42) was used to compute the monthly ET_p for 5 years at N'Djamena (Chad) and 2 years at Brazzaville (Congo Brazzaville) using the Colorado sunken pan observations. The results thus obtained are plotted versus the measured ET_p values as shown in Figure 5.10. The graph shows the scatter of the plotted points around the 1:1 line. Moreover, nearly all points are contained between the two enveloping lines with slopes 0.91:1 and 1.11:1.The computed annual ET_p values in mm for N'Djamena for the years 1964-1968 are: 1,351 (for 9 months), 1,927, 1,855, 1,872, 1,887, with an annual average of 1,879 mm. The measured values for the same years in their respective order are 1392, 1895, 1819, 1894 and 1910, with an average of **1,873 mm y^{-1}**.

A few years later, Riou (± 1975) presented some examples related to the application of radiation measurements for determining evapotranspiration in tropical climate. A network of three meteorological stations at N'Djamena (Chad), Bangui (Central African Republic) and Brazzaville (Congo Brazzaville) began radiation measurements after 1964. Later, a station was installed at Bol (Chad) on the shore of Lake Chad. Sheltered climatological stations were installed for measuring soil temperature, insolation, wind speed, open water evaporation (Colorado sunken pan, Class A pan and **4 m^2** tanks), and

evapotranspiration (4 m^2 square tanks placed inside a field covered with exuberant grass at a distance of no less than 400 m^2 from the edge). More stations have been added to the network: F. Largeau, Ba-Illi and Bebedjia in Chad, and Bossangoa in Central African Republic, The regional study of *ET* prompted the addition of three stations in Congo Brazzaville, namely: Ouesso, Pointe Noire and Impfondo to compute *ET* using the derived methods. The locations of all stations already mentioned are shown on the map in Figure 5.11.

The theoretical approaches used were essentially the radiation balance and the combined method of Penman describing evaporation from a free water surface. The available annual ET_p values when compared to Penman's evaporation E_P shows that the ratio $ET_p/E_P = 0.82$ for N'Djamena (average of 5 years), 0.81 for Bangui (1969) and 0.775 for Brazzaville (average of 2 years).

To avoid the difficulties encountered in applying Penman's method, the long record of insulation at the four stations in Congo Brazzaville; Brazzaville, Pointe Noire, Ouesso and Impfondo, has been worked out to develop a tentative calculation method. This can be expressed by a relation of the form:

$$\varphi R_s = \lambda + \delta(SS_o)_m \qquad (5.43)$$

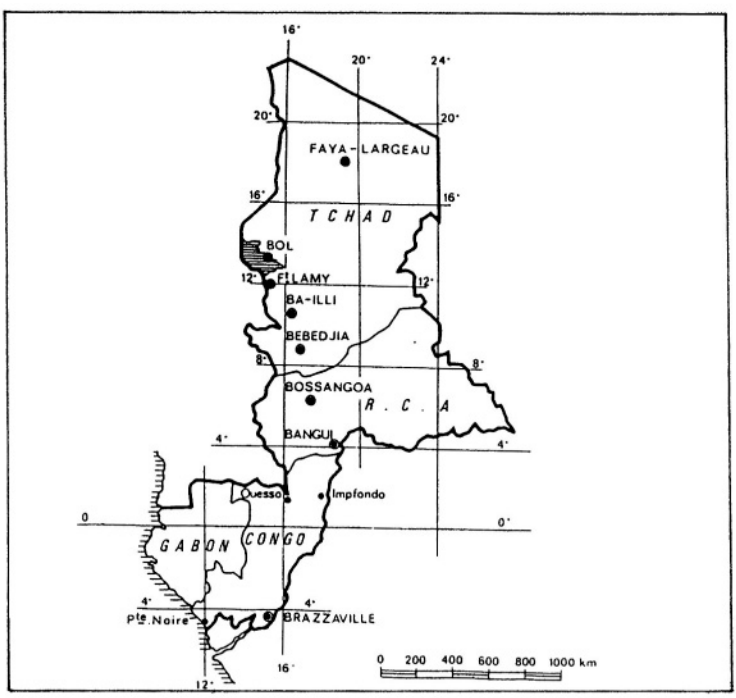

Figure 5.11- Locations of climatological stations of O.R.S.T.O.M. used in the study of evapotranspiration (Riou, ±1975)

where φ, λ and δ are coefficients depending on the global radiation, number of actual sunshine hours, and $(SS_o)_m$ is the mean number of observed sunshine hours. The coefficients λ and δ for Brazzaville (average for 5 years) were found to be 0.64 and 0.054 respectively. Furthermore, the wind speed had to be reduced by 0.75 in the rainy season and by 0.85 in the dry season.

Monthly and annual estimates of ET_p in mm obtained from the radiation-insolation measurements at the four stations in Congo Brazzaville are given in Table 5.8. The four annual estimates are highly consistent. However, they are about 5% larger than the annual loss from the nearby river basins. Probably this is caused by the difference in albedo between the environment surrounding the lysimeters and the forests, which occupy a large proportion of the basins.

It has been repeatedly mentioned that some of the climate parameters needed for the application of Penman's formula are not usually available. In such situations, the application of a simpler formula will be highly appreciated. Potential evapotranspiration in the Equatorial zone appears to depend strongly on the amount of global radiation. The data available at Brazzaville showed with a high correlation that ET_p in $mm\ d^{-1}$ can be taken as $0.45\ R_s$, where R_s is expressed in mm equivalent depth of evaporation. The calculated monthly and annual ET_p in mm for Brazzaville (Station No. 175) are included in the lower part of Table 5.8. These figures when compared to the corresponding measured ET_p figures, they show a maximum difference of about 12% for September, the end of the dry season. Investigation of the remaining stations in Congo Brazzaville has shown that they can better be served by applying a factor equal to 0.48, 0.43 and 0.44 for Pointe Noire, Ouesso and Impfondo respectively, instead of 0.45 found for Brazzaville. The ratio ET_p/R_s for N'Djamena (Chad, more arid) appeared to decrease during the rainy season from 0.69 to 0.61, 0.53 and 0.45 for April, May, June and July respectively.

The above summarized research work dealt also with the relationship between the actual and potential evapotranspiration. The ratio ET_a/R_s for Brazzaville as obtained from lysimeter measurements declined gradually during the dry season from 0.40 around mid June to 0.23 at the end of July and further to 0.15 close to the end of August. These ratios can be expressed in terms of $ET_p = 0.45\ R_s$, i.e., $ET_a/ET_p = 0.89$, 0.50 and 0.33 for the given dates in their respective order. Theoretical elaboration of the relationship between ET_a and ET_p has led to the following expression:

$$ET_a / ET_p = 1 - b(w_k - w) \qquad (5.44)$$

where b = slope of curve describing the variation of ET_a/ET_p with the moisture available in the soil, w = actual moisture storage in the soil, w_k = minimum amount of soil moisture to sustain the processs of evapotranspiration, i.e.,

$$ET_a = ET_p \; ; \; w \geq w_k \tag{5.45}$$

A much simpler expression relating the ET_a, ET_p and the soil moisture deficit, *S,* in percent, has been developed by Riou (±1975) as:

$$ET_a / ET_p = 1 - 0.0046S \tag{5.46}$$

According to Eq. (5.46), the ratio ET_a/ET_p equals 0.908, 0.77 and 0.632 as S becomes 20, 50 and 80%, respectively.

5.5.7 Tunisia- The results of the research work on irrigation with saline water in Tunisia, 1962-1969, are published in a Technical Report of UNESCO/UNDP (SF) TUN. 5 (1970). The report shows that the difference in consumptive use of tomatoes between the lysimeter and the field is about 30% for the period 26.08.1968-04.09.1968, as obtained by the energy balance method. The measurements carried out by the water balance method are in good agreement if one considers the results obtained at the end of August and the beginning of September. Since these results only cover a few days in one growing season of one crop only, it is certainly difficult to assess their practical significance.

Combremont (1972) upon commenting on the results obtained from the experimental work conducted on evapotranspiration in Tunisia stated that:

- Thornthwaite's formula does not seem to be reasonable, especially in the spring time,
- Blaney-Criddle's formula tends to give the potential evapotranspiration, ET_p, rates,
- Penman's formula, though needs adjustment, is to be preferred since it takes into account a larger number of climatic factors,
- the sunken pan agrees fairly well with Penman as far as winter is concerned. In summer, it gives values that are slightly lower on the coast or slightly higher in the interior,
- the lysimeters give reasonably correct values in winter. In summer, they are likely to give incorrect measurements due to advective heat,
- measuring devices such as evaporation tanks and lysimeters do measure the degree of crop water consumption rather than the actual value of the crop water use.

In order to determine the actual evapotranspiration, the soil moisture balance method was used. In this method, samples were taken every 10 cm to a depth of 80 cm, then every 20 cm to a total depth of 140 cm (under which drains are placed). The results obtained from those experiments were reported by Combremont (1972) and are presented in summarized form in Table 5.9. The tabulated figures cover a number of winter crops as well as summer crops.

5.5.8-Morroco: The soil moisture depletion method was applied to determine the consumptive use of water by cotton in Morocco in the period 1956-1965. Morocco's National Committee, ICID (International Commission on Irrigation and Drainage, 1973), reported the results of experiments at four stations. Experiments were carried out under different irrigation quantities as well as different available soil moisture contents just before irrigation. A review of the results obtained shows that there were marked differences between one year and another, and between an irrigation treatment and another. However, a global average for each station is given briefly in Table 5.10.

5.5.9 Congo (Kinshasa), Rwanda and Burundi- Potential evapotranspiration rates for Congo (Kinshasa), Rwanda and Burundi have been measured using tank lysimeters, $4\ m^2$ in size, planted with Bahia grass (Paspalum notatum). The annual ET_p values averaged over the number of years of record are plotted on a map of the three countries and lines of equal annual potential evapotranspiration are drawn as shown on the map, Figure 5.12 (Bultot, 1971). The work presented by Bultot was preceded by an investigation carried out by the National Institute for Agronomical Studies in the Belgian Congo (INEAC) and reported by Dupriez (1959). That study was conducted at 24 stations distributed between Congo (Kinshasa), Rwanda and Burundi. It covered measurements using lysimeters, $4m^2$, square tanks planted with Paspalum notatum) and simple barrels, and estimates using the formulas of Thornthwaite and Penman. Some of the measurements and estimates obtained from that study is included in Table 13_a of Appendix A. The most noteworthy conclusions that the study reached were:

- the lysimeters used ($4\ m^2$ square tanks) gave with good precision monthly evapotranspiration figures. However, they are unsuitable to follow evapotranspiration day by day,
- in certain studies on grassy formations of low development, it is cheaper and easier to use, ordinary gasoline drums as lysimeters,
- Penman's formula is satisfactory to give an estimate of evaporation from a free water surface. An empirical formula was developed for computing evaporation under the local conditions of the Congo,
- Thornthwaite's formula could not be applied in the Congo because it does not take into account the saturation deficit and the altitude of the location under study. From the figures obtained for the stations presented in Table 13_a, Appendix A, the ratio between the measured and calculated evapotranspiration varies from less than 50% to more than 150% for monthly values and from 66% to 136% for annual values.

The entire area shown in Figure 5.12 is covered by ET_p contour lines of between $1{,}000\ mm\ y^{-1}$ and $1{,}300\ mm\ y^{-1}$, except for a very small part close to the Atlantic Ocean. The potential evapotranspiration in that area around the

Table 5.9- Consumptive use of water by winter and summer crops in Tunisia° as obtained from soil moisture studies (after Combremont, 1972)

Crop	Jan	Feb	Mar	Apr		May		Jun		Jul		Aug		Sep		Oct	Nov	Dec
				1st H	2nd H	1st H	2nd H	1st H	2nd H	1st H	2nd H	1st H	2nd H	1st H	2nd H			
Winter crops																		
Barley	1.5	3.0															1.5	1.5
Ray grass	2.0	3.0	3.0														2.5	2.0
Bersim*	2.0	2.5	2.5	5.5													3.0	2.0
Wheat	2.0	3,5	4.0	5.0														2.0
Artichokes	2.0	2.5	4.0	6.0								4.5		4.5		3.5	3.0	2.0
Fescue grass	2.5	2.5	3,0	4.0													2.5	2.5
Penman**	1.1	1.7	2.6	3.9		5.5		6.4		7.4		6.4		4.5		3.2	1.7	1.4
Summer crops																		
Lucerne					4.5	4.5	5.5	6.0	7.0	7.0	7.0	7.0	7.0					
Maize							2.5	3.0	5.0	7.0	7.0	7.0						
Sorghum+							3.5	3.5	6.0	7.0	8.5	8.5	7.5					
Tomatoes						2.0	3.0	4.5	5.5	6.0	8.0	7.0	6.0	4.5				
Cotton						2.0	2.5	4.5	5.5	4.0	7.5	7.5	6.0					

Explanation

° Data are obtained from Cherfech experimental station (latitude 36° 50' N and longitude 10° 00' E)

**Berseem is an Egyptian clover, ** Estimate of open water evaporation and + Sorghum for forage.*

The figures listed in the above table are in mm d^{-1}.

Table 5.10- Average consumptive use of water consumption by cotton at four experimental stations in Morocco (ICID, 1973, ed. Framji and Mahagan)

Month	Decade No.	Duration, days	O.G*. day	O.G*. decade	Tr** day	Tr** decade	O.F°. day	O.F°. decade	S.S.°° day	S.S.°° decade
Mar	1	10								
	2	10	1.5	15						
	3	11	1.8	19.8	1.6	17.6	1.6	17.6	1.7	18.7
Apr	1	10	1.9	19	1.6	16	1.6	16	1.8	18
	2	10	2	20	2.2	22	2.1	21	2	20
	3	10	2.1	21	2.3	23	2.2	22	2.1	21
May	1	10	2.6	26	2.6	26	2.5	25	2.5	25
	2	10	2.8	28	2.8	28	2.6	26	2.7	27
	3	11	3.2	35.2	3	33	3.4	37.4	3.3	36.3
Jun	1	10	3	30	3.3	33	4.2	42	4.1	41
	2	10	4.9	49	3.5	35	5.4	54	5.1	51
	3	10	6	60	3.7	37	5.4	54	5.8	58
Jul	1	10	6.2	62	3.9	39	5.5	55	5.9	59
	2	10	7	70	4	40	6.2	62	6.6	66
	3	11	8.4	92.4	4.1	45.1	6.4	70.4	7.4	81.4
Aug	1	10	8	80	8.1	81	7.8	78	7.9	79
	2	10	8	80	8.1	81	7.8	78	7.9	79
	3	11	7.5	82.5	9.2	101.2	9.3	102.3	8.4	92.4
Sep	1	10	4.6	46	6.7	67	9.1	91	6.9	69
	2	10	3.2	32	6.3	63	4.7	47	4	40
	3	10	2	20	3.4	34	2.5	25	2.3	23
Oct	1	10	1.5	15	3.2	32	2	20	1.8	18
	2	10	1.2	12	2.2	22	1.7	17	1.6	16
	3	11	1	11	1.1	12.1	1.4	15.4	1.2	13.2
Nov	1	10	0.8	8						
	2	10	0.7	7						
	3	10	0.6	6						
Season				955		873		962		949

Explanation

O.G. = Ouled Gnaou, Tr** = Triffa, O.F.° = Ouled Frej and S. S.°° = Sidi Slimane*

Zaire River on the Ocean varies between 1,000 and 850 mm y^{-1}. The map of ET_p prepared by Kurzon (Figure 2.13, Chapter 2) shows that the annual potential evapotranspiration for the area under discussion varies between 1,250 and 1,500 mm y^{-1}. This is 10-15% larger than that given by Bultot (1971). For example, the map of Kurzon (1978) gives annual ET_p of 1,280 mm for Brazzaville. This value is about 15% greater than what can be found from either Figure 5.12 or what was obtained by Riou (±1975) from his extensive experimental and theoretical research work, already summarized in subsection 5.5.6.

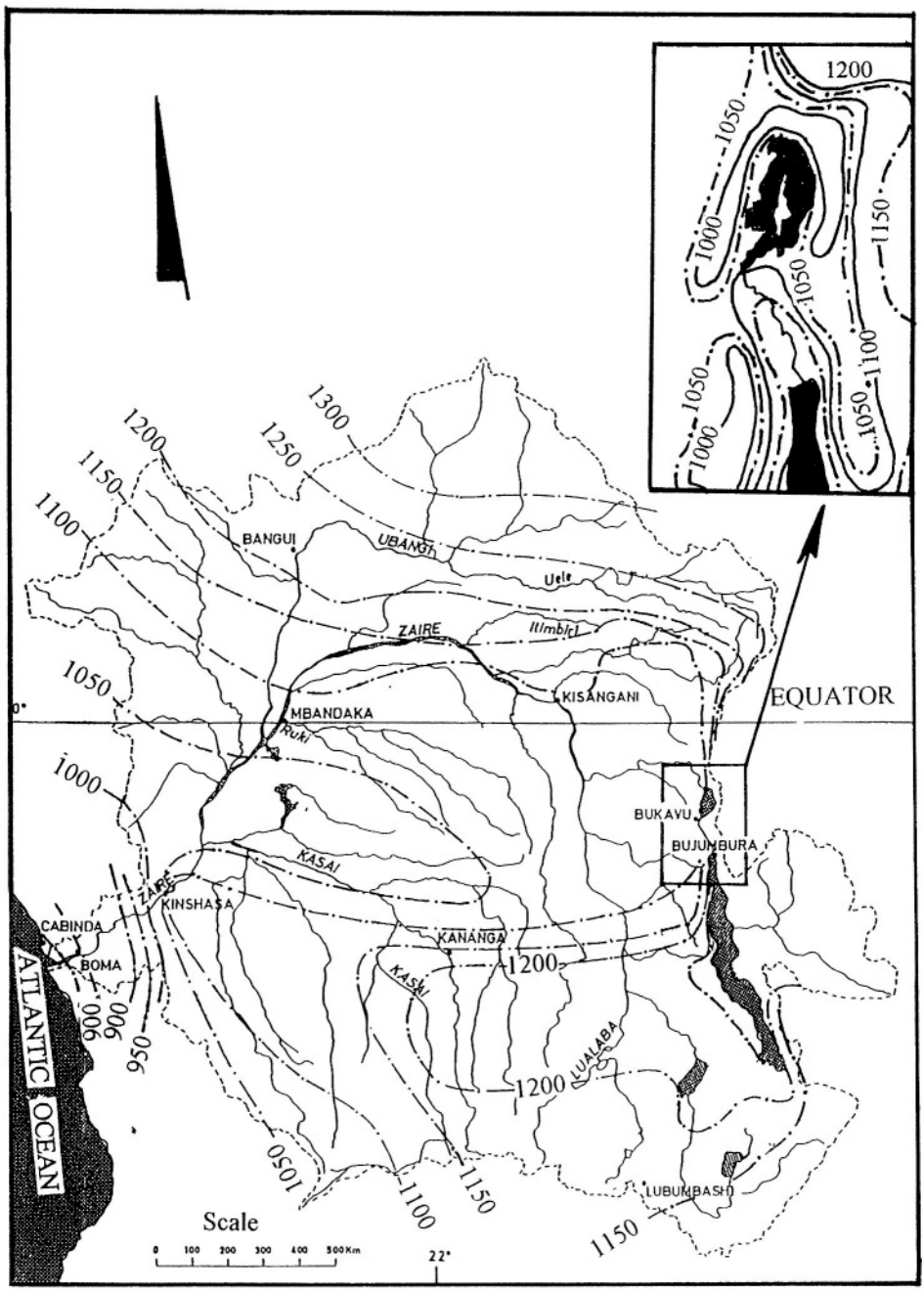

Figure 5.12- Map showing lines of equal ET_p in mm for the area covered by Congo (Kinshasa), Rwanda and Burundi (reproduced from the Atlas of climatic data by Bultot, 1971)

The average annual ET_p over the entire area of Congo (Kinshasa), Rwanda and Burundi, as obtained from Figure 5.12, falls between 1,100-1,150 mm. The corresponding overall areal average as given by Figure 2.13 is 1,350-1,400 mm y^{-1}. According to Kurzon (1978) annual ET_p is estimated at 1,370 and 1,420 mm for geographic latitudes of 10-0°N and 0-10°S respectively. The latter ET_p figures were determined by Budyko's method, which is different from the method based on lysimeter measurements used by Bultot. Budyko's method takes into account the radiation balance, air temperature and moisture content. Monthly estimates of ET_p computed by this method are likely to contain an average error of 7-10% to 15-20% depending on the season. Additionally, it has been reported that the errors of computed annual potential evapotranspiration values make 4-5% (Kurzon, 1978).

The same reference, i.e. Kurzon (1978), gives the distribution of the actual evapotranspiration by latitudinal zones. The annual rate for the zone from 0° to 10°N is 950 mm increasing to 1,020 mm for the zone from 0° to 10°S. The largest part of the surface covered by the Congo (Kinshasa) is traversed by contour lines of ET_a of 1,000 and 1,250 mm. Again, the very small area around the mouth of the River Zaire close to the Atlantic Ocean shows an ET_a of 600-800 mm y^{-1}. The actual evapotranspiration in the area to the east, covered by Rwanda and Burundi, varies between 900 and 1,000 mm y^{-1}. These figures indicate that the ratio ET_a/ET_p is close to 0.70, which is not too different from the values found for the Congo Brazzaville, in subsection 5 5.6. Despite the discrepancy between the annual values one finds that the distribution patterns of monthly ET_p in both sources of information are reasonably similar to each other.

5.5.10- Uganda and Kenya: Hanna (1971) upon studying the effect of water availability on tea yield in Uganda concluded that ET_p from a full cover of tea is nearly 0.85 Penman's evaporation. In East Africa, the best estimate of potential evapotranspiration is derived from Penman's equation. The network of stations at Entebbe, Kabanyolo, Jinja and Kituza for which the 10-day means of Penman evaporation were reported by Hanna to allow for a reasonably accurate estimate of Et_p within a narrow zone adjacent to Lake Victoria. North of Kabanyolo is situated the Cotton Research Station at Namulonge (0° 32'N, 32° 27'E and z = 1100 m). Evapotranspiration from a papyrus swamp in the neighbourhood of this station was observed by Rijks (1969) and shall be presented in the next section. More results obtained from evapotranspiration studies on swamps, grasses and evergreen forests will also be presented in the next section.

The seasonal ET_p from a field covered with maize at Muguga, Kenya, was reported as 560 mm. The free water evaporation for the same season was 840 mm (estimated by Penman's method), i.e. $ET_p / E = 0.67$. When Penman's evaporation becomes in the range 5-6 mm d^{-1}, the ratio rises to 0.75.

While involved in a water resources assessment study in Kiambu District, a few kilometers northwest of Nairobi, Kenya, Heederik et al. (1984) reported that

detailed information on the cropping pattern and water consumed by the various crops was not available. In that study recharge to the ground water aquifer was taken as the difference between the precipitation P and the actual evapotranspiration ET_a. The available monthly pan evaporation E_P values were multiplied by 0.8 to estimate the reference evapotranspiration ET_r. The estimates thus obtained were multiplied by a monthly crop coefficient k_c and another monthly coefficient k_a depending on the availability of soil moisture to obtain monthly estimates of ET_a. The monthly and total estimates of ET_r, ET_p and ET_a obtained through this procedure are listed in Table 5.11. The Atlas of Water Resources of the World (Kurzon, 1978) gives annual values for ET_p and ET_a at the Kiambu District of about 1,500 mm and 800 mm respectively. The difference between these two figures and the corresponding estimates, Table 5.11, is about 7% for ET_a and 22.5% for ET_p. However, it should be well remembered that the tabulated results, in view of the various assumptions, should be regarded as approximate only.

Much earlier to the Kiambu District study, the moisture balance in the soil of the Coffee Research Station at Ruiru was followed annually in the period from 1951 to 1960. The station is located at latitude 1° 06'S, longitude 36° 56'E and elevation of 1,608 m, thus too close to Kiambu. The annual free water surface evaporation for the years 1951, 1952,...,1960 was 1,571, 1,539, 1,597, 1,586, 1,538, 1,368, 1,341, 1,426, 1,565 and 1,684 mm, with an annual average of 1,519 mm. For those years, in their respective order, the ET_a was found from the moisture balance as 702, 941, 844, 734, 870, 862, 837, 933, 818, 1, 018 mm respectively, with an annual mean of 856 mm. It is remarkable that the last figure is exactly the same as the estimate for ET_a given in Table 5.11 for Kiambu District. The two sets of results for Kiambu and Ruiru give the pan coefficient E/E_P as 0.88, which is within the long-established range of values for the said coefficient.

5.5.11 Zambia, Zimbabwe, and Malawi- Consumptive use of water for cotton in Zimbabwe is related to evaporation from US Class A pan and Penman evaporation An average ratio of 0.72-0.75 between these two variables was obtained for the entire growing season. It starts from 0.22 at planting and increases to almost 1.0 during the period of boll-formation, which is from 9 to 17 weeks after planting cotton in the Lowveld (ICID, 1973).

In Zambia, the ratio between the water use of a closed canopy crop and the corresponding pan evaporation was found to be 0.88. Water balance calculation shows that annual evapotranspiration outside each of the Bangweulu swamp, Kafu flats and Lukanga swamp is 890, 785 and 908 mm (Balek, 1977). It goes without saying that these figures represent actual evapotranspiration. The Atlas of World Water Resources (Kurzon, 1978) gives 800 mm and 1,600 mm as average annual figures for ET_a and ET_p for the area occupied by these swamps.

Evapotranspiration figures for the swamps themselves will be presented in the next section.

According to Griffith's (1972), "of the standard evaporation formulas tested, the most successful is undoubtedly that of Penman. While it underestimates the high evaporation rates in the period September-November, and slightly overestimates in winter, the form of the annual curve matches observed conditions quite closely, and gives reasonable agreement on annual totals." Potential evapotranspiration calculated from the Penman formula is shown in Figure 5.13. Amounts are least in the extreme north of Zambia, where the rainy season is longest, and in the mountain areas of Malawi and Zimbabwe. They annual ET_p values are greater in the major river valleys, especially the Limpopo and Sabi in Zimbabwe, the Zambezi below Livingstone, and the Shire.

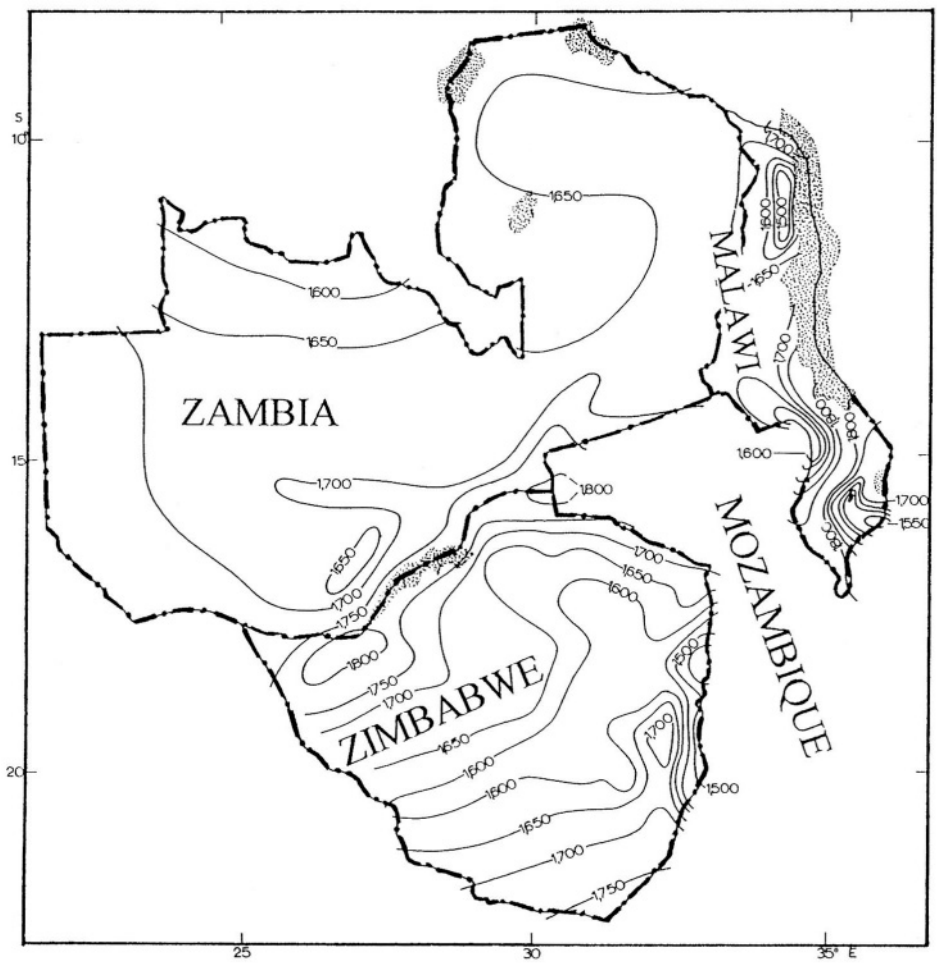

Figure 5.13- Lines of equal ET_p for Malawi, Zambia and Zimbabwe, based on Penman's evaporation (after Griffith's, 1972)

Table 5.11-Estimation of ET_r, ET_p and ET_a for the Kiambu District in Kenya (Heederik et al., 1984)

Month	P, mm	E_P, mm	ET_r, mm	k_c	ET_p, mm	k_a	ET_a,mm
January	59	193	154	0.69	106.3	0.50	53.2
February	40	202	162	0.60	115.2	0.20	23.0
March	72	201	161	0.85	136.9	0.75	102.7
April	242	140	112	0.93	104.2	1.00	104.2
May	173	103	82	1.11	91.0	1.00	91.0
June	43	90	72	0.83	63.9	1.00	63.9
July	25	83	66	0.69	45.5	0.75	34.1
August	24	96	77	0.60	46.2	0.75	34.7
September	28	138	110	0.85	93.5	0.50	46.8
October	52	176	141	0.93	131.1	0.75	98.3
November	123	119	111	1.11	123.2	1.00	123.2
December	76	162	129	0.83	107.1	0.75	80.3
Total	958	1,726	1,377		1,164		855

Explanation

P = precipitation, E_p = pan evaporation, ET_r = reference evapotranspiration = 0.80 x E_P, k_c = crop coefficient, ET_p = potential evapotranspiration, ET_a = actual evapotranspiration and $k_a = ET_a / ET_p$

It is remarkable that the rates appearing in Figure 5.13 agree quite well with the rates shown for the same area on the map of potential evapotranspiration for Africa (Kurzon, 1978). Additionally the ET_p rates for that part in Figure 5.13 for Zimbabwe are more or less similar to the evaporation rates shown in Figure 4.11 multiplied by about 0.8.

5.5.12 South Africa- Evapotranspiration in South Africa is measured using lysimeters. Mostly, however, it is estimated using evaporation rates obtained from evaporation pans or calculated by Penman's formula. These rates are then adjusted to yield crop water use or evapotranspiration rates using the relevant crop coefficients. Table 5.12 is an example of the average crop (sugar) coefficient as obtained from three experimental farms (Chaka's Kraal, Tongaat and Illovo) all located in the sugar belt. The total evaporation is 1,180 mm (360 days) and the total evapotranspiration for the same period is 1,028 mm, giving an overall coefficient for the growing season of 1.085. The periodic values as given in Table 5.12 vanes from a minimum of 0.35 to a maximum of 1.41. These figures are not too different from the single crop coefficient to be multiplied by the reference evapotranspiration to obtain the crop evapotranspiration. This coefficient starts as 0.40 at the beginning of growing season to reach 1.25 at the middle of the season and ends by 0.75 (FAO-Paper No. 56, 1998).

Table 5.12- Free water evaporation, E, consumptive use of water by sugar, CU and crop coefficient K_c average of three experiment stations*, S. Africa

Period from - to	E, mm	CU, mm	K_c	Period from - to	E, mm	CU, mm	K_c
Oct 05-Nov 04	112.6	40.5	0.35	Apr 17-May 14	66.2	90.8	1.40
Nov 05-Dec 01	101.9	67.5	0.67	May 15-Jun 11	60.1	69.3	1.16
Dec 2-Dec 27	121.0	121.5	1.01	Jun 12-Jul 09	48.9	69.6	1.41
Dec 28-Jan 23	134.8	160.5	1.19	Jul 10-Aug 06	62.4	72.4	1.16
Jan 24-Feb 20	122.0	168.7	1.39	Aug 07-Sep 03	61.7	74.7	1.22
Feb 21-Mar 19	115.9	130.5	1.12	Sep 04-Sep 30	80.0	86.6	1.08
Mar 20-Apr 16	89.7	122.6	1.37	Total	1.177	1.275	1.085

Explanation

** The three stations are; Chaka's Kraal, Tongaat and Illovo, all in the sugar belt of South Africa, near the coast of the Indian Ocean overlooking Mozambique Channel.*

Figure 4.12 (Chapter 4 "Evaporation") shows lines of equal Class A pan evaporation for South Africa and the nearby parts of the adjacent countries. According to FAO-Irrigation and Drainage Paper No. 56 (Allen et al., 1998) the reference evapotranspiration ET can be estimated by multiplying the pan evaporation E_p by a pan coefficient k_p as already given by Eq. (5.29). The magnitude of the coefficient k_p, according to the same reference, depends on the pan surroundings being either green or fallow, relative humidity and wind speed. In general it varies between 0.40 and 0.8

A comparison between the annual pan evaporation shown in Figure 4.12 and the annual potential evapotranspiration indicated in the Atlas of the World Water Resources (Kurzon, 1978) shows that the two sets of data are related by a pan coefficient of 0.5-0.6. It is evident from these sources of information that the largest ET_p rates occur in the western part of Botswana and the eastern part of Namibia around the boundary between these two countries. In Namibia, the ET_p decreases gradually from more than $2{,}000\ mm\ y^{-1}$ in the extreme east to reach say $1{,}200\ mm\ y^{-1}$ along the Atlantic coast in the west.

5.6- Evapotranspiration from Wetlands

5.6.1 Brief description and background- By wetland we mean a surface covered by a perennial and/or intermittent swamp or marsh. In Africa, there are numerous swamps occupying a large surface, e.g. the "Central Basin" of Zaire includes large swampy areas and Lake Chad is largely made up of swamps. Swamps also occur in headwater lowlands, for example in the high lands of Rwanda and Madagascar and in Sierra Leone.

The distinction between swamps and marshes is based on the concept that marshes are wetlands with predominantly grassy vegetation. They are often

called "wet meadows". Herbaceous swamps can be distinguished from marshes by their higher vegetation. Papyrus swamps are generally more typical of African herbaceous swamps, although *Typha* (sedge) swamps can be found there too. The Okavango Delta lies in Ngamiland, which is named after the floating reed swamps commonly occurring in the region. The difference between rooted swamp and floating swamp can be seen from Figure 5.14 (redrawn from Howard Williamas & Gaudet, in Denny, 1985).

Intermittent swamps or dambos, as they are usually called in Africa, are streamless grassy depressions that are periodically inundated. Dambos can be found at the headwater of a drainage system in a region of dry forest or bush vegetation (Ackerman, 1936). More details, including drawings and geographical maps relevant to the occurrence, physiography and hydrology of African wetlands, are given with the hydrology of lakes in a subsequent chapter.

Some investigators suggest that the total surface area of swamps in Africa could be greater than the area covered by open water. Table 5.13, quoted from Balek (1977), lists the main African swamps, for which the country of location, mainstream and surface area of each swamp is included. Water hyacinth fills many of river and stream channels as well as storage reservoirs in tropical and subtropical regions of the world, and Africa is no exception to this. Due to its high consumption of water, water hyacinth is usually regarded as a source of water loss. Some authorities (e.g. Timmer and Weldon, 1967) claim that water

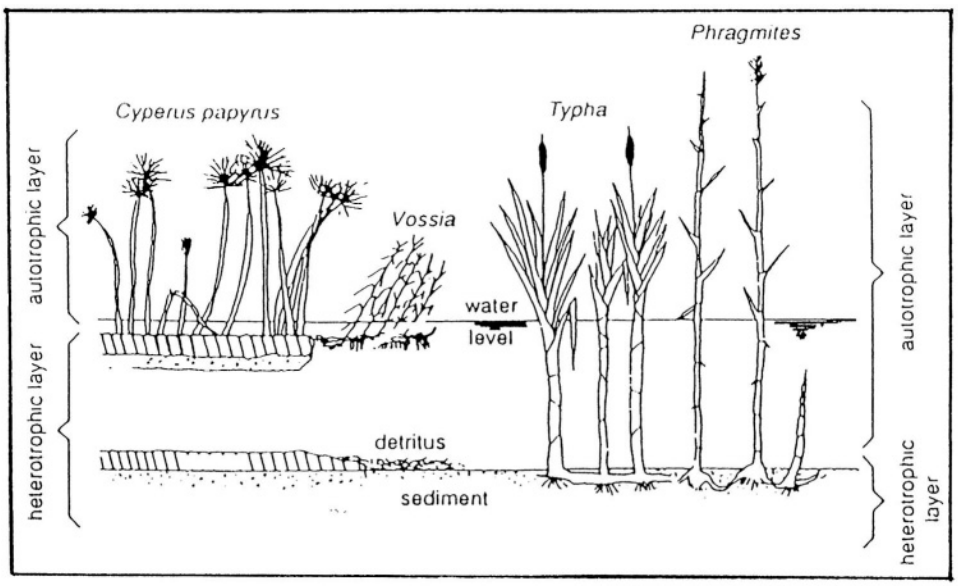

Figure 5.14- Floating swamp and rooted swamp (from Howard-Williams & Gaudet, 1985)

Table 5.13- Main African swamps (after Balek, 1977)

Swamp	Country	Main stream	Area, km^2
1- Bahr el-Jabal/Bahr el-Ghazal (Sudd)	Sudan	White Nile	64,000
2- Central Congo swamps	Congo	Zaire	40,550
3- Lake Chad swamps	Chad	Chari	32,650
4- Bahr Balamat	Chad	Chari	27,000
5- Okavango	Botswana	Okavango/ Botletle	26,750
6- Upper Lualba swamps	Congo	Lualba	25,750
7- Lake Kyoga swamps	Uganda	Victoria Nile	21,875
8- Lake Mweru swamp	Zambia/Congo	Luapula	17,000
9- Lake Mweru Wantipa swamp	Zambia	Mofwe	16,500
10- Lake Bangweulu swamps	Zambia	Chambeshi	15,875
11- Kenamuke/Kabonen	Sudan		13,955
12- Lotagipi	Sudan/Kenya	Tarach	12,937
13- Malagarasi	Tanzania	Malagarasi	7,357
14- Nyong	Cameroon	Nyong	6,688
15- Albert Nile swamps	Sudan	Albert Nile	5,200
16- Kafue flats	Zambia	Kafue	2,600
17- Lukanga	Zambia	Kafue	2,600

lost by evapotranspiration can be as high as 3.7 times the evaporation from a free water surface. In view of the importance of this matter to hydrology of swamps in Africa, it might be of interest to present briefly the results of a study that was carried out elsewhere to verify the validity of this high figure.

Van der Weert & Kamerling (1974) accomplished this aim by conducting experimental work in August-October, 1968, near the Agricultural Experiment Station at Paramaribo, Surinam. To avoid the border effects and the differences in microclimate between the Experiment Station and the natural environment of the water hyacinth, the measurements were repeated in the period October-December, 1968, at the Brokopondo Lake some 140 km south of Paramaribo. Evapotranspiration was measured from two water hyacinth pans forming the inner and outer components of a double cylindrical pan system. The evaporation E from a free water surface was measured using a US Class A pan and estimated from meteorological observations substituted in Penman's formula. In the Brokopondo Lake experiment water hyacinth was grown in a 2-m-diameter floating pan placed in a large field of water hyacinth. Outside this field, open water evaporation was measured from a 2-m pan having the same dimensions as the water hyacinth pan. From this study, it has been concluded that evapotranspiration from swamps basically depends on the plant species growing in the swamp. Under several climatological environments, the ratio ET/E is above unity, and under specific conditions can be very high (above 2.0 or even 3.0).

5.6.2 Swamps in southern Sudan- Migahid (1948, 1952) carried out the earliest experiments for estimating the loss of water from the swamps (Sudd) in the Upper Nile Basin. Papyrus was grown in tanks 10 m^2 in surface area and 2.5 m in depth each. The results reported in 1948 led Hurst (1950) to consider that the evapotranspiration from the papyrus growing in the swamps in southern Sudan is twice as much as free water evaporation.

Rijks (1969) commented on the Migahid's experiments saying that the mean evapotranspiration over the 6½ years from the undisturbed papyrus was 55 percent of Penman's estimate of open water evaporation for that area. He added: "Migahid notes that the 6½ year old papyrus in the tank was very poor as compared with the dense and luxuriant papyrus outside". So, it appears that the growth condition of the papyrus is the factor that dictates the extent of its evapotranspiration in relation to open water evaporation in the same location. The same conclusion has been reached later by Van der Weert & Kamerling (1974).

Sutcliffe (1974) reported the findings of a hydrological study of the southern Sudd region. Those findings did not include any estimate of the evapotranspiration from the swamps filling that region. Later, Sutcliffe and Parks (1987) while developing a water balance model of the Bahr el-Jebel (1987) referred to a discussion by Penman (1963), in which he suggested that the evapotranspiration from the papyrus and evaporation from open water would be nearly equal, i.e. *ET/E* is nearly equal to 1. As such, the suggested monthly open water evaporation (also papyrus evapotranspiration) has been estimated using the meteorological data of Bor on the Bahr el-Jebel and Penman's formula. The suggested monthly rates are: 217, 195, 205, 189, 184, 161, 142, 142, 151, 178, 189, 217 mm for January, February,..., December, respectively. The total annual evapotranspiration is 2,170 mm. These estimates have been used once more by Sutcliffe and Parks in the design of water balance model for the swamps of the Bahr el-Ghazal (1994).

5.6.3 East Africa (Kenya and Uganda)- Glover and Forsgate (1964) observed the daily evapotranspiration from a low, closely matted, perennial grass (Kikuyu grass) at Muguga (1° 14'S, 36° 38'E, altitude 2, 100 m), Kenya. Measurements were taken by means of a floating lysimeter (2.5 m by 1.25 m and 1.25 m deep steel tank) over a period of four months, which included a long drought. The daily loss of soil moisture was compared with daily evaporation from a sunken pan, E_{sp}, and with daily estimates of open water evaporation, E, using the Penman (1956) modified equation and incorporating the Glover-McCulloch (1958) estimates of radiation based on values of hours of bright sunshine *n/N*. Records of rainfall, temperature, saturation deficit, wind speed and solar radiation were available from an adjacent well-equipped meteorological station where several evaporation pans of different types were in operation.

The observed evapotranspiration appeared to vary widely between slightly

above zero to about 5 mm d^{-1}, with an average of about 3 mm d^{-1} over the period of the experiment (126 days). Some of the important results obtained from that study are given in a summarized form in Table 5.14.

Evidence suggests that evaporation from the lysimeter was very nearly the same as that from the undisturbed surroundings. The direct measurement of daily pan evaporation and the estimate of open water evaporation by means of the Penman equation (1956) have proven to be closely related to measured daily evapotranspiration by Kikuyu grass. Either the pan evaporation or the Penman evaporation would prove a useful estimate of the latter, as shown by the relevant high correlation given by r^2 in Table 5.14. Not withstanding the important information in this Table, the most striking result the experiment showed is that the Kikuyu grass did not wilt until all the soil down to the bottom of the lysimeter was depleted of available water.

Rijks (1969) examined the evapotranspiration from a valley swamp near Namulonge (0° 32'N 32° 37'E, altitude approximately 1,110 m). The swamp belongs to the Koki lake system (4,715 km^2) in southern Uganda. Rijks used the meteorological data available at the Cotton Research Station at Namulonge along with the Bowen ratio method to estimate the Penman open water evaporation, *E,* the Penman evapotranspiration from short grass, ET_r, and the evapotranspiration from the swamp, *ET.* The results obtained for three periods during the course of the experiment, March-April, 1965, are as follows:

Table 5.14 Evapotranspiration from short grass related to evaporation from a sunken pan and Penman open water evaporation using *n/N (after Glover and Forsgate, 1964)**

Month	Number of obser-vations	Lysimeter vs sunken pan	r^2	Lysimeter vs Penman	r^2
a- mm water / day					
Jul.	31	$ET = -0.18 + 0.87\ E_{sp}$	0,78	$ET = -0.92 + 0.90\ E$	0,78
Aug.	31	$ET = 0.12 + 0.76\ E_{sp}$	0,8	$ET = -1.73 + 1.13\ E$	0,8
Sep.	30	$ET = 0.10 + 0.78\ E_{sp}$	0,8	$ET = -1.55 + 1.09\ E$	0,76
Total	92	$ET = 0.03 + 0.79\ E_{sp}$	0,83	$ET = -1.43 + 1.06\ E$	0,82
b- mm water / 5-day period					
	Periods				
Overall	18	$ET = 0.17 + 0.75\ E_{sp}$	0,91	$ET = -1.17 + 1.00\ E$	0,94
c- mm water / 10-day period					
	Periods				
Overall	9	$ET = 0.06 + 0.78\ E_{sp}$	0,98	$ET = -1.35 + 1.03\ E$	0,97

Explanation

ET = Evapotranspiration from short grass, E_{sp} = evaporation from a sunken pan,

E = Penman's estimate of open water evaporation and r^2 = coefficient of determination

** n/N = relative duration of bright sunshine*

Period from	to	E mm d^{-1}	ET_r mm d^{-1}	ET mm d^{-1}	ET/E %
08.03	12.03	6.2	4.9	3.65	59
22.03	28.03	3.8	3.1	1.92	51
07.04	11.04	5.5	4.4	3.81	69

In view of the limited data, which were available then, the results obtained were limited too. From those results, however, Rijks (1969) concluded that the evapotranspiration from an old stand of papyrus, in which a fair proportion of brown and dried out heads is visible, is about 60±15 percent of the evaporation from open water.

5.6.4 Zambia- Balek and Perry (1973) investigated the hydrology of seasonally inundated African headwater swamps. The word “dambo” is generally used to refer to an African seasonal swamp, though ”mbuga” is the term used in East Africa. Four dambos in the Luano experimental catchments, near Chingola and within the Kafue River basin in Zambia were placed under intensive observation. The area of study is located at 12° 34’S, 28° 01’E and 1300 m a.m.s.l. The aim of thet investigation was to draw the water balance of those four dambos and obtain the evapotranspiration, and, consequently, its monthly and annual ratio to open water evaporation. The results obtained for the three years between 1967 and 1970 are listed in Table 5.15. The Table gives also monthly and annual estimates of potential evapotranspiration from another dambo, Itwa dambo, near Ndola close to the boundary between Zambia and Congo (Kinshasa) and about 100 km south east of Chingola (Adams and Kitching, 1979). Some of the results obtained from those two investigations are listed in Table 5.15.

Another water balance study of Zambian swamps and dambos was carried out a few years later by Balek (1977). This included the Bangweulu swamp surrounding the entrance of Lulingila River into Lake Chaya and the Lukunga swamp, a side swamp with a limited connection to the Kafue River. It also included the Kafue Flats, which are swamps located on both sides of the Kafue River, and a dambo located within the Kafue basin, surrounded by a dense forest formed mainly by grasses, which can easily evaporate any amount of water infiltrating into the soil. The results obtained on annual basis can be summarized as follows:

Swamp / dambo	E, mm	ET (outside), mm	ET (total), mm	E (total)/E %
Bangweulu	2,340	890	2,000-2,160	85-92
Lukanga	2,070	908	1,120	54
Kafue Flats	2,070	785	1,000	48
Dambo	1,710	1,320	1,075	63

Table 5.15- Monthly and annual evapotranspiration from a number of dambos in Zambia, and their ratios to open water evaporation

Year and hydrologic item	Monthly and annual *ET in* mm and the corresponding *ET/E ratios*												
	Oct	Nov	Dec	Jan	Feb	Mar	Apr	May	Jun	Jul	Aug	Sep	Year
*Dambo**													
1967-68, *ET*	29.1	124.0	65.9	99.6	71.3	55.3	26.6	10.3	9.02	6.65	5.56	5.13	508
ET/E	0.15	0.72	0.45	0.68	0.47	0.34	0.18	0.08	0/09	0/06	0.04	0.03	0.29
1968-69, *ET*	6.58	80.7	86.4	87.5	67.5	64.1	29.3	20.4	9.17	9.63	6.65	5.84	474
ET/E	0.03	0.53	0.66	0.59	0.55	0.47	0.21	0.17	0.09	0.09	0.05	0.04	0.29
1969-70, *ET*	20.1	43.8	5.3	97.4	71.8	77.7	39.4	16.8	18.5	6.02	5.46	5.28	487
ET/E	0.12	0.25	0.68	0.64	0.54	0.47	0.28	0.14	0.09	0.06	0.04	0.03	0.29
*Dambo***													
ET	174	151	135	135	123	135	144	132	116	126	149	161	1.681

Explanation

** Four dambos situated in the Luano catchments near Chingola: latitude 12° 34' S, longitude 28° 01' E and elevation 1,300 m a.m.s.l.(Balek & Perry, 1973), ** Itwa dambo near Ndola, ET is estimated from a locally adjusted form of Penman's evaporation formula (Adams & Kitching, 1979)*

5.6.5 Sénégal, Niger and Botswana- Sutcliffe and Parks (1989) reported the results of comparative water balances of selected African wetlands. These comprised the wetlands in the flood plain of the lower Sénégal, the Niger Inland Delta, the Okavango delta in Botswana and, the Sudd region of the upper Nile. Results from the last, i.e., the Sudd, have already been presented in sub-section 5.5.2. The method of analysis in every case is the same. The swamp is regarded as a reservoir whose storage volume is the mass or cumulative inflow (rainfall plus river inflow) less the mass outflow (river outflow plus evaporation and soil moisture recharge). Open water evaporation has been estimated from Penman's formula, and the rates obtained are given in Table 5.16. It should be made clear that Sutcliffe and Parks, based on previous experience, have considered that the vegetation conditions of the wetlands they investigated justify using Penman's open water evaporation as an equivalent of evapotranspiration.

5.7- Evapotranspiration From Woodlands and Forests

According to Dagg (1972) tall evergreen rain forest of the Kericho Catchment area in Kenya, lying between 2100 m and 2400 m a.m.s.l., uses about 1,500 mm of water per annum with a ratio *ET/E* of 0.90. A similar experiment with evergreen forest in the Mbeya Range in Tanzania has shown the same annual ratio, i. e., *ET/E* = 0.90, which corresponds to 1,450 mm of water use. This amount is partly obtained from rainfall and the rest is obtained from the water stored in the soil from the rainy season. Dagg (1972) adds that the mambo forest on altitude of 2400 m, where rainfall is adequate and well distributed, uses about 1, 150 mm y^{-1} at an *ET/E* = 0.75 only. He adds further that pine forests consume water with *ET/E* increasing with level of growth and density of the canopy. The ratio *ET/E* of a mature pine forest reaches 0.85.

In addition to grass and herbaceous swamps there are swamp forests. These forests are found on the lower shores of water bodies and rivers, in depressions and in some high-water riverbeds, on muddy, water logged soils. Swamp forests occupy large stretches of Central Africa, particularly in Congo (Kinshasa and Brazzaville), Gabon, Southern Cameroon and the Niger Delta. Swamp forests will be discussed further in a special chapter on lakes and wetlands.

Table 5.16- Monthly and annual estimates of open water evaporation in mm for selected wetlands in Africa (Sutcliffe & Parks, 1989)*

Swamp	Jan	Feb	Mar	Apr	May	Jun	Jul	Aug	Sep	Oct	Nov	Dec	Year
Okavongo	200	180	165	130	110	90	100	125	155	205	200	200	1860
Niger	179	172	195	225	230	218	173	128	117	158	159	146	2100
Senegal	135	177	185	233	228	222	165	171	159	200	162	163	2200

Explanation

**Figures in the table are read from the diagrams given in the above-mentioned reference.*

The relationships between forest stand structure, growth and evapotranspiration in South Africa were analyzed to determine whether forest evapotranspiration can be estimated from stand growth data. The basis for this approach is (a) that growth rates are determined by water availability and limited by the maximum water extraction potential, and (b) the stand evapotranspiration is proportional to biomass and biomass increment.

Model studies have shown that the most consistent relationship between *ET* and stand growth takes the form of a power function as (Le Maitre & Versfeld, 1997):

$$ET = aX^b \tag{5.47}$$

where X is a standard growth parameter (height, basal area or utilizable volume).

Le Maitre & Versfeld (1997) stated that the models using stand basal area, BA, gave the best mean fit over all the catchments analyzed, but gave poor results in some cases. The general form of such models is:

$$ET = c(BA+1)^d \tag{5.48}$$

where c and d are parameters varying from catchment to catchment. For the examined eight catchments a varied from a maximum of 966.43 to a minimum of 569.99 and d from 1.15144 to 0 05259. The correlation coefficient (given by r^2) varied between a maximum of 0.81 and a minimum of 0.04. The basal area BA is expressed in $m^2\ ha^{-1}$ and the evapotranspiration ET is in $mm\ y^{-1}$.

The study has also shown that the projected evapotranspiration increases steeply in the early age of the plantation, first 5 years or so. The increase continues with increasing age but with a slower rate till it becomes hardly noticeable at about 20 years of age. As such, under a high level of afforestation, the rates of evapotranspiration may increase considerably, thereby reacting negatively on streamflow. It is highly likely that streamflow will cease during droughts.

Woodlands of various types can be found in several countries, such as Angola, Zambia, Zimbabwe, Malawi, Mozambique and Tanzania. They are found in the zone of seasonal rainfall that almost surrounds the rainforest. Consequently, woodlands reflect the various ratios of the length of the dry and wet seasons.It is common to call the African tropical woodland by “miombo”. Alexandre (1977) reported the results obtained from water balance study of a miombo in the Lufira River basin, Upper Shaba region, Congo (Kinshasa). During the rainy season, *ET* is probably higher in miombo ($120\text{-}150\ mm\ mo^{-1}$) than in the moist evergreen forest ($100\ mm\ mo^{-1}$). During the dry season, *ET* is very likely to drop down to nearly one-third of its value in the rainy season.

The distribution of E and ET_p within the year is shown in Figure 5.15. Additionally, the distribution of the ratio ET_a/ET_p over the months of the year is: 138/125, 133/120, 150/136, 102/133, 81/115, 49/92, 42/100, 42/133, 39/167, 45/198, 93/154 and 126/137 for January, February up to December. The figures in the numerator are monthly ET_a rates in mm, and in the denominator are monthly ET_p rates in mm. The total values of ET_a and ET_p are 1,610 and 1,040 mm respectively, giving an ET_a/ET_p ratio of 0.65.

Table 13_c Appendix A gives monthly and annual evapotranspiration rates from woodland and transitional zones between grasslands and woodlands in Zambia for the year 1969-1970. Table 5.17 also is prepared using the results published by Balek (1977). It gives monthly rates of open water evaporation and evapotranspiration, and the monthly and annual ratios for *E/ET*.

It is quite remarkable that the results given in Table 5.17, though obtained from the water balance of the system, are exactly the same for the years 1967-68 and 1969-70, for both the woodlands and the transitive zones. Not withstanding this remark, the average annual *ET/E* ratios for the woodlands and the transitive zones are 0.77 and 0.63 respectively. The latter value depends on the percentage of grass and trees. The *ET/E* ratio for grassland (dambos) situated in the same region was 0.29, as listed in Table 5.15.

When the available *ET/E* values for all wetland systems are arranged in descending order, herbaceous swamps under certain conditions can exceed unity, forests at, a certain age have 0.85-0.90, woodlands follow with 0.75, next come transitive zones with 0.65, and finally grasslands with a low value of 0.29. Last but not least, from all case studies presented in this section, one can fairly conclude that the ratios ET_p/E and ET_a/ET_p for any wetland system depend essentially on the climate of the area, availability of water, soil moisture reserve, vegetation condition and age of plantation.

Table 5.17- Monthly evapotranspiration from woodland and transitive zones in the Central African Plateau, 1967-1970 (after Balek, 1977)

	Monthly and annual *ET in* mm, and the corresponding *ET/E* ratios												
	Oct	Nov	Dec	Jan	Feb	Mar	Apr	May	Jun	Jul	Aug	Sep	Year
Woodland													
1967-68													
A	67	153	146	146	163	198	128	87	63	61	55	47	1,314
B	0.35	0.89	1.0	1.0	1.07	1.22	0.85	0.67	0.63	0.53	0.40	0.29	0.74
1968-69													
A	49	85	129	153	164	194	193	120	82	72	68	56	1,365
B	0.24	0.56	0.99	1.03	1.32	1.42	1.39	0.99	0.83	0.67	0.52	0.36	0.83
1969-70													
A	67	153	146	146	163	198	128	87	63	61	55	47	1,314
B	0.35	0.89	1.0	1.0	1.07	1.22	0.85	0.67	0.63	0.53	0.40	0.29	0.74
Transitive zone													
1967-68													
A	67	153	146	146	153	159	87	51	40	42	44	45	1,133
B	0.35	0.89	1.0	1.0	1.0	0.98	0.57	0.39	0.40	0.37	0.33	0.28	0.64
1968-69													
A	49	85	129	153	115	132	128	54	36	37	40	40	998
B	0.24	0.56	0.99	1.03	0.93	0.96	0,92	0.45	0.36	0.35	0.31	0.26	0.61
1969-70													
A	67	153	146	146	153	159	86	51	40	42	44	45	1,132
B	0.35	0.98	1.0	1.0	1.0	0.98	0.57	0.39	0.40	0.37	0.33	0.28	0.64

Explanation

A = ET and B = ET/E

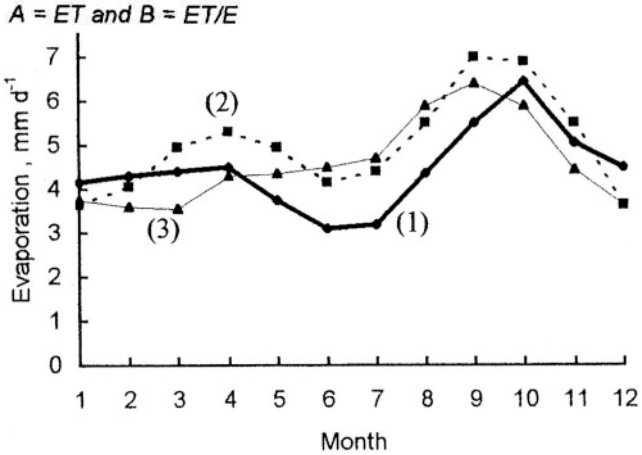

Figure 5.15- Evaporation and potential evapotranspiration throughout the year
(1) estimated using Penman formula for a thinned area in the miombo,
(2) estimated Penman evaporation using climatic data of Lubumbashi, and
(3) evaporation measured by means of Colorado sunken pan.

CHAPTER 6

RUNOFF, STREAMFLOW, EROSION AND SEDIMENTATION

6.1- Introduction

Vegetation and/or artificial surfaces such as roofs or pavements intercept a certain amount of the rain falling during the first part of a rainstorm. The rainfall that reaches the land surface evaporates, infiltrates or lies in depression storage. It does not always happen in every rain event that some water is left on the land surface after these losses are all provided for. But, if there is any surplus water left, the surface will be covered with a film of water known as surface detention, and overland flow begins downslope toward the nearest stream channel. This water upon entering a channel is referred to as surface runoff. The streams coalesce into rivers, and rivers eventually find their way down to the sea.

The rate of surface runoff is the difference between the rainfall intensity and the infiltration rate assuming that evaporation during and shortly after a rainstorm is so small that that it can be neglected without any significant error. Likewise, the depth of runoff is the difference between the rainfall depth less the depth of infiltration. These classical views as developed by Horton (1933), while being valid for a certain site, can be misleading if extended to a sizeable catchment area. Runoff into streams may occur only from certain parts of the catchment, called source areas. These source areas vary in extent and performance during the progress of a rain event.

It is the dream of every hydrologist to establish a relationship between rainfall and runoff. The ratio of the runoff to the rainfall is known as the runoff coefficient. The magnitude of this coefficient is not constant, but varies with time and in space depending on a number of factors that will be mentioned later.

It should be noted, however, that not all streamflow is a result of surface runoff. Streamflow may consist of surface runoff and subsurface runoff. L'vovich (1979) distinguishes between two types of runoff in humid zone catchments: a flood flow rapidly transferred along the river during wet periods, and a groundwater-generated base flow. The latter is less variable and provides the dependable flow source in a river. In arid zones there is hardly any base flow, since the water table is generally below the streambed.

Climate classification of Africa, and analyses and discussion of the amounts, rates and other target variables relevant to precipitation, evaporation, and evapotranspiration corresponding to each class have already been presented in various sections in Chapters 2, 3, 4, and 5. A distinction between arid and humid

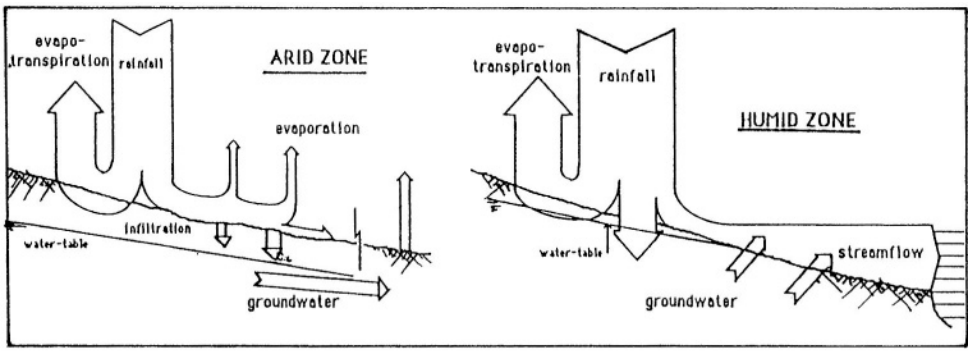

Figure 6.1- Schematic illustration of runoff formation and streamflow in arid and humid zones (Margat, 1979)

regions with regard to runoff and streamflow is shown schematically in Figure 6.1 (Margat, 1979).

Rainfall and surface runoff under certain conditions related to land slope, structure and texture of the soil together with the rain intensity and raindrop impact are responsible for soil erosion. The process of erosion consists of the detachment of soil particles from their original position in the soil mass and their movement to a nearby channel, in which they may be transported to other channels or to depressions and swales, where they are deposited.

Erosion is generally divided into dry (wind) erosion and wet (water) erosion. Water erosion has, in turn, its own subdivisions. Description of the different types of water-induced erosion, their causes and characteristics can be reviewed in any of the specialized pieces of literature (e.g.. Evans, 1980).

Erosion products, which reach streams competent of moving them, are transported as suspended sediments in the flowing water and as bed load along the channel bottom. As such, the transported matter may range from tree trunks, boulders and other trash dislodged and carried away by floods to minute particles suspended in a tranquilly flowing stream.

The relatively quiescent waters of storage reservoirs encourage the deposition of sediment transported in the flowing water. The rate at which the reservoir size is reduced depends on the rate of sediment inflow to and sediment outflow from the reservoir. The difference between the inflow and outflow, i.e. the rate at which sediments are entrapped (trap efficiency), determines the active or life age of the reservoir.

Several aspects related to runoff, streamflow, erosion and sedimentation in Africa, both at the continental or regional scale and at country scale, will be dealt with successively in the next sections. Review and discussion of these items are supported by the hydrological data contained in the Tables given in Part 1 of Appendix B and the water quality data included in the Tables of Part 2 of the same Appendix.

6.2- Runoff and Runoff Coefficient

Estimation of runoff as a percentage of storm rainfall is a widely used practice. This percentage is often referred to as the runoff coefficient. It varies from near zero to a relatively high value depending upon the topography of the catchment, magnitude and intensity of the storm rainfall, soil infiltration rate and the initial soil moisture condition.

The runoff coefficient, on a temporal scale, can be obtained for a single storm of short duration or else for all rainfall in a month, season or year. On a spatial scale, the water balance as a method for determining the runoff coefficient remains the same in every case. The difference, if any, lies in the size of the area for which the balance is drawn. The size here can vary from as large as a whole continent to a certain region or river basin or just a small experimental basin.

6.2.1 Water balance of Africa- The water balance of Africa including long-term annual data of precipitation, *P,* evaporation and evapotranspiration, *E,* and total runoff, *R,* has been drawn up by several researchers interested in world water resources. The studies they carried out have produced several estimates for the annual runoff. Some of these estimates are as follows:

Source of data	*P*, mm	*E*, mm	*R*, mm	*r*, %
Kalinin (1971)	728	525	203	28.0
Baumgartner and Reichel (1975)	696	582	114	16.4
Korzun (1978)	740	587	153	20.7
L'vovich (1979)	686	547	139	20.3
Willmott et al. (1985)	639	495	144	22.5
Budyoko (1986)	720	580	140	19.4

The average figures for the above estimates are: 701 mm for precipitation, 553 mm for evaporation and evapotranspiration, and 148 mm for total runoff. These figures give 21% as an average value of the runoff coefficient, r. The runoff coefficient is the ratio of the total runoff to the precipitation, both over the same length of time. More recently, Shiklomanov (1990) gave 151 mm as an overall figure for annual streamflow. This is not significantly different from the 148 mm, the average of the six estimates produced in the period 1971-1986. Shiklomanov stated truly that his estimate for the runoff in Africa differs by almost 32% of the estimate given by Baumgartner and Reichel (1975). Surprising enough, the runoff coefficient, which he set at 10%, is only half of the average of the earlier estimates. This immediately suggests that the long-term mean annual precipitation in Africa must be 1,510 mm, a figure that cannot be accepted by any means. The only explanation is that the term percentage of total runoff as used by Shiklomanov (1990) has a different meaning than simply the

sum of surface and groundwater runoffs divided by the effective or ground precipitation. This can also be evidenced from his figures of 306 mm and 7% for streamflow and percentage of total runoff for Europe, respectively. It is well known that the runoff coefficient for Europe is in the range of 35- 40%. As such, it seems advisable to take into account whenever necessary the average values of the runoff and runoff coefficient obtained from the early estimates, 1971-1986, instead of the figures estimated by Shiklomanov.

The annual runoff coefficient varies from place to place, with a minimum of 1% or less to more than 70%. The lines of equal runoff coefficient shown on the map in Figure 6.2 indicate the spatial distribution of the runoff coefficient in Africa. The coefficient generally increases with annual rainfall and land slope. The mountainous strip parallel to the Mediterranean Sea in Morocco has a runoff coefficient that easily reaches 30% or more. This value decreases rapidly to reach almost zero at a distance of say 300 km inland. The runoff coefficient remains at about this value up to latitude 15° N. Below this latitude the coefficient increases in southerly and westerly directions due to the improvement of the rainfall there. The runoff coefficient can easily reach 40% in the Congo and 60-70% in West Africa: Sierra Leone, Liberia and Gabon. In the east, the marked rise of the runoff coefficient in the Ethiopian Plateau is partly due to the increase of rainfall and partly to the topography of the country. The runoff coefficient in Madagascar increases from 20% in the southwest to 40% in the north, and further to 80% along the coast of the Indian Ocean in the extreme east of the island. There is a general fall in the value of the runoff coefficient moving from the land strips adjacent to Mozambique's channel in the east to Namibia in the west and down south, except for some improvement close to the southern tip of Africa.

6.2.2 Regional water balance- L'vovich (1979) applied the principle of mass balance to regions with different land cover and developed what he termed *interpolation curves.* The general balance equation used can be written as:

$$W = P - R_S,\ R_G = W - ET \text{ and } R = R_S + R_G \qquad (6.1)$$

where W = wetting of the soil surface, P = precipitation, R_S = surface runoff, R_G = ground runoff, ET = evapotranspiration and R = total runoff.

Figure 6.3 shows two sets of interpolation curves for total runoff, R, and surface runoff, R_S, both for Africa (L'vovich, 1979). Both sets are given as functions of the annual rainfall, P, with upper bound of 2,500 mm. Curves I refer to the mountain conifer forests in North Africa; curves II to the evergreen sclerophyll forests and scrub; curves III to the savannahs: a- desertic savannahs and steppes, b- arid, c- moist and d- thinly wooded without leaves in dry seasons, and curve IV denotes humid evergreen forests. All interpolation curves bear the same features. After the initial losses are made up, excess rain produces some

runoff. The runoff increases with rainfall at a rising rate above which the curve becomes parallel to the line $S = P$, i.e. all excess rainfall becomes surface runoff. The difference between one curve and another is due to the difference in magnitude of the initial losses, which vary from one land cover to another. It can be observed from Figure 6.3 that the least initial losses occur in the mountain coniferous forests in North Africa and the largest in the humid evergreen forests. The probable error in the interpolation curves is as follows:

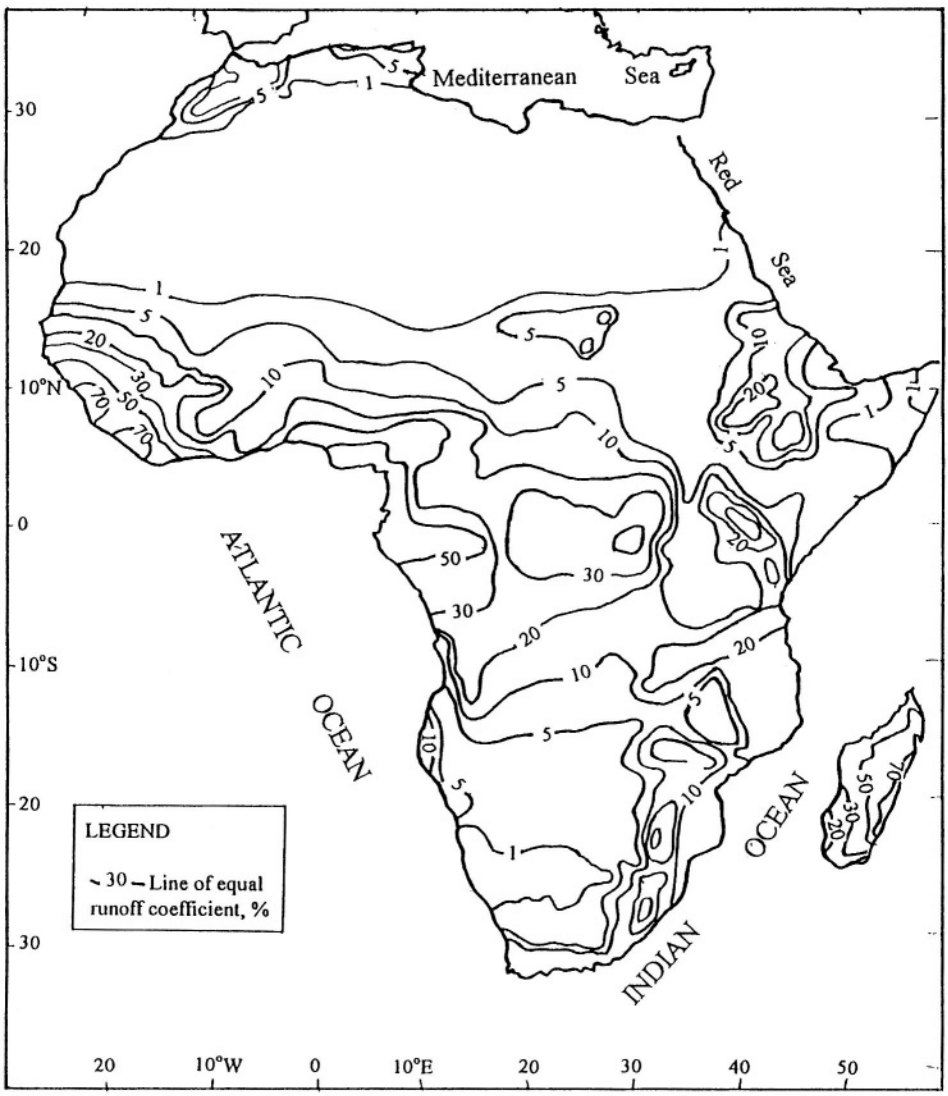

Figure 6.2- Map showing contour lines of equal runoff coefficient in Africa (from Korzun / UNESCO, 1978)

Savannahs	$W = f(P)$	Error = 15%
	$R = f(P)$	16%
Mediterranean conifer forests	$R = f(P)$	13%
	$S = f(P)$	15%
Sclerophyll forests and scrub	$R = f(P)$	15%
	$S = f(P)$	16%
Humid evergreen forests	$R = f(P)$	17%

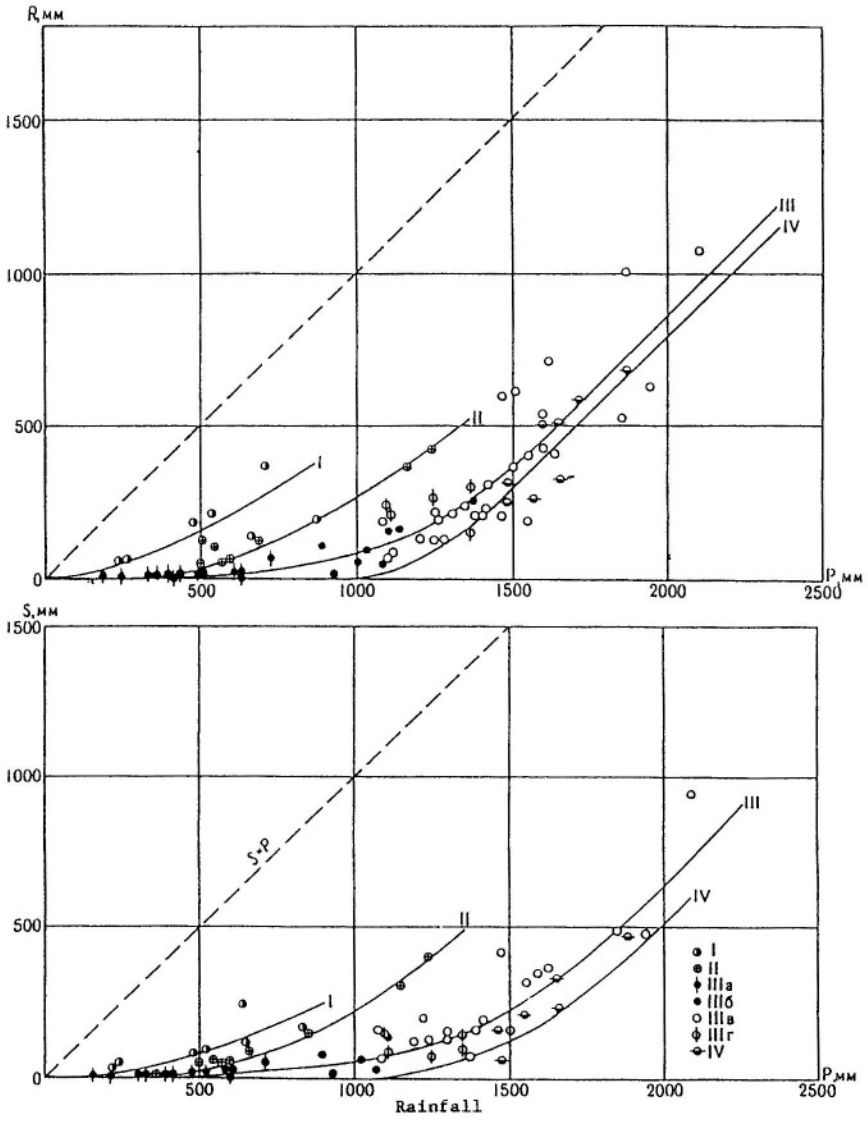

Figure 6.3- Total runoff, R, and surface runoff, S, as functions of rainfall, P, for Africa (from L'vovich, 1979)

6.2.3 River basins- The water balance of several African river basins will be reviewed in the next chapter (s). For the purpose of this sub-section, reference can be made to Tables 4, Part I / Appendix B. The contents of these Tables have been collected from different sources, thus giving a fair estimate of the annual runoff coefficient. These Tables 4 are classified as follows:

-Table 4_a gives the runoff coefficient for rivers west of the Congo river (Rodier, 1984).

-Table 4_b gives the runoff coefficient for certain parts of the Chambeshi and Congo basins located in northern Zambia (Balek, 1977).

-Table 4_c gives the runoff coefficient for certain parts of the Nile Basin (Hurst and Philips, 1938; Hurst, 1950; WMO, 1974; Balek, 1977; and Ogembo, 1977).

-Table 4_d gives the runoff coefficient of the Zambezi River system (Balek, 1977).

-Table 4e gives the runoff coefficient of some Kenyan rivers outside the Nile Basin (Ogembo, 1977)

The Tables prepared by L'vovich (1979) are somewhat different from Tables 4, Part I / Appendix B, in that the annual depth of soil wetting and separate estimates of the surface and underground runoffs are included. Table 6.1 (taken from L'vovich, 1979) also includes the groundwater runoff coefficient, K_g, which is equal to the annual groundwater runoff, R_g, as percentage of the annual depth of wetting, W, already expressed by Eq. (6.1).

For a brief explanation of the water balance studies behind the results presented in Tables 4, Part I / Appendix B, consider as an example the case of the Kagera Basin, Table 4_c. A fairly extensive hydrological study of some selected river basins was carried out by WMO (1974) as a component of the hydrometeorological study of the Equatorial Lakes.

The study aimed at determining the runoff from the basin of the Kagera River, which is the principal source of water for Lake Victoria and the Nile River system.. The surface of the Kagera Basin occupies a total area of 58,370 km^2 distributed between Burundi (22.5%), Rwanda (35.0%), Tanzania (34.5%) and Uganda (8.0%). The principal sub-basins of the Kagera are the Nyavarongo (13, 315 km^2) and the Akyanaru (5, 285 km^2), both rivers in Rwanda; the Ruvuvu (12, 300 km^2) in Burundi; and the Middle Kagera (22, 835 km^2), Mwisa (2, 035 km^2) and Ngono (2, 600 km^2) in Tanzania and Uganda. The location of these rivers can be seen from the map in Figure 6.4.

The basic elements of the said study are comprised of the mean monthly and annual rainfall, mean monthly and annual discharge and underground runoff. The number of rain gauges exceeded by far the number of stream gauges as well as the lengths of the record provided by them. Additionally, a certain proportion of the rain gauges were recording automatically, rendering the quality of rainfall data better compared to the quality of runoff data. Six normal years, from 1956-57 to 1961-62, and an exceptionally wet year, 1962-1963, all with concurrent

records, were used in the water balance calculations. Since the relationship between the surface and the underground runoff was not satisfactorily known, it has been assumed that the stream flow during the dry season was approximately equal to the infiltration water stored in the soil during the preceding wet season. The monthly and annual magnitudes of these elements were applied to each of the above-mentioned sub-basins of the Kagera River. It might be of interest to state here that the numerical difference between the rainfall and the runoff was checked against the monthly figures for evapotranspiration given by the Research Station at Rubona, Rwanda. For example, the mean annual rainfall minus runoff for the Akaynaru basin was about 1,000 mm whereas the average estimate for the period 1959-1961 as given by the Rubona Research Station was 1,046 mm. The corresponding mean annual precipitation was 1,203 mm.

6.2.4 Index catchments- Index catchments constituted another component of the Hydrometoerological Survey of the Catchments of Lakes Victoria, Kyoga and Albert (1974). The objective was to provide the necessary data for defining the

Table 6.1- Total, surface and underground runoff and the corresponding runoff coefficients for some African rivers (after L'vovich, 1979)

River	Station / No.	*P, mm*	*W, mm*	R_s	R_g	K_g	R_t	*r*
Niger	Koulikoro / 61	1,550	1,232	318	87	0.07	405	0.26
Nianden	Baro	1,940	1,468	472	170	0.11	642	0.33
Konkoure	Pt.Telimile / 82	2,100	1,169	931	159	0.13	1,090	0.52
Pendjari	Porga	1,026	924	102	12	0.01	114	0.11
Bia	Ayame	1,560	1,341	219	51	0.04	270	0.17
Wouri	Yabassi / 154	2,300	1,663	637	460	0.27	1,097	0.48
Nyong	M'Balmayo / 163	1,480	1,317	163	77	0.06	240	0.16
Lobe	Kribi	2,450	1.075	1,375	362	0.33	1,737	0.71
Lualaba	Bukama	1,250	1.182	68	72	0.06	140	0.11
Lufira	Kapalowe	1,100	1.014	86	113	0.11	199	0.18
Fulakari	Ban-de-Kimpansu / 210	1,460	1, 058	402	195	0.18	597	0.41
Lulua	Highway Br. Chikapa	1,350	1,210	140	171	0.14	311	0.23
Ouham	Bozoum	1,590	1,237	353	194	0.17	547	0.34
Orange	Prieska	503	478	25	7	0.02	32	0.06
Sakrivier	Vastrap	226	215	13	2	0.01	15	0.06
Sambiranu	Ambanja	2,148	1, 261	887	548	0.43	1,435	0.67
Dra	Zaonia-Nurbaz	234	187	47	8	0.04	55	0.24
El-Abid	Ait Ouchene / 26	394	380	14	8	0.02	22	0.06

Explanation

P = areal average annual rainfall, W = areal average depth of soil wetting,

R_s = surface water runoff, Rg = groudwater runoff, R_t = total runoff

Kg = underground coefficient of runoff and r = annual total runoff coefficient

water balance and other pertinent characteristics of certain segments of land catchment area, streamflow and the appropriate elements for estimating evapotranspiration. To achieve this objective seven catchments were considered: 4 in the Lake Victoria Basin, 2 in the Lake Kyoga Basin and 1 index catchment in the Lake Albert Basin. These basins were selected according to a number of criteria, such as location, size, hydrometeorological and physiogeographical features, and availability of certain meteorological and hydrological data. The size of the catchment area put under study varied from a minimum of 100 km^2 to a maximum of 1,161 km^2. The mean annual precipitation, runoff, and runoff coefficient of the index cathchments of the Awach-Kaboun and Ngono are listed in Table 4_c, Part I / Appendix B. The areas under study were the sub-basin of the Upper Ngono, 1,161 km^2 and the Awach-Kaboun, 558 km^2.

The water balance of the Awach-Kaboun for the year 1970 relied on a total rainfall of 1,973 mm and 353 mm total runoff, thus yielding annual runoff coefficient of 17.9%. The monthly balance yielded monthly runoff coefficients of 5,5, 7.0, 6.1, 17.4, 32.9, 39.8, 14.2, 14.2, 23.5, 22.2, 9.3 and 5.4% for months January to December successively. The corresponding coefficients for the year

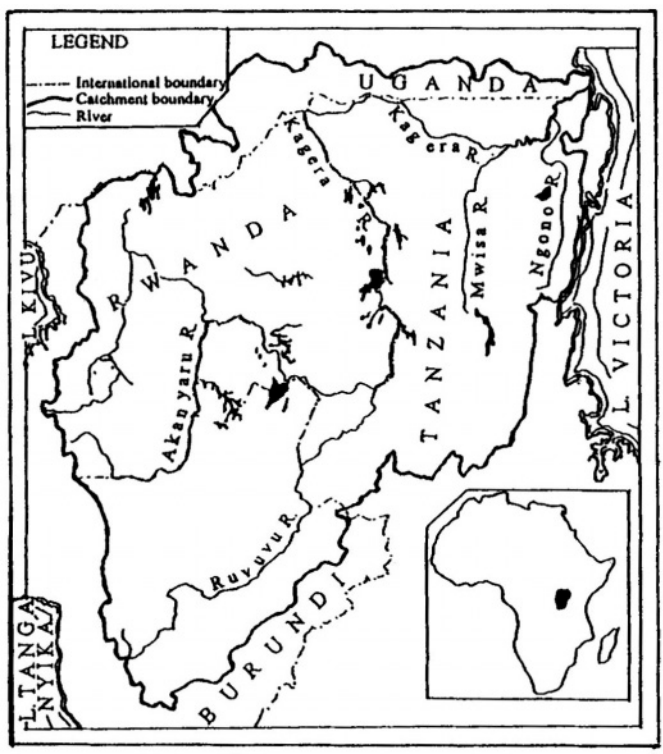

Figure 6.4- Map showing the basin of the Kagera River and its tributaries

1971 were 12.1, 18.7, 7.3, 5.2, 19.3, 26.7, 21.7, 16.2, 16.9, 20.0, 16.4 and 12.1 %. Although the annual coefficient for 1971, 17%, is close to that of 1970, the pattern of the monthly coefficients for 1971 appears to be more uniform compared to the pattern of 1970.

The monthly runoff coefficient for the Upper Ngono was 23, 44, 57, 55, 34, (-), 58, 21, 19, 16, 26 and 21% for January through December, 1970, and 26, 14, 83, 40, 30, (-), 37, 45, 24, 11, 11 and 15% for the same months in their respective order for 1971. The annual coefficients being 33 and 34% for 1970 and 1971 respectively, are too large compared to 18% given as average for the total area of the Ngono Basin (Table 4_c, Part I / Appendix B).

Similar studies were applied to the remaining index catchments. These studies included, in addition to the water balance calculations, frequency and duration curve analyses, construction of unit hydrographs, and supplementing missing data.

6.2.5 Representative basins- ORSTOM (The French Office for Scientific and Technical Research Overseas) was for some decades in charge of extensive hydrological studies in West and Central Africa. A large number of representative or experimental basins have been used in these studies. Rodier (1976a) stated that representative basins offer guide lines for computing (i) the mean annual flow, and in some cases for determining the statistical distribution of the annual flow and (ii) for computing the 10-year flood maximum discharge and volume of flow.

The representative basins, which have been studied, were classified into different categories depending on surface area: less than 100 km^2, from 100 to 1, 000 km^2 and larger than 1, 000 km^2. Those basins were further subdivided depending on climate, soil type and vegetal cover, geology and other physiograhical features. For certain studies the size of the small basins has been standardized to 25 km^2. The annual depth of rainfall, permeability of the soil, slope of the basin floor and density of drainage network were all taken into consideration.

While estimating the annual runoff from each category of basins of the dry tropical regions of West Africa, a type basin was considered. This basin was either ungauged basin or a gauged basin included in the regional network. In the former case, runoff models were applied for the reconstitution of long series of annual runoff from long time series of daily precipitation. Girard (1975) developed a simple model that permits the determination of the runoff depth for a certain flood event from the depth of the corresponding precipitation storm as well as the preceding precipitation storms, all measured at a point close to the center of area of the basin. By summing up the runoffs produced by all individual storms, one can obtain an adequate estimate of the total annual flow. The model that was suggested by Gerard (1975) can be expressed as:

$$R = K_o(P - H_o) \tag{6.2}$$

where P is the depth of rainfall in mm, R is the corresponding runoff in mm, K_o is a runoff coefficient depending on the areal extent of soil wetting, and H_o is a value depending on the soil retention capacity that can be calculated from the expression:

$$H_j = C(P_{j-1} + H_{j-1}) \tag{6.3}$$

In Eq. (6.3), H_j replaces H_o for day j, P_{j-1} is the rain on the previous day, $j-1$, H_{j-1} replaces H_o for day $j-1$ and C is an adjustment parameter varying between 0 and 1, with an average value of about 0.7.

The generated annual runoff depths were used for developing frequency distribution curves of annual runoff from the 100 dry year up to the 100 wet year. An example of the results obtained for a small catchment 25 km^2 in area and median precipitation, P_M, of 300 mm is provided by the following figures (Rodier, 1985):

Category		r_M*	R_M* in mm	Runoff in mm 10-y dry
I	Steep slope,relatively impervious soil	0.285	57	15
II	Intermediate slope, impervious soil (with less than 25% permeable soil)	0.135	27	8
III	mild slope, soils are not very permeable (with 50% permeable soil)	0.05	10	1

*r_M and R_M are the median values of runoff coefficient and runoff depth respectively.

Furthermore, the annual runoff depth, R in mm, and the corresponding runoff coefficient, r, have been estimated for a large number of representative basins for which the annual precipitation P in mm, drainage density, D_d, and global slope index, I_g, runoff coefficient were all known. A few examples of the results thus obtained (Rodier, 1976 b) from the dry tropical (Sahelian) regions in West Africa are given in Table 6.2. The tabulated results show clearly that the runoff and the corresponding runoff coefficient vary from one basin to another depending on the surface area, type of soil and vegetal cover. They also vary for the same basin from year to year depending on the corresponding annual rainfall. However, the estimation method proved to be less efficient with increasing surface of the representative basin.

Once more the characteristics of surface hydrology in arid and semi-arid areas of Africa were reviewed by Rodier (1989). In this review, the rainfall-runoff relationship for small representative basins 25 km^2 in surface area receiving different amounts of annual rainfall was considered. As stated earlier,

Table 6.2- Data about representative basins from < 100 km^2 to >1,000 km^2 surface area and annual preciptation from 690 mm up to 1,075 mm in the Sahelian regions, West africa (Rodier, 1977$_b$)

Basin type	Country	Soil	Area, km^2	D_d	I_g	Year	P, mm	R, mm	r
Godola	Cameroon	Granite	42	5.83	15.3	1968	918	299	0.33
						1969	909	147	0.16
Loure	Burkina Faso	Granite	98	2.06	4.20	1963	925	184	0.20
						1964	895	262	0.29
						1965	843	153	0.18
Taya	Chad	Granite	167	3.30	4.30	1964	875	92	0.11
Ouagadougou I	Burkina Faso	Granite/ magmitite	294	0.56	3.04	1961	835	58	0.07
							850	97.8	0.11
							680	13.4	0.02
Network stations									
Tsanaga a Maroua	Cameroon		845			1954	935	273	0.29
						1966	856	196	0.23
						1967	885	246	0.28
						1968	885	246	0,28
						1969	1,075	219	0.20
						1970	854	204	0.24
Guera-Chad	Chad		1, 200	3.20	3.40	1963	690	8.7	0.01
						1964	995	92.9	0.09
						1965	716	8,1	0.01
						1966	723	14.1	0.02

Explanation

P = annual precipitation, R = annual runoff, D_d = drainage density, I_g = global index of slope and r = runoff coefficient

next to rainfall, permeability and slope appeared to be the most effective parameters. Typical graphs have been developed for the Sahel zone. An example of such graphs is shown in Figure 6.5 (Rodier, 1989).

Bullock & Gustard (1989) upon investigating runoff characteristics in southern Africa stated that the regionalization techniques are generally poorly developed in the arid and semi-arid regions of Africa compared with temperate regions. An analysis of runoff data from 49 catchments in central Zimbabwe has indicated a strong effect of the soil type on the shape of the standardized flow (discharge expressed as percentage of average discharge) duration curve. The available major soil types were regrouped in five classes according to their annual rainfall acceptance potential (ARAP). These are very high, high, moderate, low, and very low. The runoff potential of a certain group varies inversely with it's ARAP, i.e. high ARAP corresponds to low runoff potential and very low ARAP corresponds to very high runoff potential.

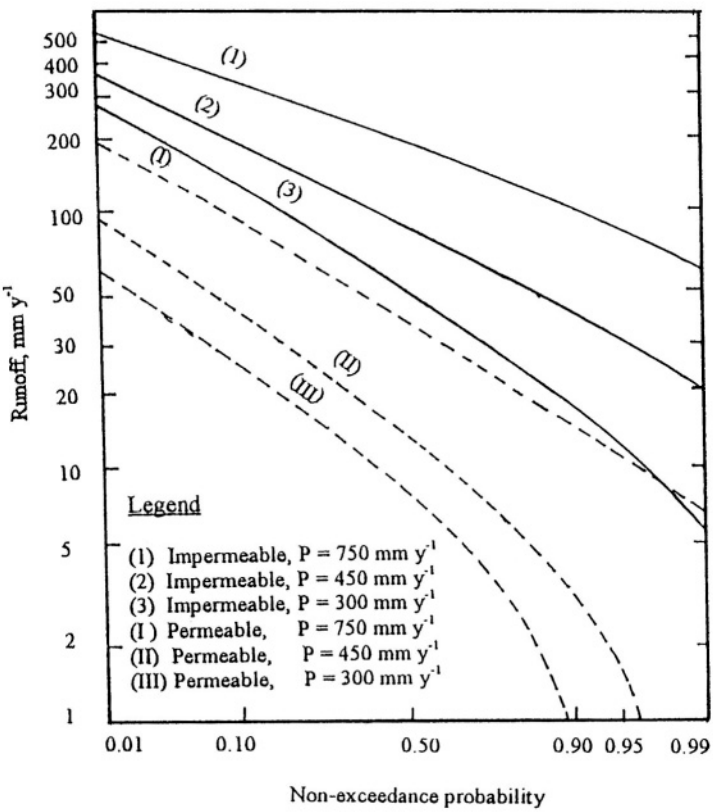

Figure 6.5- Probability of non-exceedance of a certain annual runoff depth given the states of soil permeability and annual rainfall depth (from Rodier, 1989)

Mean annual rainfall and mean annual runoff data were assembled from 171 catchments located in four countries: Zimbabwe (108), Malawi (38), Lesotho (14) and Botswana (11). The regional rainfall-runoff relationship developed using the data from these 171 catchments is presented in Figure 6.6. Preliminary estimates of mean annual runoff (R_{ma} in mm) may be derived at any ungauged site from given values of the mean annual rainfall (P_{ma} in mm) using the following regression equation calibrated from the data in Figure 6.6:

$$R_{ma} = -104.7 + 0.151P_{ma} + 0.00019(P_{ma})^2 \qquad (6.4)$$

with determination coefficient and standard error of estimate of 0.769 and 71.6 respectively.

The R_{ma}, in mm, estimated by Eq. (6.4) can be converted to average daily flow in $m^3 s^{-1}$ by multiplying it by the catchment area in km^2 divided by 31, 320. Reference to the appropriate standardized flow duration curve enables the estimation of flows with a specified exceedance probability.

6.2.6 Preliminary estimate of flood flow for a given return period- It has already been mentioned in subsection 6.2.5 that regional runoff estimates obtained from representative basins can provide guide lines for computing the 10-year flood maximum discharge and volume for small water courses (Rodier, 1976 a).

The rainfall-runoff model developed by Girard (1975) enable estimation of runoff depth for each individual flood from the depth of each rainstorm. The model equations are already given in the previous subsection. This model was tested on several representative basins in Tropical Africa west of Congo. The basin of Kadiel in Mauritania is one of those basins. With this model, it became possible to reconstruct a series of around forty values of the annual runoff, *R,* through which the parameters of the distribution function can be estimated.

As the Kadiel basin is sufficiently impermeable, it has contributed to the successful application of the model, rendering the estimated runoff values to be fairly realistic.

For basins where conditions are less favourable than those of Kadiel, the parameters of the rainfall-runoff model have been determined in terms of the physiographic characteristics of the basin and its rainfall regime. Next to rainfall, permeability and slope appear to be the most effective parameters. Where estimation of high flows is concerned, the 1 in 10-year frequency is often taken into consideration for small drainage basins. In view of the relationship between the flood flows and the surface runoff for the very high frequencies in the tropical zones, the unit hydrograph method can be easily applied. It is also possible to predetermine the runoff coefficient from the characteristics of the storm generating the flood flow.

Nearly the same approach has been used by ORSTOM for estimating the 10-year flood and its characteristics using small representative tropical forest bains.

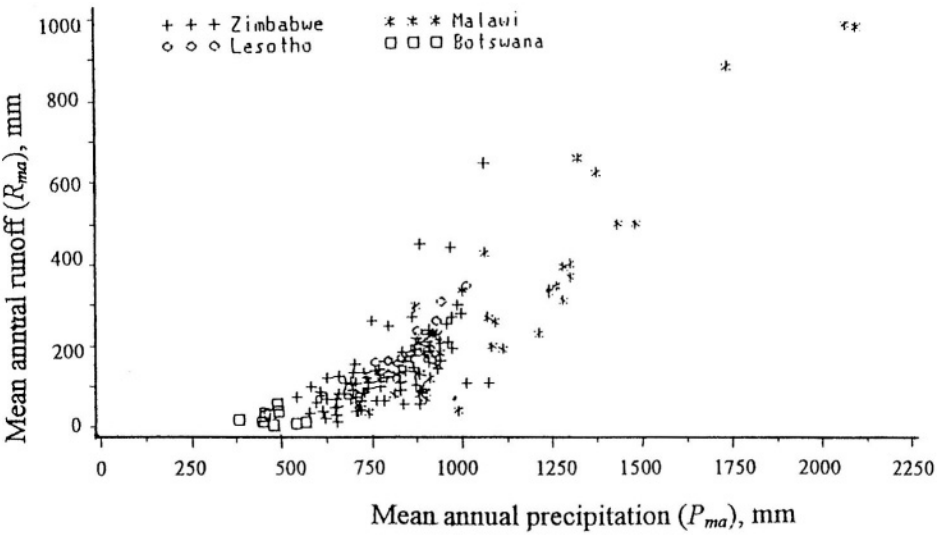

Figure 6.6- Provisional mean annual rainfall / runoff relationship for southern Africa (taken from Bullock & Gustard, 1989)

Rodier (1976 c) stated that the data collected by ORSTOM in the period 1956-1976 on 27 tropical forest basins have been processed using the same daily precipitation of 120 mm so as to obtain the maximum 10-year flood discharge. The flood hydrograph is assumed to be triangular in shape with a time to peak, T_b, base width, T_b, reduction factor, f, to convert the point rainfall to areal rainfall, annual depth and volume of rainfall, P in mm, and V_P, respectively, maximum discharge of 10-year flood hydrograph, $(Q_p)_{10}$, and M is the mean ordinate of the hydrograph.

The calculation procedure, assuming that the surface runoff coefficient, r_s, and the ratio $(Q_P)_{10} / M$ are given or known, is as follows:

- From the surface area of the catchment, A, and the global index of catchment slope, I_g, the base width, T_b, of the hydrograph is obtained.
- The volume of rainfall, V_P in m^3, is simply the point depth of rainstorm generating the 10-year flood, P_{10} in mm, reduced by the factor, f, times the catchment area, A in km^2, divided by 1, 000. The ordinate M is simply the volume V_P in m^3 multiplied by the surface runoff coefficient, r_s, divided by T_b in hours times 3, 600.
- The 10-year flood peak runoff, $(Q_p)_{10}$, is determined by multiplying the value M already obtained by the so-called coefficient of Graveluis, C, which is a function of I_g and the soil type.
- One should add to $(Q_p)_{10}$ already obtained in the previous step a certain discharge for the base flow, Q_b in $m^3 s^{-1}$, to the value $(Q_p)_{10}$ already obtained to get the total maximum 10-year flood discharge. Q_b is a function of the soil permeability and extent of surface area of the catchment in question.

Numerical example- The following data are given for a small catchment: $A = 8$ km^2, mean annual precipitation $P_{ma} = 1800$ mm, rainstorm generating 10-year flood $(P)_{10} = 140$ mm, precipitation reduction coefficient $f = 0.92$, coefficient of surface runoff $r_s = 0.08$, time to peak $T_p = 2.80$ h, base width $T_b = 8.75$ h, Graveluis coefficient $C = 2.2$ and base flow $Q_b = 0.40$ m^3 s^{-1}.
Solution- The 10-year surface runoff depth = 140 * 0.92 * 0.08 = 10.3 mm
Mean runoff, $M = 0.0103 * 8 * 106 / (8.75 * 3,600) = 2.62$ m^3 s^{-1}
Peak surface runoff ordinate, $(Q_p)_{10} = 2.2 * 2.62 = 5.67$ m^3 s^{-1}
Actual observations have shown that this method of calculation overestimates the ordinate $(Q_p)_{10}$ by about 15%. As such, the adjusted ordinate can be taken as $5.76 * 0.85 = 5.00$ m^3 s^{-1}. When a base flow of 0.40 m^3 s^{-1} is added to this amount, the total 10-year maximum flood rate becomes 5.40 m^3 s^{-1}.

The above procedure shows clearly that unless previous knowledge of calculation parameters such as the time to peak, base width and Graveluis coefficient is available or assumptions about them are made, the estimation of flood discharge will hardly be possible.

The selected river basins within the catchments of the Equatorial Lakes are different from the representative basins in West Africa in that they are all gauged. In the case of the selected basins, e.g. the Kagera River basin and it's sub-basins described earlier the procedure used is as follows:
- The period from 1940 up to 1971 was considered. This period was regarded as reasonably adequate for the purpose of frequency analysis. The conventional procedure has been followed:
- The daily maximum and minimum discharges for each year and so the maximum and minimum monthly discharges at certain stream gauging sites were assembled used in the analysis
- The distributions of Gumbel, Fuller and Frechet were used for the probabilities of occurrence of certain discharges. The latter distribution, i.e. the distribution function of Frechet proved to give the best fit to the plotted data.
- The best-fitting probability distribution function has been used for estimating the low-flows as well as the high-flows at the specified sites.

Probabilities of exceedance of certain discharges of the Kagera River in m^3 s^{-1} at Kayaka Ferry were found to be as follows (WMO, 1974):

Probability of exceedance, %	Annual flow	Daily discharge maximum	Daily discharge minimum	Mean monthly discharge maximum	Mean monthly discharge minimum
2	418	600	248	590	264
5	358	515	220	505	236
10	311	440	198	430	213
20	265	360	175	350	190

Probability of exceedance, %	Annual flow	Daily discharge maximum	Daily discharge minimum	Mean monthly discharge maximum	Mean monthly discharge minimum
50	233	320	160	310	172
80	138	160	117	152	125
90	116	127	106	120	115
95	97	105	95	100	103

A different methodology for estimating flood discharge using river channel dimensions has been recently reported. This estimation method relies on the development of relations between flood discharges, measured at gauging stations, and channel dimensions measured from natural river reaches in the vicinity of the gauge. Channel-geometry equations enable flood discharges to be estimated at ungauged locations on natural streams from measurements of channel size and by combining the index flood estimate (usually the mean annual flood) with regional flood growth factors (Wharton and Tomlinson, 1999).

The mean annual flood (MAF), Q, can be related to the channel geometry by the power equations:

$$Q = gW^h \tag{6.5}$$

and

$$Q = iA^n \tag{6.6}$$

where W and A are the channel width and cross sectional area of the channel respectively, measured at a specified reference level, and the multipliers g and i are the antilogarithms of the regression constants and the power terms (h and n) are the regression coefficients. Eqs. (6.4) and (6.5) were applied to channel conditions in Ghana, Burundi and Tanzania, and the results obtained are:

Ghana

$MAF = 1.83Wb^{1.47}$	$R^2 = 0.71$	n=12
$MAF = 1.55AREA^{0.58}$	0.76	12

Burundi

$MAF = 4.23Wb^{0.96}$	0.94	8
$MAF = 3.00AREA^{0.47}$	0.85	8

Tanzania

$$MAF = 2.14 Wb^{1.29} \qquad 0.87 \qquad 8 \qquad (6.7)$$

$$MAF = 3.29 AREA^{0.38} \qquad 0.62 \qquad 8$$

where Wb = active channel baneful width in m, $AREA$ = catchment area in km^2 and R^2 = coefficient of determination. MAF is expressed in $m^3 s^{-1}$. Eq. (6.6) shows that the power of Wb, i.e. h, varies for Ghana, Burundi and Tanzania from slightly less than 1.0 to about 1.5, whereas the power of $AREA$, i.e. n, is less than unity for the three studied countries. The correlation between MAF and Wb is stronger compared to the relation between MAF and $AREA$, except for Ghana.

The regional flood growth factors used in flood studies of the three countries are as follows:

Country	Growth factor (Q_T/ MAF) for a given return period, T, years					
	(mean)	2.0	10	20	50	100
Ghana	(1.00)	0.94	1.70	2.00	2.30	2.60
Burundi	(1.00)	0.95	1.50	-	-	2.10
Tanzania	(1.00)	0.82	1.89	2.40	3.13	3.70

These results show that the channel-geometry equations, when combined with the regional flood growth factors, can be employed as a basis for further hydrological studies in Ghana, Burundi and Tanzania. They also show how the channel dimensions might be employed to estimate flood frequency characteristics in similar situations when stream gauging stations are sparse and flow records are short.

6.3- Streamflow

In section 6.2, a number of studies and regional or country experiences about measurement and estimation of runoff depth and runoff coefficient along with the factors effecting their respective values under different physiographic, soil and climate conditions have been reviewed. While doing so, sometimes the surface runoff and the underground runoff were dealt with separately and other times both runoffs were dealt with combined as total runoff or simply runoff.

In this section as well as the forthcoming sections, no distinction will be made whether the flow is due to surface, underground or total runoff.

Streamflow or river flow is simply open channel flow where water level or stage and discharge are the items of primary interest. River channels are mostly natural though for some rivers certain reaches may be canalized. The stage-discharge relationship is important for computing any of them when the value of

the other variable is known. This relationship is often given as a mathematical expression referred to as the rating function. It is called rating table or curve depending on whether concurrent values of stage and discharge are given in a tabular or a graphical form.

Tables 9$_a$, 9$_b$, 9$_c$, 9$_d$, and 9$_e$, Part I/Appendix B, are examples of the rating table for Victoria Nile, White Nile, Congo River, Baro River, and Benue River, respectively. The rating curve and the confidence interval (95% probability) of the estimated discharges of the Congo River at Kinshasa-Kalina using the stage-discharge measurements of the period from 1955-1961 are shown in Figure 6.7 (Bultot & Dupriez, 1989). According to Demarée (1987) the rating functions can be expressed as:

$$(Q)_{est} = 0.377H^2 + 5.898H + 24.181 \qquad \text{for } H \leq 3.35 \qquad (6.8)$$

and

$$(Q)_{est} = 1.224H^2 + 0.224H + 33.683 \qquad \text{for } H > 3.35 \qquad (6.9)$$

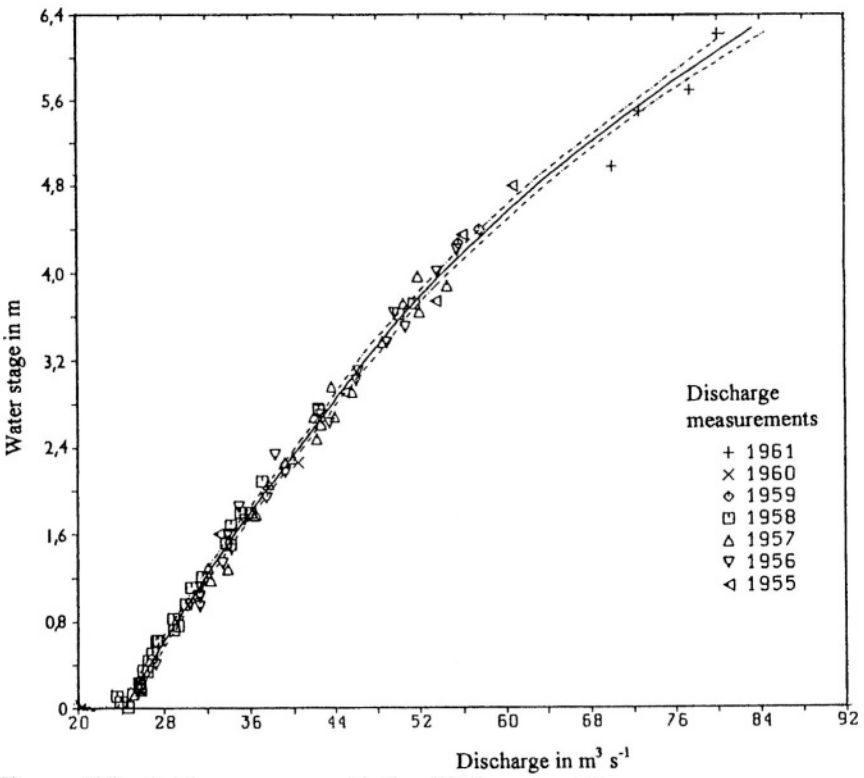

Figure 6.7- Rating curve and the 95% probability confidence interval (from Bultot & Dupriez, 1989)

Other than the parabolic equations (6.7) and (6,8), suggested for the Congo River, logarithmic functions are used at large for a wide majority of rivers all over the world.

6.3.1 Streamflow data- A relatively large number of stream-gauging stations have been employed for the purpose of this book. Table 5, Part I / Appendix B, gives the name, coordinates, country and catchment area served by each one of the 278 gauging stations referred to in a rather recent UNESCO document (1995). These stations are also located on the map of Africa in Figure 6.8.

Tables 6a, Part I / Appendix B, gives for each of the mentioned 278 stations the period of discharge record, and the mean and coefficient of variation of the annual discharge. With the exception of a few rivers, the uninterrupted length of record for many African rivers is limited to a few number of years. Tables $6b_1$, $6b_2$, $6b_3$, $6b_4$, $6b_5$, $6b_6$, and $6b_7$ are examples of moderate to long annual discharge series. These tables include the annual discharges of the Nile at Aswan (114-y), Nile tributaries in Sudan (73-y), the Niger at Niamey (50-y), Senegal at Bakel (81-y), Obangui at Bangui (55-y), Congo at Kinshasa (81-y) respectively.

Part I / Appendix B includes, in addition to the Tables already mentioned above, Tables 7 and 8. The former lists the maximum and minimum means of the annual flows at those measuring stations with length of record not less than 18 years. Table 8, on the other hand, gives mean monthly and annual discharges of selected rivers. It should be clearly stated here that the largest amount of raw data contained in these Tables have been drawn from the UNESCO reports on Discharge of selected rivers of the world (1971, 1995) and Global river discharge database (Vol. 1: Africa).

6.3.2 Patterns of mean monthly discharges- The ratio of the mean discharge of the month of (most frequently) high-flow to the mean discharge of the month of (most frequently) low-flow at a number of gauging stations is given in Table 6.3. This ratio will be referred to as the index of seasonality, $(In)_s$, of a river at a certain station. A reliable knowledge of the magnitude of this index is essential for the proper management of natural water supply of any river, particularly when storage works are thought of as an adequate measure.

Values of the index $(In)_s$ have been divided into a number of groups to each of which a rank has been assigned. Ranks I, II, III, IV, V and VI are given arbitrarily to $(In)_s$ ranges of 1-2, 2-5, 5-10, 10-20, 20-100 and > 100. Rank no. VII is kept to non-perennial streams that undergo a dry season causing the index $(In)_s$ to rise to ∞. Obviously, the months of (most frequently) high-flow and (most frequently) low-flow vary from location to location depending on the climate, especially the occurrence of rainfall topography and soil moisture conditions. Examples of the six types of the mean monthly discharge pattern are shown in Figures 6.9.

The results presented in Table 6.3 show that stations located around the Equator, except when the river supply is heavily regulated, score ranks I and II. All stations on the Nile downstream Aswan are an example of gauging sites on a strongly regulated river. On the other hand, the stations situated in regions nearly halfway the Equator and the two Tropics belong to ranks V and VI, where the seasonality index is quite high. The remaining stations, which make ranks III and IV, do not really show any specific characteristic associated with the geographic location, instead they are randomly dispersed everywhere.

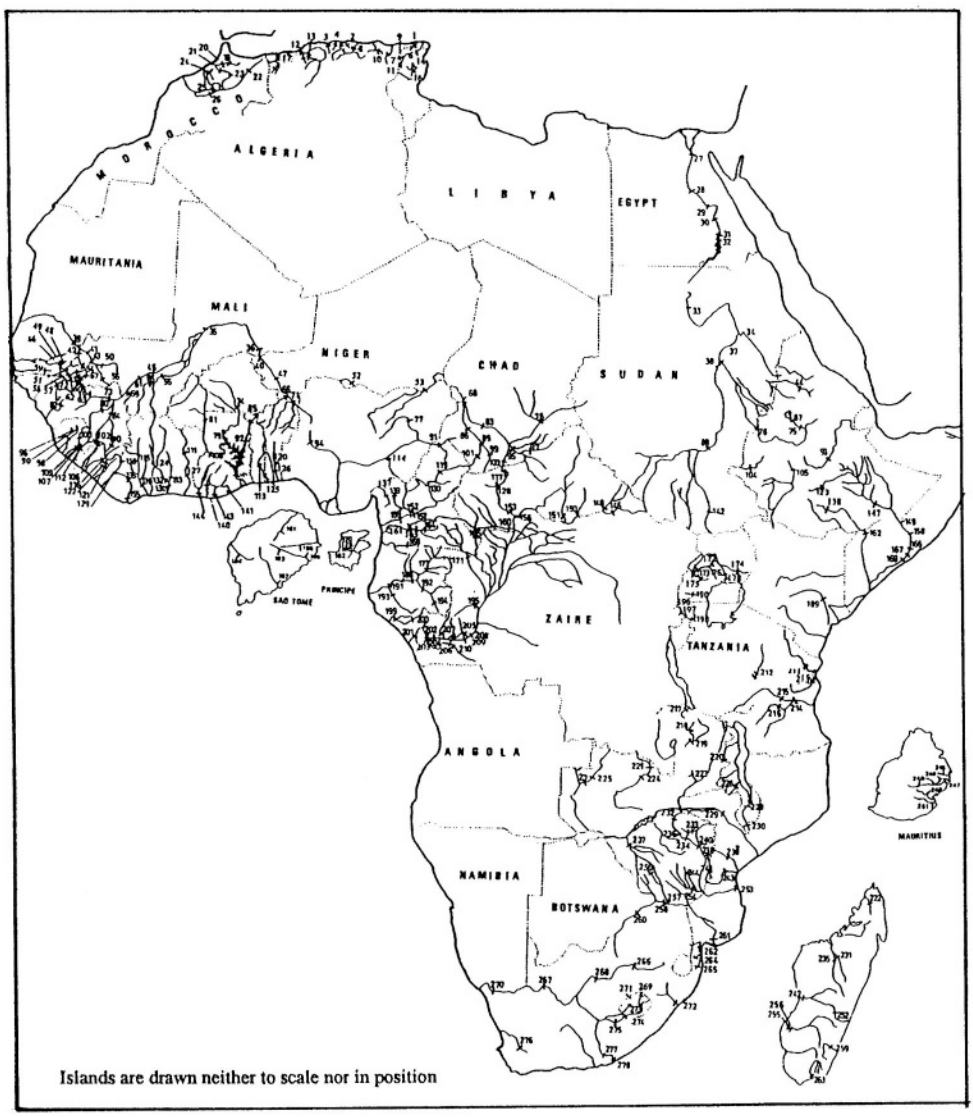

Figure 6.8- Map of Africa showing the locations of stream gauging stations

Table 6.3- Q_{mx}, Q_{mn} and seasonality index, $(In)_s$ for 90 stream gauging stations scattered over Africa

Station No.	Q_{mx}, $m^3 s^{-1}$	Q_{mn} $m^3 s^{-1}$	$(In)_s$	Rank	Station No.	Q_{mx}, $m^3 s^{-1}$	Q_{mn}, $m^3 s^{-1}$	$(In)_s$	Rank
19	159.4	2.5	63.6	V	159	5357	529	10.1	IV
20	234.9	2.5	94	V	160	500	231	2.2	II
21	113.1	23.1	4.8	II	163	347.5	51.5	6.8	III
22	40.7	3.9	10.4	IV	164	132.2	26.6	5	II
23	36.2	7.3	5	II	165	1805	373.6	4.8	II
25	59.7	15.4	3.9	II	168	594.2	90.6	6.6	III
27	1756	1072	1.6	I	171	3230	875.9	3.7	II
28	1616	1050	1.5	I	178	1245	1118	1.1	I
29	2150	1315	1.6	I	186	2.5	0.6	4.2	II
30	2345	1400	1.7	I	189	364.6	68.8	5.3	III
31	2597	1487	1.8	I	191	7619	1930	4	II
33	7867	829	9.5	III	195	230.6	195.2	1.2	I
35	2147	71.7	29.9	V	196	139.4	54.7	2.5	II
39	3138	5.2	603	VI	197	189.5	67.8	2.8	II
41	1033	3.9	265	VI	198	324.4	160.8	2	II
42	807.4	0.7	1153	VI	200	302.2	58.6	5.2	III
43	2473	7.2	344	VI	201	1326	309	4.3	II
47	1578	77	20.5	V	202	595.3	133.4	4.5	II
49	552.3	1.9	291	VI	203	48.9	11.1	4.4	II
52	34.7	0.01	347	VI	204	497.1	109.1	4.6	II
55	1814	20.4	88.9	V	207	272.6	46.7	5.8	III
58	591.2	0.1	5912	VI	209	56081	31087	1.8	I
59	11.3	0.1	113	VI	210	94.1	8.9	10.6	IV
60	411.6	0.3	1372	VI	220	8.1	0.1	81	V
61	5174	61.2	84.5	V	228	580.6	363	1.6	I
63	40.8	0.01	4080	VI	230	687	299.6	2.3	II
64	280.6	0.2	1403	VI	232	92	4.6	20	IV
68	2953	148.7	19.9	IV	233	38.5	0.2	193	VI
84	586.3	13.5	43.4	V	234	29.8	1	29.8	V
88	1288	585.3	2.2	II	235	1077	121.7	8.9	III
91	1820	2.2	827	VI	236	14.6	0.1	146	VI
95	925.8	43.8	21.1	V	237	59.3	0.1	593	VI
119	86.6	6.7	12.9	IV	238	2.5	0.2	12.5	IV
130	1063	130.7	8.1	III	240	213.3	2.8	78.2	V
131	3833	267.6	14.3	IV	244	5.6	0.01	560	VI
137	1498	62.2	24.1	V	250	4.1	0.3	13.7	IV
139	222	30.7	7.2	III	255	1621	93.3	17.4	IV
142	1258	863	1.5	I	259	691.7	122.9	5.6	III

Table 6.3- Cont'd

Station No.	Q_{mx}, $m^3 s^{-1}$	Q_{mn}, $m^3 s^{-1}$	$(ln)_s$	Rank	Station No.	Q_{mx}, $m^3 s^{-1}$	Q_{mn}, $m^3 s^{-1}$	$(ln)_s$	Rank
143	388	40.1	9.7	III	267	521.7	112,4	4.6	II
144	306.9	48.9	6.3	III	269	1.8	0.1	18	IV
145	161.7	12.5	12.9	IV	270	319.8	73.2	4.4	II
152	1918	132.6	14.5	IV	271	41	2.5	16.4	IV
154	809.4	66.6	12.2	IV	273	2.2	0.3	7.3	III
156	9542	1004	9.5	III	274	270.6	20.2	13.4	IV
157	2794	339.8	8.2	III	275	364.1	28.4	12.8	IV

6.3.3 Annual extreme discharges- Annual extreme discharges refer to the annual maximum and annual minimum discharges. As such, the series dealt with in this sub-section are simply annual series. To each series the distribution function of best fit is used for estimating flood, and drought discharges that correspond to return periods beyond the available length of record.

According to Balek (1977), only a few rivers in Africa have been observed for at least fifty years, and the numerous gaps in the records make it difficult to analyze the sequences of extremes properly for the needs of engineering designers. By the time of preparing this book, the situation has improved in just a few areas but not everywhere in Africa. As such, the analysis of extreme values has been limited to stations having a period of record of at least 24 uninterrupted years. The calculated discharges are presented in Table 6.4 includes the calculated discharges for return periods in the range from 1.053 to 100 years. Next to the tabulated results, four frequency distributions of the maxima discharges and one of the minima discharges are shown graphically. **Figure 6.10$_a$** through **6.10$_d$** show the maxima discharges of the Congo River, 1903-1983, at Kinshasa (Butlot & Dupriez, 1987), the Blue Nile, 1902-1992, at Khartoum (Sutcliffe & Parks, 1999), the Senegal River, 1904-1973, at Bakel and the Chari, 1933-1973, at N'Djamena (Roche et al., 1976). **Figure 6.10$_e$** represents the minima discharges of the Chari, 1933-1973, at N'djamena (Roche et al., 1976).

For design purposes, it is often, though not necessary, to consider the maximum discharge that is exceeded once in hundred years or more when flood control and protection works have to be constructed. On the other hand, when minimum flows are of interest, the least discharge that is not exceeded, on the average, in 100 years say is the design value. Discharge values corresponding to return periods longer than 100 years can be estimated using the same distribution functions, which proved to best fit the observed data. This technique is recommended only when ever the historical record is sufficiently long. According to Yevjevich (1972) the return period for which a value is estimated should not exceed two or three times the used length of record.

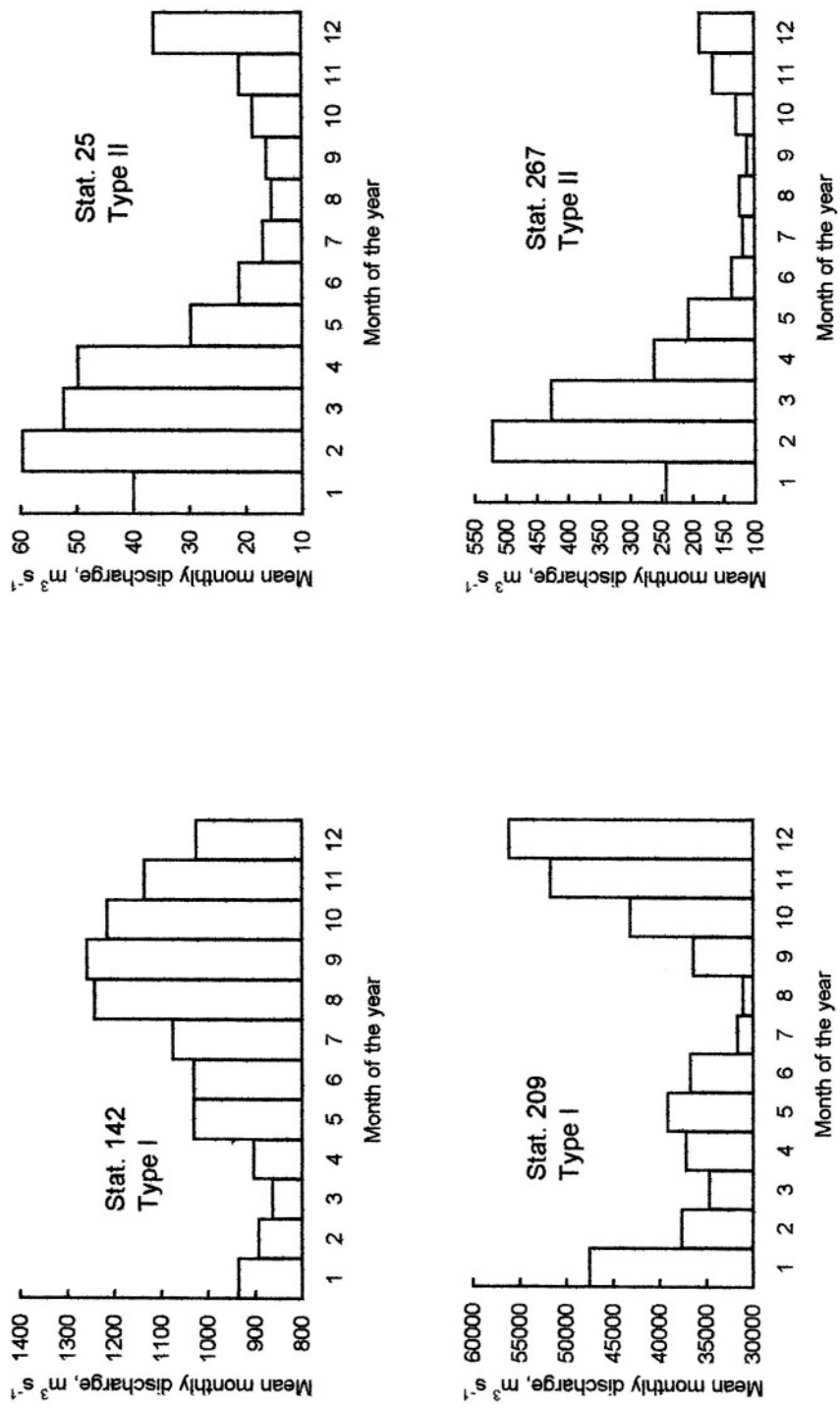

Figure 6.9- Types I and II of mean monthly discharge pattern

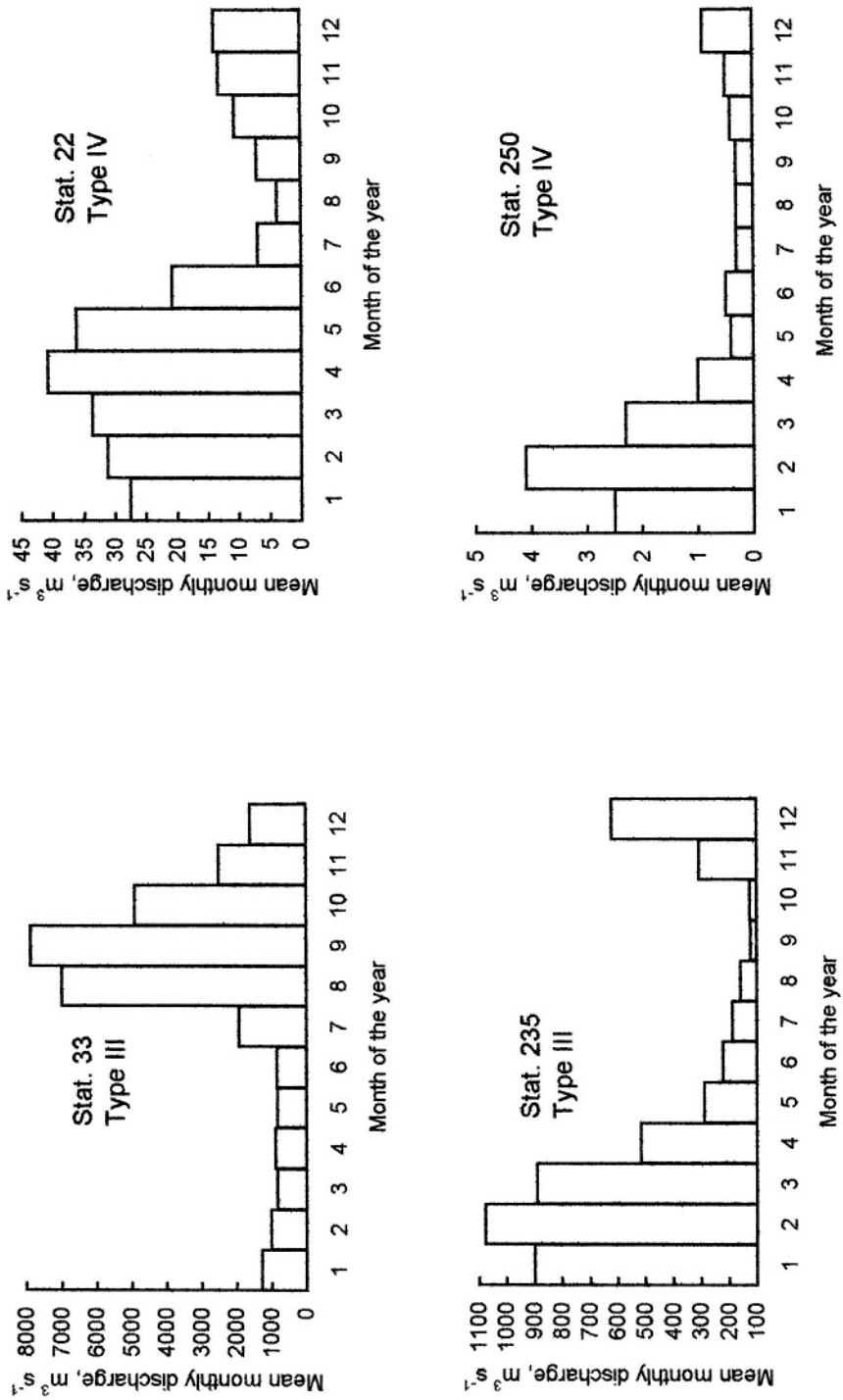

Figure 6.9 Cont'd- Types III and IV of mean monthly discharge pattern

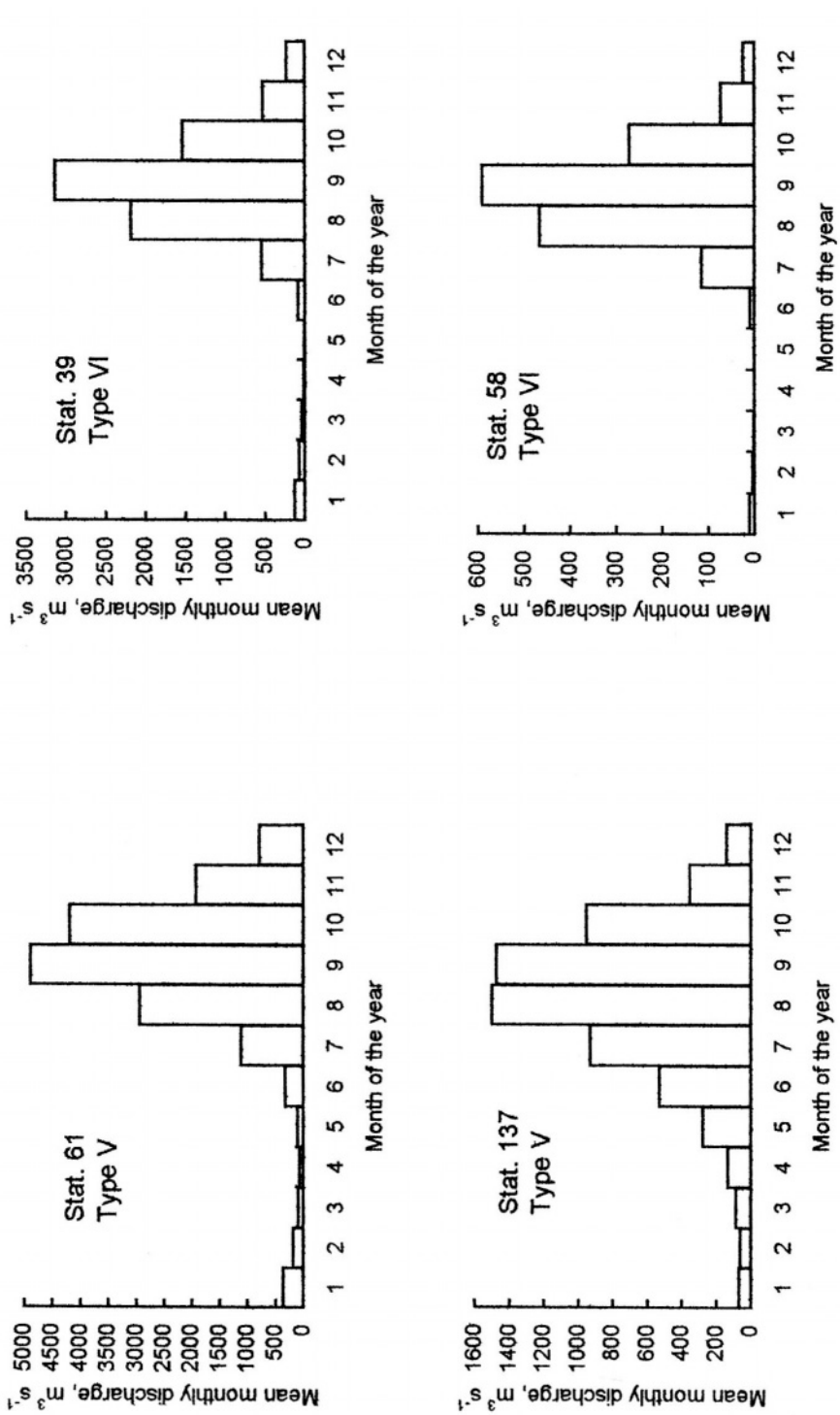

Figure 6.9 Cont'd- Types V and VI of mean monthly discharge pattern

Table 6.4- Estimated annual maxima and minima discharges for some return periods using frequency distribution functions of best fit to the observed data

Station No.	River	Length of record, y	Distribution function	Q_{mx} / Q_{mn} for return periods in years								
				1. 053	1.11	1.25	2	5	10	20	50	100
Annual flood discharges												
39	Senegal	80	Pearson III	1,733	2,119	2,941	4,365	5,960	6,865	7,648	8,571	9,210
61	Niger	73	Pearson III	4,308	4,641	5,098	6,061	7,171	7,812	8,374	9,042	9,509
91	Benoue	40	Normal	1,257	1,642	2,108	3,000	3,892	4,358	4,743	5,177	5,465
125	Mono	40	Pearson III	260	373	496	693	844	906	939	979	997
126	Oueme	28	Pearson III	254	424	612	913	1,149	1,249	1,312	1,398	1,428
145	Nkam	26	Pearson III	177	202	231	277	312	327	337	348	353
152	Mbam	25	Pearson III	7,770	1,820	2,050	2,451	2,804	2,971	3,100	3,235	3,319
154	Wouri	26	Pearson III	901	1,053	1,220	1,492	1,704	1,793	1,859	1,919	1,954
156	Oubangui	56	Normal	6,750	7,460	8,310	9,950	11,590	12,450	13,150	13,950	14,480
157	Sanaga	29	Pearson III	2,593	2,735	2,916	3,290	3,702	3,934	4,142	4,368	4,530
159	Sanaga	29	Pearson III	5,132	5,452	5,846	6,548	7,185	7,503	7,770	8,034	8,214
163	Nyong	29	Pearson III	305	316	333	375	434	472	507	551	583
168	Ntem	27	Gumbel E V I	537	577	631	757	927	1,040	1,148	1,289	1,393
171	Sangha	36	Normal	2,889	3,083	3,319	3,770	4,221	4,456	4,650	4,869	5,015
212	Bubu	24	Pearson III	11.3	22.9	35.9	58.2	76.9	85.4	92.2	98.3	102.2
Annual minimum discharges												
61	Niger	73	E V III	97.6	80.6	62.5	36.3	20.4	15.8	13.2	11.7	11.2
131	Volta	32	E V III	55.4	40.5	26.4	11.3	8	x	x	x	x
145	Nkam	25	E V III	14.8	14.1	13.1	10.8	7.6	5.4	3.3	0.2	0
156	Oubangui	55	E V III	1315	1181	1023	735	483	374	296	212	195
189	Tana	42	E V III	76	61.8	44.9	30.5	22.5	22.8	20.3	19.9	19.7

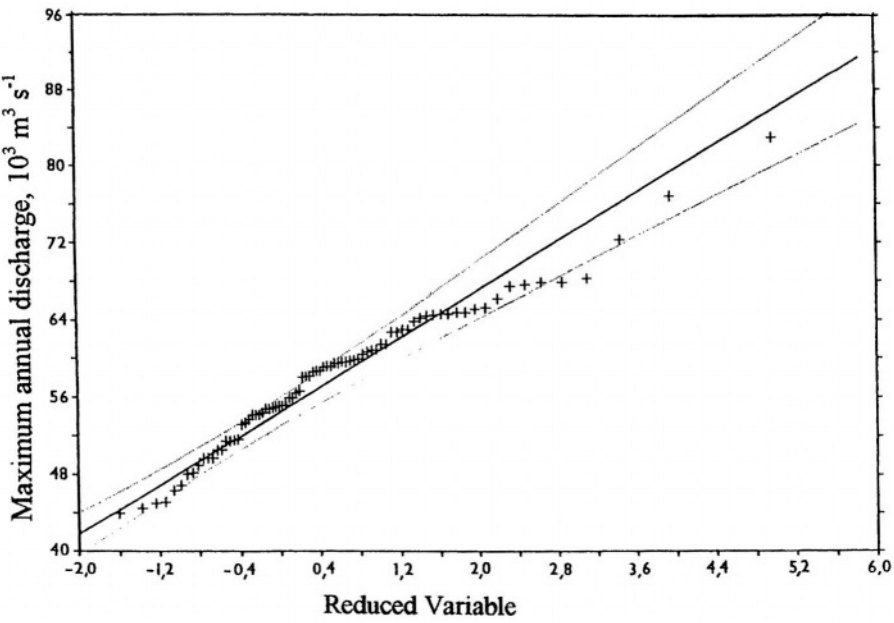

Figure 6.10$_a$- Frequency distribution and 95% confidence limits of the maxima discharges of the Congo, 1903-1983, at Kinshasa (Butlot & Dupriez, 1987)

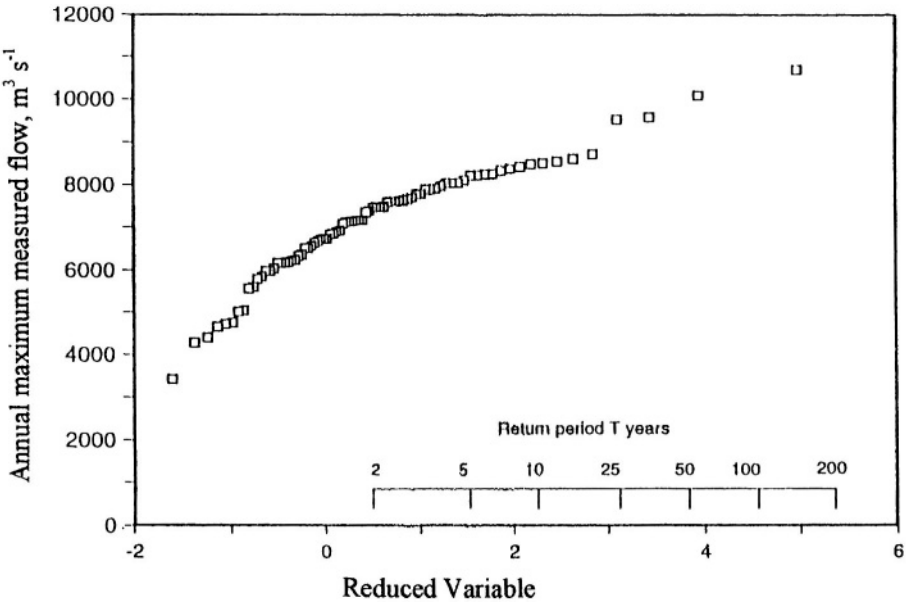

Figure 6.10$_b$- Frequency distribution of maxima discharges of the Blue Nile, 1902-1992, at Khartoum (Sutcliffe & Parks, 1999)

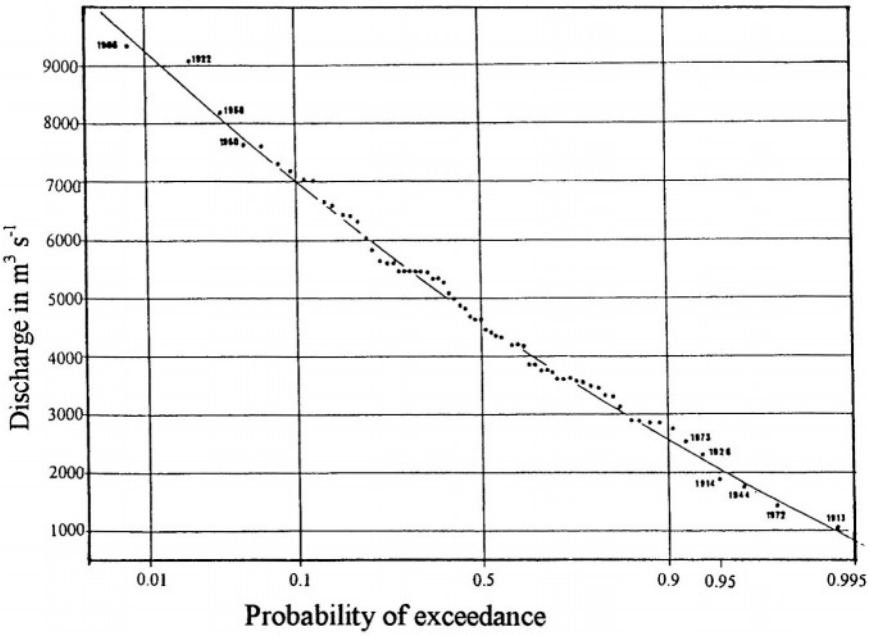

Figure 6.10$_c$- Frequency distribution of the maxima discharges of the River Senegal, 1904-1973, at Bakel (Roche et al., 1976)

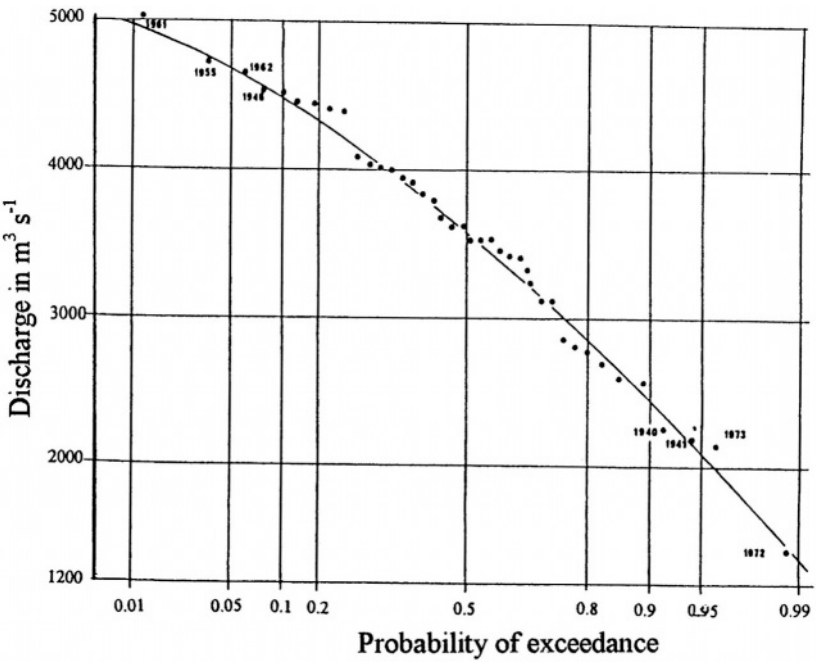

Figure 6.10$_d$- Frequency distribution of the maxima discharges of the River Chari, 1933-1973, at N'Djamena (Roche et al., 1976)

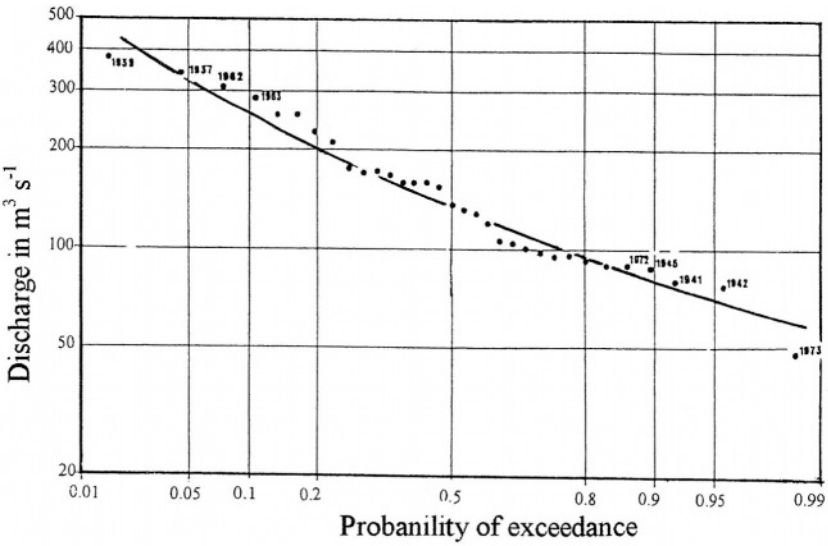

Figure 6.10$_e$- Frequency distribution of the minima discharges of River Chari, 1933-1973, at N'Djamena (Roche et al., 1976)

Balek (1977) summarized the work of Pitman and Midgley on flood discharges in South Africa. In that work the country was divided into seven regions.

1- High rainfall areas, mountainous with a high proportion of exposed rocks and covered with sclerophyllous vegetation.
2- Interior plateau, relatively high rainfall, with early summer thunderstorm belt, grassveld fairly dense drainage pattern, parts suffering from soil erosion.
3- Year-round rainfall, dense drainage pattern, high-proportion of exposed rocks or advanced soil erosion.
4- Eastern coastal strip, high rainfall, dense drainage pattern, generally well vegetated.
5- Sub-humid to semi-arid interior plateau, rains generally late summer.
6- Well-forested bushveld areas, low-rainfall well forested.
7- Arid interior and wet coast, sparse vegetation, low-drainage density.

The ratios of flood peak discharges, $(Q_{fp})_T$, given certain return periods, T, to the Mean annual flood peak discharge, $(Q_{fp})_{ma}$, are as given below:

Region	$(Q_{fp})_T / (Q_{fp})_{ma}$ for T in years				
	5	10	20	50	100
1	1.54	2.08	2.67	3.54	4.28
2	1.70	2.43	3.25	4.48	5.54
3	2.00	3.14	4.51	6.68	8.60

Region	$(Q_{fp})_T / (Q_{fp})_{ma}$ for T in years				
	5	10	20	50	100
4	1.97	3.02	4.24	6.13	7.78
5/7	2.04	3.22	4.58	6.82	8.78
6	2.46	4.40	6.82	10.75	14.26

The mean annual flood peak discharge, as related to the catchment area was analyzed for some East African catchments by Kovács (cited in Balek, 1977).
A flood analysis of Kenyan, Malawian and Nigerian rivers was carried out by Starmans. Figure 6.11 shows the relationship between the peak flood discharge and the catchment area of these rivers (cited in Balek, 1977).

Annual minimum discharges of perennial rivers can be analyzed statistically in a manner similar to the peak flood discharges. An example of this is already shown in **Figure 6.10**$_e$ for the River Chari in Chad. A similar example can be found in Balek (1977) for the River Obangui, in the Central African Republic.

The lowest discharge in the period, 1935-1968 (28 years), used in the analysis analysis was **344 m^3 s^{-1}**. This figure is somewhat less than the figure of about **395 m^3 s^{-1}**, the 1% minimum, which was calculated using the Pearson III distribution function.

6.3.4 Interannual variability of river flow and analyses of annual flow series- River flow exercises interannual variation depending essentially on the climate condition. Hydrologic records show that annual flows can be arbitrarily divided into years of moderate, normal or average flow, above average flow, extremely high flow, below average and extremely low-flow. Floods definitely have catastrophic consequences. By the way of comparison, low-flows are equally, if not more, catastrophic. Perennial rivers sometimes exercise above average flow, as well as below average flow for a number of uninterrupted years.

Since 1962, and for a series of subsequent years, the water level of the Equatorial Lakes and the flow in the river system of the Upper Nile were exceptionally high. The flood that swept over Mozambique and Madagascar in the spring of 2000 will be remembered for years to come. Likewise, the last decades have witnessed a number of severe drought events. Burkina Faso, Cape Verde Islands, Chad, Gambia, Mali, Mauritania, Niger and Senegal in Northwest and West Africa, and Djibouti, Ethiopia, Kenya, Somalia and certain parts of the Sudan in East Africa are well-known for their meteorological and hydrological droughts. During the drought which swept over the Sahel region from 1967 to 1974 the stage and discharge of the Niger and Sénégal Rivers fell down to almost unprecedented levels.

Grove (1985) presented the discharge hydrographs of the Chari, Niger and Senegal Rivers for high, average and low-flow years. From these graphs one can list the mean annual discharge of each flow year for these rivers as follows:

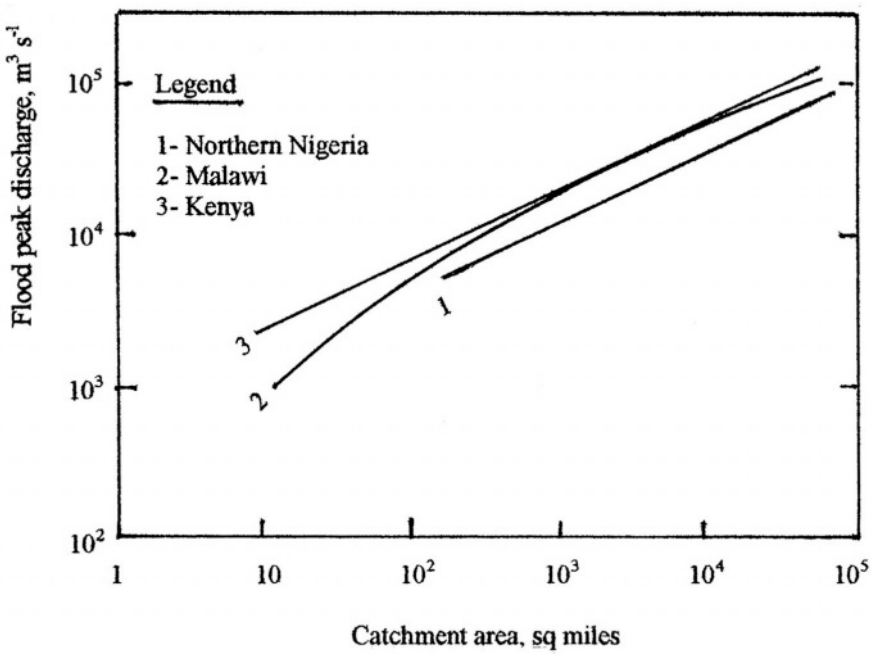

Figure 6.11- Relationship between the catchment area and the flood peak discharge for some Kenyan, Malawian and north Nigerian streams (after Starmans, cited in Balek, 1977)

Station No	River/ basin	High-flow Year	Q_m*	Average-flow Year	Q_m	Low-flow Year	Q_m*
19	Ouergha/Sebou	1963	277	1976	97	1981	27.7
32	Main Nile/Nile	1946	3299	1953	2631	1931	1441
39	Senegal/Senegal	1067	1073	1953	628	1972	256
61	Niger/Niger	1925	2304	1935	1442	1913	829
68	Chari/Chari	1961	1673	1953	1204	1973	576
88	White Nile/Nile	1964	1536	1956	941	1922	714
108	Black Volta/Volta	1963	535	1962	319	1971	107
142	Bahr el-Jebel/Nile	1964	2022	1932	1031	1922	483
156	Oubangui/Congo	1969	6131	1956	4316	1990	2187
159	Sanaga/Sanaga	1969	2679	1952	2058	1972	1440
189	Tana/Tana	1968	374	1974	159	1949	51
209	Zaire/Zaire	1962	54964	1928	40264	1919	32872
230	Shire/Zambezi	1980	945	1971	531	1973	264
235	Ikopa/Betsiboka	1965	557	1968	413	1979	218
237	Gwaai/Zambezi	1974	78.1	1977	37	1982	0.96

*Q_m = mean annual flow for the given year, $m^3 s^{-1}$

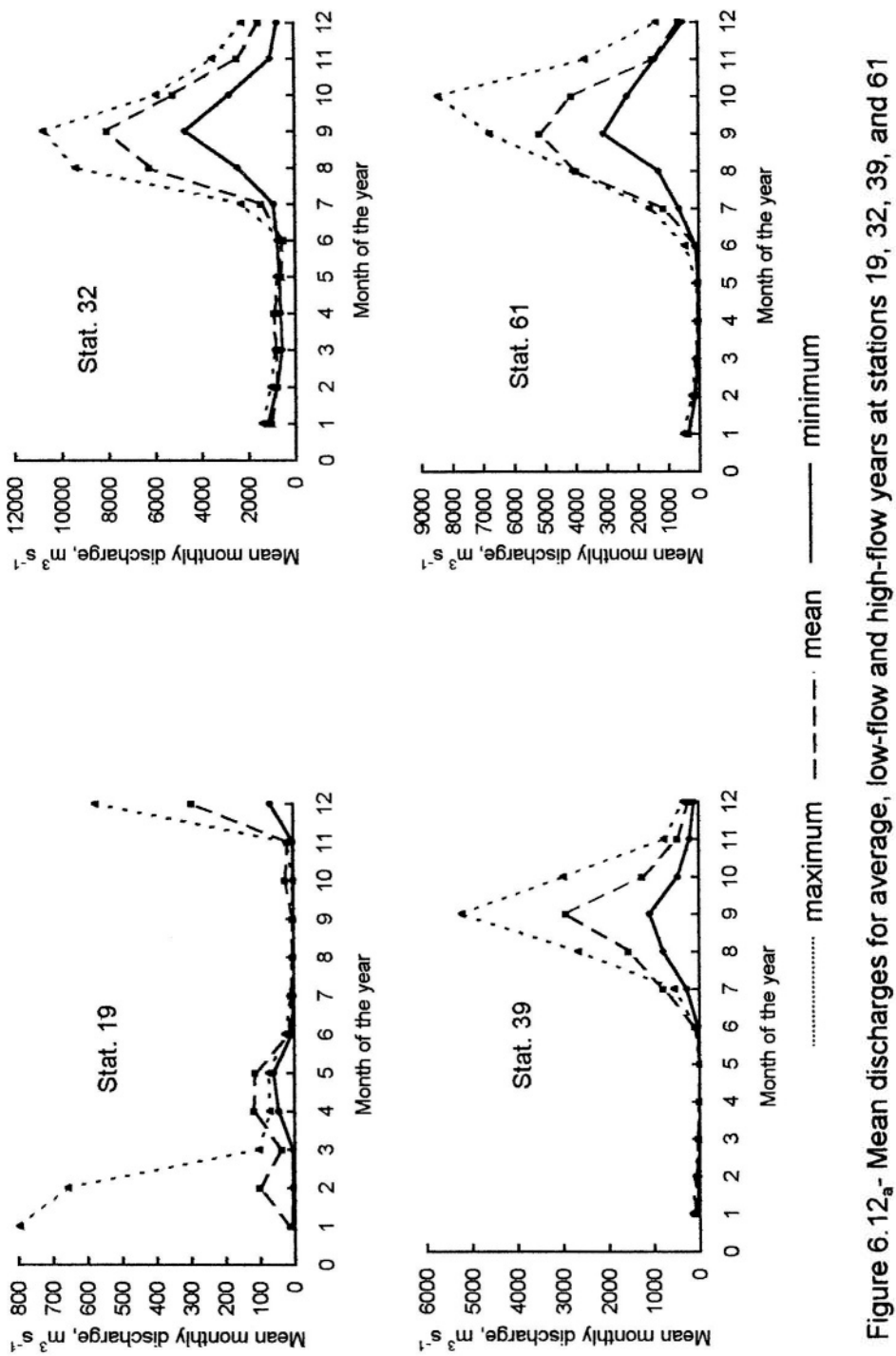

Figure 6.12$_a$- Mean discharges for average, low-flow and high-flow years at stations 19, 32, 39, and 61

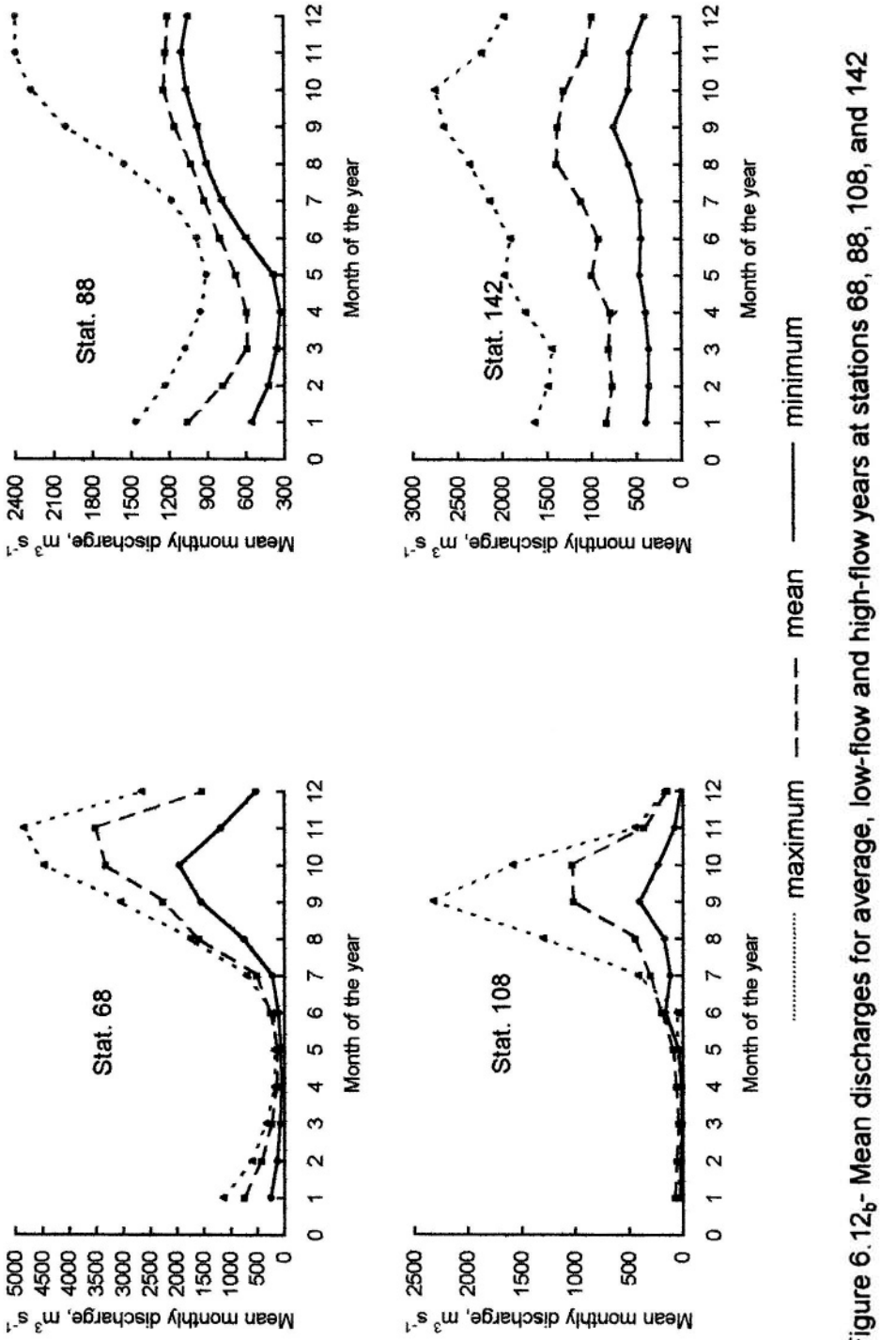

Figure 6.12b - Mean discharges for average, low-flow and high-flow years at stations 68, 88, 108, and 142

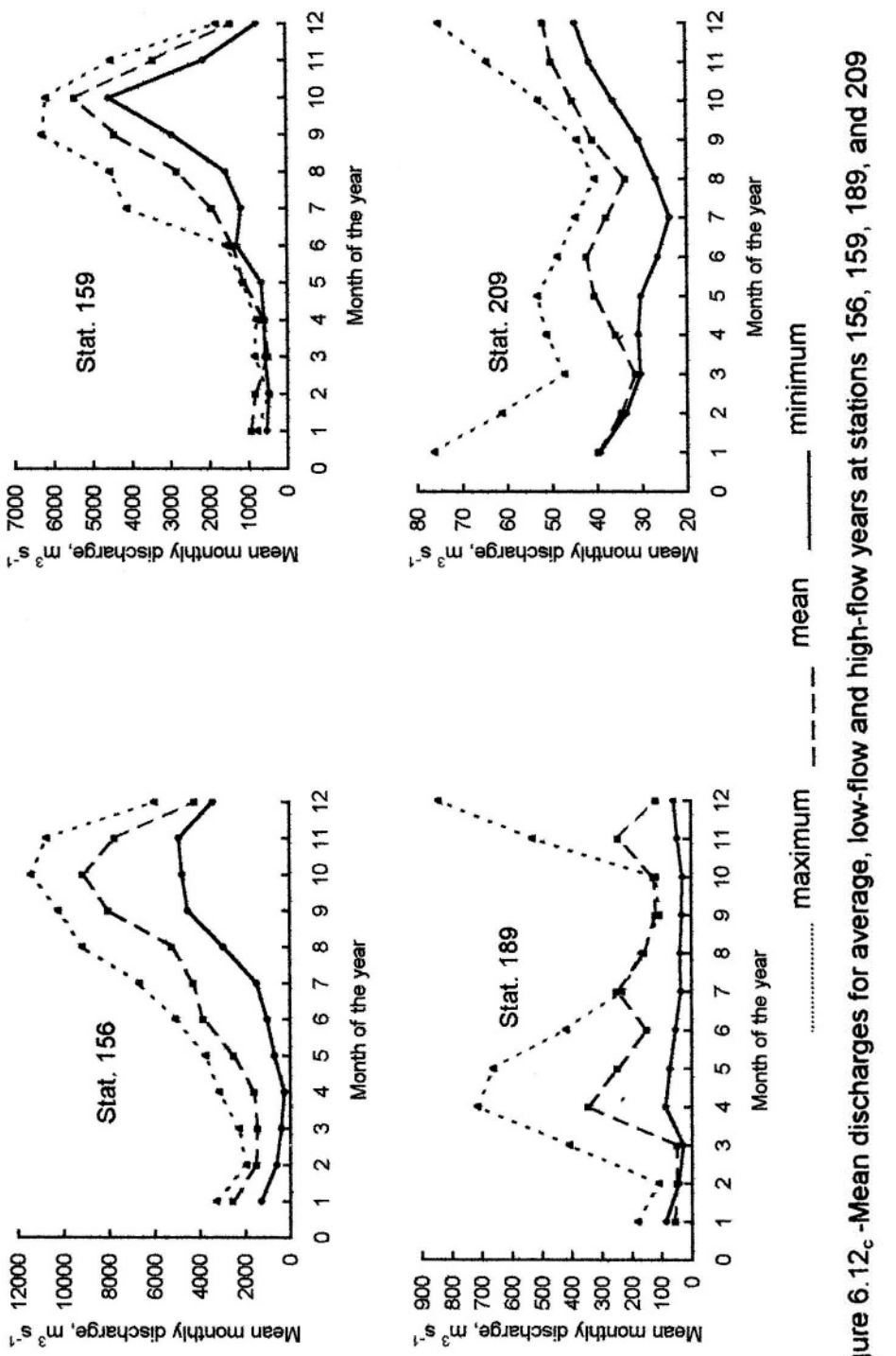

Figure 6.12c -Mean discharges for average, low-flow and high-flow years at stations 156, 159, 189, and 209

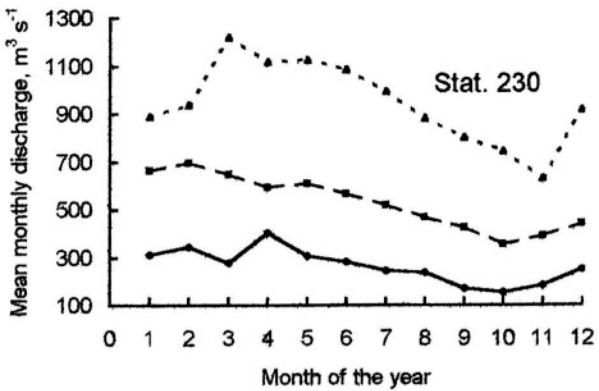

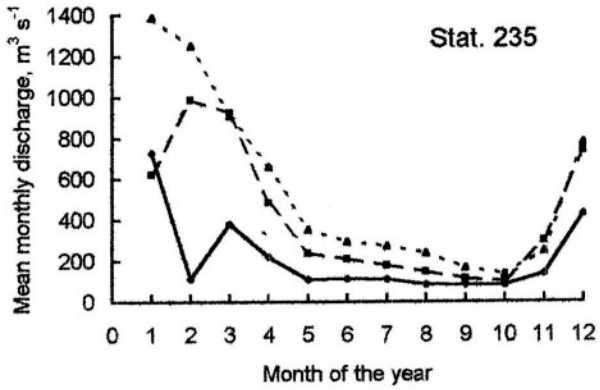

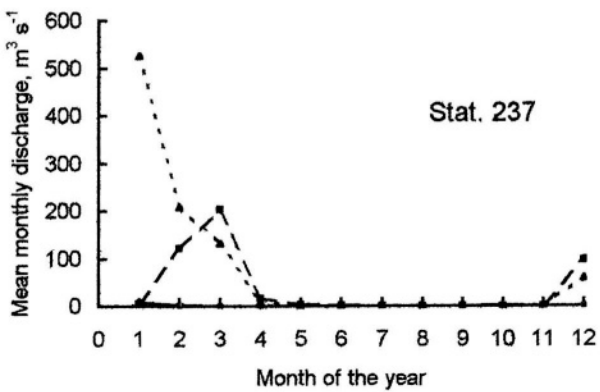

maximum mean minimum

Figure 6.12$_d$ - Mean discharges for average, low-flow and high-flow years at stations 230, 235, and 237

Generally speaking, the natural river supply in a high-flow year can be twice as much, if not more, as the natural supply in a normal (average) year. Likewise, the yield in a low-flow year may fall to less than half the natural yield in a normal year. These ratios vary from one river to another and with the length of record. The range of interannual variability for small rivers is more likely to exceed that of larger rivers for the same period of record. Station 19 on the Ouergha River, Sebou basin, Morocco, corresponds to a catchment of 4, **404** km^2. The mean river flow, which was **195** $m^3 s^{-1}$ in 1963, fell to only **17.1** $m^3 s^{-1}$ (8.76%) in 1981. The interannual variability of the discharge of the Tana River at Garissa (Station 189 and catchment area of **42, 220** km^2) is somewhat less. The mean annual discharge of 1,040 is about 13.6% of the mean annual discharge in the year 1968.

Graphical plots of the mean annual discharge series at 15 gauging stations having a length of record between 28 and 48 years are shown in Figure 6.13. Linear trends and moving averages are also plotted on these figures. The time step of the moving averages is 7 years for the length of record exceeding 50 years and 5 years for shorter records. The graphs in Figures 6.13 reveal some of features of the interannual variability of the mean discharge values. Other than the range of the (natural) annual flow, patterns of variation such as trends (gradual variation with time), jumps (abrupt variation with time) and cycles (periodic variation with time) can be observed.

Each of the annual discharge series presented in Figures 6.13 has been considered for a possible trend. The Spearman's rank correlation test was applied to the series and the computed coefficient, R_s, substituted in Eq. (6.10) to obtain the corresponding z-statistic:

$$z = Rs\sqrt{n-1} \tag{6.10}$$

which approximate a standard normal variable (for large n, say $n > 20$) and n = number of elements in the series. The results obtained are as follows:

Stat. No.	Period of record	R_s	n	z	Trend falling	Trend rising	Test of significance rejected	Test of significance not rejected
19	1952-88	0.08	37	0.47	-		-	
32	1871-1965	0.42	95	4.07	-			-
33	1912-84	0.37	73	3.14	-			-
36	1925-78	0.27	54	1.98	-			-
37	1912-83	0.41	72	3.49	-			-
39	1904-84	0.29	81	2.58	-			-
61	1907-90	0.34	84	3.06	-			-
142	1912-82	0.60	71	5.02		-		-
156	1936-90	0.57	55	4.15	-			-

Stat No	Period of record	R_s	n	z	Trend falling	rising	Test of significance rejected	not rejected
171	1953-83	0.59	31	3.23-				-
189	1934-75	0.32	42	2.05	-			-
209	1903-83	0.42	81	3.77	-			-
230	1953-81	0.69	29	3.74	-			-
235	1949-78	0.18	30	0.97-		-		
237	1956-83	0.15	28	0.75	-	-		

The above results indicate that 10 series out of 15 have been displaying a falling trend and the rest a rising trend, both during the listed periods of record. Furthermore, 12 of these trends have proven to be significantly dependent on time (5% significance level) whereas the remaining 3 trends rejected the test of significance. Whether these trends are apparent or true, the main conclusion to be derived from the trend test is that the mean annual discharge series are generally time-dependent.

Any abrupt break in the hydrologic regime of a certain river basin is reflected on the discharge series of the river in the form of a jump. A jump is defined as a sudden rise (positive) or decline (negative) in the variate value the time series is representing. Yevjevich (1972) discussed possible causes underlying the negative jump in the flow series of the Main Nile at Aswan, which occurred between 1899 and 1902 (**Figure 6.13$_a$**). The mean discharge of 3,950 $m^3 s^{-1}$ in the pre-jump period (1870-1898) dropped to 2,640 $m^3 s^{-1}$ in the post-jump period (1899-1955). The mean for the total period 1870-1955 was 2,925 $m^3 s^{-1}$. It is quite remarkable that the time of this jump coincided with the completion of construction of the Old Aswan reservoir and having it put into operation.

Table 6.5- Occurrence and amount of jump in the annual discharge series of the Nile River system at a number of key stations (after Shahin, 1983)

Station	River	Jump Year	Jump $m^3 s^{-1}$	Jump*, %	Cause(s)
Mongalla	B. el- Jebel	1961-62	840	100	Increased rainfall and improved
Malakal	White Nile	1961-62	317	37	runoff coefficient in the Equatorial Lakes Plateau
Sennar	Blue Nile	1964-65	-365	-24	Storage at Roseires and Sennar
Khartoum	Blue Nile	1964-65	-444	-26	reservoirs, and increased withdrawal from the river upstream
Atbara	Atbara	1965-66	-127	-4	Storage at Khashm el-Girba reservoirs, and increased withdrawal from the river upstream
Aswan	Main Nile	1966-67	-887	-32	Storage at the high Dam and increased share of the Sudan

** Amount of jump divided by the mean of series in the pre-jump time*

Shahin (1983) applied the model developed by Lee and Heghinian (1977) for detecting the jump in the mean annual discharge series of the Nile River system. This model was chosen as it presupposes the existence of a jump in the series dealt with, which is the case of many rivers of the Nile system in the 1960s. The data used in that study were the mean annual discharges from 1912 up to 1973 at ten key stations. The results obtained for 6 stations; Mongalla (142), Malakal (88), Sennar, Khartoum (37), Atbara (34) and Aswan (32) are summarized in Table 6.5

Carbonnel and Hubert carried out the same analysis on the mean annual discharge series of the Senegal and Niger Rivers in West Africa (1989). The analysis of these series dealt with multiple jumps (segmentation procedure) in the period of record, not a single, though major jump, as in the case of the Nile system. The regime of these two rivers can be summarized as follows:

River	Period	Average discharge, $m^3 s^{-1}$	Year of jump	Type of jump	Maximum probability, %
Senegal	1904-21	low, 685	1921-22	positive	
	1922-36	high, 887	1936-37	negative	
	1937-49	low, 591	1949-50	positive	45 (1950-51)
	1950-67	high, 880	1967-68	negative	40 (1968-69)
	1968-83	low, 430	-		
Niger	1907-23	low, 1319	1923-24	positive	
	1924-32	high, 1972	1932-33	negative	
	1933-50	low, 1354	1950-51	positive	
	1951-70	high, 1606	1970-71	negative	19 (1969-70)
	1970-85	low, 1047		negative	23 (1976-77)
				negative	37(1979-80)

The seven-year moving averages of the Sénégal River discharge from 1903 to 1979 prepared by Faure & Gac (1981) display a remarkably regular oscillation. Low values appear in the periods 1909-1919 and 1938-49 with twin peaks in 1925 and 1933, and also in 1956 and 1964. According to Grove (1985) the seven-year moving averages of the annual discharge values of the Upper Niger and Logone-Chari produce strikingly similar oscillations. This can also be evidenced from the graphical plot of the moving averages of mean annual discharge series of the Niger River at Koulikoro (station 61) and Diré (station 35)'Troughs are centred around 1925, 1954 and 1969. This information suggests that extremely high flows and extremely low flows are spaced almost 30 years apart, and that peaks and troughs alternate every 10 to 20 years. Reservoir storage and other water resources development and management projects are probably among the reasons causing this oscillation to be less regular with time.

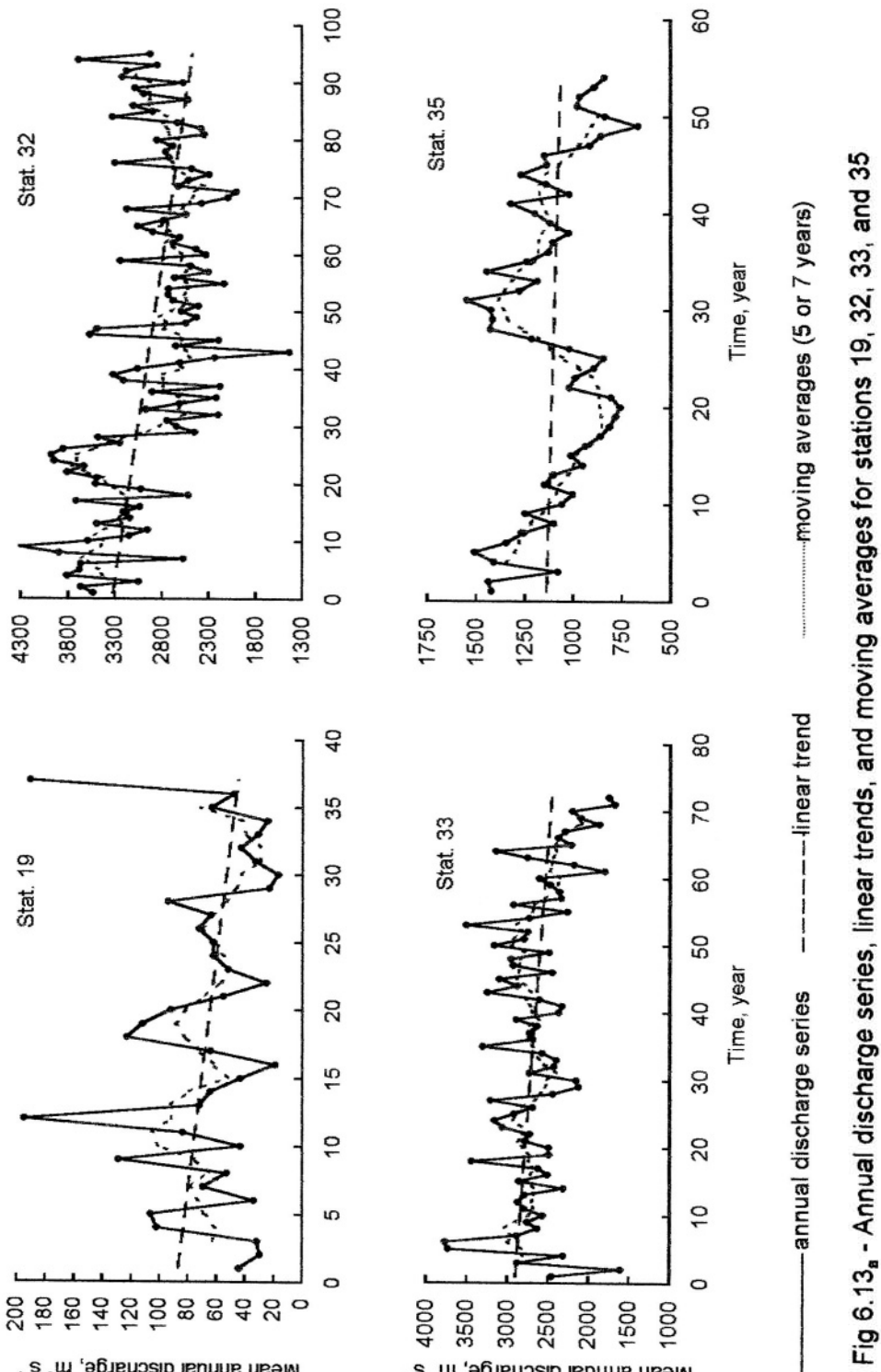

Fig 6.13a - Annual discharge series, linear trends, and moving averages for stations 19, 32, 33, and 35

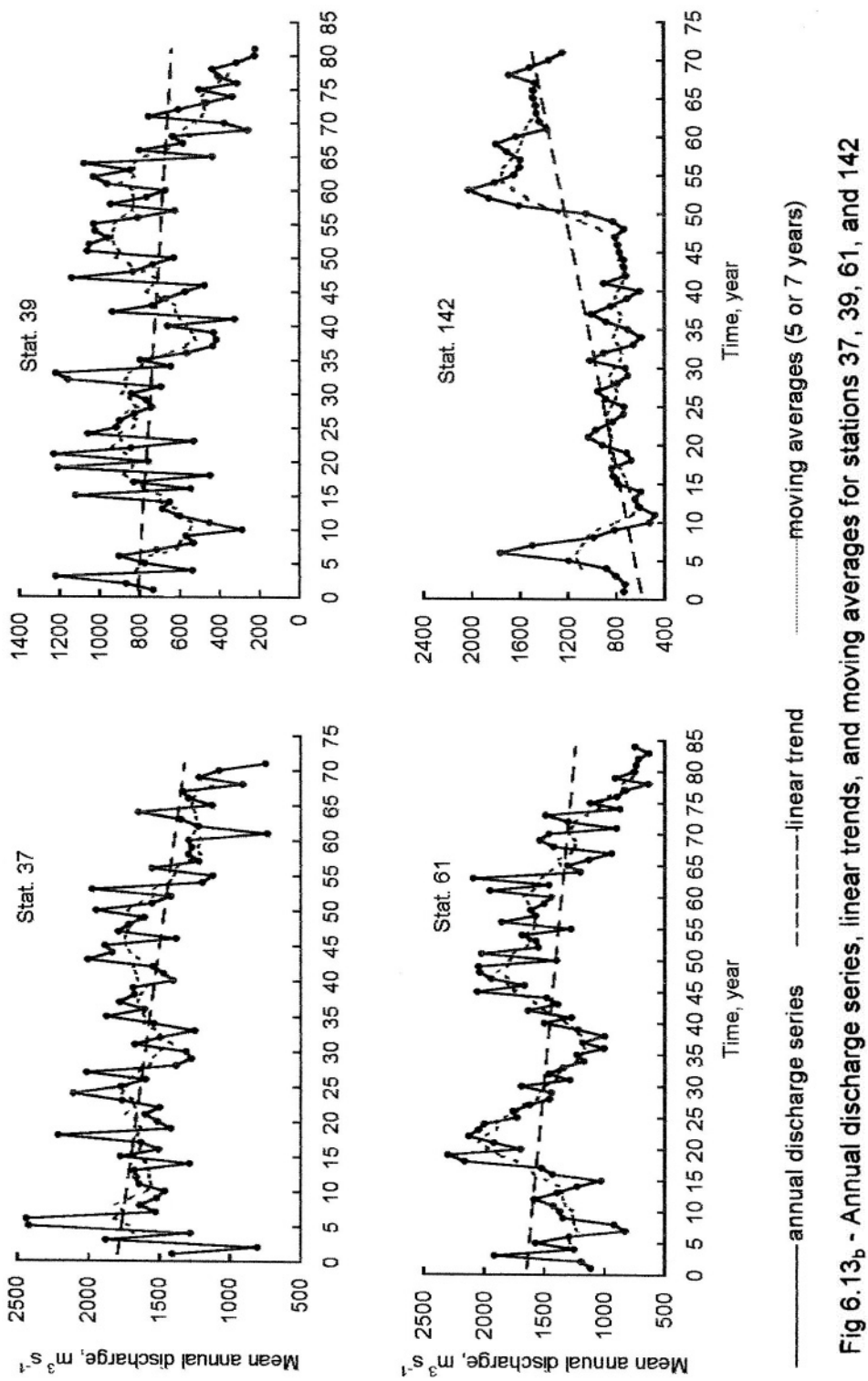

Fig 6.13$_b$ - Annual discharge series, linear trends, and moving averages for stations 37, 39, 61, and 142

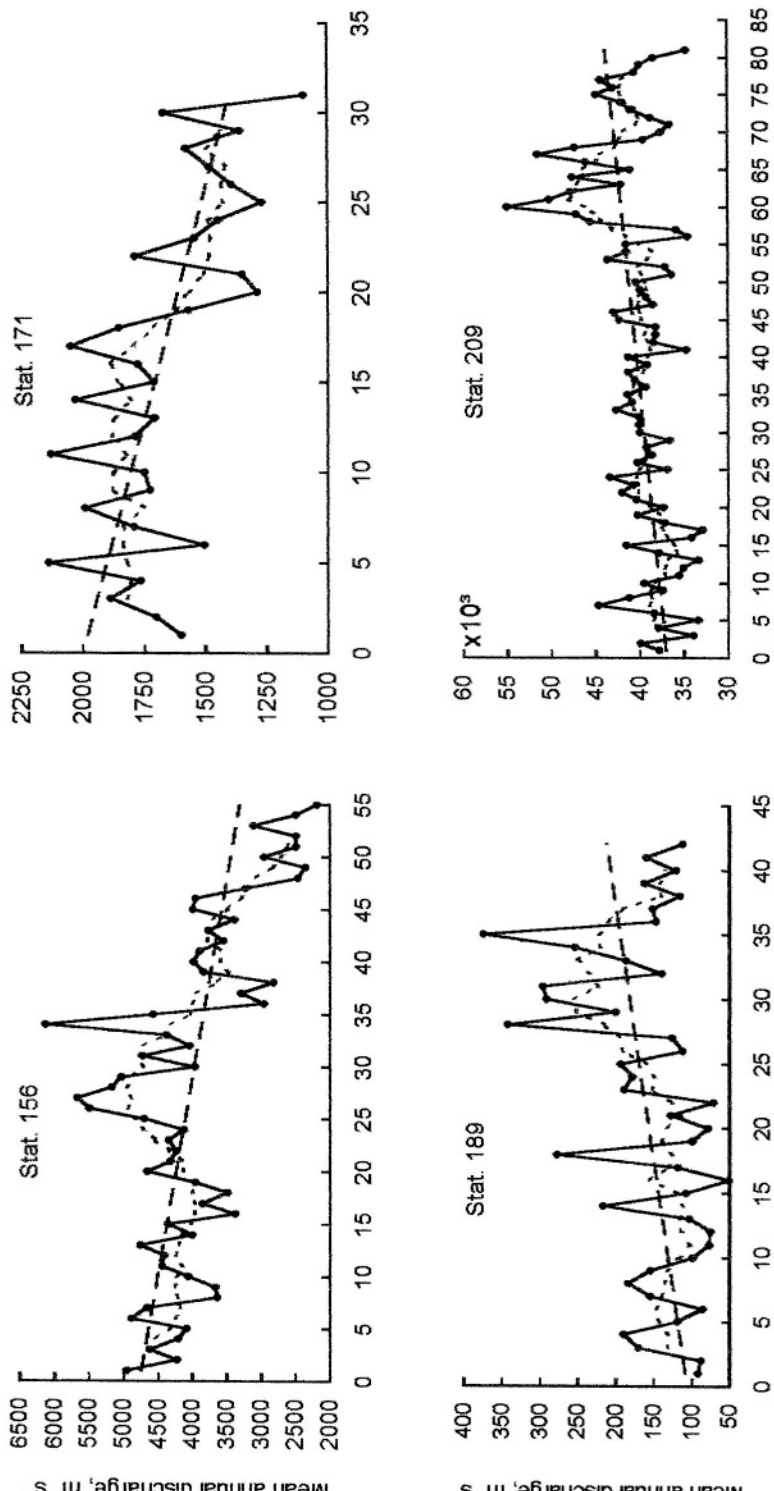

Fig 6.13$_c$ - Annual discharge series, linear trends, and moving averages for stations 156, 171, 189, and 209

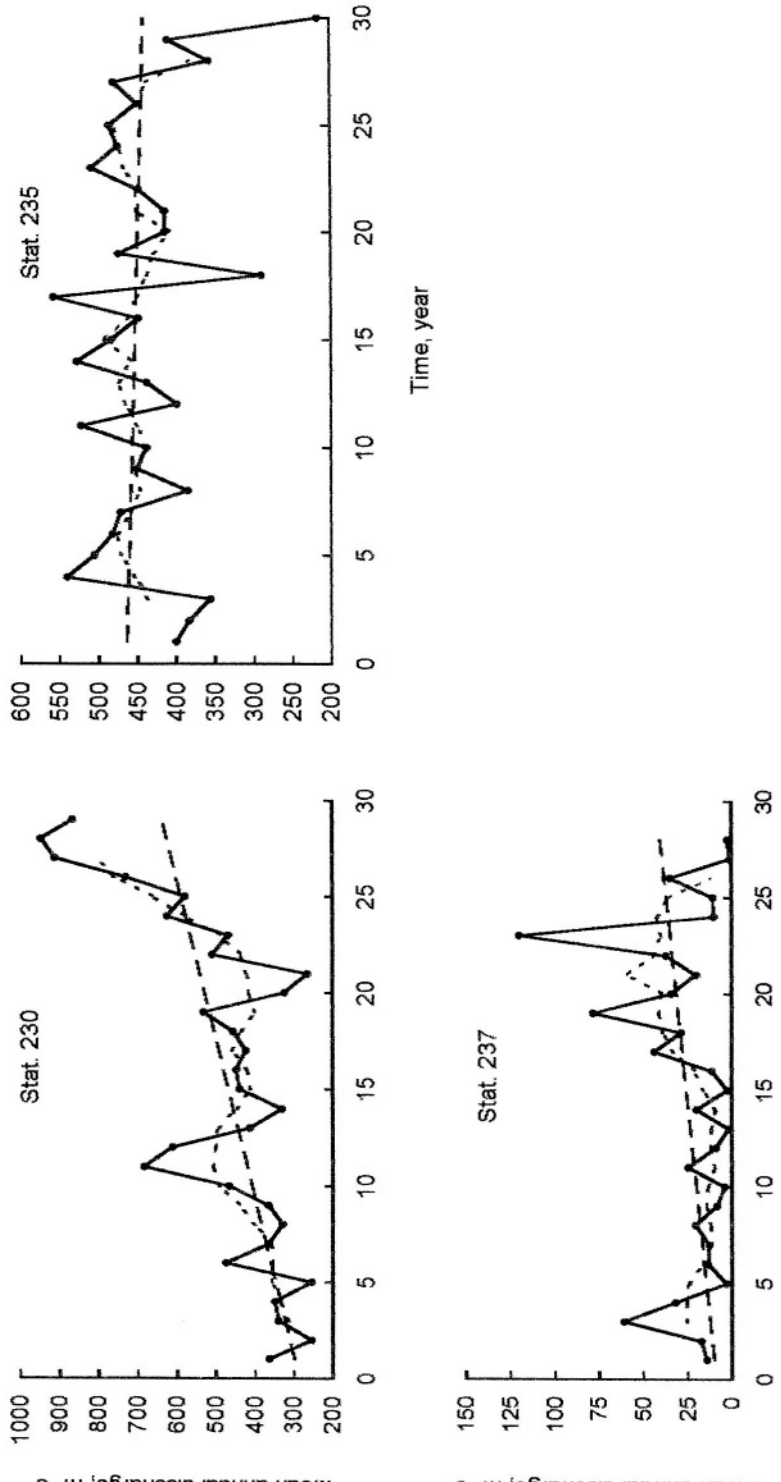

Fig 6.13$_d$ - Annual discharge series, linear trends, and moving averages for stations 230, 235, and 237

Hurst raised the issue of periodic analyses of hydrologic data when discussing the "Flood-Stage Records of the Raver Nile" by Jarvis (1935). He reported that periods varying from 2 to 240 years were found. The period of 240 years has amplitude of 0.15 m for the maxima water levels and 0.46 m for the minima levels. The average amplitude of the 76.8 years period is 0.17 m. He added "The average standard deviation of the flood levels is 0.56 m; this makes apparent the relative smallness of any periodic effects, which although of theoretical interest, are of no use to the forecaster. The principal features are the existence of fairly long terms of years when, on the whole, the floods have been high and others when have been low".

Yevjevich (1972) upon examining a large number of monthly and annual precipitation and runoff series from North America and other locations conclthat there is no significant cross correlation between these these hydrologic series and the series of sunspot numbers. The latter is well known with the 11.1-year cycle. The results of periodic analyses of discharge series of the Nile, Niger and Congo (Zaire) rivers, however, will be presented in the next chapter.

6.4- Filling Gaps or Supplementing Missing Runoff/ Streamflow Data:

The current literature contains a large amount of methods that can be used for supplementing missing data or filling gaps in runoff / sreamflow series. Boayke (1993) presented a comprehensive review of eight groups of such methods. The models and the related runoff-generating algorithms are summarized as follows:

6.4.1 Recession equation- The recession equation may take different forms, one of which can be written as:

$$Q_{t+\Delta t} = Q_t K^{\Delta t} \tag{6.11}$$

where, $Q_{\Delta t}$ is the discharge at time $t+\Delta t$, Q_t is the discharge at time t and K is the recession constant. The recession limbs in the continuous sections of the hydrographs are separated for each of the test catchments. Applying Eq. (6.11) to the selected calibration hydrographs, an average value of K can be obtained for the basin in question through optimisation using the test parameter denoted by f given by:

$$f = \Sigma_1^n (Q_{t+1} - Q_{t+1}^*)^2 \tag{6.12}$$

6.4.2 Interpolation equation- The interpolation equation can be expressed as

$$R_i = Q_o \pm \frac{1}{N}(Q_N - Q_o) \tag{6.13}$$

where R is the computed runoff for the ith day, Q_o is the observed runoff at the beginning of the gap, Q_N is the observed runoff at the end of the gap, and N is the number of missing data +1 day.

6.4.3 Recursive models- The recursive models are based on the input, storage and output of a river basin system. The models are based on the continuity and storage equations combined with a storage-runoff relationship. The latter can be the linear, log-linear or non-linear storage-runoff relationship. The equations of the model assuming the log-linear storage –runoff to hold can be expressed as:

$$Q_{t+\Delta t} = Q_t\left[\frac{B_t}{Q_t}(1-e^{-\Delta t/K})+e^{-\Delta t/K}\right] \tag{6.14}$$

where $B_t > 0$ and

$$Q_{t+\Delta t} = Q_t e^{-\Delta t/K} \tag{6.15}$$

where $B_t \leq 0$ and

$$B_t = (P_t - E_t) \tag{6.16}$$

6.4.4 Autoregressive models- Generated runoff sequences using these models basically depend on statistical properties, including frequency analysis, of the available historical runoff records. A simple model (Markov) relating the discharge at a certain time t, Q_t, and the discharge at earlier time intervals, Q_{t-i}, can be expressed by:

$$Q_t = \alpha_o + \alpha_1 Q_{t-1} + \alpha_2 Q_{t-2} + \ldots \alpha_n Q_{t-n} \tag{6.17}$$

where α_o is a constant, and α_1, $\alpha_2, \ldots$, and α_n are model parameters to be estimated from the historical record (e.g. Yevjevich, 1972, and Kottegoda & Elgy, 1977).

6.4.5 Extended autoregressive models- This class of models, as a matter of fact, is a special class of the general autoregressive models. In the extended models historical rainfall records are included. The runoff-generating algorithm is

$$Q_t = \beta_o P_t + \beta_1 P_{t-1} + \ldots + \beta_n P_{t-n} + \varepsilon \tag{6.16}$$

where $\beta_1, \beta_2, \ldots,$ and β_n are model parameters, and P_t is the precipitation at the

current time, and $P_{t-1},\ldots P_{t-n}$ are the antecedent precipitations corresponding to 1,..., n time intervals, respectively.

6.4.6 Regression models- Simple and multiple regression models are used foe extensively for establishing relationships between two or more variables. The established relationship can be used to estimate a missing value of one of the variables given the corresponding value (s) of the other variable (s). An example of *regression model without including rainfall* is:

$$Q_A = \alpha + \beta_1 Q_B + \beta_2 Q_C + \cdots + \beta_m Q_N + \varepsilon \tag{6.19}$$

where Q_A, Q_B, $Q_C,\ldots$, Q_N are the discharges at stations *A, B, C,...,* and *N* and α is constant which can be taken as representing baseflow and channel storage, and β_1, $\beta_2,\ldots$, and β_m are partial regression coefficients. Likewise, an example of *regression model with rainfall included* is:

$$Q_{A,t} = \alpha + \beta_1 Q_{B,t} + \cdots + \beta_m Q_{N,t} + \lambda 1_1 P_t + \lambda_2 P_{t-1} + \cdots + \lambda_r P_{t-r} + \varepsilon \tag{6.20}$$

where λ_1, $\lambda_2,\ldots,$ and λ_r, are additional model parameters to be associated with current and antecedent rainfall.

Some runoff models incorporate only rainfall in current and earlier time periods P_t, P_{t-1}, $P_{t-2},\ldots$.These models are either linear or non-linear. The basic equation describing a non-linear model can be written as:

$$Q(t) = \int_0^t h_1(\tau)P(t-\tau)d\tau + \int_0^t\int_0^t h_2(\tau_1,\tau_2)P(t-\tau_1)P(t-\tau_2)d\tau_1 d\tau_2 + \cdots + \cdots +$$

$$\int_0^t\int_0^t h_r(\tau_1,\tau_2,\cdots,\tau_r)P(t-\tau_1)\cdots P(t-\tau_r)d\tau_1,\cdots,d\tau_r, + \cdots \tag{6.21}$$

For the purpose of comparison between all models described in this section, Eqs. (6.19), (6.20) and (6.21) will be referred to as methods 6_a, 6_b and 6_c, respectively. The above-mentioned methods, except the recession equation, method (6.4.1), can be used for filling gaps in hydrologic data series of both yhe high-flow and low-flow seasons. The next types of models are recommended exclusively for filling gaps in the data series of the wet seasons.

6.4.7 Unit Hydrograph- A unit hydrograph (UH) is defined as the hydrograph of surface runoff which would be generated from a unit depth of rainfall excess, i.e. after all losses have been allowed for, uniformly distributed over the river basin

and occurring within a specified time interval. The theory underlying the unit hydrograph follows the theory of linear systems. The relationship between the input to the system (rainfall excess) and the output (direct surface runoff) is given by an appropriate function known as the convolution integral.

As the duration of the effective precipitation becomes infinitesimally small, the unit hydrograph is called then by the instantaneous unit hydrograph (IUH). The IUH is often referred to as the impulse-response function, *h (t),* as it appears in the expression:

$$\int_{-\infty}^{\infty} h(t)dt = 1 \tag{6.22}$$

Replacing *t* and *dt* in Eq. (6.22) by τ and $d\tau$ respectively, the convolution integral linking the input (rainfall excess) with the output (runoff) can be given by the equation:

$$Q(t) = \int_{0}^{t} h(\tau)P(t-\tau)d\tau\,; \qquad i = 1, 2, \quad n \tag{6.23}$$

Next, Eq.(6.23) can be reformulated into a discrete form as:

$$Q_i = \sum_{k=1}^{i} P_k h_{i-k+1} \tag{6.24}$$

yielding

$$Q_1 = P_1\, h_1,$$

$$Q_2 = P_2\, h_1 + P_1\, h_2,$$

$$\mathbf{Q}_i = P_i\, h_1 + P_{i-1}\, h_2 + \ldots. + P_1\, h_1 \tag{6.25}$$

A number of methods are available for the derivation of the instantaneous unit hydrograph (e.g. Singh et al., 1981). Rodriguez-Iturbe and Valdes (1979) and sometime later other researchers have contributed to the development of the concept of geomorphological hydrograph (GIUH) as alternative methodology. In this concept, the shape and scale parameters of the catchment transfer function are related to the topology and catchment's characteristics. The derivation of the GIUH depends essentially upon a set of assumptions including that for estimating the characteristic velocity. When this velocity is expressed in terms of

the kinematic wave approximation, the peak and time-to-peak of IUH may be expressed in terms of a group of catchment and channel characteristics and the intensity of rainfall excess. The hydrograph thus developed is referred to as the geomorphoclimatic instantaneous unit hydrograph (GCIUH). Studies involving the GCIUH have developed a single IUH relating to the total duration of rainfall excess. Zaki et al. (2000) have introduced some modifications to this quasi-linear approach, in which the total duration is divided into several equal time increments with separate IUHs being generated for each interval..

6.4.8 Storage models- Several storage models can be found in the current literature on hydrological models. Figure 6.14 is a schematic representation of a storage model developed by Dawdy and O'Donnell (1965) to simulate the rainfall- runoff process. The following notations are used in the model:

P_t = precipitation at time t,
E_t = evapotranspiration at time t,
SS_t = surface water storage in the catchment at time t,
GS_t = ground water storage in the catchment at time t,
RS_t = surface water release from the catchment at time t,
SM = threshold above which surface runoff begins,
QS_t = surface runoff at time t,
QG_t = groundwater contribution at time t, and
Q_t = total runoff at time t.

Boakye (1993) applied the above methods to fill the gaps in the daily discharge series of three river basins in Ghana. These basins are the Nabogo (semi-arid north, surface area of 1,950 km^2), Tano (humid south west/semi-arid north, 1,204 km^2), and Ayensu (semi-arid north, 1,657.5 km^2).

The comparison between the various models comprised both dry and wet seasons, where the length of missing data varied from 1 to 120 days. The comparison between models was based on the coefficient of variation of the residual of errors (hereafter referred to as the Y-term). For this purpose, the best Y-value (assumed zero) was computed (i.e. for the best method) and then all other values of Y have been compared with the best Y-value.

Table 6.6 specifies the best model for filling the gaps in the daily discharge series given the season and length of missing data. From the tabulated results it appears clearly that, for all three climatic regions put under investigation, the interpolation technique is the best for filling in short-term or short-duration missing data. For the filling in of long-term or long-duration missing runoff data, the regression methods including the autoregression models prove to be the best for all the climatic regions.

It has to be stated here that all the methods already mentioned above in connection with filling gaps due to missing data can also be used for forecasting hydrologic data such as river discharges, with varying degrees of reliability.

Since the group of regression, including autoregression, models is widely used for forecasting purposes, a case study from Zambia will be briefly reviewed and the main conclusions presented.

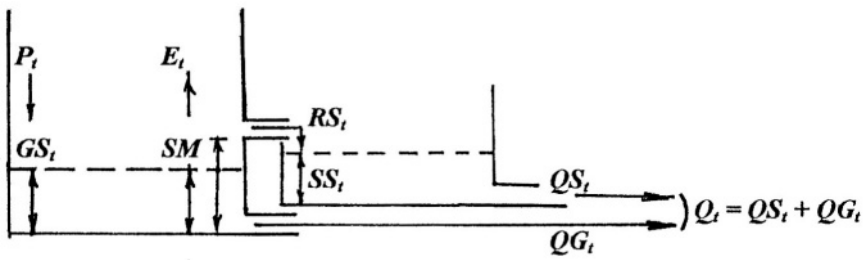

Figure 6.14- Astorage model to simulate the rainfall-runoff process (after Dawdy and O'Donnell, 1965)

Table 6.6- Comparison of different models applied to fill the gaps in the daily discharge series of three Ghanian river basins both in the dry and wet seasons (after Boakye, 1993)

	Tano basin (humid south west)		Ayensu Basin (semi-arid south)		Nabogo basin (semi-arid north)	
Rank	Up to 2 days gaps	> 2-days gaps	Up to 3 days gaps	> 3-days gaps	Up to 7 days gaps	> 7-days gaps
Dry season						
I	2	6_b	2	6_b	2	6_b
II	5	6_a	5	6_a	5	6_a
III	3		4		4	
IV	4		3		3	
V	6_b		6_b		6_b	
VI	6_a		6a		6_a	
Wet season						
Rank	Up to 2 days gaps	> 2-days gaps	Up to 2 days gaps	> 2-days gaps	Up to 4 days gaps	> 4-days gaps
I	2	8	2	7	2	8
II	3	7	3	8	3	6_b
III	5	6_b	5	6_b	5	6_a
IV	4	6_a	4	6_a	4	
V		6_c		6_c		

Explanation

Methods 2 = interpolation, 3 = recursive, 4 = autoregressive without rainfall, 5 = autoregressive with rainfall, 6_a = regression without rainfall, 6b = autoregression with rainfall, 6_c = non-linear model, 7 = unit hydrograph and 8 = storage model.

Sharma (1985) performed a study on the stochastic characteristics of the rainfall-runoff processes in Zambia. Data from 13 rainfall stations in the Kafue River basin and 10 stations in the Chambeshi basin were used for characterizations of the rainfall processes and for discrete dynamic modeling of rainfall-runoff processes. Monthly and annual runoff data from 20 gauging stations in the Kafue basin and 8 stations in the Chambeshi basin were subjected to analyses.

The monthly rainfall sequences were found to follow approximately the normal probability distribution. These sequences can be assumed to be composed of deterministic (periodic) and stochastic components. The runoff sequences tended to follow the lognormal probability distribution. The deterministic periodic component explained more than 60% of the variance in the log-transformed monthly runoff sequences. The stochastic component behaved as a random process in the monthly rainfall sequences and as an autoregressive moving average (ARMA (1,0) or ARMA (1,1)) process in the monthly runoff sequences. The annual rainfall sequences resembled a random process and the annual runoff sequences a first order autoregressive process (AR (1)).

The ARMA(1,1) and ARMA (1,0) are referred to as univariate stochastic models because a sequential value of the stochastic sequence at a certain time is generated from the sequential value (s) of earlier time step (s). Bivariate linear models incorporate monthly rainfall depths as input and the logarithms of monthly runoff depths as output. Denote the sequential values of the logarithms s of the monthly runoff by y_i and the sequential values of monthly rainfall depths by x_i, and α, δ, β_0, and β_1 the system parameters. The term ε_i a white noise sequence with zero mean and variance s^2_ε uncorrelated with the x_i sequences. Using these notations the model can be written as:

$$y_i - \alpha y_{i-1} = \delta + \beta_o x_i + \beta_1 x_{i-1} + \varepsilon_i \qquad (6.26)$$

The model structure on a yearly basis was comparable to the monthly model, Eq. (6.26), except that the variables y_i and x_i apply in this case to the yearly sequences, and the parameter β_1 is equal to zero. The univarite stochastic model performed satisfactorily in providing one-month-ahead adaptive forecasts. The performance of the model to provide 12-month-ahead forecasts was described as poor. An autoregressive AR (1) showed good results when the logarithms of annual discharge sequences were used. The bivariate model, Eq. (6.26), was used to forecast the discharge using the mean rainfall for the 12 months ahead. It was observed that forecasts based on bivariate rainfall-runoff model were closer to observed sequences when compared with a univariate model (Figure 6.15$_a$). Last, but not least, the ability of the rainfall-runoff model to fill the gaps in the monthly discharge series was also tested. The observed rainfall sequences were used for estimating discharges from October to September. The estimated and

the observed discharges compared reasonably well, as can be seen from **Figure 6.15b**. It should be noted here that Eq. (6.26) describing the model used is quite similar to the extended autoregressive model already given by Eq. (6.18), subsection 6.4.5.

6.5- Erosion and Sedimentation

Erosion phenomena acting on the surface of the earth by running water is a result of complicated natural processes together with consequences of human activities. As such, erosion can be divided into natural erosion and accelerated

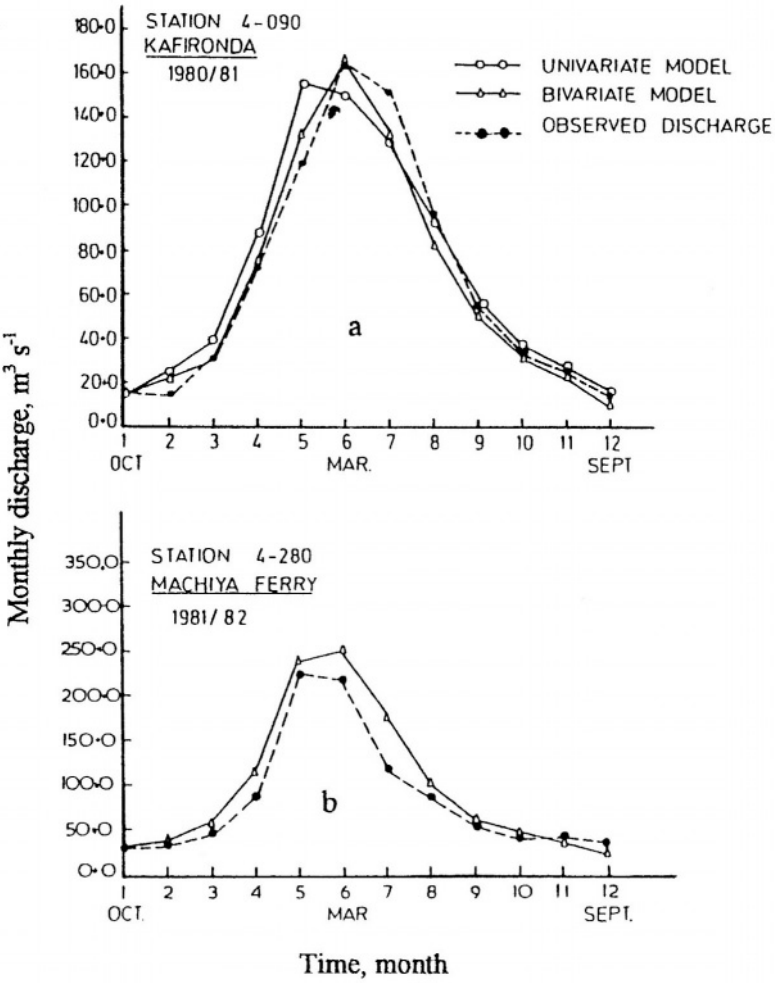

Figure 6.15-(a) One-month-ahead adaptive forecasting for the Kafue basin, (b) filling missing monthly discharges in the Kafue basin (from Sharma, 1985)

erosion. The climate, hydrology, morphology, geology, soil, and vegetation prevailing in a certain region are considered to be the most important factors influencing natural erosion. On the other hand, land management and use for agricultural, urban and other purposes are held responsible for accelerated erosion. Erosion might cause damage to land and water resources. Agricultural soil loses its fertility and become unable to sustain crop production. Erosion too brings sediments to water streams and reduces the life age of impoundments and storage reservoirs. It affects the function and operation of water structures and increases their maintenance costs.

The process of erosion consists of the detachment of soil particles from their position in the soil mass and their movement to a channel in which they may be transported for the balance of their journey. Erosion can be subdivided into gully erosion and sheet erosion. Gully erosion occurs where a small rivulet forms during heavy storms (e.g. torrents). Turbulence in the flow creates local forces capable of dislodging soil particles from the bed and banks of the channel. As the gully deepens, the profile is steepest at head causing the gully to grow headward. Sheet erosion can be defined as the removal of a relatively uniform layer of soil from the ground surface (Linsley et al., 1958).

A world evaluation of the severity of erosion and land degradation was performed by FAO (1986). The results related to Africa are summarized in Table 1_a, Part II / Appendix B. From these results it can be seen that in the humid tropics, gully erosion is generally slight to moderate in most areas, except in Kenya, where it is severe. Sheet erosion is slight to moderate in all the regions. Rates of erosion and sediment loss rates as obtained from a variety of experiments in certain parts of Africa are given in **Tables 1_b and 1_c**, Part II / Appendix B.

Sediments are the natural products of erosion. The sediment yield of a certain river basin is affected by its climate, especially rainfall, temperature, land slope, soil type and vegetal cover. As such, sediment yield varies from one part of the basin to another part, and from one time interval to another interval. Of importance here is the role the method used for measuring or estimating the sediment yield is playing. The available estimates of sediment reaching all the oceans vary from a maximum of $630\ t\ km^{-2}\ y^{-1}$ to a minimum of $137\ t\ km^{-2}\ y^{-1}$. The map prepared by Milliman and Meade (1983) gives an annual total of $530*10^6\ t$ for Africa (Figure 6.16). Assuming that one half of the surface of Africa, i.e. $15*10^6\ km^2$, supplies this amount, the sediment supply to the oceans surrounding Africa must be in the order of $35\ t\ km^{-2}\ y^{-1}$. This figure is too small compared to any of the global estimates for the whole world.

Holeman (1968) classified the sediment yield of African rivers into high, moderate, low and very low. The average production of the Medjerdah basin in Tunisia is about 700, the Cheliff in Algeria 153, the Nile about 39, the Congo 17.8 and the Niger 4.6, all in $t\ km^{-2}\ y^{-1}$. During flood storms in the arid-regions the sediment concentration is usually high, in the range 30 to $50\ g\ l^{-1}$, though

higher concentrations of 100 g l^{-1} and more have been observed. Rodier (1987) raised an interesting point about the statistical distribution of annual sediment load stating "A fifty year flood may transport a total sediment load far greater than the total load transported during the previous fifty years". He gave as an example the Oued Zeroud, Tunisia, where the sediment transport during the 1969 floods was $450*10^6$ t for an area of 9,000 km^2, while the average annual transport is in the order of $20*10^6$ t.

The concentration of suspended sediment in a river at a certain section varies considerably from one flow season to another flow season. The graphs shown in Figure 6.17 for the Atbara River, the Blue Nile and the Main Nile show clearly that the ratio of the average sediment concentration in a normal flood season is 5 to 10 times the average concentration in the low-flow season. Since the Atbara

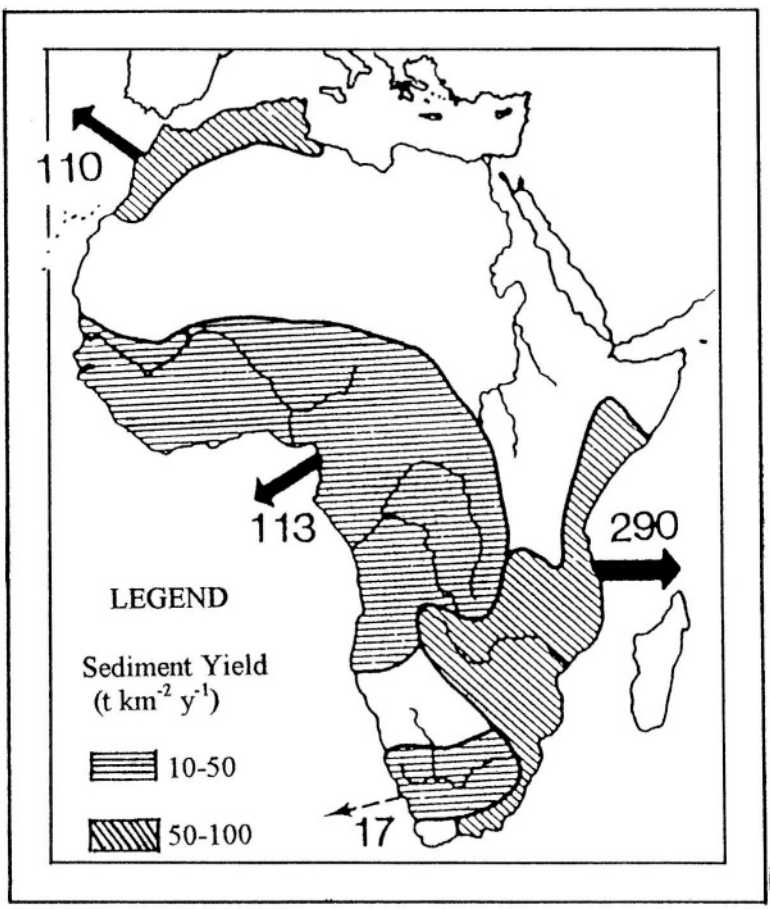

Figure 6.16- Annual discharge of suspended sediments, 10^6 t, flowing to the oceans from some drainage basins of Africa (Milliman & Meade, 1983)

basin is generally steeper than the Blue Nile basin, the concentration of its floodwater is higher than the concentration of the floodwater of the Blue Nile. Tables 2_a through 2_k, Part II / Appendix B, include a fairly large amount of data related to suspended sediments in some African countries.

According to Walling (1984), the available data suggest that the suspended sediment loads of African rivers draining basins of the order of $10{,}000\ km^2$ range between 1.0 and $4{,}000\ t\ km^{-2}\ y^{-1}$. He stressed that careful attention must be given to the accuracy of the available data. Considerations including the equipment and procedures used for collecting samples, sampling frequency, and the technique used for load calculation are important. In attempt to summarize and generalize the information currently available, he developed a tentative map of the pattern of suspended sediment yields on the African Continent.

6.5.1 Relationship between discharge and suspended sediment load- For some rivers, stage-discharge relations may not be well defined, yet the relations between sediment discharge and flow are well defined and stable. If the sediment discharge is a function of stage or discharge, a few sediment samples covering a range in stages may be used to define empirically a sediment-rating curve. This empirical relation is then used to compute the sediment discharge as a function of time, from either stage or discharge hydrograph, or to obtain long-term average annual sediment discharges using a flow duration curve.

Figure 6.18 is a logarithmic plot of all water discharges against the corresponding suspended sediment loads for the Caledon River at Maseru, Lesotho. In this graphical plot, no distinction has been made between low-flow and high-flow seasons or between rising and falling flood waves. The heavy scatter of the plotted points is a consequence of having just one relationship between the discharge and the sediment load. The sediment load corresponding to a discharge of $10\ m^3\ s^{-1}$ varies from less than $1*10^{-3}$ to more than $1*10^{-1}\ t\ s^{-1}$. The scatter grows wider with increasing water discharge.

It should be emphasized that the aforesaid procedure does not apply to all rivers at all times. In many cases, a rating curve for the same stage indicating two different discharges: one for the rising stage and the other for the falling stage. Additionally, the discharge of the rising flood wave often carries along more suspended load compared with the same discharge when the flood wave is receding. The Niger is one of the African rivers experiencing this situation. Figure 6.19 illustrates the loop-shaped sediment rating curve of the River Niger at Onitsha, Nigeria (NEDECO, 1959). The curve has two distinct branches; a rising branch and a falling one. A reasonable solution to overcome this problem is to try to establish two independent sets of relationships between stage, discharge and concentration: one for the rising flood and the other for the falling flood. Another possibility is to derive one set of stage, discharge and sediment relationships using average values for the rising and falling floods and establish a correction procedure to cope with each condition separately.

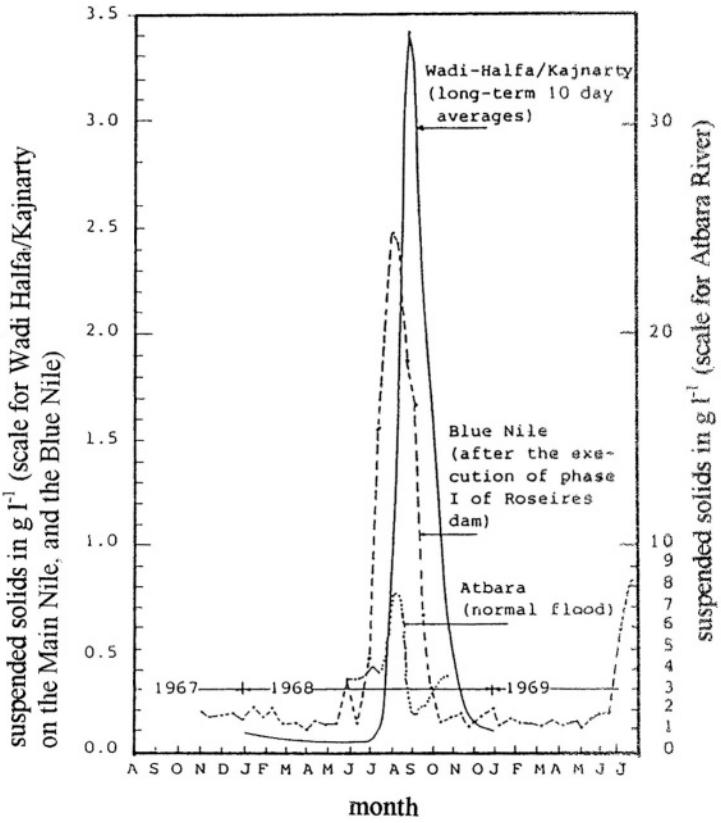

Figure 6.17- Concentration of suspended sediment in the Atbara River, Blue Nile and the Main Nile from August 1967 to July 1969 (from Shahin, 1986)

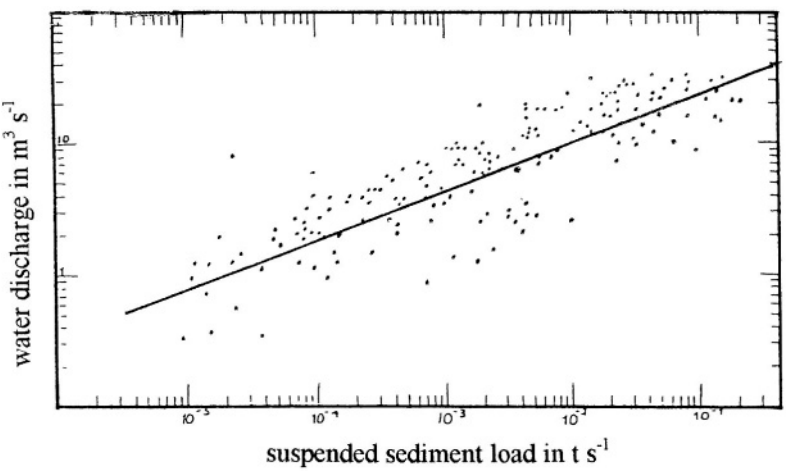

Figure 6.18- The suspended sediment rating curve For the Caledon River at Maseru, Lesotho (from Makhoalibe (1984)

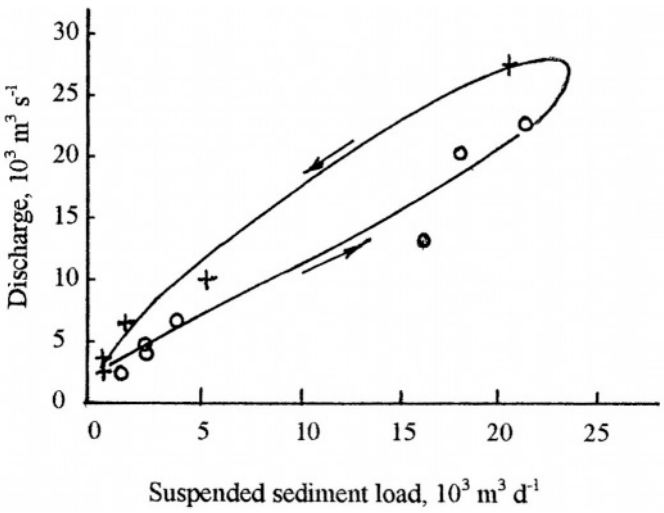

Figure 6.19- Sediment rating curve of the River Niger at Onitsha, Nigeria (NEDECO, 1959)

6.5.2 Relationship between sediment yield and drainage area- It is a widely accepted hydrometeorological concept that the intensity of a rainstorm decreases substantially with the size of the area hit by that storm. This fact often causes the specific yield of suspended sediment to decrease with increasing surface area of the drainage basin in the same climatic region. The functional relationship between the specific sediment yield and basin area appears as a straight line when they are plotted on a logarithmic paper. Makhoalibe (1984) while investigating suspended sediment transport in river basins in Lesotho obtained straight lines for the Vaal and Caledon river basins. The plot for the Senqu (Upper Orange), exceptionally, did not show as a straight line. Instead the specific sediment yield increased considerably with basin area up to 10,000 km^2. This was followed by almost a flat part for a surface area in the range from about 20,000 to 200,000 km^2, above which the specific yield of sediment began to fall with increasing area. This has been attributed to the strong diversity of the rocks underlying the basin.

6.5.3 Other factors influencing erosion and sediment yield- Heusch (1970] measured the sediment yield (global erosion) in the basin of the river Sebou and its tributaries, Morocco. The observed rates varied from 150 t km^{-2} for the plains to 2,000 t km^{-2} in the Middle Atlas (rugged) and further to 3,500 t km^{-2}. These figures led him to examine the kinetic energy of the raindrops falling on the land surface and its effect on eroding the soil Walling (1984) presented some hypothetical functional relationships between the so-called precipitation

aggresssivity index and sediment yield. He used the percentage of catchment occupied by certain rock types (Upper Cretaceous and Tertiary clays and marls) in northern Algeria as a parameter.

The slope of land surface is a major factors in the process of erosion caused by running water. Its detrimental influence can be reduced, though never be eliminated. It is therefore necessary to examine the relationship between the slope, surface runoff, soil type and vegetative cover on the rate of soil loss in attempt to bring the effect of the slope to a minimum. The work of Dunne in Kenya (1979) portrayed the role of vegetal cover and land use in tropical catchments on sediment yield. One of the important conclusions obtained is the tremendous reduction in the catchment sediment yield with the increase of the percentage of area occupied by forests.

6.5.4 Sedimentation in storage reservoirs- Patterns of the mean monthly river discharges have already been discussed in sub-section 6.3.2, and graphically illustrated by Figure 6.9. The seasonality index at a number of stream measuring stations is included in Table 6.3. Moreover, the interannual variability of river discharges has been reviewed in sub-section 6.3.4 and illustrated by Figure 6.12. The management of the natural supply of many an African river to cope with the demands on water for agriculture, electrical power, navigation and other purposes necessitates the construction of storage reservoirs. A storage reservoir is usually a natural facility where water is stored in times of excess or surplus to be released together with the natural supply during times of deficit or shortage.

Africa started to build reservoirs in the recent time since the 19^{th} century. The number of storage reservoirs has increased considerably in the course of time to the extent that Africa is sometimes referred to as the continent of dams. Dams and consequently the storage reservoirs formed by them vary so widely in their dimensions that some of them are called small dams, others large or high dams. The corresponding storage volume may vary from a few tens of million (10^6) m^3 to tens of billion or milliard (10^9) m^3. While describing African river basins in the next chapter, the hydrology of a number of the storage reservoirs will be discussed

The cross section of a reservoir is usually much wider and deeper than the cross section of the stream traversing it. This results in a considerable decrease in the average velocity of inflowing water, thereby encouraging the deposition of the transported sediment load. Tables 3_a through 3_e, Part II / Appendix B include some data on reservoir sedimentation in Africa. The rate at which the capacity of a reservoir is reduced by sedimentation depends on the rates of sediment inflow and outflow and the density of the deposited sediment. The live storage capacity of the Khashm el-Girba reservoir on the River Atbara dropped from 1,821 to 1,281 and further to 1,182, all in 10^6 m^3 in 1966, 1976 and 1981, respectively. These volumes correspond to storage level of 475 m above mean sea level. This example shows the said reservoir lost 35% of its original capacity in just 15

years. It is a generally accredited concept among water resources engineers that, when a reservoir losses 50% of its original live or conservancy volume, the reservoir has reached then a failure state. More detailed examples of reservoir sedimentation will be reviewed in the next chapter(s).

The rate at which sediment fills in a reservoir can be decreased through appropriate choice of dam and reservoir designs, certain reservoir operation rules, flushing and dredging. The reservoir engineer has to choose one or more of the reduction measures to extend the lifetime of his reservoir longer. The total storage volume of the reservoir formed by the High Aswan Dam (HAD), Egypt, was designed to accommodate the total inflowing sediment for a period of 300-500 years. As such, the total capacity has been subdivided into three volumes: one for live storage, another for dead storage (storage of sediments) and the third for flood protection. The quality of the water leaving a reservoir, where all or some of the inflowing sediment is entrapped in that reservoir, is different from the quality of water entering the reservoir. This state of affairs causes some damage, namely scour of the riverbanks and bed downstream the storage work. This damage, unless repaired effectively, might extend itself to some of the hydraulic structures on the river in question.

6.5.5 Sedimentation in canals and around hydraulic structures- The accumulation of sediments in irrigation canals represents a serious problem to all interested in land irrigation. Silt removal to clear the canals whether manually or mechanically is a tedious job. Maintenance of canal design sections to secure the proper flow of water can be costly. According to Hussein et al. (1986), about $20*10^6$ m^3 of sediment need to be cleared every season from the canals throughout the Gezirah and Managil irrigation scheme in the Sudan. Since the total area to be irrigated from this scheme is about $0.5*10^6$ ha, sediment should be removed at the rate of $40\ m^3\ ha^{-1}$.

Siltation in pumping station intakes, hydropower plants and around intakes of irrigation and water supply works imposes a serious problem. Irrigation and water supply authorities in many African countries are spending large sums of money to maintain the proper functioning of these structures. Next to sediment removal and clearance there is ongoing hydraulic research for quite sometime aiming at producing more efficient designs. The objective is avoid or reduce silt deposition at or around the critical parts of the said structures, instead to divert the sediment such that it remains transported by the water in the main stream.

CHAPTER 7

HYDROLOGY OF LARGE RIVER BASINS: Eastern and Western Africa

One of the most striking features of the African relief is the vast extent of level or gently undulating surfaces. This large extent is subdivided into a number of smaller basins separated by divides formed by fault blocks, mountain ranges and plateaus. Some of the erosion products of the divides have been deposited in these basins. Long ago the running waters began to cut their courses through the low-resistance sediment beds, thereby developing networks of streams. Major rivers such as the Congo, Zambezi, and Orange, for example, have carved out for themselves great valleys in troughs floored by the Karoo sediments (sediments of Permo-Carboniferous origin).

Seven or eight major rivers drain nearly two-thirds of the surface of Africa; much of the reminder is occupied by basins of inland drainage with no outlet to the sea (Stamp and Morgan, 1972). In this text, we shall divide the river basins "arbitrarily" according to the extent of their surface area into large, intermediate and small. The surface area of a large river basin is equal to or more than $1*10^6$ km^2, the intermediate between $1*10^5$ and $1*10^6$ km^2, and the small less than $1*10^5$ km^2. Table 3, Part I/Appendix B, includes 44 river basins. The surface area of these basins vary from $20*10^3$ km^2 to about $3.75*10^6$ km^2. It is worthwhile to mention that sometimes a river is referred to as the main river including its tributaries, i.e. what can be termed a river system. The Nile system, for example, includes the Main Nile, the White Nile, the Blue Nile, the Sobat, the Atbara, etc.

Rivers can also be classified into international and national rivers. The basin of an international river is shared by more than one state, whereas the basin of a national river is confined to just one state. The Niger and Congo are two examples of international rivers, while Tana and Pra are essentially national rivers. Rivers can also be classified according to their flow condition within the hydrologic year. Perennial rivers never run dry of water. Most of the perennial rivers have (a) high-flow season(s) and (a) low-flow season(s). The seasonality of the river discharge is expressed by the seasonality index, $(In)_s$, already discussed in Chapter 6. Table 6.3 gives the value of this index for several stations on a number of rivers. Different from perennial, there are rivers that flow only seasonally or intermittently. The index $(In)_s$ for such rivers is equal to infinity. Last, but not least, there are the so-called ephemeral streams, better known as wadis (in French the word oued is used for wadi). Wadis usually have small basins, and they carry water during and shortly after heavy rainstorms. Such streams are able to carry relatively excessive amounts of sediments along

with water during their floods. Many regions in North Africa depend largely on them for their water supply.

The present and following chapters deal only with large river basins: the Nile, Congo, Niger, Lake Chad, Zambezi and the Orange. Selected intermediate and small river basins will be dealt with in Chapter 9 whereas detailed discussion of lakes and storage reservoirs, including their hydrologic characteristics, will be reviewed together with the rest of wet lands in Chapter 10.

Chapter 7 will deal with the basins of the Nile and Niger Rivers, and Lake Chad, whereas the basins of the Congo, Zambezi and Vaal Rivers in Central and Southern Africa will be dealt with in Chapter 8. A general description of each river basin will be presented in short. This description will be followed by a discussion of the prevailing hydrological aspects of each basin.

7.1-The Nile Basin

7.1.1 Short description of the basin- The Nile Basin in its present situation covers a surface of about $2.9*10^6$ km^2, approximately one-tenth the surface area of Africa. The basin extends from 4°S to 31°N latitude and from 21° 30'E to 40° 30'E longitude. The highest and lowest points in the basin represent the top of the Ruwenzori Mountain range and the trough of the Quattarah depression, respectively. They are at elevations of 5,120 m above mean sea level (a.m.s.l.) and 159 m below mean sea level (b.m.s.l.) respectively.

The present basin of the Nile is a recent one. The river channel consists of flat reaches in certain sub-basins presently linked by steep channels. The Nile River is the second longest river in the world. Its length from the most remote source, at the head of the River Luvironza near Lake Tanganyika, to its mouth on the Mediterranean Sea is about 6,500 km. The River and its tributaries traverse ten countries, Tanzania; Uganda; Rwanda; Burundi; Congo (Kinshasa); Kenya; Ethiopia and Eritreia; the Sudan; and Egypt. The percentages of these countries in the total surface area of the Nile Basin, in their respective order, are: 3.8; 7.7; 0.7; 0.5; 0.8; 1.8; 12.1; 62.7; and 9.9% (Krishna, 1986). Some sources of information add the Republic of Central Africa as the 11^{th} riparian country. The map in Figure 7. 1 shows the Nile Basin.

The vast extent of the Nile Basin comprises areas with different climates. There are humid temper areas in the Equatorial and Abyssinian plateaus, temper because of their elevation. The northern Sudan and Upper Egypt have hot dry summers and agreeable winters. The summer along the Mediterranean Coast is dry and pleasant, and so is the winter except for light rain showers. The Tables available in Appendix A include climatic data for the different parts of the Nile Basin. Chapters 2, 3, 4, and 5 contain rather elaborate analyses of temperature, precipitation, evaporation and evapotranspiration.

The Great Rift Valley, which runs with some interruptions from Zimbabwe to the Jordan Valley including the Red Sea, is divided into two branches in the southern part of the Nile Basin. The stretch of the western branch lying within the Nile basin contains Lakes Edward, George and Albert, and continues north

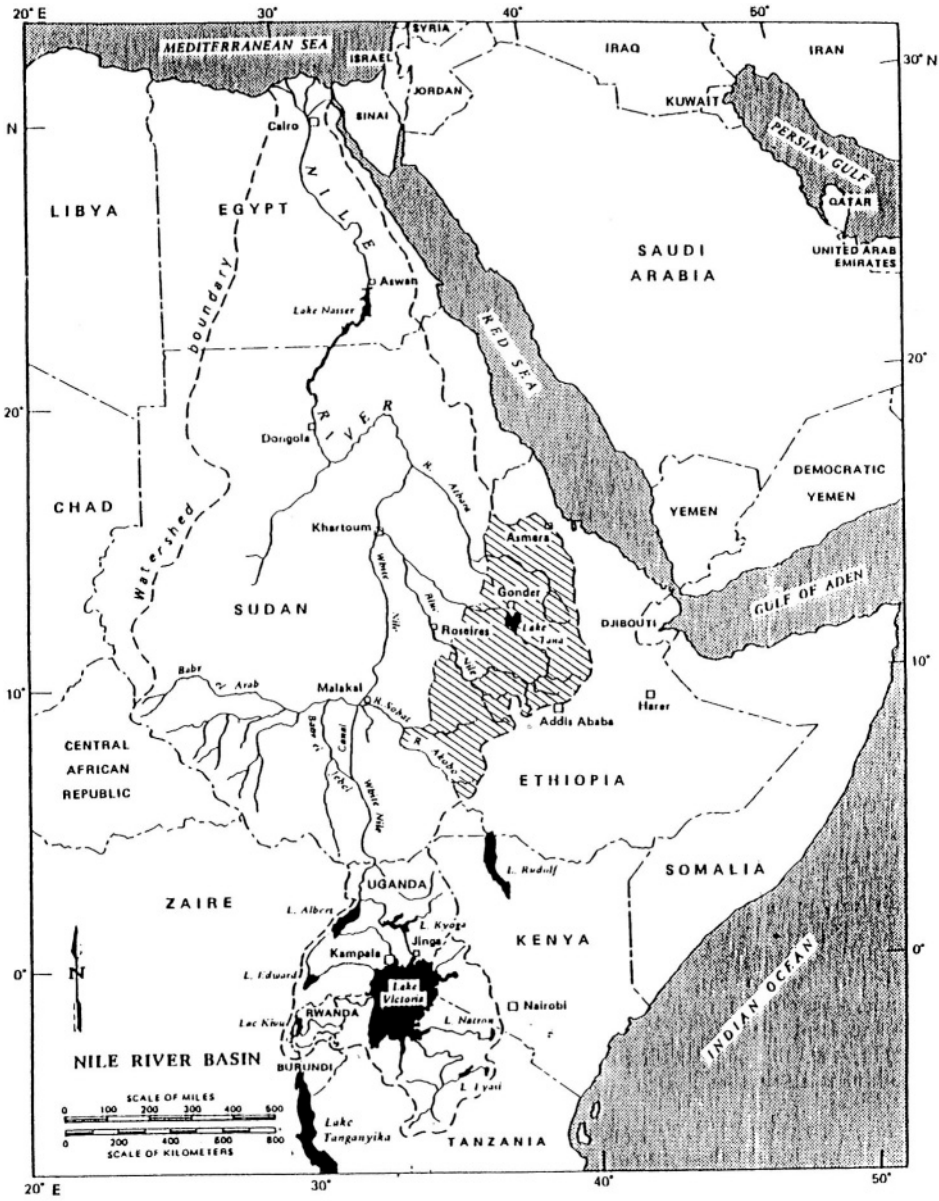

Figure 7.1- A general map of the Nile Basin. Shaded area shows parts of Ethiopia within the Nile River Basin

along Bahr el-Jebel. Lake Victoria lies shortly outside this stretch. The lake water surface covers 67,000 km^2 and has a catchment area of 193,000 km^2.

The Kagera is the most upstream tributary of the Nile and most important feeder of Lake Victoria. It has a basin of 64,000 km^2, most of it situated between 1200 and 1600 m a.m.s.l. The country level rises up to 2,500 m a.m.s.l. in the extreme west and further to 4,500 m to form the peaks of the Mufumbiro Mountain Range. The Kagera basin is a complex of streams of varying order, which are intercepted and interconnected by lakes and swamps. This complex includes the Luvironza/Ruvuvu, Nyavarongo, Akanyaru and Nyaranda rivers from the west and south, and the Kalangasa and Kakitumba and Ngono rivers from the east. A map of the Kagera basin is already shown in Figure 6.4.

The upper Victoria Nile is the only outlet of Lake Victoria and connects it with Lake Kyoga. The water surface of the river is rather steep, especially in the upper part as the Rippon, and the Owen Falls obstruct its channel. Since 1952 the Nile leaves Lake Victoria through the turbines of the power plant annexed to the Owen Dam, which is built at the foot of the Owen Falls.

Lake Kyoga is a shallow depression, also described as a submerged river valley, having a catchment of 75,000 km^2 in area including the lake itself, which at water level 1,030 m a.m.s.l. covers an area of 6,270 km^2. A considerable part of the lake catchment is covered with swamps, causing the evaporation to be in excess of the rainfall. As a consequence, the outflow from Lake Kyoga is more than the inflow. The lake outflow runs into the Kyoga Nile, which is sometimes called the Lower Victoria Nile. The Kyoga Nile runs generally as a sluggish swampy river till it enters Lake Albert through a swampy delta. The only exception lies in a certain length of the tailrace where, after a succession of rocks and rapids, the river descends the Marchison Falls.

Lake Albert has a surface area of 5,300 km^2 at the normal level of 617 m a.m.s.l., and a drainage basin of 17,000 km^2. In some places the escarpments of the Rift Valley, where Lake Albert is located, rise steeply to reach elevations above 2,000 m a.m.s.l. a short distance from the lake. Next to the Kyoga Nile, the Semliki River supplies Lake Albert with water. The Semliki river connects Lake Edward with Lake Albert.

The Kazinga Channel connects Lakes George and Edward. The two lakes have a combined surface area of 2,500 km^2 at the normal level, 915 m a.m.s.l., and a total basin area of 20,000 km^2. The Mbuku is the principal feeder of Lake George whereas the Nyamgasani, Berarara, Ishasha, Ruchuru, and Ruindi are the main feeders, which supply Lake Edward with their flow. These tributaries can carry considerable amounts of water during the flood season. As such, the runoff from a total surface of 30,500 km^2, including Lakes George and Edward themselves, is conveyed to Lake Albert through the Simliki River. The Nile flows out of Lake Albert at the extreme north comer of the lake under the name of the Bahr el-Jebel (Bahr = sea and el-Jebel = the mountain). It is sometimes referred to as the Upper White Nile. The major affluents of the Bahr el-Jebel

and the swamps and lakes already mentioned are summarized in the altitudinal map shown in Figure 7.2 (Thompson, 1975).

From the outlet of Lake Albert down to Nimule, 225 km downstream, the Bahr el-Jebel is a rather broad, sluggish stream fringed with swamps and lagoons. A number of small streams join the river from both sides in this reach. From Nimule to Rejaf, some 155 km, the river course is narrow and interrupted by rocky rapids as the Fola and Bedan. From Nimule to Mongalla, some 60 km below Rejaf the river is supplied with a number torrential streams. Of these streams, the Assua, Kala, and the Kit are the largest. The river reach from Rejaf to Malakal on the White Nile, except at Mongalla, is not confined to a single channel. North of Bor, 120 km below Mongalla, the valley widens and becomes less defined. Extensive swamps spread out on either side of the river and continue down to Lake No. The river runs northwards between walls of papyrus and tall swampy grasses. This region is known as the Sudd (Sudd means dam or

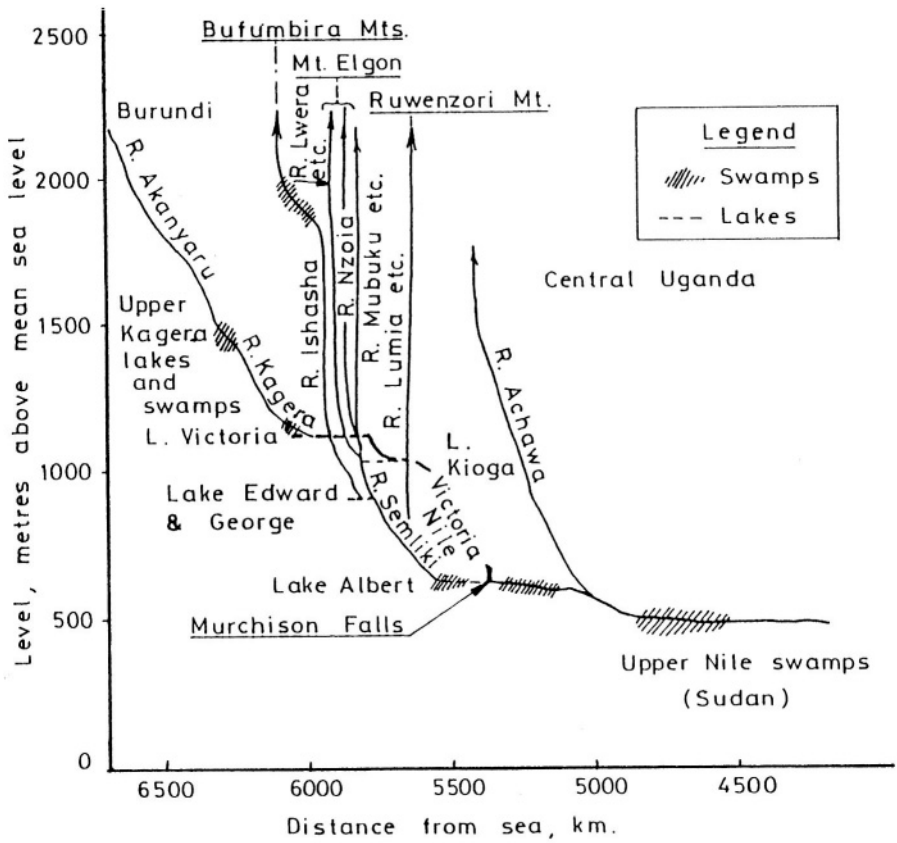

Figure 7.2- Altitudinal map of major affluents of the Upper Nile and the occurrence of swamps (based on Thompson, 1975)

blockage). Sutcliffe and Parks (1999) estimated the average monthly areas of flooding below Bor for the period 1905-83 as 12,800 km^2.

The Bahr el-Zaraf begins its own course more than 200 km below Bor at latitude 7° 20'N in the swamps east of the River Awai. The river has a winding course 280 km long up to its mouth on the White Nile, 80 km from Lake No. The flow in the Bahr el-Jebel in a normal year is divided such that 30% of it goes to Bahr el-Zaraf and the rest remains in Bahr el Jebel.

The Bahr el-Ghazal is a relatively short river with a basin of 520,000 km^2, the largest of any sub-basin in the Nile River system. While the average annual rainfall is 0.9-1.0 m the yield of this sub-basin measured at Lake No is $0.6*10^9$ m^3. All along the Bahr el-Ghazal and east of it are large areas of swamps, which are fed by a number of streams. The principal tributaries of Bahr el-Ghazal are: the Gel, the Yei or Lau, the Naam, the Meridi or Gel, the Tonj, the Jur, the Loi and Bahr el-Arab. The channels of these tributaries as shown on the map in Figure 7.3 disappear before reaching any outlet and their discharge is totally lost. Lake No is simply a shallow lagoon. At this point the sluggish Bahr el-Ghazal joins the Bahr el-Jebel, after having lost a huge volume of water in the vast swamps in its basin. The Bahr el-Jebel below Lake No changes its name to the White Nile. The Bahr el-Zaraf joins the White Nile about 65 km below Lake No. The White Nile, after a short distance, starts to change its course till it is joined by the River Sobat and the combined stream assumes gradually a northerly direction.

The Sobat Basin, approximately 225,000 km^2, includes most of the plain east of the Bahr el-Jebel and Bahr el-Zaraf, and parts of the Abyssinian mountains and the Lakes Plateau. The Sobat is formed by its principal tributaries, the Baro and the Pibor. The surface area of the basins of these two tributaries is 41,400 and 10,000 km^2, respectively. Each of these basins is intersected by a number of smaller streams, some of which can be described as swampy khors (khor is the local name for a small stream). A short distance upstream from the Baro-Pibor junction, some water leaves the Baro through khor Machar to feed a large swampy area known as Machar swamp. This swamp is a permanent source of loss from the Baro. From the Baro-Pibor junction to the mouth of the Sobat, the country is a flat plain intersected by swampy depressions or Khors. Near it's mouth, the Sobat mouth has a surface width varying from 100 to150 m and depth of section from 3.5 to 6.5 m, depending on the season.

The White Nile below the confluence of the Sobat flows due north for a distance of about 800 km from Malakal to just upstream of Khartoum, where it is joined by the Blue Nile. The river because of its too mild slope is for the larger part sluggish. Despite this state, the river is practically free of swamps and has a well-defined channel. The White Nile between Malakal and Khartoum is simply a long narrow lake without any tributary. Since the average annual evaporation is much more than the average annual precipitation, the White Nile remains a source of loss.

Some 40 km upstream the confluence of the Blue Nile at Khartoum, a dam was built at Jebel Aulia around 1937 to store water for the interest of Egypt. The rapid silting up of this reservoir and the construction of the Aswan high Dam in Egypt in 1965 have eliminated its function.

The Blue Nile Basin has an area of 324,500 km^2. This includes 17,000 km^2, which represent the surface area of the lake basin including the lake itself. Lake Tana is a fresh water body in north central Ethiopia occupying a surface of 3,400 km^2 at the normal water level. The Blue Nile and its tributaries all rise on the Ethiopian Plateau at an elevation of 2000 to 3000 m a.m.s.l (Figure 7.4). Next to direct rainfall on its surface, some feeders supply Lake Tana with water. From this lake the Blue Nile (Greater Abbai) flows in a large loop before it drops 50 m into the Tissisat Falls. A short distance downstream, the river begins to cut a deep gorge in the Plateau, which in some places is about 1200 m below land level on either side. Several rock-outcrops occur in the channel bed, the last of which are the Damazin Rapids, a few kilometers from the Roseires and about 1,000 km from the river source beyond Lake Tana. The Roseires is located about 120 km far from the frontier between Ethiopia and the Sudan. Just before crossing this frontier, the river runs through a vast clayey plain, at an average elevation of 490 m a.m.s.l. The construction of the Roseires Dam was completed in 1966. Nearly 270 km below the Roseires, there is another storage work known as Sennar or Makwar Dam. The reservoir formed by this dam has been used since 1925 for regulating the flow of the Blue Nile to supply water in time for cotton irrigation in the Gezira plain (the land located between the White and Blue Niles).

The Dinder and the Rahad join the Blue Nile in the reach between Sennar and Wad-Medani. These two rivers are strongly seasonal, with catchments of 16,000 and 8,200 km^2 respectively. The Blue Nile continues its course below the confluence of the Rahad for about 160 km before reaching Khartoum. At Khartoum, the Blue Nile joins the White Nile and the combined waters flow in the Main Nile.

The Atbara, the last tributary in the Nile system, joins the Main Nile at about 320 km downstream from the confluence of the Blue Nile. The river is 880 km long and the greater part of its catchment is in Ethiopia. Some parts of the catchment are at elevation of more than 3000 m a.m.s.l. The total catchment of the Atbara is 112,000 km^2, of which 68,000 km^2 represent the sub-catchment of the Setit, the principal tributary of the Atbara. The Atbara runs dry for 5 to 6 months each year. Its floodwater has the highest concentration of suspended sediment among all rivers in the Nile system. However, since the yield of the Atbara Basin is 20-25% the yield of the Blue Nile Basin, the total sediment yield of the Atbara is much less than the sediment yield of the Blue Nile. At a distance of about 400 km south-east the river mouth at Atbara on the Main Nile, the construction of the Khashm el-Girba Dam was completed in 1964.

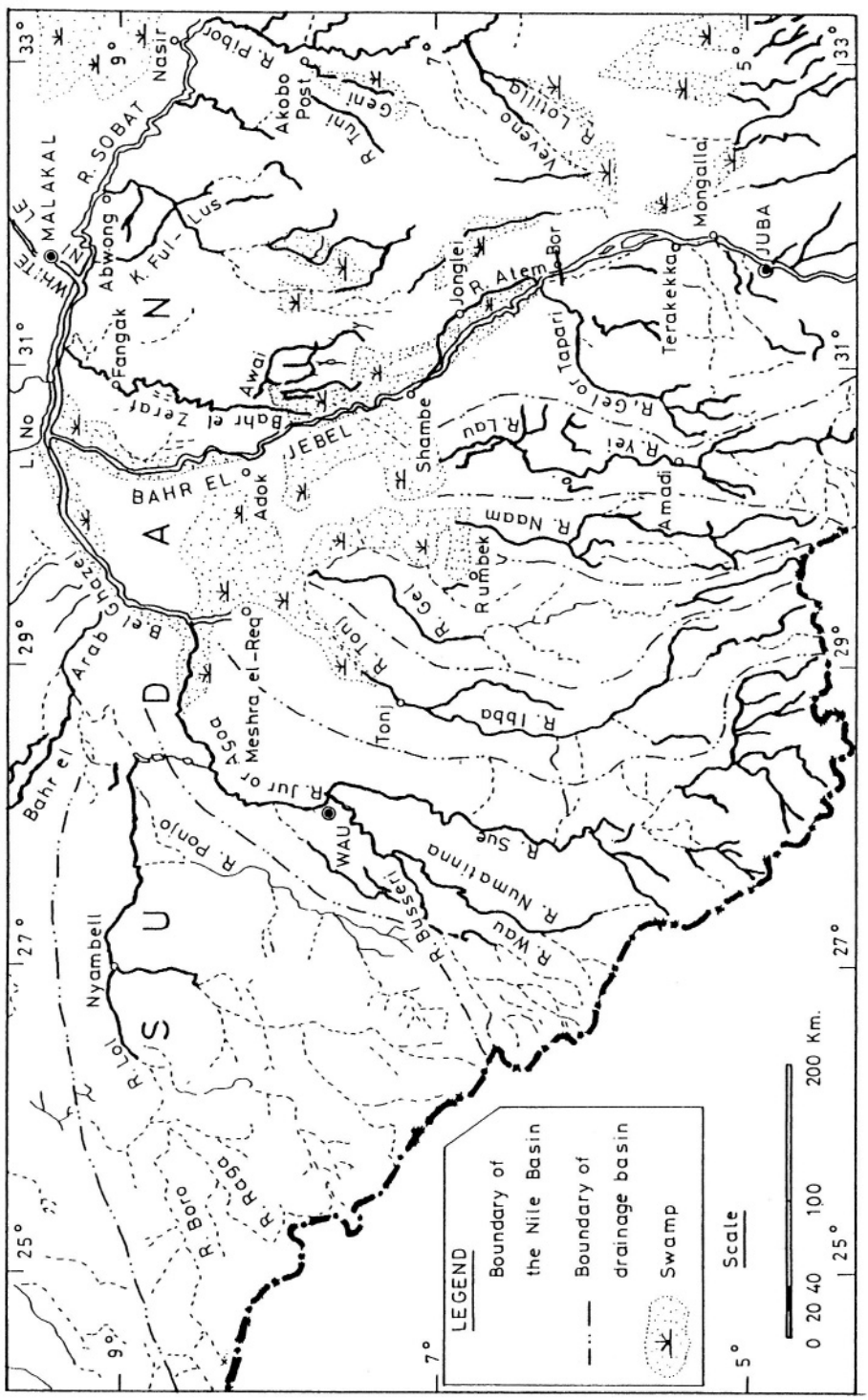

Figure 7.3- Map of the Bahr el-Jebel and Bahr el-Ghazal basins (from Shahin, 1985)

The Main Nile runs from Khartoum to Aswan in a region of Nubian sandstone overlying an eroded surface of chrystalline rocks that has been laid bare at some places in the course of the still incompletely degraded river bed. The river channel, 1,885 km long, consists of a series of placid reaches of mild slope separated by rocky rapids (cataracts). The sixth cataract (called Shabluka) is about 80 km north of Khartoum and the first one is at Aswan. A longitudinal profile of the river channel showing the locations of all six cataracts is shown in Figure 7. 5. The hydraulic section in this reach varies from a minimum of **800 m^2** to a maximum of about **7,000 m^2**, depending on the location and season of the year. The section is capable of carrying up to **$11*10^3$ m^3 s^{-1}**.

The Old Aswan Dam was built at Aswan between 1898 and 1900 and put into operation a year later. The original storage capacity was raised twice; once

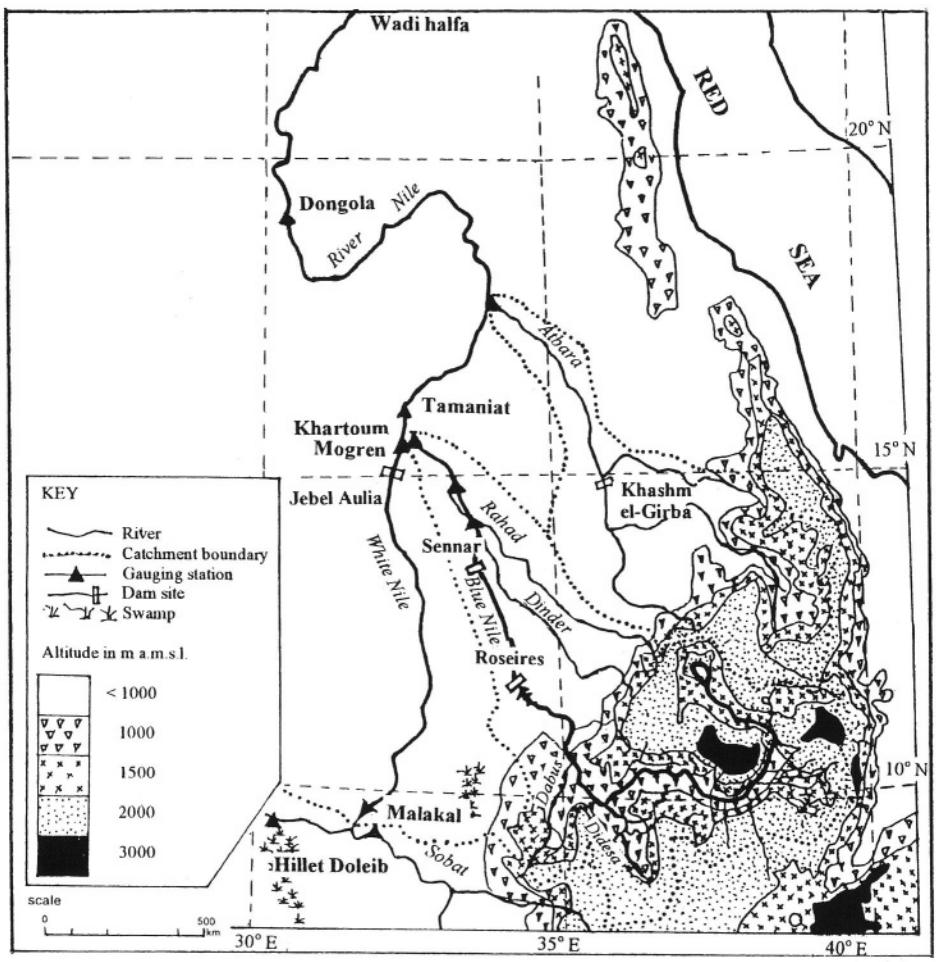

Figure 7.4- Map of the Blue Nile and the Atbara basins (based on Sutcliffe and Parks, 1999)

in 1912 and a second time in 1937. The available capacity in 1937 added to the storage capacity of the Jebel-Aulia reservoir in the Sudan used to improve the natural supply of the river in the low-flow season, basically for land irrigation. In the 1950s the total storage capacity seemed to be inadequate, and a much greater storage reservoir has to be created to cope with the interests of both Egypt and the Sudan This necessity has been fulfilled upon the construction of the Aswan High Dam around 1965. The lake formed by this dam, about 7,000 km^2 at the highest flood level, covers parts of Egypt and the Sudan. The part situated in Egypt is called Nasser Lake (after late President G. Abdel Nasser of Egypt) and the part in the Sudan is called Lake Nubia. The Nile water at Aswan, after deducting the losses, is divided between Egypt and the Sudan.

The share of Egypt in the Nile water flows below Aswan to the Delta after supplying the Nile Valley with its water needs. In its natural condition, the length of the river reach from Aswan to the apex of the Nile Delta is about 950 km. The Esna, Nag-Hammadi and Assiut barrages (open type dams) are built in this reach across the river to control the water level for the purposes of irrigation and navigation. Actually these barrages, the head regulators and the irrigation canals of the different classes are part of the well and long-established free irrigation system in Egypt. The functionality of these barrages, however, has dramatically changed due to the scour of the river section after the construction of the Aswan High Dam. The map, Figure 7.6, shows the locations of the storage and control works on the Nile and its tributaries.

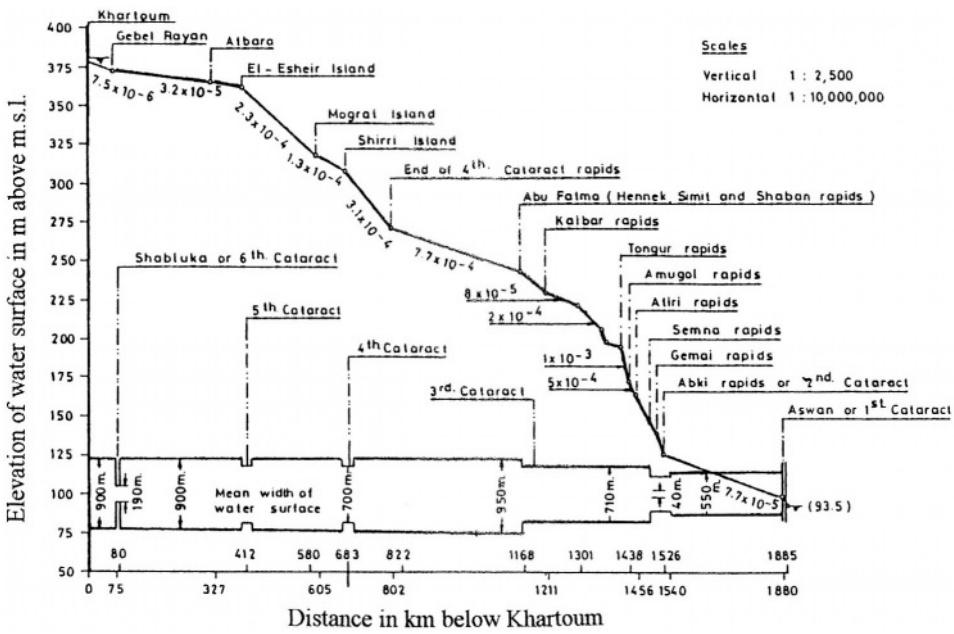

Figure 7.5- Longitudinal profile and plan view showing the water surface and cataracts in the Main Nile between Khartoum and Aswan (Shahin, 1985)

Almost 23 km north of Cairo the river bifurcates into the Rosetta and Damietta branches. At the bifurcation point the Delta barrage (formerly known as Mohammed Ali Barrage) was completed in the latter half of the 19^{th} century. Each branch is equipped with a barrage built at some distance above the promontory of the branch on the Mediterranean Sea. These barrages have certainly been of great help for irrigation in the Nile Delta area in the pre-High Dam era. Presently most of their function goes to navigation and preventing the seawater from intruding into the Nile branches in the low-flow season.

N.B. For more detailed information about the geography and physiography of the Nile Basin the reader is referred especially to the following material:

The Lake Plateau Basin of the Nile (Hurst, 1927, Paper 23)
The Nile Basin, Vol. I (Hurst & Philips, 1931)
The Nile Basin, Vol. V (Hurst & Philips, 1938)
The Nile Basin, Vol. VIII (Hurst. 1950)
The Nile Basin, Vol. IX (Hurst et al., 1959)
Hydrology of the Nile Basin (Shahin, 1985)
The River Nile (Said, 1993)
The Hydrology of the Nile (Sutcliffe & Parks, 1999)

7.1.2 Water balance of the basin- The Kagera basin supplies Lake Victoria with an average of $7.9*10^9$ m^3 (Shahin, 1985). The figure of $7.4*10^9$ m^3 has been given as average for the period 1956-1978 by WMO (1982). This figure has been based on runoff coefficient of 0.1 and annual rainfall of 1.1 to 1.2 m.

Other than the Kagera, a number of streams flow into the lake and all sources together contribute twice that from the Kagera alone (Sutcliffe and Parks, 1999). The outflow from the lake is simply the sum of the inflow to it plus the net precipitation (precipitation minus evaporation) plus the change in lake storage. The mean annual lake outflow varies significantly from one period of record to another as can be seen from the following figures (Shahin, 1985):

Period of record		Length of	Mean annual
From	to	record, y	outflow, 10^9 m^3
1896	1945	50	21.4
1906	1932	27	20.6
1946	1961	16	20.1
1962	1970	9	43.9
1946	1970	25	28.6
1896	1970	75	23.8

It is remarkable that the annual figure given by Sutcliffe and Parks (1999) for the outflow at Jinja is $28.6*10^9$ m^3 for the period from 1940 to 1977. When the tremendous rise in water level, inflow and outflow is excluded and assuming that there is no change in storage, the lake outflow can be taken equal to the

inflow. This is $15*10^9$ (inflow by the Kagera and other streams) + $67*10^9$ (water surface area) x 0.1 (direct precipitation – evaporation) = $20.7*10^9$ m^3 y^{-1}.

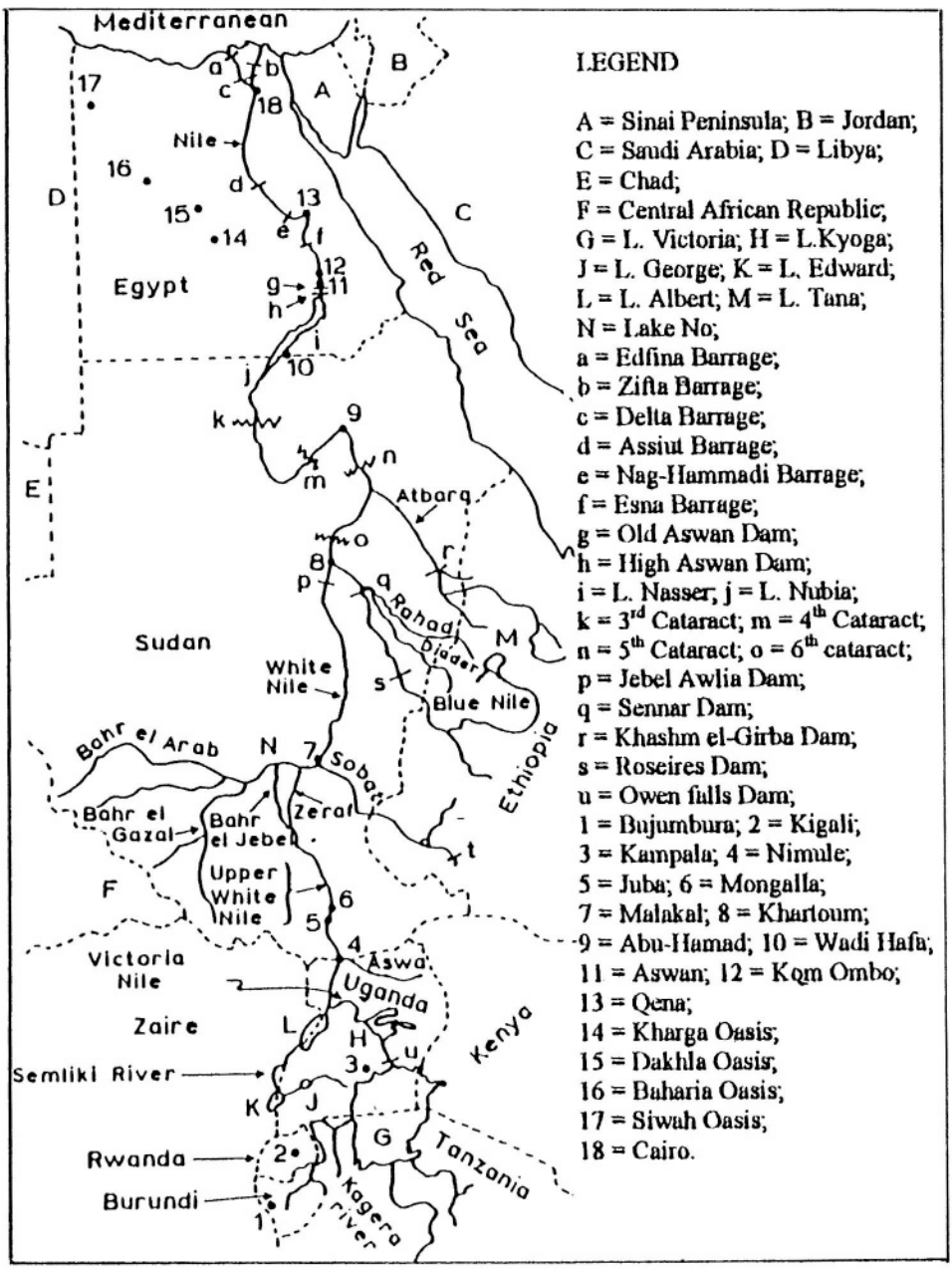

Figure 7.6- Map showing the locations of some of the major storage and control works in the Nile Basin (based on Kashef, 1981)

The monthly figures for the outflow at Jinja for the period 1940-1977 are included in Table 7.1. The same Table shows that for the same period of record, 1940-1977, the outflow of Lake Kyoga at Masindi Port is almost the same as the inflow. As a matter of fact, Lake Kyoga has never been a source of gain. On the contrary, for certain periods of time, it has been a source of loss of water. Below Masindi Port and before flowing into Lake Albert, the Kyoga Nile gains a little water thereby increasing its flow by 2-3%. The flow at Kamindi compared to the flow at Masindi Port for the same period of record verifies this conclusion.

The inflow supplied to Lake Albert by the Kyoga Nile, $29.9*10^9$, added to the runoff carried by the Semliki, $4.6*10^9$ brings the total supply to $34.5*10^9$ m^3 y^{-1}, as an average for the period 1948-1970. Albert Lake receives less water from rainfall than what it looses by evaporation. The annual loss can be estimated as $5.3*10^9*0.8 = 4.24*10^9$ m^3. From 1904 up to 1955 the outflow from Lake Albert used to be read from a rating curve established between the discharge at Mongalla on the Bahr el-Jebel and tle lake level at Butiaba. The discharge at Mongalla used to be corrected for the losses in the reach between Butiaba and Mongalla (440 km). This technique gave the mean annual outflow for the period 1904-1947 as $24.6*10^9$ m^3. Since 1956, the readings have been obtained from the Panyango-Packwach rating relationship.

The lake annual outflow is the sum of the inflow via the Kyoga Nile and the Semliki River ($34.5*109$ m^3) added to the runoff from the lake basin ($17*109*1.25*0.125=2.66*10^9$ m^3) minus the loss from the lake itself ($4.24*10^9$ m^3), and the change in storage (estimated as - $0.29*109$ m^3). This balance gives the mean annual outflow from the lake for the period 1948-1970 as $32.8*10^9$ m^3. This figure too is the same as the mean for the period 1940-1977 given in Table 7.1 by Sutcliffe and Parks (1999).

The outflow of Lake Albert flows for a distance of 225 km before it reaches Nimule. A short distance below Nimule the Assua River joins the Bahr el-Jebel. The catchment area of the Assua is 39,000 km^2 receiving annual rainfall of about 1.3 m in an average year . The Bahr el Jebel flows a distance of 440 km from the outlet of Lake Albert to Mongalla, a key hydrological station. Other torrential rivers in the reach Nimule-Mongalla together with the Assua supply Bahr el Jebel by an amount estimated at less than $3*10^9$ m^3 in a normal year. The average for the period 1940-1977, however, has been estimated as $4.7*10^9$ m^3 y^{-1} (Table 7.1).

The sum of the outflow from Lake Albert plus the supply of the torrential streams reduced by the losses, estimated as 4%, brings the average annual flow at Mongalla for the period 1940-1977 to about $36*10^9$ m^3. As a matter of fact, this figure varies from one period of record to another period as shown in Table 7.2. The largest mean flow figure, $49.56*10^9$ m^3 y^{-1}, belongs to the period 1962-1983, whereas the least flow figure, $26.63*10^9$ m^3 y^{-1} corresponds to the period 1905-61. The gratifying conclusion here is that for the two longest periods of

Table 7.1- Mean monthly and annual flows, 10^9 m^3, at a number of sites in the Equatorial Lakes Plateau, 1940-1977 (Sutcliffe and Parks, 1999)

Jan	Feb	Mar	Apr	May	Jun	Jul	Aug	Sep	Oct	Nov	Dec	Year
Victoria Nile at Jinja												
2.35	2.13	2.37	2.38	2.59	2.57	2.52	2.44	2.33	2.32	2.22	2.39	28.6
Kyoga Nile at Masindi Port												
2.33	2.05	2.18	2.12	2.34	2.37	2.52	2.57	2.53	2.60	2.47	2.49	28..6
Semliki at Bweramule												
0.35	0.29	0.32	0.35	0.41	0.37	0.39	0.42	0.41	0.42	0.44	0.42	4.6
Outflows from Lake Albert												
2.83	2.46	2.62	2.53	2.68	2.62	2.71	2.77	2.77	2.92	2.91	3.00	32.8
Torrent flows between Lake Albert and Mongalla												
0.0	0.0	0.0	0.12	0.41	0.39	0.54	0.97	0.97	0.77	0.40	0.13	4.7

record, 1912-73 (62-years) and 1905-83 (79-years), the two means are $31.38*10^9$ and $32.96*10^9$ respectively, the difference is in the order of 5%.

Salas (1981) analyzed the series of annual outflows of the Equatorial Lakes. He referred to the abrupt upward shifts in these series, which began in 1962, and remained for several years higher than the outflows during the period 1900-1961. It appears that the extreme net basin supply during 1961-1963 is the main causal factor of such shifts. He examined the possibility of using each of the ARMA, exponential autoregressive (EAR), shifting level, and the intervention models. The last model, which was chosen to simulate the outflows of Lakes Victoria and Albert and to predict their future behaviours, can be expressed as:

$$Z_t - \mu = \frac{\omega_o}{(1-\delta B)}(\xi_t - \xi_m) + \varepsilon_t \qquad (7.1)$$

where Z_t = outflow for year t, μ = mean annual outflow, ω_o = initial jump, δ = damping factor, B = backward shift operator $B\xi_t = \xi_{t-1}$, ξ_t = exogenous variable describing the effect of the extreme event, i.e. a pulse input with a mean of ξ_m and ε_t = stochastic "noise term". On the basis of stochastic analyses of the pre-1961 outflow data, an AR (2: φ_1, φ_2) was identified for the outflow series of both lakes. Subsequent diagnostic checks proved this model to be adequate for the noise component. The best results were obtained when 3 pulses and 2 pulses were used for ξ_t-series of Lakes Victoria and Albert respectively. The model parameters are as follows:

Parameter	Lake Victoria outflow (3 pulses), 10^9 m^3	Lake Albert outflow (2 pulses), 10^9 m^3
ω_o	11.592	22.601
δ	0.914	0.906
φ_1	0.827	0.854
φ_2	- 0.278	-0.303

Figure 7.7 shows the annual outflow series of Lake Albert and the fitted dynamic component of the intervention model described by Eq. (7.1) (Salas, 1981).

It is quite regrettable that discharge measurements at Mongalla have been stopped since the hydrological year 1984-85 as a consequence of the state of belligerence between the northern Sudan and southern Sudan. This situation has urged researchers to try to generate artificial flow sequences. Elwan et al. (1996) found that a stochastic model, such as ARMA (1,2), can be satisfactorily used for synthetic annual flow data at Mongalla, Hillet Doleib on the Sobat, and Malakal on the White Nile. The proposed model can be written as:

$$Z_t - \mu = \alpha(Z_{t-1} - \mu) + \varepsilon_t + \theta_1\varepsilon_{t-1} + \theta_2\varepsilon_{t-2} \qquad (7.2)$$

where Z_t = annual flow at a year t, μ = mean annual flow, Z- μ = first differenced flow, $\{\varepsilon_t\}$= a purely random process with zero mean and variance σ_ε^2. The quantities α, θ_1, and θ_2 are model parameters, and obtained as:

Station	α	θ_1	θ_2	*constant*
Mongalla	0.77	0.489	0.483	0.056
Hillet Doleib	-0.177	0.425	0.533	-0.004
Malakal	0.511	0.472	0.581	0.047

The monthly flow sequences for these stations can best be obtained by multiplying the generated annual sequences by certain weights representing the monthly distribution flow pattern, as found from the historical record.

The width of the Bahr el-Jebel swamps increases from about 3 km at Mongalla to 7 km some 30 km to the north. The width of the river valley at Bor, 140 km north of Mongalla reaches 9 km. A short distance north of Bor, the valley becomes crowded with lagoons and intersecting channels. On the eastern side appears the Atem-Awai system of rivers. They ultimately join to form the Upper Zeraf. At this point 7° 30'N the swamp occupies a width of 30 km increasing up to 35 km at latitude 7° 40'N (see the map, Figure 7.3).

Sutcliffe and Parks (1999) gave the average monthly estimated areas of flooding as 9,400 km^2 for the normal period, 1905-1960; 22,300 km^2 for the wet period, 1961-80; and 12,800 km^2 for the whole period, 1905-80. Assuming that the annual net loss (evapotranspiration minus rainfall) is 1.2-1.3 m, the corresponding estimates of losses should be $11.3*10^9$ m^3, $28.9*10^9$ m^3 and $16.6*10^9$ m^3 for the three periods of record in their respective order. Given the inflow to the swamps as 26.8, 49.2, and 33.3, all in 10^9 m^3, for 1905-60, 1961-83 and 1905-83, respectively, the swamp outflow for the same periods were given as 14.2, 20,8, and $16.1*10^9$ m^3 (Sutcliffe and Parks, 1999).

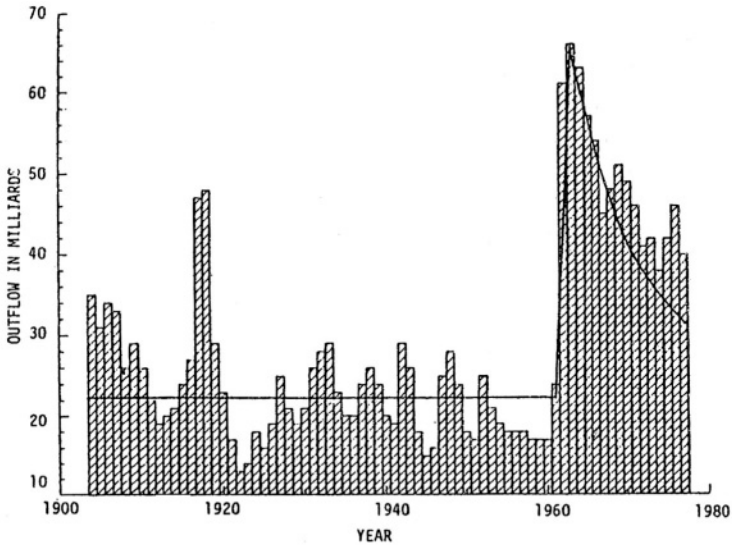

Figure 7.7- Time series of the annual outflow of Lake Albert and the fitted dynamic component of the intervention model (based on Salas, 1981)

The outflow of the swamps can be computed as the difference between the flow at Malakal on the White Nile minus the yield of the Sobat at Hillet Doleib, near the mouth on the White Nile, minus the yield of the Bahr el-Ghazal. As the last term is too small in magnitude, it is sometimes dropped from the calculation.

The differences between the inflows and outflows for the three used periods of record agree fairly well with our estimates using the annual depths of precipitation and evapotranspiration. Another approach is based on the relationship developed by Shahin (1985), which gives the water lost, L, in percent of the annual river flow at Mongalla, V_M, in 10^9 m^3:

$$L = 2.25V_M - 0.0175V_M^2 \tag{7.3}$$

According to Eq. (7.3), the losses for the aforementioned periods of record in their respective order are 47.7% ($12.8*10^9$ m^3), 68.3% ($33.6*10^9$ m^3), and 55.5% ($18.5*10^9$ m^3). The results obtained from Eq. (7.3) are slightly different from the corresponding estimates using the other methods. The Sudd monthly series of inflows and outflows for the period 1905-1983 are shown graphically in Figure 7.8 (Sutcliffe and Parks, 1999). The outflow of the Sudd swamps continue to the White Nile such that approximately 30% of the flow goes to the Bahr el-Zeraf and the rest remains in the Bahr el-Jebel.

In an attempt to reduce the losses resulting from the flooding of excessive areas in the swamps (Sudd), the excavation of a bypass canal known as Jonglei canal has been planned as early as the 1940s. Assuming that the canal flow is about 230 m^3 s^{-1}, the reduction in the total flooded areas (permanent plus

seasonal swamps) have been estimated as 4, 700, 5,800, and 5,000 km^2 for the conditions that prevailed in the periods 1905-60, 1961-80 and 1905-80, respectively. This means saving an annual volume between 5 and $6*10^9$ m^3 measured at Malakal on the White Nile.

The Bahr el Ghazal Basin is located west of the Bahr el Jebel. The mean annual depth of rain over the basin is no less than 800 mm. The area above the swamps yield a considerable amount of water distributed among the well-defined tributaries as follows (Ahmed, 1960):

River	Location	Flow, 10^9 m^3 y^{-1}
Lol	Nyamlel	4.0
Pungo	Aluk	0.5
Jur	Wau	5.0
Tonj	Tonj	1.5
Gel	Chui Bet	0.55
Naam	Mvolo	0.52
Yei	Monderi	2.0
Total		14.07

Other estimates suggest an annual yield varying between $11.3*10^9$ and $16.0*10^9$ m^3 y^{-1}. However large the yield is, it flows into the swamps and only $0.6*10^9$ m^3 y^{-1} reaches the river mouth at Lake No. A conservation scheme was planned to save a great deal of the water lost in the swamps. The scheme comprises the excavation of a deep interceptor drain to collect the above-tabulated flows. This means that the alignment of the proposed drain should pass through the points where flow measurements were taken. The water intercepted by the drain should be pumped to the Bahr el-Jebel above Mongalla. To avoid the loss of this supply, the number of channels comprising the Jonglei canal should be increased. Last, but not least, the channel of the While Nile should be reinforced to be able to carry this extra discharge. Probably, the consequences of the scheme for the ecology of the swamps of the Bahr el-Ghazal were among the reasons that this drainage scheme did not receive much attention.

The reach below Lake No to the mouth of the Sobat, 125 km in length, is joined by a number of small tributaries. This reach is a source of net loss since the gain from the tributaries discharging into it is exceeded by the losses caused by the swamps. The total net loss was estimated by Hurst and Philips (1938) as $0.875*10^9$ m^3 y^{-1}.

The Principal tributaries of the Sobat, as said earlier, are the Baro and the Pibor. The Upper Baro receives about $11.5*10^9$ m^3 in a normal year. As the slope in the lower part of the basin is much smaller than the slope of the upper part the yield of the former is about $2.6*10^9$ m^3. The losses, however, bring the total flow of the Baro at its Junction with the Pibor down to $7.6*10^9$ m^3 instead

loss of a considerable proportion of its yield. Part of the loss goes to the Machar swamps. Hurst et al. (1966) estimated the surface area of the swamps as 6,700 km^2. The inflow to the swamps is supplied through three sources, the direct rainfall, 0.9 m y^{-1}, the runoff from the eastern tributaries estimated as $1.44*10^9$ m^3 y^{-1}, and a certain part of the spillage from el-Baro estimated at about $2.67*10^9$ m^3 y^{-1}. The sum of these three sources comes to $10.1*10^9$ m^3 y^{-1}.

The yield of the Pibor at its junction with the Baro was estimated by Hurst (1950) at about $3.1*10^9$ m^3. As such, the total flow at the head of the Sobat below the confluence of the Pibor should be $10.7*10^9$ m^3 y^{-1}. The yield of Khors Fullus, Nyading, Twalor and Waku, the main tributaries of the Sobat, augments this amount to $13*10^9$ m^3 at Hillet Doleib, 9 km above the mouth, near Malakal on the White Nile. Table 7.2 shows that the discharge at Hillet Doleib is nearly constant for the three periods, 1905-61, 1962-83, and 1905-83.

The flow at Malakal is the sum of the flow of the Sobat at mouth, the flow below the swamps of Bahr el- Jebel, and at Lake No plus any possible gains and losses en route. The figures given in Table 7.2 show that the flow at Malakal in the periods 1905-61 and 1905 1995 are simply equal to the flow below the Bahr el-Jebel swamps plus the yield of the Sobat. The sum of these two flows for the period 1961-1995 is about $1.6*10^9$ m^3 more than the flow at Malakal. The flow at Malakal continues its way in the White Nile for nearly 800 km without gaining any water. On the contrary, the net flow at Mogren/Khartoum, above the confluence of the Blue Nile, is less than the upstream flow at Malakal.

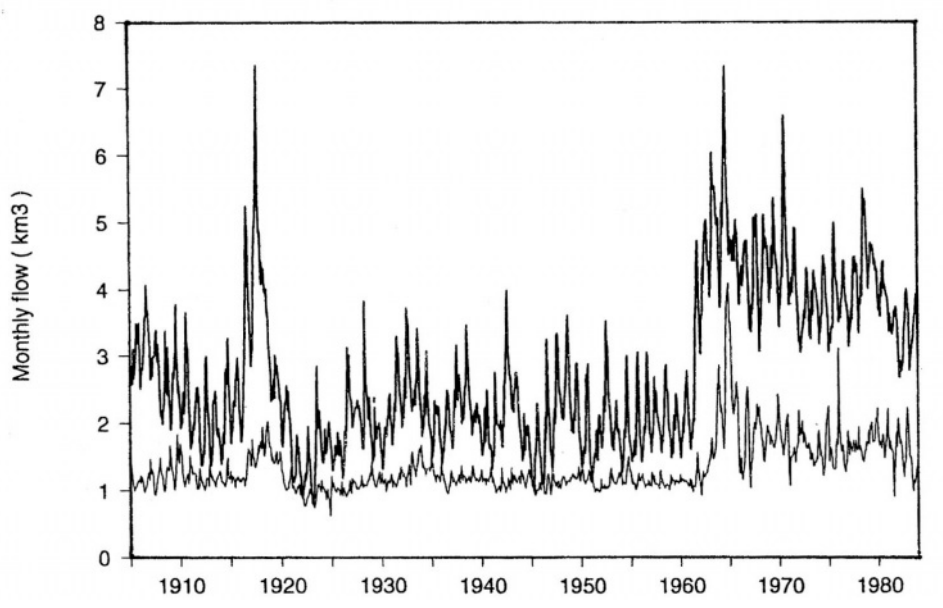

Figure 7.8- Sudd monthly inflows and outflows, 1905-1983 (based on Sutcliffe and Parks, 1999)

Table 7.2- Basic statistics of the monthly and annual flows at Mongalla, Hillet Doleib and Malakal using different periods of record

Item	Magnitude of statistic in 107 m3												
	Jan	Feb	Mar	Apr	May	Jun	Jul	Aug	Sep	Oct	Nov	Dec	Year
Mongalla / Bahr el-Jebel													
Xm (1)	233	203	214	219	263	252	273	318	312	310	278	258	3,138
Xm (2)	271	235	252	255	297	288	312	362	360	355	318	300	3,605
Xm (3)	197	169	179	183	221	212	235	271	271	265	239	218	2,663
Xm (4)	395	343	368	365	405	393	420	467	463	470	442	423	4,956
Xm (5)	252	217	231	234	272	262	287	325	324	322	295	276	3,296
s (5)	107	93	101	98	106	103	105	113	123	128	116	112	1,286
Cv (5)	0.42	0.43	0.44	0.42	0.39	0.39	0.37	0.35	0.38	0.40	0.39	0.41	0.39
Cs (5)	0.73	0.75	0.77	0.83	0.92	0.86	0.77	0.64	0.83	1.06	0.62	0.64	0.73
Hillet Doleib / The Sobat													
Xm (3)	93	36	25	22	41	87	130	160	178	201	200	175	1,348
Xm (4)	106	60	34	26	42	81	130	162	178	195	189	166	1,369
Xm (5)	97	44	27	23	41	85	130	161	178	199	196	172	1,353
s (5)	73	48	39	24	24	22	17	15	18	23	31	57	266
Cv (5)	0.74	1.07	1.29	0.92	0.55	0.25	0.13	0.09	0.10	0.12	0.16	0.33	0.20
Cs (5)	1.15	2.99	4.77	3.11	2.12	0.76	0.28	0.82	0.99	0.37	(-0.2)	(-0.1)	1.10
Malakal / White Nile													
Xm (1)	245	174	170	148	165	202	251	287	308	340	331	316	2,944
Xm (3)	227	155	148	136	154	193	241	276	296	325	314	297	2,762
Xm (4')	279	206	197	178	192	223	277	314	362	372	365	348	3,285
Xm (5')	247	175	167	152	169	204	255	291	311	343	334	0	2,965
s (5')	86	63	55	36	32	29	28	34	43	52	56	73	525
Cv (5')	0.35	0.36	0.33	0.24	0.19	0.14	0.11	0.12	0.14	0.15	0.17	0.23	0.18
Cs (5')	1.42	2.44	3.25	1.86	0.95	0.72	1.07	1.41	1.86	2.01	1.98	1.12	1.56

Explanation

Xm = mean monthly discharge; (1) = 1912-73 (Shahin, 1985); (2) 1940-77 (Sutcliffe and Parks, 1999); (3) = 1905-61; (4) = 1962-83; (5) = 1905-83 (Elwan, 1995); (4') = 1961-95; and (5') = 1905-95 (Sutcliffe and Parks, 1999); s = standard deviation; Cv = coefficient of variation; and Cs = coefficient of skewness.

Assuming that the average width of the water surface is 1.0 km and the difference between evaporation and precipitation is in the order of 2.0 m, the annual loss must be about $1.6*10^9$ m^3. This used to be the case till the Jebel Aulia Dam, 44 km above Khartoum, was completed in 1937. The lake created by the dam has quite large water surface areas at high levels. Additionally, it is very likely that some water, otherwise unaccounted for, is drawn for land irrigation.

These situations, added to the rise of the water levels of the Equatorial Lakes since 1961-1962 that lasted for more 25 years, are very likely responsible for the significant increase of the losses between Malakal and Mogren. The average annual flow was 24.64 at Mogren against 27.63 at Malakal for the period 1911-

60, 28.13 at Mogren against 32.85 at Malakal for the period 1961-95, and 26.03 at Mogren against 29.64 at Malakal for the period 1911-95, all flows are in 10^9 m^3 (Sutcliffe and Parks, 1999). One should not forget that the function of the Jebel el-Aulia as a storage reservoir has practically stopped since 1965, after the construction of the Aswan High Dam, Egypt.

The hydrology of the Blue Nile begins by Lake Tana and its basin. The lake water surface at elevation of 1800 m a.m.s.l.is 3,000 km^2 and its basin area is 13,750. The annual evaporation and precipitation are nearly balanced, both equal to about 1,500 mm. Due to its slope and cover the runoff from the lake catchment has been estimated as 0.2. This means that the outflow from the lake is in the order of $4*10^9$ m^3. The Blue Nile, below the outlet of Lake Tana, receives a number of tributaries: the Chimbili, Bashile and Jamma in the upper reach, and the Didesa, Dabus, and Balas in the lower reach. It has been observed that the flow in the Blue Nile increases gradually with distance from the outlet of Lake Tana. The average annual flow at Roseires, 935 km below Tana, for the period 1912-73 is $49.22*10^9$ m^3, with 0.1884 as a coefficient of variation (Shahin, 1985). The average flows at Roseires/Deim as given by Sutcliffe and Parks (1999) are 50.34, 46.41, and $48.66*10^9$ m^3 for the periods 1912-60, 1961-97, and 1912-97, respectively. The reduction in the annual flow in the period 1961-97 has been brought up by the drought that swept over Ethiopia in the 1970s and 1980s.

The Roseires Dam was built between 1961-66, with the aim of releasing the water stored in the flood season to the downstream when required by the Gezirah, Mangil extension and the river bank pup scheme, all for the benefit of the Sudan. The design storage capacities are $3*10^9$ m^3 and $7.6*10^9$ m^3 corresponding to the first phase (level 480 m a.m.s.l.) and the second phase (level 490 m a.m.s.l.), respectively. The discharge of the Blue Nile downstream from Er-Roseires flows a distance of 270 km before reaching Sennar without receiving any supply.

The net loss in the reach Roseires-Sennar can be reasonably assumed to be 1.85 m y^{-1}. This is equivalent to annual transmission losses of $0.5*10^9$ m^3. A storage reservoir was built at Sennar in 1925, with a design storage capacity of $0.8*10^9$ m^3, to supply water when required for cotton irrigation in the Gezirah Plain. The mean and coefficient of variation of the annual flows of the Blue Nile that passed through Sennar in the period 1912-73 are $47.2*10^9$ m^3 and 0.212 respectively (Shahin, 1985).

The Blue Nile below Sennar flows northwest for a distance of 350 km before joining the White Nile at Khartoum. In the reach Sennar-Khartoum, the Dinder and the Rahad Rivers join the Blue Nile. The drainage basin of the Dinder River is 16,000 km^2, receiving annually a rainfall depth of 800-850 mm, and has an estimated runoff coefficient of 0.22. These bring us to a basin yield of 2.9-$3.0*10^9$ m^3 in an average year. This estimate is in agreement with the old figure of $2.97*10^9$ m^3 appearing in the Nile Basin, Vol. IX, as an average for the period 1912-1950. The same reference (Hurst et. al, 1959) suggests $3.83*10^9$ m^3 for an

exceptionally high year as 1946. The calculations made by Sutcliffe and Parks (1999) resulted in the figures of 3.086, 2.374 and 2.797, all in 10^9 m^3, for the Dinder at mouth, as averages for the periods 1907-60, 1961-97 and 1907-97 respectively.

The Blue Nile below Wad Medani receives the Rahad River. The basin of the Rahad is 8,000 km^2 in area receiving annual depth of rain of 800-850 mm and having a runoff coefficient of 0.16. These figures combined give an average yield of about $1.1*10^9$ m^3. Vol IX of the Nile Basin (Hurst et. al, 1950) gave $1.08*10^9$ m^3 as an average figure for the period 1912-50. Also, Sutcliffe and Parks (1999) gave the figures of 1.145, 1.044, and 1.102 $*10^9$ m^3 y^{-1} for the periods 1908-60, 1961-97, and 1908-97, respectively. It should be well remembered here that the Dinder and Rahad are two strongly seasonal rivers. They run dry from the end of December to the end of June each year.

The river reach between Sennar and Khartoum undergoes the usual conveyance losses. Assuming that the average width of the surface water is 0.8 km, the annual evaporation less precipitation 2.25 m y^{-1}, the annual loss becomes $0.67*10^9$ m3. As such, the expected annual flow at Khartoum above the Blue Nile confluence with the White Nile should be 47.2 + 2.97 + 1.1 – 0.67 or $50.6*10^9$ m^3. The discharge measurements at Khartoum from 1912-73 give $50.37*10^9$ m^3 as the average annual flow, with 0.204 as the variation coefficient. Again, the many years with below-average flows from 1970 onwards have resulted in average annual flows of $40.2*10^9$ and $48.2*10^9$ m^3 for the periods 1961-95 and 1900-95 respectively.

The Tamaniat, the first key station on the Main Nile, is located 41 km below the confluence of the Blue Nile. The basic statistics of the annual flow series at Tamaniat from 1912 to 73 give an average of $75.56*10^9$ m^3, with variation coefficient of 0.1506. This figure is approximately 1.3% less than the sum of the $26.0*10^9$ of the White Nile and $50.6*10^9$ of the Blue Nile, which has been obtained from a number of flow measurements and estimates. Again, when the three periods 1911-60, 1961-95, and 1911-95 are considered one gets an average annual flow of 76.05, 67.69, and 72.69, all times 10^9 m^3 (Sutcliffe and Parks, 1999).

The Main Nile flows 277 km below Tamaniat in a desert country before it reaches the Hassanab station, almost 5 km above the Atbara junction. The rate of net loss in this reach can be reasonably estimated at 2.8 m y^{-1}, bringing the net volume of water lost to $1.2*10^9$ m^3 y^{-1}. As such the estimated average annual flow above the confluence of the Atbara becomes $75.4*10^9$ m^3. The corresponding average figure for the period 1912-73, based on discharge measurement only, is slightly less. The difference between the measured and estimated flows is quite similar to the flow figures at Tamaniat. The average figure obtained from discharge observations is $74.28*10^9$ m^3 with a variation coefficient of 0.134. The figures obtained by Sutcliffe and Parks (1999) for the periods 1911-60, 1961-95, and 1911-95 are 74.48, 67.33, and 72.34, all in 10^9 m^3 y^{-1}, respectively.

The Atbara basin, 100,000 km^2 in surface area, can be divided into the upper sub-basin or the basin of the Setit, 68,000 km^2 receiving an average annual rainfall of 800 mm, and the lower sub-basin, 32,000 km^2 receiving an average rainfall of 300 mm. Since the surface of the upper sub-basin is steeper in slope compared to the lower sub-basin, the runoff coefficients have been fairly assumed as 0.2 and 0.1, respectively. These pieces of information yield a total runoff of $11.84*10^9$ m^3 in a normal year (Shahin, 1985). The average flow of the Atbara at mouth amounted to $11.89*10^9$ m^3 with 0.329 as variation coefficient, both for the period 1912-73. The average annual flow for the period 1974-82 dropped to just $8.28*10^9$ m^3, i.e. 70% of the average for the period 1912-73. The drop of $3.61*10^9$ m^3 can be attributed to the losses by evaporation and leakage ($0.42*10^9$ m^3 y^{-1}), added to the withdrawal for irrigation ($1.42*10^9$ m^3 y^{-1}), all from the Khashm el-Girba reservoir put into operation since 1965. The remaining $1.77*10^9$ m^3 y^{-1} can be attributed to the harsh drought that swept over Ethiopia in the 1970s and 1980s (Shahin, 1988). This drop has recovered but slightly in the subsequent years as appears from the figures given by Sutcliffe and Parks (1999). The reported average annual flows are 12.29, and 8 62, both in 10^9 m^3, for the periods 1911-60 and 1961-94 respectively.

Dongola is the first key station on the Main Nile at a distance of 760 km below the confluence of the Atbara. The overall average width of the river channel is 400 m. The river in this reach runs in a hyper arid condition where an average rate of free water evaporation of 7.5 mm d^{-1} is not unusual. As such, the expected loss by evaporation between the mouth of the Atbara at Atbara and Dongola should be about $0.825*10^9$ m^3. The mean and coefficient of variation of the annual flow series for the period 1912-73 are $85.57*10^9$ m^3 and 0.151, respectively. The sum of the annual flows at Hassanab above the Atbara confluence and the Atbara at mouth for the same time period is 74.28 + 11.89 = $86.17*10^9$ m^3. This means that the net loss is $0.6*10^9$ m^3 y^{-1}, which is somewhat less than the evaporation loss already estimated as $0.825*10^9$ m^3 y^{-1}. The annual figures given by Sutcliffe and Parks (1999) are not very consistent, as they place Dongola with Wadi halfa and Kajnarty in one line without consideration of the fact that Wadi Halfa/Kajnarty is about 450 km downstream of Dongola. The average annual flow in the Main Nile at Wadi Halfa/Kajnarty/Dongola for the periods 1890-1910, 1911-60, 1911-95, and 1890-1995 are 97.26, 86.13, 73.09, and 84.14, all in 10^9 m^3, respectively. Assuming the average flow for the period 1890-1905 to represent 100%, the percentage flows for the other periods represent 115.6 for 1890-1910, 102.4 for 1911-60, and 86.9 for 1961-95. These figures show that despite the marked rise in the water levels and discharges of the rivers and lakes in the Equatorial Plateau in the period 1961-1995, the severe droughts that prevailed over the same period in the basins of the Abyssinian (Ethiopian) rivers have dominated the flow in the Main Nile.

The Main Nile flows a distance of 450 km downstream from Dongola before reaching Wadi-Halfa and further 345 km before reaching Aswan, the last key station on the Nile. The river thus flows between Dongola and Aswan, a total

distance of 895 km in a hyper-arid region with no precipitation to mention and annual evaporation in the order of 2.8-3.0 m. This situation means an additional loss of $(2.5\text{-}3.1)*10^9$ m^3 $y\text{-}1$. One can thus get the annual flow at Aswan by subtracting this loss from the annual flow at Dongola. The average figure given by Shahin (1985) for the period 1912-73 was $82.2*10^9$ m^3 with variation coefficient of 0.185. This average is about 4% less than the average flow arriving at Aswan in the period 1869-1992

The Aswan High Dam, which has been in operation since 1965, has created a huge reservoir for regulating the natural supply of the main Nile to safe guard the interests of Egypt and the Sudan. The average loss by evaporation from the reservoir at the high storage levels is assumed to be about 7-7.5 mm d^{-1}. Sadek et al. (1997), using estimation methods suitable for inadequate, data obtained the figure 6.0 ± 0.3 mm d^{-1}, which is 20% less than the figure in current practice. The large extent of water surfaces corresponding to high storage levels easily brings the loss by evaporation at high water levels to $(11\text{-}12)*10^9$ m^3 y^{-1}.

The flow at Aswan in the pre-High Dam era was not fully utilized. The long-term average flow was taken as $85*10^9$ m^3 y^{-1}, of which $32*10^9$ m^3 used to be released to the Mediterranean Sea to avoid flooding the country in the flood season. The remaining volume used to be shared by Egypt $(48.5*10^9)$ and the Sudan (4.5*109). The old Nile guaranteed these shared water treaties. In the post-dam era, i.e. since 1965, the control and regulation of the river flow have become complete. The total annual loss by evaporation and leakage, if any, is set at $11*10^9$ m^3. The remaining volume is divided such that the ratio of the share of Egypt to the share of the Sudan is 3 to 1. The same ratio applied to the then corresponding populations of the two countries. As such Egypt gets a total of $55.5*10^9$ m^3 and the Sudan gets $18.5*10^9$ m^3. The new shares give Egypt a gain of $7*10^9$ m^3 y^{-1} and the Sudan $14*10^9$ m^3 y^{-1}.

The water balance of the Main Nile at Aswan for the water year 1981-82 is included in the annual report (1981-82) of the Permanent Technical Joint Committee (PTJC) for the Nile waters as follows:

Total amounts withdrawn by the Sudan (estimated at Aswan) = $12.596*10^9$ m^3
Storage losses from the reservoir of the Aswan High Dam = $11.679*10^9$ m^3
Storage losses from the Jebel Aulia reservoir (estimated at Aswan) = $1.960*10^9$ m^3
Flow downstream the Aswan High Darn = $55.663*10^9$ m^3
The sum of these figures give a natural supply estimated at Aswan = $81.898*10^9$ m^3

The above-estimated supply is $0.462*10^9$ m^3 or 0.56% smaller than what is available in the record of the Nile flow at Aswan.

The share of Egypt in the Nile water in the post High Dam era is maintained at nearly the same every year ever since 1965. It flows out of the Aswan reservoir, and successively downstream of each of the Esna Barrage, the Nag-Hammadi Barrage and Assiut Barrage, all in Upper and Middle Egypt. These barrages are located on the Main Nile at distances of 166, 359, and 539 km

below Aswan, respectively (Figure 7.6). Some of the downstream flow below the Assiut Barrage is used for land irrigation and other purposes in the reach between Assiut and Cairo. The discharge passing Cairo is divided between the two branches of the Nile, the Damietta and Rosetta, and the rest goes to the major canals (Rayyahs) and main irrigation canals.

7.1.3 River stage- As already mentioned in Chapter 6, river discharge and water stages, both at the same location, are related together by a rating function. Figure 7.9 shows stage hydrographs of the Nile and its tributaries at stations 142 (Mongalla), El-Nasir on the Sobat, 88 (Malakal), 37 (Khartoum), 34 (Dongola), and 33 (Aswan). Two stage hydrographs for each station are presented, one for the average of certain years of record ending by 1977 and the other for the water year 1981-82. For more stage hydrographs at other sites and other periods of record, the reader is referred to Shahin (1985) and Sutcliffe and Parks (1999).

The longest hydrological record of river stage, maxima and minima, in existence for any river in Africa, perhaps anywhere in the world, is that of the Nile River at Roda Island near Cairo, Egypt. The maxima and minima levels, which date back to 622 AD, have been recorded by the Arab historians Taghri Birdi and Al-Hijazi. Records have been compiled by Prince Omar Tousson from 622 up to 1921 AD, by Abul-Mahasin from 641 to 1451 AD, Ibn Iyas from 769 to 1878 AD. Cap. Lyons took care of the period from the last decades of the 19^{th} century till the early part of the 20^{th} century.

The Roda Nilometer was built in 711 or 715 AD, depending on the source of information. From the time of its construction till the end of the 19^{th} century, the Nilometer has been reconstructed, renovated or repaired at least eight times, not to mention that the stage measurements for about four centuries starting from the middle of the 15^{th} century, i.e. during the Ottomans invasion of Egypt, were either neglected or destroyed. This state of affaires led Yevjevich (1984) to suggest not using the recorded sequences for any scientific purpose. Instead, he suggested keeping them for their historical and monumental value.

Popper (1951) is credited with introducing the necessary corrections to the maxima and minima series. This has made it possible for a number of investigators to analyze the corrected and undamaged data. Balek (1977) analyzed the maxima data for 849 years (Birdi and Al-Hijazi) and 663/849 years (Birdi/Al-Hijazi) in search of the periodicity in the Nile Levels. He traced periodicities from 6 y to 556 y. He also referred to the 7.3 and 20.5-32.2 y periodicities mentioned by Hurst in relation to the sequences of natural flow at Aswan. Balek (1977) fitted an autoregressive model to the Taghri Birdi minima sequence, which can be written as follows:

$$y_t = 0.42y_{t-1} + 0.10y_{t-2} + 0.06y_{t-3} + 0.10y_{t-5} + 0.02y_{t-6} + 0.04y_{t-11} +$$

$$+ 0.11y_{t-13} + \varepsilon_t \qquad (7.4)$$

where, $y = x - x_m$, x = water level, in m, above local zero level of the gauge, and x_m = mean of x = 10.80 m. Similarly, the autoregressive model fitted to the maxima can be written as:

$$y_t = 0.20y_{t-1} + 0.07y_{t-2} + 0.09y_{t-3} + 0.06y_{t-4} + 0.04y_{t-6} + 0.02y_{t-7} +$$

$$+ 0.05y_{t-8} + 0.08y_{t-9} + 0.06y_{t-10} + 0.10y_{t-13} + 0.09y_{t-17} + \varepsilon_t \qquad (7.5)$$

where, $y = x - x_m = x - 16.99$, and ε_t is a stochastic term with mean and variance as given earlier. The model results and the observed data are shown together in Figure 7.10. The author's remark is that the sum of all terms after y_{t-3} in Eq. (7.4) can be changed without significant error to $0.27\ y_{t-5}$, and all terms after y_{t-4} in Eq. (7.5) can be summed up to $0.44\ y_{t-5}$ with a little approximation.

The minima sequence recorded by Al-Hijazi covering 849 y (621-1449 AD) was analyzed and modeled by an ARMA (2,1) model (Hipel and McLoed, 1978). The same sequence has been later re-analyzed by Aguado (1987). The auto correlation function (ACF) and the partial correlation function (PCF) of the raw data suggest the possibility that the data are non-stationary. Furthermore a linear regression of the data with time indicates a significantly rising trend that can be explained by gradual siltation of the riverbed. The ARIMA model (2,2,1) that was fitted to the said sequence can be written as:

$$x_t = 1.36x_{t-1} - 0.26x_{t-2} - 0.10x_{t-3} - 0.93\varepsilon_{t-1} + \varepsilon_t \qquad (7.6)$$

Aguado (1987) gave the parameters of a wide variety of models ranging from AR (1) up to ARIMA (2,1,1). Reusing (1994), in his analysis and model building, used somewhat shorter series than the series used by either Balek (1977) or Aguado (1987). The series he considered were a complete series of 755-y (715-1469) for the maxima levels and a complete series of 756-y (715-1470) for the minima levels. The basic statistics and model parameters of the ARMA (3,1) and (2,1) are as follows:

Sequence	N, y	r_1	H	φ_1	φ_2	φ_3	θ_1
Maxima	755	0.33	0.77	1.10	-0.13	0.01	0.88
Minima (log-transformed data before modeling)	756	0.55	0.87	1.17	-0.23	-	0.76

Explanation:
N is the length of sequence, r_1 is the first serial correlation coefficient, H is the Hurst coefficient, φ_1, φ_2 and φ_3 are the parameters of the autoregressive component of the model, and θ_1 is the parameter of the moving average component of the model.

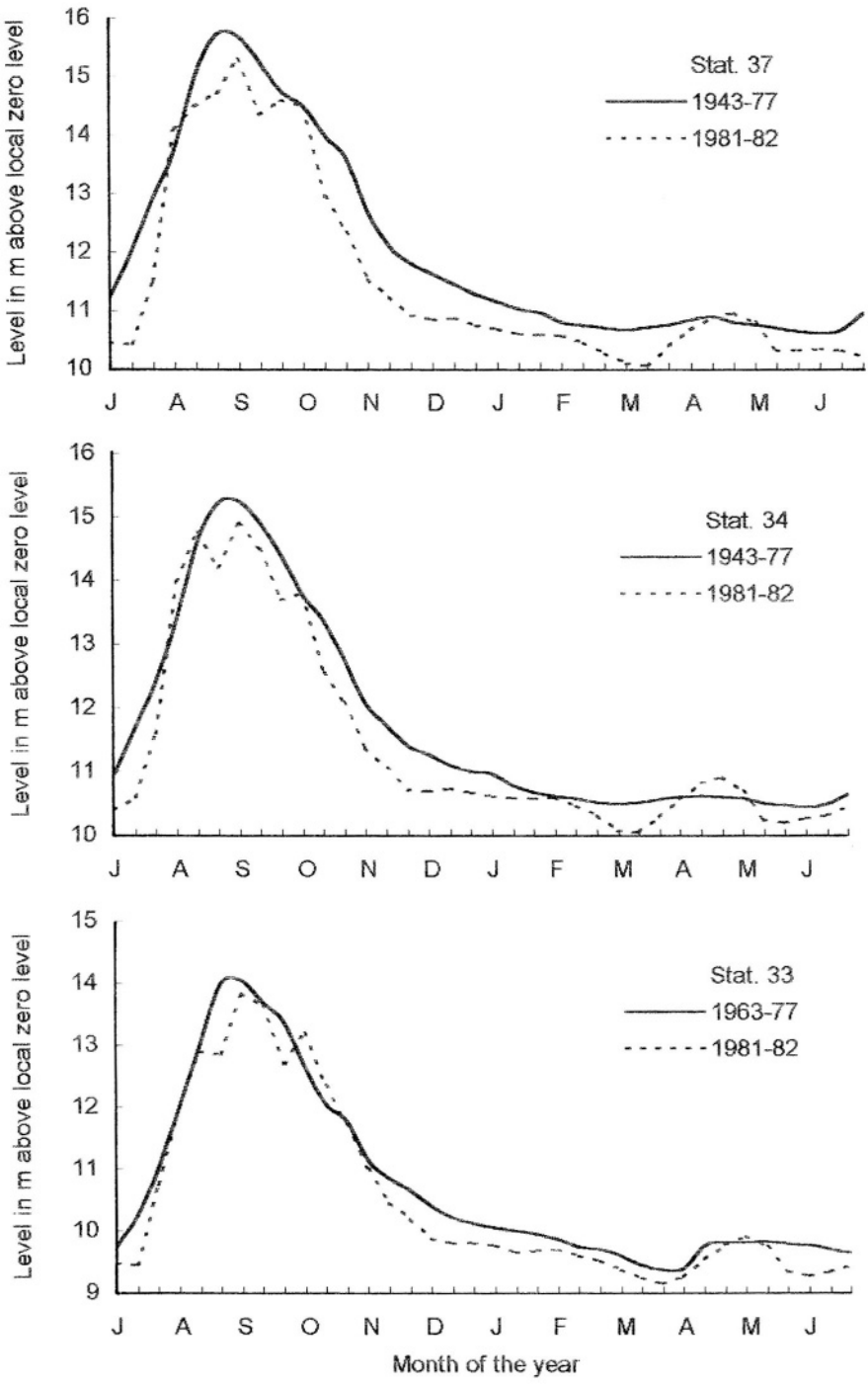

Figure 7.9- Water level hydrographs for some key stations in the Nile Basin

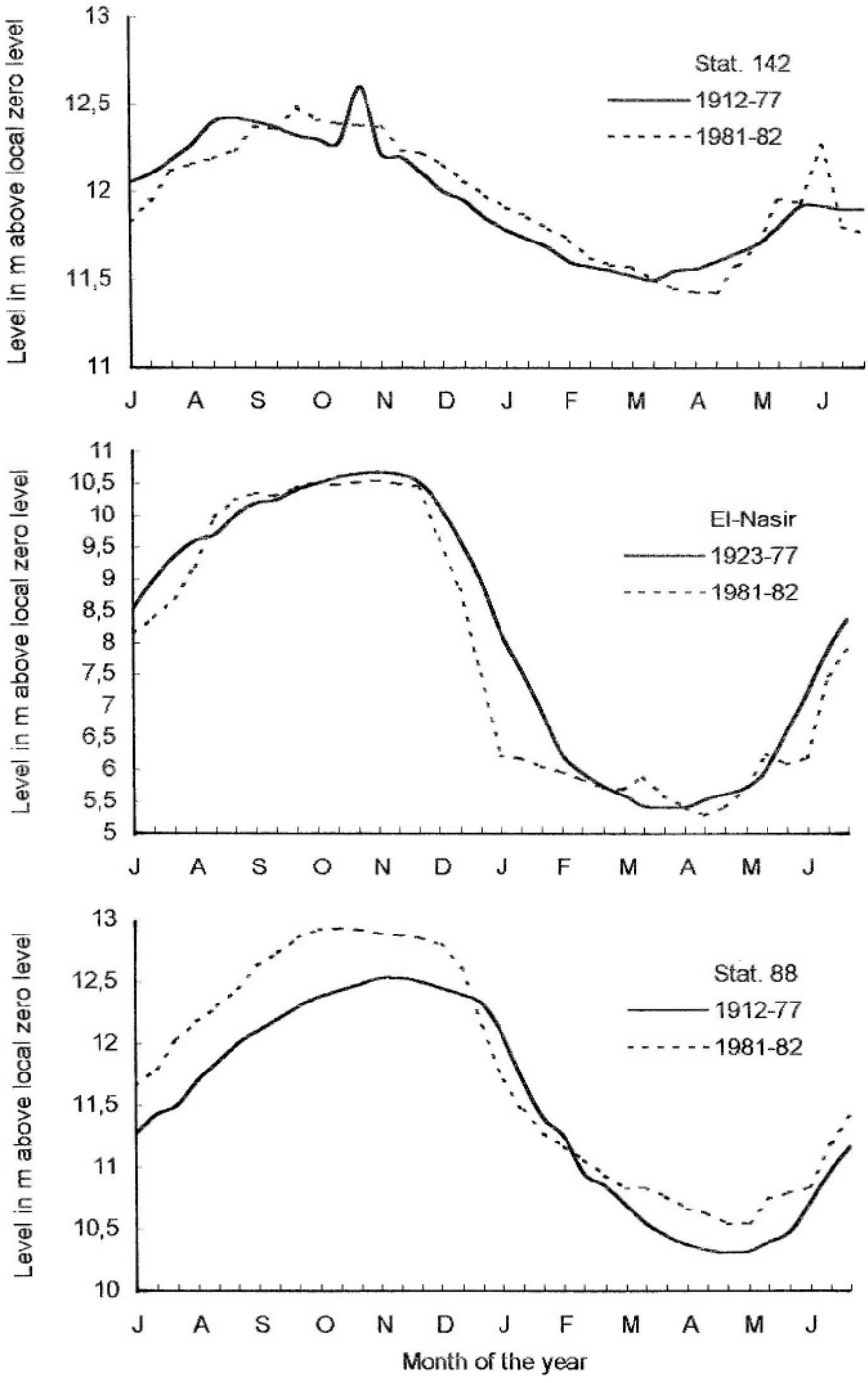

Figure 7.9 Cont'd- Water level hydrographs for key stations in the Nile Basin

The analysis of the maxima and minima series shows that strong long-term persistence is an important characteristic. This has been clearly indicated both from the range analysis, resulting in high values of the Hurst coefficient, and also from the autocorrelation analysis. The same conclusion can also be reached from the analysis performed by Balek (1977) and Aguado (1987). The research work performed by Reusing (1994) basically aimed at drought-risk analysis using the stage records at Roda. gauge, Egypt. The results obtained will be presented in the next section.

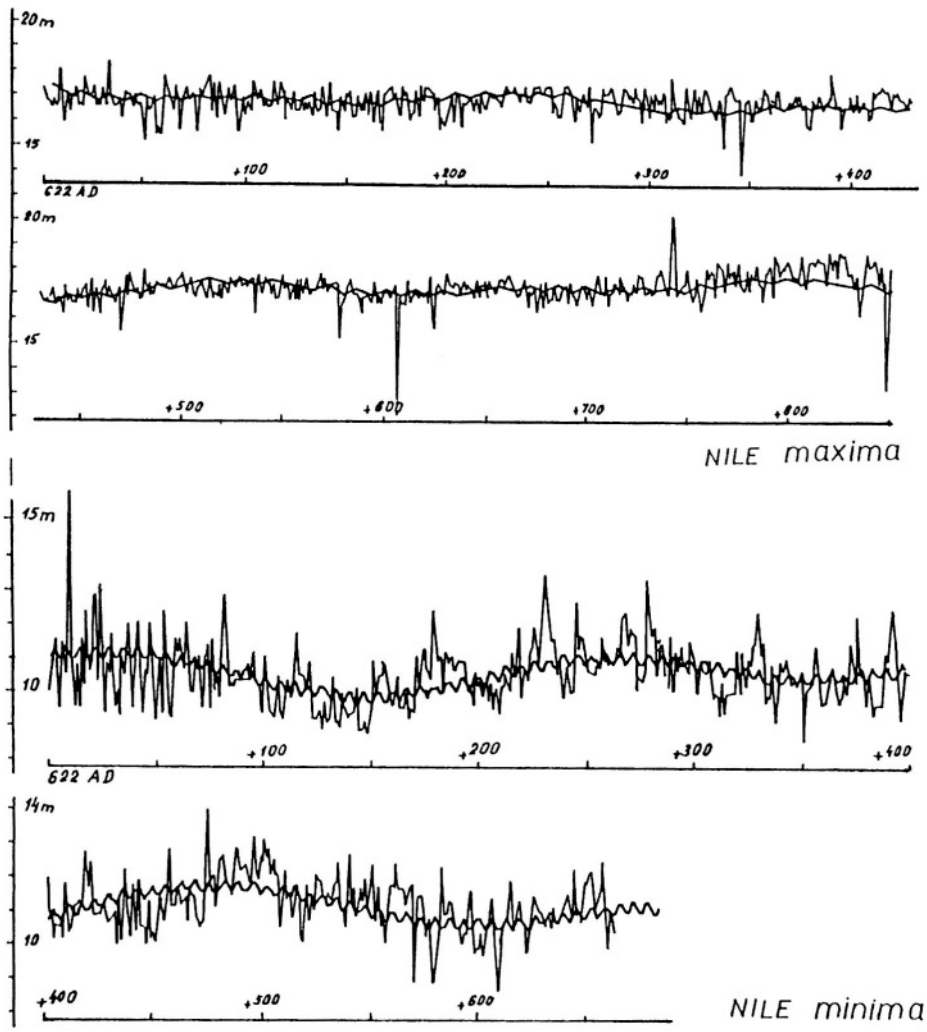

Figure 7.10- Observed sequences of Nile maxima and minima according to Taghri-Birdi and the fitted model results (based on Balek, 1977)

7.1.4 Models related to discharge and discharge forecasting- The discharges of the Nile River system in the relatively stable period, 1900-60, enabled the water resources engineers to forecast the floods in that period with a minimum of risk. Simple regression models were developed using the then available data, and the results obtained therefrom were rather satisfactory. The annual flow at Er-Roseires on the Blue Nile $(V_{BN})_R$ used to be expressed in terms of the flood volumes in June and July at the same site $(F_{BN})_R$ as:

$$(V_{BN})_R = 15.2 + 4.12(F_{BN})_R \tag{7.7}$$

where all volumes are expressed in 10^9 m^3. Eq. (7.7) was developed by Szalay (1973) using the data of the period 1918-57, and later verified by the author for the period 1912-60. In both cases, the correlation was about 0.85. The regression relation between the annual flow volume in the Main Nile at Kajenrty, $(V_{MN})_K$, and the June-July volumes of flood flow in the Blue Nile at Roseires, $(F_{BN})_R$, is as follows (Szalay, 1973):

$$(V_{MN})_K = 34.0 + 6.07(F_{BN})_R \tag{7.8}$$

with correlation about 0.65. The regression relation between the flow in the Main Nile at Dongola ,$(V_{MN})_D$, and $(F_{BN})_R$, as obtained by the author for the period 1912-60 is as follows:

$$(V_{MN})_D = 54.11 + 3.89(F_{BN})_R \tag{7.9}$$

with correlation of about 0.68.

The water level of Lake Victoria rose between October 1959 and May 1964 by more than 2.5 m. After a slight fall, the level began to rise again in 1978 and by mid-1979 had again reached almost the level of 1964. From 1981 the lake level kept fluctuating up and down around a significantly falling trend. By the end of 1995, the level was still about 0.5 m higher than the average water level when the jump started. Flohn and Burkhardt (1985) found that the average water level of Lake Victoria in the period September-December $(VL)_{9\text{-}12}$ is moderately related to the volume of water reaching Aswan in the period February-June $(A)_{2\text{-}6}$, and the regression relation is:

$$(VL)_{9-12} = 10.0 + 0.047(A)_{2-6} \tag{7.10}$$

with a correlation coefficient of 0.68. Since $(LV)_{9\text{-}12}$ is strongly correlated (0.94 correlation coefficient) with $(LV)_{annual}$, the combined relation was used to reconstruct the lake levels for the period 1870-1900. A graph showing the lake level at Jinja against time in years from 1870-1995 is shown in Chapter 10.

The flow series of the Nile above Aswan for the period 1870-1975, $(A)_{annual}$, and the annual high river levels at Roda since 1700, $(HL)_{Rd}$, have been used for verifying the possibility of short-term climatic changes in the source regions of the Nile water. The relationship obtained by (Riehl et al., 1976) can be expressed as follows:

$$(A)_{annual} = -308 + 20.8(HL)_{Rd} \qquad (7.11)$$

where $(A)_{annual}$ is in 10^9 m^3, and $(HL)_{Rd}$ is in m above Roda zero gauge. If $(HL)_{Rd}$ in a certain year happened to be 20.0 m, Eq. (7.11) yields the volume of flow above Aswan in that particular year as $108*10^9$ m^3. Eq. (7.11) was used to supplement the missing values of $(A)_{annual}$ up year 1700. The conclusion of that study is that it appears that,except for a few short periods of 10 to 20 years duration, the river flow was never "at rest" with respect to the average flow in the 275 years covered by the partly measured-partly generated series.

Ändel and Balek (1971) used the correlation-function analysis and Markov chains of high order to trace the periodic components in the flows of the Nile and the Niger Rivers. The analysis has shown that periodicities of 21; 7.6; 4.2; and 2.7 years do exist in the Nile flow above Aswan. These probably compare to the Bruckner cycle (22.2-y), Hellmann cycle (5.5-y), and Clough cycle (2-3-y), respectively.

The flow of the Nile River from Pakwach, at the outlet of Lake Albert, to Wadi Haifa at the mouth of the reservoir formed by the Aswan High Dam has been modeled by a Constrained Linear System model (CLS) developed by Fahmy et al. (1982). This model consists of six sub-models or components, which can be specified as follows:

i- The reach from Pakwach to Mongalla,
ii- Bahr el-Jebel from Mongalla to Malakal including the Sudd area and Bahr el-Ghazal swamps,
iii- Sobat basin including the Baro, the Pibor, and Machar swamps,
iv- White Nile from Malakal to Mogren,
v- Blue Nile including the Dinder and Rahad, and
vi- The Main Nile from Mogren to Dongola with Atbara included.

The different components were all modeled using linear hydrological models and the flow data at a number of key stations for the period 1912-1975 have been used for verifying the model estimating its parameters

The missing discharges at Pakwach were supplemented from the regression relation with the discharges at Mongalla. For the second component the relationship between the flows at Mongalla, Hillet Doleib and Malakal, already discussed in sub-section 7.1.2 has been used. The third component was divided into two parts; the spillage of the Baro from Gambeila to the Pibor-Baro

junction, and the routing of the flow below this junction down to Hillet Doleib, close to the mouth of the Sobat on the White Nile. The algorithm of the fourth sub-model is based on an input function, *I(t)* that can be written as:

$$I(t) = Q_{Ml}(t) - \Delta S(t) - E(t) \tag{7.12}$$

where Q_{Ml} = discharge of the White Nile at Malakal, ΔS = change in storage in the Jebel-Aulia reservoir, and E = evaporation. The basic relationship that describes the fifth component is expressed as:

$$Q_{Kh}(t) = 0.31Q_{Sn}(t) + 0.69Q_{Sn}(t-1) + Q_d(t) + Q_r(t) - 3.52 \tag{7.13}$$

where Q_{Kh} = discharge of the Blue Nile at Khartoum, Q_{Sn} = release from the Sennar reservoir, Q_d = discharge of the Dinder and Q_r = discharge of the Rahad. The sixth and last component has been expressed by the relationship:

$$Q_{WH}(t) = C + \sum_{i=0}^{5} \alpha_i Q_{Mg}(t-i) + \sum_{i=0}^{2} \beta_i Q_{Kh}(t-i) + \sum_{i=0}^{1} \gamma_i Q_{At}(t-i) \tag{7.14}$$

where Q_{WH} = discharge at Wadi Haifa, Q_{Mg} = discharge at Mogren on the White Nile upstream Khartoum, Q_{Kh} = discharge of the Blue Nile at Khartoum, and Q_{At} = discharge of the River Atbara near mouth. C is a constant equal to –5.67 whereas the model parameters α, β, and γ dependent on *i* as follows:

i	α_i	β_i	γ_i
0	0.346	0.182	0.484
1	0.263	0.720	0.516
2	0.116	-	-
3	0.120	-	-
4	0.080	-	-
5	0.075	-	-

As the flow measurement at Mogren Q_{Mg} stopped after 1988, it has been found necessary to express it in terms of the flow at Malakal, Q_{Ml}. The suggested relationship is as follows:

$$Q_{Mg} = 0.8911 + 0.8618Q_{Ml} \tag{7.15}$$

The correlation coefficient for the relationship given by Eq. (7.15) is 0.933. It should be noted here that all Q-values appearing in Eqs. (7.12) thru'(7.15) are in 10^9 m^3 y^{-1}. Eqs. (7.14) and (7.15) can be used to predict the Annual flow at Wadi Haifa, which is located at the mouth of the reservoir of the Aswan High Dam,

provided that the hydrological records are uninterrupted. Linear regression models can be used to fill in the missing data at those locations where records are discontinuous.

The maxima and minima series of the Nile level at Roda Island, Egypt, have been recently examined by Reusing (1964) as mentioned in the previous sub-section. The study has clearly shown that that the long-term persistence exhibited by long-term climate trends and corresponding fluctuations in the discharge regime are important characteristics of the hydrology of the Nile Basin. As far as the risk of hydrologic drought is concerned, models preserving the property of long-term persistence are more appropriate than those preserving only short-term persistence. Both the ARMA and ffGn (fast fraction Gaussian noise) classes of models have been used for calculating the risk estimates of the expected discharge deficits. The latter, i.e. ffGn models, have been preferred as they were found to give more conservative risk estimates. The same observation was found to hold for the Blue and White Niles. The results obtained from the ffGn models for 100 and 500 years return periods are as given below for a number of stations.

Station	Return period = 100 y		Return period = 500 y	
	(D)d, y	*(D)a mg*	*(D)d*, y	*(D)a mg*
Kagera	11	0.78	23	0.95
Outlet of Albert Lake	11	0.73	24	0.76
Mongalla	11	0.79	24	0.99
Hillet Doleib	10	0.85	15	0.95
Malakal	10	0.92	20	1.05
Mogren	10	0.85	20	0.99
Roseires	6	0.87	10	0.89
Sennar	6	0.87	11	0.90
Khartoum	7	0.94	12	1.07
Tamaniat	7	0.94	15	1.06
Hassanab	6	0.89	11	0.92
Atbara	6	0.87	9	0.92
WadiHalfa	7	0.90	12	0.99
Aswan (water arriving)	7	0.91	12	1.02

Explanation
(D)d, y = drought duration in years, (D)a mg = average magnitude of drought (deficit) below the mean in standardized form.

Upon discussing the Jarvis paper entitled "Flood Stage Records of the River Nile", Hurst (1935) mentioned the possibility that the variation of the Nile flood may be attributed to the Southern Seas Oscillation (SSO). He added that the then level of understanding and measuring technique of such an event is not developed enough to support his thinking.

Recently, El-Tahir (1996) presented the results of a study in which he used two extensive sets of data: one describing sea surface temperature (SST) of the Pacific Ocean, and the other is the flow of the Nile arriving at Aswan. The hypothesis tested in that study was that the natural variability of the Nile flow at Aswan is related to El-Niño Southern Oscillation (ENSO). The question that followed was whether such information can be used for improving the predictability of the Nile flood. Another objective of this study was to use the relation between ESNO and the Nile flow as an approach for explaining the Hurst phenomena. It has been recently suggested that ENSO events could be accurately predicted 1 or 2 years ahead using a coupled model of the ocean-atmosphere system. The predicted SST for the 17-y period 1973-89 were used to predict the annual flow volume of the Nile at Aswan using the expression:

$$(A)_{annual} = 88.5 - 8.7(ENSO_{index}) \qquad (7.16)$$

where all volumes are given in 10^9 m^3 y^{-1}. One should not forget that flood predictions are made as early as February that precedes the Nile flood of interest, i.e. 6 months ahead.

El-Tahir (1996) classified the annual volume of water arriving at Aswan into normal (between $80*10^9$ and $100*10^9$ m^3), low (less than $80*10^9$ m^3), and high (more than $100*10^9$ m^3). Of the 17 predictions obtained from Eq. (7.16) 12 were in agreement with the observed flow. In the absence of actual information about SST, the prediction of the most probable flood for any year be the average flood. According to the observations for the period 1973-89, the predictions matched 9 observations out of the 17 years. As a matter of fact, Eq. (7.16) is based on annual flow averaged over a small window of a 0.5°C centered around –1.5°C, -1.0°C, -0.5°C, 0°C, 0.5°C, 1.0°C and 1.5°C.

Last but not least, El-Tahir (1996) developed a hypothesis according to which the annual flow in the Nile varies with time following ENSO resulting in a non-stationary process and causing the Hurst phenomena. The non-stationary mean and the random fluctuation component explain 25% and 75% of the observed natural variability respectively.

7.2- The Niger Basin

7.2.1 Brief description of the basin- The real interest in exploring the River Niger can be dated back to 1788. The mission led by J. Ledyard and followed by D.F. Houghton did not meet with any success worth mentioning. In 1796, Mungo Park set out from the mouth of the Gambia River and reached the Niger at Ségou in 1796. He was able to travel through the river for 80 km only before he terminated his expedition. In 1805 he set out again on a similar route and drowned at the falls at Bussa, somewhere in what is now the State of Nigeria. According to Balek (1977), the Muslim rulers of the Hausaland (part of Nigeria)

at the beginning of the 19th century knew the route of the Niger to the ocean. He claimed that the then ruler at Sokoto, Nigeria, sketched a map of the Niger to H. Clapperton in 1824. In 1832-33, the Lower Niger up to the confluence with the Benue was explored. A few years later, W. Balfour Bikie traveled through the Niger and Benue Rivers much farther than his predecessors did. From 1850 to 1855 Heinrich Barth crossed the Sahara and traveled and studied throughout an area from Timbuktu to Cameroon. Barth navigated the headwaters of the Benue River and plotted the map of the Middle Niger, while one of his friends surveyed Lake Chad.

The Niger Basin has a large extent, which upon including the arid sections, reaches $2.2*10^6$ km^2. The basin area of the Niger alone, without including its most important tributary, the Benue River, or the and sections, is reduced to just $1.1*10^6$ km^2 (430, 000 square miles). The total length of the course of the Niger as given by the French maps is somewhat different from the length given by the English maps. Both are slightly different from the length used by the Dutch consultants (NEDECO, 1959). Whether the true length is closer to 4,000 km or 4,200 km, the Niger is the third longest river in Africa, after the Nile and the Congo. It is also the longest and largest watercourse in West Africa.

The Niger and its tributaries drain certain parts of Benin (2.25%), Burkina Faso (4.1%), Cameroon (4.1%), Central African Republic and Chad (7.45%), Guinea (4.3%), Ivory Coast (1.1), Mali (28.2%), Niger (22.3%), and Nigeria (26.4). The percentages between brackets represent the areas shared by the riparian countries in proportion of the total basin area, $2.2*106$ km^2 The percentage of the share of each country in the total basin area to the surface area of the country itself is 4.4, 29.8, 19.0, 8.6, 38.6, 8.0, 50.0, 39.0 and 63%, respectively. A general map of the Niger Basin is shown in Figure 7.11.

The river has a long plateau course, with many tributaries from the northern side, which are normally dry watercourses. The source of the Niger lies at 9° 5'N and 10° 47'W. The northernmost point of its course is at about 17° N and its mouth is located at 4° 30' N and 6° E. The main headwaters of the Niger River are in the very wet Fouta-Djallon highlands at the Guinea-Sierra Leone border, less than 300 km from the Atlantic Ocean. They are also to be found in the massif, which extends to the southwest, close to the frontier between Guinea and Liberia. A number of small and mighty tributaries join the Niger at certain points along its course. The river transports its water from source to mouth over a distance about 4,100 km, before discharging it into the Ocean. In so doing, it traverses areas with a wide diversity of climates ranging from arid Sahara lands to less arid and semi humid or humid lands. Climatic data for some parts of the basin area are already included in Appendix A.

The basin of the Niger can be subdivided into six subdivisions as follows:

i- The Upper Niger: The Niger above Koulikoro and the Bani above Mopti.
ii- The lacustrian Zone that extends to Tombouctou (Timbuktu).
iii-The Middle Niger from Boucle up to the confluence of the Benue

iv- The Upper Benue, above the dorsal, between Nigeria and Cameroon.
v- The Lower Benue up to its confluence with the Niger
vi- The Lower Niger.

The riparian countries of the main stream of the River Niger are four. Guinea possesses the upper reaches of the Niger, Mali and Niger the middle reaches including the interior delta, and Nigeria the lower course of the main river. Benin, Burkina Faso, Cameroon, Chad, and Ivory Coast are basin States, as numerous tributaries and minor streams originate in or traverse their territories.

The basin of the Upper Niger covers the area from the source of the Niger River down to Koulikoro on the Niger, about 65 km north of Bamako, and Mopti on the headwaters of the Bani River. The catchment at Koulikoro (3,270 km above mouth) is about 120,000 km^2. The Tembi River is often regarded as the main source of the river. The Upper Niger is formed by the accumulation of four tributaries; the Niger, the Niandan (320 km), the Milo (430 km) and the Tinkisso (570 km) rivers. The corresponding catchment areas of these rivers are 18,600, 12,700, 13,500, and 19,800 km^2, respectively. The Nindan and the Milo basins are privileged by their high runoff, caused by the heavy rainfall they receive and their steep slopes. The river then traverses the interior plateau in a northeasterly direction towards the Inland Delta in Mali. As it crosses the Guinea-Mali border, the Niger is joined by the Fie River (190 km) and then by the Sangarani River (575 km) near Kangare (Mali). Both of these tributaries, too, originate in Guinea and separately cross the border into Mali. The river then continues its course in a northeasterly direction towards the Inland Delta in Mali. There, an important tributary, the Bani River, joins the Niger. The Bani is formed by the convergence of the streams Baoule (685 km) and Bagoe (580 km) and of the Manadiani and Banigue Rivers, all originating in the Ivory Coast, and the Banifing River (415 km), orginating from Burkina Faso. The annual precipitation in the source areas in the Ivory Coast is about 1,600 mm in an average year. The Bani discharges its water in the Niger near Mopti in Mali.

The total surface covered by the Inland Delta can be 450 km in length and more than 200 km in width bringing its area to 80,000 km^2 in the flood season. The Delta extends from Dejna to Timbuktu, some 390 km, with Lake Débó in its middle. It is in fact a crowded network of channels, swamps and lakes. During a humid stage in the Quaternary, it had been a great lake into which the Upper Niger, then a separate river, emptied, and the lake dried up when the Middle Niger captured the Upper Niger. Again, the area occupied by the Delta is basically a swamp consisting, to a large extent, in sandy soil. The slope of the river decreases from $5*10^{-5}$ above the swamp to just $1*10^{-5}$ below it. This situation causes the river to lose nearly two-thirds of its potential flow between Ségou and Timbuktu by seepage and evaporation. The latter is aggravated by the fact that the river course becomes close to the fringes of the Sahara. The free water evaporation in this area can be estimated at between 2.0-2.5 m y^{-1}.

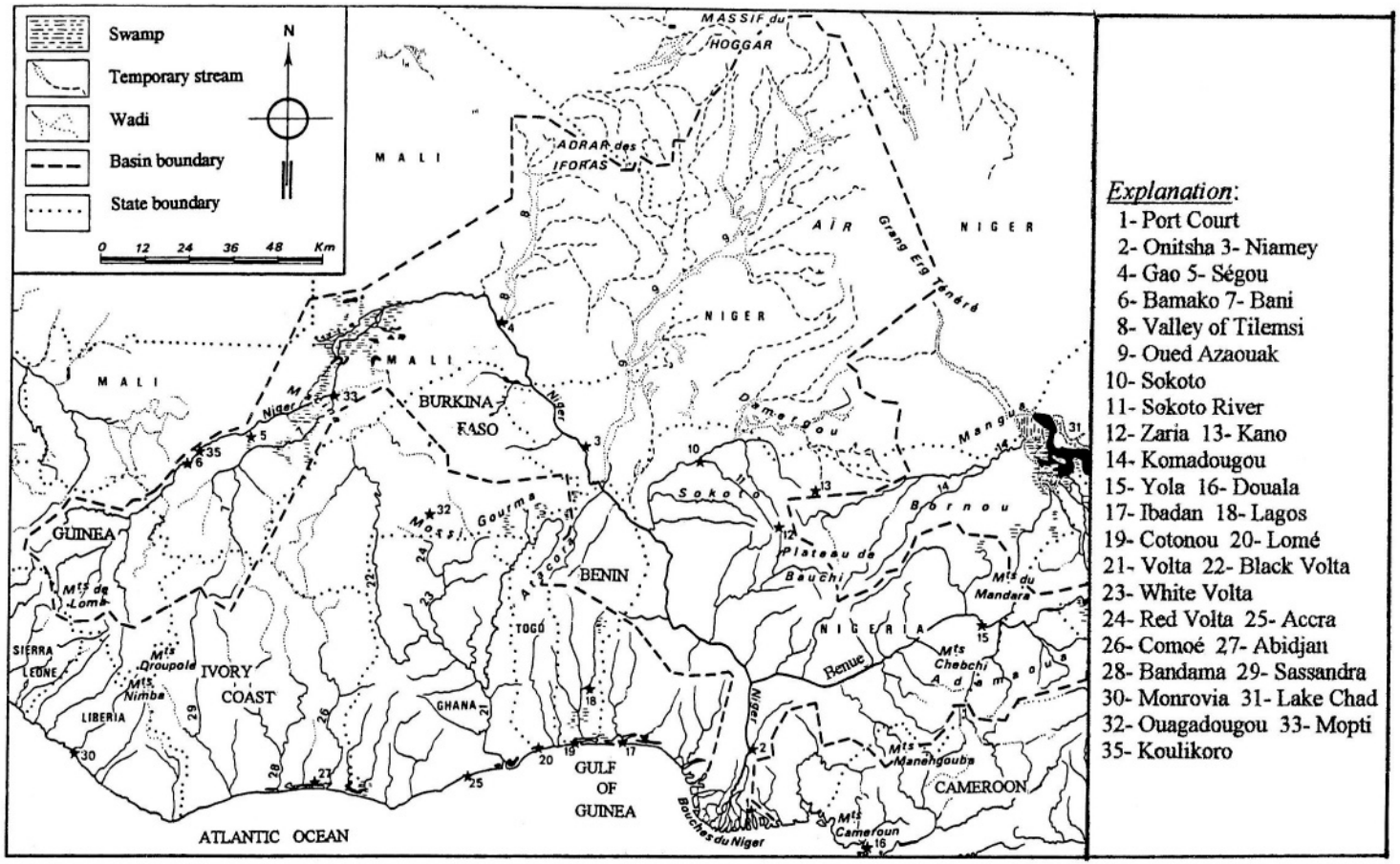

Figure 7.11- General map of the Niger Basin

The River Bara Issa, which joins the Niger just above Diré, leaves the Delta through the northern shore of Lake Débó and flows to the east. The Issa Ber, a principal arm of the lake, leaves it in a westerly direction before bending to the northeast where it joins the Bara Issa. Below Diré the Niger supplies Lake Télé, which in turn fills up Lake Faguibine (Rodier, 1964). Not far from Timbuktu, the flood plains become much smaller in size and the lacustrine zone terminates.

Downstream from the Internal Delta, below Diré and about 2,530 km above the river mouth (catchment area = 330,000 km^2), the Niger flows in a northeasterly direction before turning to the southeast to form a great bend. It then meanders through an and area before entering the Republic of Niger. In the Niger, it receives first the waters of the Faroul tributary from Burkina Faso. Further on, the waters of the Dargol (200 km) and Sirba (375 km), both are flowing from Burkina Faso, join the river while still in the Niger Republic. South of Niamey, the capital of the Niger, the Garoubi (285 km) and Tapoa (190 km) tributaries discharge into it. Some 150 km below Niamey, the Niger forms the boundary between Niger and Benin for approximately 80 km. In this reach the Mekrou River (375 km), originating in Benin, empties its water into the Niger. Thereafter, the river traverses Nigeria, where it is fed by several streams, the most important of which are the Sokoto (630 km) and its tributaries, Malendo (180 km), Kaduna (580 km), Oyi (125 km), Oro (140 km), Kampi (130 km), Oli (225 km) and Moshi rivers (205 km). The most influencial tributary of the Niger, however, is the Benue River.

The Benue rises on Adamawa Plateau in the Cameroon at an elevation of about 1,350 m above m.s.l. The average annual rainfall varies from 3,000 mm in the upper reaches to 900 mm in the middle course of the Gongola River (610 km). The river falls some 750 m over the first 35 km of its course. During the next 150 km, another 370 m, leaving for the remaining 1,130 km to the Niger confluence a fall of only 170 m. The river flows, for a certain reach of its course, through sandstone rocks. The river course is encountered with floodplains and flats where the water slope, consequently the flow velocity, drops considerably.

The Benue River is joined along its course by a number of tributaries originating in both the Cameroon and Nigeria. The most important of these tributaries, which run inside the Cameroon, are the Faro, Mayo-Kebbi and Lisaka rivers. The Faro is a transitional tropical river transporting considerable quantities of sand. Some small lakes and pools intersect the course of the Mayo Kebbi River. The Gongola, Dongo, Ankwa, Taraba, Okwa, and Katsina Ala originate and flow inside Nigeria. The Gongola is a tropical torrential stream. The average catchment area of the Taraba, Donga and Katsina Ala is in the order of 21,000 km^2.

At Lokoja, some 1,300 km from its source, the Benue joins the Niger from the east, thereby doubling up its discharge. Below the confluence, the Niger changes its course towards the south where it receives some small tributaries but with plentiful supply. The Anambra River (210 km) is the most important feeder of the Niger below Lokoja. The combined flow is discharged into the Atlantic

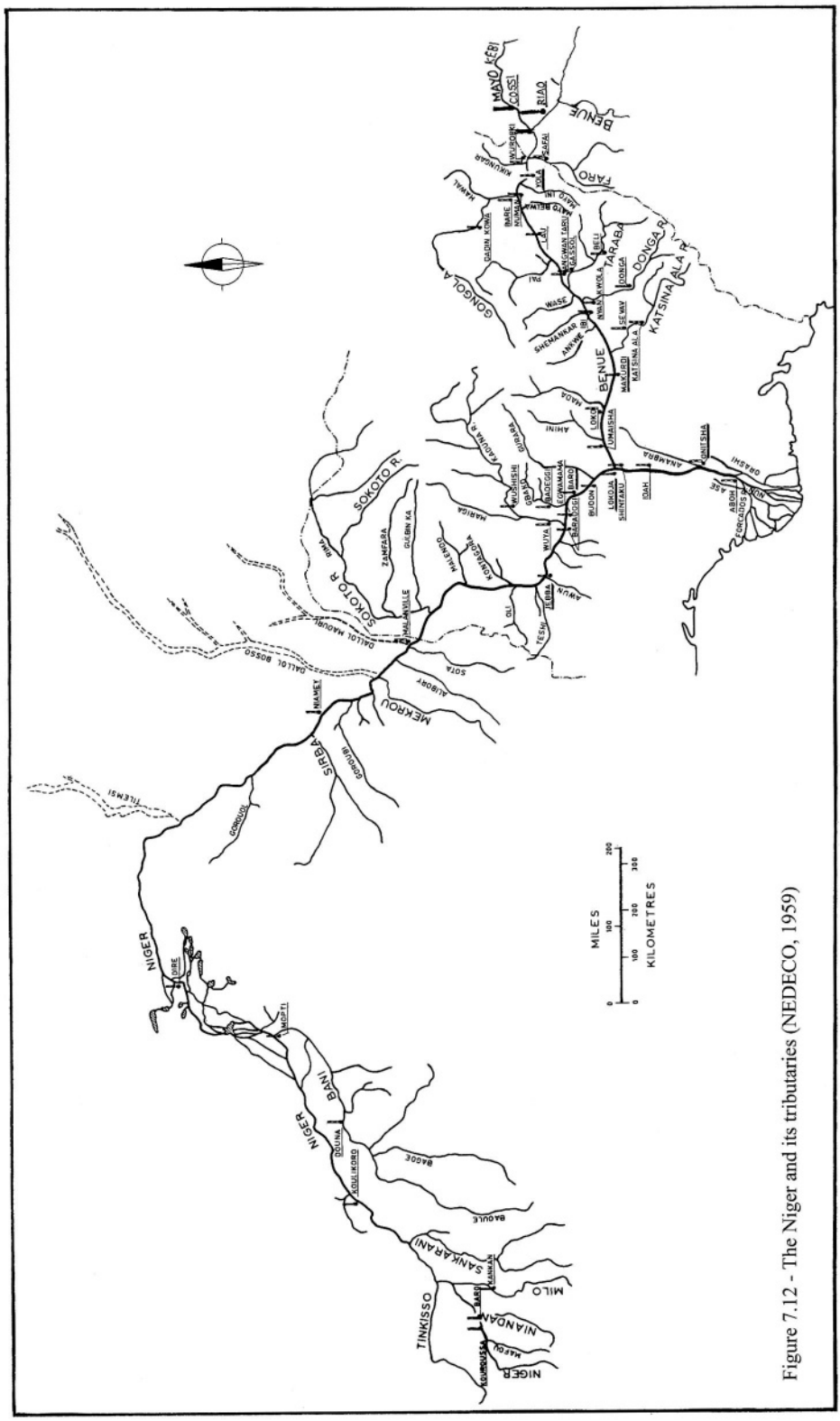

Figure 7.12 - The Niger and its tributaries (NEDECO, 1959)

Ocean in the Gulf of Guinea through a network of outlets. This network constitutes the delta of the Niger, which is about 25,000 km^2 in area.

The Niger and Benue Rivers and their respective tributaries are shown geographically and schematically in Figures 7.12 and 7.13, respectively. Additionally, the distances in kilometers between some locations and the mouth of the Niger on the Atlantic Ocean are included for reference in Figure 7.13.

7.2.2 Availability of hydrological data- Reffay (1948) prepared a leading technical note on the regime of the Niger for the Hydraulic Service of the Government of the former French West Africa. As a matter of fact, the note was intended for the former French Sudan, presently known as Mali. From this note one can get information regarding:

i- the discharge of the Niger and its tributaries at more measuring sites than those included in the UNESCO surveys (1971, 1995)
ii- the error in the available discharge measurements varied between 5 and 10%
iii- the factors affecting discharge such as evaporation and infiltration were analyzed and discussed
iv- the report contained information about the transport of solid matter.
v- the propagation of flood wave traversing the Interior Delta of the Niger was analyzed using the hydraulic methods that were available then.

A survey of certain studies in meteorology and hydrology in the Sudano-Sahelian zone of West Africa was carried out in 1973, as a consequence of the drought that hit vast areas of West and Northwest Africa since 1968 and lasted for no less than 10 years. A team of experts conducted this survey during a visit to Burkina Faso, Chad, Mali, Mauritania, Niger and Sénégal (countries of the former French West Africa). Davy (1974) described the data situation as complex, in that even within each of the individual countries there was no single centralized service controlling the networks of stations providing hydrological and meteorological observations. The same remark applied to the uniformity of standards of publishing the available data. The Davy's report included detailed lists of the gauging stations showing periods of observations that were known. The report also included the then available publications containing the data. It ended as usual with a set of recommendations. They all aimed at strengthening and improving the existing networks and urging the countries and member states of the Permanent Inter-state Committee for the Fight against Drought in the Sahel (in short CILSS in French) to make a greater effort regarding data collection, processing and publication.

In 1982, two years after the first evaluation mission on the activities of the CILSS countries, the author was invited to join the second evaluation mission. The member states of CILSS at that time grown include two more countries, the

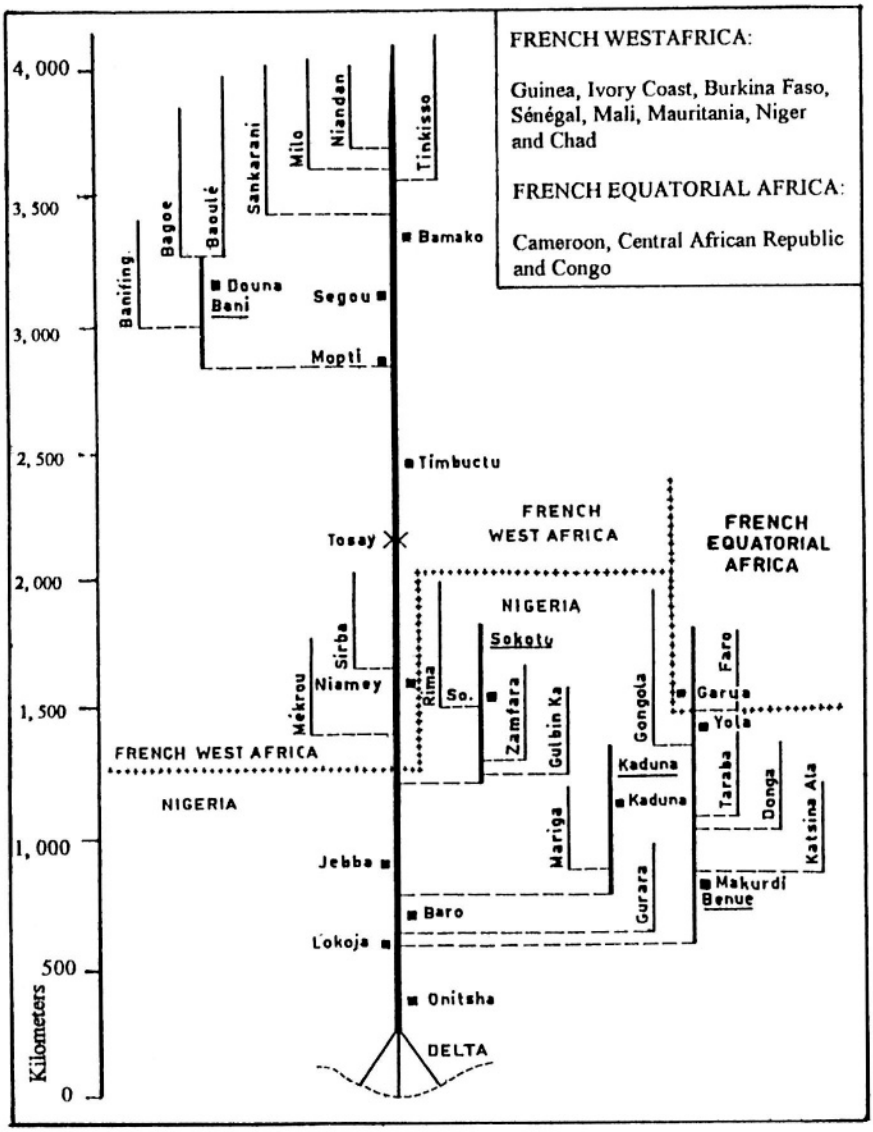

Distance in km measured from the mouth of the Niger River on the Atlantic Ocean: Onitsha, 374; Lokoja, 583; Baro, 699; Makurdi, 821; Jebba, 895; Bussa, 905; Donga, 1,104; Yelwa, 1,108; Kaduna, 1,135; Malanville, 1,306; Sokoto, 1,423; Yola, 1,430; Say, 1,538; Garoua, 1,565; Niamey, 1,602; Tillabury, 1,719; Gao, 2,045; Tosay, 2,160; Timbuktu, 2,460; Diré, 2,534; Mopti, 2,842; Ségou, 3,123; Douna, 3,160; Koulikoro, 3,286; Bamako, 3,350; Seguiri, 3,536;Kouroussa, 3,714 and source, 4,105.

Figure 7.13- Schematic presentation of the Niger and its tributaries

Gambia and Cape Verde Islands. The report of the second mission recommended the efforts undertaken by AGRHYMET for training the required staff and personnel made up of hydrologists, meteorologists and technicians. However, there was hardly any developments or improvements regarding the measurements, data collection and other fieldwork. The same conclusion applied to the measuring equipment, data publication and processing.

Katashaya (1986) examined the issue of hydrometeorological data collection for water-resource projects in Nigeria. He commented on the situation that existed then and the difficulties surrounding the improvement, maintenance and operation of the meteorological and hydrometric networks. He presented, as a case study, the project known as Gurara Inter-basin water transfer, located in northern Nigeria between latitudes 8° and 11°N and longitudes 7° 30'and 8° 30'E. The project aimed at transferring water from the Gurara River to three destinations in other basins, namely to Shiroro for hydropower generation, Abuja for water supply, and Izom for irrigation. The map in Figure 7.14 provides a strong evidence of the meager density and inadequacy of the meteorological and hydrological networks for the feasibility study and design of such projects.

The discharge data of the Niger River at Koulikoro (station 61), a key station on the Upper Niger, have been collected uninterruptedly since 1907. UNESCO published these data in 1971 and lately in 1995. The publication of 1995 includes the measurements at Diré (station 35), which is the next key station, from 1925 up to 1979 without breaks. The same publication includes the discharge data downstream of Kirango (station 45) on the Niger, Douna (station 55) on the Bani, Gouala (station 69) on the Sankarani and Dioïla (station 65) on the Baoulé. Regrettably, all these data suffer from breaks and discontinuity, which make them of limited use.

7.2.3 Hydrology of the Niger Basin- Such a vast river basin area, falling as it does within the wide latitudinal and longitudinal limits already mentioned above, cannot be expected to have uniform climate. The annual precipitation in the Guinean Highlands, which exceeds 2,000 mm, decreases considerably as the river traverses through increasing dry countries towards the Inland Delta. Table 9, Appendix A, gives the long-term average precipitation at Gao (Station 47) as only 254 mm. But as the Niger turns south, rainfall increases; by the time it gets to the Atlantic mouth, the mean annual precipitation rises again to 2,000 mm or more. One should not forget that the loss by evaporation in the dry areas is far more than evaporation in the wet areas. The non-uniformity of climate and the changing topography, physiography and land cover of the territories covered by the basin are responsible of the significant temporal and spatial variability of water level and flow in the river and its tributaries.

The sub-basins of the Upper Niger, Niandan, Milo and Tinkisso receive slightly above 2,000 mm precipitation each year. The corresponding annual runoff coefficient varies between above 30% for the Niandan and Milo to 21%

for the Upper Niger and to less than 18% for the Tinkisso. These values bring the average annual discharges to 250 $m^3 s^{-1}$ for the Upper Niger, 260 $m^3 s^{-1}$ for Niandan, 275 $m^3 s^{-1}$ for Milo and 220 $m^3 s^{-1}$ for Tinkisso.

Below Siguiri, 550 km from the source of the river, the Niger receives from the right-hand side the Fie, Sankarani and Ouassouloubalé Rivers as, shown in Figure 7.12. The Sankarani is a mighty affluent, with a catchment of 35,000 km^2. Assuming that the runoff coefficient for this river is about 20% the corresponding average runoff becomes in the order of 400 $m^3 s^{-1}$.

Rodier (1964) gave the average flow at Koulikoro, at which the catchment area reaches $120*10^3$ km^2 and the average annual precipitation 1,600 mm, as 1,545 $m^3 s^{-1}$. These figures yield an overall average runoff coefficient of 25%, which is highly consistent with the other estimates. The corresponding absolute minimum and maximum discharges are 32 $m^3 s^{-1}$ and 6,220 $m^3 s^{-1}$ respectively. The same reference gives the characteristic flood discharge as 5,840 $m^3 s^{-1}$. More recent data (UNESCO, 1995) give the mean discharge over the period 1907-90 as 1,414 $m^3 s^{-1}$, and the minimum and maximum discharges over the period 1907-79 as 16 $m^3 s^{-1}$ and 9,700 $m^3 s^{-1}$ respectively. Table 6.4 gives the estimates of annual maxima and minima discharges of the Niger for selected

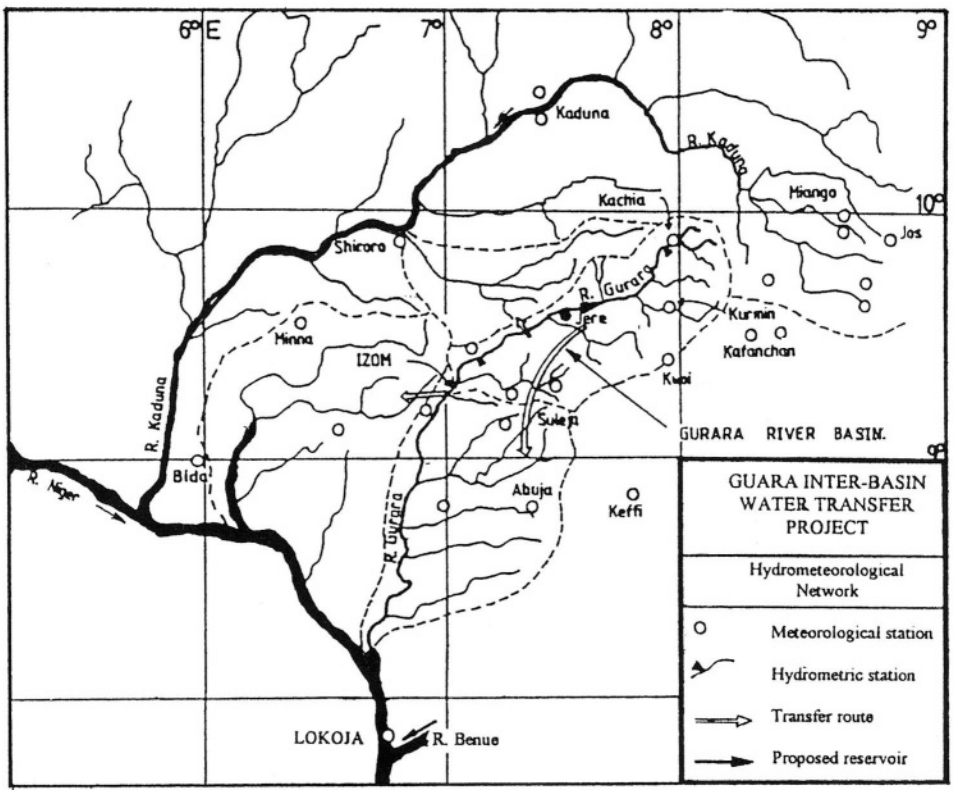

Figure 7.14- Map of the meteorological and hydrometric networks in the Guara inter-basin water transfer project area (from Katashaya, 1986)

return periods using the distribution functions of best fit to observed data. Figure 6.9 shows clearly that the river at Koulikoro runs almost dry in the February-May season. The monthly discharge variability from year to year is paralleled by the interannual variability of the flow at the same gauging site, as can be seen from Figure 6.12$_a$. Additionally, the graphical plot of the annual time series, Figure 6.13$_a$, indicates clearly the existence of a cycle superposed on a significantly falling trend. Ändel and Balek (1971) examined the existence of cyclic component(s) in the flow in the Niger. The result of that study will be presented in a forthcoming section.

The catchment area of the Bani River at Douna (station 55) is 100,000 km^2. It receives an average annual precipitation of 1,270 mm. The mean annual discharge is 670 m^3 s^{-1}, corresponding to an overall average runoff coefficient of 17%. The maximum annual discharge can be assumed as 2,980 m^3 s^{-1} and the characteristic flood discharge can be assumed as 2,900 m^3 s^{-1}. The minimum annual discharge is not exactly known. However, it has been roughly estimated as (50) m^3 s^{-1}. It should be noted here that the observations taken in the period 1952-79 (UNESCO, 1995) yield a mean of 559 m^3 s^{-1}, with a coefficient of variation of 42%.

The next key station on the Niger River, Diré, is located just downstream the Inland Delta area. Despite the large catchment area, 340,000 km^2, the tremendous losses in that particular area cause the mean annual discharge to fall down to say 1,110 m^3 s^{-1}. The situation here resembles, to some extent, the losses in the Sudd area in the Nile Basin already mentioned earlier. A much closer situation can still be found in the Upper Yobe River in northern Nigeria. The losses by open water and swamp evaporation, evapotranspiration and deep percolation to the groundwater amount to about 70% of the total annual runoff. The loss by open water and swamp evaporation alone constitutes almost 50% of the annual runoff (Sellars, 1981).

The maximum and minimum annual discharges at Diré are 2,350 m^3 s^{-1} and (50) m^3 s^{-1} respectively (Rodier, 1964). Discharge observations from 1925 up to 1978, though including the harsh drought years of the period 1965-79, give the mean annual discharge as 1,103 m^3 s^{-1} with a coefficient of variation of about 20%. Comparing the graphical plot of the annual series at Diré (Station 35), Figure 6.13$_a$, with that of the flow at Koulikoro (Station 61), Figure 6.13$_b$, one can easily realize how these two stations behave similarly.

The gauging station at Niamey (Station 47), Niger, is another key station on the Middle Niger. The catchment area at Niamey is 700,000 km^2. The mean annual discharge of the Niger at this site is very much reduced because of the increased aridity of a large part of the catchment area below Diré. Another important factor contributing to this reduction is the withdrawal of considerable volumes of water mainly for agriculture. The mean flow at Niamey up to the beginning of the 1960s was slightly above 1,000 m^3 s^{-1}. It fell down to just 882 m^3 s^{-1}, with 26.2% variation coefficient, for the period 1941-90.

The Upper Niger rises in June and falls down in December. The routing of the floodwater in the Inland Delta area together with the high losses in the summer season causes the delay of the flood in the Middle Niger. The flow in the river reaches its maximum near Timbuktu only in January. In the next section, we shall include a review of the propagation of flood wave in the transitional area between the Upper and Middle Niger.

Proceeding to Malanville (Station 71) from Niamey (Station 47), the catchment area increases to reach $1*10^6$ km^2, and the climate becomes less arid. Several tributaries flow towards the Niger from both of its sides. Those flowing from the left side do not really join the Niger; instead they feed the groundwater aquifers in the adjacent territories. Contrarily, those tributaries originating in Bénin, the Mékrou, Alibori and Sota, join the Niger on the right-hand side and supply it with about $6*10^6$ m^3 in a normal year. This volume of water helps to increase the river discharge by some 20-25%. Depending on the period over which the mean is taken, the average annual discharge varies between 1,150 and 1,250 m^3 s^{-1}.

Between Malanville and Jebba, both on the Middle Niger, the river is joined by some streams, of which the Sokoto and its tributaries, e.g. Lamfara and Ka, are the most important ones. The supply brought by this major affluent causes the river discharge to increase from say 1,250 m^3 s^{-1} to 1,600 m^3 s^{-1}, i.e. by about 30%. Due to this supply, the flood discharge, however, is nearly doubled. In 1968, the construction of the Kainji Dam on the Niger, 25 km below Yelwa, was completed. The dam is basically serving the purpose of hydro-electric power development. Originally, the dam was built with a capacity of 780 MW, but that is increased, as more generators have been added. The reservoir has a surface area of 1,280 km^2, lying between 9° 50'and 10° 57'N, in northern Nigeria. The Malendo River enters the Niger from the left side near the dam site and helps to increase the inflow to the Kainji storage reservoir As the annual evaporation from the reservoir surface is estimated at 2, 000 mm, the total evaporation loss must be 2.56*109 m^3 y^{-1}. Originally, the Kainji Dam had a capacity of 780 MW but more generators have been added later.

A short distance below Jebba, the Niger receives its second important tributary, the Kaduna. This tributary originates in the Jos Plateau, Nigeria and has a catchment area of 65,500 km^2. The Kaduna River is essentially tropical. It supplies the Niger, on the average, with 600 m^3 s^{-1}. The Jebba Dam on the Niger River was completed in 1985, with a capacity of 560 MW. Two small streams, both having a transitional tropical regime, join the Niger at Baro, a short distance below the Kaduna confluence. The flows bring the Niger's average annual discharge at Baro to no less than 2,500 m^3 s^{-1}, i. e. about twice the average annual flow at Malanville. The difference between the discharges at Baro and Malanville, about 1,200 m^3 s^{-1}, is equaled by the Sokoto and Kaduna Rivers. The contribution of the Kaduna also helps to double up the flood discharge, thus causing it to rise to 9,000 m^3 s^{-1}.

The mean annual and flood discharges of the River Benue are considered more important than the corresponding discharges of the Niger at Baro. The Benue River is joined all along its course by numerous abundant tributaries. The key gauging sites on the Benue are located at Gaorua, Yola, and Makurdi. Though climate along this reach of the river is not as harsh as that in the arid parts of the basin, a fair estimate of the loss of water by evaporation is strongly needed, especially in connection with the possibility of having water storage schemes in the vicinity of Yola.

The Benue at Garoua is supplied by the Mayo Kebbi and the Benue itself. A certain portion of the yield of these two rivers goes into the Logone River, which flows to Lake Chad. The Benue is essentially a tropical river with a mean annual discharge of about $375\ m^3\ s^{-1}$ at Garoua (Station 152). Only 75% of this amount, or $280\ m^3\ s^{-1}$, flows below the confluence. Downstream from Garoua the Benue is joined by a series of mighty streams, the Gongola from the right-hand side, and the Faro, Taraba, Donga and Katsina Ala from the left-hand side. These tributaries supply the Benue and raise its mean annual discharge to over $3{,}000\ m^3\ s^{-1}$, and its flood and low-flow discharges to 12,000 and $240\ m^3\ s^{-1}$ respectively, all discharges are measured at Makurdi. Approximately 100 km below Makurdi, the Benue River discharges its water in the Niger at Lokoja. The mean annual discharge brought by the Benue at this site is in the order of $3{,}400\ m^3\ s^{-1}$.

The Benue reaches its flood level between August and October each year. It begins to fall in October and falls rapidly in November, after which the rate of fall in the next three months becomes very slow. The water level reaches its lowest level in May, while the peak of the floodwater can attain any level from 6 m 20 m above the low-water mark. The median (50% frequency of occurrence) water stage hydrograph at Lokoja, shown in Figure 7.15, indicates that the flood level is slightly more than 8 m higher than the low-level.

The Lower Niger below the confluence of the Benue flows in a southerly direction carrying the sum of the discharges of the two rivers. The mean annual discharge at the key station Onitsha, about 150 km downstream from Lokoja, is in the order of $7{,}000\ m^3\ s^{-1}$ or $220*10^6\ m^3\ y^{-1}$. Despite the fact that the basin area of the Niger with its tributaries is nearly 75% of the basin area of the Nile and its tributaries, the mean annual discharge of the Niger is 260% greater than the mean annual discharge of the Nile at Aswan. One should not forget that the basins of both rivers include vast areas with arid climates and swamps, where excessive volumes of water are lost in them each year. The frequency distributions of the mean annual discharges at Makurdi and Onitsha are shown in Figure 7. 16.

Last but not least, the discharge data available in the recent UNESCO Publications (RivDis v 1.0, 1996) and (Discharges of selected rivers of Africa, 1995) have been used for computing the mean and variation of the mean annual discharge for the Niger Basin. The computations cover 18 stations not having the same period or length of record. These stations are number; 36, 40, 45, 47,

52, 55, 61, 65, 69, 70, 71, 73, 77, 80, 84, 91, 94 and 114. The results are to be found in Table 6a, Part A/Appendix II. Table 7.3 gives more elaborate calculations, most of them by Sutcliffe and Lazenby (1989), for 9 stations all covering the period 1951-80.

7.2.4 Some models for simulating the flow of the Niger and its tributaries- Several models have been developed for simulating the mean annual flow of the Niger River and its tributaries at a number of sites using different periods and lengths of record. The serial correlation coefficients and other values of interest of the sequences used for estimating the model parameters are included in Table 7. 4 (Shahin, 1986).This table shows that all sequences used, except the one belonging to the Benue River at Garoua, are serially correlated. The models used were AR (1), (AR 2), ARMA (1,1) and ARMA (2,1). The results obtained are given in Table 7.5. Remarkable enough, that the four models gave almost the same results for Koulikoro station (61) on the Upper Niger. The coefficient of determination, $\mathbf{R}^2$, is between 0.62 and 0.64.

The issue of periodicity in the annual flow series of some African Rivers has been briefly mentioned in subsection 6.3.4. The periodicity in the historical sequences of the water level of the Nile River at Roda Island, opposite Cairo, as obtained by Ändel and Balek (1971) has already been given in subsection 7.1.3. The same reference, using the correlation-function analysis and Makov's chains of high order for both the Nile and the Niger, concluded that at least ten previous years were found significant for the formation of the mean annual discharge in the eleventh year. For the Niger, the existence of at least one period of 25.5 y was proved at 95% significance. Periodicities of 7.3 and 3 years were also traced in the Niger sequence at Koulikoro. When the three periodicities were incorporated in the model, the result obtained was as shown in Figure 7.17.

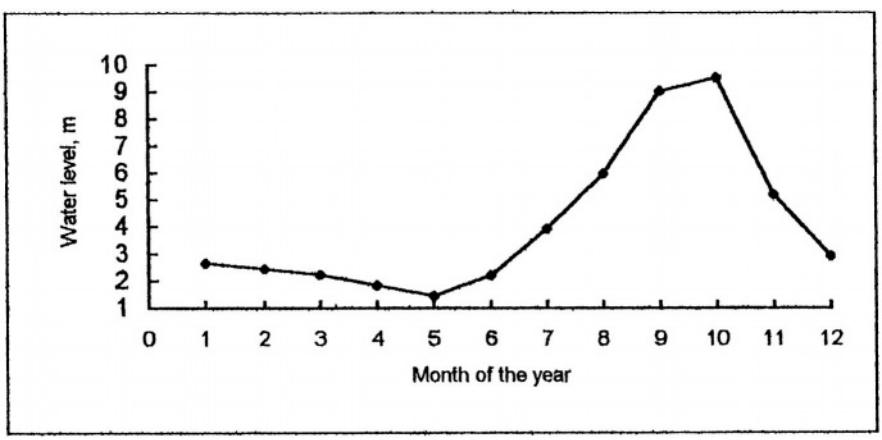

Figure 7.15- Stage hygrograph of the median monthly level of the Benue River at Lokoja

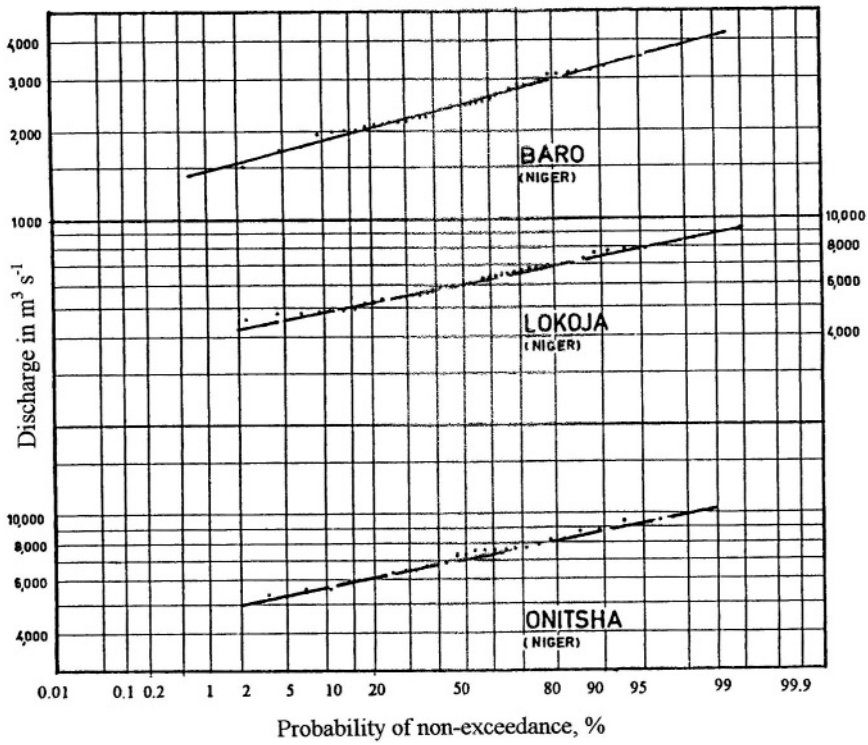

Figure 7.16- Frequency distribution of the annual mean discharge at three measuring sites along the Niger River (from NEDECO, 1959)

Table 7.3- Mean flow statistics for the Niger River, 1951-1980 (based on Sutcliffe and Lazenby, 1989)

Station	River	area, km^2	$(P)_m$, mm	$(Q)_m$, mm	Cv %	r	R^2
Koulikoro	Niger	120, 000	1, 556	407	23,4	0,262	
Tinkisso	Tinkisso	6, 370	1, 529	400	32,7	0,621	0,706
Faranah	Niger	3, 160	1, 817	725	22,3	0,399	0,651
Kouroussa	Niger	16, 560	1, 665	460	23,2	0,276	0,808
Baro	Niandan	12, 770	1, 859	638	22,2	0,385	0,711
Kankan	Milo	9, 620	1, 877	651	21,7	0,347	0,791
Tiguibery	Niger	67, 600	1, 649	515	34,8	0,312	0,977
Mandiana	Sankarani	21, 900	1, 698	405	21,7	0,239	0,793
Dire*	Niger	340, 000	975	104	19,6	0,107	0,443

Explanation

$(P)_m$ = mean annual areal precipitation, $(Q)_m$ = mean annual runoff, Cv = coefficient of variation, r = mean areal runoff coefficient and R^2 = square of correlation coefficient between the discharge at any station and the corresponding discharge at Koulikoro. Dire is not included in the calculations given by Sutcliffe and Lazenby.

It is quite unfortunate that some models, after showing a good agreement with the actual observations for the period of record used in developing the model, fail in predicting future values. This happened to be the case here. The agreement between the model results and actual data is reasonable for the period 1907-57, used for estimating the model parameters. When the discharge observations and the model results for the period 1958-79 are plotted as shown

Table 7.4- Hurst coefficient and the first five serial correlation coefficients of the mean annual discharge series of the Niger River and its tributaries (based on Shahin,1986)

Station no/name	River	*N, y*	*H*	Serial correlation given time lag,y 1	2	3	4	5	*C*/ Uc*
61	Niger	61	0,741	0,521	0,524	0,449	0,237	0,223	*C*
Mopti	Niger	45	0,893	0,754	0,59	0,509	0,301	0,287	*C*
35	Niger	44	0,883	0,726	0,538	0,551	0,42	0,256	*C*
55	Bani	33	0,94	0,759	0,648	0,614	0,406	0,219	*C*
66	Niger	42	0,797	0,362	0,234	0,091	0,321	0,101	*C*
91	Benue	39	0,609	-0,013	-0,018	0,132	-0,199	0,148	*Uc*

Explanation

N, y = length of record in years, H = Hurst coefficent, C = serially connected and Uc = serially unconnected, both at 5% significance level.*

Table 7.5- Summary of the results obtained from different models simulating the mean annual discharge of the Niger River and its tributaries at different sites (based Shahin, 1986)

River	Station name	Period of record	Model type	Model parameters	R^2	$1-R^2$
Upper Niger	Koulikoro	1906-1957	ARMA (2,1)*	$a_1 = 0.59$, $a_2 = 0.16$, $b_1 = 0.2$	0,62	0,38
			AR (2)	$a_1 = 0.40$, $a_2 = 0.25$	0,62	0,38
			ARMA (1,1)	$a_1 = 0.82$, $b_1 = 0.40$	0,62	0,38
			AR (1)	$a_1 = 0.55$	0,66	0,34
		1908-1968	ARMA (1,1)**	$a_1 = 0.84$, $b_1 = 0.40$	0,64	0,36
Middle Niger	Mopti		AR (2)	$a_1 = 0.715$, $a_2 = 0.05$	0,52	0,48
	Dire		AR (1)	$a_1 = 0.725$	0,51	0,49
			AR (2)	$a_1 = 0.708$, $a_2 = 0.024$	0,5	0,5
	Baro		AR (2)	$a_1 = 0.32$, $a_2 = 0.12$	0,14	0,86
Bani	Douna		AR (2)°	$a_1 = 0.63$, $a_2 = 0.17$	0,63	0,37
			AR (1)°°	a1= 0.68	0,56	0,44

Explanation

** Carlson et al., 1970, ** Kottegoda, 1980 and other model results are given by Shahin (1986). ° Before removing the trend, and °° after removing the trend in the series.*

diagrammatically in Figure 7.17, the agreement turned out to be less than satisfactory. Probably the procedure of segmentation of the time series applied by Carbonnel and Hubert (1989) to the Niger and Senegal Rivers is far less risky. The shift between two consecutive segments refers to the break of stationarity in the series. Further analyses were undertaken using this procedure aimed at determining for each segment the duration, mean discharge and scatter around the mean. The results obtained from these analyses are summarized in subsection 6.3.4.

Reffay (1948) studied the correspondence between the flood level and its pattern of variation at the staff gauge of Koulikoro and the flood level and its variation pattern at the downstream gauges of Douna, Mopti, Diré, Niamey and Baro. The objective of that study was to develop guide rules for forecasting the flood at a certain gauge on the river given the flood level at a reference upstream gauge. From this method, the flood level at Mopti, for example, can be predicted as a function of the corresponding levels at Koulikoro and Douna. The flood level at Niamey can also be deduced from the correspondence between it and the flood level at Diré. Suppose that the benchmark at Diré reads a flood level of 4 m, for example. The mean duration of flood wave propagation as obtained from historical data is about 30 days. At that time the discharge of the Niger reaching Niamey is 915 m^3 s^{-1}. The characteristic-rating curve of the river at Niamey gives the corresponding flood level at 223 cm.

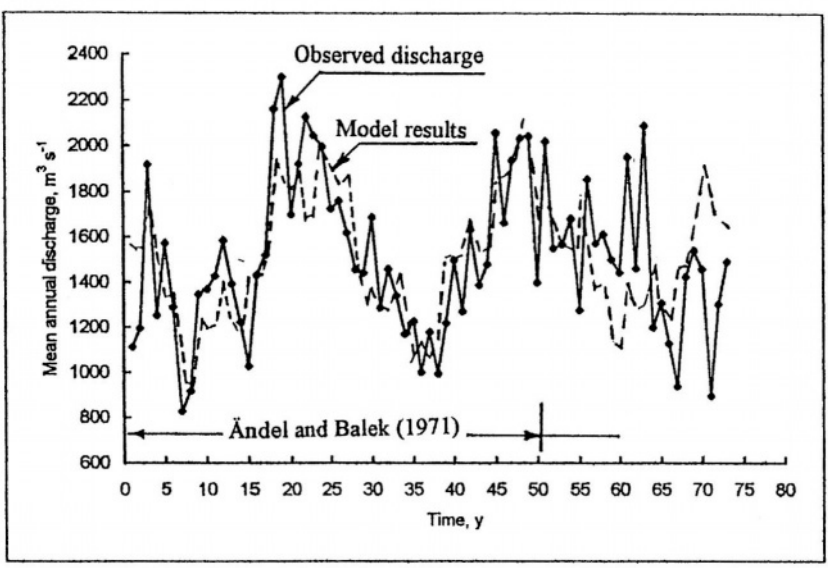

Figure 7.17- Mean annual discharge of the Niger as obtained from observations at Koulikoro, and model results, based on three periodicities (Balek, 1977)

Lamagat (1989) reported on a study program concerned with the analysis of the propagation of flood waves initiated by ORSTOM for the Sénégal and Niger Rivers. Investigation of flood levels aimed at: flow forecast, flow simulation, real-time management, and stage-discharge relationship. The methodology described by Lamagat in 1989 is about the same as that introduced by Reffay forty years earlier, except that the computer simulation models were not available in the earlier work.

The study component related to the River Niger required the development of a model for simulating the propagation of flood waves entering and leaving the inland delta in the reach between Koulikoro and Niamey. This reach can be subdivided into a number of sub-reaches. The reach Koulikoro/KeMacina, which is 275 km long, is just an example of one of these sub-reaches. The downstream flood level, H_y, has been estimated as a function of the upstream level, H_x, and the duration, T, which produce the least sum of squares of deviations between the observed and calculated levels. This can be expressed as:

$$H_y = F(H_x)$$

and

$$T = G(H_x) \qquad (7.17)$$

The model has been calibrated for the year 1979 and the agreement with the observed levels at KeMacina for the same year was found to be good.

7.2.5 Water quality- The conductivity of the Niger water has been measured since 1938 at Banankoro (Enikeff, 1950) and later at Ségou by FAO (1969) and Grove (1972). Similar measurements of the Bani water at Mopti were carried out by FAO and Grove. Grove (1972, 1985) summarized the results obtained from those studies together with results obtained from other sources, e.g. Dubreuil (1961, in Gallais, 1967) at Diré and Goundam. A set of three curves has been prepared for each measuring site: one curve for the discharge, Q, the second for the concentration, C, and the last for the total dissolved load, D. All curves have time of the year as a common abscissa. Figure 7. 18 shows one set of curves developed for the Niger near Bacita before construction of Kainji Dam (Grove 1972). The sampling of the Benue water in 1969 was reported as not successfully carried out. The mean concentration of the dissolved load, however, was roughly estimated at 40 ppm. Since the mean discharge is about $3{,}200\ m^3\ s^{-1}$, the annual transport can be estimated as 4 0 to $5.4*10^6$ t. These figures, somewhat less than that of the Niger, give a combined dissolved load past Lokoja of say $10*10^6$ t. More figures about the water chemistry of some of the tributaries in the Niger Basin are included in Table 4_g, Part II, Appendix B.

Sediment, as mentioned earlier, is the product of soil erosion in the drainage basin. The sediments are carried down into the river by the water running on the surface. Reffay in his report (1948) classified the sediments into suspended load and bed load. The suspended load consists essentially of fine material that is continuously in suspension and does not sink down. The bed load consists of the larger grains of the material that cannot be carried by flowing water and hardly rise from the bottom. The Companie Générale des Colonies carried out a series of suspended load measurements at Koulikoro in 1923, on the basis of two determinations each month. The conclusion drawn was that the concentration of the suspended load in the Niger water is too low compared to other rivers. Whereas the mean annual concentration of the Nile varies between 135 to 205 g m^{-3}, the concentration of the Niger varies between 40 and 80 g m^{-3}. For comparison the reader can be referred to Tables 2, Part B, Appendix II.

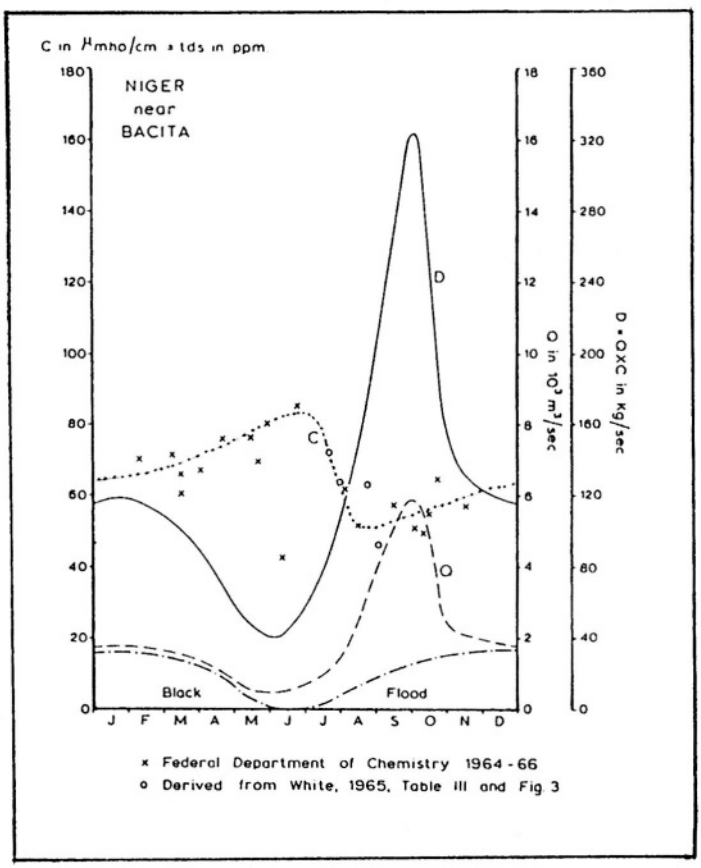

Figure 7.18- Seasonal variation of discharge and dissolved load of Niger near Bacita before the construction of the Kainji Dam (Grove, 1972)

Due to the flat plains and depressions along its course together with its mild slope, the Mayo Kebbi does not carry much sediment to the Benue. Contrastingly, the Faro transports a heavy sediment load. Consequently, the 200,000 $m^3 y^{-1}$ passing Garoua increases to 600,000 $m^3 y^{-1}$ downstream from the confluence of the Faro. The Gongola, similar to the Faro, supplies the Benue each year with a considerable sediment load, thus hampering navigation (Rodier, 1964).

The NEDECO report (1959) classified the solid transport to three classes. The first and third are similar to the first and second in the classification by Reffay (1948). NEDECO added the so-called saltation load. In this class the grains are somewhat larger in size than those in the suspended load. The grains cannot remain in suspension because their weight takes them down to the bottom. Occasionally, however, great turbulent vortices exert sudden forces in such a way that the solids more or less jump up and down, although finally returning normally to the riverbed. Hundreds of samples were taken from the Niger and the Benue; both the bed load, including saltation load, and the suspended load were determined for the years 1956 and 1957. The results obtained were added to earlier measurements and an average value for the transport each year was calculated. The average volume of each type of load at some measuring sites are listed in Table 7.6

7.3- Lake Chad Basin

7.3.1 Brief Description of the Basin- It has been mentioned in subsection 7.2.1 that Heinrich Barth crossed the Sahara and traveled the Middle Niger in his expeditions from 1850 to 1855. At the same time, one of Barth's companions, Adolf Overweg, surveyed Lake Chad. The Chad Basin, named after Lake Chad, is a vast basin that can be described as a closed hydrological system. It extends from about 24° 50'N to 5° 30'N latitudes and from 7° 50'E to 24° 10'E longitudes. The basin, from the geographical standpoint, occupies over $1*10^6$ km^2 of the southern Sahara and a similar area of savanna and forest extending

Table 7.6- Mean annual volumes of sediment transport on the Niger and Benue Rivers (based on NEDECO, 1959)

Station	River	Bed load*		Suspended load		Wash load		Total	Period
		10^6 m^3	% **	10^6 m^3	%	10^6 m^3	%	10^6 m^3	
Baro	Niger	0,31	6,5	0,55	11	4	82,6	4,9	1915-57
Yola	Benue	0,2	6	0,17	5	3	89	3,3	1934-57
Makurdi	Benue	0,61	5	0,95	8	10	87	12	1932-57
Shintaku	Niger	0,88	5	1,3	8	15	87	17	1915-57
Onitsha	Niger	1	5,5	1,7	9	16	85,5	19	1925-57

Explanation

** = including saltation load, ** = percent of total*

south to the Congo (Zaire) watershed (Grove, 1985). The total basin area is shared between seven countries: Algeria, the Cameroon, Chad, Niger, Central African Republic, Nigeria and the Sudan. However, only four countries: Chad, Cameroon, Niger, and Nigeria share the surface of Lake Chad. The map in Figure 7.19 shows the boundaries of both the geographical and the conventional basins. The Conventional Basin of Lake Chad is the area under the mandate of the Lake Chad Basin Commission. It covers 427,000 km^2 stretching from latitude 9°30'N to latitude 16°00'N.

The waters of the Logone and Chari (Shari) Rivers, which are supplied by tributaries rising in a wide arc from Cameroon to Jebel Marra, flow across the gently sloping plains of north central Africa for several hundred kilometers and eventually spread to form Lake Chad. In the geological past, Lake Chad had a surface area of around 300,000 km^2 and a depth of more than 150 m. It is believed that the waters of the lake then overflowed into the Benue valley to reach the Atlantic. Presently the surface area of the lake varies between 5,000 km^2 and 23,000 km^2, depending on the annual inflow of the River Shari. The diminution in the size of the lake after it was first seen by Europeans supported the hypothesis of desiccation in Africa, but subsequent fluctuations in level suggested a more variable regime (Stamp and Morgan, 1972).

The lowest portion of the Chad Basin is situated in the Bodélé depression at an elevation of about 160 m a.m.s.l. The present lake is located 500 km to the south of the Bodélé depression at an elevation of 278-283 m a.m.s.l. The lake is currently a vast sheet of water only a few meters deep (Grove, 1985). Over the last 100 years or so, Lake Chad receded more than 5 m, 3 to 4 m of which have taken place since 1965. Furthermore, the complicated shape of the northeast side of the lake and the numerous elongated low islands within it are believed to be the remains of ancient sand dunes, formed in a drier period, several thousands of years ago and flooded by the southern rivers. From the southeast comer of the lake, a broad shallow channel known as the Bahr el-Ghazal (this is different from the Bahr el-Ghazal described in connection with the Nile Basin) can be traced northeast for more than 300 km to the lowest part of the basin. This is known as the Bodelé depression, lying at about 155 m a. m. s. l. The Republic of Chad itself is close to the western rim of the lake basin at a level of about 280 m. It is very likely that Lake Chad's waters have at times spilled northeast, along the Bahr el-Ghazal as well as eastwards into the Benue in still more humid periods.

Although the salinity of water at the southern edge of the lake is quite low, it increases gradually towards the northern edge, as evaporation becomes higher, around 2.25 m y^{-1}. Along the sandy northern shores, salts crystallize out. Obviously, the salt concentration varies throughout the year. It depends on the inflow, the direct rainfall on the lake, and the distance of the sampling site from the Chari River, the most important freshwater feeder to the lake.

The main source area for the rivers entering the basin is the upland country, about 1000 m a.m.s.l. extending eastwards from the lava-capped Adamaoua

Plateau in northern Cameroon to the chrystalline highlands of Central African Republic. Further east, the altitude increases to 1600 m a.m.s.l. in the massif de Guera, and 3000 m in Jebel Marra in the Sudan Repulic (Grove, 1985).

The Gribingui and the Bamingui Rivers combine to form the Chari River. These two streams originate in the Central African Republic. The Chari, below the confluence of these two streams is a tropical river in transition with a catchment area of about **45,000 km²**. A short distance below the confluence the Bangoran River joins the Chari from the right bank. The Bangoran also springs

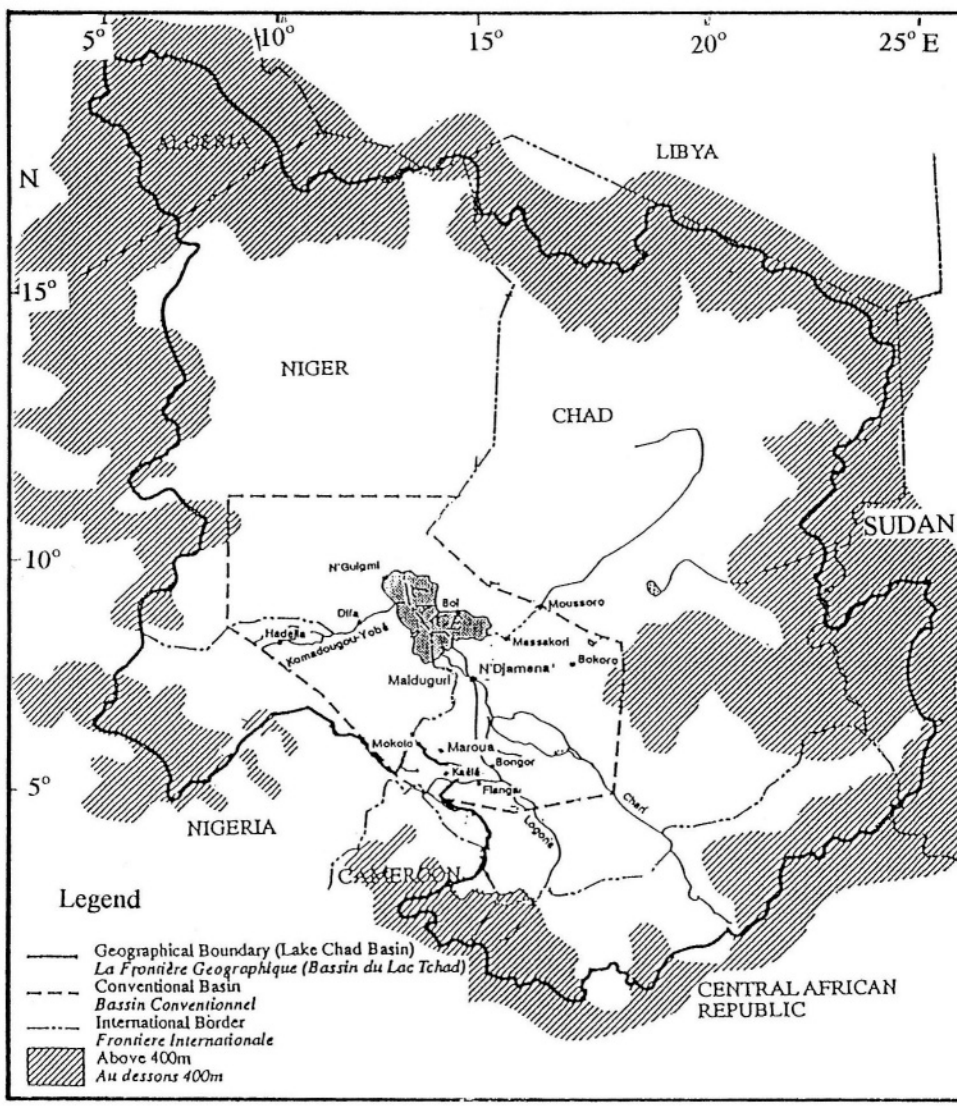

Figure 7.19- Geographical and conventional basins of Lake Chad

in the Central African Republic and has a regime that hardly differs from the regime of the Gribingui and the Bamingui.

The Chari, below the junction of the Bangoran by a short distance, receives on its right bank the Aouk, an important affluent. The Aouk springs in the Dar Fougoro at the boundary of the Sahelian zone, also the international boundary between the Central African Republic and Chad, and runs from east to west. All along its course, the Aouk traverses immense flood plains below which it enters rapidly the Chadian basin and joins the Chari. Below the confluence of the Aouk, the Bahr Keita (Bahr is the Arabic word for sea, locally meant to be any body of water) also joins the Chari.

Halfway along its course, the Chari receives on its left bank the Bahr Kamer, with its abundant supply. Both Bahr Kamer and Bahr Aouk receive on their left side all their tributaries. They traverse a large flood plain before joining the principal river course. The most important tributary is the Ouandjia, which springs from the mountainous region between the basins of the Chari and the Obangui. The course of the Chari assumes a northerly direction to Sarh (formerly known as Fort Archambault). At this point the catchment area of the Upper Chari is estimated at 193,000 km^2, of which 125,000 km^2 belong to the Bahr Aouk.

Downstream from Sarh the Chari receives its most important tributary, Bahr Sara, on its left shore near the confluence of Bahr Keita. The Ouham River is the principal branch of Bahr Sara, rising from the eastern Adamaoua heights in the western part of the African Central Republic. The Ouham, in turn, has important affluents, the Fafa and Nana Barya. A few kilometers below this confluence, the Bahr Salamat joins the Chari on the right side. The supply of the Bahr Salamat is not abundant. It originates in the Jebel Marra (altitude: 3,000 m a.m.s.l.) in the Sudan under the name of Bahr Azoum. As a result of the high elevation and the steep slope of the ground, the Bahr Azoum and its tributaries escape the total degradation, which affects the neighboring watercourses. These streams are, in fact, wadies with sandy beds that usually run dry for nine months each year. An important site on Bahr Azoum is Am Timan. Just below this site, the Bahr Azoum disappears in an inland delta, below which the river is regenerated under the name of Bahr Salamat. The river is nourished by a series of sahelian streams (wadies) rising from Abou Deia.

Below the confluence of Bahr Salamat, the Cahri develops an important flood plain on the right shore, and some affluents join its course. The most important one, Bahr Erguig, rejoins the Chari after a large distance, but not without losses. From here, the Chari flows due north, and a few kilometers before reaching N'Djamena (formerly Fort-Lamey) is joined on its left shore by the Logone River (Rodier, 1964)

The Logone rises from the northeast border of the Adamaoua massif. The Wina and Mbéré Rivers combined together form the course of the Logone River. The Logone receives the Pende (sometimes called the eastern Logone) River on its right shore below Moundou. The Logone runs in a northwesterly

direction. The discharge measuring site at Lai is located a few kilometers downstraem from the confluence of the Pende on the Logone. Below Lai, the river undergoes immense losses by flowing onto the floodplains and supplying water to its effluent streams. The most important effluents are the Ba Illi and those effluents which are captured by the Benue. The Ba Illi separates itself from the Logone downstream of Lai, winds up its course between the Chari and Logone Rivers till it disappears in the marshes between them below Bongor.

Below Bongor, the Logone flows across a vast floodplain, the Grand Yaéré, for a reach longer than 70 km. Some of the overspill water in these floodplains feed El-Beid Ebeli stream., which joins Lake Chad directly. The Serbewel, an effluent stream of the Chari River, is another important stream that is fed from the overspill of the Logone. On the other hand, the Logone receives a number of the torrential rivulets or mayos running from northern Cameroon. After traversing these swamps, the Logone rejoins the Chari after losing about 30% of its annual supply. The combined river continues its course in a northwesterly direction for approximately 110 km before discharging its water into Lake Chad.

The eastern part of the Lake Chad Basin is crowded with a number of Wadies (ouadi is the local word for wadi, which is an intermittent flowing stream) rising in the eastern provinces of Chad; Biltine, Ouadai, and Batha. These wadies flow from east to west and two of them, Ouadi el-Ouadey and Batha, discharge their water into Lake Fitri, some 250 km east of the southeastern edge of Lake Chad. Further to the northeast of Chad, several ouadies spring from the Ennedi Plateau. These comprise the Ouadi Kandor, Sata, Chili, Oum Hadier, Haouach and Yedinga. All these wadies disappear in the desert before reaching an outlet on a river or lake.

From the Jos-Kano highlands in northeast Nigeria, the Komadougou-Yobe river system flows westward and discharges its water into Lake Chad. The amount that reaches the lake does not exceed 1% of the total inflow to the lake. Additionally, two seasonal streams, the Yedseram and the Ngadda, originating in Nigeria, discharge very small amounts into the lake.

Most of the rivers and places mentioned in this subsection are shown on the detailed map in Figure 7.20.

7.3.2 Hydrology of Lake Chad Basin- The mean annual precipitation in Lake Chad Basin varies between more than 1,400 mm in the source area to less than 50 mm in the Saharan areas in the northeast. Tables 9 and 10_a in Appendix A give some information about monthly and annual precipitation. The long-term mean average precipitation in Faya Largeau (station 39), Arbéchér (station 63) and Moundou (station 111), all in Chad, are 16, 466, and 1,194 mm, respectively. Jäkel (1984) prepared a number of profiles representing the annual rainfall depth versus distance from Bongassou south of the Central African Republic in the south to Faya Largeau in northern Chad. The same study has shown a strong and direct correlation between the basin rainfall and the gauge

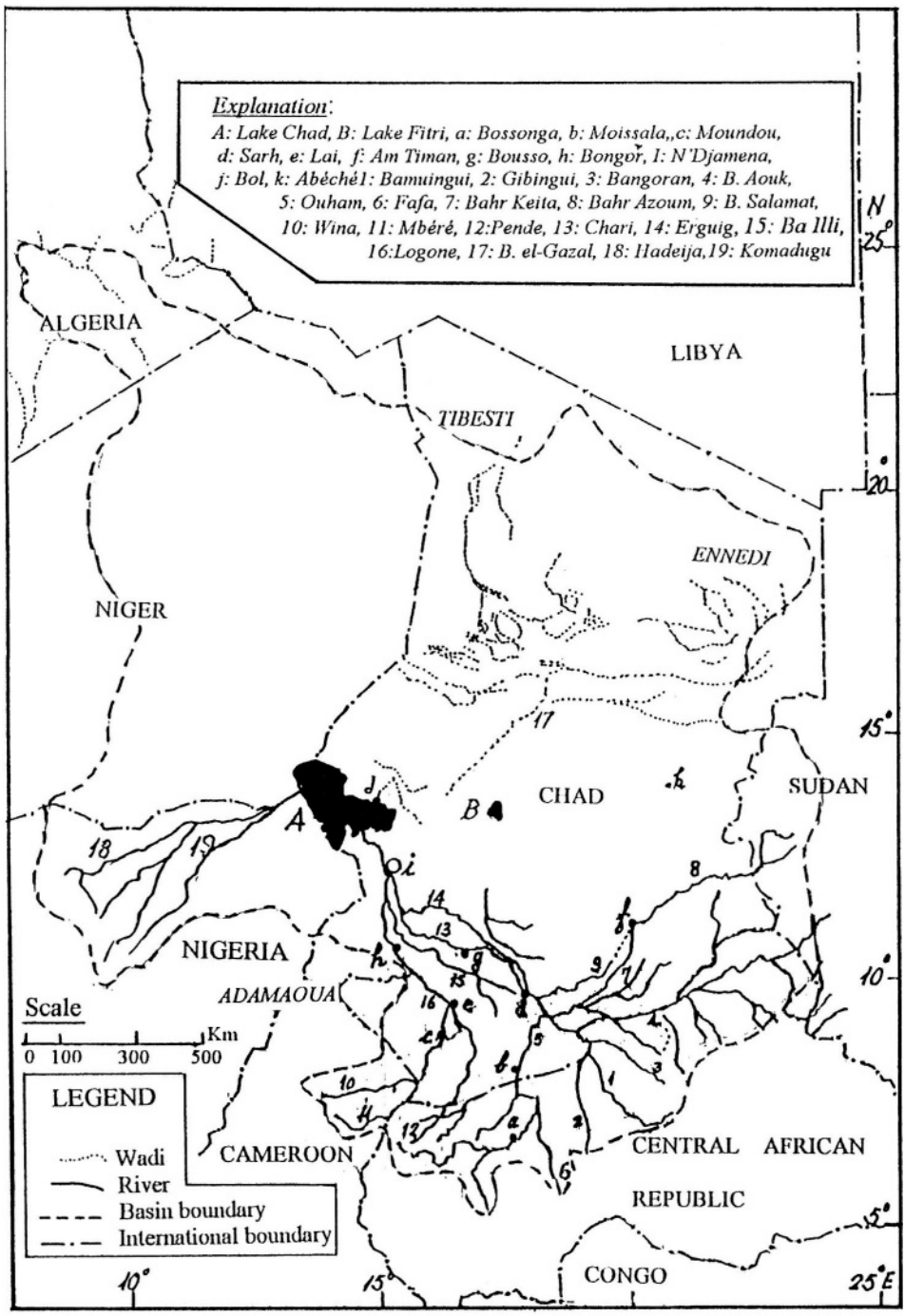

Figure 7.20- The Chari and Logone Rivers with their principal tributaries and other major streams traversing the Lake Chad Basin

height at Bol between 1936 and 1973. Furthermore, the pieces of information obtained from that study have helped in developing an integrated basin mean precipitation. Not withstanding the extreme interannual variability in the rainfall, the estimate for the Republic of Chad alone is around 350 mm y^{-1}, 790 mm y^{-1} for the conventional basin, and 850 mm y^{-1} for the geographic basin.

Pouyaud (1989) presented the monthly and annual evaporation rates from three lakes subject to Sudano-Sahelian climate. Lake Chad happened to be one of those lakes. The calculations were carried out for the period 1965-78. The methods used for calculating the evaporation rates were the water balance, evaporation pans, energy-based methods and the bulk-aerodynamic approach. The results obtained from the water balance method are included in Table 4.13. The minimum evaporation, 4.4 mm d^{-1}, occurs in January; the maximum is 7.6 mm d^{-1}, and the annual 5.95 mm d^{-1} (2,166 mm y^{-1}). The results obtained from Penman's method, upon introducing an appropriate value for the albedo and adjusting the term expressing the advective heat, are quite good. The rates of evaporation in the source areas of the Chari and Logone Rivers, as a result of the high humidity and less temperature during the summer, are less than those from Lake Chad and its surroundings. On these grounds, the annual evaporation drops to say 1,500 mm y^{-1}

The Atlas of World Water Balance (ed. Korzoun/ UNESCO, 1977) shows that the runoff coefficient in the Basin of Lake Chad varies from more than 40% to less than 5%. It also shows that the runoff coefficient generally decreases from west to east and from south to north. It increases, as one should expect, with land slope and wetness of the soil.

Gischler (1967) presented a hydrologic synthesis for the Basin of Lake Chad In that synthesis, Gischler described the number of publications containing information about the cartography, geology, pedology and hydrology of the lake that appeared since 1905 as immense. The Office of Scientific and Technical Research for Overseas (ORSTOM) started in 1947 a large number of studies covering the hydrological, geophysical and pedological aspects of the Republic of Chad. The hydrological investigations that have been performed were not confined to Lake Chad alone, but extended to cover the Chari and Logone Rivers and their respective basins.

The surface area, water level and depth, and salinity of Lake Chad are, as already mentioned, under investigation for quite some time. Despite this fact, the hydrological observations in the Chad Basin, other than the lake itself, are meager when compared to those of the Nile or the Niger. The report entitled "Discharge of Selected Rivers in Africa (UNESCO, 1995)" gives the mean monthly and annual discharges, as well as the minimum and maximum discharges of the Chari, Logone and their tributaries as tabulated below.

The tabulated figures show clearly that the percentage of missing data is quite high. The years that followed the independence of Chad from France in 1960, and the long internal fights between the different factions in the country, added to the inadequate technological levels among the nationals, have resulted

River	Gauging station Name	No.	Record from	to	Missing length of record, %
Chari	N'Djaamena	68	1933	1991	18.65
Chari	Sarh	95	1938	1986	40.82
Logone	Bongor	86	1948	1986	56.41
Bahr Azoum	Am Timan	76	1953	1976	45.83
Chari	Bousso	83	1936	1985	68.00
Logone	Moundou	101	1935	1985	78.3
Pende	Doba	99	1947	1975	58.62
Logone	Lai	89	1948	1986	66.67
Bahr Sara	Moissala	103	1951	1984	47.06

in several breaks and discontinuities in the data. As an example, the data with few minor breaks at Bousso station cover the period from 1954 to 1972, whereas the listed period of record is from 1936 to 1985. After this review of the status and availability of the data, it becomes easier to present the hydrology of the Lake Chad Basin.

The Gribingui and the Bamingui Rivers, which together form the Chari River, have the characteristics of Guinean rivers; prolonged high flow season without too high flood peaks, abundance of water in the low-flow season and limited interannual variability. The mean annual flow of the Chari at this point is in the order of magnitude of $160\ m^3\ s^{-1}$.

The Bahr Aouk at the confluence with the Chari has a catchment area of $25{,}000\ km^2$. Nonetheless, the enormous losses bring its share in the discharge of the Chari at Sarh (catchment area $193{,}000\ km^2$) to just one-third, i.e $100\ m^3\ s^{-1}$. As the overall mean annual rainfall on the basin of the Chari up to Sarh is about 1,070 mm and the mean runoff coefficient approximately 5%, the average discharge at Sarh (first key station on the Chari) is around $300\ m^3\ s^{-1}$ ($10*10^9\ m^3\ y^{-1}$). The difference between the two discharge figures represents the combined discharge of the Bamingui, Gribingui, and Bangoran Rivers (total catchment area of $68{,}000\ km^2$). Table 6_a, Part I/Appendix B, shows that the mean discharge for the period 1952-75 is $273\ m^3\ s^{-1}$ with a coefficient of variation of 38%. The UNESCO Publication (Riv Dis v 1.0, 1996) gives a mean annual discharge of $286\ m^3\ s^{-1}$, using a length of record of 357 months within the period 1938-75. Both figures are close to each other and not beyond expectation, as the rainfall in the actual period was about 10% less than the annual rainfall in average years. Some of the years between 1965 and 1975 were years of drought, brutal drought indeed. In the pre-drought period the maximum annual discharge were $1{,}120\ m^3\ s^{-1}$ and the 100-y flood discharge was estimated as $1{,}800\ m^3\ s^{-1}$ (Rodier, 1964).

The Chari, below Sarh, receives its principal tributary, Bahr Sara. The Ouham is the main branch of Bahr Sara. After flowing some distance to the

northeast, it is joined on the left bank at Moïssala by Nana Barya, another principal tributary. The catchment area of Bahr Sara at Moïssala is 67,500 km^2, and the mean annual discharge is about 500 $m^3 s^{-1}$ or $16*10^9$ $m^3 y^{-1}$ (Rodier, 1964). This is quite reasonable since under the normal rainfall depth of 1, 400 mm y^{-1} the runoff coefficient varies between 15 and 20%. With this figure in mind the Bahr Sara must be regarded as the parent branch of the Chari.

At some distance downstream from the confluence of Bahr Sara, the Chari receives the Bahr Salamat. The upper reach of this sahelian river is known by as Bahr Azoum. This is a wadi-like river, which carries its annual flood in just a matter of hours from July to September each year and runs empty of water for nine months. Other than the flash flood, the river during its flow season carries some base flow and the runoff generated by some isolated storms. By the time the flood arrives at Am Timan station, half of the discharge would have been lost through the spill of water into a number of effluent streams. The mean annual flow at Am Timan is about 45 $m^3 s^{-1}$ ($1.4*109$ $m^3 y^{-1}$). The flood discharge varies between 225 and 350 $m^3 s^{-1}$. The flood season usually begins before the end of July and can last till mid-November.

Below Am Timan, the water left in Bahr Azoum is totally lost in the Inland Delta, and is regenerated under the name of Bahr Salamat. This occurs by way of a series of affluents originating in the surroundings of Aboudeïa. The discharge hydrograph of Bahr Salamat resembles the hydrograph at Am Timan, though to a different scale. It is probably closer to that of Bahr Aouk, except that the discharges are much less. This makes the contribution of Bahr Salamat to the flow in the Chari quite inferior.

The water in the Chari, downstream from the confluence of Bahr Salamat, flows across flood plains and spills into effluent streams, of which the Erguig is the most important one. The Erguig rejoins the Chari after flowing in its own course for some distance, but not without losses. The hydrograph at Bousso is somewhat more uniform than that at Sarh, with a mean annual discharge of 890 $m^3 s^{-1}$ ($28*10^9$ $m^3 s^{-1}$). The corresponding figure for the annual flood discharge is, on average, 2,600 $m^3 s^{-1}$.

The second important river system traversing the Chad Basin is the Logone. Moundou is the first key station, (station no. 101), on the Logone. The available data give the mean annual discharge as 355 $m^3 s^{-1}$, with variation coefficient of 24.9%. Below Moundou, the Logone receives on its left shore the Pende, which brings at Doba (station no. 99) an average discharge of 123 $m^3 s^{-1}$, with variation coefficient of 35.3%. The combined discharge of the Logone and Pende amounts to 478 m3 s^{-1} ($15.1*10^9$ $m^3 y^{-1}$). The mean annual discharge in the pre-drought period, 1948-60, used to be about 10% larger or $16.27*10^9$ $m^3 y^{-1}$ at Laï. This figure corresponds to a catchment area of 56,700 km^2, an overall average precipitation depth of 1,420 mm y^{-1} and annual runoff coefficient about 20%. According to Roche et al. (1976) the deviation of the individual years from the mean figure, 513 m3 s^{-1}, is – 6, + 22, + 13, - 20, - 53 and - 48 for the years 1968, 1969, 1970, 1971, 1972 and 1973 respectively.

The Logone downstream of Laï undergoes significant losses while traversing the floodplains and by over-spilling water to some effluents, notably the Ba Illi and those effluents captured by the Benue River. The Ba Illi, after separating itself from the Logone, runs its course in the wet lands between the Chari and Logone. After some distance and losing a considerable portion of its flow it rejoins the Logone below Bongor.

Below Bongor, the Logone enters into the Grand Yaéré, a flood plain whose length exceeds 70 km. A certain reach of this flood plain supplies El-Beid tributary with water, which is eventually and directly discharged into Lake Chad. Contrarily, the flood plains receive the discharges of some small torrential streams (mayos in local language) originating in north Cameroon.

The Logone, after traversing the marshy land, rejoins the Chari bringing with it about $12.5*10^9$ m3 y^{-1}, after having $5*10^9$ m^3 y^{-1} lost en route. As such, the mean annual flow earned by the Chari at N'Djamena for the period 1933-1991 would have been $33*10^9$ m^3 (equivalent to 1,048 m^3 s^{-1}, coefficient of variation of 35.5%). This figure is 15% less than the figure of 1,230 m^3 s^{-1} given by Rodier (1964) as a mean for the period 1933-60. Again, according to Roche et al. (1976) the deviation of the actual measurements from the mean, 1,230 m3 s^{-1}, is- 17, -22, -4, -21, -56 and –44% for the years 1968, 1969, 1970, 1971, 1972 and 1973 respectively. The maximum and minimum of the annual mean discharges in the period 1933-91 were 1,673 m^3 s^{-1} and 236 m^3 s^{-1}, respectively. Figures 6.10_a and 6.10_b give the maximum and minimum annual mean discharges as 4,900 m^3 s^{-1} and 236 m^3 s^{-1} respectively, both for 100 years return period. The discharge of the Chari into Lake Chad is hardly different from its discharge at N'Djamena. Figure 7.21 is a simplified flow chart of the Chari and Logone and their principal tributaries.

Other than the Chari and Logone Rivers, which drain the southern part of the basin, there is the Komadougou-Yobe river syetem flowing to the basin from the Kano-Jos highlands of Nigeria. The contribution of this system to the inflow of Lake Chad is quite small, in the order of 1% of the total inflow. Next to the perennial rivers there is a number of intermittent streams or wadies, which cover some of the local needs for water in the Saharan/Sahelian zone in the north of the basin.

7.3.3 Water quality- The map prepared by Milliman and Maede (1983), though general, indicates that the sediment yield in the southern part of the Lake Chad Basin varies between 10 and 50 t km^{-2} y^{-1}. The annual sediment yield anywhere else in the basin is less than 10 t km^{-2}. Tables 2_a and 2_b, Part II/Appendix B, give some data about the sediments of the water carried by the Chari (sometimes written Shari) River. Table 2_b, for example, shows that the sediment yield of the Chari is 0.93 t km^{-2} y^{-1} and of Bahr Sara 8.4 t km^{-2} y^{-1}, thus in agreement with that map.

According to Gac (ORSTOM, 1981), the annual average dissolved sediment is $2*10^6$ t and the corresponding density is 59 mg l^{-1}. The annual amount of

solids is $3*10^6$ t and the corresponding density is 87 mg l^{-1}, all based on a total annual flow of $40*10^9$ m^3. These values are not too different from the values listed in Table 2_a, Part II/Appendix B, bearing in mind that they are based on an annual flow of $41.65*10^9$ m^3 y^{-1}.

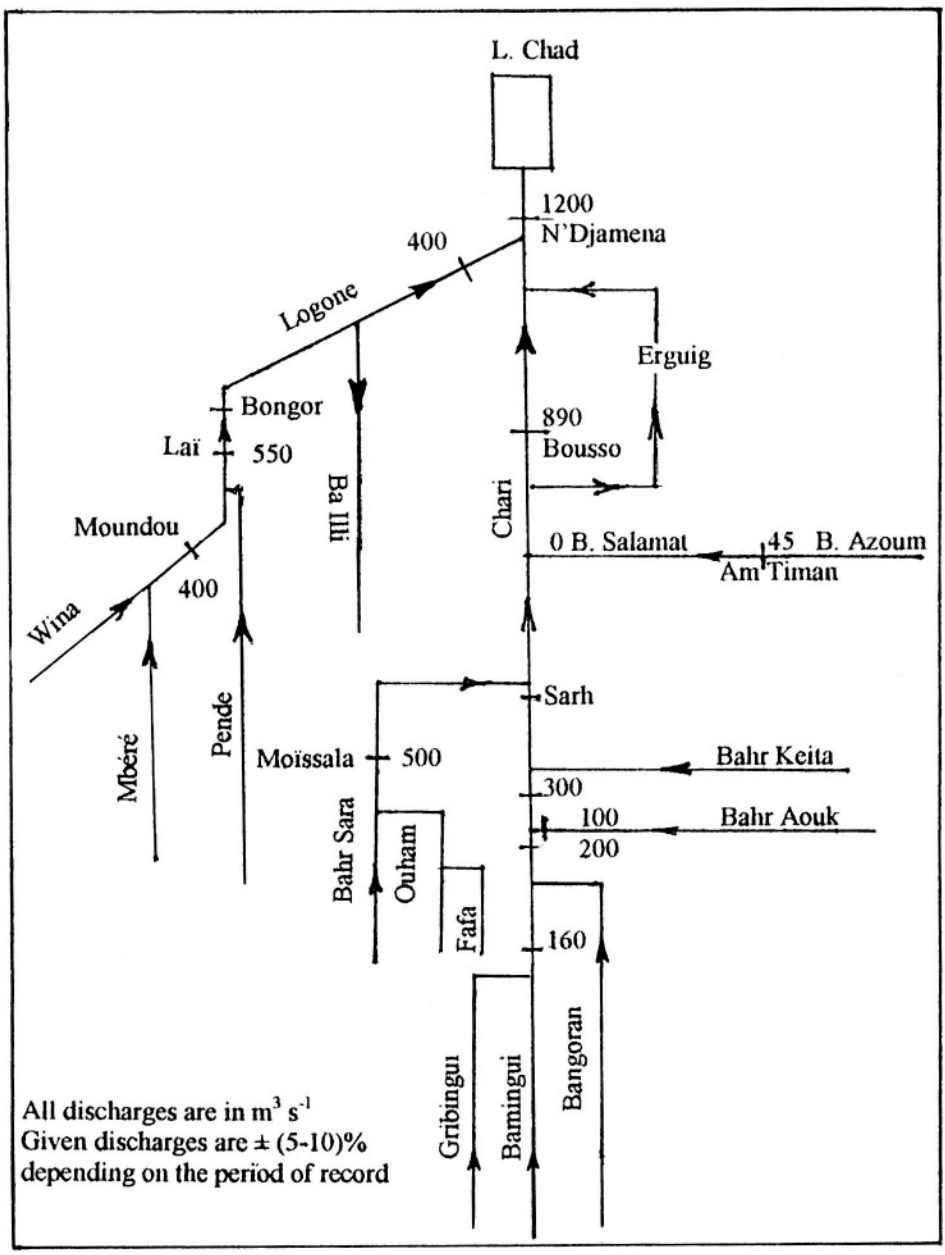

Figure 7.21- Flow chart of the Chari and Logone and their principal tributaries

The total dissolved solids in the waters flowing across the Continental Terminal (sedimentary beds of Cenozoic age) past Moundou, Doba, Munda and Sarh are $2.4*10^6$ t y^{-1}. This is equivalent to 88% of the amounts finally delivered to Lake Chad. The total particulate load at those points, average for the period 1969-72, is $3.25*10^6$ t. In their lower reaches, the Logone and Chari lose, on the average, about 25% of their discharges by evaporation and spilling over the banks. They lose also, on the average, about 25% of their dissolved load and 40% of their sediment load in suspension. The spillage of water from both rivers over the flood plains results in loss of water and retardation of the flood peak. Together with this, on average, a million tons of sediment are filtered out of the floodwater by the reeds and grasses each year and added to the Quaternary deposits south of the lake (Grove, 1985).

The dissolved load has its lowest concentration in July-August during the early rains, when values are about 35 ppm, rising slowly to a peak value at the end of the dry season in May, about 80 ppm, and then falling sharply. As the mean concentration of the dissolved load is 50 ppm, the mean annual supply of dissolved solids to the lake should be around $2*10^6$ t assuming an annual input of $40*10^9$ m^3. Roche (1972) estimated the concentration at N'Djamena, average for 1968 and 1969, as 57 ppm.

The concentration of the suspended sediment load in the discharge of the Chari increases from a small value, 25 ppm, in the dry season, and increases rapidly to more than 250 ppm in the early part of the rainy season. With the progress of the rainy season, the river loses much of its floodwater through spillage over its banks and flow into the flood plains. The loss is not limited to water but extends to the solid load. At this stage the water still left in the Chari is fairly clear. The total solid load brought to the confluence annually is $2.4*10^6$ t, of which $1.4*10^6$ t by the Chari and $1.0*10^6$ t by the Logone. As can be seen in Table 2b, Part II/Appendix B, Bahr Sara (Ouham) supplies the major portion of the sediment load carried by the Chari. This tributary originates in a highland covered with crystalline rocks. The solid material brought by the Ouham consists of about 65% clay (kaolinite and illite) and 17% quartz and feldspar. This composition changes to about 50% clay (kaolinite and illite), 10% quartz, 11% smectites and a considerable percentage of organic matter in the lower reach of the Chari.

The chemical composition of water is included in Table 4_g, Part II/Appendix B. Those data are somewhat different from the data published by Carmouze and Pedro (1977), which gives the prevalence of cations present in the order Ca^{2+}, Mg^{2+}, Na^+ and K^+. The same order but for the old data (Grove, 1972) is Ca^{2+}, Na^+, Mg^{2+} and K^+. Roche (1981) developed Figure 7.22 to show the monthly variation of, among others, the cations present in the Chari at N"Djamena.

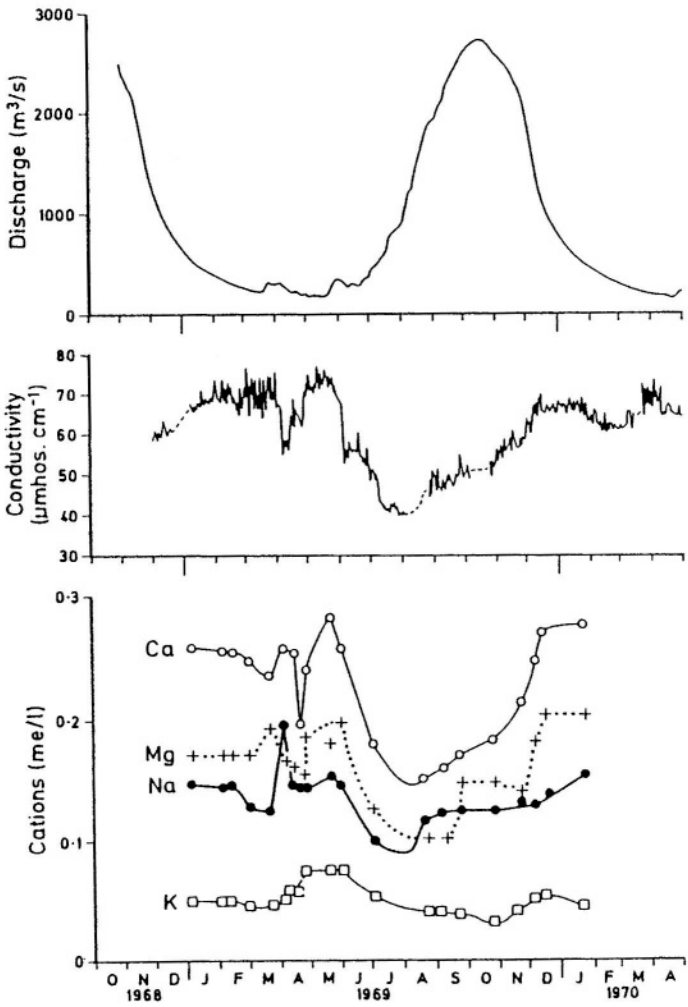

Figure 7.22- Discharge, conductivity and cations of the Chari and Logone versus time in month at N'Djamena (from Roche, 1981)

CHAPTER 8

HYROLOGY OF LARGE RIVER BASINS: Central and Southern Africa

This chapter is merely a continuation of Chapter 7, where three more large river basins will be dealt with. These are the basins of the Congo or Zaïre River, essentially in Central Africa, and the Zambezi and the Orange in southern Africa.

8.1- The Congo (Zaire) Basin

8.1.1 General description of the basin- The Portuguese explorer Diego Cão is claimed to be the first European to have set a foot on the bank of the Congo River. That event took place in 1483 while being on a trip to discover Angola. Three centuries later another explorer, Mungo Park, sailed in the Congo down mistaking it for the Niger River. In his second expedition (1874-1877), Stanley circumnavigated Lake Victoria, passed down the Lualaba, a tributary of the Congo, to where it becomes the Congo and then down that mighty river to the ocean. Wissman is accredited with mapping the Kasai, another tributary of the Congo, whereas many southern tributaries were explored and mapped by Grenfell. In the 1880s, de Brazza extended his trips to the regions beyond the confluence of the Ubangi (sometimes written Ubangui or Oubangui) and the Congo Rivers. Meanwhile Crampel was busy exploring the Sangha River Basin.

The basin extends from latitude 09°15'N in the Central African Republic to 13° 28'S in Angola and Zambia, and from longitude 31° 10'E through the Great African Lakes in the East African Rift to 11° 18'E on the Atlantic Ocean. Other sources of information (e.g. Bultot and Dupriez, 1987) show that a small area in the extreme east of the basin extends to 34° 02'E. This enormous geographical extent covers a surface area of about $3.8*10^6$ km^2 situated in the middle of Africa. Approximately one-third of the basin is located in the Northern Hemisphere, the other two-thirds in the Southern Hemisphere. It should be noted here, however, that the surface area varies from as small as $3.6*10^6$ km^2 to as large as $4.1*10^6$ km^2, depending on the source of information.

The Congo Basin is an enormously broad flat basin in the great Central African Plateau. The basin is simply a shallow depression bordered from the northwest by the Adamaoua Mountains, the northern equatorial ridge from the north, and the East African Highland from the east. The Crystal Mountain forms the western boundary of the basin and the southern equatorial ridge bounds it from the south.

The Congo Basin is geologically very ancient. The recent alluvium borders the main river whereas the lower core of the basin is occupied by older alluvium. These old sediments give place on the higher ground to vast stretches of soft sandstone. Older than these are the Koundeloungou beds, which are by far the oldest rocks found resting on the ancient massif. They are probably Permian-Triassic in age and have been folded by the tectonic movements responsible for the folded mountains of the cape in the extreme southwest of Africa. These beds include limestone, shale, and sandstone (Stamp and Morgan, 1972).

The Congo basin is shared between nine African countries. These are Angola, Burundi, Cameroon, Central African Republic, Congo (Brazzaville), Congo (Kinshasa), Rwanda, Tanzania and Zambia. In the extreme northeast the water divide between the Congo Basin and the Bahr el-Ghazal Basin of the Nile system is the frontier with the Republic of the Sudan. Further to the east, the basin extends to Lake Tanganyika, and in the extreme south the water divide with the Zambezi is in part the frontier with Zambia. Figure 8.1 is a map showing the boundaries between the countries sharing the Congo Basin.

The entire surface area of Congo (Kinshasa) and most of the surface of the Congo Brazzaville are located within the river basin. We are going to distinguish between the two Congos by annexing the name of the capital city to each state. As such, instead of the Democratic Republic of Congo and the Congo Republic, we shall call them by Congo Kinshasa and Congo Brazzaville respectively.

The heart of the basin area enjoys an equatorial climate with no dry season. The rainfall in this part varies between 1,500 and 2,000 mm y^{-1}. For example, the total rainfall at Bangui (station 136) is 1,560 mm; Bambesa (station 143) 1,782 mm; and Ouesso (station 154) 1,792 mm. As tropical rainforest is limited to areas with annual rainfall exceeding 1,400 mm, and temperature between 21°C and 32°C, one can easily realize that wide areas of the Zaïre drainage basin are tropical rainforest regions. Data about monthly and annual rainfall at many more stations in the basin can be found in Tables 9 and 10, of Appendix A. In the subequatorial region in the northern part of the basin, maxima rainfall occur in May-June and September-October, and the minima in December and January. The months of maxima and minima rainfall in the southern subequatorial region are March and November, and from June to September, respectively.

The facts that most of the basin area does not suffer from high temperature all the year round and the relative humidity of the air is generally too high render the annual potential evapotranspiration limited to between 1,200 and 1,400 mm. As such, the percentage of the total area that enjoys water surplus or excess (precipitation > potential evapotranspiration) in the Congo Basin is not competed by any other large river basin in Africa. This conclusion is supported by the finding of Riou (1975) that the actual and potential rates of evapotranspiration are practically the same for the region of Central Africa situated between latitudes 5°N and 5°S. Figure 8.2 shows the distribution of the monthly rainfall and potential evapotranspiration at Bambesa station.

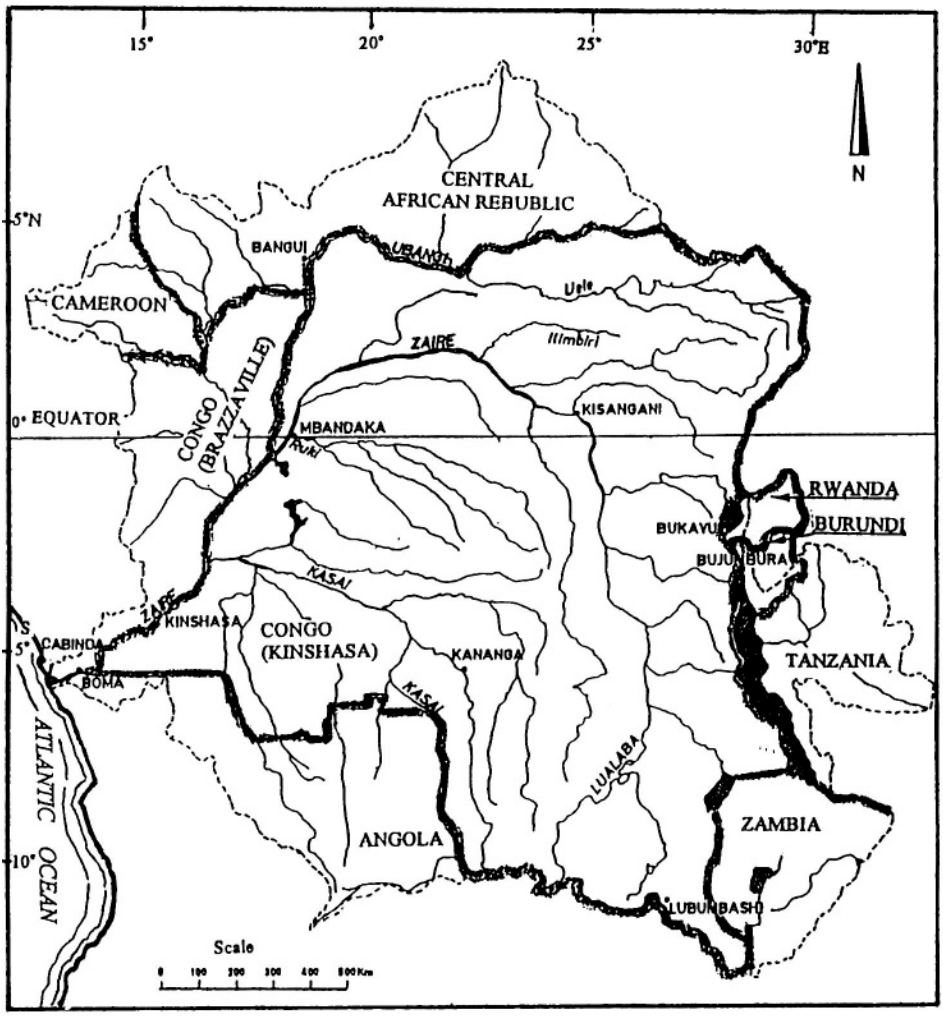

Figure 8.1- The Congo (Zaïre) River Basin

As the soil surface of the major part of the basin is nearly always wet and the soil texture is generally heavy, the loss by infiltration is rather limited. This causes the runoff coefficient to fairly high, falling in the range of 20-25%, except where marshy spots or swamps are encountered. Such a range is relatively large in comparison with the runoff coefficient for the Nile, Chari and most of the Niger basin, already discussed in Chapter 7.

The Congo (Zaïre) River traverses the surface of the basin for a length estimated at between 4,700 and 5,100 km. It loops through the country, plunging over numerous rapids and cataracts making uninterrupted navigation impossible. From Kinshasa to Kisangani, however, and from Kinshasa to Ilebo, the Congo

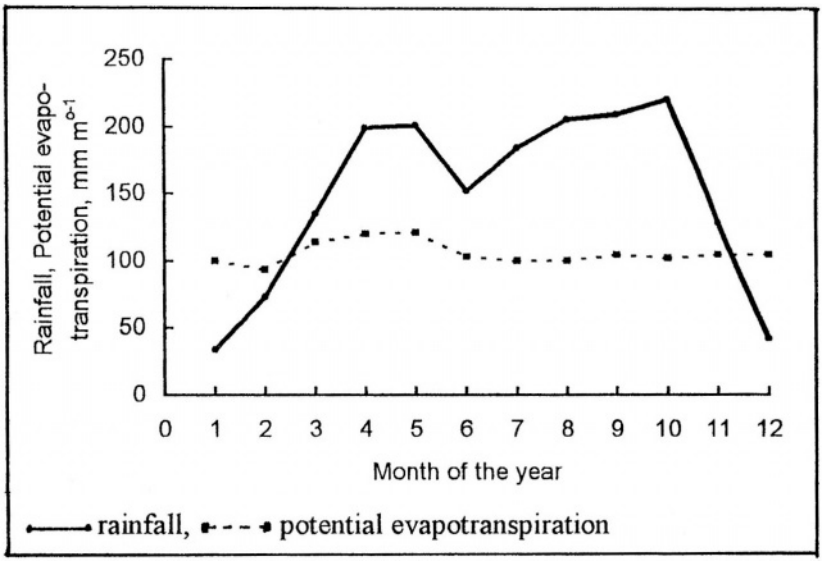

Figure 8.2-Average rainfall and potential evapotranspiration at Bambesa station

and its major tributary the Kasai are navigable for 1,740 and 820 km respectively. The stretch of the river water separating Kinshasa and Brazzaville, the capitals of the two states is known as Malebo (Stanley Pool). Here the river widens to say 20 km before plunging over the first cataract of the Livingstone Falls, 32 in total. From this point downwards to the ocean, the river flows through a narrow gorge obstructed by the cataracts, thus descending some 270 m before reaching Matadi, which lies some 300 km further downstream at the head of the estuary. The most impressive rapids are those at the Inga site (latitude 5° 30'S), where there is a fall of 98 m between the Island of Sikila and the confluence of the Bundi River. The Inga Dam has been constructed with the aim of benefiting from this huge drop in developing hydropower

The Congo (Zaïre) is, after the Amazone, the second largest river of the world and the largest in Africa. It drains one of the largest tropical forests of the world. The average annual flow of the river at Kinshasa represents 38% of the total drainage of all African rivers to the surrounding oceans. Flowing as it does through the heart of Africa, the Congo is a more constant river compared to the Nile or the Niger. Despite this statement, the flow of the Congo over the years shows that it is subject to interannual variability. July and August are the months of low flow, whereas December is month of high flow. The tributaries from the south, such as the Kasai, have two periods of low water and two of high in the year, but the tributaries from the north, such as the Ubangi, have a single maximum. Consequently, the regime of the main river varies from place to place.

According to Balek (1977) the source of the river is thought to be the Chambeshi River, rising south of Lake Tanganyika and transferred by the Bangweulu Lake into the Luapula River. Before entering into Lake Mweru, the Luapula is joined by tributaries like the Wiswila on the left shore and the Luongo, above Johnston Falls, on the right shore. The Kalungwishi flow in a northwesterly direction to feed Lake Mweru from the east. After flowing through Lake Mweru, the Luapula joins the Lualaba. Above the confluence, the Lualaba flows through Lake Kisala and is joined by the Lufira River. Lake Tanganyika joins the Congo system through the Lukuga River. The Lomami, a mighty tributary, joins the Lualaba at about 100 km below Kisangani (formerly called Stanleyville). The catchment area of the Congo at the confluence Lomami-Lualaba is slightly over $1*10^6$ km^2.

The two principal tributaries of the Congo, other than the Lualaba, are the Kasai flowing from the south and the Ubangi from the north. All the tributaries of the Ubangi, e.g. the Chiko, Bari, Ouaka, Lobay and Mbaéré, originate in the Central African Republic. The catchment area just below the confluence of the Ubangi increases to $2.3*10^6$ km^2. The Sangha River and its tributaries originate in the extreme northwest of the Congo Basin. Less important, yet powerful, tributaries are the Aruwimi, Itimbiri, Mongala, Lulonga, Momboyo and the stream draining Lake Tumba. The Kasai is formed by the Sankuru, Lulua, Lusiko, Inzia, Kwango and Kwili / Kwa Rivers.

Figure 8.3 is a map showing some of the principal tributaries, lakes and falls in the Congo system. Figure 8.4 is a more detailed map showing many more tributaries of the Congo River in the reach between Kinshasa and the estuary connecting it to the Atlantic Ocean.

8.1.2 Hydrology of the Congo Basin- From the data appearing in the UNESCO Publication "Discharge of selected rivers of Africa (1995)",one finds discharge measurements at 14 gauging sites in the Congo Basin. Obviously, this number is infinitely small for a basin of about $3.8*10^6$ km^2. The 14 sites are distributed between four countries: 1 (station 164) in the Cameroon, 7 (stations 146, 148, 151, 153, 156, 160 and 165) in the Central African Republic, 5 in Congo Brazzaville (stations 171, 195, 205, 208 and 210), and 1 (station 209) in Congo Kinshasa. The length of uninterrupted record at these stations varies between a maximum of 81-y for Kinshasa (station 209) to a minimum of 6-y at each of Zémio (station 146) and Bossélé Bali. The mean monthly and annual discharges of stations no. 148, 151, 156, 165, 171, 205, 209 and 210 are given in Table 8, Part I / Appendix B, whereas the mean annual discharge and the coefficient of variation at all 14 stations are included in Table 6, of the same Appendix.

The mean annual discharges of those 14 stations, despite the large differences between their respective lengths of record, are strongly correlated each with the catchment area at the corresponding measuring site. This might be attributed to the limited differences between the mean annual rainfall and runoff coefficient

from sub-basin to sub-basin. The relationship between the mean annual discharge, $(Q)_m$, in $m^3 s^{-1}$, and the catchment area A in km^2 can be written as:

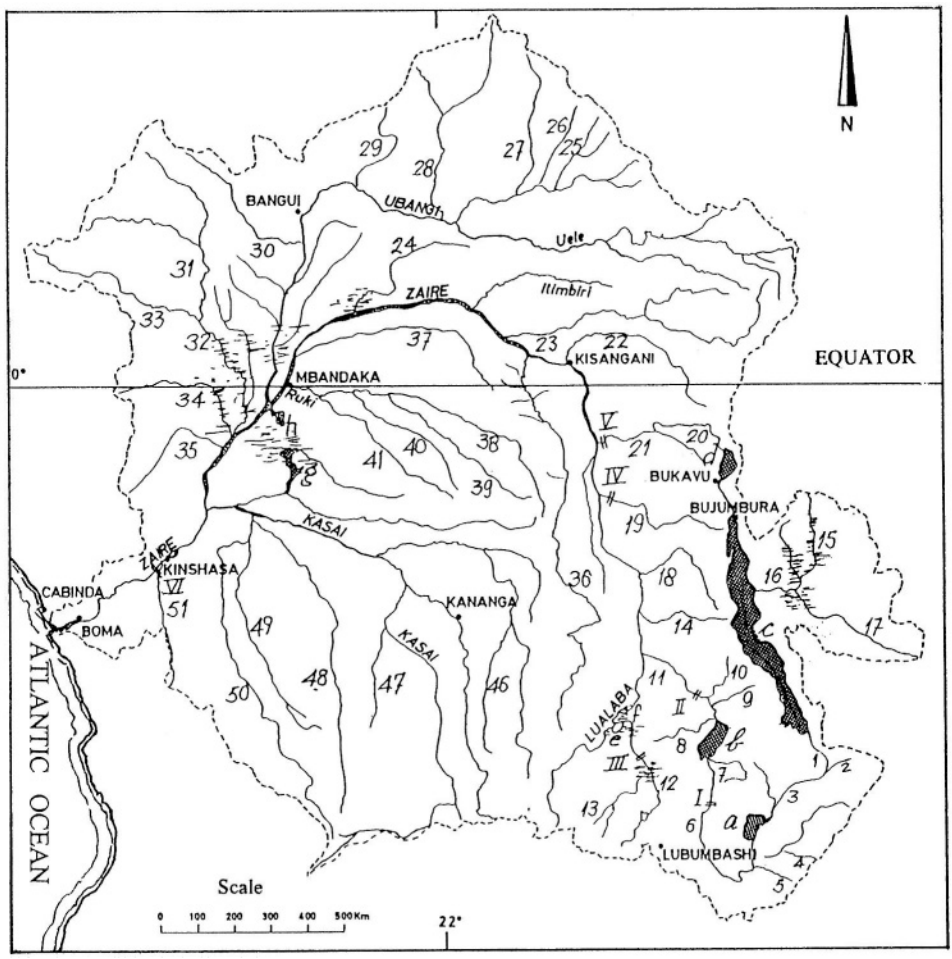

Figure 8.3- Some of the rivers, lakes and falls covering the Congo drainage basin

Explanation of the notations on the map

***Rivers**: 1-Chambeshi, 2-Kalungu, 3-Chambezi, 4-Lukulu, 5-Lulimala, 6-Luapulu, 7-Kalungwishi, 8-Lubule, 9-Luvunzo, 10-Lukumbi, 11-Luvua, 12-Lufira, 13-Dikuluwe, 14-Lukuge, 15-Moyowasi, 16-Malagarsi, 17-Ugalla, 18-Luama, 19-Elila, 20-Lugulu, 21-Ulindi, 22-Nia Nia, 23-Lulu, 24-Ebola, 25-Duarte, 26-Chiko, 27-Bori, 28-Kotto, 29-Ouake, 30-Loboya, 31-Boumba, 32-Sangha, 33-Dja, 34-Likouala, 35-Aima, 36-Loman, 37-Lopari, 38-Lomela, 39-Satonga, 40-Luilako, 41-Lokoto, 42-Lokoro, 43-Lukenie, 44-Lubefu, 45-Lulua, 46-Chikopa, 47-Loange, 48-Kwilu, 49-Inzia, 50-Kwango, 51-Inkis.*

***Lakes**: a-Bangweulu, b-Mweru, c-Tanganyika, d-Kivu, e-Upemba, f-Lukanga, g-MaiNdombe, h-Tumba*

***Falls**: I-Johnston Falls, II-Luvua Falls, III-Kiubo Falls, IV-Elila Falls, V-Ulindi falls, VI-Livingstone Falls.*

$$(Q)_m = 0.0287A^{0.9155} \quad (8.1)$$

The correlation as expressed by R^2 is 0.9588.

Balek, using older data than what is available in the UNESCO Publication (1995), drew the water balance of 19 sub-basins next to the principal tributaries and the main river (1977). The results obtained from that study are given in Table 8.1. From this Table, it is clear that the range of variation of each of the mean annual precipitation, *P,* evapotranspiration, *(ET),* and runoff coefficient, *r,* for these sub-basins is much wider than the corresponding ranges in the aforementioned 14 sub-basins. In the set of 19 sub-basins used by Balek (1977), the runoff coefficient varies between 3% and 32% and the annual rainfall from about 1,100 mm in the Lualaba Basin to an average of 1,700 mm in the Ubangi Basin. Again, the mean annual discharge, $y = (Q)_m$, and the catchment area, $x = A$, using the data of the two sets of sub-basins, are plotted to a logarithmic scale as shown in Figure 8.5. The low points are essentially those for the sub-basins with small runoff coefficients. This is the case when the tributary traverses a swampy area like the interbasin the Bangweulu Swamps and the sub-basin of the Lukuga. The line of best fit to the plotted data can be written as:

$$(Q)_m = 0.0119A^{0.9649} \quad (8.2)$$

with correlation, R^2, of 0.8607. The less uniformity of the data in the set of the 19 sub-basins compared to the former set of the 14 sub-basins is responsible for the lower correlation associated with Eq. (8.2) compared to Eq. (8.1). The comparison shows clearly that the regression relation must contain, in addition to *A*, terms related to each of *P* and *r*.

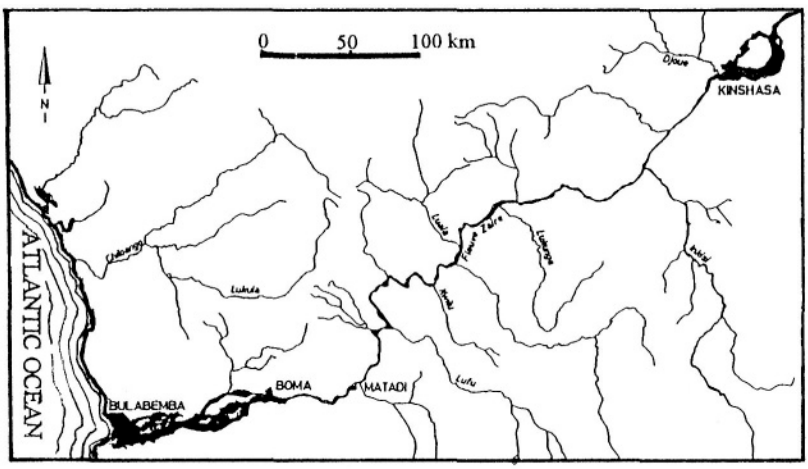

Figure 8.4- Tributaries of the Congo River in the reach Boma-Kinshasa

Table 8.1- Water balance of the major rivers and tributaries in the Congo Basin (after Balek, 1977)

River	Location	A	P	R	(ET)	r	$(Q)_m$
Chambeshi	above Bang.S.	43,830	1,143	241	902	0.21	337
Interbasin	Bang.Swamps	57,664	1,229	59	1,170	0.05	110
Lupula	*below Bang.S.*	*101,494*	*1,191*	*138*	*1,053*	*0.12*	*441*
Interbasin	Bang.S.-L. Mweru	71,372	1,165	136	1,029	0.12	307
Lupula	*at Mweru Lake*	*172,866*	*1,181*	*138*	*1,029*	*0.12*	*754*
Kalungwishi	Mweru (mouth to)	26,696	1,143	164	929	0.14	139
Interbasin	Kalung.-Lualaba	123,734	1,160	132	1,028	0.11	520
Luvua	*confluence with Lualaba*	*296,600*	*1,172*	*136*	*1,036*	*0.12*	*1,274*
Lualaba	Uzilo	16,300	1,100	200	906	0.18	103
Lufira	Cornet Falls	11,980	1,180	126	1,054	0.11	48
Lualaba	above Luvuua	187,800	1,130	110	1,020	0.10	651
Lualaba	*below Luvua*	*484,400*	*1,156*	*126*	*1,030*	*0.11*	*1,931*
Interbasin	Luvua-Lukuga	7,200	1,125	108	1,017	0.10	24
Lualaba	*above Lukuga*	*491,600*	*1,155*	*125*	*1,030*	*0.11*	*1,955*
Lukuga	mouth to Lualaba	270,900	1,062	32	1,030	0.03	271
Lualaba	*below Lukuga*	*762,500*	*1,122*	*91*	*1,031*	*0.08*	*2,226*
Interbasin	Lukuga-Lomami	227,083	1,905	602	1,303	0.32	5,295
Lualaba	*above Lomami*	*989,583*	*1,399*	*239*	*1,160*	*0.17*	*7,521*
Lomami	mouth	95,830	1,675	274	1,401	0.16	837
Congo	*conf. Lomami-Lualaba*	*1,085,413*	*1,422*	249	*1,790*	*0.17*	*8,358*
Interbasin	conf.-Ubangi	463,000	1,875	482	1,393	0.26	7,128
Congo	*above Ubangi*	*1,548,413*	*1,559*	*315*	*1,244*	*0.20*	*15,484*
Ubangi	mouth	754,830	1,597	248	1,349	0.16	5,936
Congo	below Ubangi	*2,303,243*	*1,568*	*293*	*1,276*	*0.19*	*21,420*
Interbasin	Ubangi-Sangha	9,58	1,750	355	1,395	0.20	108
Congo	*above Sangha*	*2,312,823*	*1,561*	293	*1,268*	*0.19*	*21,528*
Sangha	mouth	213,40	1,580	362	1,218	0.23	2,471
Interbasin	Sangha-Kwa	109,50	1,750	375	1,375	0.21	1,304
Congo	*Kwa*	*2,635,723*	*1,581*	301	1,280	0.19	3,303
Kwa	mouth	881,89	1,538	350	1,180	0.23	9,873
Congo	*below Kwa*	*3,517,610*	*1,570*	*314*	*1,256*	*0.20*	*25,176*
Interbasin	Kwa-mouth of Congo	89,84	1,300	220	1,080	0.17	629
Congo	*mouth*	*3,607,450*	*1,561*	*313*	*1,246*	*0.20*	*38,805*

Explanation

A = drainage area in km^2; P = precipitation in mm y^{-1}; R = runoff in mm y^{-1}; (ET) = evapotranspiration in mm y^{-1}; r = runoff coefficient; and $(Q)_m$ = mean annual discharge in m^3 s^{-1}.

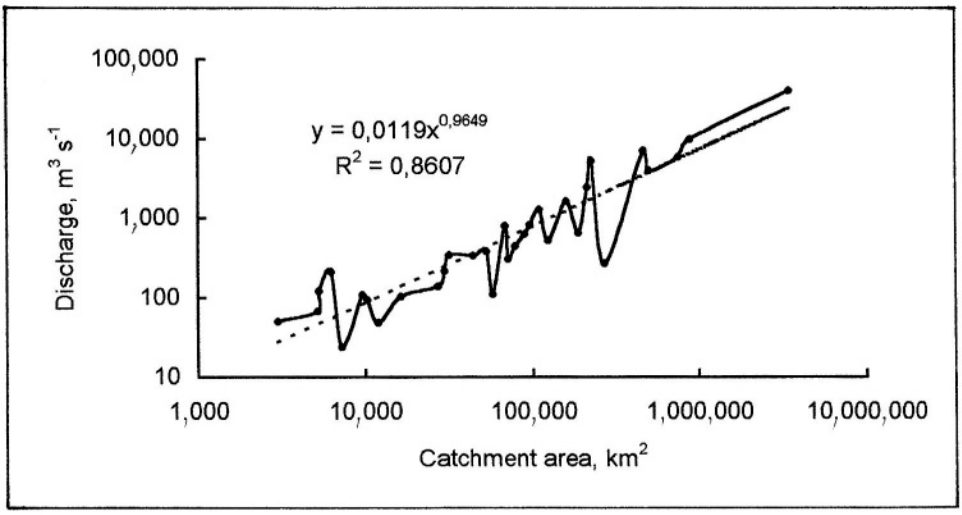

Figure 8.5- The mean annual discharge against catchment area for 33 sub-basins in the Congo Basin

According to Bultot and Dupriéz (1987), the average annual figures for the Congo (Zaïre) basin are P = 1,550 mm and (ET) = 1,200 mm yielding runoff, R, = 350 mm. As this runoff depth corresponds to a long-term mean annual discharge, $(Q)_m$, of 40,000 $m^3 s^{-1}$ at Kinshasa, the basin area must then be $3.6*10^6$ km^2. This figure for the runoff, R, however, should be reduced to about 330, 315, and 307 mm y^{-1} would the surface area of the basin increases to 3.8, 4.0 and $4.1*10^6$ km^2 respectively. The same reference analyzed the 1903-83 series of daily river stage at Kinshasa-East and a series of 85 actual discharge measurements (1987).

A summary of the results obtained from the analysis of the river stage series is given in Table 8.2. The tabulated results show that the highest mean monthly level, 6.11 m, took place in December 1961, and the lowest, - 0.32 m, in July 1905. As the river stage series is sufficiently long, it has been possible to define the annual regime not only by the mean daily level each year, but also by their enveloping values using different probability levels (e.g. extreme values corresponding to 5% and 95% frequencies). Moreover, the water level series have been adjusted by means of Taylor series to turn them from discrete to continuous.

The rating curve, Figure 6.7, for the Congo River at Kinshasa has been established using a series of 85 discharge measurements at Kinshasa-Kalina taken in the period 1955-61. Two pairs of equations have been suggested, each for describing the rating function. The pair described by Eqs. (6.7) and (6.8) has been used for calculating the daily discharges corresponding to the daily water levels.

Table 8.2- Mean , maximum and minimum monthly and annual water levels in m for the period 1903-83 at Kinshasa (from Blutot and Dupriez, 1987)

Item	J	F	M	A	M	J	J	A	S	O	N	D
I- Mean monthly												
a	3.2	1.99	1.6	1.93	2.19	1.86	1.16	1.08	1.83	2.72	3.7	4.13
b	0.75	0.7	0.62	0.68	0.75	0.76	0.67	0.54	0.51	0.53	0.57	0.69
c	0.23	0.35	0.39	0.35	0.34	0.41	0.58	0.51	0.28	0.19	0.15	0.17
d	5.81	4.63	3.28	3.84	3.91	3.76	2.94	2.74	3.09	3.86	5.02	6.11
e	1.41	0.45	0.5	0.85	0.85	0.31	-0.32	-0.03	0.64	1.56	2.46	2.45
II- Maximum monthly												
a	3.85	2.45	1.82	2.26	2.39	2.13	1.55	1.43	2.26	3.2	4.12	4.32
b	0.74	0.78	0.63	0.74	0.73	0.72	0.77	0.51	0.52	0.55	0.63	0.68
c	0.19	0.32	0.35	0.33	0.3	0.34	0.5	0.36	0.23	0.17	0.15	0.16
d	6.17	5.35	3.69	4.16	4.18	3.88	3.59	3.04	3.3	4.41	5.73	6.26
III- Minimum monthly												
a	2.49	1.64	1.42	1.61	1.97	1.5	0.84	0.82	1.4	2.28	3.23	3.8
b	0.79	0.66	0.64	0.65	0.76	0.81	0.62	0.59	0.52	0.52	0.55	0.69
c	0.32	0.4	0.45	0.4	0.39	0.54	0.73	0.72	0.37	0.23	0.17	0.18
e	0.76	0.3	0.36	0.55	0.56	-0.17	-0.47	-0.29	-0.24	1.06	2.04	2

Explanation

a = arithmetic mean, in m, b = standard deviation, in m, c = coefficient of variation, d = maximum and e = minimum. The zero level is at 272.12 m above the mean level of the Atlantic Ocean .

Annual values: I, a = 2.28 m; b = 0.52 m; c = 0.23; d = 3.95 m; and e = 1.31 m
II, a = 4.48 m; b = 0.60 m; c = 0.13; and d = 6.26 m.
III, a = 0.72 m; b = 0.58 m; c = 0.80; and e = -0.47 m.

Table 8.3 gives the basic statistics of the monthly and annual discharge series at Kinshasa for the period 1903-1983. The statistics included in this Table are the monthly and annual mean, maximum and minimum. The interannual variability is in the range 10-15%. The mean annual discharge plotted as a time series for the period 1903-83 is shown in figure 6.13_c. This plot shows a rising trend for the entire period, except after 1975 till the end of the record. There seems to be some cyclic fluctuation, which shall be described and discussed in the next subsection. The frequency distribution with confidence limits of the annual maximum discharge for the same period is shown graphically in Figure 6.10_a. The 1 in 100 y flood discharge, as can be read from this Figure is $83.5*10^3$ m^3 s^{-1} ($\pm$ $5.0*10^3$ m3 s^{-1}). The same discharge was reached once, in December 1961, during the period of record.

The July discharge exceeded $24.5*10^3$ m^3 s^{-1} in 95% of the cases, and exceeded $41.5*10^3$ m^3 s^{-1} in just 5% of the cases. The highest mean monthly discharge, 80.8 m^3 s^{-1}, was observed in December 1961 and the least, $21.5*10^3$ m^3 s^{-1}, in July 1905.

Table 8.3- Mean, maximum and minimum monthly and annual discharges in $m^3 s^{-1}$ of the Congo River at Kinshasa for the period 1903-83 (Bultot and Dupriez, 1987)

Item	J	F	M	A	M	J	J	A	S	O	N	D	year
I- Mean monthly													
a	47,490	37,650	34,710	37,170	39,150	36,720	31,710	31,090	36,370	43,170	51,710	56,080	40,250
b	6,890	5,530	4,530	5,140	5,760	5,670	4,680	3,690	3,660	4,220	5,410	7,150	4,150
c	0.15	0.15	0.13	0.14	0.15	0.15	0.15	0.12	0.10	0.10	0.10	0.13	0.10
d	76,310	61,210	47,560	52,690	53,230	51,800	44,830	43,170	45,980	52,930	65,910	80,830	54,960
e	33,330	26,910	27,230	29,230	29,470	26,080	22,350	23,990	28,120	34,450	41,010	40,930	32,870
II- Maximum monthly													
a	53,320	41,210	36,310	39,660	40,670	38,630	34,440	33,450	39,540	47,070	55,870	58,050	59,710
b	7,420	6,450	4,750	5,760	5,730	5,510	5,590	3,610	3,960	4,660	6,510	7,370	6,850
c	0.14	0.16	0.13	0.15	0.14	0.14	0.16	0.11	0.10	0.10	0.12	0.13	0.11
d	81,660	69,910	51,170	55,810	56,010	52,980	50,260	45,610	47,750	58,470	75,150	83,050	83,050
III- Minimum monthly													
a	41,500	35,020	33,470	34,840	37,450	34,110	29,560	29,370	33,310	39,710	47,350	52,680	28,730
b	6,590	4,880	4,560	4,770	5,690	5,840	4,110	3,870	3,580	3,970	4,710	6,740	3,810
c	0.16	0.14	0.14	0.14	0.15	0.17	0.14	0.13	0.11	0.10	0.10	0.13	0.13
e	28,880	25,980	26,350	27,540	27,610	23,190	21,490	22,500	25,620	30,860	37,780	37,480	21,490

Explanation

a = arithmetic mean, b = standard deviation, c = coefficient of variation, d = maximum and e = minimum

The first and second stream gauging stations after Kinshasa in the Congo Basin as far as publication of discharge measurement is concerned are Bangui on the Oubangui River, Central African Republic and Ouesso on the Sangha River, Congo Brazzaville, respectively. The length of record at each station has already been given in the beginning of the present sub-section. The corresponding catchment areas are 500,000 and 158,350 km^2 respectively.

As the regime of the Ubangui is transitional between tropical and equatorial, the ratio of the mean monthly flow in October (month of largest flow) to the mean monthly flow in March (month of smallest flow) is larger compared to the same ratio at Kinshasa. The ratio for Ubangui is 8, 818 $m^3 s^{-1}$ to 963 $m^3 s^{-1}$, or 9.16, and $56.08*10^3$ $m^3 s^{-1}$ to $34.71*103$ $m^3 s^{-1}$, or 1.62, for the Congo at Kinshasa. Additionally, whereas for both rivers, March is the month of smallest flow, the months of largest flow are October for the Ubangui and December for the Congo respectively. Depending on the surface area of the Congo Basin, the average specific yield of the Congo at Kinshasa falls in the range 9.8-11.6 l s^{-1} km^{-2}. It is likely that the corresponding figure for the Ubangui at Bangui is slightly different.

The mean specific discharge of the Sangha at Ouesso, being 8.3 l s^{-1} km^{-2}, is very close to that of the Ubangui at Bangui. It appears to be somewhat smaller than the specific yield of the Congo at Kinshasa. The comparison, however, is questionable as the periods of record for the three stations are not the same. Whereas the major part of the mean annual discharge series of the Congo at Kinshasa shows a rising trend the series of both the Ubangui and the Sangha show a falling trend. This can be observed from the time series plots, Figure 6.10$_c$. The regime of the Sangha, though not exactly similar to that of the Ubangui, yet is closer to it than to the Congo. The largest mean monthly discharge, 3,230 $m^3 s^{-1}$, occurs in November and the smallest, 852 $m^3 s^{-1}$, in February. These figures bring the ratio between the mean discharges in these two months to 3.79.

8.1.3 Stochastic analysis of the mean monthly discharge series, 1903-83, of the Congo River at Kinshasa- The interannual fluctuations of the Congo at Kinshasa have been studied by Molinier and Mbemba (1979) and later by Probst and Tardy (1987). They concluded that in the pre-1960 period, the climate of the basin suffered four cycles of average and below average discharges, whereas since 1960, above average discharges have been the rule with the exception of the Sahelian drought in 1973 when the Congo fell back to the average discharges.

The autocorrelation analysis of the monthly discharge series, 1903-83, performed by Bultot and Dupriéz (1987) has clearly indicated that the annual (12 months) and seasonal (six months) cycles are the principal cyclic components of the data. Furthermore, analysis of the residuals left after removing the annual and seasonal components has shown that these residuals suffer from a strong

persistence. The application of the Mann as well as other tests has pointed out to the occurrence of a jump in the series around August 1959. Applying the same tests to the two sub-series 03.1903-08.1959 and 09.1959-12.1983 has detected a jump (not significant) about April 1920 and another jump (significant) about November 1970. These jumps can be clearly observed in Figure 8.6. In conclusion, the reference series has been declared as non-stationary of the first and the second orders.

The autocorrelation analysis already summarized was complemented by the spectral analysis of the monthly mean discharge series, 1903-83. The objective of the latter analysis is to calculate the contribution $V(\omega)$ caused by a cycle with a certain frequency ω to the variance of the observed discharges. This contribution can be determined from the expression:

$$V(\omega) = 100x\frac{SSR(\omega)}{TSS} \tag{8.3}$$

where TSS = total sum of squares of observations and $SSR(\omega)$ = sum of squares of the periodic term with frequency ω adjusted to the observations.

The percentage contribution has been determined for 25 cyclic fluctuations with periodicity ranging from 2.4 month up to 461 month. The six largest contributions were found to correspond to periods of 12, 6, 461, 89, 162 and 4 months. The corresponding contributions expressed as percentage of the long-term mean annual discharge ($40.34*10^3$ m^3 s^{-1}) are 20.8, 15.7, 5.8, 5.6, 4.8 and 3.6 respectively. The sum of squares of the contributions of the 12 and 6-mo cycles amounts to 87% of the sum of squares of the contributions of the six periods and 80.5% of all 25 periods. These results confirm the findings obtained from the autocorrelation analysis that the annual and seasonal cycles have the largest influence on the variance of the observations included in the series.

The sum of the amplitudes of the cyclic oscillations with periods of 89 month (7 y 5 mo) and 162 month (13 y 6 mo) is slightly above 10% of the mean annual discharge. Since the amplitude of each oscillation alone is about 5% they can be regarded as significant. It is likely to find an explanation of the power of the amplitudes of these two oscillations in connection with the solar and lunar activities. On the grounds of these results a trigonometric-type model, Eq. (8.4), has been suggested for simulating the monthly discharge series.

$$y_i = M + \Sigma_{k=1}^{m} A_k \cos(\omega_k t_i + \phi_k) + \varepsilon_i \tag{8.4}$$

where m = 25 is the total number of periods, P_k, $\omega_k = 2\pi/P_k$ is the pulsation of the kth component, k = 1, 2, …, 25 is the number of component, M = constant, A_k and φ_k are the amplitude and phase of the kth component, and ε_i is the standard error of estimate of the observed discharge at time t_i.

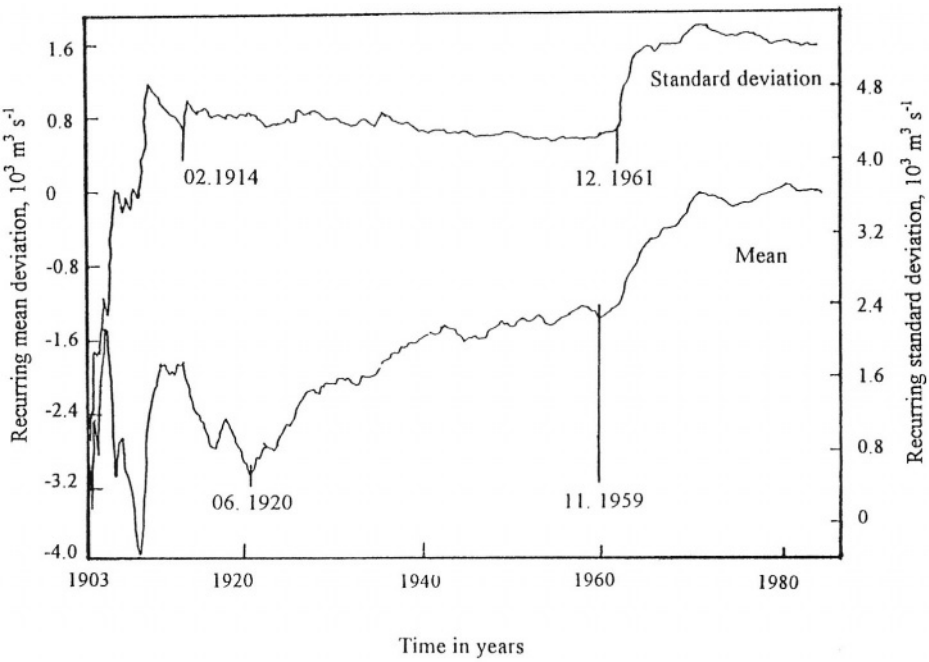

Figure 8.6- Time series of recurring means and standard deviations of monthly discharges after removing the annual seasonal components (Bultot and Dupriéz, 1987)

The above findings have been used to develop an autoregressive model for forecasting the monthly discharges. The estimated mean monthly discharge, Q'_t, where *t* corresponds to *mth* month of the year, is the sum of the three components appearing in the right-hand side of Eq. (8.5)

$$Q'_t = P'_m + R'_t + E'_t \qquad (8.5)$$

where P'_m is the specific belonging to the month m, to be estimated from a sub-model that represents the mean periodic variation of the monthly discharge throughout the year, R'_t is the sum of the effects caused by perturbations and noise, to be estimated with the help of an autoregressive sub-model, and *E't* is an estimate of the random error at time *t*.

The parameters of the trigonometric sub-model have been determined using a sliding sequence with a duration of 7 years. Despite the fact that not all of the four harmonics, 12, 6, 4 and 3 mo, are significant yet they have been used in that sub-model. The proportion of the variance explained by these four harmonics varied, depending on the sequence throughout the period 1903-83, from 57 to 81%. The standard error of estimate for the ensemble covering the period 1910-83 reached $\pm 2{,}459\ \mathrm{m^{-3}\ s^{1}}$ or 6.1% of the mean discharge.

To test the validity of the forecasted discharges, the discharge data of the 1903-09 period have been considered as a primary series. The forecasted discharges were then obtained for lead periods of 1, 2, 3,..., 12 months. As the mean error did not exceed, on the average, 0.2 % of the mean observed discharge, the agreement has been considered excellent. Furthermore, the standard deviation of error between the estimated and the corresponding observed discharges has been found to increase rather rapidly from about 7 % for 1 month-ahead to 12.1% for 6 months-ahead, followed by a slow increase to 12.7 % for 12 months-ahead. As a 3 months-ahead forecast is regarded quite sufficient from the practical point of view, the corresponding standard error is in the order of ± (8-12) % of the observed values. For more accurate estimates of the discharge in the flood months, however, it is recommended to repeat the estimates using shorter intervals.

8.1.4 Water quality- The average concentrations of the suspended sediment load in the Congo River as given by various investigators are smaller than 60 ppm. The average figure as obtained from a larger number of samples is just $37\ mg\ l^{-1}$, corresponding to about $48*10^6\ t\ y^{-1}$ or $12\text{-}13\ t\ km^{-2}\ y^{-1}$. The bedload transport amounts only to $3*10^6\ m^3\ y^{-1}$.

The concentration of the suspended load in the Congo River is too small compared to the concentrations in other large rivers of the world. As the total tonnage of suspended sediments from the African Continent is $530*10^6\ t\ y^{-1}$, the yield of the Congo Basin represents only 9.4% of the total yield of Africa. Bearing in mind that the water yield of the Congo Basin represents 38% of the total water yield of Africa, the ratio of the suspended sediment to water for the Congo is just one-fourth the general figure for Africa. The smallness of the concentration of the suspended load can be attributed to three factors. These are the protection of the soil by the rainforest against erosion by rainwater, the flatness of the land, in general, and the presence of lakes and wetlands traversed by the river, in which suspended sediments can settle (Nkounkou and Probst, 1987).

According to Meybeck (1976) the river basins having low relief and tropical climate like the Congo and the Niger, have a dissolved transport, T_d, in the range of 3 to $20\ t\ km^{-2}\ y^{-1}$ and solid transport, T_s, in the range of 1 to $10\ t\ km^{-2}\ y^{-1}$. As such they have a total transport, T_d, in the range of 4 to $30\ t\ km^{-2}\ y^{-1}$.

On the basis of monthly sampling during the period 1987-89, the geochemistry of the Congo and it's tributary, the Ubangi, was studied for two reasons. The first was to get insight into the seasonal variation of the physico-chemical parameters of their waters, and the second to estimate the annual dissolved fluxes exported by the two rivers (Probst et al., 1992). Some of the results obtained from that study are given in Table 4 j, Part II/Appendix B.

The composition of the suspended sediment of the Congo River with regard to major elements as analyzed by various researchers is somewhat variable.

Relative to the Amazon River, the suspended material of the Congo is enriched in *Fe, Al* and *P* and depleted in *Si, Ca, K* and *Mg*. According to Nkounkou and Probst (1987), the ratio $R' = SiO_2 / (Al_2O_2+Fe_2O_3)$, for example, varies from 1.16 to 2.0, depending on whose data the calculation is based

The water of the Congo River appears to be more diluted than the water of the Ubangi River, the concentrations being 34 mg l^{-1} and 42 mg l^{-1} respectively. The main constituents of the inorganic dissolved load in both rivers are HCO^-_3 and SiO_2. In view of the geological composition of its catchment area, the proportions of HCO^-_3 and Ca^{2+} in the water of the Ubangi are higher than in the Congo. Periodic analysis of water samples taken from both rivers has shown that the composition of water in either river does not change with time. On a seasonal scale, however, the concentration of dissolved anions and cations, except silica, varies inversely with discharge.

In conclusion, using three different methods, the estimated annual inorganic dissolved flux of the Congo varies from $39*10^6$ to $44*10^6$ t, depending on the year. Nearly 10% of this amount is coming from the Ubangi drainage basin.

8.2- The Zambezi Basin

8.2.1- General description of the basin- The explorer Antonio Fernandes, while searching in 1514-16 for new routes in the interior of Africa, followed the courses of the Sabi and Zambezi Rivers. The Zambezi River is plotted as the Cauna or Zambere River on the map prepared around 1700 AD by Modern. Moreover, Lake Zaïre can be identified as the presently Lake Tanganyika and the Zambere River as the Luapula already discussed in connection with the Congo River. The Portuguese explorers carried out further expeditions in the 18^{th} and 19^{th} centuries. They discovered the Luangua Valley and the course of the Upper Zambezi (Balek, 1977). Livingstone visited the Victoria Falls during his first trip to Africa in 1855, and reached the Chobe River and the northern Zambezi. In 1866, Holub, a Czech explorer, surveyed the Kafue Basin and carried out the first hydrological measurements ever to be done in this area.

According to Matondo & Mortensen (1998) the Zambezi Basin drains a total surface of $1.8*10^6$ km^2 when the Cuando-Chobe and the Okavango Basins are included. When these two basins are not included, the surface area reduces to $1.3*10^6$ km^2. The Zambezi Basin drains eight riparian countries, namely: Angola (18.3 %), Botswana (2.8 %), Malawi (7.7 %), Mozambique (11.4 %) Namibia (1.2 %), Tanzania (7.7 %), Zambia (40.7 %) and Zimbabwe (15.9 %). The basin area covers 93% of the total surface area of Malawi, 72% of Zambia and 64% of Zimbabwe. The contributing areas in Namibia and Tanzania do not exceed 3%.

The Zambezi Basin ranks as the fourth largest river basin in Africa. It extends between latitudes 10° and 20°S and between longitudes 20° and 37°E.The Zambezi River is by far the largest African stream flowing into the Indian

Ocean. It is often described as a "typical" African river. Its upper course drains a huge shallow basin, floored with alluvial deposits, in the Central African Plateau. In the 2,740 km of its course the Zambezi River flows through three distinct regions. The first is its plateau course, lying in Angola, partly in Zambia, but receiving also intermittent streams from the Okovango Swamps of northern Botswana. The second part of its course is the Middle Zambezi or Gwembe trough, essentially the part lying below Victoria Falls. There, the river flows through a narrow gorge excavated in crushed rock produced by successive fault lines and obstructed by waterfalls and rapids. At the lower end of its middle course the river passes through the Kariba gorge, where the Zambezi narrows to less than 30 m as it cuts through a rocky barrier. Shortly below, it reaches its third course through the Mozambique Plain (Stamp and Morgan, 1972).

In the upper part of its course, the Zambezi flows southward and is joined by the Lungue-Bungo, Kabompo and Luanginga Rivers. Shortly after bending its course to the east, the river is joined by the Chobe River. The Chobe system is composed of the Cuando and Okavango Rivers. The Okavango-Chobe river system joins the Zambezi River through the Okavango-Chobe Lake. The connection between the Chobe and the Zambezi can occur in either direction (Balek, 1977). In its middle course, the river continues its flow in a northeasterly direction. The Kafue River joins the Zambezi a short distance below the Kariba Reservoir. The Kariba Reservoir is a very huge lake formed by the Kariba Dam. Next to the regulation of the river flow, the primary objective of the dam is hydropower generation. Some 150 km downstream from the confluence with the Kafue, the Luangua River and its tributaries join the course of the Zambezi. After a long journey of 2,600-3,000 km the Zambezi, in fact the lower part of its course, downstream from the Cabora Bassa Reservoir, flows southeast to discharge its water into the Indian Ocean below its confluence with the Shire. The Cabora Bassa Reservoir, though not as huge as the Kariba, is quite huge with a total capacity of $66*10^9$ m^3. The map in Figure 8.7 shows the network of streams covering the basin of the Zambezi River.

The Zambezi Basin, occupying such a vast surface as $1.8*10^6$ km^2, has three distinct climatic seasons: cool and dry (April-August), warm and dry (September and October), and warm and wet season (November-March). The annual precipitation varies considerably from location to location. For example, the annual rainfall at Zomba and Lilongwe, Malawi (stations no. 215 and 207) is 1,367 and 838 mm respectively whereas at Bulawayo, Zimbabwe (station no. 232) is just 596 mm. More data about annual and monthly precipitation can be found in Tables 9 and 10, of Appendix A. The average annual rainfall over the whole basin is estimated as 990 mm and the annual evaporation as 870 mm. The annual rainfall varies considerably across the full extent of the basin. The northern parts have an annual rainfall of 1,200 mm, while the average for the southern and southwestern parts is about 700 mm. Likewise the actual evapotranspitration or feed-back varies from 1,000 mm in the Luangwa, Shire

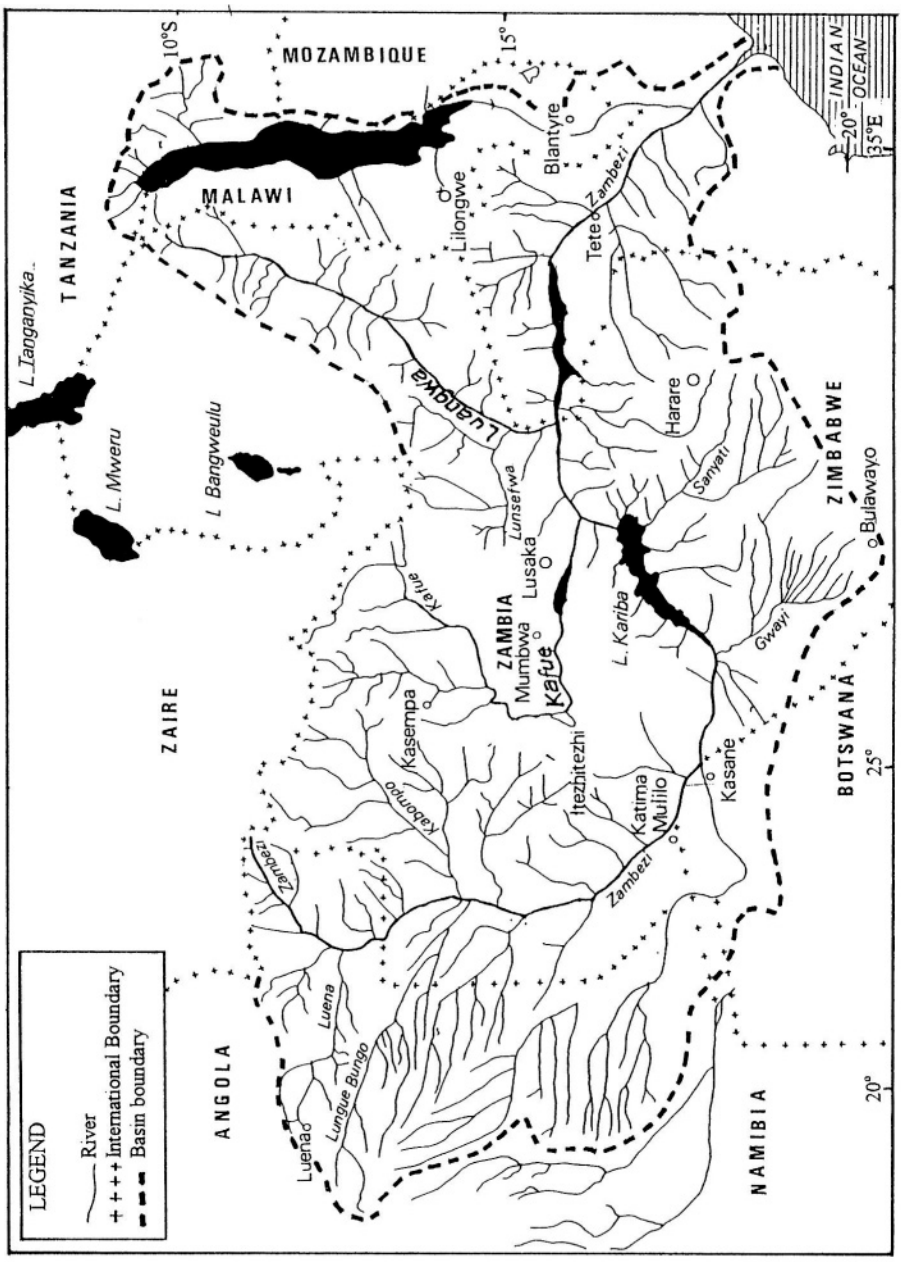

Figure 8.7- Map of the Zambezi basin showing the Zambezi and its tributaries

and the lower parts of the basin down to 500 mm in the southwestern areas of the basin.

The annual runoff coefficient varies from a small percentage as 1-2% in and around the swampy areas to more than 15% in other parts of the basin, especially the Upper Zambezi. The work of Balek in the Central African Plateau has shown that when the swampy area is 5% of the total catchment area the runoff coefficient reduces from 0.18 to 0.10 and further to 0.02 corresponding to annual rainfall of 1,250, 1,000 and 750 mm respectively (1983). The same coefficient decreases to 0.13, 0.07 and 0.10 for the same annual rainfalls would the area covered by the swamps be increased to 10% of the catchment area. These seasonal and spatial variations in rainfall, evapotranspiration and runoff coefficient have made the eventual runoff rather complex and the annual runoff volumes, at least in certain parts of the basin, quite limited.

8.2.2 Hydrology of the Zambezi basin- The UNESCO Publications on African River Discharges (1995, 1996) include monthly and annual discharges at 15 gauging stations in the Zambezi Basin. These stations are distributed such that 5 are situated in each of Zambia (stations no. 221, 223, 224, 225, 227), and Zimbabwe (stations no. 232, 233, 234, 236, 237), 1 in Mozambique (station no. 229) and 4 in Malawi (stations no. 220, 226, 228, 230). The mean annual discharge and its variation coefficient for the discharge series at these stations are included in Table 6, Part I/Appendix B.

Balek (1977), using mean annual figures for precipitation, $(P)_m$, and actual evapotranspiration, $(ET)_a$, at a number of locations in the basin, was able to draw the water balance, sub-basin wise. As the unit of time used in balance calculations, the runoff was considered as the difference between $(P)_m$ and $(ET)_a$. The basic data used and the results obtained are listed in Table 8.4. The specific yield of the Zambezi Basin according to those results is $1.4\ l\ s^{-1}\ km^{-2}$, compared to 9.9, 6.3 and $0.9\ l\ s^{-1}\ km^{-2}$ for the Congo, the Niger and the Nile Basins, respectively.

The Zambezi basin drains a large surface of the tropical wet and dry highland, and a much larger surface of the semi-desert area of Northern Kalahari. As a considerable portion of the rainfall in that part of the semi-desert area is lost in the desert itself, its contribution to the river flow is rather insignificant. This results in greatly reduced values of the discharge below the mouth of the Chobe River, which flows from the Kalahari Desert. This can be seen from Table 8.4. Matondo and Mortensen (1998) carried out a more elaborate study of the water balance of the Zambezi Basin compared to that of Balek, already summarized in Table 8.4. The data used for water balance calculation cover the period 1959/60-90/91. This period is fairly long to yield reasonable average figures. It includes two extreme years; 1972/73 a typical dry year, and 1977/78 a typical wet year. To perform the water balance the basin area has been divided into 21 sub-basins varying in surface area from 18,870

Table 8.4- Water balance of the Zambezi Basin (based on Balek, 1977)

River	Location	A, km^2	$(P)_m$, mm	$(ET)_a$, mm	R, mm	r	$(Q)_m$, $m^3 s^{-1}$
Zambezi	Chavuma Falls*	75, 967	1,288	1,057	231	0.18	555
Interbasin	Chavuma F.-Choba	284,538	1,030	969	61	0.06	541
Zambezi	above Chobe	360,505	1,085	990	95	0.09	1,096
Chobe	mouth**	870,758	625	622	3	0.01	135
Zambezi	below Chobe	1,231,263	760	730	30	0.05	1,231
Interbasin	Chobe Victoria F	5,317	605	584	21	0.03	6
Zambezi	Victoria Falls	1,236,580	759	729	30	0.04	1,237
Kafue	Victoria Falls-Kafue	163,380	718	664	54	0.08	261
Zambezi	above kafue	1,399,960	754	720	34	0.05	1,498
Kafue	mouth to Zambezi	154,856	1,023	938	85	0.08	417
Zambezi	below Kafue	1,554,816	782	744	38	0.05	1,915
Interbasin	Kafue-Luangwa	19,091	1,198	1, 173	25	0.02	151
Zambezi	above mouth Luangwa	1,573,907	787	746	41	0.05	2,066
Luangwa	mouth	148,326	925	834	91	0.11	436
Zambezi	below Luangwa	1,722,233	799	755	44	0.06	2,501

Explanation

A = drainage area, $(P)_m$ = mean annual precipitation, $(ET)_a$ = actual evapotrans-, piration, R = annual runoff, r = runoff coefficient and $(Q)_m$ = mean annual discharge

** at the boundary between Angola and Zambia and ** including northern Kalahari, the mean annual rainfall in Chobe basin alone is 798 mm.*

km^2 to 234,000 km^2. The locations and names of these 21 sub-basins are shown on the map in Figure 8.8. The number of each sub-basin in this map is written between brackets and the average discharge is expressed in $m^3 s^{-1}$. The mean annual rainfall, actual evapotranspiration, runoff coefficient, specific yield, discharge and storage losses are included in Table 8.5. The same table includes also the sub-basin specific yields in the typical wet and dry years.

The method of water balance calculations is essentially based on the long-term mean annual rainfall, $(P)_m$, and evapotranspiration, $(ET)_a$. The annual runoff, the runoff coefficients and the mean annual discharge, $(Q)_m$, are obtained from the simple expressions:

$$R = (P)_m - (ET)_a \tag{8.6}$$

$$r = R/(P)_m \tag{8.7}$$

and

$$(Q)_m = R.A/31.5576*10^3 \tag{8.8}$$

where, $(P)_m$, $(ET)_a$ and R are in mm, A = catchment area in km^2 and $(Q)_m$ is in $m^3 s^{-1}$.

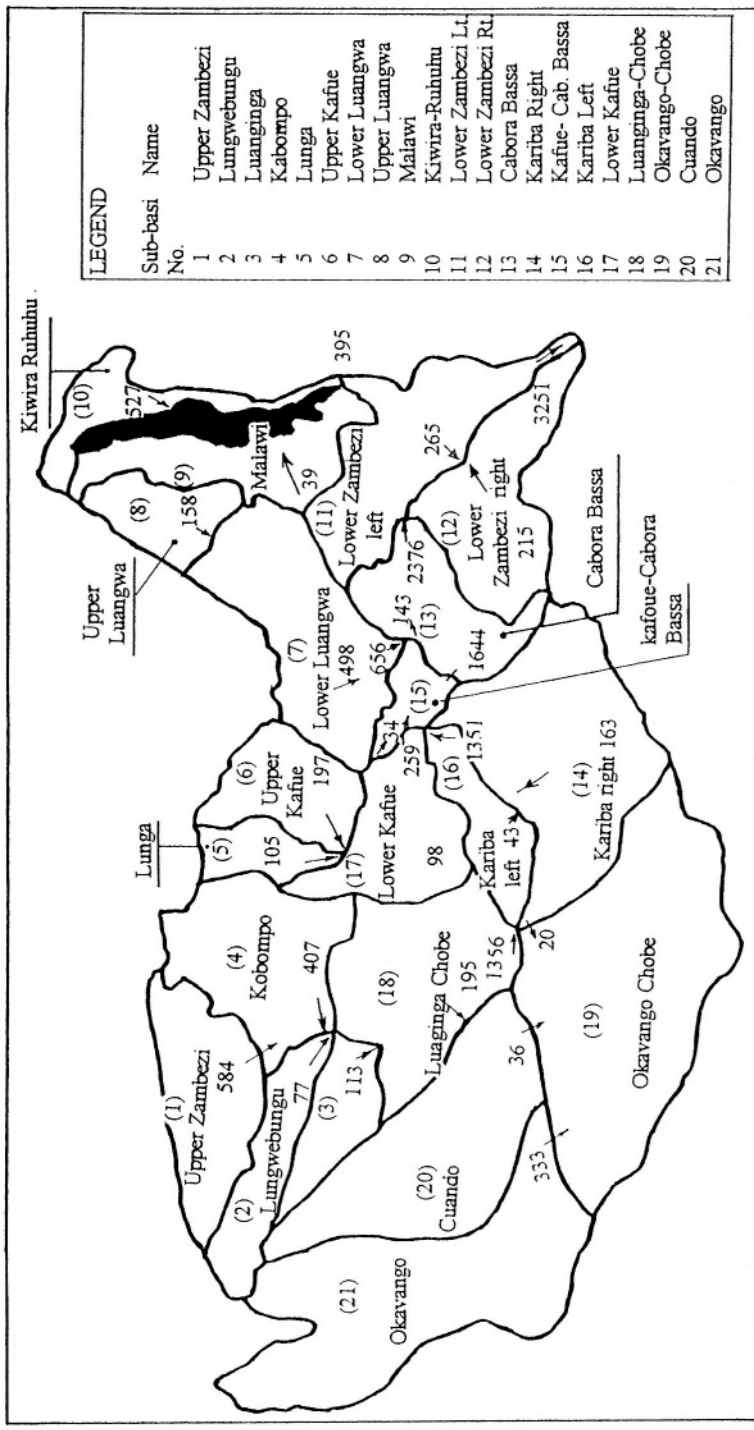

Figure 8.8- Map showing the 21 sub-basins of the Zambezi Basin used for calculating the water balance (Matondo and Mortensen, 1998)

The water balance of the Kariba Reservoir is simply the discharges coming from sub-basins No.1 (584), 2 (77), 3 (113), 4 (407) and 18 (195) less 19 (20) = 1,356 $m^3 s^{-1}$. To this amount the inflows coming from Kariba right No. 14 (163) and Kariba left No. 16 (43) should be added bringing the total inflow to 1,562 $m^3 s^{-1}$. As the net evaporation from the reservoir is 211 $m^3 s^{-1}$ the total net inflow to the reservoir reduces to 1,351 $m^3 s^{-1}$.

The second water balance is that of the Kafue flats. The inflow is simply the sum of the discharges from sub-basins 5 (105), 6 (197) and 17 (98) minus the losses, estimated as 141 $m^3 s^{-1}$, bringing the outflow to 259 $m^3 s^{-1}$. The third balance is that of the Cabora Bassa. The inflow is the sum of the discharges supplied by the sub-basins No. 8 (168), 7 (488), 17 (259), 15 (34), 13 (143) and 16 (1,351) minus the loss of 67 $m^3 s^{-1}$. This balance brings the mean annual outflow from the Cabora Bassa Reservoir to 2,376 $m^3 s^{-1}$.

The fourth and last part of the basin for which the water balance has been calculated is the eastern part bringing water from Malawi and Tanzania via the Shire River to the Indian Ocean. The inflow to the Shire from Lake Malawi is 395 $m^3 s^{-1}$. The mean annual discharge of the Shire for the period 1965-1984 at Liwonde (station No. 228) was 472 $m^3 s^{-1}$ with coefficient of variation of 0.41, and for the period 1953-80 at Chiromo (station No. 230) was 481 $m^3 s^{-1}$ with coefficient of variation of 0.37. For the purpose of consistency, however, we shall add here the value of 395 $m^3 s^{-1}$ to the runoff from sub-basins No. 11 and 12, (265 and 215 respectively) plus the outflow from the Cabora Bassa Reservoir (2,376). As such, the total discharge earned by the Zambezi to the Indian Ocean becomes 3,251 $m^3 s^{-1}$.

Table 8.5 includes values of the maximum specific yield, $(q)_{mx}$, and the minimum specific yield, $(q)_{mn}$, for each one of the 21 sub-basins as obtained for the period of record 1959/60-90/91. The ratio $(q)_{mx}$ to $(q)_{mn}$ varies widely from sub-basin to sub-basin. The range extends from 1.6 to 20, with 4 as an average ratio for the entire basin. The discharge flowing to the Indian Ocean varies from 6,994 $m^3 s^{-1}$ for the wet year 1977/78 to 1,753 $m^3 s^{-1}$ for the dry year 1972/73. The average for the 32-y length of record is 3,251$m^3 s^{-1}$. It should not be forgotten, however, that Table 8.4 gives this average but for a different period of record as 2,501 m3 s-1.

The interannual variation of the mean discharge of the Zambezi River at Victoria Falls for the period 1908-1992 can be seen from the graphic plot of the discharge series in Figure 8.9. This figure shows clearly that the series enjoyed a steadily rising trend from the beginning till about 1958, after which the discharges have fallen down till the end of the series. According to Grove (1998), the mean annual discharge of the Zambezi at Victoria Falls was $45*10^9$ m^3 (1426 $m^3 s^{-1}$) between 1948 and 1980 as compared with a mean of less than $30*10^9$ m^3 (950 $m^3 s^{-1}$) over the preceding 40 years.

A significant correlation between the air temperature at sites in the northern and southern extremities of Lake Tanganyika, and the sea surface temperature

(SST) of the Pacific Ocean has been reported by Plisnier (1998), as described in Chapter 2. Similarly, a strong connection between fluctuations in the Southern Oscillation Index (SOI), the occurrence of the Niño event, and rainfall in Africa. Low values of the index were accompanied by reduced precipitation and river discharges in the Sudan zone in 1913/14, 1940/41, 1972/73, 1984/85 and 1992/95. Similar occurrences of El- Niño event were observed in the basin of Lake Tanganyika in 1954, 1958, 1966, 1973, 1983, 1988 and 1991/94. It is clear

Table 8.5- Water balances for the sub-basins pf the Zambezi River based on data for the period 1959/60-90/91(from Matondo and Mortensen, 1998)

Sub-basin		$(P)_m$	$(ET)_a$	r	$(Q)_m$ in	Yield, q, in l s^{-1} km^{-2}			Loss in
No.	A in km^2	in mm	in mm		m^3 s^{-1}	$(q)_m$	$(q)_{mx}$	$(q)_{mn}$	m^3 s^{-1}
1	73,630	1,285	1,035	0.20	584	7.9	9.9	4.7	
2	47,030	1,150	1,098	0.05	77	1.6	2.0	0.1	
3	67,650	1,087	1,034	0.05	113	1.7	2.2	0.4	
4	86,610	1,150	1,002	0.13	407	4.7	6.3	2.1	
5	23,990	1,247	1,109	0.11	105	4.3	11.6	1.4	
6	53,810	1,150	1,035	0.10	197	3.7	7.2	1.1	
7	112,020	900	763	0.15	488	4.2	8.0	2.3	
8	38,570	950	813	0.14	168	4.1	7.4	2.1	
9	64,372	1,140	949	0.17	391	6.1	10.8	3.9	281[+]
10	33,368	1,430	932	0.35	527	15.8	28.0	10.0	
11	103,45	900	819	0.09	265	2.6	5.6	1.3	
12	93,900	770	698	0.09	215	2.2	5.0	1.2	
13	59,310	880	724	0.10	143	2.4	NA	NA	67[x]
14	164,410	737	698	0.04	163	1.0	4.6	0.9	
15	18,870	754	694	0.08	34	1.8	NA	NA	211*
16	42,830	700	661	0.05	43	1.0	4.6	0.9	
17	75,260	887	841	0.05	98	1.5	3.9	0.5	141[o]
18	81,730	828	753	0.09	195	2.4	6.0	1.5	
19	227,530	500	500	(-)	0	NA	NA	NA	
20	170,000	900	893	0.01	36	NA	NA	NA	
21	234,000	798	753	0.06	333	1.4	1.6	1.0	

Explanation

*$(P)_m$ = mean annual rainfall, $(ET)_a$ = actual evapotranspiration, r = runoff coefficient, $(Q)_m$ = mean annual discharge, $(q)_m$ = mean specific yield, $(q)_{mx}$ = maximum specific yield, $(q)_{mn}$ = minimum specific yield, all for the period of record, 1959/60-1990/91, [+] = net evaporation from Lake Malawi [x] = net evaporation from Cabora Bassa Reservoir, * = net evaporation from Kariba Reservoir, and [o] = net evaporation from the Itezihtezih Reservoir and Kafue flats.*

from Figure 8.9 that the years 1914/15 and 1948/49 were probably the driest years in the 20th century and the year 1957/58 the wettest one as far as the discharge of the Zambezi at Victoria Falls is concerned.

The apparent trend in the series in Figure 8.9, whether rising or falling, is surmounted by cyclic oscillations. The tact that neither the successive peaks nor the successive troughs show a regular pattern makes it difficult to use the characteristics of the past oscillations for flow prediction purposes. It is evident, however, that any significant change in rainfall is reflected on the river runoff either directly or after some time lag. If concrete relationships can be established between the El Niño index and rainfall on one hand, and between rainfall and runoff on the other hand, predicted values of the El Niño index can be used to predict streamflow values. El-Tahir (1996) followed these lines, except that instead of rainfall he used air temperature, in attempt to forecast Nile floods. The final result he reached is given by Eq. (7.16). A model for predicting cyclic rainfall and streamflow in South Africa, without reference to the El Niño events, has been reported by Paling and Stephenson (1988). This model will be described in connection with hydrology of the Orange and Vaal Rivers, sec. 8.3.

As the Zambezi Basin is draining wet, semi-arid and dry areas, the river discharge shows a relatively high seasonality. At Chavuma Falls the flood peak occurs in March and the lowflow from July up to November-December. The March flood peak on the Upper Zambezi is delayed by no less than 3 months at Lake Kariba, approximately at a distance of 1,200 km. The mean monthly discharge hydrograph at Victoria Falls, based on a 59-year average is shown in Figure 8.10.

Figure 8.10, which has been developed by Borchert and Kempe 1985), shows three hydrographs The middlemost hydrograph is for the mean monthly volumes of flow, the uppermost gives the mean plus one standard deviation and the third for the mean less one standard deviation. They all show that the April is the month of peak flow and October and November are the months of the lowest flow. The coefficient of variation of the monthly flow is certainly high, not less than 40%.

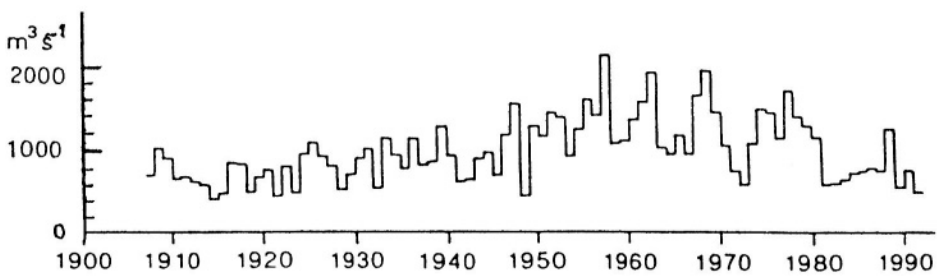

Figure 8.9- Annual discharge series of the Zambezi River at Victoria Falls, 1908-92

8.2.3 Water quality of the Zambezi River- Leopold (1962) obtained some sediment data of the Zambezi River. These data appear in reference papers by Holeman (1968) and Meybeck (1976). They are briefly included in Table 2_a, Part II/Appendix B. The remarkable thing is that those data have been based on a mean annual discharge at mouth of $7{,}100\ m^3\ s^{-1}$ or annual volume of about $225*10^9\ m^3$. According to Martins and Probst (1991), if the discharge rate of $225*109\ m^3\ y^{-1}$ is used to calculate the transport rate of dissolved elements, then the river exports $25*10^6\ t$ of dissolved load into the Indian Ocean. The results associated with this assumption are: average concentration figures of $113\ mg\ l^{-1}$ for the total dissolved substance, TDS, and $90\ mg\ l^{-1}$ for the total soluble substance, TSS, bringing the total dissolved and soluble load transports to 25.2 and $20*10^6\ t\ y^{-1}$ respectively. The ratio between the two concentrations, TSS/TDS is close to 0.8. Additionally, Hall et al. and Milliman and Meade (cited in Martins and Probst, 1991) give the figures of 21 and $16.7\ t\ km^{-2}\ y^{-1}$ for the chemical and mechanical specific transports respectively. It should be noted, however, that the dissolved inorganic carbon, present mostly as bicarbonate ion, constitutes more than 50% of the TDS.

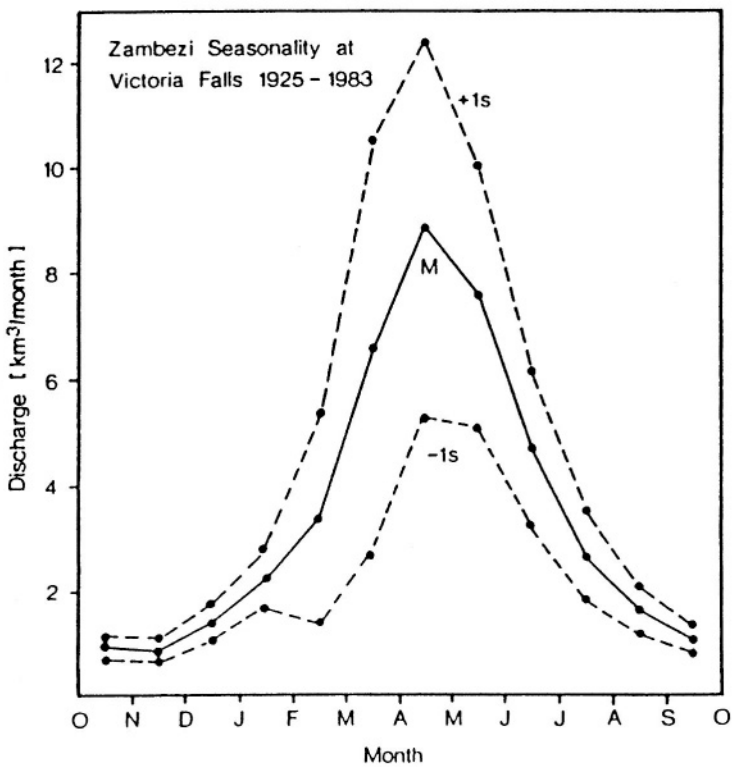

Figure 8.10- The hydrograph of the Zambezi monthly discharge at Victoria Falls, 59-year average (Brochert and Kempe, 1985)

In the previous sub-section, 8.2.2, it has been shown that the investigation reported by Matondo and Mortensen, 1998) has shown that the discharge brought by the Zambezi, averaged over the period 1959/60-90/91, is 3,251 $m^3 s^{-1}$ ($103*10^9 m^3 y^{-1}$). The results available at the Zambezi River authority give a very close figure, 3,600 $m^3 s^{-1}$ ($114*10^9 m^3 y^{-1}$). The average of the discharge observations taken before 1960 gives a figure less than this. As such, the old transport load calculations need to be corrected. The TDS load transported by the Zambezi to the Indian Ocean when based on an annual flow volume of $100*10^9$ m^3 is reduced to $11.2*10^6$ t y^{-1} and the corresponding TSS transport load to $8.9*10^6$ t y^{-1}. These estimates bring the specific transport rate to about 6.2 t km^{-2} y^{-1}. The difference between this rate and the annual rate of $15.4*10^6$ t originally given by Leopold (1962) is directly proportional to the ratio of the two flow volumes, i.e. 225 and $100*10^6 m^3 y^{-1}$.

Bolton (1984), while investigating the sediment deposition in major reservoirs in the Zambezi Basin, examined the results obtained from the studies performed on the Gwaai and the Umsweswe Rivers, two tributaries of Lake Kariba, between 1975 and 1979. He suggested that the sediment yield of the two basins were similar at about 40 t $km^{-2} y^{-1}$. The mean sediment concentrations differed significantly, approximately 1,600 mg l^{-1} for the Gwaai and 500 mg l^{-1} for the Umsweswe. Further analysis of the results of that study has shown that the average sediment yield of the drainage basin of Lake Kariba downstream of Victoria Falls lies in the range 40 to 400 t km-^{2} y^{-1}. The sediment input to Lake Cabora Bassa was thought of to be supplied by the basin tributaries in Zimbabwe ($42*10^3$ km^2), minor tributaries in Zambia and Mozambique ($35*10^3 km^2$) and the Luangwa Basin ($148*10^3$ km^2). The total sediment discharge from all these tributaries into Lake Cabora Bassa probably lies in the range 20 to $200*10^6$ t y^{-1}.

The poor land use and conservation practices caused by the social-economic conditions in the Zambezi Basin have led to widespread catchment degradation, water resources degradation and pollution. As a consequence, there are some serious soil erosion and increased flash runoff problems, with rivers flooding more frequently and their hydrographs receding or drying much faster than before. The prevalent flash runoff diminishes groundwater recharge, increases sediment loads and some times induces excessive leaching of agrochemicals into streams and rivers. It is quite unfortunate that most of the farmers suffer from lack of capital, a situation that makes it almost impossible to deal with the land and associated water resources degradation and pollution (Dutch Ministry of Foreign Affairs, 1998).

8.3-The Orange Basin

8.3.1 Brief description of the basin- By 1652 the Dutch boers (boer = farmer in Dutch/African languages), who used to work in East India (nowadays Indonesia)

and preferred not to return back home after their retirement, had succeeded in establishing a settlement at Cape Town. After long-lasting disputes with the British because of the slavery and other affairs, they consented to move from Cape Town to the interior. The first white man known to have explored any south African river was Coetsee, who reached the mouth of the Groot River (Great River) in 1760. The later expeditions in the 18^{th} century explored the river reach from its middle section to its mouth. As most of the explorers were from the Dutch settlers they named the river Orange, after the Dutch Monarch House.

In 1836, the Great Trek began; the boers (actually in Dutch proper the plural of boer is boeren not boers) set off into the interior and crossed another great river, a chief tributary of the Orange, and called it the Vaal. In the same year the French missionaries Arbousset and Dumas reached the source of the Orange.

The Orange River is about 2,200 km long. As such, it is the longest river in southern Africa south of the Zambezi. The headwaters rise at an altitude of about 3,300 m a.m.s.l.on a plateau formed by the Highlands in Lesotho that extends from the Drakensberg escarpment in the east to the Maluti Mountains in the west. The river headwaters are situated nearby the Thabantshoyana mountain peak (3,480 m a.m.s.l.). There are three sources to the river, the main source of which is known as the Senqu River, rises in the eastern edge of the escarpment. The second source, the Seati headwater, originates near Mont-aux-Sources to the north. The third lies farther north in the Malibamatso headwater (The New Encyclopædia Britannica, Vol. 13, 1988). The Orange River on its way to the Atlantic Ocean, passes over the Great Falls, but its bed is usually dry before the ocean is reached through the coastal desert belt of the Namib. Even in the damper parts of the High Veld (in Dutch/African languages veld means field) the streams are frequently non-perennial (Stamp and Morgan, 1972).

The basin of the Orange drains nearly all the surface of the southern African Plateau. The estimate of the surface area of the basin ranges from $0.85*10^6$ km^2 to $1.02*10^6$ km^2 of arid and semi-arid areas. This is the largest river basin south of the Zambezi. More than half of the basin area lies in the Republic of South Africa (RSA). The southern half of the Kalahari Desert in Botswana lies in the same drainage basin, but the watercourses are nearly always dry. The remainder of the basin occupies parts of Lesotho and Namibia. As such, the riparian countries are South Africa, Botswana, Lesotho and Namibia.

The headwaters of the Orange traverse the lava-covered surface of the Drakensberg and cut its gorge in the underlying sedimentary rocks. After entering South Africa, the river runs south and west through a country whose surface is covered with sandstones, mudstones and shales. Amidst these formations hard rock outcrops form hills and flat-topped mountains. The Orange River, at some locations, has carved out for itself a great valley in the Karoo sediments of low resistance. In general, the wide contrast in the resistance of the surface deposits and the underlying material to erosion causes the width and depth of the river channel to vary considerably from one place to another.

A number of tributaries keep feeding the Upper Orange from both sides at several points along its course. The Orange, after leaving the border between Lesotho and South Africa by about 180 km, enters the Verwoerd Reservoir from the southeastern corner at a distance of about 50 km below Aliwal North. The construction of the Verwoerd Dam was completed in 1971 and put into function in 1972. The reservoir created by this dam has a surface area of $374\ km^2$ and gross storage capacity of $5.96*10^9\ m^3$. The ultimate generating capacity at the dam's power station has been estimated at 320 MW.

The Caledon River is the second principal tributary of the Orange after the Vaal. It rises in the Drakensberg, on the Lesotho-South Africa border, in southeastern Africa. It flows generally southwest for about 480 km to join the Orange near Bethulie before entering the Verwoerd Reservoir. The Caledon River has a number of tributaries reaching it from the right and left banks. The supply of these tributaries, however, is limited.

The Orange after leaving the reservoir swings to the northeast down to its confluence with the Vaal River. Almost half way along the distance between the Verwoerd Reservoir and the confluence of the Vaal on the Orange, the P.K. Le Roux Dam has been built on the Orange River around 1976. The Vaal, the chief tributary of the Orange, originates in southeastern Transvaal at an elevation of about 1,800 m a.m.s.l. It flows about 1,200 km before reaching its confluence with the Orange. Basically a plateau river, the Vaal occupies a shallow bed, with mouth at about 1,050 m a.m.s.l. The difference in levels means that the average slope of the Vaal is about $0.625*10^{-3}$. The major tributaries of the Vaal: the Klip, Wilge, Valsche, Vet, and the Riet Rivers are on the left bank. The Skoon and the Harts on the right bank are of little significance to the flow of the Vaal. The Vaal Dam takes care of the regulation of the river flow. The dam was built in 1938 and heightened about two decades later. With the building of the Bloemhof Dam, 478 km downstream of the Vaal Dam, the demand on the latter for irrigation water has been reduced. The Vaal River is regarded as the second River in Africa, after the Nile, to be nearly completely regulated.

Below its confluence with the Vaal at Douglas, the Orange turns southwest and flows over limestone shale-covered terrain. It keeps alternating its course through deep gorges and broad valleys. At Prieska farther downstream, some 130 km far from Douglas, the Orange makes another sharp bend to the northwest, some 220 km, before reaching Upington. This bend marks the beginning of the Middle Orange. Less than half the distance between Prieska and Upington the Boegbergdam was built in 1931 to help irrigate a considerable area raising cotton on both sides of the river. At Upington, the river spreads out over a granite surface where it splits up into innumerable channels circumscribing a large number of small islands. The river section in this stretch can be as wide as 6 km, which after a short distance is suddenly narrowed to about 650 m. At Kakamas, some 80 km southwest of Upington, the Sak River has its confluence with the Orange. The Sak and its tributaries descend from the Neweveld

Mountains in the southwest of South Africa. They flow intermittently from south to north depending on the rainfall conditions in the area. Approximately 40 km below Kakamas, the Orange River-again flowing in several channels-forms the Augrabies Falls. The falls occur where the river leaves a plateau formation of resistant granite. The main fall of water is 90 m, and the total fall is about 190 m. The width of the Falls at flood time extends over several kilometers with 19 separate waterfalls tumbling into a ravine 18 km long (Encyclopædia Britannica, Vol. 13, 1988).

The Lower Orange, down the Augrabies Falls to the ocean, is sometimes called the Gorge Tract. The dimensions and form of the river section depends on resistance of the surface rock. Where the surface is soft the river valley is generally open. Oppositely, when it is hard igneous rock, the river is confined between deep vertical cliffs. Upon traversing the Northveld region of South Africa, the Orange defines the southern limit of the Kalahari and bisects the southern Namib before draining into the Atlantic Ocean at Alexander Bay.

The last tributary is the Fish River (Vis Rivier in African language). It joins the Orange at a short distance, less than 100 km, above the mouth on the Atlantic Ocean. The Fish River rises in Namaqualand and flows in a southerly direction across the Great Namaqualand Plateau, where it cuts a gorge 300 to 700 m deep. It runs for about 600 km before discharging its water into the Orange. It should be noted, however, that the Fish River flows intermittently, not perennially.

Most of the rivers and tributaries mentioned in this section are shown on the map in Figure 8.11.

The extent of the Orange Basin covers most of the width of Africa in South Africa. In this large, extent the climate varies from Equatorial Tropical in Lesotho to Desert in Namibia. Above the Vaal confluence, the source area of the headwaters receives annual precipitation, which includes some snowfall, in the range between 1,500 and 2,000 mm, with a potential evapotranspiration around 1,200 mm y^{-1}. Quite differently, in the vicinity of the river mouth where potential evapotranspiration exceeds 2,500 mm y^{-1}, the annual rainfall averages less than 50 mm y^{-1}. The mean annual rainfall at Germiston (station No. 251), Upington (station No. 256) and Alexander Bay (station No. 257) is 710, 207 and 45 mm respectively. Tables 9 and 10, in Appendix A include the mean monthly and annual precipitation data for a number of sites within the drainage basin. The mean annual precipitation on the basin, estimated at 400 mm, is arid by world norms. The runoff depends on the climatic data together with the prevailing values of the runoff coefficient.

8.3.2 Hydrology of the Orange basin- The Orange River is a wild and unpredictable river. Its flood follows no pattern. Heavy rains in the catchment area can cause a raging torrent that crashes over the riverbanks, taking everything with it and annually washes invaluable tons of fertile soil into the sea. The UNESCO Publications (1995 and 1996) give the mean monthly and annual

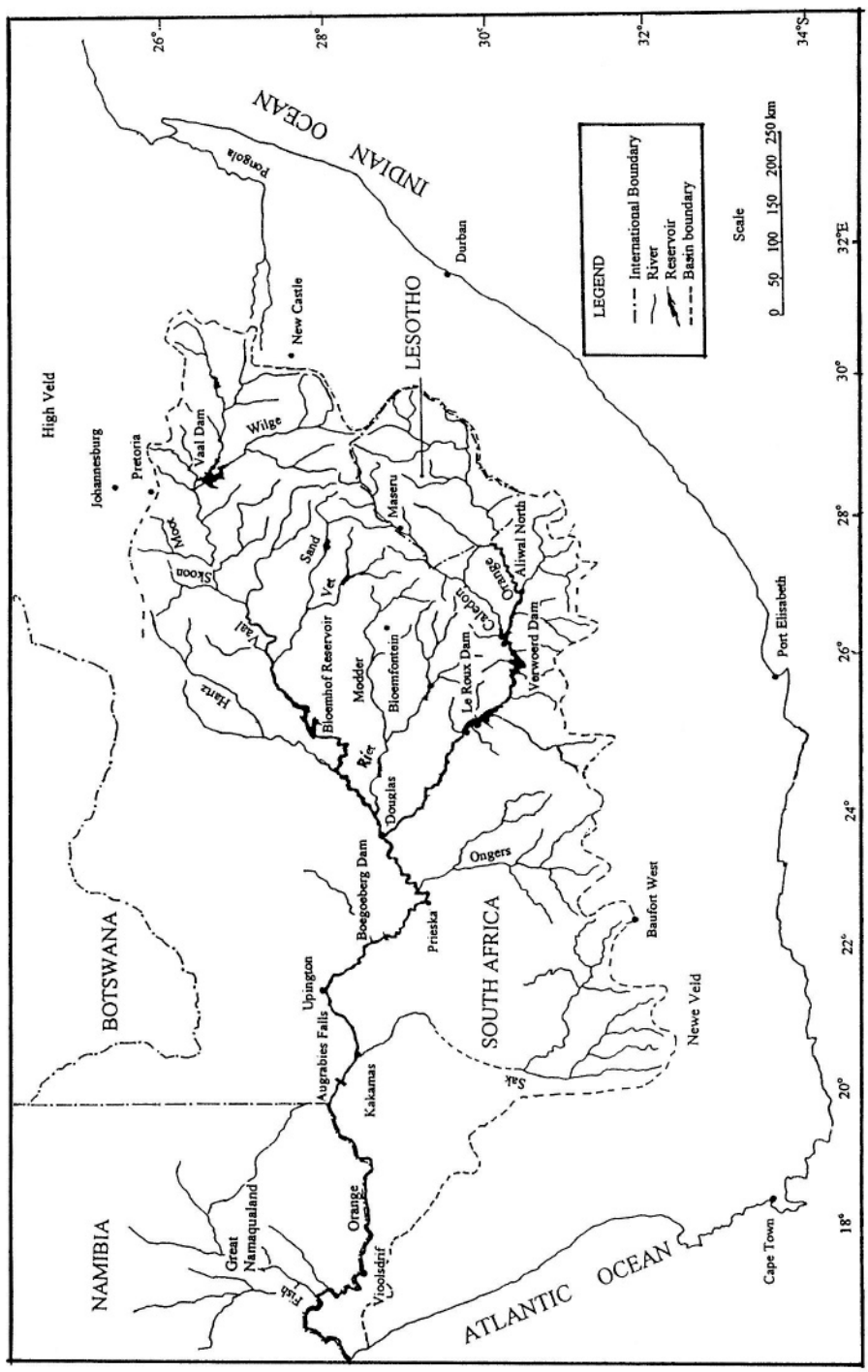

Figure 8.11- Map of the basin of the Orange River and its tributaries

discharge of the Orange and its tributaries at four stations: 269, 271, 273 and 274 in Lesotho, and five stations: 266, 267, 268, 270 and 275 in South Africa. The stations 266 and 268 are located on the Vaal, stations 267, 270 and 275 on the Orange River, station 269 on the Tshalanyane, station 271 on the Caledon, station 273 on the Makhalang, and station 274 on the Senqu River. The maximum published record for any of these stations does not exceed 20 years. This situation should not be misinterpreted, as discharge observations in the Orange basin, especially within South Africa, are abundant both spatially and temporally. Additionally, before presenting and discussing the hydrologic characteristics, it is worthwhile mentioning that the Orange Basin is crowded with large and small dams, many of which have been built in connection with development projects.

The annual discharge of the Upper Orange (Senqu) at Seaka (station No. 274) is $120\ m^3\ s^{-1}$, with 0.66 as coefficient of variation, averaged over the years 1973-84. The catchment area at this station is about $20{,}000\ km^2$ and the specific runoff is about $0.19\ m\ km^{-2}\ y^{-1}$. The tributaries feeding the river from the left side bring the annual mean discharge at Aliwal North (station No. 275) to an average of $148\ m^3\ s^{-1}$, with a coefficient of variation of 0.75. The discharge of the Caledon River at Mohlokagala (station 271), averaged over the period 1970-84, is 19.3 $m^3\ s^{-1}$, with a coefficient of variation of 0.70. The combined flow plus any amount supplied by the smaller tributaries minus the conveyance loss forms the inflow to the Verwoerd Reservoir, the outflow of which serves as inflow to Le Roux Reservoir. Water from both reservoirs is withdrawn basically for irrigation and land development purposes.

The runoff from the Upper Vaal, in the Republic of South Africa, and from Lesotho, supplies the Orange annually with a considerable proportion of its flow. The flow of the Vaal River for most of the year is minimal, but the winter season, October to March, can create the muddy torrents for which the Vaal is reputed. The mean annual discharge at Engelbrachtsdrift (station No. 266), averaged over the period 1965-85, was $42.1\ m^3\ s^{-1}$, with a coefficient of variation of 1.0. This small discharge is caused by the low value of the runoff coefficient, less than 5%, coupled with the limited rainfall. The annual flow can differ considerably from year to year (Figure 8.12). Due to the losses from the Vaal Reservoir and the withdrawal of some of its water the average discharge at De Hoop 65 (station No. 268), over the period 1969-85, was $5.2\ m^3\ s^{-1}$, with variation coefficient of 0.25.

A few kilometers above Prieska, the Ongers River with its tributaries join the tail section of the Middle Orange. Downstream at Prieska the Orange has an annual runoff of about $6.9*10^9\ m^3$ ($218\ m^3\ s^{-1}$). The available data for the period 1975-85 at Upington (station No. 267) give a mean annual discharge of $224\ m^3\ s^{-1}$, with variation coefficient of 112%.

The long-term average discharge of the Orange River is $360\ m^3\ s^{-1}$ or $11.4*10^9\ m^3\ y^{-1}$. The time series plot of the annual flow at Vioolsdrift (station

No. 270) has been composed of the data for the period 1940-70 gathered by Hart (1985), and up to 1985 as published by UNESCO (1995). This graphic plot is shown in Figure 8.13. As a result of the heavy withdrawal of water for the development of the Vaal Basin as well as other parts of the Orange Basin, only about half of the annual runoff now reaches the ocean, although the amount varies widely. In 1988, the wettest recorded year, it was estimated at $26*10^9$ m^3, while the average annual flow for the two driest years was estimated at only $1.1*10^9$ m^3

The same Figure 8.13 shows a falling trend over the full length of the series together with cyclic occurrence of high flows in the years 1944, 1950, 1958, 1967 and 1976, i.e. once every 6 to 9 years. The periodic oscillation of the streamflow in South Africa and its relation to rainfall will be discussed in sub-section 8.3.3. In this discussion, the basin of the Upper Pongola River is used in the analysis. Though it lies outside the Orange Basin, yet its proximity warrants its use.

Although Botswana lies partly within the basin, the nearest point of its border is 200 km far from the Orange River, to which it has yielded no significant flow.

The Namibian Desert at the downstream end of the river also yields very little water, except from the Fish River near the estuary, and mostly during occasional floods (The Dutch Ministry of Foreign Affairs, 1998).

The patterns of mean monthly river discharges have already been discussed in sub-section 6.3.2. The ratio between the mean monthly maximum to the mean

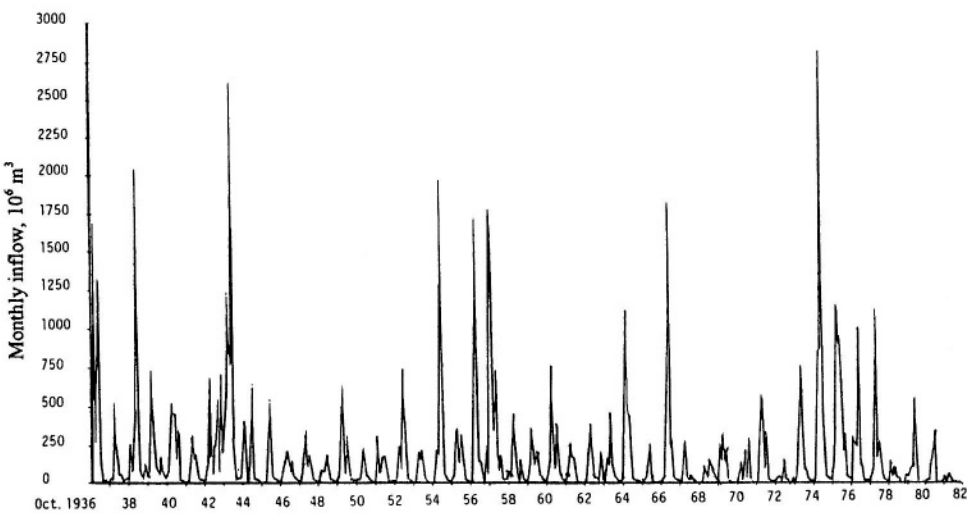

Figure 8.12- Monthly inflow to the Vaal Reservoir in the period from 1936 to 1982 (from Paling, 1984)

The patterns of mean monthly river discharges have already been discussed in sub-section 6.3.2. The ratio between the mean monthly maximum to the mean monthly minimum, termed seasonality index, $(In)_s$, for seven stations: 267, 269, 270, 271, 273, 274 and 275 located in the Orange basin is included in Table 6.3. The index for stations No 269, 271, 274 and 275 belongs to Type IV, in the range 10-20. The index for station No 273 belongs to Type III, in the range 5-10, and the index for stations 267 and 270 being 4.6 and 4.4 respectively belong to Type II. It should be well remembered, however, that the mentioned index values do not merely reflect the prevailing climate. They are strongly affected by the length and period of the record as well as the extent of river regulation

The annual maximum flood discharge varies considerably from year to year. The flood peak data for the period 1965-85 at Vioolsdrift (station No.270), as an example, have a mean, coefficient of variation, skewness and kurtosis of 1,057.5 $m^3 s^{-1}$, 1.09, 2.03 and 8.08 respectively. Should these data be distributed like Pearson Type 3, the frequency factor, K, for return periods of 100 and 200 y must be around 3.6 and 4.3 respectively, and the corresponding flood discharges 5,190 and 6,000 $m^3 s^{-1}$. Rodier (1985) suggested that return periods of 1,000 to 2,000 y corresponding to K-values of about 5 for three arid zones of South Africa is an overestimation.

Water resources management in South Africa has prompted the research authorities interested in the relevant hydrological problems to recommend to the design engineers the most appropriate approaches of design flood determination.

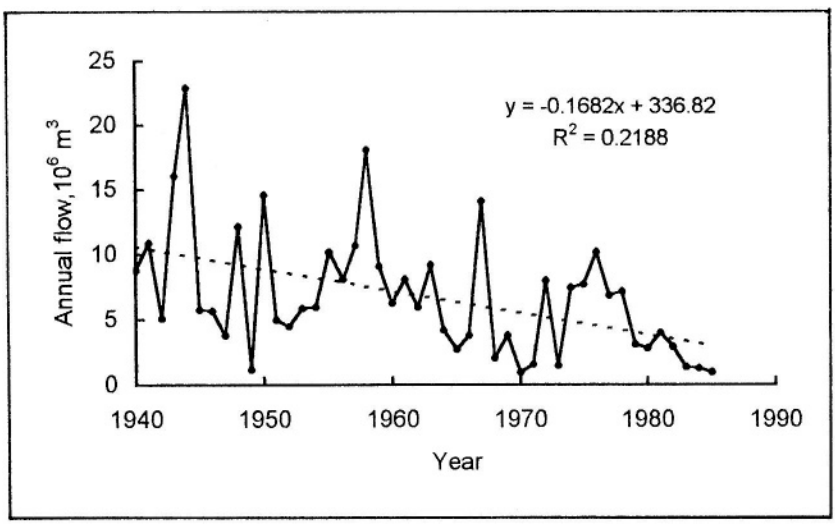

Figure 8.13- Annual flow series of the Orange River at Vioolsdrift (station No. 270), South Africa

The surface of the country, including the Orange Basin, was thus subdivided into regions of winter, summer, and year-round rainfall. The rational method has been recommended to small catchments up to 5 mi^2 (about 13 km^2) in area. The unit graph approach has been recommended to intermediate catchments of area each between 5 mi^2 (about 13 km^2) and 2,000 mi^2 (about 5,180 km^2). The unit graph method has not been recommended to catchments larger than 5,180 km^2 before subdividing them into sub-catcments each not exceeding 5,180 km^2. For this purpose the country has been subdivided into 22 large units. Each large unit, in turn, has been further subdivided into a number of smaller units. The technical reports prepared by Midgley et al. (1969) prescribe and describe the method to be used in each case together with some worked out examples.

The catchment of the Upper Wilge River has been used as a case study of an intermediate catchment. The catchment area is 710 km^2 with annual rainfall between 800 and 1, 200 mm y^{-1} and a mean annual precipitation of 950 mm. The calculation procedure begins by caculating a catchment index using the stream length, the distance between the center of area and the outlet, and the average slope of the catchment area. Using tabulated figures based on actual observations and local experiences, the point rainfall corresponding to selected storm durations and recurrence intervals are determined. The point rainfall is then multiplied by a reduction factor to convert it to areal rainfall depth. The effective rain is estimated by deducting from the areal rain a certain depth expressing the storm loss corresponding to each duration and recurrence interval. The next step is to select the relevant dimensionless one-hour unit hydrograph, already available, and compute its peak discharge, Q_p, using the critical storm duration, T_L, catcment area, A, and a constant, K_u, depending on the zone where the catchment lies. For any time, T, the ratio Q/Q_p is computed for the corresponding ratio T/T_L which when multiplied by Q_p gives the discharge Q.

The synthetic unit graph method has shown to give flood peak discharges for recurrence periods of 20, 50 and 100 y about 20% higher than the values listed in the flood manual for South Africa. As such, the results obtained from the synthetic hydrograph method have been described as plausible (Pullen, 1969) and recommended for design purposes.

8.3.3 Cyclic oscillation of streamflow and runoff prediction- The alternation of dry and wet hydroclimatic periods is evident in the historical discharge record. According to Martins and Probst (1991), the discharge fluctuations of African rivers flowing in the Southern hemisphere show some lag and even oppositions between the hydroclimatic periods when compared to those of the rivers in the Northern hemisphere.

Paling and Stephenson (1988) claimed that Tyson studied the cyclic variations in rainfall in South Africa in depth, and from that study he has been able to identify long-term and “9-year” cycles These cycles can be attributed to physical phenomena such as ocean temperatures, atmospheric pressure

oscillation in the Southern hemisphere and possibly solar activity. The cyclic oscillations in precipitation definitely react on basin runoff and river flow. In order to predict streamflows further ahead in time than the lag time of the catchment, a rainfall model was developed and used jointly with a rainfall-runoff model.

For the purpose of the study in question, a catchment area was chosen in the relevant summer-rainfall region. To facilitate the comparison between historical and calculated runoff data, preference was given to catchment in the upper reach of the Pongola River. This catchment also has about the same conditions as the upper basin of the Vaal River. The annual rainfall for the period 1921-75 averaged over the catchment area and expressed as a percentage of the mean annual precipitation (MAP), is shown in Figure 8.14$_a$. The same figure shows the runoff at a certain stream gauge located within the chosen catchment for the period 1929-67. The spatial rainfall data were filtered using a 5-term binomial filter and a 9-y moving average. Both filters seem to support the idea of having an 18.5-y cycle in the annual rainfall data. Cycles with shorter wavelength have been disregarded in the analysis under description.

The cyclic component in the annual rainfall expressed as a percentage of the MAP has been formulated as:

$$17 * \sin\left[(2\pi(i-1934)/18.65\right] \tag{8.9}$$

where i is the year of interest and 1934 is the origin for the sine curve. So, if i is taken as 1940, say, the cyclic component according to Eq. (8.9) will be 15.3%. Further elaboration of Eq (8.9) gave the best fit of the annual precipitation AP(i)

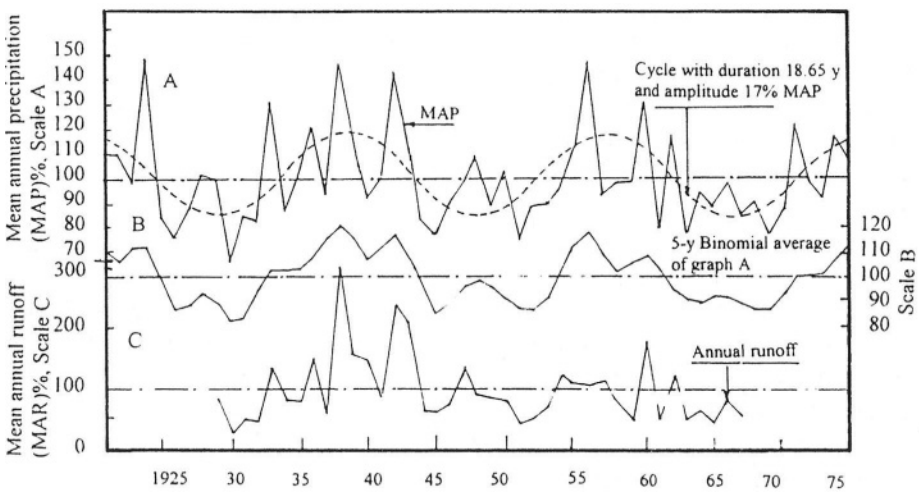

Figure 8.14$_a$- Annual rainfall and runoff series for a certain part of the basin of the Pongola River, South Africa (based on Paling and Stephensen, 1988)

at year *i* as:

$$AP(i) = 100 + \left[17 * \sin(2\pi(i - 1934)/(18.65)\right] - 29 + rnd * 74, \qquad (\%\text{MAP}) \tag{8.10}$$

where *rnd* is a random number between 0 and 1. So, for the same year, i.e., 1940, the range of *AP(i)* is from 86.3 to 160.3 (% MAP) corresponding to *rnd* at 0 and 1, respectively.

A prediction of the monthly rainfall would be determined from the predicted annual rainfall in combination with the average monthly distribution based on the historical rainfall record. The variation of runoff in a certain month in the course of years might best be represented by a suitable distribution function like the gamma or 2-parameter lognormal function. In the present study, however, the range of variation was kept, for simplicity, to between 0.5 and 1.5 times the average monthly runoff percentage. As such, the predicted monthly runoff in year I and month j can be written as:

$$MR(i, j) = 0.16 * \left[(0.5 + rnd) * MP(j, i)\right]/100 * AP(i) * 7.122 \tag{8.11}$$

where *MR(i, j)* = monthly runoff in 10^6 m^3 for year *i* and month *j*, *MP(j)* = % rainfall in month *j*, *AP(i)* = annual rainfall in mm, and *rnd* as before.

The rainfall-runoff model described by Eq. (8.11) has been used to predicting the monthly runoff for the period 1985-94. Figure 8.14_b shows the actual and simulated monthly flows for the period 1930-39 and the predicted monthly flows

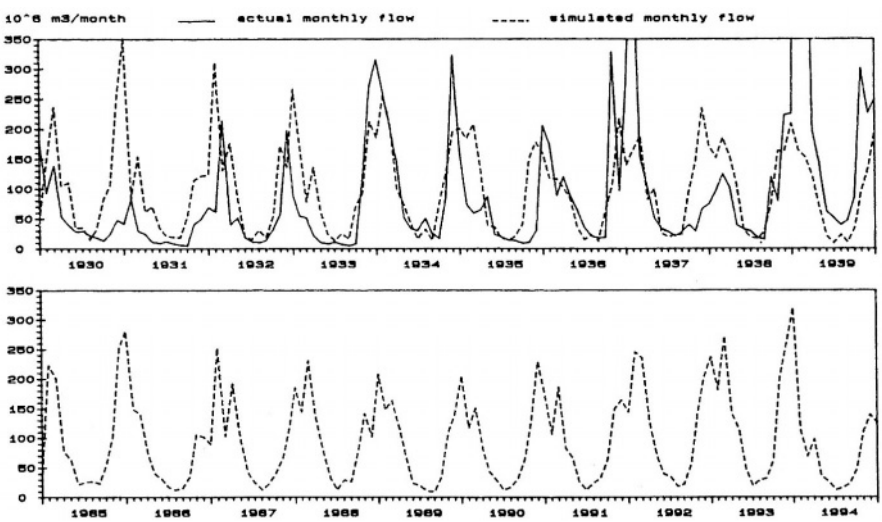

Figure 8. 14_b- Actual and predicted monthly flow (from Paling and Stephenson, 1988)

for the period 1985-1994. It would have been interesting to have the actual discharge observations of the upper reach of the Pongola River available for comparison with the predicted values. Unfortunately this is not the case.

Visual examination of Figure 8.14$_b$ shows that the agreement between the observed monthly flow and the simulated flow for most of the months in the period 1930-39 is not satisfactory. The several approximations introduced in constructing the simulation model, like describing the variation of the annual precipitation by a simple sine wave and the restriction of the range of runoff variation to just between 0.5 and 1.5 the mean annual runoff, are very likely responsible for this result. The inadequate performance of the model has led Paling and Stephenson (1988) to hint at the possibility of using a model of a different type. They suggested a stochastic model incorporating serial correlation and monthly variations, like the one developed by Thomas and Fiering (1962) or a more recent version of it.

8.3.4 Response of streamflow to land use- The results of experimental and analytical works on the response of streamflow to land use in South Africa has been recently reported by Scott and Lesch (1997). The study has been carried out in the Mokobulaan research catchments on the Drakensberg escarpment. The experimental area is located less than 100 km from the source of the Vaal River and 350 km northeast of the site of the Vaal Dam. The climate there is subtropical with more than 80% of the annual rainfall, 1,167 mm, falling in the summer. The mean annual A-pan evaporation at a nearby forest is 1,723 mm.

The streamflow in the experimental area has exercised significant reduction following the afforestation of grassland with *Eucaliptus grandis* and *Pinus patula.* The original runoff depth, 236 mm, in the catchment afforested with *eucalyptus* started to experience significant reduction beginning in the third year after planting and resulting in the stream becoming completely dried up by the 9th year. The peak reduction of 470 mm took place in the seventh and ninth years of the rotation. The eucalyptus was clearfelled when 16 years old but full perennial streamflow did not return until 5 years later.

Before the other catchment has been forested with pine trees the runoff used to be 217 mm. This amount decreased significantly in the fourth year after planting and by the twelfth year the stream dried up completely. The peak reductions of 205 and 257 mm occurred in the ninth and twentieth years of the rotation.

The reduction in runoff was not unexpected in view of the bigger consumption of water by the eucalyptus and pine trees compared to the grassland. The percentage flow reductions over time follow a typical sigmoidal growth curve. By fitting an equation to these points, general predictive equations of the flow reduction as a function of plantation have been developed.

8.3.5 Water quality- Table 2_a, Part II/Appendix B includes, among other items, the total mineral content, dissolved transport and solid transport in the waters of the Orange River. More recent data presented by Martins and Probst (1991) give the total suspended sediments, *TSS,* as 57 mg l^{-1} and total dissolved sediments, *TDS,* as 140 mg l^{-1}, and the ratio *TSS/TDS* 0.41. After the Nile, the Orange is the major African river with highest total dissolved salts in its water. However, the concentrations of the Dissolved Organic Carbon, *DOC,* being 2.3 mg l^{-1}, Particulate Organic Carbon, *POC,* 0.9 mg l^{-1}, and Total Organic Carbon, *TOC,* 3.2 mg l^{-1} are the lowest compared to the water of all other major rivers so far discussed.

Hart (1985) has been observing the variation of the values of some of the physico-chemical parameters of the water in the Orange for the period 1981-84. He concluded that the seasonal variability of most of the observed parameters has been severely depressed. This state of affairs has been largely attributed to the stabilizing influence of the water in P.K. Le Roux Reservoir. As already mentioned in sub-section 8.3.1 the construction of Le Roux Reservoir has been completed in 1976, five years after the completion of Verwoerd Reservoir. The Le Roux Reservoir has a storage capacity of $2.9*10^9$ m^3 and covers a surface of 128 km^2. The reservoir was operated at 80%-90% of its full capacity level during the first eight months of the study period. Conductivity, pH and alkalinity showed conservative variation of around 15-17 mS m^{-1}, 8.0 and 1.3 meq l^{-1}, respectively. The change of these parameters in the course of time is diagrammatically illustrated in Figure 8.15.

Makhoalibe (1984) reported on suspended sediment transport measurement in Lesotho. The paper discusses the suspended data collected during the period 1976-1982. The data covered the basins of the Senqu and Caledon Rivers. Some of the data obtained are summarized in Table 2_c of Part II/Appendix B. The results obtained show that annual suspended sediment yields range from less than 10 t km^{-2} in the igneous rock region to more than 2,000 t km^{-2}. Three curves for the sediment yield versus drainage area have been developed; one for the Caledon Basin, the second for the Vaal and the last for the Senqu (Upper Orange). These curves show clearly that the highest sediment yield given drainage area is obtained from the curve belonging to the Caledon Basin. The first and second curves show, as most of river basins do, that the sediment yield decreases with increasing drainage area. The curve describing the Senqu shows a rapid increase of suspended sediment yield with increasing drainage area, followed by declining rate of increase with further increase in the area up to say 10,000 km^2. Beyond this area, the yield stays unchanged till the area becomes 100,000 km^2 or so, after which the yield reduces with increasing drainage area. For drainage areas larger than 100,000 km^2, the three graphs coincide on each other and become one single curve.

It may be of interest to summarize some of the results obtained from an experimental study carried out during the period 1979-80 in two neighboring and

physiographically comparable drainage basins in the Natal Drakensberg (Watson, 1984). One of the basins will be termed the control basin and the other the experimental basin. The aim of the study was to investigate the effect of the autumn bum treatment of the grassland, a land management practice viewed as the most efficient means of insuring the highest sustained yields of sediment free water. The parameters monitored in this study were rainfall, vegetation cover, stream discharge, sediment yield and the organic and dissolved solids components of the total stream load. Both drainage basins were monitored for a period prior to the application of an autumn burn treatment to the experimental one, and a full annual cycle after the treatment.

The results obtained showed no significant change in the distributions of the rainfall events and their characteristics such as amount, duration and intensity.

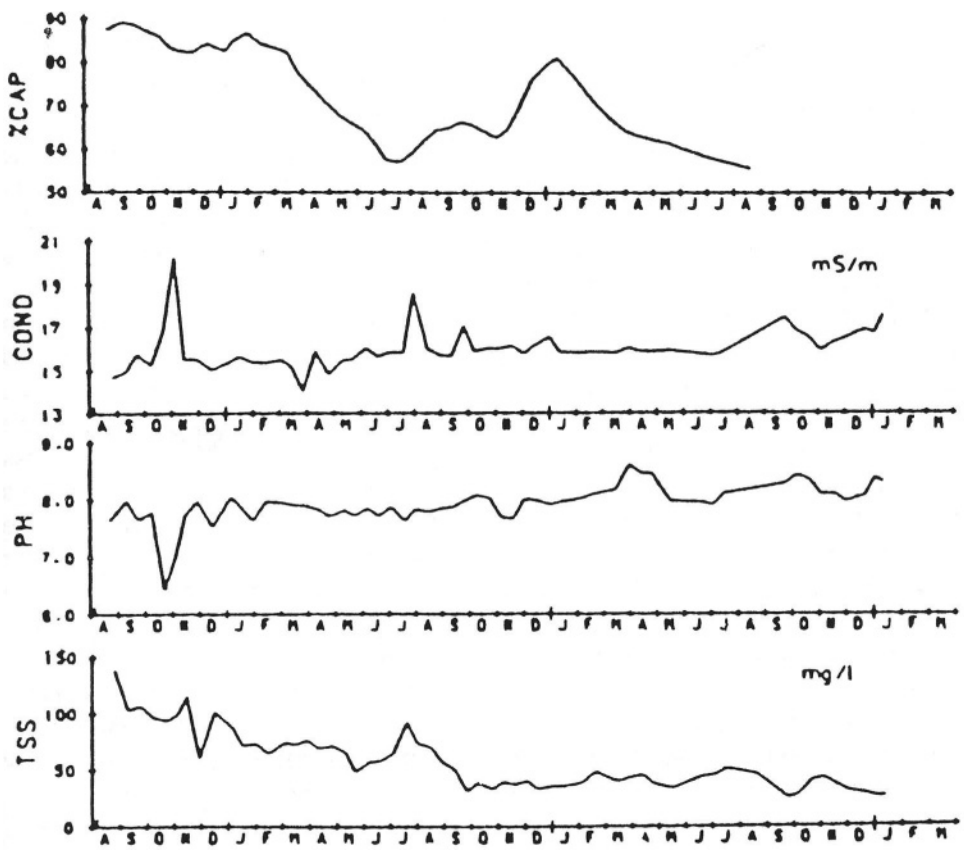

Figure 8.15- Seasonal variation of the capacity of Le Roux Reservoir on the Orange River, and of the conductivity, pH and total suspended sediments of the outflow water in the period 1981-84 (from Hart, 1985)

The runoff of the two basins before the application of the firebreak treatment was the same. The differences in streamflow became significant throughout the annual cycle following the treatment.

Prior to treatment the total sediment yield, the suspended sediment yield and the yield of sand-sized particles from the experimental drainage basin were all significantly greater than those from the control basin. the yield of sediment from the experimental drainage basin The yield of sediment from the experimental drainage basin throughout the annual cycle following the treatment was significantly less than the yield of the control basin. During winter, the yield of sediment from the experimental basin steadily decreased in direct contrast to the steady increase in yield from the control. Bed load components made a major contribution to the yield of the experimental drainage basin.

The total dissolved solids yield from the experimental drainage basin was significantly lower than the yield from the control. The mean concentration of the dissolved solids in the experimental basin started as 92 mg l^{-1} in autumn 1979 and dropped to just 54 mg l^{-1} in winter 1980, then increased to 88 mg l^{-1} in the spring of the same year. Again, the concentration dropped in the summer to 73 mg l^{-1} to rise up to 90 mg l^{-1} by autumn of 1980. The figures for the mean concentration of the dissolved sediments in the control drainage basin for the same seasons in their respective order were 102, 34, 100, 118 and 92 mg l^{-1} respectively. The percentage of organic yield to the total yield, inorganic plus organic is 0.4 in both drainage basins (Watson, 1984).

The above-summarized case study is a unique example showing how the quality of surface water can be strongly influenced by a certain practice of land management.

8.4- Summary Statistics of Large African Basins

Six large river basins in Africa have already been described with emphasis on their hydrological and water quality characteristics These large basins are; the Nile, Niger and Lake Chad in Chapter 7, and the Congo or Zaïre, Zambezi and the Orange in Chapter 8. It might be useful to end this chapter by summarizing the characteristics of these large basins in a Table listing the long-term average values of their basic statistics. The statistics appearing in Table 8.6, next to describing each basin alone, can also be used for comparison between the basins. As an example, the order of magnitude of the long-term average specific yield of the said basins, starting with the largest ending with the smallest is the Congo, Niger, Chari, Zambezi, Nile and Orange. The corresponding values, in l km^{-2} s^{-1}, are 10.59, 2.81, 2.05, 1.81, 0.95 and 0.35, respectively. Needless to say many more examples can be given using other parameters.

Table 8.6- Summary statistics of the largest six African River Basins; Nile, Niger, Chad, Zaire, Zambezi, and Orange

Item	River basin					
	Nile	Niger	Lake Chad	Zaire (Congo)	Zambezi	Orange
Basin Area, 10^6 km^2	2.88	2.2	2.3	3.8	1.8	1.02
Riparian countries of the river basin	Burundi Congo Egypt Ethiopia Kenya Rwanda Sudan Tanzania Uganda	Benin Burkina Faso Cameroon C.A.Republic Chad Guinea Ivory Coast Mali Niger Nigeria	Algeria Cameroon Chad Niger C.A. Republic Nigeria Sudan	Angola Burundi Cameroon C.A.Republic Congo (Brazzaville) Congo (Kinshasa) Rwanda Tanzania Zambia	Angola Botswana Malawi Mozambique Namibia Tanzania Zambia Zimbabwe	Botswana Lesotho Namibia S. Africa
Hemisphere	Northern and southern hemispheres	Northern hemisphere	Northern hemisphere	Northern and southern hemispheres	Southern hemisphere	Southern hemisphere
Length of river in km	6,500	4,100	1,300 (Chari)°	4,700-5,100	2,700-3,000	2,200
Outlet	Mediterranean Sea	Atlantic Ocean	Inland Lake Chad	Atlantic Ocean	Indian Ocean	Atlantic Ocean
MAP in mm	510	1, 140	870	1, 560	800	400
MAR in mm	30	124	65	336	57	12
$MA(ET)_a$, in mm	480	1,016	805	1,224	743	388
q in l km^{-2} s^{-1}	0.95	2.81	2.05	10.59	1.81	0.35
r in %	5.5	10.9	7.5	21.5	7.1	3

Explanation

MAP = mean annual precipitaion, MAR = mean annual runoff, $MA(ET)_a$ = mean annual actual evapotranspiration, q = specific runoff, and r = runoff coefficient = MAR/MAP, and ° basin area of the Chari at N'Djamena is 600, 000 km^2

Table 8.6- Cont'd.

Item	River basin					
	Nile	Niger	Lake Chad	Zaire	Zambezi	Orange
Gauging station	Aswan	Lokoja	N'Djamena	Kinshasa	Mutarara	Vioolsdrift
Q_m in $m^3 s^{-1}$	2,742	6,200	1,230	40,251	3,250	360
Q_{mx} in $m^3 s^{-1}$	4,327	17,800	3,570	54,964	6,994	500
Q_{mn} in $m^3 s^{-1}$	1, 441	1, 335	180	32, 872	1, 753	63
TSS in 10^6 t	67	25.4	3	50	42	0.7
Concentration mg l^{-1}	755	127	87	42	324	57
TDS in 10^6 t	18	14	2	37	20	1.6
Concentration mg l^{-1}	200	67	59	31	149	140
TSS/TDS	3.72	1.86	1.47	1.35	2.17	0.41

Explanation

Q_m = mean annual discharge, Q_{mx} = Maximum annual discharge, Q_{mn} = minimum annual discharge, TSS = total suspended solids, and TDS = total dissolved solids

CHAPTER 9

HYDROLOGY OF SELECTED INTERMEDIATE AND SMALL RIVER BASINS

This chapter deals with a number of intermediate river basins, between $1*10^5$ and $1*10^6$ km^2, and small river basins, less than $1*10^5$ km^2. Of the intermediate river basins, we shall discuss the Sénégal, Volta, Sanaga, Ogooué and Limpopo Rivers. The small river basins that we are going to discuss will be of the Oued (Wadi) Zeroud, Oued (Wadi) Sebou, the Gambia River and the Tana River.

9.1- The Sénégal River Basin

9.1.1 Brief description of the basin- After the Niger River, the Sénégal is the second most important river in West Africa. Four riparian states, Guinea, Mali, Mauritania and Sénégal, share the basin of the Sénégal River. The river forms the Mauritania-Mali and the Mauritania-Sénégal international boundaries. The Sénégal drainage basin lies between latitudes 10°20' and 17°30'N and longitudinal lines 7° and 16° 30'E.

The Séněngal River is about 1,790 km long from source to mouth. The drop in elevation is around 800 m, giving an average slope of about $0.45*10^{-3}$. As a matter of fact, the slope changes substantially from location to location depending, for example, on the presence of rapids and falls. The drop in the upper reach of the river, Bafing-Bakel, is 789 m in a length of 1,006 km, giving an average slope of $0.78*10^{-3}$. Totally different from this figure is the average slope in the lower reach of the river, between Bakel and the river mouth at St. Louis, which is 12 m in a distance of 784 km, i.e. $0.01.5*10^{-3}$.

The Sénégal Basin is often subdivided into two sub-basins, the upper and the lower sub-basin. The former is drained by the river reach from the source area up to the key gauging station of Bakel, whereas the lower part is drained by the river reach below Bakel up to the mouth on the Atlantic Ocean. Each sub-basin has its own rivers and tributaries. The upper sub-basin comprises the Bafing, the Bakoye, the Baoulé (sometimes written Bafoulé), the Falémé, the Kolimbine and the Karakoro. The lower sub-basin is drained essentially by Wadi type (intermittent) streams such as Oued Ghorfa, the Black and White Gorgols and Oued Savalel. This reach is connected with Lakes Guiers and Rkiz. Figure 9.1 shows a map of the Sénégal Basin.

The Bafing originates in the massive mountain rise of the Fouta Djallon, Guinea. Many rapids and falls obstruct the river course in its upper source area.

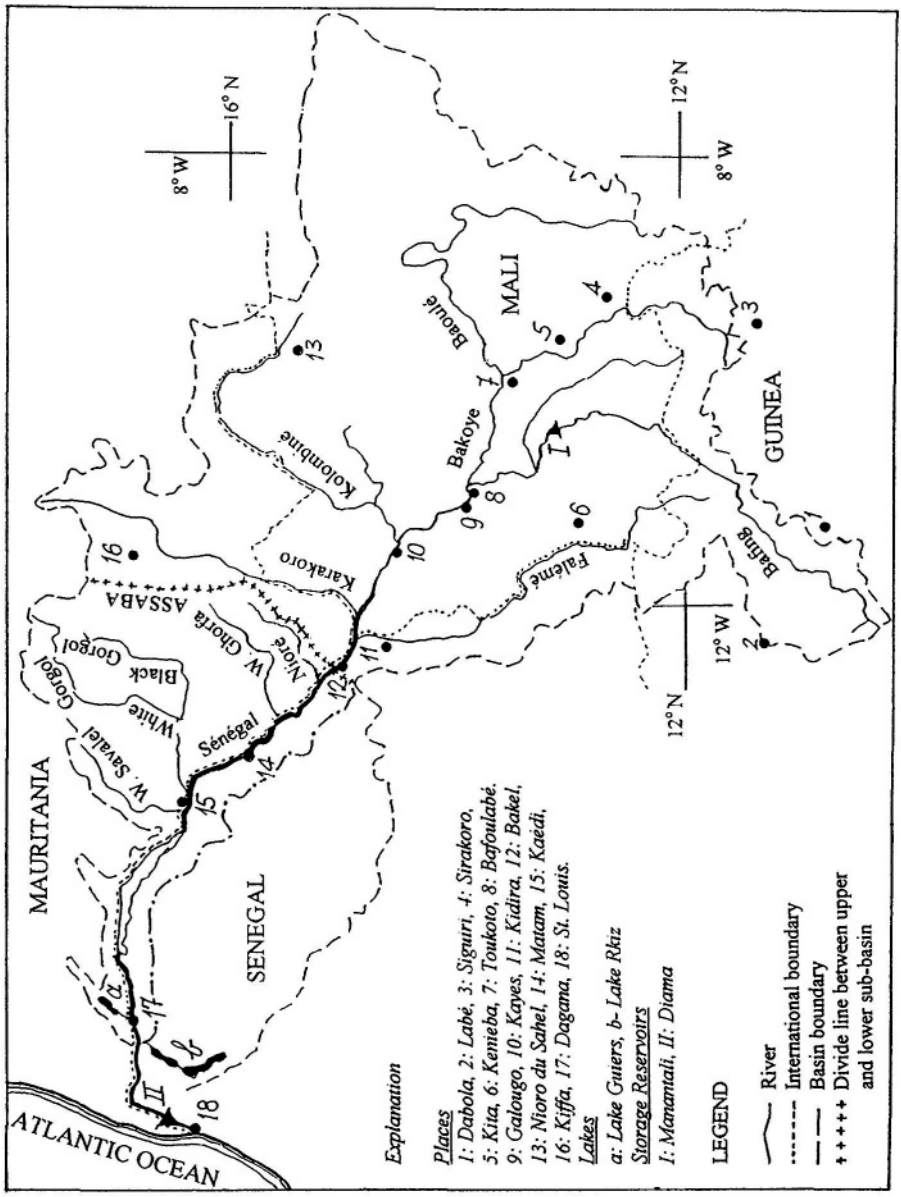

Figure 9.1- Map of the Sénégal River Basin

The total length of the Bafing up to Bakel is 1,006 km. The two principal tributaries of this River are the Téné and the Kiona. The Téné has its source at Dalaba, at an altitude of 1,000 m a.m.s.l., and after some 135 km empties into the Bafing. Out of the 38,400 km^2 drainage basin only 17,000 km^2 are situated in Guinea. The Kiona takes its source on the same mountain near Labé, at an altitude of about 800 m. It drains an area of 2, 000 km^2 and after 93 km pours into the Bafing at Balabori (Rochette, ORSTOM, 1974).

The Bakoye tributary has a catchment area of 85,000 km^2. The source area of this river lies in the mountainous region of the Meinen Mountains at an elevation of 760 m a.m.s.l. The water level drops rapidly and reaches 400 m at Kilometer 14 due to the series of rapids that obstruct the course of the river. The Bakoye, after crossing the Mandinga Plateau, receives the Bafoulé, and joins the Bafing at km 561. The Bafoulé is an important tributary originating in the southwest of Mali at elevation of 750 m a.m.s.l. The length of this tributary is 632 m, and it's and catchment area is 59,500 km^2.

The two rivers, Bakoye and Bafing, flow below their confluence at Bafoulabé (sometimes written Bafoualabé) as one stream under the name of Sénégal River from Bakel to the mouth on the Atlantic Ocean. The total catchment area of the Sénégal at Bafoulabé is 124,700 km^2. It is worthwhile to mention that the contribution of the Bafing to the flow of the Sénégal River is superior to the contribution of the Bakoye.

The Kolimbiné is the continuation of the Ouadou River, bringing the total length of the stream to 450 km. The Kolimbiné rises in the southeast of Nioro du Sahel, Mali, at an elevation of 300 m a.m.s.l. The lower reach of the river traverses the swampy depression of Magui before pouring into the Sénégal, a few kilometers above the town of Kayes. Since the Kolimbiné is basically a sahelian river its contribution to the discharge of the Sénégal is quite limited. However, it brings the catchment of the Sénégal at Kayes to 157,400 km^2.

The last major tributary in the upper sub-basin is the Falémé. It has a catchment area of 28,900 km^2 and length of 625 km. It rises at elevation of 800 m a.m.s.l. in the region of the deloritic plateaus, Bowal, Seguree and Fougou, and joins the Sénégal on the left side. The Falémé discharges its yield into the Sénégal some 50 km above Bakel.

The last tributary in the upper basin is the Karakoro. It originates in the region of Kiffa, Mauritania, at altitude of 130 m. After flowing in a rather dry region for about 300 km it joins the Sénégal at Lami-Tounka on the right side. Again, as the basin of the Karakoro is situated in a sahelian climate its yield, if any, adds but little to the flow of the Sénégal (Rodier, 1964). The basin of the Karakoro brings the area of the upper sub-basin of the Sénégal River at Bakel to 218,000 km^2.

The lower sub-basin in the west, where the Sénégal flows sluggishly, is covered by a vast plain formed by recent sediments. The Assaba massive can be regarded as the divide line between the upper and lower sub-basins. The surface

area of the lower sub-basin is debatable Some maps in the "Monographies Hydrologiques ORSTOM No. 1" (Rochette, 1974) show that the catchment area at Dagana, a few kilometers above the river mouth is 268,000 km^2 and the total basin area at St. Louis on the ocean is 270, 000 km^2. Other maps in the same reference as well as other sources claim that the lower part of the basin reaches as much as 100,000 km^2. Both basin boundaries are shown in Figure 9.1.

The length of the Sénégal River between Bakel and St. Louis is 784 km. The principal streams forming the drainage network in the lower sub-basin are the Niorde (sometimes written Nioré), Ghorfa and Savalel wadis and the Gorgol River, formed by the junction of the White (Blanc) Gorgol and the Black (Noir) Gorgol. The Ghofra Wadi originates in the Assaba massive at elevation of 318 m a.m.s.l. It runs a distance of about 190 km before joining the Sénégal at a point 40 km below Ouaunde. The junction of the Black Gorgol (194 km long and 95 m fall) and the White Gorgol (346 km long and 336 m fall) forms the main Gorgol. Again, as all tributaries in the lower sub-basin rise in fairly dry areas their contribution to the flow in the Sénégal River is quite limited. For practical purposes, it could be said that, at Bakel, the river has received all the contributions it can count on. For some distance, the Sénégal River forms the international boundary between Sénégal and Mauritania, and thus becomes a contiguous river. It finally pours into the Atlantic Ocean through a delta some 40 km from the port of St. Louis.

9.1.2 Hydrology of the Sénégal Basin- The basin of the Sénégal is probably the most well-studied basin of all the rivers in West Africa. Stage and discharge measurements began as early as 1903. Staff gauges and other stage measuring devices kept changing and updated in the course of time, at least till 1965. Rochette (1974) produced a technical report containing an extremely detailed inventory of stage and discharge measurement sites, measuring equipment, observations and the hydrological services taking care of them. A short summary of that inventory is given in Table 9.1. According to this inventory, some of the measuring sites were not operative all the time, and some stations even ceased to operate and had to be stopped.

UNESCO Publications concerned with discharge of selected rivers of Africa lists discharge data at eight stations. Three stations (No. 39, 41and 43) are on the Sénégal River, three (No. 42, 54 and 67) on the Falémé, one (No. 56) on the Bafing, and one (No.50) on the Bakoye. The monthly, annual, flood and low-flow series at these stations suffer from breaks of different duration. This state of affairs does not make it easy to detect, for example, the temporal variation of the basin yield, or to perform flood and low-flow frequency analysis at a sufficient number of reasonably spaced points. Despite these shortcomings, some of the sites do have adequate record that helps to produce a fair evaluation of the basin's hydrologic parameters. Particularly, the stations at Bakel (No. 39), Kayes (No. 41) and Kidira (No. 42) can be regarded as key measuring sites.

Table 9.1- Summary of the stage and discharge gauging stations in the Senegal Basin (Rochette, 1974)

Tributary	Gauging station	Coordinates	Area[x], 10^3 km^2	Start of record	End of record
Faleme	Fadougou	11°23' W, 12°31' N	9,3	1945	
	Gourbassi	11°38' W, 13°24' N	17,1	1954	
	Kidira	12°13' W, 14°27' N	28,9	1930	
Bafing	Balabori	11°20' W, 11°17' N	11,6	1955	after 1956
	D. Saidou	10°37' W, 11°57' N	15,7	1952	
	B. Makana	10°17' W, 12°33' N	22,0	1955	
	Dibia	10°48' W, 13°14' N	33,5	1956	1960
	Degurre	10°50' W, 13°39' N	37,9	1951	
	Mahina	10°50' W, 13°45' N	38,4	1904	
Bakoye	Toukoto	9°53' W, 13°27' N	16,5	1903	
	Oualia	10°23' W, 13°36' N	84,7	1954	
	Dioubeba	10°30' W, 13°38' N	84,9	1904	
	Kale	10°39' W, 13°43' N	85,6	1951	after 1959
Middle	Bafoulabe	10°50' W, 13°49' N	124,7	1904/30	
Senegal	Galougo	11°03' W, 13°51' N	128,4	1904	
Bafoulabe-	Gouina	11°06' W, 14°00' N	128,6	1929	
Ambidedi	Felou	11°21' W, 14°21' N	131,5	1950	
	Kayes	11°27' W, 14°27' N	157,4	1903	
	Ambidedi	11°47' W, 14°35' N	159,0	1909/37	
Lower	Bakel	12°27' W, 14°54' N	218,0	1901/06	
Senegal	Ouaounde	12°52' W, 15°15' N	222,0	1951	interruptions
	Matatm	13°15' W, 15°39' N	230,0	1904	
	N'Guiguilone	13°21' W, 15°56' N	232,5	1950	
	Kaedi	13°30' W, 16°08' N	253,0	1903	
	Diorbivol	13°43' W, 16°07' N		1914	1943
	Salde	13°52' W, 16°10' N	259,5	1903	
	Diolde-Diabe	13°58' W, 16°20' N	260,0	1951	
	Boghe	14°17' W, 16°35' N	263,0	1908/33	
	Sarepoli	14°34' W,16° 37' N		1951	
	Podor	14°57' W, 16°39' N	266,0	1903/06	
	Dagana	15°30' W, 16°31' N	268,0	1903/06	
Delta of	Richard Toll	15o42'W, 16o27'N		1906	
Senegal	Guiers Lake			1950	
	Rosso	15°48' W, 16°30' N		1951	
	Gueylobe			1955	

Table 9.1- Cont'd.

Tributary	Gauging station	Coordinates	Area[x] 10^3 km^2	Start of record	End of record
Delta of Senegal	Saint-Louis	16°30' W, 16°02' N		1931	
	Gandiole			1961	
Doue	N'Goui	13°55' W, 16°09' N		1955	
	Madina	14°08' W, 16°18' N		1952	
	Guede	14°47' W, 16°33' N		1940	

Explanation

[x] *Catchment area from source up to the station in question*

Table 9.2 gives the mean monthly and annual discharges at 14 sites over different periods, all of them before 1965. When the discharge measurements were considered sure for certain years, the averages for those years only have been included in Table 9.2.

Before embarking upon any discussion of the hydrology of the Sénégal Basin, however, one should always bear in mind some important basin characteristics. Firstly, the mean annual precipitation decreases gradually from 2,000 mm or more in the source area of the river in the extreme south to 300 mm or less at the location of the river mouth in the extreme north. A few examples can be cited here; the annual rainfall, averaged over the period 1904-60, was 1,750 mm at Labé decreasing to 750 mm at Kayes, 410 mm at Kaédi, and further to 300 mm at Dagana. Quite oppositely, the annual evaporation along the course of the river increases from say 1.5-1.8 m in the uppermost part of the basin to 2.2-2.5 m or more in the lowermost part. The geometry of the basin's form is such that the width in the upper basin is small compared to the width in the middle or the lower basin. Under such conditions, one should expect that the increase of the basin runoff with distance from the location of the headwaters must be at a declining rate.

The three stations on the Falémé River show a gradual increase in discharge from 122 $m^3 s^{-1}$ (station No. 67) to 153 $m^3 s^{-1}$ (station No. 54) and further to 177 $m^3 s^{-1}$ (station 42) corresponding to catchment areas of 9,300, 17,100 and 28,900 km^2 respectively. The given mean annual discharge values and the corresponding variation coefficients are given in Table 6a, Part I/Appendix B. These values pertain, however, to the period 1951-78. The discharge of the Falémé River at the same stations but for the sure years in the pre-1965 period, are given in Table 9.2 as 134, 183 and 221 $m^3 s^{-1}$ respectively. A comparison between the two sets of results shows that the more recent data are between 10 and 20% less than the pre-1965 figures. Additionally, the pre-1965 discharges when compared to the annual rainfall then yield a runoff coefficient varying from 27 to 22% depending on the distance from the source area of the Falémé tributary.

Table 9.2- Mean monthly and annual discharges in $m^3 s^{-1}$ of the Senegal and its tributaries in the period before 1965 summarized from Rochette, 1974)

Tributary	Station	May	Jun	Jul	Aug	Sep	Oct	Nov	Dec	Jan	Feb	Mar	Apr	year	Remarks
Faleme	Fadougou	2.7	22.3	147	502	498	246	88	47	25.7	13.2	6.8	3.3	134	11 y sure[x]
	Gourbassi	1.2	25.8	164	669	843	306	96	43	22.3	11.3	5.5	2.1	183	11 y sure
	Kidira	0.9	26.3	146	693	940	400	109	40	18.6	9.2	4.3	1.8	200	29 y
		0.7	23.9	149	704	1,100	464	115	46	20.9	9.9	4.9	2.0	221	14 y sure
Bafing	Dakka Saidou	27.2	107	381	975	1,042	659	280	123	61	38	24.2	17.4	313	12 y
	Dibia-Degurre	12.5	75	355	1,371	1,769	1,179	458	170	91	51	28	14.4	466	10 y
Bakoye	Toukoto	0.8	17.3	68	325	409	281	80	33	17.7	10.3	6.5	2.0	105	08 y
	Kale-Oualia	0.6	25	136	632	821	403	104	44	24	12.9	5.9	1.8	185	12 y
Senegal	Galougo	12.1	128	599	2,184	2,789	1,552	545	242	134	75	39	17.3	699	14 y sure
	Gouina	12.6	131	575	2,081	2,766	1,568	557	256	143	78	37	14	695	13 y
	Kayes	9.2	122	525	2,048	2,633	1,283	462	219	168	70	32	11.6	631	58 y
		9.6	115	562	2,190	2,910	1,590	546	245	138	78	37	14.3	705	14 y sure
	Bakel	9.4	112	615	2,445	3,949	2,118	691	296	163	96	53	23	884	15 y sure
	Matam	7.8	74	512	2,094	3,434	1,961	638	269	146	83	46	18.6	776	62 y
		7.2	74	563	2,226	3,874	2,892	804	323	175	100	52	21	893	15 y sure
Senegal+	Salde	15,0	56	441	1,637	2,836	2,434	939	318	172	105	61	30	757	13 y sure
Doue	Dagana	17.5	33	417	1,223	1,998	2,301	1,405	438	201	113	62	31	691	62 y

Explanation

[x] = *number of years of sure record, I.e. no doubt about measurements being correct.*

The pre-1965 discharges show a mean annual discharge at Toukoto of 105 $m^3 s^{-1}$, increasing to 185 $m^3 s^{-1}$ at Oualia, both in the sub-basin of the Bakoye tributary. The large increase in the surface area from 16,500 km^2 to 84,700 km^2 is not paralleled by a proportionate increase in the mean annual discharge. This can be attributed to the smaller rainfall in the large area compared to the rainfall depth in the smaller catchment. This too is coupled with smaller runoff coefficient for the large catchment compared to the runoff coefficient for the smaller one. The annual discharge at Oualia, averaged over the 1951-78, was 157 $m^3 s^{-1}$, with coefficient of variation of 0.42, i.e. about 15% less than the mean annual discharge for the pre-1965 period.

Galougo is situated a short distance below the confluence of the Bafing and the Bakoye Rivers. Again, the interannual variability of the discharge affects the value of the mean discharge for the period over which the mean is computed. This explains the difference between the average over the period 1952-76, 603 $m^3 s^{-1}$, and the average for 14 sure years in the pre-1965 period, 699 $m^3 s^{-1}$.
The mean annual discharge for the same 14 sure years but at Kayes (station No. 41) was 705 $m^3 s^{-1}$. The corresponding figure for the period 1952-1976 fell to 609 $m^3 s^{-1}$ and further to 491 $m^3 s^{-1}$ over the period 1952-1988, illustrating the severe effect of the harsh drought the hit the Sahelian countries from 1968 and lasted at least till the mid-eighties. Considering an average precipitation over the catchment area up to Kayes, 157,400 km^2, of 1,100-1,200 mm and a mean discharge of 700 $m^3 s^{-1}$, the corresponding runoff coefficient must be 12%.

The issue of the interannual variation of the annual discharge at Bakel station (No. 39) has been receiving some attention, especially in connection with the severe drought that struck the Sahel region from 1968 up to 1985. Here below the mean annual discharge and the corresponding period are tabulated:

Period	Mean annual discharge, $m^3 s^{-1}$	High/Low	Source
1904-21	685	low	Carbonnel & Hubert
1922-36	887	high	
1937-49	591	low	
1950-67	880	high	
1968-83	430	low	
1904-83	732	average	Sutcliffe & Lazenby
1913-61	768	above average	Rodier
1926-65	787	above average	
1903-64	770	above average	Rochette
1950-64	884 (15 sure years)	high	
1951-84	665 (Cv = 0.415)	below average	(Table 6_a, Part I/Appndix B)

The above listed figures show that the annual discharge assumes an alternating pattern of low and high flows. The amplitude of jump of the mean discharge from one period to another is quite sensitive to the rainfall variability, Figure 6.13_b shows the annual flow series at Bakel together with the 5-y moving average and a linear trend line. From this figure, one can easily observe that the annual discharge series can be approximately represented by a succession of cyclic fluctuations of opposite signs superposed on a downward sloping line.

Figure 6.12_a illustrates three distinct discharge hydrographs, one for a low-flood year, another for a normal-flood year and a third for a high-flood year. The peak ordinate of a high-flow year can simply exceed two times the corresponding ordinate in a normal-flood year whereas the peak ordinate of the low-flow year can hardly reach half of the latter. The long-term average discharge shows, however, that an annual areal precipitation of 900 mm on the catchment up to Bakel produces nearly 106 mm of runoff, i.e. the average annual runoff coefficient counts to about 12%, and the specific yield is nearly 10.5 l km^{-2} s^{-1}. Discussion of the extreme water levels and discharges of the Sénégal River will be presented in the following sub-section.

The mean monthly flow of the Sénégal is characterized by a high seasonality index. The value of this index, which expresses the ratio of the maximum monthly discharge to the minimum monthly discharge, is in the order of 500. The peak flood flow usually occurs in September, after which the discharge begins to fall in October to reach the minimum flow by mid-May. The river flow begins to augment in June and reaches its new flood in the next September.

Matam is the next important station after Bakel. The corresponding catchment area at these two stations is 230,000 and 218,000 km^2 respectively. Despite this difference, the annual discharge averaged over the 62-y period, 1904-65, was very much the same at the two stations. The volume of water supplied annually to the Sénégal by the two tributaries, Nioré and Wadi Ghorfa, located between Bakel and Matam is limited. Additionally, the river stretch between these two stations belongs to the river reach traversing the and part of the basin where evaporation is far larger than precipitation.

The same 62 years of record, as that recorded at Bakel and Matam produced a mean annual discharge at Dagana (268,000 km^2) of 691 m^3 s^{-1} (see Table 9.2). This figure is nearly 10% less than the corresponding figure for Bakel or Matam. The reduction in the mean annual discharge despite the increase in the catchment area is a mere reflection of the aridity in the area traversed by the Lower Sénégal. This situation brings the specific yield of the Sénégal Basin at Dagana to just 2.6 l km^{-2} s^{-1}.

Before bringing the present sub-section to it's end, it might be worthwhile to report here that the water management plans of the "highly irregular" Sénégal River included, among other items, the construction of the Manantali Dam on the Bafing River in Mali, and the Diama Barrage near Saint Louis in Sénégal.

The construction of the Manantali Dam was completed in 1986 and the reservoir was put into operation during 1987. The reservoir created behind the dam has a surface area of $477\ km^2$ at full storage level, and a design capacity of $11*10^9\ m^3$. This large capacity helps to provide 800 GWh per year and regulated artificial flood of $2{,}500\ m^3\ s^{-1}$. As such, the dam controls about 50% of the flow down the Sénégal Valley and will help irrigate more than 250,000 ha of arable land.

ORSTOM (1964) reported the results obtained from a study of the oceanic tidal movement and the subsequent penetration of the saline water wedge into the Delta of the Sénégal. These results were summarized by Rochette in 1974. Among the important results that were obtained is the relationship between the river discharge and the length of the saltwater wedge. For example, a length of 100 km of the wedge corresponds to a discharge of $1{,}850\ m^3\ s^{-1}$, whereas a smaller discharge of say $360\ m^3\ s^{-1}$ corresponds to a length of 285 km. The length of the wedge reaches 440 km under zero discharge. The results of that study have been helpful in prompting the plans of the Diama Barrage, near the river mouth. This hydraulic undertaking has been designed essentially to reduce the penetration of saltwater into the river. The barrage that has been completed in the 1990s with a design capacity of $0.25*10^9\ m^3$ and a surface area of $235\ km^2$ at full reservoir makes it also possible to irrigate up to 42,000 ha of land

9.1.3 Extreme values of stage and discharge of the Sénégal River- The Sénégal has often been described as a highly irregular river. The height of the flood peak level above a reference zero datum at several sites in the upper, middle and lower Sénégal were collected up to 1965 and reported by Rochette (1974). An appropriate frequency distribution function has been fitted to the data of each site and the characteristic heights corresponding to a number of frequencies of exceedance have been computed. The results obtained are listed in Table 9.3, where they are expressed as ratios of the median height, i.e. ratios of the height corresponding to frequency of exceedance of 50%. The advantage of this presentation is that it gives a clear picture of the growth of the median water height at each site, especially against extreme frequency values. It also serves as a basis for comparison between two or more observation sites. A glance to Table 9.3 will show that the departure from the median value at Kayes is greater than the corresponding departure at Kaédi or Boghe for the same frequency of exceedance. The ratio to the median height given F = 1% say is 1.422 at Kayes and 1.145 for Kaédi, whereas the same ratio for F = 99% is 0.476 and 0.618 for the two stations in their respective order.

The flood discharge and the height of floodwater are interconnected by the rating function of the gauging site under consideration. Figure 9.2 shows the distribution of the maximum annual discharges at Kayes and Dagana using the same 62-y of record. The distribution of best fit to the observations at Kayes is steeper compared to the slope of the line fitted to the observations at Dagana.

Table 9.3- Frequency distribution of maximum annual flood levels at a number of observation sites in the Senegal Basin (raw data are taken from Rochette, 1974)

F, %	Factor to be multiplied by H_{50} to estimate the height of peak flood water above reference zero datum that corresponds to a given frequency of exceedance at a certain observation site exceedance at a number of observation sites in the Senegal Basin										
	Kidira	Bafou-labe	Galougo	Kayes	Ambi-dedi	Bakel	Matam	Kaedi	Boghe	Podor	Dagana
0.5	1.330	1.372	1.472	1.465	1.397	1.247	1.203	1.158	1.165	1.355	1.355
1	1.303	1.326	1.415	1.422	1.358	1.228	1.186	1.145	1.154	1.198	1.329
2	1.277	1.291	1.371	1.380	1.324	1.212	1.175	1.133	1.142	1.190	1.297
5	1.223	1.221	1.289	1.305	1.263	1.183	1.141	1.115	1.125	1.164	1.250
10	1.181	1.163	1.214	1.241	1.212	1.153	1.113	1.091	1.106	1.129	1.197
20	1.117	1.105	1.138	1.161	1.145	1.111	1.073	1.067	1.072	1.095	1.132
25	1.096	1.081	1.113	1.128	1.117	1.096	1.062	1.055	1.062	1.078	1.105
40	1.037	1.028	1.038	1.048	1.051	1.041	1.023	1.018	1.025	1.026	1.039
50	1.000	1.000	1.000	1.000	1.000	1.000	1.000	1.000	1.000	1.000	1.000
60	0.957	0.965	0.950	0.947	0.944	0.968	0.972	0.976	0.977	0.974	0.955
75	0.883	0.907	0.868	0.861	0.855	0.89	0.927	0.933	0.938	0.914	0.882
80	0.851	0.884	0.843	0.829	0.827	0.877	0.91	0.915	0.921	0.888	0.847
90	0.761	0.849	0.755	0.733	0.726	0.799	0.836	0.855	0.868	0.810	0.763
95	0.665	0.779	0.686	0.647	0.637	0.721	0.768	0.782	0.798	0.724	0.684
98	0.542	0.709	0.585	0.545	0.531	0.616	0.667	0.691	0.704	0.603	0.592
99	0.452	0.663	0.522	0.476	0.458	0.557	0.593	0.618	0.631	0.517	0.526
99.5	0.352	0.605	0.440	0.401	0.385	0.502	0.520	0.552	0.574	0.430	0.474
$^{x}H_{50\%}$	940	430	795	935	895	1095	885	825	871	580	380

Explanation

F = Frequency of exceedance, $^{x}H_{50}$ = Height in cm corresponding to F = 50%. Accordingly, the height corresponding to F = 20%, for example, at Matam should be 1.073 x 885 = 950 cm.

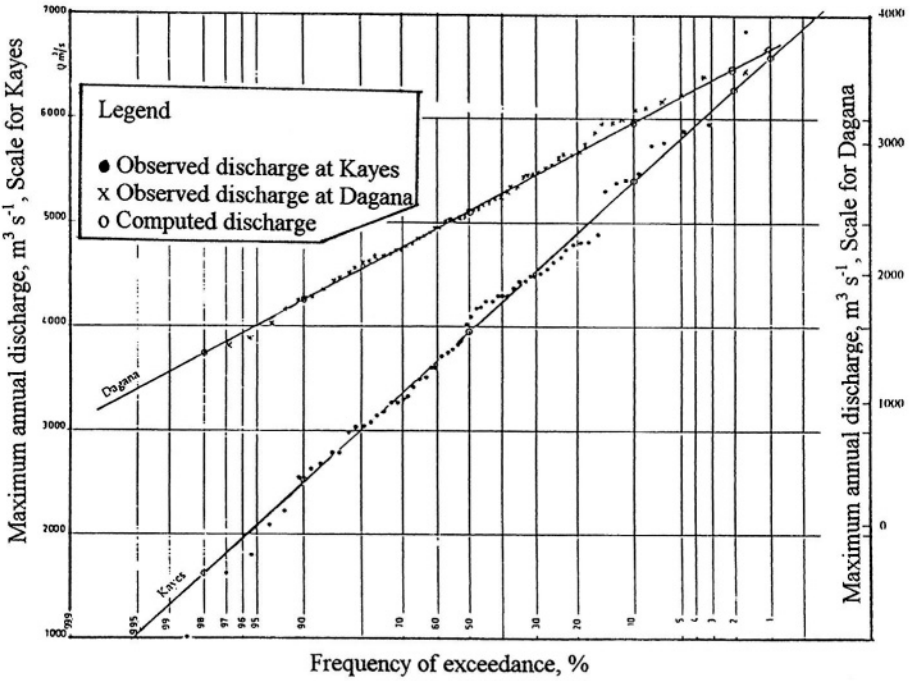

Figure 9.2- Frequency distribution of maximum annual discharge at Kayes and Dagana on the Sénégal River (based on Rochette, 1974)

The ratios of the 1% and 99% maximum discharges to the 50% discharge are 1.67 and 0.33 for Kayes, and 1.5 and 0.5 for Dagana respectively. Roche et al. (1976) increased the length of record up to 70 y, i.e. 1904-73. The incorporation of some of the Sahelian drought years had an effect on the distribution of the maximum annual flows at Bakel, as can be seen from Figure 6.10_c. From this figure it can be seen that the ratios of the discharges at 1% and 99% frequencies of exceedance and the median flood discharge are 2.07 and 0.24 respectively. It goes without saying that these ratios and the underlying frequency distributions are valuable for the management of the river's water.

9.1.4 Water quality- Tables 2_i and 2_j, Part II/Appendix B, give the monthly and annual suspended sediment load and concentration figures for water in the Sénégal River at Bakel for the 5-y period, 1979-1983, respectively. The listed figures show that the mean annual concentration of suspended sediment in the given period varied between 156 and 239 mg l^{-1}, with an average of 185 mg l^{-1}. The mean annual load is $1908*10^3$ t and the corresponding specific load is 8.75 t km^{-2} y^{-1}.

Grove (1972) published the results obtained from the analysis of water samples taken from different sites located at increasing distances from St.

Louis, all in October 1969, at the end of the rainy season. Those results have shown clearly that the conductance, in mhos, at 25° C, decreased from 52 at Diama (29 km) to 40 at Podor (268 km) and further to 33 at Tiguéré (610 km). Exceptionally, the sample obtained from the site at the confluence of the Falémeé (825 km) rose to 42 mhos. The sum of the sodium and magnesium contents and therefore the chlorinity decrease from Diama next to the ocean to Sénégal inland without any exception.

In the low-flow season, between February and June in the pre-Diama era, when the mean discharge used to fall to less than $100\ m^3\ s^{-1}$, the seawater wedge advanced up the river for 300 km or more as already mentioned in sub-section 9.1.2. With the arrival of the flood-season in July, the large incoming freshwater helped to flush the stagnant saltwater down the river that by the end of August the Sénégal above the mouth at St. Louis became once more clear of salt.

Most of the total dissolved load is carried out by the river in the flood season. Considering the mean discharge as $750\ m^3\ s^{-1}$ and the concentration as 40 ppm, the dissolved load carried in an average year would be around $1*10^6$ t. According to Grove (1972), the greater part of this load is derived from a small area in the headwater zone of about $75{,}000\ km^2$, with over 1,000 mm rainfall, indicating a specific yield of $10\text{-}15\ t\ km^{-2}\ y^{-1}$ from that area.

9.2- The Volta Basin

9.2.1 Brief description of the Volta Basin- The lower course of the Volta River has been known to the Europeans since the 15th-century explorations of the Portuguese. They called the river by the name Volta, meaning "turn", because of its twisting course. Anyhow, it was not before the end of the 19th century that the full size and extent of the Volta Basin were drawn on maps. The Volta Basin, which lies south of the Niger Basin, occupies a surface area of $394,000\ km^2$. This area is shared between five riparian countries: Benin, Burkina Faso, Ghana, Ivory Coast and Mali. In fact, most of the country area of each of Ghana and Burkina Faso falls within the Volta Basin

The Volta River is 1,600 km long. However, the total length of the affluent streams of the Volta Basin in Burkina Faso alone is about 3,000 km (Traore, 1989). The Volta River has two main upper branches, the Black and White Voltas, both of which rise on crystalline rocks in the open plateaus of Burkina Faso and unite in North-central Ghana, some 480 km north of the sea. The Red Volta and the Sisili are the principal tributaries joining the channel of the White Volta on its right bank. Likewise, the Tui and the Bougouriba join the Black Volta from the right bank too. The Volta flows generally southward through Ghana, discharging its water in the Gulf of Guinea. However, before reaching the sea, some tributaries like the Sorri, Mole, Kalurakun, Daka, Pru, the Oti (Pandjari) and the Afram flow into Lake Volta. The most important of these

tributaries are the Oti and the Afiram. Figure 9.3 shows the Volta Basin and the Volta River system.

Lake Volta is a huge lake that has been formed after the construction of the Akosombo Dam in 1965. The dam is located south of Ajena, some 60 km above the river mouth. The lake itself extends from Akosombo to Yapei, beyond the former confluence of the Black and White Voltas. It is 400 km long and covers a surface of $8{,}500\ km^2$, or 3% of the surface area of Ghana, thus impounding a huge reservoir having a capacity of $148*10^9\ m^3$. The dam was built with the aim of river flow regulation and hydropower development.

The Lower Volta, below the Akosombo Dam, emerges from a gorge in the Akwapim Hills and traverses a series of rock bars to reach the sea by a single channel cutting across the western part of an ancient delta of the Volta. The seaward side of the Volta Delta is a complex of Lagoons and barrier beaches with extensive plains extending northwards to an old cliff line (Grove, 1985)

The Volta Basin enjoys a wide variety of climates The climate in the extreme north of the Basin in Burkina Faso is sahelian, where the annual precipitation varies from 300 to 500 mm. This zone is followed by a succession of narrow bands of steadily increasing annual precipitation: 500-750 mm, 750-900 mm, 900-1,200 mm and 1,200-1,500 mm and more. The mean annual precipitation increases further to more than 2,100 mm in the extreme southwest of Ghana. Contrarily, it decreases rapidly to less than 800 mm in the southeast comer of Ghana. The long-term average annual precipitation is about 800 mm in Ouagadougou and 1,130 mm at Bobo Dioulasso, both in Burkina Faso. It is quite remarkable that the annual rainfall at Axim is 2,170 mm and 827 mm in Accra, both sites are in southern Ghana along the coast of the Gulf of Guinea and spaced 300 km apart. One should not forget, however, that the area in southwest Ghana receiving too much rainfall lies outside the Volta Basin.

The areas relatively rich in rainfall are characterized by their high relative humidity and cloudiness, and limited sunshine hours. These factors together bring the annual potential evapotranspiration to a relatively low value, 1.5 m say. The corresponding figure for drier areas lies between 2.0-2.25 m.

A narrow coastal savanna plain overlooking the Gulf of Guinea bounds the Volta Basin from the south. Behind this plain lies an undulating upland rising gradually to the Ashanti Plateau with its exposures of ancient crystalline rocks. Northwards from the crest the land falls to the broad valley occupying the northern part of Ghana. The basin extends its surface further to the north in Burkina Faso, where it is mostly flat and relatively dry savanna country. Obviously, a basin with such a relief should not be expected to have a high runoff coefficient.

9.2.2 Hydrology of the Volta Basin- The Volta River as already mentioned is a confluence of the Black Volta (Mou Houn in local language and Volta Noire in French) and the White Volta (Nakambe in local language and Volta Blanche in

French). It flows southwards into the Gulf of Guinea. The lower part of the basin in southeast Ghana is partly covered by the Volta Lake, which has been formed by the Akosombo Dam.

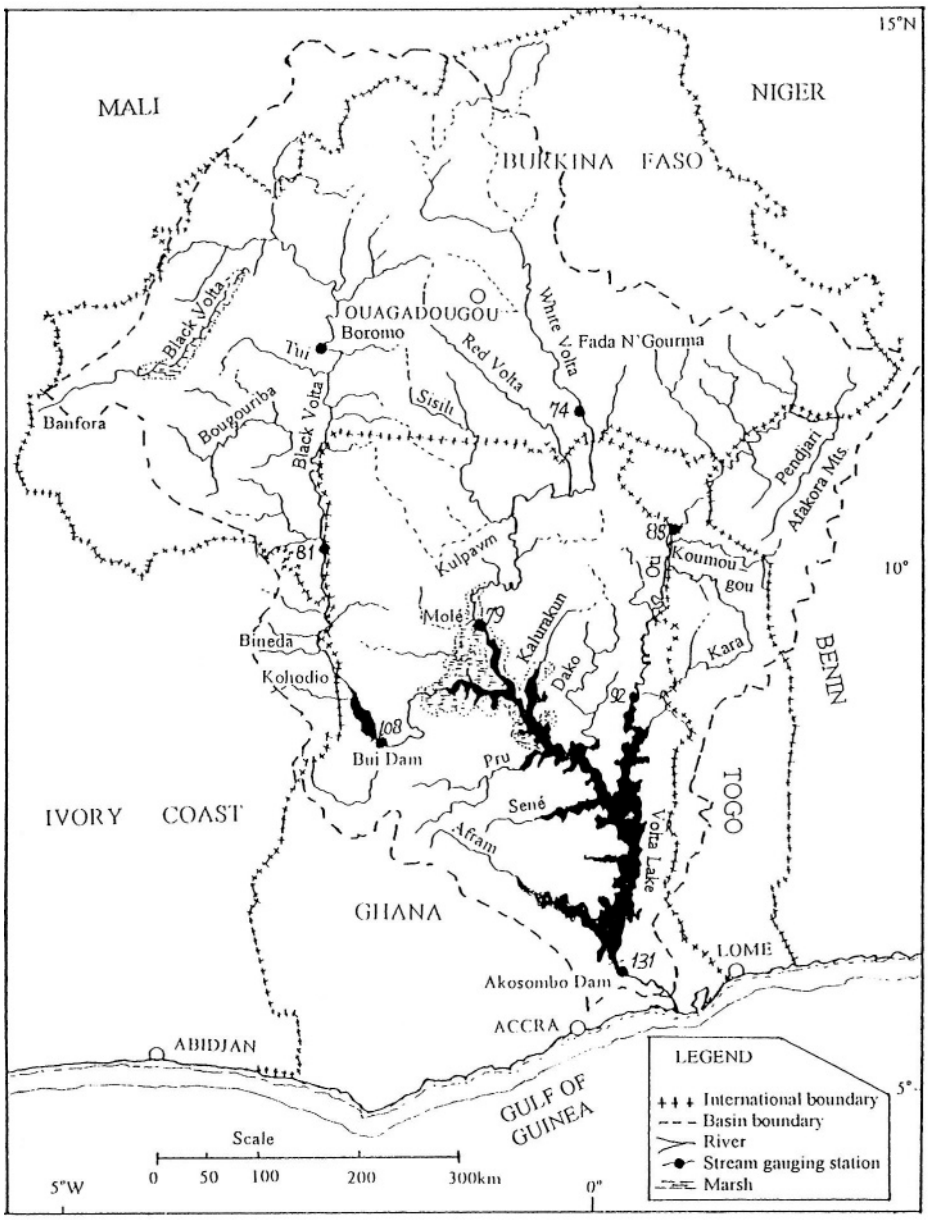

Figure 9.3- Map of the Volta Basin

The Black Volta, below its head water source in the Banfora Cliffs, flows northeastwards, where it receives on its left bank some Sahelian streams providing the main river with limited supply. The river traverses on the left bank side the Sourou, which is a north-south depression, thereby loosing a considerable proportion of the water received from the highland. This depression functions similar to the lacustrine depression in the basin of the Upper Niger in that it helps to route the flood wave of the river and also retain much of its sediment load (Rodier, 1964). Below the depression, the river flows, generally, in a southerly direction with a number of meanders in its course.

At the station of Boromo (see Figure 9.3), the flow regime of the river can be described by well-defined characteristics. The first characteristic is the extremely small value of the mean annual discharge. The catchment area at Boromo is about 58,000 km^2 receiving, on the average, 920 mm annual rainfall, yet the mean annual discharge is about 50 $m^3 s^{-1}$, i.e. the runoff coefficient is less than 3%. This can be attributed to the Sourou depression and the flat slope of the terrain. The flood peak discharge in a normal year varies between 140-150 $m^3 s^{-1}$ and the low-flow discharge can be less than 10 $m^3 s^{-1}$. Statistical analysis of the annual discharge series at Boromo predicts the 10-y flood at about 200 $m^3 s^{-1}$. The second characteristic is concerned with the regularity of the annual hydrograph, whereas the third characteristic is concerned with the small interannual variability that can be attributed to the regularizing effect of the overflowing water.

The Black Volta, while flowing down south, is joined by a series of small streams having a transient-tropical regime, of which the Bougoun is the most important one. Dopola is the next gauging station (No. 81) on the Black Volta within the frontiers of Bukina Faso. The catchment area at this point is 66,540 km^2, and the average annual precipitation is about 0.95 m. The mean annual discharge over the period 1952-86 is 116 $m^3 s^{-1}$. This figure corresponds to an average runoff coefficient of 5.8%, which is nearly twice as much as the average coefficient for the catchment area at Boromo. The range of values in which the mean annual discharge at Dopola varied is definitely wide. In those 35 years of record, the minimum discharge was 27.2 $m^3 s^{-1}$ and the maximum 576 $m^3 s^{-1}$, causing the interannual variability to be as much as 0.77. Statistical analysis of the said annual series estimates the 10-y and 100-y discharges at about 220 and 540 $m^3 s^{-1}$.

The Black Volta after reaching Bamboi, the last measuring station (No. 108), makes a sharp bend while flowing from west to east. A few kilometers above Bamboi, the Black Volta traverses the lake created by the Bui Dam. After some distance, the river used to join the White Volta. Since the construction of the Volta Dam, the Black and the White Voltas do not join each other any more, instead each river enters the lake through a separate channel.

The UNESCO Publication on discharge of selected rivers in Africa (1995) gives the annual series of the mean annual discharge at Bamboi station for 23-y,

1951-73. Table 6a, Part I/Appendix B, gives the mean annual discharge for that period as 267 $m^3 s^{-1}$, with a variation coefficient of around 0.44. The given figure of the mean discharge hardly reaches one-fourth the total yield of the Volta Basin. As such, one can fairly conclude that despite its length and surface area of its sub-basin, the yield of the Black Volta is rather limited.

The upper basins of the White Volta and its tributary the Red Volta carry limited supplies of water. Their river channels are nearly flat and covered with swamps. Additionally, their flow regime is typically tropical, hardly receiving any water in the period from January to June. This period is followed by a short high-flow season, from July to mid- October. At the end of the flood season the hydrograph assumes a long recession curve till the discharge reaches almost null. The first gauging station on the White Volta is at Yakala (station No. 74), a short distance before the river crosses the boundary between Burkina Faso and Ghana. The available period of record, 1957-73, gives a mean annual discharge of 32 $m^3 s^{-1}$, with a variation coefficient of about 0.41. As the catchment area at this measuring site is 33,000 km^2, receiving on the average an annual precipitation of 800 mm, the average overall run coefficient must be around 3.8%. Again, like the case at Boromo on the Black Volta, the magnitude of the coefficient is quite small.

Below its confluence the river flows in a southerly direction and is joined from the right bank by a number of streams of a tropical regime. The gauging station of Yarugu (No. 79) is located on the river at a short distance before entering the Volta Lake. The available period of record is from 1967 to 1973, i.e. 7 years only. The catchment area at Yarugu is 41,550 km^2 receiving an annual precipitation of no less than 900 mm. The mean and variation coefficient are 73 $m^3 s^{-1}$ and 0.3 respectively. The corresponding runoff coefficient being 6.2% is still small, yet 60% more than that at Yakala.

The Oti River is probably the most important tributary in the whole Volta River system. It originates in the Fada N'Gourma Plateau, southeast of Burkina Faso. It receives on the left bank the Pandjari River, which is often considered as the Oti itself. The Pandjari rises in the massif of Atakora in the northwestern corner of Benin. There are two discharge-measuring sites on the Oti. The upstream one is at Mango (station No. 85). Two sets of data are available for this station. The results obtained from the first set as given by Rodier (1964) are 131 $m^3 s^{-1}$ for the mean annual discharge, and 1,000 and 1,400 $m^3 s^{-1}$ as estimates for the annual and 10-y flood discharges. The results given in Table 6a, Part I/ Appendix B, give the mean annual discharge for the period 1954-73 as 135 $m^3 s^{-1}$, with a coefficient of variation of 0.42. The catchment area at Mango is 35,650 km^2 and the average annual precipitation is 1,000 mm. These figures bring the corresponding average annual runoff coefficient close to 12%, a value that is much higher compared to the values already obtained for the Black and White Voltas.

The second or downstream station (No. 92) is at Sabari before the river enters the Volta Lake. The available discharge data for the period 1960-73 gives a mean annual discharge of 357 $m^3 s^{-1}$, with a variation coefficient of about 0.38. The catchment area at Sabari is 59,500 km^2 receiving an average precipitation of 1,150 mm y^{-1} and has a runoff coefficient of 16.5%. The monthly distribution of the annual discharge at Sabari is rather similar to the distribution pattern at Mango and the other stations. The low-flow season extends from January to June, followed by a high-flow season covering the period from July to mid-October. The maximum flood discharge usually occurs in September. From the end of October the discharge rapidly diminishes till the next low-flow season begins again in January.

The water flowing out of the Volta Lake runs in just one channel known as the Volta River. Before the construction of the Akasombo Dam the river flow was extremely irregular, hardly any trickle of water in the dry season, with flood peaks varying enormously from year to year. The total annual discharge at Senchi (Halcrow) reached $94.5*10^9$ m^3 in 1963, whereas in 1958 it was only $11.3*10^9$ m^3. The filling of the reservoir (lake) took four years, 1964-68, after the completion of the dam construction. The Volta Reservoir has since then helped to stabilize the outflow reaching the most downstream and key station at Senchi (No. 131). Figure 9.4, partly prepared by Grove (1985) and completed by the author using the UNESCO data (1995), emphasizes the impact of the reservoir on flow regulation. The Volta at Akosombo has a catchment area of 292,000 km^2 receiving, on the average, annual precipitation of 1,200 mm and yielding a mean annual discharge of 1, 180 $m^3 s^{-1}$ (Rodier, 1964).

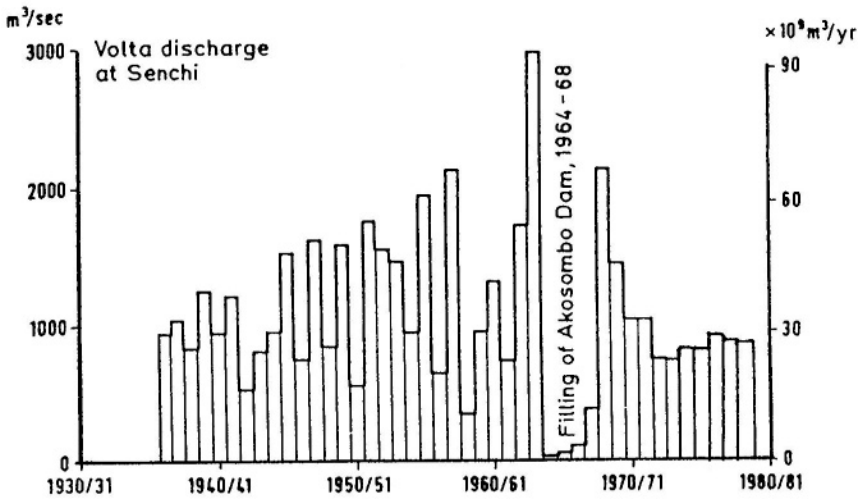

Figure 9.4-The annual discharge series of the Volta River at Senchi before and after the construction of the Akosombo Dam

The same source gives the mean flood discharge as 6,500 $m^3 s^{-1}$, the 1-in 100-y flood discharge as 15, 000 $m^3 s^{-1}$ and the minimum annual discharge as 28 $m^3 s^{-1}$. The mean annual discharge for the period 1937-79 (Table 6_a, Part I/Appendix B) is 1,125 $m^3 s^{-1}$, with coefficient of variation of 0.53. Actually the discharge in the last eight or nine years of record represents the controlled outflow from the reservoir rather than the natural supply to the river. From the data in the pre-dam era, it can be concluded that the yield of the Volta Basin is $37.2*10^9$ $m^3 y^{-1}$ and its specific yield 4.0 l $km^{-2} s^{-1}$. The basin overall runoff coefficient is around 10%.

The Lower Volta below the Akosombo Dam receives a number of small streams of the transient-equatorial type. These streams hardly add any water to the Volta itself, instead they feed the lagoons in the south of the basin. These lagoons fill or dry up according to their respective water balance. The Volta River bends its course abruptly to the east before emptying its discharge into the Gulf of Guinea after completing a journey of 1,200 km.

9.2.3 Water Quality- The interest in sediment discharge data in the Volta River system in Ghana has begun not long ago. Reports based on investigation of individual water resources projects form one source of information, whereas reports derived from planned networks comprise the other source (Akrasi and Ayabotele, 1984).

The maximum and minimum concentrations of the suspended sediment load, as obtained by FAO, are given in Table 2_f, Part II/Appendix B. A few more data, which were obtained at about the same time by Nippon Koei Consulting Engineers, are included in Table 2_h of the same Appendix. From these data, it appears that the water of the White Volta has the highest maximum and minimum concentrations. This has to be expected as most of the sediment load brought by the Black Volta from the head sources is deposited in the Sourou depression.

9.3- Sanaga River Basin

9.3.1 Brief description of the basin- The drainage basin of the Sanaga River is confined to Cameroon only and has a size of about 135,000 km^2. It is situated southeast of the Niger Basin and extends from northeast to southwest. The particular situation of this basin is quite important, as a large part of it is mountainous and often exposed to the masses of humid air blowing from the Gulf of Guinea. The southern regions of the Sanaga Basin have a transient-tropical climate and flow regime. Despite the small size of its basin, the Sanaga River judged by its specific yield is an abundant African water resource. The next sub-section will review and discuss some of the hydrologic characteristics of the basin at a number of locations.

The Sanaga is formed by the junction of the Lom and the Djérem Rivers. Both rivers rise in the Adamaoua Plateau, in the central part of the Cameroon, whose altitude ranges between 1,000 and 1,200 m a.m.s.l. The Djérem is more important compared to the Lom, yet it is the less known tributary of the two.

The Lom is joined on its right bank by the Panjar, an important tributary. The Sanaga is the name given to the Djérem after flowing out of the dam on Mbakaou Lake. Other than the Djérem, a number of streams, of which the Meng is an important feeder, supply the lake with water. The Sanaga before joining the Lom receives water from two tributaries. The tributary coming from the right, known as Mekie, is the richer one. The confluence of the Sanaga on the Lom is about 20 km below the confluence of the Panjar. The river reach for a distance of 180 km below the confluence is obstructed by some falls and rapids, as can be seen from the map in Figure 9.5. The river is further supplied with water discharging from a number of tributaries as the Ndo and the Ndieké.

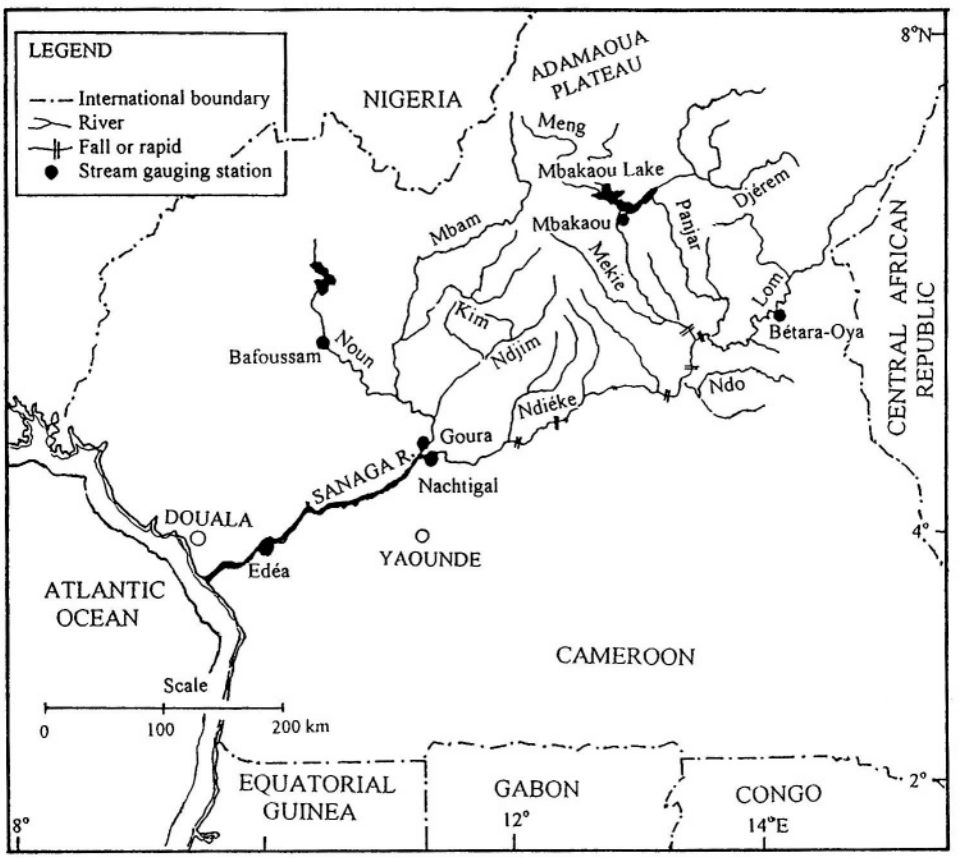

Figure 9.5- Map of the Sanaga River system

The Sanaga below Nachtigal is joined by its principal tributary, the Mbam River. The Mbam drains the mountainous region between Nigeria and Cameroon. Its main tributaries are the Kim and Ndjim rivers. The flow regime of the Mbam is about the same as that of the Lom and the Djérém. Before its confluence with the Sanaga, the Mbam receives on its right bank the Noun River.

Below the confluence of the Mbam, the course of the Sanaga traverses a zone of rapids and falls. These obstructions, of which the Herbert and the Edéa Falls are the most spectacular cause a drop of 350 m of the water level in a distance of 140 km. In this reach, a number of small streams of equatorial regime join the Sanaga. Their supplies, however, are so limited that they do not produce any sensible change in the flow regime of the Sanaga. Below Edéa down to the ocean, the river slope is very mild and hardly receives any additional supply

9.3.2 Hydrology of the Sanaga Basin- The Sanaga Basin despite its small surface area, about 135,000km^2, varies in elevation from about 1,500 m a.m.s.l. near the headwater sources to sea level at the river mouth. There are reaches of considerable slope, basically obstructed by rapids and waterfalls, and other reaches with extremely mild slope. The annual rainfall, though generally high, varies considerably from place to place. The long-term mean annual figures are 1,550 mm at Batouri (station No. 135), 4,000 mm at Douala (station No. 138), 1,650 mm at Yaounde (station No. 140) and 2,930 mm at Kribi (station No. 147). More figures for monthly and annual rainfall are available in Tables 9 and 10_a of Appendix A. The potential evapotranspiration on the other hand is limited, 1,250 mm and less, rendering the entire area covered by the Sanaga Basin into a region of excess water. Another important feature of the basin is that certain parts of it are relatively steep, causing the runoff coefficient to be generally higher compared to of the basins so far discussed.

The discharge data, which are available in the current publications, cover five measuring sites. Four of them are provided by UNESCO Publications (1971 and 1995) and the fifth is given by Rodier (1964). The last site, Bétaré-Oya, is located on the Lom River and has a catchment area of 10,680 km^2. It receives on the average 1,480 mm annual rainfall and yields a mean annual discharge of 182 $m^3 s^{-1}$ or 363 mm runoff, corresponding to 24.5% runoff coefficient. The low-flow and flood discharges are 42 $m^3 s^{-1}$ and 560 $m^3 s^{-1}$ respectively.

The measuring site (station No. 130) on the Djérem just below the Mbakaou Lake has a catchment area of 20,390 km^2, at an altitude of 826 m, receiving an the average annual precipitation of about 1,500 mm. The annual discharge in the available record, 1960-79, varies from a minimum of 258 $m^3 s^{-1}$ to a maximum of 560 $m^3 s^{-1}$. The mean annual discharge is 391 $m^3 s^{-1}$ with interannual

variation of 16.6%. The corresponding runoff depth and runoff coefficient are 605 mm and 40%, respectively.

Records are available at two measuring sites, one on the Mbam (station No. 152) and the other (station 139) on its tributary the Noun. The Goura on the Mbam has a catcment area of 42,300 km^2, at 396 m altitude, receiving on the average annual rainfall of 1,750 mm and yielding a mean annual discharge of 707 $m^3 s^{-1}$ with interannual variability of 15.1%. The given mean annual discharge corresponds to the period 1952-79. The mean discharge over an earlier period happened to be 780 $m^3 s^{-1}$, i.e. 10% larger (Rodier, 1964). The same source gives the low-flow and high-flow discharges for that earlier period at 96 and 2,750 $m^3 s^{-1}$ respectively. The average of mean discharge figures corresponds to annual runoff depth of about 550 mm and an average runoff coefficient of 32%.

The station at Bafoussam (No. 139) is located on the Noun River in the highland at elevation of 987 m a.m.s.l. The catchment area is 4,700 km^2, receiving, on the average, annual rainfall of 1,700 mm and yielding a mean annual discharge of 104 $m^3 s^{-1}$ with 14.9% as coefficient of variation. The corresponding specific yield is 22 l $km^{-2} s^{-1}$ and runoff coefficient is 0.41.

The last two measuring stations are located on the Sanaga River itself. The station at Nachtigal (No. 157) has a catchment area of 76,000 km2 receiving an average rainfall of 1,570 mm y^{-1}. The corresponding mean annual discharge according to Rodier (1964) is 1,190 $m^3 s^{-1}$. Table 6_a, Part I/Appendix B, using more recent observations, gives 1,072 $m^3 s^{-1}$, with interannual variability of 15.6%. This means that the two sets of data produce two mean values with 10% difference. Actually this difference should be reduced to 8.5% to account for the difference in catchment area between the two results. The same situation is repeated in the second station (No. 159), which is located at Edéa. The old result given by Rodier (1964) is 2,158 $m^3 s^{-1}$ as a mean annual discharge produced by 1, 630 mm annual precipitation on a catchment area of 135,000 km^2. The data given by UNESCO (1995) results in a mean annual discharge of 1986 $m^3 s^{-1}$, with 14.6% interannual variability. Taking into account 2.5% difference in catchment area, the net difference between the two mean annual discharges becomes in the order of 5%. As such, one can conclude that the Sanaga Basin has an annual yield of 62.5 to 68.1*10^9 m^3, corresponding to annual runoff of 475-504 mm, specific yield of 15 to 16 l $km^{-2} s^{-1}$ and annual runoff coefficient of 30%. These figures show clearly that the specific yield of the Sanaga Basin is nearly 60% larger than the corresponding yield of the Zaïre River.

It is worthwhile to mention here that the Mbam River supplies more than one-third of the discharge of the Sanaga at Edéa. The low-flow median discharge at the same site is 390 $m^3 s^{-1}$, whereas the annual and the 10-y maximum flood discharges are 6,700 and 7,300 $m^3 s^{-1}$, respectively.

The Sanaga River and its tributaries get their highest discharge in October. The discharge starts to diminish at the end of October till it reaches the lowest

value in March. The flow begins to improve slightly in April followed by a steeper rise in May till the peak is reached once more the next October. The mean October discharge for the period 1944-79 is 5,430 $m^3 s^{-1}$ and the mean discharge in March for the same period was is 529 $m^3 s^{-1}$. The ratio of the mean maximum to the mean minimum, which expresses the seasonality $(In)_s$, is equal to 10.1 (Table 6.3, sub-section 6.3.2).

9.4- Ogooué River Basin

9.4.1 Brief description of the basin- The Ogooué Basin is basically confined between the Sanaga Basin in the north and the Zaïre basin in the south. The basin is practically confined to Gabon. However, since certain areas of the basin, though too small, lie in the Cameroon in the north and Congo (Brazzaville) in the south, they too are regarded as riparian countries.

Pierre Savorgnan de Brazza navigated the entire course of the Ogooué in the period 1875-83), locating its source in 1877. The Ogooué (sometimes spelled Ogwe) River is a mighty equatorial river of West-central Africa. It flows in Gabon for almost its entire course, and its basin drains an area estimated at about 223,000 km^2. The river rises in the Congo on the eastern slopes of the Massif of Chaillu and flows northwest through Gabon past Franceville and Lastourville; it then turns west and southwest past Booué, Ndjolé and Lambaréné, collecting water from numerous lakes above Lambaréné. The Ogooué forms a delta and empties its water into the Atlantic Ocean south of Port Gentil, after a course of 1,200 km.

The navigable parts of the river are heavily used for shipping goods to the ocean coast. Although interrupted by rapids and waterfalls along its upper course, the Ogooué is navigable as far as Lambaréné (185 km upstream the mouth) throughout the year, and to Ndjolé (250 km upstream) from October to May. Shallow-draft boots can ply the river from Booué to Latoursville between mid-November and mid-June; and its two major tributaries, the N'Gounié and the Ivindo, have seasonal navigable stretches. Other tributaries of the Ogooué River are the Mpassa, the Sébé, the Djadié, the Okano, the Abanga, the Lolo, and the Offoué. Between the N'Gounié and the Ogooué Rivers, the Massif of Chaillu, the country's main watershed, rises to more than 1,000 m. The map, Figure 9.6 shows the location of the principal tributaries within the Ogooué River system.

The climate of the basin is equatorial with an average rainfall of no less than 2.0 m with 2 to 3 dry months each year. The annual potential evapotranspiration varies between 1,000 and 1,250 mm bringing the excess water to between 500 and 1,000 $mm\ y^{-1}$.

9.4.2 Hydrology of the Ogooué Basin- The available literature gives the monthly and annual discharge of the Ogooué and its tributaries at six observation sites. These are the stations at Lambaréné (No. 191), Booué (No. 188), Lastourville (No. 192) and Franceville (No. 194) on the Ogooué, the station at Fougamaou (No. 193) on the N'Gounié and at Loa-Loa (No. 177) on the Ivindo. All stations, except the one at Lambaréné, hardly have 8 years of uninterrupted record, all beginning from 1965 or 1966. The station at Lambaréné has complete records since January 1930, with the exception of four missing years, 1950, 1951, 1952 and 1953.

The catchment area of the Ivindo River at Loa-Loa (station No. 177) is about **48,500 km^2**. It receives an average rainfall of about **1,900 mm y^{-1}** and yields a mean annual discharge of **789 m^3 s^{-1}**. The small sample represented by the short record from September 1965 up to March 1974 has a relatively wide range of variation between a minimum annual discharge of **585 m^3 s^{-1}** and a maximum of

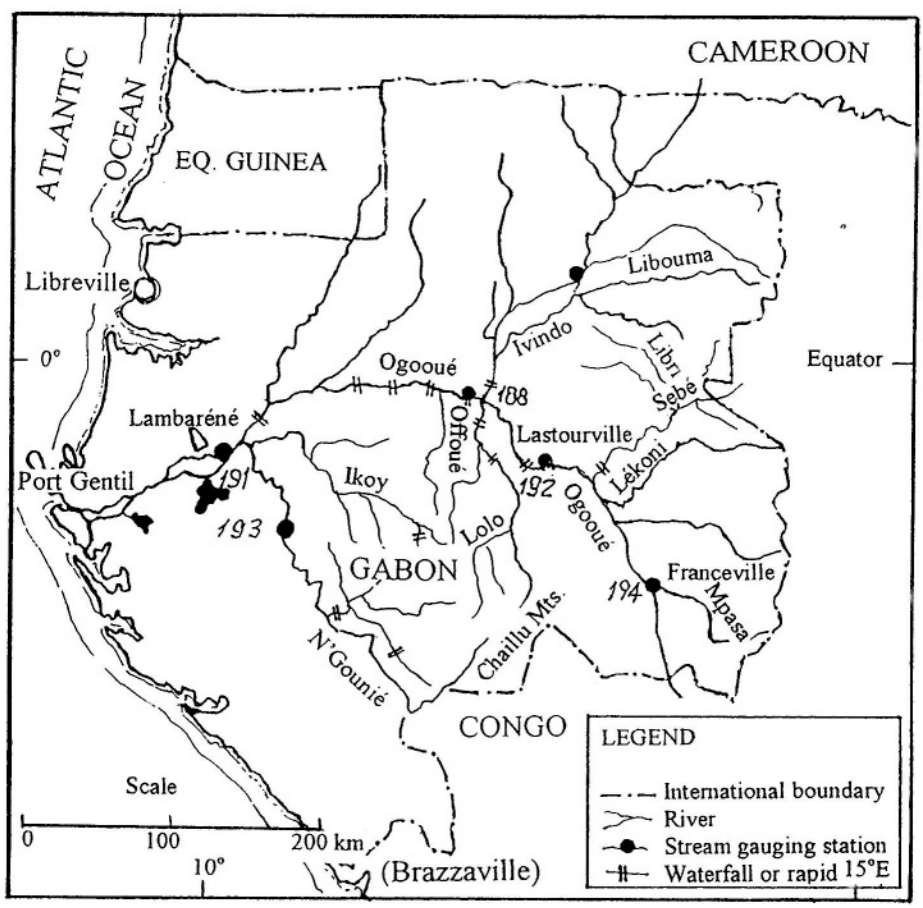

Figure 9.6- Map of the Ogooué River system

1,051 $m^3 s^{-1}$, bringing the interannual variability of the annual discharge to 0.233. The mean, which is close to the median of the annual discharge, corresponds to annual runoff depth of 513 mm and runoff coefficient of 27%.

The catchment area of the second tributary, i.e. N'Gounié, at station No. 193 is 22,000 km^2, receiving annual rainfall of about 2,000 mm. The mean annual discharge is 716 $m^3 s^{-1}$ with annual coefficient of variation of 0.157. These figures correspond to annual runoff of 1,027 mm and runoff coefficient of 51%. Both figures are nearly twice as much as those for the sub-basin of the Ivindo .

The stream gauging stations No. 194 and 192 are located on the upper reach of the Ogooué. The corresponding catchment areas are 8,700 and 47,700 km^2 respectively both receiving, on the average, about 2,000 mm annual rainfall. The available discharge records (UNESCO, 1995) give mean annual discharges of 260 $m^3 s^{-1}$ and 1,276 $m^3 s^{-1}$, respectively. These figures correspond to annual runoff of say 930 and 884 mm and annual runoff coefficient of 46.5 and 44.2% for the two stations in their respective order.

The station No. 188, situated at Booué, is located below the confluence of the Ivindo and its tributary system. The catchment area is 129,600 km^2 receiving, on the average, 1,950 mm annual rainfall. It yields a mean annual discharge of 2,707 $m^3 s^{-1}$, with coefficient of variation of 15.2%. The corresponding annual runoff depth and runoff coefficient are 659 mm and 34% respectively. These figures, in comparison with those for the stations in the upstream, are relatively low. This can be attributed to the characteristics of the flow supplied by the Ivindo River and its tributaries, as shown by station No. 177. The situation is somewhat improved at station No. 191. At this site, the catchment area reaches 205,000 km^2 receiving, on the average, 1,900 mm annual rainfall and yielding a mean annual discharge of 4,659 $m^3 s^{-1}$, with annual variability of 15.1%. The corresponding figures for the annual runoff depth and coefficient are 722 mm and 38% respectively. Actually, the mean and maximum annual discharges for the period 1930-49 were 4,672 and 5,912 $m^3 s^{-1}$ respectively, and 4649.4 and 5970 $m^3 s^{-1}$ for the period 1954-75. These figures show that the mean and maximum annual discharges are about the same for the pre-break and post-break periods. Oppositely, the minimum annual discharge for the post-break period, being 3,093 $m^3 s^{-1}$, is considerably less than the corresponding discharge, 3,569 $m^3 s^{-1}$, for the pre-break period.

The above-mentioned figures lead to the conclusion that the annual yield of the Ogooué Basin is about 148*109 m^3 and the corresponding mean specific yield around 23.0 l $km^{-2} s^{-1}$. The last figure is at least 30% larger than the specific yield of the Sanaga Basin and 250% larger than that of the Congo Basin.

9.5- Limpopo Basin

9.5.1 Brief description of the basin- The Limpopo Basin covers a surface area of about 412,000 km^2 shared between Mozambique (19%), South Africa (47%), Zimbabwe (16%) and Botswana (18%). The mouth of the Limpopo River on the Indian Ocean was explored in 1498 by Vasco da Gama, who named it Espiritu Santo River (Holy Ghost River). St. Vincent Erskine explored the lower course of the river in 1868-69, and J. Elton traveled down its middle course in 1870. The river rises at an altitude of about 2,300 m a.m.s.l in northeast South Africa (Witwatersrand = Whitewater edge) near the Indian Ocean where it is known as the Crocodile River. From there it drops into the alluvial plain in Mozambique. It flows in a semicircular course 1,770 km long before emptying its water into the Indian Ocean. For much of its course the Limpopo forms the boundary between the Transvaal on the south, Botswana on the west, and Zimbabwe on the north.

From its source, the river flows northward to the Magaliesberg Mountains, traversing the Hartbeespoort Gap, then across the fertile Bushveld area to open granite country, where the Marcio River joins it on the left bank. From there, the river becomes known as the Limpopo. Flowing northeastward, the river forms the boundary between the Transvaal and Botswana. In this reach of about 400 km, the river receives some tributaries, most of which flow intermittently. The Limpopo upon receiving the Sashi River, one of its two important tributaries, flows some 250 km to Mozambique, where it reaches the fall line. In this zone the Limpopo drops 250 m, most of this drop is concentrated in a line of rapids

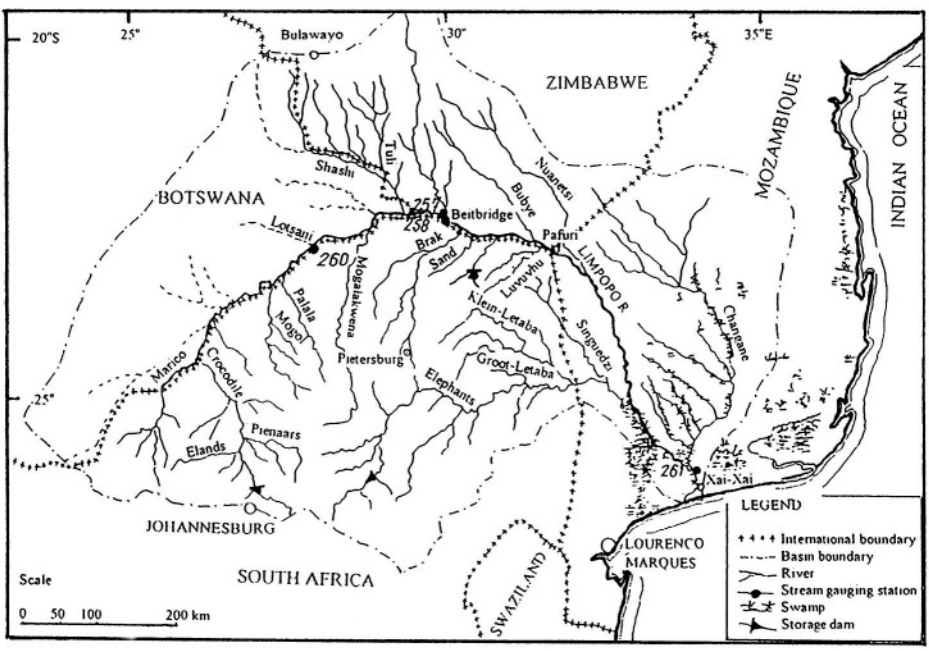

Figure 9.7- Map of the Limpopo Basin

40 km long. The second important tributary is the Olifants (Elephants) River. The Limpopo River is navigable below the confluence of the Olifants, 200 km from the coast. Figure 9.7 is a map showing the Limpopo Basin.

The annual rainfall in the basin area increases generally from north to south and from west to east. This can be evidenced from the long-term average figures for Messina or Beitbridge, 340 mm, Pafuri 380 mm, Pietersburg 480 mm, and Nelspruit, 805 mm. More examples can be found in Tables 9 and 10, of Appendix A. The annual evaporation varies between 2,250 and 3,000 mm depending on the location and the measuring device or estimation method used.

9.5.2 Hydrology of the Limpopo Basin- The Limpopo is known to be one of Africa's lesser rivers. It has been recently found that the Limpopo in Mozambique virtually runs dry in the cold season even in years with normal rainfall, whereas this was not the case before 1975. The Limpopo Basin, however, drains a well-watered country eastward to the Indian Ocean.

The Crocodile headwaters at Hartbeespoort Dam have a mean annual discharge of $0.152*10^9$ m^3 y^{-1}, with maximum discharge in February and minimum in August. The average annual flow at the border near Combomune is about $3.25*10^9$ m^3 y^{-1}, while the normal average inflow to Missinger Dam is $1.23*10^9$ m^3 y^{-1}. According to the report describing the experiences of SADC and EU (Dutch Ministry of Foreign Affairs, 1998) there are 13 storage dams in the Limpopo Basin with a storage capacity exceeding $100*10^6$ m^3. Of this number there is one dam in Mozambique, eight in South Africa, three in Zimbabwe and one in Botswana.

The data published by UNESCO (1995) give the monthly and annual discharges of the Limpopo and its tributaries at four measuring sites: Beit Bridge in Zimbabwe (station No. 257), Beitbrug and Oxenham Ranch in South Africa (stations No. 258 and 260, respectively), and Chokwe in Mozambique (station No. 261)

The most upstream measuring station is No. 260, situated on the river inside South Africa. The available record, which extends from October 1964 to April 1980, is incomplete, as it contains 20 missing monthly values. This brings the net number of years with complete record down to nine. Those nine years show a minimum of say 2 m^3 s^{-1} in 1970 to a maximum of about 57 m^3 s^{-1} in 1976. One should not forget that the river runs dry, at least in some years, for three months or more. Based on this short-term data, the mean annual discharge is 26.3 m^3 s^{-1} with 83.8% interannual variability. This mean discharge value is too small for a catchment area of 98,160 km^2, as it corresponds to just 8.5 mm annual runoff depth and 3% or so runoff coefficient.

The discharge data for station No. 257, Zimbabwe, cover the period from October 1959 to September 1980, with a total of 7 missing months. Table 6, in Part I/Appendix B gives the mean annual discharge for the said period as 91 m^3 s^{-1}. The annual discharge varied from as little as 8.37 m^3 s^{-1} in 1965 to as much

as 463 $m^3 s^{-1}$ in 1975, i.e. fifty five fold in about 10 years. No wonder then that the mean annual discharge is associated with a variation coefficient of 121%. It should be well remembered also that the period of zero discharge each year occupies at least three months, from July to October. The zero flow period in a meager year, such as 1965, lasted from April to October, i.e. seven uninterrupted months. As the catchment area at station No. 257 is 196, 000 km^2 receiving, on the average, 450 mm annual rainfall, the annual runoff must be then 15 mm and the coefficient of runoff about 3%.

Station No. 258, South Africa, lies on the other side of the river opposite to station No. 257. The available discharge data at station No. 258 covers the period from October 1964 to December 1980 with 16 missing monthly values. The catchment area at Beitbrug, 205,000 km^2, is slightly larger (4.6%) than the area corresponding to station 257 in Zimbabwe. One should expect that the catchment yield at these two stations must be close to each other. Remarkable enough that this was not the case, as the data of station 258 give an annual mean discharge of 45.1 $m^3 s^{-1}$, which is about half that at station 257. An investigation of the two sets of data has shown that there are six common years with complete observations. Of those six years, five, 1968, 1970, 1971, 1973, 1974, have almost similar discharges with a mean value of 38.37 $m^3 s^{-1}$ for station 257 and 40.63 $m^3 s^{-1}$ for station 258. In the sixth year, 1975, The discharges in the sixth year, 1975, for stations 257 and 258 are too different, 463 $m^3 s^{-1}$ for station 257 and 115 $m^3 s^{-1}$ for station 258. The 1975 data included the figures of 297 $m^3 s^{-1}$ and 3,920 $m^3 s^{-1}$ as average discharge for March at stations 258 and 257 respectively. The difference between these two values for just one month reacts on the mean annual discharge by 300 $m^3 s^{-1}$ or 86% of the difference between the two stations. As a matter of fact, the highest discharge ever reached at station 258 in that particular year was 744 $m^3 s^{-1}$ and took place on 21.02.

The above figures show clearly that the quantity and quality of the hydrological data of the Limpopo Basin are inadequate to draw any firm conclusion. There is another measuring station (No. 250) on the Limpopo in Zimbabwe. The station, called Ncema Dam U/S G/W, has a published record extending from October 1964 to May 1984. Would the available observations be trusted one can find the mean annual discharge as 1.1 $m^3 s^{-1}$, with interannual variation of 105%. As the catchment area at the location of the measuring site is 640 km^2, the annual runoff must be about 54 mm and the runoff coefficient as around 10%.

The last measuring site in the Limpopo Basin, which is station No.261, is located at Chokwe, Mozambique. The published data cover 38 months only, four years of which ten months are missing. The mean annual discharge computed from these meager data is 370 $m^3 s^{-1}$. The catchment area corresponding to this station is 342,000 km^2 receiving, on the average, 550 mm annual rainfall. From these figures, the specific yield of the Limpopo Basin can be found as 1.08 1 l $km^{-2} s^{-1}$, the annual runoff as 34 mm and the runoff

coefficient as 6%. The annual total basin yield corresponding to the given specific yield is thus close to $14*10^9$ m^3. This figure should be regarded as approximate and be used with care. The report of the Dutch Ministry of Foreign Affairs (1998) gives the annual yield of the Limpopo Basin as $7.3*10^9$ m^3.

It can be generally stated that the maximum discharge of the Limpopo River occurs in March and the minimum discharge in August. The inaccuracy of, at least, some of the published observations cause many breaks in this general rule. It is hoped that, with future cooperation between the Southern African Development Community (SADC), especially in relation to shared water resources, more care will be focused on data collection and publication.

The next tabulation gives a summary list of the specific yield figures of the five intermediate river basins already discussed above.

Basin	location	Area, km^2	Specific yield $l\ km^{-2}\ s^{-1}$	Annual yield $10^9\ m^3$
Sénégal	Dagana	268,000	2.6	22
Volta	Akosombo	292,000	4.0	37
Sanaga	Edéa	131,500	16	67
Ogooué	Lambaréné	205,000	23	148
Limpopo	Mouth	412,000	(1)	(7-14)

9.6- The Oued (Wadi) Zeroud Basin

9.6.1 Brief description of the basin- The sub-basin of Oued Zeroud (sometimes written Zurud)at Sidi Saad is a part of a larger basin known as the Sebkha Kelbia catchment. This catchment (14,400 km^2) includes, next to Zeroud, the basins of Merguellil, Nebhana, and the southern sector. Most of the sub-basin of Oued Zeroud penetrates into the Kairouan plain in the northern central part of Tunisia. The Zeroud Basin at Sidi Saad covers a surface of 8,650 km^2 totally inside Tunisia. It is often represented by a square 93 km side length, with diagonals extending north-south and east-west. The highest point in the basin is at elevation 1,544 m, the lowest at 230 m, and the median at 650 m, all a.m.s.l.

The yield of Oued (Wadi) Zeroud counts for just 4% of the total yield of surface water resources in Tunisia. This percentage, however small, constitutes 55% of the total surface water resources of the central part of Tunisia. As such, it is rightfully considered to be the most important resource of water for that part of Tunisia.

The Oued Zeroud has two branches. These are Oued Hathob, the northern branch, and Oued Hadjel, the southern branch. The basin formations of the northern branch rest on the southern slopes of the Tunisian Dorsal and form a continuous, generally high relief. The relief of the basin of the southern branch,

on the contrary, comprises isolated and separate slopes, which are more or less penetrated by alluvial bands. The northern branch of the oued is 120 km long, whereas the southern one is no less than 200 km. Each of these two branches has its own feeders on both the right and left sides.

Table 9.4 lists the major feeders of each branch together with their respective catchment areas. The map in Figure 9.8 shows the drainage network of the basin of Oued Zeroud up to the measuring station of Sidi Saad. Most of the water

Table 9.4- The principal affluents of Oued Zeroud, Tunisia (based on Bouzaiane and Lafforgue, 1986)

River bank	Sub-basin of the northern branch	Basin area,
	Oued Hathob	km^2
Right	Oued Sguifa	176
	Babouch	330
	Sbiba	487
	Lamedj	306
	Zerga	
Left	Oued Messenga	176
Northern branch		3,004
	Sub-basin of the southern branch	
	Oued Hatab	
Right	Oued Erriah	180
	Cherchara	295
	Battoum	160
	Derb	295
	Andlou	
	Fekka	
Left	Oued Guergour	
	Baidah	
	Brika	
	Oude Fekka	
Right	Oued Hchim	360
	Hallouf	790
Left		
	Oued Negada	
Right		
Left	Oued Sbeitla	916,0
	Djilma	140,0
	Oude Hadjel	
Right		
Left		
Southern branch		5,551
Intermediate sub-basin		95,0
Oued Zeroud at Sidi Saad		8,650

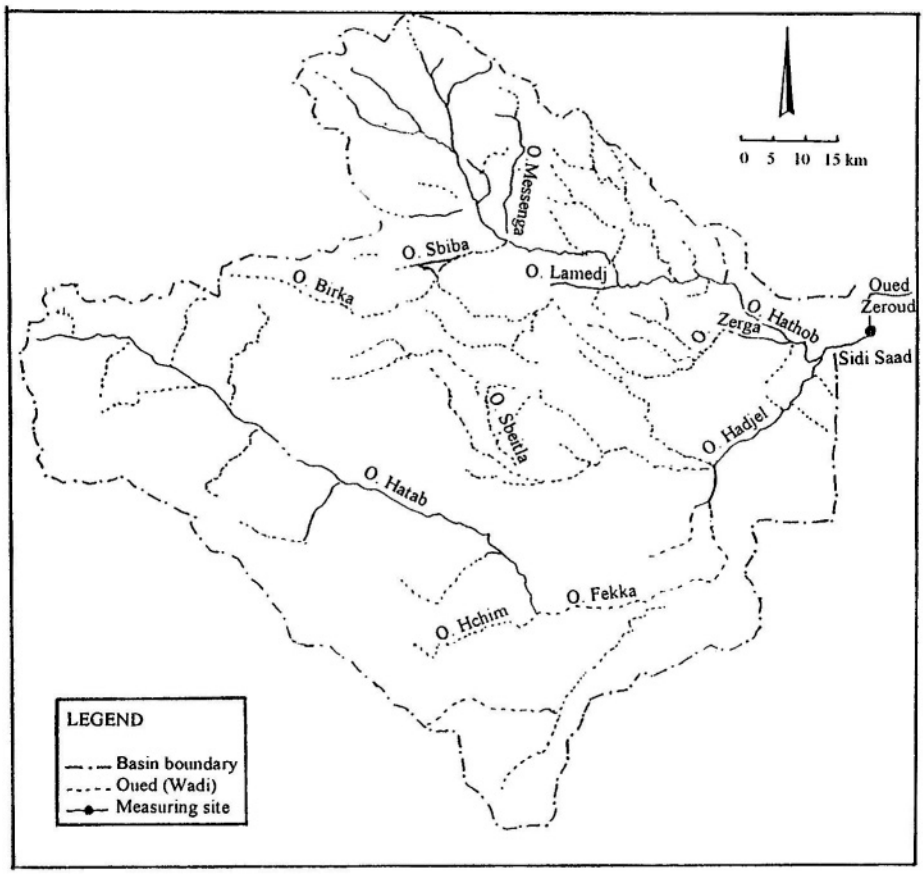

Figure 9.8- Map of the drainage basin of Oued Zeroud, Tunisia

courses in this map, contrary to the previously discussed river basins, are indicated by dotted lines, which is conventionally used for intermittent streams. The average annual rainfall in the Oued Zaroud is around 300 mm and the annual potential evaporatranspiration is between 1,500 and 1,800 mm. The calcmagnesic soil and the associated erodible soils constitute the predominant soil types. They occupy 31% and 28% of the surface of the basin respectively.

9.6.2 Hydrology of the Oued Zeroud Basin- The hydrometric observations in the Oued Zeroud dates back to 1945. The location of the measuring site has changed a number of times. The observations comprise stage and discharge measurements and calculations, with emphasis on low-flow as well as flood.

The report produced by Bouzaiane and Lafforgue (1986) deals with the measurements taken between 1949 and 1974. The locations of the measuring site, frequency of measurements, measuring techniques and methods of calculation are well reviewed in the said report. Unfortunately, the UNESCO

Publications (1995, 1996) present the monthly and annual discharges only for the three-year period 1976-78.

The report of Bouzaiane and Lafforgue (1986) lists the mean monthly and annual base flow for the period 1949-78 two times, once including the excessively wet year 1969/1970 and another time excluding it. The mean monthly values in the second case vary from slightly less than $1*10^6$ m^3 in August to a maximum of about $1.8*10^6$ m^3 in December, with an annual total of $17.5*10^6$ m^3. The coefficient of variation of the annual values is close to 0.4. The mean annual total runoff (base + surface) of the basin, as will be discussed in the subsequent paragraphs, is in the order of $95*10^6$ m^3. These figures lead to the conclusion that the base flow constitutes about 18.5% of the total basin yield.

The heterogeneity of the soil covering the basin surface makes the study of the process of surface runoff rather difficult and inconclusive. The severe floods, however, generally occur in the autumn and spring. The cyclones blowing in these seasons can cause the rainfall intensity to be quite high. A survey of the number of floods that occurred annually in the period 1949/50-1977/78 varied from a minimum of 6 to a maximum of 19, with an average of 13 per year. The maximum discharge in those 346 floods varied in an extremely wide range from a minimum of 98 m^3 s^{-1} (1959/60) to a maximum of 17,050 m^3 s^{-1} (1969/1970). Statistical analysis of the sample of maximum flood discharges over the 27-y period, 1949/50-1977/78, has yielded the following results: mean = 1518 m^3 s^{-1}, median = 610 m^3 s^{-1}, standard deviation = 3,421 m^3 s^{-1}, and coefficient of variation = 2.25. These results show that the peak flood discharges in the given sample are heavily skewed with a wide range of variation. The sample data with their statistical descriptors can be worked out further using the general frequency formula developed by Chow (1951):

$$X_T = (X)_m + K_T s \tag{9.1}$$

where $(X)_T$ = flood peak discharge corresponding to T years return period, $(X)_m$ = mean flood peak discharge, K_T = frequency factor corresponding to the same return period and s = standard deviation. The lognormal distribution predicts the 1 in 100-y flood peak as 17,118 m^3 s^{-1} (K = 4.56), which is close to the 17, 050 m^3 s^{-1} already observed in the 27-y record. This state of affairs has led Rodier (1989) to suggest 5.63 as a value for K for an extreme flood peak discharge without identifying the return period in years.

The wadi flow is basically characterized by a number of floods occurring each year. The number, as mentioned above, varies from one year to another and the volume of water varies from one flood event to another. The discharge carried by the wadi between two consecutive events is extremely limited and mostly sustained by the base flow. A typical example of the discharge hydrograph of Oued Zeroud just before, during and just after the flood event of

6 October 1957 is illustrated by Figure 9.9. Additionally, the flood studies over the 27-y period, 1949-78, have shown that the contribution of the largest flood each year counts, on the average, to 44% of the annual runoff volume.

The term mean annual discharge of a wadi with too high and too low discharges does not have the same weight as a perennially flowing river. It does make better sense to consider the annual total volume of flow (base + direct). The unpublished flow data of Oued Zeroud at Sidi Saad for the period 1949/50-1979/80 gives a mean annual volume of $93.8*10^6$ m^3 with a standard deviation of $56.6*10^6$ m^3, once the most exceptional year 1969/70 is excluded. Under this condition the annual volume varies in the range from $26.4*10^6$ m^3 up to $229.8*10^6$ m^3. Taking that special year into consideration the range will change from $26.4*10^6$ m^3 up to 2, $700*10^6$ m^3, with a mean value of $190.3*10^6$ m^3 and standard deviation of $504*10^6$ m^3.

The report on the Oued Zeroud by Bouzaiane and Lafforgue (1986) contains a considerable amount of statistical analysis of base, direct and total monthly and annual volumes of flow. Figure 9.10 shows graphical plots of monthly volumes of total flow corresponding to 10 and 50-y return periods

9.6.3 Water quality- A large number of water samples are collected for the purpose of measuring the electrical conductivity, and a fewer number of samples are collected for determining the major ion constituents such as Ca^{++}, Mg^{++}, Na^{+}, SO_4^{--}, Cl^{-} and CO_3H^{-}. The results over the period 1949/50-1979/80 have shown that the salinity varies between 0.43 g l^{-1} and 19.3 g l^{-1}, with 87.7% of the total samples (5,353 out of 6,103) have salinity between 1.5 and 5.5 g l^{-1}.

Further elaboration of the results of analysis has shown that the overall average salinity of the low-flow is 4.6 g l-l. Three-quarters of the salt carried by Oued Zeroud is supplied by its northern branch, 3.58 g l-1, and one-quarter by the southern branch, 8.19 g l^{-1}. These figures correspond with $14.5*10^6$ m^3 mean annual volume of low-flow (27-y) carrying a salt load of $66.8*10^3$ t y^{-1}, with a mean salinity of 4.61g l^{-1}. The removal of the exceptional year 1969/70 from the calculations changes these figures a little to become $13.2*10^6$, $60.5*10^3$ and 4.58 respectively.

The salinity of the floodwater has shown to vary with the volume of flood. The salinity of floodwater events varied between a minimum 1.33 g l^{-1} and a maximum of 6.8 g l^{-1}. The overall relationship between the salt load and the volume of flood can be written as:

$$A_s = 3.58(V_f)^{0.89} \qquad (9.2)$$

The average salinity as obtained from the annual volume of floodwater and the corresponding annual salt load falls in a narrower range compared to the salinity obtained from individual flood events. It varies from a minimum of say (1) to a maximum of 2.54 g l^{-1}. Table 4_i, Part II/ Appendix B gives the annual salinity

figures over the period 1949/50-1978/79. Last but not least, the annual salinity figure corresponding to the annual total flow has also been computed for the same period as the floodwater, and was found to vary between say (1) and 3.8 g l^{-1}, with a mean value of 2.44 g l^{-1}. The expression relating the total annual flow volume, V in 10^6 m^3, and the annual salt load, A_s in 10^3 t, can be written as:

$$A_s = 6.89V^{0.28} \tag{9.3}$$

The chemical analysis of the water samples has shown some differences in composition between the floodwater and the low-flow water. Regardless of these differences, the percentages of cations and anions were as follows:

Cations:	Ca^{++} = 30.8%	$Na^{+} + K^{+}$ = 50%	Mg^{++} = 19.5%
Anions:	SO_4^{--} = 46.2%	Cl^{-} = 45.1%	CO_3H^{-} = 8.7%

In conclusion, it can be firmly stated that the waters of Oued Zeroud are highly charged with Sodium, and the Calcium sulfates are present in larger amounts in the floodwater compared to those in the low-flow water.

The discharge carried by Oued Zeroud in its low-flow season is practically free of any suspended sediment. This is not the case with floodwater. The analysis of results obtained from the samples collected during 27 successive years has shown that the most frequent range of sediments is from 20 to 50 g l^{-1}, which is the case with light and moderate floods. Severe floods have much higher sediment concentration that can fall in the range 200-347 g l^{-1}. The concentration-time curve during a heavy flood lags behind the discharge-time curve. The method of least squares has been worked out to develop a relationship between the available annual flood volume and the corresponding sediment load data. The resulting expression can be written as:

$$T_s = 37.41(Vf)^{1.1} \tag{9.4}$$

where Ts = annual sediment load brought by the floods in 10^3 t. According to Eq. (9.4) an annual flood volume of $80.2*10^6$ m3 transports an annual load of about $4,651*10^3$ t, with an average concentration of 58 g l^{-1}.

A series of devastating floods swept over the middle and south of Tunisia in the autumn of 1969. Remarkable enough, the channel of Oued (Wadi) Zeroud was able to carry excessive flood discharges. From the end of August up to the end of October 1969, the basin received an average rain depth of 678 mm. The total runoff during those two months alone reached $2.636*10^9$ m^3. This volume was occupied by both sediments and water such that the volume of the sediment discharge ($0.240*10^9$ m^3) formed 10% of the water discharge ($2.40*10^9$ m^3).

According to Rodier (1989), a 50-y flood may transport a total sediment load far greater than the total transported during the previous fifty years. Anyhow, it

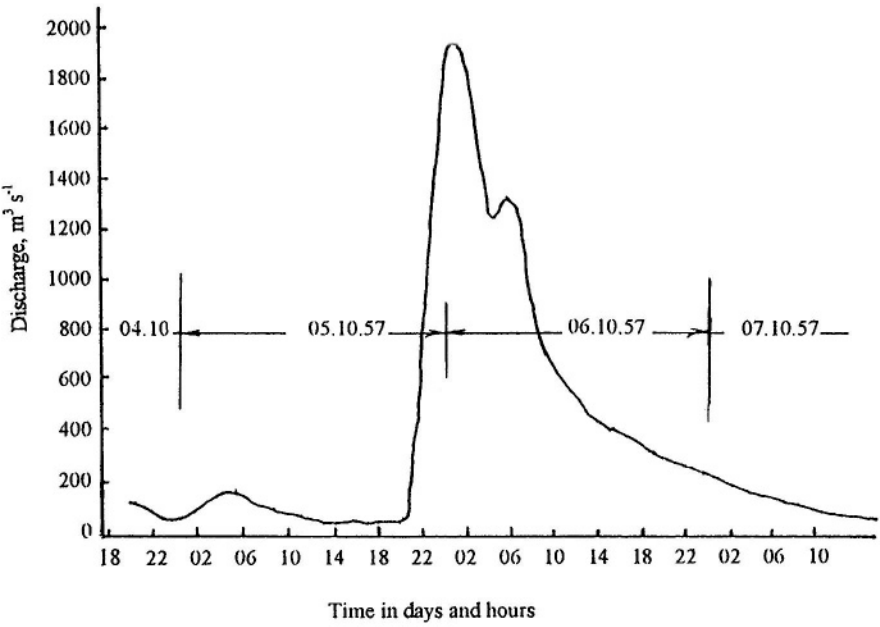

Figure 9.9- Hydrograph of the flood event of 6 October 1957 at Sidi Saad, Oued Zeroud, Tunisia

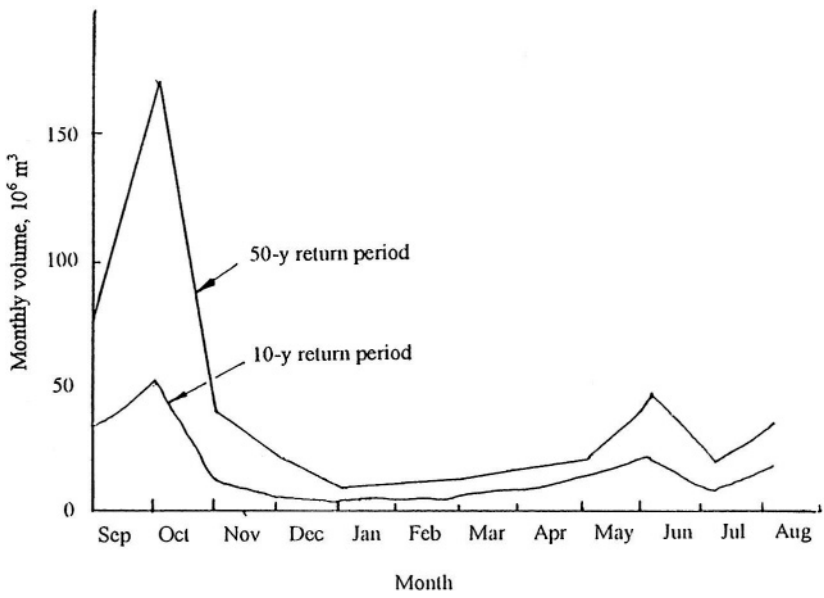

Figure 9.10- Estimated monthly flow volumes of Oued Zeroud corresponding to 10 and 50-y return periods

has been reported that the total sediment transported by the Oued Zeroud during the 1969 floods was $450*10^6$ t, whereas the average sediment load in an average year is around $6.0*10^6$ t.

9.7- The Oued (Wadi)-Sebou Basin

9.7.1 Brief description of the basin of Oued (Wadi) Sebou- The Oued or Wadi Sebou is an important river in northern Morocco, draining part of the Atlas Mountains and Rharb plain into the Atlantic Ocean. The basin, which is about 37,000 km^2, is an important agricultural area. Furthermore, the coastal town of Kenitra, 16 km upstream from Mehdiya, the mouth of the river, is a busy port at the head of navigation for oceangoing vessels.

The Sebou Basin in its upper part has an elevation of no less than 1,000 m a.m.s.l. falling to almost zero at the mouth of the river. As such the average overall slope of the oued is in the order of $2*10^{-3}$, which is rather steep. From its source as Oued Guigou in the Middle Atlas, the stream flows northward to Fès. Along the bend of its course eastward, the Sebou is joined by Oued Lebene from the right side. At some 10 km above the confluence, the Oued Inaouène, after traversing the Idriss Reservoir, joins the Oued Lebene.

The Sebou in its course northward to the Ocean is joined by several tributaries and feeders from both sides. Almost three kilometers above the stream measuring station Azib Soltane, the Oued Mikkes joins the Sebou. Below this confluence, the Oued Ouerrha (sometimes written Ouergha) also joins the Sebou. The Ouerrah is a major tributary of the Sebou and has its own drainage basin, which includes, among others, Oued Sra, Amzez, Aoulai, Aoudour, Aoudiar, and M'Jara Reservoir. Again, the Oued Sebou bends its course and assumes the shape of an arch. It receives on its right bank both Oueds Rdat and Et-tnine, whereas the left side receives the mightiest tributaries, Oued Rdom and Oued Beth. Figure 9.11 shows a map of the drainage basin of Oued Sebou and its tributaries.

The Sebou at the end of a 500 km journey reaches the Atlantic Ocean, where it discharges its water at Mehdiya. The Rharb coastal plain, formed by the alluvial deposits of the Oued Sebou, is often flooded by the heavy floods, originating from the Sebou and its main tributary the Oued Ouerrha.

The climate of the Sebou Basin varies along its extent from source to mouth. The annual rainfall is in the range from above 1,200 mm to below 400 mm, with a basin average of around 600 mm. Fès, Meknes and highland stations experience snow almost every year. Hail occurs often above 1,000 m elevation, being associated mainly with local cyclonic storms during middle and late spring. This makes Oued Sebou the mightiest surface water resource in Morocco. The basin yield counts to 28.5% of the total river water supply in the whole country and 40% of all the Middle Atlas basins.

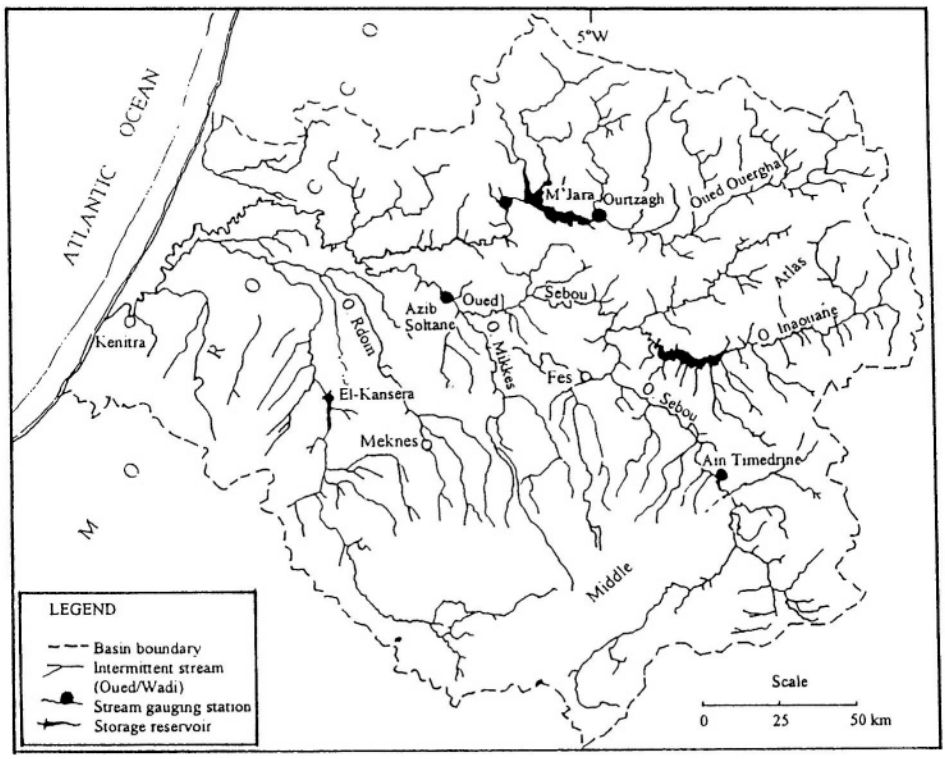

Figure 9.11- Map of the drainage basin of Oued Sebou

According to the map of the world distribution of arid regions (UNESCO, 1979) the ratio of the annual precipitation to the annual potential evapotranspiration for this basin falls in the range 0.20-0.50. The monthly free water evaporation at El-Kansera in the southwest of the basin as measured by a Colorado evaporation pan in a moderate year was: 47, 47, 77, 79, 104, 139, 183, 183, 144, 119, 82 and 79 mm for the months from January to December respectively. The sum of these monthly figures gives the annualevaporation at 1,283 mm. Obviously, the annual evaporation increases sensibly in a warmer and/or drier year.

What makes the Sebou basin more important is that it is located in an area rich in groundwater. The groundwater reservoir underlying the Middle Atlas is free, and the reservoir under Fès-Meknas plain is artesian as, it is overlain by an impermeable stratum.

9.7.2 Hydrology of the Sebou Basin- The map in Figure 9.11 shows the locations of four stream gauging stations, the Ain Timedrine (station No. 23) and Azib Soltane (station 21) on the Oued Sebou, and the Ourtzegh (station No.

19) and M'Jara (station No. 20) on the Oued Ouergha. The four stations have periods of record varying from 19 to 39 years. The records, which have a few breaks, include monthly and annual, as well as extreme annual discharges.

Station No. 23 is the station with the shortest record, 1965-83. The catchment area corresponding to it is just 4, 392 km^2. Table 6., Part I/Appendix B, gives a mean annual discharge of 16.8 $m^3 s^{-1}$ with 36.9% coefficient of variation. These figures bring the runoff to 120 mm and the runoff coefficient to about 15%. The station at Azib Soltane (No. 21) has a much longer record than station No.23. The mean annual discharge over the period 1960-88, which is published by UNESCO (1995), is 57.3 $m^3 s^{-1}$ with interannual variability of 61.6%. The monthly and annual discharge of the Sebou at Azib Soltane dates back to 1933. The Report on the Development of the Sebou Basin (NEDECO, 1975) includes some interesting hydrological data. After checking the 1960-73 period in the said report against the corresponding data in the UNESCO Report (1995), it has been decided to extend the discharge record to 1934. The calculation of the basic descriptors of the 55-y sample, 1934-88, has yielded a mean annual discharge as 62.8 $m^3 s^{-1}$ with interannual variability of 54.2%. The difference between the means and coefficients of variation of the two records, 1960-88 and 1934-88, indicates the reduction of the annual flow carried by the Sebou.

Figure 9.12 shows a graphical plot of the annual discharge series together with a falling trend line fitted to it by the method of least squares. The reduction in the annual discharge reaching Azib Soltane is considerable. This can partly be explained by the natural decrease of the rainfall in the second half of the period of record, and partly by the withdrawal of increasing volumes of water for land irrigation and the associated reservoir storage losses. The catchment area of the Oued Sebou at Azib Soltane is 17,250 km^2. The annual runoff as obtained from the larger sample is around 115 mm and the runoff coefficient between 12 and 14%.

The two measuring stations on the Oued Ouergha are No. 19 and 20. The catchment area at station No. 19 is 4,404 km^2 increasing to 6,190 km^2 at station No. 20. The mean annual discharge over the period 1952-88 is 62 $m^3 s^{-1}$, with coefficient of variation of 60.7%, and 95 $m^3 s^{-1}$, with coefficient of variation of 58.2%, for the two stations in their respective order. These figures lead to annual runoffs of about 440 and 480 mm, or an average of 460 mm, and a runoff coefficient of more than 40%. This considerable runoff joins the flow in the Oued Sebou below Azib Soltane. Additionally, the Sebou on its course to the ocean receives supplies from the Oued R'dat, R'dom, Beth and Tiflet.

The total yield of the Sebou Basin is $6.61*10^9$ $m^3 y^{-1}$ (Country Report of Morocco, 1986), corresponding to a runoff depth of almost 178 mm. According to Rodier (1989), the average runoff of Wadi Oum er R'bia (3,360 km^2), which is located far southwest of Wadi Sebou, is 283 mm. Despite the difference of climate between the two basins, one should not forget that the runoff generally

decreases with increasing basin area. The total yield of the Sebou basin corresponds to 5.6 1 km^{-2} s^{-1} average specific yield. The last figure when compared to the specific yield of the Wadi Zeroud , 0.3451 km^{-2} s^{-1}, is about 15 times as much. This large difference is essentially caused by the difference in annual precipitation in the two basins.

The high flows are mostly concentrated in the winter and spring as a result of rainfall and snowmelt. The remaining months get much less water and rarely reach zero, except for the small tributaries. The extreme flood values as experienced by the Oued Ouergha at station No. 20 exceeded 6,000 m^3 s^{-1} in 1970 and 1977 during the period of record 1952-88. The flood peaks in the Sebou at Azib Soltane during the same period were small compared to those of the Oued Ouergha. Furthermore, from the annual flood volumes carried by the Oued Sebou at the confluence Sebou-R'Dat in the period 1934-71, which are available in the NEDECO Report of 1975, it has been possible to compute the mean flood discharge that corresponds to the maximum flood event in each year. The duration of this event varied from one year to another. The shortest duration was 2-days in 1937 and the maximum 25-days 1969/1970. The minimum, mean and maximum for the mean flood discharge series thus obtained are 1,180, 2,030 and 3,160 m^3 s^{-1}, respectively.

9.7.3 Erosion and sedimentation- Studies on the erosion and sedimentation in certain parts of Morocco were undertaken as early as 1933. Heusch and Millies-Lacroix (1971, cited in Walling, 1984) have suggested that, in low precipitation environments, about 400 mm y^{-1}, erosion rates are likely to be around 100 t km^{-2} y^{-1} However, this rate can reach 4,000 t km^{-2} y^{-1} with precipitation in the order of 1,500 mm y^{-1}.

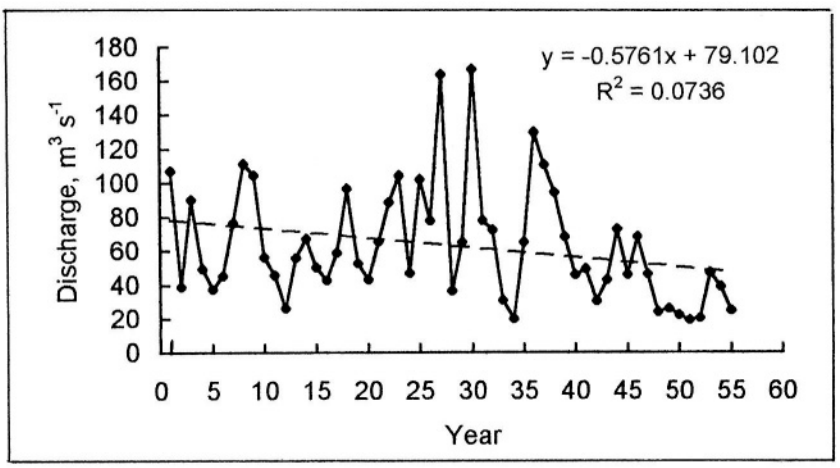

Figure 9.12- Annual discharge series of the Oued Sebou at Azib Soltane, Morocco (year 1 = 1934, year 2 = 1935,..., and year 55 = 1988)

The suspended sediment yield of the Oued Ouerrha and Oued M'Jara are included in Table 2_b, Part II/Appendix B. The listed sediment yields, 3,500 and 2,910 t km^{-2} y^{-1} respectively, can be regarded among the highest in Africa. Many more figures have been reported by Heusch and Cayla (1986). For example, the average sediment discharge over the period 1933-62 in the Inaouene catchment (3,384 km^2) was 1,110 t km^{-2} y^{-1} and the Lebene (792 km^2), with 830 mm precipitation, was 2,250 t km^{-2} y^{-1}. Such high rates of erosion and sedimentation can be attributed to the steep unstable terrain, the highly erodible rocks, the relatively high annual precipitation (500-1,000 mm) in many areas, and vegetation removal by human activity The role of precipitation and runoff has been firmly emphasized by Heusch and Cayla (1986). They stated: "As a general rule, even if concentration decreases while rainfall and runoff increase, specific erosion increases linearly with rainfall, at least up to an average depth of 1,300 mm of rain per year, but with wide fluctuations from one catchment to another". The high yields give rise to a major problem of reservoir sedimentation in the mountainous Maghreb (western) region of Morocco, Algeria and Tunisia (Walling, 1984). This is especially true for Morocco, which has a relatively large number of existing storage reservoirs and some more planned for construction in future.

9.8- The Gambia River Basin

9.8.1 Brief description of the basin- Around 1455, Portuguese sailors landed in the coastal part of the Gambia Basin along the Atlantic Ocean. They used it as a trading post for shipping precious metals outside Africa, as well as a port of call on their route to the Far East. This post was sold to British authorities around about 1665. Despite this early history, sources of the Gambia and the Sénégal Rivers were discovered only in 1818 by a Frenchman called Gaspard Mollien.

The Gambia Basin is located between 10°55'and 14°30'N latitudes and between 16° 15'and 11°10'W longitudes. It extends from the ocean coast in the west to the inland, covering a surface area of about 77,000 km^2. This area occupies all the surface of the Gambia and parts of the Sénégal and Guinea. This can be seen from the map of the drainage basin shown in Figure 9.13.

The Gambia River is the main surface water supplier to Gambia and to some extent to Sénégal. It rises in the water-rich Fouta Djalon heights in Guinea and flows westward across a plateau with elevations between 25 and 75 m a.m.s.l. The river course is about 1,000 km long. The Upper River traverses a region of light sandy soils where narrow valleys are separated by broad, low hills The Middle River has tracts of alluvium liable to river floods throughout the Gambia flanked by sandstone terraces yielding sandy soils. The lower part of the basin, is comprised of low-lying areas liable to flooding and uplands that are unlikely to be flooded. Low sand hills alternate with depressions that often form sand-

filled plains. The soils of the upper and middle sections of the river basin are generally more fertile than those of the lower river basin.

Compared to the Sénégal River, the channel of the Gambia River has a great depth, making it a better waterway. Even in the dry season the river is tidal and navigable for a distance of 500 km, i.e. about half of its length

The average annual rainfall in Gambia was about 960 mm in 1990. There is some evidence of a steady decline in rainfall from 1875 onwards, which still continues and which is causing increased salinity in the lowlands and increased salinity in the uplands. Hutchinson (1985) investigated five rainfall stations in Gambia with records from 1946 up to 1982. The average decline of the rainfall in that period is found to vary from one location to another. The range of decline has a minimum of $3.3\ mm\ y^{-1}$ at Basse ($\varphi = 13^{\circ}\ 19'\ N$, $\lambda = 14^{\circ}\ 13'\ W$ and $z = 14$ m) and a maximum of $22.7\ mm\ y^{-1}$ at Bansang ($\varphi = 13^{\circ}\ 26'\ N$, $\lambda = 14^{\circ}\ 40'\ W$ and $z = 2$m). The potential evapotranspiration and free water evaporation rates experience less interannual variation compared to rainfall.

9.8.2 Hydrology of the Gambia Basin- The map in Figure 9.13 shows the location of 10 discharge-measuring stations in the Gambia Basin. These are stations No. 46, 48, 49, 51, 57, 58, 60, 62, 63 and 64. All these stations have records from 1971 to 1984, mostly with breaks and gaps. The stations at Gouloumbou (No. 49) and Kedougou (No. 64) are the only stations with 14 uninterrupted years of record.

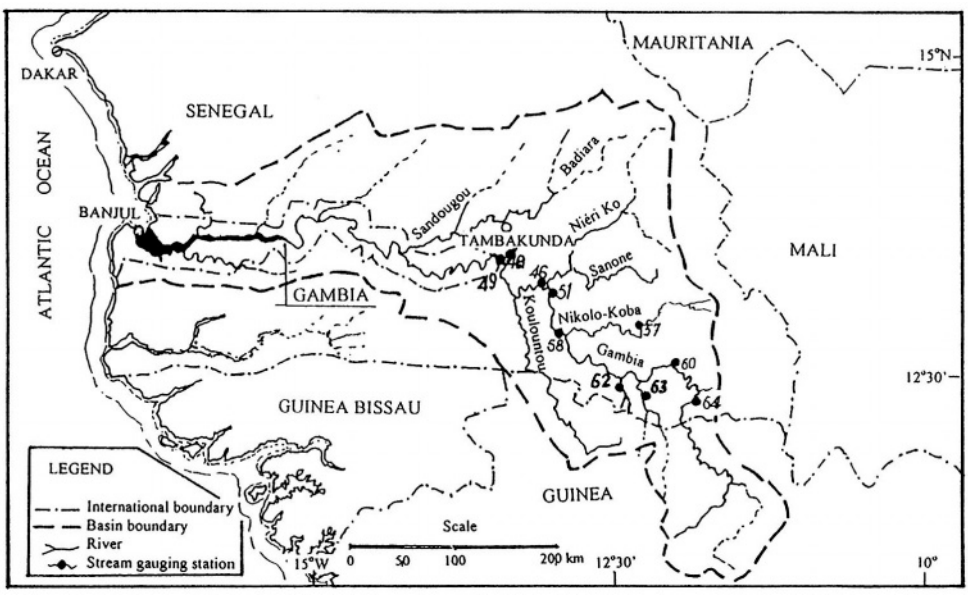

Figure 9.13- Map of the drainage basin of the Gambia River

Station No. 64 is the most upstream station on the Gambia River. The catchment area at this station is 7,550 km^2 yielding a mean annual discharge of 75 $m^3 s^{-1}$ with interannual variability of 24%. These figures correspond to about 315 mm runoff and a runoff coefficient of approximately 25%. The catchment area at the second upstream station on the Gambia, No. 60, is 10,450 km^2 and the mean annual discharge rises to 88 $m^3 s^{-1}$, with a coefficient of variation of 27%. The catchment runoff thus decreases from 315 to 265 mm. The mean annual discharge at Stations No. 63 and 62 on the neighbouring branches, Thiokoye and Diarha, is 9.1 and 7.5 $m^3 s^{-1}$ respectively. Though relatively small, these two discharges strengthen the flow downstream Station 60. This is further supported by a mean discharge of 6.8 $m^3 s^{-1}$ produced by the catchment of Nikolo-Koba (3,000 km^2) at station 57. Nikolo-Kobo is a tributary joining the Gambia on the right bank. These three additional sources plus the runoff from the sub-basin of the Gambia itself bring the mean annual discharge at Simenti (station No.58) to 124 $m^3 s^{-1}$, with variation coefficient of 35%. The basin runoff at this station (catchment area = 20,500 km^2) is further reduced to 191 mm.

A few kilometers below Simenti, the mean annual discharge of the Gambia upstream Wassadou (station No. 51) reaches 125 $m^3 s^{-1}$, which is hardly any different from that at Simenti. A slight increase can be noticed at station No. 46, which is located downstream from Wassadou, where the mean annual discharge increases to 129 $m^3 s^{-1}$. Given the catchment area at this location as 33,500 km^2 the corresponding annual runoff depth should be around 122 mm.

A very small tributary known as Niaoule joins the Gambia on the right bank and hardly adds any supply to it. The last measuring site on the Gambia whose data are available is at Gouloumbou (station No.49), just below the confluence of the Niaoule. The mean annual discharge over the period 1971-84 is 143 $m^3 s^{-1}$, with 47.5% coefficient of variation. The catchment area at Gouloumbou is 42,000 km^2 yielding an annual runoff of 107 mm. Considering the average areal precipitation during the said period is about 800 mm y^{-1}, the annual runoff coefficient must have been in the range of 12-14% and the mean specific yield 3.4 l $km^{-2} s^{-1}$. The last figure is about 31% larger than that of the Sénégal Basin at Dagana. It is very unfortunate that the record that has been used is too short, at best 14 years, and that some of those years fall in the harsh drought period that swept over West Africa in the late 1960s and lasted for more than 10 years. The data cited in Martins and Probst (1991) give 1,100 mm for precipitation, 210 mm for rainfall and 20% as runoff coefficient. From these figures, one can easily obtain the specific yield for The Gambia Basin as 6.6 l $km^{-2} s^{-1}$, a figure that is about twice as much as the one obtained from the short record.

9.8.3 Water quality of the Gambia River- The total suspended solids, *TSS,* in the Gambia River has been found as 19.5 mg l^{-1}, and the total dissolved solids, *TDS,* to be 17 mg l^{-1}, giving the ratio *TSS/TDS* as 1.1. The corresponding transport

figures are 0.9 and $0.8*10^6$ t, respectively. It should be strongly stated that these figures are averages computed from monthly samples covering one year, 1983. All the water samples have been taken from the same place, Gouloumbou. The salinity of water increases between May and July, dropping sharply towards the end of the year, as shown in Figure 9.14. It goes without saying that the salinity concentration increases as the distance from the ocean decreases. Also, for the same location, the concentration in the low-flow season is higher than the high-flow season. Plans have already been laid down for quite some time in order to construct a salt-protection barrier on the river mouth so as to improve the quality of the river water.

9.9- The Tana Basin

9.9.1 Brief description of the Tana Basin- The major features of the drainage pattern of Kenya were created by the ancient crustal deformation of a great oval dome that arose in the west-central part of the country and created the Central Rift. This dome produced a primeval watershed from which rivers once drained eastward to the Indian Ocean and westward to the Zaïre system and the Atlantic

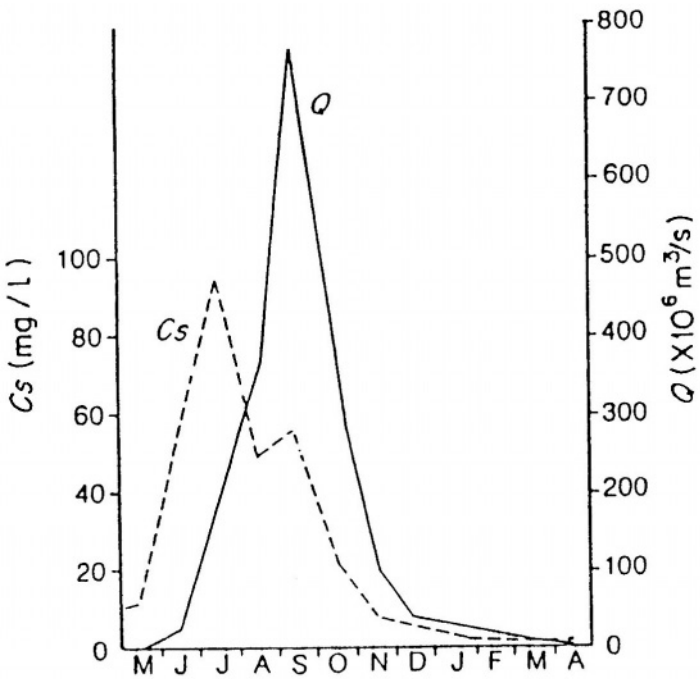

Figure 9.14- Salinity and Discharge of the Gambia River at Gouloumbou, 1983 (from Martins and Probst, 1991)

Ocean. The Tana River is still following this ancient pattern. The river arises in the eastern-highlands of Kenya and flows roughly southeast to the Indian Ocean, after a journey of about 700 km in different Kenyan landscapes.

The coastal plain of Kenya, which runs for about 400 km along the Indian Ocean, is a narrow strip in the south. In the Tana Basin lowlands to the north, it broadens to 160 km. The coastal zone is distinguished by greater rainfall and lower altitudes than the plateau behind it. Inland are the arid plains and plateau made up of the sedimentary basin of the Tana embayment. The areas circumscribed by square brackets in Figure 9.15 are deserts and semi-deserts. Most of the streams in this area are of the intermittent type. This can be recognized from the streams indicated by dotted lines in Figure 9.16.

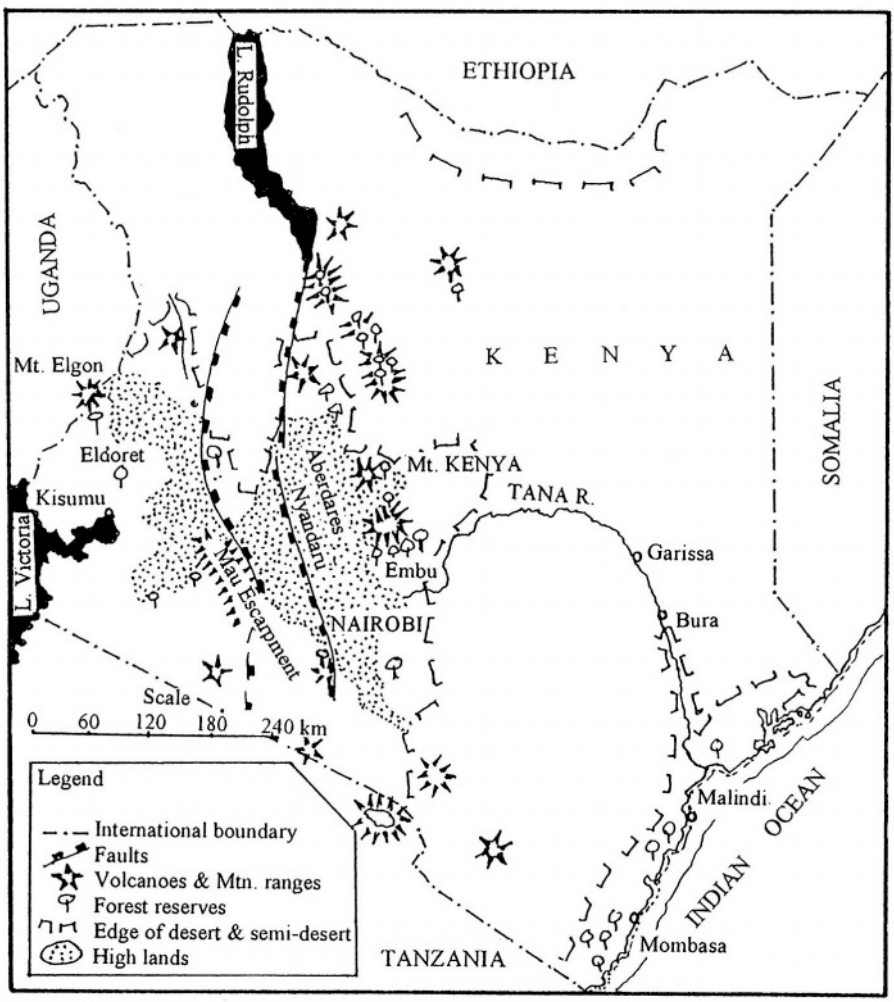

Figure 9.15- Map of Kenya showing the course of the Tana River

In contrast, the tributaries in the upper basin are of perennial nature, tributaries in the Upper basin are of perennial nature.

The natural complexity of landscape as shown by the map in Figure 9.15, added to the absence of contour mapping of a vast desert area makes it difficult to delineate the boundary of the basin accurately, at least for certain reaches of the river. Besides, the basin of the Lower Tana is crowded with many swampy streams (lagos), some of which disappear in the swamps before reaching the channel of the main river. All these factors render a thorough survey of the total surface covered by the Tana Basin so far unaffordable. However, areas such as 132,000 km^2 and 120,000 km^2 have been given by Krhoda (1989) and Ongwenyi et al. (1993a) respectively. Most of the published hydrological studies are confined to that part of the basin up to Garissa, where the catchment area is 42,220 km^2. Moreover, the Tana Basin is confined to Kenya alone, a fact that gives the basin a national not international character. For all these reasons it has been found more relevant to place this river basin in the same class as the other small rivers.

9.9.2 Hydrology of the Tana basin- The Tana River has been harnessed to a much greater extent than Kenya's other major arid watersheds. The high mountain ranges receive up to and even more than 2,000 mm annual precipitation. As an example, the mean annual rainfall at Kericho (meteorological station No. 165) is 1,861 mm. This amount drops to 330 mm at Garissa and further to less than 200 mm y^{-1} in the desert areas. The average rainfall that the drainage basin receives is estimated at 562 mm.

Like precipitation, the annual evaporation rate depends on the altitude and general environment of the location. In arid low-lying areas, it can be as high as 2,300 mm whereas the average open water evaporation in the wet highlands is much less. For example, the annual evaporation over the period 1951-60 at the Coffee Research Station, Ruiru (φ = 1° 06'S, λ = 36° 56'E and z = 1, 608 m), was 1,520 mm. The long-term pan evaporation in the Ndeiya-Karai area west of Nairobi is 1,720 mm corresponding to approximately 1,370 mm y^{-1} (Heedrik et al., 1984).

The runoff data available in the UNESCO Publication (1995) belongs to the discharge observation site at Garissa (station No. 189). The available discharge data covers the period 1934-75. The old literature provides some information about rainfall and runoff in the Upper Tana catchment at Kamburu. We shall introduce some of this information in a summarized form before expanding it.

The Tana River rises in the highland of Kenya known as Nyandarua Ranges. In its upper basin, the Tana is joined on the right bank by the Thika River, a principal tributary, and below the confluence on the left bank by the Thiba River, another principal tributary. Five storage reservoirs have been built at

Massinga, Kamburu, Gitaru, Kindaruma and Kiambere to regulate the flow in that part of the Basin.

The Upper Tana catchment receives an average annual rainfall of 630 mm at about 1,000 m a.m.s.l. increasing to 2,000 mm at about 2, 450 m a.m.s.l. on the Mount Kenya and Aberdare Ranges. The average precipitation on the catchment up to Kamburu, 8,240 km^2, is 1,170 mm. Sutcliffe and Rangeley (1960) used the available precipitation data to divide the precipitation stations into groups, and for each group, they calculated the average of the station indices for each year of record. Again, the average of all groups for each year was used to define the yearly catchment index. The term index here means that annual precipitation is expressed in a modular form, i.e. the individual value divided by the average value of the whole period of record. This was done for the 50-y period, 1908-57.

The average annual rainfall depth over the whole catchment was estimated by multiplying the long-term mean rainfall by the catchment index for the year in question. The figures so derived have been compared with measured runoff for the period which 1947-57. The comparison has shown that the loss from the river basin increases with the annual rainfall This result can be attributed to the fact that potential evapotranspiration exceeds precipitation over most of the Tana Basin, so that only the higher parts of the catchment contribute significant runoff.

A linear relationship between precipitation and runoff was established and used for estimating the runoff for the missing period 1908-46 (Sutcliffe and Rangeley, 1960). From the runoff estimates, 1908-46, and the discharge measurements over the period 1947-57, we calculated the basic statistical descriptors of the sample covering the period 1908-57. The mean annual discharge, standard deviation and skewness are 76.65 $m^3 s^{-1}$, 23.09 $m^3 s^{-1}$ and 0.45 respectively. The mean annual runoff and the runoff coefficient as obtained from these figures are 293 mm and 26.5% respectively.

The mean annual discharges over the period 1934-57 have been used to establish a linear relationship between the runoff at Kamburu and Garissa stations, some 250 km apart. The correlation between the two stations, as expressed by the coefficient R^2 has proven to be 0.844. The relationship thus obtained has been used for expanding the record at Kamburu up to 1975. As such, the annual discharge series at Kamburu comprises 3 segments: 1908-46 estimated using rainfall, and runoff data of Kamburu, 1947-57 measured discharges, and 1958-1975 estimated from the relationship between the runoff at Kamburu and Garissa. Figure 9.17 shows a graphical plot of the annual discharge series, the 5-y moving average and a rising trend line

The Tana after leaving Kamburu traverses its middle basin, where the annual rainfall decreases till it becomes 332 mm at Garissa (meteorological station No. 166). Table 10_a in Appendix A, gives this figure as an average for the period 1931-80. The mean annual discharge at Garissa for the period 1934-75, as included in Table 6_a, Part I/Appendix B, is 157 $m^3 s^{-1}$ with interannual

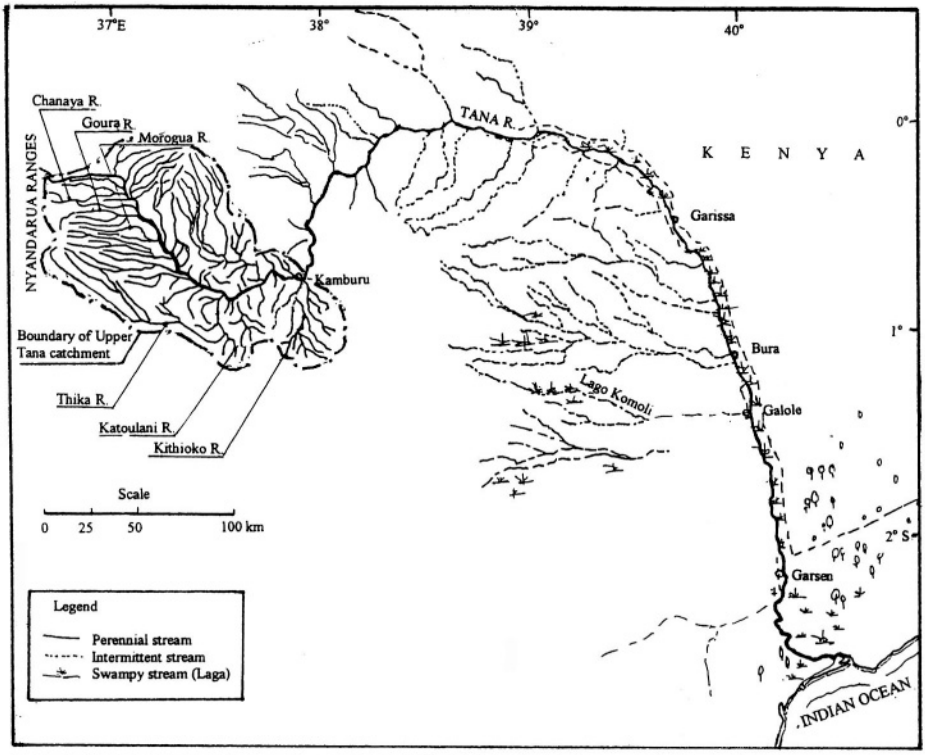

Figure 9.16-Map of the Tana Basin

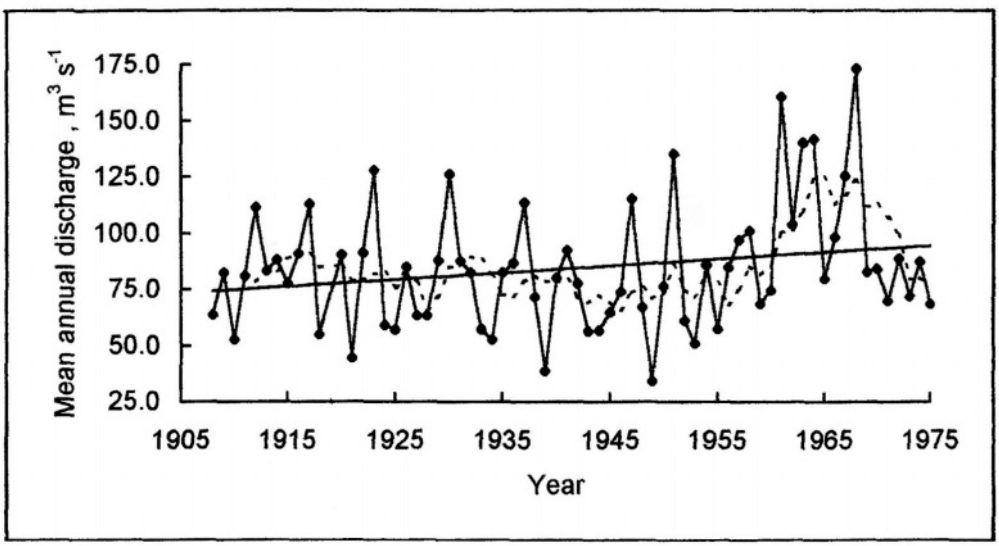

Figure 9.17- Annual discharge series, 1908-75, for Kamburu on the Tana

variability of 47.9%. Since the catchment area at Garissa is 42,220 km^2, and the overall average precipitation is 650 mm, the annual runoff depth and the runoff coefficient reduce to 117 mm and 18% respectively. Furthermore, the mean annual volume of water, based on a mean annual discharge of 157 $m^3 s^{-1}$, is close to $5*10^9$ m^3. This figure is 5.5% higher than the figure of $4.7*10^9$ m^3 given by Ogembo (1977) and Ongwenyi et al. (1993a). The yield of the Tana Basin at Garissa constitutes almost 24% of the total internal renewable water resources of Kenya.

Some of the runoff characteristics at Garissa (station No. 189) have already been given as examples when certain aspects of stream flow were being discussed in Chapter 6. First of all, the annual discharge series together with the trend line and 5-y moving average are presented in Figure 6.13_c. From this graphical plot, it is obvious that the annual discharge in the period of record 1934-75 has been undergoing a significant upward trend. It is unfortunate that the discharge after 1975 is not available so as to decide whether this trend has continued, and if so till when. Was it a part of a long cycle? It is not possible to tell.

The index of seasonality, $(In)_s$, is given in Table 6.3 and the probability distribution of the minimum flow in Table 6.4. Additionally, the distribution patterns of monthly discharge in a low-flow year, average and high-flow year are presented in Figure 6.12_c. The distribution pattern of the monthly discharge of the Tana River at Garissa is bimodal. The first and larger maximum discharge occurs in May and the second and smaller in November, i.e. six months later. Likewise, the first minimum discharge occurs in February and the second in September. The bimodal nature of monthly discharge is a mere reflection of the two rainy seasons, March-June and October-November, resulting from the movement of the Intertropical Convergence Zone.

Below Garissa the river traverses its lower basin on its way to the ocean. In this section of the river basin the annual rainfall increases till it reaches more than 1,000 mm along the coast. The other feature is that the land level falls to between 200 and zero m a.m.s.l, thereby creating many swamps. Several rivers, coming from the west cross the lowland and disappear in the swamps before reaching the Tana River. The two main rivers that are able to join the Tana are the Hiraman and the Galole. Most of the supply of the tributaries in the lower Tana Basin is lost by evapotranspiration, spilling and infiltration. There is hardly any net contribution added to the river flow below Garissa. As such, it is not unrealistic to conclude that the average yield of the Tana Basin remains between 4.7 and $5.0*10^9$ $m^3 y^{-1}$ and the average specific yield between 1.2 and 1.3 l $km^{-2} s^{-1}$.

The special features of land and water resources in the lower Tana Basin have led the Kenyan authorities together with some of the international development aid agencies to plan some projects under the title of Tana Delta development. Of these projects, the reclamation of wetlands, rice irrigation,

development of freshwater and marine fisheries and tourism are noteworthy. Unfortunately, the weak economy and problematic internal affairs of the country make any progress in these projects, if there is any at all, quite slow.

9.9.3 Sediment yield of the Tana Basin- The areas that experience the highest erosion risk in Kenya coincide with the most productive areas in the country. These include the Highlands, the Lake Victoria Basin, Kiyui and Embu Districts and some parts of the coastal zone. **Table 1_c,** Part II/Appendix B, gives soil erosion data from selected catchments (Ongwenyi et al., 1993b).

Several estimates of the suspended sediment load in the Upper Tana Basin have been carried out by a number of investigators at different time intervals. Those estimates have been collected, presented and discussed by Walling (1984). The disagreement between the various estimates is quite large. The yield of the basin at Kamburu, as obtained from river water samples, varied from $0.4*10^6$ t y^{-1} to $7.6*10^6$ t y^{-1}. The summation of the tributary loads varied between 3.0 and $5.6*10^6$ t y^{-1}. These wide discrepancies can be attributed to the different sampling and estimation techniques. Of much importance is that they indicate the possibility of having considerable inaccuracy in the available sediment load data.

The above-mentioned possibility of having inaccurate data, however, does not eliminate the fact that there have been increased rates of sedimentation in the multipurpose reservoirs constructed across the Tana River. This finding can be attributed to the continuous increase in rainfall, subsequently the runoff, both for the available periods of record, as explained in sub-section 9.9.2. The construction of the reservoirs themselves seems to be another major factor. Judging by the unexpectedly increasing rates of sedimentation of the Missinga, Kindaruma and the Kamburu reservoirs, the impacts of dam construction are becoming alarming. There is a strong fear that the design age for electricity development will be reduced, reservoirs will be filled much earlier than planned, fish and aquatic life in the created reservoirs will be destroyed and flooding of the upstream river reaches will be a real menace (Ongwenyi et al., 1993b).

CHAPTER 10

HYDROLOGY OF WETLANDS AND NATURAL LAKES

Wetlands have been defined loosely as vegetation areas that are flooded, either permanently or seasonally. There may be areas of open water (shallow lakes) in a wetland, but these are generally smaller than the areas of vegetation (Denny, 1985). Kuusisto (1985) mentioned that a lake should satisfy the following conditions:

- fill completely or partially a basin or a number of connected basins,
- have essentially the same water level in all parts unless affected occasionally by wind or large inflow,
- have a large volume compared to the average inflow that a considerable portion of the suspended sediment is deposited, and
- have a size exceeding a specified area, e.g. $0.01\ km^2$.

In the present chapter, only wetlands and natural lakes will be dealt with. Artificial or man-made lakes, such as the storage reservoirs that are excavated or created as a result to the construction of dams, e.g. Akosombo on the Volta, Kariba on the Zambezi, etc., will be presented and discussed in the next chapter.

10.1-Wetlands

10.1.1 Definitions and physical features- Wetlands are characterized by the presence of aquatic plants (emergent or submerged vegetation; plants with floating leaves). They can be subdivided into swamps, marshes, dambos and flood plains. The growth of such plants is encouraged by the presence, for most of the time, of shallow stagnant water (in the case of a swamp) or muddy water logged soil (in the case of a marsh). Swamps and marshes never dry out.

Swamps can be subdivided into herbaceous, Taypha (sedge) and forest swamps. Herbaceous swamps are distinguished from the marshes by their taller vegetation. Papyrus swamps (e.g. in Southern Sudan) are generally more typical of African herbaceous swamps, although Typha swamps are present as well (e.g. Okavango swamps in Botswana). Swamps can be found in several parts of Africa such as the Central Basin of Zaïre, Sierra Leone, Madagascar, etc. The map, Figure 10.1, shows the approximate locations of swamps in Africa.

As marshes are wetlands with permanent grassy vegetation they are often referred to as ‘wet meadows’. The kafue Flats in Zambia are typical marshes that are dominated by Oryza vegetation. Other vegetation communities can be found in West and Central Africa.

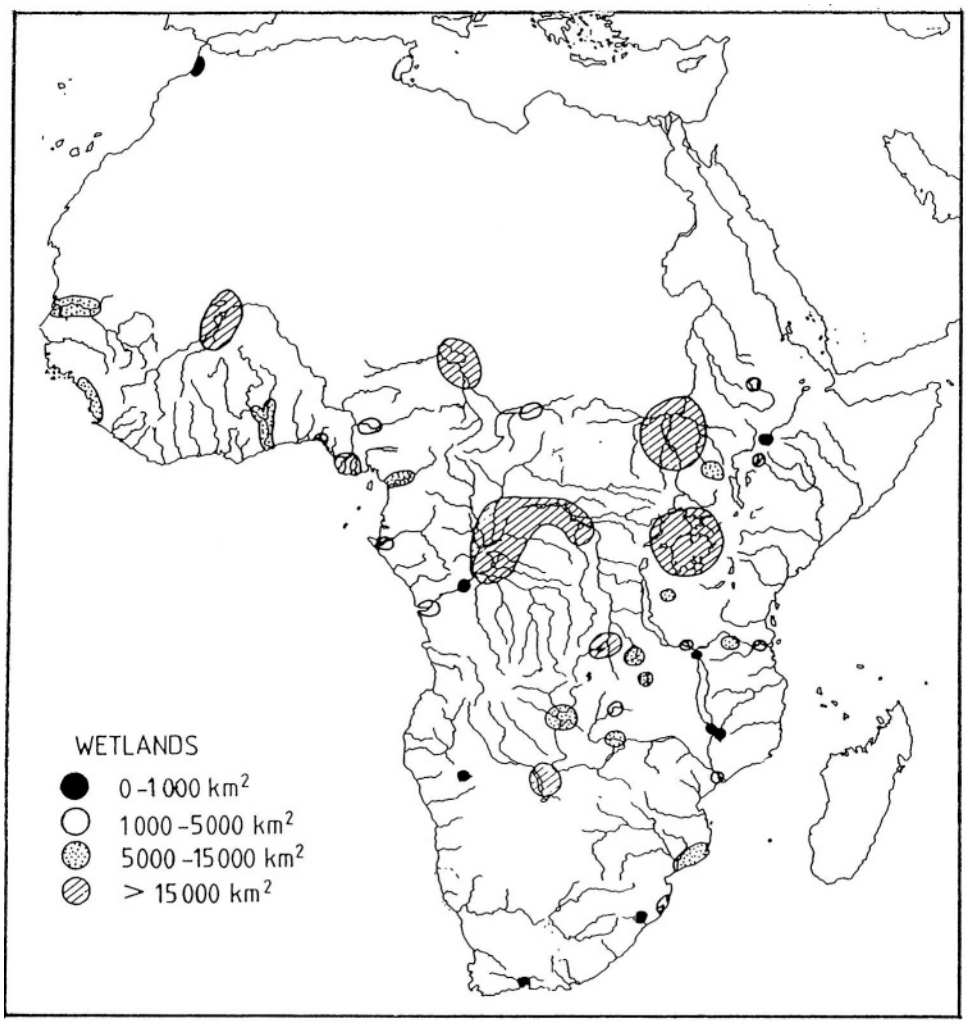

Figure 10.1- Major areas of permanent and seasonal wetlands in Africa (from Denny, 1985)

Intermittent swamps are called dambos (Balek, 1977). A dambo according to a number of authorities on African swamps is a"... seasonally waterlogged, grass covered treeless area bordering a drainage line". Figure 10.2$_a$ illustrates the difference between a floating swamp and a rooted swamp, whereas Figure 10.2$_b$ shows the difference between a swamp and a dambo. It might be of interest to refer here to the findings of Balek (1983) concerning the loss of water by evapotranspiration from the permanent Bangweulu swamp in Zambia, and from the headwater intermittent swamp located in the nearby area. The evapotranspiration from the permanent swamp is 2,156 mm y^{-1} whereas that

from the intermittent swamp is 494 mm, although the rainfall is almost the same in both swamps. The annual free water evaporation from Lake Bangweulu is already given in Table 4.13 as 1,642 mm. In general, water consumption by the vegetation is much higher in the perennial swamp during both the dry and the wet periods, although during the latter, flooded areas are found in both types of swamps. During the dry period, the watered area in the permanent swamp gradually decreases and the evapotranspiration is greatly reduced.

Swamp forests are found on the lower shores of water bodies and rivers, in depressions and in some high-water riverbeds, on muddy, waterlogged soils. They occupy vast areas in Central Africa, particularly in Zaïre, Gabon, Southern Cameroon and the Niger Delta.

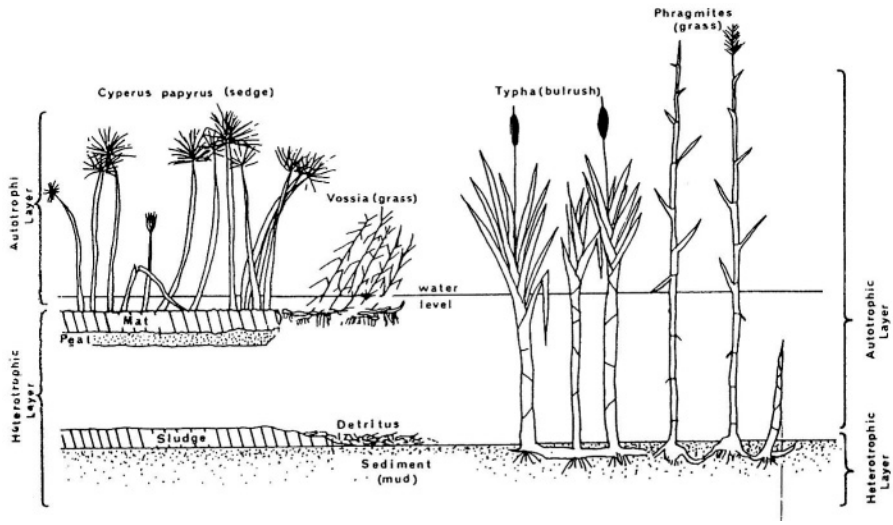

Figure 10.2$_a$- Comparison of floating and rooted tropical swamps showing differences in general structure (from Williams and Gaudlet in Denny, 1985)

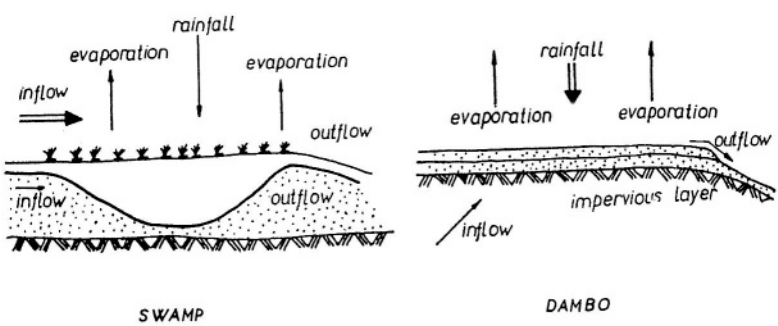

Figure 10.2$_b$- Comparison of perennial and headwater (dambo) swamps (from Balek, 1977)

Wetlands function as very shallow reservoirs with relatively extensive surface areas, thereby offering resistance to flow. As such wetlands have the capacity to regulate runoff, reduce flood peaks, recharge the groundwater, thus improving the base flow and entrap much of the suspended sediment load. Wetlands often have a stabilizing effect on the sediment as the roots of their dense vegetation have anti-erosive function. On the other hand, wetlands are a source of loss of water where evaporation and mostly high evapotranspiration rates take place. Additionally, some soils in arid and semi-arid areas tend to accumulate salts where groundwater rises to the surface or comes close to it. This process is accelerated by high evaporation. Regular flooding of these soils, however, allows the salt to become dissolved and washed out.

River floodplains are susceptible to having their flooding patterns changed, whether naturally as in case of drought or due to human activities. Interference in the natural flooding processes through construction of storage reservoirs and flood-protection works, or considerable withdrawal of water for irrigation and/or other purposes might have detrimental impacts. Figure 10.3 shows the impact of drought and withdrawal of water of irrigation on the flooding pattern on the Logone floodplain in the Cameroon (after Drijver and van Wetten, 1992).

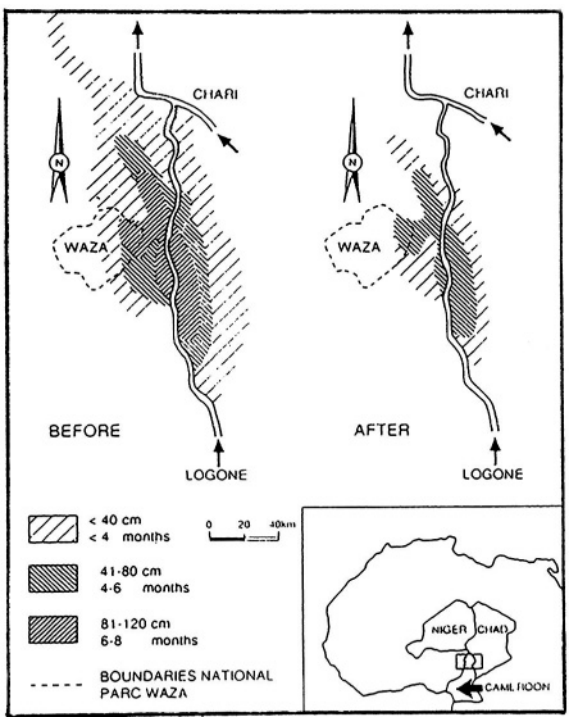

Figure 10.3-Potential impact of drought and (planned and existing) irrigation schemes on the flooding pattern of the Logone floodplain in Cameroon

The total area covered by freshwater wetlands in Africa is estimated at about 345,000 km^2 or 1.15% of the total land area of Africa. Most of the permanent and seasonal wetlands fall into three broad categories: (a) Endorheic systems (e.g. Okavango, Chad), (b) Upper floodplains of major rivers (e.g. Nile, Niger, Zaïre), (c) Coastal riverine floodplains (e.g. Sénégal, Zambezi, Incomati). There is a fourth category (d) Mountain wetlands (e.g. Drakensburg, Rwanda, Burundi and Mount Kenya). Table 10.1 contains some relevant information about the larger freshwater wetlands of Africa (Balek, 1977 and Denny, 1985). The following subsections summarize a number of case studies.

10.1.2 El-Sudd area in Southern Sudan- (Figure 7.3): From the outlet of Lake Albert down to Nimule, at the frontier between Uganda and the Sudan, the Bahr el-Jebel (Albert Nile) is a rather broad, sluggish, stream fringed with swamps and lagoons. It meanders east and west through a narrow floodplain between hilly country on either side, so that the area of the swamp is well defined. The river between Nimule and Rejaf, a distance of 155 km, flows in a narrow valley interrupted by rocky rapids. The Bahr el-Jebel in the reach between Nimule and Mongalla receives a number of small but torrential streams, which run full after heavy rains. In the reach from Rejaf to Malakal on the White Nile, the river is not confined to a single channel, except at Mongalla where it is one channel at low stage. The valley in this reach is wide, flat and swampy, with many channels leaving the river into the swamps and returning to the river. Due to the high resistance offered to flow by the swamp vegetation, it has been considered as a barrier or dam blocking the flow. The Arabic word for a dam is Sudd, from here the area used to be called the Sudd area.

Hurst and Philips (1938) estimated the area of the Bahr el-Jebel swamp in 1931/1932 as 8,300 km^2. Another estimate was reported in 1938 as 7,300 km^2 using air photography. Furthermore, the annual evapotranspiration from a tank with Papyrus was estimated as 1,530 mm. Further studies indicated the need to improve this figure. As Bahr el-Jebel loses each year half of it's water in the swamps, some years more, the diversion canal known as the Jonglei canal was designed to bypass the Sudd area, thus saving a considerable portion of the loss. Figure 10.4 shows the growth of the Bahr el-Jebel swamp between 1950 and 1980 and the proposed alignment of the Jonglei Canal (Howell et al., 1988). According to Sutcliffe and Parks (1999), the mean total area of the permanent and seasonal swamps "toich" in the Bahr el-Jebel basin was 12,900 km^2 in 1905-61 and increased to 28,900 km^2 in 1962-80, with an overall average area of 16,900 km^2 for the whole period 1905-80. All these figures are in the absence of the Jonglei canal. A diversion canal with a daily flow of $25*10^6$ m^3 can reduce the flooded area by up to 40%.

The Baht el-Ghazal is the waterway from Meshra er-Req to Lake No (see Figure 7.3). The basin area of this river is approximately 526,000 km^2 and the average annual precipitation is in the order of 800 mm. All along the river and

Table 10.1- Main African freshwater wetlands (according to Balek, 1977 and Denny, 1985)

Drainage system	Name	Locality	wetland type	Area, 10^3 km^2
Zaire Congo system	Middle Congo swamps	Zaire/Congo	Riv. Sw.and fld.pln.	40,550
	Kifulula depression	Zaire/Zambia	Swamps, fld. Pln.	1,502
	Mweru (Luapula river)	Zambia/Zaire	Shallow lake	4,580
	Bangweulu	Zambia	Shallow lake, sw. and fld.pln.	8,800
	Kamulondo depression	Zaire	Shallow lake, sw. and fld.pln.	18,840
	Mweru Wantipa	Zambia	Shallow lake, sw.	1,504
	Tumba, Cheshi, Maji	Zaire	Shallow lakes	3,402
	Rukwa	Tanzania	Shallow lake	2,300
	Malgarasi	Tanzania	Floodplain, swamp	7,357
Subtotal				88,835
Niger Benue system	Niger central delta	Mali	Floodplain, swamp and shallow lakes	23,900
	Niger river	Niger	Floodplain	1,177
		Benin	Floodplain	0,306
		Nigeria	Floodplain	6,600
	Sokoto, Benue and Anambra rivers	Nigeria	Floodplains	4,740
Subtotal				36,723
Nile system	Upper Nile sw.(Sudd)	Sudan	Swamps, fld.pln.	102,000
	Upper, Lower Kajera rivers	Burundi/Rwanda/ Tanzania	Shallow lakes, fld plains, swamps	0,520
	Ankola and Koki Lakes	Uganda	Shallow lake, fld.pln	0,570
	Kenamuka swamp	Sudan	Swamp	13,955
	Lotagipi	Sudan/Kenya	Swamp	12,900
	L. Kyoga, Bisinia, Kwanya,..	Uganda	Shallow lakes, swamps	5,025
	Lake Tana	Ethiopia	Shallow lake	3,500
	Yala, S. Ahero swamp	Kenya	Swamp, delta	0,280
Subtotal				138,750
Zambezi system	Zambezi floodplain	Zambia	Floodplain	9,700
	Liuwa, Busanga plains, Lukanga swamp	Zambia	Floodplain, swamp	6,300
	Kafue flats	Zambia	Marsh, floodplain	6,000
	Chobe-Linyanti	Botswana/ Namibia	Swamp	0,200

Table 10.1- Cont'd.

Drainage system	Name	Locality	Wetland type	Area, $10^3 km^2$
Zambezi system (Cont'd)	Lake Malombe	Malawi	Shallow lake, sw.	0,390
	Shire R. Eleph.t marsh	Malawi	Swamp	0,600
	Ndini marsh	Malawi	Swamp	0,170
		Mozambique	Swamp	0,060
Subtotal				23,480
North west Africa	Iriki	Morocco	Seasonal swamp	0,200
	Lakes of Middle Atlas	Morocco	Shallow lakes	0,014
	Ichkeul, Kelbia, Chott,	Tunisia	Shallow lakes, sw.	0,750
Subtotal				0,964
Western syatem	Oueme	Benin/Nigeria	Floodplain, delta	0,948
	Ogun and Oshun rivers	Nigeria	Floodplain	0,145
	White Volta river	Ghana	Floodplain	9,552
	Oti-Pendjari river	Burk.F/Benin	Floodplain	4,810
	Senegal river	Seng./Maurt.	Floodplain, delta	12,970
	Lake Guiers	Senegal	Shallow lake	0,170
	Lake Rkiz	Mauritania	Shallow lake	0,120
Subtotal				28,715
West equatorial system	Nyong river	Cameroon	Swamp forest	6,688
	L.Onangue, L.Mandje	Gabon	Shallow lake	0,400
Subtotal				7,088
Eastern system	Lake Chilwa	Malawi/Moz.	Shallow lake, sw.	2,100
	L.Chiuta, L. Amaramba	Malawi/Moz.	Shallow lake, sw.	0,163
	Usango, Kilombero, Rufiji river	Tanzania	Floodplain, swamp	8,704
	Lorrain sw., I. Naivasha	Kenya	Shallow lake, sw.	0,240
Subtotal				11,207
Chad system	Lake Chad	Chad/Niger/ Nigeria/Cam.n	Shallow lake, sw.	13,800
	Yaeres	Chad/Cam.n	Floodplain	5,957
	Iro	Chad	Shallow lake, sw.	0,195
Okavongo system	Okavongo delta	Botswana	Swamps	19,120
	Ngami, Dow	Botswana	Shallow lake	0,900
Rudolph system	Abaya, Awasa	Ethiopia	Shallow lake, sw.	1,363
	Shamo, Ziway	Ethiopia	Shallow lake	0,988
	Baringo	Kenya	Shallow lake	0,130
Madagas-car	Alaotra	Madagascar	Shallow lake, sw.	1,200
	L.Itasy, L. Kinkony,...	Madagascar	Shallow lake	0,150
Subtotal				43,803
Total				379,565

to the south and east of it are large swamps that are fed by a number of streams. Most of the flow of these tributaries is lost in the swamps, and the net contribution of this basin to the Nile flow is limited to just $0.6*10^9$ m^3 y^{-1} measured at Lake No.

Hurst and Philips (1938) gave an early estimate of the swamp area in Bahr el-Ghazal basin as 16, 600 km^2. Sources of information suggest a physical link between the swamps of Bahr el-Jebel and Bahr el-Ghazal north of Hillet Neur are connected by depressions full of Papyrus plants. In addition, there is an annual spill of $6*10^9$ m^3 from the Bahr el Jebel north of Shambe westwards to the Bahr el-Ghazal swamps. The tributary inflows to the swamps, $15*10^9$ m^3, less the outflow at Lake No, $0.6*10^9$ m^3, gives a net inflow of $14.4*10^9$ m^3. This figure added to the spill, when divided by the surface area of the swamps, 16, 600 km^2, gives a net loss of 1.23 m y^{-1}, representing the annual evapotranspiration less rainfall. As the annual rainfall is about 0 85 m, the evapotranspiration from the Bahr el-Ghazal swamps can be fairly estimated at 2.08m.

The water balance model has shown that after 1970 the estimated areas of flooding decreased fairly steadily, and after 1976 they varied seasonally between about 4, 600-11, 000 km^2 and 1, 400-4, 800 km^2. Sutcliffe and Parks (1999) indicated that using further satellite imagery, given a resumption of flow measurements, could in future refine the model.

The water balance of the Sudd area has been represented by a model developed by Sutcliffe and Parks (1987). This model employs measured rainfall, tributary inflows, evaporation and outflows to reproduce volumes and areas of flooding over the historical record. The model makes allowance for soil moisture recharge on newly inundated areas. The model is based on the principle of balance between the input to and output from the system (wetland) for a certain time interval δt. This principle can be expressed as:

$$\delta V = [I - O + A(P - E)]\delta t - r\delta A \qquad (10.1)$$

where V = volume of flooding, I = tributary inflow, O = Outflow from the swamp, A is the flooded area, and r = soil moisture recharge, which is positive when δA is positive and zero when δA is negative Assume that $A = kV$ and denote any arbitrary month by i. Mathematical manipulation of Eq (10.1) after introducing the relation between A and V and r leads to the model equation:

$$V_{i+1} = \{V_i[1 + k(r_i - (E_i - P_i)/2] + I_i - O_i\}/\{1 + k[r_i + (E_i - P_i)/2]\} \quad (10.2)$$

The data used in the balance model were: initial storage at the beginning of 1905, $8*10^9$ m^3; average rainfall, 870 mm, and evapotranspiration from the swamp equal to Penman's free water evaporation, 2,150 mm. Measured inflows and outflows were used in the model. Storage volumes and flooded areas were

estimated at monthly intervals up to the end of 1980. The model results were converted into water levels and compared with the river levels at Shambe in the middle of the Sudd. The seasonal fluctuation of the flooding and the ratio of seasonal to permanent flooding were obtained and compared to other wetlands.

According to Sutcliffe and Parks (1989), "the model was able to reproduce the timing of seasonal fluctuations reasonably, and also corresponded with areas of flooding measured at six dates from air photography, satellite imagery or vegetation maps".

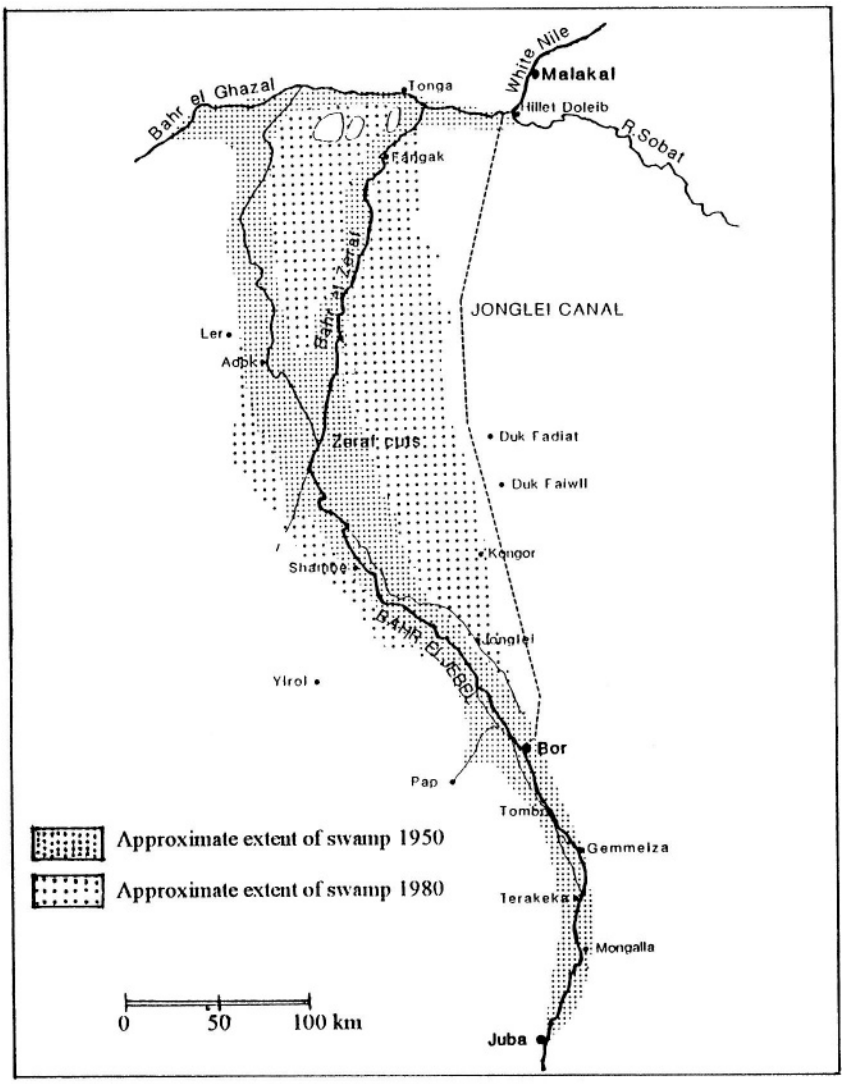

Figure 10.4- Map of the Sudd area (from Howell et al., 1988)

10.1.3 Wetlands in West Africa- This subsection outlines the water balance of the wetlands in the inland delta of the Niger River.

The principal physiographic and hydrologic aspects of the Niger River Basin have already been discussed in section 7.2. The River Niger below the weir at Sansanding (Km 3, 086) enters a large swamp area, which is the remainder of an old Interior Delta, where the slope of the river drops from $5*10^{-5}$ to $1*10^{-5}$. Much of the Niger water is lost in this area by evaporation and infiltration, such that at Diré (Km 2,533) only 35% of the annual discharge of the Niger is left.

The principal items needed for the water balance are the rainfall, evaporation, inflow and outflow. The first two items are estimated as 425 mm and 2,200 mm y^{-1} respectively. The sum of the flows of the Niger at Koulikoro and the Bani at Douna give the river inflow to the delta and the flow at Tosay the outflow from the delta (Sutcliffe and Parks, 1989). The inflow hydrographs at Segou and Douna and the outflow hydrograph at Diré are also shown in Figure 10.5 (Grove, 1985).

The results of the water balance performed by Sutcliffe and Parks (1989) give flooded areas varying on average from 4,600 to 32,000 km^2, and absolute range from 2,000 to 47,000 km^2. According to these authors, the given ranges compare reasonably well to the range of 20,000 to 30,000 km2 for the annually flooded areas between Mopti and Tombouctou obtained by Grove (1985).

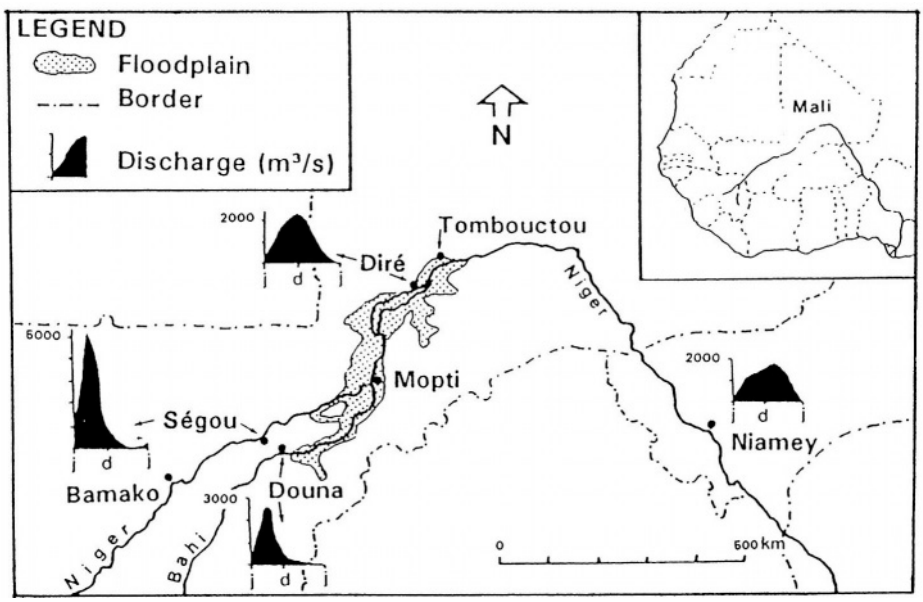

Figure 10.5- Discharge hydrographs of the Niger River upstream and downstream of the Interior Delta

10.1.4 Wetlands in Southern Africa- This subsection will discuss the water balances of the Okavango swamps, Botswana, and the Kafue Flats, Zambia.

1- *Okavango Swamp*: This large swamp occupies a large part of the delta of the Okavango River in northeast Botswana at about 20°S latitude and 23°E longitude. The Okavango Drainage Basin is 97,000 km^2 in area and the river delta area is about 20,000 km^2 at altitude of between 930 and 1,000 m a.m.s.l. The Okavango Swamp has a mean area of 10,000 km^2, varying seasonally between 6,000 and 12,000 km^2.

From the geological point of view, the Precambrian crystalline basement of the Okavango basin is overlain by deposits belonging to the Karoo series. Recent to Tertiary sand deposits of up to 300 m thick overlie this series. The Delta and Swamp rest on these deposits.

The estimates of precipitation and evaporation as adopted by Dincer et al., (1987) and Sutcliffe and Parks (1989) are about the same, 491-500 mm y^{-1} for rainfall and 1,860 mm y^{-1} for Penman's evaporation. The annual inflow to the swamps has been estimated as $10*10^9$ m^3. The swamps have five potential outlets as shown on the map in Figure 10.6. The Thamalakane river is by far the most important outlet. It carries an annual outflow between 30 and $1{,}000*10^6$ m^3 to the Boteti River. According to Dincer et al. (1987), it is reasonable to assume that the main output is evapotranspiration, amounting to more than 95% of the total input to the swamp. With these figures in mind, they were able to draw the annual water balance of the Okavango Swamp as follows.

Lake precipitation	=	$5.0*10^9$ m^3
River (Okavango) inflow	=	$10.0*10^9$ m^3
Evapotranspiration	=	$15.5*10^9$ m^3
Surface outflow (Thamalakane River)	=	$0.3*10^9$ m^3
Groundwater outflow	=	$0.2*10^9$ m^3

According to Sutcliffe and Parks (1989), the best estimate of monthly outflow, $(O)_i$, can be obtained through a linear regression with the monthly inflow with a lag of four months, $(I)_{i-4}$. The relationship can be written as:

$$(O)_i = 0.501(I)_{i-4} - 14.76 \qquad (10.3)$$

where i = month and all items in Eq (10.3) are in 10^6 m^3.

The Okavango River is claimed to bring annually 660, 000 t of sediments, occupying 400,000 m^3, to the river delta. The salinity of water at the inlet of the swamp is very low, some 30 ppm. Despite the large amount of salts entering the swamp each year, 300,000 t, the salinity at terminal areas and outlets of the swamp remains limited to just 120 ppm.

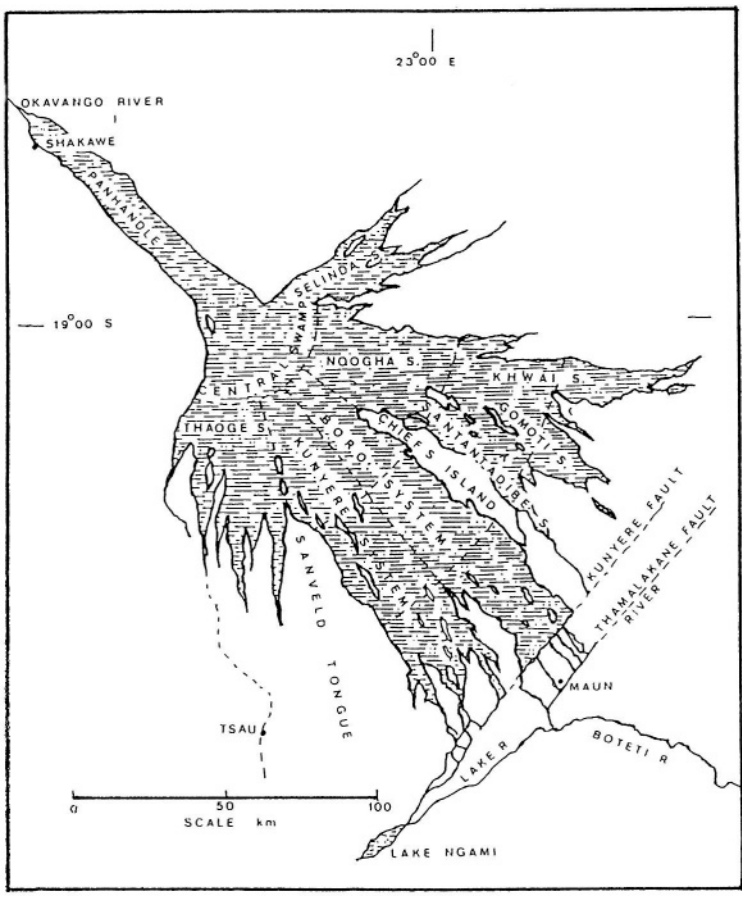

Figure 10.6- Okavango Swamp according to the satellite imagery of July 1984 (redrawn from Dincer et al., 1987)

2- *Kafue Flats*: The Kafue Basin has been briefly described in connection with the hydrology of the Zambezi River Basin in Chapter 8. The Kafue River, a tributary of the Zambezi, is 1, 500 km long and has a basin area of 154,000 km^2. The Kafue River, southwest of Lusaka slowly meanders through the flood plain extending laterally from the Itezhi-Tezhi Reservoir in the west to Kafue Gorge in the east, a distance of about 220 km. Flood plains, swamps and marshy areas provide a noticeable feature of the main part of the basin The swamps located on both banks of the river are saturated every year during the flood season of the river and dry out slowly during the dry season. Figure 10.7 shows a typical cross section of the Kafue Flats, and the flooded areas before and after flow regulation.

The isohyetal map of the Kafue Basin (Burke and Jones, 1993) shows that, whereas the basin receives annually about 1,100 mm rainfall, it loses annually

986 mm by evapotranspiration. The Flats receive less than 900 mm annual rainfall. The annual evapotranspiration outside the swamps was estimated as 785 mm and from the swamps alone as 1,005 mm (Balek, 1977). Additionally, measurements taken on the free water surface indicated that 2,070 mm of water are evaporated in a year. The same reference concludes that the water lost in the Kafue Flats represents 4% of the inflow.

The results obtained by Burke and Jones (1993) show that the unregulated flow at Itezhi-Tezhi amounts to 95 mm depth of water. This flow reduces to just 66 mm at the tail after traversing an area of 45,000 km^2 covered by the Kafue Flats. That is to say the loss upon traversing the Flats amounts to 30%

Mutale (1994) gave a brief description of the KAFLEX and WAFLEX spreadsheet models, and their application to simulate the available water resources and water use in the Kafue Basin. The overall setup of the KAFLEX model comprises ten main elements: the water supply module, water demand module, reservoir operation module, water quality parameter module, flux module, water quality-simulate flow module, river inflow, water quality parameter input, output, and macro programme. The model as such needs some adjustment to be able to show the impact of the Flats on the water balance of the basin taking into consideration different scenarios of releases from the Itezhi-Tezhi reservoir.

According to Matando and Motensen (1998), the basin of the Kafue River is subdivided into the Upper Kafue and Lower Kafue, with areas of 53,810 km^2 and 75,260 km^2 in area. The same reference gives for the Lower Kafue 887 mm annual rainfall, 841 mm evapotranspiration and the rest, i.e. 36 mm goes as runoff. Ellenbroek (1987) reported that the water balance of the Flats largely depends on the discharges at Itezhi-Tezhi.

The carrying capacity of the channel of the Kafue River in the Flats area is claimed to be 170 $m^3 s^{-1}$. As the discharge at Itezhi-Tezhi exceeds this capacity, when flooding occurs. However, the capacity of the channel between Itezhi-Tezhi and Namwala (Figure 10.8) is believed to be 250 $m^3 s^{-1}$, which means that releases less than 250 $m^3 s^{-1}$ are likely to be confined in the river channel, and no flooding occurs, Figure 10.8 also shows the flooded areas of the Kafue Flats before and after regulation (Ellenbroek, 1987). It is equally interesting to examine the maps produced by Drijver and Marchand (1985) showing the flooding areas in normal and dry years with a return period of 20 years before and after regulation.

10.2- Natural Lakes

10.2.1 Definitions and physical aspects- Lakes can be defined genetically into tectonic, volcanic, alluvial, glacial, etc. East African lakes are the result of tectonic movements and volcanic activities during the Miocene (25-12 million

years B.P.). Those movements and activities created depressions and minor lake basins, orientated approximately in the north-south direction. The wide stretch of land extending from Eritrea in the north to the Zambezi basin in the south was lifted up more than 1,000 m. Later this stretch exercised sagging in its middle part and Lake Victoria was formed. This sagging caused the two shoulders to be uplifted, thus forming the Great Rift Valleys. Further tectonic movements in the area formed a series of splits in the earth's crust, of which some were more than 1, 000 m deep and became gradually filled with water.

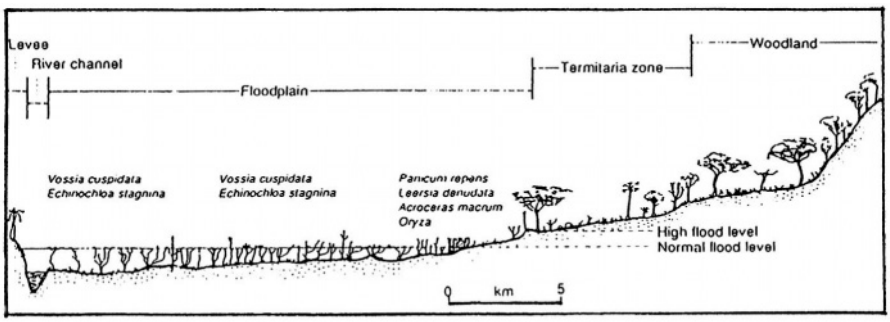

Figure 10.7- Cross section of the Kafue Flats (from Drijver and Marchand, 1985)

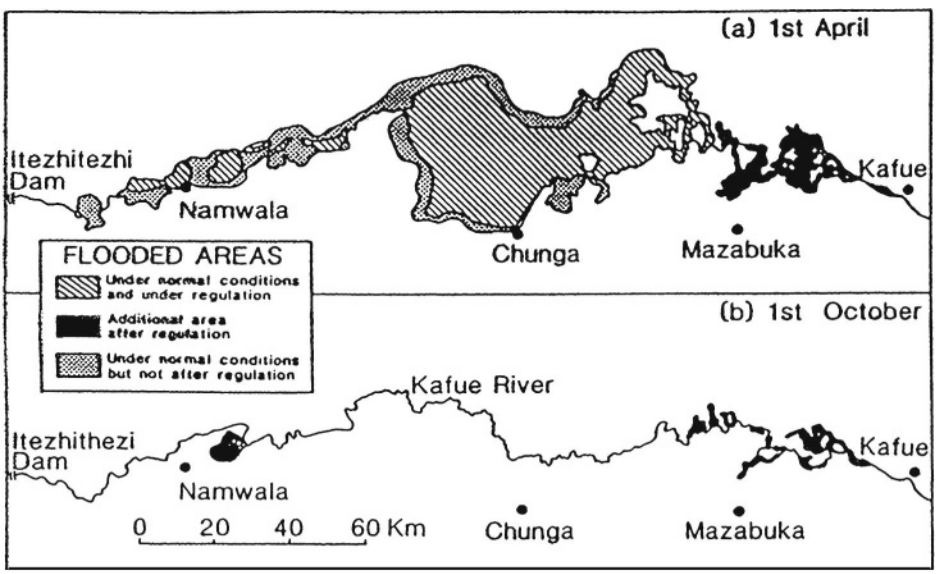

Figure 10.8- Flooded areas of the Kafue Flats before and after regulation (from Drijver and Marchand, 1985)

The Western Rift Valley comprises the Lakes Mobutu, Edward, George, Kivu, Tanganyika, Rukwa, Chiuta, and Chiwa. Of the lakes in the Eastern Rift Valley are the Ethiopian Rift Lakes, Lake Turkana and a number of shallow saline lakes in Kenya and Tanzania (Crul, 1997). The map, Figure 10.9, shows the locations of the East African Lakes.

In order to acquire a better understanding of a lake as an important water resource it is of interest here to review some of the morphometric properties of a lake and the relationships between them. Besides, a thorough knowledge of the water and thermal budgets of a lake and the parameters included in each of them is certainly important.

The main items that enter into the morphometric description of a lake are: the maximum length, L_{mx}; maximum width, B_{mx}; maximum depth, D_{mx}; mean length, L_m; mean width, B_m; mean depth, D_m; effective length (unobsructed straight line distance between an arbitrary position on the lake to the most distant point on the shoreline), L_s; relative depth, D_r; lake area, A; lake volume, V; volume development, V_d and the hypsometric relationship describing the change of surface area with depth. The following expressions are some of the widely used relationships: (Hutchinson, 1957, Kuusisto, 1985)

$$D_r = \frac{D_{mx}}{2\sqrt{\frac{A}{\pi}}}(\%) \tag{10.4}$$

$$V = \sum_{i=0}^{n} \frac{l_c}{2}(A_i + A_{i+1}) \tag{10.5}$$

$$V_d = \frac{3D_m}{D_{mx}} \tag{10.6}$$

where l_c = contour line interval, A_i = cumulative area within the limits of the contour line i, and n = number of contour lines and the remaining notations are as defined earlier.

The mass balance equation of any system, water, heat, salts, etc., is simply an expression that brings into equilibrium the input, output and change in storage in the system dealt with, all over a certain period of time known as the balance period. The inflow to a water body such as a lake comprise the surface runoff brought by rivers and streams, the groundwater supply from the underlying and surrounding aquifers and the direct precipitation on the lake. The outflow comprises the loss of water by evaporation, surface water abstractions and recharge to groundwater. The change in storage is the difference between the storage at the beginning and end of the balance period.

The dynamic processes in lakes have been classified by Starosolszky (1974) into surface forces produced by wind waves, surface oscillations and waves caused by discharge fluctuation, currents caused by flow through the lake and currents caused by surface movement and transport processes such as diffusion, mixing and stratification.

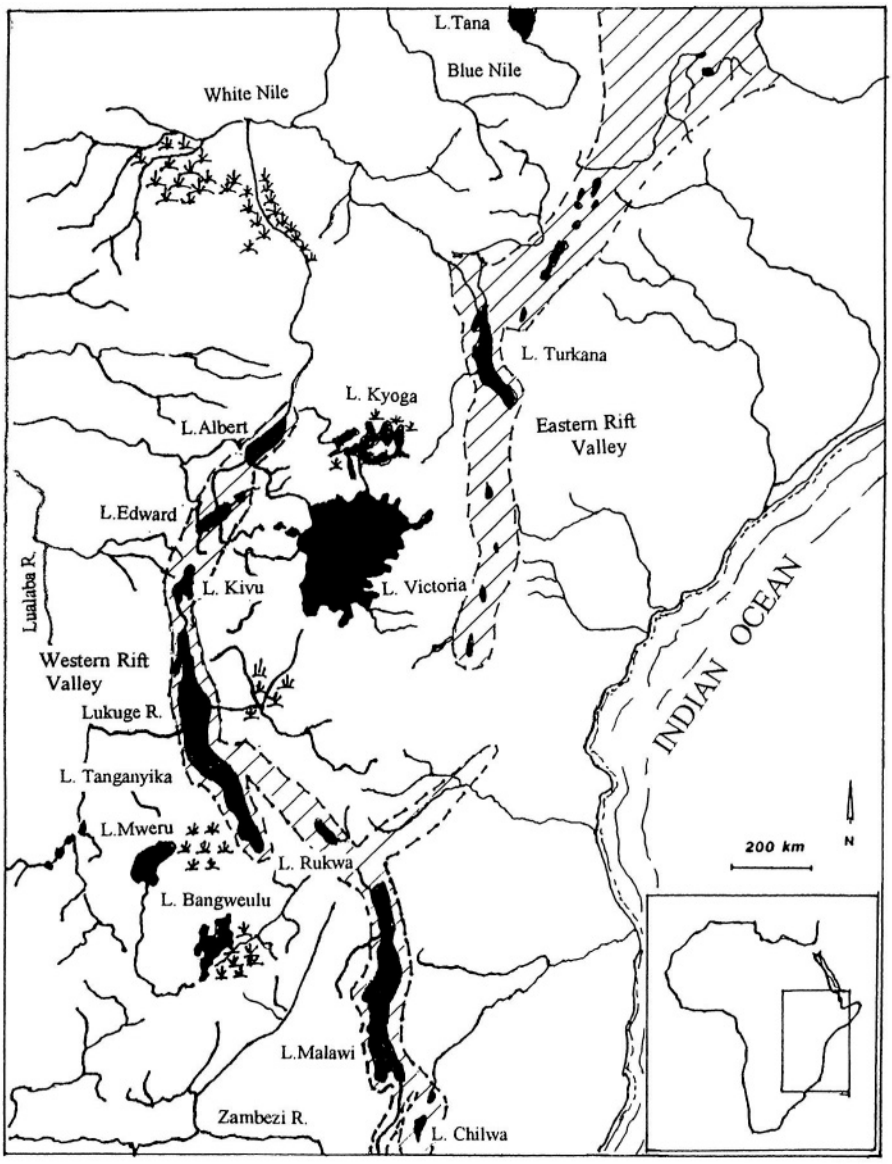

Figure 10.9- Map of Eastern Africa showing the Rift Valleys and their lakes (redrawn from Crul, 1997)

Thermal classification is perhaps the most important physical event in a lake's annual cycle. The sun heats the water surface and its density decreases. This results in a layer of less dense water overlying a denser, cool layer of water. As such, the water mass is classified into epilimnion, the warmer less dense upper water layer and the hypolimnion, the cool denser lower water layer. Between epilimnion and hypolimnion is a transition layer, called thermocline or metalimnion. Shallow tropical lakes, such as Lake George in Uganda, stratify and destratify more than twice a year and are polymictic. Very deep tropical lakes, such as Lakes Tanganyika and Malawi do not completely mix and are called meromictic. Next to climatic conditions, Golterman (1975) adds a morphometric factor determining whether or not stratification will occur. This is the ratio between the depth of water layer that can be mixed by wind action and the total depth of the lake.

While reviewing the thermal conditions in a lake distinction must be made between surface heat transfer and internal heat transfer. The heat balance of the surface can be expressed as:

$$\Delta H = H_{sn} + H_{ln} - H_b + H_{lh} + H_{sh} + H_P \qquad (10.7)$$

where H_{sn} = net short-wave radiation, H_{ln} = net long-wave radiation, H_b = back radiation, H_{lh} = latent heat flux, H_{sh} = sensible heat flux and H_P = heat flux from precipitation. The reader is advised to consult a more specialized book or publication (e.g. Plate and Wengefeld, 1979) about the expressions needed for computing the various items in Eq. (10.7).

Internal heat transfer depends on a number of physical processes, climatic and morphometric. These processes are absorption of short-wave radiation, wind-induced mixing, advective and convective mixing. These processes are graphically indicated in Figure 10.10.

Sediments keep accumulating year after year in lakes and other water bodies. The response of a certain lake to climatological or man made changes can be observed in the thickness of its sediment layers (varves), in their composition and in the rate at which they have been accumulating. In fact one of the methods that can be used for gathering information about the past annual runoff series in a certain area is to examine cores extracted from a closed lake in that area. Periodic bathymetric survey is the technique most often used to detect the changes in the bed levels of a certain lake.

10.2.2- Sahelian lakes: In this subsection the physical description, water balance and water quality of Lakes Chad and Guiers will be outlined. Besides, the impact of two storage reservoirs built on the Sénégal River on the hydrological regime of Lake Guiers and some of the environmental conditions are given.

The case of Lake Faguibine in the Central Delta of the Niger River will be given as an example illustrating the extent of the hydraulic connection between

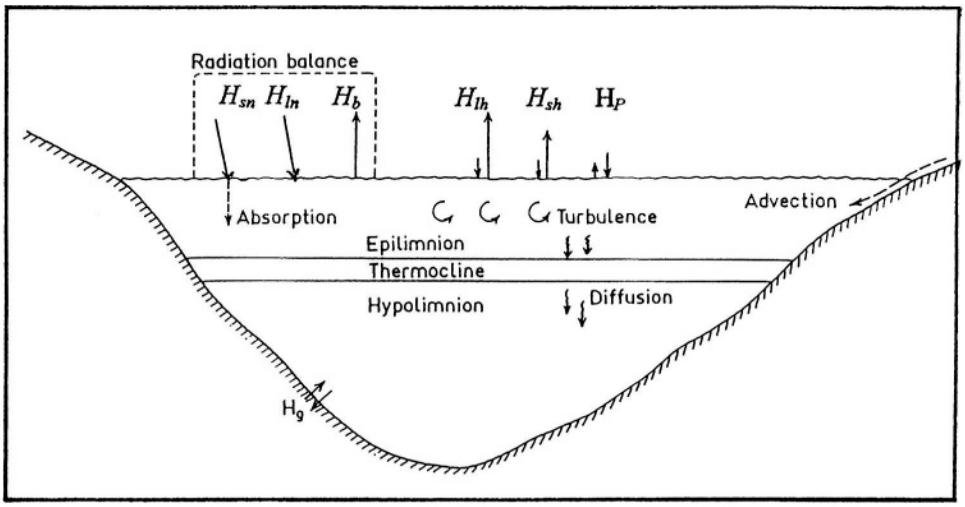

Figure 10.10- The energy balance of water surface and the physical processes affecting the thermal conditions of a lake (Kuusisto, 1985)

the water level in the River Niger and the level of the chain of lakes surrounding the delta.

1- *Lake Chad*: This lake is located between latitudes 06° and 24°N and longitudes 10° and 23°E. The drainage basin of the lake is an endorheic basin covering almost $2.5*10^6$ km^2. The present lake is shared by Chad, Niger and Nigeria, whereas the lake basin is shared by Chad, the Sudan, Central African Republic, Cameroon, Nigeria, Niger and Algeria (Figure 7.19). The lake is generally shallow, 2 to 5 m deep. Depending on the inflow to the lake, the volume varies between 20 and $90*10^6$ m^3.

In the recent times, for which hydrological records are available, the surface area of the lake has fluctuated between 15,000 and 20,000 km^2, with a minimum of 10,000 and a maximum of 25,000 km^2. However, during the 1981 drought, the surface area of the lake shrank to 4,000 km^2. As a matter of fact Lake Chad is particularly susceptible to short-term climatic changes. By contrast the surface area in the geological past was around 300,000 km^2 (Faloci, 1984).

The level of Lake Chad is a good indicator of precipitation fluctuations in the central Sahara and neighbouring areas (Borzenkova, 1980). The highest Lake Chad levels correspond to the warming of the Northern Hemisphere as a whole, while a drop in temperature produces a decrease in precipitation and a drop in lake level. Dry episodes in the Sahara and Sahel zone correspond to epochs of cooling of the Northern Hemisphere as a whole, and sufficiently wet episodes to epochs of warming. Figure 10.11, shows an approximate plot of the

lake level against time in the period from 1100 up to 1980, whereas Figure 10. 11_b shows a more detailed plot of the change in water level from 1956 up to 1977.

The climate that prevails in the northern part of the basin of Lake Chad is Saharan with annual rainfall less than 200 mm, e.g. the mean over the period 1931-1980 at Faya Largeau (station No. 39) was 16 mm y^{-1}. The corresponding figure for the same period was 466 mm y^{-1} at Abécher (station No. 63), increasing to 640 mm y^{-1} at N'Djamena, a few kilometers before the Chari River enters the lake. The annual rainfall, moving further to the south of the basin, reaches approximately 1,129 mm at Sarh and 1,215 mm at Moundou (Sircoulon/ORSTOM, 1976), as the climate becomes strongly tropical. The annual rainfall on the lake varies from year to year from a little more than 100 mm to as much as 450 mm with a long-term mean of 310 mm y^{-1}. The annual rate of evaporation from the lake surface varies from say 2,250 mm to 2,450 mm (Grove, 1985)

The Chari and Logone Rivers supply Lake Chad with water and dissolved load as already explained in sec. 7.3. This supply renders the lake water fresh in the southern part. As water moves to the drier north, where the rate of loss of water by evaporation increases steadily, the northern part of the lake turns out to be more saline than the southern part. Nevertheless, the overall salinity of the lake remains unexpectedly low. There is a strong possibility that this is caused by a substantial inflow of groundwater to the lake.

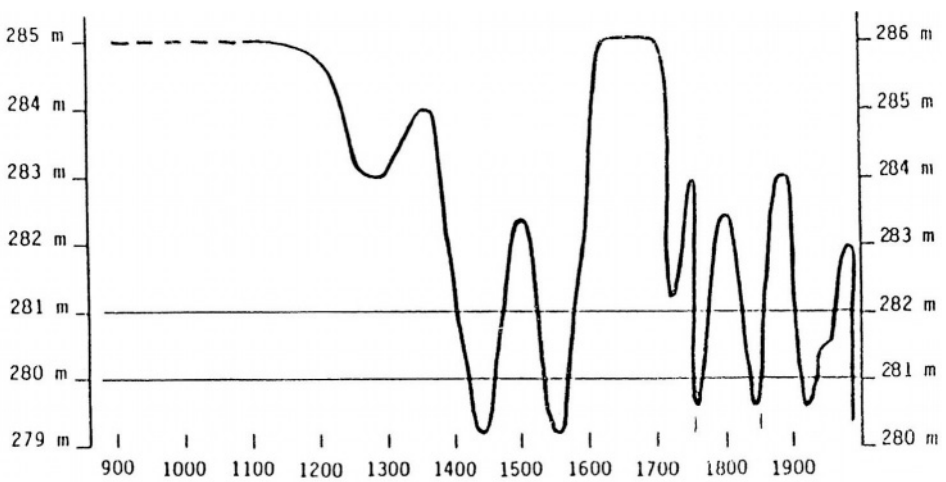

Figure 10.11_a- Fluctuation of the level of Lake Chad from 1100 A.D. up to 1980. The shift of 1 m between the recent shoreline and that of 900 A.D. reflects the accumulation of sediments in the southern basin of the lake during the last 1,000 years.

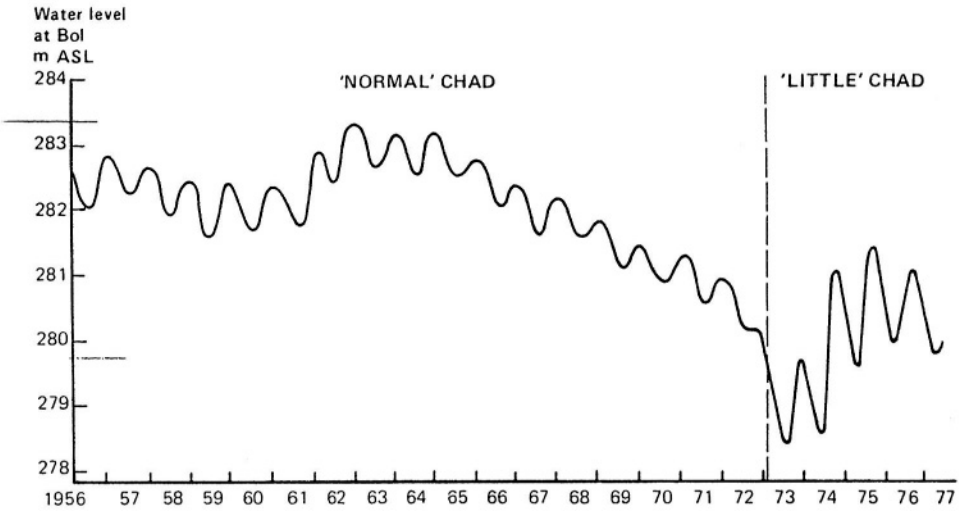

Figure 10.11$_b$-Water levels of Lake Chad recorded at Bol. From 1973 onwards the north and south basins were separated and the area of open water was drastically reduced ('Little'Chad) (Chouret, 1978, in Crul, 1998)

The water supplied by the Logone and Chari is largely derived from eastern Adamaoua in the Cameroon and the Congo watershed in the Central African Republic (Figure 7.20). The estimates of the average annual inflow brought to the lake at N'Djamena by these two rivers has been given in subsection 7.3.2 as $33*10^9$ m^3 y^{-1} for the period 1933-91 and $38*10^9$ m^3 y^{-1} for the period 1933-60 (Rodier, 1964). Faloci (1984) estimated the inflow to the lake averaged over the period 1933-67 as $35*10^6$ m^3 y^{-1}. Lake Chad receives water and dissolved material from other sources than the Chari and Logone. The Yobe River, flowing from Nigeria, has extremely variable discharge and dissolved load. The mean annual volume of water is about $1*10^9$ m^3.

The above mentioned figures can be used to draw an approximate water balance without including surface water abstraction, groundwater inflow to or outflow from the lake or change in its lake storage. The net loss (evaporation-precipitation) from the lake taken as 2,000 mm y^{-1} is compensated by the river inflow to lake, $35*10^9$ m^3 y^{-1}. The assumed condition of no change in the lake level can be verified only when the surface area is equal to 17,500 km^2. A decline in the water level and, consequently, the surface area of the lake, without any change in the groundwater balance or withdrawal from the lake water means an increased rate of loss. Field observations have shown that the surface area of the lake was almost constant from 1956 to 1961 followed by a limited rise between 1962 and 1965. From 1965 to 1972, the lake surface witnessed a drop of about 3.5 m. The level of water underwent heavy ups and

downs in the period starting from 1973, where the lake became known as little Chad. In 1981 the surface area of the lake reached a minimum record of 4,000 km^2.

In a normal year a considerable proportion of the lake water is replenished during the rainy season with the peak inflows occurring in October. The maximum lake level is reached about three months later, i.e. in December. As the lake water falls to a level of 279 m a.m.s.l., a ridge known as the Grand Barrière becomes exposed and divides the lake into northern and southern pools. Although the lake waters in the period 1975-85 rose above the 279 m level, they have failed to re-establish the connection between the two pools (UK Consultant MacDonald, 1985). As a matter of fact, vegetation began to grow rapidly on the exposed sediments in the south pool, and on the Grand Barrière. The flow was obstructed by that vegetation and reduced basically by excessive evaporation, so that only a small amount of water reached the north pool during 1975. A few shallow patches remained and these disappeared by the end of the year. The next season's flood was even higher but only a small amount of water crossed the Barrière (Crul, 1998).

Considering the mean annual concentration of dissolved solids supplied to the lake by the Chari and Logone Rivers to be 50 ppm, the mean annual supply of dissolved solids becomes about $1.8*10^6$ t. The concentration fluctuates between a minimum of 35 ppm in the rainy season and 90 ppm in the dry season. The dissolved load brought by the Yobe to Lake Chad is estimated at about $1*10^5$ t. In spite of the annual supply of $2*10^6$ t of dissolved solids by the Chari and possibly a similar amount from other sources such as dust, the mean conductivity of Lake Chad is only about 250 μmhos, which is about 5 times the conductivity of the Chari. The total amount of solids dissolved in the lake water is probably more than $20*10^6$ t, less than 10 years' supply! (Grove, 1972).

2- *Lake Guiers*: This is a freshwater lake in the west of Sénégal, centered by latitude 16°09'N and 15°52'W longitude. The lake, on the average, is 50 km long, 6 km wide and 2 m deep. Lake Guiers is located in the Sahelian part of the Sénégal, some 80 km east of the Atlantic Coast.

Lake Guiers received in the 1972-94 period a mean annual rainfall of 190 mm and lost by evaporation an average of 2,250 mm. The annual rainfall, however, is quite irregular and varies between 50 and 300 mm. The inflow to the lake is supplied from the Sénégal River via the Taoué canal. A dyke separates the southern part of the lake from the Ferlo Valley, as can be seen in the map labeled Figure 10.12.

Some of the lake water was used for irrigating crops and as drinking water for urban centers including Daker. A certain quantity is released each year to supply the Ferlo Valley with water. The drainage water of the irrigated areas flows back to the lake. These items compose the input and output components

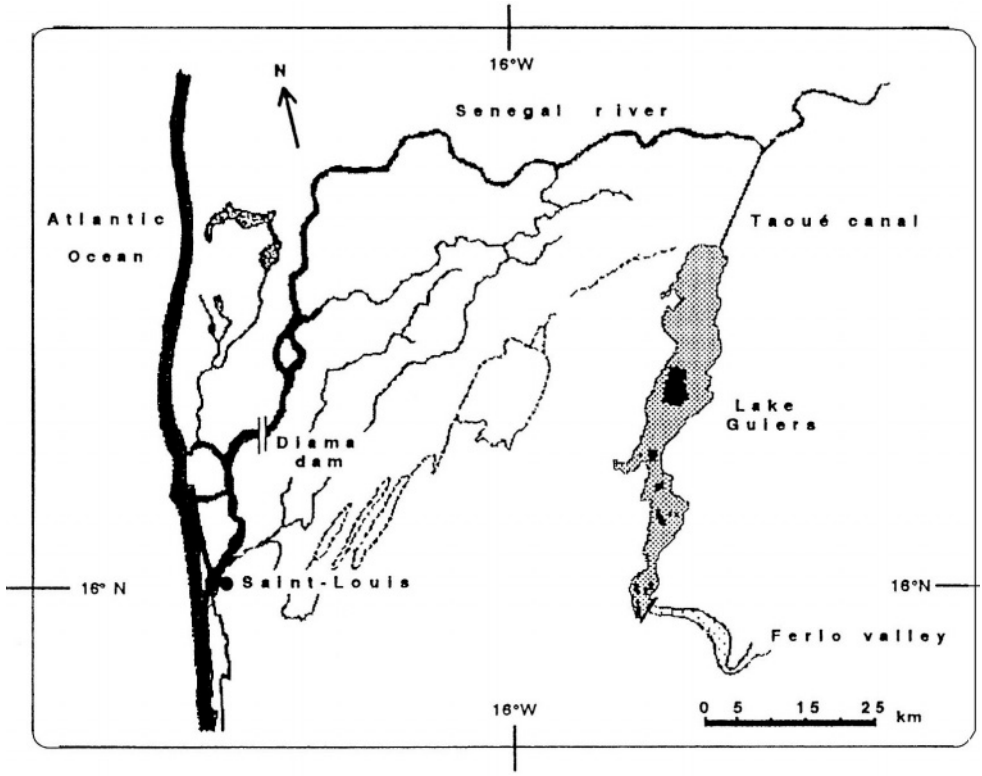

Figure 10.12- Geographical location of River Sénégal, Lake Guiers and Diama Dam (Cogels et al., 1997)

of the water balance of the lake, without including groundwater inflow to or outflow from the lake.

One should not forget that the Sénégal water at the location of the lake used to be salty, at least during the low-flow season. The interesting point here is that the hydrological regime of Lake Guiers has undergone some changes due to the operation of the Diama Dam after 1986 and the Manantali after 1989. The Diama Dam is located at a distance of 100 km downstream from the Taoué-lake junction, and the Manantali Dam is located in Mali more than 1,000 km upstream of the lake. The following is a summary of the environmental impacts of these two dams on the hydrology of the lake

- The average water level, H_m in m, before the Diama Reservoir began to operate in 1986, was 0.42, with annual mean range of variation, dH, equal to 2.13 m. After the operation of the reservoir in 1986 and up to 1991, just as prior to 1986, the lake used to be filled only once a year during the annual flood season. However, the average level, H_m, increased to 0.86 m and the range, dH, reduced to 1.82 m. This changed has been joined by another change caused by the operation of the Manantali Reservoir beginning in 1992. From 1992 to 1994 the parameter H_m increased to 1.50 m and the range dH reduced further to 0.96

m (Cogels et al., 1997). These figures lead to the conclusion that the average lake level has become higher and its range of fluctuation narrower due to the operation of the reservoirs.

The availability of water has encouraged the private initiatives with all merits and demerits. The low-water agriculture has been rapidly replaced by irrigated agriculture. The ensuing problems highlighted an important lag between plans for regional development and the benefits for rural inhabitants, who are not well prepared for such changes. Before 1986, the annual drying up of a large proportion of the lake's shores limited the development of aquatic vegetation. The present hydrological regime of the lake has led to the invasion of the shallow part of the lake in the south by vegetation.

- The change in the hydrological regime of the lake has led to direct as well as indirect changes in the water quality. The calculation of the mean salinity was based on 60 sampling series carried out from 1979-82 and from 1989 to 1992 at 13 stations distributed over the lake. The average salinity of water did not change appreciably in the period 1977-91, instead it remained almost constant at 360 mg l^{-1}. A substantial reduction in the salinity took place from 1992-96, in which the average salinity dropped to 240 mg l^{-1}. Besides, the salinity of water is not homogeneous over the entire surface of the lake. The slope of the north-south salinity gradient depends on the prevailing hydrologic conditions in the year under consideration. The improvement of the water quality has improved the life-pattern of the lakeside inhabitants, especially in the southern zone. On the other hand the improved quality of water has accelerated the development of low-tolerance aquatic plants. Another kind of aquatic vegetation has rapidly developed in the northern part of Lake Guiers, especially in the deep zones that are permanently submerged (Cogels et al., 1997).

Other case studies related to impacts on the environment due to changes in hydrological conditions of river basins originated by construction of dams and creation of artificial lakes will be outlined in Chapter 11.

3- *Lake Fagubine*: This lake is one of the chain of lakes surrounding the Central Delta area in the Niger Basin, Mali. It is located at 16°40'N latitude and 03° 52' W longitude. The geographical location of this lake can be seen on the map in Figure 10.13.

As a result of evaporation and infiltration, the water level of the lakes drops every year about 1.6 m and rises about the same amount during the flood of the Niger. As the water level of this chain of lakes is always below that of the Niger, the flow of water is always in one direction, i. e. from the Niger into the lakes. This inflow starts as soon as the water level at Diré rises above a certain level. The inflow to the lakes is closely linked with the height and duration of

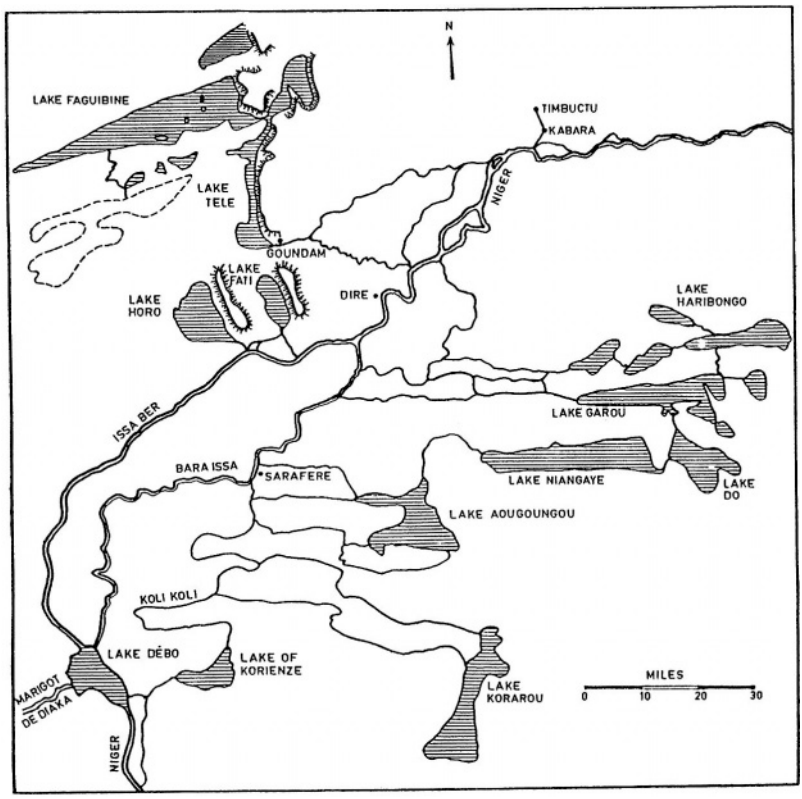

Figure 10.13- Central Delta area of the Niger showing Lake Faguibine and other lakes (from NEDECO, 1959)

the flood of the Niger at Diré. The inflow varies between $0.15*10^9$ and $3.5*10^9$ $m^3\ y^{-1}$ during a low and a high flood respectively (NEDECO, 1959).

A series of wet years results in a rise from year to year of the water level of the lakes and a sequence of low floods of the Niger gives a gradual drop of the water level. The variation of the water level of Lake Faguibine is generally parallel to the fluctuation of the average discharges of the Niger at Diré.

10.2.3 Nile Basin lakes- In this subsection the physical setting, water balance and quality of water of the lakes situated within the Nile Basin will be reviewed.

1- *Lake Victoria*: Lake Victoria is the largest African Lake. It is much younger than Lakes Tanganyika and Malawi. The lake is a depression whose area covers a surface of $68{,}800\ km^2$, at level of 1,134 m a.m.s.l. The surface covered with water is about $67{,}000\ km^2$, the difference between the two surfaces represents the areas occupied by the islands in the northwestern and southeastern extreme ends of the lake. The lake has an O-shaped surface extending from 3°0'S to 0°20'N latitude and from about 31°40'E to 34°53'E longitude. The mean depth

of the lake is only 40 m whereas the maximum depth is 92 m, and the shoreline length is 3,440 km. The catchment area of the lake is estimated as 194,000 km^2 shared between five riparian countries. These are Uganda (32,100 km^2), Rwanda and Burundi (33,600 km^2), Kenya (44,000 km^2) and Tanzania (84,200 km^2). The location of the lake amongst the East African lakes is shown in the map labeled Figure 10.9.

The climate of the lake catchment by virtue of its geographical location is tropical. The climate of the lake itself and the Ugandan part of the basin area is wet whereas the rest of the lake basin area is dry and wet Savanna. The highly elevated parts of Kenya, Rwanda and Burundi enjoy a moderate climate due to their altitude. The average lake rainfall, and so the catchment rainfall, varies depending on the period over which the annual rainfall is averaged. The data included in Table 10., Appendix A, give mean annual rainfalls of 1,122 mm, 1,039 mm and 2,084 mm for Kisumu (station No. 163), Mwanza (station No.171) and Bukoba (station No. 169) respectively. These averages correspond to the periods 1899-1980, 1921-70, and 1921-72 respectively. Piper et al. (1986) gave the averages over the period 1956-78 as 1,278 mm and 1,083 mm and 2,147 mm for the three stations in their respective order. The average annual evaporation is affected too, though very likely to a lesser extent. Table 4.9 includes 11 monthly and annual estimates for evaporation from Lake Victoria. The average of these data, after excluding the first two estimates, is 1,545 mm. Victoria Lake receives inflow from 17 tributaries, the largest of which is the Kagera, whose basin is 68,000 km^2. The Rivers Sio, Nzoia, Nyala, Migori, Mara, Simiyu, etc. join the lake from the east and southeast coming from Kenya and Tanzania. The Victoria Nile is the only river that flows out of the lake. A map of the catchment area of Lake Victoria is shown in Figure 10.14.

The considerable increase of the rainfall over the lake and in its catchment near the end of 1961 has brought excessive inflows to Lake Victoria as well other lakes in East Africa. It is important to remember that before the runoff coefficient attains a constant value it keeps increasing with rainfall till this constant value is reached. As a simple example, assume that the runoff coefficient corresponding to 1,200 mm rainfall is 10%, increasing to 12% with rainfall increase up to 1,500 mm. The runoff depth corresponding to the higher rainfall is 180 mm, whereas the runoff before the rainfall increases is 120 mm only. Under the given conditions, an increase of 25% in rainfall results in 50% increase in the runoff.

The level of Lake Victoria rose by over 2.5 m between October 1959 and May 1964. Following a slight fall the lake began to rise again in 1978 and by mid 1979 had again reached almost to the level of 1964 (see Figure 10.15). Kite (1981) concludead that neither a simple water balance nor a lake routing model had been able to pinpoint the exact cause. The calculated level for the period 1977-80 was in good agreement with the observed level when the model rainfall

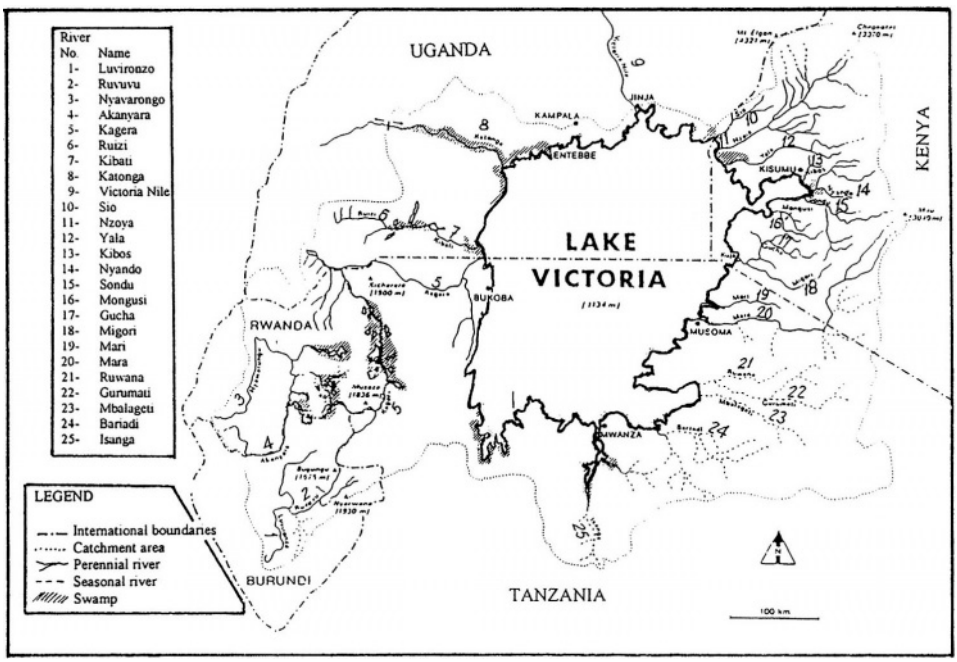

Figure 10.14- Catchment area of Lake Victoria

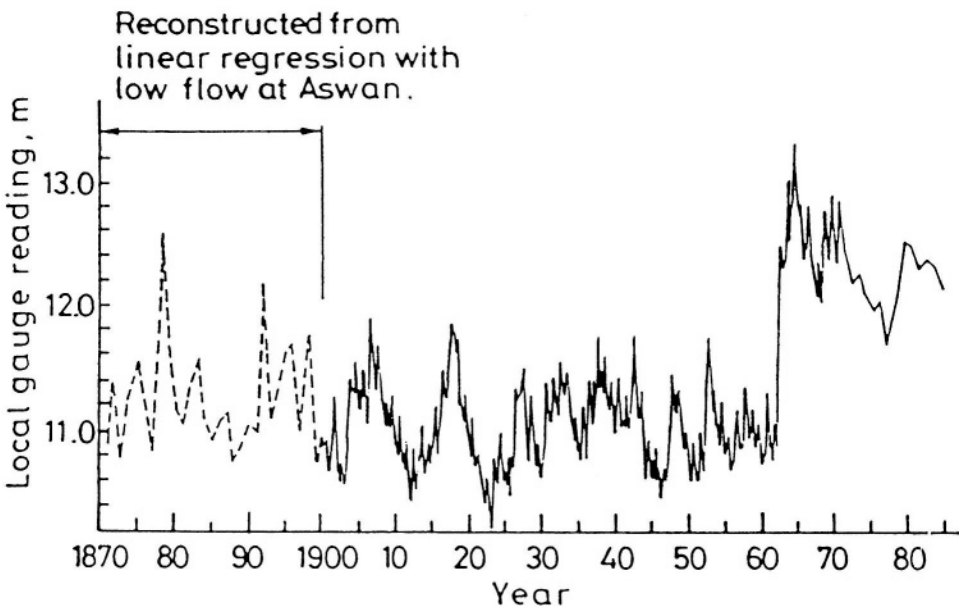

Figure 10.15- Historical and reconstructed water level series of Lake Victoria at Jinga (after Flohn and Burkhardt, 1985)

exceeded the recorded rainfall by 25% in 1977 and 1978 and by 30% in 1979. To the author's opinion the rise can be attributed to the substantial increase of the lake and catchment rainfall, growth of runoff coefficient, reduction of lake evaporation due to increased humidity and decreased cloudiness, and controlled outflow from the lake. Furthermore, the high ratio of the water surface to land surface, which is about 0.35, added to the extensive surface covered by water, makes the lake rainfall very difficult to assess.

Flohn (1987) stated: "The excessive rainy season 1961-62 over East Africa – causing a discontinuous rise of Lake Victoria and the discharge of the White Nile lasting at least 20 years – coincides with an even larger anomaly of sea surface temperature, surface winds and convective cloudiness at the western equatorial Indian Ocean". The high jump of the water level of Victoria Lake and other lakes in East Africa motivated the investigation of any other similar jumps that might have happened before 1896, when the measurement of lake water level began. Flohn and Burkhardt (1985) developed a two-step linear regression model. The relationship between average water level, the local gauge of Lake Victoria in m, in the season September-December, $(V)_{9\text{-}12}$, and the volume of water reaching Aswan in the period from February to June, denoted by $(A)_{2\text{-}5}$ and expressed in 10^9 m^3, can be written as:

$$(V)_{9-12} = 10.0 + 0.0047(A)_{2-5}, \quad (R^2 = 0.44) \tag{10.8}$$

As the discharge data at Aswan is available since the water year 1869/70, Eq. (10.8) was used to reconstruct $(V)_{9\text{-}12}$, which is highly correlated $(R^2 = 0.88)$ with the annual level, $(V)_{annual}$, for the period 1870-98. With this two-step method, the extension of the annual water level series at Jinja from 1870 to 1898 became possible. The series from 1870 up to 1985 is shown in Figure 10.15. The high water levels around 1878 and 1892 were reported earlier by Lamb (1966).

The earliest attempt to draw the water balance of Lake Victoria appears in the work of Hurst and Philips (1938). The formulation of the water balance and the quantification of its various terms over different periods of time appear frequently in the literature that has been published since then. Yin and Nicholson (1998) gave a brief review of 12 published estimates of the mean water balance using different reference periods. In those 12 balances, the estimates of the annual rainfall were in the range 1,145-1,850 mm, lake inflow in the range 215-420 mm, evaporation from 1,130 to 1,595 mm and the outflow from 305 to 570 mm. Despite the considerable width of all ranges of estimates, the range of evaporation estimates remains the smallest.

Extensive studies of the components of the water balance over the period 1956-78 were carried out. They included the use of a relatively large number, 19, of rainfall stations distributed over the catchment together with satellite estimates of direct rainfall over the lake itself. Additionally, the sensitivity of lake evaporation to climatological input data has been evaluated. The results

obtained yield average values of 1,791 mm, 328 mm, 1,532 mm and 524 mm for lake rainfall, runoff to the lake, lake evaporation and outflow from the lake respectively (Yin and Nicholson, 1998). The difference between the input and output, 63 mm, is the average annual rise of the lake level.

Suctcliffe and Parks (1999) also gathered evidence related to the rise of the lake water level in the period before its measurement began in 1896. The same reference summarized the results obtained by the Institute of Hydrology, Walingford, of the water balance estimates over the period 1956-78. The values of 1,858, 343, 1,595 and 524.4 mm have been suggested as average values of lake rainfall, tributary inflow to the lake, lake evaporation and outflow from the lake. The input exceeds the output by 81.6 mm y^{-1}. The observed rise in the balance period was 12.56-10.91 = 1.65 m or about 71.7 mm y^{-1}. The assessment by Howell et al. (1988) of the balance components differs from the figures of the Institute of Hydrology, appearing in Sutcliffe and Parks (1999), in the estimate of lake rainfall only, 1,810 mm y^{-1}. This figure brings the average annual rise of the lake level down to 36 mm.

Each one of the above mentioned water balances, and probably the average of the three can serve as a reasonable description of the high-level period 1956-78. This period does not really represent all states of lake level from 1898 till present. The water balance is unavoidably associated with the period over which the balance is drawn,47.86 pt better with the average lake level in that period.

The lake temperature varies from one location to another and from season to season. The large geographical extent of the lake and the temperature of the tributary inflow are behind the spatial variation of the lake water temperature. The widest range of variation of surface water temperature, as obtained from observations without considering extreme values, is from 23° to 29° C and from 22° to 27° C for the bottom temperature. Not withstanding these ranges of variation, the shallow depth of the lake is the reason underlying the absence of temperature stratification. Instead, complete mixing of water occurs and water temperature varies between 23.8° and 26.0° C, depending on the time of the year (Talling, 1966).

He dissolved oxygen content in the surface water varies between 6 and 10 mg l^{-1} and between 3 and 7 mg l^{-1} for bottom water. The conductivity of water varies from 100 to 179 µS cm-1, the pH from 7.8 to 9.0 for surface water and from 6.9 to 8.6 for bottom water. For more information the reader is referred to Tables 4_a and 4_b, Part II/Appendix B and recent UNESCO Publications (e.g.Crul, 1998).

2- *Lake Kyoga*: In the past pluvial episodes, Lake Kyoga was a larger lake than at present. It is a shallow depression consisting of a number of arms, many of which are filled with swamp vegetation. The geographic locations of Lake Kyoga and its catchment area are shown on the map in Figure 10. 16_a. The catchment is situated between 00°10'and 03°38'N latitudes, and 31°00' and

34°53'E longitudes, all in Ugandan territory. The catchment area is 74,713 km^2 including 4,735 km^2, which represent the surfaces permanently covered by water and permanently and seasonally covered by swamps. The catchment area, with the exception of the Debasien Mountains and the western part of the Elgon Mountain, is characterized by a series of low hills and flat valleys with impeded drainage. This characteristic renders the catchment runoff quite small. The depth of the lake at its western end is from 3 to 5 m, and the maximum recorded depth is 7 m.

The lake rainfall was estimated by Shahin (1985) as 1,220 mm for an average year as well as for the period 1948-70. The estimates for the two years 1969 and 1970 were 1,160 and 1,238 mm respectively (WMO, 1974). The average catchment rainfall for the period 1968-72 is around 1,275 mm (The Nile Basin, Vol. VI, Supplement 7, 1979).

Table 4.10 gives three different estimates for evaporation from Lake Kyoga. Hurst and Philips (1931) estimated the annual evaporation from the water balance over the period 1902-23 as 1,425 mm. The second estimate was developed by the WMO (1974) as 1,546 mm, also using the lake water balance too, but over the period 1946-70. The third estimate, 1,623 mm, was obtained by the author using Penman's method. It is worthwhile to remember that the second estimate, WMO (1974), is just 3% less than the figure for evaporation used in the three water balances of Lake Victoria over the period 1956-78.

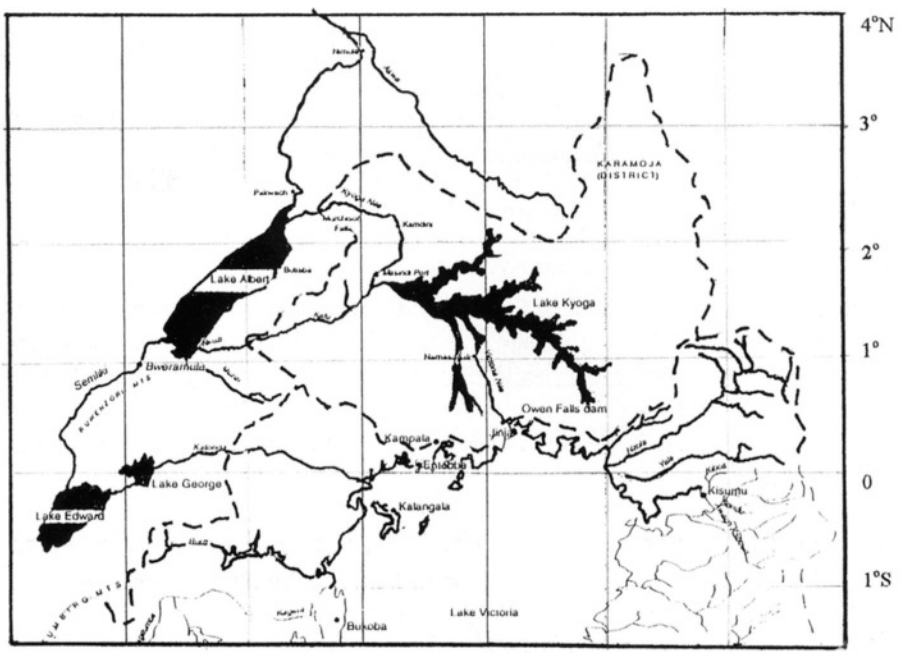

Figure 10.16.- Catchment area of Lake Kyoga

The outflow from Lake Victoria is conveyed to Lake Kyoga through the Upper Victoria Nile and the outflow from Kyoga. is transported through the Lower Victoria Nile up to Lake Albert. The optimum regression expression linking inflow, I in 10^6 m^3 mo^{-1}, and outflow, O in 10^6 m^3 mo^{-1}, can be written as (Sutcliffe and Parks, 1999):

$$O_{(t)} = 1.1331 I_{(t-1)} - 242 \quad , (R^2 = 0.9365) \tag{10.9}$$

where t is the month for which the outflow is considered, length of month is ignored.

The different water balances of Lake Kyoga are summarized in Table 10.2. The last row in this Table shows the average rise or fall per year of the lake level. The change in the gauge readings at Bugondo for the periods 1928-1939 and 1942-70 have been presented by Shahin (1985), and for the period 1912-75 at Masindi Port by Sutcliffe and Parks (1999). As the gauge at Masindi Port has the most complete record of the lake level, it is shown here by Figure 10.16$_b$.

It has already been mentioned that Lake Kyoga is a very shallow lake. As such, there is no chance for any thermal stratification in this lake. A few samples were collected for identifying the chemical characteristics of the lake water (WMO, 1974) The results obtained are included in Table 4c, Part II/Appendix B.

3- *Lakes George and Edward*: The outflow from Lake Kyoga is transported by the Lower Victoria or Kyoga Nile to Lake Albert in the west as shown in the map, Figure 10.15. Lake Albert also receives water from another system consisting of Lakes George and Edward, and the Semliki River and its catchment. The hydrologic characteristics of this system will be discussed in this subsection.

Table 10.2- Water balance of Lake Kyoga (after, WMO, 1974; Shahin, 1985; and Sutcliffe and Parks, 1999)

Component of water balance	Period of water balance				
	1948-70*	1969°	1970°	1951-60^x	1961-75^x
Lake rainfall	1,220	1,160	1,238	1,257	1,328
Inflow	6,861	9,59	9,53	4, 492	9,141
Lake evaporation	1,700	1,425	1,377	1,595	1,595
Lake outflow	6,331	9,475	9,281	4,061	8,902
Change in storage	50	-150	110	93	-28

Explanation

All items of water balance are in mm y^{-1} over a lake surface area of 4,700 km^2

** Shahin (1985) using the data of the Nile Basin, ° WMO (1974) and ^{x} Sutcliffe and Parks (1999).*

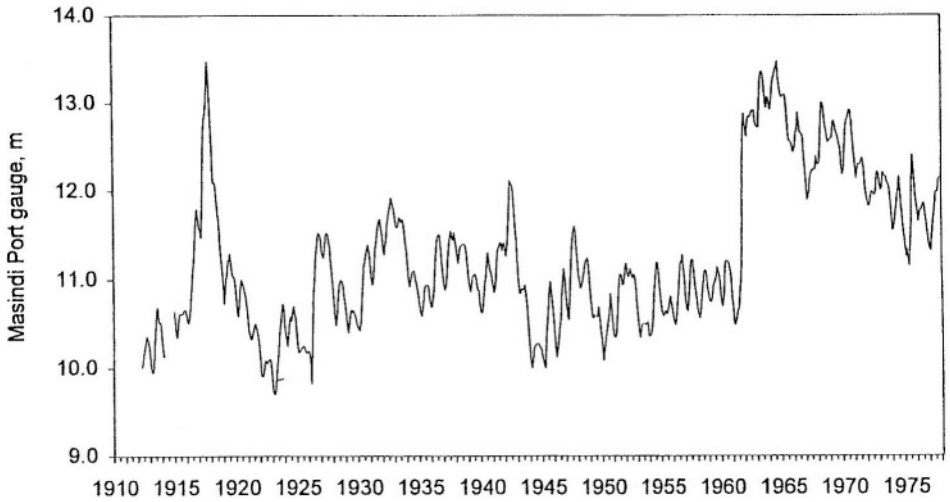

Figure 10.16$_b$- Water level series of Lake Kyoga at Masindi Port

Lake Edward is connected to Lake George by the Kazinga channel. Lake George is situated on the Equator and has a surface area of 300 km^2 at elevation 915 m a.m.s.l. The catchment area of the lake, 8, 000 km^2, is drained by a number of streams flowing down from Ruwenzori Mountain into the Papyrus-covered swamps of the northern end of the lake. Lake George is a shallow lake with a mean depth of 2.5 m. The principal tributary, the Mbuku, carries a considerable inflow to the lake during the flood.

The outflow from Lake George is transported to Lake Edward through the Kazinga channel. Lake Edward lies in the western Rift Valley, and has a surface area of 2, 200 km^2 at elevation 915 m a.m.s.l. The catchment area of Edward Lake, 12, 000 km^2, is traversed by a number of streams often fringed by thick forests at their low ends. The main streams discharging their waters into Lake Edward are: Nyamgasani flowing down the Ruwenzori Range northeast of the lake, the Berarara and Ishasha flowing from the east in a northerly direction towards the lake, a system of streams pouring into the Ruchuru River running down the Mufumbiro Mountains towards the lake in a southerly direction, and the River Ruindi reaching the lake at its southwest corner.

The Semliki River carries the outflow from Lake Edward in addition to the runoff from its own catchment to Lake Albert. The catchment area of the Semliki River is 8,000 km^2 bringing the total area of the George-Edward-Semliki system to 30,500 km^2. The Semliki River after leaving Lake Edward flows a distance of 250 km down the Rift Valley to the west of the Ruwenzori Mountain. The drop of water level between the two ends of the river caused by the rapids in the upper part of its course is 295 m. Discharges of the River Semliki have been measured regularly at Bweramule near Lake Albert from 1940 to 1978.

The old regime of the Nile Basin, as reported by Hurst and his co-workers, considered the lake and catchment rainfall equal to 1,365 mm y^{-1}, and the lake evaporation equal to 1,300 mm y^{-1}. Additionally, the runoff coefficient of the catchment area was taken as 12.5%, and no change in storage was taken into account. As such, the outflow from Lake Edward was estimated as $3.65*10^9$ m^3 y^{-1}. In addition to this volume, the Semliki River receives an annual volume of $2.05*10^9$ m^3 from its own sub-catchment, bringing a total annual inflow of $5.7*10^9$ m^3 to Albert Lake. The values adopted by Shahin (1985) for the period 1948-70 are somewhat different from what is already given. The annual rainfall on the lakes and their sub-catchments was taken as 1,400 mm, lake evaporation as 1,800 mm and the runoff coefficient as 13%. The average rainfall on the sub-catchment of the Semliki itself for the said period was estimated as 1,600 mm and the runoff coefficient as 16%. According to these estimates, the total inflow brought by the Semliki River to Albert Lake must have been $4.69*10^9$ m^3 y^{-1}. The mean annual inflow for the period 1948-70 happened to be 150.6 m^3 s^{-1} or $4.75*10^9$ m^3 y^{-1} with 51% interannual variability.

The comparison between the annual discharge of the Semliki and either the Victoria Nile or the Kyoga Nile shows that the response of the Semliki catchment to the wet spell 1961-70 was much less than the Victoria or Kyoga Nile. The strong response of the Semliki lasted only for the three-year period 1962-64.

The chemistry of the water of Lake Edward is too different from that of Lake George. The salinity of Lake Edward is 600 ppm whereas that of Lake George is limited to 100 ppm. The corresponding dissolved solids are 170 and 670 ppm respectively.

4- *Lake Albert*: The lake is oblong-shaped with a southwest-northeast orientation. It is divided along its major axis between Uganda and Zaïre, located between 01°00' and 02°22'N latitudes and 30°16'and 31°23'E longitudes. The surface area of the lake at elevation 617 m a.m.s.l is 5,300 km^2. The western side of the lake rises steeply up to 2,000 m a.m.s.l. or higher a short distance inland. The bathymetric map of the lake, Figure 10.17, shows that the lake depth at some locations reaches 50 m. The large volume in proportion to surface area makes this lake an attractive storage site.

The drainage basin of Lake Albert is 17,000 km^2. The inflow to the lake consists of the supply brought by the Lower Victoria or Kyoga Nile, the supply brought by the Semliki and the runoff from the lake catchment. These inflows combined with the lake rainfall constitute the input component of the lake water balance. On the other hand, the lake evaporation and the lake outflow through the Albert Nile constitute the outflow component of the balance. The change in lake storage or lake level brings the two components into balance. The old estimates given by Hurst and Philips (1938) were $18.0*10^9$ m^3 y^{-1} as inflow to the lake from the Kyoga Nile, $5.7*10^9$ m^3 y^{-1} the inflow brought by the Semliki

and $2.56*10^9$ m^3 y^{-1} the runoff from the catchment. The annual lake rainfall and evaporation were assessed as 0.81 m and 1.2 m respectively, and the average rise of the lake level as 60 mm y^{-1}. The given figures were used to draw the water balance of the lake over the period 1915-32 (Hurst and Philips, 1938).

The water balance and the values of the items forming the input and output components as mentioned earlier vary from period to period and from one year to another. Table 10.3 summarizes the results obtained from the water balance using more recent data over a number of more recent periods of time. The monthly lake levels at Butiaba gauge for the period 1904-81 are shown in Figure 10.18. The rise in the period 1961-64 exceeded 3 m.

Contrary to the other Equatorial lakes, which have already been discussed, the water of Lake Albert is far more saline. The water conductivity at 20° C is 711 µmohs cm^{-1}, whereas the water conductivity of the other lakes are in the order of 200 µmohs cm^{-1}. The Natrium (Sodium) content in Albert's water is 89.2 mg l^{-1} compared to 26.3 mg l^{-1}, as given in Table 4_c, Part II/ Appendix B (WMO, 1974). This situation has developed basically by the fact that the lake evaporation is far more than the direct precipitation on the lake in addition to the particular morphometric properties of the lake.

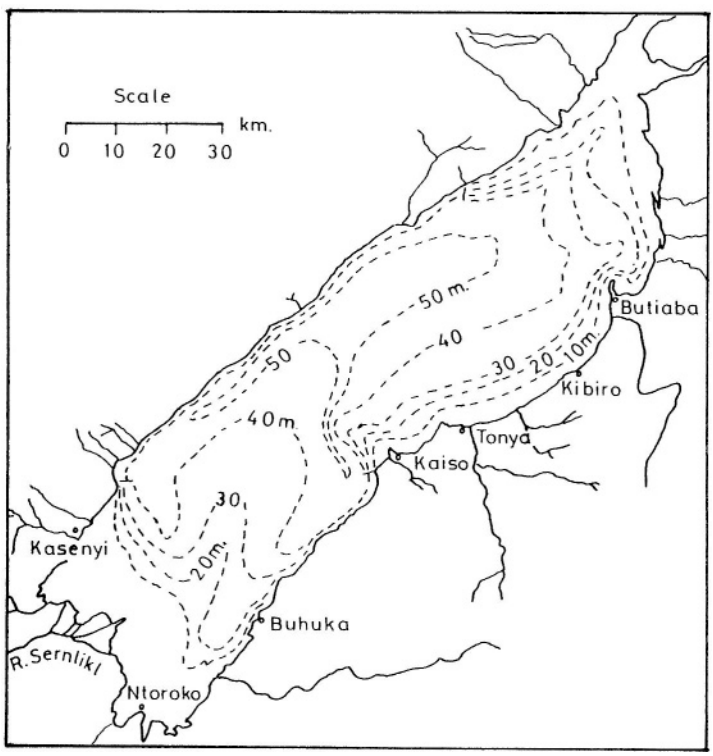

Figure 10.17- Bathymetric map of Lake Albert (Rzóska, 1977)

5- *Lake Tana*: This is the last lake within the Nile River system that is directly connected to the river or any of its tributaries. It is the largest lake in Ethiopia, situated in a depression of the northwest plateau, 1,829 m a.m.s.l. It forms the main reservoir for the Blue Nile (Abbay). Hurst (1950) reported that the source of the Blue Nile is a small spring at a height of 2,900 m and at a distance of about 135 km from Lake Tana. From this spring the Little (Gilgel in local language) Abbay flows down to Lake Tana. There are 60 affluents of Lake Tana, of which the Little Abbay is usually regarded as the most important.

Table 10.3- Water balance of Lake Albert (based on WMO, 1974; Shahin, 1985; and Sutcliffe and Parks, 1999)

Component	Period of water balance				
of water balance	1948-1070*	1969°	1970°	1951-1960ˣ	1966-1975ˣ
Lake rainfall	800	766	1,021	643	766
Kyoga Nile	5,642	8,990	8,799	3,601	7,895
Local inflow	included in the next item			425	504
Semliki River	865	849	1,026	762	904
Lake evaporation	1,431	1,913	2,223	1,595	1,595
Albert Nile	6,364	9,49	9,081	3,781	8,494
Change in storage	42	-260	120	55	-20

Explanation

All items of water balance are in mm y^{-1} over a lake surface area of 5,300 km^2

** Shahin (1985) using the data of the Nile Basin, ° WMO (1974) and ˣ Sutcliffe and Parks (1999).*

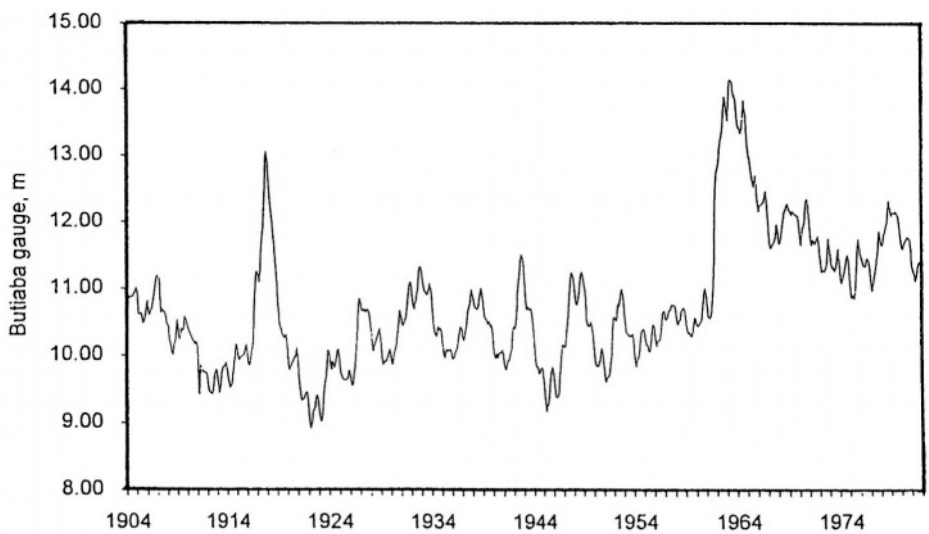

Figure 10.18- Monthly water level series of Lake Albert

The lake surface covers an area of about $3{,}000\ km^2$ with a maximum depth of 14 m (see Figure 10.19). The shoreline of the lake contains some swamps dominated by Cyperus papyrus vegetation. There are geological evidences that the lake was at one time larger than at present. Near Bahr Dar, the lake is dammed off by a lava barrier over which the Blue Nile pours, dropping 43 m to form the spectacular Tisisat Falls. The lake water level in the period 1920-33 fluctuated within a range of 2.0 m. The lake catchment, not including the lake itself, is $13{,}750\ km^2$. The average lake rainfall, being in the order of 1,300 mm, is nearly balanced by the lake evaporation. Considering the catchment rainfall as $1{,}300\ mm\ y^{-1}$ and the runoff coefficient as 22% the catchment runoff to the lake has to be $3.93*10^9\ m^3\ y^{-1}$. This figure happens to be only 2% larger than the average outflow, $3.85*10^9\ m^3\ y^{-1}$, of Lake Tana over the period 1920-33.

The amount of dissolved solids in the water of Lake Tana is the same as that of Lake George, each is much less than either Lake Edward or Albert. The conductivity and chemical composition of the lake water were examined in the period from 08.12.1965-18.04.1966 and reported by Rzóska (1976). A summary of the results obtained is included in Table 4_d, Part II/Appendix B.

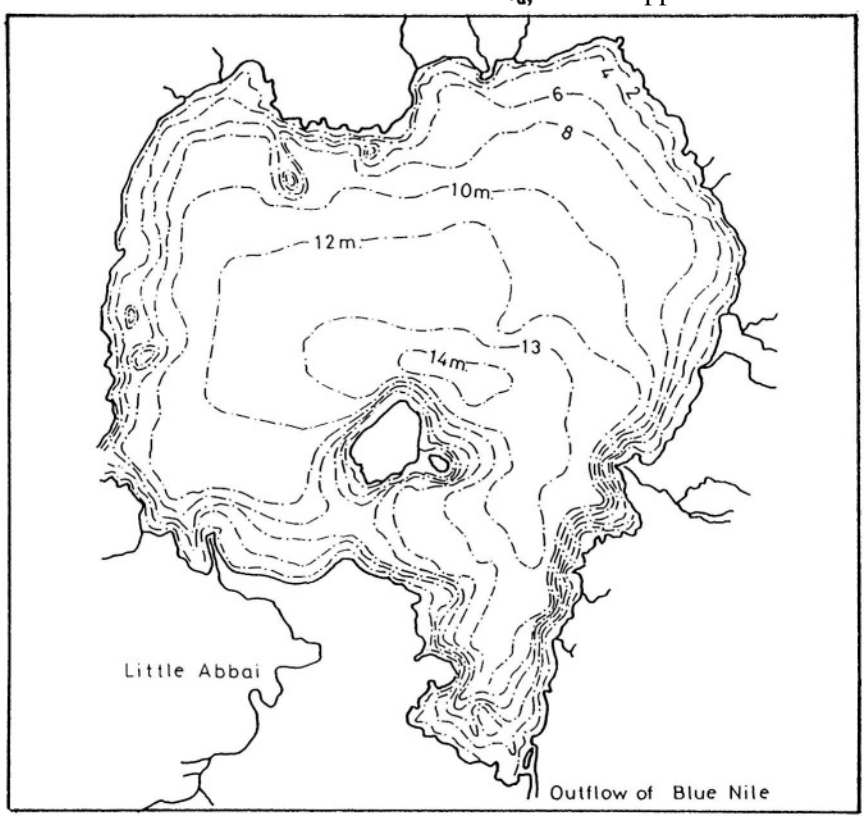

Figure 10.19- Bathymetric map of Lake Tana (Moradini, 1940)

10.2.4 Kenyan Lakes- In this subsection, we shall present two lakes of the Kenyan Rift Valley located outside the Nile Basin. One of these two, Lake Naivasha, has been selected on purpose to show how the water balance even for a small lake can be ambiguous, if not tricky.

1- *Lake Turkana (Rudolf)*: After Lakes Victoria, Tanganyika and Malawi Lake Turkana (Rudolf or Rudolph) is the fourth largest of all East African Lakes. It is situated in the eastern branch of East Africa's Rift Valley, its northern end stretching from Kenya into Ethiopia (Figure 10.9). The surface of the lake is about $9{,}000\ km^2$ at an elevation of 375 m a.m.s.l. Together with Lake Baringo in the south, Lake Rudolf once formed a larger body of water drained by the Sobat River into the Nile system.

Earth movements during the Pleistocene Epoch ($2.5*10^6$-$1*10^4$ years ago), however, created a smaller lake of independent inland drainage. Analyses of late Pleistocene sediment cores indicate that there was a high lake level at some time prior to 20, 000 B.P. This was followed by a very dry period up to at least 12,000 B.P., in which the lake level fell considerably. Furthermore, volcanic outcrops have given rise to rocky shores in the east and south, while the lower western and southern shores consist of sand dunes, sand spits and mud flats (The New Encyclopædia Britannica, Vol. 10, 1988). The lake at present has an oblong shape 300 km long, 25-60 km wide and with a maximum depth of over 75 m.

The climate of the catchment is hot and, except in the extreme north, arid. Lodwar is a key meteorological station (No. 146) located on the Turkwel River in the western part of the lake catchment. Table 10_a Appendix A, gives the mean annual rainfall over the period 1930-80 at this location as 197 mm with a coefficient of variation of 47%. The annual temperature is 29.2° C, varying between 28.2°C in July and 30.2°C in March. The corresponding East African (Kenya) pan evaporation rates are 12.4, 10.3 and $13.6\ mm\ d^{-1}$ average, minimum and maximum for the year respectively. A short description of this pan is given in Chapter 4. According to WMO T.P.105 (1966) the assumption that the Kenya pan reading be considered as 0.75 times the Class A pan reading is satisfactory. Even if the estimate of the Kenya pan is assumed to be 20% higher than evaporation from a free water body, the lake evaporation must be $3.65\ m\ y^{-1}$, quite high indeed.

Despite the fact that a very small part of the lake lies in Ethiopia, the major contribution to the lake inflow comes from there. In fact, the only perennial tributary, the Omo River, flows from Ethiopia. The Kerio and the Turkwel are the most important of the other tributaries to the lake. These tributaries originate in the highlands of Kenya and flow northwards to join the lake from the west. The flow of these streams, which is extremely irregular, is dependent on the local weather. There are however several permanent springs that flow into the lake from below the escarpments, and holes dug into the dry river beds can

fortunately provide a good source of drinking water instead of the undrinkable water of the lake.

Having no outlet, the lake's waters are brackish. As a matter fact the salinity of water of this lake is higher than that of any of the other very large African lakes. Crul (1998) gathered data about conductivity, salinity and alkalinity of water over the period 1931-75 given by different sources. The data have been obtained from samples taken in mid lake, offshore from Furguson's Gulf. The average figures are 3,036 for the conductivity (K_{20}), 2,300 mg l^{-1} for salinity and 22.06 meq l^{-1} for alkalinity. As such the quality of lake water can be described as saline-alkaline.

2- *Lake Nivasha*: This lake is also small, when compared to Lake Rudolf (Turkana) described above. However, it is probably the best known of all Kenyan Lakes due to fact that it is easily reachable, being at a relatively short distance from Nairobi (see the map, Figure 10. 20). Lake Naivasha is a freshwater lake lying at the bottom of Kenya's Rift Valley, just south of the Equator at an altitude of about 1,885 m a.m.s.l. The lake does not have any visible outlet rendering the existence of underground outlets practically the only possibility.

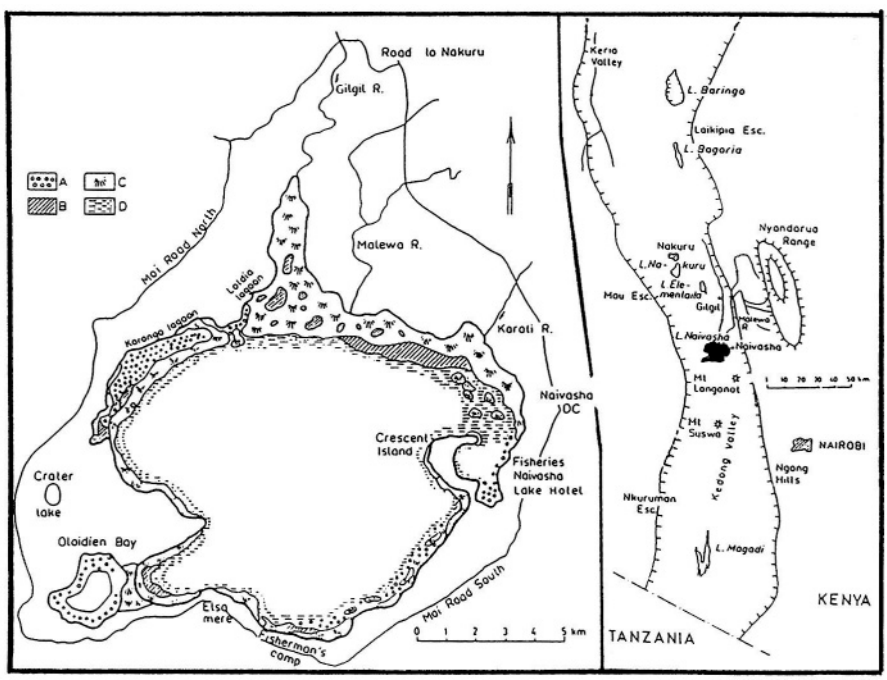

Figure 10.20- Right: Location map. Left: map showing vegetation zones along the shores of Lake Naivasha (1974-1975). Key: A = water lilies, B = Salvinia, C = Papyrus, D = submerged vegetation (cited from Åse, 1987)

Figure 10.20 shows that the different vegetation zones along the periphery of the lake were covered with vegetation, like Papyrus, Salvinia, etc, in the year 1974-75 (cited from Åse, 1987).

The water balance of the Lake Naivasha has been drawn for the period 1936-76 expressing each item as a depth of water in $mm\ y^{-1}$ distributed uniformly over the lake surface. The lake rainfall is 639, the inflow to the lake (Maleva and Gilgil streams) 2,230, lake evaporation/evapotranspiration 1,657 and the fall in lake level 37 mm (Figure 10.21). An annual depth of 1,175 is needed to bring the input and output components into balance. What does this amount represent? Does it represent the (unmeasured) underground outflow, or does evapotranspiration from the vegetation-covered surface exceed the evaporation from the lake water surface, or both? A third question that still holds here is, to what extent one has to trust the value of 0.8 as a proper pan factor?

The study performed by Åse (1987) brought him to the conclusion that evaporation and transpiration from samples of the floating fern (Salvinia) approximately equal the potential evaporation from a free water surface under similar conditions. For Papyrus, the corresponding figure is about 250-300%. As such, the influence of Papyrus, on the water budget of the lake cannot be disregarded. Accepting 0.8 as a pan factor, 10% of the surface covered with Cyperus papyrus, and the potential evapotranspiration of the Papyrus as 300% times the evaporation from the free water surface, the evaporation/ evapotranspiration term in the water balance should be increased to 2,073 mm. This figure reduces the unexplainable depth to $759\ mm\ y^{-1}$. Despite this result, the water budget and water chemistry studies of the lake give strong support to the theory suggesting the existence of an underground outlet of the lake.

10.2.5 Southeast African Lakes- In this subsection the physiography, water balance and water quality of a number of the African Rift Lakes all in the southern hemisphere are reviewed.

1- *Lake Kivu*: This lake is situated in the region of volcanic activity in East Africa. It is almost rectangular in shape, 96 km in length and 48 km in width. The total surface area covered by the lake, $2{,}850\ km^2$, is shared between Rwanda and Zaïre. Lake Kivu has an average depth of 485 m and surface water elevation at 1,460 m a.m.s.l. The Ruzizi River connects Lake Kivu to Lake Tanganyika in the south. The average slope of this river is quite steep, in the order of $5*10^{-3}$, conveying $3\text{-}4*10^{9}\ m^3\ y^{-1}$ to Lake Tanganyika. It might be interesting to note that temperature stratification has been observed in this lake. From a depth of 70 m down to the lake bottom an increase in temperature has been measured, reaching 25.3°C at a depth of 375 m. This observation has been attributed to the contact between the bottom with warm mineral water flowing from the underlying volcanic rock. The warmer mineral water remains stored at the bottom (Balek, 1977).

3- *Lake Tanganyika*: Lake Tanganyika occupies a deep, narrow trough of the western branch of the Rift Valley in East Africa. The lake is located between 03°30'and 8°50'S latitudes and 29°05'and 31°15'E longitudes. The geographical location of the lake among the series of East African lakes is shown in the map labeled Figure 10.9.

Lake Tanganyika is the second largest lake in Africa after Lake Victoria. It is a fresh water lake 673 km long, with a shoreline length of 1,838 km and a mean width of 48 km. The mean depth of the lake is 570 m and the maximum depth, 1,470 m, can be found in the most southern one third of the lake. The present altitude of the lake surface, which is about 773 m a.m.s.l., is 400 to 600 m higher than the altitude 40,000 years ago.

The given dimensions show that the lake has a surface area of **32,600 km^2**, basin area of **231,000 km^2** and a volume of **18,800*10^9 m^3**. The lake is shared between Zaire (45%), Tanzania (41%), Burundi (8%) and Zambia (6%). In addition to these four countries, Rwanda also has a share in the lake basin area (Coulter and Spiegel, 1991).

The catchment area of Lake Tanganyika enjoys a tropical climate. The annual rainfall is limited to about 8 months distributed between two seasons and interrupted by a dry period from May-June to August- September. The overall annual rainfall does not reach 1,000 mm, e.g. at Bujumbura (station No. 172) it

Figure 10.21- Water level series of Lake Naivasha 1880-1980. Symbols as they appear in the reference: F = Fisher, v. H. = von Höhnel, H = Hobley, R = Railway records, TD = Thompson and Dodson, R = Records start, C = comparison between two maps, M = Map value (cited from Åse, 1987)

is 848 mm, with 12% coefficient of variation, and at Kigoma (station No. 178) 977 mm. More data are given in Table 10, Appendix A.

Plisnier (1998), in a study on Lake Tanganyika, concluded that the average air temperature in the lake area has increased in the period from 1964 to 1990 by 0.7 to $0.9°C\ y^{-1}$, while the speed of surface winds has decreased, particularly since the 1970s. Beside the general trend of increase in the air temperature, oscillations around the mean have been observed. These oscillations can be linked to the ENSO phenomena. The correlation between the air temperature at each of Bujumbura and Mbala and the sea surface temperature (SST) has already been discussed in Chapter 2.

During a year of strong winds, the southeast trade wind piles up more epilimnion water in the northern section of the lake and causes a strong up welling in the south. Contrarily, in a year of weaker winds, the dynamics of the whole ecosystem is reduced. The tilting of the epilimnion by the southeast trades becomes less marked in the north and the upwelling in the southern end gets weaker.

The average estimate of Penman's evaporation using the climatic data of three lakeshore stations is about 1,525 mm. This estimate was reduced to 1,350 mm to represent the free water evaporation from the lake for the purpose of water balance calculation (Crul, 1997). Balek (1977) gave $1{,}696\ mm\ y^{-1}$ as another estimate for lake evaporation using Thornthwaite's formula. He added that September is the month of maximum evaporation (167 mm) and February as the month of minimum evaporation (124 mm)

Figure 10.22 shows the lake basin and the affluent streams supplying it with runoff from the riparian countries. It also shows the effluent stream, Lukuga River, taking off water from the lake and supplying it to the Lualaba River. The inflow to and outflow from the lake by these streams are taken into account together with lake precipitation and evaporation from the lake to set up it's water balance.

The annual water balance of the lake presented by Crul (1997) is based on the works of Coulter and Spiegel (1991) and Edmond et al. (1993). In both studies, there is no mention of the groundwater inflow and outflow or of any change in the lake storage. Furthermore, none of the two water balances is accompanied by a sensitivity analysis. Figure 10.23, which covers the period 1909-92, shows clearly that the lake level has never been at rest. Remembering that the surface area is $32{,}600\ km^2$, a change in lake level of just 1.0 cm is equivalent to $0.326*10^9\ m^3$. It is true that the balance suggested by Coulter and Spiegel (1991) shows that the inflow exceeds the outflow by $1.7*10^9\ m^3$, but no explanation is given,

The water balance suggested by Edmond et al. (1993) is given below. In view of the above-mentioned remarks it should be considered as approximate.

Lake precipitation $= 29.0*10^9\ m^3\ y^{-1}$
Inflow to the lake $= 18.2*10^9\ m^3\ y^{-1}$

Lake evaporation $= 43.0*10^9\ m^3\ y^{-1}$
Outflow from the lake $= 4.2*10^9\ m^3\ y^{-1}$

The Ruzizi River supplies water from Lake Kivu in the north to Tanganyika in the south. The annual supply has been estimated as $3.2*10^9\ m^3$. The annual estimates of the lake inflow by the Malagarazi River and other rivers were $6.9*10^9$ and $8.1*10^9\ m^3$ respectively. These figures bring the sum of the stream inflow to $18.2*10^9\ m^3\ y^{-1}$. The lake outflow is equal to $29 + 18.2 - 43 = 4.2*10^9\ m^3\ y^{-1}$. It is claimed that the outflow to the Lukuga, amounting to $4.2*10^9\ m^3\ y^{-1}$, is in agreement with observed discharges.

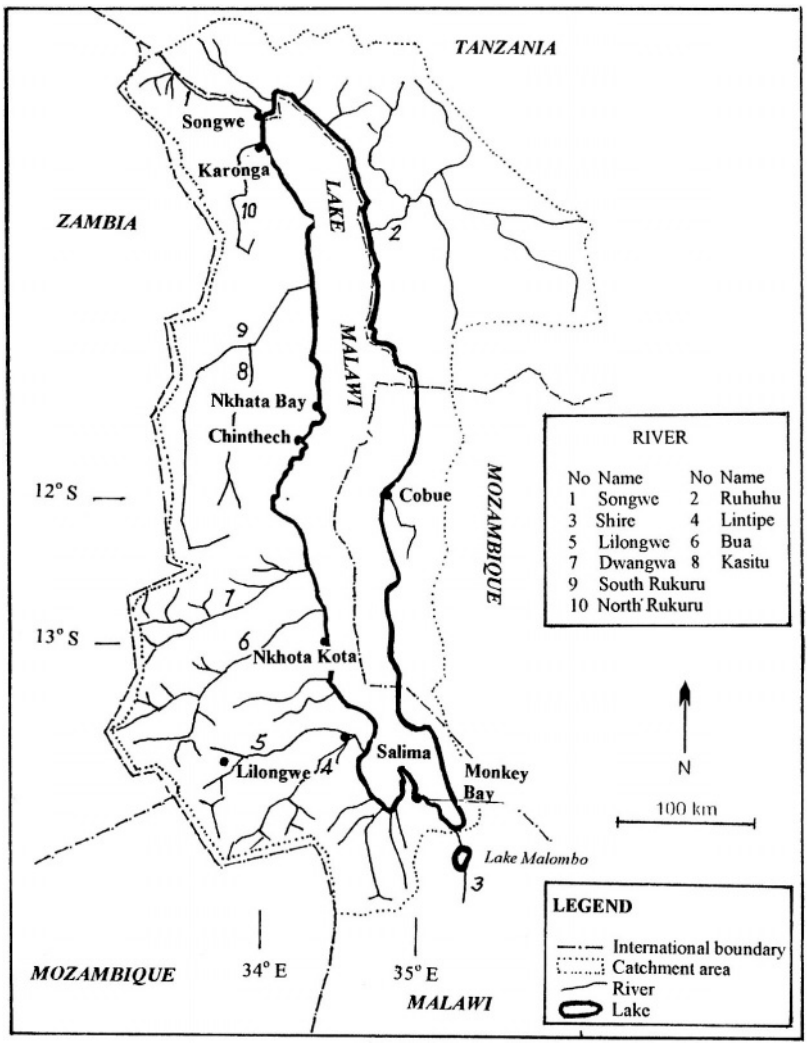

Figure 10.22- Map of the drainage basin of Lake Tanganyika (from Crul, 1997)

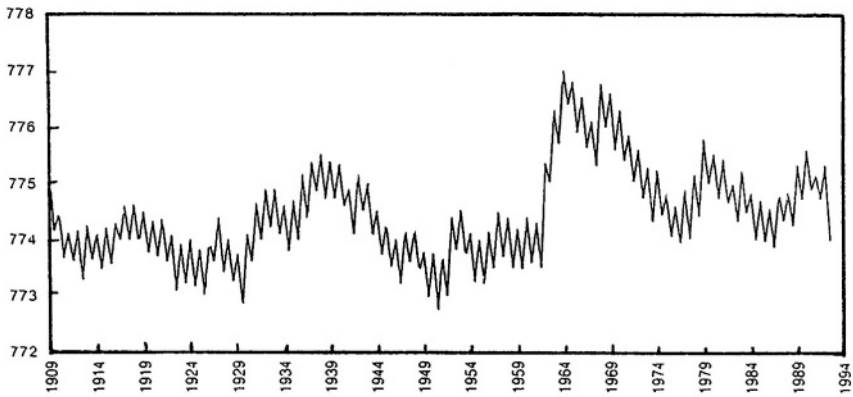

Figure 10.23- Water level series of Lake Tanganyika at Bujunbura (from Crul, 1997)

The lake surface water temperature varies between 23.5 and 26.5° C, whereas the hypolimnion temperature varies in a narrow range between 23.0 and 23.1°C. The depth to the top surface of the hypolimnion layer varies from about 120 m in the northern section of the lake to about 250 m in the southern section of the lake (Golterman, 1975). The surface water conductivity, K_{20}, varies from less than 600 $\mu S\ cm^{-1}$ to more than 750 $\mu S\ cm^{-1}$, and the pH from 9 at the surface to about 8.5 at a depth of 100 m. Obviously these values change from one location to another.

Studies on sediment accumulation in the lake have been ongoing for quite sometime. The accumulated sediments consist of various organic and inorganic substances. The permanently anoxic conditions in the deep waters of Lake Tanganyika coupled with the seasonal pattern of primary production in its pelagic zone encourage the deposition and preservation of finely laminated mud. These layers, used to be called varves in the past, can provide useful information about long-term climatic fluctuations.

The recent sediments are linked to both the whole catchment and the lacustrine basin of the lake. The sediments linked to the catchment are mainly formed by debris originating from weathering and erosion of geological formations. These formations consist of granites, gneisses, quartizites, etc., formed in the Precambrian age. The lacustrine-linked sediments are basically carbonite deposits and other sediments and can be found in the deeper parts of the lake.

3- *Lake Malawi (formerly Nyasa)*: This is the third largest African Lake after Lakes Victoria and Tanganyika. The lake is bounded by 09°30'and 14°30'S latitudes, and 33°50' 35°20'E longitudes. Lake Malawi is another tectonic lake whose geographic location within the chain of the East African Lakes is shown on the map in Figure 10.9. It is thought that Lake Malawi has come into being after Lake Tanganyika.

Lake Malawi is 579 km long, 25-80 km wide, maximum depth of 700-785 m, mean depth 292 m and shoreline length of about 1,500 km. The lake has a surface area of $28,800\ km^2$ and a volume of about $8,400*10^9\ m^3$. The catchment area, including the lake, being $126,500\ km^2$, covers parts of Malawi, Mozambique and Tanzania. The lake itself is only shared by Malawi (80%) and Mozambique (20%) only. The present lake surface is at 472 m a.m.s.l. The level of Lake Malawi, like all East African Lakes, underwent considerable changes at several times in the past. The level 25,000 years B.P. was 250-500 m lower than the level today. These changes seem to be linked to climatic changes.

The lake and its catchment area are situated within the tropical region of Southern Africa. Monthly and annual temperature, rainfall, etc. data at Karong (station No. 189), Nkhota Kota (station No. 202), Mzimba (station No.197) and Lilongwe (station No. 207) are included in Appendix A. The third and fourth stations are located at short distances from the catchment boundary. The UNESCO Report on Lake Malawi (Crul, 1997) describes the climate using the data of Nkhata Bay (Malawi) and Cobuè station (Tanzania). Furthermore, the said report lists temperature and rainfall data from other stations: Chitedzi, Mzuzu, Chitipa, Mulanje, Bvumbwe and Chileka. The figure for lake precipitation used in the water balance is $1,414\ mm\ y^{-1}$.

The annual potential evapotranspiration as estimated by using Penman's method is about 1,340 mm at Nkhata Bay and 1,660 mm at Cobuè. The annual evaporation depth already used in the water balance of the lake is $1,872\ mm\ y^{-1}$ (Crul, 1997).

Figure 10.24 is a map of the catchment of the lake showing the affluent streams supplying it with water. The major inflowing rivers are: the Songwe, Lufra, Rukuru (north and south), Dwangwa, Bua and Lilongwe from Malawi, the Songwe and Ruhuhu from Tanzania and Cobuè and other smaller streams from Mozambique. The Shire is the only river flowing out from Lake Malawi, it joins the Zambezi River above its mouth on the Indian Ocean.

The above-mentioned data have been applied by Owen et al. to the water balance of the lake over the period 1954-80 (cited from Crul, 1997). The groundwater inflow to the lake has been estimated as between 0.2 and $0.6*10^9\ m^3\ y^{-1}$, and the increase in lake storage as $3*10^9\ m^3\ y^{-1}$. The last term corresponds to an increase in the lake water level by about 3 m over the 27-y period of the balance, which can be seen in Figure 10.25. The lake balance, without taking groundwater flow to or from the lake into account, can be written down as follows:

Lake precipitation	=	$40.7*10^9\ m^3\ y^{-1}$	or 1,414 mm
Inflow to the lake	=	$28.8*10^9\ m^3\ y^{-1}$	or 1,000 mm
Lake evaporation	=	$53.8*10^9\ m^3\ y^{-1}$	or 1,872 mm
Outflow from the lake	=	$12.0*10^9\ m^3\ y^{-1}$	or 418 mm
Increase in lake storage	=	$3.2*10^9\ m^3\ y^{-1}$	or 112 mm

The depths in mm already given above are the corresponding annual volumes divided by the lake area.

Neuland (1984) calculated the water balance of Lake Malawi for the period 1954-79 on a yearly basis. The average values for that 26-y period are somewhat different from the above-listed values.

Item	Mean	Standard deviation
Lake precipitation	1,374 mm	236 mm
Inflow to the lake	693 mm	206 mm
Lake evaporation	1,605 mm	61 mm
Outflow from the lake	404 mm	150 mm
Error in the prediction of the minimum water level	0.11 m a.m.s.l	0.09

The analysis carried out by Neuland (1984) on 52 rainfall stations has indicated the presence of a long cycle. Using a sine function with its maximum and minimum at years 1907 and 1959 respectively, with amplitude equal to 26 y of linear rise of the trend line, the annual rainfall series can be written as:

$$P(t) = 42.0 + 2.3\sin(\frac{360^o}{104}t + 214^o) + \sigma\varepsilon(t) \qquad (10.10)$$

where $P(t)$ = annual rainfall at year t, ε = random component normally distributed with zero mean and unity standard deviation, σ = standard deviation and t = time in years. Evaporation is the largest single component in the water balance, yet it is the one that varies least.

Further investigation of the water balance has revealed that, in the first place, rainfall over the catchement, consequently runoff and also rainfall over the lake, can cause high lake levels. These observations have been indicated and supported by both time series and probability analyses. Probability analysis of the lake levels has indicated that the chance the level will reach 477.8 m a.m.s.l. is remote. Under various pessimistic scenarios concerning the hydroclimate of the catchment, the level remains below 477 m. Future assessed lake levels show a tendency to fall approaching gradually an equilibrium around 475 m a.m.s.l.

Drayton (1984) also considered the lake water balance over the period 1953-74. This period is slightly different from the one considered by Neuland, 1954-79. The annual values applied to the inflow and outflow components of this water balance were: lake precipitation 1,350 mm, inflow = 693 mm, lake evaporation = 1,610 mm, outflow = 334 mm and change in lake storage = + 59 mm. Drayton (1984) applied monthly lake precipitation and inflow values to a certain model aiming at predicting the annual maximum monthly level. The lake evaporation and the outflow rating were assumed to remain unchanging. The agreement

between the predicted and observed changes in lake level has been regarded as satisfactory and the model use is consequently justified.

Calder et al. (1995) studied the impact of land use on the water level of Lake Malawi using a water balance model. The investigators claimed that the major fluctuations in lake level both seasonally and annually over the period 1896-1967 have been well described by this model, except for the period 1935-45.
The agreement between observed and predicted levels over the period 1954-94 was also good when the forest cover of the catchment in the period 1967-90 was reduced by 13%. The predicted level, without introducing this reduction into the

Figure 10.24- Catchment area of Lake Malawi (from Crul, 1997)

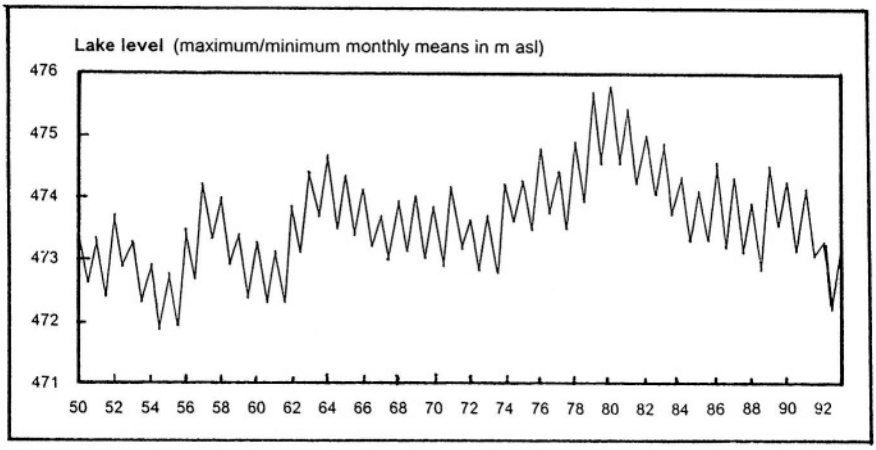

Figure 10.25- Monthly levels of Lake Malawi (Crul, 1997)

model input data would have been about 1 m lower than that observed during the southern African drought of 1992.

The model predictions of lake level have shown to be sensitive not only to uncertainties in the input data but also to uncertainties in the values of the model parameters. The estimation of forest cover and lake precipitation are of particular concern.

Lake Malawi is a thermally stratified body of water, with an epilimnion layer 125 m thick followed by a metalimnion layer down to 230 m below which is the hypolimnion layer. Like Tanganyika Lake, the water of Lake Malawi does not completely mix, i.e. meromictic, with a warmer layer of water overlying cooler water. The data compiled in the UNESCO Report (Crul, 1997) shows that the conductivity increases slightly from 215-225 $\mu S\ cm^{-1}$ at the surface to 220-230 $\mu S\ cm^{-1}$ at 300 m depth. Oppositely, the pH figure falls from 7.9-9.1 at the surface to 7.8 at 300 m below the lake surface.

From ancient times, sediments have been accumulating on the lake bottom, creating layers of mud and sands of various organic and inorganic substances. Presently, deforestation of the lake catchment, especially for agricultural purposes, constitutes a menace to the lake through soil erosion. It has already affected the quality of water of the rivers flowing into the lake.

4- *Lakes Mweru*: This lake is situated in Central Africa, where it is bordered on the east by Zambia and on the west by Zaïre. As such, the lake is shared between Zaïre and Zambia. It lies also in the northwest of the Mweru-Luapula-Bangweulu plain, southwest of Lake Tanganyika (Figure 10.9). The greatest length of the lake is 122 km, average width is 50 km and surface area of 4,920 km^2. The lake's shores are generally flat, except on the rocky western coast.

The Luapula River, the main feeder of the lake enters it on the south, and the Luvua leaves it on the north, flowing northwest to join the Lualaba River. The

extensive Bangweulu Swamps adjoin it to the east and south. The lake surface at normal conditions is at altitude 917 m a.m.s.l. The water level of Lake Mweru, similar to other East African Lakes, has undergone a rise of no less than 2.5 m in the period 1959-62.

5- *Lake Chilwa*: This lake is located at the extreme south of the western branch of the Rift Valley in Malawi, as shown in Figure 10.9. The lake used to be part of a larger lake combining it with Chitua Lake, a short distance to the north. At the present time the accumulation of salt in the lake is due mainly to evaporation of the inflow of freshwater and direct rainfall. It is not known whether this has always been the case since the isolation from Lake Chiuta. The ancient intrusive rocks of the region are rich in minerals and may have contributed much of the salts in the lake.

Lake Chilwa is probably the only exception of all Africa's Rift Valley Lakes as far as the rise of water level in the early 1960s is concerned. On the contrary, despite the limited rise between 1960 and 1963 the lake failed to reach the pre-1959 levels. The change of level against time from 1949 to 1971 as indicated in Figure 10.26, shows a general decline in the water level between 1963 and 1967. In 1968, the Chilwa Lake became totally dry. This was followed by a rise from 1968 till the end of the series in 1971.

The Sombani and Phalobe, two of the important watercourses flowing into Lake Chilwa, descend from the same mountain range. The Sombani traverses dense swamps before reaching the lake, whereas the Phalombe flows through farmlands. It is of interest to observe that the Phalombe, in comparison with the Sombani, discharges close to 840 times more sediment per square kilometer of catchment area (Starmans, 1970, in Crul, 1998).

The water salinity and other parameters of water chemistry during the critical period, 1966-1970, reached unprecedented levels. The range of water salinity was 0.3-16.7‰, alkalinity 1.9-88 meq l^{-1} and pH 8.4-10.8. The increasing salinity was a major factor in changing the composition of the fauna and flora and finally destroying most of them (Crul, 1998).

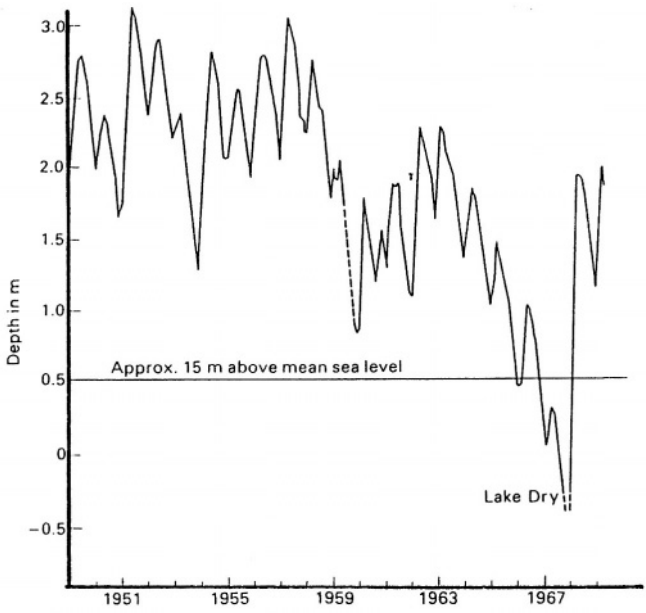

Figure 10.26- Mean monthly water level of Lake Chilwa at Kachulu (cited from Crul, 1998)

CHAPTER 11

LARGE DAMS AND STORAGE RESERVOIRS, AND THEIR IMPACTS

11.1-Introduction

Dams are constructed for such purposes as protection against floods, irrigation, hydropower development, water supply, navigation and transportation, fishing, recreation and water sport. Dam building is traditionally thought to be an effective means of river water management, especially where population is bulging with dramatic increase. Water and energy are the keys to development, this is especially true in Africa. As such, no wonder that many dams have been constructed in the past. It is likely that more dams will be constructed in the future. The diagram shown in Figure 11.1 is a striking example of the growth of the number of large dams in Zimbabwe from just one in 1902 to over sixty by 1973. There are several definitions of a large dam. One of these definitions is that the dam height from the foundation to the crest has to be not less than 15m.

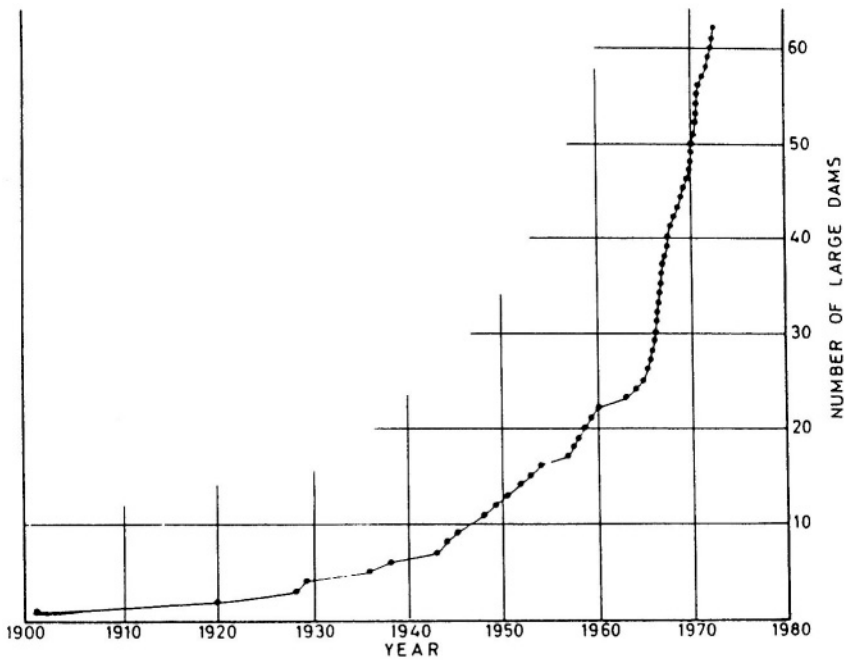

Figure 11.1- Exponential increase in number of large dams in Zimbabwe from 1900-73 (Denny, 1985)

Major dams have their vociferous critics, often because of the severity of geographically remote and unintended side effects, whether ecological, economic or social (Grove, 1985). Hori (1991) classified items of important environmental influences of dam construction on nature and on society as follows:

Influences on nature:

(1) *Area around dam and reservoir*

Micro-climate change	Water leakage
Induced earthquake	Land sliding

(2) *Interior of reservoir*

Water temperature change	Turbidity
Eutrophication	Sedimentation

(3) *Downstream the dam*

Riverbed change	Bank erosion
Salt accumulation in River Delta soils	Deterioration of soil fertility
Seawater intrusion	Coastal erosion

(4) *Others*

Impact on fish	Impact on wildlife

Influences on society:

(1) *Area in around reservoir*

Problems during construction	Displacement of population
Landscape preservation and recreation	Protection of archeological relics

(2) *Whole river basin*

Water-borne and water-related diseases

It should be well understood here that not all of the above-listed items have adverse impacts on nature and /or society. Sediment trapping and inundation of archeological and monumental relics are two examples of the negative impacts of dam construction, whereas hydroelectric power generation and flood protection are examples of positive impacts. Some of the impacts, whether positive and negative, will be given in details in section 11.3 along with description of reservoirs created by a number of large dams in Africa.

11.2- Some Methods of Determining the Capacity of a Storage Reservoir

11.2.1 Seasonal/annual storage- The basic principle is to store all or most of the surplus water carried by a certain river during it's high-flow season in a storage facility and to release it into the river during it's low-flow season. Both operations, i.e. reservoir filling and emptying take place in the same water year. The aim is to regulate the natural supply to meet a given demand for a single or multiple purpose(s). As such, the reservoir capacity should be adequate to store a certain volume of water under a given set of conditions. Additionally, the

reservoir must be kept empty at the beginning of the high-flow season so as to be able to store the excess (surplus) water.

The initial condition (supposedly empty reservoir) for any year *i,* where $i = 1, 2, 3, \ldots, n\text{-}1$, is assumed to be the same for all years. The outflow from the reservoir in this hypothetical, idealized case is assumed equal to the net inflow to the reservoir. No consideration will be given here to the sediments carried by the river and deposited fully or partly in the reservoir.

The monthly inflow and outflow data of an example typifying the case mentioned above are given in the second and fourth columns of Table 11.1 respectively. The third and fifth columns of the same table contain the cumulative or mass inflows and outflows, whereas the last column gives the accumulated inflow minus the accumulated outflow at the end of the same month. The difference between the maximum and minimum cumulative difference between supply and demand represents the required storage capacity. In the case of the example in Table 11.1, the reservoir capacity is $165*10^6\ m^3$.

Quite often it is convenient to plot the third and fifth columns of Table 11.1 against time and measure the largest ordinate difference between the two mass or cumulative curves. This technique is known as the Rippl-diagram method. The so-called differential mass curve is even more convenient as it shows in a clear way the capacity, the filling and emptying phases of the reservoir. The data given in Table 11.1 are illustrated graphically in Figures 11.2_a and 11.2_b.

Table 11.1- Monthly and cumulative supply and demand and difference between cumulative supply and demand for the case of a reservoir with and without initial storage (Shahin, 1985)

Month	Monthly supply	Cumulative supply	Monthly demand	Cumulative demand	Cumulative supply minus cumulative demand	
					a	b
Aug	10	10	45	45	-35	20
Sep	15	25	35	80	-55	0
Oct	30	55	30	110	-55	0
Nov	60	115	15	125	-10	45
Dec	80	195	10	135	60	115
Jan	50	245	5	140	105	160
Feb	20	265	10	150	115	170
Mar	10	275	15	165	110	165
Apr	10	285	25	190	95	150
May	5	290	30	220	70	125
Jun	5	295	35	255	40	95
Jul	5	300	45	300	0	0

Explanation

All listed figures are in $10^6\ m^3$ at the end of the respective months, a = without initial storage, and b = reservoir with initial storage.

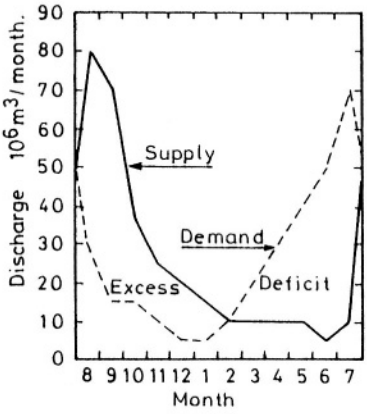

Figure 11.2$_a$- Hydrographs of natural supply and demand

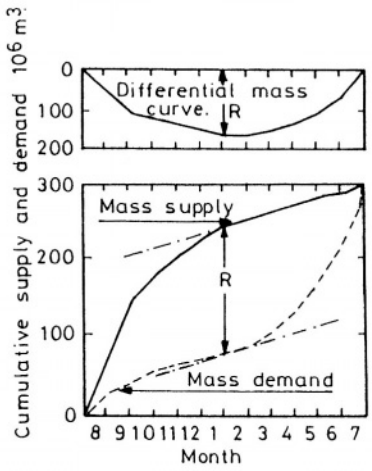

Figure 11.2$_b$- Mass curves of supply and demand, and differential mass curve

11.2.2 Long-term Storage- The Rippl method can also be used to determine the capacity of a long-term storage reservoir. Let the annual flows be $X_1, X_2, X_3, \ldots, X_n$, with a mean of X_m, and the annual outflow be constant equal to αX_m. The draft ratio of the reservoir, α ($\alpha \leq 1$), is the annual outflow in proportion of annual inflow as expressed by Eq. (11.4). The symbols 1, 2, 3, …, n denote the year number in a sequence of n-years. According to Kottegoda (1980) one needs to determine the earliest year, j, in the sequence, which satisfies the condition:

$$X_j \geq \alpha X_m > X_{j+1} \quad , j = 1, 2, 3, \ldots, n\text{-}1 \tag{11.1}$$

Suppose that the condition described by Eq. (11.1) is fulfilled at year $j = K_1$, it has been suggested that two computations must then be made:

1- The length l_1 of depletion period in which the reservoir level remains below the level at time K_1. The notation l_1 represents the maximum duration l for which the following constraint is satisfied

$$\alpha X_m l - \left[\sum_{t=1}^{l} X_{K_1+t}\right] \geq 0 \tag{11.2}$$

2- The deficit D is given by the equation:

$$D_1 = \max_{1 \leq r \leq l_1} [\alpha X_m r - \sum_{t=1}^{r} X_{K_1+t}] \tag{11.3}$$

Let the value of r that maximizes Eq. (11.2) be r_1. In order to find the next value of j, where $j = K_2$, after time l_1+K_1, Eq. (11.1) has to be applied for the years $j = K_1+l_1+1$, $K_1+l_1+2,\ldots$, n-1, until the constraint it represents is satisfied. Eqs. (11.2) and (11.3) are used to determine l_2, r_2 and D_2. This procedure is repeated for the whole sequence and the following statistics evaluated.

The maximum deficit $: \overset{(\alpha)}{\underset{\max}{D}} = D_j = \max(D_i), i = 1,2.3,\ldots.$

The maximum duration $: r_{\max} = r_j$, and

The longest depletion period $: \overset{(\alpha)}{\underset{\max}{l}} = l_j = \max(l_i), i = 1,2,3,\ldots.$

The above three expressions are for a withdrawal rate = αX_m, where X_m is the mean of the inflow sequence. The main design requirement here is the maximum deficit, $\overset{(\alpha)}{\underset{\max}{D}}$, which is the minimum reservoir capacity required to supply αX_m per unit time. Of interest too is the length of the longest depletion period $\overset{(\alpha)}{\underset{\max}{l}}$.

Kottegoda (1980) considered, as an example, the annual flow sequence of the Niger River for the period 1906-56 at Koulikoro station, Mali. The flow sequence was reduced to a unit mean, i.e. the flows were expressed in a modular form. Computations have shown that $\overset{(0.85)}{\underset{\max}{D}} = 0.67$ and $\overset{(0.85)}{\underset{\max}{l}} = 12$. Suppose that the mean annual flow for the given period is $45*10^9$ m^3, the maximum deficit corresponding to $\alpha = 0.85$ should be $0.67*45*10^9$ or $30*10^9$ m^3.

11.2.3 Rippl method applied to synthetically-generated flow data- The Rippl method can be applied as well to synthetic data having statistical properties identical to those of the available historical sequence, which are used to generate the synthetic data. Assume that Q_t denotes the release from the reservoir and $(Q)_m$ is the mean inflow over the record denoted by T- years. The draft ratio or extent of reservoir development, α, can be expressed by the relationship:

$$\alpha = \int_0^T Q_t dt \Big/ \int_0^T (Q)_m dt \qquad (11.4)$$

with the constraint $0 \leq \alpha \leq 1$. Again, consider the simple case of draft ratio $\alpha = 1$ and the reservoir release is constant with time, i.e.

$$Q_t = \text{constant} = Q \tag{11.5}$$

and the cumulative curve, C_t, of the inflow, I_t, as used in the Rippl method is expressed by the relation:

$$C_t = \int_0^t I_t dt \tag{11.6}$$

Eq. (11.6) can be rewritten for a sequence, n, of discrete time increments of one month, Δt, as:

$$C_t = \sum_{t=1}^{t} I_t \Delta t, \qquad t = 1,2,3,\ldots,n \tag{11.6'}$$

Schultz (1976) applied Eq.(11.6') to the 20-y (240-mo), 1947-66, flow sequence of the Kinzig River, Germany. Assuming that the release from the reservoir is maintained constant at $Q = 20.9\ m^3\ s^{-1}$, which is equal to the mean inflow (α =100%), the reservoir capacity, R, will be $785.4*10^6\ m^3$. He concluded that a reservoir of a total capacity of $785.4*10^6\ m^3$ with an initial storage of $536.8*10^6\ m^3$ will never fail to meet the set demand if the same inflow time series (1947-66) would occur again, a condition that can hardly be realized in practice.

In general, two important conclusions can be drawn from the above example. The first is that there is an unknown probability that the reservoir will fail in meeting the target yield, and the second is that the reservoir capacity is dependent on the length of record. For example, the reservoir size that corresponds to the first ten years of the series, 1947-56, is $546.3*10^6\ m^3$ and to the 20-y series is $785.4*10^6\ m^3$. In fact these two conclusions illustrate the basic deficiencies in the Rippl-diagram method.

Again, Schultz (1976) suggested incorporating synthetically generated data to increase the number of sequences that have to be worked out by the Rippl-diagram method. A formula developed by Thomas & Fiering (in Mass et al., 1962); Fiering and Jackson, 1971) can be reasonably used to generate as many streamflow sequences as needed. The formula can be written as:

$$I_{i,j} = (I_m)_j + r_{j,j-1}[I_{i,j-1} - (I_m)_{j-1}]\frac{s_j}{s_{j-1}} + \varepsilon_{i,j} s_j \sqrt{1 - r^2_{j,j-1}} \tag{11.7}$$

where I = inflow, i = year number, j = month number = 1,2 ,3 …, 12, $(I_m)_j$ = mean inflow of the jth month of the year, rj,j-1 = correlation coefficient between flows in month j and j-1, s_j = standard deviation of the flows in month j and $\varepsilon_{i,j}$ = standard normalized random variable corresponding to year i and month j.

Sequences of 100-y of data were generated using Eq. (11.7), one time using historical data of 20-y in length, and another time using data of 45-y in length. The number of simulation runs was 100 for the generated sequences based on 20-y historical data and 150 for those sequences based on 45-y historical data. The mean reservoir size derived from the 100 simulations of sequences based on 20-y historical data was $2.02*10^9$ m^3 and from the 150 simulation runs of sequences based on 45-y historical data was $2.19*10^9$ m^3. This example shows that the range values obtained from synthetic data are practically independent of the length of observation period, a fact that eliminates one of the major deficiencies of the conventional Rippl method (Schultz, 1976).

11.2.4 Century storage and the Hurst phenomenon- While embarking on water storage in the Nile Basin, long-term storage is often referred to as century storage. This type of storage has been frequently examined in relation to Nile Control projects aiming at the full utilization of the Nile water.

Hurst and Phillips (1938) in Volume V of the Nile Basin, pp 81-90, discussed the old proposal of Sir William Garstin regarding the possibility of constructing a dam below the outlet of Lake Albert so as to convert the lake into a huge reservoir. This proposal, among other projects, was also included by Sir Murdoch MacDonald in his report on the Nile Control. In that discussion, one finds mention of the mean and standard deviation of the outflow discharge of the lake, range of accumulated departure from the mean, accumulated deficit and difference between the draft and the mean. In the same discussion, empirical relationships have been suggested and some calculations worked out using the then available sequences of the Nile discharge Nile at Aswan, outflow of Lake Albert and rainfall at the city of Milan, etc.

In our review of the theorem of century storage, we shall adhere as much as possible to the original notations used by Hurst and his co-workers while formulating their theorem. Some of these notations are different from what have appeared in the previous subsections.

The design and implementation of Nile control projects came to a halt during the Second World War, 1939-45, and the few years that followed. That period, however, was not wasted. On the contrary it led Hurst and his co-workers Black and Simaika to formulate and verify the theorem of long-term or century storage using a wide diversity of geophysical and other phenomena. The next paragraphs contain a brief description of the basics underlying this theorem.

The crude range, R_n, of a given sequence X_1, X_2, …., X_n having a mean or expected value $E(X) = \mu$ can be obtained from the expression:

$$R_n = \max\{0, \max_{1\le i\le n}(X_1 + X_2 + \ldots + X_i - i\mu)\} - \min\{0, \min_{1\le i\le n}(X_1 + X_2 + \ldots + X_i - i\mu)\} \quad (11.8)$$

It is often practical to compute the difference between the cumulative positive departure from the mean, D_n^+, and the cumulative negative departure from the mean, D_n^-, where the mean as used by Hurst and his co-workers is denoted by $M = \sum_1^n X_i / n$. As such the adjusted range, R_n^*, can be given by the equation:

$$R_n^* = \max_{1\le i\le n}(X_1 + X_2 + \ldots + X_i - iM) - \min_{1\le i\le n}(X_1 + X_2 + \ldots + X_i - M) = D_n^+ + \left|D_n^-\right| \quad (11.9)$$

In order to compare the results obtained from different sequences, one has to compare their re-scaled ranges. A re-scaled range is the adjusted range given by Eq. (11.9) divided by the standard deviation, s_n, of the sequence, i.e.

$$R_n^{**} = R_n^* / s_n = R_n^* / \{\sum_{i=1}^n (X_i - M)^2 / n\}^{1/2} \quad (11.10)$$

Feller (1951) found that the expected range of stationary independent random variables can be given by the asymptotic expression:

$$E(R_n^*) = \sqrt{\pi/2}(n)^{1/2} \approx 1.2533(n)^{1/2} \quad (11.11)$$

Hurst (1956) reached the same result through his coin-tossing experiments. The result given by Eq. (11.11) is valid when n is large enough, i.e. 1, 000 or more. He also showed that the variance of the re-scaled adjusted range is

$$Var(R_n^{**}) = 0.07414n \quad (11.12)$$

Eq. (11.12) holds for n ≥50-values. Of important significance is the relation connecting the rescaled range and the length of the sequence given by:

$$R_n^{**} = (n/2)^k \quad (11.13)$$

where k varies from a minimum of 0.46 and 0.96 with a mean of 0.73 and standard deviation of 0.092 for the sequences examined by Hurst.

Analogous to Eq. (11.13) is the general expression suggested by Mandelbrot and Wallis (1968) given by:

$$E(R_n^{**}) = C(n)^H \tag{11.14}$$

where, C is a constant ≈ 0.71 for streamflow sequences and H is the sample estimate of Hurst coefficient h. The fact that values of $H \neq 0.5$ are found in natural sequences as air temperature, river stage, discharge, etc., whereas for normal independent processes the asymptotic value, h, of H is 0.5, which has become known as Hurst phenomena. From the 1950s till the present, the literature on stochastic processes in hydrology is full of a large amount of research papers and publications relevant to the range and deficit analyses and their application to the theorem of century storage.

11.3- Large Dams and Reservoirs in Africa

Ten of the largest dams in Africa, all on perennial rivers, are outlined in this section. The reservoirs created after the construction of these dams have surface areas in the wide range from about $200\ km^2$ to over $8{,}000\ km^2$ under normal operation conditions. The reservoirs as shown on the map, Figure 11.3, are situated in the following areas:

- Three storage dams are located in the Nile Basin. These are the Aswan High-Dam on the Main Nile in Egypt, Er-Roseires on the Blue Nile, Sudan, and the Owen Falls Dam on Victoria Nile in Uganda.
- Three storage dams are located in West Africa. These are the Manantali on the Bafing River in Mali, the Akosombo on the Volta River in Ghana, and the Kainji Dam on the Niger River, Nigeria.
- The Inga Dam is located on the Zaire River in the Congo Basin, Congo (Kinshasa), Central Africa.
- Three dams are located in Southern Africa. These are the Kariba Dam and the Cabora Bassa Dam, both on the Zambezi River in Zimbabwe, Zambia and Mozambique, and Gariep Dam on the Orange River, South Africa.

11.3.1 Aswan High Dam- This dam is located on the Nile River, Egypt. The construction of the dam began in 1960 and continued till 1968 and the hydroelectric power plant from 1967 to 1972. It is a rock-fill dam 111-m high, provided with a grout curtain 213 m deep as shown in the cross section, Figure 11.4. The dam is equipped with a diversion canal on the eastern bank of the river designed to pass a discharge up to $11{,}000\ m^3\ s^{-1}$. It consists of open canal reaches in the upstream and downstream parts joined in the middle by the main control tunnels under the dam body.

The reservoir at its storage level, 183 m a.m.s.l. is located between latitudes 23°58'N in Egypt and 20°27'N at the Dal Cataract in the Sudan, and between longitudes 30°07'E and 33°17É. The reservoir is about 496 km long and includes two sections: Lake Nasser in Egypt and Lake Nubia in the Sudan. The combined surface area varies from about 3, 000 km^2 at level 163 m to 6, 200 km^2 at level 180 m to 6, 750 km^2 at level 183 m, all a.m.s.l. The depth of water varies from a mean of 21 to 25 m and the maximum depth from 110 to 130 corresponding to surface water levels of 160 and 180 m. a.m.s.l. respectively. There are two sets of estimates for the capacity of the reservoir. The first is 65.9 and 156.9, 10^{*9} m^3 (Entz, 1976), and the second 61.5 and 149.5, in 10^{*9} m^3 (Abul-Atta, 1978), each pair of values corresponds to 160 m and 180 m a.m.s.l. respectively.

Rewriting Eq. (11.14) as:

$$R_n^{**} = 0.61(n)^{0.72} \qquad (11.14')$$

Eq. (11.14) can be rewritten as:

$$R_n^{**} = 0.61(n)^{0.72} \qquad (11.14')$$

Substituting 100-y for n and $19.3*10^9$ m^3 y^{-1} for the standard deviation, s, the range can be determined from Eq. (11.14') as $325*10^9$ m^3. This volume is too large to be considered for live capacity of a century-storage reservoir guaranteeing a draft equal to the mean, $92*10^9$ m^3 y^{-1}. In addition, a storage facility with capacity that much, added to other volumes needed for dead storage and flood storage, does not exist in Egypt.

Hurst et al. (1951) reviewed their calculations, using the original data sequences added to them other new sequences, aiming at developing an expression for the storage capacity of a reservoir guaranteeing a draft, B, less than the mean. One of the expressions they developed can be written as:

$$\log_{10}(S / R_n^*) = -0.08 - 1.00(X_m - B)/s \qquad (11.15)$$

Substituting $90*10^9$ m^3 for S, Eq. (11.15) gives the quantity B as $83*10^9$ m^3 y^{-1}. This draft is close to the long-term average natural supply at Aswan. Bearing in mind that the storage losses are, on the average, about $11*10^9$ m^3 y^{-1}, leaves a net draft of $72*10^9$ m^3 y^{-1} to be shared between Egypt and the Sudan.

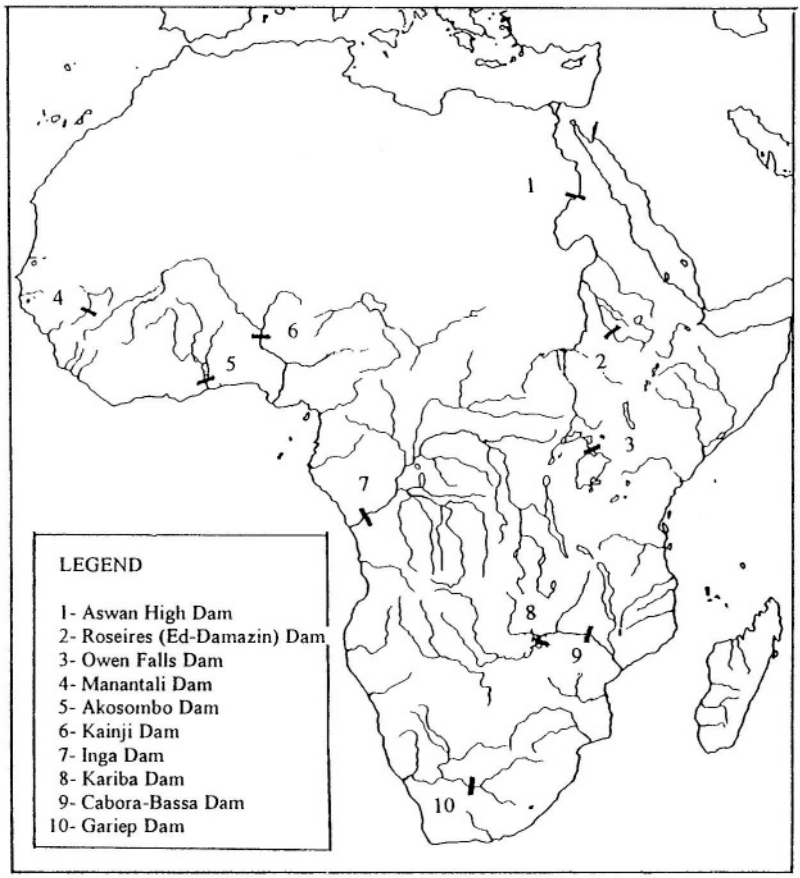

Figure 11.3- Map of Africa showing the locations of ten of its largest dams

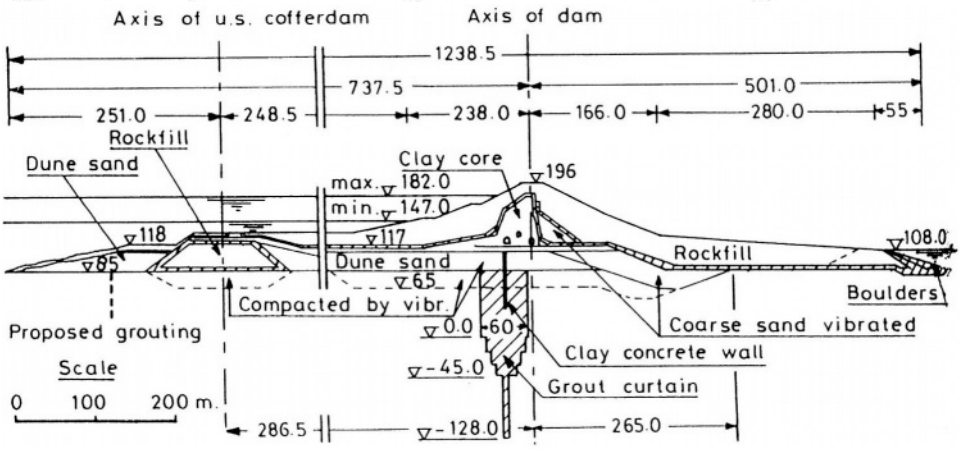

Figure 11.4- Cross section of the Aswan High Dam

The shares of Egypt and the Sudan in the Nile water at Aswan in the pre-High Dam era used to be $48.5*10^9$ m^3 y^{-1} and $4.5*10^9$ m^3 y^{-1} respectively. The difference between the sum of these two quantities and the total natural supply that reached Aswan used to be thrown into the sea, an average of $32*10^9$ m^3 y^{-1}. The annual saving of $21*10^9$ m^3, produced by storage of all floodwater in the reservoir, has been subdivided such that Egypt gets $7.0*10^9$ m^3 and the Sudan $14*10^9$ m^3. As such, the shares of Egypt and the Sudan in the Nile water at Aswan in the post-High Dam era become $55.5*10^9$ m^3 and $18.5*10^9$ m^3 y^{-1} respectively. As no water is left to flow to the sea since the reservoir began its function, the difference between the sum of the two shares and the natural supply of the Nile represents the storage losses. The ratio of the two shares, i.e. $55.5*10^9$ m^3 to $18.5*10^9$ m^3, which is 3 to 1, equaled the ratio of the population of Egypt to the population of the Sudan at the time of division. The ratio of the population of the two countries then has been the criterion stipulated by the Nile water agreement of 1959 and its amendment in 1965 for dividing the Nile water between Egypt and the Sudan.

The total capacity of the reservoir comprises the live or conservancy storage along with the dead or inactive storage and the storage of exceptionally high floods. The live storage has been set as $90*10^9$ m^3 as already mentioned above. Hurst et al. published in Vol. IX of the Nile Basin (Hurst et al, 1959) data of the suspended silt in the Nile water both upstream as well as downstream the Old Aswan Dam. Some of the published results are included in Table 2_k, Part II/Appendix B. From those data, it appeared that the long-term average content of suspended sediment in the Nile water is about $120*10^6$ t, occupying a volume of $60*10^6$ m^3. As the life age of the reservoir has been assumed as 500 y and the silt trap efficiency of the reservoir is 100%, the volume needed for dead or inactive storage was taken as $30*10^9$ m^3. The volume needed for storing exceptionally high floods was estimated as $31*10^9$ m^3. The total storage thus becomes $(90 + 30 + 31)*10^9$ or $151*10^9$ m^3.

The reservoir was put into function in June 1964. An example of the monthly water balance of the reservoir for the hydrologic year 1981-82 is given in Table 11.2. The total reservoir losses, mainly evaporation, in that particular hydrologic year have been estimated from the balance equation as $11.679*10^9$ m3. Table 4.7 gives a number of evaporation estimates obtained from various methods. Sadek et al. (1997) using these estimates concluded that, under the prevailing condition of limited data, the daily evaporation from the reservoir can be taken as 6.0 ± 0.3 mm d^{-1}, equivalent to 2.1-2.3 m y^{-1}. The average level of the reservoir surface in the year 1981-82 was 175 m and the corresponding area is 5,000 km^2. The loss by evaporation according to the given estimate is in the order of $11*10^9$ m^3, which is close enough to the total loss (evaporation and leakage) obtained from the water balance method.

Reservoir storage contents can be converted into water levels Figure 11.5 shows the reservoir levels in the period 1968-90. From this Figure it can be seen

that the reservoir remained at high levels in the period 1976-82. Higher levels were even reached around the end of the 1990s. The drawback of this situation is the risk of failure in storing future floodwater should high inflows persist. Increased reservoir storage losses are certain to occur. The advantage is the development of hydropower at full capacity of the turbines. Contrarily, the reservoir level reached its low levels between 1986 and 1988. The advantage of that situation is the reduction of the risk of flood and storage losses, whereas the interests of power production and land irrigation could have been adversely affected.

The High Dam and the reservoir it created have resulted in a number of what can be called as side effects, some of which are positive and the rest are detrimental, both to nature and society. Protection against floods, larger irrigated surface and increased water supplies for domestic and industrial purposes and production of clean energy provided by the greater shares in the Nile water made available to Egypt and the Sudan are positive impacts. The foremost drastic effect is the entrapping of the full silt load of the Nile water in the reservoir and its subsequent effect on the downstream. Sediment investigations in the post-dam era have shown that the mean annual suspended load is between 125 and 135 10^6 t y^{-1} corresponding to a volume of about $92*10^6$ m^3 y^{-1} (Shalash and Makary, 1986). This annual rate combined with a trap efficiency of 98% brings the life-age of the reservoir to 350 y, instead of the design figure of 500 y. An amount of 2, $800*10^6$ t of sediments have been

Table 11.2- Water balance of the reservoir of the Aswan High Dam for the water year 1981/1982 (from the Yearbook 1981/1982, PTJC)

Year	Month	Flow at Dongola	Trans-mission losses°	Inflow to reservoir	Release to down stream	Difference in storage contents	Storage losses*
1981	Aug	16412	119	16293	6080	7910	2303
	Sep	16950	156	16794	4550	10950	1339
	Oct	10298	136	10162	4340	4940	882
	Nov	3926	35	3891	4200	-1196	887
	Dec	3036	32	3004	4340	-2236	900
1982	Jan	2703	23	2680	4340	-2081	421
	Feb	2256	22	2234	4030	-2443	647
	Mar	1976	21	1955	4485	-3584	1054
	Apr	2690	23	2667	4220	-2400	847
	May	2519	23	2496	5030	-3174	640
	Jun	2172	21	2151	6470	-4976	657
	Jul	3044	29	3015	6915	-5002	1102
Total		67982	640	67342	59000	-3337	11679

Explanation

*All figures are in 10^6 m^3 mo^{-1}, ° = transmission losses in the Nile reach between Dongola and the reservoir, and * = reservoir storage losses.*

deposited in the reservoir from 1964 to 1989. This amount has led the original river bed to rise in the course of years to what is shown in Figure 11.6. This figure shows that the accumulation of sediments up to the year 1990 has been confined to the upper 270 km of the reservoir.

The Nile is a silt-bearing river and the Nile Delta and Valley in Egypt are made up of its' sediments. The rate of sedimentation in the pre-High Dam era was estimated as 0.6 to 1.5 mm y^{-1}, with an average rate of 0.8 mm y^{-1}, used to cover the surface of agricultural soil in Egypt. Since 1964, this annual rate ceased to reach the soil surface, with the following consequences.

- The loss of a unique source of natural nourishment to the soil
- The loss of supply of fresh soil, thereby eliminating the chance of natural rise of the land level, consequently the depth to water table
- Drastic change in the characteristics of the water leaving the reservoir.

The last factor has been the primary cause underlying the degradation of the riverbed for a long distance below the reservoir. This can be clearly witnessed in the scour under the barrages (open-type dams) built on the Nile, Figure 11.7. The profiles drawn in this Figure (Hartung, 1978) represent the drop in surface water level corresponding to discharge of $100*10^6$ m^3 d^{-1}, which is below the mean annual discharge. The quasi dynamic equilibrium between the annual sediment load that used to go to the Mediterranean Sea during the flood season of the river and the littoral drift and other sea currents was disturbed each time a major hydraulic undertaking was built across the Nile. The retreat of the shoreline at the promontories of the Rosetta and Damietta branches of the Nile on the Mediterranean Sea during the period 1898 and 1960 has been mapped by

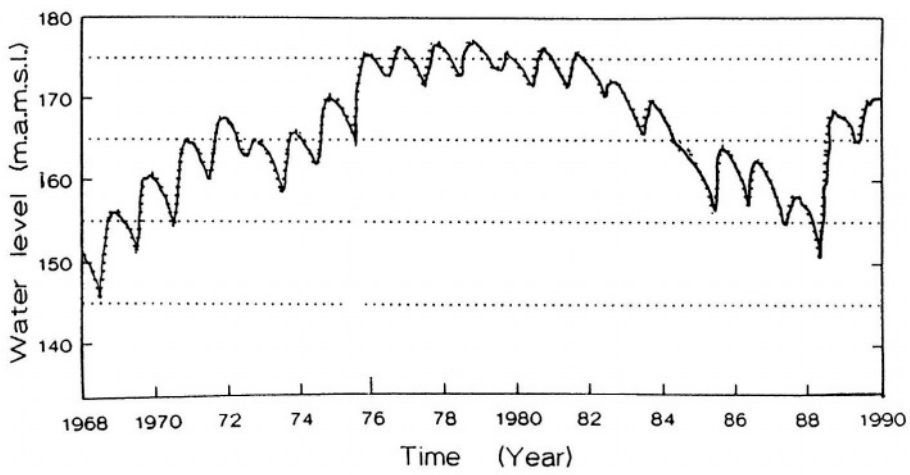

Figure 11.5- Water level of the reservoir of the Aswan High Dam, 1968-89

Wassing (1964) as shown in Figure 11.8. The fact that that the Nile does not supply water to the seashore after 1964 is causing an imbalance in the near-coast sediment budget, thereby making the coast more vulnerable to erosion. The available observations show that the average retreat of the shoreline after the construction of the High Dam is about **29 m y^{-1}**.

Latif (1980) gave a comprehensive review of the characteristics of reservoir water (Nasser and Nubia Lakes) and some of the changes in water quality developed as a result to the construction of the Aswan High Dam. The items described relate to the study of major cations and anions, nutrients, transparency, plankton, aquatic insects and bottom fauna, fish, macrophytes, and shore plants. The interested reader is strongly advised to review the results of that work.

11.3.2 The Roseires Dam- The Roseires Dam is located on the Blue Nile some 630 km above Khartoum and 120 km from the international boundary between Ethiopia and the Sudan. The dam construction began 1961 and by 1966 was complete. The dam consists of 1-km long concrete section and 15-km long earth shoulders. It has 5 low-level sluices, 7 high-level spillways and the intakes for 7 turbines in the hydroelectric power station. A typical section in a deep sluice of the dam is shown in Figure 11.9.

The total storage capacity of the reservoir is **3, 024*10^6 m^3**. The operating range between levels 467 m and 481 m (480 m before 1984), both a.m.s.l., provides a live storage of **2,300*10^6 m^3**. The planned second phase of dam construction allows for the heightening of the maximum storage level by 9 m, i.e. from 481 m to 490 m a.m.s.l., bringing the total storage to **7, 600*10^6 m^3** and the live storage up to **6,400 *10^6 m^3**. The present surface area of the reservoir is **188 km^2**, supposed to reach **381 km^2** upon the construction of the

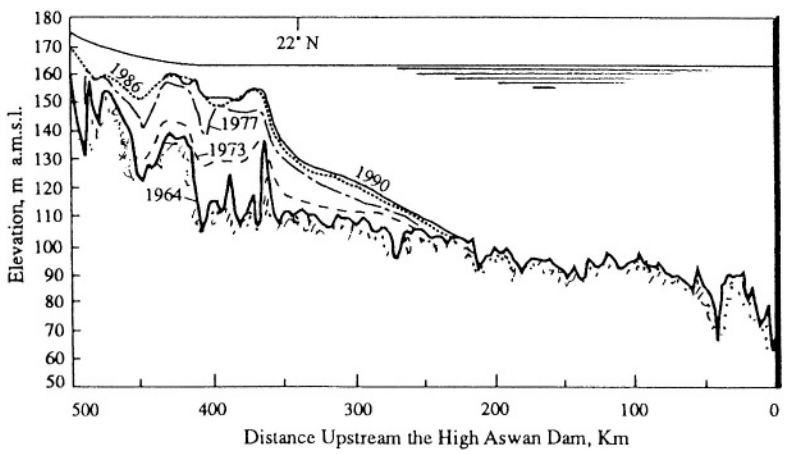

Figure 11.6- Sediment accumulation in the reservoir of the High Aswan Dam

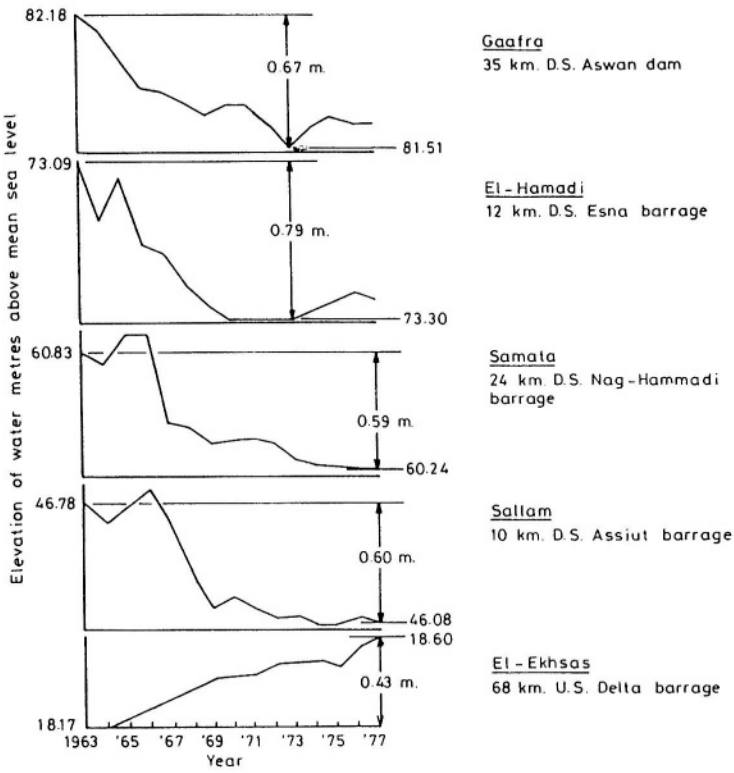

Figure 11.7- Drop of the Nile Water level in the period 1963-1977 at five sites, corresponding to discharge of $100*10^6$ m^3 d^{-1} (Hartung, 1978)

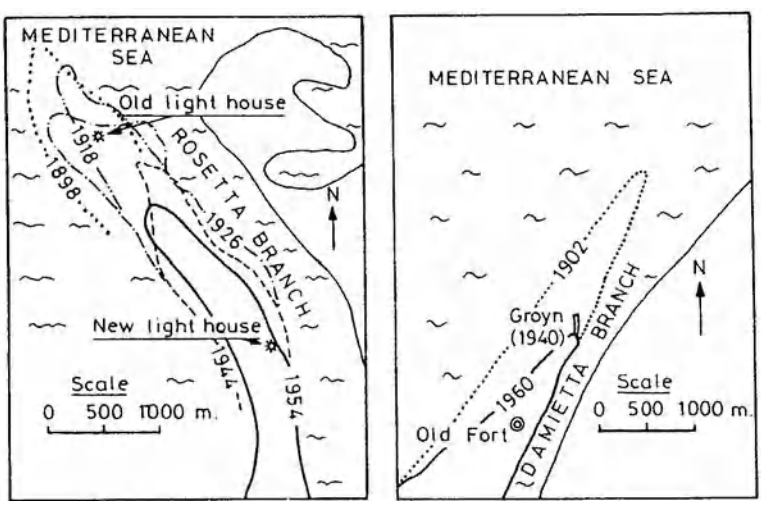

Figure 11.8- Retreat of the shoreline near the promontories of the Rosetta and Damietta Branches of the Nile between 1898 and 1960 (Wassing, 1964)

The total storage capacity of the reservoir is $3,024*10^6$ m^3. The operating range between levels 467 m and 481 m (480 m before 1984), both a.m.s.l., provides a live storage of $2,300*10^6$ m^3. The planned second phase of dam construction allows for the heightening of the maximum storage level by 9 m, i.e. from 481 m to 490 m a.m.s.l., bringing the total storage to $7,600*10^6$ m^3 and the live storage up to $6,400*10^6$ m^3. The present surface area of the reservoir is 188 km^2, supposed to reach 381 km^2 upon the construction of the second phase. Table 11.3 gives the total loss from the reservoir as 2.23 m y^{-1}. Some unpublished reports claim that annual evaporation is limited to 1.97 m. This is 85% of the Penman evaporation, 2.3 m y^{-1} estimated by Shahin (1985).

The net head for hydropower development is 27.8 m in the first phase and 30.5 m in the second phase. The installed power capacity is 210 MW expected to increase up to 250 MW upon heightening the dam.

Since its construction the Roseires Reservoir is operated jointly with Sennar Reservoir for irrigation and power generation in the Sudan. The Sennar Dam was built in 1925 on the Blue Nile at a distance of 280 below the Roseires Dam. The filling of the Roseires Reservoir begins in the second half of September when the discharge of the Blue Nile falls to or below $325*10^6$ m^3 d^{-1} (3, 760 m^3 s^{-1}). This is done with the aim to store sediment-free water. By the end of October, the reservoir is completely full and remains so till the beginning of

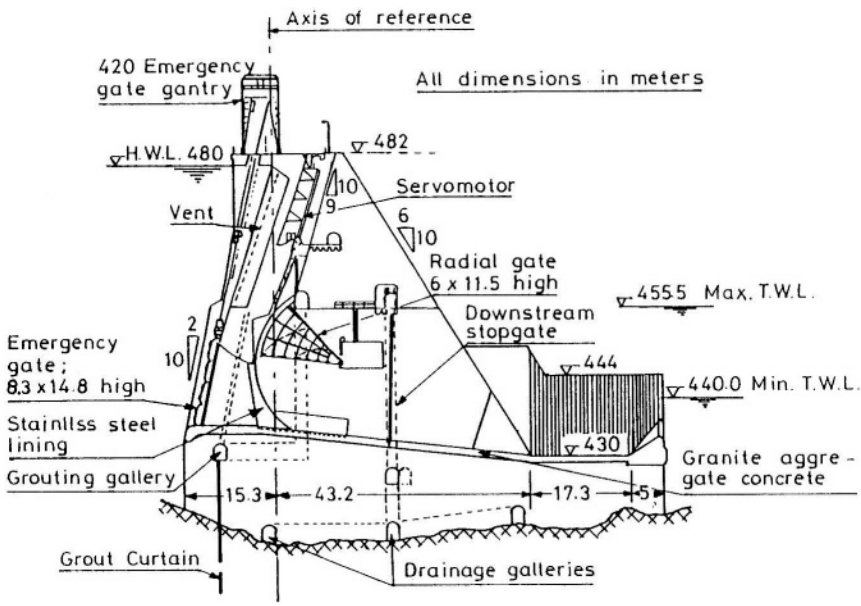

Figure 11.9- Typical section through a deep sluice of Er-Roseires Dam on the Blue Nile, The Sudan

December, after which the water in storage is drawn down gradually till it reaches the minimum storage level by mid-June.

Despite the deep sluices in the dam body, Figure 11.9, to help flush the sediments deposited in the reservoir, the problem of reservoir sedimentation remains alarming. The total storage capacity at the full reservoir level has been reduced by 21% in the period 1966-81. The reduction in storage contents at different reservoir levels can be observed from Figure 11.10 (Shahin 1993). To overcome this problem the maximum storage level has been increased since 1984 by 1-m, and the maximum discharge at the beginning of the filling operation increased to $500*10^6$ m^3 d^{-1} (5, 790 m^3 s^{-1}). This policy did not lead to any real improvement. Contrarily, it led to further accumulation of sediments.

El-Sheikh et al. (1991) studied the relationship between the sediment load and river flow for 22 years at Ed-Deim on the Blue Nile at the Sudanese-Ethiopian border. Two types of relationships have been suggested, one is linear and the other quadratic. Denoting the sediment discharge by Q_s, t s^{-1}, $Y = \log Q_s$, Q_w = river discharge, m^3 s^{-1}, and $X = \log Q_w$, the two relationships can be expressed as:

$$Y = a + bX \tag{11.16}$$

and

$$Y = c_o + c_1 X + c_2 X^2 \tag{11.17}$$

respectively where, a, b, c_o, c_1 and c_2 are regression parameters estimated from the available sets of data for the different stages of the inflow hydrograph. For example, the parameters of the Eq (11.16) for the period from 1 to 31 July are a = –7.55 and b = 2.45 and of Eq. (11.17) for the same period are c_o = -23.67, c_1 = 12.08 and c_2 = -1.43. The coefficient of correlation for both expressions is 0.95 Beside Eqs. (11.16) and (11.17) a third equation has been introduced to determine the net trap efficiency of the reservoir

$$N_{tr} = 1 - (1 - V_r)\exp - \{\phi V_r /(1 - V_r)\} \tag{11.18}$$

where N_{tr} = trap efficiency, V_r = ratio of reservoir capacity to streamflow, $\Phi = w$ T_s /D, w = fall velocity of the sediment particles, in m s^{-1}, T_s = duration of spilling, in s, and D = mean depth of reservoir, in m. The computed sediments using Eq. (11.18), which have accumulated over the period 1966-88, were in reasonable agreement with sediment thickness obtained from the bathymetric surveys of the reservoir. This agreement has led to the conclusion that $39.1*10^6$ m^3 y^{-1} can be accepted as an average rate of sedimentation instead of the $15*10^6$ m^3 y^{-1} originally adopted by the dam designers.

Table 11.3- Water balance of the reservoir formed by Er-Roseires Dam, The Sudan, for the water year 1981/82 (from the Yearbook 1981/82 PTJC)

Period	(H)US[oo], m, a.m.s.l.	Volume of contents	Change in storage	Reservoir loss[xx]	Release to downstream	Inflow to reservoir
1981						
30-jun	467.03	153.5				
01-10 Jul	466.90	146.0	-75.5	2.7	676.0	671.2
11-21 Jul	467.90	157.5	-11.5	2.7	1,352	1,366
21-31 Jul	466.89	145.5	-12	2.9	380.7	3,797
01-10 Aug.	466.94	148.0	2.5	2.0	4,298	4,303
11-20 Aug	467.12	160.0	12	2.1	3,987	4,001
21-31 Aug	466.87	144.0	-16	2.3	505.0	5,036
01-10 Sep*	470.88	565.0	421	2.6	3,750	4,173
11-20 Sep	474.10	1,098	533	4.2	3,501	4,038
21-30 Sep	475.36	1,344	246	4.4	3,397	4,647
01-10 Oct	479.09	2,219	874	8.5	1,822	2,705
11-21 Oct	480.42	2,599	380.5	9.7	1,274	1,664
21-31 Oct	480.96	2,766	176	10.9	881.0	1,059
01-10 Nov[o]	480.99	2,776	10	16.0	717.0	793
11-20 Nov	480.98	2,773	-3	16.0	557.0	570.0
21-30 Nov	481.01	2,782	9	16.0	425.0	450.0
01-10 Dec[+]	480.95	2,763	-19	18.6	395.0	394.6
11-20 Dec	480.61	2,656	-107	18.6	387	298.6
21-31 Dec	480.14	2,515	-141	20.5	396	275.5
1982						
01-10 Jan	479.96	2,463	52	19.6	246.0	213.6
11-20 Jan	479.93	2,454	-9	19.6	188.0	198.6
21-31 Jan	479.68	2,382	-72	21.5	239.0	188.5
01-10 Feb	478.64	2,100	-282	20.6	378.0	116.6
11-20 Feb	477.98	1,932	-168	19.4	256.0	107.4
21-28 Feb	477.55	1,828	-103	14.9	178.0	89.4
01-10 Mar	474.25	1,676	-153	19.5	245.0	112.0
11-20 Mar	476.27	1,536	-140	18.7	236.0	114.7
21-31 Mar	475.17	1,305	-231	19.2	289.0	77.2
01-10 Apr	474.25	1,126	-179	15.8	229.0	65.8
11-20 Apr	473.17	930	-196	14.6	240.0	58.6
21-30 Apr	471.69	687	-243.5	13.3	285.0	54.8
01-10 may	470.32	485	-201.5	10.0	258.0	66.5
11-20 May	469.04	325	-160	9.0	263.0	112.0
21-31 May	467.3	172	-153	8.8	241.0	96.8
01-10 Jun	466.96	149	-23	4.9	261.0	242.9
11-20 Jun	467.69	201	52	5.0	220.0	277.0
21-30 Jun[x]	467.82	211	10	5.2	415.0	430.2

Table 11.3- Cont'd.

Period	(H)US[oo] m, a.m.s.l.	Volume of contents	Change in storage	Reservoir loss[xx]	Release to downstream	Inflow to reservoir
Total			57.5	420.3	41,339	41,817

Explanation

** = Beginning of reservoir filling on 07.09 1981, ° = end of filling on 02.11.1981, + = beginning of emptying on 05.12.1981 and x = end of emptying on 11.06.1982, oo = measured at Ed-Deim near the frontier between Sudan and Ethiopia, and xx = mainly evaporation loss. All quantities listed in the table are in 10^6 m^3.*

In an attempt to decelerate the rate of reservoir sedimentation, Ali (1990) suggested different operation policies to balance hydropower production and reservoir sedimentation, which he formulated while assuming that the Roseires and Sennar Reservoirs followed the same operation rules. The response of the system, basically the deposited silt and the generated power, was determined. The operation rules in each scenario had two parameters: date of beginning of reservoir filling and rate of reservoir filling or date of end of filling operation Thirty-three scenarios were run to simulate the conditions in the 20-y period, 1968-87. The scenario that produced the least reservoir sedimentation gave an average rate of $33.4*10^6$ m^3 y^{-1} instead of $39.1*10^6$ m^3 y^{-1}, the average for the period of record.

11.3.3 Owen Falls Dam/Lake Victoria- The Owen Falls Dam is built at the foot of the Owen Falls and below the Rippon Falls on the Victoria Nile, about 3 km downstream its exit from Lake Victoria. The dam, constructed in the period 1948-50, is a mass concrete gravity type dam with steel reinforcements around the sluices. A cross section of the dam is shown in Figure 11.11. The dam has six sluices each 5 m high by 3 m wide, i.e. a total opening area of 90 m^2, with a combined discharging capacity of $1,275$ m^3 s^{-1}. The average operating head for the turbines is 20 m.

The Owen Falls Dam can be regarded as the first long-term storage work built on the Nile River. The storage reservoir was designed with the idea of raising the normal level of Lake Victoria by 3 m, thereby increasing the volume of water in the lake by $207*10^9$ m^3. This additional volume was thought of in the early 1950s to be too difficult for the lake to accommodate, except over a large span of time. Secondly the losses in the Sudd area increase tremendously with increasing flow out of the lake as already discussed in Chapters 7 and 10. Thirdly, the outflow of the lake has to travel thousands of kilometers before reaching Malakal in the Sudan, not to mention Aswan, Egypt. All these factors render the possibility that this storage work will lead to any substantial development of the Nile water reaching the Sudan and/or Egypt highly questionable.

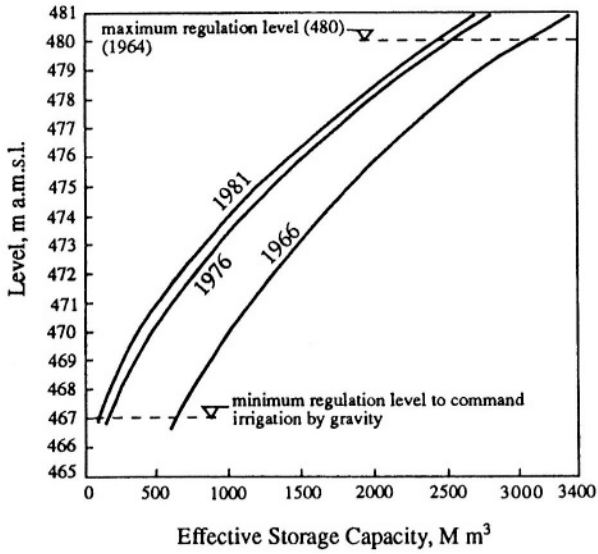

Figure 11.10- Decrease of the storage capacity of the Roseires Reservoir in the period 1966-81

Ten turbines have been installed with a combined capacity of 150 MW. Uganda alone is using the dam, since it has been opened, for hydropower production. The generated power (Westlake et al., 1954) is used to satisfy the local needs of Uganda for electricity and the rest is transmitted to Nairobi to be exported to Kenya.

Table 11.4 is an example of the monthly outflow from Lake Victoria in the period from July 1981 up to June 1983 (PTJC, 1981/82 and 1982/83). The outflows from the lake are estimated by two different methods. The first is to convert the calculated average monthly level at the gauge of Jinja to discharge using the rating curve at the same location. The second method is by estimating the outflow from the sluices of the dam and the turbines. The two methods give very close results, yet not exactly the same. The rating curve method gave for the years 1981/1982 and 1982/1983 total discharges greater than those obtained from the second method by almost 3.3% and 2.5% respectively.

11.3.4 Manantali Dam- The Manantali dam is located on the Bafing River, a tributary of the Senegal River, in Mali The reservoir, Figure 11.12, covers about $480\ km^2$ and has a design capacity of $11*10^9\ m^3$. This capacity helps to provide 800 GWh (Gigawatt hours) of hydroelectric power per year and a regulated artificial flood of $2,\ 500\ m^3\ s^{-1}$. The reservoir was put into operation in 1989 to regulate the river flow. By mid 1997, the World Bank approved a loan to help finance the installation and operation of the dam's turbines (Pottinger,

1997). The generated power is supposed to be shared by the Sénégal, Mali and Mauritania. It is expected that the energy price in these countries will become cheaper when the thermal energy is substituted by the hydroelectric power generated from the dam. When this becomes the case, industry in Mali and Sénégal will sure profit from the dam.

The Manantali Dam has terminated the ancient flood-recession farming practice (i.e., the cultivation of riverbank areas enriched by silt deposited while the floodwater is receding). Instead, since the dam construction it has been converted to irrigated agriculture. This conversion of farming practice has proven to be costly and unfamiliar to the most of the farmers, at least the simple ones. Those who are benefiting from irrigated-agriculture are the rich landholders. Besides, irrigated agriculture is contributing to the spread of water-borne diseases via irrigation canals and water storage areas. These are negative environmental and social impacts. The impact of dam construction on Lake Guiers, near the Sénégal Delta, has already been discussed in Chapter 10.

11.3.5 Akosombo Dam/Volta Reservoir- The damming of the Volta River by the Akosombo Dam just south of Ajena, Ghana, which began in 1961 was completed in 1965. A rock-fill type dam 70 m high impounds Lake Volta as shown in Figure 9.3. The dam is situated in a gorge where the river leaves a sandstone and shale basin that occupies much of southeastern Ghana and cuts across an intrusive dyke complex that form the Akwapim Hills (Grove, 1985).

The dam has created a reservoir extending upstream from the dam site to Yapei, beyond the former confluence of the Black Volta and White Volta Rivers

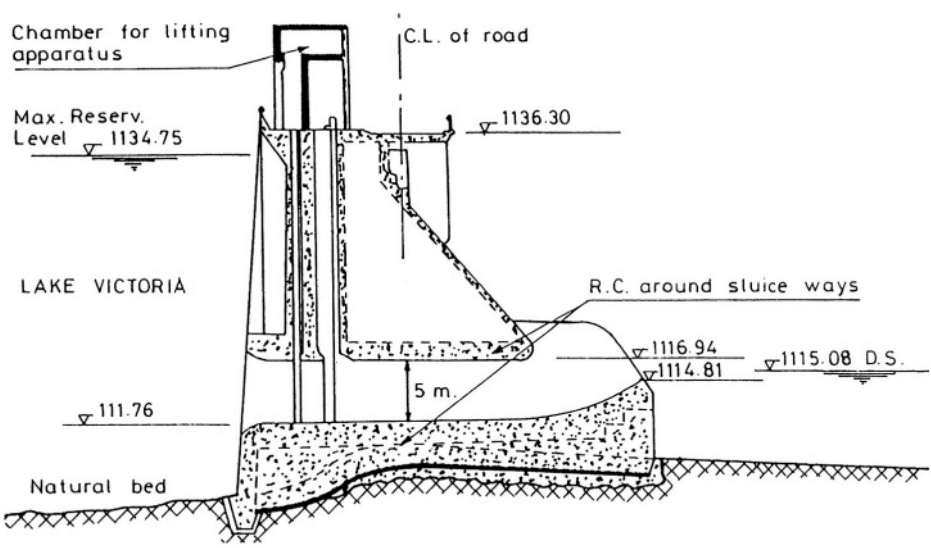

Figure 11.11- Cross section of Owen Falls Dam (redrawn from Olivier, 1977)

Table 11.4- Flow regulation sheet of the discharges passing through the sluices of Owen Falls Dam and the turbines of the annexed power plant (extracted from the PTJC 1981-82 and 1982-83 year books)

Year	Month	Lake Victoria average[x] reading	Lake Victoria discharge 10^6 m^3 mo^{-1}	Outflow from sluices and turbines	Surplus or deficit
1981	July	12.09	3046,71	3269,25	222,54
	August	12.09	3045,88	3100,38	54,50
	September	11.9	2724,77	2982,97	258,10
	October	11.88	2786,57	2735,00	-51,57
	November	11.84	2643,70	2165,81	-477,89
	December	11.83	2721,89	1550,98	-1170,91
1982	January	11.86	2753,62	2365,27	-388,35
	February	11.82	2448,02	2016,61	-431,41
	March	11.77	2641,65	2699,54	57,89
	April	11.77	2555,02	2692,86	137,84
	May	11.98	2906,12	3321,98	415,86
	June	12.06	2917,54	3205,74	288,20
Total			33191,49	32106,29	-1085,20
	July	11.99	2931,13	2648,77	-282,36
	August	11.91	2926,06	2639,54	-186,52
	September	11.85	2658,52	2645,06	-13,46
	October	11.83	2718,15	3032,93	314,78
	November	11.95	2778,18	2791,11	12,03
	December	12.15	3128,35	3035,48	-92,87
1983	January	12.15	3124,46	3314,91	190,45
	February	12.10	2767,14	2958,47	191,33
	March	12.03	2978,34	3299,15	320,81
	April	12.05	2897,43	2215,29	-682,14
	May	12.04	2989,30	2618,93	-370,37
	June	12.04	2894,62	2648,12	-246,50
Total			34691,68	33847,76	-943,92

Explanation

[x] = *average monthly local gauge reading at Jinja in m, and - = deficit*

The Volta Reservoir is about 400 km long with a mean depth of 70 m, covering a surface of $8{,}500\ km^2$. It has a storage capacity of $153*10^9\ m^3$. The installed hydroelectric power is 912 MW (megawatt, mega = 10^6). The reservoir powers also the 148 MW Kpong Dam, a low-head generating plant 50 km downstream. The large electric-power generating capacity of the Akosombo Dam meets Ghana's needs and provides a surplus for sale to neighbouring countries. A considerable part of Ghana's needs for energy is used by the aluminum smelter located at the port of Tema on the Gulf of Guinea.

The Volta Reservoir helps to regulate the flow of the Volta River, supplies irrigation for farmland in the dry Accra Plains situated below the dam site. In addition, the reservoir is a major fishing facility next to it's use for inland navigation. The lake is navigable and provides a cheap route for transportation linking Ghana's northern savanna region with the coast. The potential productivity of agriculture in the drawdown zone of the reservoir is high. The gross income from drawdown farms on the Volta Lake has shown to be 1.4 times that of upland farms per unit area. As such, the drawdown can go some way to replace the flooded fertile floodplain land. These are all positive social and economic impacts. On the other hand, the inundation of homes, villages and displacement of inhabitants are adverse impacts. The displaced population has been estimated as 84,000.

In the years that followed the construction of the Akosombo Dam, Ghana has reaped considerable benefits from the generation of electricity and from the fishing industry. The lake produced as much as 40,000 t of fish per year. The

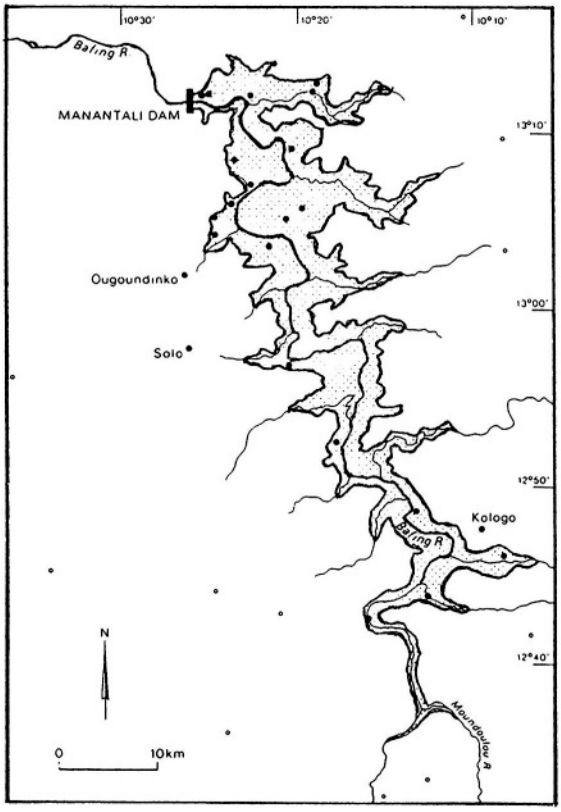

Figure 11.12- The Manantali Dam on the Upper Sénégal River (Club du Sahel/CILSS, 1979)

growth and decline of the catch, and the change of fish from insectivorous in the Volta River to herbivorous and plankton-feeding fish in the Volta Lake are described by Grove (1985). A few years after the dam construction and for more than ten consecutive years, Ghana was hit by below-average rainfall. That drought affected the inflow to the lake and caused its level to fall by over 1.5 m annually. For the first time since it's creation, the lake level fell below the minimum operating level of 75.6 m in 1979. By 1983, the level reached the lowest ever-observed minimum of 71.85 m. The Government had to enforce severe cutbacks in energy supply of up to 60% and reduce the power sold to neighbouring Benin and Togo by 50%. Waterworks along the lake became inoperative as the water level fell well below their intake points. Fishing, farming, and navigation interests were all adversely affected by that drought.

11.3.6 Kainji Dam- The dam is located on the Niger River in western Nigeria at a distance of about 1,010 km from the sea. The location of the Kainji dam is an example of dam sites that are near geological fall lines where rivers descending from crystalline uplands to sedimentary plains have cut headwards to produce rapids and water falls.

The dam construction began in 1964 and the reservoir it created was put into operation in 1969. The 85 m-high dam consists of two parts; a main dam built of concrete and rock fills and a saddle dam built of rock fills. The saddle dam is built with the aim of protecting the main dam during severe floods. There are four spillways provided with hydraulically operated gates. The gates are 17.4 m by 17.4 m, which could be opened to control the floodwater and release it for use at Jebba dam downstream.

The reservoir stretches for about 136 km along the Niger River covering an area of $1{,}300\ km^2$. The average width of the lake is about 10 km and the maximum width is 24 km. The reservoir is supplied with water from the Upper Niger. The gross capacity of the reservoir at the full storage level is about $15*10^9\ m^3$. The reservoir is used extensively for land irrigation and fishing. It is also used for hydropower development and inland navigation. The creation of the reservoir has led to inundation of many riverine settlements and part of the old town of Yelwa as well as displacement of several thousands of people.

Grove (1985) reviewed the results obtained from a study on the discharge reduction between Kowara, upstream of the Kainji Reservoir and Kainji stations. The peak flows of the Niger River in the post-impoundment years (1970-1976) at the height of the period September-October of the Sahelian drought years in the early 1970s were on the average only 75% of the peak rates in 1960 (the base year). Although the reduction in floods was most in 1972 and 1973, the worst drought years, there was an overall reduction of 60% in discharge over the period 1970-976.

Studies below Kainji in the immediately post-impoundment period demonstrated significantly reduced catch. A similar decline in fisheries

following impoundment has been recorded elsewhere in Nigeria. On the other hand, there are evidences that a viable fishery has been established in the dam area, in contrast with that further downstream (Grove, 1985).

It is repeatedly claimed that the Kainji Dam is suffering from lack or poor maintenance. The dam was equipped with flood and disaster forecasting devices. Unfortunately these devices have become outdated and malfunctioning. There are no funds for maintaining the dam that is showing signs of shifting. The Kainji Dam is presently referred to as a shifting dam: an impending calamity. However, instead of maintaining the dam and bringing it to function properly design works and feasibility studies of other dams like Zungeru and Mambila are ready for implementation.

Some of the recommendations stressed by the Environmental Rights Action (ERA, Friends of the Earth Nigeria) in its field report No. 19 (1999) were:

- NO NEW DAMS should be built in Nigeria
- Adequate and prompt maintenance of existing dams
- Immediate salvaging Kainji Dam to avert national calamity

In conclusion it seems that there is hardly any evidence that the Kainji Dam has brought Nigeria enough positive environmental, social or economic impacts.

11.3.7 Inga Dam- The dam is located at Inga Falls, which are rapids on the Lower Zaïre (Congo) River in Zaïre, Central Africa. It is one of the world's largest hydroelectric dams. The dam site is located 40 km above the port of Matadi. There, the river Falls 98 m in a distance of 15 km, i.e. at an average slope of $6*10^{-3}$. The Zaïre River, thanks to its geographical position astride the Equator, enjoys an exceptionally stable hydrologic regime. Long-term flow data show that the river flows at an average rate of about $40{,}000\ m^3\ s^{-1}$ (Chapter 8). The mean annual discharge of $26{,}400\ m^3\ s^{-1}$ is exceeded 98% of the time.

The so-called Inga scheme comprises the construction of a main dam on the Zaïre River, the Inga I, Inga II and Inga III Dams, power stations, and a number of ancillary works. The map, Figure 11.13 shows the locations of these structures. The first phase of the hydroelectric project has been completed in 1972. Figure 11.14 shows a section of the Inga I Dam and the annexed power station. The latter provides power mainly for industrial purposes, and so does the second phase. The Inga I has a guaranteed capacity of 300 MW and generates 2,400 GWh. As such, Inga II was added in 1982 with installed capacity of 1,400 MW, guaranteed availability of 1,100 MW and generated energy of $9.6*10^9$ kWh. The total installed capacity of Inga I and Inga II together is 12,000 GWh or 12 TWh (Tetrawatthours, $T = 1*10^{12}$). It is possible to carry on this development by constructing the Inga III, which would consist of one possibly two power stations capable of doubling or even tripling this output. *The Grand Inga Scheme* involves damming the main river so as to

divertits waters into a certain valley and thus exploit the whole of the river flow under a head of 150 m. The proposed installed capacity of 52 units amounting to 39 GW will make it the biggest single hydroelectric enterprise in Africa (Olivier, 1977).

It is unfortunate that the Congo has been for quite some years till a short while ago torn by civil wars, in which each fighting faction is supported by armed forces from one or more of the surrounding countries. The unstable internal situation coupled with provocative external affairs has brought the economy of the country to an extremely low level. The energy generated by Inga I and Inga II has never gone above 50% of their installed capacity. Plans to sell part of its energy to South Africa, Nigeria and Egypt need first of all the return of stability to the political and economical situations of the country. This is unavoidable before the installed capacities of the Inga's are fully exploited. After that a more serious thinking of implementing Inga III would follow.

11.3.8 Kariba Dam- It is a 100-m high, double-curved concrete arch dam built across the Zambezi River at the Kariba Gorge on the border between Zambia and Zimbabwe. The dam is situated some 385 km downstream Victoria Falls. The construction of the dam was completed in 1959.

The reservoir (Lake Kariba) created by the dam has a surface area of $5{,}200\ km^2$ at normal operation level. The Kariba Reservoir is 280 km long, has an average width of 18.5 km and a maximum depth of 116 m. The total storage capacity corresponding to the maximum flood level is $185*10^9\ m^3$. This capacity is divided between live storage, $44*10^9\ m^3$, dead storage, $116*10^9\ m^3$ and flood storage, $25*10^9\ m^3$. The normal operating range of the reservoir water level is 9.4 m. The dam body is provided with six sluice gates having a capacity of $9{,}515\ m^3\ s^{-1}$ at maximum flood level. The catchment area of the reservoir is $663{,}000\ km^2$ and the mean annual river flow is $444\ m^3\ s^{-1}$ ($14*10^9\ m^3\ y^{-1}$). The lake supplies 6, 700 GWh (gigawatthours, $giga = 1*10^9$) of electricity annually.

The dam was designed primarily as a hydroelectric project to serve the electrical energy needs of Zambia and Zimbabwe.

A major concern in the design of the Kariba Dam was the dissipation of energy of the water discharged through the sluice gates. A series of model tests indicated that a scour hole of 55 m would be formed in the gneiss rock. By 1966 this depth was approached and the scour hole appeared to be stabilized as predicted by the model tests (Olivier, 1977). Figure 11.15 is a cross section of the dam showing the development of the scour hole with spilling.

The operation of a reservoir can be approximately viewed as a sequential decision process. Decisions concerning a single reservoir or a multi-reservoir system are needed in a time sequence. In view of its sequential nature, reservoir operation, as an optimization problem, can be adequately solved by algorithms explicitly exploiting the sequential characteristics of the said problem. Dynamic programming (DP) is a solution-seeking concept that can be used in reservoir

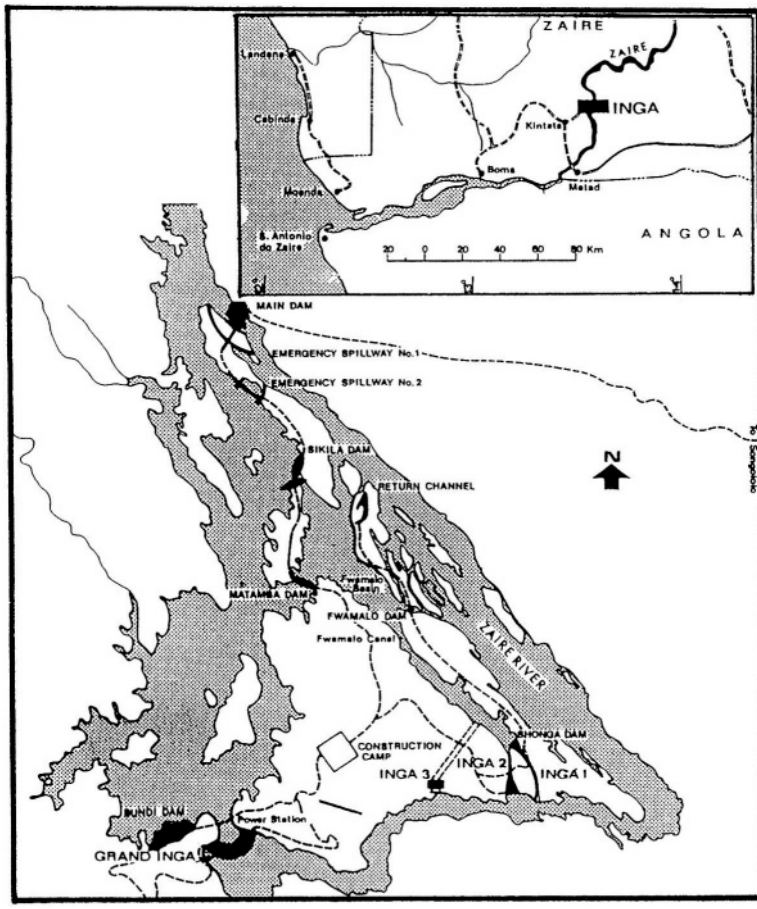

Figure 11.13- Location map of the Inga Scheme, Zaïre (after Olivier, 1977)

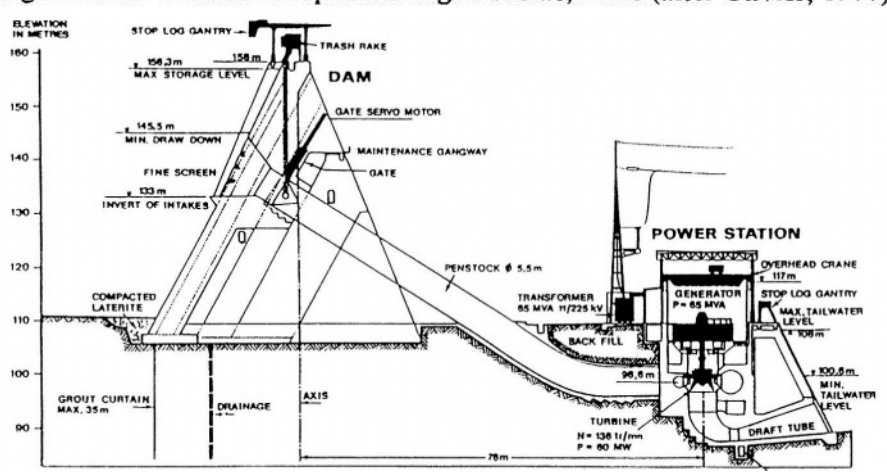

Figure 11.14- The Inga I Dam and the annexed power station (Olivier, 1977)

management (Bellman, 1957). The potential drawback of the Dynamic Programming (DP) approach originates from the number of state and decision variables. Bogardi and Nandalal (1989) reported that by considering discrete values for both the state and decision variables the number of combinations to be considered in the state transformation may be excessively large. As a matter of fact, it can exceed the capacity of powerful computers. This is often referred to as the curse of dimensionality. This curse unfortunately is present in problems related to water resources systems.

There are a few approaches to overcome the above-mentioned limitation. One of these approaches is known as the successive approximation method. Larson (1968) developed the incremental dynamic programming (IDP) technique with the aim of overcoming the shortcomings of the successive approximation method. Bogardi and Nandalal (1989) selected this technique as a tool for developing an optimum energy generating operation for the Kariba Reservoir. Historic operation of the reservoir considers the actual demand while the optimal operation of IDP is based on maximizing the energy output without consideration to the actual energy demand. The energies generated as obtained from the historic operation in the periods 1966-75, 1978-83 and 1962-1983 are 46.33, 45.03 and 148, all times 10^6 MWh. The corresponding results obtained from the IDP operation for the same periods in the same order are 47.30, 50.66 and 202.03, all times 10^6 MWh. The installed capacities of the hydropower plant are 600 MW for 1966-75 and 1,200 MW for the periods 1978-83 and 1962-83. In those years 1966, 1968, 1972 and the period 1966-1975 some of the water had to be spilled without being used for generating power due to the limitation imposed by the then installed capacity of the power plant. The conclusion to be drawn is that the results obtained from the IDP-based optimal operation indicate the maximum power output potential for the given or known inflow time series

The reservoir (Kariba Lake) is used as a commercial fishing facility. In 1967 Kapenta fish, sardine-like fish, was introduced from Lake Tanganyika into the reservoir to alleviate the food shortage in Zambia. Its exceptionally high protein content privileges the Kapenta as a nourishing stuff. The Kapenta fish multiplied at considerable rate, except that it was at the expense of the old ecology of the lake. The Tiger fish started instead to feed on the Kapenta and left the Bream, which it used to feed on earlier, alone. Large-scale fishing operations with a catch of $11*10^3$ t y^{-1} are causing light pollution of the lake.

11.3.9 Cabora Bassa Dam- This is basically a hydroelectric facility on the Zambezi River. The dam site is located 125 km north west of the township of Tete, Mozambique. The location of the Cabora Bassa with respect to the Kariba, both dams and reservoirs is shown on the map in Figure 11.16. The Cabora Bassa is a double curved concrete arch dam, with a maximum height of 160 m above the foundation. The construction of the dam began in 1969, and in 1974 it

became ready for operation. The last of five 425-MW was installed in 1979. The dam is provided with eight segmental gates each with a discharge capacity of 1,650 $m^3 s^{-1}$, i.e. a total discharge capacity of 13,200 $m^3 s^{-1}$. A section through the dam and sluice gates is shown in Figure 11. 17.

The reservoir formed by the dam is 270 km long having a shoreline 246 km long and average depth of 20 9 m. It consists of five basins covering a total surface area of 2,740 km^2. The total storage capacity of the reservoir is $66*10^9$ m^3 divided between live or conservancy storage, $48*10^9$ m^3, dead storage, $4*10^9$ m^3, and flood or surcharge storage, $14*10^9$ m^3.

The catchment area of the Cabora Bassa reservoir is $1.2*10^6$ km^2 shared between Mozambique; 137,000 km^2, Angola, 140, 000 km^2 and the remaining area is in Zambia. At the dam site, the average annual inflow is 2,800 $m^3 s^{-1}$, i.e. nearly twice the discharge upstream the site of the Kariba dam. The rivers flowing out of the reservoir are the Luangwa, Hunyani, Messenguerzi and the Shire.

Cabora Bassa Dam is quite often described as Africa's most powerful hydroelectric scheme. The final stage of construction of the dam, the power station and the installation of the turbo-generators and the power transmission lines was originally planned to be completed by 1979. That would bring the installed capacity up to 2, 000 MW. For some reasons, however, that plan was

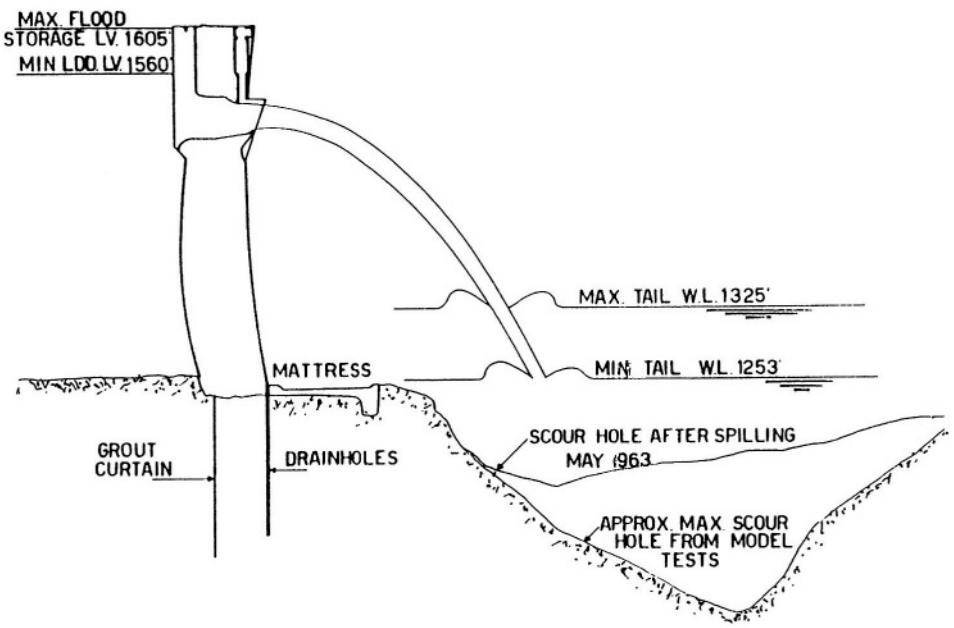

Figure 11.15- Cross section of the Kariba Dam showing formation of the scour hole with spilling of water (Olivier, 1977)

not realized in the set time. After two decades of disruption, new power lines had to be installed and the generators have become ready to deliver full power. Since 1998, South Africa has become in a position to purchase three-quarters of the total capacity of the giant 2, 000 MW dam.

The Water of the Zambezi River before construction of the dam had a low content of total dissolved salts (average $TDS = 90\ mg\ l^{-1}$), a pH of 7.6, and a too low figure (0.57) for calcium carbonate. The highest river level upstream of the dam in the period 1979-89 fluctuated between 312 m and 326 m. The content of total dissolved salts shortly after the reservoir filling became slightly higher compared to the TDS content before reservoir filling. The pH is showing slight oscillation around the mean 7.6. Concomitantly, the index of aggressiveness to calcium carbonate, consequently to the concrete of the structures, has become moderate (Henriques and Silva, 1991). The same source, i.e. Henriques and Silva (1991), upon studying the impacts of the Cabora Bassa Dam on nature and society, reached the following conclusions:

- There has been an improvement in the climate of the region caused by increased atmospheric humidity.
- The increase in air humidity and refuge zones have created better conditions for the development of wildlife.
- There is hardly any significant change in the quality of water compared to the pre-dam condition.
- The availability of water for irrigation and the increase in fishing resources have reacted favourably on the economic conditions of the lakeside population.

11.3.10 Gariep Dam- The Gariep Dam (formerly called H. Verwoerd Dam) is located on the Orange River in South Africa. It is a principal component of the Orange River Development Project. The project that began in 1928 involves freshwater supply, hydropower development, irrigation, fishing and recreation. The approximate location of the dam and the reservoir are shown on the maps in Figures 11.18_a and 11.18_b respectively. The dam itself is a concrete structure, a combined gravity and arch dam 88-m high. The construction of the dam began in 1966 and was commissioned in 1971.

The reservoir surface area at full storage level is of $374\ km^2$, with and a gross storage capacity of $5.943*10^9\ m^3$ (Olivier, 1977). The mean annual inflow to the reservoir in the period 1970-95 was $7.84*10^9\ m^3$. The runoff varied from a minimum of less than $100*10^6\ m^3$ in July to a maximum of $1{,}300*10^6\ m^3$ in February (Jury, 1998). The monthly inflows to the dam show a marked seasonality, which is a reflection of the seasonality of rainfall in the reservoir catchment.

Water from the dam is released to the downstream through four generators, each capable of producing 90 MW, thus an ultimate generating capacity of 360 MW. The dam wall incorporates two huge outlet structures on the upstream side

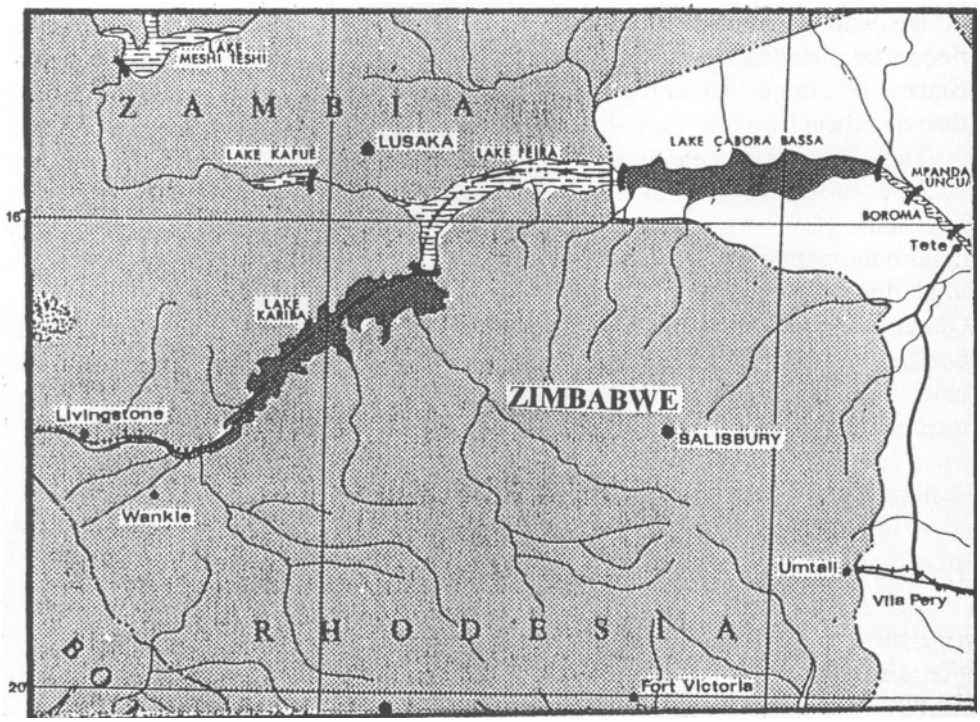

Figure 11.16- Locations of the Kariba and Cabora Bassa Dams and Reservoirs

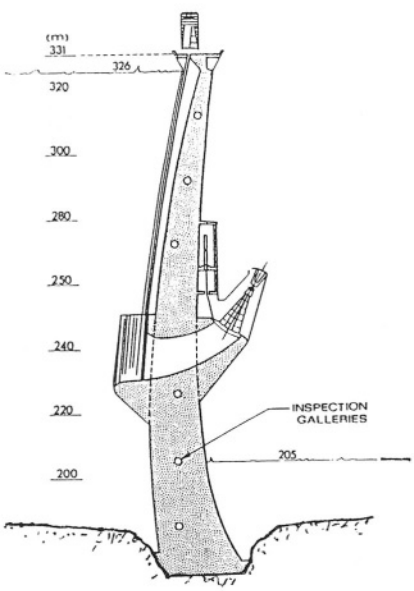

Figure 11.17- Cross section of the Cabora Bassa Dam

of the wall. There are six radial gates, three on each side, for discharging floodwaters into six concrete chutes, which lead the water into the downstream channel of the river away from the base of the dam wall. With this design, the risk of erosion to the base of the dam wall is strongly minimized. A section through one of the floodgate openings is shown in Figure 11.19.

Jury (1998) developed a model for predicting the inflow to the Gariep reservoir. Three types of predictors are used in the multivariate algorithm describing that hydrological model. These are the surface Meridional wind over West Angola, *aVang,* **(φ = 5° S, λ = 5° E),** air pressure on the South Indian Ocean, *oSIp,* **(φ = 12° S, λ = 55°-77° E)** and sea surface temperature of the Southern Ocean, *oSocnS,* **(φ = 45° S, λ = 10°-40° E)**. The predictor **areas > 10^6 km^2**, and the notations *a and o* correspond to JAS and SON months respectively. The model suggested for the inflow to the Gariep Reservoir is:

$$+0.39(aVang) - 0.78(oSIp) - 0.45(oSocnS) \qquad (11.19)$$

The correlation coefficient between the observed and predicted inflows is 0.84.

The construction of the Van der Kloof (formerly P. K. le Roux) was completed in 1977. The dam is located 145 km downstream of the Gariep Dam. Water from the four generators of the Gariep Dam is released into the Van der Kloof Dam as mentioned earlier. The two dams have been well equipped to deal with heavy silt accumulation in their reservoirs. They have deep dead-storage

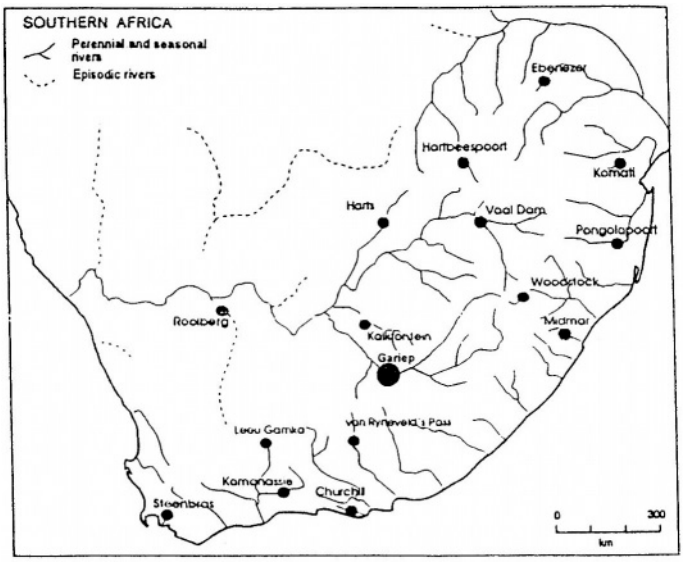

Figure 11.18,- Locations of the Gariep Dam and other major dams within South Africa

areas, and their high walls can be raised if necessary to allow for higher water levels. The Gariep Dam wall and the Gariep Nature Reserve are regarded among the top tourist attractions in South Africa.

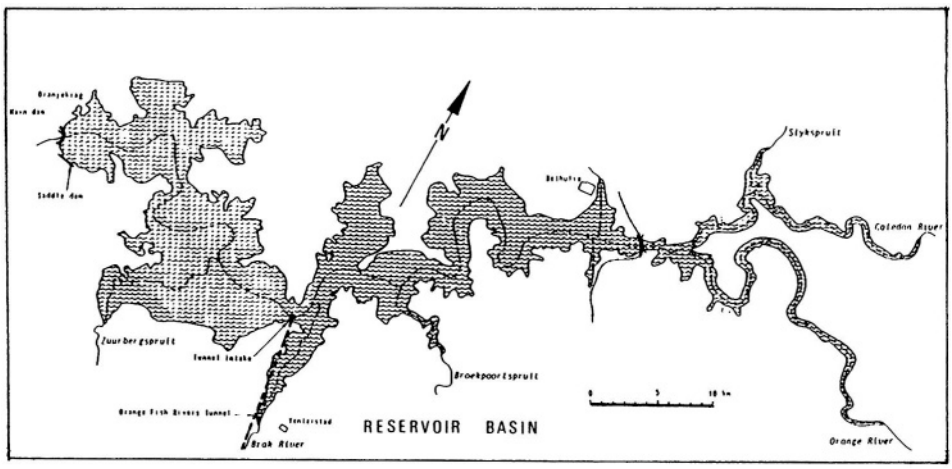

Figure 11.18$_b$- Map of the Cabora Bassa Reservoir

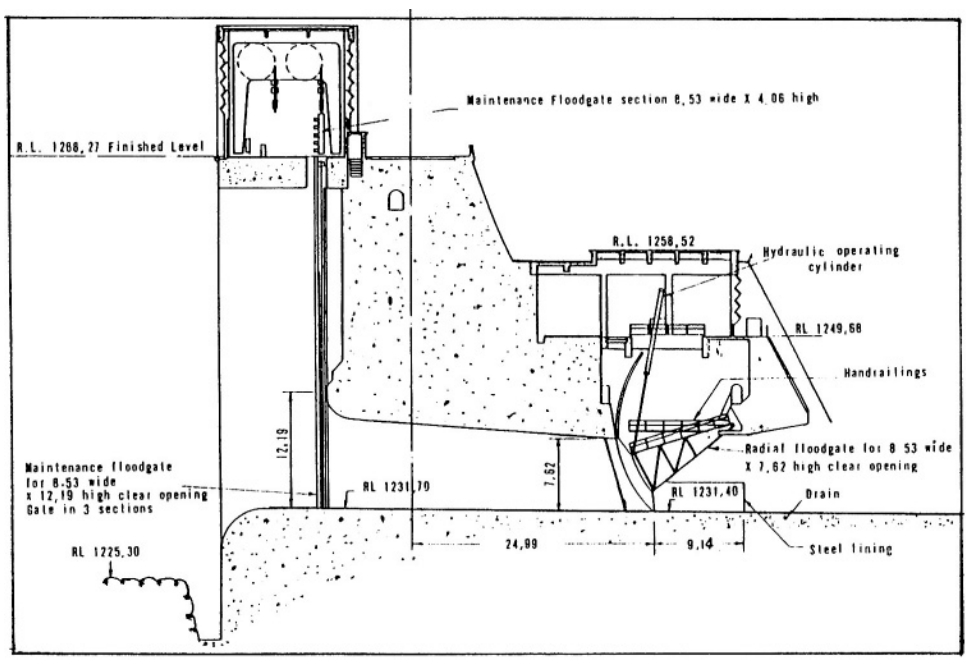

Figure 11.19- Cross section of the Gariep Dam

CHAPTER 12

GROUNDWATER RESOURCES OF AFRICA

12.1- Introduction

Aquifers (water-bearing formations) serve within water resources systems as 1) water resources, 2) water storage facilities, and 3) mean of water quality upgrading (Schwarz, 1989). In areas where precipitation is limited and/or its occurrence is seasonal, the availability of water during the long dry season (s) depends on the storage of water in the underground reservoirs. Groundwater as a source of water is thus extremely important in arid and semi-arid zones. In other climates the problem originates from the pattern of distribution of the surface water that does not match the demand on water, which could be the case in semi-humid and humid zones. Groundwater can be used in this situation as a source for alleviating the problem. Groundwater, unless contaminated, is generally of a better quality than surface water.

Groundwater has a number of unique features rendering it particularly suitable as a water supply, including the following (Coughanowr, 1994):

- Groundwater has excellent natural quality. It is generally free of pathogens, colour and turbidity and can be consumed directly without treatment;
- Groundwater is widely distributed and can frequently be developed in close proximity to needs;
- Groundwater sources are dependable and are relatively unaffected by short droughts; and
- Groundwater can be developed incrementally, at points near the water demand, thus avoiding the need for large-scale storage, treatment and distribution systems.

The same reference, i.e. Coughanowr (1994), estimated the groundwater use as 25% of the total water supply in each of Ghana and Comoros Islands, and as 40% in Mauritius Island. The groundwater use in Egypt amounts to about of 10% of the total use of water. In fact, the irrigation of vast areas of arable land with groundwater from wells and deep boreholes has become widespread in many countries like Libya, Chad, the Sudan and South Africa.

The fast development and exploitation of groundwater resources, however, is giving rise to a number of problems. Groundwater exploration and extraction in areas located within or in the vicinity of the African Shield, where the ground is covered by Precambrian rocks or by a thin veneer of sediments, is a difficult, expensive and time-consuming process. In many African rural areas,

groundwater is obtained from the basement rocks, from cracks, fissures, joints of the igneous and metamorphic rocks and from layers of weathered basement rocks. The salinity of this water is often fairly high. Water is also obtained from alluvium deposits and aquifers in coastal plains. Excessive withdrawal of groundwater from these coastal aquifers principally for potable water, can lead to salt water intrusion and eventually to deterioration of the pumped aquifers (Ishag, 1976). Once this happens it becomes exceedingly hard to restore the quality of water. So, while planning any groundwater extraction scheme the above-mentioned arguments, positive and negative, should be taken into consideration.

Groundwater bodies are replenished by infiltration from rainwater, irrigation water or seepage from surface watercourses or other aquifers. A range of aquifer pollutants result from various agricultural practices. These include pesticides, fertilizers, and toxic substances, and effluent from dairy sheds and cattle feedlots. As a result of these harmful sunstances, cases of polluted aquifers have been detected in several locations. This situation is often referred to as agricultural menace to groundwater quality. Since the late 1970s, steady advances in understanding the influence of agricultural cultivation on the quality of groundwater recharge seems to have been made (Foster and Chilton 1996).

The (former) Soviet Water Resources Research Laboratories subdivided the water resources of the continents into three zones (cited in Balek, 1983):

i- an active zone in the upper part of the earth's crust to a depth of 200 m and above the erosion base

ii- a less active zone, with a depth above the sea level, interacting with various extensive depressions and deep valleys; and

iii- a zone below the sea or ocean surface to a depth up to 2,000 m below sea level.

In Africa the above-listed divisions are 200, 400 and 2000 m in depth respectively. The corresponding storage volumes, in the same order, are 1.0, 1.5 and 3.0, all times 10^{15} m^3, with a total of $5.5*10^{15}$ m^3. Additionally, the annual outflow from the three zones together has been estimated as $1.6*10^{12}$ m^3. Abstraction of groundwater is mostly (above 90%) confined to the top zone and the rest to the middle zone. There is hardly any water abstraction from the zone below the ocean surface.

The greater part of the surface of Africa is covered by a Precambrian crystalline and metamorphic shield. Precambrian crystalline formations date back to much more than 350 million years B.P. Within the older crystalline formations, a number of independent orogenic cycles, affecting these rocks, having been detected. Precambrian formations of the large peneplains in West Africa and the highlands in East Africa have their water-bearing units mainly in weathered fractures. The upper horizon is frequently formed by laterites and

sands imbedded in clay temporarily containing groundwater. The lowest horizon consists of weathered sections of bedrock holding water under a certain head. The material composing these sections and the pressure head to which it is subjected affect the yield of this horizon. The outcroppings of the crystalline rock and metamorphic shield correspond to the uplift areas encircling the depressed basins filled with sedimentary formations such as those of the Niger, Chad, Nile, Congo and Kalahari. Metamorphic rocks in East Africa comprise a wide surface of about 620, 000 km^2. This surface extends from the Sudan-Ethiopian border in the north to the Mozambique border in the south, thus covering vast areas in Ethiopia, Kenya, Tanzania and Uganda.

Cambrian and Infracambrian formations of marine origin, composed mainly of calcareo-dolomitic rocks and calcareous shale have been identified. They are found mainly in the Central African Plateau south of the equator in certain parts of Zaïre and Zambia. Some rich water bearing units can be found in the Infracambrian and Paleozoic formations. Younger formations consist of relatively thick layers of shale and sandstone with some limestone and clay beds. Some of these deposits, as in the Chad region and northern Nigeria, contain strong groundwater resources of artesian nature.

Some of the coastal sedimentary basins, including the Somalian Plateau in the Horn of Africa, were once inundated in the Jurassic and Early Cretaceous times. During the inundation period, known as the Continental Intercalary, formations of sandstones were deposited in most of the basins. The water yield of the Mesozoic plateau of Ethiopia and Somalia is highly variable. Formations of sandstone continued to be deposited in the Tertiary period while eruptions occurred on the breaking lines along the Rift Valley during the Miocene and Pliocene periods.

Figure 1.2 is a generalized map showing the geohydrological provinces of Africa (taken from Wright, 1983). This map shows that Sedimentary Basins occupy approximately 57% (15% unconsolidated and 42% consolidated sediments) and the Basement Shield approximately 32%. The rest is divided between the volcanic terrain, 7% and the folded mountains, 4%, along the coasts of North and South Africa.

12.2- Types of Aquifers and their Hydrogeological Characteristics

12.2 1 Types of aquifers- Groundwater occurs in permeable geologic formations known as *aquifers.* Aquifers have structures that permit appreciable amounts of water to move through them under ordinary field conditions. In contradistinction, an *aquiclude* is an impermeable formation, which may contain water but is incapable of transmitting significant water quantities. An *aquifuge* is an impermeable formation neither containing nor transmitting water. Clay is an example of aquiclude while solid granite is an example of the aquifuge (Todd, 1959).

Most aquifers are of large areal extent and, in a way, can be regarded as groundwater storage reservoirs. When the reservoir consists of a number of aquifers separated by impermeable or semi-permeable layers it is referred to as aquifer system. The aquifer system of the Nubian Sandstone Basin in the Western Desert in Libya and Egypt consists of six or seven aquifers at certain locations. Whether the reservoir consists of a single aquifer or multi aquifers, aquifers can be classed into three different types.

An unconfined aquifer is one where a water table serves as the upper surface of saturation, or the surface of zero pressure, i.e. atmospheric. It is also called a free, water table, or phreatic aquifer. A rise or fall in the water table level corresponds to the change in the volume of water in storage within the aquifer.

A confined, sometimes called piezometric or pressure aquifer, is found where groundwater is confined under pressure greater than the atmospheric pressure by an overlying and underlying aquicludes, which are completely impermeable layers or strata. When such an aquifer is penetrated by a well, the water level will rise above the lower face of the confining layer. If the pressure head is so high that the water level rises above the land surface, the aquifer is referred to as an artesian aquifer and the well as an artesian well. In a number of situations the pressure becomes less with time, and water instead of flowing freely has to be pumped. Such a change in the way with which groundwater is obtained causes the cost of having water to increase sharply with time.

The third type of aquifers is known as semi-confined or leaky aquifer. This type occurs when the aquifer material, instead of being bounded by an impermeable layer or aquiclude, is bounded by a weakly permeable layer known as *aquitard.* Figure 12.1 shows the different types of aquifers as sketched by Wilson (1983).

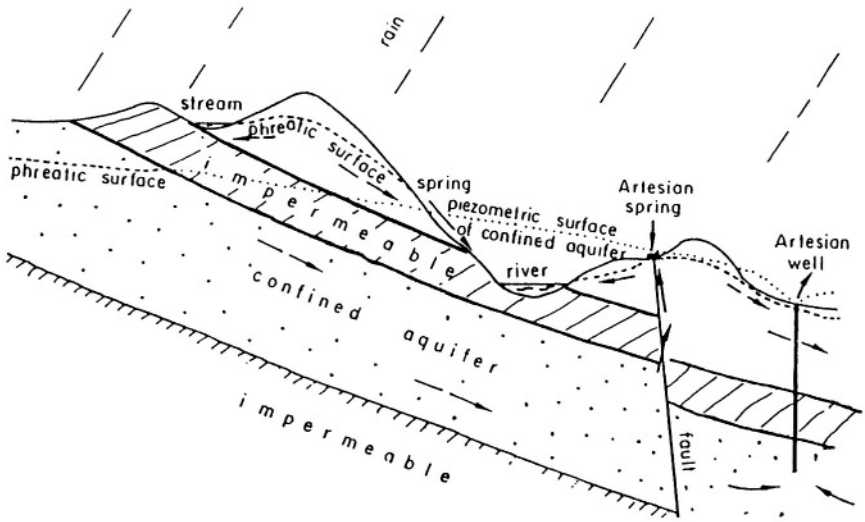

Figure 12.1- Modes of occurrence of groundwater (Wilson, 1983)

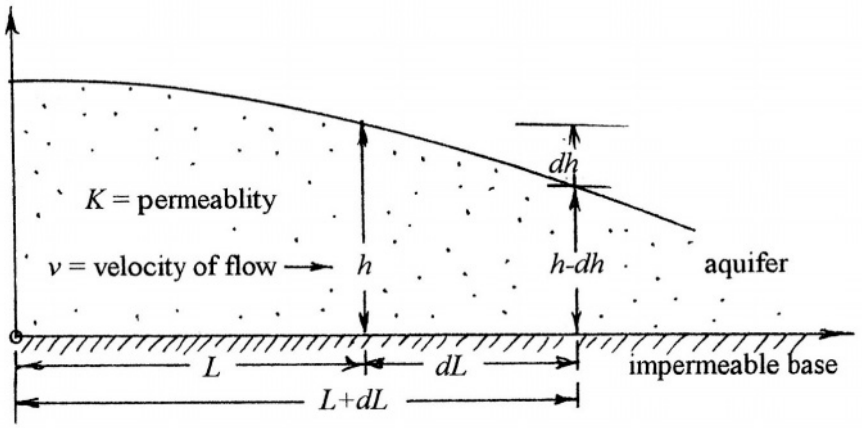

Figure 12.2- Definition sketch

12.2.2 Hydrogeologic constants- Referring to Figure 12.2, denote the drop in head over a distance *dL* by *dh.* The quantity *dh/dL* is called the hydraulic gradient. Assuming that Reynolds number does not exceed the allowable limit for laminar flow, the average velocity of flow, *v*, is related to the hydraulic gradient, *dh/dL,* according to Darcy's law by the relationship:

$$v = Kdh/dL \tag{12.1}$$

where *K* is a proportionality constant known as coefficient of permeability. This coefficient has the dimensions of velocity, and is often expressed in $\mathbf{m\ d^{-1}}$. As the thickness, *H,* of the aquifer is usually too large compared to the difference of head, *dh,* it can be taken as $(h_1+h_2)/2$ with a little approximation. The coefficient of transmissibility or the transmissivity of the aquifer, *T,* and the aquifer's resistance, *C,* can be expressed by Eqs. (12.2) and (12.3) as follows:

$$T = K(h_1 + h_2)/2 = KH \tag{12.2}$$

and

$$C = H/K \tag{12.3}$$

respectively. The transmissivity, *T,* is often expressed in $\mathbf{m^2\ s^{-1}}$ or $\mathbf{m^2\ d^{-1}}$ whereas the hydraulic resistance, *C,* is expressed in units of times such as days or years.

Aquifers are also characterized by their coefficient of storage or storativity, *S.* This coefficient can be defined as the volume of water that an aquifer releases or takes into storage per unit surface area of aquifer per unit change in the component of head normal to that surface. The storage coefficient for an

unconfined aquifer is its specific yield or free porosity. It varies between 0.05 and 0. 20 depending on the material composing the aquifer. In confined aquifers the storage coefficient equals the volume of water released when the piezometric surface declines one unit head. In most confined aquifers, values of S fall in the range 0.00005-0.005 (Todd, 1959). Analysis of pumping test results is the standard procedure for determining the aquifer constants.

Semi-confined or leaky aquifers can be defined by their leakage factor λ given by the equation (Verruijt, 1970):

$$\lambda = \sqrt{KHc} \tag{12.4}$$

In order to maintain a groundwater resource indefinitely, an equilibrium must exist between the inflow and outflow of the basin. In the meanwhile, economic, legal and water quality aspects should be taken into account. As such, the term safe yield has been developed to quantify the basin draft (release or outflow) that ensures indefinite supply of groundwater supply under a given set of conditions without endangering the basin or the right of any its users. Any withdrawal in excess of the safe yield is termed overdraft.

The next tabulation gives approximate figures for the average and maximum yield of various formations as suggested by the Resources and Transport Division of the United Nations (cited in Balek, 1983)

Formation	Average yield $m^3 h^{-1}$	Maximum yield $m^3 h^{-1}$
Precambrian		
Granitogneiss	2-5	20 and more
Schists, rhyolites, diorites	less than 1	NI
Infracambrian and Paleozoic		
Shale-limestone and calcero dolomite	10-100	NI
West African Shales and shale-limestones	NI	NI
Large Sedimentary basins of Central Africa		
Karoo sands	1	200
Artesian waters of northern Nigeria	NI	1000
Kalahari sands	1-10	50
Congo and Chad basins	1	NI
Continental Intercalaire	NI	100 or more
Alluvium	small	up to 1000 in the Nile region
Sedimentary coastal basins	20	300

12.2.3 Recharge- Adequate recharge to an aquifer system is necessary to sustain a groundwater resource. Recharge occurs as a result of rain or irrigation water

infiltrating through the ground surface at a rate that is able to make up and exceed the soil moisture deficit. The excess water joins the ground water body, and the process is termed direct recharge. An aquifer system, instead of being vertically recharged, can get lateral recharge through seepage from another water-bearing formation. Recharge can also occur by way of runoff or ponding resultant of precipitation, and the process is termed then indirect recharge.

Recharge can be estimated from the saturated water balance of an aquifer, which can be expressed by the balance equation given by Lloyd (1999):

$$RE_{eff} = Q_{abs} + S_y \Delta V + Q_o - Q_i \qquad (12.5)$$

where RE_{eff} = effective recharge after evapotranspiration losses from the aquifer have been accounted for, Q_{abs} = groundwater abstraction by pumpage or free flow, S_y = specific yield, ΔV = change in saturated storage volume, Q_o = lateral flow to lower aquifers and Q_i = lateral flow from higher aquifers.

In many semi-arid areas there exists the possibility of reducing the loss of water by evaporation. There are short periods in the rainy season where water excess occurs. The excess water can be collected in depressions (recharge ponds, stream beds, artificial lakes) by small channels, drainage pipes, etc. From these depressions, water is fed to the aquifers via recharge wells. The storage of excess rainwater in deep aquifers saves it from being lost by evaporation. This idea has been supported by the findings obtained from indirect recharge of the aquifers in the area of Borno State, which is located in the northeastern part of Nigeria and the southeastern part of the Lake Chad Basin. The aquifer system in this area consists of three aquifers. The total withdrawal from the three aquifers amounted to $82.9*10^6$ m^3 y^{-1}. To reduce the accelerated depletion of groundwater resources as a consequence of the increasing demand on water, artificial recharge using recharge wells has been experimented and the results were encouraging (Jacenkow, 1984).

Lloyd (1986) suggested some empirical relationships between recharge and annual rainfall for arid, semi-arid and other climates, and direct as well as indirect recharge method. The suggested relationships are shown in Figure 12.3. Again, Lloyd (1994) reported that recharge in the semi-arid and arid areas is often limited or non-existent. In these areas, fresh groundwater resources are non-sustainable, or only partly so, and water supplies are dependent upon groundwater mining and/or desalination of seawater or brackish groundwater, or other water sources.

12.3- Groundwater Provinces and Basins

The term hydrogeological province is meant to reflect the hydrological aspects of a geological unit. Hydrogeological provinces thus relate closely to geology.

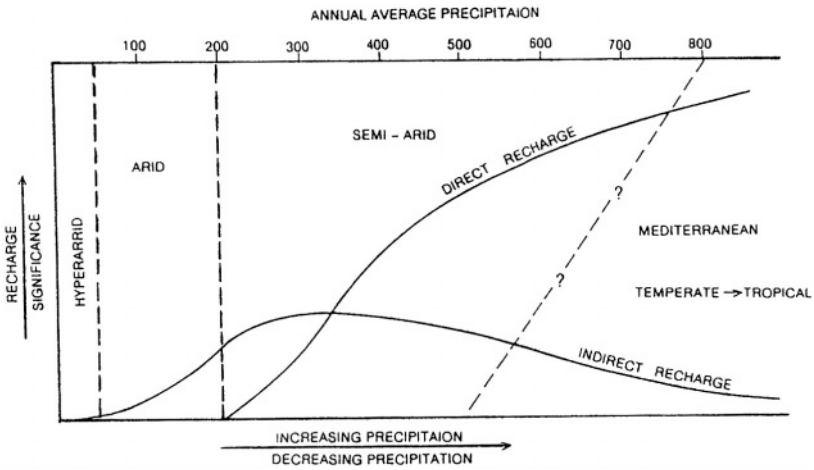

Figure 12.3- Suggested relationship between aridity and recharge (Lloyd, 1986)

The generalized map in Figure 1.2 shows the African geohydrological provinces as suggested by Wright (1983). In this map the provinces are classified into four: the fold mountains in northwest and south of the continent, the volcanic province east and south of the southern part of the Red Sea, the basement complex in East, Central and West Africa, and the rest of the continent is occupied by the sedimentary province. This last province can be subdivided into mainly consolidated and mainly unconsolidated zones.

A groundwater basin is a body smaller in size than a province, and usually consists of a number of groundwater formations. A basin, by definition, has one or more natural recharge area(s) and one or more discharge area(s). The term basin, according to Todd (1959), is used very loosely in practice, and, because of its vagueness, it has no clear general definition. However, it implies an area containing a large volume of groundwater capable of furnishing a substantial water supply. The prevailing climate, geohydrological properties of the surface formations and the underlying aquifers largely influence the basin characteristics. Furthermore, the groundwater abstraction and recharge dictate the state of equilibrium of the basin.

The groundwater basins covering most of the surface extending from North Africa to the Sudan can be found in the Atlas region, the Great Desert region and the Nile Valley and Delta region. The Atlas region includes the Tell Atlas, Upper Plateau, Reef, Atlas Coastal Plain, Upper and Middle Atlas, and the Desert Atlas. The Great Atlas Region comprises the Tarfaya-Dakhla, Nouakchot, Sénégal, Taoudeni, Great Erg (Occidental Erg = Continental Intercalary and Oriental Erg = Complex Terminal), Niger, Murzuq, Hamada Al-Hamra and Jifara. The Nile Valley region comprises the Western Desert, Nile Delta and Coastal Plain, Red Sea and Sinai, Umm Ruwaba and Western Sudan

and African Horn. Figure 12.4 is a map showing the locations of the groundwater basins in the Sahara Desert (Margat and Saad, 1984), while the flow lines and the water levels in the same Desert are shown in the map Figure 12.5 (redrawn from Alam, 1989).

Artesian groundwater has a special importance in arid tropics. This is particularly true in Algeria, Libya, Egypt's Oases, Sénégal, etc. In this context, it should be pointed out that that the African desert areas, with annual rainfall less than 250 mm, have one of the of the world's greatest aquifers.

The next subsections describe in somewhat detail the extensive groundwater provinces, basins and formations in Africa. These comprise the Basement Complex, Sedimentary rock, Nubian Sandstone and basins of mixed water-bearing formations. Table 10, Part I/Appendix B, includes approximate figures for the areal extent, aquifer depth, geohydrological constants, etc. of these basins. Additionally, as the lithology of a certain water-bearing formation is connected to its geologic age, the geological succession specified by Lloyd (1990) will be adopted here:

Age	Lithology
Quaternary	Lacustrine deposits, Sebkhas, sand dunes and alluvium
Miocene	Sands, interbedded clays and sandstones
Oligocene	Sands, sandstones, clays, limestone and basalts
Eocene	Limestones, dolomites, marls and sandstones
Upper Cretaceous	Shales with some sandstones and limestones
Lower Cretaceous	Sandstones, interbedded shales and clays (Nubian)
Undifferentiated Paleozoics	Shales and sandstones
Cambro-Ordovician	Sandstones and quartizites

12.3.1 The Basement Shield- Crystalline and metamorphic rock aquifers cover approximately one third of the surface area of Africa, as can be seen from the map in Figure 1.3. These rocks show varying degrees of weathering. Outcrops of unweathered rocks are interspersed by deeply weathered rock. The water-bearing formations or aquifers are heterogeneous, as their hydraulic characteristics vary widely over short distances. Locally, they constitute isolated groundwater basins with hardly any inter-basin exchange. The weathering process has been for sometime aggressively acting on the decomposed rock, at least in certain zones, thereby creating openings along which groundwater may circulate. The water-bearing capacity of these zones may be further enhanced by the presence of fractured quartz veins (Bannerman and Ayibotele, 1984). Fracturing is the factor that imparts the essential but highly variable secondary hydraulic conductivity and porosity without which hard rocks would have no sensible aquifer potential (Lloyd, 1999).

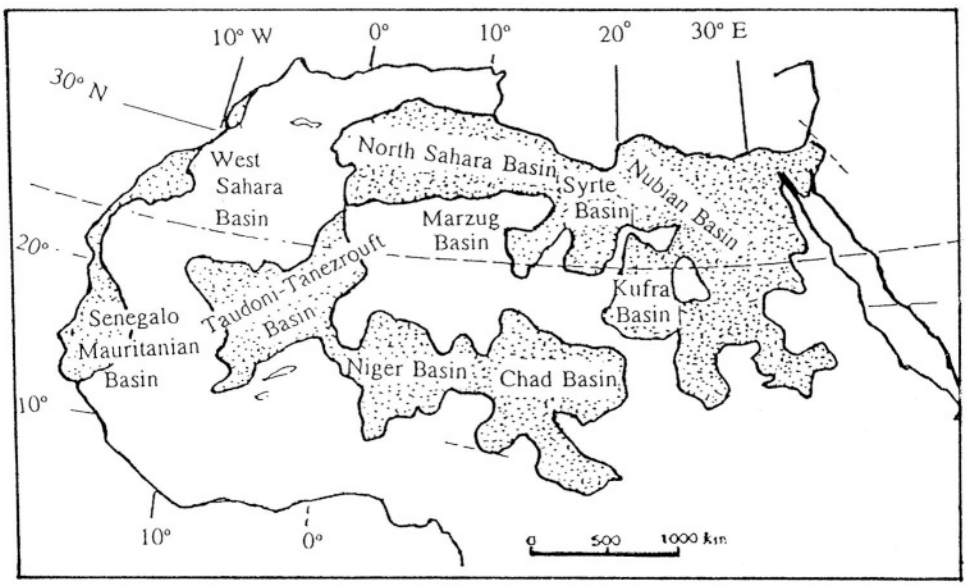

Figure 12.4- Location map of groundwater basins in North Africa (Margat and Saad, 1984)

The rock-fracturing network influences the distribution of the radon gas in the soil underlain by crystalline and metamorphic rocks. As such, the radon exploration method allows the detection of the most productive areas for groundwater abstraction. This observation has been confirmed by an experimental survey on a number of boreholes in Burkina Faso (Mathieu et al., 1989). The depth of the decomposed zone varies widely, but generally it is less than 40 m. On rare occasions the depth reaches 60 m. The aquifers are generally characterized by low transmissivities coupled with low storativities. As a consequence, the yields from boreholes are generally in the range from low to moderate depending on the lithology of the rock. Figure 12. 6 shows the results obtained by Barrat and Puyoo (1984) from a survey of a large number of boreholes and wells in Niger. The data available on the yield of wells and boreholes from many locations in arid and semi-arid areas do not really distinguish any particular hard rock as being potentially a better aquifer material than any other.

12.3.2. Sedimentary Province (Sandy formations)- Sandstone formations are abundant along the margins of the ancient shields. They are the result of the continuous deposition of sands through geological eras in regional sedimentary basins. The sedimentary basins were mainly continental terrestrial, and the sands were deposited as aeolian dunes, which were later consolidated to pressure and precipitates. Some of the sandstones were deposited in marine basins where the clay content augmented to a large extent and formed basins

made up of continuous and thick aquicludes. Where the paleo-environments arid were, the more continuous and homogeneous the aquifer system is.

On a regional scale, thick and continuous phreatic aquifers are found in regions bordering the ancient crystalline shield causing the aquifer recharge to take place along the contact lines and the margins of the basement shield. Local rain provides the direct recharge, while indirect recharge is supplied from the rivers draining the shields. By contrast, the sandstone sequence in the direction towards the ancient seas or lakes subdivides itself into secondary, confined aquifers. The flow of water in the confined regions is slow and the residence time of water in the aquifers exceeds thousands of years. Natural recharge of these aquifers is of no significance. In fact, the recharge to such extensive aquifers is limited to certain episodes in the geological history of the basin. The effective historical recharge rates have been caused by excessively wet climatological conditions different from the current ones. As the storage capacity of the basins comprising these aquifers is quite tremendous, the residence time is the main characteristic, indicating that the paleo-climatic effects are considerable, if not decisive.

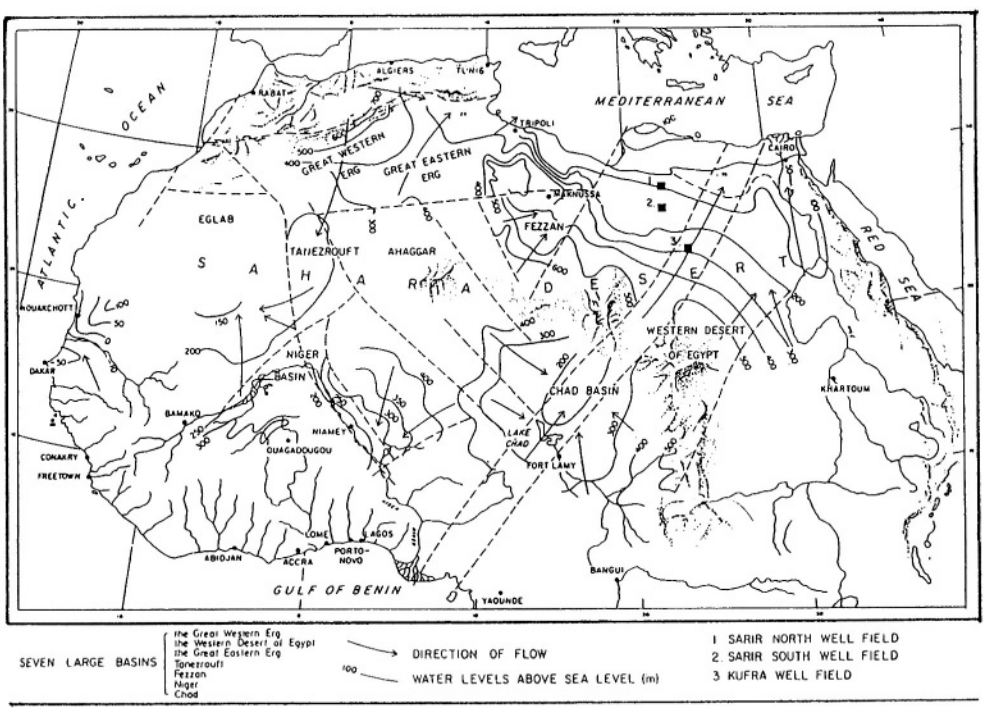

Figure 12.5- The Sahara Desert showing seven large basins and Libyan well fields (prepared by Ambroggi, 1966 and modified by Ahmad, 1981 and cited in Alam, 1989)

An example combining the above-mentioned situations is the sedimentary basin underlying Mali, Niger and Nigeria. This area has an arid climate with an average rainfall of 0-50 mm y^{-1}. The multi-layer aquifer consists of sand, sandstone and argillaceous sand. It is unconfined at the edge and becomes confined towards the center and in the south. The average thickness is in the range of 240-300 m in Nigeria and around 500 m in Niger. Recharge to the basin occurs in the Niger through outcrops into the unconfined zone and is estimated as $850*10^6$ m^3 y^{-1} (20 m^3 s^{-1}).

12.3.2$_b$ Sedimentary Province (Nubian Sandstone)- This basin constitutes part of the sedimentary province. The basin is a complex of clastic sediments, discordantly and transgressively laid on the level paleorelief of predominantly Precambrian rocks, i.e. the sandstone randomly overlies the Basement Rocks. The name Nubian Sandstone derives from the outcrops in Nubia in the north of the Sudan and south of Egypt. As this formation extends in the region of the Nubian Desert and the wider area of the Sahara-Arabian plateau, it is truly regarded as one of the most extensive artesian basins of the world. It covers northeast Chad, south and east Libya, the Western and the Eastern Deserts of Egypt and northwest of the Sudan. What is called Nubian Sandstone in North and East Africa is commonly known as Intercalary Continental in West Africa. The total surface covered by the Nubian Sandstone in these four countries is $1.8*10^6$ km^2. The thickness of the aquifer system varies from less than 500 m to

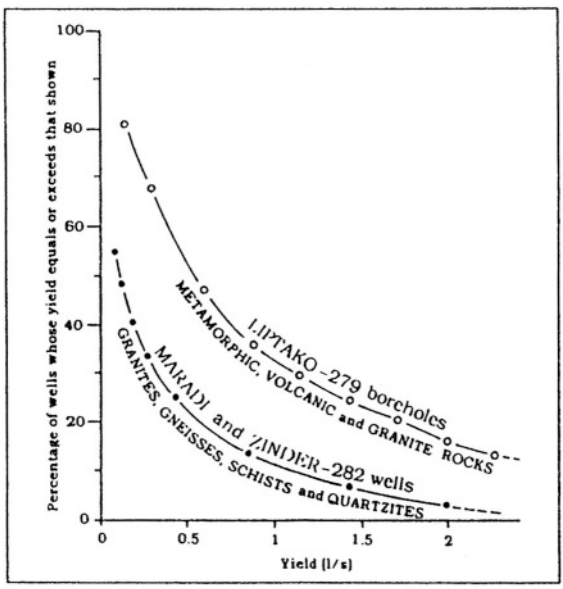

Figure 12.6- Relationship between well yield and hard rock lithology in Niger (Barratt and Puyoo, 1984)

over 3,000 m. Nubian Sandstone and equivalent formations occur also at a depth less than 200 m and are exposed in the recharged areas. The complex of sandstone has been deposited in extensive geosynclinal basins that act as regional hydrogeological basins. The storage of water in such basins took place in situ during one or more of the pluvial episodes of the Late Pleistocene age. Nace (1969) estimated that in the Nubian Sandstone and the Continental Intercalary Basins, on an area of $6.5*10^6$ km^2, about $600*10^{12}$ m^3 of water are stored. These basins were recharged during the pluvial episode (s) some 40,000 to 30,000 years B.P. The current recharge of these reservoirs is very limited.

12.3.2$_c$ Sedimentary Province (Limestone formations)- Limestone and dolostone (dolomites) are sediments of a rather shallow and warm marine environment. Aquifers made up of these rocks are generally homogeneous and thick. They extend over extensive areas to great depths. These formations are characterized by extending themselves over the global belts that have undergone folding movements, thus forming mountain chains. The Atlas Mountains in North Africa constitute an example. They receive a fairly heavy annual precipitation, which recharges the underlying thick aquifer, and flows out along the arid foothills as big springs. Quite often, limestones and dolostones form secondary aquifers, which under extreme cases can develop into karstic formations and, as a result, bring the aquifer permeability and recharge to a maximum. The studies that were carried out on limestone structures in Tunisia have shown large variations in the infiltration rate. The parameters affecting the infiltration rate are the groundwater reserves at the end of the dry season, the total depth of rain and the precipitation intensity.

12.3.3 The Volcanic Province- This province comprises vast formations of the Mesozoic plateau of Ethiopia-Somalia, the lava fields of Ethiopia, the volcano-detrital deposits of Djibouti, and the Rift valleys of East Africa. The Volcanic terrain compared to the surface area of the terrain occupied by the Basement Shield or the Sedimentary Province is small.

The performance of the aquifer systems in a Vesuvian type basalt terrain is determined by the alterations between pyroclastic (fragmental volcanic rock such as volcanic ash) and basalt flows, and the alternating episodes of lava flow and volcanic bursts. The period between each active phase is important, as it allows the soil forming processes and the development of the impermeable layers to take place.

The properties of most of the volcanic formations are still to be explored. The investigation carried out in Djibouti has shown that volcano-detrital deposits cover almost the whole country. The surface network at present consists of intermittent wadis. Properties of the groundwater systems are governed by geological and sedimentological features of the corresponding area. Only where the lavas are fractured that precipitation and water can

infiltrate and accumulate within sediments in the depressions, where permeability and porosity are too low due to the high concentration of clay. The depth to the piezometric level of groundwater below land surface varies from 30 m in the coastal strip to 200 m in the north of the country

From the groundwater samples of the basaltic outcrops, it was found that the aquifers are rapidly recharged through their cracks and fractures. The occurrence of recent recharge indicates that the aquifer storage is too limited.

12.3.4 The Chad Basin- This groundwater basin, with Lake Chad at its lowest level, constitutes a vast reservoir of groundwater. Extending over an almost continuous surface of $1.4*10^6$ km^2, the vast groundwater body surrounding the lake has different hydraulic characteristics and depth over the basin. The basin can be subdivided into three main aquifer systems or groundwater zones.

i- The groundwater in the top or uppermost is zone is free or phreatic. Flow rate tests were run on boreholes penetrating the entire thickness of the aquifer system in this zone and four transmissivity values ranging from 37 to 375 m^2 d^{-1} were obtained. A storage coefficient of 0.15 may be assigned to the aquifer system in this zone.

ii- The middle zone aquifer is essentially composed of sand and clay. It underlies a surface of 35,000 km^2 in Niger and 50,000 km^2 in northeast Nigeria. This aquifer system is confined and separated from the upper aquifer zone by a thick clay layer that ranges from 60 to over 300 m. The aquifer consists of fine to coarse-grained water bearing sand, cemented or clayey sand, sandy clay and clay. The depth below the ground surface to the upper surface of the aquifer in the areas where artesian water is found varies between 150 and 375 m. The transmissivity of the aquifer system in this zone, being around 800 m^2 d^{-1}, is quite high compared to the aquifer in the top zone. The storage coefficient is $2*10^{-3}$.

iii- The third aquifer system occupies the lowest groundwater zone and belongs to the Continental Intercalary. This aquifer system is also confined, and a substantial volume of water in the aquifer is artesian. The average transmissivity of this zone is in the range 50-100 m^2 d^{-1} (Ahmad, 1986). As little information is known about this deep aquifer, one cannot confirm the supposition that it is probably the best aquifer for groundwater abstraction.

12.4- Groundwater in Selected Regions and Countries

12.4.1 The Nile Basin Region-

i- Egypt: The main aquifer systems in Egypt are shown on the map in Figure 12.7. They can be grouped into six groups as follows:

- The Nile aquifer system is formed by the alluvial deposits of the Quaternary and Late Tertiary sand and gravel beds intercalated with clay lenses. The water-bearing formation is located between an impermeable bed at the bottom and sides of the valley and a relatively thin semi-impermeable clay layer at the top.
- The Nubian sandstone belongs to the Paleozoic-Mesozoic Eras and occupies a thin though a long slice of the Eastern Desert and a large part of the Western Desert in Egypt.
- The Moghra aquifer system belongs to the Lower Miocene (post-Nubian) and occupies a vast area between the western edge of the Nile Delta and Qattara Depression. The aquifer is composed of sand and sandy shale with a thickness varying from 500-900 m. The aquifer is phreatic with water table level between 10 m a.m.s.l. at the side bordering the Nile Delta and 60 m b.m.s.l. at the Qattara Depression in the west. The aquifer water is thought to be partly renewable and partly non-renewable. The salinity increases from 1,000 ppm near the Delta in the east to 5,000 ppm near the depression in the west. The aquifer is recharged, among others, by the lateral seepage from the aquifer underlying the Nile Delta at an annual rate of $50\text{-}100*10^6\ m^3$.

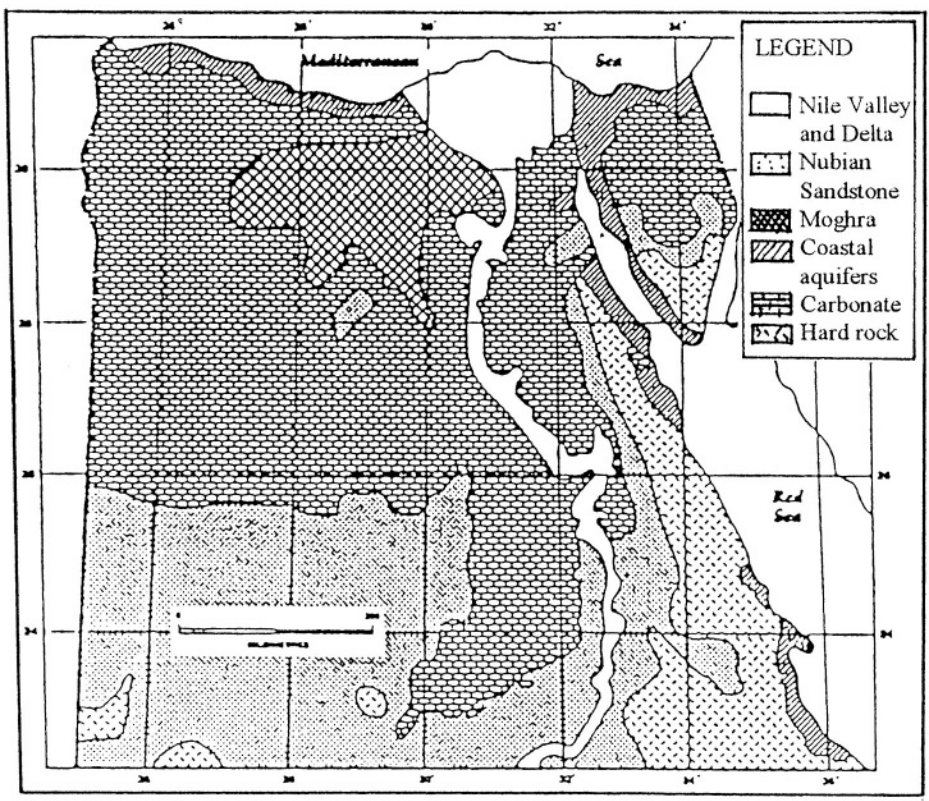

Figure 12.7- The aquifer systems of Egypt

- The coastal aquifer system, which belongs to the late Tertiary and Quaternary, and occupies the northern and western coasts.
- The Carbonatic aquifer system belongs to the Upper Cretaceous Era. It consists of fissured and karstified Carbonatic rocks. The aquifer covers the northern half of the Western Desert and northern Sinai, thus occupying more than 50% of the surface area of Egypt.
- The fissured and weathered hard rock aquifer system belongs to the Pre-Cambrian. It covers most of the surface of the Eastern Desert and South Sinai. Weathered hard rock acts occasionally as a water-bearing media through cracks and fractures. The water abstracted from this formation is used on a small local scale for domestic purpose and for tourism.

As groundwater abstraction in Egypt occurs from the Nile Delta and Valley, and the Nubian aquifer systems, the characteristics of these two systems will be reviewed in the next paragraphs in more details.

The Nubian sandstone in Egypt. The water levels in the various wells scattered in the Oases in the Western Desert suggest that they belong to one huge body of groundwater. Several investigators prepared maps showing the equipotential lines of the groundwater under this desert. Figure 12.8 is one of the recent attempts (Ezzat, 1976). The coefficients of permeability, transmissivity and storage as obtained from the analysis of pumping test results showed that they are in the ranges of 2-20 m d^{-1}, 1,000-1,800 m^2 d^{-1} and $2\text{-}4*10^{-4}$ respectively.

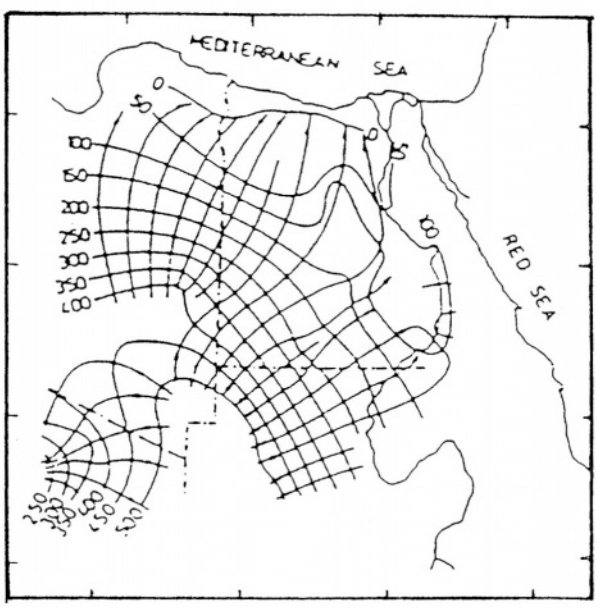

Figure 12.8- Equipotential lines of the Nubian Sandstone aquifer in the Western Desert of Egypt (Ezzat, 1976)

The depth below ground surface to the top face of the aquifer in and around the desert oases varies from 0 to 20 m. In some locations the water is even flowing freely. The total abstraction from the oases of the Western Desert in Egypt around 1975 was estimated as $0.38*10^9$ m^3 y^{-1}. The inventories of 1984 and 1990 were $0.45*10^9$ and $0.54*10^9$ m^3 respectively. The total abstraction from the Nubian Sandstone in Egypt is expected to reach $3.5*10^9$ m^3 by the year 2025. This corresponds to a total withdrawal of about $100*10^9$ m^3 from the volume in storage.

The Aquifer underlying the Nile Valley and Delta. The aquifers underlying the Nile Valley and the Nile Delta can be regarded as similar in their character. Both are composed of Quaternary and Late Tertiary sands and gravels with intercalated clay lenses and underlain by Pliocene clays. The thickness of the aquifer decreases from 300 m or more in Upper Egypt to a few meters, 70 m, around Cairo. It increases in a northerly direction and reaches 1,000 m along the Mediterranean coast. Table 12.1 includes values of the hydrogeological constants of the Nile Valley and Delta aquifers as obtained from the analysis of well pumping tests. These values show that the transmissivities of the aquifers are generally high and the groundwater quality is fair to good.

ii- **The Sudan**: The water bearing-formations in the Sudan are diverse. The Basement rock of the Precambrian age covers the areas occupied by the Nubian mountains and the mountains along the Red Sea, a total of $1.077*10^6$ km^2 or 43 % of the total surface area of the Sudan. There is hardly water to be abstracted from these rocks except where there are fractures and faults. The volcanic masses cover some $228*10^3$ km^2 or 9.1 % of the surface area of the country.

Table 12.1- Summary of the hydrogeological constants of the aquifers underlying the Nile Valley and Delta (Shahin, 1983_b and Hefny et al., 1991)

Location	*D*, m	*H*, 10^2 m	*h*, m	*K*, m d^{-1}	*S*, %	*T* = *KH*, $10^3 m^2 d^{-1}$	*C* = *H*/*K*, d	*TDS*, ppm
Nile Valley	0-20	(0.1-2)	0-5	50-70	15-25	0.5-2	1-5	<1500
Nile Delta (south)	0-20	(1-5)	0-5	50-100	15-25	5-25	1-5	<1000
Nile Delta (north)	20-100	(5-10)	0-2	<50		>10	>50	>5000
Semi-confined+		(1-2.5)		25-100	0.1-0.01	2.5-25	3000-15000	<2000

Explanation

D = depth to top face of the aquifer, H = saturated thickness, h = depth to water table, K = permeability, S = storativity, T = transmissivity, C = resistance, TDS = total dissolved salts, and + applies for both Nile Valley and Nile Delta areas.

The groundwater in the volcanic formations are generally saline with total dissolved salts varying from 1, 500 to 3, 000 ppm. The Umm-Rawaba Series of the Pliocene to Pleistocene ages can be found south of latitude 14°N. The series covers a total surface area of $515*10^3$ km^2 or 20.5% of the country's surface area. The water is of relatively good quality, as the total dissolved salts range between 400 to 600 ppm. The last water-bearing formation comprises the Nubian Sandstone. It covers an area of $704*10^3$ km^2 or 28.1% of the surface area of the Sudan, extending north of 10°N latitude.

The total volume of groundwater in storage has been estimated as $41.8*10^9$ m^3, receiving annual recharge of $1.38*10^9$ m^3. The annual abstraction till a few years ago did not exceed $0.2*10^9$ m^3 (Hedayat/Country Report of the Sudan, 1986). There is, however, a growing tendency to augment the abstraction to cope with the growing demand on water for future domestic as well as (small-scale) irrigation purposes. A few more details about the properties of some of the water-bearing formations and the local groundwater reservoirs are included in Table 12.2.

Groundwater in small quantities from a number of areas in the Sudan is currently withdrawn for domestic and other purposes. Some examples of groundwater abstraction from the alluvial sediments are presented in the next subsections.

Table 12.2- Some data about the water-bearing formations in the Sudan (from the Country Report of the Sudan, 1986)

Water-bearing formation	Area, 10^3 km^2	Groundwater basin	Storage capacity, 10^9 m^3	Recharge, 10^6 m^3 y^{-1}	Abstraction, 10^6 m^3 y^{-1}
		Nubian sandstone	5.500	3.7-136	1.2
		Sahara Nilotic	9. 740	20.6-20.6	7.4
Nubian	660	Central Darfur	0.794	12.8-47.6	5.6
		An-Nahud	0.136	1.5-15.4	2.5
		Saq-An'naam	0.134	1.2-14.8	1.5
		Atbara R.mouth	0.240	3.7-23.0	0.5
Total	660		16. 544	43.5-257.4	18.7
Umm-Rawaba	420	Swamps area	11.000	50.8-341	1.9
		East Kordufan	1.710	2.3-15.8	4.5
Total	420		12.710	53.1-356.8	6.4
Nubian/Umm-Rawaba	210	Albaqaara	7.110	22.7-155	11.9
		Blue Nile	2.270	10.4-70.9	21.6
Total	210		9.380	33.1-225.9	33.5
Nubian/basaltic	128	Gedaref	0.700	6.1-41.7	4.2
		Shaqra	0.005	1.1-1.0	0.7
XXXXXX	XXXX	Nayala-Azzum-Barakat-etc.	XXX	45-500	80.0

Alluvial Sediments in the Sudan: The volcanic areas of the Darfur Province, Western Sudan, generally have water in the joints of the lava, but deeper lavas do not have open joints and are dry. As an example, the town of Nyala in the Darfur region depends for its water supply on the groundwater in the alluvial sediments of Wadi Nyala (see location map, Figure 12.9). The aquifer there consists of alluvial sediments, mainly medium to coarse sand, not more than 10 m thick. The geometry of the aquifer is long and narrow, consisting mainly of medium to coarse sands. It is recharged in the wet season by infiltration of the wadi surface runoff. A groundwater model was used for assessing the possibilities of increased abstraction for drinking water and irrigation from the Wadi's alluvial aquifer. The permeability and storativity values used in the model were 20 and $50\ m\ d^{-1}$ and 0.1 and 0.2, respectively. The model results have shown that an annual abstraction from the aquifer of $4*10^6\ m^3$, reduced to $3*10^6\ m^3$ in a dry year, will help to cover the local needs for domestic and industrial purposes (van der Linden, 1986).

Another example can be found in groundwater abstraction from the Kassala-Gash Basin, located in the eastern part of the Sudan. Water supply by wells is widely practiced for domestic purposes and for raising livestock in the Gash Delta in Kassala Province. The area under investigation extends from the apex of the Gash River northwards along the river for almost 50 km The water resources occur in an aquifer system in the alluvial deposits of the Gash River. This aquifer system is underlain by impervious Precambrian basement rock and laterally supported against the impervious Tertiary-Pleistocene clays of the Sudan Plain. The most productive part of the aquifer system is that part close where the deposits are generally coarse and the replenishment is most intensive. Groundwater abstraction is partly used for domestic water supply, but the major part goes actually for supplementary irrigation (Senden and Saleh, 1986).

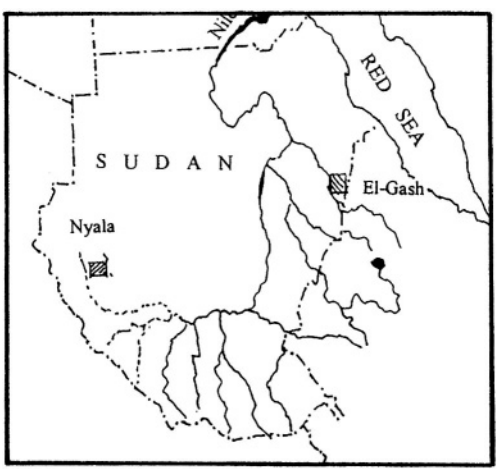

Figure 12.9- Map showing the locations of Nyala and El-Gash areas

A detailed field investigation (Hussein, 1986) reported that the Gash aquifer is composed of a heterogeneous detrital assemblage dominated by coarse sand, gravel, clayey sand and silt. The depth to water varies from 3 m near the Gash River to 30 m at the fringes of the aquifer. The general flow is towards the northeast with an average hydraulic gradient of 0.002 Transmissivity and storativity values range between 1.0 to 5, 850 m^2 d^{-1}, and 0.002 to 0.2 respectively. The groundwater is generally of excellent quality with total dissolved solids between 180 and 260 mg l^{-1}.

The Nubian Sandstone in the Sudan: In the northern desert region of the Sudan there is a permanent groundwater reservoir in the sandstone of the Nubian series. It usually exists at a fairly large depth below ground surface, though it could be locally bared by erosion to form some oases resting on a mudstone layer. The available information shows that the Nubian Sandstone system covers a surface of $660*10^3$ km^2 in the Sudan. This area comprises a number of basins with an estimated storage capacity of $16.5*10^9$ m^3. The recharge ranges between 43.5 and $257*10^9$ m^3 y^{-1} as can be seen in Table 10, Part I/Appendix B, and Table 12.2. Furthermore, Figure 12.10 shows the groundwater heads in the Nubian Sandstone in the Sudan (Countryt Report/Hedayat, 1986), after some adjustment to fit with the groundwater heads in the neighbouring countries.

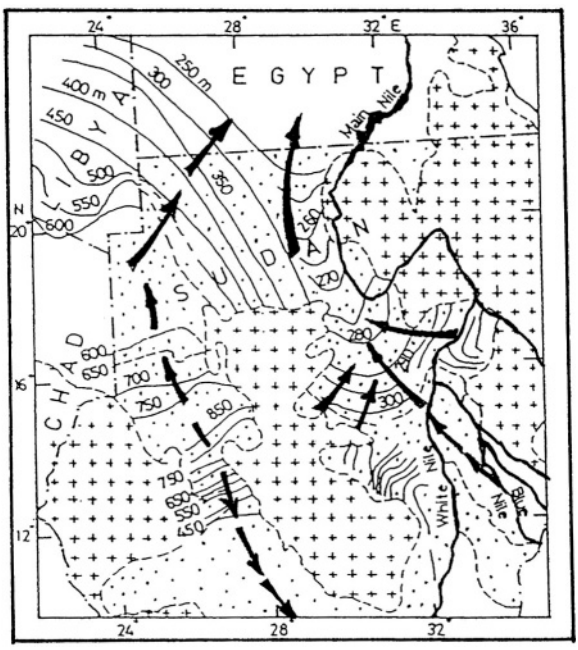

Figure 12.10- Groundwater heads in the Nubian Sandstone in the Sudan (Country Report of the Sudan/Hedayat, 1986)

12.4.2 North and West Africa- In this section, we shall present some characteristics of groundwater aquifers and groundwater exploitation in a number of North and West African countries.

i- Libya: Over 90% of the surface of Libya is covered by deserts. The areas receiving annual rainfall above 100 mm barely reach 6% of the total surface area of the country. In view of the limited surface water resources, more than 98% of the total water consumption is supplied by groundwater. The surface of Libya is covered by five main groundwater basins: Gefara or Jifara (200), Jebel Akhdar (200), Hamada (230), Murzuk (1,200), and Kufra-Sarir (1,600). The figures in parentheses are the volumes of the available water expressed in 10^6 m^3 y^{-1}. The last two basins, i.e. Murzuk basin in the southwest and the Kufra-Sarir basin in the southeast, are major basins as they together contain 81.6% of the total volume of available groundwater.

The Murzuk Basin: This basin extends over a surface area of more than 350,000 km^2 in southwest Libya. It contains two aquifer systems, a lower system comprising Cambrian, Ordovician and Divonian aquifers (Paleozoic aquifer system), and an upper system made up of Permo-Teriassic and Upper Jurassic-Lower Cretaceous aquifers (Nubian aquifer system). The two aquifers are separated by a carboniferous aquitard, allowing each system to behave as a group of independent aquifers.

The main water-bearing formations in the Paleozoic system are the Cambro-Ordovician and the Devonian. Their respective thickness varies from 200 to 1,400 m and from 40 to 60 m. The transmissivity values for the accessible areas in the northeast and southwest are between 500 and 2, 500 m^2 d^{-1}. The storage coefficient ranges from $5*10^{-3}$ to $1*10^{-5}$. There is no current recharge to the aquifer, and the current depletion of the aquifer system is at a rate of between 0.1 and 1.0 mm y^{-1}. The total solid salts are generally below 1,000 mg l^{-1} (Salem, 1991).

A Nubian Sandstone aquifer occupying some 190,000 km^2 is located in the middle part of Murzuk Basin as shown in Figure 12.11. It consists of thick series of sandstones intercalated with clay. The maximum thickness of the aquifer is about 1,000 m at the center and 200 m at the edges. Transmissivity values at the northern boundary of the aquifer range from 250 to 1,200 m^2 d^{-1}. The total dissolved solids in the shallow layers fall in the range 1,000-4,000 mg l^{-1} and 160-480 mg l^{-1} in the deep layers.

The Kufra-Sarir Basin: The surface area covered by the Kufra-Sarir Basin is about 675,000 km^2 located in southeast Libya. The water bearing-formations of the Kufra basin belong to the Cambrian-Lower Cretaceous ages and consist of Continental sandstones with intercalated clays and silts. The saturated thickness of the aquifer system is nearly 3,000 m in the middle as shown in Figure 12.12.

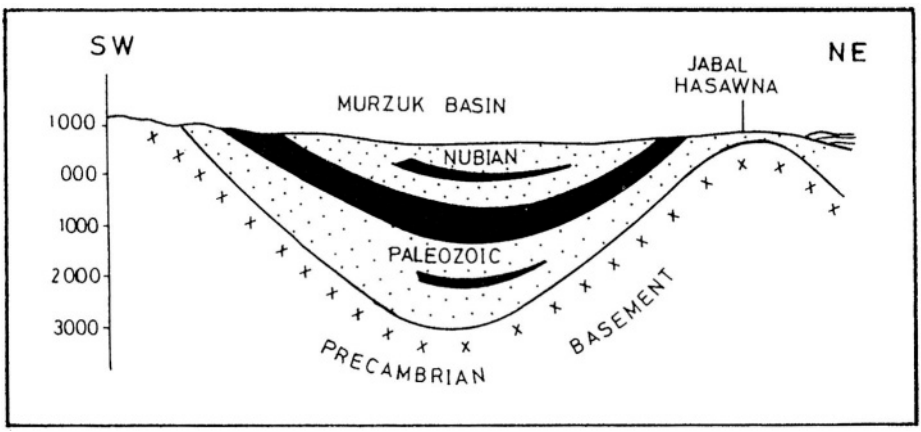

Figure 12.11- Southwest-northeast cross section through Murzuk Basin, Libya

The top middle part of the basin is occupied by Nubian Sandstone aquifer of the Teriassic-Lower Cretaceous ages. The groundwater in the Nubian aquifer emerges at the surface as an oasis owing to a topographic low in the regionally unconfined area. The aquifer transmissivity varies from 300 to 3,500 $m^2 d^{-1}$ and storativity from $1.5*10^{-2}$ to $1.1*10^{-4}$. The total dissolved salts in the water obtained from deep wells fall in the range of 180-300 mg l^{-1}.

The Sarir Basin is situated north and west of the Kufra Basin. The water-bearing formations of this basin belong to the Post Eocene with two main aquifers: the Post-Middle Miocene (PMM) and the Lower and Middle Miocene (LMM) and Oligocene. The PMM aquifer has a thickness varying from a few meters to over 200 m consisting of coarse sand and calcareous sandstones with interbedded clays. The thickness of the LMM, being in the range of 150-880 m, is much thicker than the PMM aquifer. The LMM consists of interbedded clays, fluvial sands and sandstones The Oligocene is in contact with the LMM, as can be seen from Figure 12.12. It consists of Calcareous sandstones, limestones, clays and evaporates with a thickness ranging from 250 to 730 m. Field tests have shown that the transmissivity varies from 500 to 6,000 $m^2 d^{-1}$ and the storativity from $5*10^{-2}$ and $5*10^{-4}$, depending on the aquifer material. The total dissolved salts increase from north to south and from aquifer to aquifer. The salinity falls in a wide range of 500 to more than 5,000 mg l^{-1} (Salem, 1999)

As a result of the availability of abundant groundwater of good to moderate quality the implementation of the Great Man-Made River Project was begun in the early 1970s. Hundreds of wells have been drilled mainly for irrigation in Sarir, Kufra and Murzuk basins. The implementation of the whole project requires a number of construction phases, the first of which has already been completed some years ago. It included two well fields supplying $2*10^6$ $m^3 d^{-1}$. One of the well fields is situated in the Sarir area. It comprises 126 production wells with an average depth of about 450 m, tapping the Post Eocene aquifer

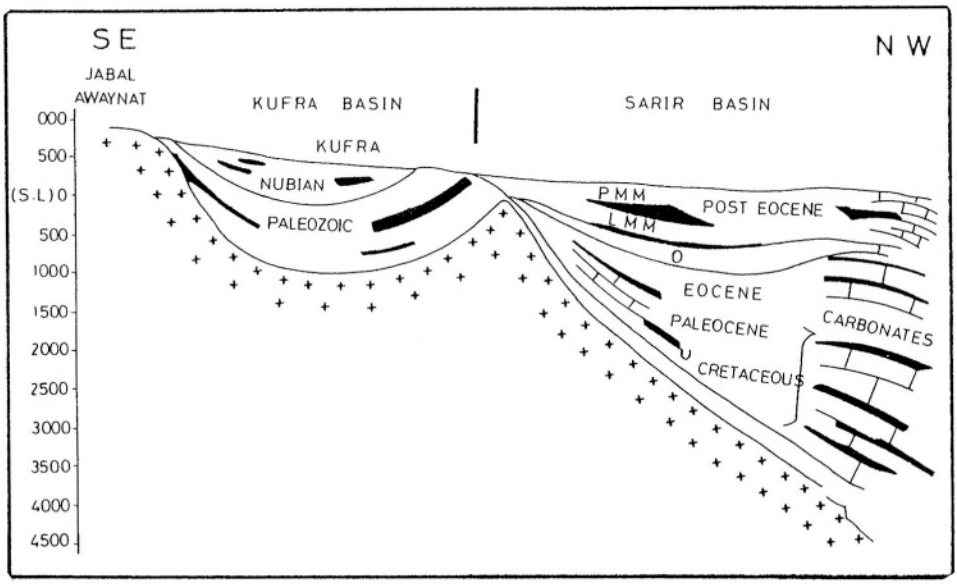

Figure 12.12- Southeast-northwest cross-section through the Kufra-Sarir Basins, Libya (Salem, 1991)

The second well field is located at Tazerbo southwest of Sarir. It comprises 108 production wells tapping the Paleozoic aquifer. The well depth varies from 500 to 800 m. The yield of the two fields is conveyed to the coastal area extending from Benghazi in the east to Sirt, some 530 km to the west. Figure 12.13 (Salem, 1991) shows the groundwater heads in the Nubian Sandstone in Libya .

The next phases of the project comprise exploitation of $2.5*10^9$ m^3 y^{-1} from the Cambro-Ordovician aquifer in the northeast of Murzuk Basin and conveying this amount to the Gefara Plain in the northwest near the seacoast. Plans require the drilling of more than 500 wells with a depth varying from 400 to 800 m to abstract the required amount. Additionally, there are plans to introduce some extensions to the conveyance lines of phase I

ii-**Mauritania**: This too is a large country with a surface area exceeding $1*10^6$ km^2, two thirds of which are practically desert. The annual rainfall on the country is estimated as $100*10^9$ m^3. Of this amount $1.0\text{-}1.5*10^9$ m^3 runs as surface runoff and contributes to the flow in the Senegal River, and $3\text{-}5*10^9$ m^3 flows inland, and of this amount $0.5\text{-}1.5*10^9$ m^3 goes as recharge to the groundwater aquifers. The remaining say $95*10^9$ m^3 represents direct or indirect loss by evaporation.

The water-bearing formations in Mauritania are generally made up of the Basement Complex and Sedimentary deposits. These are distributed among 15 reservoirs, as shown in the map labeled Figure 12.14, which contains a brief description of each aquifer.

The available information about well discharges is given in Table 12.3. Little is known about the hydrogeological parameters of the different aquifers. A study has been carried out by Ould el-Joud (1993) on the hydrology and hydrogeology of the Idini aquifer in the Sedimentary basin southwest of Mauritania. The values obtained are 5% for the porosity and $1*10^{-7}$-$1*10^{-9}$ m s^{-1} for the clay aquitard separating the phreatic and semi-confined aquifers of the reservoir. The permeability of the semi-confined aquifer is $1*10^{-5}$ m s^{-1}. These figures bring the average transmissivity of the Idni to $3*10^{-3}$ m^2 s^{-1} or about 260 m^2 d^{-1}. Moving east, one finds a limited part of the aquifer with a transmissivity of up to 1,730 m^2 d^{-1}. The storativity of the aquifer is certainly lass than 1-2%.

iii- **Burkina Faso** : This is a landlocked country, situated in the Sudano-Sahelian zone of Africa. The northern part, which is Sahelian, has a mean annual temperature of 28°C. It receives annual rainfall of less than 650 mm, and it has a potential evapotranspiration of more than 2,500 mm. The middle part of Burkina Faso is north Sudanian, receiving annual rainfall between 650 and 1,000mm.

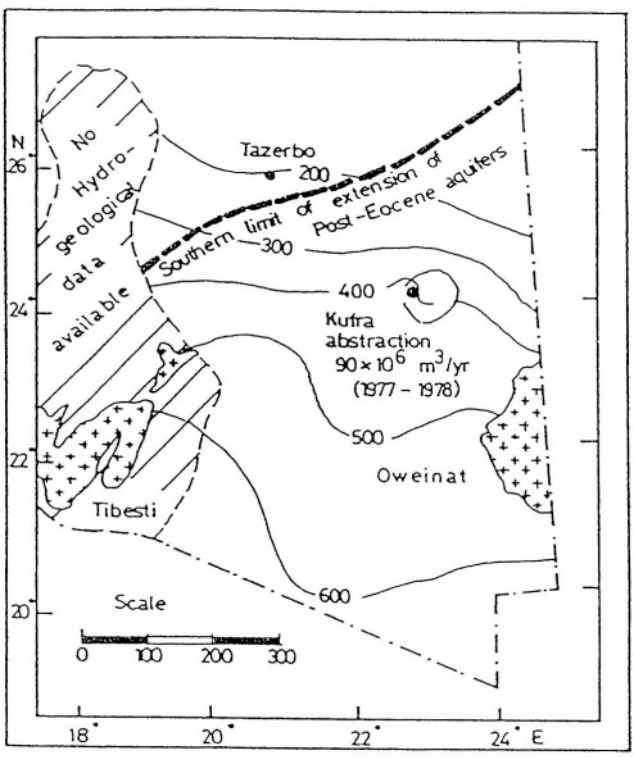

Figure 12.13- Groundwater heads in the Nubian Sandstone in Libya (Salem, 1991)

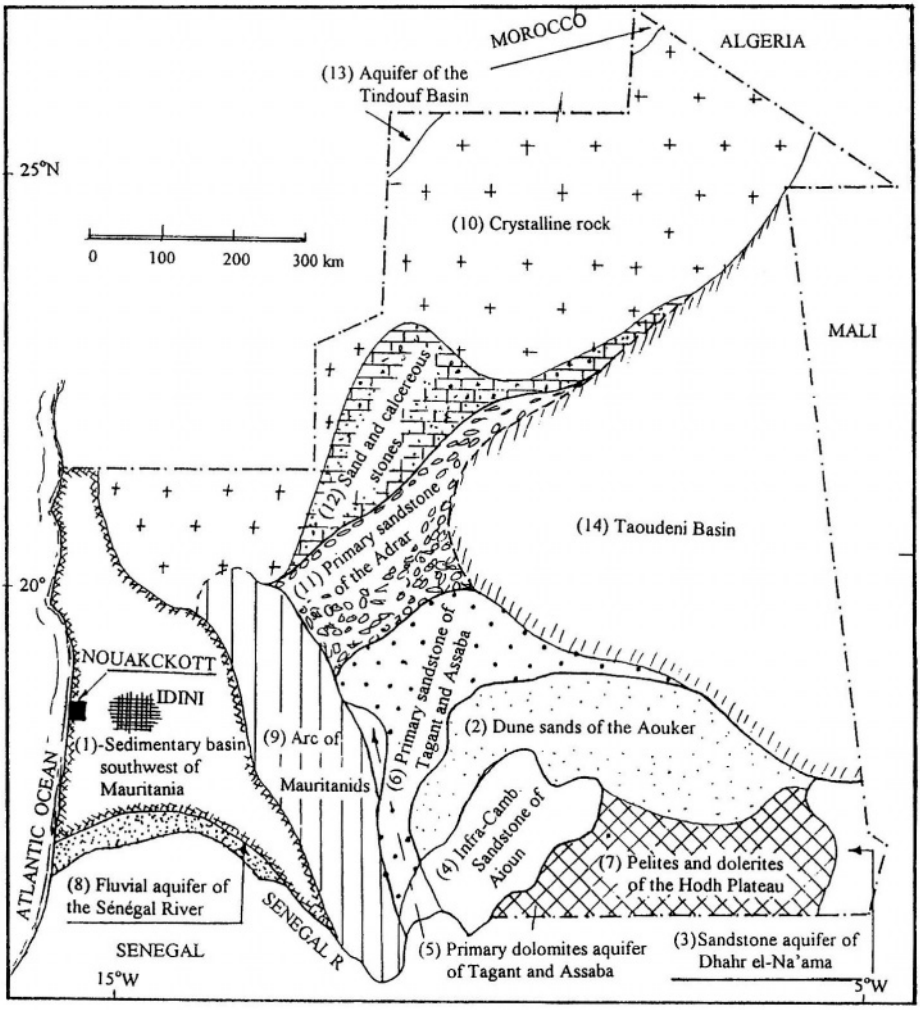

Figure 12.14- Map showing the water bearing-formations in Mauritania (from the Country Report of Mauritania, 1986)

The climate of the southern part of Burkina is south Sudanian, where the annual rainfall can be as much as 1,350 mm, with 24°C mean annual temperature and potential evapotranspiration of from 1,900 to 2,250 mm.

Crystalline and metamorphic rocks of the West African Shield cover more than 80% of the territory of Burkina Faso, as can be seen from the map in Figure 12.15. The matrices making up these rocks are essentially impermeable. However, tectonic movements in the course of time have developed networks of fractures and channels to enable the transmission and storage of groundwater

Table 12.3- Some data about the groundwater reservoirs in Mauritania (from Country paper of Mauritania, 1986)

Basin No./name	Surface area, km^2	Exploitable resource. 10^9 m^3	Depth, m below surface	Depth of well, m	Well discharge, m^3 h^{-1}	Lithology	Remarks
1- Sedimentary basin south east of Mauritania	90 000	25-55	5-80	40-150 10-70	10-70 2-5	Sandstone	Artesian
2- Sandy aquifer of the Aoukar	130 000	22-47	15-30	20-40	2-5	Sand	
3- Continental Intercalary sand-stones of Dhahr el-Naama	13 000	3-6	50-70	10-20 50-70	10-20 1-4	Sandstone Sandy clay	
4- Sandstone aquifers of the Infra-Cambrian (Al-Aioun)	35 000	2-5	5-35	60-100 25-40	5-50 2-6	Sandstone Fractured sandstone	
5- Primary dolomites aquifer at the foot of the Tagant and Assaba plateau	400	60-120	10-15	20-40 12-20	60-150 2-6	Fractured and karstified dolomites	Artesian
6- Primary sandstone aquifer of the Tagant and Assaba plateau	15 000	N I	N I	100-120	5-20	Fractured sandstone	
7- Discontinuous aquifers (Pelites and dolomites	50 000	50-100		50-70 15-30 70 + / 20	1-10 1-4 4-6	Fractured Pelites / dolomites	
8- Alluvial aquifers at or near the ground surface	8 500	300-800	5-10	15-30 10-25	10-25 0.5-10	Silt, gravely sands and clays	Recharge by seepage from Senegal River
9- Discontinuous aquifers of the Mauritanide arch	55 000	N I	N I	50-70 70 + / 20	N I	Fractured Schistes	
10- Discontinuous aquifers of the crystalline rock, north of Mauritania	250 000	N I	N I	50-70	N I	Crystalline rock	

Table 12 3- Cont'd

Basin No./name	Surface area, km^2	Exploitable resource, 10^6 m^3	Depth, m below surface	Depth of well, m	Well discharge, m^3 h^{-1}	Lithology	Remarks
11- Primary sandstone aquifer of the Adrar	50 000	N I	N I	50-100		Fractured sandstone	
12- Pre-Cambrian sandstone and calcareous aquifers of the Adrar	35 000	N I	N I	40-?	5-15	Calcareous sandstone	
13- Aquifers of the primary formations of Tindouf Basin	1 200	N I	N I	N I	N I	N I	
14- Aquifers of the primary and secondary groups of the Taoudeni Basin	300 000	N I	N I	N I	N I	N I	
15- Deep aquifers (Maastrichtian)	N I	N I	N I	N I	N I	N I	
Total groundwater sources	1 000 000						

Explanation

NI = No information

Much of the basement is usually covered by a weathered zone. The character and thickness of this zone relate to the lithology of the baserock, climatic conditions and intensity of fracture. The basement and its weathered zone form a two-layer aquifer from 25 m below the ground surface and 35-40 m thick. Abstraction from the network of fractures results in the movement of water contained in the weathered zone, which represents more than 90% of the volume available in the system. The weathered layer is often covered by layers of sand, sandy clays and clays of some 25 m in thickness.

The yields of 8,000 bore holes were classified and found to vary between 0 and > 10 $m^3 h^{-1}$. 30% of the boreholes were non-exploitable, 56% yielded between 0.5 and 5 $m^3 h^{-1}$, 9% between 5 and 10 $m^3 h^{-1}$ and the remaining 5% more than 10 $m^3 h^{-1}$. A regional modeling of short-duration (6 h) pumping tests showed that the transmissivity of the weathered aquifer varies between about 0.5 and 25 $m^2 d^{-1}$. The average regional value can be taken as 0.9 $m^2 d^{-1}$ and the value corresponding to the boreholes with maximum discharge as 8.5 $m^2 d^{-1}$. The values of storage coefficient deduced from the pumping tests are generally low, $1*10^{-5}$ to $1*10^{-3}$. The specific yield of the weathered zone is 1 to $5*10^{-2}$ depending on the lithology.

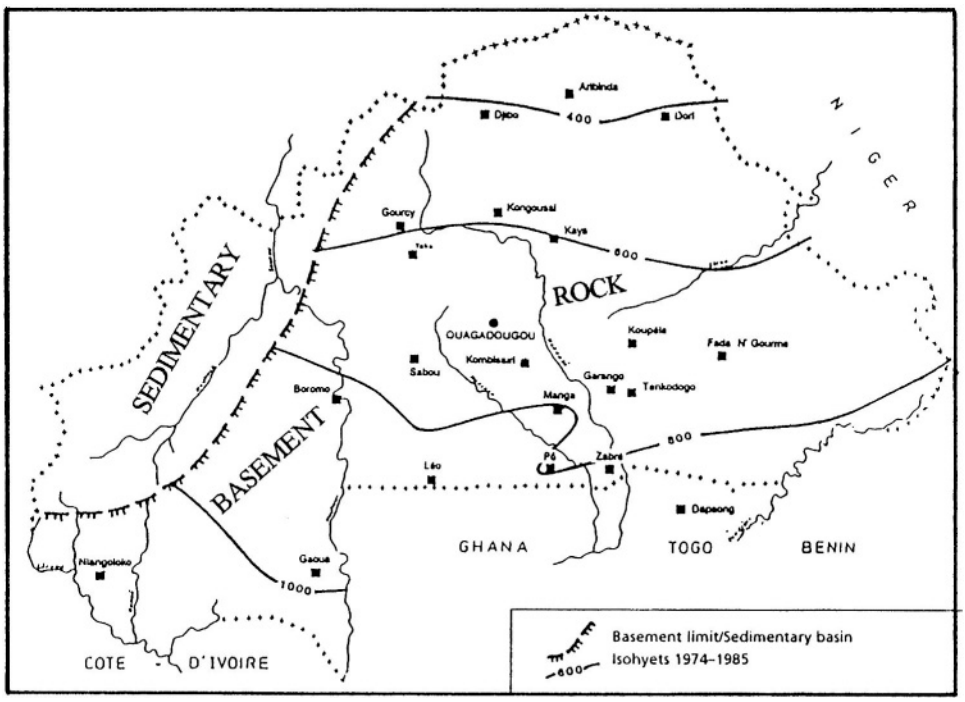

Figure 12.15- Areas covered by the Basement rock and Sedimentary formations in Burkina Faso

The recharge as found for those areas with annual rainfall between 520 and 620 mm accounted for 3-11% of the rainfall. These percentages are believed to be more accurate than those reported by Dieng (1989). According to this source the recharge as a percent of the mean annual rainfall (513 mm) in the northern part of the country is 26.5. The percentage increases in the middle of the country where the mean annual rainfall is 807 mm to reach 27.4-31.1. Beyond that it falls to 24.7 % in the south where the mean annual rainfall increases to 1,076 mm. These figures have been obtained from water balance models in which evapotranspiration was estimated from Thornthwaite's method.

iv- **Ghana:** This West African country is located south of Burkina Faso with the coastline of the Atlantic Ocean forming it's southern boundary. The movement pattern of the Inter-Tropical Convergence Zone (ITCZ) brings in two rainy seasons to the southern part of Ghana, while the northern part gets one rainy season only. As a consequence, the annual precipitation varies from about 800 in the north mm to slightly over 2,000 mm in the south. Due to the prevailing climate, the annual pan evaporation ranges from 1,200 mm to 2,600 mm respectively.

There are two hydrogeological provinces in Ghana, the Basement Complex, comprising the Precambrian crystalline igneous and metamorphic rocks, and the Paleozoic consolidated sedimentary formations. The Precambrian rocks show unequal degrees of weathering. The average depth of the decomposed zone is around 40 m. Aquifers are generally characterized by low transmissivities, 7.5-30 $m^2 d^{-1}$, coupled with low storativities, 0.003-0.008. The yields of boreholes as a consequence are as low as 3-24 $m^3 h^{-1}$ (Bannerman and Ayibotele, 1984). The sedimentary formation, which underlies the Vofta Basin and thus known as the Voltanian formation, consists of sandstone, shale, mudstone, sandy and pebbly beds, and limestones. The surface occupied by the Basement Complex constitutes 54% of the surface area of Ghana and the Sedimentary basin 45% (see the map, Figure 12.16). The remaining 1% is made up of Cenozoic sediments, which consist of unconsolidated alluvial sediments, beach sand, sandy clay gravels, marine shale and limestone (Boakye, 2001).

Infiltration of rainwater through fractured and faulty zones as well as sandy portions of the weathered formation is the direct means of recharge to all aquifer systems. Some recharge, though much smaller, occurs indirectly through seepage from ephemeral stream channels during the rainy seasons.

v- **Chad**: The country is a land-locked country in the heart of Africa. It generally has a warm winter climate and a hot harsh summer The annual precipitation drops from 1,200 mm or more in the south to less than 200 mm in the north. The annual potential evapotranspiration increases from about 1,400 mm in Sarh in the south to 1,950 mm at N'Djamena. The Chari River and its tributary the Logone, are the perennial rivers in the country, discharging their

waters into Lake Chad. Discharge data about these rives are available in Chapter 7.

Groundwater in Chad is usually found at depths between 20 and 40 m below the ground surface. Depending on the geological units, three major type of aquifers can be distinguished. These are the plateau aquifers belonging to the Paleozoic and Cretaceous sandstone of Tibesti, the Chad basin aquifers, and the massive crystalline aquifers.

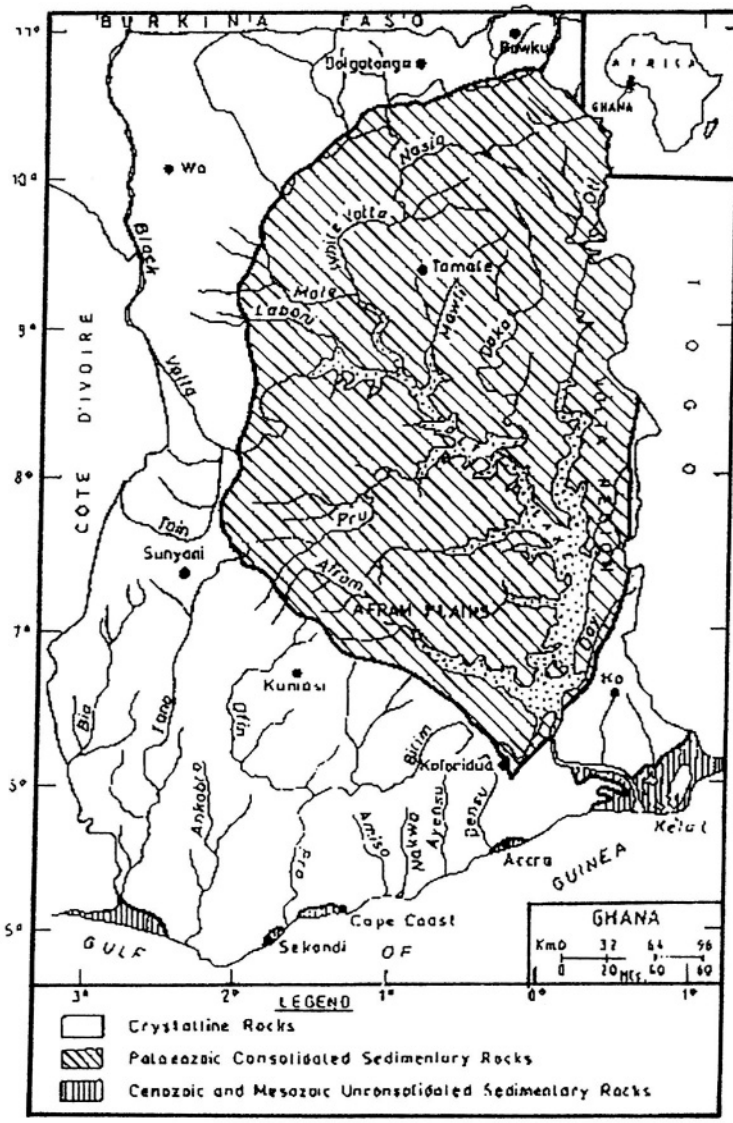

Figure 12.16- Hydrogeological provinces of Ghana (Boakye, 2001)

The Paleozoic and Creaceous sandstone aquifers are found in the most arid part of the country where the annual rainfall is than less 100 mm. These can be subdivided into three types; the kaolinic sandstone covering an area of 115,000 km^2, with a maximum thickness of 800 m: sandstone, marl and limestone covering a surface of about 20, 000 km^2; and Nubian sandstone covering an area of 73, 000 km^2. Despite the lack of adequate information, the Nubian sandstone is supposed to form the most important groundwater reservoir in Chad.

The Tertiary and Quaternary sedimentary formations of the Chad basin extend over 525,000 km^2 and contain the principal aquifers of Chad. These also can be classified into three types: the Quaternary fluvial-lacustrine and aelioan deposits forming unconfined aquifers; the Pliocene sedimentary aquifers; and the Continental Terminal sediment aquifers.

The main groundwater reservoirs can also be found in the fractured rocks of crystalline series and Pre-Cambrian granites. These reservoirs cover a surface area of 220,000 km^2.

The locations of the various aquifer subdivisions in Chad are indicated on the map in Figure 12.17 (redrawn from Terap, 1991).

vi- **Nigeria**: The two main rock formations in Nigeria are the Basement Complex (mainly Pre-Cambrian and Paleozoic rocks and Jurassic granites) and Sedimentary deposits (Post-Cambrian deposits). The extent of these formations over the surface of Nigeria is shown on the map in Figure 12.18.

The Basement Complex serves chiefly as a source for headwaters of various rivers and recharge zones, while the sedimentary formations have both surface water and groundwater of valuable economic interest. Ojiako (1985) referred to nine hydrogeological provinces in Nigeria as specified by Egboka These are the Chad Basin (sec. 12.3.3), Iullemeden Basin, Basement Complex, Benue Basin, Nsukka-Awgu, Aiyetoro-Ijebu Ode-Fugar, Ameki-Ogwashi-Asaba, Imo River Basin and the coastal plains. Figure 12.19 is a map showing the locations of these divisions together with the area occupied by the volcanic rocks (Basalt) included.

Hard rock aquifers in southwestern Nigeria: A study was conducted in the district of Ilesha, southwest Nigeria by Owoade et al. (1989). Geoelectric measurements have shown that the topsoil layer, 0.9 m thick, is underlain by a dry regolith (weathered rock) down to a depth of 7.2 m below the ground surface. The regolith is succeeded by a saturated zone down to 34.5 m, resting on the bedrock. The viability of weathered rock to groundwater storage has been found to depend largely on the development of adequate weathering in depth. This, in turn, depends on climate, environment and lethologic characteristics of the formation. Analysis of recovery test results on a large diameter well gave a permeability figure of 1.2 m d^{-1}. Despite this low value it has been concluded that storage capacity as represented by the specific yield is high

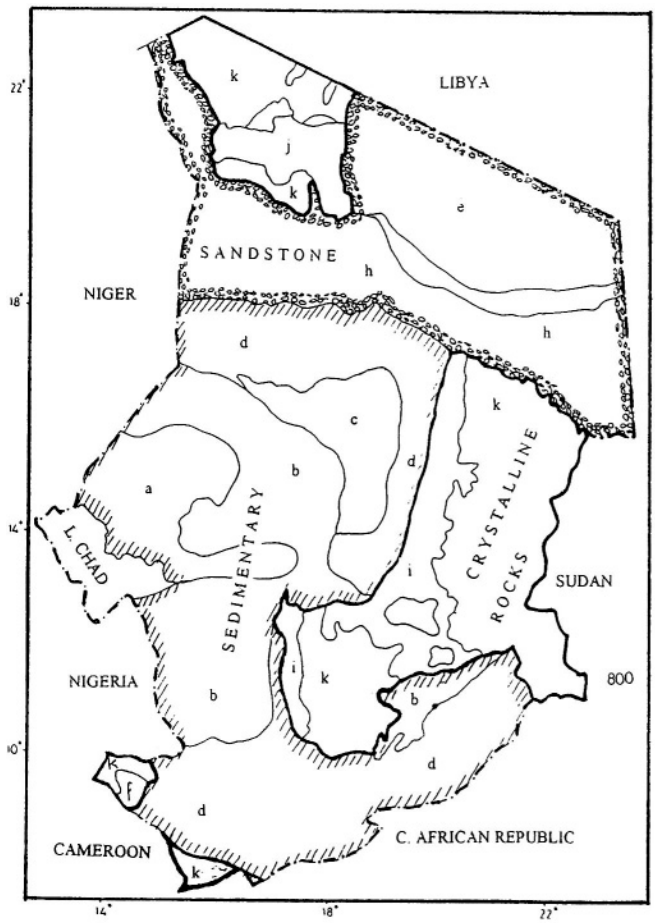

LEGEND

Sedimentary deposit aquifers

a - Phreatic level in middle Quaternary formations and eolian deposits
b - Phreatic level in old Quaternary fluvial-lacustrine formations
c - Phreatic level in Pliocene fluvial-lacustrine
d - Phreatic level in Continental Terminal Oligocene-Miocene fluvial-lacustrine

Sandstones

e - Phreatic level in Nubian Sandstone and kolinic sandstone
f - Phreatic level in conglomerate and cilcerous sandstone of Aptien-Turouien origin
h - Phreatic level of Cambrian kaolinic sandstone

Crystalline rock

i - Local levels in Tertiary and Quaternary pockets and base rock
j - Non-continuous levels in Tertiary and Quaternary rock of volcanic origin
k - Non-continuous levels in exposed in exposed crystalline rock

Figure 12.17- Hydrogeological provinces of Chad (Schneider, 1960; cited in Terap, 1991)

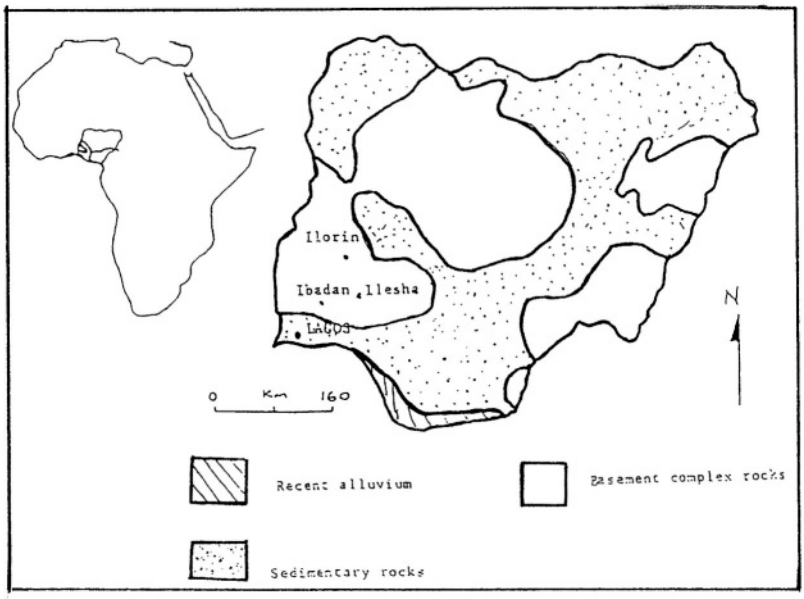

Figure 12.18- Water-bearing formations of Nigeria (Owoade et al., 1989)

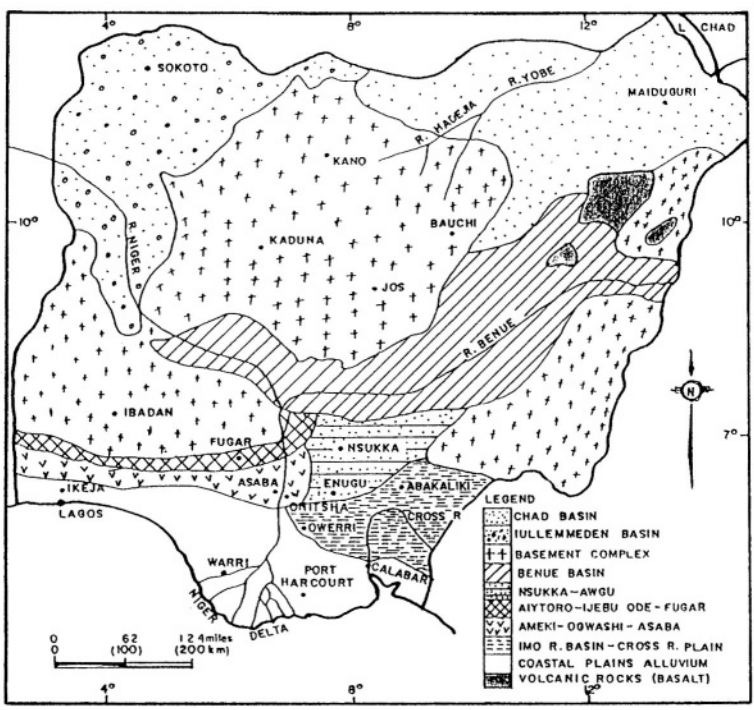

Figure 12.19- Hydrogeological provinces (Egboka; cited in Ojiako, 1985)

12.4.3- East Africa:

i- **Kenya**: The aquifer systems in Kenya are made up of three hydrogeological provinces: the Volcanic, the Basement rock and the Sedimentary provinces. Figure 12.20 is a cross-section extending from the glaciers capping Mount Kenya at elevation 5,180 m through montane moist forest near Meru at elevation 1, 830 m, and further to desert conditions in the vicinity of the Ewas Nyiro River. This cross-section gives a general idea about the conditions of groundwater (Grove, 1970).

The Sedimentary rocks deposits underlie the northeastern and eastern parts of Kenya, thus covering about one-third of the surface area of the country These areas are characterized by arid and semi-arid climates with low and variable rainfall. The western province, contrary to the eastern and northeastern parts of Kenya, is made up basically of granite rocks. Other main geological structures are the Nyanzian volcanics, Kavirondian sediments, Tertiary volcanics, and the Pleiocene and recent deposits. The western province, as can be seen from the map in Figure 12.21, constitutes part of the catchment area of Lake Victoria.

Groundwater in the Western Province: Shallow groundwater can be found at depth of 2.5 to 5.0 m below ground surface. This is found in shallow aquifers in weathered bedrocks, and sometimes as perched water that has no connection with deep groundwater. Boreholes are mostly hand-dug with average depth of 8.0 m. The annual fluctuation of the groundwater level is considerable, 2 to 3 m, requiring frequent need to deepen some of the already dug wells and boreholes.

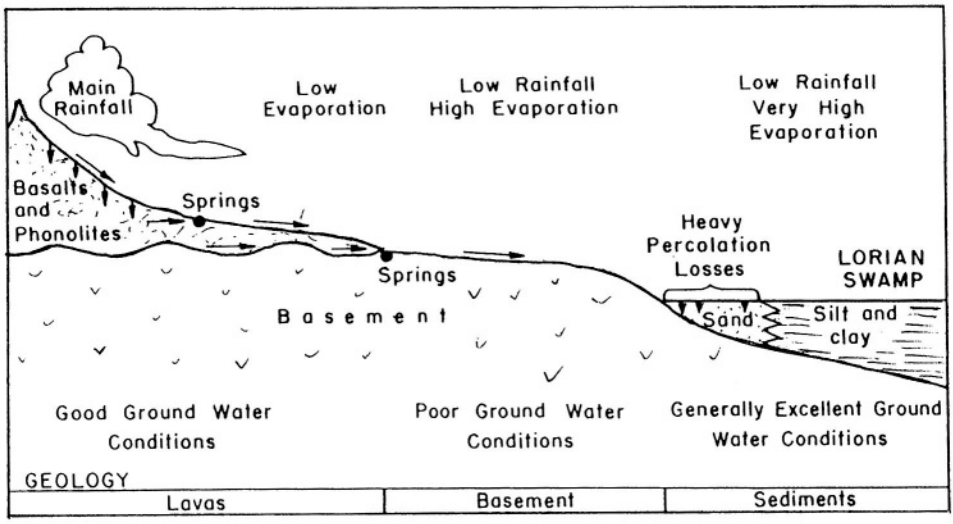

Figure 12.20- Cross-section from west to east Kenya giving general idea about geology and groundwater conditions of the country (Grove, 1970)

Shallow groundwater has a low concentration of dissolved solids with average conductivity of 110 $\mu S\ cm^{-1}$. Water is very soft and has a high concentration of dissolved carbon dioxide and a mean pH-value of 6.1.

Deep groundwater can only be utilized by boreholes or wells, and is never perched water. The static deep water level varies generally between 10 and 15 m in most of the area. The static level in sediments and volcanic deposits, varying from 11 to 13 m, is somewhat deeper than in granites. The average thickness of the aquifer tails in the range 1-52 m, with an average 8 m. Additionally, the thickness of the weathered layer in the area is about 20 m. In areas where sedimentary rocks are predominant, the weathered layer is remarkably thicker (27 m).

Transmissivity values as obtained from the analysis of the results of pumping tests carried on the aquifers in the Western Province range from less than 10 $m^2\ d^{-1}$ to over 100 $m^2\ d^{-1}$. An aquifer with transmissivity less than 10 $m^2\ d^{-1}$ can only supply water for domestic wells, while aquifers with transmissivity above 100 $m^2\ d^{-1}$ are adequate formations for industrial or municipal purposes.

Deep groundwater quality mostly meets the drinking water standards set by the World Health Organization guidelines. It usually has an average conductivity of 310 $\mu S\ cm^{-1}$ and average pH of 6.5. The last figure shows that the pH lies in the acidic range, making water aggressive to ferrous materials as has been indicated by severe corrosion of pump structures (Chengoli, 1999).

The eastern sedimentary province of Kenya. The geology of east and northeast Kenya (Figure 12.21) is made up of sedimentary deposits ranging in age from Jurassic to Quaternary periods. These deposits form two main series, the limestone series and the Cretaceous series. The limestone series can be as thick as 1,200 m. Marine-deltaic-deposited Cretaceous sediments, which are confined in certain parts, overlie these series. The rest of the remaining portion of East Kenya comprises Tertiary and Quaternary deposits composed of intercalated semi-consolidated gravel, grit, sand, silt and clay. Quaternary deposits consist mainly of alluvial accumulation with patches of limestone, gypsum, sandstones, ironstones and conglomerates (Krhoda, 1989).

12.4.4 Equatorial Africa-

i- **Congo**: The geological structure of the Congo Basin is rather simple. The outermost areas of the basin are very ancient geologically. Recent alluvium borders the Congo River and stretches around Lake Tanganyika. Older alluvium, once the bed of a great lake, occupies the heart of the basin. These give place in the higher country to vast stretches of soft sandstone known as the Lubilache Beds. Older than these beds are the Kundelunga Beds, which are sparsely scattered in the north, southeast and southwest of the basin, as can be seen from the map in Figure 12.22 (Stamp and Morgan, 1972).

Figure 12.21- Location of the eastern, northeastern and western provinces of Kenya

The Kundelunga Beds are the oldest Sedimentary rocks in the basin found resting on the ancient massif. It has been suggested that these beds, which consist of shales, limestones and sandstones, are likely to be Permian-Triassic in age. They were folded by the same movements that led to the folded mountains of the Cape in the extreme southeast of Africa.

The aquifer underlying Brazzaville: This aquifer is a tiny part of an extensive hydrogeological province made up of a huge water-bearing formation, out of which large rivers of the Congo and Gabon are springing. In view of the surplus surface water, the abstracted groundwater is mainly used for domestic purposes. The inadequacy of the sanitation facilities in Brazzaville and its environs caused contamination of the said aquifer An area of 270 km^2 was selected to conduct the necessary hydrological and water quality investigation (Moukolo, 1986).

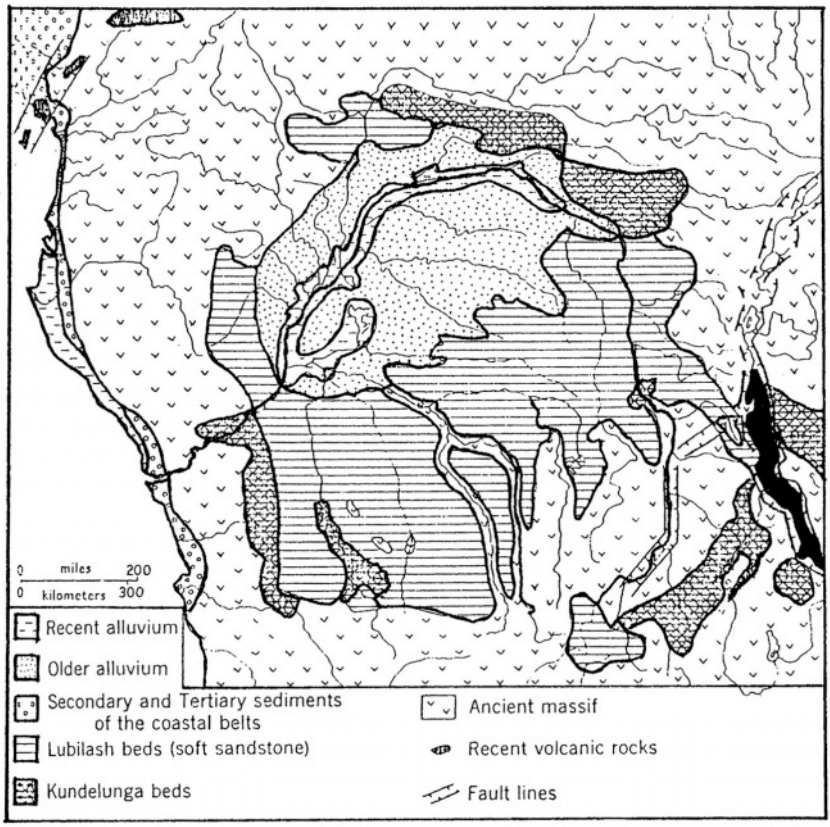

Figure 12.22- A simplified geological map of the Congo River Basin (Stamp and Morgan, 1972)

Chemical as well as physical analyses of water samples abstracted from 35 water points in the period between November 1985 and March 1988 have shown that about half of the samples were unsuitable. The chemical and physical properties of water are included in Table 5_6, Part II/Appendix B.

From the hydrogeological point of view, the piezometric surface of groundwater constitutes the upper surface of the aquifer The substrata are made up of sandy layers overlying accumulations of clays, sandstone and mudstone. The permeability coefficient of the sandstone varies from $1*10^{-5}$ to $1*10^{-4}$ m s^{-1}. The productive aquifers, which can be up to 100 m thick, are formed of unstratified fine sand, sandstone and gravel. At certain locations, however, the sandy layers of the aquifer can be interrupted by impermeable clay lenses or siliceous sandstone banks offering high resistance to the movement of water. The aquifer yield in this case is generally small, less than 0.04 m^3 h^{-1}.

The aquifer is a source of supply to many perennial streams and several traditional wells in the surroundings of Brazzaville. The direct

recharge occurs through infiltration. The mean annual infiltration in the period from 1943 to 1981 has been estimated as 460 mm of water, corresponding to an annual volume of $124*10^6$ m^3. The preliminary studies carried out on the Brazzaville aquifer have yielded a mean annual discharge of $110*10^6$ m^3, of which $13*10^6$ m^3 is a base flow and the rest is surface runoff. The groundwater reserve, *W,* can be estimated from the relationship:

$$W = Vp_e \tag{12.6}$$

where V = saturated section of aquifer under consideration and p_e = effective porosity of the aquifer material. Assuming the average saturated thickness of the aquifer to be 40 m, the range of fluctuation of the water table as 4 m and the effective porosity as 10% one gets the following results:

- Total reserve $W_T = 1,100*10^6$ m^3,
- Regulated reserve $W_R = 110*10^6$ m^3,
- Permanent reserve $W_P = 990*10^6$ m^3,
- Rate of renewal = 10-12%

12.4.5 Southern Africa-

i- **Malawi**: Most of the country in Malawi is underlain by igneous and crystalline metamorphic rocks of the Precambrian-Lower Palaeozoic age, better known as the Basement complex. The extreme northern corner, middle and southern bend of the western shore of Lake Malawi are underlain by Quaternary allvium as shown on the map in Figure 12.23. An important and extensive erosion surface in Malawi belongs to the late Cretaceous to Miocene African surface. It takes the form of a plateau at a general elevation of 1,000-1,200 m a.m.s.l. The surface of this plateau is characterized by a layer of unconsolidated material produced by the weathering of the bedrock. The tectonic activities associated with the Rift Valley have resulted in increased erosion, and much of the unconsolidated, weathered material has been removed (Chilton & Smith-Carington, 1984).

The weathered Basement rocks provide a thin, 15-30 m, yet extensive and continuous aquifer, which provides a source of water for domestic purposes. In contrast, the underlying unweathered bedrock is hardly significant as a source of water. The boreholes dug in the weathered basement aquifer produced yields in the range from 1-7 m^3 h^{-1}, depending mainly on the aquifer thickness. The corresponding drawdown varied from 5 to 25 m. The obtained yield is adequate for handpumps supplying water for domestic purposes and very limited irrigated agriculture. Good yields are often obtained where major fractures or faults in the bedrock have allowed the weathering processes to penetrate deeply. The results

obtained from the borehole tests have shown that the specific capacity and transmissivity of this aquifer varied from 0.25 to 0.70 $m^3 h^{-1} m^{-1}$, and 7 to 35 $m^2 d^{-1}$ respectively (Chilton & Smith-Carington, 1984).

ii- **Zambia**: As much as 70% of the terrain in Zambia is made up of the Cambrian Basement Complex, which is generally characterized by its uniform, low permeability. This complex, which outcrops in the east and south of the country, is basically built up of gneiss, schist and migmatite. The yield of wells and boreholes withdrawing water from this formation is quite small and rarely exceeds 1 to 2 $l s^{-1}$.

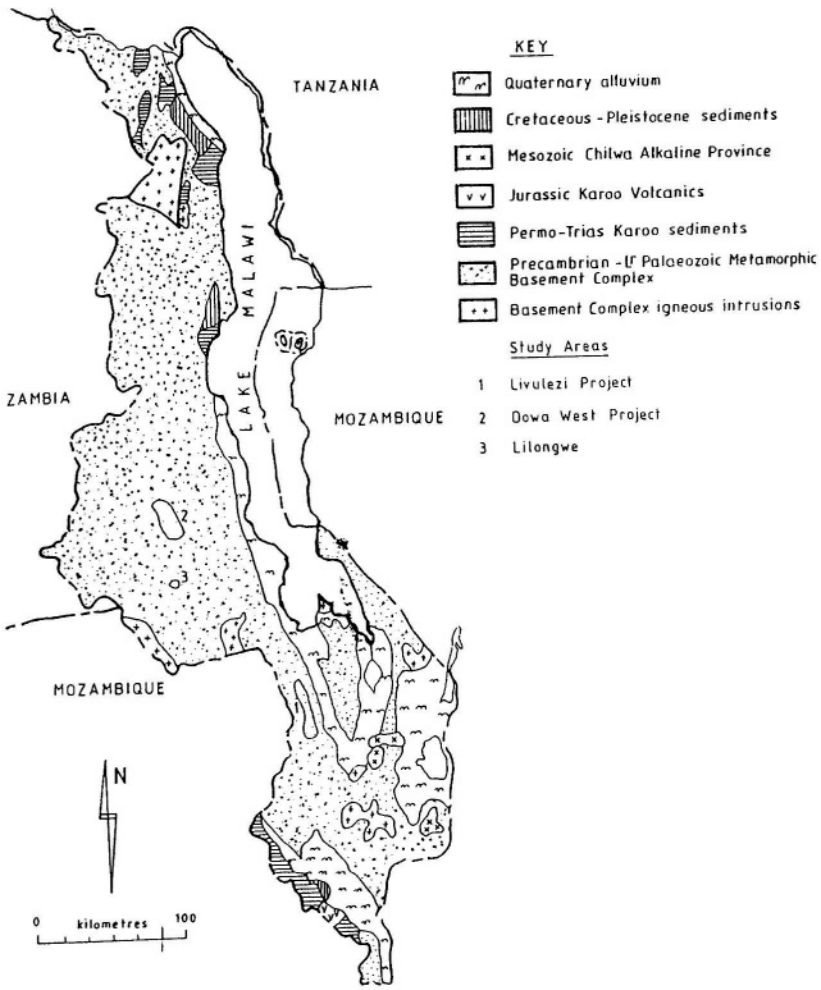

Figure 12.23- Geology of Malawi (Chilton and Carington, 1984)

A considerable part of the Basement Complex is often covered by more recent formations such as the deposits of the Paleozoic age, usually referred to as *Katanga System.* Sandstone, quartizite and shale are associated with limestone, dolomite and fluvio-glacial beds. The *Katanga System* covers 30% of the country, 5% of which are occupied by limestone and dolomite aquifers. Where these aquifers exist, they are often exploited as they are characterized by a relatively high yield, 15-30 l s^{-1} per well, as compared to 3-5 l s^{-1} in the conglomerate and quartizite aquifers (Stretta, 1983).

The *Karoo System,* which is made up of a complex of volcanic and detritic rocks, such as sandstone, marl, grit and mudstone, can be found in the more recent geological succession. This system covers about 5% of the country and belongs to the Permian, Triassic and Jurassic times. Unfortunately, their water potential is hardly better to that of the Basement Complex, i.e. 1 to 2 l s^{-1}.

Groundwater in a dolomite-limestone aquifer: The Itawa-Mwateshi basin is situated to the northeast of the town of Ndola. The northeastern boundary of the basin coincides with the international boundary between Zambia and Zaïre. The aquifer consists of Kakontwe formation of Pre-Cambrian age. This formation belongs to the Lower Kundelungu System already mentioned in connection with the geological structure of Zaïre. It occurs as a major synclinal fold structure of dolomite and limestone beds penetrating northwest into Zaïre, as shown in the cross-section provided by Figure 12.24. The flow through the aquifer occurs along open fissures and through caverns developed along joints and faults in the rock. The aquifer seems to be recharged by direct infiltration in areas of rock outcropping and shallow soils, and indirectly by seepage from neighbouring aquifers.

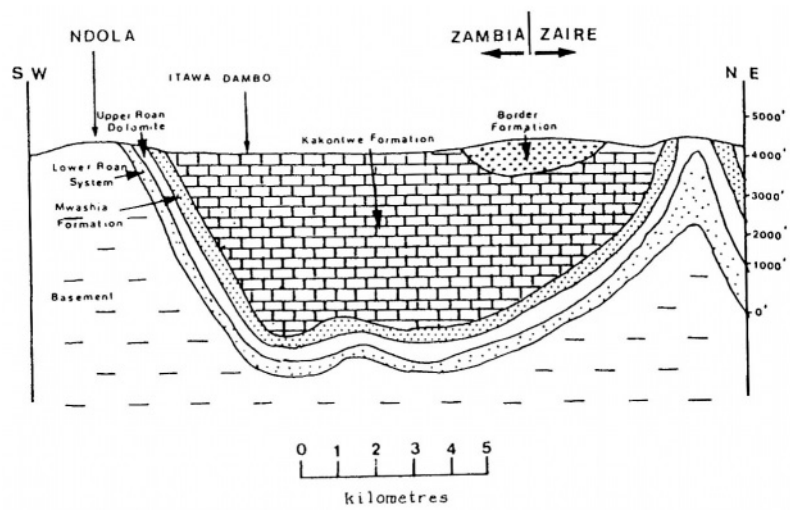

Figure 12.24- Cross-section of the Kakontwe Basin (Adams and Kitching, 1979)

The monthly rainfall in the aquifer area is 275, 285, 186, 83, 21, 0, 0, 0, 0, 6, 79, and 286 mm for the months from January to December. The corresponding monthly evapotranspiration is 135, 123, 135, 144, 132, 116, 126, 149, 161, 174, 151, 135 mm. These two sets of monthly figures bring the annual rainfall and evapotranspiration to 1,221 and 1,681 mm respectively.

Adams and Kitching (1979) carried out a study on the simulation of transmissivity, storativity and evapotranspiration by a digital model of a fissured dolomite aquifer near Ndola. The model was calibrated by comparing its behaviour with field observations. Realistic adjustments were introduced to the input parameters until the agreement between the observed and model obtained groundwater levels became satisfactory.

Another recharge model was applied to the dolomitic aquifer at Kabwe, 180 km southwest of Ndola. This aquifer, probably an extension of the Ndola aquifer, is a Pre-Cambrian dolomitic limestone situated in a complex syncline and outcrops over $40\ km^2$. The dolomite is overlain by permeable lateritic silts and sandy pockets ranging in thickness from 5 to 20 m. The average transmissivity is $1{,}000\ m^2\ d^{-1}$, with a maximum of $3{,}500\ m^2\ d^{-1}$. The aquifer is phreatic with specific yield of about 14%, receiving annual rainfall of 937 mm (average of 70 years). The infiltration rate is generally above $75\ mm\ h^{-1}$. The average recharge as obtained from the model, under different conditions of soil moisture extraction from the root zone, was found to be about $2.8\ mm\ d^{-1}$.

iii- **Botswana**: The country is a landlocked, flat country in Southern Africa. The climate is arid to semi-arid, with annual rainfall increasing gradually from 250 mm in the southwest to about 700 mm in the northeast. Table 10a, Appendix I, gives an average rainfall of 294 mm at Tsabonge (station 250) and 484 mm at Mahalapye (station 242). The annual rainfall is highly seasonal, with more than 90% of the rain falling in the period October-April. With the exception of three months during winter, temperatures are high with the average daily maximum temperature above 30°C from September to April. The annual potential evapotranspiration is about 2,000 mm. In general, there is hardly any surface runoff in the west and center of the country. The annual recharge resulting from rainfall reaches a maximum of about 40 mm in small areas in the north but less than 1 mm in most of the Kalahari region (Sekwale & Selaolo, 1991).

Almost all groundwater in Botswana occurs in bedrock and must be abstracted by deep boreholes. Hand-dug wells or shallow boreholes (20-30 m) can only be used in a few sand rivers and in other limited areas. In some places, however, the groundwater is too deep, too unreliable or too saline. The depths of boreholes range from 30-60 m and the quality of water varies with different degrees of salinity (Ganesan, 2001). As such, it is fairly safe to conclude that groundwater resources of Botswana are generally meager. Some villages in Eastern Botswana get their water supply from fractured aquifers developed in the area underlain by the basement rock. This is granitic quartz-biotite gneiss

about $2,600*10^6$ years old. Consolidated sediments cover the rest of the country. In view of the aridity of the country and the absence of perennial rivers the aquifer recharge is negligible as already mentioned. One of the major problems related to management of surface water resources is that the suitable dam sites are not close to the demand centers, a difficulty that renders groundwater extraction a pressing need and can eventually lead to mining of the aquifer. It is estimated that the extractable volume of groundwater is $100*10^9$ m^3 However, only one percent of this amount is rechargeable by rainfall. The map in Figure 12.25, shows that the depth to groundwater varies from less than 10 m to more than 60 m, while the yield varies between < 3 and >10 $m^3 h^{-1}$.

Buckley and Zeil (1984) conducted an investigation in Eastern Botswana aiming to define the character of fractured rock aquifers. The results obtained have indicated that the most promising location for borehole sites is at the major intersections of the separate channels in the fractured aquifer. Major groundwater flow paths occupy the main fracture and crush zones. These zones, on a larger scale, act as a drainage conduit of the rock mass. In all boreholes that were tested, the groundwater rose 10-20 m after being struck to within the weathered zone, approximately 20-30 m below the ground surface. This, however, is not a definite proof that the aquifer can be regarded as confined.

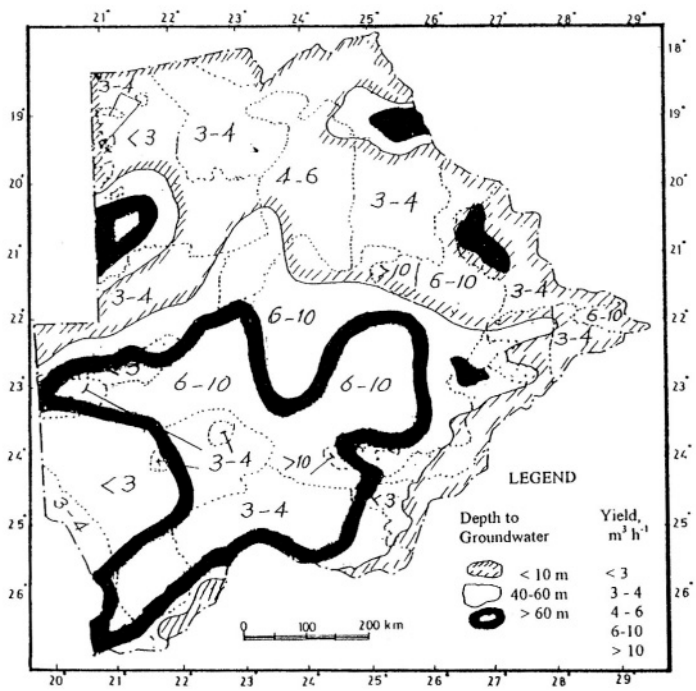

Figure 12.25- Depth to groundwater and aquifer yield (from Skwale and Selaolo, 1991)

The standard analysis of pumping test data showed that the transmissivity, *T*, of the fractured aquifer showed to be widely variable; values ranging from less than 5 to 60 $m^2 d^{-1}$ were obtained. Other methods of analysis have shown that *T* kept falling down with time during abstraction, consistent with linear flow. Figure 12.26 is a semi-log plot of long-term time-drawdown response due to abstraction from two boreholes P_1 (550 $m^3 d^{-1}$) and P_5 (450 $m^3 d^{-1}$) in Nnywane Basin as developed by De Vries (1985 and 1994, in Lloyd/UNESCO, 1999). This is an important conclusion, as *T* by definition is a constant value for any aquifer where the flow occurs through porous media. That is to say that aquifers in fractured rocks behave differently from aquifers made up of porous media. According to Lloyd (1995), it is difficult to understand the application in hard rock studies of the characteristics of hydraulic conductivity and storage as normally perceived for non-fractured or dominantly inter-granular porous aquifers.

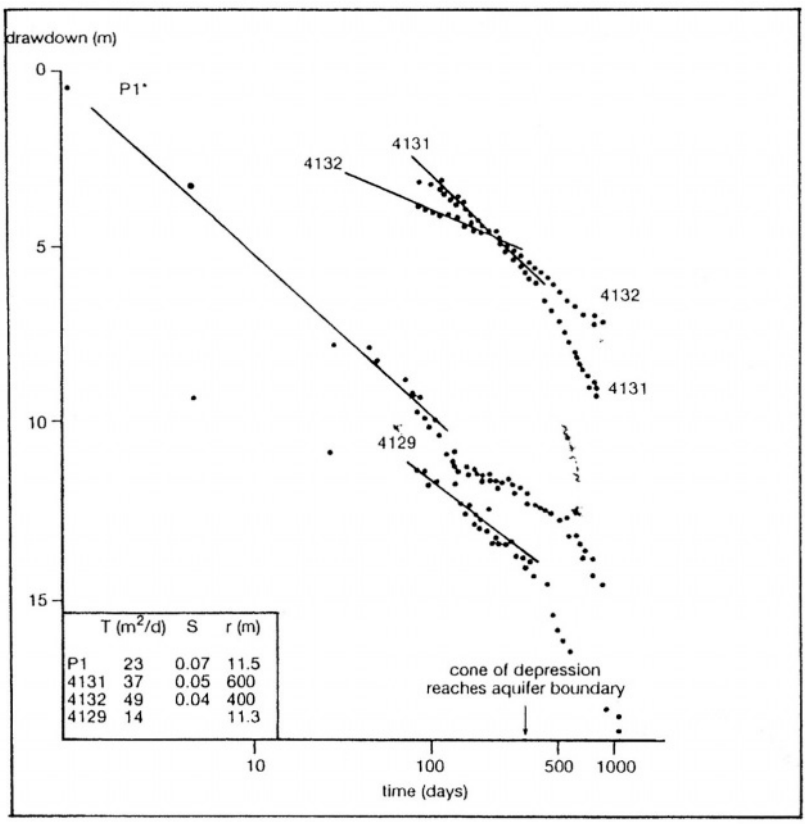

Figure 12.26- Long-term time-drawdown response due to extraction from two wells in Nnywane Basin, Botswana (De Vries, 1985 and De Vries, 1994, in Lloyd/ UNESCO, 1999)

iv- **South Africa**: This country is poor in groundwater resources as it is mainly underlain by hard rock formations. There is hardly any major groundwater aquifer that could be utilized on a national scale. Nevertheless, groundwater continues to be used for rural development of the country. Compared to most, if not all, African countries, South Africa has done and is still doing extensive amount of research work in the field of groundwater. Table 12.4 gives some general information about the aquifers in South Africa. The next paragraphs are added to give some more detailed information about a few specific topics.

Consolidated Sedimentary rocks of The Port Elizabeth Area: This area is located between latitudes 33°S and 34° 14'S, and longitudes 24°E and 28°S as shown in Figure 12.27. This area is mainly underlain by sedimentary rocks of the Cape Fold Belt (CFB). The consolidated hard rocks cover approximately 90% of the area. The geological units within the CFB comprising the fractured rocks have the glacial sedimentary, sedimentary, meta-sedimentary and extrusive as geological origin. The arenaceous: argillaceous material ratio varies from about 20 to 85. The average frequencies of the borehole yield of the different units are 14.4, 34.5, 31.4, 12.7 and 7.0% corresponding to yield classes of 0.0-0.1, 0.1-0.5, 0.5-2.0, 2.0-5.0 and >5.0 $l\ s^{-1}$. The overall mean is around 1.3 $l\ s^{-1}$.

Intergranular aquifers cover the remaining 10% of the area under discussion. These aquifers can be subdivided into coastal and alluvial aquifers. The coastal aquifers are basically made up of silt and fine-grained sand with a maximum thickness varying from 10 to 250 m. Remarkable enough is that the overall average yield of boreholes in the coastal aquifer is hardly distinguishable from that of the fractured rock aquifer, i.e. 1.3 $l\ s^{-1}$. The alluvial deposits occur principally along the flood plains of the Sundays, Gamtoos and Swartkops Rivers. The aquifer consists of an assemblage of unsorted boulders, pebbles, sand and clay. The borehole yields range from 0.1 to 15 $l\ s^{-1}$. The overall average borehole yield is slightly above 2.9 $l\ s^{-1}$ (Meyer, 1989).

The physical and chemical characteristics of groundwater in the above-mentioned aquifers are given in Table 5_h, Part II/ Appendix B.

The Dolomite Aquifer: Two case studies will be briefly reviewed here. These are the dolomite aquifers in the Kuruman and Pretoria regions.

The surface area of the dolomite in the Ghaap Plateau near Kuruman is about 1,140 km^2. The rocks consist largely of dolomite with lenses of chert and limestone. A small part, about 10%, is covered with sand. The water level in the dolomite varies between the ground surface and about 200 m below it. The region investigated receives, on the average, 450 mm y^{-1} rainfall.

The aquifer recharge was calculated by different methods. The method based on spring flow has given it as 4% of the rainfall depth in the period 1963-70.

Table 12.4- Hydrogeological information of groundwater aquifers in South Africa (Meyer, 1998)

Type of aquifer	Description of aquifer	Example
Inter-granular	Generally unconsolidated but occasionally semi-consolidated. Groundwater occurs within intergranular interstices in porous medium. Moderate areal extent.	Tertiary-Quaternary coastal deposits, along river terraces.
Fractured	Fissured and fractured bed-rock resulting from decomposition and/or tectonic action. Groundwater occurs predominantly within fissures and fractures. Aquifers are large in areal extent.	Sedimentary and metamorphic rocks with very limited overlying unsaturated residual weathered products.
Fractured and inter-granular	Sandstone and shale, intruded by mainly dolerite sills of varying thicknesses. Groundwater is contained in intergranular interstices and in fissures and fractures. Very limited in areal extent.	Sedimentary and igneous rocks with significant thickness of overlying saturated residual products of weathering.

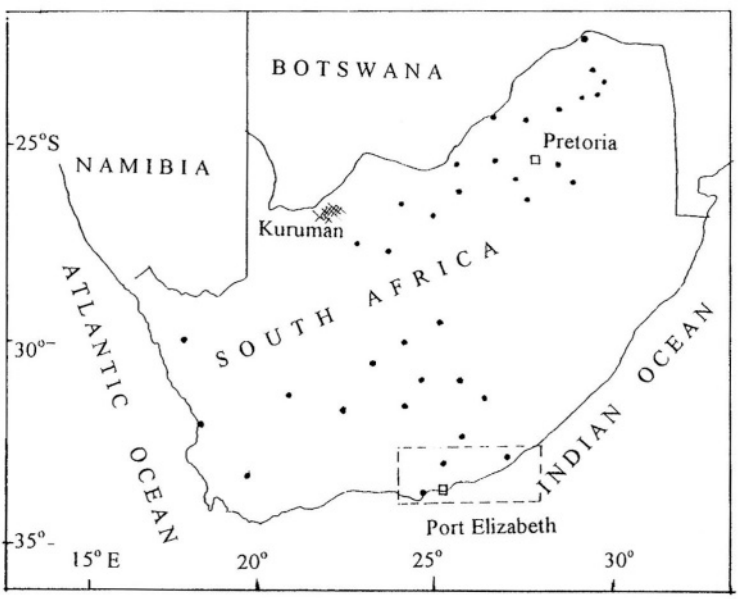

Figure 12.27- Map showing the study areas and the regional spread (indicated by closed circles) of the best cumulative rainfall departure relationships for groundwater monitoring points in South Africa (Bredenkamp, 1999)

The recharge calculation using the water balance of the aquifer in which the evapotranspiration had been estimated using Thornthwait's method gave zero recharge. This result has indicated that Thornthwaite's method for estimating evapotranspiration is not generally appropriate for the average rainfall conditions prevailing in the region under investigation. When the years of high rainfall only were considered, the areal mean ratio of recharge to rainfall was found to be in the order of 3%, a value that seems to be reasonable.

The second case study is the Pretoria region, which forms part of a large karstic basin, extending from Pretoria to the western border of Transvaal. The main aquifer material consists of crystalline dolormtic limestone. The thickness of the dolomite is widely variable and can exceed 1,200 m. The region receives, on the average, about $560\ \text{mm y}^{-1}$ The aquifer recharge was calculated from the average yield of a certain spring, which forms the main outlet of the aquifer. The annual recharge was thus estimated as $458\ \text{m}^3\ \text{h}^{-1}$. Since the area underlain by the aquifer is $225\ \text{km}^2$ the annual recharge depth becomes 17.8 mm and the average recharge: rainfall ratio is 3.2%. This ratio is not significantly different from the same ratio for the Kuruman region.

The recharge and rainfall data as obtained from different studies in South Africa, when brought together can be fitted by the following exponential regression relation:

$$R_{pc} = 0.49\exp(0.0045P) \tag{12.7}$$

where R_{pc} is the percentage of discharge and P is the mean annual precipitation in mm.

Effect of Aquifer Recharge on Groundwater Level: The variation in response of the cumulative rainfall departures (CRD), depending on the selected time interval, could be determined from the rainfalls for intervals such as 1, 3, 6 months or even periods of 12 months. The CRD can be calculated from the following relationship:

$$^{m}_{n}CRD_i = \frac{1}{m}\sum_{j=i-m+1}^{j=1} Rf_j + \frac{1}{n}\sum_{j=i-n+1}^{j=i} Rf_j \tag{12.8}$$

where Rf is the rainfall, i is the time increment, j is the status of the aquifer at a particular time in relation to the average condition over the preceding period comprising i time increments, m is the number of months representing the antecedent rainfall conditions of the aquifer, referred to as the short-term memory of the system, and n is the period which signifies the average condition

of the system determining the loss factor, also referred to as the long-term memory of the system.

The response of the piezometric level, h_i, is controlled by recharge, RE_i, and the recession, assuming that the recharge is added at the end of the chosen time interval, i, which can be expressed by:

$$h_i = h_{i-1}.c + RE_i = h_{i-1}.c + a(Rf_i - b) \tag{12.9}$$

where a and b are the regression parameters of the recharge-rainfall relationship, and c is a damping factor describing the recession curve of the hydrograph of the piezometric head. Further elaboration of Eq. (12.9) leads to:

$$h_i = \frac{a}{S_y} \sum_{j=i}^{j=i-n+1} Rf_j - C \tag{12.10}$$

where a/S_y is a proportionality coefficient between groundwater levels and CRD and C is the maximum depth of aquifer.

The above study as reported by Bredenkamp (in Lloyd/UNESCO, 1999) reached the conclusion that the interval, m, varying between 1 and 6 months in relation to the moving average rainfall over the preceding long-term memory, n, between 72 and 100 months has produced the best simulations of the groundwater levels. Figure 12.28 shows the groundwater levels at Wondergat versus moving average rainfall over preceding 72 months.

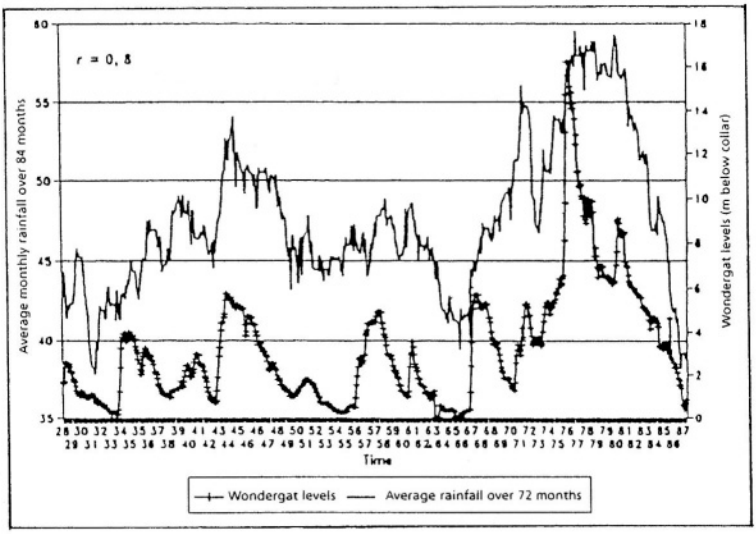

Figure 12.28- Wondergat groundwater level versus moving average rainfall over preceding 72 months (Bredenkamp, in Lloyd/UNESCO, 1999)

12.5- Vulnerability and Impacts of Groundwater Exploitation:

12.5.1 Vulnerability of groundwater- By vulnerability here is meant the vulnerability of groundwater to pollution or contamination by one or more external source(s). Three main sources of groundwater pollution in Africa are highlighted in this section.

i-Agriculture in Africa is by far the primary threat to the groundwater there. Ever increasing quantities of inorganic fertilizers and diverse pesticides, next to increasing the cropping frequencies in arid and semi-arid zones, are heavily applied for intensifying the production of agricultural land. These factors, unless properly controlled and the role of each on aquifer contamination is investigated, might turn such a source of water into a calamity.

Attia (1996) used the thickness of the clay cap overlying the aquifers in the agricultural land of Egypt as a parameter for defining the extent of groundwater vulnerability to pollution. The vulnerability increases from low in the northern part of the Nile Delta to moderate in the southern part and to high along the Desert- Delta fringes. The thickness of the clay cap decreases in the same order of the three parts. This parameter alone might be adequate if the movement of the contaminants below the surface to the groundwater body is vertical only. However, in the case of the northern and central parts of the Nile Delta area, it should be modified to take into account the proximity of the aquifer to the Mediterranean Sea.

ii- The proximity of saline water bodies such as salt lakes, seas and oceans is a source of threat to coastal aquifers. An aquifer is termed coastal when the seacoast, say, is one of its boundaries. Groundwater in coastal aquifers is highly susceptible to salinization due to the menace of seawater encroachment as a consequence to any disturbance in the state of equilibrium between seawater and freshwater. One should always keep in mind that as little as 5 percent of seawater mixed with freshwater will render the latter inadequate for human consumption.

Figure 12.29 shows a hydrogeological section of the coastal aquifer at Sidi Kreir, 30 km west of Alexandria, Egypt. It is of interest to observe in the section shown how shallow the freshwater lenses at this location are.

iii- The proximity of inadequate sanitation facilities, waste-dumping sites, or untreated harmful industrial wastes to a productive aquifer is another source of groundwater contamination. In this respect, we shall consider the situation of the aquifer used for supplying drinking water to certain districts in Brazzaville and its outskirts

Bacterial Contamination of Groundwater in Congo Brazzaville: Mention has been given to this case earlier in sec. 12.4.4. What can be added here is that the inadequate sanitary as well as poor social conditions prevailing in the outskirts of Brazzaville are closely linked to the unhealthy quality of the drinking water.

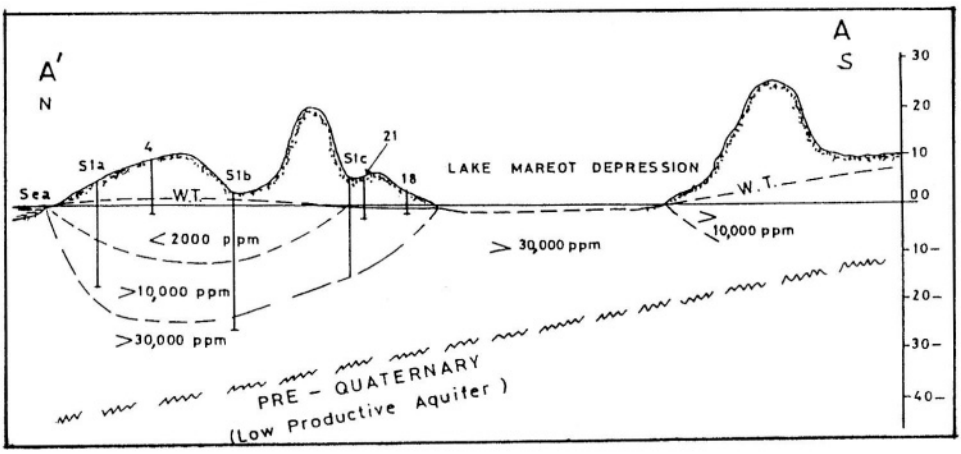

Figure 12.29- Hydrogeological section at Sidi Kreir, Egypt, showing the zones of saline groundwater (Shata, 1995)

In those areas, which are not equipped with water supply systems, water-associated diseases such as bacillary dysentery and, acute diarrhea are the prime causes of morbidity. Further examination of ground water pollution in that area ruled out the existence of industrial wastes or agricultural activities based on the use of chemical fertilizers and pesticides. Parameters of interest in this situation are the nature of the discharge point (dug well, borehole or spring), the proximity of the discharge well to the source of contamination, the particulars of the well such as depth and diameter, and the utilization of the well.

12.5.2 Impacts of groundwater exploitation- It is essential to test the quality of groundwater before exploiting the aquifer containing it. The physico-chemical and bacterial compositions of groundwater play a major role not only because of their health impacts but also in terms of user acceptance and effects on technical aspects of groundwater exploitation. Groundwater at certain locations by the nature of chemical composition of the formations there or other local circumstances might not be suitable for (direct) use by human beings. Two case studies from Kenya and West African countries in which the quality of groundwater is not favourable are briefly outlined in the following paragraphs.

The Occurrence and Distribution of Fluoride in Groundwater in Kenya: The fluoride level in groundwater samples from 1,286 boreholes in Kenya was surveyed. The samples analyzed were collected from all provinces of the country (see the map in Figure 12.21). The highest fluoride concentration was found in areas coinciding with the geographic locations of volcanic rock in and around the Rift Valley region. The results obtained by Nair et al. (1984) showed that there is a strong need to defluoridate groundwater in most regions of the

country for the health of the majority of the Kenyan population, if groundwater resources have to be exploited.

Corrosivity of Groundwater in West Africa: The problem of corrosive groundwater in drilled wells is causing serious concern throughout the Sahelian areas of West Africa. Many groundwater investigations in Mali, Burkina Faso, Sénégal, Niger, and Ivory Coast have clearly indicated to the presence of the corrosion phenomena in their groundwaters. The quality of the rural supplies in these countries is being seriously threatened by the corrosive nature of the groundwaters. This phenomenon leads to corrosion of the submerged parts of the pumps, as well as a high concentration of iron the waters themselves.

The main physical and chemical characteristics of a potentially corrosive groundwater are: low pH-value, low mineralization, relatively high temperature of water, and buffering action of some salts. The so-called Langelier index or saturation index is one of the methods that can be used to get an idea about the water corrosivity of the water. The index *i* can be obtained from the equation:

$$i = (pH)_o - (pH)_s \tag{12.11}$$

where $(pH)_o$ is the initial *pH* of water when sampled and $(pH)_s$ is the saturated or equilibrium *pH* as affected by total alkalinity (in mg l^{-1} of $CaCo_3$), calcium concentration (mg l^{-1}), dry residue (mg l^{-1}) and water temperature (°C). If *i* is less than 0, water is regarded as corrosive, between 0 and -1.0 the corrosivity is tolerable, and below -1.0 the corrosivity should be seriously considered. Guidelines for assessing the corrosivity of groundwaters in a certain region have been described in relation to the rural water supply projects in the Sahelian West Africa by Zoppis et al. (1989).

The exploitation of good-quality groundwater does not yield unfavourable impacts as long as the discharge and the recharge are equal. This is the case of safe yield that has been discussed in subsection 12.2.2. The unfavourable impacts take place when the discharge exceeds the recharge, i.e. the exploitation turns to be overexploitation or mining of groundwater resource. The impacts of overexploitation basically comprise the decline of the water table or piezometric level depending on the type of the aquifer and encroachment of saline or seawater.

i- Decline of water table levels in unconfined aquifers and piezometric levels in confined aquifers is one of the foremost negative impacts of overexploitation of groundwater aquifers. This situation leads to a gradually increasing lift heads, consequently more energy for lifting water, causing a perpetual rise of the unit price of groundwater. If this happens, the economy of the project for which water is being pumped will be disturbed. Besides, the decline of groundwater levels can lead to soil subsidence, thus affecting all what is on the ground surface. Bangkok, the capital of Thailand has been suffering from this problem

until strict measures regarding pumping of groundwater have been lately undertaken. Fortunately, there are hardly cases in African countries where this phenomenon has been observed.

Exploitation of Groundwater for Desert Irrigation in Egypt: In the 1950s a plan was laid down for a implementing a project known as the "New Valley". The project aims at expanding the agricultural land in and around the oases of the Western Desert, Egypt, through land irrigation from free-flowing groundwater. To fulfill this objective new deep wells, hundreds of meters in depth, have been drilled and many of the old wells have been properly cleaned and brought again into function. The immediate result of these works was the growing abstraction of groundwater from the deep aquifer systems underlying the Kharga and Dakhla Oases. The annual abstraction increased from $20*10^6$ m^3 in 1956 to $55*10^6$ m^3 in 1960 and further to $210*10^6$ m^3 in 1968. The obvious consequence is the rapid fall of the groundwater head by 30 m between 1962 and 1969. The factor that encouraged the heavy abstraction is the good quality of water. The major trouble here is that water stopped to flow freely; instead it has to be pumped for relatively high heads. This factor added extra expenses to the project cost, thereby affecting the overall economic aspect of the irrigation project. The overexploitation of the groundwater resource had been slowed down, such that the period from 1970 to 1975 did not witness except any further fall in the head except 3.0 m. Figure 12.30 shows the abstraction rate and the decline in groundwater head from 1956 to 1975 (Margat and Saad, 1984).

The Coastal Aquifer in Libya: Most of the water requirements for the coastal zone in Libya have been met till present from the coastal aquifer. The demand on water is ever increasing and the aquifer recharge is limited. The two factors combined are leading to overexploitation of the aquifer. Salem (1991) gave a diagram showing the decline of the water level with time from 1972 to 1989. Figure 12.31, is a reproduction of that diagram combined with a similar diagram given by Pallas (1979) for the period from 1958 to 1971. The combined diagram (Figure 12.31) shows that the water level south of Tripoli has declined by 74 m in the period from 1958 to 1989, i.e. at a rate of more than 2.3 $m\ y^{-1}$.

The Alluvial Aquifer of Kori, Teloua, Agadez, Niger: The alluvial aquifer supplying water to the city of Agadez, Niger, is located at the foot of the Air massif. By virtue of its location south of the massif, the Teloua Valley includes to some extent the structure of the Basement granite rock of the massif. This is made up of detritic alluvium, and encounters at the rim of the massif foot the border formations, which are of sandstone and mudstone of the secondary age.

The groundwater level has shown a total drop of 10.0 m in just 5 years, 1983-1988 (Figure 12.32). This is essentially due to the deviation of floodwater from the infiltration zone. It appears from the geological structure of the aquifer

and the distribution of the permeability within it that the position and direction of the dykes are not favourable for aquifer recharge (Balmer and Müller, 1989)

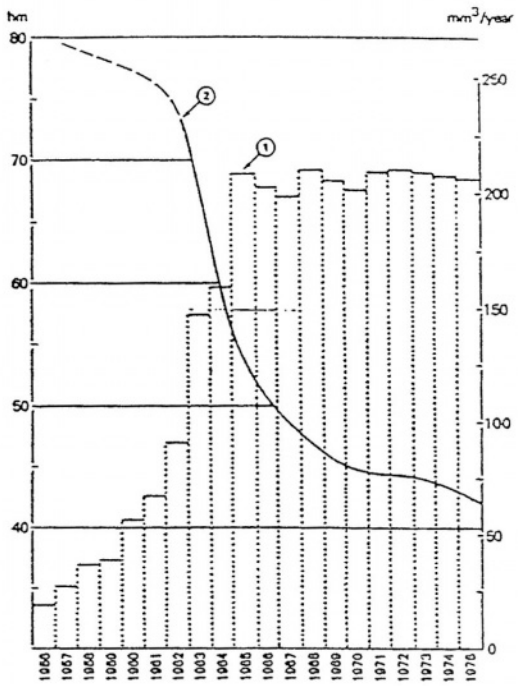

Figure 12.30- Change of abstraction rate and decline of groundwater head in the artesian aquifer underlying the Kharga and Dakhla Oases, Egypt, 1956-1975 (Margat and Saad, 1984)

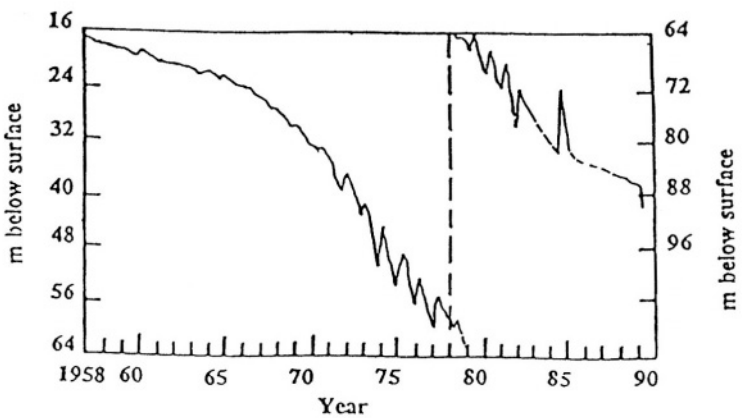

Figure 12.31 Decline of water level in an observation well at Ben Gashir, south of Tripoli, Libya (Pallas, 1979 and Salem, 1991)

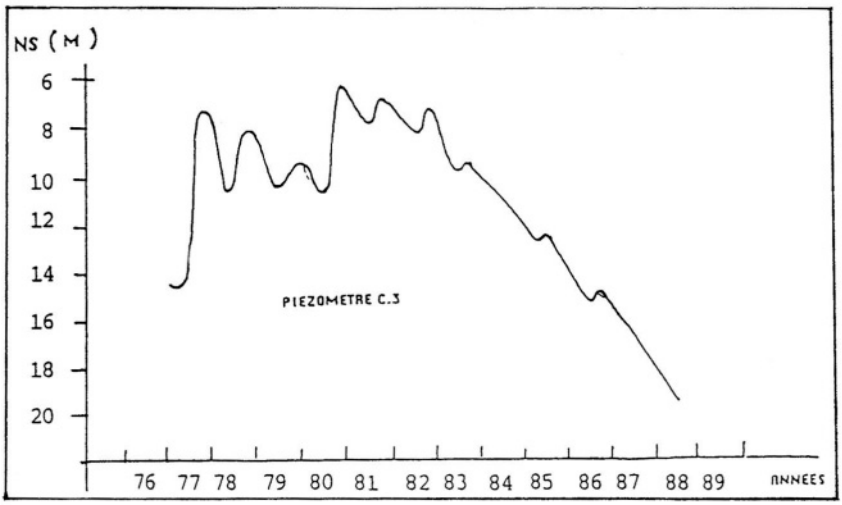

Figure 12.32- Fluctuation of the groundwater level in the aquifer of Agadez, Niger (ORSTOM, cited in Balmer and Müller, 1989)

Groundwater Level in Borno State, Nigeria: The groundwater in Borno State is abstracted from the so-called Chad formation. The hydrogeological characteristics of this formation have been described as case (vi) in subsection 12.4.2. All boreholes for which data were collected have shown a steady decline in piezometric head. The largest decline had been observed in the lowest aquifer and reaches **5-10 m y^{-1}**, as shown in Figure 12.33. According to Jacenkow (1984), the efficiency of the existing wells declined as a result, and a number of them had to be shut down because of the loss of yield. The demand on water is increasing, and the depletion of the groundwater resource is accelerating.

ii- Sea water intrusion has already been mentioned in the previous section as a source of threat to the quality of groundwater in coastal aquifers. Because two fluids of different densities are involved, a boundary surface, or interface, is formed wherever the fluids are in contact. The hydrodynamic balance of the fresh and salt waters governs the shape and movement of the interface between the two waters. Furthermore, the difference between the densities of saltwater and freshwater causes the saltwater to be found at a depth, h_s, below sea level of 30-40 times the height, h_f, of the freshwater above the sea level. This result is obtained from the Ghyben-Herzberg principle given by the relation:

$$h_s = \frac{\rho_f}{\rho_s - \rho_f} h_f \qquad (12.12)$$

where ρ_s is the density of seawater and ρ_f is the density of freshwater. As an example, a 1-m drawdown of the water table level due to freshwater abstraction

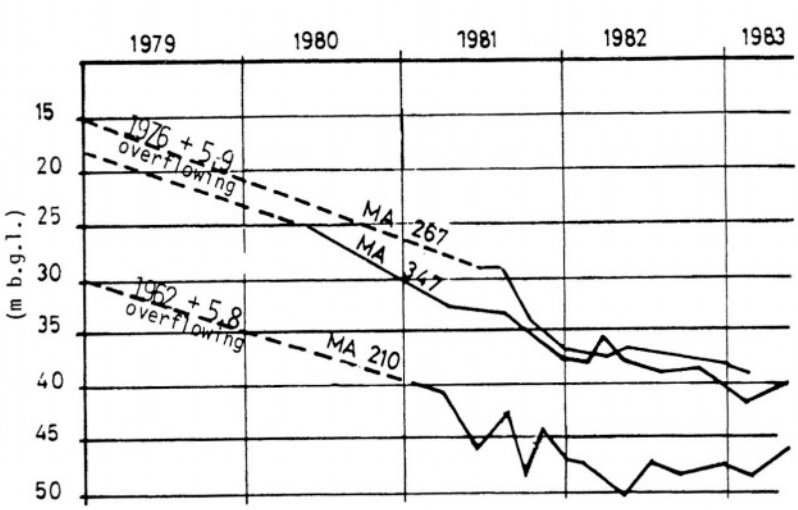

Figure 12.33- Groundwater levels in three observation wells in the lower aquifer of Borno State, Nigeria (after Jacenkow, 1984)

will result in rise of the interface between the saline and freshwater (upconing) by 30 to 40 m. Further abstraction of fresh groundwater will increase the upcoming till the two water bodies mix and the freshwater is no longer fresh.

Theoretical approaches describing more of the mechanics of seawater intrusion and the relevant models can be found in many specialized references (e.g. Pinder, 1973, Sherif et al., 1990, Senger and Fogg, 1990). As an example of seawater intrusion in a North African aquifer here below the case of a coastal aquifer in Libya is outlined.

Seawater Intrusion in a Coastal Aquifer West of Tripoli, Libya: The Quaternary aquifer, mostly referred to as the first aquifer, in the Jifara (Gefara) plain, northwest Libya, is a typical coastal plain aquifer. It is composed of calcarenite (calcareous sandstone) interbedded with silty and clayey lenses changing southwards into detrital limestone, marl, clay, sandy limestone with evaporitic lenses of Pliocene-Miocene age as shown in Figure 12.34.

The porosity and hydraulic conductivity of the aquifer material near the seacoast are high. The groundwater wells range in depth from 30 to 90 m below ground surface. Till a few decades ago, the quality of the aquifer water used to

be described by being relatively good, with an average total dissolved solids of 500 mg l^{-1} and chloride concentration of less than 150 mg l^{-1} In view of the climate of the area, especially the limited annual rainfall (< 300 mm), the direct recharge from rainfall and the indirect from wadi floods is very little. The limited amount of the available surface water has led to have more than 95% of the water supply at present coming from the Quaternary aquifer.

As a consequence to the ever-increasing abstraction of groundwater coupled with limited recharge, the aquifer began to show signs of saline water intrusion in the coastal strip as well as other parts of the Jifara Plain. The cross section in Figure 12.34 shows lines of equal salinity (Belaid, 1995). From the figure, it is clear that the depths below mean sea level to the 2,000 chlorinity line is 35 and 55 in at distances of 0.62 and 1.1 km from the coastal line respectively.

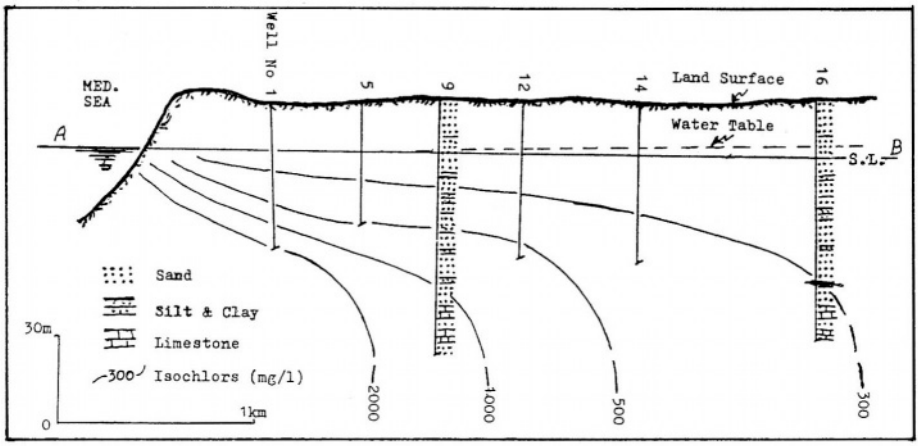

Figure 12.34- Hydrogeological cross-section of the coastal aquifer of the Jifara Plain, west Libya showing the salinization zone (Belaid, 1995)

CHAPTER 13

HYDROLOGY AND WATER RESOURCES OF AFRICAN ISLANDS

13.1- Introduction

Most of what has been presented and/or discussed in the previous chapters relates mainly to the of African mainland. Islands of the world, including those in Africa, can be subdivided according to their size. The surface area defining the upper limit of a small island is assumed here as 2,000 km^2. This figure is in conformity with the classification appearing in the relevant UNESCO Reports (Falkland, 1991 and 1992). According to this classification, one can easily conclude that all the islands in Africa, except Madagascar, have to be regarded as small islands. Small islands have the following characteristics:

i- They are volcanic, limestone, coral atoll, bedrock, unconsolidated or mixed in nature. Practically all small islands of Africa are volcanic in origin.
ii- Volcanic islands are typically high in structure, while the coral atolls are low in elevation.
iii- The volcanic islands have some surface water resources in the form of streams and rivers, while the atolls seldom experience surface runoff.
iv- Small tropical islands undergo a range of weather conditions, which have short-, medium-, and long-term cycles. They experience from time to time destruction caused by devastating tropical cyclones. Those islands, which are greatly influenced by summer monsoons, have distinct wet and dry periods, while others are less influenced by the seasons.
v- The soil cover of an island affects its water resources by influencing surface runoff, evaporation and transpiration. Besides, the water-retention capacity of the soil affects the groundwater recharge.
vi- The type and density of vegetal cover also affect an island's water supply. The trees, shrubs and grasses intercept a part of the rainfall; they participate on transpiration; they slow the runoff and they reduce soil erosion. Slowing runoff helps increase infiltration, and reduction of erosion helps conserve soil fertility (Falkland, UNESCO, 1992).

The islands of Africa, geographically speaking, can be subdivided into Atlantic Ocean Islands and Indian Ocean Islands. The Atlantic Ocean Islands are, in turn, subdivided into North Atlantic Islands and South Atlantic Ocean. Regardless of their locations, some islands serve as tourist centres, some others are used for collecting meteorological or other data, and most of the rest serve as military and marine bases for the super powers.

13.2- North Atlantic Islands

By North Atlantic Islands it is those islands located north of the Equator that are being referred to. In terms of the geographical extent of this ocean, they can better be termed Mid Atlantic Ocean Islands. Whether we call them North Atlantic or Mid Atlantic they consist of four sets of islands. These are the Azores (Açores), the Madeiras, the Canaries, and Cape Verde Islands.

13.2.1 The Azores (Açores) Islands- This set comprises nine islands forming an archipelago lying between latitudes 37°N and 39ºN. Though the shortest distance between any of the islands, Santa Maria, and Portugal is 1,300 km, yet the Azores are considered as an integral part of Portugal. The islands from north to south, as shown on the map in Figure 13.1, are Flores, Graciosa, São Jorge, Terceira, Faial, Pico, São Miguel, Formigas, and Santa Maria. The total surface area of the nine islands is $2{,}247\ km^2$ (Encyclopædia Britannic, 2001).

The islands are volcanic, well known for their numerous earthquakes and volcanic activities. The shores are therefore covered with rock and pebble debris. They rise from the ocean floors and reach a height of 2,350 m at Pico. The climate of the Azores is subtropical with about 14°C and 23°C as mean temperatures of January and August respectively. The mean monthly and mean annual temperatures at Horta (station No. 1) in the Faial Island and Punta Delgada (station No. 2) in São Miguel are listed in Table 3, Appendix A. The air humidity of all nine islands is quite high.

Table 10_a, Appendix A, give the mean annual rainfall at these two stations as 960 mm and 1,025 mm, with variation coefficient of 15% Such annual amounts of precipitation coupled with moderate temperatures and high humidity have resulted in an abundant fauna of the Mediterranean and European types, including mixed types of forests. The runoff coefficient as a result of the steep slope of the ground exceeds 25% in those locations where the infiltration is too low. The streams (rivulets) are generally small and shallow. Surface water is used for raising intensive agriculture, especially wheat, maize, vegetables and fruit. Additionally, the Azores produces adequate quantities of cattle products and sea fish.

13.2.2 The Madeira (Funchal or Madeiras) Islands- The archipelago of Madeira comprises eight islands scattered between 30°N and 33° 30'N, as shown in Figure 13.2. The total surface area covered by the eight islands is about $800\ km^2$. All eight islands are of volcanic origin covered with layers of basalt and ashes. Porto Santo and Madeira are the only inhabited islands. The Island of Madeira rises from the ocean floor and reaches elevation an of 1,860 m a.m.s.l. at Santana Peak in the middle of the island.

The Madeiras have a subtropical/Mediterranean climate with limited variation in temperature from one month to another. The mean August (warmest

month) temperature at Funchal (station No. 15) is 22.1°C, decreasing to 16.0° C in February (coldest month), bringing the mean annual temperature to 18.5° C. The mean annual rainfall at the same station, i.e. Funchal is 650 mm for the period 1931-80, is 651 mm, with variation coefficient of 24%. Stamp and Morgan (1972) gave the mean annual rainfall over a different period as 760 mm.

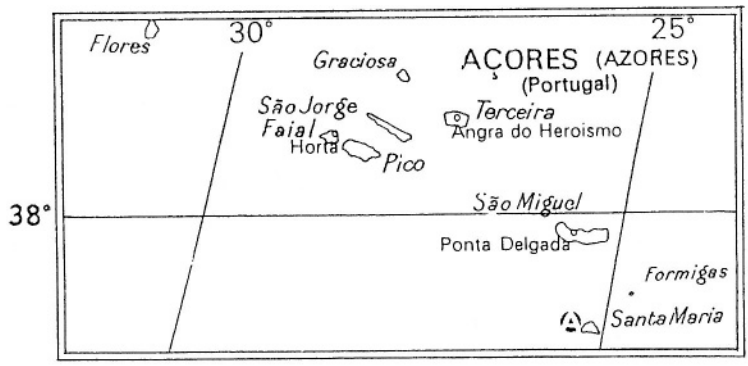

Figure 13.1- Location map of the Azores Islands (from the Times Concise Atlas of the World, 1980)

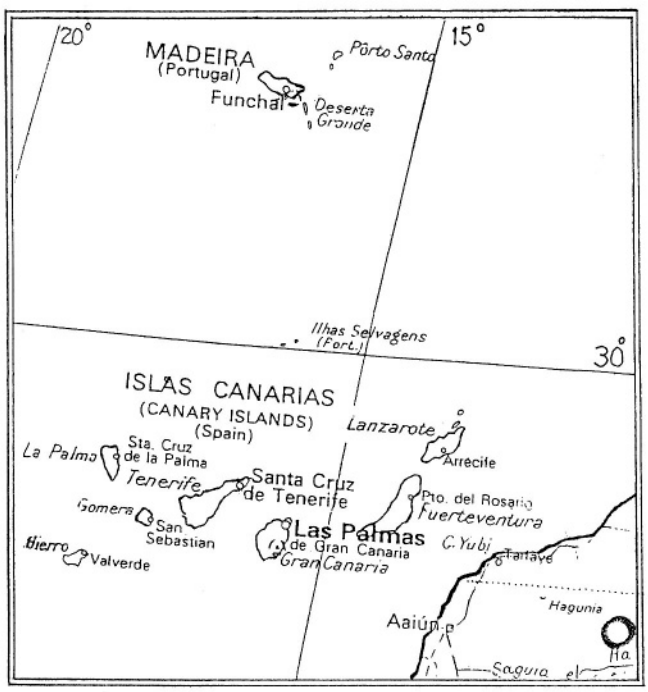

Figure 13.2- Location map of the Madeiras and Canaries (from the Times Concise Atlas of the World, 1980)

According to the World Weather Records, the mean annual rainfall during the dry period, 1971-80, at Porto Santo, 42 km north east of Madeira, was just 340 mm. The rainy season for the Madeira Islands is from October to March-April, while the dry season covers the months June-August-September.

Production of Madeira wine, sugar and vegetables, supported by limited tourism, handicrafts and fishing, forms the backbone of the Madeiran economy

13.2.3- The Canary Islands (Canaries): Despite their geographic locations in the North Atlantic Ocean and being an integral part of Spain, the Canary Islands or the Canaries, are usually viewed as African Islands This set consists of two groups of islands. The western group consists of five islands: Gran Canaria; Tenerife; Las Palmas (1,533 km^2), Gomera and Ferro (Hierro), whereas the eastern islands group comprises Lazarote and Fuerteventura (1,730 km^2). The geographical locations of the Canaries are shown on the map in Figure 13.2.

The Canaries, by origin, are volcanic islands rising from the deep ocean floor and cover a surface area of about 4, 500 km^2 at mean ocean level. The ground elevation rises from zero at the seacoast and reaches over 3,700 m above the mean ocean level at the top of the snow-capped volcano, Pico de Teide, in the island of Tenerife. The highest points in the other islands are above 1,200 m a.m.s.l

The Canary Islands enjoy a subtropical agreeable climate with limited temperature variation. Table 3, Appendix A, gives a mean monthly temperature of 17.9° C in January and 25.0° C at Santa Cruz de Tenerif (station 28), with 20.9° C as mean annual temperature. The corresponding temperatures at Las Palmas (station No. 29) are about 0.5°C below those at Santa Cruz. The topographic features of the islands make the annual rainfall increasing considerably from the coast to the higher ground. Table 10_a, Appendix A, gives the mean annual rainfall for the period 1931-80 at station No. 28 as 245 mm, with variation coefficient of 36%, and 32 as the number of rainy days per year. The mean annual rainfall over the years 1961-80 at station No.29 is 107 mm, with variation coefficient of 56%. Higher locations receive more rain up to 750 mm or more, and the number of rainy days is greater. Despite the aridity of the low-lying areas, they are hardly short of freshwater because of the plentiful supply provided by the freshwater springs.

13.2.4- Cape Verde Islands: This set is formed of 13 islands, nine of which are inhabited. These islands are Boa Vista, Maio, Sal, Fogo, Santo Antão, São Tiago, São Nicolau, and São Vincente. All thirteen islands are situated between 15°N and 17°N latitudes as shown on the map in Figure 13.3. This set is closer to Africa than any of the previous sets, as the shortest distance between any of its islands and Sénégal on the main land is about 600 km. The whole set is composed of volcanic islands and has a total surface area of 4,030 km^2. Cape

Verde Islands, like the Azores and Madeiras, are under Portuguese administration.

The climate is generally warm and arid. The mean temperature at Praia (station No. 53) is 22°C in February (coldest month) increasing up to 27°C in September (warmest month), with a mean annual temperature of 24.5°C. The nine inhabited islands can be subdivided into two groups; the northern group is relatively wet compared to the dry southern group. The mean annual rainfall in the southern or dry group is in the order of 60 mm. Table 10_b, Appendix A, gives a long-term series of annual rainfall at Praia station covering the period 1885-1973. The mean over this period is close to 260 mm. The mean annual rainfall at low-lying locations like Sal (station No. 44) can be as little as 126 mm at Porto Grande in Mindelo and 63 mm in Sal. On the other hand, the annual rainfall on the higher ground can reach 500 mm or more. These figures bring the overall average to 228 mm y^{-1} ($918*10^6$ m^3 y^{-1}). The rainy season usually lasts from August till end of November.

There are a few watercourses that run all year, except at the end of the dry season. The remaining watercourses are ephemeral, i.e. they fill up a short time during the short, intense rainstorms. Rain spells tend to occur as torrential storms causing severe soil erosion thus rendering the soil infertile and unsuitable for agriculture. Groundwater is the primary source of domestic water supply, though not all of it is of suitable quality. The amount of desalinated water is limited to $2*10^6$ m^3 y^{-1}.

The FAO Report entitled *Irrigation in Africa in Figures* (1995) estimates the renewable water resources to be $300*10^6$ m^3 y^{-1}. The surface water resources are estimated as $180*10^6$ m^3, indicating a surface runoff coefficient of about 20%. However, it is the yield of the groundwater resources, which is estimated as $120*10^6$ m^3 y^{-1}, that is currently being exploited. A small percentage, 8.6%, of the total sum of $300*10^6$ m^3, is used for agriculture and industrial purposes.

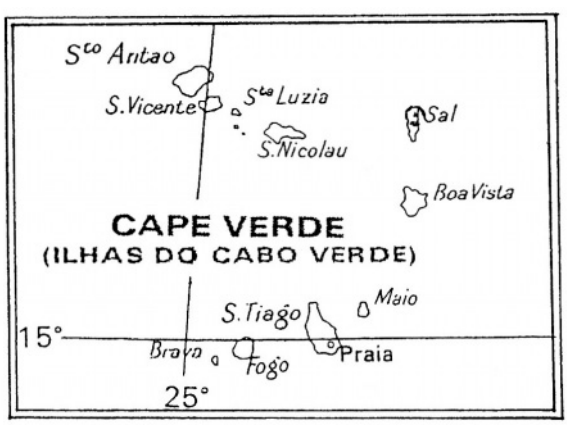

Figure 13.3- Location map of the Cape Verde Islands (from the Times Concise Atlas of the World, 1980)

Nearly 25% of the land area of the islands is volcanic, being covered with basalt stone. Additionally, over 60% is covered with sand and limestone outcrops. The remaining 15% is fertile land and can be used in agriculture. In fact, the area actually under cultivation does not exceed 370 km^2 or 9% of the surface area of the islands. Sugar and sugar cane, tubers and flowers are the main produce of the islands. Grains and fruit are grown to a limited scale.

13.3- Equatorial Islands

13.3.1 Principe and São Tomé- These two islands, as can be seen from the map, Figure 13.4$_a$, are located near the Equator in the Gulf of Guinea. The distance between São Tomé and Gabon in the mainland is 300 km. Príncipe is the smaller island, 115 km^2, whereas São Tomé is the larger one, 845 km^2. The combined area of the two islands together with a number of islets reaches 1,001 km^2. In view of their proximity to each other, spaced 150 km apart, and the smallness of their respective areas, the two islands are usually considered as a single unit. The islands are of volcanic origin with mountain peaks up to 2,000 m above mean ocean level. The mountains slope steeply towards the south but descend gradually to small plains in the northeast.

The climate is equatorial oceanic, dominated by the monsoon winds blowing from the south, the warm stream of the Gulf of Guinea, and the relief of the islands. Table 3, Appendix A, gives the mean monthly temperature of July as 23.9°C increasing to 26.3°C in March and April at São Tomé (station 162). The mean annual temperature is 25.4°C. These figures do not change the fact that the mean daily temperature can vary between 19° and 32°C. The islands, because of their geographic location are too humid, with mean relative humidity of the air constantly above 80%. The annual rainfall varies basically with height above the ocean level. The range of variation, from less than 1,000 mm to about 7,000 mm, is high indeed. The station at São Tomé, because of its position at a height of 8 m a.m.s.l., receives an average of 908 mm y^{-1}, with 19% variation coefficient, for the period 1961-80. The mean annual rainfall over the same period at Príncipe (station No. 153) was 1972 mm, with variation coefficient of 16%. The annual volume of rain falling on the two islands is $3.1*10^9$ m^3 corresponding to an average depth of 3,200 mm.

The islands have a number of steep, perennial rivers carrying heavy discharges for their cross sections The two maps, Figure 13.4$_b$, show six rivers in São Tomé and one river in Príncipe. The locations of discharge measurements on these rivers are shown as well. The inadequacies here are firstly; the available measurements cover a short period and secondly; there are some gaps in the data. The mean annual discharges, without paying attention to these inadequacies, are 0.42, 0.58, 2.4, 0.42, 1.4 and 6.9 m^3 s^{-1} corresponding to stations No. 181, 183, 184, 185, 186 and 187 in São Tomé respectively, and 3.8 m^3 s^{-1} for station No. 170 in Príncipe. The sum of these discharges brings the

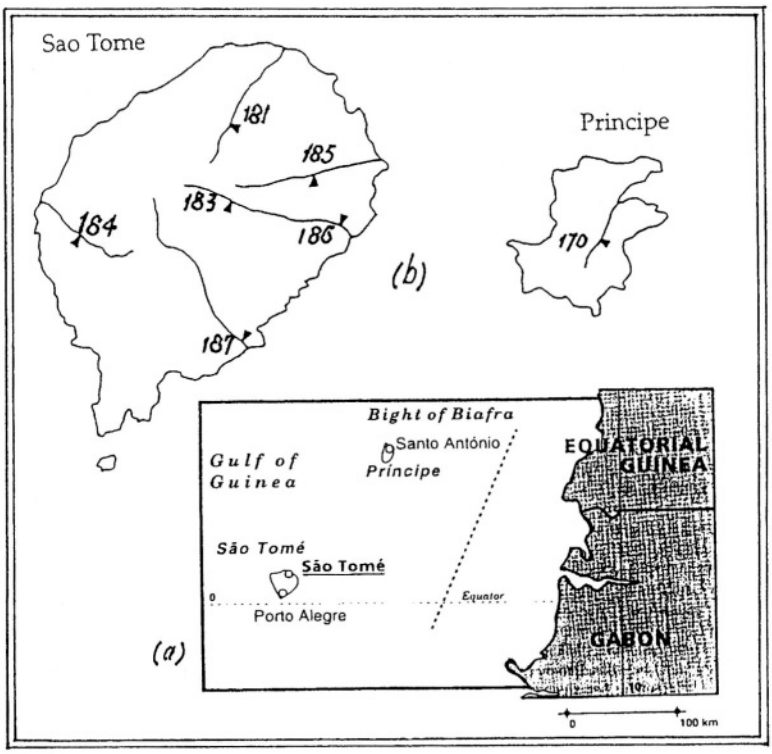

Figure 13.4- São Tomé and Príncipe Islands; (a) geographic locations (from the Times Concise Atlas of the World, 1980) and (b) discharge measuring stations (from UNESCO Studies and reports in hydrology No. 52, 1995)

total surface water yield for São Tomé to at least 12.1 $m^3 s^{-1}$ ($383*10^6 m^3 y^{-1}$) and 3.8 $m^3 s^{-1}$ ($120*10^6 m^3 y^{-1}$) for Príncipe. When these figures are compared to the annual rainfall, the surface runoff coefficient can be obtained as 15 and 30% for São Tomé and Príncipe respectively.

The renewable internal water resources have been estimated as $2.18*10^9 m^3 y^{-1}$, of which $0.18*10^9$ are for Príncipe and $2.0*10^9 m^3 y^{-1}$ for São Tomé. Nineteen small dams of a total capacity of $19*10^6 m^3$ and a single larger dam of $20*10^6 m^3$ capacity have been built in 1980. The total water requirements of the two islands were estimated in 1994 as $7*10^6 m^3 y^{-1}$, which is a small percent of the available water.

13.4- South Atlantic Islands

The South Atlantic Islands are those islands located in the Atlantic Ocean south of the Equator. These are Ascension, Saint Helena, and the island group called Tristan da Cunha.

13.4.1- Ascension Island: This is a small (88 km^2), isolated volcanic island at about 8° south of the Equator. The geographic location of Ascension Island is shown on the map, Figure 13.5. The island is a dependency of the British colony of St. Helena, about 1,100 km to the southeast. As some rain falls on the high ground, such as the heights of the Green Mountain, vegetables and fruit grow there and livestock is raised. The rest of the area is simply a desert. The surface streams hardly run full with good-quality water, except during a few months on the higher ground only. Most of the demand on freshwater is supplied from desalination plants. The island serves principally as air and naval base.

13.4.2 Saint Helena Island- This too is an isolated volcanic island, with a surface area of 122 km^2. The island as shown on the map in Figure 13.6 is located on latitude 16° south of the Equator. The hilly cliffs rise almost vertically and bring the peak height of the island up to 820 m above the mean ocean level.

Table 3 of Appendix A gives the mean monthly temperature as 14.1-14.2°C for August-September (coldest months) and 19.2-19.3oC for February-March (warmest months), both at Hullsgate (station No.219) The air humidity is high all year round, especially in the low-lying areas. The mean annual precipitation over the period 1961-70 at Hullsgate is 874 mm, with variation coefficient of 14%. The mean and coefficient of variation over the 10-y period 1971-80 at another location are 677 mm and 30.8% respectively. Generally speaking, the mean annual rainfall varies from 200 mm at sea level to more than 750 mm at the island's centre. It is worthwhile to mention here that the station at Hullsgate is located at a height of 627 m a.m.s.l.

Dispersed, water-cut gorges run south of the mountains and turn into deep valleys near the ocean side. Most of the demand on water is suppliedfrom the numerous springs that crowd the island. Trees and vegetation grow in the central part of the island.

13.4.3 Tristan da Cunha Islands- This group of islands has since 1938 formed a dependency of the British colony of Saint Helena. The group comprises six islands, all situated south of 37° S as shown on the map in Figure 13.7. The island of Tristan da Cunha is the largest in surface area (98 km^2), and the only inhabited one. This island, like the rest of the group, is of volcanic origin. The volcano in its middle rises up high to 2,600 m a.m.s.l.

The climate of the island can be described as cold, stormy and wet. The annual rainfall at the Edinburgh settlement on the northeast coast has been estimated as about 1, 675 mm. However, there is hardly any hydrological data published about this island. Due to the very small population, the main occupation of the island's inhabitants is confined to growing potatoes and fishing. Plant and animal life includes elephant seals and other species not found elsewhere in the world. The remaining islands serve as a natural sanctuaries of certain kinds of birds (Encyclopædia Brittanica, 2001).

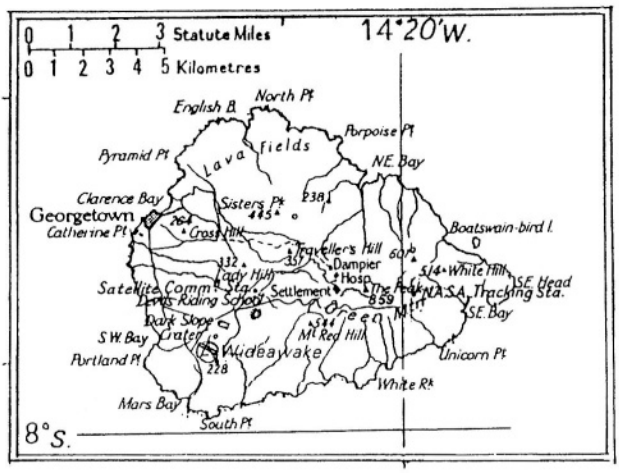

Figure 13.5- Location map of Ascension Island (from the Times Concise Atlas of the World, 1980)

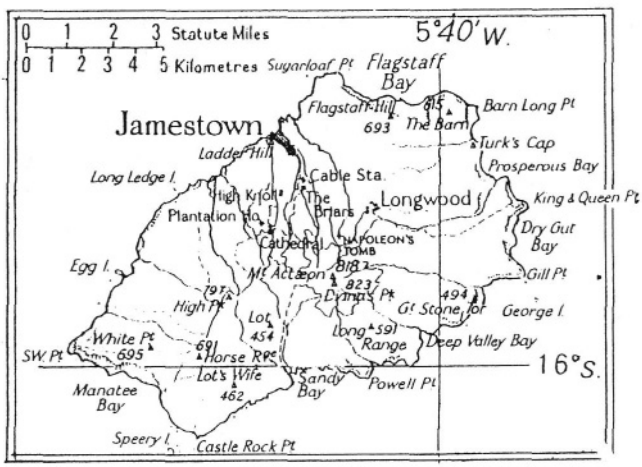

Figure 13.6- Location map of Saint Helena Island (from the Times Concise Atlas of the World, 1980)

13.5- Indian Ocean Islands

Indian Ocean Islands, which are considered to be African, mainly comprise Seychelles, Comoros, and Mascarene Islands (Mascarenas). The latter consists of Mauritius and Réunion. All these islands are small in size, except Réunion, which is slightly larger than the limit set for small islands, i.e. 2,000 km^2. Unlike the islands of the Atlantic Ocean, Madagascar a single island in the Indian Ocean is one of the largest islands of the world.

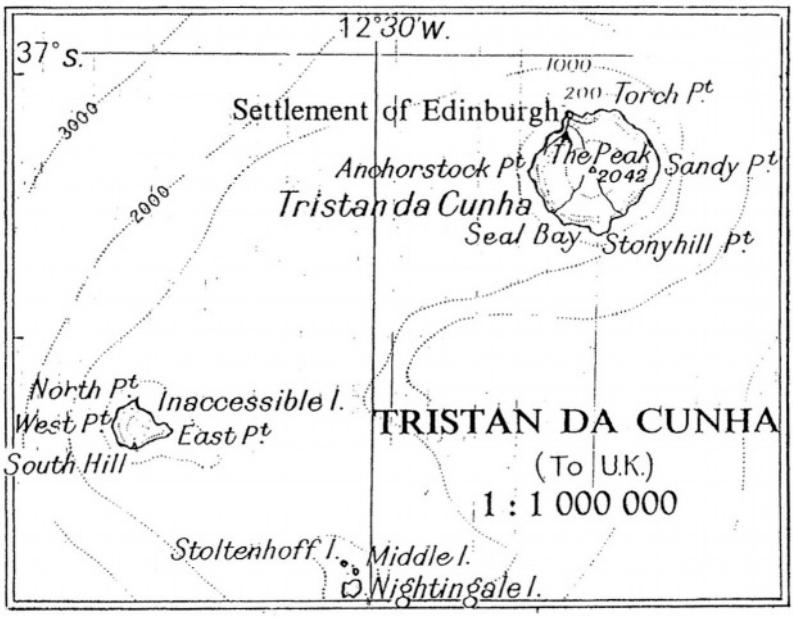

Figure 13.7- Location map of Tristan da Cunha Islands (from the Times Concise Atlas of the World, 1980)

13.5.1- Seychelles Islands: These are a group of islands situated between 3°S and 11°S. The total surface area of all the islands combined is about **453 km²**. Most of the islands in the southwest are coral, rising only a little above mean sea level. The largest of the corals is Aldabra, a large atoll. The islands lying furthest northeast, forming the Seychelles Archipelago, are built of granite, and have hills and mountains rising up to 1,000 m a.m.s.l. Mahé is the largest individual island of the group, with a surface area of about **130 km²**. The location map, Figure 13.8, while showing the important islands of the group, does not show all territorial waters of the Republic of Seychelles.

The climate of the Seychelles, judged by the data available at Victoria, the capital of Mahé, is pleasantly warm, with a slight change in temperature from month to month. The mean annual temperature is 27°C, while the monthly temperature ranges between 26 and 28°C. Table **10$_a$**, Appendix A, gives the mean annual rainfall for the period 1961-70 at the same location (station 177) as 2, 644 mm, with variation coefficient of 23%. This is about 10% higher than the mean over the period 1909-70 at Long Pier Mahé, 2,328 mm (UNESCO, 1991) The same reference gives the annual potential evapotranspiration Et_p as 1,688 mm, and the free water evaporation E_o as 1,980 mm, both figures as means over the period 1971-78. The mean monthly values fall in the range of the annual mean ± 10% for ET_p and the annual mean ± 12% for E_o.

The surface of the island of Mahé is covered with numerous, swift flowing, steep, small streams. These streams meet the need for potable water. Mahé Island has 32 catchments totaling **56 km^2**. The La Digue Island, north east of Mahé, gets most of its water needs from groundwater.

Groundwater investigation in Mahé, Praslin and La Digue Islands has been limited to the coastal plateau. The aquifers there are of limited areal extent, in the order of **2 km^2**. They are shallow too, not exceeding 20 m in thickness. The groundwater moves towards the ocean under the influence of rather small gradient, hi addition, the aquifer's permeability and storativity are **10 m d^{-1}** and 0.10, respectively. Abstraction of groundwater is carried out using well-point systems and interception ditches.

The Seychelles began to be inhabited in the last quarter of the **18th** century after the French navy established the first settlement in Mahé. Within a few years the exuberant forests of the island had been destroyed. The slaves the French imported from Mauritius introduced crop agriculture. The main crops raised in the inhabited islands are coconuts, cinnamon, and vanilla. These products go to pay for imported foodstuffs, above all rice, flour, and sugar, on which the islanders depend, plus cotton piece goods. Local production of some of the imported items can reduce the dependence on imported foodstuff. A substantial development in the islands' economy has followed the construction of a United States Air Force tracking station for satellites (Grove, 1970).

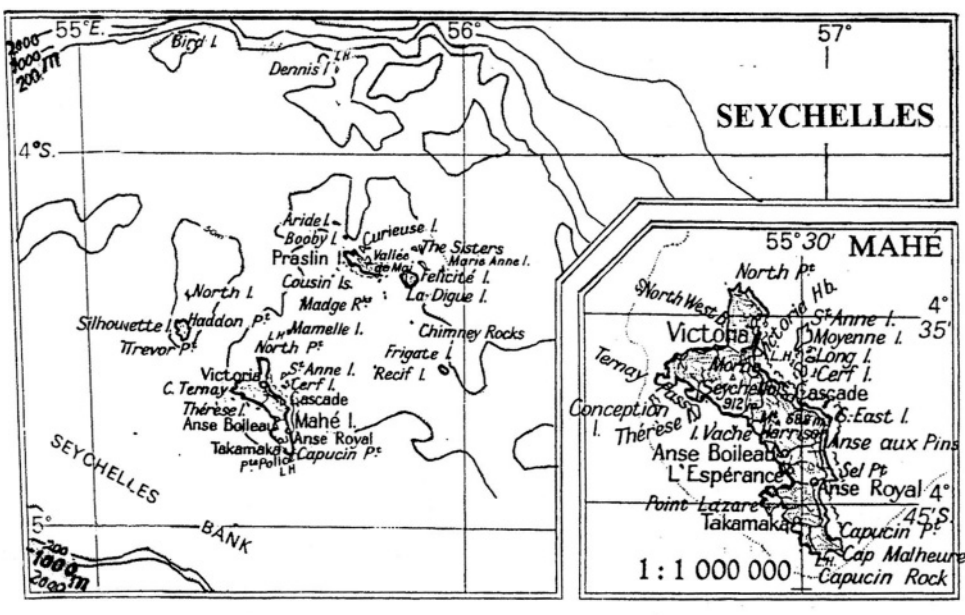

Figure 13.8- Location map of the Seychelles Islands (from the Times Concise Atlas of the World, 1980)

13.5.2- The Comoro Islands (Comoros): This too is a group of small volcanic islands between Madagascar and the African mainland. The islands are located between 11° and 13° south of the Equator. The main islands, as shown on the map in Figure 13.9, are Grand Comoro (1,148 km^2), Mayotte (374 km^2), Anjouan, and Mohéli. The Comoro Islands used to be administered by France. However, they have since long been subject to Arabic influences and the Islamic faith. After independence, the Republic of Comoros has become an Arab State and member of the Arab League. Moroni is the capital of the Republic as well as of the Grand Comoro Island.

The climate of the islands is wet tropical. Judged by the meteorological data from Moroni (station No. 195) and Ouani (station 198), the weather is usually rather warm, with a mean annual temperature of 25.5°C for both stations. The mean monthly temperatures fluctuate around the annual mean by ± 1.5-2.0°C. The mean annual rainfall at Moroni (16-y) is 2,695 mm with 27% coefficient of variation. The mean at Ouani (10-y) is 1,839 mm. Table 9, Appendix A, shows that in Moroni there is always rainfall each month of the year. The least rainfall occurs in September and the heaviest in January and April.

The natural forests have been largely cleared for agriculture. Sugar cane was a leading crop, but it has suffered from more effective production elsewhere. The principal export crops are vanilla and essential oils. Cocoa, coconuts, sisal and rice are also grown (Stamp and Morgan, 1972).

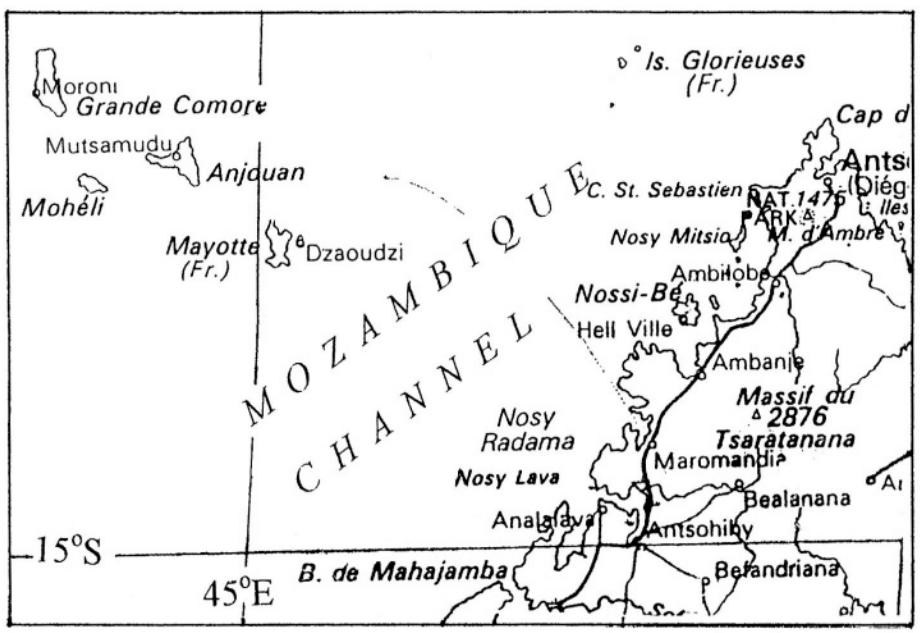

Figure 13.9- Location map of the Comoro Islands (from the Times Concise Atlas of the World, 1980)

13.5.3 Mauritius Island- The island of Mauritius, together with Réunion (Burbon) and Rodriguez Islands, form one chain of volcanic islands called the Mascarene (Mascarenhas) Islands, after their Portuguese discoverer Mascarenhas. Mauritius is an island country with a total area of 2,040 km^2, consisting of the island of Mauritius itself (1, 845 km^2), Rodriguez Island (107 km^2), and the distant Cargados Carajos shoals and Agalega Islands.

Mauritius Island as can be seen from the map in Figure 13.10$_a$, is situated in the southwest of the Indian Ocean between latitudes 19° 58'and 20° 32'S and longitudes 57° 17'and 57° 46'E. The island has a gently sloping central plateau, five mountain ranges rising up to a maximum of 825 m. The undulating coastal plains are mostly in the east and the north of the island. The Island is of volcanic origin and its geology is the result of old lava flows, intermediate lava flows and younger lava series. The old lava flows have resulted in impermeable formations, whereas the younger formations are relatively permeable in view of the fissures penetrating them.

Tables 3, 9, and 10$_a$, Appendix A, include temperature and rainfall data, respectively, at Agalega (station No. 192), Brandon (station No 222) and Plaisance (station No. 233). The mean annual temperatures at the three stations in their resopective order are 26.5°C, 25.7°C, and 23.4°C. The differences are probably due to the difference in latitude with respect to the Equator as well as the elevation with respect to mean sea level. Agalega is located on 10°26'S (2 m high), Brandon is on 16°27'S (2 m high) and Plaisance on 20°26'S (55 m high). The mean temperature in the warmest months, February and March, are about 1.2° for Agelago and about 3°C for Brandon and Plaisance, all above the annual mean. Similarly, the mean temperature in the coldest months, August and September, are about 1.2° and 3°C below the annual mean, respectively. Besides, the mean monthly temperature varies from 17°C to 22°C on the Central Plateau. The mean annual rainfall over the period 1951-60 on Mauritius Island varies from less than 1,000 mm along the coast to 3,600 on the central and most elevated part of the island. Table 10$_a$, Appendix A, gives the following results for the period 1961-1980:

Location	Mean, mm	Coefficient of variation, %
Agalega (station No. 192)	1,623	23
Brandon (station No. 222)	904	24
Plaisance (station No. 233)	1,784	36

Most rivers rise in the Central Plateau and flow to the ocean. The drainage network consists of 21 main rivers, with catchment areas varying from a minimum of 10.2 km^2 to a maximum of 164 km^2. The map, Figure 13.10$_b$, shows some of these rivers and the corresponding discharge measuring sites. Table 6$_a$, Part I/Appendix B, gives the mean annual discharge, coefficient of variation and the period over which the measurements were taken. The discharge varies from a few litres per second in the dry season to several cubic

meters per second during the wet season. The total discharge brought by those five rivers is $17\ m^3\ s^{-1}$, as a mean over the period 1976-84. The sum of the catchment areas is $344\ km^2$. Assuming the annual rainfall depth as 2.5 m, the corresponding runoff coefficient can be estimated as 62%. This figure is probably the highest for the country, In affition, the results obtained from analyses of surface water samples show that it's quality is very good.

According to information given in UNESCO Report in Hydrology, No. 49 (Falkland, 1991), the groundwater resources of the island are abundant. There are nine groundwater basins where the water table is between 5 and 20 m deep and the quality of their waters is very good too, and no treatment is required. Groundwater is pumped into the mains, and chlorine is added as a precaution. Both groundwater and surface waters are used to satisfy the demands on water for domestic and irrigation purposes. Next to the forests, which are still left uncut, the island has sugar and tea plantations, tropical fruit and greenery.

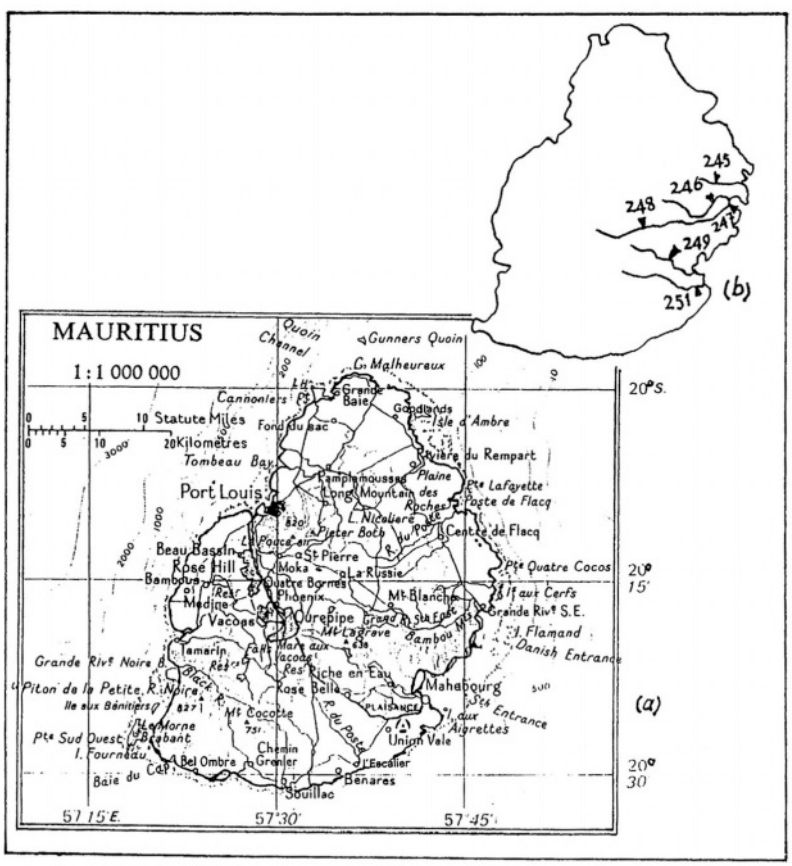

Figure 13.10- Mauritius Island; (a)- location map (from the Times Concise Atlas of the World, 1980); and (b) discharge measuring stations on some rivers (from UNESCO Hydrology Report No. 52, 1995)

13.5.4 Rodriguez Island- This island is situated far northeast of Mauritius Island near latitude 19°45'S and between the longitudinal lines 63°15' and 63° 30'E. The surface area of the island is quite small (104 km^2). The few inhabitants of the island engage themselves in the cultivation of few crops and fishing for their subsistence. There is a limited export of salted fish, animals and crops like chilies and onions.

13.5.5 Réunion (Bourbon) Island- This island is situated in the western Indian Ocean about 175 km southwest of Mauritius Island and 720 km east of Madagascar. The island has the shape of an ellipse with major and minor axes of about 65 and 48 km respectively, bringing its surface area to say 2,510 km^2. Saint Denis, the capital of Réunion, is located in the northern extremity of the island, as can be seen from the map in Figure 13.11.

The island is of volcanic origin and consists mostly of rugged mountains in an advanced state of dissection by short torrential rivers. Compared to Mauritius Island, Réunion is smaller and more mountainous. Volcanoes have developed along the island's northwest-southeast fault. The volcanic activity of the central massif ceased in the Pliocene Epoch some $3*10^6$ to $7*10^6$ years ago. Cones, rising up to 3,000 m, dominate the landscape of the island.

The climatic data available at St. Denis (station 234) show that the annual mean temperature is 23.8°C, and the mean monthly temperature fluctuates between 26.5°C in February and 21.1°C in August. The Southeast Trades, from April to October, augmented by frequent tropical cyclones, cause abundant rainfall. This can reach up to 8,000 mm at the high altitudes in the south and east of the island. Because of the high relief, rainfall totals are much higher than on Mauritius. The north and west parts of Réunion, however, receive as little as 650 mm y^{-1}. The average annual precipitation at Saint Denis over the period 1961-80, as given in Table 10_a, Appendix A, is 1,655 mm, with a variation coefficient of 26%. The average annual rainfall at Saint Pierre, on the southern shore, is 1, 037 mm but for the period 1961-70. It is expected that the mean annual rainfall on the island as a whole is much more than any of these figures.

The economy of the island is based on planting sugar cane and the sugar industry.

13.5.6 Madagascar Island- In contrast to all previous islands of the Atlantic as well as the Indian Ocean, Madagascar is not a small island. In fact, it is the fourth largest island in the world, with a surface area exceeding 587,000 km^2. The island is located in the southeastern Indian Ocean, separated from the coast of the mainland of Africa by the 400-km wide Mozambique Channel. The physical separation of Madagascar from Africa, better to say from the ancient continent of Gondwanaland, seems to have taken place as long ago as the Mesozoic era. (Grove, 1970).

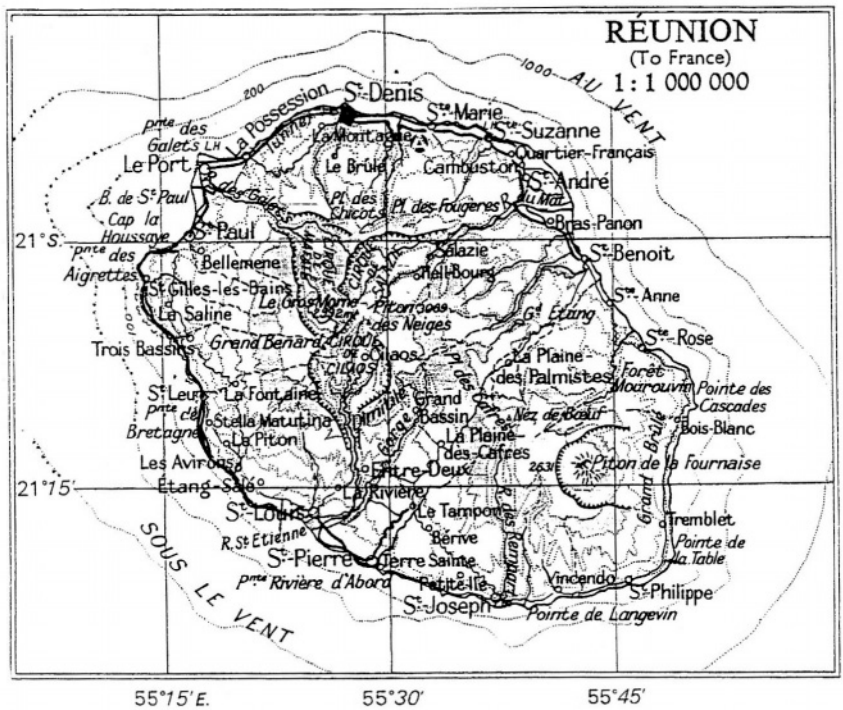

Figure 13.11- Location map of Réunion Island (from the Times Concise Atlas of the World, 1980)

The island, as can be seen from the map in Figure 13.12a, is contained between latitudes 12°S and 26°S and longitudinal lines of 43°E and 51°E. The eastern half of the island consists of a high plateau of ancient crystalline rock, covered locally by volcanic rocks. The crest of the plateau lies nearer to the east than the west, and outcrops of volcanic rock give rise to high ground reaching 2,876 m at Maromokotro. Around the crystalline plateau, sedimentary rocks have been deposited. These sediments are closely related to those of the Tanzania coast, further north. From the crest of the plateau, the ground slopes steeply to the east coast, but to the west the slope is generally milder. The east coast is an almost string of lagoons between the coral beaches and the steep rise island (Stamp and Morgan, 1972).

Meteorological data at ten stations widely spread on the island are listed in Appendix A. Since most stations are located close to the ocean, the range of variation of their annual mean temperatures is rather small, 22.8°C in the south and 26.5°C in the north. The annual mean temperature at Antananarivo or Tananarive (station No. 227) is 17.4°C. The mean temperature of the coldest month (July) is 13.5°C and in the warmest period (January-February) 19.9°C, both at station No. 227. The monthly mean temperature at the stations near the ocean coast fluctuates around their respective annual mean by ± 1° to 3°C.

The total rainfall is very much affected by the location of the point where rainfall is measured. The mean annual rainfall over the period 1931-80 at the mentioned stations varies from a minimum of 384 mm at Tulear (station No. 243) on the southwest coast to a maximum of 3,442 mm at Tamatave (station No. 226) on the northeast coast. The rainfall generally decreases from the eastern slopes and coast, where it is generally 2,500-3,500 mm, to the west and southwest, where the prevailing winds are descending from the plateau and become warm in the process. These winds deposit little rain, 200-400 mm, rendering the south and southwest coasts of the island into arid zones. As a consequence of the significant difference in rainfall amounts between the different parts, four main regions in the island are to be distinguished from west to east. These are: (1) the semi-arid country in the southwest; (2) the western savanna lands; (3) the grassland of the plateaus and highlands; and (4) the humid forest country along the east coast. These regions are indicated on the small map in Figure 13.12_b.

Table 6_a, Part I/Appendix B, gives monthly and annual discharge data for some of the rivers in Madagascar. The locations of these rivers and the discharge measuring stations are shown in Figure 13.12_a. The mean annual yields of the rivers under observation reflect clearly the effects of the location of their catchment areas and the annual precipitation they receive. The specific yields at stations No. 222 in the extreme north and 252 in the east are around 45 and 51 $l\ s^{-1}\ km^{-2}$ respectively, whereas in the southern extremity as represented by station No. 263, it is barely 5 $l\ s^{-1}\ km^{-2}$.

By comparing the above-mentioned yield figures to the corresponding annual rainfall figures, a fair estimate of the annual runoff coefficients of a number of river basins in Madagascar has been obtained. The two central river basins of Betsiboka and Ikopa, the western river basin of Mangoky and the southeastern basin of Mananara show an average runoff coefficient of about 30%. The mid-western river of Tsiribihina and the eastern basin of Mananjary, both yield an annual runoff coefficient of 60%. The river basins in the extreme north, the Mahavary North, and in the extreme south, the Mandrara, yield runoff coefficients of about 85% and 12% respectively.

Assuming that the average annual precipitation is 1,700 mm and the average runoff coefficient over the surface of the island to be 35%, the total surface water must be close to $350*10^9\ m^3\ y^{-1}$. This figure agrees quite well with the $337*10^9\ m^3\ y^{-1}$ representing the annually renewable water resource of the island (FAO Report on Irrigation in Africa, 1995). The same reference mentions that the cultivable area is about 80,000 km^2 or 14% of the total surface area of the country. The area actually under cultivation is 26,000 km^2 or slightly above 4% of the island's area. The principal crops grown in Madagascar are rice, cassava, sorghum, beans and sugar cane, whereas coffee is by far the most valuable export. The water requirement for agriculture has been estimated as $16.14*10^9\ m^3\ y^{-1}$. This amount, according to FAO (1995), seems to be an overestimate.

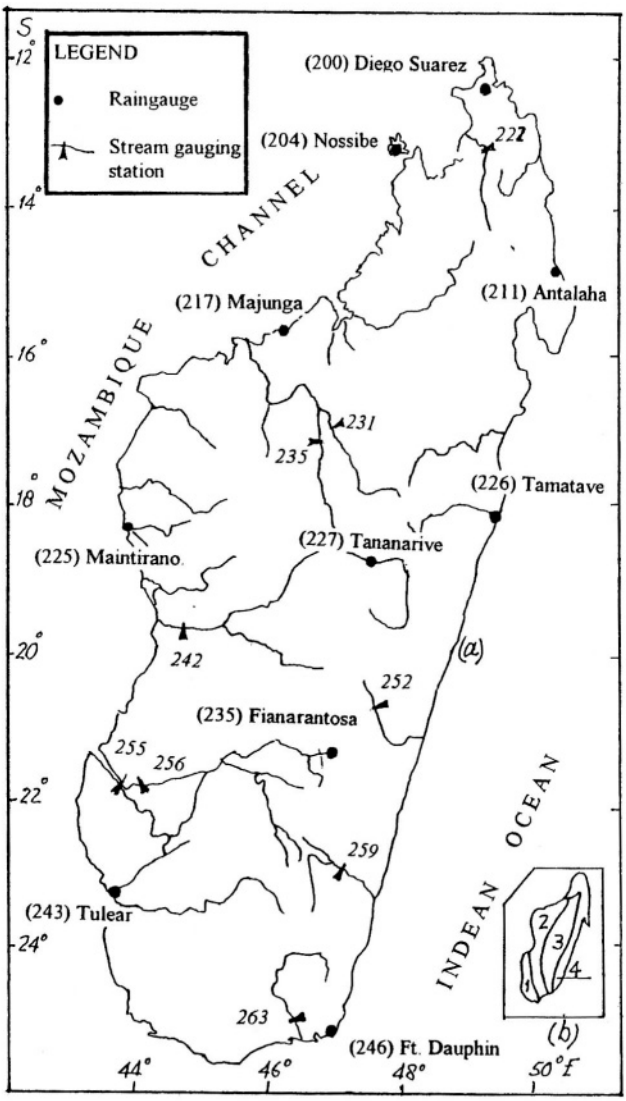

Figure13.12- Map of Madagascar showing the locations of meteorological and discharge measurement stations.

Part of the remaining volume of surface runoff finds its way to the ocean, and another part goes to the underlying aquifers and joins the groundwater body. The eastern half of Madagascar as already mentioned consists of ancient crystalline rocks, covered locally by volcanic rocks. It has been suggested that some parts of the sedimentary coastal basins in the island are rich in groundwater. No information is available about the yield of such basins. However, an estimate of **300 $m^3 h^{-1}$ (83.3 l s^{-1})** has been given by Balek (1977) as a maximum yield.

Chapter 14

WATER RESOURCES AND DEVELOPMENT OF AFRICA

The previous chapters of the book have been dealing with several aspects of climate, topography and relief, soils and vegetal cover, geology and hydrology of the mainland and insular Africa. Obviously, emphasis in most parts of these chapters has been laid on hydrology and water resources. After all, these two areas of interest are what the book is supposed to cover. In attempt to link the development of Africa with water resources development and management, it is important to assess the present situation in Africa, the effects of water resources development and management projects pending the last century, and finally discussion of what should be done in order to bring Africa to a better level of development.

14.1- Africa at Present

14.1.1 Africa's population and gross national product- The total surface area of the lands and islands of Africa is about $30.65*10^6$ km^2. The details of this figure are given in details in Tables 1.2_a and 1.2_b respectively. Despite the ongoing of losses and wastes, by internal and external powers, Africa is still rich in natural resources and in development potential. It is certain that both control of water and efficient transport are the solid foundation for all development in Africa. Water is a precious natural resource. It is an indispensable commodity; every living creature needs water for its survival. Man needs water to drink, and for domestic purposes, irrigation of arable land, hydropower development for industrial and domestic purposes, navigation and fishing.

Before dwelling upon the broad outlines of water resources and their role in the development of Africa, it might be of interest to throw some light on the population of Africa and its growth over time. After all, it is the inhabitants themselves who are the water users and consumers. Furthermore, the extent of management and efficient use of water resources in a certain country is, to some degree, reflected in the state of wealth or poverty of that country.

The estimates of population of Africa for 1990 and 1994, as given in Table 1.6, are close to $632*10^6$ and $707*10^6$ inhabitants respectively. The available statistics show that the growth rate of population in certain parts of continent is still above 3%. Assuming, at best, that the population growth rate will continue at medium rate of 2.5% in the coming two decades or so, the population of Africa will then reach $1{,}040*10^6$ and $1{,}492*10^6$ inhabitants by the years 2010

and 2025 respectively. It is with great pleasure to note that the last decades are experiencing a significant fall in the mortality rate among the children in the under 5-year-old age group. These statistics lead to the conclusion that while the mortality rate among children needs to be further reduced, the net growth rate of the population in many parts of Africa needs strict control.

Africa is poor and according to some authorities in world economy is getting poorer. This statement is true, at least for the larger part of the continent. Most Africans living in the rural areas are working in agriculture, forestry and fishery. The percentage of Africans, men and women, working in these sectors to the total working force fell from 74% in 1972 to 63% in 1990. The corresponding world figures then were 55 and 47% respectively.

The parameter known as Gross National Production (GNP) or Gross Domestic Production (GDP), expressed in $ US per capita per year, is used as an indicator to the wealth or poverty of a certain country. The $ US is generally accepted as a reference currency for the purpose of standardization and ease of comparison between countries and periods of time. The 1990 World Development Report (the World Bank, 1990) estimated the GNP of Tropical Africa in 1988 as $ US 330 per capita per year. This figure is nearly twice as much as the GNP for a number of countries in East Africa, e.g. Ethiopia, Djibouti and Somalia, and in Southern Africa, e.g. Malawi and Mozambique. These countries by far are amongst the poorest countries all over the world. Many African countries appear in the list of "low-income" economies prepared by the World Bank, and the rest appear under the title "lower middle-income" economies. Only South Africa, Nigeria, Egypt, Morocco and the Ivory Coast have GNP's large enough to get them on a list of the world's 100 largest economies (Griffiths, 1984).

14.1.2 Agriculture, forestry, fishing and food- The area of cultivated land in Africa at the end of the 1980s was 1,433,485 km^2 or 4.6% of the total surface area of the continent and the islands. According to the FAO report on irrigation in Africa (1995), the area that is actually under cultivation does not represent except 22.7% of the potential cultivable area. Furthermore, the yield of the cultivated area is not always at the high level, as there are always problems related to land drainage, quality of seeds, pesticides, and fertilizers, not to mention the fluctuation of climate from year to year.

Quite often the sizes of the land holdings are so small that modern, mechanized farming is limited to large land ownerships only. Farming on a small-scale is done following traditional practices. In fact, it is not all bad as traditional cultivation and land irrigation are both labour-intensive. The price of tropical and equatorial fruits and crops like coffee, tea, cocoa, cotton, etc. is dictated to the farmers by the world market in which the African farmers themselves have no say. The same situation applies to the prices of the different kinds of wood. Financing a large irrigation or land development scheme is often

beyond the means of the country in which the scheme has to be implemented. Bank loans are not easy to obtain and often means foreign interference in the policy of the land in question. According to O'Connor (1991), " political strife may remain just as intense as ever, and the richer countries of the world will probably remain just as mean and self-centred as ever". Besides, the costs of irrigation projects are increasing steadily and high revenues are not always guaranteed.

The World Resources Report 1994-95 estimated the cropland in Africa for 1991 as $181.62*10^6$ ha ($1.8162*10^6$ km^2), which represents just 6% of the world total. Since the population of Africa ranges between 11% and 12% of the world's population, the share per African capita in the cropland is almost 50% of the world share per capita. In this context, cropland refers to land under temporary and permanent crops, temporary meadows, market and kitchen gardens, and temporary fallow.

The average production of cereals over the period 1990-92 was estimated as $90.225*10^6$ m t or 4.68% of the world production. This figure is about 22% higher than the average for the period 1980-82. Furthermore, the average yield, which was 1,168 kg ha^{-1}, represented 42.4% of the world yield then. The yield of roots and tubers for the same period was 7,441 kg ha^{-1} or 61% of the world average (12,197 kg ha^{-1}). The grain fed to livestock as percentage of total grain consumption increased from 5 in 1972 to 16 in 1982.

It is remarkable that the area of irrigated land, as percentage of the cropped land remained unchanged, 6%, during the observation period from 1979 to 1991. Assuming that the index of agricultural production in the years 1979-81 was 100%, the average for the period 1990-92 rose to 128% while the index per capita declined from 99% to 93% for the periods 1980-82 and 1990-92 respectively.

The available figures on irrigation potential cannot be totaled due to possible double counting of shared water resources. Despite this constraint, the total can be roughly estimated as $500*10^3$ km^2. The ten countries with the highest irrigation potential are: Angola, Sudan, Egypt, Zaïre, Ethiopia, Mozambique, Nigeria, Ghana, Central African Republic, and Mauritania.

The 1994-95 Report on World Resources estimates the total extent of forests in continental and insular Africa in 1990 as $527.6*10^6$ ha ($5.276*10^6$ km^2). This extent is subdivided into rainforest (16.38%), moist deciduous (47.64%), dry deciduous (17.54%), hill and montane (6.68%), very dry (11.12%), and desert (0.64%). Based on the studies reported by FAO (1993), Africa has lost in the decade 1981-90, on the average, 0.7% y^{-1} of this extent. Of the $3.7*10^6$ ha annual total loss, $470*10^3$ ha were from the rainforest alone, mainly from Zaïre, Cameroon and Gabon. The Sudan has been losing each year a total area of $0.38*10^6$ ha (3,800 km^2) of its moist deciduous, dry deciduous forest and very dry forests. As a result of this loss, the average annual net trade in roundwood dropped from $5.286*10^6$ m^3 for the period 1979-1981 to $4.098*10^6$ m^3 for the

period 1989-91, i.e. about 23%. Evidence from West Africa suggests that forest degradation and fragmentation may play a more important role than outright conversion of forestland to other uses in the loss of wooded habitat. In Africa, forest conversion from 1981 to 1990 accounted for only about one fourth of the changes in forest cover (FAO Report 1993).

Despite its high protein content and importance for many Africans, especially those living in forest areas, fish still constitutes a small part of their diet. African sea fisheries have not been fully exploited by traditional methods. However, fishing along the coast extending from Morocco south to Sénégal and along southwest Africa has recently attracted the attention of commercial companies. These companies use well-equipped fishing boats and up-to-date techniques. Some of the fish caught is consumed in the interior, but most of it is exported to countries outside Africa in the form of canned fish and seafood, as well as oil. Fishing extends to natural lakes, reservoirs, rivers and swamps. According to Grove (1970), fish farms have been since 1946 established in several African countries, especially in the Congo.

Assuming that the index of food production in the period 1979-81 was 100%, the index rose from 102% in the years 1980-82 to 129% in the period 1990-92. The index of food production per capita for those two periods fell from 99% to 94%, respectively. From all these figures, it is clear that the rise in agricultural and food production has been overweighed by the growth of population and that the share per capita declined by 5 to 6% in the 10-y period of observation. These results show beyond doubt the urgent need to exercise all acceptable measures for suppressing the population rate of growth to the extent that allows the rates of agricultural and food productions to exceed it (World Resources 1994-1995).

14.1.3 Water resources- Water is an indispensable commodity; every living creature needs water for its survival. Man needs water to drink, as well as for domestic purposes, the irrigation of arable land to grow crops, hydropower development, industry, navigation, and fishing. In simple words, there is no life without water. It is customary to express the availability of water resources in a certain area by the annual share in cubic metres per capita or in litres per day per capita. As such, a thorough knowledge of the number of inhabitants or water consumers in that area and its change over time are unavoidable to assess this share properly.

Hyper-arid and arid zones, including, desert areas, cover almost one third of the Continent's surface. The climate of the remaining two-thirds ranges from semi-arid to Equatorial rainforest. This brings the average precipitation depth in the continent together with its islands to $701\ mm\ y^{-1}$, or a total volume of $21.2*10^{12}\ m^3\ y^{-1}$. The sum of actual evaporation and evapotranspiration is estimated as 78.9% of the precipitation. The remaining $148\ mm\ y^{-1}$ ($4.5*10^{12}\ m^3\ y^{-1}$) flows as runoff. Part of this amount, infiltrates through the soil and

reaches the water-bearing formations. In this way, it helps recharge the groundwater aquifers. The surface runoff joins the drainage networks, which have been formed some time ago under various geological, geomorphological, relief, and climatic conditions, and developed what is known as river basins. Some of these basins are large, others are medium and the rest are small, judged by their areal extent. Some of these river basins, regardless of their areal extent, are international and others are national. They are also subdivided into perennial and intermittent or ephemeral (wadis), depending on their flow condition. Approximately 48% of the continent is drained into the ocean, 12% of the drainage goes to the internal basins, and the remaining is without surface drainage.

The total annual withdrawal of water for agricultural, industrial and domestic purposes has been estimated as $150*10^9$ m^3. This amount represents only 3.76% of the internal renewable resources. Agriculture alone consumes 85% of the total withdrawn water. According to Balek (1977), the mean annual river discharge is estimated at $105.4*10^3$ m^3 s^{-1} ($3.33*10^{12}$ m^3 y^{-1}) flowing from an actual area of $18.7*10^6$ km^2. One should not forget that one-third of the continent is not contributing any runoff to mention. The remarkable feature of the discharge of most rivers, no matter the annual mean value or size of their respective drainage basins, is its strong seasonality. This state of affairs suggests the need for discharge storage and regulation to adapt the natural supply to the demand on water. Another feature of the stream flow is the low suspended sediment yield. The total annual suspended sediment yield from the continent is estimated close to $1.4*10^9$ t. The annual yield of dissolved matter is as low as $0.76*10^9$ t.

The lakes of Africa contain $36*10^{12}$ m^3 of water, which represents 30% of the world freshwater total. No wonder then that the world of tropical Africa is not dominated by its rivers, but rather by its lakes. The lakes together with other forms of wetlands have already been dealt with in Chapter 10.

Groundwater reservoirs are available in several parts of Africa. The water-bearing formations can be found in fissured and fractured hard rocks, in sedimentary basins and, to a very limited extent, in volcanic deposits. Some of the aquifers are of the water table type; others are confined or semi-confined. The saturated thickness of the aquifer, the depth to water, the yield and recharge of the aquifer varies from one location to location. Nevertheless, they form a huge resource, largely of good quality water. Urban water supply to many cities in Africa comes from groundwater.

The need to reduce the rate of population growth has already been mentioned in the previous section. Without such control, the share per capita in water resources will be reduced drastically from about 5,650 m^3 y^{-1} in 1994 to 3,840 m^3 y^{-1} in 2010, and further to 2,670 m^3 y^{-1} in the year 2025.

The above summary relates to normal conditions. Several parts in West and East Africa have witnessed drought spells, some of which lasted longer than a

decade. On the other hand, there were periods of excessive rainfall, as a result of which lake levels and river flows reached extremely high values. Despite the fact that droughts have been recurring in the Sahel and other parts of Africa for centuries, the current literature in climate and water resources keeps referring to climate change and even to desertification (saharization).

Before embarking upon discussion of the water resources of individual African countries, it is worthwhile to remember that the manner with which the continent has been divided by the former colonizing powers into individual countries can be described, in the least, as irresponsible. This has made some of the countries too rich in water resources and left other countries without any water resources to mention.

The above summary leads to the main conclusion that Africa's water resources need proper management, with sharing of water resources as an essential component.

14.1.4 Water-Related Diseases- In Africa today, more than half of the population lives without safe drinking water and two-thirds lack adequate sanitary means of excreta disposal. During the decade, 1981-90, sub-Saharan Africa witnessed an increase in water supply coverage from 32% to 46%, while sanitation coverage increased from 28% to 36%. Since then, however, progress has come to a halt and more people are without adequate services in Africa today than in 1990. There is a large number of water-related diseases. They are usually classified by the microbe causing them. Table 14.1 classifies infective diseases in relation to water supplies (Bradley, 1978). Besides, some statistics and figures about the results of bacteriological analyses of water samples, and water-related diseases in a number of African countries are included in Tables 6_a, 6_b and 6_c, and Tables 7_a, 7_b and 7_c, all in Part II/Appendix B for illustration.

Sleeping sickness is inevitably fatal unless treated. It exists in sub-Saharan Africa, west and central Africa. Most of the African countries lying between 14° of the Equator, and situated below 1,200 m a.m.s.l., are infested with tsetse-flies of different species. The disease is associated with watercourses, especially at the end of the dry hot season, where man and flies congregate around these courses searching for food and agreeable environment. Eradication of riverine vegetation is likely to increase erosion, increase the loss of water by evaporation and affect the nutrient cycle of the system adversely. Certain drugs have been used to treat the disease in human beings for sometime. More recently preventive inoculation is used for man, and animals like horses, cattle and many domestic animals. Aerial applications of insecticides (e.g. DDT) to riverine forests and savanna woodland drainage lines are helpful in reducing the recorded cases of sleeping sickness. Judging by the past situation of this disease, it is fair to conclude that the infested areas have in a certain way influenced the geographical distribution of population in Africa strongly.

Table 14.1- Classification of infective diseases in relation to water supplies (Bradely, 1978)

Category	Examples	Relevant water improvements
I- Water-borne infections		
(a) Classical	Typhoid, cholera	Microbiological sterlity
(b) Non-classical	Infective hepatitis	Microbiological improvement
II- Water-washed infections		
(a)Skin and eyes	Scabies, trachoma	Greater volume available
(b) Diarrhoeal diseases	Bacillary dysantery	Greater volume available
III- water-based infections		
(a) Penetrating skin	Schistosomiasis	Protection of user
(b) Ingested	Guinea worm	Protection of source
IV- Infections with water-related insect vectors		
(a) Biting near water	Sleeping sickness	Water piped from source
(b) Breeding in water	Yellow fever	Water piped to site of use
V- Infections primarily of defective sanitation	Hookworm	Sanitary faecal disposal

Onchocerciasis, also known as River Blindiness, is a parasitic disease occurring widely in tropical Africa. It is widely spread in wet savanna and forest areas in West Africa. According to Walsh (1985), the foci of the disease occur along all major river valleys, wherever rapids are a prominent feature of the river geomorphology. As such, areas where the Niger, Sénégal river systems flow over the outcropping Pre-Cambrian basement complex provide the ideal environment and ground for breeding the bloodsucking black flies. The disease is transmitted from person to person by the bite of any of these flies. The disease can lead to complete blindness, visual impairment, debility or severe skin damage.

It is strongly recommended to wear trousers, long socks and solid footwear to reduce the man-fly contact. The provision of a domestic water supply, like with many more diseases, discourages the consumers from taking their water directly from the river, thus reduces their contact with the flies causing the disease. The onchocerciasis control campaigns launched in many countries in West Africa include hundreds of flying hours both by helicopter and fixed wing planes, along with the dispensing of many thousands of litres of insecticides. So far, it is believed that onchocerciasis still exists and has serious socio-economic consequences. As such, it is recommended that the control programmes are maintained for a number of years in order to eliminate the disease from at least a large area in West Africa.

Schistosomiasis or Bilharzia is a worm afflicting millions of people living in many river basins in Africa, particularly in western Africa. The presence of blood in urine is a well-known symptom of infection by Bilharzia. Impounds of water in reservoirs, floodplains, isolated seasonal pools and slow-flowing water in irrigation canals are major sources of this parasitic disease. According to Brown and Wright (1985), a dramatic rise in the prevalence of urinary schistosomiasis around Lake Volta occurred within a few years of its formation. Similar findings were observed in relation to the Kainji Reservoir in Nigeria, Lake Kossou in Ivory Coast and in the coastal lagoons in Ghana.

The results obtained from a study on the control of schistosomiasis mansoni in communities living on the Cuando River floodplain of East Caprivi, Namibia were published by Schutte et al. (1995). Although the intervention programme was a 6-y project, the published results were those mainly obtained during the first 3 years of intervention. Treatment with biltricide was conducted at 6-month intervals. It took 3 years for prevalence to decline from > 80% to 20% because of lack of sanitary facilities and piped water supplies and high rates of absenteeism and re-infection.

In general, spatial, epidemiological and ecological information is important for the control of schistosomiasis because all three components of the life cycle (humans, the parasite and snail intermediate hosts) must converge in space and time at suitable water bodies for transmission to occur. Thus, intensity of infection is influenced considerably by the frequency, duration and intensity of human contact with infective water (Kloos, et al., 1998).

Cholera incidence and mortality in sub-Saharan Africa have the highest reported rates in the world. In 1996, Africa reported the largest number of cholera cases in the world, with 108,535 cases, more than three times the number in the rest of the world combined. The multivariate analysis of the cases reported during the outbreak in Kenya, which began in June 1997, showed that risk factors for cholera were drinking water from Lake Victoria or from a stream, use of unsafe water and sharing food with a person with watery diarrhea. Cholera has become an important public health concern in western Kenya, and may become an endemic pathogen in the region (Shapiro et al., 1999).

Amongst the worms living in the intestines of many Africans is the *hookworm.* Improved sanitary facilities and avoiding contact with unsafe water can easily treat the affliction. Another kind of worm, *guinea worm,* is very active in West Africa. The infection, unless treated, causes ulceration of the limbs leading to incapacitation of the body. The current literature on the subject is full of many more water-related diseases like, *malaria, typhoid,* etc. It also provides results of surveys, medical studies, disease control programmes and medical treatment. The effects of these diseases on the ability of the community members to enjoy a healthy and productive life are of much interest to many professionals, especially development planners and water resources specialists.

14.2- Water Resources Development and Management Projects in the 20th century

The aforementioned sub-sections, 14.1.1 thru' 14.1.4, can serve as a platform for asserting the living conditions of the vast majority of the African populations, particularly in rural areas.

i- Africa is poor and very likely getting poorer with time, and the GNP per capita is the lowest among all continents of the world. Realistic development plans must realistically assume that poverty will persist to a large extent.

ii- The share per capita in land under cultivation and food production is at a low level, leaving the majority of people suffering from under-nourishment.

iii- Water-related diseases are infecting a large percentage of the peoples of Africa; nonetheless the rate of population growth is quite high.

While presenting this unpleasant portrait of Africa to the reader, it is worthwhile to mention that some of the prevailing problems, such as the expansive growth of population, are not connected to water resources in the least. This particular problem is simply the resultant of cultural, social, economic and medical factors. Household density has been found to be the only socioeconomic factor significantly associated with skin disease in the rural parts of Tanzania. Reduction of household density is an attainable intervention that could reduce the prevalence of skin diseases in rural African populations (Gibbs, 1996). Another striking example is that transmission by hands has been found to be the most important mode of dysentery infections in several parts of Rwanda, Burundi, Zaire, etc. This finding suggests that community-based interventions aimed at interrupting faecal-oral transmission by increased hand washing with soap and water, particularly after defecation and before food preparation, may be effective measures for controlling dysentery epidemics in Africa (Birmingham et al., 1997).

The present state of development of Africa, in all fairness, would have been much worse without the implementation of a wide range of water resources development and management projects, especially in the 20th century. In Chapter 11 the characteristics as well as functions of ten of the largest dams in Africa have been outlined. The ten dams described were the High Aswan Dam, Egypt; Roseires, the Sudan; Owen Falls, Uganda; Manantali, Mali; Akosombo, Ghana; Kainji, Nigeria; Inga, Zaïre; Kariba, Zimbabwe; Cabora Bassa,; and Gariep, South Africa. Most of the discussion that will follow relies to a considerable extent on water resources development and management works including these storage works.

14.2.1 River flow regulation for land irrigation- The present state of development of Africa would have been much worse without the

implementation of a wide range of water resources development and management projects, especially in the 20^{th} century.

i- Irrigation in Egypt- Up to the beginning of the twentieth century the amount of water that could be used for irrigating the summer crops in Egypt was almost limited to the natural supply of the Main Nile. Such an amount in a low-flow year was hardly sufficient for irrigating $1.5*10^6$ acres ($6{,}300\ km^2$). The construction of the Old Aswan Dam (1898-1900), its heightening twice (1912 and 1934), the Grand Barrages on the Nile in Egypt, and the Jebel Aulia Dam on the White Nile in the Sudan for the benefit of Egypt (1937) helped to convert land cultivation from seasonal to more frequent cropping per year. These storage and control works have brought the area under cultivation by the end of 1940s to $6*10^6$ acres ($25{,}200\ km^2$) and increased the frequency of land cropping significantly. The construction of the High Aswan Dam in the 1960s helped further to increase the area actually under cultivation to more than $8*10^6$ acres ($>33{,}600\ km^2$).

ii- Irrigation in the Sudan- The greater part of the Central Sudan, which covers the country between the White and Blue Niles and continues eastwards to the foothills of Ethiopia, is a clay plain. The idea of irrigating a considerable area of the Gezira, the country in the angle formed by the two Niles had been suggested as early as 1904 (Hurst, 1952). The construction of the Sennar (Makwar) Dam on the Blue Nile was completed in 1925 and irrigation of the Gezira began in the same year. This dam serves two purposes: it allows the level of the Blue Nile to be raised so that water can flow into the main Gezira canal, and it also stores the water above this level, which is used later when the natural flow of the river must be passed to Egypt. The Gezira area responded marvelously to irrigation, and around the beginning of the 1950s, the total irrigated area became as much as $1.0*10^6$ acres ($4,\ 200\ km^2$). More than half of this area is growing irrigated Gezira cotton, which is the chief means of earning foreign currency for the Sudan.

iii- Irrigation in South Africa- About 60% of the land in South Africa receives normally less than $500\ mm\ y^{-1}$, and it is estimated that only 8% of the rainfall reaches the Orange River. Of this, half is lost through floods and evaporation. The Orange River flows through the semi-desert covering the central part of the country. Despite the growing demand for water, the river used to carry annually an amount of $6.5*10^9\ m^3$ to the sea. The Orange, as explained earlier, is a wild and unpredictable river, rendering the pattern of its flood highly variable. The so-called Orange River Project (ORP) entailed the construction of the Gariep (formerly H. Verwoerd) Dam, the Orange-Fish tunnel, the P.K. Le Roux Dam and its canal system, as well as other water resources development projects.

Thousands of hectares of fertile land are situated along the banks of the river. These areas, for about four decades, have depended totally on the river water for irrigation and no longer affected by droughts or scarcity of water. The purpose

of the Orange-Fish tunnel is the inter-basin transfer of water from the Orange to the Fish River Valley in the east of South Africa. It is an 82.5 km long tunnel and has a lined diameter of 5.35 m, carrying a maximum discharge of $57\ m^3\ s^{-1}$. The P. K. Le Roux Dam, in addition to its other functions of storing and releasing water to the Lower Orange River, diverts water to a network of irrigation canals on both banks of the river. As in the case of the ORP, the Tugela-Vaal (TV) scheme is a major example of a multi-purpose, inter-regional project in Southern Africa.

Generally, it can be stated that the Republic of South Africa is covered with a large number of large, medium and small dams. The majority of these water storage and regulation works serve, among other purposes, to secure water for land irrigation, making South Africa a leading African nation in agriculture. The 1990 statistics show that $123.56*10^3\ km^2$ are already under intensive cultivation. This area represents 10.12% of the total area of the country, $1{,}221*10^3\ km^2$, and 212% of the overall average for Africa. The average production of cereals in 1990-92 was $1{,}568\ kg\ ha^{-1}$ or 135.6% the overall average for Africa, and of roots and tubers $15{,}026\ kg\ ha^{-1}$ or 202% the average for Africa.

14.2.2 Management of river flow for hydropower development- All reservoirs formed by the ten dams, mentioned earlier, and many more dams also in Africa are basically multi-purpose reservoirs. Hydropower development is one of the purposes underlying their construction. Hydroelectric power generation is linked to economic and social development, and the demand for power keeps increasing. This used to be the case in the 1950s and the 1960s. In those years, the rate of growth of energy consumption was in the order of 25% per year. In the subsequent decades, as the internal disputes began to affect the development in many countries adversely, the growth rate retreated to less than 5%.

The available statistics show that the installed capacity of the hydropower plants associated with those ten dams is 8,125 MW, of which 50%, at best, is actually used for generating power. The sum of the already installed capacities of Inga I and II on the Zaïre River is 1,400 MW. This figure is just 3.6% of the potential of this river, 39,000 MW, and 2.32% of the hydropower potential of the Zaïre and all other rivers in the Congo Republic. Next to these figures, it is worthwhile to add that there are many more dams of various sizes and power production capacities. In the Ivory Coast, as an example, the Kossou Dam on the Bandama River (completed in 1972) has been followed by the Taabo Dam (210 MW) on the same river and the Buyo Dam on the Sassandra River (165 MW). The Kafue Gorge hydropower plant (completed 1972) in Zambia, with an installed capacity of 600 MW, is another example.

The hydropower developed from a certain dam can be shared between a number of countries. Part of the power developed from the Owen Falls Dam, Uganda, is consumed locally and the rest is transmitted to Nairobi to be sold to Kenya. Likewise, the energy developed from the Akosombo Reservoir, Ghana,

is used within Ghana itself, basically for the aluminum industry, and the rest is sold to neighbouring Benin and Togo. Industry is the major consumer of the hydropower developed from storage dams. The power generated by the Aswan High Dam is largely used for producing fertilizers (ammonia). The production is partly used for fertilizing the agricultural lands that have lost the natural nourishment due to silt deposition in the reservoir. The rest of the production is sold in foreign markets. The Volta Aluminum Company (VALCO) is probably the largest power consumer in Ghana.

Some of the environmental impacts of dam construction have been reviewed in Chapter 11, and some others will follow in this section. Despite their adverse effects, building more dams for developing more hydropower seems to be as yet the most attractive solution.

14.2.3 River flow regulation and flood protection- One of the purposes of having a reservoir formed by dam construction is to be able to regulate the river flow downstream the dam. This is quite obvious since the flow of most African rivers is highly seasonal.

Before the completion of the Aswan High Dam in 1968, the Main Nile in Egypt used to have a high flood once every 7 or 8 years. The floods of 1938, 1946, 1954 and 1962 were notably high. Many acres of land as well as river islands were flooded, and certain reaches of the river embankment washed out by floodwater causing deaths and loss of property. Since 1968, all floods are stored in the reservoir and the outflow regulated.

Likewise, the floods of the Limpopo River have been largely controlled after building a 70 m dam, which also provides water for irrigation. The Kariba Dam was built essentially for generating hydropower, which is shared between Zambia and Zimbabwe. The reservoir also insures some control over the Zambizi floods. The same can be said about the effect of the Diamma and Manantali Dams on the hydrologic regime of the Sénégal River.

14.2.4 Effect of storage reservoirs on fish- Reservoirs, as relatively large bodies of water, provide a fish-breeding facility. Damming off a river leads to the transformation of shallow flowing water into a deep body of still water. The resulting change in the ecosystem causes the original fish, which used to live in the river, to migrate downstream searching for a suitable environment. The change in water characteristics like temperature, salinity, chemical composition, turbidity, etc renders the catch too small compared to the catch in the pre-dam condition. In the case of the Kariba, for instance, the total catch became six times smaller in two years time. It is possible, however, to use the shallow parts of the reservoir for breeding new fish species, such as in the Volta Reservoir, Ghana, and the High Aswan Dam, Egypt, and many more dams in the world. It is also important to breed fish species which appeal to the taste of the consumer. Transporting the fish to the markets of consumption is another vital matter.

14.2.5 Impacts of storage reservoirs on the upstream and downstream of rivers- As a result of the retention of water, the suspended sediments carried by the river traversing the reservoir fall down and begin to accumulate, unless flushed away completely. With more accumulation of sediments in the reservoir, a delta begins to form in the upstream behind the dam itself. This process has been discussed in Chapter 11. In addition, the upstream water level rises as a result of retaining the floodwater and a backwater curve is formed. The length of this curve can be hundreds of kilometers long depending on the hydraulic characteristics of the river and storage reservoir. The population used to live along the river shore has to shifted elsewhere and live in a different environment.

Agricultural land, after the construction of a reservoir entrapping the suspended sediment load carried by the inflow water, no longer benefits from sediment-laden irrigation water as in the pre-reservoir time. The entrapped sediments used to serve as a natural fertilizer to the land, and unless replaced by artificial amendments the soil fertility deteriorates. The relatively clear water flowing out of the dam is likely to erode the downstream reach of the river in attempt to regain its original sediment charge. This process results in a gradual degradation of the downstream river channel, which eventually becomes weak and unable to carry the same discharge as in the pre-reservoir time.

A few years after the construction of the Aswan High Dam, it appeared that the safe discharge that can be carried by the Main Nile in Egypt below the dam is limited by $300*10^6$ m^3 d^{-1} compared to $1{,}000*10^6$ m^3 d^{-1} in the pre-dam period. Additionally, the degradation of the river channel has adversely affected the foundation of some of the Grand Barrages on the river.

14.2.6 Impacts of large-scale river management schemes on water-related diseases- Observations have indicated that large reservoirs like the Akosombo, Ghana; Kainji, Nigeria; Kussou, Ivory Coast; etc. were largely effective in eliminating the breeding of the fly causing the onchocerciasis. Apart from flooding the breeding sites, dam construction may greatly modify the breeding the fly in the downstream reach for a long stretch of the river.

However, the building of dams is not always an advantage from the point of view of control of vector disease, including onchocerciasis. This is often the case with small dams and barrages. Impoundment of water in reservoirs and irrigation canals is a major source of the parasitic disease of schistosomiasis.

14.2.7 Social impacts of reservoir construction- Resettlement of the inhabitants who used to live along the river shores upstream from a dam site is one of the common problems associated with building reservoirs, especially large ones.
In Africa, resettlement projects, which should be prepared before the start of construction work, are realized in a hurry at the last moment and without giving due thought to sociological aspects. The people are shifted a distance of several

kilometers to a strange country, where adaptation to new conditions can be extremely difficult. One should never forget that it is likely to be too difficult to find suitable jobs for the re-settled population.

According to Balek (1977) this happened during the construction of the Kariba Dam to the tribes who had been living in the fertile river valley for many years. Additionally, some of the rural population leaves for the big towns and becomes a burden on the inhabitants there. Similar situations have developed after the construction of the Akosombo and the Kainji dams, in Ghana and Nigeria respectively. In the case of the High Aswan Dam in Egypt, the Nubians who used to live in Aswan Province next to the dam site were moved hundreds of kilometers south to areas where the climate is quite different from what they used to have. Despite the material compensation, many of the re-settlers always felt uncomfortable.

14.3- Future Development and Management of Water Resources

Water resource development is an action that uses the water resources of a certain region to meet the demands of people and industry for water of adequate quantity and quality, to protect people from the hazards of floods and droughts, and to safeguard people and nature from pollutants (Plate, 1993). Implementation of such an action needs time and know-how to collect the necessary data, the political urge to plan, construct and operate water resource development projects in a sustainable way. Sufficient finances are unavoidable to carry out all needed steps carefully. Last, but not least, all side effects should be thoroughly observed, and effective measures taken to eliminate them, or at least suppress the harm they inflict.

According to Biswas & Biswas (1976), " no doubt that the primary effects of the vast majority of dams around the world have been beneficial. Equally, however, there is no doubt that many of these dams have contributed to unanticipated secondary effects, many of which could have been eliminated by a proper planning process". One can conservatively say that until a more favourable solution can be found, having more dams will remain the gateway to development. Ancillary structures such as power plants, turbines, fish ladders, navigation sluices and lock chambers, river embankments, harbours for inland navigation, irrigation and drainage canals, etc. are equally necessary.

14.3.1 Combating water-related diseases- This measure, as reported earlier, will increase the working capacity, especially in rural communities. In 1925, the inspector general of public health for Cairo, Egypt, estimated the annual loss in the national income then by some 4 million Egyptian pounds due to the poor health condition of many Egyptian farmers as a result of bilharzia infection alone. This amount at present, considering the increase of the number of infected farmers, is no less than one billion US $. The economic benefits of

tsetse eradication in terms of an increase in production and in economic return on investment have recently been stressed. It must however be emphasized that it is necessary to adopt long-term programmes with eradication as the objective, for control is likely to be a continuing commitment which may not necessarily be economic. However, vaccines to prevent some of the vector-borne diseases as malaria, schitosomiasis and yellow fever, or drugs to treat them are not always available. The reason, in a small part, is that disease organisms are formidable adversaries, and, in a larger part, they are not on the priority list of the large pharmaceutical companies. The same can be said about other diseases.

Environmental interventions to contain the insects that transmit disease can occur at a range of levels, such as household, community, or region. Improvements in and around home, and application of private and public hygiene standards can make a tremendous difference in controlling vector populations and reducing the incidence of infectious diseases.

14.3.2 Sharing water resources- Water sharing within one country or between a number of countries in a certain region is a vital issue. This is true, especially when certain parts of a region are arid or frequently stricken by droughts.

It has already been described in an earlier part of this book that rainfall generally increases from the northern and southern extremities of the continent towards the Equator. River basins, which are approximately rectangular in form with the longer side along the north-south or south-north direction, have wet parts near the Equator and dry parts farther from it. Typical examples are the Chad and Nile basins. In other cases, the major variation takes place from east to west, as in the coastal strip of southwest Africa and in Madagascar. Substantial difference in elevation also causes a pronounced variation in rainfall within the same basin. The Tana and Blue Nile Basins are typical examples.

As early as 1942, it became clear that the only solution to the problems encountered with irrigation in the Eastern Cape Province of South Africa would be the importation of water from the Orange River. An 83-km long tunnel draws off water from the Orange and transfers it to the Fish River, where it serves the fertile areas in the Fish Valley. The tunnel became operational in 1975. This is an example of transfer of water within the same country.

In Africa, there is a growing tendency among riparian countries sharing a river basin to exercise cooperation between themselves. The Chad Basin Commission was established in 1964. This commission comprises Chad, Niger, Nigeria and Cameroon. The recommendations of the Master Plan for the development and environmentally sound management of the resources of the conventional Lake Chad Basin includes 15 articles. One of the recommendations is: “To promote multi-purpose and integrated projects”. Another important article is: “ Develop a preparedness scheme for the basin that would combine irrigated agriculture, food storage at all levels and the

mobilization of national funds for supplementary investments in case of crop failures".

Two organizations were established in the 1970s to direct the resources of the Sénégal and Gambia River Basins to the economic development of the populations sharing these basins. The organization known as the Organization pour la Mise en Valeur du Fleuve Sénégal (OMVS) is comprised of Sénégal, Mali and Mauritania, whereas the second organization, known as the Organization pour la Mise en Valeur du Fleuve Gambie (OMVG), comprises the Sénégal and the Gambia. Likewise, the countries sharing the Nile Basin are members of the Permanent Technical Joint Committee of the Nile water.

The last example worth mentioning here is the group of countries known as Southern African Development Community (SADC). This group comprises Angola, Botswana, Lesotho, Malawi, Mozambique, Namibia, South Africa, Swaziland, Tanzania, Zambia and Zimbabwe. These eleven riparian countries share a total area of $3.32*10^6$ km^2 divided between the basins of the Incomati, Limpopo, Okavango, Orange and Zambezi Rivers. The policies and strategies for the management of the Zambezi and the other rivers, as emerging from the aspiration of SADC, are supposed to converge towards economic integration with joint and cross border water resources investments between or among the riparian countries. Again, irrigation, hydropower generation and flood control are on the top of the priority list of development projects. One of the striking comments about the situation in Mozambique is that "there are a few large reservoirs in the country to allow regulation of flows, which show sharp variations not only through the year but also from year to year, as is the characteristic of the rivers in these regions" (Dutch Ministry of Foreign Affairs, 1998).

14.3.3 Water management for irrigation- The potential for irrigation in West Africa is enormous, but the proportion of the land irrigated is still small. In 1965, 0.7% of the annually cropped area, was irrigated. The area under irrigation in some countries increased rapidly after that time to reach 7% in Gambia, 10% in Mali, 3% in Nigeria, 8% in Senegal and 5% in Sierra Leone, all by 1990. The countries in southwestern Africa also need to expand their irrigated areas.

Improved irrigation efficiency means higher crop yield per unit of water. Modern irrigation methods can help in this respect, though the chance is limited. The lack of skilled irrigators and equipment such as that required for sprinkler irrigation, as well as the small size of holdings are among the obstacles.

Intermittent streams (wadis) receive plenty of water during and shortly after intense rainstorms. Most of this water is lost, especially by evaporation. Small check dams are built at suitable sections across such streams to reduce the losses by retaining the floodwater till it infiltrates through the sides and beds, and eventually join the underlying groundwater. Groundwater is used in many

countries for domestic water supply. The last decades are witnessing a steady increase in the use of groundwater for irrigation. Examples can be found in Egypt, Sudan, Libya, Kenya, Botswana, etc. This has been discussed in details in Chapter 12.

14.3.4 Water management for hydropower development- Despite the large number of dams already built in Africa for generating hydropower, what is currently generated represents a small fraction of the hydroelectric potential. According to Balek (1977), those parts of Africa with 1,500 mm annual rainfall and which are located at more than 300 m a.m.s.l. are the most favourable for major schemes.

The estimated power to be generated from the gigantic scheme known as Inga III (Grand Inga) in Congo is 39,000 MW, to be generated by 52 units each 750 MW. This alone is about two times the hydropower presently generated in all Africa. Exporting a considerable proportion of this energy to countries outside Africa will be a considerable investment.

The topography and relief of the terrain in Ethiopia added to the precipitation on its highland render its hydropower potential quite high. Unfortunately, so far there is hardly anything being done about that. The major work in operation is the Koka Dam on the River Awash, with installed capacity of 46 MW. Actually, the operation policy of this reservoir has never been successful due to the conflict of interest between generating the maximum power, availability of water for irrigation, and sediment control of the reservoir (Imru, 1992).

At present there are some 4,500 MW of electricity generated from installed power plants at Kariba, Cabora Bassa, Victoria Falls, Kafue Gorge, and the Lunsefwa and Shire Rivers, all in Southern Africa. The remaining potential of the Zambezi proper, which is not developed, is estimated as 11,000 MW. It is also expected to increase hydropower generating capacity of the Cabora Bassa to 4,000 MW. The future power, upon utilizing the existing potentials, will be not less than five times the present hydropower capacity.

14.3.5 River (inland) navigation as a means of development- It has been repeatedly mentioned that water resource management and adequate transport facilities are unavoidable for Africa's development. Improved river navigation requires management of river levels and discharges. With proper management navigation can provide adequate transport of passengers and goods. The present state of inland or river navigation in many parts of Africa is not satisfactory. This, however, does not eliminate the fact that river navigation in certain areas is the only means of transport, whether for passengers or cargo. Nevertheless, a lot more has to be done, and any ambitious plan aimed at the overall development of Africa must include the upgrading of river navigability.

Shallow depth of water, obstruction of river waterways by man-made dams and barrages, and naturally by falls, rapids and cataracts are the main factors

causing inefficient river navigability. The cost of dredging the shallow parts to an appropriate depth is likely to be compensated in a short time by the revenue from increased passenger and cargo transport. Furthermore, difficulties in navigation imposed by natural barriers such as rapids and falls, as well as man-made reservoirs can be overcome by digging navigable channels and/or ship lifts whenever feasible.

Most of the great African Rivers discharge their waters into the sea or ocean. The hydraulic and geomorphologic conditions of both the ocean and river at the mouth of a certain river affect the extent of connection between the ocean and the interior. Sandbars, shifting sands and wind surfs are among such conditions.

Some examples illustrating the present state of navigability in a number of rivers are as follows:

- Navigation in the Nile between the Sudan and Egypt is interrupted by six cataracts obstructing the river channel between Khartoum and Aswan (1,885 km). The Old Aswan Dam, built between 1898 and 1900, created a maximum drop of 32 m between the upstream and downstream sides of the dam. A set of five lock chambers was built within a navigable channel to facilitate navigation. The White Nile is navigable for some 150 km above Khartoum, and about 300 km of the Blue Nile are navigable too. The rapids, falls and swamps limit the navigability of the rivers in the Upper Nile system.

- The Sénégal River is navigable from its mouth on the Atlantic Ocean up to a distance of 800 km, at least for boats up to a certain draft and tonnage. The Saloum and Gambia Rivers together with their tributaries form a network of navigable waterways, though for limited-size boats.

- The Niger River is sometimes but not always navigable up to Jebba, 895 km upstream of the river mouth (see Figure 7.13). The Benue is navigable by shallow-draft vessels. The middle Niger is divided by the rapids at Bamako and Koulikoro into two sections. The gross river system to the east of the Niger River can transport small vessels for 500 km upstream (Balek, 1977).

- The Zaïre (Congo) is navigable from the mouth on the Atlantic Ocean up to a distance of 130 km. The navigable section of the river is divided into five sections. The Zaïre River system, however, has 13,000 km of navigable waterways, of which 3,500 km can be traveled by large barges. The streams south of the Zaïre are navigable from the ocean only for a few weeks each year.

- The traditional navigation services on the Lower Shire and Zambezi were stopped due to security problems and shallow water depths. There are long standing studies to change the current situation and to re-establish navigation services on these rivers.

- Passenger and cargo navigation services are mainly practiced on Lake Malawi, having ports and boat facilities that handle more than 150,000 t and 300,000 persons per year respectively.

The above-listed examples illustrate the current inadequate situation of river navigability in Africa. It is hoped that they, together with similar examples of other rivers, will urge the concerned authorities to prompt the implementation of improved navigation plans for enhancing the overall development of Africa.

REFERENCES

Abdel Warith, M. 1965. Consumptive use and irrigation requirements for cotton plant in Egypt. *M.Sc. Thesis,* Faculty of Engineering, Cairo University, Cairo, Egypt.

Abdulai, B.I. 1989. Evaporation calculations from Lake Sennar (Sudan): a search for a meteorological minimum input approach. *M.Sc.Thesis,* Wageningen Agricultural University, Wageningen, The Netherlands.

Abul-Atta, A. 1978. *Egypt and the Nile after the High Dam* (text in Arabic). Ministry of Public Works and Water Resources, Cairo, Egypt.

Ackermann, E. 1936. Dambos in Northern Rhodesia (Zambia) 1936. *Wiss. Veroff.* Leipzig **4** (1): 149-157.

Adams, B. & R. Kitching 1979. The simulation of transmissivity, storativity and evapotranspiration in a digital model of a fissured dolomite aquifer near Ndola, Zambia. *Hydrol. Sci. Bull.* **24** (4): 487-498.

Afouda, A. 1989. Development of theoretical hydrology in West Africa. In: *Proc. Sahel Forum: The State-of-the-Art of Hydrology and Hydrogeology in the Arid and Semi-arid Areas of Africa,* Ouagadougou, Burkina Faso, pp 1-14.

Aguado, E. 1987. A time-series analysis of the Nile River low flows. *Ann. Assoc. Amer. Geogr.* **72** (1): 109-119.

Ahmad. M.U. 1981. The role of the Sahara in food production. *Wat. Int.* **6**: 126-129.

---------- 1986. Groundwater resources; the key to combat drought in Africa. In*: Proc. Int. Conf. on Water Resources Needs and Planning in Drought- Prone Areas,* Khartoum, the Sudan, Part 1: 47-63.

Akrasi, S. A. & N.B. Ayibotele 1984. An appraisal of sediment transport measurement in Ghanian Rivers. In: *Proc. Harare Symp.*: *Challenges in African hydrology and Water resources. IAHS Publ.* **144**: 301-312.

Alam, M. 1989. Water resources of the Middle East and North Africa with particular reference to deep artesian groundwater resources of the area. *Wat. Int.* **14** (3): 122-127.

Alexandre, J. 1977. Le bilan de l'eau dans le miombo (forêt claire tropicale). *Bull. Soc. Géo. Liège,* **13** (Ann. 13): 107-126.

Ali, Y.A.M. 1990. Simulation and optimization of the Blue Nile double reservoir system. *M.Sc. Thesis,* Int. Inst. for Infrastruc., Hydr. and Env. Eng. (IHE), Delft, The Netherlands. .

Allen, R.G. & W.O. Pruitt 1991. FAO-24 reference evapotranspiration factors. *J. Irr Dr. Div., ASCE,* **117** (IR 5): 758-773.

Allen, R.G., M. Smith, A. Perrier & L.S. Pereira 1994. An update for the definition of reference evapotranspiration. *ICID Bull.* **43**: 1-92.

Allen, R.G., L.S. Pereira, D. Raes & M. Smith 1998. Crop evapotranspiration guidelines for computing crop water requirements. *FAO Irrigation and Drainage Paper* **56**. Food and Agriculture Organization of the United Nations, Rome.

Ambroggi, R.P. 1966. Water under the Sahara. *Sci.Amer.* **214** (5): 22-23.

Ančel, J. & J. Balek 1971. Analysis of periodicity in hydrological sequences. *J. Hydrol.* **14**: 66-82.

Ångström, A. 1924. Solar and atmospheric radiation. *Q. J. R. Meteo. Soc.* **50** (210): 121-125.

Anyadike, R.N.C. 1992. Regional variations in fluctuations of seasonal rainfall over Nigeria. *Theo. Appl. Climatol.* **45**: 285-292.

Åse, L.E. 1987. A note on the water budget of Lake Naivasha, Kenya. *Geogr. Ann,* **69** A (3-4): 415-429.

Attia, B., F. El-Shibini & D.P. Carr 1979. Lake Nasser simulation studies. In: *Proc. Int. Conf. on Water Resources Planning in Egypt,* Cairo, Egypt, pp 65-83.

Attia, F.A.R. 1996. Agricultural threats to groundwater, the Egyptian situation. In: *Agricultural Threats to Groundwater Quality.* In: *Proc. of the Zaragoza. Workshop,* Zaragoza, Spain, pp 191-201.

Aubreville, A. et al. 1959. *Vegetation Map of Africa South of the Tropic of Cancer.* Calrendon Press, Oxford.

Ayibotele, N.B. 1984. Problems of African hydrology and water resources. *Lecture notes in River Basin Management (unpublished) to the International Course in Water Resources Management.* Wat. Resour. Res. & Doc. Cen., Perugia, Italy.

Ayoade, J.O. 1976. A preliminary study of the magnitude, frequency and distribution of intense rainfall in Nigeria. *Hydrol. Sc. Bull.* **XXI** (3): 419-429.

Bagnouls, F. & H. Gaussen 1959. Saison sèche et régime xèrothermique. *Ann. de Gèogr.* **66,** Toulouse, France, pp 193-229.

Balek, J. & J. Perry 1973. Hydrology of African headwater swamp. *J. Hydrol.* **19**: 227-249.

Balek, J. 1977. *Hydrology and WaterRresources in Tropical Africa.* Develop. Wat. Sci. **8**, Elsevier Sci. Publ. Co., Amsterdam, Oxford, New York.

---------- 1983. *Hydrology and Water Resources in Tropical Countries.* Develop. Wat. Sci. **18**, Elsevier Sci. Publ. Co., Amsterdam, Oxford, New York.

Balmer, F. & I. Müller 1989. Etude hydrogéologique et géophysique électromagnitique de la nappe alluviale du Kori Teloua, Agadez, Niger. In: *Proc. Sahel Forum*: *The State-of-the-Art of Hydrology and Hydrogeology in the Arid and Semi-arid Areas of Africa,* Ouagadougou, Burkina Faso, pp 426-424.

Bannerman, R. & N. Ayibotele 1984. Some critical issues with monitoring crystalline rock aquifers for groundwater management in rural areas. *IAHS Publ.* **144**: 47-56.

Barratt, J.M. & S. Puyoo 1984. Hydrological analysis using statistical methods in the 1000-borehole Programme in Niger. *BRGM Report* **84**, SGN 309 EAW/AGE, 82 p.

Bartholomew, J.C. (editorial director) 1980. *The Times Concise Atlas of the World* (revised edition). Times Books Ltd., London.

Baumgartner, A. & E. Reichel 1975. *The world Water Balance: Mean Annual Global, Continental and Maritime Precipitation, Evaporation and Runoff.* Elsevier Publ. Co., Amsterdam.

Belaid, M.N. 1995. Seawater intrusion into a Quaternary aquifer wet of Tripoli, Libya. In: *Proc. Int. Conf. on Water Resources Management in Arid Countries,* Muscat, Vol. **2**: 547-552. The Sultanate of Oman.

Bellman, R. 1957. *Dynamic Programming.* Princeton University Press, New Jersey, USA.

Belloum, A. 1993. Hydrologie agricole en Algérie – une double problématique. *Hydrol. Sc. J.* **38** (6): 479-495.

Birmingham, M.E., L.A. Lee, M. Ntakibirora, F. Bizimana & M.S. Deming 1997. A household survey of dysentery in Burundi: implications for the current pandemic in sub-Saharan Africa. *Bull. WHO* **75** (1): 45-53. World Health Organization, Geneva.

Biswas, A.K. & M.R. Biswas 1976. Hydropower and the environment. *Water Power & Dam Construction.* May: 40-43.

Blaney, H.F. & W.D. Criddle 1950 (slightly revised in 1952). Determining water requirements in irrigated areas from climatological and irrigation data. *USDA, SCS Tech. Paper* **96**.

----------1966. Determining consumptive use for water developments. In: *Proc. ASCE (Irr. & Dr. Spec.) Conf.*: *Methods for Eestimating Evapotranspiration,* Las Vegas, USA, pp 1-34.

Boakye, P.G. 1993. Filling gaps in hydrological runoff data series in West Africa. *Ph. D. Thesis,* University of Bochum, Germany.

---------- 2001. Sources of rural water supply in Ghana. *Wat. Int.* **26** (1)*:* 96-103.

Bogardi, J. & K.D.W. Nandalal 1989. Deterministic dynamic programming and its application to reservoir management. In: *Proc. Sem.-Workshop on Conflict Analysis in Reservoir Management* (ed. J. Bogardi). Bangkok, Thailand, pp 59-108.

Bolton, B. 1984. Sediment deposition in major reservoirs in the Zambezi Basin. In: *Proc. Harare Symp.; Challenges in African Hydrology and Water Resources. IAHS Publ.* **144**: 559-567.

Boonyatharokul, W. & W.R. Walker 1979. Evapotranspiration under depleting soil moisture. *J. Irr. Dr. Div. ASCE,* **105** (IR 4): 391-402.

Borchert, G. & S. Kempe 1985: A Zambezi aqueduct. In: *Transport of Carbon and Minerals in Major world Rivers* (eds. E. T. Degens, S. Kempe & R. Herera). Part 3, *Mitt.* Geol.-Paläont. Inst., Universität Hamburg. SCOPE/UNEP **58**: 443-457.

Borzenkova, I.I. 1980. Precipitation fluctuations in the Sahara and neighboring regions in the last 20, 000 years. *Sov. Hydro.: Selected Papers* **19** (2): 120-125.

Bouchet, R.J. 1963. Evapotranspiration réelle et potentielle, signification climatique. *Gen. Assem. Berkley, Intl. Assoc. Sci. Hydrol.* **62**: 134-142.

Bouzaiane, S. & A. Lafforgue 1986. Interpretatiion des données hydrologiques du Bassin de l'Oued Zeroud. *Mono. Hydrolo. des Oudes Zeroud et Merguellil* **III**, Direc. Centr. des Resourc.en Eau/Inst. Français de Rech. Sci. pour le Develop, en Coopération, Ministère de l' Agriculture, Tunisie, pp 474-604.

Bradely, D.J. 1978. Health aspects of water supplies in Tropical Africa. Chapter 1. In: *Water, Wastes and Health in Hot Climates* (eds. R. Feachem, M. McGarry & D. Mara). Wiley Intersci. Publ., Chichester, pp 3-17.

Bredenkamp, D.B. 1999. Recharge: Part of chapter 4 resources assessment. In: *Water Resources of Hard Rock Aquifers in Arid and Semi-arid Zones* (ed. J. W. Lloyd). Studies and Reports in Hydrology **58**: 159-180, UNESCO, Paris.

Brown, D.S. & C.A. Right 1985. Schistosomiasis: Bilharzia. Chapter 11. In: *The Niger and its Neighbours* (ed. A.T. Grove), pp 295-317. A. A. Balkema Publishers, Rotterdam/Boston.

Bruin, H. A.R. de & J.Q. Keijman 1979. The Priestley-Taylor evaporation model applied to a shallow large lake in the Netherlands. *J. Appl. Meteo.* **18**: 898-903.

Brutsaert, W.H. 1982. *Evaporation into the Atmosphere.* D. Reidel Publ. Co., Dordrecht, The Netherlands.

Buckley, D.K. & P. Zeil 1984. The character of fractured rock aquifers in Eastern Botswana. *IAHS Publ.* **184**: 25-36.

Budyko, M.I. 1956. *The Heat Balance of the Earth's Surface* (translated from Russian). U.S.W.B., Washington, DC, USA.

Budyko, M.I. 1986. *The Evolution of the Earth's Biosphere.* D. Reidel Publ. Co., Dordrecht, The Netherlands.

Bullock, A. & A. Gustard 1989. Towards a regional water resource study of arid and semi-arid Africa. In: *Proc. Sahel Forum: The State-of-the-Art of Hydrology and Hydrogeology in the Arid and Semi-arid Areas of Africa,* Ouagadougou, Burkina Faso, pp 118-125.

Bultot, F. 1971. *Atlas climatique du Bassin Congolais.* **1-4**, Inst. Nat. pour l'Etude Agronomique du Congo, Kinshasa.

Bultot, F. & G.L. Dupriéz 1987. Niveaux et débits du fleuve Zaïre à Kinshasa. *Kon. Acad. Overzeese Wetenschap.* **VI**: pp 1-49, Brussels, Belgium.

Bunting, A.H., M.D. Dennet, J. Elston & J. R. Milford 1976. Rainfall trends in West African Sahel. *Q. J. R. Meteo. Soc.* **102**: 59-64.

Bunting, A.H. 1987. Irrigation in Africa's agriculture future. *ICID Bull.* **36**, (2): 12-23.

Burke, J.J. & M. Jones 1993. *Report on the Kafue Basin Action Plan.* New York, USA.

Burman, R. & I.O. Pochop 1994. Evaporation, evapotranspiration and climatic data. Develop. Atm. Sci. **22**, Elsevier; Amsterdam, New York, Tokyo.

Butzer, K.W. 1966. Climatic changes in the arid zones of Africa during early to mid-Holocene times. *Roy Meteo. Soc.*: In: *Proc. World Climate from 8, 000 to 0 BC.* London, UK, pp 72-83.

Calder, I.R., L.R. Hall, H.G. Bastable, H.M. Gunston, O. .Shela, A. Chirwa & K. Robinson 1995. The impact of land use on water resources in sub-Saharan Africa: a modeling study of Lake Malawi. *J. Hydrol.* **170**: 123-135.

Carbonnel, J.P. & P. Hubert 1989. Analyse de la non-stationnarité des series pluviométriques et hydrologiques d'Afrique de l'Ouest. In: *Proc. Sahel Forum: The State-of-the-Art of Hydrology and Hydrogeology in the Arid and Semi-arid Areas of Africa,* Ouagadougou, Burkina Faso, pp 192-201.

Carmouze, J.P. & G. Pedro 1977. Influence du climat sur le type de régulation saline du Lac Tchad: relations avec les modes de sedimentation lacustre. *Strasbourg Sci. Géol. Bull.* **30**: 33-49.

Chengoli, R.W. 1999. Water supply development in Western Province, an overview. *Country Paper of Kenya submitted to the 7th Nile 2002 Conference,* Cairo, Egypt.

Chilton, P.J. & A.K. Smith-Carington 1984. Characteristics of the weathered basement aquifer in Malawi in relation to water supplies. In: *Proc. Harare Symp.*: *Challenges in African Hydrology and Water Resources. IAHS Publ.* **144**: 57-72.

Chow, V.T. 1951. A general formula for hydrologic frequency analysis. *Trans. Amer. Geophs. Un.* **32**: 231-237.

Christiansen, J.E. 1966. Estimating pan evaporation and evapotranspiration from climatic data. In: *Proc. ASCE (Irr. & Dr. Spec.) Conf.*: *Methods for estimating Evapotranspiration,* Las Vegas, USA, pp 193-231.

Club du Sahel 1979. *Development of Irrigated Agriculture in Mali: General Overview and Prospects.* Permanent Interstate Committee for drought Control in the Sahel (CILSS), Niamey, Niger.

Cogels, F.X., A. Coly & A. Niang 1997. Impact of dam construction on the hydrological regime and quality of a Sahelian lake in the River Sénégal Basin. In: *Regulated Rivers: Research and Management* **13**: 27-41.

Combremont, R. 1972. Crop water requirements in Tunisia. *Paper No.* **13**, *Water Use Seminar, Damascus, FAO Irr. & Dr. Div.,* pp 138-141.

Conrad, V. 1946. Usual formulas of continentality and their limits of validity. *Trans. Amer. Geophys. Union* **27**.

Coughanower, C. 1994. Groundwater. *IHP Humid Tropics Programme Series* **8**, UNESCO Publishing, Paris.

Coulter, G.W. & R.H. Spiegel 1991. Hydrodynamics. In: *Lake Tanganyika and its Life* (ed. G.W. Coulter). Oxford University Press, UK, pp 49-75.

COWAR (prepared by Jordan, J., E.J. Plate, E. Prins & J. Veltrop) 1993. Water in our common future: a research agenda for sustainable development of water resources. *Report prepared by the Committee on Water Research (COWAR) to the Int. Hydrol. Progr.* (IMP), UNESCO, Paris.

Crul, C.R. 1997. Limnology and hydrology of lakes Tanganyika and Malawi. *UNESCO Studies and Reports in Hydrology* **54**, UNESCO Publishing, Paris.

Crul, C.R. 1998. Management and conservation of the African Great Lakes. *UNESCO Studies and Reports in Hydrology* **59**, UNESCO Publishing, Paris.

Dagg, M. 1972. Water requirements. Chapter 10. In: *East Africa: It's Peoples and Resources* (ed. W.T. Morgan). Oxford University Press, London, pp 119-125.

Davy, E.G. 1974. A survey of meteorological and hydrological data available in six Sahelian countries of West Africa/A survey of studies in meteorology and hydrology in the Sudano-Sahelian zone of West Africa. *WMO Publ.* **379**. World Meteorological Organization, Geneva.

Dawdy, D.R. & T. O'Donnel 1965. Mathematical models of catchment behaviour. *J. Hydr. Div., ASCE, Paper* **4410** (HY4): 91-123.

Demarée, G. 1987. Application of non-linear regression techniques to the determination of rating curves consisting of one or two branch. *IRM Publ. Ser. A.,* Brussels, Belgium.

Demarée, G.R. & C. Nicolis 1990. Onset of Sahelian drought viewed as a fluctuation-induced transition. *Q. J. R. Meteo. Soc.* **116**: 221-238.

Dennett, M.D., J. Elston & J.A. Rodgers 1985. A reappraisal of rainfall trends in the Sahel. *J. Climat.,* **5**: 353-361.

Denny, P. (ed.) 1985. *The Ecology and Management of African Wetland Vegetation.* Dr W. Junk Publishers., Dordrecht, Boston, Lancaster.

Dieng, B. 1989. Transfer d'eau en milieu poreux non-saturé, recharge des nappes en climat Soudano-Sahelian. In: *Proc. Sahel Forum: The State-of-the-Art ofHydrology and Hydrogeology in the Arid and Semi-arid Areas of Africa,* Ouagadougou, Burkina Faso, pp 387-396.

Dincer, T., S. Child & B. Khupe 1987. A simple mathematical model of a complex hydrologic system – Okavango Swamp, Botswana. *J. Hydrol.* **93**: 41-65.

Doorenbos, J. & A.H. Kassam 1979. Yield response to water. *FAO Irr. & Dr.Paper* **24**. Food and Agriculture Organization of the United Nations, Rome.

Doorenbos, J. & W.O. Pruitt 1977. Guidelines for predicting crop water requirements, *FAO Irr.& Dr. Paper* **24**, Food and Agriculture Organization of the United Nations, Rome.

Doyle, P. 1990. Modelling catchment evaporation: an objective comparison of the Penman and Morton approaches. *J. Hydrol.* **121**: 257-276.

Drayton, R.S. 1984. Variations in the level of Lake Malawi. *J. Hydrol. Sci.* **29** (1): 1-10.

Drijver, C.A. & M. Marchand 1985. *Taming the Floods, Environmental Aspects of Floodplain Development in Africa.* Report for the Commission of European Union Communities, Brussels. Center of Environmental Science (CML), Leiden, The Netherlands

Drijver, C.A. & J.C.J. van Wetten (eds.) 1992. *Report on Sahel Wetlands 2020: Changing Development Policies on losing Sahel's Best Resources.* Centre of Environmental Science (CML), Leiden, The Netherlands.

Dubreuil, P. 1961. Aménagement des lacs Télé et Faguibine. Etude hydroclimatique. *Cahiers de L 'O.R.S.T.O.M., Série Hydrologie, O.R.S.T.O.M.*

Dunne, T. 1979. Sediment yield and land use in tropical catchments *J. Hydrol.* **42**: 281-300.

Dupriéz, G.I. 1959. La cuve lysimétrique de Thornthwaite, comme instrument de mesure de l'évapotranspiration en régions équatorials. In: *Proc. Symp. Hannoversch-Münden* **II** (Lysimeters)*, IASH Publ.* **49**: 84-98.

Dutch Ministry of Foreign Affairs 1998. The management of shared river basins: experiences from SADC and EU (eds. H. Savenjie & P. van der Zaag). *Focus on Development* **8**, The Hague, The Netherlands.

Edmond, J.M., R.F. Stallard, H. Craig, V. Craig, R.F. Wees & G.W. Coulter 1993. Nutrient chemistry of the water column of Lake Tanganyika. *Limnol. Oceanogr.***38** (4): 725-738.

EL-Agib, N.A. 1995. Study of hydrological variations, drought and desertification in the Sudan. *M.Sc. Thesis,* University of Bahrain, Bahrain.

El-Bakry, M.M. 1975. Evaporation from Lake Victoria. *Meteo. Res. Bull.* **7** (1): 21-47. The Meteorological Authority of Egypt. Cairo.

El-Gibali, A. 1966. Irrigation requirements and frequency of late corn. *Agr. Res. Rev.* **44** (1): 139-157, Cairo, Egypt.

Ellenbroek, G.A. 1987. *Ecology and Productivity of an African Wetland System.* University of Utrecht. Dr W. Junk Publishers, The Hague, The Netherlands.

El-Nokrashy, M.A. 1963. Effect of frequency of irrigation on quality and quantity of bearing-orange varieties budded on three root stocks in loamy clay soil. *M.Sc. Thesis,* Faculty of Agriculture, Cairo University, Cairo, Egypt.

El-Shal, M.I. 1966. Consumptive use and water requirements for some major crops in Egypt. *Ph.D. Thesis,* Faculty of Engineering, Cairo University, Egypt.

El-Sheikh, S., A. Kaikai & K. Andah 1991. Intensive sediment transport from the Upper Nile Basin and water resources management in Sudan. *IAHS Publ.* **201**: 291-300.

Eltahir, E.A.B. 1996. El-Niño and the natural variability in the flow of the Nile River. *Wat. Resourc. Res.* **32** (1): 131-137.

Elwan, M.Y. 1995. Synthetic generation of missing runoff data of the White Nile, River Sobat and Bahr el-Jebel. *M.Sc. Thesis,* Int. Inst Infrastruct., Hydr. and Env. Eng. (IHE), Delft, The Netherlands.

Elwan, M.Y., M. Shahin & M.J. Hall 1996 Synthetic generation of missing runoff data for the White Nile, Sobat River and Bahr el-Jebel. In: *Proc. 17th IAHR Intl. Symp. Stochastic Hydraulics,* Mackay, Australia, pp 333-340.

Encyclopaedia Britannica 1988. *(The New) Encyclopædia Britannica, Different Volumes.* 15th edition, Chicago-Auckland-London-Paris- Rome-Tokyo.

---------- 2001. *Encyclopædia Britannica,* Inc. de Luxe ed. CD Rom.

Engelman, R. & P. Le Roy 1995. *Sustaining Water*: *an Update to Population and the Future of Renewable Water Supplies* (updated version of the 1993 report). Population and Environment Program/Population Action International, Washington, D.C.

Enikeff, M.G. 1950. Le transport de sels par le Niger en 1938. C. *R. 1er Conf. Inst. des Africanists de l'Ouest, Paris* **1**: 106-107.

Entz, B.A.G. 1976. Lake Nasser and Lake Nubia. Chapter. 19a In: *The Nile, Biology of an Ancient River* (ed. J. Rzóska). Dr W. Junk Publishers B. V. The Hague, pp 271-298.

Environmental Rights Action [ERA; Friends of the Earth, Nigeria] 1999. Power shift at the dam is a looming disaster. *The Kainji Dam Flood: an ERA Field Report.* ERA Field Report **19**, Benin City, Nigeria.

Evans, R. 1980. Mechanics of water erosion and their spatial and temporal controls: an empirical viewpoint. In: *Soil Erosion* (ed. M.J. Kirkby). J. Wiley & Sons Inc, New York, pp 109-128.

Evans, T. 1994. History of Nile flows. In: *The Nile sharing a scarce resource* (eds. P.P. Howell & J. A. Allan). Cambridge University Press, pp 27-61.

Ezzat, M.A. 1976 Regional groundwater models, Wadi el-Gadid project. *Working Document* **2**, *UNDP/FAO Report, AGON: EGY 71/561,* Cairo, Egypt.

Fahmy, A., L. Panattoni & E. Toddini 1982. A mathematical model of the River Nile. In: *Engineering Applications of Computational Hydraulics,* Vol. **I** (eds. M.B. Abbott & J. A. Cunge).Pitman Advanced Publ. Progr. UK, pp 111-130.

Faloci, M.L. 1984. A new chance for Lake Chad. *Short Note, Natural Resources Forum © United Nations,* New York, pp **175-177**.

FAO 1979. *A Provisional methodology for Soil Degradation Assessment.* Food and Agriculture Organization of the United Nations, Rome.

------ 1981. *Forestry and Rural Development. FAO Forestry Paper* **26**, Food and Agriculture Organization of the United Nations, Rome.

------ 1986. African agriculture, the next 25 years. In: *Atlas of Agriculture.* Food and Agriculture Organization of the United Nations, Rome.

------ 1987. *Irrigation and Water Resources Potential for Africa.* Food and Agriculture Organization of the United Nations, Rome.

------ 1989. *Manual for CROPWAT Computer Programme.* FAO Land and Wat. Develop. Div., Food and Agriculture Organization, Rome.

------ 1993. Forest resources assessment, 1990. In. *Tropical Countries. FAO Forestry Paper* **112**. Food and Agriculture Organization of the United Nations, Rome.

------ 1995. *Irrigation in Africa in Figures. Water Report* 7, Food and Agriculture Organization of the United Nations, Rome.

Fathi, A.M. 1995. Water consumptive use and crop coefficient for some field crops in desert sandy soils using simple field volumetric lysimeters. In: *Proc. Int. Conf. Wat. Resour. Mgmt. in Arid Countries.* Muscat, The Sultanate of Oman, Vol. **l**, pp 106-113.

Faure, H. & J. Gac 1981. Senegal river runoff. *Nature* **293**: 414-419.

Fiering, M.B. & B.B.Jackson 1971. *Synthetic Streamflows. Wat. Resourc. Monogr. Ser.* **1**, Amer. Geophys. Un., Washington, D.C.

Flohn, H. & H. Wittenberg 1980. Die Verdunstung als Wassewirtscahfliche Schlüsselgröβe zum Qattara-Projekt. *Wasser und Boden* **8**: 352-358.

Flohn, H. & Th. Burkhardt 1985. Nile runoff at Aswan and Lake Victoria: a case of discontinuous climate time-series. Z. für Gleitsch, Glazialgeol. **21**: 125-130.

Flohn, H. 1987. East African rains of 1961/62 and the abrupt change of the White Nile discharge. In: *Palæoecology of Africa and the Surrounding Islands,* Vol.**l8** (ed. J.A. Coetzee). A.A. Balkema Publishers, Rotterdam, Brookfield, pp 3-18.

Foster, S.S.D. & P.J. Chilton 1998. As the land so the water, the effects of agricultural cultivation on groundwater. In: *Agricultural Threats to Groundwater Quality* (eds. L. Candela & A. Aureli). Workshop Proc., IHP/UNESCO/ IAMZ/CIHEAM, Zaragoza, Spain, pp 15-43.

Gac, J.Y. 1981. Géochemie du basin du Lac Chad: bilan de l'altération de l'érosion et de la sédimentation. *Traveaux et documents de l 'O.R.S.T.O.M.* **123**, O.R.S.T.O.M.

Gallais, J. 1967. Le delta intérieur du Niger et ses bourdures. *Mém.et doc. Centre de Recherches et documentation Cartographiques et Géographiques* **3**. *C.N.R.S.,* Paris,

Gamachu, D. 1977. Aspects of climate and water budget in Ethiopia. *Tech. Monogr.,* Addis Ababa University Press. Addis Ababa, Ethiopia.

Ganesan, C.T. 2001. Water resources development and management, a challenging task for Botswana. *Wat. Int.* **26** (1): 80-85.

Gautier, F., H. Lubes-Niel, R. Sabatier, J.M. Masson, J.E. Paturel & E Servat 1998 Variabilité du régime pluviométrique de l'Afrique de l'Ouest non sahélienne entre 1950 et 1989. *J. Hydrol. Sci.* **43** (6): 921-935.

Gentilli, J. 1972. *Australian Climate Patterns.* T. Nelson, Melbourne, Australia

Gibbs, S. 1996. Skin disease and socioeconomic conditions in rural Africa: Tanzania. *Int. J. Dermatol.* **35** (9): 633-639.

Girard, G. 1975. Modèles mathématiques pour l'évaluation des lames écoulées en zone sahélienne et leurs contraintes. *Cahiers de l'O.R.S.T.O.M., Série Hydrologie,* **XII** (3), O.R.S.T.O.M., Bondy.

Gischler, C.E. 1967. Synthèse hydrologique du basin du Lac Chad. *Nat. & Resourc.* **III** (3): 10-16.

Glantz, M.H. 1987. Drought in Africa. *Sci. Amer.* **256** (6): 34-40

Gleick, P.H. 1993. *Water in Crisis: a Guide to the World's Freshwater Resources.* Pacific Inst. Stud. Dev., Env. and Secur. /Stockholm Env. Inst. Oxford University Press, Oxford, New York.

Glover, J.N. & J.S. McCulloch 1958. The empirical relation between solar radiation and hours of sunshine. *Q. J. Roy. Met. Soc.* **84**: 172-175.

Glover, J. & J. Forsgate 1964. Transpiration from short grass. *Q. J. Meteo. Soc.* 90: 320-324.

Golterman, H.L. 1975. *Physical Limnology.* Dev. Wat. Sci. **2**, Elsevier Sci. Publ. Co., Amsterdam, New York, Oxford.

Griffiths, I.L. 1984. *An Atlas of African Affairs.* Metheun, London.

Griffiths, J.F. 1972. Climates of Africa (ed. J. F. Griffiths). Chapter 10. In: *World Survey of Climatology.* Elsevier Publ. Co., Amsterdam, New York.

Grove, AT. 1970. *Africa South of the Sahara.* 2nd Edition, Oxford University Press, London, UK.

---------- 1972. The dissolved and solid load carried by some West African rivers: Sénégal, Niger, Benue and Shari. *J. Hydrol.* **16** (4): 277-300.

Grove, A.T. 1978. *Africa.* Oxford University Press, London, UK.

---------- (ed.) 1985. *The Niger and its Neighbours.* A.A. Balkema Publishers, Rotterdam, Boston.

---------- 1998. Variability of African River discharges and lake levels. In: *Proc. 1nt. Conf. Trop. Climatology, Meteorology and Hydrology* (eds. G. Demarée, J. Alexandre & M. de Dapper). Roy. Inst. Trop. (KIT), Brussels, Belgium, pp 470-478.

Hall, A., I. Maria, C.B.S. Valente & B.R. Davies 1977. The Zambezi river in Mozambique: the physico-chemical status of the Middle and Lower Zambezi prior to the closure of the Cabora Bassa Dam. *Freshwater Biol.* 7: 187-296.

Hall, M.J., A.F. Zaki & M. Shahin 2001. Regional analysis using the geomorpho-climatic instantaneous unit hydrograph. *Hydrol. Earth Sys. Sci.* **5**(1): 93-102.

Hanna, L.W. 1971. The effects of water availability on tea yields in Uganda. *J. App. Eco.* **VIII**: 791-813.

Hargreaves, G.H. 1956. Irrigation requirements based on climatic data. *Paper* **1105**, *Proc. ASCE, J. Irr. Dr. Div.* **82** (IR 3): 1-10.

Hargreaves, G.H. 1975. Moisture availability and crop production. *Trans. Amer. Soc. Agr. Engrs. (ASAE)* **18**(5): 980-984.

Hargreaves, G.H. & Z.A. Samani 1982. Estimating potential evapotranspiration. *J. Irr. Dr. Div. ASCE,* Vol **108** (IR 3): 223-230.

Hargreaves, G.L., G.H. Hargreaves & J.P. Riley 1985. Agricultural benefits for Senegal River Basin. *Paper No.* **19800**, *J. Irr. Dr. Div., ASCE* **111** (2 IR): 113-124.

Harrold, L.L. 1966. Measuring evapotranspiration by lyisemetry. In: *Proc Conf. on Evapotranspiration and its Role in Water Resources Management, ASAE,* Michigan, pp 28-33.

Hart, R.C. 1985. Aspects of hydrogeochemistry of the Upper Orange River. In: *Transport of Carbon and Minerals in Major World Rivers,* Part **3** (eds. E. T. Degens, S. Kempe & R. Herrera). Mitt. Geol-Paläont. Inst., Universität Hamburg, SCOPE/UNEP **58**: 435-442.

Hartung, F. 1978. 75 Jahre Nilstau bei Assuan, Entwicklung und Fehlentwicklung. Bericht **40**, Versuchanstalt für Wasserbau der Technischen Universität München, Oskar von Miller Institute, (West) Germany.

Hastenrath, S. & R. Kruss 1992. Greenhouse indicators in Kenya. *Nature* **335**: 503-504.

Heederik, J.P., N. Gathuru, F.I. Majanga & P.G. van Dongen 1984. Water recources assessment study in Kiambu district, Kenya. In: *Proc. Harare Symp: Challenges in African Hydrology and Water Resources, IAHS Publ.* **144**: 95-110.

Hefny, K., M.S. Farid & M. Hussein 1991. Groundwater assessment in Egypt. In: *Round Table Meeting on Planning for Groundwater Development in Arid and Semi-arid Regions,* Cairo, Egypt, pp 93-104.

Henriques, A.G. & H.S. Silva 1991. *7th Congress on Large Dams,* Vienna, Austria. Q. **64**, R. 25: 427-442.

Herbst, P.H., D.B. Bredenkamp & H.G. Barker 1966. A technique for the evaluation of drought from rainfall data. *J. Hydrol.,* **4**: **264-272.**

Heusch, B. 1970. L'érosion par les eaux de pluie au Maroc. In: *Proc. Int. Wat. Eros. Symp., ICID,* Prague (Czechoslovakia), **III,** pp131-138.

Heusch, B. & A. Milliés-Lacroix 1971. Une méthode pour estimer l'écoulement et l'érosion dans un basin: application au Maghreb. *Mines et Géologie,* Rabat, Morocco **33**, pp 21-39.

Heusch, B. & O. Cayala 1986. Assessment of sediment discharge measurements in the Maghreb countries. *J. Wat. Resour.* **5** (1): 349-366, Baghdad, Iraq.

Hillel, D. 1980. *Fundamentals of Soil Physics.* Academic Press, New York.

Hipel, K.W. & A.I. McLoed 1978. Preservation of the rescaled adjusted range: 2: simulation studies using Box-Jenkins models. *Wat. Resourc. Res.* **14** (3): 509-518.

Holeman, J.N. 1965. The sediment yield of major rivers of the world. *Wat. Resourc. Res.* **4** (4): 737-747.

Hori, H. 1991. Environmental influences of dam construction on nature and society *7th Congress on Large Dams,* Vienna, Austria. Q. **64** (R. 19): 323-340.

Horton, R.E. 1933. The role of infiltration in the hydrologic cycle. *Trans Amer. Geophys. Un.* **4***:* 443-460.

Howard-Williams & J.J. Gaudet 1985. In: *The Ecology and Management of African Wetland Vegetation* (ed. P. Denny). Dr W. Junk Publishers, The Hague, The Netherlands.

Howell, P.P., J.M. Lock & S.M. Cobbs (eds.) 1988. *The Jonglei Canal: Impacts and Opportunity.* Cambridge University Press, Cambridge, UK.

Hubert, P. & J.P. Carbonnel 1987. Approche statistique de l'aridification de l'Afrique de l'Ouest. *J. Hydrol.* **95**: 165-183.

Hurst, H.E. 1927. The Lake Plateau Basin of the Nile, 2nd Part. *Phys. Dept. Paper* **23**, Government Press, Cairo, Egypt.

---------- 1935. Discussion of the paper: flood stage records of the River Nile by C.S. Jarvis, *Trans. ASCE, Paper* **1944**: 1036-1040.

---------- 1950. The Nile Basin, Vol. VIII. *The hydrology of the Sobat and White Nile and the topography of the Blue Nile and Atbara. Phys. Dept. Paper* **55**, Government Press, Cairo, Egypt.

---------- 1952. *The Nile: A General Account of the River and the Utilization of its Waters.* Constable and Company Ltd., London.

---------- 1956. Methods of using long-term storage in reservoirs (with discussion). *Proc. Inst. Civil Engrs., Part I, Paper* **6059**: 519-590, London.

Hurst, H.E., R.P. Black, & Y.M. Simaika 1951. The Nile Basin Vol. VII. *The Future Conservation of the Nile. Phys. Dept. Paper* **51**, Eastern Press, Cairo, Egypt.

---------- 1959. The Nile Basin, Vol. IX. *The Hydrology of the Blue Nile and the Atbara and of the Main Nile at Aswan, with some Reference to Projects. Nile Control Department, Paper* **12**. The General Organization for Government Printing Office, Cairo, Egypt.

---------- 1966. The Nile Basin, Vol. X. *The Major Nile Projects. Nile Control Department Paper* **23**. General Organization of Government Printing Offices, Cairo, Egypt.

Hurst, H.E. & P. Philips 1931. The Nile Basin, Vol. I. *General Description of the Basin, Meteorology and Topography of the White Nile Basin, Phys.Dept. Paper* **26**. Government Press, Cairo, Egypt.

---------- 1938. The Nile Basin, Vol. V. *The Hydrology of the Lake Plateau and Bahr el-Jebel. Phys. Dept. Paper* **35**, Schneider's Press, Cairo, Egypt.

Hussein, A.S., A.A. Ahmed & S.E. Ahmed 1986. Sedimentation problems in the Geziera scheme. In: *Proc. Int. Conf. on Water Resources Needs & Planning in Drought Prone Areas,* Khartoum, the Sudan, pp 947-953.

Hussein, A.S. & A.K. El-Daw 1989. Evapotranspiration in Sudan Gezeira irrigation scheme. *J. Irr. Dr. Div., ASCE* **115** (6): 1018-1033.

Hussein, M.T. 1986 Groundwater potentialities of the eastern region of the Sudan. In: *Proc. Int. Conf. on Water Resources Needs and Planning in Drought Prone Areas,* Khartoum, The Sudan, Vol. **II**, pp 1141-1151.

Hutchinson, G.E. 1957. *A treatise on Limnology.* Vol. **I**. John Wiley & Sons, New York.

Hutchinson, P. 1985. Rainfall analysis of the Sahelian Drought in the Gambia. *J. Climatol.* **5**: 665-672.

Ibrahim, AM., M.M. Ibrahim, S.A.Gaheen & S.M. Ismail 1995. Role of irrigation management on water parameters and yield of sugar beet in shallow water table soils of the Nile Delta. In: *Proc. Int. Conf. on Water Resources Management in Arid Countries,* Muskat, Vol. **1**, pp 98-105. The Sultanate of Oman.

ICID 1973. Consumptive use of water for irrigated cotton under different soil and climatic conditions (Morocco's Country paper). In: *Irrigated Cotton, a World-wide Survey* (eds. K. Framji & I. Mahajan). New Delhi, pp 98-110.

--------1973. Consumptive use of water for irrigated cotton under different soil and climatic conditions (Zambia's Country paper). In: *Irrigated Cotton, a World-wide Survey* (eds. K. Feamji & I, Mahajan). New Delhi, pp 76-77.

Imru, M. 1992. Sedimentation in the Koka Reservoir, Ethiopia: possibilities of prediction and control. *M.Sc. Thesis,* Int. Inst. Infrastruct., Hydr. and Env. Eng., (IHE), Delft, The Netherlands.

Ishag, A.S. 1976. Problems of groundwater in the rural areas of Africa. Nature & Resources **XII**(4): 33-34, UNESCO, Paris.

Israelsen, O.W. 1956. *Irrigation Principles and Practices,* 2nd ed. John Wiley & Sons Inc., New York.

Jacenkow, O.B. 1984. Artificial recharge of groundwater resources in semiarid regions. In: *Proc. Harare Symp.: Challenges in African Hydrology and Water Resources. lAHS Publ.* **144**: 111-119.

Jäkel, D. 1984. Rainfall patterns and lake level variations at Lake Chad. In: *Climatic Changes on a Yearly and Millenial Basis* (eds. N.A. Mörner & W Karlén). D. Reidel Publ. Co., Dordrecht, The Netherlands, pp 191-200.

Jarvis, C.S. 1935. Flood-stage records of the River Nile. *Trans. Amer. Soc. Civ. Engrs., Paper* **1944**: 1012-1030.

Jenkinson, A.F. 1973. A note on variations in May to September rainfall in West African marginal rainfall areas. In: *Report of the 1973 Symp. on Drought in Africa* (eds. D. Dalby & R.J. Harrison Church). Centre for Africa Studies, School of Oriental and African Studies, UK, pp 31-32

Jensen, M.E. & H.R. Haise 1963. Estimating evapotranspiration from solar radiation. *J. Irr. Dr. Div. ASCE* **89** (IR4): 15-41.

Jensen, M.E. 1966. Empirical methods of estimating or predicting evapotranspiration using radiation. In: *Proc. Conf. on Evapotranspiration and its Role in Water Resources Management, ASAE,* Chicago, Illinois, pp 49-53.

Jensen, M.E., R.D. Burman, R.G. Allen (eds.) 1990. Evapotranspiration and irrigation water requirements. *ASCE Manuals and Reports on Engineering Practices* **70**.

Johnson P.A. & P.D. Curtis 1994. Water balance Blue Nile Basin in Ethiopia. *Paper* **4807**, *J. Irr. Dr. Div. ASCE,* Vol. **120** (IR3): 573-589.

Jury, M.R. 1998. Forecasting water resources in South Africa. *IAHS Publ.* **252**: 275-279.

Kalinin, G.P. 1971. *Global Hydrology* (translated from Russian to English/Israel Program for Scientific Translation). Leningrad/Jerusalem. Amer. Geophys. Un.

Kamutanda, K. 1979. Contribution à l'étude de l'intensité des pluies à Lubumbashi (Shabe, Zaïre). *Géo-Eco-Trop.* **3** (3): 159-167.

Kashef, A.Z. 1981. The Nile – one river and nine countries. *J. Hydrol.* **53**: 53-71.

Katashaya, G.G. 1986. Hydrometeorological data collection for water resources planning: a case study. In: *Proc. Int. Conf. on Water Resources Needs and Planning in Drought-Prone Areas,* Khartoum, The Sudan, Part **II**: 741-758.

Katul, G.G., R.H. Cuenca, P. Grebet, J.L. Wright & W.O. Pruitt 1992. Analysis of evaporative flux data for various climates. *Paper No.* **2194**, *J. Irr. Dr. Div., ASCE* **114** (IR4): 601-618.

King, K.M., C.B. Tanner & V.E. Suomi 1956. A floating lysimeter and its evaporation recorder. *Trans. Amer. Geophys. Un.* **37** (6): 738-742.

Kite, G.W. 1981. Recent change in level of Lake Victoria. *Hydrol. Sci. J.* **26** (3): 233-243.

---------- 1984. Regulation of the White Nile. *Hydrol. Sci. J.* **29** (2): 191-201.

Kloos, H., A. Gazzinelli & P. van Zuyle 1998. Microgeographical patterns of Schistosomiasis and water contact; examples from Africa and Brazil. *Mem. Inst. Oswaldo Cruz,* Rio de Janero, Vol. **93**, Suppl. (1): 37-50.

Kohler, M.A., T. J. Nordenson & W.E. Fox 1955. Evaporation from pans and lakes, *U.S. Weath. Bur. Res., Paper* **38**.

Kohler, M. A. & I.H. Parmele 1967. Generalized estimates of the free-water evaporation. *Wat. Resour. Res.* **3**: 997-1005.

Köppen, W. 1931. *Die Klimat der Erde.* Walter de Gruyter Publ. Co., The Netherlands.

Kottegoda, N.T. & J. Elgy 1977. Infilling missing flow data. In: *Modelling Hydrologic Processes* (eds. J. Hubert et al.). In: *Proc. Ft. Collins 3rd Int. Hydrol. Symp. on Theor. & Appl. Hydrol.,* Colorado State University, Ft. Collins, Colorado.

Kottegoda, N.T. 1980. *Stochastic Water Resources Technology.* The MacMillan Press Ltd, London.

Krhoda, G.O. 1989. Aquifer characteristics in the sedimentary basin of the semi-arid areas of Kenya. In: *Proc. Sahel Forum: The State-of-the-Art of Hydrology and Hydrogeology of the Arid and Semi-arid Areas of Africa,* Ouagadougou, Burkina Faso, IWRA, pp 492-501.

Krishna, R. 1986. The Nile River Basin. Paper prepared for the Near East Studies Program and its conference "*U.S. Foreign Policy on Water Resources in the Middle East for Peace and Development*". Washington, D.C.

Kurzon. Y. 1978. *World Water Balance and Water Resources of the Earth,* (translated from Russian, original printing in 1974). UNESCO Press, Paris.

Kuusisto, E.E. 1985. Lakes: their physical aspects. Chapter 6. In: *Facets of Hydrology* II (ed. J. C. Rodda). John Wiley & Sons. New York. London, pp 153-181

Lamagat, J.P. 1989. Analyse de la vitesse de propagation des ondes de crues. In: *Proc. Sahel Forum: The State-of-the-Art of Hydrology and Hydrogeology in the Arid and Semi-arid Areas of Africa,* Ouagadougou, Burkina Faso, pp 292-305.

Lamb, H.H. 1966. Climate in the 1960's. *Geogr. J.* **132**: 183-212.

---------- 1973. Some comments on atmospheric pressure variations in the northern hemisphere. In: *Report of the 1973 Symp. on Drought in Africa* (ed D. Dalby and R. J. Harrison Church). Centre for African Studies, School of Oriental and African Studies, UK, pp 27-28

Latif, A.F. 1984. Lake Nasser – the new-man-made lake in Egypt (with reference to Lake Nubia, Chapter 16. In: *Ecosystems of the World.* Vol. **23**, *Lakes and Reservoirs* (ed. F.B. Taub). Elsevier, Amsterdam, pp 385-410.

Lee, A.F.S. & S.M. Heghinian 1977. A shift of the mean level in a sequence of independent normal random variables: a Bayesian approach. *Technometrics* **19**: 503-506.

Le Maître, D.C. & D.B. Versfeld 1997. Forest evaporation models: relationships between stand growth and evaporation. *J. Hydrol.* **193**: 240-257.

Leopold, L.B. 1962. Rivers. *Amer. Sci.* **50** (4): 511-537.

Linden, W. van der 1986. Groundwater modeling and the optimum operation of the Wadi Nyala aquifer. In: *Proc. Int. Conf. on Water Resources Needs and Planning in Drought Prone Areas,* Khartoum, the Sudan, Vol. **I**: 455-466.

Linsley, R.K., M.A. Kohler & J.L. Paulhus 1958. *Hydrology for Engineers.* McGraw Book Co., Inc. New York, Toronto, London.

Lloyd, J.W. 1986. A review of aridity of groundwater. *Hydrogeol. Proc.* **1**: 63-78.

---------- 1990. Groundwater conditions and development of the Eastern Sahara. *J. Hydrol.* **119**: 71-87. Elsevier Publ. Co., Amsterdam, New York, Tokyo.

---------- 1994. Groundwater management problems in the developing world. *J. Appl. Hydrogeol.* **4**: 35-48.

---------- 1995. The reality of recharge in semi-arid and arid areas. In: *Proc. Int. Conf. on Water Resources Management in Arid Countries,* Muscat, Vol. **2**: 466-479. The Sultanate of Oman.

---------- (ed.) 1999. Water resources of hard rock aquifers in arid and semi-arid zones. *Studies and Reports in Hydrology* 58, UNESCO, Paris.

L'vovich, M.I. 1979. *World Water Resources and Their Future* (translated from Russian by AGU, ed. R. Nace). The Russian edition was published in 1974 by Mysl'P.H., Moscow.

Mahé, G. & J.C. Olivry 1995. Variations des précipitations et des écoulements en Afrique de l'Ouest et Centrale de 1951 à 1989. *Sécheresse* **6**: 109-117.

Makholibe, S. 1984. Suspended sediment transport measurement in Lesotho. In: *Proc. Harare Symp.; Challenges in African Hydrology and Water Resources. IAHS Publ.* **144**:313-321.

Mandelbrot, B.B. & J.R. Wallis 1968. Noah, Joseph and operational hydrology. *Wat. Resour. Res.* 4: 909-918.

Mankarious, W.F. 1979. Hydrology of Lake Qarun, Egypt. *M.Sc. Thesis,* Faculty of Engineering, Cairo University, Cairo, Egypt.

Margat, J. 1979. Aridité et resources en eau. CIEH/CEFIGRE, Sémin. Intern. Politique de l'eau pour l'agriculture en zones arides et semi-arides, Niamey, Niger; et doc. BRGM 79 SGN **255** HYD, Orléans.

Margat, J. & K.F. Saad 1984. Deep-lying aquifers: water mines under the desert? *Nature & Resources* **XX** (2): 7-13.

Martins, O. & J.L. Probst 1991. Biogeochemistry of major African rivers: carbon and mineral transport. Chapter 6. In: *Biogeochemistry of Major World Rivers* (eds. E.T. Degens, S. Kempe & J.E. Richey), SCOPE. John Wiley & Sons Ltd., New York.

Martonne, E. de 1926. Aréisme et indice d'aridité. C. *R. Acad Sci. (Paris).* **182**:1395-1398.

Martyn, D. 1992. *Climates of the World.* Dev. in Atm. Sci. **18**, Elsevier Publ. Co., Amsterdam, New York and PWN, Polish Sci. Publ., Warsaw.

Mathieu, R. et al. 1989. Prospection des fractures aquifers du socle cristalin par dosage du gaz Radon contenue dans le sol. In: *Proc. Sahel Forum: The State-of-the-Art of Hydrology and Hydrogeology in The Arid and Semi-arid Areas of Africa,* Ouagadougou, Burkina Faso, pp 435-447.

Matondo, J.I. & P. Mortensen 1998. Water resource assessment for the Zambezi River Basin. *Wat. Int.* **23** (4): 256-262.

Meigs, P. 1951. La répartition mondiale des zones arides ou semi-arides. *UNESCO, NS AZ* **37**, UNESCO, Paris.

Meybeck, M. 1976. Total mineral dissolved transport by world major rivers. *J. Hydrol. Sci.* **21** (2): 265-284.

Meyer, P.S. 1998 An explanation of the 1: 500 000 general hydrological map, Port Elizabeth 3324. *Directorate: Hydrogeology, Department of Water Affairs and Forestry,* Pretoria, South Africa.

Midgley, D.C., R.A. Pullen & W.V. Pitman 1969. *Report* 4/69 *on Design Flood Determination in South Africa.* Department of. Civil Engineering, University of the Witwatersrand, South Africa.

Migahid, A.M. 1948. *Report on a Botanical Excursion to the Sudd Region.* Fouad I University Press, Cairo, Egypt.

---------- 1952. *Further Observations on the Flow and Loss of Water in the "Sudd" Swamps of the Upper Nile.* Fouad I University Press, Cairo, Egypt.

Milliman, J.D. & R.H. Meade 1983. Worldwide delivery of river sediment to the oceans. *J. Geo.* **91**: 1-21.

Molinier, M. & E. Mbemba 1979. The Congo-Zaïre River Basin. In: *The Great Rivers of the World,* Part 2. *Wat. Qual. Bull.* **4**: 83-85 and 97.

Moorehead, A. 1983. *The White Nile.* Penguin Books Ltd., Harmondsworth, U.K.

Moradini, G. 1940. *Missione di Studio al Logo Tana.* Ricerche Limnilogische, Vol. **III** (1). Rome, Addis Ababa.

Morocco 1986. Country report on the water resources of Morocco and their utilization (in Arabic). In: *Proc. Symp. on Water Resources in the Arab World and their Utilizations.* ACSAD-AFESD-KFAED, Kuwait.

Morton, F.I. 1979. Climatological estimates of lake evaporation. *Wat. Resour. Res.* **15** (1): 64-76.

---------- 1983. Operational estimates of lake evaporation. *J. Hydrol.* **66**: 76-100

---------- 1986. Practical estimate of lake evaporation. *J. Theor. Appl. Climatol.* **25**: 371-387.

Moukolo, N. 1989. Problèmes de vulnerabilité de la nappe de Brazzaville et risques de contamination par les rejets domestiques. In: *Proc. Sahel Forum: The-State-of- the-Art of Hydrology and Hydrogeology in the Arid and Semi-arid Areas of Africa,* Ouagadougou, Burkina Faso, pp 605-626.

Mutale, M. 1994. Assessment of water resources with the help of water quality: a case study of the Kafue Basin in Zambia. *M.Sc. Thesis.* Int. Inst. Infrastruc., Hydr. & Env. Eng. (IHE), Delft, The Netherlands.

Nace, R.C. 1969. Human use of groundwater. In: *Water, Earth and Man.* Methuen & Co., London.

Nair, K.R., F. Manji & J. N. Gitonga 1984. The occurrence and distribution of fluoride in groundwaters of Kenya. *IAHS Publ.* 144: 75-86.

Nash, I.E. 1989. Potential evaporation and the complementary relation. *J. Hydrol.* 111: 1-7.

NEDECO 1959. *River Studies and Recommendations on Improvement of Niger and Benue.* North Holland Publishing Company, Amsterdam.

NEDECO 1975. Flood control study. *Final Report for Mission 2; Development of the Sebou River.* Netherlands Engineering Consultants, The Hague, The Netherlands.

Neuland, H. 1984. Abnormal high water levels of Lake Malawi? – An attempt to assess the future behaviour of the lake water levels. *J. Geol.,* **9** (4): 323-334.

Nicholson, S.E. 1983. Sub-Saharan rainfall in the years 1976–80: evidence of continued drought. *Monthly Weather Review* 107: 1646-1654.

---------- 1985. Sub-Saharan rainfall 1981–1984. *J. Clim. Appl. Meteo.* **24**: 1388-1391.

---------- 1986. The spatial coherence of African rainfall anomalies: interhemispheric teleconnections. *J. Clim. Appl. Meteo.* **25**: 1365-1381.

Nieuwolt, S. 1977. *Tropical Climatology: an Introduction to the Climates of the Low Latitudes.* John Wiley & Sons, London, New York, Sydney.

Nile Control Staff 1979. *Monthly and Annual Rainfall Totals and Number of Rainy Days at Stations in and near the Nile Basin for the Period 1968–1972, and Normals up to 1972.* The Nile Basin; 7th supplement to Volume VI. *Nile Control Paper* **33**. Nile Control Department, Cairo, Egypt.

Nkounkou, R.R. & J.L. Probst 1987. Hydrology and geochemistry of the Congo River system. In: *Transport of Carbon and Minerals in Major World Rivers* (eds. E. T. Degens et al.). Part 4 *Mitt. Geol-Paläont. Inst.,* Universität Hamburg, SCOPE/ UNEP Sond. **64**: 483-508.

O'Conner, A.M. 1991. *Poverty in Africa: A Geographical Approach.* Belhaven Press, London.

Ogembo, V.G. 1977. Kenya's water problems (English translation from Russian). *Vodny Resursy* **2**: 171-176.

Ojiako, G.U. 1985, Nigerian water resources and their management. *Wat. Int.* **10**: 64-72.

Olivier, H. 1961. *Irrigation and Climate.* Edward Arnold Publishers Ltd., London.

---------- 1977. *Great Dams in Southern Africa.* Purnell, Cape Town, Johannesburg, London, New York.

Omar, M.H. & M.M. El-Bakry 1970. Estimation of evaporation from Lake Nasser. *Met. Res. Bull,* **II** (1): 1-27, Meteorological Authority of Egypt, Cairo.

---------- 1981. Estimation of evaporation from the lake of the Aswan Dam (Lake Nasser) based on measurements over the lake. *Agr. Met.* **23**: 293-308, Elsevier Publ. Co., The Netherlands.

Ongwenyi, G.S., S.M. Kithiia, F.E. Denga & P.O.Abwao 1993(a). Environmental and hydrological implications of the development of multipurpose reservoirs in some catchments of Kenya: meeting Kenya's water demands by the year 2010. In: *Proc. Yokohama Inl. Symp. on Sediment Problems. IAHS Publ.* 217: 207-215.

---------- 1993(b). An overview of the soil erosion and sedimentation problems in Kenya. In: *Proc. Yokohama Intl. Symp. on Sediment Problems. IAHS Publ.* 217: 217-224.

Ould El-Joud, M.Y. 1993. Cadre gélogique et hydrologique de la nappe d'Idni (Mauritanie), *M.Sc. Thesis* in Geologie, Faculty of Sciences, University of Liège, Liège, Belgium.

Owoade, A., L.G. Hutton, W. S. Moffat & M. D. Bako 1989. Hydrogeology and water chemistry in the weathered crystalline rocks of southwestern Nigeria. *IAHS Publ.* 188: 201-214.

Oyebande, L. 1962 Deriving rainfall intensity-duration-frequency relationships and estimates for regions with inadequate data. *Hydrol. Sci. J.* **27** (3): 353-367.

Paffen, K. 1966. Die täglichen Temperaturschwankungen als geographisches Klima-karakteristikum. *Erdkunde* **20**: 252-265.

Paling, W.A.J. 1988. Optimization of conjunctive use of groundwater and surface water resources in the Vaal Basin. In*: Proc. Harare Symp.*: *Challenges in African Hydrology and Water Resources. IAHS Publ.* No. **144**: 121-128.

Paling, W.A.J. & D. Stephens 1988. Prediction of cyclic rainfall and streamflow. In: *Proc. 1st Intl. Conf. on Computer Methods and Water Resources, Morocco,* Vol. **3** *Computational Hydrology* (eds. D. Oazar et al.). Computational Mechanics Publ., Southhampton, Boston and Springer-Verlag, Berlin, New York, London, Tokyo, pp 141-156.

Pallas, P. 1978. Water resources of the Socialist People's Libyan Arab Jamahiriya. *Document No. PP/mr, TF 9184/79/23* prepared for the Food and Agriculture Organization of the United Nations (FAO), Rome/Tripoli.

Paulhus, J.L.E. 1965. Indian Ocean and Taiwan rainfalls set new records. *Monthly Weather Review* **93**: 331.

Penman, H.L. 1948. Natural evaporation from open water, bare soil and grass. *Proc. Roy. Soc.*(London) **193**: 120-145.

Penman, H.L. 1956. Evaporation: an introductory survey *Nether. J. Agr. Sci.* **4**: 9-29.

Pinder, G.F. 1973. A Galerkin finite element simulation of groundwater concentration on Long Island. *Wat. Resour. Res.* **9** (6): 1657-1669.

Piper, B.S., D.T. Plinston & J.V. Sutcliffe 1986. The water balance of Lake Victoria. *Hydrol. Sci. J.* **31** (1): 25-47.

Plate, E.J. 1993. Sustainable water resources development, In: IAHR moving towards the 21st Century. *Memorial Seminar for the Silver Jubilee on the Occasion of the XXV IAHR Biennal Congress,* Tokyo, Japan, pp 37-47.

Plate, E.J. & P. Wengefeld 1979. Exchange processes at the water surface. In: *Hydrodynamics of Lakes. Develop. Wat. Sci.* **11**, Elsevier, Amsterdam, pp 277-301.

Plisnier, P.D. 1996. Lake Tanganyika: recent climate changes and tele-comunications with ENSO. *Proc. Intl. Conf. on Tropical Climate, Meteorology and Hydrology,* Brussels, Belgium, pp 228-250.

Popper, W. 1951. *The Cairo Nilometer, Studies in the Ibn Taghri Birdi's Chronicles of Egypt.* University of California Publications in Semitic Philology, I, Vol. **12**, University of California Press.

Postel, S. 1992. *Last Oasis: Facing Water Scarcity.* W.W. Norton & Co., New York.

---------- 1993. Water and Agriculture. Chapter 5. In: *Water in Crisis* (ed. P. Gleick). Pacific Inst. Stud. Dev., Env. And Secur./Stockholm Env. Inst. Oxford University Press, Oxford, New York.

Pottinger, L. 1997. Manantali Dam changes will make a bad situation worse. *World Rivers Rev.,* Publ. International Rivers Network. Encyclopædia Britannica, Inc.

Pouyaud, B. 1989. Evaporation from free water surfaces in the Sudano-Sahelian climate. In: *Proc. Sahel Forum: The State-of-The-Art-of Hydrology and Hydrogeology in the Arid and Semi-arid Areas of Africa,* Ouagadougou, Burkina Faso, pp 169-180.

Probst, J.L. & Y. Tardy 1987. Long range streamflow and world continental runoff fluctuations since the beginning of this century. *J. Hydrol.* **94**: 289-311.

Probst, J.L., R.R. Nkounkou, G. Krempp, J.P. Bricquet, J.P. Thiébaux & J.C. Olivry 1992. Dissolved major elements exported by the Congo and the Ubangi rivers during the period 1987-1989. *J. Hydrol.* **135**: 237-257.

PTJC 1982. *Yearbook 1981-1982.* Permanent Technical Joint Committee on the Nile Waters. Cairo-Khartoum.

------- 1983. *Yearbook 1982-1983.* Permanent Technical Joint Committee on the Nile Waters, Cairo-Khartoum.

------- 1984, *Yearbook 1983-1984.* Permanent Technical Joint Committee on the Nile Waters, Cairo-Khartoum.

Quaye, G. 1993. Drought analysis of the Sahel Region, Africa. *M.Sc. Thesis,* Int. Inst. Infrastruct., Hydr. and Env. Eng. (IHE), Delft, The Netherlands.

Reffay, L. 1948. *Le régime du Niger.* Technical document prepared for the Niger River Commission. Hydraulic Service of the former French West Africa. Bamakoe, Republic of Mali.

République Islamique de Mauritanie 1986. Les resources en eau de la République Islamique de Mauritanie et leur mise en valeur. In: *Proc. Symp.* on *Water Resources in the Arab World and their Utilizations* (Country Paper, text in Arabic and French). ACSAD-AFESD-KFAED, Kuwait.

Reusing, G. 1994. Contribution to the risk analysis of hydrologic droughts based on hydrologic time-series of the River Nile. Berliner Geowissenschaftliche Abhandlungen, Reihe D, Band 7, Technical University of Berlin, Berlin.

Riehl, H., M. El-Bakry & J. Meitín 1979. Nile River discharge. *Amer. Meteo. Soc. Mon. Wea. Rev.***107**: 1546-1553.

Rijks, D.A. 1967. Water use by irrigated cotton in Sudan, I: reflection of short wave radiation. *J. App. Eco.* **4** (2): 561-568.

---------- 1968. Water use by irrigated cotton in Sudan, II: net radiation and soil heat flux. *J. App. Eco.* **5** (2): 685-706.

---------- 1969. Evaporation from a papyrus swamp. *Q. J. Roy. Meteo. Soc.* **95**: 643-640.

---------- 1971. Water use by irrigated cotton in Sudan, III: Bowen ratios and advective energy. *J. App. Eco.* **III**: 643-663..

Riou, C. 1970. Evaporation en bac et évapotranspiration potentielle: expression de l'évaporation d'une petite nappe d'eau en fonction des données sous abri. *Cahiers de l 'O.R.S.T.O.M., Série Hydrologie,* pp 73-85.

---------- (± 1975). Quelques examples d'application des mesures de rayonnement à la determination de l'evapotranspiration en climat tropical. *Cahiers de l 'O.R.S. T.O.M. Sér. Hydrolo..* **11**: pp 19-37.

---------- 1975. La determination pratique de l'evaporation: application à l'Afrique Centrale. *Mém. de l'O.R.S.T.O.M.* **88**, O.R.S.T.O.M., Bondy.

Roche, M. A. 1969. Evolution dans l'espace et le temps de la conductivité électrique des eaux du Lac Tchad d'après les resultats de 1908, 1957, 1962 à Mars 1968. *Cahiers de l'O.R.S.T.O.M., Sér Hydrolo.* **6**: 35-78, O.R.S.T.O.M

---------- 1975. Geochemistry and the natural ionic and isotopic tracing: two complementary ways to study the natural salinity regime of the hydrological system of Lake Chad. *J. Hydrol.* **26**: 153-172.

---------- 1981. Tracage naturel salin et isotopique des eaux au système hydrologique du Lac Tchad. *Traveaux et documents de l'O.R.S.T.O.M.* **117**. O.R.S.T.O.M., Paris.

Roche, M.A., J. Rodier & J. Sircoulon 1976. Les aspects hydrologiques de la sécheresse recente en Afrique de l'Ouest. *Hydrol Sc. Bull.* **XXI** (2): 315-332.

Rochette, C. 1974. Le Bassin du Fleuve Sénégal. *Monographies Hydrologiques de l'O.R.S.T.O.M.* **1**, O.R.S.T.O.M., Paris

Rodier, J. 1964. Régimes hydrologiques de l'Afrique Noire à l'Ouest du Congo. *Mém. O.R.S.T.O.M.* **6**.

---------- 1976(a). Utilization of the results from representative and experimental basins with a view to the management of water resources. *Bull. Hydrol. Sci.,* **XXI** (4): 531-544.

---------- 1976(b). Evaluation of annual surface runoff in the dry tropical (Sahelian) regions in West Africa. *Cahiers de l'O.R.S.T.O.M., Série Hydrologie,* **XIII** (4): 269-306, O.R.S.T.O.M., Bondy.

---------- 1976(c). Estimation des débits de crues décennales pour les petits basins versants en Afrique tropicale. *Cahiers de l'O.R.S.T.O.M., Série Hydrologie* **XIII** (4): 243-267, O.R.S.T.O.M., Bondy.

---------- 1985. Aspects of arid-zone hydrology. Chapter 8. In: *Facets of Hydrology* Volume **II** (ed. J.C. Rodda). John Wiley & Sons, pp 205-247.

---------- 1989. General characteristics of surface hydrology in arid and semi-arid areas of Africa and their consequences for development. In: *Proc. Sahel Forum: State-of-the-Art of Hydrology and Hydrogeology in the Arid and Semi-arid Areas of Africa,* Ouagadougou, Burkina Faso, pp 15-34.

Rodriguez-Iturbe, I. & J.B. Valdes 1979. The geomorphologic structure of hydrologic response. *Wat. Resour. Res.* **15**: 1409-1420.

Rzóska, J. (ed.) 1976. *The Nile, Biology of an Ancient River.* Dr Junk Publishers B.V., The Hague, The Netherlands.

Sadek. M.F. 1992. Evaporation from the reservoir of the High Aswan Dam, Egypt: a comparison of relevant methods with limited data. *M.Sc. Thesis,* Int. Inst. Infrastruct, Hydr. and Env. Eng. (IHE), Delft, The Netherlands.

Sadek, M.F., M. Shahin & C.J. Stigter 1997. Evaporation from the reservoir of the High Aswan Dam, Egypt, a new comparison of relevant methods with limited data. *J. Theor. Appl. Climatol.* **56**: 57-66.

Said, R. 1993. *The River Nile; Geology, Hydrology and Utilization.* Pergamon Press, Oxford, New York, Seoul, Tokyo.

Salas, J.D., J.B. Obeysekera & D.C. Boes 1981. Modeling of the Equatorial Lakes outflows. In: *Proc. Int. Symp. Rainfall – Runoff Modelling* (ed. V.P. Singh), Mississippi. Water Resources Publications, Littleton, Colorado, pp 431-440.

Salem, O.M. 1991. The Great Man-made river project: a partial solution to Libya's future water supply. In: *Round Table Meeting on Planning for Groundwater development in Arid and Semi-arid regions,* Cairo, Egypt, pp 221-238.

Schaake, J.C. & L. Chunzehn 1989. Development and application of simple water balance models to understand the relationship between climate and water resources. *IAHS Publ.* 181: 343-352.

Schultz, G.A. 1976. Determination of deficiencies of the Rippl-diagram method for reservoir sizing by use of synthetically generated runoff data. ICLD, 12th Congress, Mexico, Q **46** R(1): 1-19.

Schutte, C.H., A.C. Evans, M.D. Pammenter, E. Gouws, P.L. Jooste, C.J. Badenhorst & J.J. Joubert 1995. Epidemiology and control of *Schistosomiasis mansoni* in communities living on the Cuando River floodplain of East Caprivi, Namibia. *Ann. Trop. Med. Parasitol.* **89** (6): 631-644.

Schwarz, J. 1989. Aquifers as components of water resources systems. *IASH Publ.* **188**: 433-441.

Scott, D.F. & W. Lesch 1997. Streamflow responses to afforestation with *Eucaliptus grandis* and *Pinus patula* and to felling in the Mokobulaan experimental catchments, South Africa. *J. Hydrol.* **199**: 360-377.

Sekwale, M. & E.T. Selaolo 1991. An overview of the groundwater resources of Botswana as portrayed by the hydrogeological maps and the recently completed national water master study. In: *Round Table Meeting on Planning for Groundwater Development in Arid and Semi-arid Regions,* Cairo, Egypt, pp 179-197.

Sellars, C.D. 1981. A floodplain storage model used to determine evaporation losses in the Upper Yobe River, Northern Nigeria. *J. Hydrol.* **52**: 257-268.

Semaika, M.R. & M.A. Rady 1988. On the irrigation management of cotton in Egypt. In: *Proc. VIth IWRA World Congress on Wat. Resourc. (Water for World Development),* Ottawa, Vol. **III** pp 184-193.

Senden, W. & K.M. Saleh 1986. Groundwater assessment and management in Sudan. In: *Proc. Intl. Conf. on Water Resources Needs and Planning in Drought Prone Areas.* Khartoum, Sudan, Vol **I** pp 467-478.

Shahin, M. 1959. Tile drainage of irrigated lands in Egypt. *Ph.D. Thesis,* Faculty of Engineering, Cairo University, Cairo, Egypt.

---------- 1969. Analysis of evaporation pan data in U.A.R. (Egypt). *ICID Ann. Bull.,* New Delhi, pp 53-69.

---------- 1983(a). Effect of storage works in the Nile River system on the homogeneity in the annual flow series. In: *Proc. Conf. on Optimal Utilization of Water Resources,* Varna, Bulgaria, pp 11-23.

---------- 1983(b). *Consultant report on a TOKTEN/UNDP mission to the Groundwater Research Institute of Egypt.* Acd. Sci. Tech./UNDP, Cairo, Egypt.

---------- 1985. *Hydrology of the Nile Basin.* Dev. Wat. Sci. **21**, Elsevier, Amsterdam, New York, Tokyo.

---------- 1986(a). Prediction of the concentration of suspended matter in the Main Nile between Halfa and Aswan. *J. Wat. Resourc.* **5** (1): 683-704, Baghdad, Iraq.

---------- 1986(b). Stochastic structure of the annual discharge series of some African rivers. In: *Proc. Int. Conf. on Water Resources Needs and Planning in Drought-Prone Areas,* Khartoum, the Sudan, Part **II**, pp189-210.

---------- 1993. An overview of reservoir sedimentation in some African river basins. *IAHS Publ.* 217: 93-100.

---------- 1994.The state-of-the-art of drought analysis and assessment: case studies from Africa. *9th Congress of the Asian and Pacific Division of IAHR, Singapore,* Part **1**: pp 32-39.

---------- 1999. Resources hydriques et modification du climat au Moyen-Orient. *Bull. de la Soc. Géo. de Liège* **37** (2): 75-90.

Shahin, M. & M.I. El-Shal 1969. An investigation of the consumptive use of water for crops and the frequency of irrigation in the United Arab Republic (Egypt). *Trans. 7th congress ICID, New Mexico,* R. **2**, Q. 23: 27-51.

Shahin, M., H.J. van Oorschot & S.J. de Lange 1993. *Statistical Analysis in Water Resources Engineering.* A.A. Balkema Publishers, Rotterdam.

Shalash, S. & A. Makary 1986. Mathematical modeling for sedimentation process in the High Aswan Dam Reservoir. *J. Wat. Resourc.* **5** (1): 654-682, Baghdad, Iraq.

Shapiro, R., M. Otieno, P. Adcock, P. Philips-Howard, W.A. Hawley, L. Kumar, P. Waiykai, B. Nahlen & L. Slutsker 1999. Transmission of epidimic *Vibro Cholerae O1* in rural Western Kenya associated with drinking water from Lake Victoria: an environmental reservoir for cholera? *Amer. J. Trop. Med. Hyg.* **60** (2): 271-276.

Sharma, T.C. 1985. Stochastic characteristics of rainfall-runoff processes in Zambia. *Hydrol. Sci J.* **30** (4): 497-512.

Shata, A.A. 1995. Management of the shallow aquifer systems in some desert coastal desert areas. In: *Proc. Int. Conf. on Water Resources Management in Arid Countries,* Muscat, Vol. **2**: pp 539-546. The Sultanate of Oman.

Shaw, E.M. 1984. *Hydrology in Practice.* Van Nostrand Reinhold Co. Ltd, UK.

Shenouda, R., A. El Gibali, A. Taudros & M. Gamal 1966. Irrigation requirement of early com and the best irrigation frequency for the crop with a comparative study for the plant requirements of early corn and late corn in Middle Egypt. *Agr. Res. Rev.* **44** (1): 159-170, Cairo, Egypt.

Sherif, M.M., V.P. Singh & A.M. Amer 1990. A two-dimensional finite element model for dispersion (2D-FED) in coastal aquifers. *J. Hydrol.* **118**: 343-356.

Shih, S.F. 1984. Data requirement for evapotranspiration estimation. *J. Irr. Dr. Div.* 110 (IR 3), *ASCE Paper* 19142. 263-274.

Shiklomanov, I.A. 1990. Global water resources. *Nature & Resources* **26**, (3): 34-43.

Singh, V.P., A. Banijklewicz & R.S. Ram 1981. Some empirical methods of determining the unit hydrograph. In: *Rainfall-runoff Relationship.* In: *Proc. Int. Symp. on rainfall–runoff modelling* (ed. P.V. Singh), Mississippi. Water Resources Publications, Colorado, USA, pp 67-90.

Sircoulon, J. 1976. Les données hydropluviométriques de la sécheresse récente en Afrique intertropicale; comparaison avec les sécheresses «1913» et «1940». *Cahiers de l'O.R.S.T.O.M., Sér. Hydrol.,* **XII** (2): 75-174, O.R.S.T.O.M.

Sivakumar, M.V.K., A. Maidoukia & R.D. Stern 1993. *Agroclimatology of West Africa: Niger, ICRISAT, Info. Bull.* **5**, Anddhra Pradesh, India.

Snijders, T.A.B. 1986. Interstation correlations and nonstationarity of Burkina Faso rainfall. *J. Clim.Appl. Meteo.* **25**: 524-531.

Stamp, L.D. & W.T. Morgan 1972. *Africa: a Study in Tropical Development.* John Wiley and Sons, Inc. New York, London, Sydney.

Starmans, G.A. 1970. Soil erosion of selected African and Asian catchments. In: *Proc. Inl. Wat. Eros. Symp.* (ICID), Prague, Czech Republic.

Stigter, C.J. & E.A.C, Kisamo 1978. Evaporation determinations by Penmama's methods: a rational and up-to-date approach for Tanzanian conditions. *Univ. Sci. J.* **4**: 53-72, Dar es Salam, Tanzania.

Straosolszky, Ö. 1974. Lake hydraulics. *IAHS Bull.* **19** (1): 99-114.

Stretta, P. 1983. Assignment report on the water resources of Zambia. *RP/1981–1983/2/7.3/03, FMR/SC/HYD/83/117,* UNESCO. Paris/Lusaka.

Sudan, The (ed. A. Hedayat) 1986. Country report on the water resources of the Sudan and their utilization (in Arabic). In: *Proc. Symp. Water Resources in the Arab World and their Utilizations.* ACSAD-AFSED-KFAED, Kuwait.

Sutcliffe, J.V. & J.B.C. Lazenby 1989. Hydrology and river control on the Niger and Senegal. In: *Proc. Sahel Forum: The State-of-The-Art of Hydrology and Hydrogeology in the Arid and Semi-Arid Areas of Africa,* Ouagadougou, Burkina Faso, pp 846-856.

Sutcliffe, J.V. & Y.P. Parks 1987. Hydrological modeling of the Sudd and Jonglei Canal. *J. Hydrol. Sci.***32** (2): 143-159.

---------- 1989. Comparative water balances of selected African wetlands. *Hydrol. Sci. J.* **34** (1): 49-62.

---------- 1994. The water balance of the Bahr el-Ghazal swamps. In: *The Nile: Sharing a Scarce Resource* (eds P.P. Howell & J.A. Allen), Cambridge University Press, Cambridge, UK, pp 281-298.

---------- 1999. The hydrology of the Nile, *IAHS Publ.* **5**, pp 179.

Sutcliffe, J.V. & W.R. Rangeley 1960. Variability of annual river flow related to rainfall records. *IASH, Comm. Surf. Wat., Gen. Assem, Helsinki,* pp 182-192.

Sutton, L.J. 1950. *Climatological Normals for Egypt and the Sudan, Cyprus and Palestine.* Phys. Dept., Ministry of Public Works of Egypt, Cairo, Egypt.

Sweers, H.E. 1976. A nomogram to estimate the heat-exchange coefficient at air-water interface as a function of wind speed and temperature: a critical survey of some literature. *J. Hydrol.* **30**: 375-401.

Szalay, M. 1973. Forecasting of flood characteristics of the Nile. In: *Proc. IAHR Int. Symp. Riv. Mechs.,* Bangkok, pp 443-454.

Tailing, J.F. 1966. The annual cycle of stratification and phytoplankton growth in Lake Victoria (East Africa). *Int. Rev. Hydrob.* **51**: 545-621.

Tanner, C.B. 1967. Measurement of evaporation. Chapter 29. In: *Irrigation of Agricultural Land* (eds. R. Hagan et al.). Amer. Soc. Agro., Wisconsin,. pp 534-574.

Terap, M.M. 1991. Water resources of Chad. In: *Round Table Meeting on Planning for Groundwater Development in Arid and Semi-arid Regions,* Cairo, Egypt, pp 205-211.

Thomas, H.A. & M.B. Fiering 1962. Mathematical synthesis of streamflow sequences for the analysis of river basins by simulation. Chapter 12. In: *Design of Water Resources Systems* (eds. A. Maass et al.). Harvard University Press, Cambridge, Massachusettes, U.S.A.

Thompson, B.W. 1965. *Climate of Africa.* Oxford University Press, London.

Thompson, K. 1975. Productivity of Cyperus papyrus L. In: *Photo-synthesis and Productivity in Different Environments* (ed. J. P. Cooper). *I. B. P. Synthesis Series* **3**, Cambridge University Press, Cambridge, UK.

Thornthwaite, C.W. 1948. An approach toward a rational classification of climate. *Geogr. Rev.* **38** (1): 55-94.

Timberlake, L. 1985. *Africa in Crisis: the Causes, the Cures of Environmental Bankruptcy.* Earthscan Publ. Ltd., London

Timmer, C.E. &L.W. Weldon 1967. Evapotranspiration and pollution of water by water hyacinth. *Hyacinth Control J.,* 34-37.

Todd, D.K. 1959. *Groundwater Hydrology.* John Wiley & Sons, Inc., New York, London.

Sudan, The (ed. A. Hedayat) 1986 Country report on the water resources of the Sudan and their utilization (in Arabic). In: *Proc. Symp. Water Resources in the Arab World and their Utilizations.* ACSAD-AFSED-KFAED, Kuwait.

Sutcliffe, J.V. & J.B.C. Lazenby 1989. Hydrology and river control on the Niger and Senegal. In: *Proc. Sahel Forum: The State-of-The-Art of Hydrology and Hydrogeology in the Arid and Semi-Arid Areas of Africa,* Ouagadougou, Burkina Faso, pp 846-856.

Sutcliffe, J.V. & Y.P. Parks 1987. Hydrological modeling of the Sudd and Jonglei Canal. *J. Hydrol. Sci.***32** (2): 143-159.

---------- 1989. Comparative water balances of selected African wetlands. *Hydrol. Sci. J.* **34** (1): 49-62.

---------- 1994. The water balance of the Bahr el-Ghazal swamps. In: *The Nile: Sharing a Scarce Resource* (eds P.P. Howell & J.A. Allen), Cambridge University Press, Cambridge, UK, pp 281-298.

---------- 1999. The hydrology of the Nile, *IAHS Publ.* **5**, pp 179.

Sutcliffe, J.V. & W.R. Rangeley 1960. Variability of annual river flow related to rainfall records. *IASH, Comm. Surf. Wat., Gen. Assem, Helsinki,* pp 182-192.

Sutton, L.J. 1950. *Climatological Normals for Egypt and the Sudan, Cyprus and Palestine.* Phys. Dept., Ministry of Public Works of Egypt, Cairo, Egypt.

Sweers, H.E. 1976. A nomogram to estimate the heat-exchange coefficient at air-water interface as a function of wind speed and temperature: a critical survey of some literature. *J. Hydrol.* **30**: 375-401.

Szalay, M. 1973. Forecasting of flood characteristics of the Nile. In: *Proc. IAHR Int. Symp. Riv. Mechs.,* Bangkok, pp 443-454.

Talling, J.F. 1966. The annual cycle of stratification and phytoplankton growth in Lake Victoria (East Africa). *Int. Rev. Hydrob.* **51**: 545-621.

Tanner, C.B. 1967. Measurement of evaporation. Chapter 29. In: *Irrigation of Agricultural Land* (eds. R. Hagan et al.). Amer. Soc. Agro., Wisconsin,. pp 534-574.

Terap, M.M. 1991. Water resources of Chad. In: *Round Table Meeting on Planning for Groundwater Development in Arid and Semi-arid Regions,* Cairo, Egypt, pp 205-211.

Thomas, H.A. & M.B. Fiering 1962. Mathematical synthesis of streamflow sequences for the analysis of river basins by simulation. Chapter 12. In: *Design of Water Resources Systems* (eds. A. Maass et al.). Harvard University Press, Cambridge, Massachusettes, U.S.A.

Thompson, B. W. 1965. *Climate of Africa.* Oxford University Press, London.

Thompson, K. 1975. Productivity of Cyperus papyrus L. In: *Photo-synthesis and Productivity in Different Environments* (ed. J. P. Cooper). *I. B. P. Synthesis Series* **3**, Cambridge University Press, Cambridge, UK.

Thornthwaite, C.W. 1948. An approach toward a rational classification of climate. *Geogr. Rev.* **38** (1): 55-94.

Timberlake, L. 1985. *Africa in Crisis: the Causes, the Cures of Environmental Bankruptcy.* Earthscan Publ. Ltd., London

Timmer, C.E. & L.W. Weldon 1967. Evapotranspiration and pollution of water by water hyacinth. *Hyacinth Control J.,* June, pp 34-37.

Todd, D.K. 1959. *Groundwater Hydrology.* John Wiley & Sons, Inc., New York, London.

Traora, S. 1989. Impact de l'hydrologie sur les projets hydrauliques au Burkina. In: *Proc. Sahel Forum: The State-of-the-Art of Hydrology and Hydrogeology in the Arid and Semi-arid Areas of Africa,* Ouagadougou, Burkina Faso, pp 871-888.

Trewartha, G.T. 1962. *The Earth's Problem Climates.* Madison, University of Wisconsin Press.

U.K. Consultant; Mac Donald, M. 1985. Lake Chad at risk if drought goes on. *World Water,* Vol. **8** (7): 34, Thomas Telford Ltd. Publishers, UK.

UNEP 1985. *Report of the Executive director of UNEP.* African Environmental UNEP Conference, Cairo, Egypt.

------- 1993. Poverty and environment. Information Document for the International Environment Day for the Year 1993 (text in Arabic). United Nations Environmental Programme, Regional Office for West Asia, Bahrain, pp 6-7.

UNESCO 1970. Study of water resources in the Chad Lake. *Nature & Resources* **VI** (2): 6-10, UNESCO, Paris.

---------- 1971. Discharge of selected rivers of the world. *Studies and Reports in Hydrology,* No. **5**, UNESCO, Paris.

---------- 1979. Map of the world distribution of arid lands. *MAB Tech. Note* **7,** UNESCO, Paris.

---------- 1981. Methods of computation of the water balance of large lakes and reservoirs (eds. H.L. Ferguson & V.A. Znamensky). *A Contribution to the International Hydrological Programme,* UNESCO, Paris.

---------- 1991. Hydrology and water resources of small islands: a practical guide (ed. A. Falkland). *Studies and Reports in Hydrology* **49**. UNESCO, Paris.

---------- 1995. Discharge of selected rivers of Africa. *Studies and Reports in Hydrology* **52** UNESCO, Paris.

---------- 1996. Global river discharge data base (RivDIS v1.0), Vol **I**. Africa, *Technical Documents in Hydrology, International Hydrological Programme (IHP),* UNESCO, Paris.

UNESCO/IHP/MaB 1992. Small tropical islands: water resources of paradises lost (ed. A. Falkland). *IHP Humid Tropics Programme, Series* **2**. UNESCO, Paris.

UNESCO/UNDP 1970. Research and training on irrigation with saline water, 1962 - 1969. *Tech. Rep./UNESCO/UNDP (SP) TUN 5,* Paris.

USBR 1964. *Land and Water Resources of the Blue Nile Basin.* U.S. Bureau of Reclamation, United States Department of the Interior, Washington, D.C.

USDA/SCS 1967. Irrigation water requirement. *Tech. Release* **21**, *Eng. Div. Soil Conservation Service, Department of Agriculture,* USA.

Verruijt, A. 1970. *Theory of Groundwater Flow.* MacMillan and Co. Ltd., London.

Wallén, C.C. 1968. Agroclimatological studies in the Levant. In: *Agricultural Methods, Proc. Reading Symp.,* Reading: pp 225-233.

Walling, D.E. 1984. The sediment yields of African Rivers. In: *Proc. Harare Symp.: Challenges in African Hydrology and Water Resources. IAHS Publ.* No. **144**: 265-283.

Walsh, J.F. 1985. Onchocerciasis: river blindness, Chapter **10**. In: *The Niger and its Neighbours* (ed. A. T. Grove). A.A. Balkema Publishers, Rotterdam/ Boston, pp 269-294.

Walton, K. 1969. *The Arid Zones.* Hutchinson University Library, London.

Wassing, F. 1964. Coastal engineering problems in the Delta region of UAR (Egypt). *Memoranda W1-W6, Reports of UN Expert to the Department of Ports and Lighthouses,* Alexandria, Egypt.

Watson, H.K. 1984. Veld burning and sediment yield from small drainage basins. In: *Proc. Harare Symp.: Challenges in African Hydrology and Water Resources. IAHS Publ.* **144**: pp 323-333.

Weert, R. van der & G.E. Kamberling 1974. Evapotranspiration of water hyacinth *(Eichhornia crassipes). J. Hydrol.* **22**: 201-212.

Westlake, C.R. Mountain & T. Paton 1954. Owen Falls, Uganda, hydroelectric development. In: *Proc. Inst. Civ. Engrs.* 3, Part **1**, *Paper* **6007** (with discussions): pp 630-669, London.

Wharton, G. & J.J. Tomlinson 1999. Flood discharge estimation from river channel dimensions: results of applications in Java, Burundi, Ghana and Tanzania. *Hydrol. Sci. J.* **44** (1): 97-111.

Whittington, D. & G. Guarisso 1983. *Water Management Models in Practice: A Case Study of the Aswan High Dam.* Dev. Env. Model. **2**, Elsevier Publ. Co., Amsterdam. The Netherlands.

Willmott, C.J., C.M. Rowe & Y. Mintz 1985. Climatology of the terrestrial seasonal water cycle. *J. Climatol* **5**: 589-606.

Wilson, E.M. 1983. *Engineering Hydrology* (3rd ed). MacMillan Education Ltd., London, UK.

Wisler, C.O. & E.F. Brater 1957. *Hydrology.* John Wiley & Sons, New York, London.

WMO 1966. Measurement and estimation of evaporation and evapo-transpiration, WMO-No. **201**.TP. **105**, World Meteorological Organization, Geneva.

---------- 1973. Map of the distribution of arid regions. *Tech. Rep.,* World Meteorological Organization of the United Nations, Geneva, Switzerland.

---------- 1974. Hydrometeorological survey of the catchments of Lakes Victoria, Kyoga and Albert. Volumes I, II III and IV, United Nations Development Programme/ World Meteorological Organization, Geneva.

---------- 1976. The CIMO International evaporimeter comparisons. Final Report, *WMO* **449**, World Meteorological Organization, Geneva.

-------- 1983. Guide to hydrological practices. *WMO Tech. Note.***126**, World Meteorological Organization, Geneva.

World Bank 1990. *World Development Report 1989–1990,* Oxford, Oxford University Press.

World Guide 1997. World Guide 1997–1998, A View from the South. New Internationalist Publications Ltd., U.K.

World Resources Institute/UNEP/UNDP 1994. *World Resources 1994–1995*. Oxford University Press, Oxford, New York.

Wright, J.L. 1982. New evapotranspiration crop coefficients. *J. Irr. Dr. Div. ASCE,* **108** (IR2): 57-74.

Wright, E.P. 1983. Groundwater development. In: *Proc. ICE Conference on World Water 83* (London), pp 63-71 (and discussions).

Yevjevich, V. 1967. An objective approach, definitions and investigations of hydrologic droughts. *Hydrology Paper* **23,** Ft. Collins, Colorado.

---------- 1972. Stochastic processes in hydrology. *Wat. Resour. Publ.,* Ft. Collins, Colorado, U.S.A.

---------- 1983. The Nile River Basin: hardcore and soft core water projects. *Wat. Intl.* **8** (1): 23-34, Lausanne.

Yin, X. & S.E. Nicholson 1998. The water balance of lake Victoria. *Hydrol. Sci.Bull.* **43** (3): 789-811.

Z.D.M.S. 1981. *Climate Handbook of Zimbabwe.* Department of Meteorological Services of Zimbabwe, Harare (Salisbury), Zimbabwe.

Zoppis, L. & R. Zoppis 1989. Corrosivity problems in rural water supply projects in Sahelian areas of West Africa. In: *Proc. Sahel Forum: The State-of-the-Art of Hydrology and Hydrogeology in The Arid and Semi-arid Areas of Africa,* Ouagadougou, Burkina Faso, pp 586-593.

GUIDE TO METEOROLOGICAL, HYDROMETRIC AND WATER QUALITY DATA USED IN THE BOOK

NOTE TO THE READER

Before bringing the book to its end, it is worthwhile to remind the reader of the purpose of the next few pages. A list of abbreviations of the countries and islands of Africa are listed below, and so are the nomenclature and units that are used in Appendixes A and B as well as the chapters of the book.

The analyses and discussions covered in the fourteen chapters of the book have been depending, to a fairly large extent, on various types of data. The large majority, but not all, of these data is classified into two Appendixes, A and B. Appendix A contains the meteorological data arranged in a series of 13 Tables with subdivisions. The hydrometric and water quality data are arranged in Parts I and II of Appendix B respectively. The hydrometric data occupy 10 Tables with subdivisions, whereas the water quality data occupy 7 Tables with subdivisions. The headings of all these Tables are given in the next few pages.

The Tables and their subdivisions fill more than 150 pages and the references and sources of information fill 6 pages, bringing the total to about 160 pages. To avoid having this heavy bulk of pages at the end of the book, it has been found easier and lighter to put them separately on a compact disc (CD-Rom) to be made available with the book. In order to browse the files containing the tables of data, the user needs to have MS EXCEL installed on his computer.

It is sincerely hoped that, with this arrangement the user will be able to achieve the utmost benefit of the book with a minimum effort.

The author

Abbreviation of Country and Island Names

Name	Abbreviation	Name	Abbreviation
Algeria	Alg	Libya	Lib
Angola	Ang	Madagascar	Mad
Ascension Island	AsI	Madeira Islands	MdI
Azores Islands	AzI	Mali	Mal
Benin	Ben	Malawi	Mlw
Botswana	Bot	Mauritania	Mrt
Burkina Faso	BrF	Mauritius Island	MtI
Burundi	Bur	Morocco	Mor
Cameroon	Cmn	Mozambique	Moz
Canary Islands	CnI	Namibia	Nam
Cape Verde Islands	CvI	Niger	Ngr
Central African Republic	CAf	Nigeria	Nig
Chad	Chd	Réunion Island	RnI
Comoros Islands	CmI	Rwanda	Rwd
Congo (Brazzaville)	CnB	São Tome & Principe	STP
Congo (Kinshassa)	CnK	Senegal	Sng
Djibouti	Djb	Seychelles Island	Syl
Egypt	Egy	Sierra Léeone	SrL
Equatorial Guinea	EqG	Somalia	Som
Eritreia	Ert	South Africa	SAf
Ethiopia	Eth	St Helena Island	SHI
Gabo	Gab	Sudan, The	Sud
Gambia, The	Gmb	Swaziland	Swz
Ghana	Ghn	Tanzania	Tnz
Guniea	Gun	Togo	Tog
Guinea Bissau	GnB	Tunisia	Tun
Ivory Coast	IvC	Uganda	Ugd
Kenya	Ken	West Sahara	WSh
Lesotho	Les	Zambia	Zmb
Liberia	Lib	Zimbabwe	Zmw

Nomenclature and Units used in Appendixes A and B

C = Concentration
Ca = Calcium
°C = Degree centigrade
Cl = Chloride
CO = Carbon monoxide
CO_2 = Carbon dioxide
Cv = Coefficient of variation
E =East
EC = Electrical conductivity
FC = Faecal coliform (per 100 ml)
Fe = Iron
Fs = Faecal streptococcus (per 100 ml)
H = Water level (stage)
HCO_3 = Bicarbonate
H_2S = Hydrogen sulphid
K = Potassium
K_{20} = Electrical conductivity at 20°C
Mg = Magnesium
N = North
Na = Sodium
NO_3 = Nitrate

O_2 = Oxygen
P = Precipitation
Q = Discharge
S = South
SiO_2 = Silicates
SO4 = Sulphate
TDS = Total dissolved solids
W =West
Z = Height

cal = Calorie
cal - = Calories per square
cm^{-2} d^{-1} centimeter per day
cm = Centimeter
cm^2 = Centimeter square
cm^3 = Centimeter cube

d = day
g = Gram
$g\ l^{-1}$ = Gram per liter
h = hour
ha = Hectare (10^4 m^2)
kg = Kilogram (10^3 g)
km = Kilometer (10^3 m)
km^2 = Kilometer sq. (10^6 m^2)
km^3 = Kilometer cube (10^9 m^3)
$km\ h^{-1}$ = Kilometer per hour
l = Liter (10^3 cm^3)
m = Meter
m^2 = Meter square (10^4 cm^2)
m^3 = Meter cube (10^6 cm^3)
$meq\ l^{-1}$ = Milliequivalent per liter
mg = Milligram
$mg\ l^{-1}$ = Milligram per liter
min = Minute
mm = Millimeter
$mm\ d^{-1}$ = Millimeter per day
mmhos-cm^{-1} = Millimohs per centi-meter
mo = Month
$m^3\ s^{-1}$ = Cubic meter per second
$m\ S\ m^{-1}$ = Milli Simens per meter
pH = Measure of alkalinity
ppm = Parts per million
s = Second
t = Ton(10^3 kg)
$t\ km^{-3}$ = Ton per cubic kilometer
$t\ km^{-2}$ - y^{-1} = Ton per square kilometer per year
y = year
Φ = Latitude
λ = Longitude
μ_{20} = see k_{20}
µmhos = Micromohs
μSm^{-1} = Micro Simens per meter

Appendix A: Key to Meteorological Data

Table 1- Names and coordinates of meteorological stations (a map showing the location of these stations is included in the text)

Table 2- Mean daily and total daytime hours of the year

Table 3- Mean monthly and annual surface air temperature

Table 4- Mean monthly and annual relative humidity

Table 5- Mean monthly and annual global radiation

Table 6- Mean monthly and annual duration of sunshine

Table 7- Mean monthly and annual degree of cloudiness

Table 8- Mean monthly and annual wind speed

Table 9- Mean monthly and annual rainfall

Table 10.- Annual mean and coefficient of variation of rainfall depth
Table 10_b- Annual rainfall series of 50 or more (uninterrupted) years of record

Table 11_a- Mean monthly and annual number of days
Table 11_b- Maximum monthly and annual rainfall for the used years of record
Table 11_c- Minimum monthly and annual rainfall for the used years of record

Table 12- Measured/estimated rates of evaporation from free water surfaces

Table 13_a- Measured/estimated rates of potential evapotranspiration
Table 13_b- Estimates of Thornthwaite's potential evapotranspiration at some additional stations
Table 13_c- Estimates of potential evapotranspiration from grasslands, woodlands, forests, swamps and wetlands

Appendix B: Key to Hydro and Water Quality Data

Part I- Hydro Data

Table 1- Estimates of fresh water resources potential

Table 2- Subdivision of fresh water resources potential into surface and groundwater

Table 3- Approximate surface areas of river basins larger than 20,000 km^2, and the names of countries sharing these basins (riparian countries)

Table 4_a- Runoff coefficients of the river basins west of the Congo River
Table 4_b- Runoff coefficients of the Chambeshi basin and the Congo headwaters, northern Zambia
Table 4_c- Runoff coefficients for certain parts of the Nile River system
Table 4_d- Runoff coefficients of the Zambezi River system
Table 4_e- Runoff coefficients of river basins in Kenya outside the Nile Basin

Table 5- Names and coordinates of stream gauging stations and the corresponding catchment areas

Table 6_a- Mean and coefficient of variation of annual river discharges
Table 6_b- Annual mean discharge series of 50 or more (uninterrupted years) of record (this title applies to Tables 6_{b1} thru' 6_{b7})
Table 6_{b1}- The Nile at Aswan
Table 6_{b2}- The Nile tributaries in the Sudan
Table 6_{b3}- The Niger at Koulikoro, Mali
Table 6_{b4}- The Niger at Niamey, Niger
Table 6_{b5}- The Sénégal at Bakél, Sénégal
Table 6_{b6}- The Obangui at Bangui, Central African Republic
Table 6_{b7}- The Congo at Kinshasa, Congo Democratic Republic

Table 7- Maximum and minimum average annual discharges at stations having complete record for at least 18 years

Table 8- Mean monthly and annual discharges of selected rivers

Table 9_a- Discharge and gauge measurements of Victoria Nile at Mbulamati
Table 9_b- Discharge and gauge measurements of the White Nile at Malakal
Table 9_c- Discharge and gauge measurements of the Congo at Kinshasa

Part I- Cont'd

Table 9_d- Discharge and gauge measurements of the Baro (tributary of the Niger) at Niandan
Table 9_e- Discharge and gauge measurements of the Benue near Yola

Table 10 - Principal groundwater formations/basins/aquifers and their hydrogeological parameters

Part II- Water Quality Data

Table 1_a- Erosion and land degradation in Africa
Table 1_b- Selected erosion rates in Africa
Table 1_c- Rate of sediment loss as a function of land use type for certain drainage basins in Kenya

Table 2_a- Sediment data of selected rivers in Africa
Table 2_b- Maximum and minimum annual sediment yields recorded for drainage basins ranging from ca 2,500 to 190,000 km^2
Table 2_c- Suspended sediment yield data for Lesotho
Table 2_d- Silt and dissolved data for some Malawian Rivers
Table 2_e- Average suspended sediment concentration of the Awash River water, Ethiopia
Table 2_f- Suspended sediment loads in the Volta Basin, Ghana, 1965
Table 2_g- Annual sediment load carried by the flood of Oued Zeroud at Sidi Saad, Tunisia
Table 2_h- Concentration and sediment yield, maximum and minimum values, for some rivers in Ghana
Table 2_i- Monthly and annual sediment loads in the Sénégal River at Bakel, Sénégal
Table 2_j- Monthly concentration of suspended sediment in the Sénégal River at Bakel, Sénégal
Table 2_k- Concentration of suspended load of floodwater in the Main Nile at Gaafra, 1955-63

Table 3_a- Sedimentation in storage reservoirs, Morocco
Table 3_b- Sedimentation in storage reservoirs, Tunisia
Table 3_c- Deposited sediment volumes in the high Aswan Dam Reservoir, Egypt, 1964-89
Table 3_d- Average rates and cumulative volumes of sediments deposited in the Roseires, Khashm el-Girba and Koka Reservoirs

Part II- Cont'd

Table 3_e- Average rates of sedimentation in 14 storage reservoirs in South Africa

Table 4_a- Salinity and dissolved solids in various sections of the Nile Basin
Table 4_b- Average values of some physical and chemical characteristics of water samples from Lake Victoria
Table 4_c- Water characteristics of the Equatorial Lakes other than Lake Victoria
Table 4_d- Water characteristics of Lake Tana, Blue Nile, Sobat, and Atbara Rivers
Table 4_e- Water characteristics of the White and Main Niles and Nubia and Nasser Lakes
Table 4_f- Chemical composition of the Niger River discharge
Table 4_g- Chemical composition of the discharges of some rivers in West Africa
Table 4_h- Chemical composition of the discharges of some rivers in the Upper part of Ghana
Table 4_i- Annual salt carried by the flood of Oued Zeroud at Sidi Saad, Tunisia
Table 4j- Chemical composition of the Congo and Bangui river Discharges

Table 5_a- Chemical composition of groundwater in rural areas of some West African countries
Table 5_b- Chemical characteristics of groundwater samples in the Niger Delta, Nigeria
Table 5_c- Chemical composition of groundwater in the outskirts of Cairo, Egypt
Table 5_d- Chemical analysis of shallow groundwater in the Moro area, Kwara State, Nigeria
Table 5_e- Conditions in shallow wells in the south coastal region of Kenya
Table 5_f- Physical and chemical characteristics of groundwater in the outskirts of Brazzaville, Congo Brazzaville
Table 5_g- Chemical characteristics of groundwater samples from Djibouti, Sénégal, and Khartoum Province, The Sudan
Table 5_h- Chemical characteristics of groundwater samples from different formations in the area of Port Elizabeth, South Africa

Table 6_a- Results of bacteriological water quality testing, Lesotho
Table 6_b- Bacteriological analysis of groundwater in the aquifer underlying the Greater Cairo District, and two villages in the Nile Delta area

Part II- Cont'd

Table 6_c- General bacteriological analysis of river waters in Ghana, The Sudan and Egypt

Table 7_a- Brief review of water-related diseases in Central Africa, Tanzania and Burundi

Table 7_b- Incidence of water-related diseases in rural areas of The Sudan and Nigeria

REFERENCES INDEX

Abdel Warith, M. 1965: 177
Abdulai, B.I. 1989: 117, 119, 134
Abel Afouda 1989: 102, 103
Abul-Atta, A. 1978: 484
Ackermann, E. 1936: 203
Adams, B. & E. Kitching 1979: 207, 548, 549
Aguado, E. 1987: 295, 298
Ahmad, M.U. 1981: 419
---------- 1986: 522
Akrasi, S.A. & N.B. Ayibotele 1984: 395
Alam, M. 1989: 517, 519
Alexandre, J. 1977: 210
Ali, Y.A.M. 1990: 134, 494
Allen, R.G. & W.O. Pruitt 1991: 166
Allen, R. G. et al. 1994: 157, 169
---------- 1998: 172, 173, 201, 202
Ambroggi, R.P. 1966: 519
Aňdel, J. & J. Balek 1971: 300, 313, 316
Angstrom, A. 1924: 41
Anyadike, R.N.C. 1992: 80, 82
Åse, L.E. 1987: 463-65
Attia, B. et al. 1979: 133
Attia, F.A.R. 1996: 556
Aubreville, A. et al. 1959: 9
Ayibotele, N.B 1984: 57
Ayoade, J.O. 1976: 99

Bagnouls, F. & H. Gaussen 1959: 56
Balek, J. & J. Perry 1973: 207
Balek, J. 1977: 9, 119, 121, 136, 144, 199, 203, 204, 207, 211, 212, 219, 235, 242-44, 294, 298, 303, 319, 339, 341, 350, 351, 353, 354, 428, 431-33, 439, 464, 466, 587, 596, 599, 600
---------- 1983: 428, 429, 510, 514, 582
Balmer, F. & I. Müller 1989: 560, 561
Bannerman, R. & N. Ayibotele 1984: 517, 537
Barratt, J.M. & S. Puyoo 1984: 518, 520
Bartholomew, J.C. (ed. director) 1980: 567, 569, 571, 573-76, 580
Baumgartner, A. & E. Reichel 1975: 215
Belaid, M.N. 1995: 563
Bellman, R. 1957: 503
Belloum, A. 1993: 98, 99,105, 106
Birmingham, M.E. et al. 1997: 591
Biswas, A.K. & M.R. Biswas 1976: 596
Blaney, H.F.& W.D. Criddle 1950: 164
---------- 1966: 164, 165
Boakye, P.G. 1993: 256, 260, 261
---------- 2001: 537, 538
Bogardi, J. & K.D.W. Nandalal 1989: 503
Bolton, B. 1984: 360
Boonyatharokul, W. & W.R. Walker 1979: 170, 172
Borchert, G. & S. Kempe 1985: 358, 359
Borzenkova, I.I. 1980: 65, 444
Bouchet, R.J. 1963: 129
Bouzaiane, S. & A. Lafforgue 1986: 406-09
Bradely, D.J. 1978: 588
Bredenkamp, D.B. 1999: 553
Brown, D.S. & C.A. Right 1985: 590
Bruin, H.A.R. de & J.Q. Keijman 1979: 126
Brutsaert, W.H. 1982: 41, 128
Buckley, D.K. & P. Zeil 1984: 550
Budyko, M.I. 1956: 57, 61
---------- 1986: 215
Bullock, A. & A. Gustard 1989: 225, 227
Bultot, F. 1971: 39, 194, 196, 197
Bultot, F. & G.L. Dupriez 1987: 231, 235, 240, 335, 343-45, 348
Bunting, A.H. et al. 1976: 67
Bunting, A.H. 1987: 19, 20
Burke, J.J. & M. Jones 1993: 438, 439
Burman, R. & I.O. Pochop 1994: 157, 158
Butzer, K.W. 1966: 66

Calder, I.R. et al. 1995: 144, 471
Carbonnel, J.P. & P. Hubert 1989: 251, 319, 384
Carmouze, J.P. & G. Pedro 1977: 333
Chengoli, R.W. 1999: 543
Chilton, P.J. & A.K. Smith-Carington 1984 546, 547
Chow, V.T. 1951: 100, 408
Christiansen, J.E. 1966: 39
Club du Sahel 1979: 498
Cogels, F.X. et al. 1997: 448, 449
Combremont, R. 1972: 193, 195
Conrad, V. 1946: 33
Coughanower, C. 1994: 509
Coulter, G.W. & R.H. Spiegel 1991: 465, 466
COWAR 1993: 18

Crul, C.R. 1997: 14, 137, 441, 442, 466-69, 471, 472
---------- 1998: 446, 447, 454, 463, 473, 474

Dagg, M. 1972: 209
Davy, E.G. 1974: 309
Dawdy, D.R. & T. O'Donnel 1965: 260, 261
Demarée, G. 1987: 231
Demarée, G.R. & C. Nicolis 1990: 72, 73
Dennet, M.D. et al. 1985: 67
Denny, P. (ed.) 1985: 203, 427-29, 431, 433, 475
Dieng, B. 1989: 537
Dincer, T. et al. 1987: 437, 438
Doorenbos, J. & A.H. Kassam 1979: 188
Doorenbos, J. & W.O. Pruitt 1977: 41, 157, 165, 166, 170, 176, 178, 188
Doyle, P. 1990: 129
Drayton, R.S. 1984: 470
Drijver, C.A. & M. Marchand 1985: 439, 440
Drijver, C.A. & J.C.J. van Wetten (eds.) 1992: 430
Dubreuil, P. 1961: 320
Dunne, T. 1979: 269
Dupriez, G.I. 1959: 161, 194
Dutch Ministry of Foreign Affairs 1998: 360, 366, 403, 405, 598

Edmond, J.M. et al. 1993: 466
El-Agib, N.A. 1995: 34, 140, 141
El-Bakry, M.M. 1975: 126, 134
El-Gibali, A. 1966: 177
Ellenbroek, G.A. 1987: 439
El-Nokrashy, M.A. 1963: 178
El-Shal, M.I. 1966: 177
El-Sheikh, S. et al. 1991: 492
Eltahir, E.A.B. 1996: 303, 358
Elwan, M.Y. 1995: 289
Elwan, et al. 1996: 285
Encyclopaedia Britannica *(The New)* 1988: 361, 363, 462
---------- 2001: 565, 572
Engelman, R. & P. Le Roy 1995: 19, 22, 23
Enikeff, M.G. 1950: 320
Entz, B.A.G. 1976: 484
Environmental Rights Action 1999: 500
Evans, R. 1980: 214
Evans, T. 1994: 66
Ezzat, M.A. 1976: 524

Fahmy, A. et al. 1982: 300
Faloci, M.L. 1984: 444, 446
FAO 1979: 188
------- 1981: 9
------- 1986: 264
------- 1987: 4, 6, 18, 19, 20, 23, 87
------- 1989: 176
------- 1993: 585, 586
------- 1995: 569, 581, 584
Fathi, A.M. 1995: 176, 178
Faure, H. & J. Gac 1981: 251
Fiering, M.B. & B.B. Jackson 1971: 480
Flohn, H. & H. Wittenberg 1980: 139, 140
Flohn, H. & Th. Burkhardt 1985: 299, 452, 453
Flohn, H. 1987: 453
Foster, S.S.D. & P.J. Chilton 1998: 510

Gac, J.Y. 1981: 331
Gallais, J. 1967: 320
Gamachu, D. 1977: 183, 184
Ganesan, C.T. 2001: 549
Gautier, F. et al. 1998: 74
Gentilli, J. 1972: 55
Gibbs, S. 1996: 591
Girard, G. 1975: 222, 226
Gischler, C.E. 1967: 328
Glantz, M.H. 1987: 67
Gleick, P.H. 1993: 23
Glover, J.N. & J.S. McCulloch 1958: 42, 205
Glover, J. & J. Forsgate 1964: 206
Golterman, H.L. 1975: 468
Griffiths, J.F. 1972: 25-27, 30, 50, 60, 88, 90, 98, 99, 145, 146, 154, 155, 200
Griffiths, I.L. 1984: 584
Grove, A.T. 1970: 542, 575, 579, 586
---------- 1972: 320, 321, 333, 386, 389, 447
---------- 1978: 9
---------- (ed.) 1985: 243, 251, 320, 323, 324, 333, 390, 394, 436, 445, 476, 496, 499, 500
---------- 1998: 356

Hall, A. et al. 1977: 359
Hall, M.J. et al. 2001: 260
Hanna, L.W. 1971: 198
Hargreaves, G.H. 1956: 166
---------- 1975: 188
Hargreaves, G.H. & Z.A. Samani 1982: 166
Hargreaves, G.L.et al. 1985: 188
Harrold, L.L. 1966: 159

Hart, R.C. 1985: 372, 373
Hartung, F. 1978: 488, 490
Hastenrath, S. & R. Kruss 1992: 34
Heederik, J.P. et al. 1984: 198, 200, 421
Heny, K. et al. 1991: 525
Henriques, A.G. & H.S. Silva 1991: 505
Herbst, P.H. et al. 1966: 75
Heusch, B. 1970: 268
Heusch, B. & A. Milliés-Lacroix 1971: 415
Heusch, B. & O. Cayala 1986: 416
Hillel, D. 1980: 170
Hipel, K.W. & A.I. McLoed 1978: 295
Holeman, J.N. 1965: 264, 359
Hori, H. 1991:476
Morton, R.E. 1933: 213
Howard-Williams & P. Gaudet 1985: 203
Howell, P.P. et al. (eds.) 1988: 431, 435
Hubert, P. & J.P. Carbonnel 1987: 73
Hurst, H.E. 1927: 281
---------- 1935: 302
---------- 1950: 205, 219, 281, 288, 291, 460
---------- 1952: 592
---------- 1956: 482
Hurst, H.E. et al. 1951: 484
---------- 1959: 133, 134, 281, 290, 486
---------- 1966: 288
Hurst, H.E. & P. Philips 1931: 121, 123, 133-35, 184, 281, 455
---------- 1938: 134, 219, 281, 287, 431, 434, 453, 458, 459, 481
Hussein, A.S. et al. 1986: 270
Hussein, A.S. & A.K. El-Daw 1989: 181, 183, 184
Hussein, M.T. 1986: 528
Hutchinson, G.E. 1957: 441
Hutchinson, P. 1985: 417

Ibrahim et al. 1995: 176
ICID 1973: 194, 199
------ 1987: 18, 19
Imru, M. 1992: 599
Ishag, A.S. 1976: 510
Israelsen, O.W. 1956: 159

Jacenkow, O.B. 1984: 516, 561, 562
Jäkel, D. 1984: 326
Jarvis, C.S. 1935: 256
Jenkinson, A.F. 1973: 67
Jensen, M.E. & H.R. Haise 1963: 167
Jensen, M.E. 1966: 168, 170
Jensen, M.E. et al. (eds.) 1990: 166, 168-70, 172
Johnson, P.A. & P.D. Curtis 1994: 183, 184, 186
Jury, M.R. 1998: 505, 507

Kalinin, G.P. 1971: 215
Kamutanda, K. 1979: 106-08
Kashef, A.Z. 1981: 282
Katashaya, G.G. 1986: 311, 312
Katul, G.G. et al. 1992: 158
King, K.M. et al. 1956: 160
Kite, G.W. 1981: 134, 451
---------- 1984:
Kloos, H. et al. 1998: 590
Kohler, M.A. et al. 1955: 128, 129
Kohler, M.A. & I.H. Parmele 1967: 128, 129
Köppen, W. 1931: 55
Kottegoda N.T. & J. Elgy 1977: 257
Kottegoda, N.T. 1980: 478, 479
Krhoda, G.O. 1989: 421, 543
Krishna, R. 1986: 272
Kurzon, Y. 1978: 53, 54, 57, 196, 198, 199, 201, 202, 215, 217, 328
Kuusisto, E.E. 1985: 427, 441,

Lamagat, J.P. 1989: 320
Lamb, H.H. 1966: 453
---------- 1973: 80
Latif, A.F. 1984: 489
Lee, A.F.S. & S.M. Heghinian 1977: 251
Le Maître, D.C. & D.B. Versfeld 1997: 210
Leopold, L.B. 1962: 359, 360
Linden, van der W. 1986: 527
Linsley, R.K. et al. 1958: 113, 121, 264
Lloyd, J.W. 1986: 515
---------- 1990: 517
---------- 1994: 515, 516
---------- 1995: 551
---------- (ed.) 1999: 515, 551, 555
L'vovich, M.I. 1979: 23, 51, 113, 137, 213, 215, 216, 218, 220
Mahé, G. & J.C. Olivry 1995: 74, 75
Makholibe, S. 1984: 267, 269, 372
Mandelbrot, B.B. & J.R. Wallis 1968: 483
Mankarious, W.F. 1979: 135, 137, 139
Margat, J. 1979: 214
Margat, J. & K.F. Saad 1984: 517, 518, 559, 560
Martins, O. & J.L. Probst 1991: 2, 359, 368, 372, 418, 419
Martonne, E. de 1926: 55

Martyn, D. 1992: 32, 46, 88, 92
Mathieu, R. et al. 1989: 518
Matondo, J.I. & P. Mortensen 1998: 350, 353, 355, 357, 360, 439
Mauritania 1986: 533-535
Meigs, P. 1951: 56
Meybeck, M. 1976: 349, 359
Meyer, P.S. 1998: 552, 553
Midgley, D.C. et al. 1969: 368
Migahid, A.M. 1948: 205
---------- 1952: 205
Milliman, J.D. & R.H. Meade 1983: 264, 265, 331
Molinier, M. & E. Mbemba 1979: 346
Moorehead, A. 1983: 15, 16
Moradini, G. 1940: 461
Morocco 1986: 196, 414
Morton, F.I. 1979: 122, 128, 133
---------- 1983: 126, 128, 130, 133, 174
---------- 1986: 131
Moukolo, N. 1989: 544
Mutale, M. 1994: 439

Nace, R.C. 1969: 521
Nair, K.R. et al. 1984: 557
Nash, I.E. 1989: 129, 174
NEDECO 1959: 266, 268, 304, 317, 322, 450
---------- 1975: 414, 415
Neuland, H. 1984: 137, 470
Nicholson, S.E. 1983: 70, 80
---------- 1985: 68
---------- 1986: 80, 81
Nieuwolt, S. 1977: 5, 36, 37
Nile Control Staff 1979: 455
Nkounkou, R.R. & J.L. Probst 1987: 349, 350

O'Conner, A.M. 1991: 585
Ogembo, V.G. 1977: 219, 424
Ojiako, G.U. 1985: 539, 541
Olivier, H. 1961: 120, 179, 180
---------- 1977: 496, 501, 502, 504, 505
Omar, M.H. & M.M. El-Bakry 1970: 133
---------- 1981: 126, 131, 133
Ongwenyi, G.S. et al. 1993(a): 421, 424
---------- 1993(b): 425
OuldEl-Joud, M.Y. 1993: 154, 532
Owoade, A. et al. 1989: 539, 541
Oyebande, L. 1962: 110, 111

Paffen, K. 1966: 5
Paling, W.A.J. 1988: 366
Paling, W.A.J. & D. Stephens 1988: 85, 358, 368-71
Pallas, P. 1978: 559, 560
Paulhus, J.L.E. 1965: 104
Penman, H.L. 1948: 113, 126, 128, 129, 168, 181, 183, 184
---------- 1956: 127, 130, 205, 206
Pinder, G.F. 1973: 562
Piper, B.S. et al. 1986: 134, 451
Plate, E.J. 1993: 596
Plate, E.J. & P. Wengefeld 1979: 443
Plisnier, P.D. 1996: 34, 35, 357, 466
Popper, W. 1951:294
Postel, S. 1992: 18
---------- 1993: 18
Pottinger, L. 1997: 495, 496
Pouyaud, B. 1989: 136, 152, 328
Probst, J.L. & Y. Tardy 1987: 346
Probst, J.L. et al. 1992: 349
PTJC 1982: 293, 487, 493, 494, 497
------- 1983: 495, 497
------- 1984: 496

Quaye, G. 1993: 74, 76, 77

Reffay, L. 1948: 309, 319, 321, 322
République Islamique de Mauritanie 1986: 533
Reusing, G. 1994: 295, 298, 302
Riehl, H. et al. 1979: 300
Rijks, D.A. 1967: 179
---------- 1968: 179
---------- 1969: 179, 198, 205-07
---------- 1971: 179, 180, 182
Riou, C. 1970: 189, 190
---------- (±1975): 148, 151, 152, 190, 191, 193, 196
---------- 1975: 336
Roche, M.A. 1969: 333
---------- 1975: 152, 333
Roche, M.A. 1981: 333, 334
Roche, M.A. et al. 1976: 66, 67, 71, 232, 241, 242, 330, 331
Rochette, C. 1974: 379-381, 383, 384, 386-388
Rodier, J. 1964: 5, 219, 307, 312, 313, 322, 325, 329-31, 379, 384, 388, 392-94, 397, 398, 446
---------- 1976(a): 222, 226
---------- 1976(b): 223, 224
---------- 1976(c): 227
---------- 1985: 223, 265, 367

Rodier, J. 1989: 223, 225, 410, 414
Rodriguez Iturbe, I. & J.B. Valdes 1979: 259
Rzóska, J. (ed.) 1976: 459, 461

Sadek, M.F. 1992: 42, 124, 127, 128, 130, 131, 134
Sadek, M.F. et al. 1997: 131, 293, 286
Said, R. 1993: 281
Salas, J. D. et al. 1981: 284-86
Salem, O.M. 1991: 529-32, 559, 560
Schaake, J.C. & L. Chunzehn 1989: 186
Schultz, G.A. 1976: 480, 481
Schutte, C.H. et al. 1995: 590
Schwarz, J. 1989: 509
Scott, D.F. & W. Lesch 1997: 371
Sekwale, M. & E.T. Selaolo 1991: 549, 550
Sellars, C.D. 1981: 313
Semaika, M.R. & M.A. Rady 1988: 176
Senden, W. & K.M. Saleh 1986: 527
Shahin, M. 1959: 178
---------- 1969: 139, 140
---------- 1983(a):251
---------- 1983(b): 525
---------- 1985: 33, 36, 42, 134, 136, 159, 180, 184, 250, 278, 280, 281, 286, 289, 290, 292-94, 455, 456, 458, 477, 491
---------- 1986(a): 267
---------- 1986(b): 316, 318
---------- 1993: 492
---------- 1994: 292
---------- 1999: 34, 35
Shahin, M. & M.I. El-Shal 1969: 177
Shahin, M. et al. 1993: 93
Shalash, S. & A. Makary 1986: 487
Shapiro, R. et al. 1999: 590
Sharma, T.C. 1985: 262, 263
Shata, A.A. 1995: 557
Shaw, E.M. 1984: 107, 114
Shenouda, R. et al. 1966: 177
Sherif, M.M. et al. 1990: 562
Shih, S.F. 1984: 158, 162
Shiklomanov, I.A. 1990: 137, 215
Singh, V.P. et al. 1981: 259
Sircoulon, J. 1976: 445
Sivakumar, M.V.K. et al. 1993: 185-187
Snijders, T.A.B. 1986: 73
Stamp, L.D. & W.T. Morgan 1972: 13, 19, 22, 43, 44, 46, 323, 336, 351, 361, 543, 545, 567, 576, 580
Starmans, G.A. 1970: 473
Stigter, C.J. & E.A.C. Kisamo 1978: 113, 127
Straosolszky, Ö. 1974: 442
Stretta, P. 1983: 548
Sudan, The (ed. A. Hedayat) 1986: 526, 528
Sutcliffe, J.V. 1974: 205
Sutcliffe, J.V. & J.B.C. Lazenby 1989: 316, 317, 384
Sutcliffe J.V. & Y.P. Parks 1987: 205, 434
---------- 1989: 209, 435-37
---------- 1994: 141, 205
---------- 1999: 235, 237, 276, 279, 281, 283-86, 288, 290-92, 294, 431, 434, 454, 456
Sutcliffe, J.V. & W.R. Rangeley 1960: 422
Sutton, L.J. 1950: 138
Sweers, H.E. 1976: 130
Szalay, M. 1973: 299

Talling, J.F. 1966: 454
Tanner, C.B. 1967: 170, 171
Terap, M.M. 1991: 539, 540
Thomas, H.A. & M.B. Fiering 1962: 371
Thompson, B.W. 1965: 88, 90
Thompson, K. 1975: 275
Thornthwaite, C.W. 1948: 56, 166
Timberlake, L. 1985: 16
Timmer, C.E. & L.W. Weldon 1967: 203
Todd, D.K. 1959: 511, 514, 516
Traora, S. 1989: 389
Trewartha, G.T. 1962: 62, 64

U.K. Consultant; Mac Donald, M. 1985: 447
UNEP 1985: 9
------- 1993: 56
UNESCO 1970: 137, 153, 193
---------- 1971: 232, 309, 311, 397
---------- 1979:413
---------- 1981: 123
---------- 1991: 565, 574, 578
---------- 1995: 232, 309, 311-13, 328, 339, 341, 353, 363, 366, 392, 394, 397, 398,401, 403, 414, 421, 571, 578
---------- 1996: 232, 315, 329, 353, 363
UNESCO/IHP/MaB 1992: 565
UNESCO/UNDP 1970: 154
USBR 1964: 158
USDA/SCS 1967: 165

Verruijt, A. 1970: 514

Wallén, C.C. 1968: 91

Walling, D.E. 1984: 266, 268, 415, 416, 425
Walsh, J.F. 1985: 589
Walton, K. 1969: 55
Wassing, F. 1964: 489, 490
Watson, H.K. 1984: 373, 374
Weert, R. van der & G. E. Kamberling 1974: 204, 205
Westlake, C.et al. 1954: 495
Wharton, G. & J.J. Tomlinson 1999: 229
Whittington, D. & G. Guarisso 1983: 133
Willmott, C.J. et al. 1985: 215
Wilson, E.M. 1983: 512
Wisler, C.O. & E. F. Brater 1957: 513
WMO 1966: 115, 157, 160, 161,462
------- 1973: 7
------- 1974: 94, 97, 100, 107, 109, 118, 123, 126, 129, 134, 135, 219, 220, 228, 455, 456, 458, 459
WMO 1976: 118
------- 1983: 122, 124, 281
World Bank 1990: 584
World Guide 1977: 4, 19, 22
World Resources Institute/UNEP/UNDP 1994: 585, 586
Wright, J.L. 1982: 158
Wright, E.P. 1983: 7, 8, 511, 516

Yevjevich, V. 1967: 75
---------- 1972: 235, 250, 256, 257
---------- 1983: 294
Yen, X. & S.E. Nicholson 1998: 42, 128, 135, 453, 454

Z.D.M.S. 1981: 39, 47, 102, 103, 108, 110, 142, 143
Zoppis, L. & R. Zoppis 1989: 558

GEOGRAPHICAL INDEX

The Geographical Index includes the names of places; countries, cities, seas, oceans, rivers, mountain ranges, islands, dams and reservoirs, and meteorlogical and hydrometric stations that appear in the text of the book. Opposite each of these names the corresponding page numbers are listed. The following abbreviations have been adopted:

Afr.	= Africa	Mt.	= Mountain
Agr.	= Agriculture	N.	= North
Atl.	= Atlantic	Oas.	= Oasis
Bas.	= Basin	Oc.	= Ocean
Catch.	= Catchment	Plat.	= Plateau
Depr.	= Depression	R.	= River, water course
Des.	= Desert	Reg.	= Region
E.	= East	Reserv.	= Reservoir
Exp.	= Experimental	Val.	= Valley
Fl. Pl.	= Flood plain	S.	= South
H.	= Hydrometric	St.	= Station
Ind.	= Indian	Sw.	= Swamp, marsh
Isl.	= Island	Torr.	= Torrent
Kh.	= Khor (torrential stream)	W.	= West
L.	= Lake	Wad.	= Wadi (intermittent stream)
M.	= Meteorological		

The abbreviated function of each item is given between parentheses followed by / and the country to which it belongs or from which it originates, all in italic type letters. Whenever the item has another name it is also included between the parentheses.

Abanga *(Ibanga, H. St./Gab)*: 399
Abaya *(L. Sw./Eth)*: 433
Abecher *(M. St./Chd)*: 59, 326, 327, 445
Aberdar *(Mt./Ken)*: 422
Abidjan *(M. St./IvC)*: 3
Abuja *(Nig)*: 3, 312
Accra *(M. St./Ghn)*: 3, 498
Adamawa Plateau *(Highland/Cmn)*: 307, 325, 335, 396, 446
Addis Ababa *(M. St./Eth)*: 3
Adrar *(Reg./Alg, Mrt)*: 535
Afakora *(Mts./Tog)*: 391
Afram *(R./Ghn)*: 389, 390, 538
African Horn *(Reg./E. Afr.)*: 50
Agades *(M. St./Ngr)*: 58, 559
Agadir *(M. St./Mor)*: 32, 58
Agalega *(M. St./MtI)*: 82, 577
Ahaggar Massif *(Alg)*:2
Ain Timedrine *(H. St./Mor)*: 413
Ait Ochene *(H. St./Mor)*: 220
Aiyetoro-Ijebu *(Bas./Nig)*: 539
Ajena *(Ghn)*: 390, 496
Akanyoro *(R./Ugd)*: 219, 229, 274, 452, 591
Akobo *(R./Eth)*: 278
Akosombo Dam *(Volta, Reserv./Ghn)*: 390, 391, 394, 395, 405, 427, 483, 496-98, 593, 595, 596
Akwapim Hills *(Ghn)*: 390, 496
Al-Aioun *(WSh)*: 4
Alaotra *(Sw./Mdg)*: 433
Albaqaara *(Sud)*: 526
Albert *(L./Ugd, CnK)*: 7, 13, 17, 123, 124, 129, 221, 273-75, 283, 284, 300, 302, 456-61
Albert Nile *(R./Ugd)*431, 458
Aldabra *(Atol./SyI)*: 574
Alexander Bay *(M. St./SAf)*: 60, 363
Alexandria *(M. St./Egy)*: 58, 139, 556
ALGERIA: 3, 5, 7, 21, 23, 98, 264, 269, 323, 416, 444, 517
Algiers *(M. St./Alg)*: 3, 38
Alibori *(R./Ben)*: 314
Aliwal Noord *(R., H. St./SAf)*: 362, 365
Al-Minya *(M. St./Egy)*: 34
Alsace-Lorrine *(France)*: 3
Al-Taiyba *(M. St./Sud)*: 95, 96
Amaramba *(L., Sw./Mlw, Moz)*: 433
Amazone *(R./S. America)*: 338, 350
Ambanja *(H. St./Mdg)*: 220
Ambidedi *(H. St./Mal)*: 381, 387
Ambilobe *(H. St./Mdg)*: 576
Ameki-Ogwashi-Asaba *(Bas./Nig)*: 539
Am Timan *(H. St./Chd)*: 329, 330
Anambra *(R./Nig)*: 307, 432
Andiou *(Wad./Tun)*: 406
ANGOLA: 3, 9, 21, 23, 39, 45, 74, 87, 210, 335, 336, 504, 585, 598
Ankobra *(R./Ghn)*: 538
Ankola *(L./Ugd)*: 432
Ankwa *(R. /Nig)*: 307
An-Nahud *(Sud)*: 526
Antalaha *(M. St./Mdg)*: 52, 582
Antananarivo *(Mdg)*: 52,580
Aruwimi *(R./CnK)*: 339
Ascension Island *(AsI,/S. Atl. Oc.)*: 57, 572, 573
Ashanti *(Plat./Ghn)*: 390
Asmara *(M. St./Ert)*: 3, 58
Assab *(M. St./Ert)*: 59
Assab Massif *(Highland/Mrt)*: 379, 380
Assiut Barrage *(M. St., H. St./Egy)*: 58, 280, 293, 294
Assua *(Torr. R./Sud)*: 275, 283
Aswan *(M. St./Egy)*: 17, 32, 38, 58, 138
Aswan High Dam *(Reserv.,H.St./Egy)*: 113, 124, 126, 232, 233, 251, 270, 277, 280, 290, 293, 294, 300, 302, 303, 315, 453, 483, 485, 486, 489, 494, 591, 594-96
Aswan Old Dam *(Reserv./Egy)*: 279, 486, 592, 606
Atakora Massif *(Highland, Ben)*: 393
Atakpamé *(M. St./Tog)*: 83
Atar *(M. St. /Mrt)*: 32, 58, 189
Atbara *(M. St./Sud)*: 13, 58, 267, 271, 277
Atbara *(R., H.St./Sud., Eth)*: 17, 251, 291, 292, 300, 302
Atem *(Tor. str./Sud)*: 285, 278
Atlantic Ocean: 11, 25, 45, 194, 198, 304, 309, 335, 361, 363, 377, 380, 399, 412, 416, 537, 573, 600
Atlas *(Mts./Mor)*: 28, 268, 412, 413, 516, 521
Augrabies *(Falls/SAf)*: 363
Awach-Kaboun *(Catch. /Ken)*: 221
Awai *(R. /Sud)*: 276, 278
Awasa *(Sw./Eth)*:433
Awash *(R., H. St./ Eth)*: 599
Aweil *(M. St./Sud)*: 285
Ayame *(H. St. /Nig)*: 220
Ayensu *(R., Bas./Ghn)*: 260
Azib Soltane *(H. St. /Mor)*: 412-15
Azores Islands *(AzI/N. Atl. Oc.)*: 43, 566, 567, 569
Azzaba (*M. St./ Alg)*: 105, 106

Babouch *(Wad./Tun)*: 406
Bafing *(R./Gun, Mal)*: 377, 379, 380, 384, 385, 483, 495
Bafoulabé *(Bafoulabé, R., H. St./Mal)*: 378, 379, 381, 387
Bafoussam *(H. St./Cmn)*: 398
Bagoe *(R./Mal)*: 305
Bahr Aouk *(R./CAf,Chd)*: 325, 327, 329
Bahr Azoum *(R./Sud, Chd)*: 325, 327, 329, 331
Bahr Dar *(M. St./Eth)*: 461
Bahr el-Arab *(R./Sud)*: 276, 278
Bahr el-Ghazal *(R.,Sw./Sud)*: 141, 205, 276, 278, 286, 287, 300, 323, 327, 336, 431, 434
Bahr el-Jebel *(R.,Sw./Sud)*: 17, 205, 244, 274, 276, 278, 283, 285-88, 431, 434
Bahr el-Zaraf *(R, Sw./Sud)*: 276, 278, 286
Bahr Erguig *(R./Chd)*: 325, 327, 330
Bahr Kamer *(R./Chd)*: 325
Bahr Keita *(R./Chd)*: 325, 327
Bahr Sara *(R./Chd)*: 325, 329-31, 333
Bahr Salamat *(Chd)*: 325, 327, 330
Bahteem *(Agr. Exp. St./Egy)*: 176
Ba-Illi *(R./Chd)*: 191, 326, 327, 331
Bakel *(H. St./Sng)*: 17, 232, 235, 241, 377, 379, 380, 386, 387
Bakoye *(R. Mai)*: 377, 379, 380, 384
Balabori *(H. St./Mal)*: 379, 381
Balas *(Kh./Eth)*: 290
Bamako *(Mal)*: 3, 305, 310, 600
Bambesa *(M. St./CnK)*: 336
Bamboi *(H. St./Ghn)*: 392
Bamingui *(R./CAf)*: 324, 325, 327, 329
Bandama *(R./IvC)*: 306, 593
Banfora Cliffs *(Highland/BrF)*: 392
Banghazi *(M. St./Lib)*: 58, 531
Bangoran *(R./CAf)*: 324, 325, 327
Bangui *(M. St., H. St./CAf)*: 3, 17, 190, 191, 232, 336, 346
Bangweulu *(L., Sw./Zmb)*: 13, 199, 207, 339-41, 428, 429, 472, 473
Bani *(R./Mal)*: 304, 305, 313, 436
Banifing *(R./BrF)*: 305
Banigue *(R./IvC)*: 305
Banjul *(M. St./Gmb)*: 3
Baoulé *(Bafoulé,R./Mal)*: 305, 377
Bara Issa *(R./Mal)*: 307
Barakat *(Sud)*: 526
Bari *(R./CAf)*: 339, 340
Baringo *(L./Ken)*: 433
Baro *(R./Eth)*: 287, 288, 300
Baro *(H. St./Nig)*: 276, 310, 314, 315, 317
Barou *(*H. *St./Ben)*:318
Bashile *(Kh./Eth)*: 290
Bata *(Eq. Gun)*: 3
Batha *(Wad./Chd)*: 326
Batouri *(M. St./Cmn)*: 397
Battoum *(Wad./Tun)*: 406
Beaufort West *(M. St./SAf)*: 60
Bebedjia *(Chd)*: 191
Beitbridge *(M. St., H. St./Zmw)*: 32, 50, 403
Beitbrug *(H. St./SAf)*: 403, 404
BELGIUM: 14
BENIN: 3, 9, 13, 21, 38, 74, 304, 305, 307, 389, 393, 499, 594
Bénoué *(R./Cmn)*: 239
Benue *(R./Nig)*: 304, 307, 309, 315, 316, 320, 322, 331, 600
Benue *(Bas./Nig)*: 307, 326, 539
Berarara *(R./Ugd)*: 274, 457
Berbera *(M. St./Som)*: 59
Bétaré-Oya *(M. St., H. St./Cmn)*: 397
Bethulie *(SAf)*: 362
Betsiboka *(R.Mdg)*: 244, 581
Bilma (*M. St./Ngr)*: 32, 58
Biltine *(Wad./Chd)*: 326
Birao *(M. St./CAf)*: 89
Biskra (*M. St./Alg)*: 58
Bissao *(GnB)*: 3
Black Gorgol *(Wad./Mrt)*: 377, 400
Black Volta *(Moun Houn, V. Noire, R./BrF, Ghn)*: 244, 389, 390, 392, 393, 496
Blantyre *(M. St./Mlw)*: 145
Bloemhof Dam *(Reserv./SAf)*: 362
Blue Nile *(Abbay R./Eth., Sud)*: 17, 117, 119, 179, 184, 185, 235, 240, 266, 267, 271, 276, 277, 288, 291, 299, 301, 460, 483, 489, 491, 492, 592, 597, 600
Boa Vista *(CVI)*: 568
Bobo Dioulasso *(M. St./BrF)*: 49, 390
Bodelé *(Depr./Chad)*: 323
Boegoeberg Dam *(Reserv./SAf)*: 362
Boghe *(H. St./Sng)*: 381, 387, 388
Bolama *(M. St./GnB)*: 52
Bol-Dune *(M. St./Chd)*: 148, 150
Boma *(CnK)*: 341
Bongor *(H. St./Chd)*: 326, 327, 329, 331
Booué *(H. St./Gab)*: 399-401
Bor *(H. St./Sud)*: 275, 277
Boromo *(M. St./BrF)*: 32, 392, 393, 536
Bossangoa *(H. St./CAf)*: 191, 327
Bossélé-Bali *(H. St./CAf)*: 339
Boteti *(R./Bot)*: 437

BOTSWANA: 3, 21, 23, 45, 47, 115, 202, 209, 226, 350, 351, 361, 366, 402, 427, 437, 549, 598, 599
Bouati Mahmoud *(M. St./Alg)*: 105
Bougouni *(M. St./Mal)*: 96
Bougouri *(R./BrF)*: 392
Bougouriba *(R./BrF)*: 389
Bousso *(H. St./Chd)*: 329
Boutilimit *(M. St./Mrt)*: 58
Bozoum *(H. St./Chd): 220*
Brazzaville (*M. St, H. St./CnB)*: 148, 149, 190-92, 338, 445, 556
Brokopondo *(L./Sur)*: 204
Bua *(R./Mlw)*: 469
Bubu *(H. St./Tnz)*: 239
Bugondo *(H. St./Ugd)*: 456
Bui Dam *(Reserv./Ghn)*: 391, 392
Bujumbura *(M. St./Bnd)*: 34-36, 465, 466
Bukama *(H. St./CnK)*: 220
Bukoba *(M. St./Tnz)*: 97, 451
Bulawayo *(M. St./Zmw)*: 50, 351
Bundi *(R./CnK)*: 338
BURKINA FASO: 3, 9, 21, 23, 38, 67, 73, 74, 242, 304, 305, 307, 309, 389, 390, 392, 393, 518, 532, 533, 536, 537, 538
BURUNDI: 3, 21, 23, 161, 194, 198, 229, 230, 272, 336, 431, 451, 465
Butiaba *(H. St./Ugd)*: 17, 129, 283, 459
Buyo Dam *(Reserv./IvC)*: 593
Bvumbwe *(M. St./Mlw)*: 469
Bweramule *(H. St./Bnd/Ugd)*: 284, 457

C. Bachar *(M. St./Alg)*: 58
Cabora Bassa Dam *(Reserv./Moz)*: 351, 356, 483, 503-06, 508, 591, 599
Cairo *(Egy)*: 3, 11, 138, 281, 294, 316, 524, 596
Caledon *(R./Les, SAf)*: 266-68, 362, 365, 371
Cameronian Range *(Mts./Cmn): 2*
CAMEROON: 3, 9, 21, 23, 38, 47, 74, 209, 304, 305, 307, 323, 324, 326, 331, 336, 339, 395, 396, 392, 399, 429, 430, 444, 445, 585, 597
Canary Islands *(Canaries, CnI/N. Atl. Oc.)*: 1, 4, 21, 566-68
Cape Hafun *(Alg)*: 1
Cape Town *(M. St./SAf)*: 12, 32, 361
CAPE VERDE *(Isls./N. At. Oc.)*: 1, 4, 21, 24, 243, 311, 566, 568, 569
Casablanca *(M. St./Mor)*: 58
Central Africa *(Reg.)*: 28, 65, 74, 76, 87, 222, 336, 351, 427, 472, 483, 500, 511
CENTRAL AFRICAN REPUBLIC: 3, 20, 21, 24, 32, 38, 74, 189, 304, 323-26, 335, 336, 339, 346, 444, 446, 585
Central Delta *(Mal)*: 305, 307, 436, 443, 449
CHAD: 3, 7, 8, 20, 21, 24, 67, 74, 148, 189, 243, 304, 305, 309, 323, 325, 326, 328, 431, 444, 509, 511, 520, 537, 539, 540
Chad *(L./Bas.)*: 2, 5, 6, 20, 32, 65, 137, 150, 152, 202, 272, 304, 315, 322, 323, 327-29, 331, 443-447, 515, 522, 538, 597
Chaka's Kraal *(Exp. Farm/SAf)*: 201
Challiu Massif *(Mts./Gab, CnB)*: 399
Chambeshi *(R., Bas./Zmb)*: 219, 262, 339
Chan *(R./Chd)*: 17, 235, 241, 243, 244. 251, 323-29, 331-34, 374, 445-47, 537
Chavuma Falls *(Zmb)*: 358
Chaya *(L./Zmb)*: 207
Cheliff *(R./Alg)*: 264
Cherchera *(Wad./Tun)*: 406
Cherfech *(Agr. Expt. St./Tun)*: 152, 153
Chikapa *(H. St./CnK)*: 220, 340
Chiko *(R./CAf)*: 339, 340
Chileka *(M. St./Mlw)*: 469
Chili *(Wad./Chd)*: 326
Chilwa *(L., Sw./Mlw, Moz)*: 433, 441, 473. 474
Chimbili *(Kh./Eth)*: 290
Chingola *(Exp. Bas./Zmb)*: 207
Chipata *(M. St./Zmb)*: 145, 469
Chiromo *(H. St./Mlw)*: 356
Chitedzi *(M. St./Mlw)*: 469
Chiuta *(L. Sw./Mlw, Moz)*: 433, 441, 473
Chobe *(R., Sw./Bot)*: 350, 351, 353
Chokwe *(H. St./Moz)*: 403, 404
Chott *(Wetland/Tun, Alg)*: 5, 433
Cobuè *(R., M. St./Tnz)*: 469
Comoro Islands *(Comoros, CmI/ Ind. Oc.)*: 1, 4, 21, 24, 509, 576
Conakry *(M. St./Gun)*: 3
Congo *(R., Bas.)*: 1, 5-7, 14, 17, 20, 25, 38, 39, 46, 219, 231, 232, 235, 240, 264, 271, 272, 304, 323, 335, 337, 341, 343, 346, 349, 353, 374, 399, 401, 427, 446, 483, 543, 545
CONGO Brazzaville *(Congo)*: 3, 9, 21, 24, 74, 148, 189, 209, 336, 339, 346, 399, 544, 556
CONGO Kinshasa *(Con. Dem. Rep.,Zaïre)*: 3, 9, 21, 24, 32, 47, 74, 119, 161, 194, 198, 209, 272, 336, 339, 429, 458, 464,

CONGO Kinshasa (Cont'd): 465, 472, 483, 501, 502, 511, 544, 548, 585, 591, 593, 599
Cotonou *(M. St./Ben)*: 103
Crocodile *(R./SAf)*: 402, 403
Cuando *(R/Ang, Nmb)*: 351, 580

Dabus *(Kh./Eth)*: 290
Dagana *(H. St./Sng)*: 378, 380-82, 385-88, 405, 418
Daka *(R./Ghn)*: 389, 538
Dakar *(Sng)*: 3, 13, 78, 447
Dakhla *(Oas./Egy)*: 517, 559, 560
Dakka Saidou *(H. St./Mal)*: 381, 382
Dal Cataract *(3rd Cat./Sud)*: 484
Damazin Rapids *(Eth)*: 34, 277
Damietta *(Br. of R.Nile/Egy)*: 281, 488, 490
Dar es-Salaam *(M. St./Tnz)*: 90
Dar Fougoro *(Headwater/CAf)*: 325
Darfur *(Sud)*: 527
Dargol *(R./BrF)*: 307
De Hoop 65 *(H. St./SAf)*: 365
Debasien *(Mts./Ken, Ugd)*: 455
Debra Marcos *(M. St./Eth)*: 30, 185
Débò *(L./Mal)*: 305, 307
Degurre *(H. St.Mal)*: 381
Dejna *(Mal)*: 305
Derb *(Wad./Tun)*: 406
Derna *(M. St./Lib)*: 58
Diama Barrage *(Sng)*: 378, 385, 388, 389, 448, 594
Diarha *(R./Sng)*: 418
Dibia *(H. St./Mal)*: 381
Diedessa *(Kh./Eth)*: 290
Diego Suarez *(M. St./Mdg)*: 82, 582
Digue, La *(Syl)*: 575
Dinder *(R./Sud)*: 277, 291, 300, 301
Dioïla *(H. St./Mal)*: 311
Diolde-Diabe *(H. St./Mrt)*: 381
Diorbivol *(H. St./Sng)*: 381
Dioubeba *(H. St./Mal)*: 381
Diré *(H. St/Mal)*: 251, 310, 311, 313, 319, 320, 436
Dire Dawa *(M. St./Eth)*: 59
Djerem *(R./Cmn)*: 396, 397
DJIBOUTI: 3, 21, 24, 45, 46, 243, 521, 584
Djibouti S. *(M. St./Djibouti)*: 3, 37, 59
Djilma *(Wad./Tun)*:406
Doba *(H.St./Chd)*: 329, 339
Donga *(H.St./Nig)*: 307, 310, 315
Dongola *(H.St./Sud)*: 292-94, 300
Dopola *(H. St./BrF)*: 392
Dori *(M. St/BrF)*: 59, 536
Douala *(M. St./Cmn)*: 39, 397
Douglas *(SAf)*: 362
Douna *(H. St./Mal)*: 310, 311, 313, 319, 436
Dow *(Sw./Bot)*: 433
Dra *(Draa,R./Alg,Mor)*: 220
Drakensberg *(Mts./SAf)*: 361, 362, 371, 373, 431
Durban *(M.St./SAf)*: 90
Dwangwa *(R./Mlw)*: 469

East Africa *(E. Afr., Reg.)*: 7, 19, 28, 42, 76, 78, 87, 127, 160, 198, 205, 243, 451, 465, 510, 584, 587
Eastern Desert *(Egy)*: 520, 523, 524
Edéa *(Falls, H. St./Cam)*: 17, 397, 398, 405
Edinburgh *(Tristan de Cunha Isl)*: 572
Edward *(L./CnK)*: 4, 7, 273, 274, 441, 456-58, 461
EGYPT: 3, 5, 7, 18, 21, 24, 44, 117, 137, 161, 174, 175, 272, 280, 293, 294, 298, 302, 483, 484, 486, 494, 501, 509, 512, 522, 524, 556, 559, 584, 591, 592, 595, 596, 599, 600
El-Abid *(Wad./Mor)*: 220
El-Akhsas *(H. St./Egy)*: 490
El-Fasher *(M. St./Sud)*: 33, 34, 58
El-Fayoum *(M. St./Egy)*: 58
El-Gash *(Wad./Sud)*: 527-29
Elgon *(Mt./Ken)*: 4, 7, 455
El-Nassir *(H. St./Sud)*: 294, 296
El-Obeid *(M. St./Sud)*: 34, 58, 78, 79
El-Tahrir *(M. St./Egy)*: 139
Engelbrechsdrift *(H. St./SAf)*: 365
Ennedi Plateau *(Highland/Chd)*: 326
Entebbe *(M. St./Ugd)*: 118, 198
Equator: 25, 38,43, 80, 233, 597
EQUATORIAL GUINEA: 1, 3, 9, 21, 24
Erigavo *(M. St./Som)*: 59
ERITRIA: 3, 12, 21, 24, 38, 272, 440
Esna Barrage(*H. St./Egy)*: 280, 293
Estcourt *(M. St./SAf)*: 49
ETHIOPIA: 3, 9, 21, 24, 45, 46, 183, 243, 272, 277, 292, 460, 462, 489, 511, 521, 584, 585, 592, 599
Ethiopian Plateau *(Abyssinian Plat.)*: 38, 272, 277

Fada N'Gourma *(Plat., M. St./BrF)*: 393, 536
Fadougou *(H. St./Mal)*: 381

Fafa *(R./CAf)*: 327
Faguibine *(L./Mal)*: 307, 441, 449, 450
Faial *(AzI)*: 566
Falémé *(R./Mal, Sng)*: 17, 377, 380, 382, 389
Faro *(R/Cmn)*: 307, 315, 322
Faroul *(R./BrF)*: 307
Faya Largeau *M. St./Chd)*: 58, 191, 326, 445
Fekka *(Wad./Tun)*: 406
Felou *(H. St./Mal)*: 381
Ferlo Valley *(Sng)*: 447
Ferro *(Hierro/CnI)*: 568
Fès *(Mor)*:412, 413
Fie *(R.Mal)*: 312
Fitri *(L./Chad)*: 326, 327
Flanarntosa *(M. St./Mdg)*: 582
Flores *(AzI)*: 566
Fogo *(CVI)*: 568
Fougamaou *(H. St./Gab)*: 400
Fouta-Djallon *(Highlands/Gun, SrL)*: 304, 377, 416
FRANCE: 13, 14, 328
Franceville *(H. St./Gab)*: 399, 400
Freetown *(M. St./SrL)*: 3
Ft. Dauphin *(M. St./Mdg)*: 146, 582
Ft. Victoria *(Zmw)*: 78, 84
Fuerteventura *(CnI)*: 568
Fulakari *(R./CnB)*: 220
Fullus *(Kh./Sud)*: 278, 288
Funchal (*M. St./MdI)*: 4, 32, 58, 566, 567

Ga'afra (*H. St./Egy)*: 590
Gabes *(M. St./Lib)*: 58
GABON: 3, 9, 21, 24, 45, 209, 216, 399, 429, 544, 570, 585
Gaborone *(Bot)*: 3
Gafsa *(M. St./Lib)*: 58
Galcaio *(M. St./Som)*: 59
Galougo *(H. St.Mal)*: 378, 384, 387
GAMBIA: 3, 11, 21, 24, 243, 311, 416, 598
Gambia *(R./Sng)*: 12, 303, 377, 416-19, 598, 600
Gandiole *(H. St./Sng)*: 381
Garissa (*H. St./Ken)*: 17, 59, 249, 421, 422, 424
Gao *(M. St./Mal)*: 59, 310, 311
Gaoua *M. St./BrF)*: 536
Gariep Dam *(Verwoerd, Reserv./SAf)*: 362, 365, 372, 483, 505, 507, 508, 591, 592
Garoua *(H. St./Cmn)*: 310, 315, 316, 322
Garoubi *(R./Ngr)*: 307
Gedaref *(M. St./Sud)*: 34, 45, 59, 526
Gel *(Tapari. R./Sud)*: 276, 278, 287
George *(L./Ugd)*: 4, 273, 274, 441, 443, 456-58, 461
GERMANY: 13, 14, 480
Germiston *(M. St./SAf)*: 363
Gezira *(Reg./Sud)*: 179, 181, 182, 184, 270, 290, 592
Ghaap Plateau *(SAf)*: 552
Ghadames *(M. St./Lib)*: 58
GHANA: 3, 9, 21, 24, 74, 229, 230, 260, 389-91, 393, 395, 483, 496, 498, 499, 509, 537, 538, 585, 590, 591, 593-96
Ghanzi *(M. St. /Bot)*: 39, 60
Gharsa *(Wetland/Tun)*: *5*
Gitaru Dam *(Reserv./Ken)*: 422
Giza *(Agr.Exp. St., M. St./Egy)*: 58, 138, 139, 164
Gomera *(CnI)*: 568
Gondar *(M. St./Eth)*: 90
Gongola *(R./Nig)*: 307, 315, 322
Gouala (*H. St./Mal)*: 311
Gouina (*H. St./Mal)*: 381
Gouloumbou (*H. St./Sng)*: 417-19
Goundam *(Mal)*: 320
Goura (*H. St./Cmn)*: 398
Gourbassi (*H. St.Mal)*: 381
Graciosa *(AzI)*: 566
Gran Canaria *(CnI)*: 568
Grand Barriére *(L.Chd./Chd)*: 447
Grand Comoro *(CmI)*: 576
GREAT BRITAIN: 13, 14
Great Rift *(Val./E. Afr.)*: 20, 273, 274, 419, 440, 441, 457, 462, 473, 511, 521, 546, 557
Gribingui *(R./CAf)*: 324, 327, 329
Groot Fontein *(M. St./SAf)*: 30, 32, 60
Groot *(R./SAf)*: 361
Groot Aughrabies Falls *(SAf)*: 363, 364
Guede(*H. St./Sng)*: 381
Gueylobe (*H. St./Sng)*: 381
Guiers *(L./Mrt)*: 377, 378, 381, 433, 443, 447, 448, 496
GUINEA: 3, 9, 21, 24, 38, 45, 74, 304, 305, 377, 416
GUINEA BISSAU: 1, 3, 9, 21, 24, 74
Guinean Highlands *(Mts./Gun)*: 2, 311
Gulu *(M. St./Ugd)*: 97, 107, 109
Gurara *(R, Nig)*: 311
Gwaai *(R./Zmw)*: 244, 360

Halluf (*Wad./Tun)*: 406
Hamada Al-Hamra *(Desert/Alg)*: 516, 529

Haouach *(Wad./Chd):* 326
Harare *(Zmw)*: 4, 47, 102
Hargeisa *(M. St./Som)*: 59
Hartbeespoort Dam *(Reserv./SAf)*: 402, 403
Harts *(R./SAJ)*: 362
Hassanab *(H. St./Sud)*: 291, 292, 302
Herbert Falls *(Cmn)*: 397
Hillet Doleib *(H. St./Sud)*: 285, 286, 301, 302
Hillet Nueir *(H. St./Sud)*: 434
Horta *(M. St./AzI)*: 566
Huambo *(M. St./Ang)*: 89
Hunyani *(R./Zmw)*: 504
Huttsgate *(M. St./SHI)*: 573

Ibadan *(Nig)*: 101
Ichkeul (*L., Sw./Tun*): 433
Ikopa *(R./M/g)*: 244, 581
Ilebo *(CnK)*: 337
Illovo *(Exp.Farm/SAf)*: 201
Imo (*R. Bas./Nig*): 539
Impfondo (M. *St./CnB)*: 191, 192
Incomati *(R./Moz)*: 431, 598
Indian Ocean: 2, 11, 25, 43, 45, 46, 49, 350, 351, 356, 402, 403, 419, 469, 577, 579.
Inga Dam *(Reserv./CnK)*: 338, 483, 500, 502, 591
Inzia *(R./CnK)*: 339, 340
Ió Grande *(R./STP)*: 571
Iriki *(Sw./Mor)*: 433
Iro *(Sw./Chd)*: 433
Ishasha *(R./Ugd)*: 274, 457
ITALY: 14
Itasy *(L./Mdg):* 433
Itezhi-Tezhi Dam *(Reserv./Zmb):* 438, 439
Itimbiri *(R. CnK)*: 339
Iullemeden *(Bas./Nig)*: 539
Ivindo *(R./Gab)*: 399, 400, 401
IVORY COAST. 3, 9, 13, 21, 24, 38, 74, 304, 305, 389, 558, 584, 590, 593, 595
Izé-Agua *(H. St./STP)*: 571

Jamma *(R./Eth):* 290
Jebba Dam *(Reserv., H. St./Nig)*: 314
Jebel-Aulia Dam *(Reserv., H. St./Sud)*: 277, 280, 289, 301
Jebel Marra *(Sud)*: 323
Jerid *(Wetland/Tun)*: 5
Jifara *(Gefara/Lib)*: 516, 529, 531, 562, 563
Jijiga *(M. St./Eth)*:*98*
Jinja *(M. St., H. St./Ugd)*: 17, 281, 283, 453
Jonglei Canal *(Div. Can/Sud)*: 278, 431
Jordan Valley *(Jordan)*: 7, 273
Jos (M. *St./Nig)*: 47
Juba *(R./Som)*: 5, 6, 20
Juba *(R., M. St./Sud)*: 34
Jur *(R./Sud)*: 276, 287

Kabanyolo *(M. St./Ugd)*: 198
Kabompo *(R./Zmb)*: 351
Kadiel (Exp. *Bas./Mrt)*: 226
Kaduna(*R.*,M. *St./Nig)*: 307, 310, 314
Kaédi *(M. St., H. St./Mrt)*: 72, 73, 381, 382, 388
Kafironda *(H. St./Zmb)*: 263
Kafue *(R./Zmb)*: 207, 262, 351, 438, 593, 599
Kafue Flats *(Sw./Zmb)*: 199, 207, 263, 350, 351, 356, 427, 437-39
Kainji Dam *(Reserv.,H. St./Nig)*: 147, 314, 320, 321, 483, 498, 500, 590, 591, 595, 596
Kairawan Plain *(Tun)*: 405
Kajera *(R., Bas./Rwd, Ugd)*: 219, 220, 228, 281, 302, 451, 452
Kajnarty *(H. St./Sud)*: 292, 299
Kakamas *(SAf)*: 362, 363
Kakitumba *(R./Tnz)*: 274
Kala *(Torr Stream/Sud)*: 275
Kalahari Desert *(Bot)*: 7, 38, 47, 80, 359, 361, 363, 511, 549
Kalangasa *(R./Tnz)*: 274
Kale *(H. St./Mal)*: 381
Kalungwishi *(R./Zmb)*: 339
Kalurakun *(R./Ghn)*: 389
Kamadougou-Yobe *(R. Sys./Ngr, Nig)*: 326, 327, 331
Kamburu Dam *(Reserv., H. St./Ken)*: 421-23, 425
Kamindi (H.St./Ugd):283
Kampala *(Ugd)*: 4, 90
Kampi *(R./Nig)*: 307
Kamulondo *(Depr. Sw., Fl.Pl./CnK):* 432
Kananga *(M. St./CnK)*: 89
Kandor *(Wad./Chd)*: 326
Kangare *(Mai)*: 305
Kankan (*H. St./Gun)*: 317
Kano *(M. St/Nig):* 47
Kaolack *(M. St. Sng)*: 103
Kapalowe *(H. St. CnK)*: 220
Karakoro *(R./Mrt, Mal)*: 377, 379

Kariba Dam *(Reserv./Zmw, Zmb)*: 351, 356, 358, 427, 483, 501, 503, 504, 506, 591, 594, 596, 599
Karonga (*M. St./Mlw)*: 145, 469
Kasai *(R./CnK)*: 335, 337, 338
Kassala *(Sud)*: 34, 59, 527
Kastina Ala *(R./Nig)*: 307, 315
Kayes *(H. St./Mal)*: 378-80, 382, 384, 386-388
Kazinga *(Connecting channel)*: 274, 275
Kedougou *(H. St./Sng)*: 417
Keetmanshoop *(M. St./Nmb)*: 60
Kelbia *(Sw./Tun)*: 433
KeMacina *(H. St./Mal)*: 320
Kenamuka *(Sw./Sud)*: 204, 432
Kenitra *(Mor)*: 412
KENYA: 3, 7, 9, 21, 24, 46, 88, 115, 117, 243, 264, 269, 272, 419-21, 424, 425, 441, 451, 462, 495, 511, 542, 543, 557, 590, 593, 599
Kenya Mt. *(Ken)*: 7, 420, 422, 425, 43 1
Kericho *(M. St./Ken)*: 87, 421
Kerio *(R./Ken)*: 462
Kharga *(Oasis/Egy)*: 139, 517, 559, 560
Khartoum (*M. St., H. St./Sud)*: 3, 17, 34, 45, 59, 65, 138, 140, 181, 235, 240, 251, 276, 277, 279, 288-91, 294, 301, 302, 489, 600
Khashm el-Girba Dam *(Reserv./Sud)*: 269, 292
Kiambere Dam *(Reserv./Ken)*: 422
Kiambu *(Ken)*: 198, 199
Kidira *(H. St./Sng)*: 17, 378, 380, 381, 387
Kiffa *(M. St./Mrt)*: 58, 189, 378, 379
Kifulula *(Sw., Fl. PI./ Zmb, CnK)*: 432
Kigali *(H. St./Rwd)*: 3
Kigoma *(M. St./Tnz)*: 466
Kilimanjaro *(Mt./Ken)*: 4, 7
Kilo 3 *(H. St./Sud)*: 17
Kilombero *(R., Sw./Tnz)*: 433
Kim *(R./Cmn)*: 397
Kimberly (M. *St./SAf)*: 60, 90
Kimpanzou *(H. St./CnB)*: 220
Kindanima Dam *(Reserv./Ken)*: 422, 425
Kinkony *(L./Mdg)*: 433
Kinshasa *(M. St., H. St./CnK)*: 3, 17, 231, 232, 235, 240, 337, 338, 343, 344
Kinzing *(R./Germany)*: 480
Kiona *(R./Gun)*: 379
Kirango D.S. *(H. St./Mal)*: 311
Kisala *(L./CnK)*: 339
Kisingani *(Stanleyville/CnK)*: 337, 339
Kisumu *(M. St., H. St./Ken)*: 97, 101, 451
Kit *(Torr. str./Sud)*: 275, 377
Kita *(Exp. Farm/Mal)*: 188, 189
Kituza *(M.St./Ugd)*: 198
Kivu *(L./CnK, Rwd)*: 340, 441, 464, 467
Klip *(R./SAf)*: 362
Koka Dam *(Reserv./Eth)*: 599
Koki *(L./Ugd)*: 206, 432
Kolimbine *(R./Mal)*: 377, 379
Konkouré *(R. Gun)*: 220
Kossou Dam *(Reserv./IvC)*: 590, 593, 595
Koulikoro *(H. St./Mal)*: 17, 251, 304, 305, 310-13, 316, 319-21, 436, 479, 600
Kouroussa *(M. St./Gun)*: 310
Kribi *(M. St./Cmn)*: 37, 52, 88, 397
Ksar Geriss *(Agr.Exp. St./Tun)*: 152, 153
Kufra *(M. St., Oas./Lib)*: 33, 58, 529-31
Kuotiala *(M. St./Mal)*: 32
Kurdufan *(Sud)*: 526
Kuruman *(Reg./SAf)*: 552, 554
Kwania *(L./Ugd)*: 432
Kwango *(R./CnK)*: 339, 340
Kwili-kwa *(R./CnK)*: 339
Kyaka Ferry *(H. St./Tnz)*: 228
Kyoga *(L./Ugd)*: 123, 129, 221, 274, 454, 455, 456

Labé *(Gun)*: 378, 379, 382
Laghouat *(M. St./Alg)*: 58
Lagos *(M. St./Nig)*. 38, 101, 111, 147
Laï *(H. St./Chd):* 326, 327, 329
Lambaréné *(H. St./Gab):* 17, 399, 400, 405
Lamedje *(Wad./Tun)*: 406
Lamfara *(R./Nig):* 314
Lami-Tounka *(Mal)*: 379
La Pipe *(H. St./MtI)*: 571
Lastourville *(H. St./Gab)*: 399, 400
Lau *(R./Sud)*: 276
Lazarote *(CnI)*: 568
Lembá *(R./STP)*: 571
LESOTHO: 3, 4, 20, 21, 24, 45, 115, 226, 266, 267, 361-63, 365, 372, 598
LIBERIA: 3, 9, 14, 21, 24, 38, 74, 216, 304
Libcrville *(M. St./Gab)*: 3
LIBYA: 3, 7, 21, 24, 32, 44, 509, 512, 517, 520, 529, 531, 532, 559, 562, 563, 599
Lilongwe *(R., M. St./Mlw)*: 3, 145, 351
Limpopo *(R. Bot)*: 5, 6, 20, 377. 401. 402. 404, 405, 594, 598
Linthipe *(R./Mlw)*:471
Linyanti *(Sw./Bot)*: 432
Lisaka *(R./Cmn)*: 307
Liuwa *(Sw./Zmb)*: 432
Livingstone *(M. St./Zmb)*: 145

Livingstone Falls *(CnK)*: 338, 340
Liwonde *(H. St./Mlw)*: 356
Loa-Loa *(H. St./Gab)*: 400
Lobay *(CAf)*: 339
Lobito *(M. St./Ang)*: 59
Lodwar *(M. St./Ken)*: 59
Logone *(R./Chd)*: 251, 315, 323, 325-30, 332-34, 430, 446, 447, 537
Lokoja *(Nig)*: 307, 310, 315
Lol *(R./Sud)*: 276,187
Lolo *(R./Gab)*: 399
Lom *(R./Cmn)*: 396, 397
Lomami *(R./CnK)*: 339
Lomé *(M. St./Tog)*: 3, 306
Lorrain Swamps *(Ken)*: 433
Lotagipi *(Sw./Sud, Ken)*: 204, 432
Lottila *(R./Sud)*: 278
Lualaba *(R./CnK)*: 14, 335, 339, 341, 472
Luanda *(M. St./Ang)*: 3, 59
Luanginga *(R./Ang)*: 351
Luangwa *(R./Zmb)*: 350, 351, 360, 504
Luano *(Exp. Catch./Zmb)*: 119, 144, 207
Luapula *(R./CnK. Zmb)*: 339, 340, 472
Lubumbashi *(M. St./CnK)*: 89, 106-08, 212
Lüderitz Bay *(M. St./Nmb)*: 60
Lufira *(R./CnK, Mlw)*: 210, 339, 340, 469
Luigi Ferrandi *(M. St./Som)*: 59
Lukanga *(Sw./Zmb)*: 199, 207, 340, 332
Lukuja *(R./CnK)*: 339-41
Lulonga *(R./CnK)*: 339
Lulua *(R./CnK)*: 220, 339, 340
Lungue-Bungo *(R./Ang)*: 315
Lunsefwa *(R./Zmb)*: 599
Luongo *(R./Zmb)*: 339
Lusaka (M. *St./Zmb)*: 4, 36, 37, 438
Lusiko *(R./CnK)*: 339
Luvironzo *(R./CnK)*: 272, 274, 502
Luvua *(R./CnK)*: 340, 472
Lydenburg *(M. St./SAf)*: 119, 120

Machar *(Kh.,Sw./Eth)*: 300
Machiya Ferry (*H. St./Zmb)*: 263
MADAGASCAR: 1, 4, 12, 24, 39, 45, 47, 87, 88, 146, 202, 216, 427, 565, 573, 579, 581, 582, 597
Madeira Islands *(Madeiras, Mdl/N. Atl. Oc.)*: 4, 21, 566-69
Madina *(H. St./Sng)*: 381
Maghreb *(Mt. Reg./Alg., Mor)*: 416
Magui *(Depr./Mal)*: 379
Mahalapye *(M. St./Bot)*: 60, 549
Mahavary North *(R./Mdg)*: 581
Mané *(SyI)*: 574, 575
Mahina *(H. St./Mal)*: 381
Maiduguri *(M. St./Nig)*: 47
Main Nile *(R./Sud, Egy)*: 244, 250, 265, 277, 291, 300, 483, 595
Maintirano *(M. St./Mdg)*: 582
Maio *(CVI)*: 568
Maji *(L./CnK)*: 432
Majunga (*M. St./Mdg)*: 582
Makhalang (*R.*/Les): 365
Makoholi *(M. St./Zmw)*: 342
Makona *(R./Gun)*: 381
Makurdi *(H. St./Nig)*: 147, 310, 315
Malagarasi *(Malagarazi, R., Sw./Tnz)*: 340, 432, 467
Malakal *(M. St., H. St./Sud)*: 17, 34, 138, 179, 251, 275, 276, 285-89, 294, 300-02, 431, 494
Malanville *(H. St./Ben)*: 314
MALAWI: 3, 21, 24, 39, 45, 144, 145, 199, 200, 226, 350-53, 356, 469, 546, 547, 584, 598
Malawi *(Nyassa, L. Mlw, Moz)*: 7, 13, 17, 136, 137, 144, 210, 356, 443, 450, 462, 468-72, 546, 600
Malebo *(Stanley Pool/Cnk, CnB)*: 338
Malendo *(R./Nig)*: 307, 314
MALI: 3, 7, 9, 21, 24, 67, 74, 87, 188, 243, 304, 305, 309, 377, 379, 385, 389, 448, 449, 479, 483, 495, 496, 520, 558, 591, 598
Malimbamatso *(R. headwater/Les)*: 351
Malombe *(L.Mlw)*: 433
Manadiani *(R./IvC)*: 305
Managil *(Irr. Scheme/Sud)*: 270, 290
Mananara *(R., Bas./Mdg)*: 581
Mananjary *(R./Mdg)*: 581
Manantali Dam *(Reserv./Mal, Sng, Mrt)*: 378, 385, 388, 448, 483, 495, 496, 498, 591, 594
Mandinga *(Plat./Mal)*: 379
Mandje *(L./Gab)*: 433
Mango *(M. St., H. St./Tog)*: 393
Mangoky *(R., Bas./Mdg)*: 581
Mansoura *(M. St./Egy)*: 58
Maputo *(R,,M. St./Moz)*: 3
Mara *(R./Ken, Tnz)*: 451, 452
Marchison *(Falls/Ugd)*: 274
Marico *(R./SAf)*: 402
Maromokotro *(RnI)*: 580
Marrakesh *(M. St./Mor)*: 58
Mascarena Islands *(Mascarenas, Ind.Oc.)*: 573
Maseru *(Les)*: 3, 266, 267

Masindi Port *(H. St./Ugd)*: 283
Massaka *(M. St./Ugd)*: 97
Massawa *(M. St./Ert)*: 59
Massinga Dam *(Reserv./Ken)*: 422
Matadi *(CnK)*: 338
Matam *(M. St., H. St./Sng)*: 59, 79, 95, 96, 378, 381, 385, 387
Maun *(M. St./Bot)*: 59
MAURITANIA: 3, 7, 8, 21, 38, 67, 74, 87, 163, 188, 243, 309, 377, 380, 496, 531, 585
Mauritius Island *(MtI/lnd. Oc.)*: 1, 4, 21, 24, 509, 573, 577-79
Mayo-Kebbi *(R./Cmn)*: 307, 315, 322
Mbabane *(M. St./Swz)*: 3
Mbaéré *(R./CAf)*: 325, 339
Mbakaou Dam *(Reserv., H. St./Cmn)*: 396, 397
Mbala *(M. St./Zmb)*: 34-36, 466
Mbalmayo *(H. St./Cmn)*: 220
Mbam *(R./Nig, Cmn)*: 397, 398
Mbarara *(M. St., H. St./Ugd)*: 97
Mbeya Range *(M. St./Tnz)*: 209
Mbuku *(R./Ugd)*: 457
Mediterranean Sea: 11, 33, 281, 293, 488
Mehdiya *(Mor)*: 412
Meinen *(Mts./Mal)*: 379
Mejerdah *(Wad./Tun)*: 152, 264
Mekie *(R./Cmn)*: 396
Meknas *(Mor)*: 412, 413
Mekrou *(R./Ben, Ngr)*: 307, 314
Mellila *(Mor)*: 98
Merguellil *(Wad./Tun)*: 405
Meridi *(R./Sud)*: 276, 278
Meshraer-Req *(Sud)*: 278, 431
Messina *(M. St./Saf)*: 60, 403
Messoudia *(Agr. Exp. St./Tun)*: 152, 153
Milo *(R./Gun)*: 305, 311, 312
Mindelo *(CVI)*: 569
Missinger Dam *(Reserv./SAf)*: 403, 425
Misurata *(M. St./Lib)*: 58
M'jara *(Reserv., H. St./Mor)*: 412, 413
Mlanje *(M. St./Mlw)*: 145
Mogadiscio *(M. St./Som)*: 3, 59, 61
Mogren *(H. St./Sud)*: 288, 289, 301, 302
Mohlokaqala *(H. St./Les)*: 365
Moïssala *(H. St./Chd)*: 327, 329, 330
Mole *(R. Ghn)*: 389, 538
Mombasa *(M. St./Ken)*: 420
Momboya *(R./CnK)*: 339
Mongala *(R./CnK)*: 339
Mongalla *(H. St./Sud)*: 17, 251, 275, 283, 285-87, 294, 300, 302, 431
Mongu *(M. St./Zmb)*: 145
Mono *(R./Ben,Tog)*: 239
Monrovia *(M. St./Lbr)*: 3, 168
Mopti *(H. St./Mal)*: 304, 305, 310, 319, 320, 436
MOROCCO: 3, 7, 13, 21, 24, 194, 268, 412, 415, 416, 584, 586
Moroni *(M. St./CmI)*: 4, 576
Moshi *(R./Nig)*: 307
Mossamedes *(M. St./Ang)*: 59
Moundou *(M. St., H. St./Chd)*: 325-27, 329, 330, 333
MOZAMBIQUE: 1, 3, 9, 11, 16, 20, 21, 24, 45, 47, 210, 350, 353, 360, 402-04, 469, 483, 503, 504, 511, 584, 585, 598
Mozambique Channel: 579
Mpassa *(R./Gab)*: 579
Mtwara *(M. St./Tnz)*: 49
Mufumbiro Range *(Mts./ Rwd)*: 457
Muguga *(Exp. St./Ken)*: 198, 205
Mulanje *(M. St./Mlw)*: 469
Murzuq *(Bas./Lib)*: 529-31, 576
Mwanza *(M. St.,/Tnz)*: 97, 451
Mweru *(L./CnK, Zmb)*: 5, 13, 339, 340, 472, 473
Mweru-Wantipa *(Sw./Zmb)*: 204
Mwisa *(R./Tnz)*: 219
Mzimba *(M. St./Mlw)*:¦145, 469
Mzuzu *(M. St./Mlw)*: 469

Na'am *(R./Sud)*: 276, 278, 287
Nabogo *(R., Bas./Ghn)*: 260
Nachtigal *(H. St./Cmn)*: 396
Nag-Hammadi Barrage *(H. St. Egy)*: 280, 293
Nairobi *(Ken)*: 3, 198, 361, 421, 463, 495, 593
Naivasha *(L./Ken)*: 433, 462-64
Nakta *(Agr. Exp. St./Tun)*: 152, 153
Namaqualand *(Plat./SAf)*: 363
Namib Desert *(Nmb)*: 7, 43, 363
NAMIBIA: 3, 21, 24, 45, 47, 202, 350, 363, 590, 598
Namulonge *(Cot.Exp. St., Sw./Ugd)*: 118, 198, 206
Namwala *(Zmb)*: 439
Nana Barya *(R./CAf)*: 325, 330
Nasser Lake *(Reserv./Egy)*: 137, 280, 484, 489
Natal *(Province/SAf)*: 373
Ncema *(R./Zmw)*: 404
Ncema Dam *(Reserv., H. St./Zmw)*: 404
Ndeiya-Karai *(Ken)*: 421

Ndieké *(R./Cmn)*: 396
Ndini Mrash *(Sw./Mlw)*: 433
N'Djamena *(H. St./Chd)*: 3, 17, 78, 148, 149, 151, 190, 191, 235, 241, 242, 321, 325, 327, 329
N' Djim *(R./Cmn)*: 397
Ndjolé *(Gab)*: 399
Ndo *(R./Cmn)*: 396
Ndola *(M. St./Zmb)*: 52, 207, 549
Nebhana *(Wad./Tun)*: 405
Negelli *(M. St./Eth)*: 59
Nelsptuit *(M. St./SAf)*: 403
Nema *(M. St./Mrt)*: 30, 59
Nero de Sahel *(M. St./Mal)*: 378
New Valley *(El-Wadi'l Gedied/Egy)*: 559
New Veld *(Mts./SAf)*: 362
Ngadda *(Wad./Nig)*: 326
Ngami *(L./Bot)*: 203, 433
Ngono *(R./Tnz)*: 219, 221, 222, 274
N'Goui *(H. St./Sng)*: 381
Ngounié *(R./Gab)*: 399, 400, 401
N'Guiguilone *(H. St./Sng)*: 381
N'Guini *(M. St./Ngr)*: 59
Niamey *(M. St., H. St./Ngr)*: 3, 37, 232, 307, 310, 313, 314, 319, 320
Niandan *(R./Mal)*: 305, 311, 312
Niaoule *(R./Sng)*: 418
Niaoule Tanou *(H. St./Sng)*: 418
NIGER: 3, 20, 21, 67, 73, 300, 304, 305, 307, 309, 323, 429, 444, 511, 518, 520, 557
Niger *(R./W. Afr.)*: 2, 5-8, 17, 20, 24, 209, 232, 239, 243, 244, 251, 264, 266, 271, 272, 303-06, 312-17, 319, 320, 322, 337, 338, 349, 353, 374, 395, 431, 436, 443, 449, 450, 479, 483, 499, 589, 597, 600
NIGERIA: 3, 8, 9, 20, 21, 24, 38, 47, 67, 80, 82, 100, 115, 147, 161, 268, 303, 304, 307, 311, 323, 326, 396, 444, 446, 483, 501, 515, 520, 522, 539, 541, 561, 562, 584, 590, 591, 595-98
Nikolo-Koba *(R./Sng)*: 418
Nile *(R. Sys., Bas./E. Afr.)*: 1, 5-7, 11, 17, 20, 219, 232, 244, 267, 271, 338, 353, 374, 431, 460, 597
Nimule *(Sud)*: 275, 283, 431
Nkam *(R./Cmn)*: 239
Nkhata Bay (M. *St./Mlw)*: 469
Nkhota-Kota *(M. St./Mlw)*: 145, 469
No *(L./Sud)*: 276, 287, 288, 431, 434
Noiré *(Niord, Wad./Mrt)*: 380, 385
North Africa *(Reg./N. Afr.)*: 7, 45, 53, 72, 88, 216
Nossibe *(M. St./Mdg)*: 90, 582, 576
Nouakchott *(Mrt)*: 3, 154, 516
Noun *(R./Cmn)*: 398
Nsukka-Awgu *(Bas./Nig)*: 539
Ntem *(R./Cmn)*: 239
Nubia Lake *(Reserv./Sud)*: 280, 434, 489
Nyaborongo *(R./Rwd)*: 274, 452
Nyala *(Wad./Sud, Ken)*: 34, 59, 451, 527
Nyamgasani *(R./CnK)*: 274, 457
Nyamllel *(Sud)*: 278, 287
Nyandarua Ranges *(Mts./Ken)*: 421
Nyanding *(Kh. Sud)*: 288
Nyaranda *(R. Rwd/Bnd)*: 274
Nyong *(R., Sw./Cmn)*: 239, 433
Nzoya *(R./Ken)*: 451, 452

Offoué *(R./Gab)*: 399
Ogooué *(Ogwe. R./Gab)*: 17, 377, 399-401, 405
Okano *(R./Gab)*: 399
Okavango *(R./Nmb)*: 6, 20, 351, 437, 598
Okavango Basin *(Delta, Sw./Bot)*: 6, 203, 209, 350, 351, 427, 431, 437, 438
Okiep *(M. St./SAf)*: 60
Okwa *(R./Nig)*: 307
Oli *(R./Nig)*: 307
Olifants *(Elephants, R/SAf)*: 405
Omo *(R./Eth)*: 462
Onangue *(L./Gab)*: 433
Ongers *(Str./SAf)*: 364
Onitsha *(H. St./Nig)*: 266, 268, 310, 315
Orange River *(SAf, Nmb)*: 5, 6, 20, 268, 271, 272, 358, 361-68, 372, 374, 483, 505, 592, 593, 597, 598
Oro *(R./Nig)*: 307
Oti *(Pandjari, R./Ben., Tog)*: 389, 390
Ouadai *(Wad./Chd)*: 326
Ouagadougou *(BrF)*: 3, 390
Ouahigouya *(M. St./BrF)*: 78
Ouaka *(R./CAf)*: 339, 340
Oualia *(H. St./Mal)*: 381, 384
Ouandjia *(Head-water-/CAf)*: 325
Ouani *(M. St./CmI)*: 576
Ouaounde *(H. St./Sng)*: 380, 381
Ouassouloubalé *(R./Mal)*: 312
Oudtshoorn *(M. St./SAf)*: 60
Oued Amzez *(Wad./Mor)*: 412
Oued Aoudiar *(Wad./Mor)*: 412
Oued Aoudour *(Wad./Mor)*: 412
Oued Aoulai *(Wad./Mor)*: 412
Oued Beth *(Wad./Mor)*: 412, 414
Oued el-Abtal *(H. St./Alg)*: 412
Oued Erriah *(Wad./Tun)*: 406

Oued Fekka *(Wad./Tun)*: 406
Oued Ghorfa *(Wad./Mrt)*: 377, 380, 385
Oued Guergour *(Wad./Tun)*: 406
Oued Guigou *(Wad./Mor)*: 412
Oued Hadjel *(Wad./Tun)*: 405
Oued Hatab *(Wad./Tun)*: 406
Oued Hathob *(Wad./Tun)*: 405
Oued Hchim *(Wad./Tun)*: 406
Oued Lebene *(Wad.Mor)*: 412, 416
Oued Messenga *(Wad./Tun)*: 406
Oued Mikkes *(Wad./Mor)*: 412
Oued M'Jara *(Wad.Mor)*: 412, 414, 416
Oued Negada *(Wad./Tun)*: 406
Oued Ouerrha *(Ouergha, Wad./Mor)*: 244, 249, 412, 414-16
Oued R'dat *(Wad./Mor)*: 412, 414, 415
Oued R'dom *(Wad./Mor)*: 412, 414
Oued Savalel *(Wad./Mrt)*: 377, 380
Oued Sbeitla *(Wad./Tun)*: 405
Oued Sguifa *(Wad./Tun)*: 406
Oued Sra *(Wad./Mor)*: 412
Ouémé *(R., Fl. Pl./Ben)*: 239, 433
Ouesso *(M. St.. H. St./CnB)*: 191, 192, 336, 346
Ouham *(R./CAf)*: 325, 327, 329, 333
Oum er Rebia *(Wad./Mor)*: 414
Oum Hadier *(Wad./Chd)*: 326
Ouro *(R./STP)*: 571
Ourtzagh *(H. St./Mor)*: 413
Owen Falls Dam0*(Reserv., H. St.,/Ugd)*: 274, 483, 496
Owen Falls *(Ugd)*: 274, 494, 591, 593
Oxenham Ranch *(H. St./SAf)*: 403
Oyi *(R./Nig)*: 307

Pafuri (*M. St./Moz)*: 60, 403
Palmas, Las *(Isl., M. St./CnI)*: *4,* 58, 568
Panda *(M. St./Moz)*: 32
Pangani *(R./Tnz)*: 393
Panjar *(R./Cmn)*: 396
Panyango-Packwach *(H. St./Ugd)*: 283
Papegeio *(R./STP)*: 571
Paramaribo *(Agr. Exp. St./Sur)*: 204
Pendé *(R./Cam, Chd)*: 325-27, 329, 330
Phalobe *(R./Mlw, Moz)*: 473
Pian Pian *(H. St./STP)*: 571
Pibor *(R./Sud)*: 276, 287, 288, 300
Pico *(AzI)*: 566
Pietersberg *(M. St./SAf)*: 60, 403
Plaisance *(M. St./MtI)*: 577
Podor *(H. St./Sng)*: 389, 381, 387
Pointe Noire *(M. St./CnB)*: 191, 192
Pongola *(R./SAf)*: 366, 369, 371
Pont de Télimelé *(H. St./Gun)*: 220
Pont Lardier *(H. St./MtI)*: 571
Port Elizabeth *(M. St./SAf)*: 522
Port Gentil *(Gab)*: 399
Port Louis *(MtI)*: 4
Port Sudan *(Sud)*: 3, 4, 59,141
Porto Grande *(M. St./CVI)*: 58, 59
Porto Novo *(M. St./Ben)*: 3
Porto Santo *(MdI)*: 566
PORTUGAL: 14, 566
Pra *(R./Ghn)*: 271
Praia *(M. St./CVI)*: 4, 59, 569
Praslin *(SyI)*: 575
Pretoria *(SAf)*: 3, 552, 554
Prieska *(H. St./SAf)*: 220, 362, 365,
Principe (Isl., *M. St./STP)*: 570, 571
Pru *(R./Ghn)*: 369
Pungoé *(R./Moz)*: 287
Punta Delgada *(M. St./AzI)*: 566

Quaroun *(L., H. St./Egy)*: 136, 138, 139
Quattara *(Depr./Egy)*: 139, 272, 523

Rabat *(Mor)*: 3
Raga *(M. St./Sud):* 33
Rahad *(R./Eth, Sud)*: 277, 290, 291, 300, 301
Ras-Dashen *(Eth)*: 4
Red Sea: 7, 25, 516, 525
Red Volta *(R./BrF)*: 389, 391, 393
Reef (Mor): 516
Rejaf *(Sud)*: 275,431
Reunion Island *(Burbon/RnI)*: 1, 4, 21, 573, 577, 579, 580
Rharb Plains *(Mor)*: 412
Richard Toll *(H. St./Sng)*: 381
Riche en Eau *(H. St./Mtl)*: 571
Riet *(R./SAf)*: 362, 364
Rippon Falls *(Ugd)*: 274, 494
Rkiz *(L./Sng)*: 377, 378, 433
Roda Nilometer *(Egy)*: 17, 294, 298, 300, 302, 316
Rodriguez Island *(Mtl)*: 577, 579
Roseires *(M. St.. H. St./Sud)*: 45, 290, 299, 302
Roseires Dam *(Reserv./Sud)*: 277, 290, 483, 489, 491, 494, 495, 591
Rosetta *(Branch of Nile/Egy)*: 281, 488, 490
Rosso *(H. St./Sng)*: 381
Rubona *(M. St., Exp. St./Rwd)*: 220
Ruchuru *(R./Ugd)*: 274, 457
Rufiji *(R./Tnz)*: *9,* 433

Ruhuhu *(R./Tnz)*: 469
Ruindi *(R./Ugd)*: 274, 457
Ruiru *(Coff. Res. St./Ken)*: 199, 421
Rukuru *(R./Tnz)*: 469
Rukwa *(L./Tnz)*: 432, 441
Ruvuvu *(Luvironzo, R./Rwd, Bnd)*: 219, 274, 452
Ruwenzori Range *(Mts/Ugd)*: 4, 272, 457
Ruzizi *(R./Rwd, Bnd, CnK)*: 464, 467
RWANDA: 3, 21, 24, 161, 194, 198, 202, 272, 336, 431, 451, 464
Rwizi *(R./Ugd)*: 452

Sabari *(H. St./Ghn)*: 394
Sabhat Guzzzayil *(Wetland/Tun)*: 5
Sahara *(Desert/N. Afr.)*: 25, 32, 43, 45, 53, 65, 304, 305, 322, 444, 517, 519
Sahel *(Reg./NW, W. Afr.)*: 68, 80, 225, 379, 444
Saint Helena Island *(SHI, S. Atl. Oc.)*: 571-573
Sak *(R./SAf)*: 220, 362
Sal *(M St./CVI)*: 58, 569
Salde *(H. St./Sng)*: 381
Saloum *(R./Sng)*: 600
Sanaga *(R./Cmn)*: 239, 244, 337, 395, 396, 398, 405
Sand *(R./SAf)*: 364
Sangha *(R./CnB)*: 239, 336, 339, 340, 346
Sankarani *(Sangarani, R./Mal)*: 305, 312
Sankuru *(R./CnK)*: 339
Santa Maria *(AzI)*: 566
Santo Antão *(CVI)*: 568
Saõ Jorge *(AzI)*: 566
Saõ Miguel *(AzI)*: 566
Saõ Nicolau *(CVI)*: 568
Saõ Tiago *(CVI)*: 568
Saõ Tomé *(Isl., M. St./STP)*: 4, 570, 571
Saõ Tomé & Principe Islands *(Equator/STP)*: 1, 4, 21, 571
Saõ Vincent *(CVI)*: 568
Sarepoli *(H. St./Sng)*: 381
Sarh *(Ft. Archambeault, H. St./Chd)*: 325, 327, 329, 333, 537
Sarir *(Lib)*: 529-31
Sassandra *(R./IvC)*: 593
Sata *(Wad./Chd)*: 326
Sbiba *(Wad./Tun)*: 406
Seaka *(H. St./Les)*: 365
Seati *(R. headwater/Les)*: 361
Sébé *(R./Gab)*: 399
Sebkha Kelbia *(Catch./Tun)* 405
Sebou *(R., Wad./Mor)*: 244, 249, 268, 412-415
Seche *(R./MtI)*: 578
Ségou *(H. St./Mal)*: 303, 305, 310, 320, 377, 436
Semliki *(R., L. Edw.-L. Alb./CnK)*: 274, 283, 456-58
Senchi *(Halcrow, H. St./Ghn)*: 393
SENEGAL: 3. 8, 9, 13, 21, 24, 73, 188, 209, 243, 309, 377, 379, 380, 385, 416, 447, 496, 517, 558, 586, 598
Sénégal *(R./Mal., Sng, Mrt)*: 1, 5, 6, 17, 20, 72, 188, 232, 235, 239, 241, 243, 244, 251, 319, 320, 377, 378, 380, 382, 386, 389, 405, 416-18, 431, 448, 495, 589, 594, 598, 600
Sennar Dam *(Reserv., H. St./Sud)*: 117, 119, 138, 277, 290, 291, 302, 491, 494
Senqu *(Upp. Orange, R./Les)*: 361, 365, 372
Setit *(Takaze, R./Sud)*: 277, 292
Seychelles Islands *(SyI, Ind. Oc.)*: 1, 4, 22, 573-75
Sfax *(M. St./Tun)*: 33, 58
Shabluka Cataract *(6th Catar./Sud)*: 279
Shambe *(H. St./Sud)*: 278, 434, 435
Shamo *(L./Eth)*: 433
Shibeli *(R./Som, Eth)*: 5, 6, 20
Shire *(R./Mlw)*: 13, 244, 356, 469, 504, 599, 600
Shire Highlands *(Mlw)*: 13
Sidi Saad *(H. St./Tun)*: 405, 406, 409, 411
SIERRA LEONE: 3, 9, 21, 24, 45, 74, 202, 216, 304, 427, 598
Siguiri *(Mal)*: 312, 378
Simenti *(H. St./Sng)*: 418
Simiyu *(R./Tnz)*: 451
Sinai Peninsula *(Egy)*: 11, 516, 524
Singa *(M. St./Sud)*: 509
Sio *(R./Ken)*: 451, 452
Sirba *(R./BrF)*: 307
Sirte *(M. St./Lib)*: 52, 58, 88
Sisili *(R./BrF)*: 389
S. José *(H. St./STP)*: 571
Skikda (M, H. St./Alg): 98, 99
Skoon *(R./SAf)*: 362
Sobat *(R./ Eth, Sud)*: 271, 276, 285-88, 300, 301
Sokodé *(M. St./Tog)*: 83
Sokoto *(R., M. St./Nig)*: 147, 304, 307, 310, 314
SOMALIA: 1-3, 8, , 20, 21, 24, 32, 45, 46, 88, 243, 511, 584

Sombani *(R./Mlw, Moz)*: 473
Songwe *(R./Mlw)*: 469
Sota *(R./Ben)*: 314
SOUTH AFRICA: 3, 7, 14, 21, 24, 32, 38, 47, 87, 115, 119, 145, 146, 201, 361-63, 365-68, 371, 402, 404, 483, 501, 505, 508, 509, 553, 584, 591, 593, 597, 598
Southern Africa *(Reg./S. Afr.)*: 19, 76, 88, 227, 469, 483, 549, 584, 599
SPAIN: 14, 568
St. Brandon *(M. St./MtI)*: 577
St. Cruz de Tenerif *(M. St./CnI)*: 58, 568
St. Denis *(M. St./RnI)*: 4, 579
St. Isabel *(M. St./EGn)*: 39
St. Louis *(Sng)*: 13, 78, 83, 84, 377, 378, 380, 381, 385, 389
SUDAN, The: 3, 7-9, 16, 18, 21, 24, 38, 43, 68, 95, 117, 138, 139, 160, 179, 232, 243, 272, 280, 293, 336, 431, 483, 484, 486, 489, 494, 509, 525-28, 581, 585, 591, 592, 599, 600
Sudd (Sw./Sud): 141, 205, 209, 275, 286, 313, 431, 434, 435, 494
SURINAME: 204
Swakopmund *(M. St./Nmb)*: 60, 89, 90
SWAZILAND: 3, 21, 24, 115

Tabou *(Reserv., M. St./IvC)*: 593
Tahoua *(M. St./Ngr)*: 59, 185
Tamale *(M. St./Ghn)*: 538
Tamaniat *(H. St./Sud)*: 291, 302
Tamanrasset *(M. St./Mor)*: 89
Tamatave *(M. St./Mdg)*: 581
Tana *(L., H. St./Eth)*: 290, 460, 461
Tana *(R./Ken)*: 9, 17, 239, 244, 249, 271, 377, 419-24, 597
Tananarive *(M. St./Mdg)*: 4, 580
Tanganyika *(L./E. Afr.)*: 7, 13, 17, 34, 137, 272, 336, 339, 340, 350, 356, 357, 441, 443, 450, 462, 464-68, 472, 503
Tanger *(M. St./Mor)*: 49, 98
Tano *(R., Bas./Ghn)*: 260, 538
TANZANIA: 3, 20, 21, 24, 115, 210, 229, 230, 272, 336, 350, 356, 441, 451, 465, 469, 511, 580, 598
Taoudeni *(Ngr)*: 516
Taoué Canal *(Sng)*: 447
Tapoa *(R./Ngr)*: 307
Taraba *(R./Nig)*: 307, 315
Tarfaya Dakhla *(Atlas Reg./Alg, Mrt)*: 516
Tazerbo *(Lib)*: 531
Télé *(L./Mal)*: 307
Tembi *(R./Gun)*: 305
Téné *(R./Gun)*: 379
Tenerife *(CnI)*: 568
Terceira *(Azl)*: 566
Tessalit *(M. St./Mal)*: 58
Tete *(M. St./Moz)*: 503
Thamalakane *(R./Bot)*: 437
Thiba *(R./Ken)*: 421
Thika *(R./Ken)*: 421
Thiokoye *(R./Sng)*: 418
Tibesti Massif *(Lib, Chd)*: 2, 538
Tidjikia *(M. St./Mrt)*: 58
Tiguéré *(Sng)*: 389
Tillabery *(M. St./Ngr)*: 32, 59, 185, 310
Timbuktu *(Tombouktou/Mal)*: 304, 305. 307, 310, 314, 436
Tindouf *(Bas./Alg)*: 535
Tinkisso *(R./ Gun)*: 305, 311, 312
Tissisat Falls *(Eth)*: 277, 461
TOGO: 3, 9, 22, 24, 38, 499
Tongaat *(Exp. Farm/SAf)*: 201
Tonj *(R./Sud)*: 276, 287
TouKoto *(H. St./Mal)*: 384
Tozeur *(Agr. Exp. St./Tun)*: 152, 153
Tripoli *(M, St. Lib)*: 3, 58, 559, 560
Tristan da Cunha Islands *(TCI, S. Atl. Oc.)*: 571, 572, 574
Tsabong (M. *St./Bot)*: 32, 60, 549
Tsehlanyane *(R./Les)*: 365
Tsiribihina *(R./Mdg)*: 581
Tsumeb (M. *St./Nmb)*: 59
Tulear *(M. St./Mdg)*: 60, 146, 581
Tumba *(L./CnK)*: 339, 340
Tunis *(M. St./Tun)*: 4
TUNISIA: 4, 5, 7, 22, 24, 152, 154, 193, 264, 405, 410, 411, 416, 521
Turkana *(Rudolf, L./Ken, Eth)*: 441, 462, 463
Turkwel *(R./Ken)*: 462

Ubangi *(Ubangui, Oubangui, R./CAf, CnK)*: 5, 6, 17, 20, 232, 239, 244, 325, 335, 338, 339, 341, 346, 349, 350
UGANDA: 4, 11, 20, 22, 24. 47, 115, 117, 272, 431, 443, 451, 458, 483, 495, 511, 591, 593,
Upington *(M. St., H. St./SAf)*: 60, 361, 363, 365

Vaal *(R./SAf)*: 5, 12, 268, 272, 358, 361, 362, 365, 366, 371, 372
Vaal Dam *(Reserv./SAf)*: 362, 366, 371
Vallon, Beau *(H. St./MtI)*: 578
Valsche *(R./SAf)*: 362

Van der Kloof Dam *(P.K. Le Roux, Reserv./SAf)*: 362, 365, 372, 507, 592, 593
Vastrap *(H. St./SAf)*: 220
Versailles *(France)*: 149
Vet *(R./SAf)*: 362
Veveno *(R./Sud)*: 278
Victoria *(L./E. Afr.)*: 5, 12, 13, 17, 42, 66, 113, 123, 126, 128, 129, 198, 219, 221, 274, 284, 299, 335, 425, 440, 450-53, 455, 456, 462, 465, 468, 494, 495, 542, 590
Victoria *(M. St./SyI)*: 574, 575
Victoria Falls *(H. St./Zmw)*: 13, 350, 351, 353, 358, 360, 501, 599
Victoria Nile *(R./Ugd)*: 451, 452, 456, 458, 483, 494
Villa Cisneros *(M. St./WSh)*: 58
Vioolsdrift *(H. St./SAf)*: 365, 367
Vis *(Fish, R./SAf)*: 362, 593, 597
Volta *(Reserv., R./Ghn)*: 239, 377, 389, 390, 391, 394, 395, 405, 427, 483, 496-99, 537, 590, 594

Wad Medani *(M. St./Sud)*: 33, 34, 59, 83, 96, 140, 179, 181, 182, 277, 291
Wadi Halfa *(M. St./Sud)*: 58, 131, 138, 292, 300-02
Wassadou D.S. *(H. St./Sng)*: 418
Wassadou U.S. *(H. St./Sng)*: 418
Wau *(M. St./Sud)*: 34, 141, 278, 287
West Africa *(Reg./W. Afr.)*: 19, 28, 43, 45, 53, 67, 74, 76, 87, 188, 216, 222, 228, 309, 377, 380, 418, 427, 483, 510, 558, 586, 88, 590
Western Desert *(Lib, Egy)*: 5, 6, 139, 516, 523, 524, 559
WESTERN SAHARA: 4, 22
White Gorgol *(Wad./Mrt)*: 377, 380
White Nile *(Sud)*: 17, 65, 179, 271, 274, 277, 285, 286, 287, 290, 291, 301, 592, 600
White Volta *(Nakambe, V. Blanche, R./BrF, Ghn)*: 389, 390, 393, 496
Wideawake *(M. St./AsI)*: 59
Wilge *(R./SAf)*: 362, 368
Wina *(R./Cmn)*: 325, 327
Windhoek *(M. St./Nmb)*: 3, 39, 60
Wiswila *(R./CnK)*: 339
Wouri *(R./Cmn)*: 220, 239

Yabassi *(H. St./Cmn)*: 220
Yaeres *(Fl. Pl./Chd, Cmn)*: 326, 331, 433
Yakala *(H. St./BrF)*: 393
Yala *(Sw./Ken)*: 432, 452
Yangambe *(M. St./CnK)*: 33
Yaounde *(M. St./Cmn)*: 3, 397
Yapei *(Ghn)*: 390, 496
Yarugu *(H. St./Ghn)*: 393
Yedinga *(Wad./Chd)*: 326
Yedseram *(Wad./Nig)*: 326
Yei *(R., M. St./Sud)*: 278, 287
Yelwa *(Nig)*: 147, 310, 499
Yobe *(R./Nig)*: 313, 446, 447
Yola *(H.St./Nig)*: 310, 315

Zaïre *(R./Congo)*: 198, 244, 336, 343, 398, 419, 431, 500, 593, 600
Zambezi *(R./Zmb, Zmw, Moz)*: 5-7, 12, 13, 20, 219, 271, 336, 350, 351, 356, 358, 359, 361, 374, 427, 431, 438, 440, 469, 483, 501, 503, 505, 598-600
ZAMBIA: 22, 24, 32, 39, 45, 47, 87, 88, 115, 119, 144, 145, 199, 200, 210, 211, 261, 262, 335, 336, 350, 353, 360, 427, 437, 465, 472, 483, 501, 503, 504, 511, 547, 548, 593, 594, 598
Zanzibar *(Tnz)*: 13
Zaonia-Nurbaz *(H. St./Alg, Mor)*: 220
Zeerust *(M. St./SAf)*: 60
Zémio *(H. St./CAf)*: 339
Zerga *(Wad./Tun)*: 400
Zeroud *(Wad./Tun)*: 265, 377, 405-11,415
ZIMBABWE: 4, 9, 22, 24, 39, 45, 47, 78, 87, 115, 142-44, 199, 201, 210, 225, 226, 273, 350, 351, 353, 402-04, 475, 483, 501, 591, 594, 598
Zinder *(M. St./Ngr)*: 96, 185
Ziway *(L./Eth)*: 433
Zomba *(M. St./Mlw)*: 165, 351

Water Science and Technology Library

1. A.S. Eikum and R.W. Seabloom (eds.): *Alternative Wastewater Treatment.* Low-Cost Small Systems, Research and Development. Proceedings of the Conference held in Oslo, Norway (7–10 September 1981). 1982 ISBN 90-277-1430-4
2. W. Brutsaert and G.H. Jirka (eds.): *Gas Transfer at Water Surfaces.* 1984 ISBN 90-277-1697-8
3. D.A. Kraijenhoff and J.R. Moll (eds.): *River Flow Modelling and Forecasting.* 1986 ISBN 90-277-2082-7
4. World Meteorological Organization (ed.): *Microprocessors in Operational Hydrology.* Proceedings of a Conference held in Geneva (4–5 September 1984). 1986 ISBN 90-277-2156-4
5. J. Němec: *Hydrological Forecasting.* Design and Operation of Hydrological Forecasting Systems. 1986 ISBN 90-277-2259-5
6. V.K. Gupta, I. Rodríguez-Iturbe and E.F. Wood (eds.): *Scale Problems in Hydrology.* Runoff Generation and Basin Response. 1986 ISBN 90-277-2258-7
7. D.C. Major and H.E. Schwarz: *Large-Scale Regional Water Resources Planning.* The North Atlantic Regional Study. 1990 ISBN 0-7923-0711-9
8. W.H. Hager: *Energy Dissipators and Hydraulic Jump.* 1992 ISBN 0-7923-1508-1
9. V.P. Singh and M. Fiorentino (eds.): *Entropy and Energy Dissipation in Water Resources.* 1992 ISBN 0-7923-1696-7
10. K.W. Hipel (ed.): *Stochastic and Statistical Methods in Hydrology and Environmental Engineering.* A Four Volume Work Resulting from the International Conference in Honour of Professor T. E. Unny (21–23 June 1993). 1994
    10/1: Extreme values: floods and droughts ISBN 0-7923-2756-X
    10/2: Stochastic and statistical modelling with groundwater and surface water applications ISBN 0-7923-2757-8
    10/3: Time series analysis in hydrology and environmental engineering ISBN 0-7923-2758-6
    10/4: Effective environmental management for sustainable development ISBN 0-7923-2759-4
    Set 10/1–10/4: ISBN 0-7923-2760-8
11. S.N. Rodionov: *Global and Regional Climate Interaction: The Caspian Sea Experience.* 1994 ISBN 0-7923-2784-5
12. A. Peters, G. Wittum, B. Herrling, U. Meissner, C.A. Brebbia, W.G. Gray and G.F. Pinder (eds.): *Computational Methods in Water Resources X.* 1994
    Set 12/1–12/2: ISBN 0-7923-2937-6
13. C.B. Vreugdenhil: *Numerical Methods for Shallow-Water Flow.* 1994 ISBN 0-7923-3164-8
14. E. Cabrera and A.F. Vela (eds.): *Improving Efficiency and Reliability in Water Distribution Systems.* 1995 ISBN 0-7923-3536-8
15. V.P. Singh (ed.): *Environmental Hydrology.* 1995 ISBN 0-7923-3549-X
16. V.P. Singh and B. Kumar (eds.): *Proceedings of the International Conference on Hydrology and Water Resources* (New Delhi, 1993). 1996
    16/1: Surface-water hydrology ISBN 0-7923-3650-X
    16/2: Subsurface-water hydrology ISBN 0-7923-3651-8

16/3: Water-quality hydrology ISBN 0-7923-3652-6
16/4: Water resources planning and management ISBN 0-7923-3653-4
Set 16/1–16/4 ISBN 0-7923-3654-2

17. V.P. Singh: *Dam Breach Modeling Technology.* 1996 ISBN 0-7923-3925-8
18. Z. Kaczmarek, K.M. Strzepek, L. Somlyódy and V. Priazhinskaya (eds.): *Water Resources Management in the Face of Climatic/Hydrologic Uncertainties.* 1996 ISBN 0-7923-3927-4
19. V.P. Singh and W.H. Hager (eds.): *Environmental Hydraulics.* 1996 ISBN 0-7923-3983-5
20. G.B. Engelen and F.H. Kloosterman: *Hydrological Systems Analysis.* Methods and Applications. 1996 ISBN 0-7923-3986-X
21. A.S. Issar and S.D. Resnick (eds.): *Runoff, Infiltration and Subsurface Flow of Water in Arid and Semi-Arid Regions.* 1996 ISBN 0-7923-4034-5
22. M.B. Abbott and J.C. Refsgaard (eds.): *Distributed Hydrological Modelling.* 1996 ISBN 0-7923-4042-6
23. J. Gottlieb and P. DuChateau (eds.): *Parameter Identification and Inverse Problems in Hydrology, Geology and Ecology.* 1996 ISBN 0-7923-4089-2
24. V.P. Singh (ed.): *Hydrology of Disasters.* 1996 ISBN 0-7923-4092-2
25. A. Gianguzza, E. Pelizzetti and S. Sammartano (eds.): *Marine Chemistry.* An Environmental Analytical Chemistry Approach. 1997 ISBN 0-7923-4622-X
26. V.P. Singh and M. Fiorentino (eds.): *Geographical Information Systems in Hydrology.* 1996 ISBN 0-7923-4226-7
27. N.B. Harmancioglu, V.P. Singh and M.N. Alpaslan (eds.): *Environmental Data Management.* 1998 ISBN 0-7923-4857-5
28. G. Gambolati (ed.): *CENAS. Coastline Evolution of the Upper Adriatic Sea Due to Sea Level Rise and Natural and Anthropogenic Land Subsidence.* 1998 ISBN 0-7923-5119-3
29. D. Stephenson: *Water Supply Management.* 1998 ISBN 0-7923-5136-3
30. V.P. Singh: *Entropy-Based Parameter Estimation in Hydrology.* 1998 ISBN 0-7923-5224-6
31. A.S. Issar and N. Brown (eds.): *Water, Environment and Society in Times of Climatic Change.* 1998 ISBN 0-7923-5282-3
32. E. Cabrera and J. García-Serra (eds.): *Drought Management Planning in Water Supply Systems.* 1999 ISBN 0-7923-5294-7
33. N.B. Harmancioglu, O. Fistikoglu, S.D. Ozkul, V.P. Singh and M.N. Alpaslan: *Water Quality Monitoring Network Design.* 1999 ISBN 0-7923-5506-7
34. I. Stober and K. Bucher (eds): *Hydrogeology of Crystalline Rocks.* 2000 ISBN 0-7923-6082-6
35. J.S. Whitmore: *Drought Management on Farmland.* 2000 ISBN 0-7923-5998-4
36. R.S. Govindaraju and A. Ramachandra Rao (eds.): *Artificial Neural Networks in Hydrology.* 2000 ISBN 0-7923-6226-8
37. P. Singh and V.P. Singh: *Snow and Glacier Hydrology.* 2001 ISBN 0-7923-6767-7
38. B.E. Vieux: *Distributed Hydrologic Modeling Using GIS.* 2001 ISBN 0-7923-7002-3

39. I.V. Nagy, K. Asante-Duah and I. Zsuffa: *Hydrological Dimensioning and Operation of Reservoirs.* Practical Design Concepts and Principles. 2002 ISBN 1-4020-0438-9
40. I. Stober and K. Bucher (eds.): *Water-Rock Interaction.* 2002 ISBN 1-4020-0497-4
41. M. Shahin: *Hydrology and Water Resources of Africa.* 2002 ISBN -4020-0866-X